emc2016

11 - 15 September

2nd European Mineralogical Conference

rimini, italy

Minerals, rocks and fluids: alphabet and words of planet Earth

Book of Abstracts

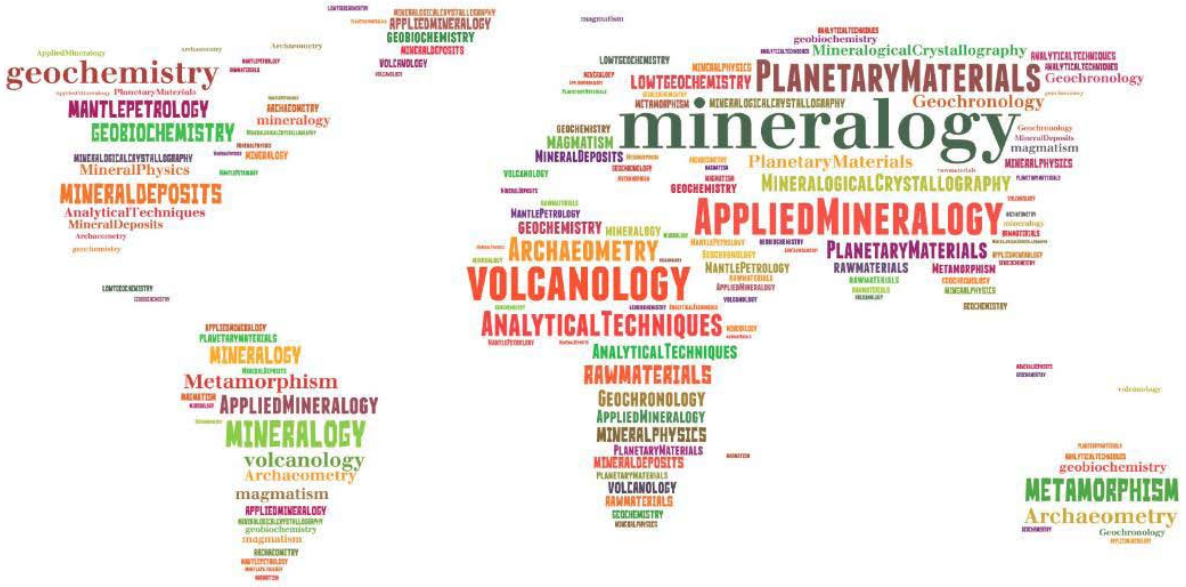

Editors: Bernardo Carmina and Marco Pasero

Thermo SCIENTIFIC

A Thermo Fisher Scientific Brand

Research without boundaries

To answer your scientific questions, the Thermo Scientific™ portfolio of isotope analysis instruments provides you with the right analytical solutions. See us at **EMC 2016** and discover the field-proven portfolio, that offers you state of the art technologies for your analytical needs in the lab and in the field.

for the lab and in the field

• thermofisher.com/geosciences

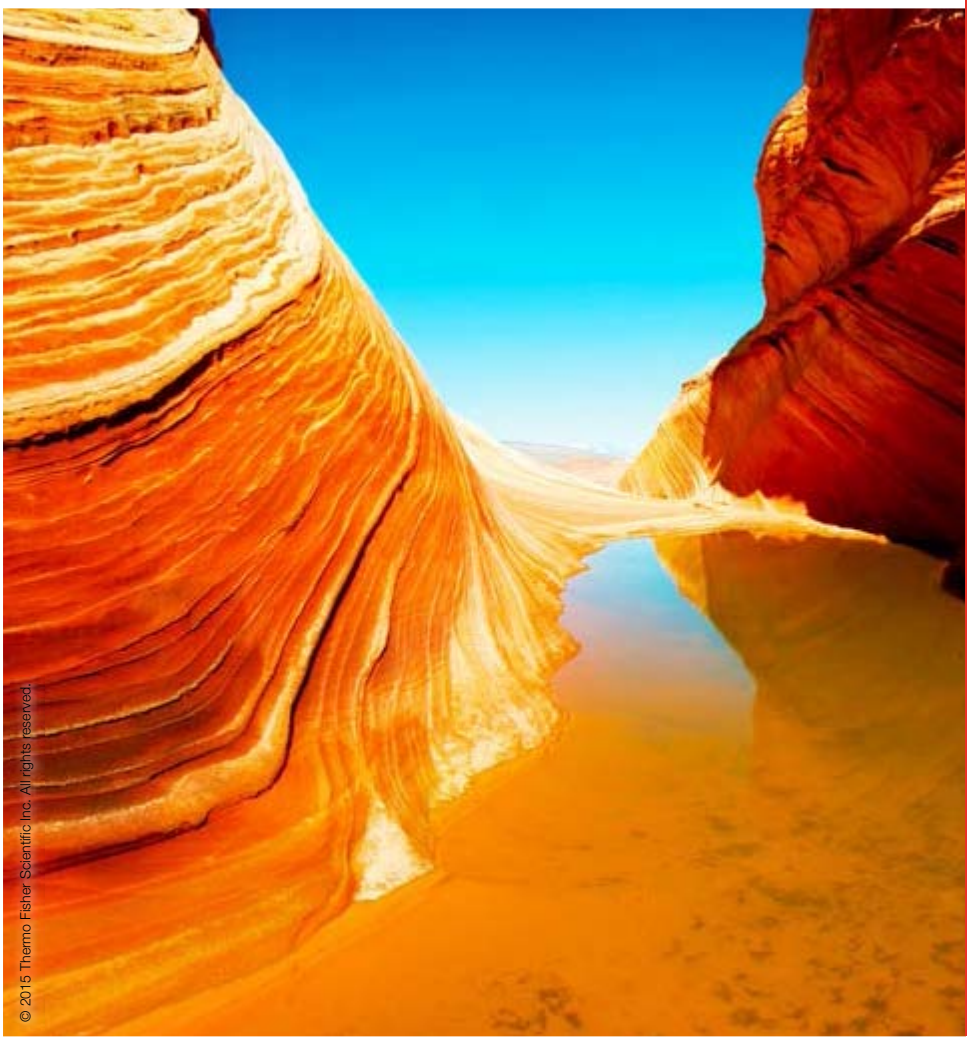

Thermo Scientific™ Delta Ray™
Isotope Ratio Infrared
Spectrometry with
URI Connect

Thermo Scientific™ 253 Plus™
10 kV Isotope Ratio MS

Thermo Scientific™
NEPTUNE Plus™
High resolution
Multicollector ICP-MS

Thermo Scientific™ 253 Ultra™
High Resolution
Isotope Ratio MS

The moment correlation completes the picture

ZEISS Geoscience Solutions

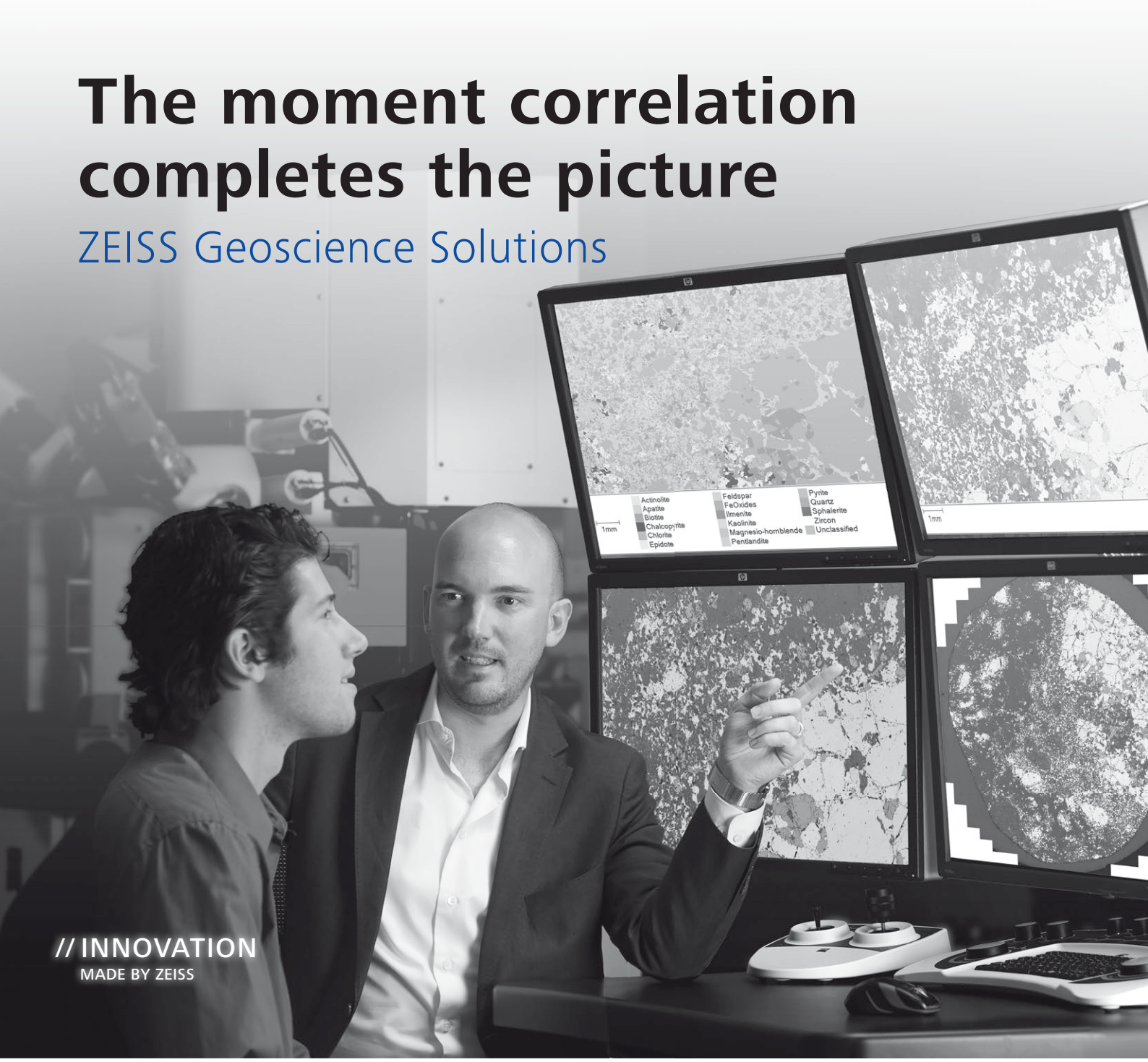

Images of a nickel sulphide ore. Sample courtesy of Leicester University, UK.

Correlative Microscopy Solutions from ZEISS

Integrate images and data from multiple sources for rapid and accurate mineralogical analysis with ZEISS correlative workflows.

Incorporate optical, electron and X-ray microscopy with automated mineralogy to link the micro and nano worlds in 2D and 3D. Correlation from ZEISS gives you the complete picture.

www.zeiss.com/mineralogic

ZEISS

HORIBA Scientific

JOBIN YVON Technology

Raman Family

Range of Instruments

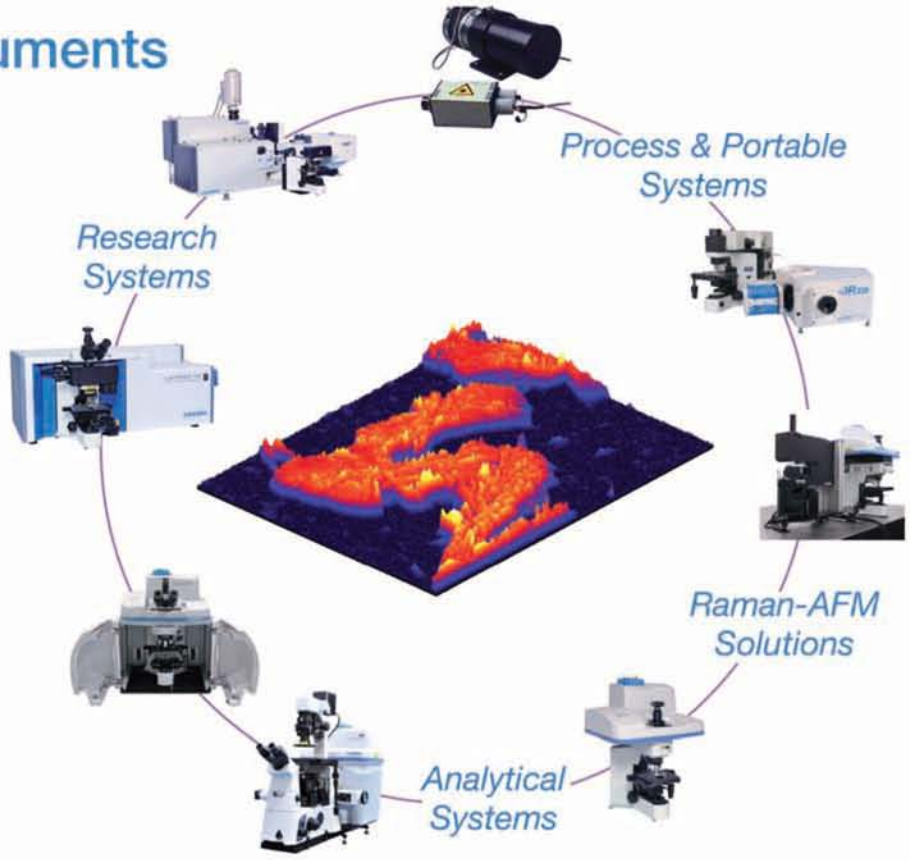

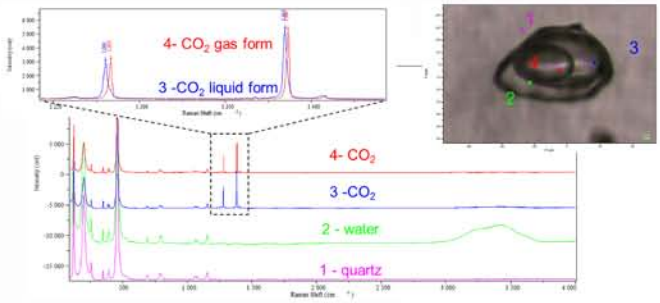

Inclusion Analysis-confocal depth profiling

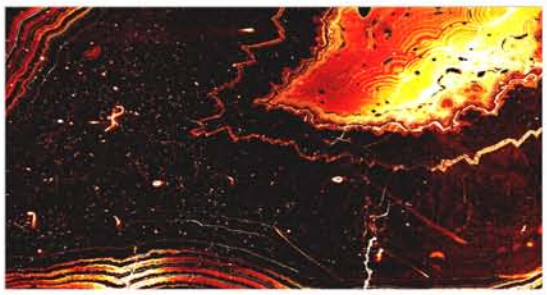

Fast High resolution maps
(4001 x 2800 spectra of a
20 mm x 14 mm Geological rock sample)

Multivariate analysis of spectra (Meteorite reconstruction)

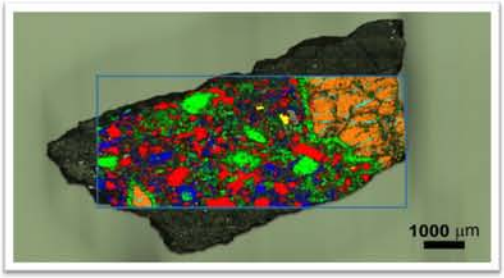

OLYMPUS

Your Vision, Our Future

Making Mineralogy Faster and Easier

With the Olympus Microscopy, X-Ray Fluorescence and Diffraction Systems

Olympus is the perfect partner for your research with our expert knowledge and experience in microscopy, X-ray fluorescence and diffraction systems. Our high performance portable and benchtop solutions save time and provide confident results, enabling accurate and rapid analysis of mineral and rock samples at the bench and in the field.

Introducing the new modular BX3M system - the most flexible and easy to use microscope in the lab:

- Intuitive Aperture and field stop control
- Easy stage movement for large panoramic view
- Extended focus imaging
- Advanced automatic calibration

Discover high performance portable X-ray Fluorescence and X-ray Diffraction analyzers for rapid and precise elemental chemistry, quantitative mineralogy and mineral phase identification.

Find out more at www.olympus-ims.com

OLYMPUS ITALIA S.R.L.
Via Modigliani, 45 – 20090 Segrate (MI), Italia | Tel.: +39 0 22 69 721 | Fax: +39 0 22 69 72 355
www.olympus-ims.com | infoindustrial.italia@olympus-europa.com

LYNXEYE XE-T: Energy dispersive 0D/1D/2D XRD

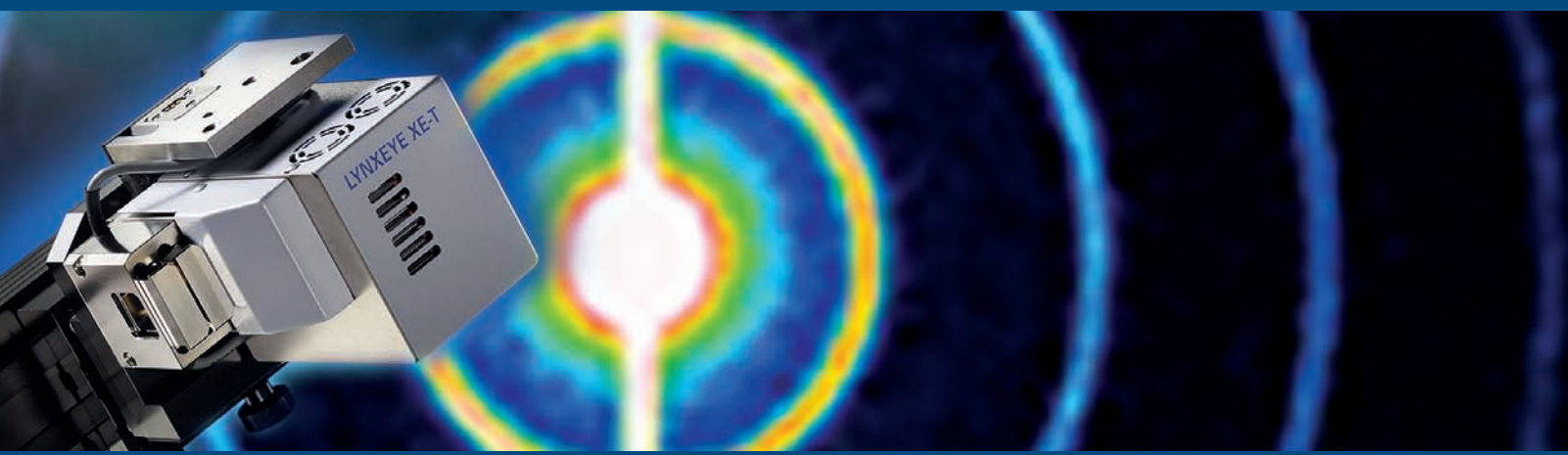

The 1st and only detector on the market enabling energy dispersive zero-, one- and two-dimensional diffraction

- Superb energy resolution better than 380 eV, eliminating the need for Kß filters, mirrors and secondary monochromators
  → Unrivalled filtering of sample fluorescense, white radiation, and Kß radiation
- Operation with all common characteristic X-ray emission lines (Cr, Co, Cu, Mo, and Ag radiation)
- Variable sample to detector distance to optimize 2θ- and γ-coverage
- No defective strips at delivery time - guaranteed
- Full integration in DIFFRAC.SUITE

Dynamic Beam Optimization

Superior suppression of instrument background, specifically of air scatter at low angles 2θ

- Motorized Anti Scatter Screen: Fully software controlled retraction of the knife to prevent any cropping of the beam
  - Fully compatible with both the Bragg-Brentano geometry (fixed as well as variable divergence slits) and the parallel beam geometry
- Variable Active Detector Window: Fully software controlled switching on of individual strips to open the detector window as a function of 2θ
- Acquisition of diffraction data with virtually no instrument background starting at angles as low as about 0.2° 2θ
- Full integration in DIFFRAC.SUITE

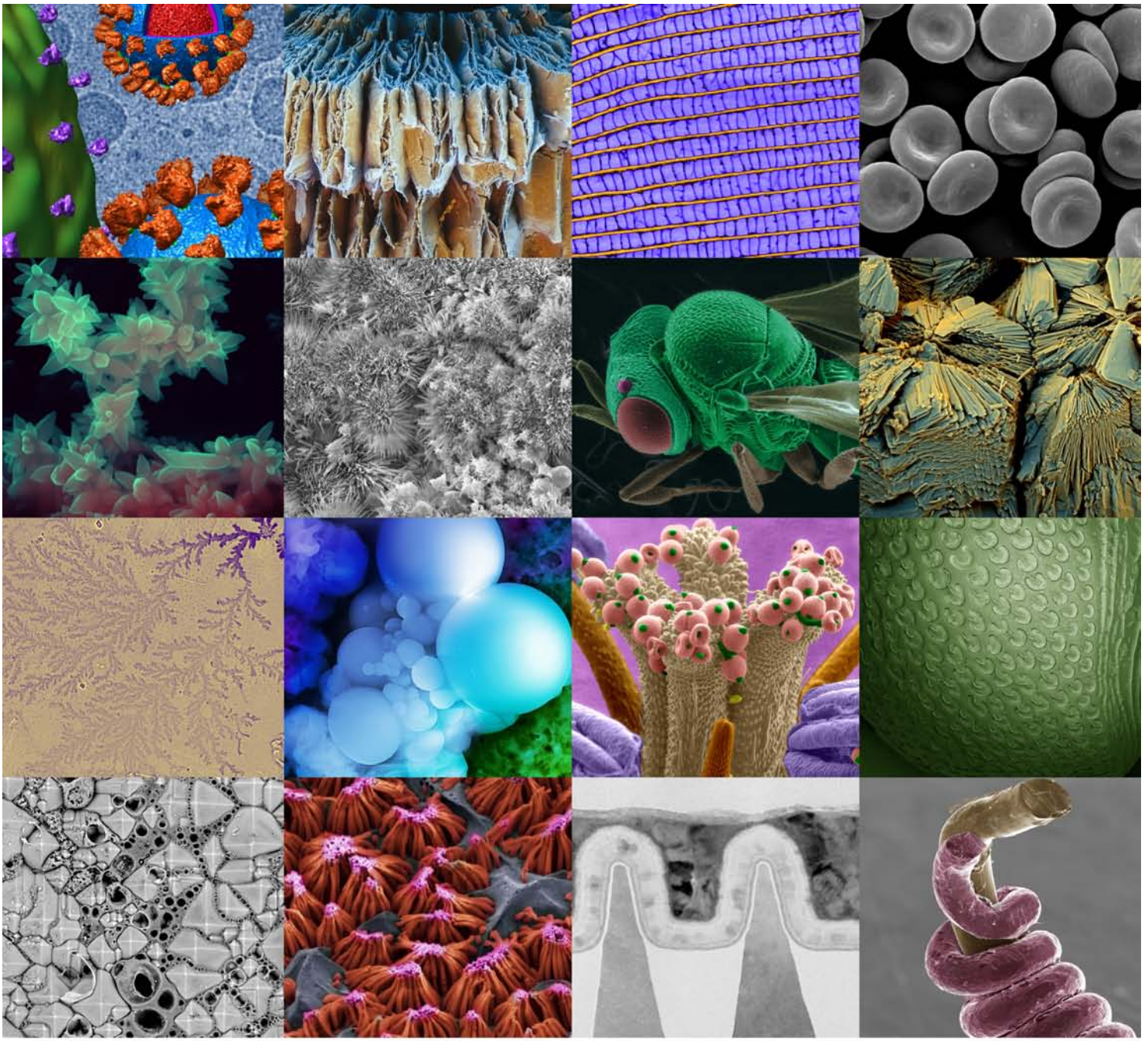

Collection of images from FEI customers. To learn more about the images above, visit FEI.com/BetterWorld.

FEI customers create a better world

Founded in 1971, FEI reveals the unseen world via powerful microscopes and software that help researchers understand things at the nano-scale. Our customers seek to improve the quality of life for everyone by solving global challenges that will lead to cures for diseases, new materials to make vehicles safer and more eco-friendly, longer-lasting batteries for mobile devices, and so much more.

Discover more at FEI.com/BetterWorld

FEI™

Explore. Discover. Resolve.

HUMAN HEALTH

ENVIRONMENTAL HEALTH

ONE RUN LETS YOU SEE IT ALL

Nanoparticle concentration, composition, size and distribution, dissolution and agglomeration tracking – all in under a minute.

Nanoparticles' unique characteristics and increasing usage in consumer products will inevitably lead to their release into the environment. Characterizing them required hours of analysis time and manual calculations – until now. The NexION® 350 ICP-MS single-particle analyzer combines best-in-class data acquisition rates with proprietary software to deliver full characterization in one run – *that's 60 seconds or less*. Want to understand more from your nanoparticle research? Just give us a minute.

www.perkinelmer.com/NexIONnano

PerkinElmer®
For the Better

INDEX

Plenary lectures

NEW PERSPECTIVES FOR MINERAL SCIENCES USING FOURTH GENERATION LIGHT SOURCES

Appel K.*[1]
[1] European X-Ray Free-Electron Laser Facility, Schenefeld, Germany
Corresponding email: karen.appel@xfel.eu

Keywords: FEL, pump-probe experiments, dynamic compression

Free-electron laser facilities (FEL) i.e. fourth generation light sources enable new applications in the field of time-resolved studies including mineralogical research. The pulse length of the X-rays of these FELs is in the regime of a few to a few 100 fs and the repetition rate is 50 Hz - 4.5 MHz. The high intensity and the time structure of the FEL X-ray beam allow single shot images of the exposed material. With the principle of pump-probe experiments, reactions of materials can be studied with a time resolution down to femtoseconds. First FELs operated in the VUV regime (FLASH and FERMI), but since a few years, FELs in the hard X-ray regime are available (LCLS and SACLA) and several are planned to become operative within the next couple of years (SwissFEL, PAL-XFEL) as well as the European X-ray Free Electron Laser (XFEL) in Schenefeld. Since the X-rays allow to probe short-lived states, high-energy optical long pulse lasers have been installed at SACLA and LCLS to study materials at extreme conditions of pressure and temperature. One obvious application in mineralogy using optical high-energy long pulse lasers as a pump is for dynamic compression experiments in high-pressure research. By modifying the pulse shape of the optical long pulse laser, either the Hugoniot behavior of a material can be studied with shock compression, or the regions below the Hugoniot line in the P-T diagram with ramp compression. In this contribution, an overview of recent experiments in this field will be given. European XFEL is a new user facility which will open to the users in late 2016. It will provide soft to hard X-rays of up to 25 k*e*V and can be operated up to 4.5 MHz. Six baseline experiments are currently being build, one of them is dedicated to High Energy Density Science (HED). At this scientific instrument several pump systems are foreseen including a high-energy long pulse laser (100 J, 2-15 ns). This will allow to realize P-T conditions in the Earth core and of rocky planets of several Earth masses. X-rays with up to 25 k*e*V will be available, thus enabling also diamond anvil cell experiments at a unprecedented repetition rate. On top of that, chemical reactions can be studied in-situ at a time resolution of up to 4.5 MHz. In this contribution, we present the actual status of the facility, the capabilities of European XFEL with respect to mineralogy, compare this to state-of-the-art techniques and will show planned first experiments.

THE JOYS OF MAKING OR BREAKING BONDS IN MINERALS: A MOLECULAR PERSPECTIVE

Benning L.G.*[1-2]
[1] Helmholtz Zentrum Potsdam, GFZ Deutsches GeoForschungsZentrum, Potsdam, Germany
[2] School of Earth and Environment, University of Leeds, United Kingdom
Corresponding email: benning@gfz-potsdam.de

Keywords: mineral-fluid interfaces, nanoparticles, weathering

Reactions leading to the formation or dissolutions of mineral phases control most biogeochemical element cycles on Earth and as far as we know also elsewhere. Surprisingly, to quantitatively asses the molecular level reactions that lead to bonds between atoms in minerals to be made or broken - essentially to nucleate, grow, transform or dissolve a mineral phase - is harder to measure than you may think. In the last decade our ability to follow such complex and highly dynamic reactions has massively improved, yet we still lack quite a lot of fundamental theoretical knowledge about nanoscale processes, and we lack experimental validations of reactions that have been inferred from observations of natural processes. Bases on examples I will discuss how we can today not just quantitatively follow such complex and often multiple steps reactions in solution, but also how we use this knowledge to further develop, test and validate new sample preparation / handling approaches, and or *in situ*, time resolved and high-resolution methods. This allows us to gain a better understanding of fluid-mineral-microbe interface mineral reactions at more realistic chemical and physical conditions representative of natural processes in aquatic media, soils, sediments, aerosol or other geo-bio systems. I will show how mineral formation and transformations in the carbonates (Bots et al., 2012) and sulphate (Stawski et al., 2016; Van Driessche et al., 2012) occurs, what the role of biology in mineral weathering and soil formation is (Bonneville et al., 2016), or how we assessed if and why the delivery of iron-rich nanoparticles into the ocean (Hawkings et al., 2014) teaches us something about nutrient cycling, primary productivity and mineral chemistry in modern or ancient geological settings.

Bonneville, S., Bray, A.W., Benning, L.G. (2016): Structural Fe(II) oxidation in biotite by an ectomycorrhizal fungi drives mechanical forcing. *Environ. Sci. Technol.*, **50**, 5589-5596.

Bots, P., Benning, L.G., Rodriguez-Blanco, J.-D., Roncal-Herrero, T., Shaw, S. (2012): Mechanistic insights into the crystallization of amorphous calcium carbonate (ACC). *Cryst. Growth Des.*, **12**, 3806-3814.

Hawkings, J.R., Wadham, J.L, Tranter, M., Raiswell, B., Benning, L.G., Statham, P.J., Tedstone, A., Nienow, P., Lee, K., Telling, J. (2014): Ice sheets as a significant source of highly reactive nanoparticulate iron to the oceans. *Nature Commun.*, **5**, 3929.

Stawski, T.M., van Driessche, A.E.S., Ossorio, M., Rodriguez-Blanco, J.D., Besselink, R., Benning, L.G. (2016): Formation of calcium sulfate through the aggregation of sub-3 nanometre primary species. *Nature Commun.*, **7**, 11177.

Van Driessche, A.E., Benning, L.G., Rodriguez-Blanco, J.D., Ossorio, M., Bots, P., García-Ruiz, J.M. (2012): The role and implications of bassanite as a stable precursor phase to gypsum precipitation. *Science*, **336**, 69-72.

RADIATION EFFECTS IN MINERALS

Ewing R.C.*[1]
[1] Department of Geological Sciences, Stanford University, CA, USA
Corresponding email: rewing1@stanford.edu

Keywords: radiation, metamict, amorphous

The earliest description of a change in mineral property caused by radiation damage was by Jöns Jacob Berzelius in 1814. Berzelius discovered that some U- and Th-bearing minerals glowed on heating, releasing stored energy. In 1893, Brøgger defined "metamikte" as a third class of naturally occurring, amorphous materials. Metamict minerals were recognized as being amorphous due to their conchoidal fracture and isotropic optical properties; however, well-developed crystal faces evidenced their prior crystalline state. Thus, radiation effects in minerals were well recognized even before the discovery of radioactivity in 1896 by Henri Becquerel. During the first one hundred years of investigation of metamict minerals substantial progress was made in understanding radiation-induced damage in minerals and materials (Ewing, 1994). During the past 25 years, much of the progress in understanding radiation damage in minerals has been made by the use of ion beams to simulate different types of damage, mainly alpha-decay and fission fragment damage (Ewing et al., 2000). These investigations have been stimulated by an interest in the effect of radiation on nuclear waste forms (Ewing & Weber, 2010), the formation and annealing mechanisms of fission tracks, and the diffusion and subsequent retention or loss of U, Pb and He in minerals used for age-dating and thermochronology (Li et al., 2012). A variety of materials, with mineral analogues, have been investigated because they have a high capacity to incorporate actinides, are chemically durable, and in some cases, are resistant to radiation damage. There has been substantial interest in isometric pyrochlore, $A_2B_2O_7$ (A = rare earths, actinides; B = Ti, Zr, Sn, Hf), for the immobilization of transuranium elements. Four radiation-induced transformations occur: i) periodic-aperiodic, ii) order-disorder, iii) crystalline-to-crystalline, and iv) chemical decomposition. Certain pyrochlore compositions (B = Zr, Hf) remain crystalline to very high doses of alpha-decay event dose, which is mainly caused by ballistic interactions with the alpha-recoil nucleus. The radiation-response of pyrochlore and zircon have been investigated using relativistic heavy ions for which high energy deposition occurs by electronic excitation. Energetic ions deposit exceptional amounts of kinetic energy (G*e*V) within an exceedingly short time (less that a femtosecond) into nano-scale volumes. Energy deposition is up to tens of *e*V/atom, creating damage tracks, very similar to fission tracks in zircon and apatite. Some irradiations have been done at high pressures (> 50 Gpa) and temperatures (up to 500°C) within a diamond anvil cell (Lang et al., 2009). The combined use of advanced *in situ* (synchrotron X-ray diffraction and Raman spectroscopy) and ex situ (transmission electron microscopy) characterization techniques has shown that normal phase relations are changed by irradiation and that most materials can be amorphized. Most recently, new advances in understanding the local ordering in irradiated materials have been made by the use of neutron total scattering and pair distribution function analysis (Shamblin et al., 2016). The research horizon for metamict minerals remains broad and exciting!

Ewing, R.C. (1994): The metamict state: 1993 – the centennial. *Nucl. Instr. Meth. Phys. Res.*, **B91**, 22-29.

Ewing, R.C. & Weber, W.J. (2010): Actinide waste forms and radiation effects. *in* "The chemistry of the actinides and transactinide elements", L.R. Morss, N.M. Edelstein, J. Fuger, eds., Springer, New York, 3813-3888.

Ewing, R.C., Meldrum, A., Wang, L.M., Wang, S.X. (2000): Radiation-induced amorphization. *Rev. Mineral. Geochem.*, **39**, 319-361.

Lang, M., Zhang, F.X., Lian, J., Trautmann, C., Neumann, R., Ewing, R.C. (2009): Combined high pressure and heavy-ion irradiation: a novel approach. *J. Synchr. Rad.*, **16**, 773-777.

Li, W.X., Lang, M., Gleadow, A.J.W., Zdorovets, M.V., Ewing, R.C. (2012): Thermal annealing of unetched fission tracks in apatite. *Earth Planet. Sci.Letters*, **321**, 121-127.

Shamblin, J., Feygenson, M., Neuefeind, J., Tracy, C.L., Zhang, F.X., Finkeldei, S., Bosbach, D., Zhou, H., Ewing, R.C., Lang, M. (2016): Probing disorder in isometric pyrochlore and related complex oxides. *Nature Mater.*, **15**, 507-511.

A NEW METHODOLOGICAL APPROACH FOR THE EVALUATION OF SOIL POLLUTION BY TRACE ELEMENTS

Galán E.*[1]
[1] Departamento de Cristalografía, Mineralogía y Química Agrícola, Universidad de Sevilla, Spain
Corresponding email: egalan@us.es

Keywords: soil pollution, trace elements, evaluation methodology

Soil trace elements are derived from either geogenic or anthropogenic sources. The first are directly inherited from the parent materials, or from the weathering and leaching of ore deposits. Anthropogenic trace elements enter the soil through several pathways; coming from industrial, urban and agricultural activities, including those aerial deposition and acid mine drainage. These contributions to trace elements in soils are of primary concern in pollution investigations. But, distinguishing between geogenic and anthropogenic contributions in a soil is never a simple issue. In addition, from the total concentration of soil toxic elements only the bioavailable fraction can result in a hazard to human and ecological receptors. The risk assessment is generally a complex procedure that includes many parameters, many of them difficult to assess. The proposed methodological approach for the evaluation of soil pollution by trace elements is an easier procedure to obtain a reasonable evaluation of the potential risk soil contamination by toxic metal(loid)s. This approach can be succefully applied in most of cases, avoiding a sometimes flawed risk analysis procedure, which leads to an unnecessary declaration of soil contamination, resulting in mandatory and expensive reclamation actions. The approach is primarily based on two considerations: a) the anomalous high concentration of soil toxic elements does not always mean a health risk, although they exceed the generic reference levels, b) the mobile fraction of the soil toxic elements and their bioavailability should be the base of any risk assessment. As illustrated on the attached flow-sheet, the proposal consists on a series of sucesive steps ranging from a simple investigation of available information of the history and present state of the potential polluted site (PPS) to a detailed research that dtermines reference local values, enrichment and geoacumulation factors, soil parameters, mobility, bioavailability, operational speciation, etc. For some elements, i.e. As, Hg, Cd, and Pb, particular procedures are also proposed.

Nb-Ta-Sn MINERALIZATION IN PEGMATITES AND GRANITES

Melcher F.*[1]
[1] Lehrstuhl für Geologie und Lagerstättenlehre, Montanuniversität Leoben, Austria
Corresponding email: frank.melcher@unileoben.ac.at

Keywords: rare-element pegmatite, rare-metal granite, mineralization

Rare-metal granites and granitic rare-element pegmatites account for the majority of the production of tantalum, tin, niobium, lithium, beryllium, and other raw materials. Each period of rare-metal granite and rare-element pegmatite formation in Earth history is characterised by peculiar mineralogical and geochemical features. The major and trace element composition of Ta-Nb and Sn oxides is used here to characterise these periods and to distinguish ore provinces (Melcher et al., 2015, 2016). Some of the largest rare-element pegmatite bodies are located within Archean terrains and intruded ultramafic and mafic host rocks. They are highly fractionated, of LCT (Li-Cs-Ta) affinity and yield complex mineralogical compositions. Many carry significant Li mineralization as spodumene, petalite, and amblygonite. In the Paleoproterozoic, syn- to post-orogenic LCT-family pegmatites intruded variable lithologies within a variety of structural settings. Minor and trace element signatures in columbite-tantalite are similar to those from Archean pegmatites, although some are characterized by considerable REE enrichment along with Sc and Y, being transitional to NYF (Nb-Y-F)-family pegmatites. The Mesoproterozoic period is comparatively poor in rare-element pegmatites and rare-metal granites. Placer material from Colombia points to an unusual pegmatite source of NYF affinity, yielding high total REE, Sc and Th at low Li in columbite-group minerals. A major period of pegmatite formation was the Early Neoproterozoic at around 1 Ga. Pegmatite fields often display a zonal arrangement of mineralized pegmatites with respect to assumed “fertile” parent granites. They intrude metasediments, metabasites, gneiss and granite of middle to upper crustal levels and display a variety of mineralogical and chemical characteristics. Pegmatites of the Sveconorwegian and Grenville domains are usually of the NYF type. In contrast, the pegmatites of central and southwestern Africa are commonly of LCT affinity carrying spodumene, beryl, abundant Ta-Nb oxides and cassiterite. The fourth major pegmatite-forming event coincides with amalgamation of Gondwana around 550 Ma ago. Pegmatites showing both LCT and NYF affinities often intruded high-grade metamorphic terrains. Rare-metal granites of NYF affinity are locally abundant. The Alto Ligonha and Madagascar provinces are characterized by abundant REE and Sc both within Ta-Nb-oxides and as separate mineral phases. In the Phanerozoic, pegmatite formation was related to Sn-W mineralized granites during the Variscan and Alleghanian orogenies. Most of the pegmatites are of LCT affinity, although NYF and some mixed types are present as well. Nb-Ta oxides from Mesozoic pegmatites and rare-metal granites are invariably rich in REE, Sc, Y and Th. In all rare-metal granites, Ta-Nb oxides are characterized by high total REE concentrations and both, negative Eu and Y anomalies in chondrite-normalized REE diagrams.

Melcher, F., Graupner, T., Gäbler, H.-E., Sitnikova, M., Henjes-Kunst, F., Oberthür, T., Gerdes, A., Dewaele, S. (2015): Tantalum-(niobium-tin) mineralization in African pegmatites and rare metal granites: constraints from Ta-Nb oxide mineralogy, geochemistry and U-Pb geochronology. *Ore Geol. Rev.*, **64**, 667-719.

Melcher, F., Graupner, T., Gäbler, H.-E., Sitnikova, M., Oberthür, T., Gerdes, A., Badanina, E., Chudy, T. (2016): Mineralogical and chemical evolution of tantalum-(niobium-tin) mineralization in pegmatites, granites and carbonatites: Part 2: Worldwide examples (except Africa) and an overview of global metallogenic patterns. *Ore Geol. Rev.*, in press, DOI: 10.1016/j.oregeorev.2016.03.014

FLUIDS, MASS TRANSFER AND TECTONICS IN SUBDUCTION ZONES: WHAT DO WE LEARN FROM SERPENTINITE?

Scambelluri M.*[1]

[1] Dipartimento di Scienze della Terra, dell'Ambiente e della Vita, Università di Genova, Italy

Corresponding email: marco.scambelluri@dipteris.unige.it

Keywords:

Serpentinites affect major tectonic and geochemical processes on Earth. Due to their abundance in oceanic lithosphere and in subduction zones, they affect the volatile budgets and the geochemical-geophysical properties of slabs and overlying mantle (Rüpke et al., 2004). Increasing importance is now given to interface domains between subducting and overlying plates, where serpentinite either occurs in tectonic mélanges atop the slab, or forms kilometre-thick layers derived from hydration of supra-subduction mantle (Bostock et al., 2002; Bebout, 2007). In such environments, serpentinite enhances deformation channelling, fluid release, mass transfer and the buoyancy-driven uplift of eclogitic rocks (Hermann et al., 2000; Gerya et al., 2002; Hyndman & Peacock, 2003). The role of serpentinite in element cycling during subduction is debated. Sediments and altered oceanic crust are identified as the reservoirs delivering incompatible elements to arcs and it has been envisaged that element loss from such rocks is boosted by de-serpentinization fluids (Plank & Langmuir, 1993; Hermann et al., 2006; Spandler & Pirard, 2013). However, it has been shown that serpentinites incorporate volatiles and fluid-mobile elements (FME) during oceanic alteration and/or interaction with subduction fluids: once stored in serpentinite, these elements are released during prograde serpentine dehydration (Hattori & Guillot, 2003; Deschamps et al., 2013; Kendrick et al., 2011; Scambelluri et al., 2015). Serpentinite is also relevant for C storage and transport to depth in subduction zones (Kerrick & Conolly, 1998). In the subduction-zone C cycle, de-serpentinization supplies water to carbonate-bearing rocks promoting C mobility via decarbonation and carbonate dissolution. Back-reaction of serpentinite with COH fluids converts silicates to carbonate minerals, sequestering carbon from the circulating subduction fluids. To test the role of serpentinites as tracers of fluid activity in subduction interface settings, I show FME contents and B, Sr, Pb isotopes of Alpine HP-UHP serpentinites and in their dehydration products. I focus on: (i) lenses of de-serpentinized metaperidotite in the Cima di Gagnone mélange (Central Alps); (ii) HP serpentinites (Voltri Massif, Western Alps). I discuss geochemical tracers to assess fluid-rock interactions, element exchange and C-storage experienced during serpentinite subduction and accretion to plate interface settings. Uptake of As, Sb, Be and reset of B, Sr and Pb isotopes are due to interaction with sediment-derived fluids during prograde subduction metamorphism. This implies the early slicing and accretion of serpentinite (of slab and/or mantle wedge origin) to plate-interface domains, where they uptake crust- and sediment-derived fluids. Serpentinite metasomatism by sediment-derived fluids enable transfer of these elements to subarc depths and their release to de-serpentinization fluids affecting the mantle sources of arc magmas.

Bebout, G.E. (2007): Metamorphic chemical geodynamics of subduction zones. *Earth Planet. Sci. Letters*, **260**, 373-393.

Bostock, M.G., Hyndman, R.D., Rondenay, S., Peacock, S.M. (2002): An inverted continental Moho and serpentinization of the forearc mantle. *Nature*, **417**, 536-538.

Deschamps, F., Godard, M., Guillot, S., Hattori, K. (2013): Geochemistry of subduction zone serpentinites: A review. *Lithos*, **178**, 96-127.

Gerya, T.V., Stöckher, B., Perchuk, A.L. (2002): Exhumation of high-pressure metamorphic rocks in a subduction channel: A numerical simulation. *Tectonics*, **21**, 1056.

Hattori, K. & Guillot, S. (2003): Volcanic fronts as a consequence of serpentinite dehydration in mantle wedge. *Geology*, **31**, 525-528.

Hermann, J. Müntener, O., Scambelluri, M. (2000): The importance of serpentinite mylonites for subduction and exhumation of oceanic crust. *Tectonophys.*, **327**, 225-238.

Hermann, J., Spandler, C., Hack, A., Korsakov, A.V. (2006): Aqueous fluids and hydrous melts in high-pressure and ultra-high pressure rocks: implications for element transfer in subduction zones. *Lithos*, **92**, 339-417.

Hyndman, R.D. & Peacock, S.M. (2003): Serpentinization of the forearc mantle. *Earth Planet. Sci. Letters*, **212**, 417-432.

Kendrick, M.A., Scambelluri, M., Honda, M., Phillips, D. (2011): High abundances of noble gas and chlorine delivered to the mantle by serpentinite subduction. *Nature Geosci.*, **4**, 807-812.

Kerrick, D.M. & Connolly, J.A.D. (1998): Subduction of ophicarbonates and recycling of CO_2 and H_2O. *Geology*, **26**, 375-378.

Plank, T. & Langmuir, C.H. (1993): Tracing trace elements from sediment input to volcanic output at subduction zones. *Nature*, **362**, 739-743.

Rüpke, L.H., Morgan, J.P., Hort, M., Connolly, J.A.D. (2004): Serpentine and the subduction zone water cycle. *Earth Planet. Sci. Letters*, **223**, 17-34.

Scambelluri, M. Pettke, T., Cannaò, E. (2015): Fluid-related inclusions in Alpine high-pressure peridotite reveal trace element recycling during subduction-zone dehydration of serpentinized mantle (Cima di Gagnone, Swiss Alps). *Earth Planet. Sci. Letters*, **429**, 45-59.

Spandler, C. & Pirard, C. (2013): Element recycling from subducting slabs to arc crust: A review. *Lithos*, **170-171**, 208-223.

Session S1:

Diamonds: open windows in the Earth's mantle

Conveners:

Hélène Bureau (Paris – France)

Fabrizio Nestola (Padova – Italy)

Mikhail Sami (Saint Andrews – United Kingdom)

X-RAY DIFFRACTION TOPOGRAPHY, MICRO-TOMOGRAPHY AND MICRO X-RAY FLUORESCENCE OF DIAMONDS AND THEIR TRAPPED INCLUSIONS: A MULTI-ANALYTICAL APPROACH FOR NON-DESTRUCTIVE ANALYSES

Agrosì G.*[1], Tempesta G.[1], Mele D.[1], Allegretta I.[2], Terzano R.[2], Hutchison M.T.[3] & Nestola F.[4]

[1] Dipartimento di Scienze della Terra e Geoambientali, Università di Bari, Italy

[2] Dipartimento di Scienze del Suolo, della Pianta e degli Alimenti. Università di Bari, Italy

[3] Trigon GeoServices Ltd, Las Vegas, NV, USA

[4] Dipartimento di Geoscienze, Università di Padova, Italy

Corresponding email: giovanna.agrosi@uniba.it

Keywords: structural defects, inclusions, plastic deformation

The study of diamonds and the mineral inclusions trapped within them is of great interest to the Earth Sciences, since it can provide insights into deep mantle conditions and evolution (Nestola et al., 2011). Conventional techniques commonly used are destructive and thus do not allow the integration of different methods to obtain complementary results. Significant information about the growth conditions of diamonds and their inclusions should be obtained preferably by non-destructive, in-situ investigations. In this study, the use of X-ray Topography combined with X-ray Tomography and Micro-X-ray Fluorescence allowed us to obtain minero-petrogenetic information on diamonds and their inclusions, while totally preserving the diamond hosts. In particular, X-ray Diffraction Topographic images, obtained in transmission mode, provide maps of spatial distribution of lattice imperfections in the whole sample volumes, without the need for cutting the samples into slices. This technique can furnish useful information to reconstruct the crystal's growth history, in a similar fashion to diamonds from Finsch mine, South Africa (Agrosì et al., 2013) and from the Udachnaya kimberlite, Russia (Agrosì et al., 2016). In our study, this methodological approach was applied to diamonds from different provenances. Comparisons between the topographic images acquired on each studied sample allowed the characterization of structural defects and identification of different types of post-growth plastic deformation. Relationships between topographic features and different origin of diamonds were found. X-ray Tomography provided visualization of the spatial distribution and shape of the inclusions, permitting to distinguish inclusions made by a single crystal from polyphase inclusions or aggregates. Chemical maps, obtained by Micro-X-ray fluorescence, allowed for the determination of the chemical compositions of the majority of inclusions. Correlations were made between the composition of the inclusions and their different density, obtained by the X-ray absorption observed in tomographic reconstructions. The results obtained show that the plastic deformation of diamonds, the nature of the inclusions and their shape are strictly related, contributing to the characterization of the different origins of diamonds.

Agrosì, G., Tempesta, G., Scandale, E., Harris, J.W. (2013): Growth and post-growth defects of a diamond from Finsch mine (South Africa). *Eur. J. Mineral*., **25**, 551-559.

Agrosì, G., Nestola, F., Tempesta, G., Bruno, M., Scandale, E., Harris, J.W. (2016): X-ray topographic study of a diamond from Udachnaya: Implications for the genetic nature of inclusions. *Lithos*, **248-251**, 153-159.

Nestola, F., Nimis, P., Ziberna, L., Longo, M., Marzoli, A., Harris, J.W., Manghnani, M.H., Fedortchouk, Y. (2011): First crystal-structure determination of olivine in diamond: Composition and implications for provenance in the Earth's mantle. *Earth Planet. Sci. Letters*, **305**, 249-255.

JEFFBENITE (EX-"TAPP"): A HIGH-PRESSURE MARKER IN DIAMONDS

Anzolini C.*[1], Drewitt J.W.E.[2], Lord O.T.[2], Walter M.J.[2] & Nestola F.[1]
[1] Dipartimento di Geoscienze, Università di Padova, Italy
[2] School of Earth Sciences, University of Bristol, United Kingdom
Corresponding email: chiara.anzolini@studenti.unipd.it

Keywords: Jeffbenite, sub-lithospheric diamonds, inclusions

Super-deep diamonds are thought to crystallize between about 300 and 800 km (Harte, 2010) on the basis of the inclusions trapped within them. Many of the inclusions are composites of multiple minerals and show evidence of retrograde transformation from lower-mantle (LM) or transition-zone (TZ) precursors, and their depth of origin is inferred. However, due to the lack of experimental evidence relating composite inclusions directly to high-pressure precursors, their actual depth of origin has never been proven. Jeffbenite is a new official mineral (Nestola et al., 2016), previously referred to as TAPP (Tetragonal Almandine-Pyrope Phase), which occurs both in composite inclusions and as homogeneous inclusions, and may provide key information about the depth of formation of super-deep diamonds. Jeffbenite is a tetragonal phase with garnet-like stoichiometry discovered in Brazilian diamonds (Harris et al., 1997) and found exclusively in nature as inclusions in super-deep diamonds. The main argument in favour of a super-deep origin for jeffbenite is its coexistence in the same diamond with minerals, which are interpreted to have crystallized in the TZ or LM (Harris et al., 1997; Harte et al., 1999; Hutchison et al., 2001; Brenker et al., 2002; Hayman et al., 2005; Kaminsky, 2012). An origin for jeffbenite in the LM is also supported by its capacity to hold ferric iron, as it was demonstrated that in deep mantle silicates Fe^{3+} is significantly abundant (McCammon et al., 1997; Harte, 2010). By contrast, the absence of octahedral silicon in the crystal structure, which is typical of high-pressure silicates below 200 km depth, makes a LM origin difficult to explain if the jeffbenite structure is primary (Harris et al., 1997; Finger & Conrad, 2000). Thus, whether jeffbenite forms as a primary phase in the LM or is the product of retrogression from high-pressure mantle phases has been a matter of debate and is still controversial.

The only experimentally determined stability field for jeffbenite is that of Armstrong & Walter (2012), which provides a maximum pressure for jeffbenite stability of ~ 13 GPa (~ 390 km) at 1700 K. This confirms that jeffbenite is a sub-lithospheric mineral, but rules out direct incorporation of jeffbenite in diamond at the TZ-LM boundary. However, these results were obtained on a Ti-rich jeffbenite, which is usually found as part of composite inclusions, and not on a Ti-free jeffbenite, which occurs as single-phase inclusions in diamonds (Nestola et al., 2016). We therefore report here new laser heated diamond-anvil cell experiments from 5 to 30 GPa on a Ti-free jeffbenite, in order to determine the role that TiO_2 plays in the stability field of jeffbenite and to figure out if the latter can be directly incorporated into diamond in the TZ or LM. Our preliminary results show that the absence of TiO_2 extends the stability field of jeffbenite to higher pressures than previously determined.

Acknowledgements: This work was supported by Fondazione Cassa di Risparmio di Padova e Rovigo, NERC Grant NE/M000419/1 to MJW, NERC Fellowship Grant NE/J018945/1 to OTL and ERC-2012-StG 307322 to FN.

Armstrong, L.S. & Walter, M.J. (2012): Tetragonal almandine pyrope phase (TAPP): retrograde Mg-perovskite from subducted oceanic crust?. *Eur. J. Mineral.*, **24**, 587-597.

Brenker, F.E., Stachel, T., Harris, J.W. (2002): Exhumation of lower mantle inclusions in diamond: ATEM investigation of retrograde phase transitions, reactions and exsolution. *Earth Planet. Sci. Letters*, **198**, 1-9.

Finger, L.W. & Conrad, P.G. (2000): The crystal structure of "tetragonal almandine-pyrope phase" (TAPP): A reexamination. *Am. Mineral.*, **85**, 1804-1807.

Harris, J., Hutchison, M., Hursthouse, M., Light, M., Harte, B. (1997): A new tetragonal silicate mineral occurring as inclusions in lower-mantle diamonds. *Nature*, **387**, 486-488.

Harte, B. (2010): Diamond formation in the deep mantle: the record of mineral inclusions and their distribution in relation to mantle dehydration zones. *Mineral. Mag.*, **74**, 189-215.

Harte, B., Harris, J., Hutchison, M., Watt, G., Wilding, M. (1999): Lower mantle mineral associations in diamonds from Sao Luiz, Brazil. *in* "Mantle Petrology: Field Observations and High Pressure Experimentation (a Tribute to Francis R. (Joe) Boyd)", Y. Fei, C.M. Bertka, B.O. Mysen, eds., *Geochem. Soc. Spec. Publ.*, **6**, 125-153.

Hayman, P.C., Kopylova, M.G., Kaminsky, F.V. (2005): Lower mantle diamonds from Rio Soriso (Juina area, Mato Grosso, Brazil). *Contrib. Mineral. Petrol.*, **149**, 430-445.

Hutchison, M.T., Hursthouse, M., Light, M. (2001): Mineral inclusions in diamonds: associations and chemical distinctions around the 670-km discontinuity. *Contrib. Mineral. Petrol.*, **142**, 119-126.

Kaminsky, F. (2012): Mineralogy of the lower mantle: A review of 'super-deep' mineral inclusions in diamond. *Earth Sci. Rev.*, **110**, 127-147.

McCammon, C., Hutchison, M., Harris, J. (1997): Ferric iron content of mineral inclusions in diamonds from Sao Luiz: a view into the lower mantle. *Science*, **278**, 434-436.

Nestola, F., Burnham, A.D., Peruzzo, L., Tauro, L., Alvaro, M., Walter, M.J., Gunter, M., Kohn, S.C. (2016): Tetragonal Almandine-Pyrope Phase, TAPP: finally a name for it, the new mineral jeffbenite. *Mineral. Mag.*, in press.

ISOTOPIC CHARACTERIZATION OF DIAMOND GROWTH IN FLUIDS

Bureau H.*[1], Remusat L.[1], Esteve I.[1], Pinti D.L.[2], Cartigny P.[3] & Frost D.[4]

[1] Institut de Minéralogie, de Physique des Matériaux et de Cosmochimie, Sorbonne Universités, Centre National de la Recherche Scientifique, Paris, France

[2] GEOTOP, Université du Québec, Montréal, Canada

[3] Laboratoire de Géochimie des Isotopes Stables, Institut de Physique du Globe de Paris, Université D. Diderot, Centre National de la Recherche Scientifique, Paris, France

[4] Bayerisches Geoinstitut, Universität Bayreuth, Germany

Corresponding email: helene.bureau@impmc.upmc.fr

Keywords: diamond, carbon, inclusions

Inclusions trapped in diamonds are one of the few diagnostic tools to constrain diamond growth conditions in the Earth's mantle. At conditions of the upper mantle, diamonds can potentially grow from various forms of media (solid, gas, fluid). In this study, experiments have been performed to synthesize inclusion-bearing diamonds employing starting mixtures of carbonates, graphite and silicates together with diamond seeds in the presence of excess of pure water or saline fluids (H_2O-NaCl). Experiments were carried at conditions compatible with the Earth's geotherm between 6-7 GPa (1300-1675°C) in multi-anvil presses at the Bayerisches Geoinstitut, Bayreuth. Results show that within the timescale of the experiments (6 to 30 hours) diamond growth occurs on seeds if water and alkali-bearing carbonates are present. Water promotes faster diamond growth, which is favorable to the formation of inclusions (Bureau et al., 2012).

Thin sections of a few diamond seeds containing exposed inclusions were prepared using a Focus Ion Beam (about 2 to 5 µm thickness). These sections were deposited on silicon wafers and gold coated for micron-scale determination of the $\delta^{13}C$ isotopic compositions using the NanoSIMS 50 installed at the Muséum National d'Histoire Naturelle, Paris.

Carbon isotope measurement with NanoSIMS were calibrated against a natural Ia and a synthetic IIa diamond used for diamond anvil cells, whose compositions were determined by gas-source mass spectrometry at IPGP at 3.6±0.1‰ and -20.9±0.1‰, respectively. All the starting materials used for the experiments were also characterized for their $\delta^{13}C$ by the same technique at GEOTOP, Montréal.

The isotopic composition of the new diamond grown areas were measured close to the inclusions. They exhibit a different isotopic signature than that of the starting seeds (starting diamond composition: -29.6 to -30.4±1.4‰). The new diamond signatures are falling into the range of signatures of the starting carbonates used for the experiments (-4.8±0.1 to -16.2±0.1‰) when they are far away from the composition of the starting graphite (-26.4±0.1‰).

This shows that the carbon source for diamond growth must be the carbonates present either as CO_3^{2-} ions dissolved in the melt or as carbon dioxide species CO_2 in the aqueous fluid.

In the light of the results we suggest that the presence of small discrete or isolated volumes of water-carbonate-rich fluids are necessary to grow inclusion-bearing peridotitic, eclogitic, fibrous, cloudy and coated diamonds, and may also be involved in the growth of ultrahigh pressure metamorphic diamonds.

Bureau, H., Langenhorst, F., Auzende, A.-L., Frost, D.J., Estève, I., Siebert, J. (2012): The growth of fibrous, cloudy and polycrystalline diamonds. *Geochim. Cosmochim. Acta*, **77**, 202-214.

IN-SITU HIGH-RESOLUTION MICRO-RAMAN SPECTROSCOPY ON MINERAL INCLUSIONS STILL TRAPPED WITHIN DIAMONDS

Cavallo F.*[1], Romano C.[2], Vona A.[2] & Nestola F.[1]
[1] Dipartimento di Geoscienze, Università di Padova, Italy
[2] Dipartimento di Scienze, Università di Roma Tre, Italy
Corresponding email: francesca.cavallo.1@studenti.unipd.it

Keywords: diamonds, inclusions, micro-Raman

Diamonds and their mineral inclusions represent a real "probe" to the deepest regions of our Planet and this explains why they are among the most studied geological materials in Earth Sciences. The diamond-inclusion pair can provide crucial information about deep mantle conditions and its evolution (Nestola et al., 2011; Pearson et al., 2014; Nestola & Smyth, 2016). Diamonds and their inclusions are usually investigated by destructive techniques but it is evident that a non-destructive approach is in many case preferable to preserve the samples. In this work we have performed in-situ high-resolution micro-Raman mapping of some inclusions of olivines (compositions in average $Mg_{1.8}Fe_{0.2}SiO_4$) still trapped within diamonds in order to investigate the distribution of the residual pressure exerted by the diamond. Indeed, it is well known that olivine entrapped in diamonds can be under some residual pressures up to 0.5-0.6 GPa (Nestola et al., 2011) and by the knowledge of such pressure and the thermo-elastic parameters (bulk modulus, thermal expansion, etc.) of olivine-diamond pair it is possible to determine the depth of diamond formation. However, a very recent work (Nimis et al., 2016) reported the presence of a SiO_2-H_2O fluid constituting a 1.5 µm thick film around the inclusions at the interface with diamonds. Such a fluid could definitively affect the residual pressure on the inclusions and have a strong impact on the final determination of the depth of crystallization. Therefore, we have started a research project with the aim to determine if the residual pressure around the inclusions is homogeneous by studying the positions of the Raman bands of olivine at the entire interface with diamond. Such experiments could provide crucial information on the real distribution of the fluid around the inclusion as it is not clear yet if such a film is distributed all over the interface between the inclusion and the diamond or there is some contact between the two crystalline phases.

Nestola, F. & Smyth, J.R. (2016): Diamonds and water in the deep Earth: a new scenario. *Int. Geol. Rev.*, **58**, 263-276.

Nestola, F., Nimis, P., Ziberna, L., Longo, M., Marzoli, A., Harris, J.W., Manghnani, M.H., Fedortchouk, Y. (2011): First crystal-structure determination of olivine in diamond: Composition and implications for provenance in the Earth's mantle. *Earth Planet. Sci. Letters*, **305**, 249-255.

Nimis, P., Alvaro, M., Nestola, F., Angel, R.J., Marquardt, K., Rustioni, G., Harris, J.W. (2016): First evidence of hydrous silicic fluid films around solid inclusions in gem-quality diamonds. *Lithos*, in press.

Pearson, D.G., Brenker, F.E., Nestola, F., McNeill, J.C.R., Nasdala, L., Hutchison, M.T., Matveev, S., Mather, K., Silversmit, G., Schmitz, S., Vekemans, B., Vincze, L. (2014): Hydrous mantle transition zone indicated by ringwoodite included within diamond. *Nature*, **507**, 221-224.

CARBON ISOTOPE, NITROGEN ABUNDANCE AND NITROGEN AGGREGATION STATE DATA FOR DIAMONDS FROM ORAPA MINE: A CLEAR SUBDUCTION SIGNATURE?

Chinn I.*[1], Perritt S.[1] & Stiefenhofer J.[2]
[1] De Beers Exploration, De Beers Group Services (Pty) Limited, Johannesburg, South Africa
[2] Technical and Sustainability, De Beers Group Services (Pty) Limited, Johannesburg, South Africa
Corresponding email: Ingrid.chinn@debeersgroup.com

Keywords: subduction, carbon isotope

Carbon isotope and nitrogen abundance data were acquired using secondary-ion mass spectrometry (SIMS) for 198 diamonds from the Orapa Mine, Botswana. The diamonds were selected from a microdiamond sampling campaign, hence full geological control exists for the location of the diamonds with respect to the kimberlite pipe model.

The diamonds for which SIMS analyses were conducted have been thoroughly characterised in terms of colour and morphology and comprise a representative subset of more than 2000 diamonds investigated. Fourier Transform Infrared Spectrometry (FTIR) was used to determine nitrogen content and aggregation state for the whole stones before they were mounted and polished for SIMS analyses.

The individual diamonds show considerable heterogeneity in both carbon isotope and nitrogen abundance. The maximum variation in carbon isotope composition recorded for a single diamond is 17.82‰: from -24.03 ‰ in the core of diamond S016 to -6.21‰ in the rim. The largest variation in nitrogen content in a single diamond is 3156 atomic ppm, from 40 to 3196 atomic ppm. Generally, stones that show heterogeneity in carbon isotope composition and/or nitrogen abundance show clear evidence of more than one growth zone in cathodoluminescence (CL) images. In some of these instances truncation of growth zonation indicates the presence of a resorption boundary. Some diamonds appear to have had more than one resorption and growth event.

A plot of nitrogen abundance versus carbon isotope composition shows a significant proportion (17%) of the 412 analyses displaying light carbon isotope compositions and high nitrogen contents, falling well outside the limit sector curve defined by Cartigny et al. (2001). The concave trend of the limit sector relationship was used to argue against mixing of a subducted component with a primordial component for diamond growth models (Cartigny et al., 2001).

The data are consistent with the presence of a subducted component in at least some of the diamonds from Orapa. It is anticipated that this will be further confirmed with the acquisition of nitrogen isotope data which will be presented if obtained timeously.

Unfortunately, most diamonds for which carbon isotope data exist are inclusion-bearing and not representative of the run-of-mine populations, resulting in a bias. Furthermore, given the extreme heterogeneity in carbon isotope and nitrogen content recorded in individual diamonds and clearly supported by CL images, the bulk combustion analyses which comprise the majority of the global data set are inappropriate. Clearly, detailed and spatially controlled stable isotopic analyses and fully representative samples are required if the complex origins of diamonds in the mantle are to be understood.

Cartigny, P., Harris, J.W., Javoy, M. (2001): Diamond genesis, mantle fractionations and mantle nitrogen content: a study of δ^{13}C-N concentrations in diamonds. *Earth Planet. Sci. Letters*, **185**, 85-98.

DIAMOND: MESSENGERS FROM DEEP SPACE AND DEEP TIME AND OLDER THAN THE EARTH?

Jones A.*[1], Alvaro M.[2] & Nestola F.[3]
[1] Department of Earth Sciences, University College London, United Kingdom
[2] Dipartimento di Scienze della Terra e dell'Ambiente Università di Pavia, Italy
[3] Dipartimento di Geoscienze, University di Padova, Italy
Corresponding email: adrian.jones@ucl.ac.uk

Keywords: diamond, lonsdaleite, supernova

Because of its peculiar chemical and physical properties diamond can preserve clues on several planetary processes. For example, inclusions trapped in inert diamonds are the key witness of mantle state. But diamond can also preserve nanoscale traces of deformation (e.g., the hexagonal deviation from cubic symmetry commonly called lonsdaleite phase) caused by instantaneous stresses such as those produced by impact of meteorites and/or planetary bodies.

Impact cratering is undoubtedly one of the most frequent high-energetic and potentially catastrophic event occurring at the earth surface and in the planetary system. For example, the energy released from an impact occurring on the Earth's surface for a small impact crater would be 3 orders of magnitudes higher than the Hiroshima atomic bomb. These enormous energies (e.g., 624 GPa in terms of pressure have been calculated for the 100km Popigai impact crater) and the very short duration cause unique irreversible changes to rocks and minerals, are compatible with P and T conditions required to transform graphite into diamond (e.g., 4.5 GPa at 1000°C) and are also enough to induce deformation in the newly formed diamonds.

A fully integrated experimental and theoretical approach demonstrated that quantifying the amount of stacking disorder in diamonds can lead to fundamental new insight not only on impact cratering process but also on the origin of the carbon phases in our planetary system.

We have performed a completely new multi-methodological study of the stacking disorder induced on diamond using shock waves at energies comparable to those released during impact cratering at Earth's surface (e.g., 7 km/s).

The results obtained on the laboratory-shocked diamonds have been then compared with the evidence from natural diamond retrieved from Popigai impact crater allowing us to demonstrate that (i) hexagonal features can form in diamond shocked to 60 GPa so that observations of "lonsdaleite" do not require precursor graphite; (ii) Coexisting hexagonal and cubic diamond features in laboratory-shocked and impact diamond is explained by stacking disorder. Moreover, aided by first principle calculations, we extended the current state-of-the-art demonstrating that Raman spectra for hexagonal diamond can provide a marker for the presence of extended hexagonal sequences in diamond.

Furthermore, on the basis of these observation we could propose a metastable pathway for formation of mixed cubic-hexagonal carbon phases that can explain fast energetic shock formation of both lonsdaleite and impact diamond. Pure lonsdaleite has been reported in shock experiments, which for a few nanoseconds approach extreme PT conditions (~ 6000 K, ~ 230 GPa; Kraus et al., 2016) similar to the centre of the Earth. Since these very brief but energetic events can be recorded in diamonds, we can start to consider new ways to search for these important messengers of extreme conditions in planetary materials. Hypothetical formation of nanodiamond in supernovae, which might include hexagonal diamond, could in principle survive Earth-sized planetary collisions and be older than our solar system.

Acknowledgements: This work was in part supported by Leverhulme grant A20080365 Superdeep diamond and Earths atmosphere, and by ERC starting grant 307322 to F. Nestola and by the MIUR-SIR grant "MILE DEEp" (RBSI140351) to M. Alvaro.

Kraus, D., Ravasio, A., Gauthier, M., Gericke, D.O., Vorberger, J., Frydrych, S., Helfrich, J., Fletcher, L.B., Schaumann, G., Nagler, B., Barbrel, B., Bachmann, B., Gamboa, E.J., Göde, S., Granados, E., Gregori, G., Lee, H.J., Neumayer, P., Schumaker, W., Döppner, T., Falcone, R.W., Glenzer, S.H., Roth, M. (2016): Nanosecond formation of diamond and lonsdaleite by shock compression of graphite. *Nature Comm.*, **7**, 10970.

MANTLE-CARBONATITE CONCEPT OF DIAMOND ORIGIN AT 150-800 KM LEVELS

Litvin Y.A.*[1], Kuzyura A.V.[1] & Spivak A.V.[1]
[1] Institute of Experimental Mineralogy, Russian Academy of Sciences, Chernogolovka, Russia
Corresponding email: litvin@iem.ac.ru

Keywords: diamond genesis, mantle-carbonatite concept, physico-chemical experiments

Primary inclusions in diamonds are a guide to the general chemical composition of the diamond-parental media at the mantle 150-800 km levels. This is the initial information for physico-chemical experimental studies of the multicomponent heterogeneous systems which are responsible for natural diamond genesis. A coordination of mineralogical and experimental data makes it possible to unravel the chemical and phase compositions of growth melts that are effective in paragenetic origin of diamonds and their primary inclusions. The following problems are of principal significance for the diamond genetic mineralogy: a) chemical nature of growth melts for diamonds and paragenetic phases; b) physico-chemical mechanisms of diamonds and primary inclusions syngenesis; c) phase reactions which govern the origin of discrete ultrabasic and basic parageneses of mineral inclusions. The mantle-carbonatite concept of diamond origin is based on plausible solutions of the problems which follow: a) the growth melts have changeable silicate-oxide-carbonate-carbon compositions and are visualized in their generalized diagrams which are simultaneously demonstrative for the primary inclusions genetic classification as well as genetic links to the upper mantle, transition zone and lower mantle rocks; b) a labile carbon-oversaturation of the silicate-oxide-carbonate melts in respect to diamond initiates mass nucleation and crystal growth of diamonds which are capable of trapping their inclusions from the common growth melts (experimental “syngenesis” phase diagrams are evidenced about); c) the regularities of ultrabasic-basic evolution and paragenetic transitions in the diamond-forming systems are discovered by experimentally-based “syngenesis” phase diagrams under the regime of fractional crystallization; d) a physico-chemically united mode of diamond origin at the mantle 150-800 km levels with different mineralogy is demonstrated.

Acknowledgements: Program P34 of the RAS and RFBR grants 14-05-00537 and 16-05-00850.

Litvin, Y.A. (2007): High-pressure mineralogy of diamond genesis. *in*: “Advances in high-pressure mineralogy”, E. Ohtani, ed., *Geol. Soc. Am. Spec. Pap.*, **421**, 83-103.

Litvin, Y.A. (2012): Experimental study of physico-chemical conditions of natural diamond formation on an example of the eclogite-carbonatite-sulphide-diamond system. *Geol. Ore Dep.*, **54**, 523-539.

Litvin, Y.A., Spivak, A.V., Solopova, N.A., Dubrovinsky, L.S. (2014): On origin of lower-mantle diamonds and their primary inclusions. *Phys. Earth Planet. Inter*., **228**, 176-185.

EXPLORING A NEW GEOBAROMETER FOR FERROPERICLASE INCLUSIONS IN DIAMOND FROM THE LOWER MANTLE

Melai C.*[1], Marquardt K.[1], Armstrong K.[1] & McCammon C.A.[1]
[1] Bayerisches Geoinstitut, Universität Bayreuth, Germany
Corresponding email: caterina.melai@gmail.com

Keywords: diamond, magnesioferrite, ferropericlase

Ferropericlase (Mg,Fe)O is the most abundant non silicate oxide within Earth's lower mantle and is one of the most common mineral inclusions in super-deep diamonds. Magnesium-iron monoxide is the only lower mantle phase thermodynamically stable at ambient conditions. Ferropericlase can incorporate significant amount of Fe^{3+} (substituting Fe^{2+}) in structural point defects, either in tetrahedral or octahedral coordination. Under oxidizing conditions, the incorporation mechanism is controlled by a coupled cation substitution (2 Fe^{3+} for 3 Fe^{2+}) which results in an octahedral cation vacancy (McCammon et al., 2004). In synthetic samples at high-P and high oxygen fugacity the capacity of ferropericlase to accommodate Fe^{3+} is suppressed likely because of the high-P phase transition occurring in the magnetite-magnesioferrite system (McCammon, 1998). Magnesioferrite (natural occurrence) has been found as precipitates along dislocations and at the interface with the diamond and accommodates Fe^{3+} from the (Mg,Fe)O. Therefore, it has always been interpreted as the exsolution product of ferropericlase (Harte et al.,1999). The entrapment volume of the ferropericlase inclusion in the diamond is constant and because of the higher density of the spinel, the above mentioned precipitation process requires extremely high pressure conditions (Wirth et al., 2014). Another explanation for the magnesioferrite formation might be the differential stress that the ferropericlase accumulates during exhumation that leads to a large growth of dislocations that act as nucleation sites for the spinel phase, but the pressure –temperature conditions are still not well constrained. To address these issues, we aimed our investigation to bracketing the formation conditions (e.g. pressure, temperature and oxygen fugacity) of magnesioferrite from ferropericlase to provide a new barometer for lower mantle phase assemblages. We investigated the formation conditions of magnesioferrite by multianvil syntheses of ferropericlase at different pressure (15 to 25 GPa) and oxygen fugacity conditions (Re-ReO_2 buffer; Fe-FeO buffer). Combined Mössbauer and TEM analysis provides evidence and characterization of the newly formed spinel phase. The latest results will be presented with their relevance for better constraining the formation conditions of ferropericlase inclusions in diamonds.

Harte, B., Harris, J.W., Hutchinson, M.T., Watt, G.R., Wilding, M.C. (1999): Lower mantle mineral associations in diamonds from Sao Luiz, Brazil. *in* "Mantle petrology: Field observations and high pressure experimentation: A tribute to Francis R. Joe Boyd", Y. Fei, C.M. Bertka, B.O. Mysen, eds., Geochemical Society, Houston, 125-153.

McCammon, C.A., Peyronneau, J., Poirier, J.P. (1998): Low ferric iron content of (Mg,Fe)O at high pressures and temperatures. *Geophys Res. Letters*, **25**, 1589-1592.

McCammon, C.A., Stachel, T., Harris, J.W. (2004): Iron oxidation state in lower mantle mineral assemblages II. Inclusions in diamonds fram Kankan,Guinea. *Earth Planet. Sci. Letters*, **222**, 423-434.

Wirth, R., Dobrzhinetskaya, L., Harte, B., Screiber, A., Green, H.W. (2014): High-Fe (Mg,Fe)O inclusion in diamond apparently from the lowermost mantle. *Earth Planet. Sci. Letters*, **404**, 365-375.

UHP PHASES VERSUS PREPARATION MATERIALS – BE CAUTIOUS WHEN USING MICRO-RAMAN SPECTROSCOPY

Nasdala L.*[1], Dobrzhinetskaya L.F.[2], Korsakov A.V.[3], Massonne H.-J.[4], Reissner C.[1-5] & Steger S.[1]

[1] Institut für Mineralogie und Kristallographie, Universität Wien, Austria

[2] Department of Earth Sciences, University of California, Riverside, CA, USA

[3] V.S. Sobolev Institute of Geology and Mineralogy, Siberian Branch of the Russian Academy of Sciences, Novosibirsk, Russia

[4] Institut für Mineralogie und Kristallographie, Universität Stuttgart, Germany

[5] Institute for Interdisciplinary Studies, University of Amsterdam, Netherlands

Corresponding email: lutz.nasdala@univie.ac.at

Keywords: UHP diamond, abrasives, Raman spectroscopy

The identification of minute amounts of diamond and moissanite is possible with ease by means of confocal Raman spectroscopy, as both species are fairly good Raman scatterers and yield characteristic, narrow-line spectra. Further, these minerals are formed in the Earth's interior under ultra-high-pressure (UHP) conditions. The occurrence of diamond and/or moissanite as inclusions that are trapped inside rigid host minerals, such as garnet, kyanite, or zircon, is therefore commonly taken as evidence for either mantle origin or UHP metamorphism experienced by the host rock (e.g., Dobrzhinetskaya, 2012; Liou & Tsujimori, 2013, and references therein).

It however needs to be considered cautiously that both diamond and moissanite (i.e. silicon carbide) are common abrasive materials, contained in many grinding and polishing powders, pastes, and sprays that are used in the preparation of sample mounts. For this reason, the Raman-based identification of diamond and/or moissanite alone is decidedly inconclusive with respect to origin/formation of the host rock. Rather it needs to be checked most cautiously and critically whether the diamond and/or moissanite detected is of undoubted natural origin, then verifying high-pressure conditions, or might be inherited preparation debris instead. An example for the latter has been documented by Dobrzhinetskaya et al. (2014) who showed that the proposed discovery of what was assumed to represent the world's oldest diamonds (Menneken et al., 2007) merely was diamond abrasive trapped in surface voids of Hadean zircon in epoxy sample mounts. Also, diamond is contained in many tools, such as drill bits or saws. Even insufficient cleaning of rock-processing machines, such a jaw breakers, needs to be considered. Diamond detected in unpolished rock specimens, or in heavy-mineral concentrates separated from crushed and acid-processed rock material, therefore may be an inherited artefact. This has for instance been discussed by Ogasawara et al. (2011) who questioned the correctness of the proposed discovery of metamorphic diamond in the Dabie UHP terrane (e.g., Xu et al., 1992).

There have been attempts to distinguish UHP minerals and abrasives of the same material using peculiarities of Raman spectral parameters (Perraki et al., 2009; Nasdala et al., 2016). The outcome, however, is disappointing. Spectral parameters (i.e., band positions and widths) of UHP minerals and abrasives both show extensive scatter and overlap widely. In addition, there may be vast differences between the spectra of a fresh abrasive and its used analogue (Steger et al., 2013). We discuss that Raman identification is a conclusive, genuine proof of UHP diamond and/or moissanite only if it is accompanied by thorough optical microscopy and/or electron microscopy, verifying that the crystals analyzed are completely enclosed inclusions and have naturally developed connections with their host or neighboring minerals.

Dobrzhinetskaya, L.F. (2012): Microdiamonds – frontier of ultrahigh-pressure metamorphism: a review. *Gondwana Res.*, **21**, 207-223.

Dobrzhinetskaya, L., Wirth, R., Green, H. (2014): Diamonds in Earth's oldest zircons from Jack Hills conglomerate, Australia, are contamination. *Earth Planet. Sci. Letters*, **387**, 212-218.

Liou, J.G. & Tsujimori, T. (2013): The fate of subducted continental crust: evidence from recycled UHP–UHT minerals. *Elements*, **9**, 248-250.

Menneken, M., Nemchin, A.A., Geisler, T., Pidgeon, R.T., Wilde, S.A. (2007): Hadean diamonds in zircon from Jack Hills, Western Australia. *Nature*, **448**, 917-921.

Nasdala, L., Steger, S., Reissner, C. (2016): Raman study of diamond-based abrasives, and possible artefacts in detecting UHP microdiamond. *Lithos*, in press; DOI: 10.1016/j.lithos.2016.03.009.

Ogasawara, Y., Igarashi, M., Tsai, C., Iwasaki, I., Liou, J.G. (2011): Possibility of the misidentification of contaminated microdiamonds in UHP metamorphic rocks: an example of diamond grains in Dabie garnet clinopyroxenite. American Geophysical Union, Fall Meeting 2011, abstract V23E–2609.

Perraki, M., Korsakov, A.V., Smith, D.C., Mposkos, E. (2009): Raman spectroscopic and microscopic criteria for the distinction of microdiamonds in ultrahigh-pressure metamorphic rocks from diamonds in sample preparation materials. *Am. Mineral.*, **94**, 546-556.

Steger, S., Nasdala, L., Wagner, A. (2013): Raman spectra of diamond abrasives and possible artefacts in detecting UHP microdiamond. Conference on Raman and Luminescence Spectroscopy in the Earth Sciences, abstr., 95-96.

Xu, S.T., Okay, A.I., Ji, S., Sengor, A.M.C., Su, W., Liu, Y., Jiang, L. (1992): Diamond from the Dabie Shan metamorphic rocks and its implication for tectonic setting. *Science*, **256**, 80-82.

THE CRYSTALLOGRAPHIC ORIENTATIONS BETWEEN DIAMOND AND ITS Mg-CHROMITE INCLUSIONS

Nestola F.*[1], Angel R.J.[1], Nimis P.[1], Alvaro M.[2], Milani S.[1] & Harris J.W.[3]
[1] Dipartimento di Geoscienze, Università di Padova, Italy
[2] Dipartimento di Scienze della Terra e dell'Ambiente, Università di Pavia, Italy
[3] School of Geographical and Earth Sciences, University of Glasgow, United Kingdom
Corresponding email: fabrizio.nestola@unipd.it

Keywords: diamond, Mg-chromite, inclusions

The study of the crystallographic orientations and morphology of minerals included in diamonds can provide insights into the mechanisms of their incorporation and the timing of their formation relative to the host diamond (e.g., Nestola et al. 2014). The reported occurrence of non-specific orientations for some minerals in some diamonds, suggesting an epitactic relationship, has long been considered to reflect contemporaneous growth of the diamond and the inclusion. Magnesium chromites [$(Mg,Fe)Cr_2O_4$, space group *Fd*-3*m*] are the third most abundant mineral found as inclusions in diamond, representing about 14% (identical to the olivine abundance) of all the inclusions in cratonic diamonds (Stachel & Harris, 2008). We have measured the relative orientations of 23 chromites in 16 diamonds from the Udachnaya kimberlite (Siberia) and four chromites in four diamonds from Panda mine (Slave Craton, Canada) by both in-house and synchrotron *in-situ* X-ray diffraction. Allowing for the ambiguities in indexing caused by the symmetries of the Mg-chromite and diamond host, the relative orientation of each inclusion relative to its diamond, were determined with the OrientXplot software (Angel et al., 2015). The inclusions exhibit a strong tendency (more than 90% of measured inclusions) for a single (111) plane of each inclusion to be sub-parallel to a {111} plane of their diamond host, but without any statistically significant orientation of the crystallographic axes *a*, *b*, and *c*. This parallelism of (111) chromite and (111) diamond without epitaxy may reflect a mechanical control during growth of chromite and diamond octahedral crystals.

Diffraction measurements do not provide information about the morphology of the inclusions in diamonds, although such information may constrain possible growth mechanisms of the diamond and/or its inclusions. Three-dimensional imaging of 29 chromite inclusions was performed by Synchrotron Radiation X-ray Tomographic Microscopy (at TOMCAT, Swiss Light Source). The three-dimensional images revealed features such as olivine inclusions within chromite inclusions and details of the surface morphologies that could be interpreted as growth and/or dissolution features.

Acknowledgements: This work was supported by ERC starting grant 307322 to Fabrizio Nestola and by the MIUR-SIR grant "MILE DEEp" (RBSI140351) to M. Alvaro.

Angel, R.J., Milani, S., Alvaro, M., Nestola, F. (2015) OrientXplot: a program to analyse and display relative crystal orientations. *J. Appl. Crystallogr.*, **48**, 1330-1334.

Nestola, F., Nimis, P., Angel, R.J., Milani, S., Bruno, M., Prencipe, M., Harris, J.W. (2014) Olivine with diamond-imposed morphology included in diamonds. Syngenesis or protogenesis? *Int. Geol. Rev.*, **56**, 1658–1667.

Stachel, T. & Harris, J.W. (2008) The origin of cratonic diamonds – Constraints from mineral inclusions. *Ore Geol. Rev.*, **34**, 5-32.

HYDROUS SILICIC FLUID FILMS AROUND SOLID INCLUSIONS IN GEM-QUALITY DIAMONDS

Nimis P.*[1], Alvaro M.[1-2], Nestola F.[1], Angel R.J.[1], Marquardt K.[3], Rustioni G.[2] & Harris J.W.[4]
[1] Dipartimento di Geoscienze, Università di Padova, Italy
[2] Dipartimento di Scienze della Terra e dell'Ambiente, Università di Pavia, Italy
[3] Bayerisches Geoinstitut, Universität Bayreuth, Germany
[4] School of Geographical and Earth Sciences, University of Glasgow, United Kingdom
Corresponding email: paolo.nimis@unipd.it

Keywords: diamond, inclusions, fluids

Kimberlite-borne diamonds form from fluids or melts circulating at depth in the Earth's mantle. Usually, analysis of this parental material is confined to specific types of diamond, the so-called fibrous or milky varieties. Here we provide the first direct evidence of the common presence of a hydrous silicic fluid surrounding typical peridotitic and eclogitic mineral inclusions in gem-quality diamonds from the Siberian and Kaapvaal cratons. The fluid film (up to 1.5 µm thick) was identified by using confocal micro-Raman spectroscopy and Synchrotron-based X-ray Tomographic Microscopy and contains $Si_2O(OH)_6$, $Si(OH)_4$, and molecular H_2O. This observation would strongly suggest that gem-quality lithospheric diamonds from both major parageneses normally grow in the presence of a water-rich fluid. The presence of the fluid envelope should be taken into account for the interpretation of H_2O contents in solid inclusions and will need to be part of the assessment of diamond formation pressures based on residual pressures of inclusions.

Acknowledgements: This contribution was supported by ERC starting grant 307322 to Fabrizio Nestola and by the MIUR-SIR grant "MILE DEEp" (RBSI140351) to Matteo Alvaro.

EVIDENCE FOR H_2O-BEARING FLUIDS IN THE LOWER MANTLE FROM DIAMOND INCLUSION

Palot M.*[1-2], Jacobsen S.D.[3], Townsend J.P.[3], Nestola F.[4], Marquardt K.[5], Harris J.W.[6], Stachel T.[1], McCammon C.A.[5] & Pearson D.G.[1]

[1] Department of Earth and Atmospheric Sciences, University of Alberta, Edmonton, Canada
[2] Laboratoire Magmas et Volcans, Université Jean Monnet, Saint-Etienne, France
[3] Department of Earth and Planetary Sciences, Northwestern University, Evanston, IL, USA
[4] Dipartimento di Geoscienze, Università di Padova, Italy
[5] Bayerisches Geoinstitut, Universität Bayreuth, Germany
[6] School of Geographical and Earth Sciences, University of Glasgow, United Kingdom
Corresponding email: mederic.palot@gmail.com

Keywords: diamonds, water, brucite

Earth's deep water cycle plays a critical role in the long term geochemical evolution of our planet. Recent developments from high-pressure experiments and regional seismic studies (Schmandt et al., 2014), geochemical evidence from magmas, and the discovery of a natural hydrous ringwoodite (Pearson et al., 2014) affirm early theoretical predictions that the components of water can persist in minerals and melts as deep as the mantle transition zone (410-660 km depth). However, the water storage capacity of the dominant lower-mantle mineral assemblage, bridgmanite-$(Mg,Fe)(Si,Al)O_3$ (~ 80% vol.) and ferropericlase-(Mg,Fe)O (~ 20% vol.), is 10-15 times lower than in the transition zone. Contrast in H_2O storage capacity between the transition zone and lower-mantle can produce volatile-rich magmas by dehydration melting below 660 km depth and could act as a factory for diamond formation. Here we show the first direct evidence for water-bearing fluids in the uppermost lower mantle from natural ferropericlase crystal contained within a diamond from São Luíz, Brazil. The ferropericlase exhibits exsolution of magnesioferrite, which places the origin of this assemblage in the uppermost part of the lower mantle. The presence of brucite-$Mg(OH)_2$ precipitates in the ferropericlase crystal reflects the later-stage quenching of H_2O-bearing fluid likely in the transition zone, which has been trapped during the inclusion process in the lower mantle. Dehydration melting may be one of the key processes involved in transporting water across the boundary between the upper and lower mantle.

Pearson, D.G., Brenker, F.E., Nestola, F., McNeill, J., Nasdala, L., Hutchison, M.T., Matveev, S., Mather, K., Silversmit, G., Schmitz, S., Vekemans, B., Vincze, L. (2014): Hydrous mantle transition zone indicated by ringwoodite included within diamond. *Nature*, **507**, 221-224.

Schmandt, B.,Jacobsen, S.D., Becker, T.W., Liu, Z., Dueker, K.G. (2014): Dehydration melting at the top of the lower mantle. *Science*, **344**, 1265-1268.

CARBON ISOTOPIC COMPOSITION OF A JUINA DIAMOND WITH A CARBONATE INCLUSION DETERMINED BY NANOSIMS

Pinti D.L.*[1], Bureau H.[2], Ishida A.[3], Sano Y.[3] & Cartigny P.[4]
[1] Geotop, Université du Québecl, Montréal, Canada
[2] Institut de Minéralogie, de Physique des Matériaux et de Cosmochimie, Université Pierre et Marie Curie, France
[3] Atmosphere and Ocean Research Institute, University of Tokyo, Japan
[4] Institut de Physique du Globe de Paris, Université Paris Diderot, France
Corresponding email: pinti.daniele@uqam.ca

Keywords: sub-lithospheric diamonds, Juina, carbonate

Diamonds form in the lithospheric mantle at depths between 150 and 200 km. A small amount of diamonds is recognized to form in the transition zone and even in the lower mantle. These “sub-lithospheric” diamonds are particularly abundant in the Juina area, Mato Grosso, Brazil and thereby have been the subject of numerous studies. Juina diamonds present a wide spectrum of mineral inclusions, covering both peridotitic and eclogitic composition. Syngenetic mineral inclusions such as calcium silicate perovskite and magnesiowüstite point out to diamond formation at depths between 500 km up to 800 km. Among the more rare inclusions found in the Juina diamonds, carbonates are interpreted as an evidence of deep recycling of sedimentary carbon into the transition zone or the lower mantle. Yet, the $\delta^{13}C$ values measured in three FIB-TEM foils by NanoSIMS50 of an alluvial diamond with a dolomite inclusion range between -8.85±1.32‰ and -2.31±1.88‰ with a mean total value of -5.0±2.3‰. These values are in the range of typical mantle carbon, as measured in diamonds of peridotitic paragenesis. Similar $\delta^{13}C$ values from -6.6 to -4.4‰ are reported in literature for three other Juina diamonds with carbonate/dolomite inclusions. There are several hypotheses that could explain the measured “peridotitic”-like carbon isotopic composition in these diamonds but the more plausible is that these diamonds were formed from reduction of carbonatitic melts. In this case, the carbonate inclusion would be inherited from the melt and survived its reduction into diamonds. Schrauder & Navon (1994) found carbonates in fluid inclusions from peridotitic diamonds formed in the lithosphere. The trapped inclusions are cogenetic with their host-diamonds and they represent their parent fluid. Thus the implication of fluids in the precipitation of the dolomite in carbonate-bearing Juina diamonds cannot be excluded.

Schrauder, M. & Navon, O. (1994): Hydrous and carbonatitic mantle fluids in fibrous diamonds from Jwaneng, Botswana. *Geochim. Cosmochim. Acta*, **58**, 761-77

NH-BEARING NANOINCLUSIONS IN MILKY DIAMONDS FROM JUINA AREA, MATO GROSSO, BRAZIL

Rudloff-Grund J.*[1], Brenker F.E.[1], Marquardt K.[2], Howell D.[1-3-4], O'Reilly S.Y.[4] & Kaminsky F.V.[4-5]
[1] Institut für Geowissenschaften, Goethe-Universität Frankfurt am Main, Germany
[2] Bayerisches Geoinstitut, Universität Bayreuth, Germany
[3] School of Earth Sciences, University of Bristol, United Kingdom
[4] Centre of Excellence for Core to Crust Fluid Systems & National Key Centre for Geochemical Evolution and Metallogeny of Continents, Department of Earth & Planetary Science, Macquarie University, Sydney, Australia
[5] KM Diamond Exploration Ltd., West Vancouver, Canada
Corresponding email: rudloff@em.uni-frankfurt.de

Keywords: milky diamonds, nanoinclusions, ammonia

Octahedral nanoinclusions are the main characteristic defect microstructures in irregular shaped milky diamonds from Juina area, Mato Grosso, Brazil. Comprehensive chemical analysis using scanning transmission electron microscopy (STEM) combined with energy dispersive X-ray spectroscopy (EDX) with new ChemiSTEM^{TM} technology yields a high N content for all sealed nanoinclusions studied. The ChemiSTEM^{TM} design includes an X-Field emission gun (X-FEG), high-brightness, Schottky electron source and the Super-X^{TM} geometry. The latter includes four windowless silicon drift detectors (SDD) symmetrically arranged around the sample within the TEM column. This new setup provides increased light element sensitivity, handling of high count-rates with excellent energy resolution and low dead times (Schlossmacher et al., 2010; Von Harrach et al., 2010). Fourier transform infrared mapping of the milky regions, occurring within octahedral diamond growth zones, showed a strong correlation between structurally bound nitrogen, hydrogen and the abundance of nanoinclusions. We propose that the most likely phase included in these nanoinclusions is ammonia (NH_3). Although the total amount of N measured via STEM EDX cannot be calculated directly, approximations of the minimum values are possible. Assuming a detection limit for N of about 0.1 wt.% and a calculated nanoinclusion volume fraction of 0.17% results in a minimum bulk N content within the nanoinclusions of about 170 ppm. If NH_3 is the inclusion species the minimum estimate for bulk hydrogen within the nanoinclusions is about 510 ppm. Formation of these NH-bearing nanoinclusions can possibly take place by two different mechanisms at two different times during diamond host formation or evolution. They could be the result of a recovery process during a high-temperature episode and thus might represent the last stage of the nitrogen aggregation, or they may have simply grown in defects that captured a free NH-bearing fluid. Trace-element analysis of milky and non-milky areas will help to distinguish between the two suggested growth processes. Platelet breakdown would not induce higher concentrations of trace elements within the milky areas. Assuming nanoinclusions represent growth zoning, trapping the host fluids, they might have higher levels of other elements delivered by the fluid.

Schlossmacher, P., Klenov, D.O., Freitag, B., Von Harrach, H.S. (2010): Enhanced detection sensitivity with a new XEDX system for AEM based on silicon drift detector technology. *Microsc. Today*, **18**, 14-20.

Von Harrach, H., Dona, P., Freitag, B., Soltau, H., Niculae, A., Rohde, M. (2010): An integrated multiple silicon drift detector system for transmission electron microscopes. *J. Phys. Conf. Ser.*, **241**, 012015.

PRESSURE RELEASE FOR HOST – INCLUSION SYSTEMS: THE INTERPLAY BETWEEN BRITTLE FAILURE AND FLUID PHASE

Rustioni G.*[1], Angel R.J.[2], Mazzucchelli M.L.[1], Milani S.[2], Nimis P.[2], Domeneghetti M.C.[1], Marone F.[3], Harris J.W.[4], Nestola F.[2] & Alvaro M.[1]

[1] Dipartimento di Scienze della Terra e dell'Ambiente, Università di Pavia, Italy

[2] Dipartimento di Geoscienze, Università di Padova, Italy

[3] Swiss Light Source, Paul Scherrer Institut, Villigen, Switzerland

[4] School of Geographical and Earth Sciences, University of Glasgow, United Kingdom

Corresponding email: greta.rustioni@gmail.com

Keywords: diamonds, inclusions, brittle failure

Mineral inclusions entrapped in their hosts can provide fundamental information about geological processes. For example, recent developments in "elastic" geobarometry allow the retrieval of encapsulation pressures (P_{trap}) for host-inclusion pairs. In principle this method can be applied to any mineral-mineral pair as long as both the residual pressure (P_{inc}) on the inclusion, and the Equations of State (EoS) for both host and inclusion are known (Angel et al., 2015). However, this is only possible if the deformation in the host-inclusion pair is purely elastic. This excludes all inclusions that are surrounded by cracks, indicative of brittle deformation, as such weaknesses may result in partial or complete release of the Pinc. If however the effects of these cracks on pressure release could be quantitatively modelled, then the applicability of "elastic" geobarometry might be extended to a much larger number of inclusion-host pairs.

We report the results of a pilot experiment in which the residual pressures have been determined for 9 olivine inclusions still entrapped in 5 diamonds. Inclusion pressures were determined from the unit-cell volumes of the olivines measured by X-ray diffraction and the EoS suitable for their compositions as determined by in-situ X-ray structure refinement (Angel & Nestola, 2016). We quantified the actual amount of cracks surrounding the inclusions by Synchrotron Radiation X-ray Tomographic Microscopy (at TOMCAT, Swiss Light Source). Preliminary results showed that 90% of the inclusions trapped in our set of diamonds are surrounded not only by cracks, but also by a continuous fluid rim (Nimis et al., 2016). Both the volumes of cracks and rim have been determined from 3D reconstructions to an accuracy of about 4%. Our results show that the fracture intensity around the inclusions increases with increasing inclusion size. The presence of a fluid phase around the inclusions and its migration into developing cracks enhances the pressure released upon fracturing. As a confirmation of such behaviour, within an individual diamond the P_{inc} decreases with increasing crack volumes normalized over the volume of the rim. In principle, combining elastic geobarometry (e.g., EoS for host and inclusions and unit cell volumes of the inclusions at room-T and P_{inc}) together with the information on the volume of the cracks, it would be possible to reconstruct the original P_{trap} regardless of the state of fracturing.

Acknowledgements: This work is supported by ERC starting grant 307322 to F. Nestola and by the MIUR-SIR grant "MILE DEEp" (RBSI140351) to M. Alvaro.

Angel, R.J. & Nestola, F. (2016): A century of mineral structures: How well do we know them? *Am. Mineral.*, **101**, 1036-1045.

Angel, R.J., Nimis, P., Mazzucchelli, M.L., Alvaro, M., Nestola, F. (2015): How large are departures from lithostatic pressure? Constraints from host–inclusion elasticity. *J. Metam. Geol.*, **33**, 801-813.

Nimis, P., Alvaro, M., Nestola, F., Angel, R.J., Marquardt, K., Rustioni, G., Harris, J.W. (2016): First evidence of hydrous silicic fluid films around solid inclusions in gem-quality diamonds. *Lithos*, in press.

THERMOELASTIC PROPERTIES OF SILICATE GARNETS AND THEIR USE IN THE STUDY OF DIAMOND FORMATION

Scandolo L.*[2], Milani S.[1], Mazzucchelli M.L.[2], Alvaro M.[2], Di Prima M.[2], Domeneghetti M.C.[2], Nestola F.[1], Geiger C.A.[3] & Stagno V.[4]

[1] Dipartimento di Geoscienze, Università di Padova, Italy
[2] Dipartimento di Scienze della Terra e dell'Ambiente, Università di Pavia, Italy
[3] Fachbereich Chemie und Physik der Materialien, Universität Salzburg, Austria
[4] Dipartimento di Scienze della Terra, Sapienza Università di Roma, Italy
Corresponding email: lorenzo.scandolo01@universitadipavia.it

Keywords: alluminosilicate garnets, P-V-T EoS coefficients, entrapment pressures

The formation conditions of diamond can be determined by measuring the residual pressures on small, trapped mineral inclusions. Determinations of the pressure of entrapment require accurate EoS of the inclusion phases as well as diamond. Because mineral inclusions in diamonds from the subcratonic lithospheric mantle are often garnet (38% of them; Stachel et al., 2008), we have determined new sets of P-V-T EoS coefficients for various end-member aluminosilicate garnets (i.e., pyrope, almandine, grossular) and uvarovite. These compositions constituent the main components of the garnet solid solutions found as inclusion in diamonds. We test whether it is possible to determine the thermoelastic properties of intermediate compositions by linear interpolation of the end members.

We began by synthesizing four end-member garnets and one intermediate garnet composition ($Py_{51}Al_{22}Gr_{27}$) using piston-cylinder and multi anvil devices (Milani et al., 2015). The unit-cell volume for each garnet was measured as a function of pressure from 1 atm to 10 GPa and temperature from 100 to 1073 K.

Simultaneous fits of the elastic coefficients, performed using a thermal pressure Eos combined with a 3rd order Birch-Murnhagan in EoSFit7 (Angel et al., 2014), yielded the following values for the bulk modulus, its first pressure derivative and the thermal expansion coefficient:K'_O:

Uv_{100}: K_{T0} = 157.9(1.8) GPa, K'_0 = 5.4(5), and α = 2.16(3)·$10^{-5}K^{-1}$
Gr_{100}: K_{T0} = 167.0(2.0) GPa, K'_0 = 5.0(5), and α = 2.07(1)·$10^{-5}K^{-1}$
Py_{100}: K_{T0} = 163.7(1.7) GPa, K'_0 = 6.4(4), and α = 2.52(1)·$10^{-5}K^{-1}$
Al_{100}: K_{T0} = 172.6(1.5) GPa, K'_0 = 5.8(5), and α = 2.21(1)·$10^{-5}K^{-1}$

and

$Py_{51}Alm_{22}Gr_{27}$: K_{T0} = 166.2(1.9)GPa, K'_0 =5.8(5), and α = 2.45(1)·$10^{-5}K^{-1}$.

Linear interpolation from the EoS parameters of the end-members yields K_{T0} = 166.8(1.2) GPa, K'_0 = 5.9(4) and α = 2.36(1)·10-5K^{-1} for $Py_{51}Alm_{22}Gr_{27}$. The difference between interpolated and measured parameters are about 0.29 GPa for typical entrapment pressures of inclusions in diamond.

Acknowledgements: This work was supported by ERC starting grant 307322 to Fabrizio Nestola and by the MIUR-SIR grant "MILE DEEp" (RBSI140351) to M. Alvaro.

Alvaro, M., Angel, R., Marciano, C., Milani, S., Scandolo, L., Mazzucchelli, M., Zaffiro, G., Rustioni, G., Briccola, M., Domeneghetti, M.C., Nestola, F. (2015): A new micro-furnace for *in situ* high-temperature single-crystal X-ray diffraction measurements. *J. Appl. Crystallogr.*, **48**, 1192-1200.

Angel, R.J., Gonzalez-Platas, J., Alvaro, M. (2014) EosFit-7c and a Fortran module (library) for equation of state calculations. *Z. Kristallogr.*, **229**, 405-419.

Angel, R.J., Alvaro, M., Nestola, F., Mazzucchelli, M. (2015): Diamond thermoelastic properties and implications for determining the pressure of formation of diamond-inclusion systems. *Russian Geol. Geophys. J.*, **56**), 211-220.

Milani, S., Nestola, F., Alvaro, M., Pasqual, D., Mazzucchelli, M.L., Domeneghetti, M.C., Geiger, C.A. (2015): Diamond-garnet geobarometry: The role of garnet compressibility and expansivity. *Lithos*, **227**, 140-147.

Shirey, S.B., Cartigny, P., Frost, D.J., Keshav, S., Nestola, F., Nimis, P., Pearson, D.G., Sobolev, N.V., Walter, M.J. (2013): Diamonds and the geology of mantle carbon. *Rev. Mineral. Geochem.*, **75**, 355-421.

Stachel, T. & Harris, J.W. (2008): The origin of cratonic diamonds - constraints from mineral inclusions. *Ore Geol. Rev.*, **34**, 5-32.

METALLIC INCLUSIONS IN UNIQUE TYPE IIA DIAMONDS

Smith E.M.*[1], Shirey S.B.[2], Nestola F.[3] & Wang W.[1]
[1] Gemological Institute of America, New York, NY, USA
[2] Department of Terrestrial Magnetism, Carnegie Institute for Science, Washington, DC, USA
[3] Dipartimento di Geoscienze, Università di Padova, Italy
Corresponding email: evan.smith@gia.edu

Keywords: type II diamond, inclusions, Fe-Ni metal

Many of the world's largest and most famous diamonds have been noted to have very low concentrations of nitrogen, below the detection limit of infrared spectroscopy. These diamonds constitute a unique and enigmatic variety of Type II (low nitrogen) diamonds, whose origin has long remained uncertain (Moore, 2014). In addition to their nitrogen deficient character, these diamonds are generally large, inclusion poor, relatively pure, irregularly shaped, and highly resorbed. The renowned 3106 carat Cullinan diamond, discovered over a century ago, is a prime example. These Cullinan-like Type II diamonds are especially valuable as gemstones and difficult to access for research. Furthermore, they very rarely contain any inclusions that might shed light on their geological origin.

Here we report the findings of a systematic search for inclusions in large, high-quality Type IIa diamonds, which reveals the recurring appearance of metallic inclusions. Analysis using X-ray diffraction and electron microprobe shows a consistent assemblage of Fe-Ni-C-S phases within the inclusions. Such inclusions suggest that Cullinan-like, large, high-quality diamonds could represent an unrecognized, unique paragenesis with an intimate link to Fe-Ni metal in the deep mantle (Rohrbach et al., 2014; Smith & Kopylova, 2014).

Moore, A.E. (2014): The origin of large irregular gem-quality Type II diamonds and the rarity of blue Type IIb varieties. *South African J. Geol.*, **117**, 219-236.

Rohrbach, A., Ghosh, S., Schmidt, M.W., Wijbrans, C.H., Klemme, S. (2014): The stability of Fe–Ni carbides in the Earth's mantle: evidence for a low Fe–Ni–C melt fraction in the deep mantle. *Earth Planet. Sci. Letters*, **388**, 211-221.

Smith, E.M. & Kopylova, M.G. (2014): Implications of metallic iron for diamonds and nitrogen in the sublithospheric mantle. *Can. J. Earth Sci.*, **51**, 510-516.

Session S2:

Evolution of the Earth's mantle and melt generation through time

Conveners:

Costanza Bonadiman (Ferarra – Italy)

Marguerite Godard (Montpellier – France)

Carsten Münker (Münster – Germany)

Othmar Müntener (Lausanne – Switzerland)

Helen Williams (Durham – United Kingdom)

Alberto Zanetti (Pavia – Italy)

OVERVIEW OF THE TECTONIC EVOLUTION OF THE IRAQI ZAGROS THRUST ZONE: SIXTY MILLION YEARS OF CONVERGENCE IN NEOTETHYS

Ali S.A.*[1-2], Nutman A.P.[1] & Jones B.G.[1]
[1] GeoQuEST Research Centre, School of Earth & Environmental Sciences, University of Wollongong, Australia
[2] Department of Applied Geology, College of Science, Kirkuk University, Iraq
Corresponding email: sarmad@uow.edu.au

Keywords: Iraq, Zagros, Neotethys

The tectonic history in the Zagros Orogenic belt of northeastern Iraq (Kurdistan) started in the late Cretaceous and continued into the early Miocene. Two allochthonous terranes in northeast Iraq are the Upper and Lower Allochthon thrust sheets (Aziz et al., 2011). These were obducted and transported on top of the northeast of the former Arabian passive margin during the early Miocene (Aswad, 1999). Consequently the northeastern Arabian passive margin is first covered by parautochthonous flysch deposits of Late Campanian-Maastrichtian age (known as the Tanjero clastics) and then by "Tertiary Red Beds". The Tanjero clastics and Tertiary Red Beds unconformably overly the autochthonous Balambo platform carbonates and the accretionary prism of the Qulqula par-autochthonous radiolarites of oceanic provenance. The verification of a long-lived tectonism of Iraqi Zagros Suture Zone is a non-trivial task, mainly because the Arabian passive margin has been affected by incremental superimposed deformation through time. A part of the Upper Allochthon segment is the Hasanbag arc complex (Ali et al., 2012). ^{40}Ar-^{39}Ar dates on Hasanbag magmatic hornblende from volcanic arc units indicate an Albian – Cenomanian age (106-92 Ma; Ali et al., 2012). Aswad (pers. comm.) provides further insights into the extended episode of magmatism that resulted from ridge subduction by examining the tectonic evolution of the Zagros thrust at Jabal Bulfat, 30 km east of Qala Deza City. The biotite and hornblende from gabbroic and coeval granitoid components of a Bulfat composite intrusion yield ^{40}Ar-^{39}Ar ages of 39.23±0.21 and 38.87±0.24 Ma respectively. These argon ages of ~39 Ma might also represent the termination of arc related magmatism that had initiated more than sixty million years previously in the Albian-Cenomanian. Unlike the Upper Allochthon Ophiolite-bearing Terrane, the Lower Allochthon has limited extent in Iraq. Their equivalents in Iran occur in the Kamyaran area along the Sahneh-Marivan line. It is composed of the Walash- Naopurdan volcano-sedimentary groups. The ^{40}Ar-^{39}Ar data on basalt shows that the Walash- Naopurdan Groups are the major manifestations of 43.01±0.15 to 24.31±0.60 Ma magmatism i.e. with a long time span of approximately 19 million years (Ali et al., 2013). This suggests that Cenozoic subduction was proximal to the northeastern margin of the Arabian craton.

Ali, S., Buckman, B., Aswad, S., Jones, K., Ismail, S., Nutman, A. (2012): Recognition of Late Cretaceous Hasanbag ophiolite-arc rocks in the Kurdistan region of the Iraqi Zagros Thrust Zone: A missing link in the paleogeography of the closing Neo-Tethys Ocean. *Lithosphere*, **4**, 395-410.

Ali, S., Buckman, B., Aswad, S., Jones, K., Ismail, S., Nutman, A. (2013): The tectonic evolution of a Neo - Tethyan (Eocene–Oligocene) island - arc (Walash and Naopurdan groups) in the Kurdistan region of the Northeast Iraqi Zagros Suture Zone. *Island Arc*, **2**, 104-125.

Aswad, K.J. (1999): Arc-continent Collision in Northeastern Iraq as Evidenced by Mawat and Penjein Ophiolite Complexes. *Rafidain J. Sci.*, **10**, 51-61.

Aziz, N.R.H., Aswad, K.J., Koyi, H.A. (2011): Contrasting of serpentinite bodies in northwestern Zagros Suture Zone serpentinites, Kurdistan region, Iraq: tracing a "subduction signature" in serpentinite-matrix mélanges *Geol. Mag.*, **148**, 819-837.

DEFORMATION OF THE LITHOSPHERIC MANTLE BENEATH THE STYRIAN BASIN (EASTERN AUSTRIA) – A STUDY ON PERIDOTITE XENOLITHS

Aradi L.E.*[1], Hidas K.[2], Klébesz R.[1-3], Kovács I.[4], Patkó L.[1], Zanetti A.[5] & Szabó C.[1]

[1] Lithosphere Fluid Research Lab, Eötvös Loránd University, Budapest, Hungary

[2] Instituto Andaluz de Ciencias de la Tierra, Consejo Superior de Investigaciones Científicas, Universidad de Granada, Spain

[3] Geodetic and Geophysical Institute, Research Centre for Astronomy and Earth Sciences, Hungarian Academy of Sciences, Budapest, Hungary

[4] Geological and Geophysical Institute of Hungary, Budapest, Hungary

[5] Istituto di Geoscienze e Georisorse, Consiglio Nazionale delle Ricerche, Pavia, Italy

Corresponding email: aradi.laszloelod@gmail.com

Keywords: mantle, xenolith, EBSD

Plio-Pleistocene alkali basaltic volcanism occurred within the Carpathian-Pannonian Region (CPR; e.g., Szabó et al., 2004) at six distinct volcanic fields. Several lava and pyroclast outcrops contain xenoliths, however mantle xenoliths from only a few outcrops have been studied in details in the Styrian Basin Volcanic Field (SBVF, Eastern Austria and Northern Slovenia). Based on previous studies, the subcontinental lithospheric mantle (SCLM) beneath the SBVF is mainly composed of texturally homogeneous coarse granular and high temperature spinel lherzolites. In our study we present new comprehensive petrographic, crystal preferred orientation (CPO) and mineral chemistry data from 12 less-studied volcanic outcrops across the SBVF.

The studied xenoliths are mostly coarse granular lherzolites, amphiboles are present in almost every sample and often texturally replace pyroxenes and spinels. In amphibole-rich samples phlogopite, coupled with apatite, is also present. The peridotites are highly annealed, with lobate grain boundaries, and the microstructures of the constituent phases, particularly those of olivine and pyroxenes, do not suggest significant intragranular deformation (i.e., they are devoid of subgrain walls and undulose extinction).

CPO of olivines varies between the most common distributions in nature: [010]-fiber, orthogonal and [100]-fiber symmetry (Tommasi & Vauchez, 2015). The CPO of pyroxenes is usually coherent with coeval deformation with olivine, showing $[100]_{OL}$ distributed subparallel to $[001]_{OPX}$. The CPO of amphiboles suggest postkinematic epitaxial overgrowth on the precursor pyroxenes.

The studied xenoliths show a broad temperature range (850-1100°C), corresponding to mantle depths (estimation based on local geotherm) between 30 and 60 km, which coincide with the shallower part of the recent 60-80 km thick lithosphere beneath the SBVF (Bianchi et al., 2014). Equilibrium temperatures show correlation with the varying CPO symmetries and grain size: coarser xenoliths with [100]-fiber and orthorhombic symmetry and appear in the high temperature (> 1000°C) xenoliths, which is characteristic for xenoliths that have asthenospheric origin (Kovács et al., 2012). Most of the xenoliths display transitional CPO symmetry between [010]-fiber and orthogonal, which may apply lithospheric deformation under varying deformation regime from transtensional to transpressional setting (Tommasi et al., 1999). Such deformation may have been caused by the Neogene evolution of the lithosphere within the CPR. According to our calculations, a significant part of the observed seismic anisotropy under the SBVF can be generated by the SCLM beside the assumed mantle flow beneath the region (Qorbani et al., 2015).

Acknowledgements: This research was granted by the Hungarian Science Foundation (OTKA, 78425 to C. Szabó). K. Hidas' research leading to these results was funded by the European Union Framework Programme 7 (EU-FP7) Marie Curie postdoctoral grant PIEF-GA-2012- 327226.

Bianchi, I., Miller, M. S., Bokelmann, G. (2014): Insights on the upper mantle beneath the Eastern Alps. *Earth Planet. Sci. Letters*, **403**, 199-209.

Kovács, I., Falus, G., Stuart, G., Hidas, K., Szabó, C., Flower, M.F.J., Hegedűs, E., Posgay, K., Zilahi-Sebess, L. (2012): Seismic anisotropy and deformation patterns in upper mantle xenoliths from the central Carpathian–Pannonian region: Asthenospheric flow as a driving force for Cenozoic extension and extrusion?. *Tectonophys.*, **514**, 168-179.

Qorbani, E., Bianchi, I., Bokelmann, G. (2015): Slab detachment under the Eastern Alps seen by seismic anisotropy. *Earth Planet. Sci. Letters*, **409**, 96-108.

Szabó, C., Falus, G., Zajacz, Z., Kovács, I., Bali, E. (2004): Composition and evolution of lithosphere beneath the Carpathian–Pannonian Region: a review. *Tectonophys.*, **393**, 119-137.

Tommasi, A. & Vauchez, A. (2015): Heterogeneity and anisotropy in the lithospheric mantle. *Tectonophys.*, **661**, 11-37.

Tommasi, A., Tikoff, B., Vauchez, A. (1999): Upper mantle tectonics: three-dimensional deformation, olivine crystallographic fabrics and seismic properties. *Earth Planet. Sci. Letters*, **168**, 173-186.

CONSTRAINTS FROM SPREADING RIDGE-DERIVED ECLOGITES ON ARCHAEAN MANTLE POTENTIAL TEMPERATURES

Aulbach S.*[1]
[1] Institut für Geowissenschaften, Goethe-Universität Frankfurt am Main, Germany
Corresponding email: s.aulbach@em.uni-frankfurt.de

Keywords: Archaean oceanic crust, eclogite xenoliths, mantle dynamics

Earth's mantle has been cooling at least since the Mesoarchaean, but there is little agreement on the rate at which this proceeded and several models have been proposed that differ by as much as ~ 200ºC in the Mesoarchaean (Davies, 2009; Herzberg et al., 2010). Our weak grasp of the mantle thermal evolution is in stark contrast to the importance of this parameter in regulating terrestrial dynamics and geochemical cycles, ranging from controls on the peridotite solidus and consequent geochemical differentiation, to plate stiffness conducive to the operation of plate tectonics and to the recycling efficiency of volatiles in subduction zones.

High-Mg eclogite xenoliths, entrained by kimberlites from the mantle lithospheres of ancient continental cores into which they were emplaced during craton amalagamation, have elemental and isotopic compositions indicative of formation in Archaean oceanic spreading ridges. Combined with rare orogenic eclogites, exhumed or obducted during closure of ancient ocean basins, they may retain a memory of the thermal and redox state of the ancient convecting mantle sources that gave rise to their low-pressure protoliths. In contrast to modern MORB, their protoliths formed from higher-degree melts, in part from Fe-rich mantle heterogeneities, experienced orthopyroxene (opx) fractionation in addition to or instead of olivine fractionation (indicative of high pressures of crystallization), and some subsequently experienced partial melt loss upon recycling and metamorphism.

Flat MREE-HREE patterns and lack of Y or Al_2O_3 depletion relative to TiO_2 and MgO in Archaean eclogites indicate formation of protoliths from a melt that separated predominantly from a garnet-free peridotite source, implying intersection of the solidus at shallow pressures in or not far above the spinel peridotite stability field at pressures ~ 2.5 GPa. Low average melt fractions (~ 0.25) are calculated from the TiO_2 contents of the least differentiated, non-cumulate Archaean samples, assuming robustness of TiO_2 during partial melting of eclogite as supported by experiments. This again suggests shallow intersection of the solidus at ~ 3 GPa for decompression melting with productivities of ~10% per GPa and final melting pressures of 0.5 GPa. Combined with a solidus parameterisation (Hirschmann, 2000), this yields initial melting temperatures of ~1400-1520ºC, corresponding to T_P of ~ 1370 to 1480ºC. This temperature estimate is significantly lower than some estimates for the ambient convecting mantle, arguing for early plate strengthening that would support plate tectonics and topography and possibly facilitating deep volatile recycling from the Mesoarchaean onwards.

Davies, G.F. (2009): Effect of plate bending on the Urey ratio and the thermal evolution of the mantle. *Earth Planet. Sci. Letters*, **287**, 513-518.

Herzberg, C., Condie, K., Korenaga, J. (2010): Thermal history of the Earth and its petrological expression. *Earth Planet. Sci. Letters*, **292**, 79-88.

Hirschmann, M.M. (2000): Mantle solidus: Experimental constraints and the effects of peridotite composition. *Geochem. Geophys. Geosyst.*, **1**, 70.

THE SULFUR DEPLETION IN THE EARTH'S MANTLE IS NOT A HIGH PRESSURE SIGNATURE

Ballhaus C.*[1], Münker C.[2], Fonseca R.O.C.[1], Nagel T.[1-3], Speelmanns I.M.[1-4], Zirner A.[1], Vogel A.[5] & Heuser A.[1]

[1] Steinmann Institut, Universität Bonn, Germany
[2] Institut für Geologie und Mineralogie, Universität Köln, Germany
[3] Geology Department, University of Århus, Denmark
[4] Departement Erdwissenschaften, Eidgenössische Technische Hochschule, Zürich, Switzerland
[5] Bayerisches Geoinstitut, Universität Bayreuth, Germany
Corresponding email: ballhaus@uni-bonn.de

Keywords: sulfur, late veneer

The extreme depletion of the Earth's mantle in the chalcogens (S, Se, Te) is commonly seen as a signature of mantle-core equilibration at high pressure. However, in addition to S, Se, and Te, the mantle contains other elements as volatile as S that are hardly depleted relative to the volatility trend despite being potentially siderophile. Sulfur-bearing metal-silicate experiments over a wide range of metal/S ratios reported here show that the relative abundances of all moderately volatile elements cannot be reproduced with metal-silicate equilibration, neither at low nor at high pressure. Much of the volatile inventory of the Earth's mantle must have been added late in the accretion history, when core formation had become largely inactive. The great depletion in the chalcogens is attributed to the selective segregation of a late sulfide matte from an oxidized and largely crystalline mantle. We propose that the volatile abundances of the Earth's mantle may not be in redox equilibrium with the Earth's core.

HYBRID ORIGIN OF THE ERRO-TOBBIO TROCTOLITES (LIGURIAN OPHIOLITES, ITALY): STRUCTURAL AND GEOCHEMICAL EVIDENCE OF MULTI-STAGE EVOLUTION

Basch V.*[1], Rampone E.[1], Ildefonse B.[2], Godard M.[2] & Crispini L.[1]
[1] Dipartimento di Scienze della Terra, dell'Ambiente e della Vita, Università di Genova, Italy
[2] Géosciences Montpellier, Université de Montpellier, France
Corresponding email: valentin.basch@gmail.com

Keywords: Ligurian ophiolites, troctolites, melt impregnation

Recent studies of olivine-rich gabbroic rocks from the lower oceanic crust describe a hybrid origin of olivine-rich troctolites, through melt-rock interaction processes, impregnation and incorporation of mantle slivers in the lower crust (e.g., Drouin et al., 2010). The Erro-Tobbio ultramafic massif allows the study of the association between impregnated mantle peridotites and a hectometre-size ultramafic body composed of troctolite to plagioclase-bearing wehrlite. We used detailed structural analyses and in-situ mineral geochemistry to infer the formation mechanism of this mafic body. The inner troctolitic body exhibits high complexity, with a host troctolite (Troctolite A) crosscut by troctolitic tabular bodies (Troctolite B). These different generations of troctolites show distinct modal compositions and textures. The host troctolite A is characterized by a dominant millimetre-size corroded granular texture of olivine associated with dunite pods and a layering defined by poikilitic plagioclase enrichment. The contact between the mafic body and the host mantle peridotites is defined by irregular troctolite to wehrlite apophyses. The troctolite A shows microstructures and Crystallographic Preferred Orientations (CPO) indicative of a formation after impregnation of a mantle dunite by an olivine-undersaturated melt. This impregnation leads to olivine dissolution, associated with poikilitic plagioclase and clinopyroxene crystallization. This is indicated by a progressive randoming of the Axial-[100] CPO with olivine disaggregation and increasing melt input in the troctolite. The crosscutting troctolite B displays extreme olivine textural variation, from fine-grained granular to deformed coarse-grained skeletal olivine. Troctolite B shows CPO indicative of crystallization after magmatic flow, intrusive into the host troctolite A. Both troctolite types display large major and trace element variations in minerals, e.g. variation of anorthite content (An = 54-67) in plagioclase at rather constant Forsterite content in olivine, and significant Zr, Ti, HREE heterogeneity in olivine, systematically correlated with the textural variability (e.g. corroded deformed vs. undeformed granular olivine). Such features indicates an important role of reactive (rather than pure fractional) crystallization. We infer that the textural heterogeneity of olivine in the troctolite B is related to variations in the degree of undercooling and cooling rate of the melt (Faure et al., 2003). The skeletal olivine crystallization corresponds to a first influx of a primitive melt into a colder host troctolite, followed by a local reheating of the host rock and evolution of the melt leading to formation of fine-grained euhedral crystals. Overall, the results of this study suggest a poly-phase formation of this hectometre-scale troctolitic body through multiple processes: the impregnation of a mantle-derived dunitic body followed by intrusions by undercooled primitive melts.

Drouin, M., Ildefonse, B., Godard, M. (2010): A microstructural imprint of melt impregnation in slow spreading lithosphere: Olivine-rich troctolites from the Atlantis Massif, Mid-Atlantic Ridge, 30°N, IODP Hole U1309D. *Geochem. Geophys. Geosyst*., **11**, Q06003.

Faure, F., Trolliard, G., Nicollet, C., Montel, J.M. (2003): A developmental model of olivine morphology as a function of the cooling rate and the degree of undercooling. *Contrib. Mineral. Petrol.*, **145**, 251-263.

THE ALKALINE-CARBONATITE COMPLEX OF JACUPIRANGA (BRAZIL) REVISITED: MAGMA GENESIS, MODE OF EMPLACEMENT AND TECTONO-MAGMATIC SIGNIFICANCE

Beccaluva L.[1], Bianchini G.[1], Natali C.*[1] & Siena F.[1]
[1] Dipartimento di Fisica e Scienze della Terra, Università di Ferrara, Italy
Corresponding email: ntlcld@unife.it

Keywords: alkaline-carbonatite complex, tectono-magmatic significance, lithosphere/astenosphere interaction

Field, petrological and geochemical data is reported on the Jacupiranga alkaline-carbonatite complex (133-131 Ma) which, together with other alkaline complexes of southern Brazil and south-western Africa, occurs in the central part of - and is coeval with - the Paranà-Etendeka CFB province. It consists of a shallow intrusion in the Precambrian crystalline basement, and can be subdivided in two main diachronous plutonic bodies: an older dunite-gabbro-syenite in the NW and a younger clinopyroxenite – ijolite (*s.l.*) in the SE, later injected by a carbonatitic core (< 1% volume). A petrogenetic model based on bulk rock major and trace element, mineral chemistry and Sr-Nd-Pb-C isotopes indicate that the two silicate intrusions generated from different parental magmas that rose from distinct mantle sources and evolved at shallow level in two zoned cup-shaped plutonic bodies. The first intrusion was generated by OIB-like alkaline to mildly alkaline parental basalts that initially led to the formation of a dunitic adcumulate core, surrounded by gabbroic cumulates, in turn injected by subanular syenite intrusive and phonolite dikes. Mela-nephelinitic (± melilite) melts likely generated deep (≥ 3 GPa) in the lithosphere were the parental magmas of the second intrusion and gave rise to large coarse-grained clinopyroxenite ad- to meso-cumulates, in turn surrounded and partially cut, by semi-annular fine-layered melteigite-ijolite-urtite ortho-cumulates. Isotopically, carbonatites do not evidence genetic links with the associated silicate intrusions, thus suggesting either a direct mantle origin or shallow liquid immiscibility from hypothetical silicate magmas currently not observed in the complex. An important result arising from the new Sr-Nd-Pb isotopes on Jacupiranga rocks is the clear correspondence of the clinopyroxenite-ijolite *(s.l.)* intrusion with the “Gough component” recently identified as the initial plume signature that characterizes the magmatic activity since 132 Ma, encompassing the oldest part of the Walvis Ridge volcanism and the Etendeka picrite-basalt association. Therefore, a model is proposed to account for the Early Cretaceous tectonomagmatic evolution of western Gondwana, where the impinging proto-Tristan (Walvis) mantle plume caused lithospheric arching, extension and radial fracturing of the south American-African plate triggering widespread small volume alkaline-carbonatite episodes mostly coeval with the eruption of the majority of Paranà-Etendeka CFB; the model could explain the coexistence of 1) small degree alkaline melts mostly generated from lithospheric mantle sources that, for the deepest magmas such as Jacupiranga parental melanephelinites, may also record the signature of sublithospheric plume-related geochemical components; and 2) higher degree melting CFB picrites generated from the hottest and deepest sublithospheric mantle sources at the core of the plume head.

EARLY EVOLUTION OF MANTLE MELTS INTRUDING THE LOWERMOST CONTINENTAL CRUST OF THE IVREA-VERBANO ZONE: INSIGHTS FROM THE M. CAPIO PERIDOTITE-PYROXENITE LENS

Berno D.*[1], Tribuzio R.[1-2] & Zanetti A.[2]
[1] Dipartimento di Scienze della Terra e dell'Ambiente, Università di Pavia, Italy
[2] Istituto di Geoscienze e Georisorse, Consiglio Nazionale delle Ricerche, Pavia, Italy
Corresponding email: davide.berno01@universitadipavia.it

Keywords: Monte Capio, Ivrea-Verbano Zone, Val Strona

Magma chambers in the deep continental crust play a major role in modifying the compositions of ascending mantle-derived melts, through complex evolution processes involving fractional crystallization, crustal assimilation and melt-crystal mush reactions (e.g., Solano et al., 2012). To unravel the early magmatic evolution experienced by the mantle melts intruding the lowermost continental crust of the Ivrea-Verbano Zone, we carried out a petrological and geochemical study of the km-scale ultramafic lens exposed near M. Capio. This lens spreads for a few km from Strona to Sesia valleys, near the Insubric tectonic line, and has a maximum thickness of 300 m. The ultramafic lens includes Fe-Ni-Cr mineralizations (e.g., Zaccarini et al., 2014) that were exploited in the past through mine activity, and shows intrusive relationships with respect to granulite-facies metasediments of the Kinzigite Formation (Ewing et al., 2013; Redler et al., 2013). Primary magmatic relationships between the ultramafic lens and garnet-bearing gabbros are locally preserved (Ferrario et al., 1983). A U-Pb zircon date of 314±5 Ma was reported for one garnet-bearing gabbro and interpreted as the intrusion age (Klötzli et al., 2014).

The ultramafic lens mostly consists of amphibole-bearing peridotites and pyroxenites. Olivine from the peridotites (dunites to olivine-rich harzburgites/lherzolites) has forsterite molar proportions ranging from 84 to 79% and is associated with accessory Cr-poor spinel. The pyroxenites are characterized by euhedral orthopyroxene (Mg# = 82-77) as the most abundant phase and are locally plagioclase-bearing. The peridotite-pyroxenite association is locally crosscut by plagioclase-bearing hornblendite dykes. In addition, sparse amphibole-rich gabbronorite dykes were found in one of the pyroxenite exposures. Amphibole from the peridotites has relatively low TiO_2 (about 1.5 wt.%) and rather variable K_2O. In the pyroxenites and the dykes, amphibole has TiO_2 ranging from 2 to 3 wt.% and nearly constant K_2O, and plagioclase is anorthite-rich (89-75 mol%). Amphibole and clinopyroxene from the peridotites show marked variations in the incompatible trace element signature, contrary to amphibole and clinopyroxene from the pyroxenites and the dykes. The variable geochemical fingerprint of the peridotites is attributed to reactive melt migration within an olivine-rich spinel-bearing matrix. Nd-Sr isotopic analyses of mineral separates and whole-rocks are currently in progress to elucidate whether the percolating melts were differentiates mantle melts or melts contaminated by crustal components

Ewing, A.T., Hermann, J., Rubatto, D. (2013): The robustness of the Zr-in-rutile and Ti-in-zircon thermometers during high-temperature metamorphism (Ivrea-Verbano Zone, northern Italy). *Contrib. Mineral. Petrol.*, **165**, 757-779.

Ferrario, A., Garuti, G., Rossi, A., Sighinolfi, G.P. (1983): Petrographic and metallogenic outlines of the "La Balma – M. Capio" ultramafic – mafic body (Ivrea–Verbano Basic Complex, NW Italian Alps). In "Mineral Deposits of the Alps and of the Alpine Epoch in Europe" H.J. Schneider, ED., Proc. IV ISMIDA 1981, 28-40.

Klötzli, U.S., Sinigoi, S., Quick, J.E., Demarchi, G., Tassinari, C.C.G., Sato, K., Günes, Z. (2014): Duration of igneous activity in the Sesia Magmatic System and implications for high-temperature metamorphism in the Ivrea-Verbano deep crust. *Lithos*, **206-207**, 19-33.

Redler, C., Johnson, T.E., White, R.W., Kunz B.E. (2012): Phase equilibrium constraints on a deep crustal metamorphic field gradient: metapelitic rocks from the Ivrea Zone (NW Italy). *J. Metam. Geol.*, **30**, 235-254.

Solano, J.M.S., Jackson, M.D., Sparks, R.S.J., Blundy, J.D., Annen, C. (2012): Melt segregation in deep crustal hot zones: a mechanism for chemical differentiation, crustal assimilation and the formation of evolved magmas. *J. Petrol.*, **53**, 1999-2026.

Zaccarini, F., Tredoux, M., Miller, D.E., Garuti, G., Aiglsperger, T., Proenza, J.A. (2014): The occurrence of platinum-group and gold minerals in the Bon Accord Ni-oxide body, South Africa. *Am. Mineral.*, **99**, 1774-1782.

BASIC DYKES CROSSCUTTING THE CRYSTALLINE BASEMENT OF VALSUGANA (ITALY): FURTHER EVIDENCE OF EARLY TRIASSIC VOLCANISM IN THE SOUTHERN ALPS

Bianchini G.*[1], Natali C.[1], Shibata T.[2] & Yoshikawa M.[2]
[1] Dipartimento di Fisica e Scienze della Terra, Università di Ferrara, Italy
[2] Institute for Geothermal Sciences, Kyoto University, Beppu, Japan
Corresponding email: bncglc@unife.it

Keywords: basic dykes, Triassic magmatism, Southern Alps

The southern Alps in the Province of Trento (Italy) are constituded by a Paleozoic crystalline basement covered by Mesozoic sedimentary units. Volcanism is also represented, as testified by Permian (calcalkaline products, mainly rhyolitic in composition), Triassic (basic to intermediate shoshonitic products) and Paleogene (tholeiitic and Na-alkaline basalts) episodes. In this framework, the updated 1:50,000 geological map of Trento revealed in Valsugana (a lateral valley respect to the main Adige valley) the presence of a series of basic dykes crosscutting the crystalline basement, ignored by the previous researches. These dykes, outcropping close to the towns of Pergine and Levico Terme, could represent evidence for an indipendent volcanic episode so far overlooked in the literature. To discover the nature of these dykes 10 whole-rock samples have been analyzed by XRF and ICP-MS to have a major and trace element characterization, as well by TIMS for the analysis of Sr-Nd-Pb isotopes. Plotted in a Total Alkali Silica (TAS) diagram, samples include subalkaline and transitional products, that according to the K_2O *vs.* SiO_2 diagram pertain to the calcalkaline and shoshonite series, respectively. The incompatible trace element distribution invariably displays the negative anomalies in High Field Strenght Elements (HFSE) typical of subduction related magmas. The Sr-Nd-Pb isotopic composition (carried out on leached whole rock powders) displays a marked crustal signature, with $^{87}Sr/^{86}Sr$ 0.7093-0.7464, $^{143}Nd/^{144}Nd$ between 0.5122-0.5121, $^{206}Pb/^{204}Pb$ 18.6-19.6, $^{207}Pb/^{204}Pb$ 15.6-15.7, $^{208}Pb/^{204}Pb$ 38.9-40.5. Preliminary dating of two samples, performed by ActLabs, gives K-Ar ages of 236±6 and 251±7 Ma. On the whole, considering the observed spatial location, the timing, and the geochemical signature, we propose that the studied dykes represent a transition between the Permian and the Triassic volcanism that are known in neighbouring sectors of the southern Alps, as result of post-collisional magmatism following the end of the Varisic orogenic cycle. On the other hand, a possible relation between these dykes and the Cenozoic (Alpine) tectono-magmatic phases (an hypothesis proposed in the notes of the geological map) seems to be unwarranted.

SUBSOLIDUS PHASE RELATIONS IN A SECONDARY-TYPE PYROXENITE: AN EXPERIMENTAL STUDY UP TO 1.5 GPa

Borghini G.[1] & Fumagalli P.*[1]
[1] Dipartimento di Scienze della Terra "A. Desio", Università di Milano, Italy
Corresponding email: patrizia.fumagalli@unimi.it

Keywords: pyroxenites, mantle lithospheric evolution, experimental petrology

Mantle peridotites exposed in ultramafic massifs are often veined by pyroxenitic lithologies that can be originated by deep magmatic infiltration, thus representing old heterogeneities in the mantle. These pyroxenites experienced the same metamorphic evolution of the host peridotites but they are expected to develop sensibly different phase assemblages from peridotites as a result of significantly different bulk composition. Although several experimental studies have been focused on melting relations in pyroxenites over a wide compositional range, phase relations at subsolidus lithospheric conditions are still poorly experimentally investigated. This study aims to provide new experimental constraints on phase stability and mineral chemistry in pyroxenites. A natural pyroxenite from ophiolitic mantle sequence (Northern Apennine, Italy) has been chosen; this pyroxenite has a peculiar bulk composition, with relatively high X_{Mg} (0.83), high CaO (14.5 wt.%) and low Na_2O (0.48 wt.%) contents, and it is interpreted as a hybrid secondary pyroxenite originated by interaction between peridotite and pyroxenite-derived melt (Borghini et al., 2016). Experiments were performed at pressure from 0.7 to 1.5 GPa, temperatures from 1100 to 1250°C using both single stage and end-loaded piston cylinders. The starting material was prepared as an anhydrous glass obtained from the powder of the natural pyroxenite, seeded with 1% of a mixture of synthetic spinel *s.s.* (50%) and pyrope (50%). Al-rich spinel is ubiquitous in all experimental run products together with clinopyroxene, orthopyroxene and olivine. At 1100°C, a plagioclase-bearing assemblage is stable up to 0.9 GPa and a garnet-bearing assemblage is stable at 1.5 GPa and temperature between 1150 and 1230°C. The stability of plagioclase moves to slightly higher pressure than what observed in fertile lherzolite (Borghini et al., 2010). At 0.8 and 0.9 GPa, plagioclase is slightly more anorthitic than in lherzolite and its modal abundances are about 12 and 8 wt.%, respectively. We found few percent (5-6 wt.%) of a pyrope-rich garnet in experiments at 1.5 GPa; at T = 1150-1230°C the "garnet-in" curve is rather flat and located at significantly lower pressure as compared with mantle peridotites, expected to be above 1.8 GPa (Klemme & O'Neill, 2000). Pyroxenes mineral chemistry varies significantly in the plagioclase stability field and in the garnet stability field, but is rather homogeneous in the spinel pyroxenite field, as result of negligible variability of spinel composition reflecting the very low X_{Cr} of the bulk (0.01). The results of this experimental study are comparable with mineral compositions variability documented in natural samples and they can represent useful tools to trace the geothemobarometric evolution of tectonic mantle sequences.

Borghini, G., Fumagalli, P., Rampone, E. (2010): The stability of plagioclase in the upper mantle: Subsolidus experiments on fertile and depleted lherzolite. *J. Petrol.*, **51**, 229-254.

Borghini, G., Rampone, E., Zanetti, A., Class, C., Cipriani, A., Hofmann, A.W., Goldstein, S. (2016): Pyroxenite layers in the Northern Apennines' upper mantle (Italy) - Generation by pyroxenite melting and melt infiltration. *J. Petrol.*, in press, DOI: 10.1093/petrology/egv074.

Klemme, S. & ONeill, H.S.C. (2000): The near-solidus transition from garnet lherzolite to spinel lherzolite. *Contrib. Mineral. Petrol.*, **138**, 237-248.

THE ROLE OF SECONDARY PYROXENITES IN THE COMPOSITION OF MELTS FROM VEINED MANTLE SOURCES: EXPERIMENTAL CONSTRAINTS

Borghini G.*[1], Fumagalli P.[1] & Rampone E.[2]
[1] Dipartimento di Scienze della Terra "A. Desio", Università di Milano, Italy
[2] Dipartimento di Scienze della Terra, dell'Ambiente e della Vita, Università di Genova, Italy
Corresponding email: giulio.borghini@unimi.it

Keywords: pyroxenite melting, mantle heterogeneity, experimental petrology

Secondary pyroxenites can form in the deep mantle as a result of interaction between pyroxenite-derived melt and peridotite (e.g., Sobolev et al., 2005); they therefore potentially represent a melting component in the basalt sources. Although partial melting of pyroxenites has been extensively investigated at P > 2 GPa (e.g., Lambart et al., 2013), melting relations for peculiar hybrid pyroxenite compositions at P < 2 GPa is still poorly known. We have experimentally derived the extent and composition of partial melts from a secondary pyroxenite at 1 and 1.5 GPa, in order to evaluate its role in the basalts composition by combining the results of this work with experimental data on peridotites in a simple partial melting model. As starting material, we selected a pyroxenite sample from the Northern Apennine ophiolites (Italy), whose "second-stage" origin was documented by field and geochemical observations (Borghini et al., 2016). This pyroxenite has solidus temperature of 70 and 100°C lower than the solidus of moderately fertile peridotite (MM3), at 1 and 1.5 GPa respectively. It encounters very high degrees of melting (around 90%) within narrow temperature ranges (100 and 130°C, respectively), and its melt productivity, at fixed T, can be 6-7 times higher than that of a peridotite. At increasing melt fraction, orthopyroxene (± garnet), spinel and clinopyroxene are progressively consumed by melting reactions. At both pressures, olivine is the liquidus phase. Pyroxenite melts cover a wide range of X_{Mg} (0.53-0.80), with SiO_2, Al_2O_3 and Na_2O decreasing and CaO increasing with degree of melting. Profiting of experimental results we calculated melt compositions for mantle sources made by different proportions of peridotite, considering both fertile and depleted peridotite composition, and secondary pyroxenite. In this simplified model, the effect of heat transfer from peridotite towards the lower solidus-temperature pyroxenite (e.g., Phipps Morgan, 2001) has been not considered, and the two components are chemically and thermically isolated until melt mixing and extraction. At elevated melting degrees of the mixed source (F > 20%), due to the higher melt productivity of pyroxenite, the influence of pyroxenite component results in X_{Mg} similar to peridotite melts, very low Na_2O contents and CaO/Al_2O_3 higher than MORBs. At moderate melting degrees (F < 20%), computed mixed melts are highly comparable with most primitive MORBs either assuming fertile or depleted peridotite, even for high pyroxenite fraction (20-50%). In such melting scenario, the studied secondary pyroxenite would represent a "hidden" component in the mantle source, potentially capable to explain the decoupling between "enriched" trace-element/isotope and "normal" major-element compositions sometimes documented in oceanic basalts.

Borghini, G., Rampone, E., Zanetti, A., Class, C., Cipriani, A., Hofmann, A.W., Goldstein, S. (2016): Pyroxenite layers in the Northern Apennines' Upper Mantle (Italy) - Generation by pyroxenite melting and melt infiltration *J. Petrol.*, in press, DOI: 10.1093/petrology/egv074.

Lambart, S., Laporte, D., Schiano, P. (2013): Markers of the pyroxenite contribution in the major-element compositions of oceanic basalts: Review of the experimental constraints. *Lithos*, **160-161**, 14-36.

Phipps Morgan, J. (2001): Thermodynamics of pressure release melting of a veined plum pudding mantle. *Geochem. Geophys. Geosyst.*, **2**, 2000GC000049.

MANTLE XENOLITHS FROM MAROSTICANO AREA (NORTHERN ITALY): A COMPARISON WITH VENETO VOLCANIC PROVINCE LITHOSPHERIC MANTLE

Brombin V.*[1], Bonadiman C.[1], Coltorti M.[1] & Bryce J.[2]
[1] Dipartimento di Fisica e Scienze della Terra, Università di Ferrara, Italy
[2] Department of Earth Sciences, University of New Hampshire, Durham, NH, USA
Corresponding email: brmvnt@unife.it

Keywords: Veneto Volcanic Province, mantle xenoliths, metasomatism

The Tertiary Magmatic Province of Veneto, known as Veneto Volcanic Province (VVP), in the North-East of Italy, represents the most important volcanic district of the Adria Plate. It is composed by five volcanic localties: Val d'Adige, Marosticano, Mts. Lessini, Berici and Euganean Hills. Most of the volcanic products are relatively undifferentiated lavas and range in composition from nephelinites to tholeiites. Often VVP nephelinites and basanites carry mantle xenoliths (mainly harzburgites and lherzolite).

This study reports a petrological comparison between Marosticano xenoliths (new outcrop) and those from the Lessinean and Val d'Adige areas (Siena & Coltorti 1989; Beccaluva et al., 2001; Gasperini et al., 2006).

Mineral major elements analyses show that the Marosticano lherzolites and harzburgites reflect "more restitic" composition than the mantle domain beneath the other VVP districts (Lessini Mts. and Val d'Adige). Olivine and pyroxene of Marosticano xenoliths have in fact the highest mg# values of the entire district (Marosticanoà90-93; literatureà86-92). At comparable mg# (45-85 wt.%) Marosticano spinels tend to be higher in Cr_2O_3 (23-44 wt.%) contents with respect to the other VVP spinels (7-25 wt.%). Ni contents in Marosticano olivines are higher (2650-3620 ppm) than those of the Lessinean xenoliths (1500-3450 ppm), and similar to that of Val d'Adige lherzolites (3000-3500 ppm), approaching the contents of Archean cratonic mantle (Kelemen, 1998). In turn, Lessinean olivines properly fall in the Ni-mg# Phanerozoic field.

Detailed *in-situ* trace element analyses show that clinopyroxene in the Marosticano mantle xenoliths exhibits strong enrichment in Th, U and LREE, but depletion in both HREE and HFSEs (e.g., Ta, Zr and Hf). Moreover clinopyroxenes in most Marosticano mantle xenoliths have high La/Yb but low Ti/Eu ratios, suggesting a metasomatism by carbonatitic melts (Coltorti et al., 1999), while the Lessinean clinopyroxene compositions are consistent with a metasomatism by silicate melts (Beccaluva et al., 2001).

To complete this state-of-art, the equilibration temperatures and oxigen fugacities for Marosticano peridotites were estimated and compared with those of the other VVP xenoliths. At fixed pressure of 15 kbar, the equilibration temperatures of Marosticano xenoliths are similar (Brey & Köhler: 920-1120°C) to those of Lessini (O'Neill & Wall: 990-1110°C; Beccaluva et al., 2007), but higher than those of Val d'Adige (Wells: 909-956°C; Gasperini et al., 2006). Finally, Marosticano mantle fragment show similar relatively high redox conditions (Dlog fO_2: +1.2 to -0.7, Ballhaus, 1991) with respect to Lessinean and Val d'Adige xenoliths, in agreement with the range of continental lithosphere (Foley et al., 2011).

Ballhaus, C., Berry, R., Green, D. (1991): High pressure experimental calibration of the olivine-orthopyroxene-spinel oxygen geobarometer: implications for the oxidation state of the upper mantle. *Contrib. Mineral. Petrol.*,**107**, 27-40.

Beccaluva, L., Bonadiman, C., Coltorti, M., Salvini, L., Siena, F. (2001): Depletion events, nature of metasomatizing agent and timing of enrichment processes in lithospheric mantle xenoliths from the Veneto Volcanic Province *J. Petrol.*, **42**, 173-187.

Beccaluva, L., Bianchini, G., Bonadiman, C., Coltorti, M., Milani, L., Salvini, L., Siena, F., Tassinari, R. (2007): Intraplate lithospheric and sublithospheric components in the Adriatic domain: Nephelinite to tholeiite magma generation in the Paleogene Veneto Volcanic Province, Southern Alps. *Geol. Soc. Am.*, *Spec. Pap.*, 418, 131-152.

Brey, G.P. & Köhler, T.P. (1990): Geothermobarometry in four-phase lherzolites II. New thermobarometers, and pratical assessment of existing thermobarometers. *J. Petrol.*, **31**, 1353-1378.

Coltorti, M., Bonadiman, C., Hinton, R.W., Siena, F., Upton, B.G.J. (1999): Carbonatite metasomatism of the oceanic upper mantle: evidence from clinopyroxenes and glasses in ultramafic xenoliths of Grande Comore, Indian Ocean. *J. Petrol.*, **40**, 133-165.

Foley, S.F. (2011): A reappraisal of redox melting in the Earth's mantle as a function of tectonic setting and time. *J. Petrol.*, **52**, 1363-1391.

Gasperini, D., Bosch, D., Braga, R., Bondi, M., Macera, P., Morten, L. (2006): Ultramafic xenoliths from the Veneto Volcanic Province (Italy): Petrological and geochemical evidence for multiple metasomatism of the SE Alps mantle lithospere. *Geochem. J.*, **40**, 377-404.

Siena, F. & Coltorti, M. (1989): Lithospheric mantle evolution: evidences from ultramafic xenoliths in the Lessinean volcanics (Northern Itlay). *Chem. Geol.*, **77**, 347-364.

DUNITE CHANNELS IN PERIDOTITES OF LITHOSPHERIC MANTLE BENEATH LOWER SILESIA (SW POLAND)

Ćwiek M.*[1]
[1] Institute of Geological Sciences, University of Wrocław, Poland
Corresponding email: mateusz.cwiek@ing.uni.wroc.pl

Keywords: lithospheric mantle, dunite channels, Central Europe

Grodziec nephelinite is one of the mantle xenolith-bearing Cenozoic alkaline lavas in Lower Silesia (SW Poland, Central Europe). The xenoliths are represented by peridotitic and clinopyroxenitic suites. The peridotites comprise mostly spinel lherzolites, but other lithologies are present as well. Forsterite content in olivine classifies the xenoliths into four groups: A (Fo = 90.7-91.8%), A- (Fo = 89.3-89.9%), B (Fo = 85.2-86.1%), and clinopyroxenitic group C (Fo = 78.8-86.6%). Xenoliths from groups A and A- plot into OSMA field by Arai (1994) and thus represent undoubtly mantle rocks. Group B xenoliths are Cpx-bearing dunites (2-6 vol.% of Cpx) and wehrlite (15 vol.% of Cpx) and are characterized by adcumulative texture. Clinopyroxene (Mg# = 0.88-0.86) occurs in interstices as clusters or parallel layers. It is enriched in LREE ($(La/Lu)_N$ = 4.07-4.15).

Dunites can form during partial melting of primary mantle which degree exceeds 40% (Pearson et al., 2003). However, more commonly dunites originate due to reaction of harzburgite with silicate melt which result in crystallization of olivine at expense of orthopyroxene (e.g., Kelemen, 1990). The dunites may contain small amounts of clinopyroxene which crystallized from the percolating melt. Such replacive dunites are commonly observed as veins in ophiolitic complexes and are interpreted as channels through which silicate melt was transported. Our study shows that Grodziec group B xenoliths share the replacive origin with ophiolitic dunites and that group C xenoliths represent precipitates from the percolating melt in uppermost mantle conditions. Moreover, the peridotite-melt reaction caused also olivine enrichment in Fe ("Fe-metasomatism"). Dunites and wehrlites have been found in Lower Silesia (Puziewicz et al., 2015), however they were not considered as effect of dunitization. Chemical and textural features of dunite xenoliths (olivine enrichment in Fe, absence of orthopyroxene, LREE enrichment in clinopyroxene, if present), allow us to suppose that dunitization process can be more widespread in upper mantle in Central Europe.

Dunitization process is limited to narrow channels (centimeters to meters) therefore their volume in upper mantle is rather low (5 to 15%; Kelemen et al., 1995). Replacive dunites constitute 13.6% of all xenoliths from Grodziec and 3 to 9% of all xenoliths from another Lower Silesia locations. This observation suggests that proportions between "normal" and "dunitized" peridotites laying beneath Lower Silesia resemble those from the oceanic lithosphere.

Acknowledgements: This study was supported by National Centre for Scientific Research project no DEC-UMO-2014/15/B/ST10/00095.

Arai, S. (1994): Characterization of spinel peridotites by olivine -spinel compositional relationship: review and interpretation. *Chem. Geol.*, **113**, 191-204.

Kelemen, P. (1990): Reaction between ultramafic rock and fractionating basaltic magma I. Phase Relations, the origin of calc-alkaline magma series, and the formation of discordant dunite. *J. Petrol.*, **31**, 51-98.

Kelemen, P., Shimizu, N., Salters, V. (1995): Extraction of mind-ocean-ridge basalt from the upwelling mantle by focused flow of melt in dunite channels. Nature, **375**, 747-753.

Pearson, D.G., Canil, D., Shirey, S.B., Heinrich, D.H., Karl, K.T. (2003): Mantle samples included in volcanic rocks: Xenoliths and diamonds. *in* "Treatise on Geochemistry", H.D. Holland, K.K. Turekian, eds., Pergamon,Oxford, 171-275.

Puziewicz, J., Matusiak-Małek, M., Ntaflos, T., Grégoire, M., Kukuła, A. (2015): Subcontinental lithospheric mantle beneath Central Europe. *Int. J. Earth Sci.*, **104**, 1913-1924.

NEW CONSTRAINTS ON THE FORMATION OF HETEROGENEOUS OCEANIC CRUST AT SLOW SPREADING RIDGES: A DETAILED PETRO-GEOCHEMICAL STUDY OF THE OLIVINE-RICH TROCTOLITES FROM ATLANTIS MASSIF (MAR, IODP HOLE U1309D, 30°N)

Ferrando C.*[1], Godard M.[1] & Ildefonse B.[1]
[1] Géosciences Montpellier, Centre National de la Recherche Scientifique, Universitè de Montpellier, France
Corresponding email: carlotta.ferrando@gm.univ-montp2.fr

Keywords: olivine-rich troctolites, Mid-ocean ridge, lower oceanic crust

The gabbroic series drilled at IODP Hole U1309D (Mid Atlantic Ridge, IODP Expeditions 304, 305) comprise a whole range of modes from the most primitive olivine-rich troctolites to more evolved gabbros. High Mg-contents and a relatively large proportion of olivine-rich lithologies characterize this gabbroic series. *In situ* trace element geochemistry and crystallographic preferred orientation measurements of olivine-rich troctolites indicate that they record extensive melt impregnation of pre-existing olivine rich material (mantle rocks or dunitic cumulate). By studying well-preserved olivine-rich troctolites from Hole U1309D we aim at understanding their formation and the timing of re-equilibration processes. Processed EBSD maps show variable textures characterized by coarse grained and deformed olivines, and small rounded undeformed olivines. Clinopyroxene, plagioclase, and minor orthopyroxene are present as interstitial phases. *In situ* major and trace element analyses were performed in selected microstructural sites. To constrain the local conditions driving the formation of these rocks, we performed core-to-rim major and trace element analyses along the [100], [010], and [001] crystallographic axes of olivine. Adjacent clinopyroxene and plagioclase minerals were also analysed. No systematic compositional differences were observed between deformed and undeformed olivines. Cpx_{rim}-ol_{rim} analyses revealed that the two phases are in disequilibrium. Although Ni and Mn in olivine are high (Ni 1915-3537 ppm and Mn 1665-1930 ppm), olivines show low Mg# and Ca (Mg# 82.5-86 and Ca 387-800 ppm), and are relatively enriched in incompatible elements (Sc 5.72-9.03 ppm, Y 0.03-0.15 ppm, Yb 0.02-0.09 ppm). These compositions suggest that olivines were in equilibrium with an evolved MORB derived melt (Mg# 50-56) enriched in incompatible elements compared to the melt that crystallized clinopyroxene (Mg# 67-70). Major and trace elements analyses reveal flat profiles cpx_{rim}-cpx_{rim}-ol_{rim}-ol_{rim} except for Ca and Y, and only in fine grained olivines, indicating incipient subsolidus re-equilibration. We test two end-member scenarios to interpret the inter-mineral disequilibrium observed in olivine-rich troctolites; 1) formation of an Fe-rich olivine-rich cumulate after a MORB-type melt followed by the infiltration of a less evolved melt after which clinopyroxene crystallized upon cooling; 2) infiltration and dissolution of a mantle-derived olivine-rich rock by olivine-undersaturated MORB melt, followed by crystallization of plagioclase and Mg-rich clinopyroxene after the “contaminated” MORB derived melt. The consequences of the two scenarios for the architecture and composition of the oceanic crust (including MORB) at slow spreading ridges are discussed.

Drouin, M., Godard, M., Ildefonse, B., Bruguier, O., Garrido, C.J. (2009): Geochemical and petrographic evidence for magmatic impregnation in the oceanic lithosphere at Atlantis Massif, Mid-Atlantic Ridge (IODP Hole U1309D, 30°N). *Chem. Geol.*, **264**, 71-88.

Drouin, M., Ildefonse, B., Godard, M. (2010): A microstructural imprint of melt impregnation in slow-spread lithosphere: olivine-rich troctolites from the Atlantis Massif (Mid-Atlantic Ridge 30°N, IODP Hole U1309D). *Geochem. Geophys. Geosyst.*, **11**, Q06003.

Godard, M., Awaji, S., Hansen, H., Hellebrand, E., Brunelli, D., Johnson, K., Yamasaki, T., Maeda, J., Abratis, M., Christie, D., Kato, Y., Mariet, C., Rosner, M. (2009): Geochemistry of a long in situ section of intrusive slow spread oceanic lithosphere: Results from IODP Site U1309 (Atlantis Massif, 30°N Mid Atlantic Ridge). *Earth Planet. Sci. Letters*, **279**, 110-122.

OLIVINE-RICH TROCTOLITE ORIGIN THROUGH MELT-ROCK REACTION EXPERIMENTS

Francomme J.E.*[1], Fumagalli P.[1] & Borghini G.[1]
[1] Dipartimento di Scienze della Terra "A. Desio", Università di Milano, Italy
Corresponding email: justine.francomme@unimi.it

Keywords: melt-rock reactions, olivine-rich troctolite, experimental petrology

Melt-rock reaction processes are inferred to play an important role in the origin of olivine-rich troctolite at mantle-crust transition in oceanic spreading lithosphere. We performed reactive dissolution and crystallization experiments at pressure ≤ 0.7 GPa in a piston-cylinder apparatus to provide experimental constraints on textures and mineral chemistry variations of melt-rock reaction products. Experiments are carried out by using salt-Pyrex-graphite-magnesium assemblies and graphite-lined platinum capsules. Experimental charges are prepared with three layers superposed from the bottom up: (1) basalt glass powder, (2) fine powder of San Carlos olivine (Fo90) as dunite analog, and (3) vitreous carbon spheres, used as a melt trap. In order to investigate the effect of melt composition, three synthetic MORB-type glasses have been used, two tholeiitic basalts and a primitive one (X_{Mg} = Mg/(Mg+Fe^{tot}) = 0.62, 0.58 and 0.74 respectively). Experiments have been performed at 0.5 and 0.7 GPa, at temperatures from 1150 to 1300°C, at both step cooling and isothermal conditions for different run durations (12-72 hrs). Step cooling experiments resulted in layered samples in which all the initial San Carlos olivine reacted with the melt generating different lithologies from olivine-gabbro to olivine-rich troctolite (ORT). ORT has a poikilitic texture with rounded, lobate and euhedral olivine and interstitial poikilitic plagioclase and clinopyroxene; these latter showing mutual sharp contacts. Similar textures of resorption and recrystallization are observed in natural samples. Olivine shows significant chemical variations as a function of distance along the experimental sample; it ranges from Fo85 at the olivine-gabbro/ORT transition, i.e. the original melt-dunite interface, to Fo90 in the major part of the ORT layer far away from the original interface. Clinopyroxene shows X_{Mg} ranging from 84 to 90 from olivine-gabbro/ORT interface toward the ORT, plagioclase composition is An75 close to the interface, decrease along the ORT layer reaching An52. Chemical variations are observed also in the melt recognized as trapped phase all along the capsule, and not only within the vitreous carbon spheres at the top of the charge. Melt display an increase of X_{Mg} value from the bottom to the top coupled with a CaO/(CaO+NaO) decrease. In isothermal experiments only olivine and an interstitial melt are present, giving clues on the melt rock interactions that originate troctolites. Furthermore, reacted melts have been successfully trapped in the carbon spheres. They show, as expected, an increased X_{Mg} compared to the starting material (e.g., from X_{Mg} 0.62 to 0.73). Textures and mineral chemistry obtained in the present experiments are discussed in the light of natural occurrences in oceanic and ophiolitic environments.

MELT-PERIDOTITE MULTISTAGE INTERACTION AT MANTLE CONDITIONS: PETROLOGICAL AND GEOCHEMICAL EVIDENCES FROM SAPPHIRINE-APATITE-CALCITE-BEARING GABBROIC DYKES FROM THE FINERO PHLOGOPITE PERIDOTITE (IVREA-VERBANO ZONE)

Giovanardi T.[1], Zanetti A.*[2], Mazzucchelli M.[2-3], Langone A.[2] & Morishita T.[4]
[1] Institute of Geosciences, University of São Paulo, Brazil
[2] Istituto di Geoscienze e Georisorse, Consiglio Nazionale delle Ricerche, Pavia, Italy
[3] Dipartimento di Scienze Chimiche e Geologiche, Università di Modena e Reggio Emilia, Modena, Italy
[4] School of Natural System, College of Science and Engineering, Kanazawa University, Japan
Corresponding email: alberto.zanetti9@virgilio.it

Keywords:

The Finero Phlogopite-Peridotite (FPP) is a mantle unit outcropping in the northernmost part of the Ivrea-Verbano Zone (IVZ, Southern Alps). Multistage pervasive to channelled melt migrations had completely recrystallized the entire FPP. The main metasomatic event pervasively formed an association of amphibole-rich phlogopite harzburgite with subordinated phlogopite-pyroxenites which do not show geochemical gradients (Zanetti et al., 1999). Channelled migrations lately formed dunite bodies, sometimes containing stratiform chromitites and, more rarely, pyroxenite layers similar to those associated to phlogopite harzburgite. Several other lithologies, showing geochemical gradients with rocks of the main FPP association and characterized by the presence of apatite sometimes associated to carbonates (i.e. dolomite and calcite), are subordinated in volumes and abundances. Commonly these lithologies occur as dykes or veins along deformation zones. Geochronological data from apatite-calcite zircon syenites and apatite-dolomite wehrlites provide Triassic ages assumed to document the time of the melt/fluid migrations. Notwithstanding the apparent mineralogical and chemical differences with the main lithologic sequences, apatite-carbonates-bearing rocks have been frequently interpreted as cogenetic to phlogopite harzburgites and related to the main metasomatic event. Recently, apatite-calcite-bearing gabbroic dykes randomly crosscutting the FPP lithologic associations were recognized as possibly the last (or one of the last) melt migration event within the mantle unit (Giovanardi et al., 2013). The dykes show symmetrical internal layering formed by melanocratic bands towards the host peridotite dominated by titanian pargasite and a central leucocratic zone dominated by plagioclase. Magmatic sapphirine occurs in plagues at the contact of the leucocratic zone within the melanocartic bands. New field, petrographic and geochemical studies were conducted to constrain the gabbroic veins intrusion and their genetic relationships with other FPP metasomatic events. Petrographic evidences, major and trace element data and the O isotopic composition of such gabbroic veins indicate that they formed at shallow mantle conditions by multistage fractional crystallisation of a migrating melt unrelated to those forming the harzburgite-pyroxenite association and the dunite bodies. However, local strong enrichments in LILE, LREE and $\delta^{18}O$ in vein minerals confirm that such melt was deeply modified by interaction with the host phlogopite peridotite. However, the amphiboles in textural equilibrium with sapphirine show a marked M-HREE and Y depletion associated to a marked positive Eu anomaly, which support melt evolution through plagioclase assimilation. The genetic relationships with other intrusive events recorded by the FPP and the associated crustal sequence will be addressed with the aim of placing place new constraints on the petrologic and geodynamic evolution of the IVZ.

Giovanardi, T., Morishita, T., Zanetti, A., Mazzucchelli, M., Vannucci, R. (2013): Igneous sapphirine as a product of melt-peridotite interactions in the Finero Phlogopite-Peridotite Massif, Western Italian Alps. *Eur. J. Mineral.*,**25**, 17-31.

Zanetti, A., Mazzucchelli, M., Rivalenti, G., Vannucci, R. (1999): The Finero phlogopite-peridotite massif: an example of subduction-related metasomatism. *Contrib. Mineral. Petrol.*, **134**, 107-122.

REDISTRIBUTION OF TRACE ELEMENTS IN REACTIVE ABYSSAL MANTLE: A LA-ICPMS STUDY OF ODP SITE 1274 PERIDOTITES (15°20 FZ, MID-ATLANTIC RIDGE)

Godard M.*[1], Alard O.[1-2] & Gréau Y.[2]

[1] Géosciences Montpellier, Centre National de la Recherche Scientifique & Université de Montpellier, France

[2] Geochemical Evolution and Metallogeny of Continents, Macquarie University, Sydney, Australia

Corresponding email: marguerite.godard@umontpellier.fr

Keywords: peridotite, melt/rock reactions, geochemistry

Mantle peridotites sampled at ODP Site 1274 (15°20 FZ, Mid-Atlantic Ridge) are highly refractory and are interpreted as recording extensive melt extraction; yet observation of interstitial clinopyroxene and local variations in bulk compositions suggest late melt rock reactions occurred (e.g., Godard et al., 2008). In order to better understand the sequence of melt extraction and percolation processes, we carried out a geochemical study of a series of Site 1274 harzburgites using Laser Ablation HR-ICPMS for trace element analyses. *In situ* trace element composition of olivine (ol), orthopyroxene (opx) and clinopyroxene (cpx) is used to characterize the contribution of each phase to the bulk rock and to discuss to what extent the geochemical signature of peridotites can be modified by late magmatic processes in oceanic environments, in particular for petrogenetic indicators (e.g. REE).

Site 1274 peridotites are characterized by strong downhole modal and geochemical variations at ~ 80-90 mbsf, marked by a higher olivine mode in harzburgites and by an increase of the cpx Na and Ti contents (from < 0.2 to ~ 0.8 wt.% Na_2O and from < 0.1 to 0.25 wt.% TiO_2). Cpx are poor in all trace elements (e.g., Yb = 1.6-2.6 x C1-chondrites), and are preferentially depleted in LREE and MREE except for the 80-90 mbsf area, where cpx is less fractionated. These depleted compositions, amongst the most depleted analyzed until now, are consistent with high degrees of melt extraction. Yet, extended trace element patterns of cpx, opx and ol are characterized by relative enrichments in Cs, Rb, Th, U, Nb and Ta and Pb relative to LREE, suggesting addition of highly incompatible elements by post melting magmatic processes. However, these elements have similar compositions in all phases indicating that their distribution is not controlled by the mineral structure. Comparison to lattice strain models suggests that ol, opx and ol are at equilibrium only for HREE (Dy to Lu). This implies that the melt in equilibrium with these samples can be calculated only for these elements. The observed downhole variations in the less incompatible elements are consistent with an open system partial melting process except at 80-90 mbsf area, where compositions are in equilibrium with melts similar to ultra-depleted MORB melts. The 80-90 mbsf area is interpreted as a melt focusing zone.

Godard, M., Lagabrielle, Y., Alard, O., Harvey, J. (2008): Geochemistry of the highly depleted peridotites drilled at ODP Sites 1272 and 1274 (Fifteen-Twenty Fracture Zone, Mid-Atlantic Ridge): Implications for mantle dynamics beneath a slow spreading ridge. *Earth Planet. Sci. Letters*, **267**, 410-425.

FRACTIONAL CRYSTALLISATION AND Fe-ISOTOPY VARIATION OF BONINITES FROM PAPUA NEW GUINEA

Harak M.*[1], Hezel D.C.[1] & Münker C.[1]
[1] Department für Geowissenschaften, Universität Köln, Germany
Corresponding email: markus.harak@googlemail.com

Keywords: Fe-isotopes, mantle, boninites

Boninites are an extremely depleted endmember of volcanic rocks in subduction zones. In contrast to arc tholeiites that are produced from lherzolitic mantle sources, boninites are melted from refractory harzburgite residues in the presence of subduction fluids penetrating the mantle wedge. The details of boninite petrogenesis are still debated. Iron isotopes can be used as tracers to identify the processes that account for boninite formation, such as partial melting or fractional crystallisation. A number of recent studies demonstrated that partial melting of the mantle is the main process fractionating Fe-isotopes (e.g., Schoenberg & von Blanckenburg, 2006; Weyer & Ionov, 2007; Dauphas et al., 2009). This leads to a δ^{56}Fe of about +0.1 ‰ in MORB-like basalts relative to the IRMM-014 standard that has an Fe-isotope composition undistinguishable from chondrites (Craddock & Dauphas, 2010). As working hypothesis, refractory mantle sources might exhibit light Fe-isotope compositions, and therefore boninites from such sources should be isotopically lighter than arc tholeiites. Fractional crystallisation is an additional process that fractionates Fe-isotopes (e.g., Teng et al., 2008; Schuessler et al., 2007; Weyer & Seitz, 2012). The lighter Fe-isotopes preferentially enter the crystal lattice during olivine crystallisation, thereby producing an isotopically heavier melt during olivine fractionation. Thus, subsequently crystallising pyroxene should be enriched in isotopically heavier Fe.

Iron-isotopes were analysed using the ThermoFinnigan Neptune MC-ICP-MS in the joint Cologne-Bonn facility with ^{53}Cr, ^{54}Fe, ^{56}Fe, ^{57}Fe, ^{58}Fe, ^{63}Cu and ^{65}Cu ion beams measured simultaneously at medium resolution. Each sample analysis was bracketed by measurements of the IRMM-014 standard. Sample concentrations were 1 µg mL^{-1} for bulk samples and 0.5 µg mL^{-1} for mineral samples. The blank-sample ratio was below 10^{-5}. Samples and bracketing standards were doped with 1 µg mL^{-1} Cu (NIST 976) to correct for instrumental mass bias.

We studied bulk and mineral Fe-isotope composition of 12 boninites and bulk compositions of 6 associated tholeiites from the Cape Vogel locality of Papua New Guinea (König et al., 2010). Boninites display a variation in δ^{56}Fe from -0.02±0.05 ‰ (2 sd, n = 3) to +0.11±0.04 ‰ (2 sd, n = 3) with a mean of +0.04±0.03 ‰ (2 sd, n = 36). Associated tholeiites range in their δ^{56}Fe from +0.01±0.04 ‰ (2 sd, n = 3) to +0.12±0.01 ‰ (2 sd, n = 3) with a mean of +0.06±0.03 ‰ (2 sd, n = 18). Hence, boninites indeed have a slightly lighter Fe-isotope composition than tholeiites. Boninitic pyroxenes range in their δ^{56}Fe from -0.07±0.03 ‰ (2 sd, n = 2) to +0.3±0.06 ‰ (2 sd, n = 1) with a mean of +0.12±0.08 ‰ (2 sd, n = 13). Boninite glass ranges in δ^{56}Fe from -0.07±0.02 ‰ (2 sd, n = 3) to +0.27±0.09 ‰ (2 sd, n = 4) with a mean of +0.11±0.06 ‰ (2 sd, n = 23). Thus, pyroxenes and glass have almost identical δ^{56}Fe values. Boninitic olivines vary in δ^{56}Fe from -0.04±0.02 ‰ (2sd, n = 4) to +0.03±0.02 ‰ (2 sd, n = 3) with a mean of -0.01±0.04 ‰ (2 sd, n = 10). Boninitic Cr-spinels vary from -0.39±0.05 ‰ (2 sd, n = 4) to -0.14±0.05 ‰ (2 sd, n = 4) with a mean of -0.24±0.15 ‰ (2 sd, n = 12).

In summary, the lighter Fe-isotope compositions of boninites is reflecting their more depleted mantle sources. The boninites fall in two groups based on their Fe-isotope compositions. The first group shows negative correlation of δ^{56}Fe with Mg#. The second group has an more uniform and overall lower Mg# than the first group and the data shows no correlation of Mg# with δ^{56}Fe. We employed the mineral Fe-isotope compositions in a model to demonstrate that fractional crystallisation of olivine is responsible for the Fe-isotope variation in the first group. The same model can be applied to identify a sequence of combined olivine and pyroxene fractionation to explain the Fe-isotope variation in the second group of boninites.

Craddock, P.R. & Dauphas, N. (2010): Iron isotopic compositions of geological reference materials and chondrites. *Geostand. Geoanal. Res.*, **31**, 101-123.

Dauphas, N., Craddock, P.R., Asimow, P.D., Bennett, V.C., Nutman, A.P., Ohnenstetter, D. (2009): Iron isotopes may reveal the redox conditions of mantle melting from Archean to Present. *Earth Planet. Sci. Letters*, **288**, 255-267.

König, S., Münker, C., Schuth, S., Luguet, A., Hoffmann, J.E., Kuduon, J. (2010): Boninites as a window into trace element mobility in subduction zones. *Geochim. Cosmochim. Acta*, **74**, 684-704.

Schoenberg, R. & von Blankenburg, F. (2006): Modes of planetary-scale Fe isotope fractionation. *Earth Planet. Sci. Letters*, **252**, 342-359.

Schuessler, J.A., Schoenberg, R., Behrens, H., von Blanckenburg, F. (2007): The experimental calibration of the iron isotope fractionation factor between pyrrhotite and peralkaline rhyolitic melt. *Geochim. Cosmochim. Acta*,**71**, 417-433.

Teng, F.-Z., Dauphas, N., Helz, R.T. (2008): Iron isotope fractionation during magmatic differentiation in Kilauea Iki lava lake. *Science*, **320**, 1620-1622.

Weyer, S. & Ionov, D.A. (2007): Partial melting and melt percolation in the mantle: The message from Fe isotopes. *Earth Planet. Sci.Letters*, **259**, 119-133.

Weyer, S. & Seitz, H.-M. (2012): Coupled lithium- and iron isotope fractionation during magmatic differentiation. *Chem. Geol.*, **294-295**, 42-50.

EXSOLUTION OF GARNET AND KYANITE FROM AN ESKOLAITE-BEARING, Al-RICH CLINOPYROXENE IN A RUBY ECLOGITE DURING COOLING IN THE SUBCRATONIC MANTLE (KAAPVAAL-CRATON)

Heckel C.R.*[1], Brey G.P.[1], Hoefer H.E.[1] & Linckens J.[1]
[1] Institut für Geowissenschaften, Goethe-Universität Frankfurt am Main, Germany
Corresponding email: heckchri@web.de

Keywords: exsolution, eclogite, Earth mantle

We have collected a rare ruby eclogite from the Bellsbank diamond mine which is situated about 150 km NE of Kimberley on the Kaapvaal craton. The xenolith is about 4 cm in its largest dimension and consists of about 2 mm sized primary red rubies and up to 3 mm sized colourless garnets set in a matrix of green omphacite with conjugate exsolutions of colourless garnet and blue kyanite lamellae.

When projected onto a 38 mW/m^2 conductive geothermal gradient (Pollack & Chapman, 1977) the Fe-Mg exchange thermometer of Krogh (1988) gives 1050°C and 5 GPa as conditions of last equilibration in the mantle for all combinations of primary and exsolved garnet with omphacite, i.e. the Fe-Mg exchange was continuous until the time of eruption 118 Ma ago. Conversely, the CaO content in the exsolved garnet lamellae is slightly higher than in the coarse primary garnets and the REE contents differ greatly. The primary garnets have LREE depleted patterns with flat middle to heavy REE with about 4x chondritic abundances. The garnet lamellae have negatively inclined middle to heavy REE patterns with Lu abundances around 1x chondritic. The host omphacites have negatively inclined REE patterns with about 5x chondritic La up to Ho with the heavier REE being below detection limit. Host omphacite and garnet lamellae appear in equilibrium. Calculated REE patterns of an unexsolved hypothetical clinopyroxene in equilibrium with the coarse garnet gives about 10x chondritic La and 0.1x chondritic Lu. The bulk rock therefore has very low REE abundances around 1x chondritic and has no Eu anomaly.

Because of the lack of a positive Eu anomaly we postulate that the precursor rock before metamorphism was a cumulate of spinel and Al-rich clinopyroxene at elevated pressures (0.5-0.8 GPa) from a basaltic composition to generate the very Al-rich nature of the bulk rock. This inference is supported by the liquidus phase diagram of Presnall et al. (1978) for tholeiitic compositions. This Al-rich cumulate with small Cr-contents was subducted sometime in the Archean to a depth corresponding to 5 GPa where it crystallized to ruby, garnet and a clinopyroxene with high Ca-Tschermaks (ca. 32 mol%) and eskolaite (ca. 11 mol%) contents. The latter composition was calculated from the modal proportions of phases within the exsolved clinopyroxene. A temperature of about 1300°C is necessary to stabilize such a pyroxene. The subcratonic mantle is cooling since the Mid-Archean with a rate of about 0.1°C/Ma (Shu et al., 2014) and the high temperature clinopyroxene had to exsolve garnet and kyanite.

Krogh, E.J. (1988): The garnet–clinopyroxene-Fe–Mg-geothermometer – A reinterpretation of existing experimental data. *Contrib. Mineral. Petrol.*, **99**, 44-48.

Pollack, H. & Chapman, D. (1977): On the regional variation of heat flow, geotherms, and lithospheric thicknesses. *Tectonophys.*, **38**, 279-296.

Presnall, D.C., Dixon, S.A., Dixon, J.R., O'Donnell, T.H., Brenner, N.L., Schrock, R.L., Dycus, D.W. (1978): Liquidus phase relations on the join diopside-forsterite-anorthite from 1 atm to 20 kbar. Their bearing on the generation and crystallization of basaltic magma. *Contrib. Mineral. Petrol.*, **66**, 203-220.

Shu, Q., Brey, G.P., Gerdes, A., Hoefer, H.E. (2014): Mantle eclogites and garnet pyroxenites – the meaning of two-point isochrons, Sm–Nd and Lu–Hf closure temperatures and the cooling of the subcratonic mantle. *Earth Planet. Sci. Letters*, **389**, 143-154.

THE DETERMINATION OF THE OXIDATION STATE OF Fe IN CLINOPYROXENE MEGACRYSTS WITH THE "FLANK METHOD" BY EPMA: IS THE CRYSTALLOGRAPHIC ORIENTATION IMPORTANT?

Hoefer H.E.*[1], Brey G.P.[1] & Linckens J.[1]
[1] Institut für Geowissenschaften, Goethe-Universität Frankfurt am Main, Germany
Corresponding email: hoefer@em.uni-frankfurt.de

Keywords: Fe speciation, cpx, flank method

A number of methods for the *in situ* determination of the oxidation state of Fe in Earth materials with high spatial resolution has been developed over the past years like XANES, EELS and the "flank method". The "flank-method" by electron microprobe (EPMA) is based on the concomitant change of the intensity and of the wave length of the iron Fe*L*α and *L*β emission lines with the iron oxidation state and is well calibrated for garnets (Höfer & Brey, 2007). Our aim is to extend the method to clinopyroxenes.

For the extension from a cubic (garnet) to a monoclinic mineral (cpx), orientation effects may have to be considered. Such effects are known to occur in synchrotron-based *K*-edge XANES spectroscopy (Berry et al., 2010). XANES is well suited to determine the oxidation state of Fe in garnets (Yaxley et al., 2012). Its applicability is, however, hampered substantially for anisotropic minerals because of the dependency of the spectra on the crystallographic orientation (Berry et al., 2010). This is mainly due to the strongly polarized X-ray beam at the synchrotron. To test for an orientation dependency of the EPMA-based flank method, we analysed pieces from chemically homogenous cpx grains whose orientations were determined beforehand by EBSD.

We focussed on a homogenous cpx megacryst from an alkali basalt in the Biu Plateau, Nigeria (Rankenburg et al., 2004). The sample contains 5.7 wt.% total Fe with $Fe^{3+}/\Sigma Fe = 0.18$ as determined by Mössbauer spectroscopy. Randomly broken pieces from this megacryst were embedded in epoxy, polished, and their orientations determined by EBSD. Those pieces were selected for the flank method measurements whose orientation was such that prominent crystallographic directions follow the direction of the Fe*L*α and *L*β X-ray emission from its source in the sample to the analysing spectrometer crystal. The directions chosen are [100], [001] and perpendicular to (010) to get the highest probability of interaction parallel and perpendicular to the SiO_4 chains in the pyroxene crystal structure. The result of flank method measurements in these directions is that there is no significant difference in the *L*α/*L*β ratios within the analytical errors.

These results make us confident to proceed the investigation of the oxidation state of cpx with the flank method. At present our error for the determination of $Fe^{3+}/\Sigma Fe$ in cpx is significantly higher than in garnets (0.05 *vs.* 0.02). We now aim to optimize the results by processing the cpx data by multiple linear regression which appears to be the more suitable approach for the larger range of $Fe^{3+}/\Sigma Fe$ in our natural cpx, varying from 0.14 to 0.50.

Berry, A.J., Yaxley, G.M., Woodland, A.B., Foran, G.J. (2010): A XANES calibration for determining the oxidation state of iron in mantle garnet. *Chem. Geol.*, **278**, 31-37.

Höfer, H.E. & Brey, G.P. (2007): The iron oxidation state of garnet by electron microprobe: Its determination with the flank method combined with major-element analysis. *Am. Mineral.*, **92**, 873-885.

Rankenburg, K., Lassiter, J.C., Brey, G. (2004): Origin of megacrysts in volcanic rocks of the Cameroon volcanic chain – constraints on magma genesis and crustal contamination. *Contrib. Mineral. Petrol.*, **147**, 129-144.

Yaxley, G.M., Berry, A.J., Kamenetsky, V.S., Woodland, A.B., Golgovin, A. (2012): An oxygen fugacity profile through the Siberian Craton – Fe *K*-edge XANES determinations of $Fe^{3+}/\Sigma Fe$ in garnets in peridotite xenoliths from the Udachnaya East kimberlite. *Lithos*, **140-141**, 142-151.

ORTHOPYROXENE IN PRIMITIVE LAYERED GABBROS FROM HESS DEEP (EPR): FORMATION BY MANTLE/MELT INTERACTION OR FRACTIONAL CRYSTALLIZATION?

Koepke J.*[1], Zhang C.[1], Namur O.[1], Meyer R.[2] & Feig S.T.[3]
[1] Institut für Mineralogie, Leibniz Universität Hannover, Germany
[2] Oberflächennahe Geochemie, Helmholtz Zentrum Potsdam, GFZ Deutsches GeoForschungsZentrum, Potsdam, Germany
[3] Central Science Laboratory, University of Tasmania, Hobart, Australia
Corresponding email: koepke@mineralogie.uni-hannover.de

Keywords: accretion of oceanic crust, layered gabbro, stability of orthopyroxene

IODP (International Ocean Discovery Program) Expedition 345 drilled, for the first time in the history of IODP, coherent cores of layered gabbros from a fast-spreading ridge at the Hess Deep Rift in the equatorial Pacific at the East Pacific Rise (EPR). Most of the drilled cores show spectacular modal and/or grain size layering, validating for the first time the use of the Penrose model based on ophiolites for interpreting fast-spreading crust. Typical rocks of the drilled cores are primitive olivine gabbros and troctolites with Mg# varying between 75 and 89. A significant observation from this expedition is that orthopyroxene was found as an abundant cumulus phase in many of the layered primitive olivine gabbroic rocks. This was unexpected, since experiments on the liquid line of descent of MORB show that orthopyroxene always crystallizes late in the sequence of MORB-type systems, in a regime where the melt fraction is low, implying interstitial crystallization. In an ongoing project based on the investigation of natural samples drilled at Hess Deep we aim to find out what is the reason why orthopyroxene was stabilized within these primitive gabbros. Especially we focus on a model of Coogan et al. (2002), that orthopyroxene was stabilized due to interaction between MORB melts and mantle rocks.

With EPMA we analyzed more than 30 gabbros with coexisting clino- and orthopyroxene, plus about 20 olivine gabbros and troctolites without orthopyroxene. In addition we analyzed 15 orthopyroxene-bearing more evolved olivine gabbros and gabbronorites from the uppermost part of the plutonic EPR crust regarded as frozen melt. The Mg#'s of coexisting ortho- and clinopyroxenes from primitive gabbroic rocks from Hess Deep vary within a narrow range between 82-90 (clinopyroxene) and 80-86 (orthopyroxene). A good correlation between the Mg#'s of orthopyroxene and clinopyroxene implies a common evolution by co-crystallization/fractionation. Many of the analyses of orthopyroxene show Cr_2O_3 contents ≤ 0.1 wt.%, indicating that these orthopyroxenes do not correspond to relics which survived from a melt in equilibrium with mantle. First results on trace element analysis of ortho-, clinopyroxene, and plagioclase in primitive olivine gabbros and also in more evolved gabbronorites from the top of the plutonic section reveal chondrite-normalized REE patterns which are very similar for the corresponding minerals. The patterns of the gabbronorite phases are always slightly enriched, compared to those of the primitive gabbros from the base of the crust, implying an origin by fractional crystallization from the same parental melt.

Coogan, L.A., Gillis, K.M., MacLeod, C.J., Thompson, G.M., Hekinian, R. (2002): Petrology and geochemistry of the lower ocean crust formed at the East Pacific Rise and exposed at Hess Deep: A synthesis and new results. *Geochem. Geophys. Geosyst.*, **3**, DOI: 10.1029/2001GC000230.

EVIDENCE OF CARBONATITE METASOMATISM IN LITHOSPHERIC MANTLE BENEATH THE HELDBURG DIKE SWARM (HELDBURGER GANGSCHAR, CENTRAL GERMANY) SUBSET OF CENTRAL EUROPEAN VOLCANIC PROVINCE

Kukuła A.*[1], Puziewicz J.[1], Matusiak-Małek M.[1], Ntaflos T.[2] & Milke R.[3]
[1] Institute of Geological Sciences, University of Wrocław, Poland
[2] Department für Lithosphärenforschung, Universität Wien, Austria
[3] Institut für Geologische Wissenschaften, Freie Universität Berlin, Germany
Corresponding email: anna.kukula@ing.uni.wroc.pl

Keywords: lithospheric mantle, oceanic provenance, Central Europe

The Heldburg Dike Swarm (Heldburger Gangschar) at the border between Bavaria and Thuringia in Germany is one of the subsets of the Central European Volcanic Province. Some of the lavas contain the xenoliths of peridotites of subcontinental lithospheric mantle. We studied xenoliths coming from Feldstein (Thuringia) columnar outcrop, located ca. 38 km north-east of Coburg and Bramberg (Bavaria) volcanic cone, situated 30 km south-west of Coburg. The distance between them is ca. 40 km. Our study is based on 11 xenoliths from Feldstein and 7 xenoliths from Bramberg.

Three groups (A, A- and B) of spinel peridotite (mostly lherzolite) characterized by different olivine composition occur in study localities. Group A consists of olivine (89.6-91.4 Fo), orthopyroxene (Mg# 0.90-0.93, Al 0.05-0.18 a pfu), clinopyroxene (Mg# 0.87-0.95, Al 0.06-0.26 a pfu) and spinel (Cr# 0.13-0.47, Mg# 0.54-0.78). Rare earth elements (REE) patterns of clinopyroxene are S-shaped and exhibit enrichment in light REE. Clinopyroxene in some of the xenoliths has spoon-shape REE patterns. Trace element patterns show negative Nb, Ta, Zr, Hf, Ti and positive Th, U anomalies. The most magnesian clinopyroxene (xenolith 3140, Feldstein) is strongly alumina and LREE depleted; it does not show anomalies in clinopyroxene TE patterns. Group A- consists of olivine (88.9-89.5 Fo), orthopyroxene (Mg# 0.89-0.90, Al 0.10-0.13 a pfu) and clinopyroxene (Mg# 0.90-0.92, Al 0.10-0.17 a pfu). Clinopyroxene is enriched in LREE. TE patterns are similar to those of group A but anomalies are less pronounced. Group B consists of olivine (86.7-88.2 Fo), orthopyroxene (Mg# 0.88-0.89, Al 0.07-0.14 a pfu), clinopyroxene (Mg# 0.88-0.90, Al 0.10-0.26 a pfu). Clinopyroxene is enriched in LREE and TE patterns are similar to those in group A. Group B harzburgite contains Ca-Mg carbonates (up to 0.5 mm grains, located in interstices or in intergranular aggregates).

The temperatures of opx-cpx equilibration (Brey & Köhler, 1990) in single sample vary in a narrow range, but in the whole suite they are variable: 850-940 ºC for group A and 940-1010 ºC for group A-.

Orthopyroxene composition suggest 12-30% of partial melting (Upton et al., 2011) followed by carbonatite metasomatism. The gradual enrichment in LREE content with increase of mg# in clinopyroxene might suggest chromatographic fractionation of metasomatic agent. The xenolith 3140 seems not to be affected by metasomatic overprint.

Acknowledgements: This study was possible thanks to the project NCN UMO-2014/15/B/ST10/00095 of Polish National Centre for Science to JP.

Brey, G.P. & Köhler, T. (1990): Geothermobarometry in four-phase lherzolites II. New thermobarometers and practical assessment of existing thermobarometers. *J. Petrol*., **31**, 1353-1378.

Upton, B.G.J., Downes, H., Kirstein, L.A., Bonadiman, C., Hill, P.G., Ntaflos, T. (2011): The lithospheric mantle and lower crust-mantle relationships under Scotland: a xenolithic perspective*. J. Geol. Soc.*, **168**, 873-886.

GEOCHEMICAL EVOLUTION OF THE UPPER MANTLE BENEATH THE NÓGRÁD-GÖMÖR VOLCANIC FIELD (N-HUNGARY – S-SLOVAKIA) AS RECONSTRUCTED FROM SPINEL PERIDOTITE XENOLITHS

Liptai N.*[1-2], Patkó L.[1], Kovács I.[3], Hidas K.[4], O'Reilly S.Y.[2], Griffin W.L.[2], Pearson N.J.[2] & Szabó C.[1]

[1] Lithosphere Fluid Research Lab, Eötvös Loránd University, Budapest, Hungary

[2] Centre of Excellence for Core to Crust Fluid Systems and National Key Centre for Geochemical Evolution and Metallogeny of Continents, Department of Earth and Planetary Sciences, Macquarie University, Sydney, Australia

[3] Hungarian Geological and Geophysical Institute, Budapest, Hungary

[4] Instituto Andaluz de Ciencias de la Tierra, Consejo Superior de Investigaciones Científicas & Universidad de Granada, Armilla, Spain

Corresponding email: n.liptai.elte@gmail.com

Keywords: lithospheric mantle, metasomatism, xenolith

The Nógrád-Gömör Volcanic Field (NGVF) is located on the northern part of the Pannonian Basin. Upper mantle xenoliths are hosted in Plio-Pleistocene alkali basalts aged 7.0-1.7 Ma (Hurai et al., 2013). The xenolith bearing part of the volcanic field can be divided into three major domains based on the age and location of the basalts (northern, central and southern parts). This study presents geochemical properties and reconstructs processes of the discussed mantle domains.

Based on petrographic examinations, a lherzolitic and a wehrlitic series was distinguished, the latter being present only in the central part of the NGVF. The lherzolitic series contains modal amount of orthopyroxene, whereas the wehrlitic one consists of olivine- and clinopyroxene-rich aggregates and has no modal orthopyroxene. Xenoliths from the lherzolitic series were analysed for major and trace elements, and evidence for different metasomatic events (which overprint a varying degree of melt extraction in the upper mantle) have been found. These events include modal metasomatism indicated by amphibole in samples from the northern and southern part, as well as amphibole and secondary clinopyroxene in the central part. Furthermore, uncorrelated to modal composition, LREE-enrichment is shown in some of the xenoliths from all three regions, and Fe-Mn-Ti- and LREE-enrichment is present in a group of xenoliths from the central part only. This latter group is geochemically identical to xenoliths of the wehrlite series, and therefore interpreted to be linked to the same process that produced the wehrlites by forming clinopyroxenes at the expense of orthopyroxenes (Patkó et al., 2013).

It is assumed that another cryptic metasomatic event affected the xenoliths before the formation of wehrlites, resulting in varying degrees of LREE-enrichment throughout the whole NGVF. Amphibole formation likely predates this process, since REE-patterns of amphiboles follow closely those of coexisting clinopyroxenes. All of these metasomatic events are proposed to result from reaction between the peridotite wallrock and silicate melts of slightly different compositions, but similar in character to the host basalt. These melts are presumed to have generated during the Miocene extension and asthenospheric uplift in the Pannonian Basin.

Hurai, V., Danišík, M., Huraiová, M., Paquette, J.-L., Ádám, A. (2013): Combined U/Pb and (U-Th)/He geochronometry of basalt maars in Western Carpathians: implications for age of intraplate volcanism and origin of zircon metasomatism. *Contrib. Mineral. Petrol.*, **166**, 1235-1251.

Patkó, L., Aradi, L.E., Liptai, N., Bodnar, R.J., Fedele, L., Kovács, Z., Cesare, B., Vaselli, O., Fioretti, A.M., Jeffries, T., Szabó, C. (2013): Wehrlitization process within the upper mantle beneath the Northern Pannonian Basin. *Mineral. Mag.*, **77**, 1934.

PETROLOGICAL EVOLUTION OF NORTHERN VICTORIA LAND LITHOSPHERE: NEW INSIGHTS FROM HARROW PEAKS MANTLE XENOLITH

Pelorosso B.*[1], Bonadiman C.[1], Coltorti M.[1] & Gentili S.[2]
[1] Dipartimento di Fisica e Scienze della Terra, Università di Ferrara, Italy
[2] Dipartimento di Fisica e Geologia, Università di Perugia, Italy
Corresponding email: plrbrc@unife.it

Keywords: mantle xenoliths, metasomatism

A petrological study of hydrous and anhydrous mantle xenoliths from Harrow Peaks, Northern Victoria Land (Antarctica) has been carried out, aiming at mapping the evolution of this lithospheric mantle domain with respect to the presence of amphibole.

Samples vary in composition from lherzolite to harzburgite with textural evidences of matrix/melt interaction (secondary minerals and spongy textures). Olivine and orthopyroxene are mainly present as large primary grains, whereas clinopyroxene can also occur as resorbed grains or newly formed small crystals, often associated to glassy patches. Spinel is present as small anhedral crystals or larger, dendritic grains. Amphiboles occur both as disseminated and in veins; the latter frequently associated with secondary clinopyroxenes.

Considering fusible element content in orthopyroxene (i.e., Al_2O_3 in opx ~ 2.50 wt.%), Harrow Peaks lithosphere domain reflects a relatively residual character. On the other hand, Light Rare Earth Element content in clinopyroxenes (La_N from 9 to 30) evidences that they were strongly affected by enrichment processes, i.e. metasomatism.

Amphiboles from Harrow Peaks can be classified as kaersutite, magnesio-hastingsite, and ferri-kaersutite with pretty high TiO_2 contents, ranging from 2.74 wt.% to 5.30 wt.% (Gentili et al., 2015).

The comparison between Harrow Peaks and the nearby amphibole-bearing xenolith area of Baker Rocks (Coltorti et al., 2004; Bonadiman et al., 2014), allowed to reconstruct the amphibole genesis in relation to the metasomatic processes. Harrow Peaks amphibole present a lower enrichment with respect to Baker Rocks, that may be related to an incipient stage of peridotite/melt interaction.

Considering the inter mineral equilibria among the main peridotitic phases, thermobarometric estimates were constrained. Temperature values range from 800 to 1100°C at relatively reduced conditions ($\Delta \log fO_2$ (QFM) -2.78 to -0.24). The fugacity values calculated by the anhydrous parageneses strongly deviated from those obtained on the basis of amphibole dehydration equilibrium applying the dissociation reaction that record extremely oxidizing conditions (ΔQFM = +5; + 6.8; Gentili et al., 2015). This decoupling is not observed for Baker Rocks amphibole –bearing peridotites, where both methods converge to the values of ΔQFM ~ -1.78 (Bonadiman et al., 2014). This may suggest that amphibole in Harrow Peaks is in strong disequilibrium with the anhydrous parageneses recording an early stage of peridotite-metasomatic melt interaction.

Bonadiman, C., Nazzareni, S., Coltorti, M., Comodi, P., Giuli, G., Faccini, B. (2014): Crystal chemistry of amphiboles: implications for oxygen fugacity and water activity in lithospheric mantle beneath Victoria Land, Antarctica. *Contrib. Mineral. Petrol.*, **167**, 1-17.

Coltorti, M., Beccaluva, L., Bonadiman, C., Faccini, B., Ntaflos, T., Siena, F. (2004): Amphibole genesis via metasomatic reaction with clinopyroxene in mantle xenoliths from Victoria Land, Antarctica. *Lithos*, **75**, 115-139.

Gentili, S., Bonadiman, C., Biagioni, C., Comodi, P., Coltorti, M., Zucchini, A., Ottolini, L. (2015): Oxo-amphiboles in mantle xenoliths: evidence for H_2O–rich melt interacting with the lithospheric mantle of Harrow Peaks (Northern Victoria Land, Antarctica). *Mineral. Petrol.*, **109**, 741-759.

SILVER AND COPPER FRACTIONATION IN MORB

Portnyagin M.*[1-2], Sushchevskaya N.[2], Shishkina T.[2], Kamenetsky V.[3], Taylor R.N.[4] & Garbe-Schönberg D.[5]
[1] GEOMAR - Helmholtz-Zentrum für Ozeanforschung, Christian-Albrechts-Universität Kiel, Germany
[2] V.I.Vernadsky Institute of Geochemistry and Analytical Chemistry, Russian Academy of Sciences, Moscow, Russia
[3] School of Physical Sciences, University of Tasmania, Hobart, Australia
[4] Ocean and Earth Science, University of Southampton, United Kingdom
[5] Institut für Geowissenschaften, Christian-Albrechts-Universität Kiel, Germany
Corresponding email: mportnyagin@geomar.de

Keywords: MORB, sulfide, melting

Ag and Cu are strongly chalcophile elements, and their behavior in magmatic systems is highly dependent on the presence of solid or liquid sulfide phase in magmas and their sources (e.g., Li & Audetat, 2012). A recent study of Jenner & O'Neill (2010) revealed a nearly uniform 1000Ag/Cu = 0.28 ± 0.04 (2s, N = 338) in MORB glasses, similar to that in the Earth mantle (0.25-0.35; McDonough & Sun, 1995; Wang & Becker, 2015). Because Cu and Ag have very high and similar in magnitude partition coefficients between sulfide and silicate liquids (~1000; e.g., Patten et al., 2013; Li & Audetat, 2012), the constancy of Ag/Cu in MORB has been explained by a major control of sulfide liquid on the partitioning of these elements in MORB magmas during mantle melting and low-pressure fractionation (Jenner & O'Neill, 2010; Li & Audetat, 2012).

Here we report results of a new survey of Cu and Ag abundances in MORB from several active and abandoned ridge segments (e.g., Reykjanes Ridge, 15°20'N, Bouvet triple junction and TAG area in Atlantic, Macquarie Island, EPR and paleo Kula-Pacific Rift in Pacific). All samples were relatively primitive basaltic glasses with Mg# = 0.4-0.7 of N- and E-MORB types. The analyses were performed in the Institute of Geosciences at the University of Kiel by LA-ICP-MS (Agilent 7500s, 193 nm GEOLAS Pro). A thoroughly elaborated protocol for analysis allowed limit of detection below 1 ppb for Ag and long-term reproducibility within 15%.

The measured contents are 52-139 ppm Cu and 0.016-0.037 ppm Ag in N-MORB, and 35-151 ppm Cu and 0.015-0.046 ppm Ag in E-MORB. The concentrations decrease with decreasing Mg#. The highest Cu and Ag at given Mg# were found in Reykjanes Ridge glasses. Despite of the relatively wide range of concentrations, N-MORB have nearly constant 1000Ag/Cu = 0.32±0.02 (2s, N = 50), which are similar to those reported by Jenner & O'Neill (2010). E-MORB glasses have 1000Ag/Cu ranging from 0.29 to 0.61, on average 0.40±0.07 (2s, N = 43), which is significantly higher than in N-MORB. A strong positive correlation was found between Ag/Cu and indices of source enrichment in highly incompatible elements (K/Ti, La/Sm etc.).

Because Ag/Cu ratio in basalts is not easy to fractionate, we propose that the elevated Ag/Cu in E-MORB reflect the composition of their mantle source metasomatised by a melt component enriched in highly incompatible elements and Ag. The origin of such component is uncertain but may be related to small-degree low-temperature hydrous mantle melting in the presence of solid sulfide (monosulfide solid solution, mss). Because Ag is much less compatible in mss compared to Cu (e.g., Li & Audetat, 2012), such melts are expected to be enriched in Ag and have high Ag/Cu as observed in E-MORB.

Jenner, F.E. & O'Neill, H.S.C. (2012): Analysis of 60 elements in 616 ocean floor basaltic glasses. *Geochem. Geophys. Geosyst.*, **13**, Q02005.

Li, Y. & Audetat, A. (2012): Partitioning of V, Mn, Co, Ni, Cu, Zn, As, Mo, Ag, Sn, Sb, W, Au, Pb, and Bi between sulfide phases and hydrous basanite melt at upper mantle conditions. *Earth Planet. Sci. Letters*, **355**, 327-340.

McDonough, W.F. & Sun, S.S. (1995): The composition of the Earth. *Chem. Geol.*, **120**, 223-253.

Patten, C., Barnes, S.-J., Mathez, E.A., Jenner, F.E. (2013): Partition coefficients of chalcophile elements between sulfide and silicate melts and the early crystallization history of sulfide liquid: LA-ICP-MS analysis of MORB sulfide droplets. *Chem. Geol*., **358**, 170-188.

Wang, Z. & Becker, H. (2015): Abundances of Ag and Cu in mantle peridotites and the implications for the behavior of chalcophile elements in the mantle. *Geochim. Cosmochim. Acta*, **160**, 209-226.

MANTLE ROOTS OF NE PART OF THE VARISCAN OROGEN IN EUROPE: PROTOLITH PROVENANCE AND METASOMATIC STYLES

Puziewicz J.*[1], Matusiak-Małek M.[1], Ntaflos T.[2], Kukuła A.[1] & Ćwiek M.[1]
[1] Institute of Geological Sciences, University of Wrocław, Poland
[2] Department für Lithosphärenforschung, Universität Wien, Austria
Corresponding email: jacek.puziewicz@uwr.edu.pl

Keywords: lithospheric mantle, oceanic provenance, Central Europe

The subcontinental lithospheric mantle (SCLM) beneath Lower Silesia (SW Poland) and neighboring part of Upper Lusatia (SE Germany) is dominated by harzburgites (Puziewicz et al., 2015, and references therein). Clinopyroxene which occurs in these rocks, despite its primary textural appearance, is a late addition to the protoliths which are residues after extensive (up to 30%) partial melting. This clinopyroxene was added to the harzburgites in Cenozoic times by alkaline basaltic melts migrating upwards from their asthenospheric sources during rifting in the Variscan foreland of the Alpine-Carpathian chain. The pre-rifting history of the SCLM beneath the region is thus recorded in the olivine and orthopyroxene.

The forsterite content in olivine divides the Lower Silesian harzburgites into two groups: A (olivine Fo 90.5-92.0), and B (olivine Fo 84.0-90.0; Puziewicz et al., 2015). The Al content in orthopyroxene is low in A harzburgites (typically 0.05-0.10 atoms of Al per formula unit, corresponding to 0.5-2.5 wt.% Al_2O_3). Part of the B harzburgites (termed B1 in the following) contains orthopyroxene of similar Al content, whereas another part (B2 harzburgites) exhibits negative correlation between the Al content in orthopyroxene and forsterite content in olivine (up to 0.24 atoms of Al pfu, corresponding to ca. 5.7 wt.% Al_2O_3 in orthopyroxene coexisting with olivine Fo 86.5). The Al content in the B1 orthopyroxene is not correlated with forsterite content in coexisting olivine.

The low Al content in orthopyroxene, corresponding to that typical for the Lower Silesian European mantle domain, is characteristic for (1) oceanic mantle formed in the mid ocean ridges (MOR), and (2) mantle wedge affected by extreme melting in the supra-subduction zones (SSZ). The orthopyroxene from SSZ harzburgites contains usually less Al (< 2.0 wt.% Al_2O_3) than that of the MOR ones (2.0-6. 0 wt.% Al_2O_3; Bonatti & Michael, 1989). Thus, we infer that the Lower Silesian SCLM originated rather in the MOR setting.

The B harzburgites were formed by reactive basaltic melt percolation, which lowered the forsterite content in olivine and Mg# in orthopyroxene ("Fe metasomatism"). The B1 harzburgites contain orthopyroxene which is Al poor irrespectively of forsterite content of coexisting olivine. We suggest that they originated due to percolation of tholeiitic basaltic melts which originate by multiple polybaric mantle melting in MOR environment. Their percolation in oceanic mantle leads to production of low-Al orthopyroxene (e.g., in the peridotites from East Pacific Rise, Dick & Natland, 1996). Textural relationships show that the Al-enriched B2 harzburgites were also affected by "Fe metasomatism", but by alkaline basaltic melt percolating in SCLM during Cenozoic rifting.

Acknowledgements: This study was possible thanks to the project NCN UMO-2014/15/B/ST10/00095 of Polish National Centre for Science to JP.

Bonatti, M. & Michael, P. J. (1989): Mantle peridotites from continental rifts to ocean basins to subduction zones. *Earth Planet. Sci. Letters*, **91**, 297-311.

Dick, H.J.B. & Natland, J.H. (1996): Late-stage melt evolution and transport in the shallow mantle beneath the east Pacific Rise. *in* "Proceedings of the Ocean Drilling Program, Scientific Results", C. Mével, K.M. Gillis, J.F. Allan & P.S. Meyer, eds., **147**, 103-134.

Puziewicz, J., Matusiak-Małek, M., Ntaflos, T., Grégoire, M., Kukuła, A. (2015): Subcontinental lithospheric mantle beneath Central Europe. *Int. J. Earth Sci.*, **104**, 1913-1924.

MELT MIGRATION AND MELT-ROCK REACTION IN THE ALPINE-APENNINE PERIDOTITES: INSIGHTS ON MANTLE DYNAMICS IN EXTENDING LITHOSPHERE

Rampone E.*[1]

[1] Dipartimento di Scienze della Terra, dell'Ambiente e della Vita, Università di Genova, Italy

Corresponding email: betta@dipteris.unige.it

Keywords: mantle peridotites, melt-rock reaction, Alpine-Apennine ophiolites

Studies on ophiolitic and abyssal peridotites have provided evidence that the compositional variability of the lithospheric mantle at extensional settings is largely caused by the reactive percolation of uprising melts in the thermal boundary layer and in lithospheric environments. The Alpine-Apennine (A-A) ophiolites are predominantly constituted by mantle peridotites, and are widely thought to represent analogs of the oceanic lithosphere formed at ocean/continent transition and slow- to ultra-slow spreading settings (e.g., Rampone & Piccardo, 2000; Manatschal & Muentener, 2009). Structural and geochemical studies on the A-A mantle peridotites have revealed that they preserve significant small- versus large-scale textural, compositional and isotopic heterogeneity reflecting a long-lived multi-stage evolution, testified by: (i) records of old pre-Jurassic events (e.g., pyroxenite emplacement); (ii) metamorphic and deformation events related to tectonic exhumation, localized in extensional shear zones; (iii) multiple melt-rock interaction and intrusion events occurred at different lithospheric depths during progressive uplift. The A-A mantle peridotites thus constitute a unique window on mantle dynamics and lithosphere-asthenosphere interactions in very slow spreading environments. This work aims to review field, microstructural and chemical-isotopic evidence on the major stages of melt percolation and melt-rock interaction recorded by the A-A peridotites, and discuss their consequences in creating chemical-isotopic heterogeneities at variable scales, and enhancing weakening and deformation of the extending mantle. Focus will be on three most important stages: i) old (pre-Jurassic) pyroxenite emplacement, and the significant isotopic modification induced in the host mantle by pyroxenite-derived melts, thus addressing the issue of small-scale isotopic mantle heterogenity caused by pyroxenite components (Rampone & Hofmann, 2012; Borghini et al., 2013), ii) melt-peridotite interactions during Jurassic mantle exhumation, i.e. the open-system reactive porous flow at spinel facies depths causing bulk depletion (origin of reactive harzburgites and dunites), and the shallower melt impregnation which originated plagioclase-rich peridotites and an overall mantle refertilization. This latter stage had a key role in the deformation and weakening of the extending lithosphere (e.g., Kaczmarek & Muentener, 2010). Impregnating melts originating the plagioclase-rich peridotites were Silica-rich (opx-saturated), highly depleted melts, similar to what documented in abyssal peridotites (e.g., Laukert et al., 2014). The origin of such depleted signature and the primitive Si-rich composition, either acquired by reaction with depleted peridotite or reflecting a primary feature (e.g., non aggregated melt fractions, or melting of hydrous depleted peridotites) are still open questions.

Borghini, G., Rampone, E., Zanetti, A., Class, C., Cipriani, A., Hofmann, A.W., Goldstein, S.L. (2013): Meter-scale Nd isotopic heterogeneity in pyroxenite-bearing Ligurian peridotites encompasses global-scale upper mantle variability. *Geology*, **41**, 1055-1058.

Kaczmarek, M.A. & Muentener, O. (2010): The variability of peridotite composition across a mantle shear zone (Lanzo massif, Italy): interplay of melt focusing and deformation. *Contrib. Mineral. Petrol.*, **160**, 663-679.

Laukert, G., Von der Handt, A., Hellebrand, E., Snow, J., Hoppe, P., Klu, A. (2014). High-pressure reactive melt stagnation recorded in abyssal pyroxenites from the Ultraslow-spreading LenaTrough, Arctic Ocean. *J. Petrol.*, **55**, 427-458.

Manatschal, G. & Muentener, O. (2009): A type sequence across an ancient magma-poor ocean-continent transition: the example of the western Alpine Tethys ophiolites. *Tectonophys*., **473**, 4-19.

Rampone, E. & Hofmann, A.W. (2012): A global overview of isotopic heterogeneities in the oceanic mantle. *Lithos*, **148**, 247-261.

Rampone, E. & Piccardo, G.B. (2000): The ophiolite-oceanic lithosphere analogue : new insights from the Northern Apennines (Italy). *in* "Ophiolites and oceanic crust: New insights from field studies and the Oceanic Drilling Program" Y. Dilek, E.M. Moores, D. Elthon, A. Nicolas, eds., *Geol. Soc. Am. Spec. Pap.*, **349**, 21-34.

NEW PERSPECTIVES ON THE ORIGIN OF OLIVINE-RICH TROCTOLITES AND ASSOCIATED HARRISITES FROM THE LIGURIAN OPHIOLITES (ITALY)

Renna M.R.*[1], Tribuzio R.[2-3] & Ottolini L.[3]

[1] Dipartimento di Scienze Matematiche e Informatiche, Scienze Fisiche e Scienze della Terra, Università di Messina, Italy

[2] Dipartimento di Scienze della Terra e dell'Ambiente, Università di Pavia, Italy

[3] Istituto di Geoscienze e Georisorse, Consiglio Nazionale delle Ricerche, Pavia, Italy

Corresponding email: mrenna@unime.it

Keywords: Alpine Jurassic ophiolites, spinel-hosted amphibole, harrisite

The MOR-type gabbroic sequences from the Internal Ligurian ophiolites include up to tens of meters thick olivine-rich troctolite lenses. For one of the olivine-rich troctolite lenses, a meter-scale thick portion characterized by skeletal to dendritic olivines (harrisites) was observed near the contact with host gabbros. Spinels from the olivine-rich troctolites locally include hydrous silicate minerals, namely amphibole (titanian pargasite to kaersutite) frequently associated with dark mica (phlogopite to Na-phlogopite). Spinel-hosted amphibole displays chondrite-normalized REE patterns characterized by negative Eu anomaly, thereby recording a magmatic process associated with plagioclase fractionation. The amphiboles also show variable depletion of LREE relative to MREE, and HREE that are weakly enriched to depleted with respect to MREE. Crystallization of the inclusion-bearing spinels is attributed to cooling of hybrid melts originated by interaction between primitive melts and gabbro-related melts relatively rich in SiO_2 and incompatible elements. The olivine-rich troctolite lenses may thus have an entire crustal origin, in response to primitive melt injections into the growing lower crust.

Clinopyroxene and amphibole from the harrisites show extensive variability for trace element compositions, albeit characterized by subparallel incompatible element patterns. For instance, the concentrations of REE vary by a factor of ~5 and ~6 for clinopyroxene and amphibole, respectively. The REE patterns of both clinopyroxene and amphibole show LREE depletion with respect to MREE and nearly flat to slightly depleted HREE. In addition, clinopyroxene and amphibole have negative Eu-Sr anomalies deepening with increasing concentrations of trivalent REE and other incompatible trace elements. The chemical variability of clinopyroxene and amphibole from the harrisites are consistent with their rapid crystal growth related to melt undercooling, in association with olivine and plagioclase. Similarly to associated olivine-rich troctolites, the harrisites are hybrid rocks that did not form by closed-system crystallization of a primitive melt batch. We attribute the melt undercooling responsible for harrisite formation to physical and chemical interaction of a primitive melt batch with a host material made up of gabbroic crystal mush.

MANTLE MELTING, MELT EXTRACTION AND AGGREGATION BENEATH MID OCEAN RIDGES: CLUES FROM OLIVINE IN REPLACIVE DUNITES

Sanfilippo A.*[1-2], Tribuzio R.[1-2], Ottolini L.[2] & Hamada M.[3]
[1] Dipartimento di Scienze della Terra e dell'Ambiente, Università di Pavia, Italy
[2] Istituto di Geoscienze e Georisorse, Consiglio Nazionale delle Ricerche, Pavia, Italy
[3] Japan Agency for Marine-Earth Science and Technology, Yokosuka, Japan
Corresponding email: alessio.sanfilippo@unipv.it

Keywords: MORB, olivine, water

Replacive mantle dunites are considered the pathways for extraction of mantle melts from their source region (Kelemen et al., 1995). These rocks offer a unique possibility to unravel the compositional variability of the melts produced in the upper mantle, before mixing and crystal fractionation at shallow depths modify their pristine signature. Here we focus on the chemistry of the olivine in large replacive mantle dunites from the Lanzo South ophiolite (Western Alps) as probes into the variability of the melts produced in a cold thermal regime. Previous studies indicated that these dunites acted as reactive melt migration channels for melts with a MORB-like geochemical signature (e.g., Piccardo et al., 2007). The minor and trace element compositions of these olivines agree with this idea, although the chemical variability between the different bodies implies equilibration with MORB-type melts not-aggregated (i.e. not-averaged at shallow lithospheric levels). To better constraint this idea, we expand our investigation to the H_2O and lithium contents of these olivines. We show that the dunite olivine has 19-40 ppm H_2O and 0.30-0.56 ppm Li, thereby suggesting involvement of melts enriched in H_2O and depleted in lithium compared to normal MORB values. We propose that the melts transported within the Lanzo replacive dunites formed under high pressures conditions through preferential melting of a chemically enriched component in the lowermost part of the melting region. Preferential extraction of enriched melts through focused melt channels may have major role in preserving a chemical variability of melts delivered to the lower crust.

Kelemen, P.B., Shimizu, N., Salters, V.J.M. (1995): Extraction of mid-ocean-ridge basalt from the upwelling mantle by focused flow of melt in dunite channels. *Nature*, **375**, 747-753.

Piccardo, G.B., Zanetti, A., Muntener, O. (2007): Melt/peridotite interaction in the Southern Lanzo peridotite: field, textural and geochemical evidence. *Lithos*, **94**, 181-209.

SUBMARINE STRUCTURES OF THE CARIBBEAN LARGE IGNEOUS PROVINCE: AGE AND GEOCHEMISTRY OF THE BEATA RIDGE AND HESS ESCARPMENT

Schwindrofska A.*[1], Hoernle K.[1-2], van den Bogaard P.[1], Hauff F.[1] & Werner R.[1]
[1] GEOMAR - Helmholtz-Zentrum für Ozeanforschung, Christian-Albrechts-Universität Kiel, Germany
[2] Institut für Geowissenschaften, Christian-Albrechts-Universität Kiel, Germany
Corresponding email: aschwindrofska@geomar.de

Keywords: Large Igneous Province, geochemistry, geochronology

R/V Meteor cruise M81/2 mapped and sampled two prominent submarine structures of the Caribbean Plate: the Beata Ridge and the Hess Escarpment. While the Beata Ridge is commonly believed to be part of the Caribbean Large Igneous Province (CLIP), no comprehensive survey of the Hess Escarpment exists and thus its origin remains unclear. We present major element, trace element and Sr-Nd-Hf-Pb isotope data as well as $^{40}Ar/^{39}Ar$ age data including the first representative geochemical dataset for the Hess Escarpment. Unlike the proposition that the Hess Escarpment is part of the continental Chortis Block, our results show that the structure is of volcanic origin and most likely also belongs to the CLIP. The volcanic nature is also confirmed by its morphology. The Hess Escarpment represents a large fault zone but, including the area north of the Escarpment, it also consists of seamounts, guyots and ridges often located on huge plateau-like structures.

Our preliminary age determinations of Beata Ridge samples yield an age range from 94 to 86 Ma lying well within the assumed main CLIP event at 89±6 Ma that is commonly believed to be formed by large degrees of melting of a starting plume head. However, three analyses with younger ages of 79, 63 and 51 Ma question the hypothesis that large igneous provinces are the result of catastrophic short-termed magmatic events and instead support the model of prolonged volcanism over tens of millions of years with several magmatic pulses. The geochemical data show that the Beata Ridge has compositions typical for the CLIP with flat chondrite-normalized rare earth element (REE) patterns (average $(La/Yb)_N$ = 1.15) and intermediate radiogenic isotope ratios, but enriched and depleted signatures are observed as well. The Hess Escarpment, in contrast, displays mainly depleted compositions partly more depleted than normal mid ocean ridge basalt (MORB) compositions and similar to the highly depleted komatiites of Gorgona Island. The results imply that the mantle source is heterogeneous and contains two components: a highly depleted component, in our data represented in samples from the Hess Escarpment, and an enriched component trending towards HIMU compositions, which we found only on the Beata Ridge. The typical CLIP isotopic compositions can be generated by mixing of melts from the two components. We further show that these heterogeneities can occur on a small scale of only tens of kilometers within the CLIP.

AMPHIBOLE AS A PROXY OF THE SECULAR VARIATIONS IN PRIMITIVE MAGMAS

Sessa G.[1], Tiepolo M.*[1], Moroni M.[1], Fiorentini M.L.[2], Langone A.[3], Giazzi G.[4], Krotz L.[4], Ferrari E.[1] & Loucks R.R.[2]

[1] Dipartimento di Scienze della Terra "A. Desio", Università di Milano, Italy
[2] Centre for Exploration Targeting, University of Western Australia, Perth, Australia
[3] Istituto di Geoscienze e Georisorse, Consiglio Nazionale delle Ricerche, Pavia, Italy
[4] Thermo Fisher Scientific, Rodano (MI), Italy
Corresponding email: massimo.tiepolo@unimi.it

Keywords: amphibole, secular variations, Archean

In primitive hydrous arc-magmas and under pressure conditions typical of the lower crust calcic amphibole precedes the crystallisation of plagioclase and follows that of olivine, spinel and pyroxene (e.g., Muentener & Ulmer, 2006). Among the early minerals, amphibole is the sole capable to incorporate a large number of petrologically important elements (including Nb, Ta) and volatile elements such as H, Cl and F. In ultramafic igneous rocks amphibole is thus the phase preserving the most complete record of the geochemical signature of the primary magma including its volatile contents.

Hornblendites and amphibole-bearing (typically pyroxenites) ultramafic intrusive rocks occur in most Phanerozoic orogenic belts worldwide. Amphibole-bearing rocks also occur in several Archean komatiites. Hence amphibole may be considered an ideal proxy for monitoring the secular variations in primitive magma composition for a relatively large number of elements including volatiles.

For this purpose we started an ambitious project and selected amphibole-bearing ultramafic igneous rocks from different sites worldwide, form Archean to Phanerozoic in age: komatiites, pyroxenites, hornblendites. Archean samples come from Canadian, Australian and Russian greenstone belts (Abitibi, Agnew-Wiluna, Pechenga), whereas post-Archean samples include mafic and ultramafic rocks from Himalaya (Tibet and Pakistan), Zagros belt (Iran), Ross orogeny (Antarctica), Italian Alps (Ivrea-Verbano zone, Adamello, Bregaglia) and Japan arc. Magmatic sulphides and carbonates may also occur in some amphibole-bearing assemblages suggesting CO_2- and S-bearing primary magmas.

Genetic conditions in most of the samples resulted in amphibole crystallization following olivine, spinel and pyroxene and predating plagioclase. Samples of Archean and Phanerozoic age may show striking similar textural features (like olivine embedded in pyroxene or amphibole oikocrysts).

Preliminary major element analyses on amphibole-bearing assemblages indicate that amphiboles are of igneous origin and in most cases in equilibrium with associated pyroxenes. Amphiboles show relatively restricted major element composition suggesting similar petrogenetic origin, although significant differences exist between Archean and post-Archean amphiboles (e.g., TiO_2 contents). The trace element and volatile content characterization of representative amphiboles by SIMS and LA-ICP-MS is in progress. On selected amphiboles we also determined the S and C contents for a first estimate about the potential for amphibole to influence the deep volatile cycle for C and S.

We shall discuss the first results of this project with emphasis on secular variations marked by key elements and element ratios (e.g., Nb/Ta) for the Earth's evolution.

Muntener, O. & Ulmer, P. (2006): Experimentally derived high-pressure cumulates from hydrous arc magmas and consequences for the seismic velocity structure of lower arc crust. *Geophys. Res. Letters*, **33**, L21308.

THE LUNAR Mg SUITE AND THE IRON ISOTOPE COMPOSITION OF THE MOON

Sossi P.A.*[1] & Moynier F.[1]

[1] Institut de Physique du Globe de Paris, Sorbonne Paris Cité, Université Paris Diderot, Centre National de la Recherche Scientifique, Paris, France

Corresponding email: sossi@ipgp.fr

Keywords: iron isotopes, Moon, Mg Suite

Early dynamical models showed that a giant impact of a Mars-sized body with the proto-Earth could form the Moon, where most lunar material was derived from the impactor (e.g., Canup, 2004). However, the observed chemical and isotopic kinship between the Earth and its Moon has given rise to the hypothesis that the Moon is made of material primarily derived from the proto-Earth's mantle (O'Neill, 1991) or that efficient homogenisation took place in an Earth-Moon disk (Pahlevan & Stevenson, 2007). An element that appears to show significant differences between the two bodies is iron, whose concentration in mare basalts, 15-25 wt.%, greatly exceeds that found in their terrestrial counterparts (10-15 wt.%). The isotopes of iron are also apparently distinct from one another, where estimates for the Earth's mantle yield $\delta^{57}Fe$ = +0.05±0.03‰ (Sossi et al., 2016), compared with the systematically heavier low-Ti (+0.12±0.04‰) and high-Ti basalts (+0.27±0.04‰; Liu et al., 2010). This departure to heavy values relative to chondritic meteorites (homogeneous to -0.02±0.05‰) has been explained by volatile loss of Fe during the giant impact (Poitrasson et al., 2004). Iron isotopes in mare basalts correlate with TiO_2 content, implying a degree of iron isotope fractionation during lunar magma ocean crystallisation, and complicating estimation of its bulk mantle composition. To tackle this question, we have analysed 7 samples from the lunar Mg Suite (e.g., Hess, 1994) that are notable for their low TiO_2 contents (0.1-0.3 wt.%, close to estimates for the lunar mantle) and particularly high Mg#s, up to 0.88. Such high Mg/Fe ratios make them indistinguishable from the Earth's mantle (0.89; Palme and O'Neill, 2013). Therefore, the Mg Suite may be the most faithful analogue of the Moon's mantle. A single analysis of Mg Suite dunite 72415 (Wang et al., 2015) yields a very light value, -0.2‰, however we find that the Mg Suite rocks have iron isotope compositions only slightly, though systematically lighter than low-Ti mare basalts, bringing the lunar and terrestrial mantles into isotopic concordance. This result enables the Moon to be formed from the Earth's mantle during a giant impact without isotopic fractionation of iron, within analytical uncertainties. However, that isotopic fractionations are observed for more volatile elements, such as Zn (Paniello et al., 2012) may place constraints on the nature of volatile element depletion in the Earth-Moon disk.

Canup, R.M. (2004): Simulations of a late lunar-forming impact. *Icarus*, **168**, 433-456.

Hess, P.C. (1994): Petrogenesis of lunar troctolites. *J. Geophys. Res.*, **99**, 19083-19093.

Liu, Y., Spicuzza, M.J., Craddock, P.R., Day, J.M.D., Valley, J.W., Dauphas, N., Taylor, L.A. (2010): Oxygen and iron isotope constraints on near-surface fractionation effects and the composition of lunar mare basalt source regions. *Geochim. Cosmochim. Acta*, **74**, 6249-6262.

O'Neill, H.S.C. (1991): The origin of the Moon and the early history of the Earth - A chemical model. Part 1: The Moon. *Geochim. Cosmochim. Acta*, **55**, 1135-1157.

Pahlevan, K. & Stevenson, D.J. (2007): Equilibration in the aftermath of the lunar-forming giant impact. *Earth Planet. Sci. Letters*, **262**, 438-449.

Palme, H. & O'Neill, H.S.C. (2014): Cosmochemical estimates of mantle composition. *in* "Treatise on geochemistry, Vol. 2: The mantle and core", R.W. Carlson, ed., Elsevier, Amsterdam, 1-39.

Paniello, R.C., Day, J.M.D., Moynier, F. (2012): Zinc isotopic evidence for the origin of the Moon. *Nature*, **490**, 376-379.

Poitrasson, F., Halliday, A.N., Lee, D.C., Levasseur, S., Teutsch, N. (2004): Iron isotope differences between Earth, Moon, Mars and Vesta as possible records of contrasted accretion mechanisms. *Earth Planet. Sci. Letters*, **223**, 253-266.

Sossi, P.A., Nebel, O., Foden, J.D. (2016): Iron isotope systematics in planetary reservoirs. *Earth Planet. Sci. Letters*, in press.

Wang, K., Jacobsen, S.B., Sedaghatpour, F., Chen, H., Korotev, R.L. (2015): The earliest Lunar magma ocean differentiation recorded in Fe isotopes. *Earth Planet. Sci. Letters*, **430**, 202-208.

EARTH'S OLDEST MANTLE PERIDOTITES INDICATE EARLY MIXING OF THE LATE VENEER INTO THE MANTLE

van de Löcht J.[1], Li C.[2], Hoffmann J.E.[2], Wang Z.[2], Becker H.[2], Rosing M.[3], Kleinschrodt R.[1] & Münker C.*[1]
[1] Institut für Geologie und Mineralogie, Universität Köln, Germany
[2] Fachbereich Geowissenschaften, Freie Universität Berlin, Germany
[3] Natural History Museum, Copenhagen, Denmark
Corresponding email: c.muenker@uni-koeln.de

Keywords:

Only three localities worldwide have been identified as potential candidates for preserving relics of early Archean mantle, all of which are exposed in the 3.6-3.9 Ga Itsaq gneiss complex (IGC) of southern West Greenland (e.g., Friend et al., 2002). In order to gain new insights into the evolution and isotopic composition of the Eoarchean mantle, a new, carefully collected sample set was investigated in terms of its petrology and geochemistry. Samples include dunites and harzburgites from the region south of the Isua Supracrustal belt (SOISB) and from the Narssaq ultramafic body, south of Nuuk. So far, it was heavily debated, whether the proposed candidates for preserved early Archean mantle relics in the IGC are indeed of true mantle origin or whether they are ultramafic cumulates (e.g., Bennett et al., 2002; Friend et al., 2002; Rollinson, 2007; Szilas et al., 2014). Pristine mantle peridotites and ultramafic crustal cumulates can unambiguously be discriminated by their distinct fractionation patterns of PGEs. Hence, our investigations also included platinum group element (PGE) concentration and Re-Os isotope measurements. For the first time, there is now unambiguous evidence based on low Pt_N/Ir_N ratios, olivine compositions and major element compositions that at two localities in the IGC > 3.8 Ga mantle peridotites are indeed preserved. Importantly, these mantle peridotites display a clear vestige of a broadly chondritic late veneer signature, with PGE abundances similar to present-day mantle rocks, thereby showing that a chondrite-like late veneer was mixed efficiently into the sampled mantle domains by Eoarchean time. Hence, the platinum group element abundances and Re-Os isotope compositions of Earth´s oldest mantle peridotites strongly support models implying very early addition of late veneer material, and efficient mixing into the upper mantle by 3.8 Ga. Recently reported ^{182}W excesses in rocks from the Isua region (Willbold et al., 2011, Rizo et al., 2016) may therefore represent a vestige of early silicate-differentiation events. Collectively, the > 3.8 Ga mantle peridotites from southern West Greenland can now offer a direct window into Eoarchean tectonic processes and early mantle evolution.

Bennett, V.C., Nutman, A.P., Esat, T.M. (2002): Constraints on mantle evolution from $^{187}Os/^{188}Os$ isotopic compositions of Archean ultramafic rocks from southern West Greenland (3.8 Ga) and Western Australia (3.46 Ga).*Geochim. Cosmochim. Acta*, **66** 2615-2630.

Friend, C.R.L., Bennett, V.C., Nutman, A.P. (2002): Abyssal peridotites >3,800 Ma from southern West Greenland: field relationships, petrography, geochronology, whole-rock and mineral chemistry of dunite and harzburgite inclusions in the Itsaq Gneiss Complex. *Contrib. Mineral. Petrol.*, **143**, 71-92.

Rizo, H. Walker, R.J., Carlson, R.W., Touboul, M., Horan, M.F., Puchtel, I.S., Boyet, M., Rosing, M.T. (2016): Early Earth differentiation investigated through ^{142}Nd, ^{182}W, and highly siderophile element abundances in samples from Isua, Greenland. *Geochim. Cosmochim. Acta*, **175**, 319-336.

Rollinson, H (2007): Recognising early Archaean mantle: a reappraisal. *Contrib. Mineral. Petrol.*, **154**, 241-252.

Szilas, K., Kelemen, P.B., Rosing, M.T. (2015): The petrogenesis of ultramafic rocks in the > 3.8 Ga Isua supracrustal belt, southern West Greenland: Geochemical evidence for two distinct magmatic cumulate trends. *Gondwana Res.*, **28**, 565-580.

Willbold, M., Elliott, T., Moorbath, S. (2011):The tungsten isotopic composition of the Earth's mantle before the terminal bombardment. *Nature*, **477**, 195-198.

THE PRESSURE SIGNAL IN OLIVINE-BEARING GABBROIC ROCKS

Ziberna L.*[1], Green E.C.R.[2] & Blundy J.D.[1]
[1] School of Earth Science, University of Bristol, United Kingdom
[2] Institut für Geochemie und Petrologie, Eidgenössische Technische Hochschule Zürich, Switzerland
Corresponding email: luca.ziberna@bristol.ac.uk

Keywords: geobarometry, gabbroic rocks, igneous cumulates

Pressure (*P*) and temperature (*T*) of formation of gabbroic rocks are commonly estimated using thermobarometric methods based on cation exchange between minerals. Despite the obvious need of reliable and precise *P*estimates, *P* uncertainties of commonly used thermobarometers are far too high (> 3 kbar) relative to the pressure range that needs to be investigated (i.e., as small as 5 kbar for oceanic settings). Most likely, the difficulty to extract a clear *P* signal is related to the fact that most thermobarometers use either empirical formulations based on the composition of a single phase or a single reaction involving only two phases, the latter being often characterized by a relatively low volume change. A multiple-reaction approach employing an internally consistent thermodynamic model would be preferable, as it allows for all the phases in the equilibrium assemblage to be used for thermobarometry. An established method originally developed for metamorphic rocks is the so-called average P (avP) in thermocalc (Powell & Holland, 1994), which uses a least square minimization technique to calculate the optimal *P*, taking into account both uncertainties and correlations of all the reactions in an independent set. Thanks to its diagnostic utilities, it also allows the consistency of the input data used for the calculations (i.e., end-member activities and thermodynamic properties) to be evaluated. Despite its potential, this method has been only rarely applied to igneous rocks and has never been tested to evaluate its accuracy and precision.

In this work, we analysed a number of well-equilibrated natural rocks and collected a large dataset of phase equilibria experiments in basaltic systems, which allowed us to test the reliability of avP for olivine-bearing gabbroic rocks. Calculations have been performed using olivine-magnetite-clinopyroxene-plagioclase and olivine-clinopyroxene-plagioclase equilibria. Using the existing thermodynamic data and mixing models, avP is capable to predict the experimental pressures, but the uncertainties propagated from the calculations (σ_P) are unacceptably high (1.8-5.0 kbar). Thanks to the diagnostics in thermocalc and the careful selection of experimental data, we then refined the thermodynamic properties of some end-members, which allowed decreasing σ_P (1.0-2.1 kbar for experimental assemblages). If olivine-magnetite-clinopyroxene-plagioclase equilibria are used, the model is now capable to predict the experimental pressures with a confidence of 92% and the standard error of estimate of avP is 1.0 kbar. If *T* can be constrained by other methods, avP is capable to predict the pressures of natural olivine-bearing gabbros with uncertainties as low as 1.1 kbar.

Powell, R. & Holland, T.J.B. (1994): Optimal geothermometry and geobarometry. *Am. Mineral.*, **79**, 120-133.

Session S3:

Volatiles in the deep Earth: storage, mobility and implications

Conveners:

Marc Blanchard (Paris – France)

Dan Frost (Bayreuth – Germany)

István Kovács (Budapest – Hungary)

SYSTEMATIC DECREASE OF HYDROXYL DEFECT CONCENTRATION IN QUARTZ PHENOCRYST FRAGMENTS WITHIN IGNIMBRITES: IMPLICATIONS FOR POST-DEPOSITIONAL DIFFUSIONAL LOSS OF HYDROGEN

Biró T.*[1], Kovács I.[2], Karátson D.[1], Király E.[2], Falus G.[2], Fancsik T.[2] & Sándorné Kovács J.[4]

[1] Department of Physical Geography, Institute of Geography and Earth Sciences, Eötvös Loránd University, Budapest, Hungary

[2] Geochemical and Laboratory Department, Geological and Geophysical Institute of Hungary, Budapest, Hungary

[3] Department of Petrology and Geochemistry, Institute of Geography and Earth Sciences, Eötvös Loránd University, Budapest, Hungary

[4] Hungarian Institute for Forensic Sciences, Budapest, Hungary

Corresponding email: tbiro.geogr@gmail.com

Keywords: quartz, structural hydroxyl, ignimbrite

We examined the hydroxyl defect content of quartz phenocryst fragments from different vertical positions above the base of pyroclastic density current (PDC) deposits. Via this sampling and measurement strategy information on the vertical variation of hydroxyl defect concentration of quatz phenocrysts, thus an insight into potential post-depositional hydrogen loss and cooling history of PDC deposits can be gained. Quartz phenocryst fragments were collected from two different, thick ignimbrites at the Bükkalja Volcanic Field (North Hungary). Unpolarized micro-FTIR measurements on at least 23 randomly oriented crystal fragments from each site were performed on 4 different vertical levels of each ignimbrite. The hydroxyl defect content shows a clear decrease from the initial ~ 12 wt.% ppm measured just above the base to ~3 ppm within few meters towards the centre of the deposits. Ignimbrites with different physical volcanological properties (degree of welding, maximum grain size) are characterized by different hydroxyl defect concentrations of quartz phenocryst fragments at the same height above the base. The difference between the empirical and theoretical distribution of unpolarized absorbances, indicates that there may be some outlier values at or close to the base of these ignimbrites. These can be xenocrysts which were possibly ripped up and incorporated during pyroclast transport.

Our results imply that the structural hydroxyl content of quartz phenocrysts could be considered as an input for numerical modeling on the cooling speed, initial temperature, and the degree of erosion of quartz-bearing ignimbrites.

EFFECT OF IRON AND TRIVALENT CATIONS ON OH-DEFECTS IN OLIVINE

Blanchard M.*[1], Ingrin J.[2], Balan E.[1], Kovács I.[3] & Withers A.C.[4]
[1] Institut de Minéralogie, de Physique des Matériaux, et de Cosmochimie, Université Paris 06, Centre National de la Recherche Scientifique, France
[2] Unité Matériaux et Transformations, Université de Lille 1, Centre National de la Recherche Scientifique, France
[3] Geochemical and Laboratory Department, Geological and Geophysical Institute of Hungary, Budapest, Hungary
[4] Department of Earth Sciences, University of Western Ontario, London, Canada
Corresponding email: marc.blanchard@impmc.upmc.fr

Keywords: olivine, OH-defect, IR spectroscopy

Hydrogen incorporation in olivine involves many OH-defects that will control the hydrogen solubility at mantle conditions. Several of these OH-defects are identified essentially from the investigation of forsterite (the olivine Mg end-member). We study here the effect of Fe^{2+}, Fe^{3+}, Al^{3+} and Cr^{3+} on OH-defects in order to improve our understanding of the hydrogen speciation in natural olivine. Low-temperature infrared spectra are collected on synthetic and natural olivines. These spectra are then interpreted in light of the theoretical determination of the structural, vibrational and infrared spectroscopic properties of Fe-related OH-defects, using first-principles calculations based on density functional theory. The presence of Fe^{2+} changes the cationic environment around the fully protonated vacancies in forsterite, leading to a slight modification of their infrared signatures. In particular, the presence of Fe^{2+} in an octahedral site adjacent to a hydrogarnet-type defect is likely responsible for the additional bands observed at 3599 cm^{-1} and around 3520-3550 cm^{-1} in Fe-doped olivines. Results show that the OH bands between 3310 and 3380 cm^{-1} are associated with the presence of trivalent cations. Specifically, two bands at 3323 and 3358 cm^{-1}, commonly observed in natural olivine, are associated with the substitution of Mg^{2+} by Cr^{3+} while two similar bands at 3328 and 3353 cm^{-1} are associated with the substitution of Mg^{2+} by Fe^{3+}. The presence of these defects and the “titanoclinohumite” defect in natural olivine clearly underlines the prominent role of trace elements on the hydrogen incorporation in the lithospheric olivine.

WATER STORAGE IN THE TRANSITION ZONE

Bolfan-Casanova N.*[1], Schiavi F.[1], Martinek L.[1], Novella D.[1], Bureau H.[2], Raepsaet C.[3] & Demouchy S.[4]
[1] Laboratoire Magmas et Volcans, Université Blaise Pascal, Clermont-Ferrand, France
[2] Institut de Minéralogie, de Physique des Matériaux et de Cosmochimie, Paris, France
[3] Commissariat à l'énergie atomique et aux énergies alternatives Saclay, Gif-sur-Yvette, France
[4] Géosciences Montpellier, Université de Montpellier, France
Corresponding email: n.bolfan@opgc.univ-bpclermont.fr

Keywords: water, transition zone, ERDA

The transition zone is potentially an important water reservoir within the Earth. Magneto-telluric data are often interpreted as being due to 0.1 to 1 wt.% H_2O at 410 km discontinuity (Yoshino & Katsura, 2013). On the other hand, the interpretation of seismic data is still debated due to problems in measuring the water content in transition zone minerals (Chang et al., 2015). Indeed, transition zone minerals, namely wadsleyite and ringwoodite, can contain up to 3.2 wt.% H_2O by weight (Inoue et al., 1995; Ohtani et al., 2000). The recent discovery of hydrous ringwoodite (containing 2.5 wt.% H_2O) included in a deep diamond (Pearson et al., 2014) shows that experimental predictions are possible within the Earth: that is, in subduction zones, high water activities are or have been possible, allowing for the formation of hydrous transition zone minerals.

In recent years, we have been working on extending the capabilities of measurements of water in minerals using other techniques than Fourier Transform Infrared spectroscopy (FTIR) like Raman spectroscopy (Bolfan-Casanova et al., 2014) that allows the use of very small probing beams under reflection geometry, but also ERDA (Elastic Recoil detection Analysis; Bureau et al., 2009; Withers et al., 2012) that allows quantification without the use of any standards. The main problem of using FTIR on wadsleyite and ringwoodite is that these phases are often too absorbing to allow proper quantification of water. Also, whenever working on realistic, i.e., complex, compositions, samples end up having small grain sizes that are difficult to deal with FTIR when the samples are polyphasic.

We will present our new results using samples synthesized in the multi-anvil press under conditions of the transition zone. Thanks to Raman spectroscopy we were able to measure the partitioning of water between mantle phases such as olivine and wadsleyite coexisting in the same sample. Thanks to ERDA, we show that ringwoodite exhibits the same incorporation mechanism of hydrogen as wadsleyite, that is predominantly hydrogen substituting for magnesium, contrary to what was observed before.

Bolfan-Casanova, N., Montagnac, G., Reynard, B. (2014): Measurement of water contents in olivine using Raman spectroscopy. *Am. Mineral.*, **99**, 149-156.

Bureau, H., Raepsaet, C., Khodja, H., Carraro, A., Aubaud, C. (2009): Determination of hydrogen content in geological. samples using elastic recoil detection analysis (ERDA). *Geochim. Cosmochim. Acta*, **73**, 3311-3322.

Chang, Y.-Y., Jacobsen, S.D., Bina, C.R., Thomas, S.M., Smyth, J.R., Frost, D.J., Boffa Ballaran, T., McCammon, C.A., Hauri, E.H., Inoue, T., Yurimoto, H., Meng, Y., Dera, P. (2015): Comparative compressibility of hydrous wadsleyite and ringwoodite: Effect of H_2O and implications for detecting water in the transition zone. *J. Geophys. Res.*, *Solid Earth*, **120**, 8259-8280.

Inoue, T., Yurimoto, H., Kudoh, Y. (1995): Hydrous modified spinel, $Mg_{1.75}SiH_{0.5}O_4$: a new water reservoir in the mantle transition zone. *J. Geophys. Res.*, **22**, 117-120.

Ohtani, E., Mizobata, H., Yurimoto, H. (2000): Stability of dense hydrous magnesium silicate phases in the systems Mg_2SiO_4-H_2O and $MgSiO_3$-H_2O at pressures up to 27 GPa. *Phys. Chem. Minerals*, **27**, 533-544.

Pearson, D.G., Brenker, F.E., Nestola, F., McNeill, J., Nasdala, L., Hutchison, M.T., Matveev, S., Mather, K., Silversmit, G., Schmitz, S., Vekemans, B., Vincze, L. (2014): Hydrous mantle transition zone indicated by ringwoodite included within diamond. *Nature*, **507**, 221-224.

Withers, A.C., Bureau, H., Raepsaet, C., Hirschmann, M.M. (2012): Calibration of infrared spectroscopy by elastic recoil detection analysis of H in synthetic olivine. *Chem. Geol.*, **334**, 92-98.

Yoshino, T. & Katsura, T. (2013): Electrical conductivity of mantle minerals: Role of water in conductivity anomalies. *Ann. Rev. Earth Planet. Sci*., **41**, 605-628.

HYDROGEN DISTRIBUTION AND DIFFUSION IN UPPERMOST MANTLE ROCKS

Demouchy S.*[1]
[1] Geosciences Montpellier, Centre National pour la Recherche Scientifique, Université de Montpellier, France
Corresponding email: demouchy@um2.fr

Keywords: olivine, peridotite, hydrogen

The minerals constituting the Earth's uppermost mantle contain "water" in the form of hydrogen bonded to structural oxygen. Hydrogen is only present as a trace element (ppm level), decorating point defects in the mineral crystalline structure. These minerals are the so-call nominally anhydrous minerals (NAMs). Experimental petrology and mineralogy have quantified the maximum concentration under several compositional and thermodynamic conditions, but systematic studies on the hydrogen concentration in minerals from mantle-derived rocks have only recently been carried out. Here, a compilation of the distribution of hydrogen in uppermost mantle peridotite xenoliths is presented. NAMs from peridotite xenoliths (mostly in the spinel stability field) contain a few ppm wt. H_2O in their structure. From the current database, the maximum hydrogen concentrations in olivine regularly increase with increasing depth. To date, the amount of hydrogen in NAMs from peridotite xenoliths from subduction contexts does not seems higher than in other geological contexts for similar temperature and pressure conditions. The highest hydrogen concentrations are found in peridotitic olivines from cratonic mantle (Siberia) transported by kimberlitic magmas, and are likely due to the deeper depth of origin (> 5 GPa). The increasing hydrogen concentration in olivine with increasing depth is likely controlled by the increase of H partitioning into olivine at the expense of orthopyroxene as imposed by a decrease in Al content in opx with depth. However, the sparse data could also indicate that the bulk hydrogen concentration slightly increases with depth higher than 150 km. In this case, it would suggest, for at least one location (Udachnaya, Siberia), a possible increase in water fugacity due to water-rich fluid saturation. Even if the most abundant mineral in mantle rocks is olivine, and in the absence of a significant amount of amphibole (> 3%) the bulk hydrogen concentration in peridotites is controlled by the amount of hydrogen stored in pyroxenes. However, one must keep in mind that hydrogen concentration in olivine remains potentially crucial for consequences on physical properties such as rheology and electrical conductivity. At last, the questions of the preservation of hydrogen concentration in NAMs due to rapid ionic diffusion will be discussed in the light of recent results from peridotite xenoliths and diffusion models.

THE FATE OF SULFIDE DURING ADIABATIC DECOMPRESSION MELTING – IMPLICATIONS FOR SULFUR BUDGET OF MORB AND OIB SOURCE MANTLE

Ding S.*[1] & Dasgupta R.[1]
[1] Department of Earth Science, Rice University, Houston, TX, USA
Corresponding email: sd35@rice.edu

Keywords: sulfur cycle, MORB, OIB

Sulfur (S) is a key volatile element, which has fundamental impact on the planetary differentiation, elemental partitioning, volcanism and long to short term habitability of the planetary surficial environment. Yet the constraints on the S budget of the Earth's mantle are limited. Magmatism in mid-ocean ridges is the main pathway of S from the Earth's depleted mantle (DM), and magmatism in ocean islands is one of the critical probes for understanding chemical, lithological, and thermal variations in the Earth's mantle. Therefore, S content of primitive MORBs and OIBs could provide insights into the S budget of the Earth's mantle. However, the fate of sulfide during mantle melting is incompletely explored – limiting our ability to fully understand the sulfur and chalcophile element geochemistry of primitive basalts.

This study is a geochemical modeling work to constrain the extraction of S through magmatism in mid-ocean ridges and ocean islands. Compilation of MORB and OIB (e.g., Loihi, Samoa, Iceland and Galapagos) major element, Cu, and S contents from literature shows that although differentiated basalts may be sulfide saturated, basalts with MgO > 8 wt.% fall in the range of 800-1200 ppm of S, and do not show any systematic trends with major element compositions. In order to test whether primitive MORBs and OIBs can be sulfide-undersaturated, we coupled thermodynamic models (Ghiorso et al., 2002) and experimental constraints (Hirose & Kushiro, 1993; Walter, 1998) on isentropic decompression melting at different mantle potential temperatures with existing SCSS model (sulfur content at sulfide saturation; e.g., Fortin et al., 2015). The goal was to track the S contents in the partial melt and the mode of residual sulfide as a function of initial sulfur content of the mantle source, melting degree, depth, temperature, and change in partial melt composition. The fractionation of Cu, a chalcophile element, is also modeled to derive an internally consistent set of inferences about the geochemistry of both S and Cu in partial melt parental to MORB and OIB. Our modeling suggests that, for mantle potential temperature, T_P of 1380°C, the S and Cu budgets of primitive MORBs can be explained by exhaustion of 100-200 ppm S (as sulfide) from the residue by 10-20 wt.% melting, which is consistent with the estimated average to maximum *F*appropriate for MORB generation. We further discuss the effects of different SCSS models, bulk partitioning and initial abundance of Cu, and T_P of 1280-1420°C on our results. This analysis also brackets the S content in peridotite source of high-*F* (~10-25%) Icelandic basalts of 50-200 ppm for T_P of 1450-1550°C. However, the bulk S content of the heterogeneous OIB sources is likely higher and mixing of eclogite and sediment partial melt, with lower SCSS, with peridotite partial melt is critical to reconcile the measured S contents in low-*F* (<10%) OIBs from GSC, Loihi and Samoa for T_P of 1450-1650°C.

Fortin, M.-A., Riddle, J., Desjardins-Langlais, Y., Baker, D.R. (2015): The effect of water on the sulfur concentration at sulfide saturation (SCSS) in natural melts. *Geochim. Cosmochim. Acta*, **160**, 100-116.

Ghiorso, M.S., Hirschmann, M.M., Reiners, P.W., Kress, V.C. (2002): The pMELTS: A revision of MELTS for improved calculation of phase relations and major element partitioning related to partial melting of the mantle to 3 GPa. *Geochem. Geophys. Geosyst.*, **3**, 1-35.

Hirose, K. & Kushiro, I. (1993): Partial melting of dry peridotites at high pressures: Determination of compositions of melts segregated from peridotite using aggregates of diamond. *Earth Planet. Sci. Letters*, **114**, 477-489.

Walter, M.J. (1998): Melting of garnet peridotite and the origin of komatiite and depleted lithosphere. *J. Petrol.*, **39**, 29-60.

SITE-SPECIFIC HYDROGEN DIFFUSIVITY IN CLINOPYROXENE AND IMPLICATIONS FOR MANTLE XENOLITHS

Ferriss E.*[1], Plank T.[1] & Walker D.[1]
[1] Division of Geochemistry, Lamont-Doherty Earth Observatory, Columbia University, Palisades, NY, USA
Corresponding email: ferriss@ldeo.columbia.edu

Keywords: hydrogen, FTIR, clinopyroxene

Accurately quantifying the rate at which hydrogen ("water") diffuses through nominally anhydrous minerals such as clinopyroxene (cpx) and olivine is critical for interpreting measurements of water concentrations in mantle xenoliths to gain insight into ascent rates and the distribution of water in the deep earth. Here I summarize the results of recent work (Ferriss et al., 2016) dehydrating two diopsides and an augite to determine diffusivities for bulk water as well as individual hydrogen incorporation mechanisms based on FTIR peaks. In both diopsides considered, the peak at 3645 cm^{-1} diffuses the slowest, and the peak at the 3450 cm^{-1} diffuses the fastest. However, the diffusivities of bulk water and all FTIR peaks are ~ 3 orders of magnitude higher for the diopside containing more Fe, and hydrogen diffusivity in the augite is near the highest diffusivities measured in cpx. These observations support previous proposals (Hercule, 1996; Woods et al., 2000) that hydrogen diffusivity increases with Fe content up to ~ 1-2 wt.% FeO. Virtually all natural cpx contain more Fe than this threshold value, and therefore hydrogen diffusivities in xenolith cpx are expected to be fast, on the order of 10^{-9} to 10^{-11} m^2/s at 1000°C.

Such fast diffusivities have three important implications for interpreting water measurements in xenoliths. First, to explain the consistent observation of significant water loss in xenolith olivine but not in cpx, the fast "proton-polaron" mechanism must be operating in the olivine, and the diffusivities in cpx must be toward the low end of the proposed 2-order of magnitude range. These relatively low diffusivities in mantle cpx are proposed to be related to high ^{IV}Al contents. Second, because equilibration with the surroundings will take place on time-scales of hours, the water concentrations measured in cpx are more likely to be in equilibrium with the host magma than to retain mantle water signatures. Third, when interpreting time scales retrieved from water diffusion profiles, the initial depth of zonation formation is likely the depth at which water loss from the magma begins, typically 2-3 km, rather than mantle depths.

Ferriss, E., Plank, T., Walker, D. (2016): Site-specific hydrogen diffusion rates during clinopyroxene dehydration. *Contrib. Mineral. Petrol.*, DOI: 10.1007/s00410-016-1262-8.

Hercule, S. (1996): Cinétique et solubilité de l'hydrogène dans le diopside monocristallin. Université Paris-Sud, thesis, 196 p.

Woods, S., Mackwell, S., Dyar, D. (2000): Hydrogen in diopside: diffusion profiles. *Am Mineral.*, **85**, 480-487.

WATER CONCENTRATIONS AND HYDROGEN ISOTOPE COMPOSITIONS OF ALKALINE BASALT HOSTED CLINOPYROXENE MEGACRYSTS: THE IMPORTANCE OF STRUCTURAL HYDROXYL GROUPS AND MOLECULAR WATER

Kovács I.*[1], Demény A.[2], Czuppon G.[2], Lécuyer C.[3], Fourel F.[3], Xia Q.-K.[4], Liu J.[4], Pintér Z.[5-6], Király E.[1], Török K.[1], Szabó Á.[1-5], Deloule E.[7], Falus G.[1], Fancsik T.[1], Zajacz Z.[8], Sándorné Kovács J.[9] & Udvardi B.[1]

[1] Geological and Geophysical Institute of Hungary, Budapest, Hungary

[2] Institute for Geological and Geochemical Research, Research Centre for Astronomy and Earth Sciences, Hungarian Academy of Sciences, Budapest, Hungary

[3] Laboratoire de Géologie, University of Lyon, France

[4] School of Earth and Space Sciences, University of Science and Technology of China, Hefei, China

[5] Lithosphere Fluid Research Lab, Eötvös Loránd University, Budapest, Hungary

[6] Bayerisches Geoinstitut, Universität Bayreuth, Germany

[7] Centre de Recherche Pétrographiques et Géochimiques, Université de Lorraine, Vandoeuvre-lès-Nancy, France

[8] Department of Earth Sciences, University of Toronto, Canada

[9] Hungarian Institute for Forensic Sciences, Budapest, Hungary

Corresponding email: kovacs.istvan.janos@mfgi.hu

Keywords: mass spectrometry, FTIR spectrometry, nominally anhydrous minerals

We present new data on both “water” contents (as OH^- and H_2O) and δD values for several clinopyroxene megacrysts from alkaline basalts. These parameters were first obtained from five clinopyroxene megacrysts applying both the classical “off-line” vacuum extraction technique and the “on-line” high-temperature pyrolysis technique. Blanks measured with the “on-line” gas extraction technique were low enough to exclude any contamination by atmospheric moisture. The comparison of data has revealed that the “on-line” procedure is more effective for the extraction of “water” from clinopyroxenes and, consequently, this “on-line” technique was applied to eight additional clinopyroxene megacryts. δD values cover a similar range from -95‰ to -45‰ (VSMOW) regardless the studied locations, whereas the total “water” content varies from ~115 to ~2570 ppm. The structural hydroxyl content of clinopyroxene megacrysts measured by micro-FTIR spectrometry varies from ~0 to 476 ppm expressed in molecular water equivalent. The total “water” concentrations determined by mass spectrometry differs considerably from structural hydroxyl contents constrained by micro-FTIR, thus indicating that considerable fraction of the “water” may be present in (nano)-inclusions. The structural hydroxyl concentration correlates positively with the δD values of clinopyroxene megacrysts for each locality, indicating that structurally bond hydrogen in clinopyroxenes may have δD values higher than molecular water in inclusions. This implies that that there may be a significant hydrogen isotope fractionation for structural hydroxyl during crystallization of clinopyroxene, while for molecular water there may be no or only negligible isotope fractionation (Kovács et al., 2016).

Kovács, I., Demény, A., Czuppon, G., Lécuyer, C., Fourel, F., Xia, Q.-K., Liu, J., Pintér, Z., Király, E., Török, K., Szabó, Á., Deloule, E., Falus, G., Fancsik, T., Zajacz, Z., Sándorné Kovács, J., Udvardi, B. (2016): Water concentrations and hydrogen isotope compositions of alkaline basalt hosted clinopyroxene megacrysts and amphibole clinopyroxenites: the role of structural hydroxyl groups and molecular water. *Contrib. Mineral. Petrol.*, **171**, 38.

QUENCH *p*H MODELLING OF $CePO_4$-MONAZITE AND YPO_4-XENOTIME-KCl-H_2O SOLUBILITY EXPERIMENTS AT 800°C AND 1 GPa

Mair P.*[1], Tropper P.[1], Manning C.E.[2] & Harlov D.[3]
[1] Institut für Mineralogie und Petrographie, Universität Innsbruck, Austria
[2] Department of Earth and Space Sciences, University of California, Los Angeles, CA, USA
[3] Helmholtz Zentrum Potsdam, GFZ Deutsches GeoForschungsZentrum, Potsdam, Germany
Corresponding email: philipp.mair@uibk.ac.at

Keywords: monazite and xenotime solubility, experimental petrology, REE mobility

Monazite ($CePO_4$) and xenotime (YPO_4) are important accessory minerals in metamorphic and igneous rocks, and are particularly suitable for assessing the role of fluids at high pressures and temperatures, where metasomatic activity is important but poorly understood. The two phosphate minerals represent important reservoirs for light-group rare earth elements (LREE) and heavy rare earth elements (Y+HREE). Their mobilities and metasomatic activities in crustal and mantle fluids are especially important, and thus can be used to monitor elemental mass transfer in high P-T settings (Newton & Manning, 2010). We have investigated the influence KCl-H_2O aqueous fluids on the solubility behaviour of synthetic Ce-monazite, and Y-xenotime at 800°C and 1.0 GPa using 3 mm diameter / 1 cm long Pt capsules arc welded shut and the piston-cylinder apparatus (NaCl setup, cylindrical graphite oven). The experimental results indicate a weak increase in monazite and xenotime solubility for aqueous fluids with a moderate KCl mole fraction (X_{KCl}). Their solubility increases from 8 and 46 ppm in pure H_2O to 336 and 171 ppm, respectively, at X_{KCl} = 0.5. In contrast to the NaCl-H_2O system (Tropper et al., 2011), monazite and xenotime solubilities in the system KCl-H_2O are considerably lower. We also present, by means of a simple example, a comprehensive step-by step procedure to consistently derive a quench pH model of the aquatic system, based on the amount of limiting reactant to calculate the amount of product produced. The influence of the quench *p*H of the monazite-xenotime-KCl-H_2O aqueous solution (with different X_{KCl}) is calculated including the effect of equilibration of this system due to a set of acid-base reactions in local equilibrium. This possibility of quantifying influences of modelled processes on the pH generates a powerful tool for understanding the internal *p*H dynamics of the system.

Newton, R.C. & Manning, C.E. (2010): Role of saline fluids in deep-crustal and upper-mantle metasomatism: insights from experimental studies. *Geofluids*, **10**, 58-72.

Tropper, P., Manning, C.E., Harlow, D. (2011): Solubility of $CePO_4$ monazite and YPO_4 xenotime in H_2O and H_2O-NaCl at 800°C and 1 GPa: implications for REE and Y transport during high-grade metamorphism. *Chem. Geol.*, **282**, 58-66.

THERMODYNAMIC MODELING CONSTRAINTS ON INCIPIENT MELT COMPOSITIONS IN THE CARBONATED UPPER MANTLE

Massuyeau M.*[1], Le Trong E.[1], Gardés E.[2], Aulbach S.[3], Morizet Y.[4] & Gaillard F.[1]

[1] Institut des Sciences de la Terre d'Orléans, Centre National de la Recherche Scientifique, Université d'Orléans, Bureau de Recherches Géologiques et Minières, Orléans, France

[2] Centre de Recherche sur les Ions, les Matériaux et la Photonique, Centre National de la Recherche Scientifique, Commissariat à l'énergie atomique et aux énergies alternatives, Ecole Nationale Supérieure d'Ingénieurs de Caen, Université de Caen Basse Normandie, Caen, France

[3] Institut für Geowissenschaften, Goethe-Universität Frankfurt am Main, Germany

[4] Laboratoire de Planétologie et Géodynamique de Nantes, Université de Nantes, Nantes Atlantique Universités, Centre National de la Recherche Scientifique, Nantes, France

Corresponding email: malcolm.massuyeau@cnrs-orleans.fr

Keywords: thermodynamic modeling, mantle incipient melting, CO_2-H_2O volatiles

For several decades, important experimental work has improved our understanding of igneous processes, which laid the groundwork for MELTS, a series of powerful thermodynamic models computing crystal-liquid equilibria. MELTS is essentially calibrated for silicate melt compositions and intends to cover processes ranging from magma crystallization upon cooling to melting of the mantle in presence of H_2O. Here, we developed a model specifically calibrated for mantle melting in presence of CO_2 and H_2O. Numerous experimental, geochemical, petrological and geophysical studies have revealed the presence of H_2O-bearing carbonated silicate melts in the upper mantle. Such melting regimes producing low melt fractions, usually referred to as “incipient melting”, operate in a large P-T domain of the upper mantle, where carbonate, carbonated silicate and silicate melts can be equilibrated with mantle peridotites. The transition between these liquids can be sharp and operates via immiscibility between a carbonatitic melt and a carbonated silicate melt, provided that enough carbonate is present to saturate both liquids.

A first, simplified model based on the silica activity in the melt (Massuyeau et al., 2015) has shown the ability of thermodynamic modeling to describe and predict incipient melting of carbonated peridotite. Here, we report a multicomponent model defining the excess Gibbs free energy of melts ranging in composition from carbonatite to basalt.

ThermoLIQS describes the activity-composition relationships of melt components using a Margules formalism. This parameterization is calibrated on crystal-liquid, diamond/graphite-liquid, fluid-liquid and liquid-liquid equilibria obtained by experimental studies in the P-T range ~ 1-10 GPa and ~ 1000-2000°C. The strength of this model lies in the use of the experimental and thermodynamic uncertainties in the calibration, by weighting and readjusting experimental points within quoted uncertainties.

ThermoLIQS is a powerful tool to better understand and constrain the evolution of the melts at depth. A preliminary application of *ThermoLIQS* defining the dynamics of mantle melting within an ascending plume emphasizes the important role of lithosphere thickness in the transition between kimberlites and OIBs from a single plume source.

Massuyeau, M., Gardés, E., Morizet, Y., Gaillard, F. (2015): A model for the activity of silica along the carbonatite–kimberlite–mellilitite–basanite melt compositional joint. *Chem. Geol.*, **418**, 206-216.

MAGMATIC WATER CONTENT OF PICO VOLCANO (AZORES ISLAND, PORTUGAL) AS RECORDED BY CLINOPYROXENE PHENOCRYSTS

Nazzareni S.*[1], Barbarossa V.[2], Skogby H.[3], Zanon V.[4-5] & Petrelli M.[1]

[1] Dipartimento di Fisica e Geologia, Università di Perugia, Italy

[2] Department of Environmental Science, Radboud University Nijmegen, Netherlands

[3] Department of Geosciences, Swedish Museum of Natural History, Stockholm, Sweden

[4] Center for Volcanology and Geological Risks Assessment, University of the Azores, Ponta Delgada, Portugal

[5] Institut de Physique du Globe de Paris, France

Corresponding email: sabrina.nazzareni@unipg.it

Keywords: pyroxenes, magma volatile content, FTIR

The volcanic rocks of Pico Volcano (the Azores Islands, North Atlantic Ocean) commonly contain numerous clinopyroxene crystals. We used clinopyroxene crystals to reconstruct shallow magmatic processes of the central volcano, since this mineral phase may record variations of intensive parameters, like *P*, *T* and fO_2, as well as trace elements like water. This late forming phase can incorporate H^+ that may be used to calculate the water content of magma at the shallow magma ponding stages and contribute to understand the evolution processes before magma ascent.

The Pico volcanic island is formed by an almost perfect conical stratovolcano and an ESE-WNW trending elongated ridge, constituted by cinder cones, associated to fissural eruptions.

Samples are millimetric euhedral phenocrysts from a cumulitic lava flows and centimetric euhedral crystals from the Pic16 mugearite lava flow erupted during the early stages of the 1718 AD eruption. On the same crystal we carried out single-crystal polarized FTIR and Mössbauer spectroscopy, single-crystal X-ray diffraction, electron probe micro-analysis and laser-ablation ICP-MS.

Pyroxenes, that are diopside ($Wo_{45-46}\ En_{45-48}\ Fs_{06-09}$) in composition, have very weak or absent OH^- vibrational bands in the IR spectra (except in PIC16). From the integration of the OH^- vibrational bands we calculated a H_2O content from 0 to 91 ppm H_2O. These low contents are related to H^+ loss during ascent to surface or post-eruptive re-equilibration, which may occur via the redox reaction $Fe^{2+} + OH^- = Fe^{3+} + O^{2-} + ½H_2$. To recover the possibly lost H^+ we performed thermal annealing experiments under H_2 gas flux at 700 and 800°C. All the samples increased their hydrogen content and reached saturation after 65-83 hours, depending on crystal thickness. The new H_2O values reached 93-170 ppm in crystals from the cumulitic lava and 120-182 ppm in PIC16. The untreated clinopyroxenes have a Fe^{3+}/Fe_{tot} ratio between 18.8-25.8%, which after the thermal annealing remains constant or slightly decrease. Using the H-saturation values and the partition coefficients of O'Leary et al. (2010) we calculated 0.71-1.17 H_2O wt.% in melt, which is slightly lower than those measured by FTIR in melt inclusions in olivines from the Pico fissure zone (Métrich et al., 2014).

According to literature data, Pico primary magmas were produced at around 3 GPa and 1352-1362°C, by a very low melting degree of a mantle source characterized by 350-630 ppm of H_2O, then melts ascended up to 15-18 km (around 0.5 GPa), where Fo-poor olivine and clinopyroxene crystallised and accumulated in a storage areas (Métrich et al. 2014; Zanon & Frezzotti, 2013). The clinopyroxene geobarometry suggests that they crystallized at around 0.5 GPa except PIC64 that crystallized deeper at around 1 GPa. The H^+ loss occurred during the ascent or a late stage of eruption.

O'Leary, J.A., Gaetani, G.A., Hauri, E.H. (2010): The effect of tetrahedral Al^{3+} on the partitioning of water between clinopyroxene.and silicate melt. *Earth Planet. Sci. Letters*, **297**, 111-120.

Métrich, N., Zanon, V., Creon, L., Hildenbrand, A., Moreira, M., Marquez, F.O. (2014): Is the "Azores Hotspot" a wetspot? Insight from the geochemistry of fluid and melt inclusions in olivine of Pico Basalts. *J. Petrol.*, **55**, 377-393.

Zanon, V. & Frezzotti, M.L. (2013): Magma storage and ascent conditions beneath Pico and Faial islands (Azores archipelago): A study on fluid inclusions. *Geochem. Geophys. Geosyst.*, **14**, 3494-3514.

MEASURED VOLATILITIES OF IMPORTANT TRACE ELEMENTS IN THE EARTH

Norris C.A.*[1] & Wood B.[1]
[1] Department of Earth Sciences, University of Oxford, United Kingdom
Corresponding email: ashley.norris@earth.ox.ac.uk

Keywords: volatility, activity, trace elements

The loss rates of volatile elements from silicate melts are of considerable interest to a number of branches of volcanology, petrology and geochemistry. In the volcanic context emanation coefficients are used as empirical measures of the extent of loss of individual elements in the gas phase. In geochemistry and cosmochemistry relative loss rates control the pattern of element depletions during melting and core segregation on asteroids and protoplanets. Incorporation of such differentiated, pre-melted bodies probably influenced the well-known pattern of volatile element depletion in silicate Earth.

We began our study by considering the condensation of a wide range of elements from a solar gas. The calculated order of relative volatility in the case we have studied is V < Cu < Ag < Sb < Ga < Ge < Bi ~ Pb < Sn < Cd < Tl ~ In (Lodders, 2003). This does not correlate well with emanation coefficients in volcanic systems. The latter also do not correlate with the diffusion coefficients of the elements in silicate melts (Johnson & Canil, 2011). Given the latter observation we started with the hypothesis that volatile loss is more likely related to oxygen fugacity and speciation than to diffusion to the melt-gas interface. We therefore constructed a furnace to investigate relative loss-rates from well-stirred silicate melts under controlled oxygen fugacity conditions. Experiments were performed on trace-element doped basalt at 1300^{o}C and oxygen fugacities from just above FMQ to values about 6 log units below FMQ.

Almost all elements studied exhibited increasing volatility with decreasing oxygen fugacity. The order of volatility did not change significantly in this fO_2 range, however, but is dramatically different from the condensation sequence. At FMQ measured relative volatilities are V < Ga < Pb < In < Tl ~ Sb ~ Ag < Cu < Sn < Ge < Cd < Bi. The order we observe here is broadly consistent with independent activity measurements we have made on silicate melts. It is also in much better agreement with measured emanation coefficients than the condensation sequence and goes someway to explaining the high relative abundance of In in silicate Earth, i.e., In is less volatile than previously calculated.

Johnson, A. & Canil, D. (2011): The degassing behavior of Au, Tl, As, Pb, Re, Cd and Bi from silicate liquids: Experiments and applications. *Geochim. Cosmochim. Acta*, **75**, 1773-1784.

Lodders, K. (2003): Solar system abundances and condensation temperatures of the elements. *Astrophys. J.*, **591**, 1220-1247.

REDOX CONDITIONS OF A CO_2-BEARING SPINEL PERIDOTITE AS FUNCTION OF COMPOSITION, PRESSURE AND TEMPERATURE, AND THE ARCHAEAN DEEP CARBON CYCLE

Stagno V.*[1], Ziberna L.[2], Andreozzi G.B.[1], Lenaz D.[3], Lustrino M.[1], Mollo S.[1] & Scarlato P.[4]
[1] Dipartimento di Scienze della Terra, Sapienza Università di Roma, Italy
[2] School of Earth Sciences, University of Bristol, United Kingdom
[3] Dipartimento di Matematica e Geoscienze, Università di Trieste, Italy
[4] Istituto Nazionale di Geofisica e Vulcanologia, Roma, Italy
Corresponding email: vincenzo.stagno@uniroma1.it

Keywords: spinel peridotite, oxybarometry, carbon cycle

Chromium-rich spinel can be stable in peridotites down to ~ 200 km in subcratonic lithospheric roots, where diamonds usually form. Despite not being typical Fe-rich phases, mantle spinels show up to 20 wt.% FeO_{tot} and variable Fe^{3+}/Fe_{tot} ratios up to ~ 40%. This implies that this mineral can play a key role during redox processes involving C-O-H fluids, such as carbon precipitation and redox melting. A number of oxygen barometers have been calibrated to determine the fo_2 of peridotites based on the chemical equilibrium of olivine-orthopyroxene-spinel-bearing assemblages:

$$3\ Fe_2Si_2O_6 + 2\ Fe_3O_4 = 6\ Fe_2SiO_4 + O_2 \quad (1)$$

expressed as Fe end-members (Wood, 1990; Ballhaus et al., 1991). However, considering the highly variable Cr content and its effect on spinel stability at high pressures (Klemme, 2004), the accuracy of this oxy-thermobarometer would benefit of an in-depth experimental investigation.

This study aims to investigate 1) the effect of pressure and spinel composition on the fO_2 calculated using (1), and 2) the iron oxidation state of Mg-chromite equilibrated at fO_2 buffered by carbon/carbonate equilibrium (Stagno & Frost, 2010).

To this end, we performed experiments in a simplified Mg-Fe^{2+}-Fe^{3+}-Cr-Al-Si-O-C model peridotite obtained by a stoichiometric mixture of natural olivine + orthopyroxene + spinel + magnesite + graphite equilibrated at 2.5-5 GPa and 1000-1400°C. Experiments were carried out using a Walker-type multi anvil press (840 ton) available at the HP-HT Laboratory of Experimental Volcanology and Geophysics of the National Institute of Geophysics and Volcanology (INGV) in Rome (Italy). Oxygen fugacities buffered by the carbon/carbonate equilibrium, i.e., enstatite–magnesite–olivine–diamond (EMOD) buffer, were experimentally measured using as redox sensor the Ir(Pt)-Fe alloy.

Results from these experiments will allow to: 1) compare the redox conditions for carbon and carbonate stability using the Fe^{3+}/Fe_{tot} ratio of spinel-bearing peridotite rocks; 2) determine the redox conditions in spinel-bearing peridotites at pressures and temperatures where diamonds form, and 3) track the redox evolution of the upper mantle in Archean by combining thermodynamic calculations with the obtained experimental data.

Ballhaus, C., Berry, R.F., Green, D.H. (1991): High pressure experimental calibration of the olivine-orthopyroxene-spinel oxygen geobarometer: implications for the oxidation state of the upper mantle. *Contrib. Mineral. Petrol.*, **107**, 27-40.

Klemme, S. (2004): The influence of Cr on the garnet–spinel transition in the Earth's mantle: experiments in the system MgO–Cr_2O_3–SiO_2 and thermodynamic modelling. *Lithos*, **77**, 639-646.

Stagno, V. & Frost, D.J. (2010): Carbon speciation in the asthenosphere: experimental measurements of the redox conditions at which carbonate-bearing melts coexist with graphite or diamond in peridotite assemblages.*Earth Planet. Sci. Letters*, **300**, 72-84.

Wood, B.J. (1990): An experimental test of the spinel peridotite oxygen barometer. *J. Geophys. Res.*, **97**, 15845-15851.

STABILITY OF HYDROUS DEFECTS IN QUARTZ AT UPPER CRUSTAL CONDITIONS

Stalder R.*[1]
[1] Institut für Mineralogie und Petrographie, Universität Innsbruck, Austria
Corresponding email: roland.stalder@uibk.ac.at

Keywords: quartz, quartzite, hydrous defects

Quartz is a nominally anhydrous mineral that crystallizes under various rock-forming conditions in hydrous systems. As a consequence, traces of water are incorporated as hydrous defects, whose abundance and local structure depends on pressure, temperature and available metal impurities. Each type of hydrous defect gives rise to a characteristic absorption band in the infrared (IR) range. Hence, the hydrous defect inventory can be qualitatively and quantitatively characterised by IR-spectroscopy. In most metamorphic rocks, concentrations of hydrous defects are rather low, suggesting that the water fugacity was low. However, even if hydrous defects in quartz crystals from several different metamorphic rock types have been reported, so far detailed and systematic data have not been published.

In this study high-pressure experiments were performed in a cold seal pressure vessels at 3 kbar and 650°C over different temperature intervals in the system quartz – muscovite without free water fluid. The starting material contained fragments from a crushed and sieved natural hydrothermal quartz that was mixed with natural muscovite in order to simulate a water fugacity of a mica-bearing quartzite. Seven crystals from the starting material and each experimental charge were manually oriented parallel to the crystallographic *c*-axis and ground to wafers of 50-190 µm thicknesses, and polarised IR measurements parallel to the main refractive indices were performed on each grain.

Initial results show that the absorption band at 3480 cm^{-1} (Li-specific OH-defect) decrease continuously with time at the cost of the absorption band 3378 cm^{-1} (Al-specific OH-defect), while the total amount of defect water stays more or less constant. Interestingly, the rate at which the first type of band decreases is in accord with preliminary determined dehydration kinetics, suggesting that one defect is destroyed while the other type is formed from the deliberated hydrogen. It is therefore suggested that the second type of defect is stable at the run conditions of the experiments described here. The preliminary findings from this study may explain the dominance of Al-specific over Li-specific hydrous defects in natural quartz from quartzite. Further experiments will be performed in the same system at different temperatures, and in other systems containing fluid phases with different compositions. Furthermore, the dehydration kinetics of the different OH-defects has to be determined in more detail and with better precision.

NITROGEN CYCLING IN THE EARLY PRECAMBRIAN: A MAJOR PLAYER IN EARLY EVOLUTION AND GREENHOUSE WARMING

Stüeken E.E.*[1-2]
[1] Department of Earth & Space Sciences and Astrobiology Program, University of Washington, Seattle, WA, USA
[2] Department of Earth Sciences, University of California, Riverside, CA, USA
Corresponding email: evast@uw.edu

Keywords: nitrogen isotopes, Precambrian, biogeochemical nitrogen cycle

Nitrogen is an essential nutrient for all life on Earth and could have severely influenced the pace and trajectory of early evolution. Furthermore, it is the major constituent of Earth's atmosphere and significantly enhances the warming capacity of greenhouse gases through pressure broadening. Changes in atmospheric N_2 pressure could therefore have played a major role in global climate (Goldblatt et al., 2009, Som et al., 2015). A critical factor in the atmospheric N_2 budget is the onset and degree of nitrogen drawdown into sediments through time. I will present new constraints showing that (a) nitrogen burial is trivial in the absence of life, (b) nitrogen concentrations in Paleoarchean metasedimentary biotite grains are indicative of biological nitrogen utilization, and (c) nitrogen isotopes in Mesoarchean shales and carbonates reveal enzymatic N_2 fixation into biomass (Stüeken et al., 2015). These results further support an early origin of life prior to 3.8 Ga and an early origin of the molybdenum-based nitrogenase enzyme prior to 3.2 Ga. Using a numerical box model, I will show that biological nitrogen burial could thus potentially have lowered atmospheric pN_2 to a minimum of 40% modern levels in the Neoarchean, consistent with paleobarometric results from Som et al. (2015). The sequestered nitrogen would have been stored primarily in continental crust. With the onset of widespread oxidative weathering around 2.4 Ga, pN_2 would likely have rebound. New Paleoproterozoic nitrogen isotope data support the idea of a transition to a mostly aerobic nitrogen cycle at this time. The Mesoproterozoic shows a return to anaerobic conditions and stratification, as supported by isotopic data from three separate basins. A modern nitrogen cycle was probably not established until the Neoproterozoic or early Phanerozoic. In conclusion, the nitrogen cycle has been shaped markedly by the evolution of Earth's biosphere and vice versa. This has implications for evaluating measurements of nitrogen abundance and speciation on other planets.

Goldblatt, C., Claire, M.W., Lenton, T.M., Matthews, A.J., Watson, A.J., Zahnle, K.J. (2009): Nitrogen-enhanced greenhouse warming on early Earth. *Nature Geosci.*, **2**, 891-896.

Som, S., Catling, D., Buick, R. (2015): A recipe for changing terrestrial air pressure 2.7 Gyr ago: redox states, biology and plate tectonics. Astrobiology Science Conference, Chicago, abstr., #7657.

Stüeken, E.E., Buick, R., Guy, B.M., Koehler, M.C. (2015): Isotopic evidence for biological nitrogen fixation by molybdenum-nitrogenase from 3.2 Gyr. *Nature*, **520**, 666-669.

SUBDUCTION-RELATED MANTLE METASOMATISM BENEATH THE EASTERN TRANSYLVANIAN BASIN?

Szabó Á.*[1], Tóth A.[2], Hidas K.[3], Kovács Z.[1], Patkó L.[1] & Szabó C.[1]

[1] Lithosphere Fluid Research Lab, Department of Petrology and Geochemistry, Institute of Geography and Earth Sciences, Eötvös University, Budapest, Hungary

[2] Department of Environmental Sciences, Sapientia Hungarian University of Transylvania, Cluj-Napoca, Romania

[3] Instituto Andaluz de Ciencias de la Tierra, Consejo Superior de Investigaciones Científicas & Universidad de Granada, Spain

Corresponding email: abel.szabo.hu@gmail.com

Keywords: mantle xenolith, amphibole, metasomatism

The Plio-Pleistocene alkali basalts in the Carpathian–Pannonian Region (CPR) brought a large amount of lithospheric mantle xenoliths to the surface. The easternmost and youngest alkaline basaltic volcanic field is developed in the Perşani Mountains (Eastern Transylvanian Basin), where numerous peridotite and pyroxenite xenoliths have been collected (Szabó et al., 2004, and references therein). By studying these xenoliths, we may have an insight into the upper mantle regarding its chemical and physical processes, such as partial melting, metasomatism and deformation.

We selected seven amphibole bearing spinel lherzolite/hornblendite composite, and four amphibole-clinopyroxenite xenoliths for this paper in order to study mantle metasomatic processes, as well as to evaluate their possible geodynamic implications. The amphibole appears as disseminated grains in lherzolite or forms hornblendite and amphibole-pyroxenite veins/bodies. The peridotites contain small amounts of interstitial amphibole, whereas the hornblendites and amphibole-clinopyroxenites contain occasionally other OH-bearing minerals such as apatite and phlogopite as well. The amphiboles and clinopyroxenes in spinel lherzolites are depleted in incompatible trace elements, whereas the same minerals in hornblendites and amphibole-pyroxenites show elevated incompatible trace element content. These geochemical variations of the texturally defined amphiboles and their high La/Lu ratios suggest that the hornblendites and amphibole-pyroxenites formed by an incompatible element enriched mafic silicate melt (Powell et al., 2004). Since the incompatible element content of hornblendites are similar to those of amphibole-pyroxenites, it is probable that they crystallized from the same melt, depending on H_2O saturation of the liquid. Based on major and trace elements data, this melt could originate from partial melting of a previously metasomatized mantle section (Chalot-Prat & Bouiller, 1997). These features indicate a complex melt-mantle interaction beneath the study area, which can be related to the subduction of the European plate beneath the Eastern Carpathians (Wortel & Spakman, 2000) occurring in Neogene and causing extensive melt percolation and mantle metasomatism.

Chalot-Prat, F. & Bouiller, A. (1997): Metasomatism in the subcontinental mantle beneath the Eastern Carpathians (Romania): new evidence from trace element geochemistry. *Contrib. Mineral. Petrol.*, **129**, 284-307.

Powell, W., Zhang, M., O'Reilly, S.Y., Tiepolo, M. (2004): Mantle amphibole trace-element and isotopic signatures trace multiple metasomatic episodes in lithospheric mantle, western Victoria, Australia. *Lithos*, **75**, 141-171.

Szabó, C., Falus, G., Zajacz, Z., Kovács, I., Bali, E. (2004): Composition and evolution of litosphere beneath the Carpathian-Pannonian Region: a review. *Tectonophys.*, **393**, 119-137.

Wortel, M.J.R. & Spakman, W. (2000): Subduction and slab detachment in the Mediterranean-Carpathian region. *Science*, **290**, 1910-1917.

ANALYSIS OF HYDROGEN IN NOMINALLY ANHYDROUS MINERALS BY TRANSMISSION RAMAN SPECTROSCOPY

Weis F.A.*[1-2], Lazor P.[2] & Skogby H.[1]
[1] Department of Geosciences, Swedish Museum of Natural History, Stockholm, Sweden
[2] Department of Earth Science, Uppsala University, Sweden
Corresponding email: franz.weis@nrm.se

Keywords: NAMs, hydrogen, Raman spectroscopy

During growth from a hydrous magma nominally anhydrous minerals (NAMs) such as clinopyroxene include small amounts of hydrogen in structural defects (e.g., charge deficiencies) and interstitial spaces where it is bonded to oxygen and, regarded as an oxide component, can be expressed as water concentration. The amount of water present in the minerals can serve as a proxy to estimate magmatic water contents or the water content in the mantle of planetary bodies (e.g., Peslier, 2010; Weis et al.; 2015). Common methods for analysis of water in NAMs are FTIR or SIMS which, however, require orientation of the crystals, limited spatial resolution or result in the loss of sample material. An alternative method may be provided with Raman spectroscopy (e.g., Bolfan-Casanova et al., 2014) which has the advantage of very small analysis spot sizes and its non-destructive nature. Yet one problem with backscattered Raman spectroscopy may be the strong effect of fluorescence background due to heating of dark crystals which might interfere with the bands of weakly Raman active molecules such as water. In addition, the obtained Raman spectrum is only representative for a single spot within the sample. Thus we tested the analysis of known water contents in orientated, very thin and nearly transparent crystals of clinopyroxene and garnet by transmission Raman spectroscopy. By such, the quality of the Raman spectra improved as fluorescence background was reduced drastically and the Raman signal of water was increased and more representative of the whole rather than a single point within the crystal. The improved spectra can be used for an internal calibration using water and silica bands to develop a method for quantification of water in NAMs using Raman spectroscopy.

Bolfan-Casanova, N., Montagnac, G., Reynard, B. (2014): Measurement of water contents in olivine using Raman spectroscopy. *Am. Mineral.*, **99**, 149-156.

Peslier, A.H. (2010): A review of water contents of nominally anhydrous natural minerals in the mantles of Earth, Mars and the Moon. *J. Volcanol. Geotherm. Res.*, **197**, 239-258.

Weis, F.A., Skogby, H., Troll, V.R., Deegan, F.M., Darehn, B. (2015): Magmatic water contents determined through clinopyroxene: Examples from the Western Canary Islands, Spain. *Geochem. Geophys. Geosyst.*, **16**, 2127-2146.

Session S4:

Fluids in the crust

Conveners:

Maria Luce Frezzotti (Milano – Italy)

Cristoph Heinrich (Zurich – Switzerland)

Thomas Mueller (Leeds – United Kingdom)

CENTRE POSITION OF RAMAN SPECTROGRAPHIC BANDS OF GASES IN FLUID INCLUSIONS

Bakker R.J.*[1]
[1] Department Angewandte Geowissenschaften und Geophysik, Montanuniversität Leoben, Austria
Corresponding email: bakker@unileoben.ac.at

Keywords: Raman spectroscopy, fluid inclusions, CO_2-CH_4

The centre position of Raman bands of CO_2 and CH_4 has been used to estimate the density of the gases with purely empirical equations at known temperature and occasionally pressure within fluid inclusions. However, modifications of the centre position are relatively small compared to the resolution of most commercial available Raman spectrometers, therefore, a band-shape best-fit procedure with established cumulative distribution functions (DF) has been applied to apparently improve accuracy and precision of the centre positions. An error of 0.03 cm^{-1} has been claimed (Fukura et al., 2006) for Raman spectrometers with spectral resolution of 1.35 cm^{-1} (e.g., labRAM) and 0.45 cm^{-1} (e.g., labRAM HR). This approach is highly ambiguous, and not reproducible, as illustrated by Bakker (2011). There has been no attempt to standardize calibration of measurements and calculation procedures.

Raman band positions can be calibrated with emission spectrum of noble gases (e.g. Neon) or with standard Raman spectra (e.g., cyclohexane). Neon has very narrow well-defined bands, but detectors may register the signal over at least 6 to 12 pixels of the CCD camera. Consequently, the Neon bands also have to be fitted to DF's to obtain their centre position. However, most DF's do not fit well to these bands. The full width at half maximum (FWHM) of these fits is about 1.7 cm^{-1} (corresponding to a standard deviation of approximately 0.7 cm^{-1}), even for a high-resolution apparatus. Cyclohexane has relatively wide bands, and the centre position of these bands have a standard deviation of 0.3 to 1.0 cm^{-1} (e.g., McCreery Group, and NIST). Abundant publications use a double calibration method, but that is doubling the uncertainty in centre positions of Raman bands. For example, cyclohexane was calibrated with Neon emission lines, and, subsequently, the measurement was calibrated with this cyclohexane. A variety of cumulative DF's are available (e.g. Gaussian, Lorentzian, Voigt) and each function reveals a different centre position (0.2 cm^{-1} variability) and FWHM (1 cm^{-1} variability) of the same Neon band. The selected best-fit cumulative DF that were used in literature to reproduce CO_2 and CH_4Raman bands have very low R^2 numbers, i.e. they do not fit very well the morphology of the bands. For example, a CH_4 Raman band does not fit well to a Gaussian DF. The R^2 number is highly dependent on the number of pixels that are taken into account for fitting procedures. If most of these pixels represent a background signal than a R^2 close to 1 is obtained, even if those pixels that define the Raman band do not match the fit very well.

In conclusion, the uncertainty in density calculation of CO_2 and CH_4 in fluid inclusions as obtained from Raman band centre position can be as high as 40%. Microthermometry, a classical method to obtain gas densities from homogenization temperatures), reveals uncertainties of only about 0.3%, and is therefore a superior method.

Bakker, R.J. (2011): Accuracy, precision and uncertainty of peak position estimation of CO_2 and CH_4 in Raman spectra. *Ber. Geol. Bundes.*, **87**, 32-33.

Fukura, S., Mizukami, T., Odake, S., Kagi, H. (2006): Factors determining the stability, resolution, and precision of a conventional Raman spectrometer. *Appl. Spectrosc*., **60**, 946-950.

CONTROL OF STABLE ISOTOPE EXCHANGE BY NET-TRANSFER AND DISSOLUTION-RECRYSTALLIZATION REACTIONS AROUND HYDROTHERMAL VEINS IN CARBONATES

Baumgartner L.P.*[1], Bégué F.[1], Bouvier A.-S.[1], Putlitz B.[1], Vennemann T.[2] & Baumgartner C.[1]
[1] Institut des Sciences de la Terre, Université de Lausanne, Switzerland
[2] Institut des Dynamiques de la Surface Terrestre, Université de Lausanne, Switzerland
Corresponding email: lukas.baumgartner@unil.ch

Keywords: fluid flow, stable isotope exchange, SIMS

Extensive fluid flow has been documented in contact aureoles using stable isotope geochemistry (e.g., Baumgartner & Valley, 2001). Here we present a detailed petrologic, cathodoluminescence (CL) and secondary ion mass spectrometry (SIMS) study of reactions driven by infiltration of magmatic fluids in carbonate host-rocks of the Bergell and Adamello intrusions (Alps, Italy). The large difference in stable isotope composition of the original sedimentary carbonates protolith and the fluids interacting with igneous rocks permits the tracing of small amounts of reactive fluid flow in the host rocks.

Abundant veins formed in large (10 m to 100 m) carbonate xenoliths at Alpe Sissone (Malenco, Bergell; e.g., Bucher, 1998). The veins studied have a central zone interpreted to have been open cracks, now filled by olivine (ol) and calcite (cc), or tremolite (tr) and cc. The crack is surrounded by a replacement zone, where ol + cc replaced the original host dolomite (do). Gas-mass-spectrometry isotope analysis of calcite, olivine, and dolomite revealed very steep, sub-mm-sized isotope fronts for carbon of over 4‰ and oxygen of over 8‰ at the replacement front between the cc+ol zone and the dolomitic host rocks (Taylor & Bucher, 1986; Bégué 2008). Apparent oxygen isotope equilibrium between ol and cc gives a formation temperature of 540°C, in agreement with estimates from phase petrology.

However, detailed CL and SIMS studies allow us to demonstrate that the reaction front progressed several grain sizes (mm to cm) further into the host rock, recrystallizing parts of dolomite grains along grain boundaries and across grains, Sparse calcite was precipitated along some grain boundaries. Similar observations were made around rare veins crosscutting the pure dolomite host rocks in contact with the Bruffione Granodiorite in the southern Adamello (Passo di Bondolo), suggesting that our observations are general and can be used to constrain fluid-rock around veins.

Several hundred SIMS analyses in the reaction zone demonstrate that calcite grains in the vein are not zoned with respect to oxygen isotopes. No isotopic gradient towards the vein wall was observed in the cc+ol zone. In contrast, dolomite grains display abundant zoning close to the vein, with cores (dark in CL) having sedimentary isotope values. Lighter CL zones, surrounding and crosscutting the dolomite grains have isotope compositions trending towards equilibrium with the infiltrating fluid with proximity to the vein. While the zones with different CL are crystallographically continuous, there is a sharp (sub-µm scale) CL and isotopic boundary separating the zones.

We interpret the data to show that the silica front lagged behind a dolomite recrystallization front. Isotopic exchange happened through mineral reactions where silica activity is high enough to form olivine, while minerals mainly recrystallization further away from the vein. The often observed fingering of the isotopic front is controlled by this latter recrystallization of dolomite grains. To accurately model isotopic fronts it is necessary to couple them to mineral reactions due to element transport and mineral recrystallization.

Baumgartner, L.P. & Valley, J.W. (2001): Stable isotope transport and contact metamorphic fluid flow. *Rev. Mineral. Geochem.*, **43**, 415-467.

Bégué, F. (2008): Etude des veines métasomatiques dans les xénolites carbonatés de la bordure Est de l'intrusion du Bergell, Val Sissone (Italie). Master Thesis, Univ. Lausanne.

Bucher, K. (1998): Growth mechanisms of metasomatic reaction veins in dolomite marbles from the Bergell Alps. *Mineral. Petrol.*, **63**, 151-171.

Taylor, B.E. & Bucher-Nurminen, K. (1986): Oxygen and carbon isotope and cation geochemistry of metasomatic carbonales and fluids - Bergell aureole, Northern Italy. *Geochim. Cosmochim. Acta*, **50**, 1267-1279.

ION PROBE DATING OF HYDROTHERMAL CLEFT MONAZITE TRACKING EXHUMATION AND BRITTLE TECTONIC EVOLUTION IN THE CENTRAL ALPS

Bergemann C.*[1], Gnos E.[2], Berger A.[3] & Whitehouse M.[4]
[1] Département de Sciences de la Terre, Université de Genève, Switzerland
[2] Muséum d'Histoire Naturelle, Genève, Switzerland
[3] Institut für Geologie, Universität Bern, Switzerland
[4] Swedish Museum of Natural History, Stockholm, Sweden
Corresponding email: christian.bergemann@unige.ch

Keywords: monazite, Th-U-Pb dating, hydrothermal vein

In situ dating of mm-sized hydrothermal monazite by ion probe is an excellent method for understanding the low-T tectonic history of an area. Hydrothermal monazite from open alpine type fissures (clefts) has the advantage of recording the age of crystallization without the risk of diffusional lead-loss at the prevalent temperatures. Due to partial dissolution-reprecipitation, there is the added potential to record more than one age for the temperature range of ca. 350-200ºC. To capture as wide an age range recorded in the crystals as possible, 15 to more than 30 ion-probe analyses were performed on more than 20 mm-sized monazite samples according to internal zonation.

All analyzed samples come from a wide area in the Central Alps encompassing the Lepontine metamorphic dome and the eastern half of the Rhone-Simplon fault, one of the major fault systems of the Alps. The region has a complex tectonic history, with greenschist to amphibolite facies metamorphism predated by and partly overlapping with nappe stacking. This was followed by exhumation, particularly in the central part and further folding and thrusting. Later brittle deformation affecting the entire region, in combination with hydrothermal fluid flow worked to produce the famous mineralized Alpine clefts of the Lepontine area. The westernmost part of the region was dominated by dextral strike-slip deformation along the Rhone-Simplon Line.

The dating of cleft monazites revealed ^{232}Th-^{208}Pb ages between 19 and 5 Ma over several age groups. Ages generally decrease from east to west, with the westernmost areas recording significantly younger ages than the rest of the area. Almost all samples have in common that they suggest an event affecting the entire area at around 10 to 12 Ma. Combined with already published data from more local studies of the surrounding area as well as other chronological methods, the monazite data provide an overview over part of the brittle tectonic history of much of the Central Alps.

TOURMALINE'S RECORD OF FLUID HISTORY IN THE W TAUERN WINDOW

Berryman E.*[1], Kutzschbach M.[1-2], Trumbull R.B.[1], Meixner A.[3] & Franz G.[2]
[1] Chemie und Physik der Geomaterialien, Helmholtz Zentrum Potsdam, GFZ Deutsches GeoForschungsZentrum, Potsdam, Germany
[2] Fachgebiet Mineralogie-Petrologie, Technische Universität Berlin, Germany
[3] Fachbereich Geowissenschaften & Zentrum für Marine Umweltwissenschaften, Universität Bremen, Germany
Corresponding email: berryman.eleanor@gmail.com

Keywords: tourmaline, fluid history, metamorphism

Tourmaline (Tur) is a common accessory mineral in the metasedimentary Pfitsch Formation located in the Pfitscher Joch area in the W Tauern Window of the Eastern Alps. These post-Variscan metasedimentary units experienced peak metamorphic conditions of ~550°C, 1.0 GPa during the Alpine orogeny (Selverstone et al. 1984). Tur is most abundant in a ~25 m thick unit of feldspathic gneiss (~20-200 ppm B), where it occurs as idiomorphic crystals, typically 10 mm in length. The abundance and size of the Tur crystals increases near coarse-grained quartzofeldspathic segregations (~1200 ppm B), reflecting the mobilization and concentration of B by the metamorphic fluid. Near segregations, individual Tur crystals have up to three growth zones, recording pro- (~350–500°C, 0.7-1.0 GPa) and retrograde (400°C, 0.2 GPa) growth as determined by textural information and sector-zoning thermometry. Retrograde Tur occurs as individual crystals, as well as overgrowths on prograde Tur crystals, especially on the surface of extensional fractures formed by regional E-W extension during decompression.

Tur in the Pfitsch Formation is dravitic with variable Fe contents, reflecting that of the host unit. They are zoned in major and trace elements, as well as boron isotope composition. Charge balance calculations indicate that a significant proportion of their Fe is ferric, supporting the interpretation of a subaerial continental sedimentary protolith. Tur near segregations has the highest minimum ferric iron content, which decreases with crystal growth, potentially reflecting the gradual reduction of the fluid during metamorphism. The Mg/(Mg+Fe) ratio increases with prograde Tur growth and subsequently decreasing with retrograde growth, consistent with trends in metamorphic Tur zonation from the literature. In contrast, the Ca/(Ca+Na) ratio increases gradually from 0.05 to 0.20 with prograde growth and continues to increase up to <0.25. Based on the Ca-Na Tur-fluid partitioning experiments of Berryman et al. (2016), the Ca/(Ca+Na) ratios recorded in the Tur represent the maximum Ca/(Ca+Na) ratio of the fluid throughout metamorphism.

The metasediments of the Pfitsch Formation display relatively light $\delta^{11}B$ values (-15 to -34‰) with the heaviest values found near B-rich segregations, and the lightest values in B-depleted samples. This correlation reflects the preferential mobilization of ^{11}B towards the segregations. Isotopic zonation of individual tourmaline crystals with -11‰ in their cores and -20‰ in their rims suggests continuous volatilization and fractionation of B by a ^{10}B-rich precursor mineral (e.g. mica) during prograde mobilization and redistribution of B within the Pfitsch Formation. Due to the rather heavy whole rock B-isotope ratios in the neighbouring units (Variscan basement gneiss unit: -3 to -8‰; pre-Variscan basement: -10 to -17‰) contribution of external fluids during tourmaline growth is unlikely.

Berryman, E.J., Wunder, B., Rhede, D., Schettler, G., Franz, G., Heinrich, W. (2016): P-T-X controls on Ca and Na distribution between Mg-Al tourmaline and fluid. *Contrib. Mineral. Petrol.*, **171**, 1-14.

Selverstone, J., Spear, F.S., Franz, G., Morteani, G. (1984): High-pressure metamorphism in the SW Tauern Window, Austria: P-T paths from hornblende-kyanite-staurolite schists. *J. Petrol.*, **25**, 501-531.

NATURE AND ORIGIN OF Si-RICH FLUIDS AT 13°20'N SILICIFIED OCEANIC DETACHMENT FAULT (MID-ATLANTIC RIDGE)

Bonnemains D.*[1], Verlaguet A.[2], Escartin J.[1], Mével C.[1], Boiron M.-C.[3] & Andreani M.[4]
[1] Equipe de Géosciences Marines, Institut de Physique du Globe de Paris, France
[2] Institut des Sciences de la Terre de Paris, Université Pierre et Marie Curie, Paris, France
[3] Laboratoire GeoRessources, Centre de Recherches sur la Géologie des Matières, Vandoeuvre-lès-Nancy, France
[4] Laboratoire de Géologie, Université de Lyon 1, France
Corresponding email: bonnemains@ipgp.fr

Keywords: oceanic detachment fault, fault silicification, fluid inclusions

Slow-spreading ridges display a mode of accretion involving long-lived detachment faults (DFs) rooting deep below the axis. These DFs localize deformation accommodating a high proportion of the plate separation, while exhuming deep crustal and upper mantle rocks to the seafloor. They are also associated with fluid circulation that can be channelized by the fault zone. To better constrain deformation mechanisms and associated fluid circulation in such systems, we investigated the 13°20'N oceanic DF rooting at the ridge axis along the Mid-Atlantic Ridge, during the ODEMAR cruise (2013, R/V Pourquoi Pas?) with deep-sea vehicles. This DF is of particular interest as it is active, well-developed structurally, and hosts an active hydrothermal site. Seven fault outcrops were identified and sampled along the corrugated DF surface and on the flanks of microbathymetric corrugations. Deformation is highly localized along fault surfaces that systematically show subhorizontal striations subparallel to extension. Fault rocks are breccias made of basaltic clasts and rare ultramafic clasts variably silicified, that also show striated fault surfaces at the sample scale. Microstructural and petrological observations indicate pervasive syntectonic silicification during fault exhumation.

To characterize the nature and origin of silicifying fluids and constrain the conditions of fluid-rock interaction, we studied fluid inclusions (FIs) trapped in quartz grains from two highly silicified metabasaltic samples (fault mirrors), one poorly silicified metabasaltic breccia, and a silicified ultramafic sample. All FIs are biphasic. The highly silicified samples present higher homogenization temperatures (250-350°C) than those from poorly silicified ones (150-200°C). Most FIs record salinities higher than that of seawater (4-6 wt.% eq. NaCl) with one exhibiting salinities up to 10 wt.% eq. NaCl. Mineral hydration reactions alone cannot account for the formation of such high salinity fluids, which most likely formed by fluid phase separation at high temperature. Raman spectroscopy also shows that high salinity fluids contain $H_2 \pm CH_4 \pm CO_2$, suggesting an interaction of these fluids with ultramafic rocks present in the footwall of the detachment. LA-ICP-MS analyses reveal that salinity is a mixture of NaCl and KCl. We propose that these fault rocks record hydrothermal fluids that have witnessed both the hydration of ultramafic rocks, likely involving serpentinization and associated H_2 release, and phase separation in the presence of a heat source at depth. These fluids are then channelized along the fault zone, where they may interact with shallower seawater-like fluids potentially from the basaltic hanging wall. Fluid mixing and pathways along the fault plane may have been highly variable both spatially (salinity and gas content vary significantly among nearby samples) and in time (strong variations in fluid composition from core to rim of quartz crystals), and is likely tectonic.

SEAFLOOR HYDROTHERMAL VENTING AT VOLCANIC RCS AND BACKARCS

de Ronde C.E.J.*[1] & Stucker V.K.[1]
[1] Department of Marine Sciences, GNS Science, Lower Hutt, New Zealand
Corresponding email: Cornel.deRonde@gns.cri.nz

Keywords:

Arc and backarc seafloor hydrothermal systems are closely linked to subduction zones. The concomitant range in rock compositions (i.e., basalts, basaltic andesites, dacites and rhyolites) and the variable, although relatively shallow depths to vent sites (i.e., from near surface to < 2000 m water depth) mean that they have the capacity to discharge hydrothermal emissions distinct from those at mid-ocean ridges. Arc and backarc hydrothermal systems can be broadly categorized into magmatic-hydrothermal sites – which are the most prevalent and include some that are erupting – and water/rock-dominated sites. The former are characterized by gases exsolved from the underlying magma that ascend rapidly through the crust to mix with seawater, forming acid, sulfate and elemental sulfur before being expelled on the seafloor. The latter are older, have formed circulation cells, and show the effects of interaction between hydrothermal fluids and the host rocks. Both these systems have the capacity to form ore deposits.

RECONSTRUCTING THE CIRCULATION OF PALEO-FLUIDS THROUGH FLUID INCLUSION STUDIES: THE CASE OF THE IRON-MINERALIZATION OF EASTERN ELBA ISLAND

Fregola R.A.*[1], Ruggieri G.[2], Rimondi V.[2], Zucchi M.[1], Punzi C.[1], Brogi A.[1] & Liotta D.[1]
[1] Dipartimento di Scienze della Terra e Geoambientali, Università di Bari, Italy
[2] Istituto di Geoscienze e Georisorse, Consiglio Nazionale delle Ricerche, Firenze, Italy
Corresponding email: rosaanna.fregola@uniba.it

Keywords: fluid inclusions, Elba Island, hydrothermal Fe-mineralization

In eastern Elba Island (Tuscany, Italy), the mid-upper crustal Porto Azzurro granitoid (5.9 Ma) gave rise to a widespread boron-rich contact metamorphic aureole, intense hydrothermal circulation, and Fe-ore deposits (magnetite, hematite, pyrite). These hydrothermal Fe-ore deposits are considered representative of paleo-fluids that circulated in a geothermal system interpreted as the analogue of the Larderello geothermal fields.

In this presentation, fossil geothermal fluids entrapped within quartz, calcite and adularia crystals from Fe-ore bodies of eastern Elba Island have been studied by means of microthermometry, Laser Ablation Inductively Coupled Plasma Mass Spectrometry (LA-ICP-MS), and Scanning Electron Microscopy (SEM). The analysed fluid inclusions are mainly of the L-type, i.e., biphase liquid-vapor (L+V) inclusions that homogenize in the liquid phase. Multiphase (L+V+S) fluid inclusions with halite daughter-minerals (S) have been sporadically observed in calcite and adularia crystals. A database of microthermometric results based on the analyses performed up-to-now on a total number of 1100 fluid inclusions in 32 samples from seven localities (Terra Nera, Bacino, Valle Giove, Topinetti, Cala Seregola, Capo Pero, and Fornacelle) at different distances moving from the Porto Azzurro pluton to the North, has been produced. By comparing these results, a general trend characterized by decreasing homogenization temperatures (Th) and salinities of the fluids with increasing distance from Porto Azzurro has been observed.

Acknowledgements: The research leading to these results has received funding from the European Community's Seventh Framework Programme under grant agreement No. 608553 (Project IMAGE), and from PONa3_00369 SISTEMA (University of Bari).

CHARACTERIZATION OF FLUIDS AND ELEMENT TRANSFERS ASSOCIATED TO GARNET VEIN AND CORONA DEVELOPMENT DURING GRANULITIZATION

Ganzhorn A.C.*[1-2], Verlaguet A.[1] & Austrheim H.[3]

[1] Sorbonne Universités, Université Pierre et Marie Curie, Centre National de la Recherche Scientifique, Institut des Sciences de la Terre de Paris, France

[2] Laboratoire de Sciences de la Terre, Centre National de la Recherche Scientifique, Ecole Normale Supérieure, Lyon, France

[3] Department of Geosciences, University of Oslo, Norway

Corresponding email: anneceline.ganzhorn@gmail.com

Keywords: granulites, fluids, coronitic garnet

Porosity, permeability and fluid content of deep continental crustal rocks play a fundamental role on crucial properties such as rock rheology and rock ability to concentrate mineral resources. Granulitic rocks correspond to high – temperature metamorphic rocks that constitute most of the lower crust. Granulites are classically considered as dry rocks, mostly because their equilibrium P-T conditions are above the dry solidus. However, numerous studies have evidenced the presence of low water activity CO_2-rich fluids during granulitic reactions. A fundamental issue is to understand the potential role of such fluids during granulitization processes: are granulitization reactions fluid-assisted or can they occur in completely dry conditions? How do fluids influence granulitic mineral growth and associated element transfer?

To address these key questions, we studied a massif of Precambrian granulitic rocks from the Western Gneiss Region in Norway: the Flatraket massif. It corresponds to quartz-monzonites exhibiting the granulite facies assemblage garnet + plagioclase + K-feldspar + biotite ± clinopyroxene ± quartz. These rocks are considered as completely dry, due to both the absence of Caledonian eclogitic retrogression and the coronitic texture of garnets, interpreted as solid-state diffusion. However, we observed garnet veins texturally associated to these coronas, suggesting fluid-driven mass transfer. Moreover, the similar garnet composition in both textures (EMPA analyses) suggests that veins and coronas formed coevally, at granulitic P-T conditions. We performed a detailed microstructural and petrological study (EMPA, SEM, pseudosections) of these rocks that allowed deciphering the complex sequence of granulitic reactions that finally gave rise to both garnet coronas and veins. We also evidenced several kinds of fluid traces in these rocks: inclusions in both vein and coronitic garnets look like CO_2-rich fluid inclusions, whereas inclusions in feldspars and quartz are rather aqueous (or brines); moreover, myrmekites and brines-derived textures were observed at feldspar grain boundaries. We here present the results of the detailed microstructural study and of microthermometric studies of these fluid inclusions, and propose a scenario that reconciles the a priori paradoxal coeval formation of garnet veins and coronas.

IN-SITU IRON ISOTOPE STUDY OF IRON ORE AND BANDED IRON FORMATION FROM THE CARAJÁS MINERAL PROVINCE, BRAZIL

Halder S.*[1], Lehmann B.[1], Cabral A.R.[1], Horn I.[2] & Weyer S.[2]
[1] Fachgebiet Lagerstätten und Rohstoffe, Technische Universität Clausthal, Germany
[2] Institut für Mineralogie, Leibniz Universität Hannover, Germany
Corresponding email: stefan.halder@tu-clausthal.de

Keywords: BIF, iron ore, Fe isotopes

The Carajás mineral province in northern Brazil represents one of the largest iron ore districts in the world. BIF-hosted iron ore deposits, with a resource of > 18 Gt at a grade of 66 wt.% Fe, form plateaux on the northern and southern ranges of the Serra dos Carajás. We studied the Fe isotope composition of BIF from the Neoarchean Carajás Formation, friable hematite-goethite ore (so-called soft ore) and superficial iron duricrust using *in-situ* femtosecond laser ablative MC-ICP-MS.

The positive Fe isotope composition of magnetite-rich bands in oxide facies BIF samples indicates formation by either abiologic partial oxidation or biogenic oxidation by anoxygenic phototrophic bacteria. The homogeneity of δ^{56}Fe values of magnetite in a 37 cm BIF drillcore interval, which should be representative of sedimentation over a period of ≥ 2 ka, shows that the rate of iron oxidation did not change significantly over timespans of several thousand years. However, variations in the Fe isotope composition of magnetite from different BIF units point to long-term depositional changes.

The studied iron ore consists of martite – that is, hematite pseudomorphic after magnetite – microplaty hematite and goethite. Martite has homogeneous Fe isotope values similar to magnetite in fresh BIF, which suggests in-situ formation by quantitative replacement of magnetite. This shows that iron remained mostly immobile during the geological history.

The δ^{56}Fe values of microplaty hematite resemble the homogeneous Fe isotope composition of martite and magnetite. The formation of microplaty hematite requires temperatures in excess of 80°C. Such temperatures would characterize retrograde metamorphism or hydrothermal overprint, during which the stability of hematite relative to magnetite increases with decreasing temperature. The presence of trace amounts of pyrite and chalcopyrite in all samples demonstrates that such a hydrothermal overprint affected the Carajás Formation. However, this overprint occurred in a system largely closed with respect to iron, since the Fe isotope signature remained essentially unfractionated.

By contrast, goethite formed in an open system during subrecent/recent weathering and has a more variable Fe isotope composition, compared to the earlier magnetite-martite-microplaty hematite association. Significant scatter in the Fe isotope composition of goethite indicates fractionation processes in a fluid-dominated system – that is, weathering and supergene iron enrichment.

THE DEEP WATER CYCLE THROUGH THE LITHOSPHERE

Hermann J.*[1]
[1] Institut für Geologie, Universität Bern, Switzerland
Corresponding email: joerg.hermann@geo.unibe.ch

Keywords: subduction, fluids, nominally anhydrous minerals

Mass transport through the lithosphere is tightly linked to the deep water cycle as aqueous fluids and hydrous melts are key agents to mobilize elements from the small scale to km-scale. This presentation will highlight the different modes of water transport and how it influences chemical and physical processes in the lithosphere through subduction recycling.

Water is incorporated into hydrous minerals when oceanic crust reacts with seawater-derived fluids close to the ocean floor. As the hydrous phases are dragged down the subduction channel they break down due to increasing pressure and temperature. Examples will be shown from the field, experiments and from thermodynamic modelling on how water liberation occurs during the breakdown of antigorite in subducted serpentinites. New experimental data on the stability of chlorite show the importance of this phase for transporting water to depth of 100-150 km in subduction zones, depending on the thermal structure of the slab.

The water liberated from the breakdown of hydrous phases interacts with altered oceanic crust and sediments. It will be discussed at which conditions aqueous fluids, hydrous melts or supercritical fluids with intermediate composition form and how this influences the mass transport of major and trace elements from the slab into the mantle wedge.

Beyond the stability of hydrous phases, water can be transport in nominally anhydrous minerals in the mantle. The comparison of experimental results on water incorporation into olivine with natural samples from mantle xenoliths shows that H is substituting for Si in olivine, with consequences for the rheology of the upper mantle. Experiments also provide evidence that the capacity of water incorporation into mantle rocks increases with increasing pressure. Therefore the questions arise on how much water is stored in the mantle and if the global water cycle is in secular equilibrium or not. As experiments will provide only information about the storage capacity of the mantle, it is essential to gain more information from natural rocks on how and how much water is present in the lithosphere. To correctly interpret the data from natural rocks, it is necessary to know to what extent minerals are able to retain their water contents on the way back to the surface. Thus, we need to understand H transport by diffusion at the micro-scale. I will present recent results that show that H diffusion in olivine is more complex than previously thought with diffusivities depending also on the site where H is incorporated.

ISOTOPIC COMPOSITION (δD, $\delta^{34}S$, $\delta^{13}C$) OF THE ORDOVICIAN BLACK SLATES HOSTING THE RETORTILLO-SANTIDAD URANIUM DEPOSIT (SALAMANCA, SPAIN)

Huertas F.J.*[1], Gervilla F.[1-2] & Delgado-Huertas A.[1]

[1] Instituto Andaluz de Ciencias de la Tierra, Consejo Superior de Investigaciones Científicas, Universidad de Granada, Spain

[2] Departamento de Mineralogía y Petrología, Universidad de Granada, Spain

Corresponding email: javierhuertas@ugr.es

Keywords: black slates, stables isotopes, uranium deposits

The Retortillo-Santidad uranium deposit is hosted by Ordovician black slates of the Iberian zone, located near the Bañobarez granite intrusion (Salamanca province, NW Spain). It consists of three main ore assemblages: i) coffinite-pitchblende-pyrite-calcite filling veins/breccias, 2) coffinite-pitchblende fine-grained aggregates disseminated in altered zones, and 3) autunite filling cross-cutting veins. Whereas the first assemblage could be considered as primary, the distribution of the other two assemblages correlate with the alteration zoning of the host black shales. Mineralogical and geochemical characterization suggests a multi-stage genetic process starting with a primary concentration of uranium with organic matter in sediments, followed by probably two events of hydrothermal remobilization of uranium in veins and ending with supergene remobilization and concentration of uranium by downward percolating acid solutions (Huertas et al., 2013).

Isotopic composition of deuterium, organic carbon and sulfur in sulfides were analyzed to understand the deposit origin and evolution. We have found a wide spectrum of sulfur isotopic compositions in sulfides varying from -40 to +25‰ $\delta^{34}S$. Although some additional analyses will be necessary these data indicate sulfides have been altered through several processes, probably including bacterial reduction of sulfates, that have produced important isotopic fractionation in relatively open system (most negatives values) and Rayleigh processes in more close system. The sulfur isotopic composition of these sulfides overlaps with that of those reported by Both et al. (1994) ($\delta^{34}S$ = -51.3 to -10‰) in the uranium ores of Mina Fe. The euxinic nature of the environment is also supported by the C isotopic composition of graphite which shows relatively constant around -27 ‰ (V-PDB). Additionally, some disperse $\delta^{13}C$ values ranging from -22 to -33‰, probably due to organic matter maturation processes. Values of δD plot mainly between -90 and -110 ‰ (V-SMOW), with some disperse values ranging between -41 and -143‰, showed no dependence with depth or drill core and correspond to equilibrium with meteoric fluids, probably those associated with late alteration by downward percolating solutions.

Both, R.A., Arribas, A., de Saint-André, B. (1994): The origin of breccia-hosted uranium deposits in carbonaceous metasediments of the Iberian Peninsula: U-Pb geochronology and stable isotope studies of the Fe deposit, Salamanca Province, Spain. *Econ. Geol.*, **89**, 584-601.

Huertas, F.J., Gervilla, F., Gwatkin, C. (2013): Uranium mineralization in the Retortillo-Santidad area (Salamanca, Spain): Role of late alteration. Proc. 12th SGA Biennial Meeting, 4, 1594-1597.

HOT AQUEOUS FLUIDS: ARE THEY THE KEY TO HTLP REGIONAL AUREOLES?

Jessop K.*[1], Daczko N.[1] & Piazolo S.[1]
[1] Department of Earth and Planetary Sciences, Macquarie University, Sydney, Australia
Corresponding email: kim.jessop@mq.edu.qu

Keywords: hot aqueous fluids, regional aureoles, HTLP metamorphism

The Wongwibinda Metamorphic Complex in northern New South Wales, Australia, has been used as a case study to investigate the role of hot fluids in producing steep metamorphic field gradients associated with HTLP regional aureoles. The Complex is located in the Carboniferous accretionary prism of the New England Orogen, the youngest of a series of orogens that comprise the Tasmanides of eastern Australia. Metasedimentary rocks ranging in grade from bioitite facies to migmatite are associated with a wide zone of ductile shearing and S-type granitoids.

A recently mapped, structurally separated, block west of the main complex reveals a steep metamorphic field gradient (> 70°C km^{-1}) along the Aberfoyle River. The well-exposed metasedimentary rocks progressively increase in metamorphic grade from biotite- to garnet-cordierite-bearing rocks over a traverse of approximately 2 km. The Aberfoyle transect lacks the intrusive rocks that are common elsewhere in the complex.

Evidence for the role of hydrous fluids in the metamorphism is provided by whole rock XRF and isotopic analyses of samples from the Aberfoyle transect. There is strong positive correlation between metamorphic grade and potassium content, $^{87}Sr/^{86}Sr$ and $\delta^{18}O$. In contrast, there is a negative correlation between grade and sodium content, calcium content and $^{143}Nd/^{144}Nd$.

Higher-grade rocks of the main complex are exposed approximately 14 km further east in a second apparently steep metamorphic field gradient that builds to metasedimentary migmatites. The migmatites are spatially associated with a broad, probably anastomosing, shear zone. Garnet and/or cordierite surrounded by leucosome in metasedimentary rocks and abundant dykes and small bodies of two-mica granite suggest that anatectic melt formed *in situ* and was also injected into the migmatite. Muscovite-bearing granite is consistent with high water contents and links to the influx of hot aqueous fluids inferred in the Aberfoyle transect. Abundant collapse structures trace magma pathways through the migmatite.

The mechanisms of heat advection at Aberfoyle and in the migmatites of Wongwibinda are interpreted to be part of a continuum. The source of fluid is proposed to derive from the first metamorphic cycle of the accretionary complex of the New England Orogen during crustal thinning and mantle fluxing caused by subduction roll-back. Early metamorphic fluid produced in the deeper accretionary complex is channelled up fault, and other weak structural zones, advecting heat to shallower crustal levels. As metamorphism in the deep crust progresses, partial melts produce S-type magma that migrates up the same channels, further advecting heat. The decreasing availability of water in the deep crust as metamorphism progresses self arrests the system, resulting in short-lived (<1 0 m.y.) metamorphism in the shallow crust that produces steep metamorphic field gradients of narrow extent.

SUBMARINE HYDROTHERMAL PROCESSES, MIRRORING THE GEOTECTONIC EVOLUTION OF THE NE HUNGARIAN JURASSIC SZARVASKÕ UNIT

Kiss G.B.*[1], Zagyva T.[1], Pásztor D.[1] & Zaccarini F.[2]
[1] Department of Mineralogy, Eötvös Loránd University, Budapest, Hungary
[2] Department Angewandte Geowissenschaften und Geophysik, Universität Leoben, Austria
Corresponding email: gabriella.b.kiss@ttk.elte.hu

Keywords: submarine fluid-rock interaction, fluid inclusion study, mineral and rock chemistry

The Jurassic pillow basalt of the NE Hungarian Szarvaskõ Unit is a part of an incomplete ophiolitic sequence, formed in a back-arc- or marginal basin (Aigner-Torres & Koller, 1999). Different, often superimposing hydrothermal processes were studied with polarising microscopy, EPMA, fluid inclusion microthermometry, chlorite thermometry (Zang & Fyfe, 1995), Raman spectroscopy and ICP OES, aiming to characterise them and to discover their relationship with the geotectonic evolution of the region.

Closely packed pillow, pillow fragmented hyaloclastite breccia and peperitic facies were found in the studied localities. The rocks underwent a primary and a cooling related, local submarine hydrothermal process immediately after eruption. Albite, chlorite, prehnite, pyrite, quartz, calcite, pumpellyite and clay minerals precipitated in the groundmass, in cooling cracks, in small amygdales, in the matrix of the interpillow hyaloclastite and the hyaloclastite breccia facies. The chlorite formed at 183°C (st.dev. 7°C), while the minimum formation temperature of quartz and calcite was 130-170°C. The obtained salinity (4-10 NaCl eq. wt.%) revealed an evolved seawater origin, while methane content was found, where unconsolidated sediment was present nearby.

A superimposing, bigger fluid circulation system resulted in the intense alteration of the basalt to clay minerals, goethite, chlorite and quartz, as well as in the formation of mostly pyrite filled cavities, with rare galena, sphalerite, chalcopyrite, pentlandite, quartz, barite, chlorite, albite and sericite. Pyrite contains up to 0.075 mass% As, up to 0.092 mass% Co and traces of Ag, Au, Cu, Zn, Te and Se. Whole rock geochemical data shows similarities to other low temperature submarine hydrothermal sulphide deposits (Bogdanov et al., 2006).

Basalt may be completely altered to grossular (with high Mn content), chlorite and quartz. The chlorite precipitated at 190°C (st.dev. 18°C). This mineral assemblage formed by the superimposing effect of Ca-metasomatism similar to the *s. l.* rodingitization. However, here this is more likely related to processes in ridge-setting (see, e.g., Austrheim & Prestvik, 2008), differently from *s. s.* rodingites.

Epigenetic veins containing albite, quartz, chlorite, calcite, prehnite, pumpellyite and at places, datolite formed at increasing temperature 160-210°C and pressure 0.6-1.1 kbar, from a low salinity (0.2-2 NaCl eq. wt.%), methane bearing fluid. These results suggest an Alpine regional metamorphism (see Árkai, 2001) related origin.

The observed hydrothermal minerals represent several different steps of the geotectonic evolution of the Szarvasõ Unit; from the ridge setting in the back-arc/marginal basin till the subduction and obduction. Though the found mineral paragenesis are often similar, careful study can help in distinguishing the superimposing fluid-rock interaction processes.

The work was supported by the Hungarian Science Foundation (OTKA, PD 112580 to G. B. Kiss).

Aigner-Torres, M. & Koller, F. (1999): Nature of the magma source of the Szarvaskő complex (NE- Hungary). *Ofioliti*, **24**, 1-12.

Árkai, P. (2001): Alpine regional metamorphism in the main tectonic units of Hungary: a review. *Acta Geol. Hung.*, **44**, 329-344.

Austrheim, H. & Prestvik, T. (2008): Rodingitization and hydration of the oceanic lithosphere as developed in the Leka ophiolite, north-central Norway. *Lithos*, **104**, 177-198

Bogdanov, Y.A., Lisitzin, A.P., Sagalevich, A.M., Gurvich, E.G. (2006): Hydrothermal ore genesis of the ocean floor. Nauka, Moscow, 527 p.

Zang, W. & Fyfe, W.S. (1995): Chloritization of hydrothermally altered bedrock at the Igarape Bahia gold deposit, Carajas, Brazil. *Mineral. Dep.*, **30**, 30-38.

COUPLED HYDROGEN, OXYGEN AND SILICON ISOTOPE SYSTEMATICS OF GROUNDWATER-MAGMA INTERACTION IN ICELANDIC HYDROTHERMAL SYSTEMS

Kleine B.I.*[1], Stefánsson A.[1], Halldórsson S.A.[1], Whitehouse M.[2], Barnes J.D.[3], Jónasson K.[4] & Franzson H.[5]
[1] Institute of Earth Science, University of Iceland, Reykjavik, Iceland
[2] Swedish Museum of Natural History, Stockholm, Sweden
[3] Jackson School of Geoscience, University of Texas, Austin, TX, USA
[4] Icelandic Institute of Natural History, Garðarbær, Iceland
[5] Iceland Geosurvey, Reykjavik, Iceland
Corresponding email: barbarak@hi.is

Keywords: fluid-rock interaction, stable isotopes, isotope fractionation

Magma intruded in to the crust interacts with the surrounding groundwater system resulting in formation of hydrothermal fluids commonly of meteoric or seawater origin. This process may lead to contact metamorphism and elemental transport with associated elemental and isotope gradients from mantle to surface sources. Recent work suggests that the surface fluids may be a key part of metamorphism to high T (450-600°C) suggesting that classic contact metamorphic reactions like crustal hornfels may result from magma-hydrothermal fluid interaction rather than magma-magmatic fluid interaction (Ingebritsen et al., 2010).

We use stable isotopes (δD, $\delta^{18}O$ and $\delta^{30}Si$) to unravel such contact metamorphic processes and target natural analogues from both ancient and active magmatic geothermal systems throughout Iceland. Quartz grains from various hydrothermal systems, including cuttings from two drill holes fed by seawater (Reykjanes) and meteoric water (Krafla), xenoliths from the Askja central volcano and the fossil pluton at Hafnarfjall as well as quartz grains associated with low-T zeolites were analysed for $\delta^{18}O$ and $\delta^{30}Si$ *in-situ* using SIMS. Whole rock material of these samples was further analysed for δD using a thermal conversion elemental analyser coupled to an IRMS.

Our results indicate a relationship between $\delta^{30}Si$ values and formation temperature of quartz. Low-T quartz (<150°C) are dominated by negative $\delta^{30}Si$ values (-4 to +0.6‰) whereas positive $\delta^{30}Si$ values (-0.5 to +4‰) prevail in quartz precipitated at higher T (200-400°C). $\delta^{30}Si$ values of magmatic quartz clusters around 0.0‰. Combining the results from the analyses of $\delta^{18}O$ and δD allows further division of samples into (i) seawater and/or rock dominated ($\delta^{18}O$: 0 to +15‰; δD: -80 to -60‰) and (ii) meteoric water dominated ($\delta^{18}O$: -10 to +5‰; δD: -120 to -100‰) hydrothermal systems.

Modelling of δD, $\delta^{18}O$ and $\delta^{30}Si$ was used to gain insight into effects of fluid-rock interaction, fluid source and formation temperatures at the magma-groundwater contact. Comparison of analytical and model results shows that the isotope signatures are influenced by multiple processes that also affect the source fluid, water-rock ratios and temperature. In some cases, meteoric- or seawater-derived fluids penetrate the hornfels zone and cause alteration at >400°C by direct groundwater-magma heat interaction. Other cases appear to document “baked” contact zones without any groundwater involvement. This demonstrates that groundwater flow and permeability are crucial at high T (400-600°C) around natural intrusions, as indicated by recent heat and fluid transfer modelling (Scott et al., 2015).

Ingebritsen, S.E., Geiger, S., Hurwitz, S., Driesner, T. (2010): Numerical simulation of magmatic hydrothermal systems. *Rev. Geophys.*, **48**, RG1002.

Scott, S., Driesner, T., Weis, P. (2015): Geologic controls on supercritical geothermal resources above magmatic intrusions. *Nature Commun.*, **6**, DOI: 10.1038/ncomms8837.

IMPLEMENTING METAMORPHIC CONCEPTS IN REACTIVE TRANSPORT MODELLING OF GEOTHERMAL SYSTEMS: CRYSTAL SIZE DESTRIBUTIONS: IDEAL SOLID-SOLUTIONS AND MINERAL ZONING

Kuesters T.*[1-2], Mueller T.[2] & Renner J.[1]
[1] Institut für Geologie, Mineralogie und Geophysik, Ruhr-Universität Bochum, Germany
[2] Institute of Geophysics and Tectonics, School of Earth and Environmental Sciences, University of Leeds, United Kingdom
Corresponding email: tim.kuesters@rub.de

Keywords: fluid-rock interaction, reactive-transport, numerical modelling

Reactive transport models (RTM's) have become important tools for analysis and prediction of fluid-rock interaction under shallow (up to about 5 km, geothermal) and deep (up to maximum crustal depths of 100 km, metamorphic) crustal conditions. Many different RTM's have been developed, some of them attempting to describe the complete thermal-hydraulic-chemical coupling of a system, others focusing on specific processes. However, most RTM's are limited with regard to the implementation of mineral-reaction kinetics often simplified relying on transition state theory or empirical rate laws. Rate laws are typically constrained by single mineral dissolution experiments close to ambient conditions. In addition to scarcity of experimental data for higher temperatures, this approach inherently bears the problem that information on reactive-surface areas is needed to describe dissolution and precipitation kinetics. Constraining reactive-surface areas is often difficult, in particular for mineral precipitation requiring assumptions on reactive-surface area even for phases initially not present in the system.

In this study, we present a new RTM that focusses on accounting for mineral reaction kinetics and uses classical nucleation theory with continuous monitoring of crystal size distributions (CSD's) to constrain the reactive-surface areas and their effect on reaction rates. Ideal mineral-solid solutions are included for the most important mineral phases. These features give our RTM the unique ability to predict CSD's for every mineral phase (primary and secondary) along with its composition and reactive-surface area. The model was developed by coupling a self-coded FORTRAN package with PHREEQC using the iPHREEQC interface (Charlton & Parkhurst, 2011). Processes assumed to reach thermodynamic equilibrium instantaneously, i.e., speciation in the fluid and resulting mineral saturation indices are computed by PHREEQC while our code explicitly computes reaction rates (dissolution and growth), mineral nucleation, 1-D advective-diffusive transport, and changes in hydraulic transport properties. Spatial distribution and temporal evolution of fluid temperature and pressure are input parameters. Accounting for the highly non-linear relation of reaction rates to temperature, a sequential non-iterative operator splitting between transport and chemical calculations was adopted together with a dynamic time step reduction scheme to minimize computation time.

Using hydrous alteration of granite as an example, we present temporally and spatially resolved data for fluid and solid composition, modal abundance of primary and secondary minerals, CSD'S, reactive-surface areas, and their interdependence in the parameter space. The preliminary modeling results highlight the importance of incorporation of complex formulations of mineral-reactions kinetics and solid-solutions into RTM's to adequately describe the effect of fluid-rock interaction at elevated temperatures.

Charlton, S.R. & Parkhurst, D.L. (2011): Modules based on the geochemical model PHREEQC for use in scripting and programming languages. *Comput. Geosci.*, **37**, 1653-1663.

ELEMENT MOBILITY DURING FORMATION OF THE KONGSBERG SILVER DEPOSIT

Kullerud K.*[1], Kotková J.[2-3] & Škoda R.[3]
[1] Norwegian Mining Museum, Kongsberg, Norway
[2] Czech Geological Survey, Prague, Czech Republic
[3] Department of Geological Sciences, Masaryk University, Brno, Czech Republic
Corresponding email: kare.kullerud@bvm.no

Keywords: native silver, veins, mineralogy

Minerals reported from the historical silver mines at Kongsberg, Norway, include native elements (Ag, Au, As, Cu, S, C), sulphides, sulphosalts, selenides, arsenides, carbonates, sulphates, arsenates and halides, in addition to a range of silicate minerals (Neumann, 1944; Bancroft et al., 2001). The area is dominated by Proterozoic (≈ 1.6 Ga) schists and gneisses (e.g., Starmer, 1985). Typical in the area are north-south striking subvertical zones in the gneisses enriched in sulphides, predominantly pyrite and pyrrhotite. These zones are cross-cut by nearly vertical E-W trending calcite veins, inferred to be of Permian age and related to the Oslo Rift (Ihlen et al., 1984). It has been long known that the native silver mineralizations occur exclusively at the intersections between the calcite veins and the sulphide-enriched zones (e.g., Bancroft et al., 2001). Neumann (1944) described the silver-bearing veins as very narrow, varying in width from a few mm, rarely up to 0.5 m.

The ore minerals of the silver-bearing veins show complex textural relationships, suggesting several stages of mineral growth and dissolution. The presence of acanthite, polybasite and chalcopyrite as inclusions in native silver suggest that these minerals formed prior to native silver. The earliest generation of native silver often occurs as euhedral grains, commonly with a thin rim of a sulphoarsenide of composition (Ni,Co,Fe)AsS. A second generation of native silver envelopes the earliest generation with its rims of sulphoarsenide. Late minerals overgrowing native silver include polybasite, freibergite, allargentum and stephanite. Reaction textures between the vein minerals indicate significant variations in S and As of the fluid phase during formation of the veins. Fluid inclusion data (Johansen, 1985) suggests that native silver precipitated during decreasing salinity from 25 to less than 20 wt.% NaCl-equivalents at about 300-250°C.

From the compositions of the vein forming minerals, it is inferred that the ore-forming fluids contained a range of dissolved components, including Ag, Ni, Co, Fe, Cu, Pb, Zn, Ca, Ba, Sb, Se, As, S, F and C. Most likely, the origin of the fluids responsible for the silver bearing vein formation was related to the intrusive activity in the nearby Oslo Rift during Permian time. There are three potential sources for the components that were dissolved and transported by the ore-forming fluid: 1) crystallizing magma, 2) the sedimentary rocks of the Oslo Rift, and 3) the sulphide-enriched zones that were cross-cut by the silver-bearing veins. It has been suggested that Ag and C were derived from the alum shale of the Oslo Rift (Segalstad, 2008), whereas elements such as Fe, Cu, Pb, Zn, Se and S were possibly derived locally from the sulphide-enriched zones.

Bancroft, P., Nordrum, F.S., Lyckberg, P. (2001): Kongsberg revisited. *Mineral. Rec.*, **32**, 181-205.

Ihlen, P.M., Ineson, P.R., Mitchell, I.G., Vokes, F.M. (1984): K-Ar dating of dolerite dykes in the Kongsberg-Fiskum district, Norway, and their relationship with the silver and base metal veins. *Norw. J. Geol.*, **64**, 87-96.

Johansen, H (1985): Geochemistry of hydrothermal processes of the silver bearing calcite veins in Kongsberg (in Norwegian). Cand. scient. dissertation, Univ. of Oslo. 239 p.

Neumann, H. (1944): Silver deposits at Kongsberg. *Norges Geol. Unders.* **162**, 133 p.

Segalstad, T.V. (2008): Thermochemical modelling of the Kongsberg silver ore deposit, Norway. 33rd Int. Geol. Congr. Oslo, Norway (abstr).

Starmer, I.C. (1985): The evolution of the south Norwegian Proterozoic as revealed by the major and mega-tectonics of the Kongsberg and Bamle sectors. *in* "The deep Proterozoic crust in the North Atlantic Provinces", A.C. Tobi, J.L.T. Touret, eds., Reidel, Dordrecht, 259-290.

THE EFFECT OF TETRAHEDRAL B ON THE B ISOTOPE FRACTIONATION BETWEEN OLENITIC TOURMALINE AND FLUID

Kutzschbach M.*[1-2], Wunder B.[1], Trumbull R.B.[1], Meixner A.[3], Heinrich W.[1] & Franz G.[2]

[1] Chemie und Physik der Geomaterialien, Helmholtz Zentrum Potsdam, GFZ Deutsches GeoForschungsZentrum, Potsdam, Germany

[2] Fachgebiet Mineralogie-Petrologie, Technische Universität Berlin, Germany

[3] Fachbereich Geowissenschaften & MARUM - Zentrum für Marine Umweltwissenschaften, Universität Bremen, Germany

Corresponding email: mkutz@gfz-potsdam.de

Keywords: tourmaline, tetrahedral boron, boron isotopes

Tourmaline is the most important carrier of B in crustal rocks and its $^{11}B/^{10}B$ ratio is a powerful tracer for geological mass transfer (Marschall et al., 2006). The stable B isotope fractionation between tourmaline and fluid ($\Delta^{11}B_{tour\text{-}fluid}$) depends on temperature (Meyer et al., 2008). and B coordination, i.e. bond lengths (Kowalski et al., 2013). Tourmalines contain 3 B pfu in trigonal planar coordination $^{[3]}B$, but additional B can be incorporated as $^{[4]}B$ substituting for Si. Here, we present first experimental results unraveling the effect of $^{[4]}B$ on the B isotope fractionation between olenitic tourmaline and fluid.

Piston-cylinder synthesis experiments were performed in the system SiO_2-Al_2O_3-B_2O_3-NaCl-H_2O at 700°C / 40 kbar and run durations of 0.5 h, 2.5 h and 216 h, starting from quartz-Al_2O_3-H_3BO_3 mixtures and NaCl-solutions. The stable phase assemblage after 216 h is olenite + coesite + traces of $AlBO_3$. Olenite occurs as columnar (80 vol%) and acicular crystals (20 vol%). Columnar olenites are large (30 x 150 µm) and chemically homogeneous with 1.5 $^{[4]}B$ pfu. Acicular olenites are chemically zoned with the highest B-contents of 2.5-3 $^{[4]}B$ pfu found in their cores, which form from jeremejevite as a precursor phase. Rims of acicular crystals show lower B-contents similar to the columnar olenites. Columnar and rims of the acicular olenites are considered in equilibrium with the last bulk fluid.

Analyses of the fluids show an increase in $\delta^{11}B$ from -5.9‰ in the starting fluid to -5.2‰ in the final fluid after 216 h. The bulk solid run products after 216 h analyzed with MC-ICP MS show $\delta^{11}B$ of -6.8‰. Rayleigh fractionation modeling of the fluid isotope evolution results in a $\delta^{11}B_{olenite\text{-}fluid}$ of -1.4‰, in agreement with the value of -1.5‰ calculated by Kowalski et al. (2013) for B isotope fractionation between olenites with 1.5 $^{[4]}B$ pfu and fluid at 700°C / 5 kbar. B isotope ratios of the bulk solids are consistent with the Rayleigh fractionation model.

Given the fractionation coefficient derived from the Rayleigh model of the fluid isotope evolution and the $^{[4]}B$ content of the columnar olenites, the estimated $\delta^{11}B_{(olenite\text{-}fluid)}$ at 700°C is -7‰ for the $^{[4]}B$-site only and +1.4‰ for the $^{[3]}B$-site only (latter value taken from Kowalski et al., 2013). Assuming that pressure has no significant influence on isotope fractionation we can give an estimate for the intracrystalline fractionation in olenites, with $\delta^{11}B_{(^{[3]}B - ^{[4]}B)} = +8.4‰$ at 700°C, indicating that the lighter ^{10}B strongly fractionates into the tetrahedral site.

Kowalski, P.M., Wunder, B., Jahn, D. (2013): Ab initio prediction of equilibrium boron isotope fractionation between minerals and aqueous fluids at high P and T. *Geochim. Cosmochim. Acta*, **101**, 285-301.

Marschall, H.R., Ludwig, T., Altherr, R., Kalt, A. Tonarini, S. (2006): Syros metasomatic tourmaline: evidence for very high-$\delta^{11}B$ fluids in subduction zones. *J. Petrol.*, **47**, 1915-1942.

Meyer, C., Wunder, B., Meixner, A., Romer, R.L., Heinrich, W. (2008): Boron-isotope fractionation between tourmaline and fluid: an experimental re-investigation. *Contrib. Mineral. Petrol.*, **156**, 259-267.

SPECTACULAR VIDEO INSPECTIONS OF TWO-PHASE FLUID CONDITIONS AND INVERTED FLUID-DENSITY PROFILES IN OBSERVATION WELLS AT THE KETZIN CO_2 STORAGE SITE, GERMANY – AN ARTIFICIAL ANALOGUE TO VAPOUR DOMINATED GEOTHERMAL SYSTEMS?

Liebscher A.*[1], Henninges J.[2] & Möller F.[1]

[1] Sektion Geologische Speicherung, Helmholtz Zentrum Potsdam, GFZ Deutsches GeoForschungsZentrum, Potsdam, Germany

[2] Sektion Geothermische Energiesysteme, Helmholtz Zentrum Potsdam, GFZ Deutsches GeoForschungsZentrum, Potsdam, Germany

Corresponding email: axel.liebscher@gfz-potsdam.de

Keywords: two-phase fluids, geothermal systems, CO_2 storage

Immiscible fluids within the general system H_2O-salt-non-polar gases are widespread and common phenomena in magmatic, hydrothermal and geothermal systems. Due to high temperatures and great depths direct observation of fluid phase separation and segregation in such systems is in most cases impossible and information is restricted to indirect observations. These include studies of fluid inclusion, petrological and geochemical studies on ancient, now exposed systems, experimental studies and numerical simulations. Exceptions are either those systems that vent and discharge their fluids on the surface (submarine or on-shore) and are thus accessible to direct fluid sampling or geothermal systems that are exploited and are accessible via wellbores. The critical point of CO_2 is at 7.38 MPa / 30.98°C and fluid phase separation and segregation may occur already at notably less uncomfortable *P-T* conditions in CO_2 than in aqueous dominated fluids of natural magmatic, hydrothermal and geothermal systems. Natural CO_2 reservoirs or artificial geological storage of CO_2 in the frame of carbon capture and storage (CCS) activities therefore potentially provide the opportunity to study and directly observe fluid immiscibility processes that can serve as analogues to natural, less accessible systems. Here we report on results from comprehensive wellbore monitoring at the pilot-site for geological CO_2 storage at Ketzin/Havel, Germany. Regular in-well pressure-temperature-depth profiling via routine wireline logging as well as video inspection reveal CO_2 liquid-vapour two-phase conditions over most of the upper parts of the wells overlying CO_2 single-phase regions in the lower well parts. While the upper two-phase parts show heat-pipe effects with stratification into upper, vapour dominated and lower, liquid dominated regimes, the single-phase parts exhibit notable but stable inverted density profiles. The observed in-well fluid dynamics and processes share some fundamental characteristics with vapour-dominated geothermal systems. This contribution focusses on the general CO_2 in-well fluid phase relations and their evolution over more than 2.5 years of monitoring, presentation of spectacular video shoots of the in-well fluid dynamics, and potential applicability of the observed processes to natural magmatic, hydrothermal and geothermal systems.

BORON CONTENT OF ALTERED OCEANIC GABBRO: IMPLICATIONS FOR BORON FLUXES IN SUBDUCTION ZONES

McCaig A.M.*[1], Titarenko S.S.[1], Savov I.P.[1], Cliff R.A.[1], Agostini S.[2] & Boyce A.J.[3]
[1] School of Earth and Environment, University of Leeds, United Kingdom
[2] Istituto di Geoscienze e Georisorse, Consiglio Nazionale delle Ricerche, Pisa, Italy
[3] Scottish Universities Environmental Research Centre, East Kilbride, United Kingdom
Corresponding email: a.m.mccaig@leeds.ac.uk

Keywords: boron, ocean crust, subduction flux

Boron is generally enriched in subduction zone volcanic rocks, and where accompanied by positive values of $\delta^{11}B$, the source is likely to be altered oceanic crust or upper mantle. Furthermore, both [B] and $\delta^{11}B$ decrease systematically with distance from the trench in many subduction zones, and positive spikes in [B] are associated with subduction of transform faults.

We have measured [B], $\delta^{11}B$, $^{87}Sr/^{86}Sr$ and $\delta^{18}O$ in lower crustal gabbros and troctolites collected on IODP Expedition 345 to Hess Deep, immediately east of the Galapagos triple junction in the east Pacific. Olivine is pervasively altered to talc, serpentine and magnetite, and this background alteration is strongly overprinted by prehnite, chlorite and secondary clinopyroxene in the vicinity of fault zones and veins. Samples were collected on a 4km fault scarp exposing lower crustal rocks, and we consider them to be typical of fault-related alteration in the lower oceanic gabbros.

The combination of $\delta^{18}O$ values of 5-6‰ and $^{87}Sr/^{86}Sr$ ratios of 0.704 to 0.706 in prehnite-chlorite assemblages indicates alteration by seawater at 200-300ºC, although secondary clinopyroxene may indicate transient higher temperatures. [B] correlates with $\delta^{11}B$, and both correlate with primary olivine content, with the highest values (29 ppm; 26‰) in serpentinised troctolite, but all the altered gabbroic rocks show high [B] and $\delta^{11}B$ compared to fresh MORB, and we estimate an average value for fault-altered lower gabbros of 17 ppm and +17.5‰. This is much higher in [B] than estimates from either the Oman or Troodos ophiolite, and is the only available value from *in situ* fast-spread crust. Gillis et al. (2014) estimate that the lower gabbros comprise ~ 50% of the total crustal section at Hess Deep.

A major potential reservoir for boron in subducting slabs is serpentinised upper mantle, thought to be altered during bend faulting on outer rises. The usual model for bend fault serpentinistaion is single pass downward movement of fluid due to a pressure gradient set up by fixing of water in serpentine and hence lowering of partial pressure. We show by a simple mass balance calculation that in this model all boron will be taken up in the lower crust and none will reach the mantle. We have modelled hydrothermal circulation in a permeable fault slot using Comsol Multiphysics. Long-lived (> 0.5 Ma) circulation is required to introduce significant boron into the upper mantle, which is unlikely on bend faults but possible along transform faults, thus explaining the [B] anomaly seen above subducted transforms.

We conclude that while water may be introduced to the upper mantle by bend faulting, explaining intermediate earthquakes and perhaps fluxing volcanics in hotter subduction zones, boron is not. On the other hand the lower oceanic crust is a potentially significant but underestimated reservoir of heavy boron.

Gillis, K.M., Snow, J.E., Klaus, A., Abe, N., Adrião, A.B., Akizawa, N., Ceuleneer, G., Cheadle, M.J., Faa,k K., Falloon, T.J., Friedman, S.A., Godard, M., Guerin, G., Harigane, Y., Horst, A.J., Hoshide, T., Ildefonse, B., Jean, M.M., John, B.E., Koepke, J., Machi, S., Maeda, J., Marks, N.E., McCaig, A.M., Meyer, R., Morris, A., Nozaka, T., Python, M., Saha, A., Wintsch, R.P. (2014): Primitive layered gabbros from fast-spreading lower oceanic crust. *Nature*, **505**, 204-207.

INTERNALLY CONSISTENT THERMODYNAMIC DATA FOR HYDROTHERMAL MINERAL SOLUBILITY EQUILIBRIA IN THE SYSTEM Ca-Mg-Na-K-Al-Si-O-H-C-Cl

Miron G.D.*[1-3], Wagner T.[2], Kulik D.A.[3] & Heinrich C.A.[1]
[1] Institut für Geochemie und Petrologie, Eidgenössische Technische Hochschule Zürich, Switzerland
[2] Department of Geosciences and Geography, University of Helsinki, Finland
[3] Forschung für eine nachhaltige Abfallwirtschaft, Paul Scherrer Institut, Villigen, Switzerland
Corresponding email: mirondanro@yahoo.com

Keywords: fluid-rock modeling, thermodynamic database, optimization

The quality of solubility calculations relies on the robustness of thermodynamic models and on the accuracy and internal consistency of the thermodynamic dataset. The standard state Gibbs energies of aqueous ions and complexes were simultaneously refined against a large selection of critically evaluated experimental data on mineral solubility, covering the entire Ca-Mg-Na-K-Al-Si-O-H-C-Cl system over wide ranges in temperature and pressure. The procedure was done using the revised Helgeson-Kirkham-Flowers equation of state and the extended Debye-Hückel activity coefficient model (Helgeson et al., 1981). Thermodynamic properties of solubility-controlling minerals were adopted from the dataset of Holland and Powell (2002; dataset ds55; Holland & Powell 1998) which was assumed to be fully internally consistent and non-adjustable. Results from new high-precision conductance and potentiometric experiments on electrolyte association were used to derive more reliable and accurate equilibrium constants for weak complexation and to constrain the properties of complexes which are insensitive to the solubility data. The global optimization of standard Gibbs energies of aqueous species $G^{o}_{1,298}$ at 1 bar 25 C was performed with the GEMSFITS code (Miron et al., 2015). The optimization procedure was set up in such a way that the speciation equilibria for ion pairs and complexes are always maintained. These complexes and ion pairs were constrained to the freely optimized parameters through the independently derived reaction constants.

Application of our consistency-improving strategies and tools results in equal distribution of errors over the pressure, temperature and compositional space; yields confidence intervals for the optimized parameters; and permits straightforward repetition of fitting procedures when the new or improved experimental data become available. Our method provides a clear guide to future experimentation, by highlighting the most sensitive gaps in fluid-mineral phase equilibria experiments. The dataset reproduces all available fluid-mineral phase equilibria and mineral solubility data with good accuracy over a wide range in temperature, pressure and composition.

Due to the constraints used in the optimization procedure, the only way to resolve the existing discrepancies present in the fluid-mineral equilibria experiments, needed for achieving internal consistency, is to make unavoidable changes to the $G^{o}_{1,298}$ values of some freely adjusted ions. We provide an additional database in agreement with CODATA base ions. The change in $G^{o}_{1,298}$ for the aqueous ions was added with the opposite sign to the respective mineral form the Holland and Powell database, thus preserving all mineral solubilities. The new dataset can be successfully used to model complex multi-component, multi-phase chemical systems, including mineral solubility and aqueous speciation, at the levels of confidence and accuracy that was not possible before (Miron et al., 2016).

Helgeson, H.C., Kirkham, D.H., Flowers, G.C. (1981): Theoretical prediction of the thermodynamic behavior of aqueous electrolytes by high pressures and temperatures; IV, Calculation of activity coefficients, osmotic coefficients, and apparent molal and standard and relative partial molal properties to 600 degrees C and 5kb. *Am. J. Sci.*, **281**, 1249-1516.

Holland, T.J.B. & Powell, R. (1998): An internally consistent thermodynamic data set for phases of petrological interest. *J. Metam. Geol.*, **16**, 309-343.

Miron, G.D., Kulik, D.A., Dmytrieva, S.V., Wagner, T. (2015): GEMSFITS: Code package for optimization of geochemical model parameters and inverse modeling. *Appl. Geochem.*, **55**, 28-45.

Miron, G.D., Wagner, T., Kulik, D.A., Heinrich, C.A. (2016): Internally consistent thermodynamic data for aqueous species in the system Na-K-Al-Si-O-H-Cl. *Geochim. Cosmochim. Acta*, in press.

MIDAS: MODELLING KINETICALLY CONTROLLED ISOTOPE FRACTIONATION BY MASS-DEPENDENT DIFFUSION, ADVECTION AND SORPTION PROCESS

Mueller T.*[1], Kuesters T.[1], van Zuilen K.[2] & Dietzel M.[3]
[1] Institute of Geophysics and Tectonics, School of Earth and Environment, University of Leeds, United Kingdom
[2] Institut de Physique du Globe de Paris, France
[3] Institut für Angewandte Geowissenschaften, Technische Universität Graz, Austria
Corresponding email: t.mueller@leeds.ac.uk

Keywords: diffusion, kinetic isotope fractionation, reactive transport

Isotope signatures are typically used as proxies to indirectly constrain physico-chemical conditions, such as temperature or fluid composition that accompany geological processes. However, the primary isotopic composition of fluids and minerals can be altered, e.g., by diffusive transport of the isotope species in pore fluids of the hosting sediments or rocks and/or fluid-rock interactions, such as sorption processes. Therefore isotope signatures of fluids and minerals are of combined multiple fractionation processes. In order to interpret measured isotope variations correctly and to successfully infer external conditions during a given geological process, a quantitative description of each process, i.e., space- and time-dependent transport and sorption, is necessary.

In a preceding study, we developed a simplified numerical model to demonstrate the combined effect of mass-dependent diffusive transport and adsorption to successfully reproduce experimental data on Ba isotope fractionation during migration through silica gel in a pore fluid (van Zuilen et al., 2016). In this 1-D model diffusion of two Ba isotope species (^{134}Ba and ^{137}Ba) is assumed through a reservoir of silica gel mimicking a porous sediment, driven by a concentration gradient between a high-Ba source and low-Ba sink. The relative diffusivities of the isotope species were determined using an exponential beta-factor formulation (Richter et al., 1999). For the initial model we assumed a simple linear rate law to describe adsorption kinetics and neglected any possible desorption. It was found that Ba adsorption onto silica gel had only a minor effect on the overall isotope fractionation that was mainly controlled by mass-dependent diffusion of the two Ba isotopes.

Building upon this previous work, we now present a follow-up model with increased complexity to simulate mass-dependent isotope fractionation more adequately. Advection was added to the former purely diffusive transport calculation and the simple linear adsorption kinetics were replaced by different rate laws describing the dynamics of adsorption/desorption processes. Further, changes of the reservoir material, i.e., temporal and spatial evolution of solid components, their surface area and hydraulic transport properties, can be included into the simulations. The incorporation of the new features increases the number of experimental and natural scenarios suitable to be simulated by MIDAS. The model MIDAS was developed to provide a stand-alone tool that can be used for any isotope and rock system for which aqueous diffusivities of the relevant species, porosity, sorption kinetics and flow rates are known. A set of model scenarios is shown to demonstrate the capabilities of the model and to explore the parameter space given by temperature, concentration, Peclet-number and adsorption/desorption kinetics on the resulting isotope fractionation. Our model emphasizes that a quantitative assessment of these parameters and their interaction allows to evaluate the robustness of isotope proxies in low temperature settings more accurately and to justify their application under the particular conditions.

Richter, F.M., Liang, Y., Davis, A.M. (1999): Isotope fractionation by diffusion in molten oxides. *Geochim. Cosmochim. Acta*, **63**, 2853-2861.

van Zuilen, K., Müller, T., Nägler, T.F., Dietzel, M., Küsters, T. (2016): Experimental determination of barium isotope fractionation during diffusion and adsorption processes at low temperatures. *Geochim. Cosmochim. Acta*, in press.

ELEMENT MOBILITY BETWEEN GRANITE, FLUIDS AND SKARN (CAMPIGLIA MARITTIMA, TUSCANY)

Paoli G.*[1], Rocchi S.[1] & Dini A.[2]
[1] Dipartimento di Scienze della Terra, Università di Pisa, Italy
[2] Istituto di Geoscienze e Georisorse, Consiglio Nazionale delle Ricerche, Pisa, Italy
Corresponding email: gabriele.paoli@unifi.it

Keywords: hydrothermal fluid, geochemistry, metasomatism

Metasomatic rocks occur in all continents and are hosted in rocks of all types and ages, however they are most commonly found in carbonate rocks spatially related to magmatic bodies. The magmatic-hydrothermal system of Campiglia Marittima in southern Tuscany, is an ideal site to study fluid-mineral and fluid-rock interactions leading to element mobility between granite, fluids and skarn. Detailed textural and geochemical investigations have been carried out in the field, under the optical microscope and by QEMSCAN, EPMA and (LA)-ICP-MS to the products of the hydrothermal activity.

The Campiglia Marittima late Miocene granite pluton is severely affected by hydrothermal processes, locally leading to endoskarn formation. These processes are characterized by mobilization of major elements (Fe, Ti, Si, Al, P) and HFSE (e.g., Th, Nb, Zr, REE). Breakdown of biotite is common occurrence, to form variable assemblages of low-Ti phlogopite, Al-rich titanite, hydrothermal rutile, and diopside, with the latter mostly concentrated in endoskarn veins, suggesting significant Ca abundance in circulating fluids.

Between granite pluton and carbonate host rock, a metasomatic reaction front progresses into the marble. Decarbonation reactions, associated with infiltrative magmatic hydrothermal skarn reactions, are supplied by addition of Si, Al, Fe, Ti, etc. Resulting minerals are dominated by unusually REE-enriched pyroxene, garnet and epidote. At the direct granite-marble contact, significant hydrothermal apatite crystallization occurred, probably linked to the high Ca activity likely due to host rock decarbonation.

The system is clearly characterized by significant HFSE mobility throughout the hydrothermal system, likely controlled by factors such as P–T conditions, pH and chemistry of the fluid(s). The process of mobilization and concentration of HFSE is pointed out by the prominent occurrence of REE-rich minerals (e.g allanite, thorite, ekanite, uraninite) and by the high content of HFSE in several hydrothermal products (e.g., pyroxene, titanite, garnet, epidote). On the other hand, the replacement of REE-bearing minerals like ekanite ($ThCa_2Si_8O_{20}$), by thorite-quartz and fluorite-uraninite assemblages, is evidence for the mobilisation of commonly poorly mobile elements such as Th, REE, Zr, Hf, Nb. This process is likely supported by circulation of B-F enriched fluids.

These textural-mineralogical-geochemical data lay the basis to reconstruct the relative chronological framework of element mobility between granite, fluids and skarn. The emplacement of granite magma into the carbonate host rock produced thermal metamorphism and deformation of the marble host, later deformed in brittle regime as the thermal anomaly was decaying. The new fracture system allowed fluids to circulate into the granite and the marbles leading to the formation of various hydrothermal minerals, mostly calc-silicates, at the host rock front and along the fracture planes inside the granite pluton.

PLUTONIC-LEVEL HYDROTHERMAL COOLING RELATED TO OCEANIC DETACHMENT FAULTING: MINERALOGY AND FLUID ORIGIN

Pertsev A.*[1], Prokof'ev V.Y.[1], Aranovich L.[1] & Ageeva O.[1-2]
[1] Institute of Geology of Ore Deposits, Petrography, Mineralogy & Geochemistry, Russian Academy of Sciences, Moscow, Russia
[2] Department für Lithosphärenforschung, Universität Wien, Austria
Corresponding email: alexei_n@igem.ru

Keywords: gabbro, brine inclusion, magma-hydrothermal interaction

A large-scale seawater-derived hydrothermal circulation is often invoked to explain cooling of accreting oceanic crust at spreading ridges (e.g., German & Lin, 2004). However plutonic-level magma-hydrothermal interaction in different spreading environments remains poorly characterized. In slow-spreading ridges hydrothermal fluid flows can be interrelated to detachment faulting, i.e. development of large-offset extensional faults (e.g., McCaig et al., 2007), whereas vent fluid composition shows high H_2 concentrations due to seawater interaction with mantle-derived ultramafic rocks (Charlou et al., 2010).

A series of detachment faults occurs on the western slope of the Mid-Atlantic rift valley between 12°58'N and 13°35'N, where the footwall outcrops consist of unevenly hydrated mantle-derived harzburgite with minor gabbro bodies. Hydrothermal activity in these structures is manifested by active ultramafic-hosted vent fields including Ashadze at 13°N (Ondréas et al., 2012). Complex mineralogical features of gabbro from the Ashadze detachment footwall suggest a direct magmatic to hydrothermal transition.

Gabbro late magmatic assemblages include interstitial titanomagnetite, blebs of titanian hornblende enclosed in augite, and local apatite grain chains with sporadic zircon. Advection of hydrochloride brine, as documented in the apatite-hosted inclusions (30-32 wt.% $NaCl_{eq}$), resulted in mineralogical modifications at 750 to 400°C: abundant development of highly heterogeneous amphibole, decomposition of titanomagnetite due to reducing reactions, and complete re-crystallization of apatite and zircon. For instance, replacement of titanomagnetite by ilmenite in intergrowths with Cl- and Fe^{2+}-rich hornblende occurred at 600-500°C and log $\boldsymbol{f}O_2$ from -20 to -24.

Reducing nature and high salinity of the fluid could be assumed from preceeding low-temperature (≤ 400°C) seawater-harzburgite interaction within detachment shear zones, since such interaction (serpentinization) consumes 1-2 moles of H_2O and produces 0.1-1 mole of H_2 per mole of typical peridotite olivine (Andreani et al., 2007; McCollom & Bach, 2009). A similar fluid origin has been suggested for a different slow spreading setting (Pertsev et al., 2015).

Cooling of hot melt-bearing gabbroic body by the serpentinization-related fluid results in the formation of transitional (magmatic-hydrothermal) mineral composition. The transitional hornblende shows an enrichment in such residual magmatic components as K_2O (from 0.2-0.5 to 0.7-0.8 wt.%) and locally REEs (e.g., Sm from 25-53 to 77 ppm). At the same time it demonstrates a hydrochloride fluid contribution: irregular decrease in Mg# = Mg/(Mg+Fe) atomic ratio from 0.6 down to 0.2 and associated increase in Cl content from 0.03-0.05 up to 1.6 wt.%. Final hydrothermal cooling is reflected in the hornblende to actinolite compositional trend in amphibole, with depletion in K_2O to 0.3–0.1 wt. %, increase in Mg# to 0.4–0.5 and decrease in Cl content to 0.4–0.2 wt.%.

Andreani, M., Mevel, C., Boullier, A.-M., Escartin, J. (2007): Dynamic control on serpentine crystallization in veins: Constraints on hydration processes in oceanic peridotites. *Geochem. Geophys. Geosyst.*, **8**, Q02012.

Charlou, J., Donval, J., Conn, C., Ondréas, H., Fouquet, Y. (2010): High production and fluxes of H_2 and CH_4 and evidence of abiotic hydrocarbon synthesis by serpentinization in ultramafic-hosted hydrothermal systems on the Mid-Atlantic Ridge. *in* "Diversity of hydrothermal systems on slow spreading ocean ridges", P.A. Rona et al., eds., *Geophys. Monogr. Ser.*, **188**, AGU, Washington, DC, 265-296.

German, C. & Lin, J. (2004): The thermal structure of the oceanic crust, ridge-spreading and hydrothermal circulation: How well do we understand their inter-connections? *in* "Mid-ocean ridges: Hydrothermal interactions between the lithosphere and oceans", C.R. German et al., eds., *Geophys. Monogr. Ser.*, **148**, AGU, Washington, DC, 1-18.

McCaig, A.M., Cliff, R.A., Escartin, J., Fallick, A.E., MacLeod, C.J. (2007): Oceanic detachment faults focus very large volumes of black smoker fluids. *Geology*, **35**, 935-938.

McCollom, T. & Bach, W. (2009): Thermodynamic contstraints on hydrogen generation during serpentinization of ultramafic rocks. *Geochim. Cosmochim. Acta*, **73**, 856-875.

Ondréas, H., Cannat, M., Fouquet, Y., Normand, A. (2012): Geological context and vents morphology of the ultramafic - hosted Ashadze hydrothermal areas (Mid - Atlantic Ridge 13°N). *Geochem. Geophys. Geosyst.*, **13**, DOI: 10.1029/2012GC004433.

Pertsev, A., Aranovich, L., Prokofiev, V., Bortnikov, N., Cipriani, A., Simakin, S., Borisovskiy, S. (2015): Signatures of residual melts, magmatic and seawater-derived fluids in oceanic lower-crust gabbro from the Vema lithospheric section, Central Atlantic. *J. Petrol.*, **56**, 1069-1088.

REDISTRIBUTION OF MAIN ELEMENTS DURING ECLOGITE TO AMPHIBOLITE RETROGRADE MINERAL REACTIONS

Pollok K.*[1], Uhlmann L.[1], Pleuger J.[2] & Langenhorst F.[1]
[1] Institut für Geowissenschaften, Friedrich-Schiller-Universität Jena, Germany
[2] Fachbereich Geowissenschaften, Freie Universität Berlin, Germany
Corresponding email: kilian.pollok@uni-jena.de

Keywords: retrograde metamorphism, local mass balance, fluid-consuming reactions

Retrograde mineral reactions are known to be limited by the availability and accessibility of fluids (Jamtveit & Austrheim, 2010). The infiltration of fluids is often restricted to shear zones which provide incomplete local conversion of high-grade to lower-grade metamorphic rocks. While metamorphic petrology is mostly focusing on rocks that survived the retrograde path (e.g., for maximum P-T estimates), the perished rocks and their textures received much less attention. An increase in volume is immanent to these fluid-consuming reactions which either increase local stress or must be balanced by chemical transport (Jamtveit et al., 2015). The present work addresses the mass balances at thin section scale of the frequently occurring regression of eclogite to amphibolite.

An eclogite and its amphibolite facies regressed analogs were collected close to Drangovo village, Eastern Rhodopes, Bulgaria, within the Kardžali unit which is part of the upper allochthon (Kirchenbaur et al., 2012). The eclogite consists of large euhedral garnet, subhedral omphacite (Jd_{40}) with very little alteration to amphibole and plagioclase at grain boundaries, and rutile. The retrograde altered eclogite shows a strong textural inheritance but a complete replacement of primary omphacite by fine symplectites of Am and Pl (10 µm grain size with lamellar texture).

Mass balance calculations (Gresens, 1967; Godard & Mabit, 1998) were performed based on volume-for-volume replacement reactions. The omphacite breakdown reaction is perfectly suited to determine the mass transport during symplectite formation, because only three solid phases (Omp, Am, Pl) are involved none of which show signs of pronounced chemical zoning. Further, the symplectite phases are large enough to measure the chemical composition accurately by electron microprobe but likewise small enough to provide a good statistical control on the volume fractions by using greyscales of backscattered electron images. The calculations indicate that only H_2O from fluid is needed for the growth of Am (0.11 mol H_2O per 1 mol Omp). Mainly Si is released from the reaction (almost 0.5 mol per 1 mol Omp) and transported at least on thin section scale. It appears partly as free quartz. Mg and Ca are liberated to lower extent while Al and Fe are locally redistributed. Grt is found partly or fully replaced by Am, Pl, Ep, Bt and Chl, but is always defined by Am coronas which allow to locate the original grain boundaries. Furthermore, partly replaced eclogites with fully regressed Omp but minor altered Grt pinpoint the order of retrograde mineral reactions and indicate that the rock was still open to fluids, potentially even down to greenschist-facies conditions. The texture of the replaced rock evidences pervasive fluid flow at grain scale without stress gradients due to volume changes.

Godard, G. & Mabit, J.-L. (1998): Peraluminous sapphirine formed during retrogression of a kyanite-bearing eclogite from Pays de Léon, Armorican Massif, France. *Lithos*, **43**, 15-29.

Gresens, R.L. (1967): Composition-volume relationships of metasomatism. *Chem. Geol.*, **2**, 47-65.

Jamtveit, B. & Austrheim, H. (2010): Metamorphism: the role of fluids. *Elements*, **6**, 153-158.

Jamtveit, B., Austrheim, H., Putnis, A. (2015): Disequilibrium metamorphism of stressed lithosphere. *Earth Sci. Rev.*, **154**, 1-13.

CALC-SILICATE REACTIONS AND TEXTURES REVEAL METAMORPHIC-CO_2 PROCESSES AND FLUXES IN THE HIMALAYAS

Rapa G.*[1], Groppo C.[1-2], Rolfo F.[1-2] & Mosca P.[2]
[1] Dipartimento di Scienze della Terra, Università di Torino, Italy
[2] Istituto di Geoscienze e Georisorse, Consiglio Nazionale delle Ricerche, Torino, Italy
Corresponding email: giulia.rapa@unito.it

Keywords: orogenic CO_2 cycle, metamorphic CO_2, calc-silicate rocks

Decarbonation reactions during regional metamorphism in “large-hot” collisional orogens are an important source of atmospheric CO_2, able to influence global climate through geologic time (Gaillardet & Galy, 2008). The petrologic study of the CO_2-source rocks (calc-silicates, impure marbles) is therefore fundamental to understand the deep carbon cycle. So far, the incomplete knowledge of these systems hindered a reliable quantitative modeling of metamorphic CO_2 fluxes.

Previous studies aimed at constraining the metamorphic CO_2 flux related to regional metamorphism mainly used simple model reactions between end-members in simple model systems and considered Cal in excess. However, calc-silicate rocks are more complex, because of the occurrence of Ca-Mg-Fe solid solutions (garnet, clinopyroxene), K- (biotite, muscovite, K-feldspar), Ca-Na- (plagioclase, scapolite) and Ti-bearing (titanite, biotite) silicates. Moreover, Cal may be completely consumed during prograde metamorphism.

This study aims to define and quantify the CO_2-producing metamorphic reactions that occurred during Himalayan collision using a thermodynamic approach combined with the interpretation of microstructures. Phase relations and devolatilization reactions that occurred in high-grade Cpx + Kfs + Scp + Pl + Zo + Bt + Ttn ± Cal calc-silicate rocks are investigated in the complex NKC(F)MAST-HC system. The equilibria involving plagioclase and scapolite Na-Ca solid solutions, as well as biotite Mg-Ti-(Fe) solid solution are investigated using: (i) P/T-X(CO_2) pseudosections, (ii) P/T-X(CO_2) phase diagram sections and (iii) mixed-volatile P-T phase diagram projections.

We demonstrate that:

(i) the key microstructures correspond to isobaric univariant or invariant assemblages, thus suggesting that the system remained internally buffered during its prograde evolution;

(ii) although challenging and time-consuming, considering complex solid solutions (Na-Ca and Mg-Ti-(Fe)) in the modelling allows to identify CO_2-producing reactions that are otherwise hidden. Particularly relevant is the identification of Ttn-bearing equilibria involving biotite rather than rutile as the Ti-phase counterpart. We demonstrate that, in the studied sample, different Ttn generations grew through Bt-consuming and CO_2-producing reactions. Since titanite is potentially useful as a geochronometer, a detailed knowledge of the equilibria involved in its growth is fundamental for constraining the timing of different episodes of CO^2 production during the Himalayan collision.

(iii) considering Cal in excess might be not correct; the modelling of Cal-poor domains in the studied sample, in fact, highlights that the system is sensible to Cal-absent equilibria.

Gaillardet, J. & Galy, A. (2008): Himalaya-carbon sink or source? *Science*, **320**, 1727-1728.

FLUID-ASSISTED COESITE-QUARTZ TRANSITION IN THE DORA-MAIRA WHITESCHISTS, WESTERN ALPS: PETROGRAPHIC AND RAMAN STUDIES

Remigi S.[1], Ferrando S.*[2] & Frezzotti M.L.[1]
[1] Dipartimento di Scienze dell'Ambiente, del Territorio e di Scienze della Terra, Università di Milano-Bicocca, Italy
[2] Dipartimento di Scienze della Terra, Università di Torino, Italy
Corresponding email: simona.ferrando@unito.it

Keywords: coesite, quartz, Raman spectroscopy

We applied micro-Raman spectroscopy to investigate the kinetic of the coesite-quartz (Coe/Qz) transition in selected samples from the monometamorphic complex of the Brossasco-Isasca Unit, a portion of continental crust that experienced UHP Alpine metamorphism, and that is exposed in the southern sector of the Dora-Maira Massif (Pennidic domain). Whiteschists were collected at Case Parigi (Po valley), which represents the locality where natural Coe was discovered and studied for the first time (Chopin, 1984), and near Vanasca and Gilba (Varaita Valley). Dominant mineralogical phases are Prp, Ky, Tlc, Phg and Qz/Coe, in association with secondary Wag, Ell, Mg-Dum, Mg-Chl and accessory Rt, Zrn, Mnz and Ap. In studied rocks, Coe constitutes relics included in Ppr, surrounded by radial fractures. SiO_2 inclusions in Prp consist of Coe, preserved in the core, surrounded by polycrystalline Qz and, externally, by *palissade* Qz. Relic coesite is often cut by Qz microveinlets (3-5 µm thickness). Inclusions of Qz as monocrystals, and polycrystalline or *palissade* aggregates are also present in Prp, while polycrystalline and *palissade* Qz are observed in the matrix within the S_1 foliation and in the pressure shadows. The kinetics of the Coe/Qz transition has been investigated by Raman micro-spectroscopy in inclusions within Prp. Single spectra and spectral maps show that optically-homogeneous Coe in the core of the inclusions often consists of Coe incipiently transformed to quartz (mixed Coe/Qz spectra), in particular close to Qz microveins. At the inclusion rims, spectra of polycrystalline Qz generally do not show Coe vibrations, while about 30% of *palissade* Qz spectra still preserve the main coesite vibration at 521 cm^{-1}, suggesting that locally Si-O-Si bond angles did not attain 144° (i.e., 133° - Coe; Palmeri et al., 2009). Present results indicate that retrograde aqueous fluids catalysed the Coe/Qz transition, incipiently transforming relic Coe into Qtz along microfractures. Completion of the polymorphic transition is attained only at the inclusion rims, testified by *palissade* and polycrystalline Qz.

Chopin, C. (1984): Coesite and pure pyrope in high-grade blueschists of the westem Alps: a first record and some consequences. *Contrib. Mineral. Petrol.*, **86**, 107-118.

Palmeri, R., Frezzotti, M.L., Godard, G., Davies, R.J. (2009): Pressure-Induced incipient amorphization of α-quartz and transition to coesite in an eclogite from Antarctica: a first record and some consequences. *J. Metam. Geol.*, **27**, 685-705.

SLAB FLUIDS AND CONTROLS ON TRACE ELEMENT RECYCLING IN SUBDUCTION ZONES

Sanchez-Valle C.*[1], Louvel M.[2], Tsay A.[3] & Zajacz Z.[3]
[1] Institut für Mineralogie, Universität Münster, Germany
[2] School of Earth Sciences, University of Bristol, United Kingdom
[3] Department of Earth Sciences, University of Toronto, Canada
Corresponding email: sanchezm@uni-muenster.de

Keywords: slab fluids, trace elements, recycling

High pressure slab-derived fluids (aqueous fluid, hydrous melt or supercritical fluid?) are major vectors for mass transfer and element recycling in subduction zones. The quantitative estimates of mass recycling the Earth's interior are, however, limited by the poor understanding of the atomic-scale mechanims that control the mobilization and transport of elements during fluid-rock interactions in deep settings.

In the last decade, new experimental designs combining advanced micro-analytical techniques and high-pressure vessels have opened the possibility for determining *in situ* the chemical composition, the molecular-scale structure and thermodynamic quantities for high-pressure fluids. Here, we will discuss emerging views on the mechanism of mobilization and recycling of trace elements and the nature of the slab flux in the light of synchrotron-based techniques and the analysis of fluids trapped in synthetic fluid inclusions (SFI). Specifically, we present results on the speciation, solubility and partitioning of HFSE (i.e., Zr), halogens (i.e., Br) and REE on high pressure fluids that illustrate the role of coordination chemistry involving alkali or halogen ligands (e.g., Cl and F) and polymerized silicate species (Si-Al-Na) in the recycling of trace elements. We show, for instance, that Zr (and other HFSE by extension) can be efficiently mobilized by alkali-silicate bearing aqueous fluids expelled from the slab through the formation of alkali zircono-silicate Zr-O-Si/Na complexes for which we have provided direct spectroscopic evidence. These results suggest that melting of the slab is not required to mobilize HFSE in subduction zones, and that their characteristic depletion in arc magmas is mostly related to complex fluid-rock interactions at the slab-mantle interface or in the mantle wedge rather than to their immobility during slab dehydration. In addition, REE elements can be efficiently mobilized and fractionated (LREE/HREE) by aqueous fluids upon slab dehydration and Cl-bearing slab-derived aqueous fluids are likely responsible for the characteristic REE-signature (i.e., LREE/HREE fractionation) in arc magmas, particularly at low slab surface temperatures. The picture that is emerging from these studies is that ligand-bearing (Cl, Si/Al-Na clusters) aqueous phases may have comparable efficiency to hydrous silicate melts in the mobilization and fractionation of trace elements and that their role as mass transfer agents in subduction-related processes may have been underestimated until now.

RAMAN SPECTROSCOPIC STUDY OF TIN SPECIATION IN HYDROTHERMAL FLUIDS TO 600°C

Schmidt C.*[1]

[1] Helmholtz Zentrum Potsdam, GFZ Deutsches GeoForschungsZentrum, Potsdam, Germany

Corresponding email: Christian.Schmidt@gfz-potsdam.de

Keywords: tin speciation, hydrothermal fluid, Raman spectroscopy

Wilson & Eugster (1990) inferred from solubility data for cassiterite in H_2O+HCl measured in rapid-quench experiments to 700°C that $SnCl_3^+$ or $SnCl^+$ and $SnCl_2^0$ were the dominant aqueous tin species. In contrast, the interpretation of *in-situ* EXAFS spectra of Sn(IV) or Sn(II) in HCl±NaCl solutions at temperatures to 350°C resulted in different prevalent species, $SnCl_6^{2-}$ or $SnCl_3^-$ and $SnCl_4^{2-}$ (Sherman et al., 2000). Less arguable information on tin(IV) and tin(II) complexation at ambient conditions has been provided by studies combining ^{119}Sn NMR and Raman spectroscopy, i.e. techniques that are more species-fic (Taylor, 1989; Taylor & Coddington, 1992). In this study, Raman spectroscopy was used to determine aqueous tin speciation to 600°C in fluids produced by reacting cassiterite with H_2O+HCl in the sample chamber of a hydrothermal diamond-anvil cell (Bassett et al., 1993). The most abundant species were, in the case of Sn(II), always $[SnCl_3]^-$, and, in the case of Sn(IV), $[SnCl_5(H_2O)]^-$ and $[SnCl_4(H_2O)_2]^0$, with additional $[SnCl_3(H_2O)_3]^+$ or $[SnCl_6]^{2-}$. Therefore, the predominant dissolution reactions were $SnO_2 + 5HCl = [SnCl_5(H_2O)]^- + H^+ + H_2O$ and $SnO_2 + 4HCl = [SnCl_4(H_2O)_2]^0$ for Sn(IV) or $SnO_2 + 3HCl + H_2 = [SnCl_3]^- + H^+ + 2H_2O$ for Sn(II). If Ar + 1% CH_4 gas was used to flush the cell, the fluid contained mostly Sn(IV) and little or no Sn(II). If Ar + 1% H_2 gas was used for flushing, $[SnCl_3]^-$ formed at the expense of Sn(IV) species, which indicates hydrogen permeation into the sample chamber. The cassiterite solubility increased with HCl concentration and was generally high in H_2O+HCl fluids, with no strong dependence on the oxidation state of tin in the fluid. The total band intensity from Sn(IV)–Cl symmetric stretching indicated little change in the cassiterite solubility between 400 to 600°C, and decreased by only 28% after cooling from 600 to 22°C (initial HCl concentration 1.63 molal). The determined Sn(IV) solubility is in good agreement with the cassiterite solubility reported by Wilson & Eugster (1990) at 500 and 600°C and oxygen fugacities along the hematite-magnetite buffer. In summary, the results demonstrate that redox conditions and temperature have little effect on hydothermal tin transport and cassiterite precipitation, whereas HCl molality is a crucial parameter given that the solubility of cassiterite in H_2O+HCl is about two orders of magnitude lower in equimolal NaCl or HF solutions (Duc-Tin et al., 2007). Thus, important causes of cassiterite precipitation include decreasing HCl molality due to dilution or fluid-rock reactions and decreasing *p*H by HCl dissociation upon cooling.

Bassett, W.A., Shen, A.H., Bucknum, M., Chou, I-M. (1993): A new diamond-anvil cell for hydrothermal studies to 2.5 GPa and from -190 to 1200°C. *Rev. Sci. Instr.*, **64**, 2340-2345.

Duc-Tin, Q., Audétat, A., Keppler, H. (2007): Solubility of tin in (Cl,F)-bearing aqueous fluids at 700°C, 140 MPa: A LA-ICP-MS study on synthetic fluid inclusions. *Geochim. Cosmochim. Acta*, **71**, 3323-3335.

Sherman, D.M., Ragnarsdottir, K.V, Oelkers, E.H., Collins, C.R. (2000): Speciation of tin (Sn^{2+} and Sn^{4+}) in aqueous Cl solutions from 25°C to 350°C: an *in situ* EXAFS study. *Chem. Geol.*, **167**, 169-176.

Taylor, M.J. (1989): Raman spectrum of the $[SnI_3]^-$ ion and other halogenostannate(II) complexes including mixed halides. *J. Raman Spectr.*, **20**, 663-666.

Taylor, M.J. & Coddington, J.M. (1992): The constitution of aqueous tin(IV) chloride and bromide solutions and solvent extracts studies by^{119}Sn NMR and vibrational spectroscopy. *Polyhedron*, **11**, 1531-1544.

Wilson, G.A. & Eugster, H.P. (1990): Cassiterite solubility and tin speciation in supercritical chloride solutions. *Geochem. Soc. Spec. Publ.*, **2**, 179-195.

MULTICOMPONENT FLUID CHEMISTRY OF HIGH-ENTHALPY GEOTHERMAL SYSTEM

Stefánsson A.*[1]
[1] Institute of Earth Sciences, University of Iceland, Reykjavík, Iceland
Corresponding email: as@hi.is

Keywords: geothermal, modeling, fluids

Active volcanoes are commonly associated with high-enthalpy geothermal system and a magmatic heat source. The fluid temperatures range from < 200 to > 450°C with reservoir fluids being liquid only, two phase liquid and vapor. Here, a new combined hydrological and chemical model for such high-enthalpy geothermal systems across P-T conditions is demonstrated and compare fluid composition and alteration mineralogy observations for natural systems in Iceland. The model is based on combining heat and fluid mass transfer modelling with fluid-fluid and fluid-rock interactions as a function of temperature, pressure, enthalpy and composition (T-P-h-X). Within the reservoir at temperatures of 250-350°C liquid water predominates. Under these conditions, the concentrations of most major elements are controlled by equilibrium with secondary minerals formed at low pressure and < 350°C. Around the magma intrusions, supercritical fluid is formed with temperatures of ~ 400-500°C. According to the model, such fluid is produced upon heat addition by the intrusion to the surrounding geothermal fluid resulting in boiling to dryness, precipitation of non-volatiles (Si, Fe, Mg, Al, SO_4, Na, K, Ca) where volatiles (CO_2, H2S, Cl, F, B) are unaffected. By mass, quartz is observed to be the predominant secondary mineral around the intrusions. Upon ascent and depressurization of the subcritical and supercritical fluid, various processes may occur, including supercritical fluid condensation, mixing and depressurization boiling. This leads to formation of two-phase liquid and vapor fluids, dilute acid fluids produced upon supercritical fluid condensation and mixtures thereof. Such fluids are indeed observed within active high-enthalpy geothermal systems in Iceland.

THE DISTRIBUTION OF SIDEROPHILE AND CHALCOPHILE TRACE METALS IN MANTLE ROCKS (BALMUCCIA, ITALY)

Steinmann L.*[1], Lazarov M.[1], Wang Z.[2], Becker H.[2] & Weyer S.[2]
[1] Institut für Mineralogie, Leibniz Universität Hannover, Germany
[2] Institut für Geologische Wissenschaften, Freie Universität Berlin, Germany
Corresponding email: lena.steinmann@yahoo.de

Keywords: peridotite, Cu isotopes, sulfides

The Balmuccia peridotite massif (NW Italy) consists of fresh mantle rocks exposed due to tectonic extension after Hercynian orogeny. In this study, we performed *in situ* analyses of Cu isotopes and siderophile and chalcophile trace elements of four lherzolites, two clinopyroxenites and one orthopyroxenite, in order to constrain distribution of these elements between silicates and sulfides and to discuss their mobility and enrichment in Earth's mantle. Spinel bearing lherzolites are depleted, with Mg# ~90, while pyroxenites, cumulated dikes within lherzolites, have Mg# from 87 to 89 (Wang et al., 2013; Wang & Becker, 2015). All samples contain small amounts of sulfides which are, in the order of abundance, pentlandite, pyrrhotite and chalcopyrite with grain sizes *In situ* trace element concentration analyses of all silicate and sulfide minerals, and Cu isotope composition analyses of chalcopyrites were performed using UV (194 nm) femtosecond-LA coupled to ICP-MS and MC-ICP-MS, respectively.

Similar to Ni, Zn and Co are enriched in silicates, mostly in spinel, followed by pyroxene and olivine. Cobalt is highly abundant in sulfides, while Zn appears as a trace element. Cu is primarily abundant in chalcopyrite and only low Cu concentrations of a few 100 ppm can be found in pentlandite and pyrrhotite. Cadmium behaves similarly to Cu with concentrations of up to 300 ppm in chalcopyrite and ~0.5 ppm in other sulfides. Clinopyroxene is the only silicate that contains minor amounts of Cu (~ 3 ppm) and Cd (< 0.2 ppm). Both elements are lower concentrated in pyroxenites than in lherzolites. Mass balance calculations show that sulfides and especially chalcopyrite are the main carriers of Cu and Cd in the investigated samples. Compared to sulfide free lherzolites (e.g., garnet-lherzolites from the Kapvaal craton; Lazarov, 2008), the here investigated clinopyroxenes display lower Cu and Co. The PGEs, Re, Au, Ag and Sn all show high concentration in sulfides, and are below detection limits (< 20 ppb) in silicates. Ruthenium, Re, Au and Sn are especially enriched in pentlandite, whereas Pd, Ir, Pt, Rh, Os and Sn are more enriched in chalcopyrite. Except for Rh and Pd in chalcopyrites, PGE concentrations are generally lower in pyroxenites than in lherzolites.

In situ analyses of Cu isotopes in chalcopyrites show homogeneous δ^{65}Cu values of ~ 0.2‰ ±0.3 within lherzolites, however, a heterogeneous distribution in pyroxenites with a spread of more than 1‰. This may either point to the existence of several types of chalcopyrites in pyroxenites, likely as the result of late metasomatic overprint by a sulfide bearing melt or fluid, or, alternatively as stated by Acken et al. (2010), the sulfides in the pyroxenite cumulates never reach equilibrium. The observations of this study show, that sulfide bearing fluids/silicate melts are important for transport and mobility of most chalcophile and siderophile trace elements (Cu, Cd, Re, Au, Ag, Sn and PGEs) in the mantle.

Acken, D., Becker, H., Walker, R.J., McDonough, F., Wombacher, F., Ash, R.D., Piccoli, P.M. (2010): Formation of pyroxenite layers in the Totalp ultramafic massif (Swiss Alps) – Insights from highly siderophile elements and Os isotopes. *Geochim. Cosmochim. Acta*, **74**, 661-683.

Lazarov, M. (2008): Archean to present day evolution of the lithospheric mantle beneath the Kapvaal craton. Dissertation, Univ. Frankfurt, 218 p.

Wang, Z. & Becker, H. (2015): Fractionation of highly siderophile and chalcogen elements during magma transport in the mantle: Constraints from pyroxenites in the Balmuccia Peridotite Massif, *Geochim. Cosmochim. Acta*, **159**, 244-263.

Wang, Z., Becker, H., Gawronski, T (2013): Partial re-equilibration of highly siderophile elements and the chalcogens in the mantle: A case study on the Baldissero and Balmuccia peridotite massifs (Ivrea Zone, Italian Alps).*Geochim. Cosmochim. Acta*, **108**, 21-44.

SELECTIVE TRANSFER OF Li-Al-RICH PHYLLOSILICATE TO METAMORPHIC VEINS (WESTERN ALPS): LASER INDUCED BREAKDOWN SPECTROSCOPY (LIBS) COMPOSITIONAL PROFILES AND MICROSTRUCTURAL CHARACTERIZATION

Verlaguet A.*[1], Brunet F.[2], Goffé B.[3], Menut D.[4], Findling N.[2], Poinssot C.[5] & Huet B.[6]

[1] Sorbonne Universités, Université Pierre et Marie Curie, Université Paris 06, Centre National de la Recherche Scientifique, Institut des Sciences de la Terre de Paris, France

[2] Université Grenoble Alpes, Centre National de la Recherche Scientifique, Institut des Sciences de la Terre, Grenoble, France

[3] Université d'Aix-Marseille, Centre National de la Recherche Scientifique, Institut de Recherche pour le Développement, Centre de Recherche en Gestion, Aix en Provence, France

[4] Commissariat à l'énergie atomique et aux énergies alternatives, Saclay, Direction de l'Energie Nucléaire, Service de Recherches Métallurgiques Appliquées, Gif-sur-Yvette, France

[5] Commissariat à l'énergie atomique et aux énergies alternatives, Marcoule, Direction de l'Energie Nucléaire, Département RadioChimie & Procédés, Bagnols-sur-Ceze, France

[6] Department für Geodynamik und Sedimentologie, Universität Wien, Austria

Corresponding email: anne.verlaguet@upmc.fr

Keywords: LIBS profiles, lithium diffusive transfer, interconnected fluid-filled porosity

Significant amounts of aqueous fluid are released by successive dehydration reactions occurring during burial in convergent settings. This fluid phase is expected to strongly influence both rock deformation processes and the scale of mass transfer and fluid-rock interactions. Metamorphic veins, ubiquitous in mid-crustal rocks and HP/T environments, are precious witnesses of fluid-rock interactions and their structural and chemical study can provide clues about the nature, pathways, timing and scale of fluid circulation. A striking observation if that fluid-rock interactions generally result in quartz and calcite preferential transfer to metamorphic veins in classical metamarls, while phyllosilicates tend to remain in the host-rock. However, the mechanisms responsible for such a selective mass transfer are poorly discussed in the literature.

Here, we study Alpine metabauxites in which phyllosilicates (Li-Al-rich chlorite called cookeite, followed by pyrophyllite) were preferentially transferred to veins at blueschist peak P-T conditions, by a dissolution-diffusion-precipitation process, without any fluid infiltration or associated dehydration reaction. Cookeite veins formed in two steps: fibrous en-echelon veins formed by extensional shear, and part of them evolved towards thicker fluid-filled veins with euhedral cookeite crystallization.

To constrain the modalities and controlling parameters of Li-bearing mineral diffusive transfer to veins, we performed chemical profiles across host-rocks between successive cookeite veins, using Laser Induced Breakdown Spectroscopy (LIBS), associated to a microstructural study. Flat LIBS Li profiles show that about half of the initial cookeite remains homogeneously distributed in host-rocks, which suggests a diffusion distance of 2-4 cm for Li. The availability of an aqueous fluid during most of the metamorphic cycle is demonstrated here. A simple 1D reaction-diffusion model, assuming Li diffusion through a connected fluid-filled porosity network, is able to account for the observed lithium distribution assuming Li diffusion coefficients and mineral-water interaction rates consistent with literature values in fluid-bearing systems. Chemical potential gradients that drove phyllosilicate transfer to veins can be either interfacial energy driven (i.e., Ostwald ripening), the anhedral phyllosilicate microsheets maintaining high supersaturation levels in the small host-rock pores compared to veins, or stress-induced: phyllosilicates present the highest solubility variations with pressure in the Vanoise bauxites (contrary to quartz-bearing rocks), which may account for their unusual selective transfer to veins. Mineral solubility variation with pressure thus seems to be the chief controlling parameter for pressure-solution creep. Moreover, Li, which is a strategic element, was observed to preferentially migrate and segregate into veins during metamorphic processes, which may be of importance for exploration purposes.

MAGMA CHASING HYDROTHERMAL FLUIDS IN A DISTAL SKARN SYSTEM AT CAMPIGLIA MARITTIMA (TUSCANY)

Vezzoni S.*[1], Dini A.[2] & Rocchi S.[1]
[1] Dipartimento di Scienze della Terra, Università di Pisa, Italy
[2] Istituto di Geoscienze e Georisorse, Consiglio Nazionale delle Ricerche, Pisa, Italy
Corresponding email: vezzoni@dst.unipi.it

Keywords: reverse telescoping, skarn deposit, hydrothermal fluids

Metasomatic processes are associated with fluid flow in a permeable host rock and commonly result in mineralogical net transfer reactions. Skarns are one of the main group of metasomatic rocks, and the fluid composition and infiltration pathways control the resulting skarn/ore morphology/mineralogy.

The Campiglia Marittima Fe-Cu-Zn-Pb(-Ag) skarn deposit has long been regarded as a reference exoskarn example showing a symmetric outward mineralogical zoning of both skarn and ore minerals with respect to an axial mafic porphyry dike. This classical model has been recently questioned, suggesting Campiglia Marittima skarn as a prominent example of a reverse telescoping ore deposit. Indeed, the emplacement of mafic magma into a distal Zn-Pb(-Ag) skarn triggered the overprinting of high-temperature Fe-Cu sulfide ore onto the lower-temperature Zn-Pb sulfide assemblage.

This work expand the reverse telescoping model with new field, geochemical, and lead isotopic data, offering an interpretive key to understand how magmas and fluids can move in a shallow skarn system. In detail, Campiglia Marittima experienced an efficient fluid- and magma- focusing process that allowed late mafic magmas to chase earlier hydrothermal fluids, bridging the spatial gap between the deep main intrusive level and the overlying distal metasomatic bodies. Mafic magmas and Fe-Cu ore-forming fluids exploited large, empty primary pockets in the inner portions of the skarn bodies. These pockets were mostly not interconnected, so theoretically ineffective for fluid flow. However, hydraulic brecciation played a main role in ore fluid propagation. During the development of this skarn system, a geochemical and isotopic switch is recorded highlighting a distinctive metallogenic fingerprint of crustal- and mantle- derived fluid sources.

These processes are probably more common than acknowledged, as indicated by analogous late Cu overprinting on typical granite-related ores (e.g., Kamioka, Japan and Madan, Bulgaria skarn deposits; San Rafael, Peru and Cornwall, UK, Sn deposits). This work suggests that unusual metal associations can be successfully investigated with far-field geochemical-isotopic methods for unravelling complex magmatic-hydrothermal histories at depth and potentially predict the presence of blind, deep ore deposits.

HALOGENS, BARIUM AND URANIUM IN MANTLE FLUID INCLUSIONS

Villa I.M.*[1-2], Peverelli V.[1], Oglialoro E.[1], Pettke T.[2] & Frezzotti M.L.[1]
[1] Dipartimento di Scienze dell'Ambiente, del Territorio e di Scienze della Terra, Università di Milano-Bicocca, Italy
[2] Institut für Geologie, Universität Bern, Switzerland
Corresponding email: igor@geo.unibe.ch

Keywords: halogens, Br/I/Cl ratios, xenon

Halogens are an almost unexplored geochemical marker, one of the very few exceptions being the work by Yardley (e.g., Yardley, 2013). A sensitive technique to measure halogens at ng/g levels is by irradiating samples and measuring Ar, Kr and Xe (Jeffery & Reynolds, 1961; Kendrick, 2012). Absolute rare gas amounts are converted to absolute halogen amounts via the SY scapolite monitor (Kendrick, 2012). Kr-Xe systematics also yield Ba and U concentrations, via an ad-hoc laser microprobe calibration of Ba and U concentrations in SY. We combined irradiation with stepheating on carbonate-sulfate-rich fluid inclusions (FI)-bearing xenoliths from El Hierro, Canarias: a spinel harzburgite, XML-7, and a spinel dunite, XML-1 (Oglialoro et al., 2015).

Three components are recognized in the rare gas release.

(1) Atmospheric surface contamination affects all steps to 1000°C.

(2) FI decrepitation by laboratory heating is mostly observed above 1200°C (Roedder, 1965), corresponding to the release of ^{80,82}Kr and ^{128}Xe in the 1200 and 1400°C steps. The calculated Br whole-rock concentrations are 3-8 ng/g; the molar Br/Cl and I/Cl ratios in the harzburgite FI, 9 E-4 resp. 2 E-4, are identical to those in the dunite FI. This sets the halogens in our FI apart from MORB (Kendrick, 2012). Halogen-derived rare gases are closely associated to Ba-derived artificial ^{131}Xe; this is explained by the high affinity of Ba for CO_2-rich fluids. Daughter minerals in multiphase FI were identified by Raman microspectroscopy (Oglialoro et al., 2015). The calculated Ba concentrations are 2-6 µg/g.

(3) The third component is U-derived (retained radiogenic and artificial) ^{134,136}Xe and ^{86}Kr released in a spike at 1000°C, decoupled from FI. This requires a different carrier than FI, e.g. Ti oxides; given the U concentrations of 10-20 pg/g, the modal abundance of the U-bearing phase needs to be below a ppm, undetectable by petrographic observation. Retention of radiogenic Xe in a HFSE mineral at mantle conditions is not unexpected, given its large atomic radius.

Jeffery, P.M. & Reynolds, J.H. (1961): Origin of excess xenon-129 in stone meteorites. *J.Geophys. Res.*, **66**, 3582-3583.

Kendrick, M.A. (2012): High precision Cl, Br and I determinations in mineral standards using the noble gas method. *Chem. Geol.*, **292-293**, 116-126.

Oglialoro, E., Ferrando, S., Malaspina, N., Villa, I.M., Frezzotti, M.-L. (2015): CO_2-SO_3-rich (carbonate-sulfate) melt/fluids in the lithosphere beneath El Hierro, Canary Islands. AGU Fall Meeting, abstr., V21C-3046.

Roedder, E. (1965): Liquid CO_2 inclusions in olivine bearing nodules and phenocrysts from basalts. *Am. Mineral.*, **50**, 1746-1782.

Yardley, B.W.D. (2013): The chemical composition of metasomatic fluids in the crust. *in* "Metasomatism and the chemical transformation of rock - The role of fluids in terrestrial and extraterrestrial processes", D.E. Harlov, H. Austrheim, eds., Springer, Berlin, 17-51.

Session S5:

The cycling of hydrogen, carbon, and mobile elements in the subduction factory

Conveners:

Jörg Hermann (Bern – Switzerland)

Timm John (Berlin – Germany)

Marco Scambelluri (Genova – Italy)

DEEP RECYCLING OF CARBONATE-RICH SEDIMENTS IN THE MANTLE SOURCE OF VESUVIUS VOLCANO

Avanzinelli R.*[1], Casalini M.[1], Elliott T.[2] & Conticelli S.[1]
[1] Dipartimento di Scienze della Terra, Università di Firenze, Italy
[2] School of Earth Sciences, University of Bristol, United Kingdom
Corresponding email: riccardo.avanzinelli@unifi.it

Keywords: deep recycling of carbonate-rich sediments, Vesuvius volcano, U-series disequilibria

The fate of carbonate-rich sediments recycled at destructive plate margins is a key issue for constraining the budget of deep CO_2 supplied to the atmosphere by volcanism. Experimental studies have demonstrated that carbonatite-like metasomatic liquids (fluids and/or melts) can be generated during subduction by de-carbonation and partial melting of carbonate-pelitic sediments (e.g., Poli, 2015). These liquids may modify the mantle sources of subduction-related magmas that eventually recycle carbon and other elements back to the surface through magmatism. Evidence of such a process in erupted magmas is, however elusive and much debated. Magmas erupted at Vesuvius volcano show geochemical evidence of involvement with carbonate-rich lithologies, either deeply subducted and recycled into the mantle (Avanzinelli et al., 2008) or acquired through shallow level contamination with limestone (Iacono Marziano et al., 2009). Here we present new U-Th disequilibria data coupled with high precision $\delta^{238}U$ on Vesuvius lavas, demonstrating that the ^{238}U-excess of Vesuvius lavas is anomalous with respect to other subduction-related magmas and it requires a deep addition of U-rich carbonated melts generated by partial melting of calcareous sediments in the presence of residual epidote (Skora et al., 2015). The combined used of U-series disequilibria and $\delta^{238}U$ also shown that the isotope composition of Vesuvius lavas cannot be explained by shallow level crustal contamination.

Accordingly, we argue that the occurrence of ^{238}U-excess in trace element-enriched, "sediment-dominated" arc magmas, represents a unique evidence of deep recycling of carbonate sediments, hence providing constraints on the deep carbon cycling on Earth.

Avanzinelli, R., Elliott, T., Tommasini, S., Conticelli, S. (2008): Constraints on the genesis of the potassium-rich Italian volcanic rocks from U/Th disequilibrium. *J. Petrol.*, **49**, 195-223.

Iacono Marziano, G., Gaillard, F., Scaillet, B., Pichavant, M., Chiodini, G. (2009): Role of non-mantle CO_2 in the dynamics of volcano degassing: The Mount Vesuvius example. *Geology*, **37**, 319-322.

Poli, S. (2015): Carbon mobilized at shallow depths in subduction zones by carbonatitic liquids. *Nature Geosci.*, **8**, 633-637.

Skora, S, Blundy, J.D., Brooker, R.A, Green, E.C.R, de Hoog, J.C.M., Connolly, J.A.D. (2015): Hydrous phase relations and trace element partitioning behaviour in calcareous sediments at subduction-zone conditions. *J. Petrol.*, **56**, 953-980.

COHERENT RAMAN SPECTROSCOPY-BASED PT ESTIMATES TO UNRAVEL THE METAMORPHIC EVOLUTION OF A HP/UHP UNIT (SOUTHERN TIANSHAN METAMORPHIC BELT / SW CHINA)

Bayet L.*[1], Menneken M.[1], John T.[1], Agard P.[2] & Gao J.[3]
[1] Institut für Geologische Wissenschaften, Freie Universität Berlin, Germany
[2] Institut des Sciences de la Terre, Université Pierre et Marie Curie, Paris, France
[3] Chinese Academy of Sciences, Beijing, China
Corresponding email: lea.bayet@fu-berlin.de

Keywords: HP/UHP, metamorphic belt, Raman spectroscopy

During subduction lifetime, metamorphic recrystallizations, mass-transfer and deformation occur continuously or in pulses through space and time. Understanding mass transfer, in particular, requires linking all these different processes. Since only few samples having experienced high-pressure conditions are exhumed and may record mass-transfer processes, it is of prime importance to (1) find and characterize an adequate suite of high-pressure rocks (with extensive data on lithology, structures and P-T-conditions), and (2) assess whether they belong to a coherent unit (with a common P-T evolution) or to a tectonic mélange where all blocks experienced distinct pressure-temperature-deformation paths.

Pressure and temperature estimates are unfortunately often based on single outcrop samples and on a variety of methods and assumptions (e.g., assessment of equilibrium for pseudosection modeling, average P-T, etc.), which can in part account for the spread of P-T estimates over a given metamorphic belt. By contrast, we herein propose a systematic and coherent approach to estimate P-T-conditions using Raman spectroscopy (hence not relying on thermodynamic bulk equilibrium but solely on mineral structures) with wide spatial coverage.

The Chinese Tianshan metamorphic belt (TMB) is a promising area for such a study, with well-preserved high-pressure rocks and deep deformation structures. The studied area, 11x13 km wide, is composed of a large high-pressure to ultra-high-pressure unit (HUU) bounded in the North and in the South by greenschist-facies units. The HUU is mainly composed of intercalated metasediments and volcano-clastic rocks with minor carbonate lenses, which likely represent turbidites and fore-arc basin sediments interlayered with arc volcanoclastic rocks deposited on top of the incoming plate prior to subduction (and/or eroded away from the margin). The southern part of the unit, composed of pillow basalts and pelagic sediments, preserves the uppermost part of the former oceanic crust. During subduction, these rocks underwent blueschist- to eclogite- facies metamorphism as indicated by assemblages containing garnet, omphacite, and glaucophane.

To constrain pressures and temperatures, independent in-situ Raman spectroscopic methods and microprobe analysis were used on both metapelites and metabasites. Pressures were estimated in both rock types by analysing the shift of the 464 cm^{-1} A_1 Raman mode of quartz inclusions in garnet, while peak temperatures were constrained in metapelites using carbon maturity, and Zr-in rutile thermobarometry for metabasites. Estimates yield consistent and homogeneous peak P-T-conditions of 530±30°C and 2.3±3 GPa throughout the HUU, indicating depths of around 70 km, corroborated by the presence of coesite inclusions in garnet in some samples.

INSIGHTS INTO THE CARBON CYCLE IN THE LITHOSPHERE AND THE ROLE OF GRAPHITIC CARBON FROM SUBDUCTION TO EROSION

Beyssac O.*[1]

[1] Insitut de Minéralogie, Physique des Matériaux et Cosmochimie, Centre National de la Recherche Scientifique, Université Pierre et Marie Curie, Paris, France

Corresponding email: olivier.beyssac@impmc.upmc.fr

Keywords: subduction, erosion, carbon cycle

Lithosphere is a key site of the geological carbon cycle at the interface between the exosphere and the solid Earth, and where carbon is exchanged between the biomass and the mineral world. There are two carbon subcycles in the Lithosphere, organic versus inorganic cycles, which broadly corresponds to the distinction between reduced versus oxidized carbon. Interactions between the two subcycles are largely unknown, although they may have profound implications for buffering redox conditions, or controlling the speciation of deep fluids. Main lithospheric fluxes are identified: on one side, carbon is incorporated into the Lithosphere through burial of organic carbon and incorporation of carbonates in sediments or during weathering of the oceanic lithosphere. On the other side, carbon is released from the Lithosphere through degassing, erosion of continental surfaces or subduction to the deep Earth. The broad picture seems relatively simple, but field and experimental studies reveal that the reality is actually much more complex. This presentation will focus on the particular case of organic carbon which represents nearly a quarter of the total carbon entering subduction zones and which occurs mostly under the form of graphitic carbon in the lithosphere (Beyssac & Rumble 2014). A first example of this natural complexity will be discussed regarding the fate of carbon-bearing phases during subduction based on field studies in high-pressure metamorphism settings. If graphitic carbon present in bulk sediments appears as relatively inert during subduction, the situation is different as soon as fluid-rock interactions at lithological interfaces occur. Then, graphitic carbon maybe generated from calcite reduction then stabilizing carbon in graphite, or it can be devolatilized thus transferring carbon into the fluid. Another example regards the carbon budget during erosion of continental surfaces. A major point is then the fate of modern carbon deriving from the biomass: burial and trapping in sediments, or oxidation and release as CO_2 to the atmosphere? But the fate of carbonates and rock-derived organic carbon during continental erosion as well as the CO2 consumption for silicates weathering has also to be considered for a complete budget on long timescales. This is a complex factory that depends highly on the scale and dynamics of the erosion system, and that will be discussed in light of recent studies in active small-scale (Taiwan) and large-scale (Himalayas, Andes) systems.

Beyssac, O. & Rumble, D. (2014): Graphitic carbon: a ubiquitous, diverse, and useful geomaterial. *Elements*, **10**, 415-420.

STABLE ISOTOPE CHEMISTRY OF SCAPOLITE IN ULTRA-HIGH-PRESSURE ROCKS: A MONITOR OF SUBDUCTION ZONE FLUIDS?

Bryden C.D.*[1], Jamieson R.A.[1] & Robinson P.[2]
[1] Department of Earth Sciences, Dalhousie University, Halifax, Canada
[2] Geological Survey of Norway, Trondheim, Norway
Corresponding email: colin.bryden@dal.ca

Keywords: scapolite, fluids, subduction

The volatile-bearing framework silicate scapolite is an important constituent of migmatites and orthogneisses in parts of the Nordøyane ultra-high pressure (UHP) domain of the Western Gneiss Region (WGR) of Norway. These rocks record the subduction and exhumation of Baltican continental crust during the Silurian to Devonian Scandian orogeny. We present compositional data bearing on the source(s) of fluids related to the formation of scapolite in late-stage pegmatitic leucosomes. Based on a combination of field relationships, textures, and mineral chemistry, three types of scapolite pegmatite have been identified. In Type 1 pegmatites, found on Haramsøya and Flemsøya, scapolite forms macrographic intergrowths with quartz, as part of a hornblende-plagioclase-scapolite-quartz assemblage. These scapolites are sulphate-rich meionite (silvialite), with high C (0.53-0.71 apfu) and S (0.21-0.44 apfu) and low Cl (0.01-0.09 apfu). Type 2 scapolites, encountered only on the small island of Ulla Fyr, have a bladed morphology and contain inclusions of chalcopyrite. Although still containing some S (0.08-0.26 apfu) and significant C (0.34-0.47 apfu), these are the most Cl-rich (0.33-0.47 apfu) of all the scapolites in the study area. Type 3 pegmatite scapolite, found on Finnøya, displays both macrographic and prismatic textures and has lower C (0.45-0.54 apfu) and higher Cl (0.07-0.12 apfu) and S (0.39-0.44 apfu) contents than Type 1 examples. In addition, scapolite of varying silvialitic to meionitic composition, and commonly showing signs of alteration, is found locally in basement orthogneisses on Haramsøya, Flemsøya, and Harøya. The Finnøya pegmatite has been dated at ca. 396 Ma (Gordon et al., 2013), suggesting that it formed during late-stage amphibolite facies metamorphism. Ages of other scapolite-bearing pegmatites are not yet known. Several hypotheses have been advanced to explain the source of fluids related to scapolite crystallization in these pegmatites, including: a) scapolite or scapolite-forming fluids were already present in metasomatised crust prior to subduction, and were remobilized during Scandian metamorphism and anataxis; b) fluids expelled from sedimentary cover rocks infiltrated the basement during subduction; and c) mantle fluids were introduced to the crust during subduction. Preliminary stable isotope data are compatible with a mantle fluid source for at least some scapolites.

Gordon, S.M., Whitney, D.L., Teyssier, C., Fossen, H. (2013): U-Pb dates and trace-element geochemistry of zircon from migmatite, Western Gneiss Region, Norway: Significance for history of partial melting in continental subduction. *Lithos*, **170-171**, 35-53.

TEXTURAL AND GEOCHEMICAL EVOLUTION OF OPHICARBONATES FROM OCEAN TO DEEP SUBDUCTION

Cannaò E.*[1-2], Bebout G.E.[3], Agostini S.[2] & Scambelluri M.[1-2]
[1] Dipartimento di Scienze della Terra, dell'Ambiente e della Vita, Università di Genova, Italy
[2] Istituto di Geoscienze e Georisorse, Consiglio Nazionale delle Ricerche, Pisa, Italy
[3] Department of Earth and Environmental Sciences, Lehigh University, Bethlehem, PA, USA
Corresponding email: enrico.cannao@unige.it

Keywords: ophicarbonates, carbon cycle, subduction zone fluids

Understanding how oceanic lithosphere is affected by chemical and physical processes in the subduction factory is key to elucidating the cycling of elements on Earth. In particular, the deep carbon (C) cycle and C mobility in the subduction environment are topics of recent debate in the scientific community.

Here, we present textural and geochemical data for ophicarbonate rocks (i.e., carbonate-bearing serpentinites) re-equilibrated at differing *P-T* conditions as representing a prograde subduction history. In order of increasing peak *P-T* conditions, we focus on the N. Apennines (Italy) ophicarbonates (not subducted), sub-blueschist and blueschist-facies ophicarbonates from the Voltri Massif (bVM) and the Queyras (Q), respectively (W. Alps), and eclogite-facies ophicabonates from the Voltri Massif (eVM).

The oceanic ophicarbonates display breccia-like textures linked to hydrothermal and sedimentary origin. Their carbonate geochemical signatures for $\delta^{18}O$ and $\delta^{13}C$ are +15.6 to +18.2‰ and +1.1 to +2.5‰, respectively, and their $^{87}Sr/^{86}Sr$ (0.7058 to 07068) appears to reflect equilibration with seawater during Jurassic time. Intense shear deformation characterizes the ophicarbonate rocks from bVM and Q, where strong calcite recrystallization occurred, potentially by dissolution and reprecipitation. The isotopic compositions of the bVM overlap those of the oceanic ophicarbonates, whereas the most deformed samples from the Q show enrichment in radiogenic Sr (0.7075), depletion in $\delta^{13}C$ (to as low as -2.0‰), with $\delta^{18}O$ approaching +20‰ (Collins et al., 2015). These textural and geochemical features suggest that the bVM and deformed Q rocks experienced interaction with fluids in closed and open system, respectively. High-pressure-metamorphosed eVM ophicarbonates show strong shear textures, with coexisting antigorite and dolomite and, in some cases, relict nodules of magnesite enclosed in the foliation are still recognizable. Dolomite-bearing rocks have $\delta^{13}C$ of +0.4 to 1.0‰ and $\delta^{18}O$ of +11.6 to +12.1‰ and the magnesite-bearing samples have comparable isotopic signatures. The Sr isotopic ratios for these rocks are 0.7080 and 0.7097, respectively. These data seemingly reflect interaction with externally-derived, hot metamorphic fluids with radiogenic Sr component and high O:C ratios.

We suggest that the infiltration of fluids during early stages of subduction can trigger the dissolution of the carbonate minerals, thus allowing mobilization of C. The ability of these new carbonates to record the composition of the fluids, allow us to determinate their origin (i.e., closed *vs.* open system). The dissolution/precipitation process can be monitored and tracked by C-O and radiogenic Sr isotopes and may have important implications in our understanding of the subduction factory processes and to better evaluate the global and deep C cycle.

Collins, N.C., Bebout, G.E., Angiboust, S., Agard, P., Scambelluri, M., Crispini, L., John, T. (2015): Subduction-zone metamorphic pathway for deep carbon cycling: II. Evidence from HP/UHP metabasaltic rocks and ophicarbonates. *Chem Geol.*, **412**, 132-150.

GEOMETRY AND CONNECTIVITY OF HYDROUS-CARBONATITIC LIQUIDS IN THE MANTLE: AN EXPERIMENTAL MODEL

Capizzi L.S.*[1], Fumagalli P.[1], Ildefonse B.[2], Poli S.[1] & Tumiati S.[1]
[1] Dipartimento di Scienze della Terra "A. Desio", Università di Milano, Italy
[2] Géosciences Montpellier, Université de Montpellier, France
Corresponding email: luca.capizzi@unimi.it

Keywords: dihedral angle, peridotite, experiments

The mobility and infiltration rates of carbonatitic liquids, together with their influence on the annealing of mantle peridotites, are processes poorly constrained. Although natural carbonatitic magmas are complex chemical systems, bearing H_2O as a major chemical component, previous work has been performed in anhydrous model systems. The aim of this work is to quantitatively assess the variables controlling the percolation of hydrous carbonatitic liquids in peridotites, and their bearing on the mobility of melts.

The percolation of melts and the interconnectivity of melt pockets are investigated by placing a cylindrical dunite rod against a liquid reservoir. Thick graphite cylindrical inner capsules control the redox conditions and prevent Fe-loss to the outer Pt capsules. We used a synthetic dunite, pre-sintered in a Mo capsule starting from natural San Carlos olivine, previously sieved to 38-64 µm. Sintering has been performed in a single stage piston-cylinder apparatus at P = 0.8 GPa and T = 1200°C. As natural carbonatitic magmas in equilibrium with a mantle assemblage are mainly dolomitic, the composition ($Ca_{0.541}$, $Mg_{0.389}$, $Fe_{0.069}$) CO_3 was prepared from a powder mixture of carbonates, using free water as hydrous source (5 wt.% of mix). Time resolved experiments were performed employing an end loaded piston-cylinder apparatus, at T= 1200°C, P = 2.5 GPa and run times from 3 to 300 hours, according to the experimental phase diagram retrieved by Tumiati et al. (2013). In order to account for the different roles of gravity, chemical diffusion, and Ludwig-Soret diffusion we used two different geometries, first placing the dunite rod at the top of the capsule above the carbonate mix, then reversing the stack to have the carbonate mixture at the top, hot end of the capsule.

Hydrous carbonatitic melt pockets (> 3 µm) were found along olivine grain boundaries. BSE images and X-ray maps of elements allow quantifying the dihedral angle between the liquid and olivine. The apparent dihedral was measured through a Mathematica™ routine based on X-ray maps of elements. A true dihedral angle was estimated by the median of frequency distribution of the apparent angles. The results of approximately 400 measurements (for run durations of 300 hours), 130 meas. (for 30 hours) and 300 meas. (for 3 hours) provide a dihedral angle of ~ 40°, ~ 34° and ~ 31°, respectively. These values are larger compared to the dihedral angle found for anhydrous carbonatitic liquids (25°-28°; Hunter & McKenzie, 1989). The volume fraction of melts in the peridotitic matrix was ~ 16% and ~ 2.3% for 300 hours experiment, the larger volume proportion retrieved close to the carbonatitic reservoir; ~ 10.5% for 30 hours experiment, and ~ 8.5% for 3 hours experiment. These values are significantly lower than those observed in anhydrous experiments (e.g. 18 % in Hammouda & Laporte, 2000), therefore grossly in agreement with the relatively high dihedral angle measured (Park & Yoon, 1985).

Hammouda, T. & Laporte, D. (2000): Ultrafast mantle impregnation by carbonatite melts. *Geology*, **28**, 283-285.

Hunter, R.H. & McKenzie, D. (1989): The equilibrium geometry of carbonate melts in rocks of mantle composition. *Earth Planet. Sci. Letters*, **92**, 347-356.

Park, H.H. & Yoon, D.N. (1985): Effect of dihedral angle on the morphology of grains in a matrix phase. *Metall. Trans. A*, **16**, 923-928.

Tumiati, S., Fumagalli, P., Tiraboschi, C., Poli, S. (2013): An experimental study on COH-bearing peridotite up to 3.2 GPa and implications for crust-mantle recycling. *J. Petrol.*, **54**, 453-479.

CRUSTAL CARBONATE ASSIMILATION AS A SOURCE OF MAGMATIC CO_2 RELEASE AT CONTINENTAL ARCS

Carter L.B.*[1] & Dasgupta R.[1]
[1] Department of Earth Science, Rice University, Houston, TX, USA
Corresponding email: laura.b.carter@rice.edu

Keywords: assimilation, skarns, CO_2

Carbon transported to the Earth's surface through endogenic magmatic processes in subduction zones can be augmented during ascent by thermal breakdown and assimilation of crustal carbonate. The extent of this decarbonation relies on the intrinsic properties of the interaction – pressure, temperature, composition. Comparing melt composition and mineralogy in natural volcanic systems – Etna, Vesuvius, Merapi, Popocatepetl – with experiments (see Carter & Dasgupta, 2015) allows estimates of proportion of ingested material (< 20% calcite, ≤ 40% contaminated melt), as well as extrapolation to extinct volcanic arcs through time, plutonic intrusions with skarns, or systems of varying composition.

We have performed several series of experiments using a piston cylinder apparatus at Rice University, USA, to investigate the effects of differing melt compositions interacted with carbonate of variable calcite-dolomite content at mid- to lower-crustal pressures and liquidus to subliquidus temperatures. Phase assembly and composition of melt-carbonate reactions, layered in a 1:1 weight ratio, are compared to melt liquid lines of descent and carbonate stability at identical *P-T* conditions.

Pressure and temperature affects melt fraction and the more melt available, the more calcite is consumed. Evolved to andesite, the intruding melt assimilates more (≤ 65%) than basalt (≤ 48%) at similar melt fractions, and dissolves more of the C-O-H volatiles (~ 14 vs. ~ 9 wt.% by EMPA total deficit) in the contaminated silica-undersaturated, ultracalcic melt. Dacite assimilates ≤ 17% and has minimal volatile solubility (< 2.5 wt.%), which may facilitate hydrothermal skarnification. Increasing the MgO/CaO ratio in the carbonate layer increases decarbonation (≤ 70% assimilation) due to the additional thermal instability of dolomite that breaks down into calcite, periclase and CO_2 at moderate temperatures (≤ 750°C at 0.5 GPa) without chemical reaction with melt.

In addition to the Ca-rich, Si-poor melts and C-O-H vesicles, melt-carbonate reactions produce a Ca-rich mineral assemblage consisting of clinopyroxene (diopside to Ca-Tschermak, stable to higher T, raising liquidi), plagioclase (anorthitic), ±trace spinel, ±scapolite, ±olivine, ±wollastonite. A typical skarn mineral, scapolite forms here at previously unprecedented temperatures (> 500°C, Aitken, 1983), but is small in proportion (< 10% modal abundance), leaving most of the released CO_2 to partition into the vapor ± melt, depending on solubility, which may easily degas at low pressure into the atmosphere from volcanic vent. Sub-arc melt-carbonate reaction can release as much as ~Mt/y of CO_2 with a steady magma recharge rate (10^{12} g/y; White et al., 2006) and may affect long-term climate. Matching CO_2 outgassing measurements at presently active carbonate-assimilating volcanoes (see Carter & Dasgupta, 2015), we estimate ≤ ~ half of the ascending magma becomes carbonate-contaminated.

Aitken, B.G. (1983): T-XCO_2 stability relations and phase equilibria of a calcic carbonate scapolite. *Geochim. Cosmochim. Acta*, **47**, 351-362.

Carter, L.B. & Dasgupta, R. (2015): Hydrous basalt–limestone interaction at crustal conditions: Implications for generation of ultracalcic melts and outflux of CO_2 at volcanic arcs. *Earth Planet. Sci. Letters*, **427**, 202-214.

White, S.M., Crisp, J.A., Spera, F.J. (2006): Long-term volumetric eruption rates and magma budgets. *Geochem. Geophys. Geosyst.*, **7**, Q03010.

MOLYBDENUM ISOTOPES AS TRACERS FOR SUBDUCTION COMPONENTS: THE CASE OF ROMAN MAGMATIC PROVINCE MAGMAS

Casalini M.*[1], Avanzinelli R.[1], Elliott T.[2], Tommasini S.[1] & Conticelli S.[1]
[1] Dipartimento di Scienze della Terra, Università di Firenze, Italy
[2] School of Earth Sciences, University of Bristol, United Kingdom
Corresponding email: martina.casalini@unifi.it

Keywords: molybdenum isotopes, sediments recycling, Roman Magmatic Province

Understanding the fate of recycled material into the convecting mantle is important to provide new constraints on the chemical budget of subduction zones. Molybdenum isotopes have been shown to fractionate during the incorporation into oceanic sediments (Freymuth et al., 2015), being perceptive to ocean redox condition. Indeed, the Mo isotope variability offers the opportunity to use these isotopes as tracers of recycled material into the mantle.

The occurrence in the Middle Latin Valley volcanic region of extremely variable products in terms of geochemical and isotopic compositions, makes this area a perfect case study to tackle the role of different subduction-related metasomatic agents. In this magmatic region, the compositional variability of the recycled sedimentary component into the mantle wedge during subduction, has been proposed to explain the distinct geochemical signature of volcanic products (Avanzinelli et al., 2009).

Here we present the first results of high precision Mo isotopic compositions for Italian magmatic rocks, demonstrating that the isotopically heavy δ^{98}Mo is anomalous with respect to other subduction-related magmas. In order to reproduce such heavy isotopic composition, organic carbon-rich material, in addition to the sedimentary component, is required, revealing the potential of Mo isotopes as tracers of the fate of organic carbon in subduction zones.

Avanzinelli, R., Lustrino, M., Mattei, M., Melluso, L., Conticelli, S. (2009): Potassic and ultrapotassic magmatism in the circum-Tyrrhenian region: Significance of carbonated pelitic *vs*. pelitic sediment recycling at destructive plate margins. *Lithos*, **113**, 213-227.

Freymuth, H., Vils, F., Willbold, M., Taylor, R.N., Elliott, T. (2015): Molybdenum mobility and isotopic fractionation during subduction at the Mariana arc. *Earth Planet. Sci. Letters*, **432**, 176-186.

THE BEHAVIOR OF RHODOCHROSITE ($MnCO_3$) AT EXTREME CONDITIONS

Chariton S.*[1], Bykova E.[2], Cerantola V.[1-3], Bykov M.[2], Ismailova L.[1-5], Kupenko I.[4], Aprilis G.[5], McCammon C.A.[1] & Dubrovinsky L.[1]

[1] Bayerisches Geoinstitut, Universität Bayreuth, Germany
[2] Deutsches Elektronen-Synchrotron, Hamburg, Germany
[3] European Synchrotron Radiation Facility, Grenoble, France
[4] Institut für Mineralogie, Universität Münster, Germany
[5] Lehrstuhl für Kristallographie, Universität Bayreuth, Germany
Corresponding email: stellachariton@hotmail.com

Keywords: rhodochrosite, high-pressure, high-temperature

Many studies have reported direct evidence of carbonate presence at great depths, such as carbonate inclusions in diamonds (Wang et al., 1996; Brenker et al., 2007), carbonate melt-pockets in xenoliths (Liu et al., 2015) or exhumed carbonate metamorphic rocks (Becker & Altherr, 1992). Therefore, most of the attention was focused on studies of calcite ($CaCO_3$), magnesite ($MgCO_3$) and siderite ($FeCO_3$) at extreme conditions (e.g., Isshiki et al., 2004; Lavina et al., 2009; Merlini et al., 2012). However, these carbonates behave differently to each other at mantle conditions. Studying the rarer transition metal carbonates, such as rhodochrosite ($MnCO_3$), can therefore be useful to identify systematics in carbonate behavior at high pressures and high temperatures.

While $MnCO_3$ is already the focus of intense scientific research (Farfan et al., 2013; Boulard et al., 2015; Merlini et al., 2015), the published data are controversial. Contradictory results may arise from variations in samples in different studies, i.e., natural (not endmember) and powdered samples (subject to non-hydrostatic stress at high pressure). Therefore, we synthesized chemically pure $MnCO_3$ single crystals and studied them by means of Raman spectroscopy and synchrotron X-ray single crystal diffraction (XRD). Our XRD experiments were conducted at the ID09A beamline at ESRF, Grenoble, France.

Diamond anvil cells were employed for the generation of pressures up to ~ 67 GPa. In addition, we utilized a double-sided laser-heating system (Kupenko et al., 2012) in order to reach temperatures of about 2000 K.

The results of both methods reveal clear evidence of a phase transition at about 44 GPa from the calcite-type (*R*-3*c*) to the triclinic structure (*P*-1) of $MnCO_3$-II, which is isostructural to $CaCO_3$-VI (Merlini et al., 2012; Boulard et al., 2015; Merlini et al., 2015). Our findings by XRD are in good agreement with a previous report on natural $MnCO_3$ single crystals (Merlini et al., 2015). Moreover, we have found that at uppermost lower mantle conditions, the triclinic $MnCO_3$-II phase will decompose into the novel oxide Mn_5O_7 and a new monoclinic (*C*12/*m*1) carbonate $MnCO_3$ phase.

We will present our latest results and discuss how studies on transition metal carbonates, such as rhodochrosite, can provide insight into the high-pressure crystal chemistry of carbonates and the effect of alkaline-earth cation (i.e., Ca^{2+}, M^{g2+}) substitution by a 3d transition metal on the stability field of carbonates.

Becker, H. & Altherr, R. (1992): Evidence from ultra-high-pressure marbles for recycling of sediments into the mantle. *Nature*, **358**, 745-748.

Boulard, E., Goncharov, A.F., Blanchard, M., Mao, W.L. (2015): Pressure-induced phase transition in $MnCO_3$ and its implications on the deep carbon cycle. *J. Geophys. Res.*, *Solid Earth*, **120**, B011901.

Brenker, F.E., Vollmer, C., Vincze, L., Vekemans, B., Szymanski, A., Janssens, K., Szaloki, I., Nasdala, L., Joswig, W., Kaminsky, F. (2007): Carbonates from the lower part of the transition zone or even the lower mantle. *Earth Planet. Sci. Letters*, **260**, 1-9.

Farfan, G.A., Boulard, E., Wang, S., Mao, W.L. (2013): Bonding and electronic changes in rhodochrosite at high pressure. *Am. Mineral.*, **98**, 1817-1823.

Isshiki, M., Irifune, T., Hirose, K., Ono, S., Ohishi, Y., Watanuki, T., Nishibori, E., Takata, M., Sakata, M. (2004): Stability of magnesite and its high-pressure form in the lowermost mantle. *Nature*, **427**, 60-63.

Kupenko, I., Dubrovinsky, L., Dubrovinskaia, N., McCammon, C., Glazyrin, K., Bykova, E., Boffa-Ballaran, T., Sinmyo, R., Chumakov, A., Potapkin, V., Kantor, A., Rüffer, R., Hanfland, M., Chrichton, W., Merlini, M. (2012): Portable double-sided laser-heating system for Mössbauer spectroscopy and X-ray diffraction experiments at synchrotron facilities with diamond anvil cells. *Rev. Sci. Instrum.*, **83**, 124501.

Lavina, B., Dera, P., Downs, R.T., Prakapenka, V., Rivers, M., Sutton, S., Nicol, M. (2009): Siderite at lower mantle conditions and the effects of the pressure-induced spin-pairing transition. *Geophys. Res. Letters*, **36**, L23306.

Liu, Y., He, D., Gao, C., Foley, S., Gao, S., Hu, Z., Zong, K., Chen, H. (2015): First direct evidences of sedimentary carbonate recycling in subduction-related xenoliths. *Sci. Rep.*, **5**, 11547.

Merlini, M., Hanfland, M., Crichton, W.A. (2012): $CaCO_3$-III and $CaCO_3$-VI, high-pressure polymorphs of calcite: possible host structures for carbon in the Earth's mantle. *Earth Planet. Sci. Letters*, **333-334**, 265-271.

Merlini, M., Hanfland, M., Gemmi, M. (2015): The $MnCO_3$-II high-pressure polymorph of rhodochrosite. *Am. Mineral.*, **100**, 2625-2629.

Wang, A., Pasteris, J.D., Meyer, H.O.A., Dele-Duboi, M.L. (1996): Magnesite-bearing inclusion assemblange in natural diamond. *Earth Planet. Sci. Letters*, **141**, 293-306.

LOCAL STRESS FIELD DURING SERPENTINE DEHYDRATION INFERRED FROM ORTHOPYROXENE INVERSION TO CLINOENSTATITE

Clément M.*[1], Padrón-Navarta J.A.[1], Tommasi A.[1] & Mainprice D.[1]
[1] Géosciences Montpellier, Centre National de la Recherche Scientifique & Université de Montpellier, France
Corresponding email: mxmeclmnt@gmail.com

Keywords: clinoenstatite, dehydration reactions, local stress

The release of fluid during dehydration reactions has important consequences for the subduction dynamics, since fluids might affect the rheology of the mantle wedge and the subduction interface. Additionally fluids control large scale chemical recycling through arc magmatism. How dehydration reactions and fluid transport proceed at the microscopic scale is however poorly constrained. Under poorly drained conditions, fluid pressure gradients are produced during dehydration creating small-scale variations in the stress magnitude and orientation. These local stress variations might be recorded in minerals such as orthopyroxene where shear stresses on (100) planes parallel to the [100] direction result in the inversion to low clinoenstatite (i.e., martensitic transformation). Experiments show that maximum critical resolved shear stress is reached by applying axial compression at 45° to the *a* and *c* axes (Coe & Kirby, 1975). Occurrence of clinoenstatite has been reported in natural peridotites (Frost, 1978; Padrón-Navarta et al., 2015) and Padrón-Navarta et al. (2015) showed that clinoenstatite might be produced by flexural deformation of elongated enstatite crystals.

We have studied calcium-free low temperature clinoenstatite (LCen, $P2_1/c$) lamellae in orthoenstatite (Oen, *Pbca*) in peridotites produced by dehydration of serpentinites from Cerro del Almirez (Spain) (Padrón-Navarta et al., 2015) to determine stress orientations. Optical microscopy and EBSD analyses were used to determine the orientations of both the host orthoenstatite and the clinoenstatite lamellae. LCen lamellae are observed in almost all OEn crystals oriented with the axis roughly normal to the thin section. For each Oen-LCen pair, we infer the orientation of the main principal compressional stress. The orientation of the compressional stress at the sample scale is highly variable. Based on these observations we conclude that dehydration reactions and the associated compaction generate local stresses with variable orientation and magnitudes sufficient to produce the inversion of orthoenstatite to clinoenstatite by a martensitic transformation.

Coe, R.S. & Kirby, S.H. (1975): The orthoenstatite to clinoenstatite transformation by shearing and reversion by annealing: Mechanism and potential applications. *Contrib. Mineral. Petrol.*, **52**, 29-55.

Frost, B.R., Coe, R.S. Okamura, F.P. (1978): Principal stress directions from a natural occurrence of stress-induced clinoenstatite. *Contrib. Mineral. Petrol.*, **67**, 119-126.

Padrón-Navarta, J.A., Tommasi, A., Garrido, C.J., Mainprice, D. (2015): On topotaxy and compaction during antigorite and chlorite dehydration: an experimental and natural study. *Contrib. Mineral. Petrol.*, **169**, 35.

SUBDUCTION EFFICIENCY OF CARBONATES THROUGH GEOLOGIC TIME AND THE ROLE OF SLAB-DERIVED MELTS IN TRANSPORTING CO_2 TO VOLCANIC ARCS

Dasgupta R.*[1], Duncan M.S.[1-2], Tsuno K.[1] & Muth M.[1]
[1] Department of Earth Science, Rice University, Houston, TX, USA
[2] Geophysical Laboratories, Carnegie Institution for Science, Washington, DC, USA
Corresponding email: rajdeep.dasgupta@rice.edu

Keywords: subduction, deep carbon cycle, CO_2 flux in arcs

The long-term flux of carbon dioxide into and out of the solid Earth is critical for the habitability of surface environment as well as the redox, thermal, and dynamical evolution of the Earth's interior. Constraining such long-term influx and outflux of CO_2, however, requires critical consideration of a number of factors including stability of carbon-bearing phases in different deep environments as well as the partitioning and solubility of solid carbon-rich phases in mobile agents such as silicate melts and aqueous fluids. Because subduction zones provide the most important pathway for carbon influx into the Earth, in order to understand the long-term balance of CO_2, it is critical to constrain the fate of all carbon-bearing phases hosted in different subducting lithologies.

In this presentation we will review the phase relations of various subducting lithologies constrained in the presence of carbonates over the past twenty years through laboratory experiments and thermodynamic modeling. By comparison with recent models of subduction zone thermal structures, we will show that carbonates hosted in metapelitic sediments are most prone to breakdown and release by fluid-present or fluid-absent melting for intermediate to hot subduction zones in the modern Earth. However, carbonated melting of crustal lithologies, if at all, occurs at depths well past the depth beneath volcanic arcs (e.g., Grassi & Schmidt, 2011; Tsuno et al., 2012). This behavior of carbonates might have been quite different in ancient hotter subduction zones, where shallow decarbonation was likely a norm (Dasgupta, 2013). Although significant decarbonation or melting is restricted for most slab-top lithologies where carbonates are concentrated in the downgoing slab, hydrous silicic partial melt generated in the presence or absence of aqueous fluid could potentially be the necessary carrier of CO_2 to arc source regions. To evaluate the potential of rhyolitic partial melt generated by fluid-fluxed melting of downgoing slab, we will also discuss our recent experimental data and developed thermodynamic model on the solubility of CO_2 in hydrous rhyolitic melts at depths and temperature conditions relevant for subduction zones (e.g., Duncan & Dasgupta, 2015). We will show that although carbonates in the top few hundred meters of subducting basalts and sediments are largely recycled deeper, silicic partial melts possess sufficient carrying capacity of CO_2 to explain the arc flux of CO_2. Only few weight percent of sediment partial melt is necessary to elevate the mantle wedge carbon budget over a depleted mantle carbon content such that modern arc flux of CO_2 can be reconciled.

Dasgupta, R. (2013): Ingassing, storage, and outgassing of terrestrial carbon through geologic time. *Rev. Mineral. Geochem.*, **75**, 183-229.

Duncan, M.S. & Dasgupta, R. (2014): Pressure and temperature dependence of CO_2 solubility in hydrous rhyolitic melt – Implications for carbon transfer to mantle source of volcanic arcs via partial melt of subducting crustal lithologies. *Contrib. Mineral. Petrol.*, **169**, 1-19.

Grassi, D. & Schmidt, M.W. (2011): The melting of carbonated pelites from 70 to 700 km depths. *J. Petrol.*, **52**, 765-789.

Tsuno, K., Dasgupta, R., Danielson, L., Righter, K. (2012): Flux of carbonate melt from deeply subducted pelitic sediments – geophysical and geochemical implications for the source of Central American volcanic arc. *Geophys. Res. Letters*, **39**, L16307.

MULTI-STAGE CARBONATION AND DECARBONATION IN THE MANTLE-WEDGE: STABLE-ISOTOPE COMPOSITIONS OF CARBONATE PHASES IN ULTRAMAFIC ROCKS OF THE ULTEN ZONE (EASTERN ALPS, ITALY)

Förster B.*[1], Bebout G.E.[2], Bianchini G.[3], Natali C.[3], Aulbach S.[4], Braga R.[1] & Scambelluri M.[5]

[1] Dipartimento di Scienze Biologiche, Geologiche e Ambientali, Università di Bologna, Italy

[2] Department of Earth and Environmental Sciences, Lehigh University, Bethlehem, PA, USA

[3] Dipartimento di Fisica e Scienze della Terra, Università di Ferrara, Italy

[4] Institut für Geowissenschaften, Goethe-Universität Frankfurt am Main, Germany

[5] Dipartimento di Scienze della Terra, dell'Ambiente e della Vita, Università di Genova, Italy

Corresponding email: bibiana.forster2@unibo.it

Keywords: mantle-wedge peridotites, carbon-cycle, decarbonation

The cycling of carbon (C) among Earth's reservoirs, and especially the fate of C in subduction-related environments, are still under debate. Of particular importance are the origin and fluxes of C at convergent margins, in which CHO-bearing fluids released by the downgoing slabs introduce C into mantle-wedges where dolomite is stable and might act as a C-host.

Orogenic ultramafic rocks of the Ulten Zone (UZ, Eastern Alps, Italy) consist of peridotites from a supra-subduction zone mantle wedge that were captured by the crustal portion of a subducting slab and subsequently exhumed during the Late Paleozoic Variscan orogeny (Scambelluri et al., 2006). These rocks were metasomatized by aqueous-carbonic fluids sourced by the crustal slab (Rampone & Morten, 2001; Scambelluri et al., 2006). Such metasomatism potentially enables large-scale C-mobility and transfer into the high-pressure eclogite-facies assemblage and, indeed, Sapienza et al. (2009) documented occurrence of dolomite in fine-grained garnet + amphibole peridotites.

Using UZ peridotites, we follow up on these initial reports and present an integrated textural/chemical study aimed at obtaining new insights into the origin and fate of C in the mantle wedge. A survey of a large number of new samples (~100) reveals the occurrence of diverse carbonate phases in various microtextural settings (discrete grains to intergrowths to veins). Fine-grained garnet + amphibole peridotites that are feebly serpentinized contain, according to Sapienza et al. (2009), discrete dolomite grains, while in the serpentinized ones abundant calcite-brucite-intergrowths are closely related to serpentine veins. These intergrowths have been suggested to be dedolomitization products in mantle-derived rocks (Berg et al., 1986). Such decarbonation of mantle-wedge peridotite during serpentinization-related fluid-rock interactions results in the release of C and potentially enables large-scale C-mobility and transfer.

Whole-rock analyses performed at the University of Ferrara reveal relatively uniform total-C concentrations (0.06 wt-% to 0.08 wt-%) and low $\delta^{13}C_{VPDB}$ of -17.2‰ to -11.1‰. Preliminary C and O isotope data for microsampled carbonates, obtained at Lehigh University, show more variable $\delta^{13}C$, with values ranging from -14 to -2‰, and $\delta^{18}O_{VSMOW}$ of +6 to +20‰. This isotopic variability and the overall low $\delta^{13}C$ of the UZ carbonates will be discussed in light of textural evidence for carbonation and decarbonation reactions in the mantle wedge, and in the context of the multiple processes that are known to have modified the UZ mantle-wedge, based on trace element constraints (Scambelluri et al., 2006; Sapienza et al., 2009). This systematic study of textures and stable isotopic signatures of carbonates will enhance our understanding of possible C sources and crust-mantle interactions affecting the cycling of C in collisional subduction-zone settings.

Berg, G.W. (1986): Evidence for carbonate in the mantle. *Nature*, **324**, 59-60.

Rampone, E. & Morten, L. (2001): Records of Crustal Metasomatism in the Garnet Peridotites of the Ulten Zone (Upper Austroalpine, Eastern Alps). *J. Petrol.*, **42**, 207-219.

Sapienza, G.T., Scambelluri, M., Braga, R. (2009): Dolomite-bearing orogenic garnet peridotites witness fluid-mediated carbon recycling in a mantle wedge (Ulten Zone, Eastern Alps, Italy). *Contrib. Mineral. Petrol.*, **158**, 401-420.

Scambelluri, M., Hermann, J., Morten, L., Rampone, E. (2006): Melt- versus fluid-induced metasomatism in spinel to garnet wedge peridotites (Ulten Zone, Eastern Italian Alps): clues from trace element and Li abundances. *Contrib. Mineral. Petrol.*, **151**, 372-394.

SERPENTINITE-DRIVEN EXHUMATION OF THE UHP LAGO DI CIGNANA UNIT IN THE FOSSIL ALPINE PLATE INTERFACE

Gilio M.*[1], Scambelluri M.[1], Agostini S.[2], Pettke T.[3] & Godard M.[4]
[1] Dipartimento di Scienze della Terra, dell'Ambiente e della Vita, Università di Genova, Italy
[2] Instituto di Geoscienze e Georisorse, Consiglio Nazionale delle Ricerche, Pisa, Italy
[3] Institut für Geologie, Universität Bern, Switzerland
[4] Geosciences Montpellier, Université de Montpellier IV, France
Corresponding email: mattia.gilio@edu.unige.it

Keywords: serpentinite, fluid rock exchange, UHP metamorphism

The Lago di Cignana Unit (LCU) is a coesite- (Reinecke, 1998) and diamond-bearing (Frezzotti et al., 2011) slice of oceanic-derived eclogites and metasediments recording Alpine UHP metamorphism at 600°C - 3.2 GPa (~110 km depth; Groppo et al., 2009). The LCU is tectonically sandwiched between the eclogitic Zermatt-Saas Zone (ZSZ; 540°C - 3.2 GPa; Angiboust et al., 2009) and the blueschist Combin Zone (400°C - 0.9 GPa; Reddy et al., 1999) along a tectonic structure joining HP units recording a ~ 1.2 GPa (40 km) pressure difference. So far, the ZSZ has been attributed to normal HP conditions and the mechanism driving exhumation and accretion of the LCU in its present structural position is not fully understood.

We performed petrography, bulk-rock trace element and Sr, Pb and Nd isotopic analyses of rocks from LCU and ZSZ serpentinites. While serpentinites in the core of the ZSZ show normal subduction zone trace elements and REE's patterns, the Ol+Ti-chu+Chl veins and host serpentinites enveloping the LCU are strongly enriched in oceanic crust-derived fluid-mobile elements (U, Th, Nb, Ta, Ce, Y, As, Sb) and REE's: their patterns well match those of the closely associated LCU-UHP rocks. Furthermore, serpentinites from the ZSZ display Sr and Pb isotopic values typical for oceanic serpentinization, with limited fluid infiltration during subduction and exhumation. Instead, serpentinites around the LCU record significant reset of Sr and Pb isotopes from oceanic crust-derived metamorphic fluids which occurred during subduction and UHP metamorphism.

Serpentinites in direct contact with the UHP Lago di Cignana Unit are highly enriched in crust-derived fluid mobile elements. This evidence, together with Pb, Sr and Nd isotopic data, suggests that tectonic coupling and fluid exchange between serpentinite and LCU crustal rocks occurred during subduction up to peak UHP metamorphic conditions. As such, the buoyancy force originating from the relatively light serpentinites might have fuelled the exhumation of the Lago di Cignana Unit, on top of the lower pressure Zermatt-Saas zone along a tectonic plate interface surface.

Angiboust, S., Agard, P., Jolivet, L., Beyssac, O. (2009): The Zermatt - Saas ophiolite: the largest (60 - km wide) and deepest (c. 70–80 km) continuous slice of oceanic lithosphere detached from a subduction zone? *Terra Nova*, **21**, 171-180.

Frezzotti, M.L., Selverstone, J., Sharp, Z.D., Compagnoni, R. (2011): Carbonate dissolution during subduction revealed by diamond-bearing rocks from the Alps. *Nature Geosci.*, **4**, 703-706.

Groppo, C., Beltrando, M., Compagnoni, R. (2009): The P–T path of the ultra-high pressure Lago di Cignana and adjoining high-pressure meta-ophiolitic units: insights into the evolution of the subducting Tethyan slab. *J. Metam. Geol.*, **27**, 207-231.

Reddy, S.M., Wheeler, J., Cliff, R.A. (1999): The geometry and timing of orogenic extension: an example from the Western Italian Alps. *J. Metam. Geol.*, **17**, 573-589.

Reinecke, T. (1998): Prograde high-to ultrahigh-pressure metamorphism and exhumation of oceanic sediments at Lago di Cignana, Zermatt-Saas Zone, western Alps. *Lithos*, **42**, 147-189.

METASOMATISM IN THE MANTLE WEDGE: MULTIPLE ISOTOPE CONSTRAINTS FROM OROGENIC PERIDOTITES OF THE ULTEN ZONE (N ITALY)

Gudelius D.*[1-2], Aulbach S.[2], Seitz H.-M.[2] & Braga R.[3]
[1] Institut für Angewandte Geowissenschaften, Karlsruhe Institut für Technologie, Germany
[2] Institut für Geowissenschaften, Goethe-Universität Frankfurt am Main, Germany
[3] Dipartimento di Scienze della Terra e Geologico-Ambientali, Università di Bologna, Italy
Corresponding email: dominik.gudelius@kit.edu

Keywords: orogenic peridotites, subduction fluids, mantle metasomatism

The high-grade basement rocks of the Ulten Zone (Upper Austroalpine, N Italy) contain peridotite bodies that sample a subduction-modified Variscan mantle wedge. Textural differences record a multi-stage metasomatic evolution: (1) Infiltration of melts in the shallow mantle wedge causing enrichment of coarse-grained spinel-peridotites, (2) reaction with crust-derived siliceous liquids after cooling and pressure increase generating coarse-grained garnet-amphibole-peridotites, (3) recrystallization and formation of amphibole (± dolomite) as a consequence of interaction with crustal aqueous fluids during and/or after peak metamorphism (850°C / 2.5 GPa) at 330 Ma (Tumiati et al., 2003) creating abundant fine-grained garnet-amphibole-peridotites, (4) further hydration during retrogression resulting in spinel-chlorite-amphibole-peridotites (Nimis & Morten, 2000; Scambelluri et al., 2006). Whole rock Lu-Hf, Sm-Nd, Sr, Li and garnet O isotope compositions constrain the nature of metasomatism at various stages as these isotope systems display different susceptibilities to metasomatism by melts and aqueous fluids (Kessel et al., 2005). The transition from coarse- to fine-grained peridotites is marked by a significant decrease in $^{147}Sm/^{144}Nd$ accompanied by addition of unradiogenic Nd causing overall homogeneous Sm-Nd isotope compositions. Only some coarse-grained samples have retained radiogenic εNd (up to +15.9) and mantle-like $^{147}Sm/^{144}Nd$ (~0.362). In contrast, $^{176}Lu/^{177}Hf$ records a gradual response dependent on the degree of Lu loss due to garnet-consuming reactions. Contrary to Nd, this finally generated a large spread of present-day εHf values (-2.3 to +41) and a distinct mixing line in the Lu-Hf isochron diagram. In both Lu-Hf and Sm-Nd systems, the parent-daughter ratios and isotope ratios calculated for 330 Ma decrease with increasing contents of fluid-mobile elements and modal amphibole. This indicates that the crustal isotopic signature mostly resulted from pervasive metasomatism during and/or after the high-pressure stage. In contrast, enrichment in radiogenic $^{87}Sr/^{86}Sr$ is independent from textural types and is only weakly correlated with contents of fluid-mobile, light elements (Li, B and Be). Enrichment in Li is accompanied with a decrease in δ^7Li from DM-like values (+3 to +5 ‰, Tang et al., 2007) to -4.2 ‰. This may reflect kinetic Li isotope fractionation due to faster diffusive transport of ^6Li into the peridotites during reaction with Li-rich retrograde fluids (Halama et al., 2011). Irrespective of textural types, $\delta^{18}O$ values of garnet separates (+5.3 to +5.8 ‰) lie mostly within the DM average (+5.5 ±0.2 ‰), indicating that enrichment by crustal fluids was largely buffered by mantle-derived oxygen (Eiler 2001). Furthermore, metasomatism was variable within the Ulten Zone: The samples from Samerberg are more serpentinized and LREE-/LILE-enriched but display more mantle-like δ^7Li and $^{176}Lu/^{177}Hf$ values compared to those from Seefeld area.

Eiler, J.M. (2001): Oxygen isotope variations of basaltic lavas and upper mantle rocks. *in* "Stable isotope geochemistry", J.W. Valley, D.R. Cole, eds., *Rev. Mineral. Geochem.*, **48**, 319-364.

Halama, R., John, T., Herms, P., Hauff, F., Schenk, V. (2011): A stable (Li, O) and radiogenic (Sr, Nd) isotope perspective on metasomatic processes in a subducting slab. *Chem. Geol.*, **281**, 151-166.

Kessel, R., Schmidt, M.W., Ulmer, P., Pettke, T. (2005): Trace element signature of subduction-zone fluids, melts and supercritical liquids at 120-180 km depth. *Nature*, **437**, 724-727.

Nimis, P. & Morten, L. (2000): P-T evolution of "crustal" garnet peridotites and included pyroxenites from Nonsberg area (upper Austroalpine), NE Italy: from the wedge to the slab. *J. Geodyn.*, **30**, 93-115.

Scambelluri, M., Hermann, J., Morten, L., Rampone, E. (2006): Melt- versus fluid-induced metasomatism in spinel to garnet wedge peridotites (Ulten Zone, Eastern Italian Alps): clues from trace element and Li

Tang, Y.-J., Zhang, H.-F., Ying, J.-F. (2007): Review of the Lithium Isotope System as a Geochemical Tracer. *Int. Geol. Rev.*, **49**, 374-388.

Tumiati, S., Thöni, M., Nimis, P., Martin, S., Mair, V. (2003): Mantle-crust interactions during Variscan subduction in the Eastern Alps (Nonsberg-Ulten zone): geochronology and new petrological constraints. *Earth Planet. Sci. Letters*, **210**, 509-526.

HYDRATION OF ECLOGITE AT THE PLATE INTERFACE: AN EXAMPLE OF FLUID INFILTRATION INTO A DRY ROCK

John T.*[1] & Vrijmoed J.C.[2]
[1] Institut für Geologische Wissenschaften, Freie Universität Berlin, Germany
[2] Institut für Geochemie und Petrologie, Eidgenössische Technische Hochschule Zürich, Switzerland
Corresponding email: timm.john@fu-berlin.de

Keywords: fluids, eclogite - blueschist, plate interface

An important feature observed in subduction zones worldwide is that eclogites can become hydrated and transform into blueschists (e.g., van der Straaten et al., 2008). This process occurs at the slab-wedge interface during exhumation of the rock and allows probing of the fluid that is likely not making its way into arc magma but leaving the sudduction system via the subduction channel. Beside its impact on balancing chemical subduction zone fluxes, this transformation expresses the general problem of how fluids infiltrate into a system that is expected to swell by the fluid uptake of the newly formed hydrous minerals. We found eclogitic pillow lavas that are partly transformed to blueschists along their rims due to blueschist-facies overprinting during retrograde metamorphism. Field observations and petrological data indicate two different fluid flow regimes during retrogression, one major fluid pathway system between the pillows characterized by high fluid fluxes and a second one related to fluid migration into the pillow interiors. We found that the inward-propagating reaction front is always associated with a reaction zone about 2 cm wide. Mass-balance calculations for this reaction front and zone display an overall mass loss and a calculated volume loss during eclogite-blueschist transformation. Thus, fluid infiltration resulted in shrinkage rather than expansion.

We hypothesize that the propagation of the blueschist-front is controlled by fluid migration driven by the volume loss at the reaction front. This volume loss is caused by element transport driven by chemical gradients in the connected fluid system. This indicates that for such a dynamic system the flux of elements out of the system must be high enough to keep up with the rate of mineral formation at the reaction front.

To test this we developed a reactive flow model including transport of aqueous species at high pressure (*P*) and temperature (*T*) to quantify reaction rates and element fluxes during blueschist formation from the pre-existing eclogite. The modelling approach is based on mass conservation and porous flow and treats porosity evolution due to deformation and reaction. Minerals and fluid are compressible, and variable pressure is used in calculating local equilibrium. Solid reactions are computed using Gibbs free energy minimization allowing for any possible reaction at each local equilibrium domain. Local equilibrium is calculated using minerals and melts from the Holland & Powell (1998) database and aqueous species from the SUPCRT92 database (Johnson et al., 1992) extended to high *P-T* following Sverjensky et al. (2014). Up to date solid solutions are included in a general formulation. The local equilibrium computations are combined in a fully coupled approach with diffusion and advection of chemical species leading to changes in composition at any location in the modelled domain and results in the conversion from eclogite to blueschist.

Holland, T.J.B. & Powell, R. (1998): An internally consisten thermodynamic data set for phases of petrological interest. *J. Metam. Geol.*, **16**, 309-343.

Johnson, J.W., Oelkers, E.H., Helgeson, H.C. (1992): A software package for calculating the standard molal thermodynamic properties of minerals, gases, aqueous species, and reactions from 1 to 5000 bar and 0 to 1000°C. *Comput. Geosci.*, **18**, 899-947.

Sverjensky, D.A., Harrison, B., Azzolini, D. (2014): Water in the deep Earth: The dielectric constant and the solubilities of quartz and corundum to 60 kb and 1200°C. *Geochim. Cosmochim. Acta*, **129**, 125-145.

van der Straaten, F., Schenk V., John, T., Gao, J. (2008): Blueschist-facies rehydration of eclogites (Tian Shan, NW-China): Implications for fluid-rock interaction in the subduction channel. *Chem. Geol.*, **255**, 195-219.

ORTHOPYROXENE-ENRICHED, DUNITE VEINED UPPER MANTLE XENOLITHS FROM MINDSZENTKÁLLA (BAKONY-BALATON HIGHLAND, WESTERN PANNONIAN BASIN): TRACES OF A SUBDUCTED SLAB?

Kovács Z.[1], Patkó L.[1], Aradi L.E.[1], Klébesz R.[1-2], Hidas K.[3], Garrido C.J.[2], Creon-Bocquet L.*[4-5] & Szabó C.[1]

[1] Lithosphere Fluid Research Lab, Department of Petrology and Geochemistry, Eötvös Loránd University, Budapest, Hungary

[2] Geodetic and Geophysical Institute, Sopron, Hungary

[3] Instituto Andaluz de Ciencias de la Tierra, Consejo Superior de Investigaciones Científicas, Universidad de Granada, Armilla, Spain

[4] Department Geosciences, IFP – Energies nouvelles, Rueil-Malmaison, France

[5] Centro de Geociencias, Universidad Nacional Autónoma de México, Juriquilla, Mexico

Corresponding email: kozraat@gmail.com

Keywords: mantle xenoliths, Carpathian-Pannonian region, mantle metasomatism

There are seven occurrences in the Bakony-Balaton Highland Volcanic Field (BBHVF, Central Pannonian Basin, Hungary) where Plio-Pleistocene alkali basalts host great number of upper mantle xenoliths. Most of these occurrences are dominated by lherzolites (Szabó et al., 2004, and references therein), however, harzburgites are prevalent in the Mindszentkálla locality. In addition to the homogeneous coarse-grained harzburgite xenoliths, composite mantle rocks, which represent small scale heterogeneities, were also collected. Harzburgite, interpreted as the wallrock, is crosscut by dunitic and occasionally apatite-bearing websteritic and amphibole-phlogopite-bearing glassy veins. X-ray microtomographic investigations revealed dunite veins inside four out of six examined xenoliths, which confirmed the petrographic observations.

In order to understand the evolution of the conspicuously complex mantle beneath Mindszentkálla, *in situ* major and trace element analyses were also carried out on all rock forming minerals. The major element chemistry of silicate minerals in harzburgite wallrock and in dunite veins shows a relatively lower content of TiO_2, FeO and Na_2O compared to the predominant lherzolitic xenoliths of the BBHVF. The rare earth elements display flat or U-shaped distributions in harzburgitic clinopyroxenes, whereas the websteritic clinopyroxene and the amphibole of the amphibole-phlogopite vein rather depict enrichment of light rare earth elements.

According to the textural and geochemical features, the Mindszentkálla xenoliths could have gone through significant mineralogical and compositional modifications at least in two stages. During the first event, the lherzolitic mantle was metasomatized probably by a boninite-like (MgO- and SiO_2-rich) melt. It could have resulted in orthopyroxene-rich lithology (Kelemen et al., 1992), the formation of dunite veins (Kelemen & Dick, 1995), depletion in incompatible elements of rock forming silicates of the harzburgites, and the U-shaped rare earth element distributions of the harzburgitic clinopyroxenes (Sharma & Wasserburg, 1996). Boninitic melts are exclusively known from subduction zones (Taylor et al., 1994), hence we deduce these results as proofs for a formerly present subducted slab at proximity of the study area.

The second metasomatic event lead to the formation of the apatite-bearing websterite and amphibole-phlogopite bearing glassy veins, which are known in the BBHVF area, and are interpreted as the products of asthenospheric melts similar to the host alkali basalts of the xenoliths (Dobosi et al., 2003). Thus, the websterite and amphibole-phlogopite veins in the Mindszentkálla xenoliths probably represent alkali mafic melts with highly variable volatile content, which were intruded in the dunitic veined harzburgite mantle prior to the xenolith entrapment during the Late-Pleistocene volcanism.

Dobosi, G., Downes, H., Embey-Isztin, A., Jenner, G.A. (2003): Origin of megacrysts and pyroxenite xenoliths from the Pliocene alkali basalts of the Pannonian Basin (Hungary). *N. Jb. Mineral. Abh.*, **178**, 217-238.

Kelemen, P.B., Dick, H.J.B., Quick, J.E. (1992): Formation of harzburgite by pervasive melt/rock reaction in the upper mantle. *Nature*, **358**, 635-641.

Kelemen, P.B. & Dick, H.J.B. (1995): Focused melt flow and localized deformation in the upper mantle: juxtaposition of replacive dunite and ductile shear zones in the Josephine peridotite, SW Oregon. *J. Geophys. Res.*,**100**, 423-438.

Sharma, M. & Wasserburg, G.J. (1996): The neodymium isotopic compositions and rare earth patterns in highly depleted ultramafic rocks. *Geochim. Cosmochim. Acta*, **60**, 4537-4550.

Szabó, C., Falus, G., Zajacz, Z., Kovács, I., Bali, E. (2004): Composition and evolution of lithosphere beneath the Carpathian-Pannonian Region: a review. *Tectonophys.*, **393**, 119-137.

Taylor, R.N., Nesbitt, R.W., Vidal, P., Harmon, R.S., Auvray, B., Croudace, I.W. (1994): Mineralogy, chemistry, and genesis of the boninite series volcanics, Chichijima, Bonin Islands, Japan. *J. Petrol.*, **35**, 577-617.

ECLOGITIC BRECCIA FROM THE MONVISO META-OPHIOLITE COMPLEX: FIELD AND PETROGRAPHIC EVIDENCES OF MULTIPLE-STAGE ECLOGITE-FACIES BRECCIATION

Locatelli M.*[1], Verlaguet A.[1], Agard P.[1] & Federico L.[2]
[1] Institut des Sciences de la Terre de Paris, Université Pierre et Marie Curie, Paris, France
[2] Dipartimento di Scienze della Terra, dell'Ambiente e della Vita, Università di Genova, Italy
Corresponding email: michele.locatelli@upmc.fr

Keywords: eclogite, breccia, Monviso

The Monviso meta-ophiolite complex (Northern Italy, Western Alps) derive from a portion of Tethys oceanic lithosphere metamorphosed up to eclogite-facies peak metamorphic conditions during the Alpine orogeny (2.6 GPa - 550°C, Lago Superiore Uni). It exhibits from bottom to top a thick serpentinite sole capped by Mg-Al-rich metagabbros, Fe-Ti-metagabbros and metabasalts with dispersed metasediments lenses. Three main shear zones cut this section: in our study we focus on the Lower Shear Zone (LSZ), extending from the serpentinite sole (to the East) to the Mg-metagabbro bodies (to the West). Here blocks of variably brecciated Fe-Ti and Mg-Al metagabbros are embedded, together with metasedimentary blocks, in a talc and tremolite-rich serpentinite matrix. Their origin is debated, being interpreted either as eclogitic breccias resulting from (potentially seismic) intermediate-depth rupture or as inheritance from Tethyan Oceanic Core Complex. Here we present new field and petrographic data that demonstrate their univocal genesis at eclogite-facies conditions. In the 16 km-long LSZ the occurrence of eclogite blocks is uniform along the strike of the shear-zone, which thickness varies from 500 to 200 meters with a marked decrease in block size from top to base. Here three types of eclogitic blocks can be distinguished: I, intact (not brecciated) blocks of Fe-Ti-metagabbros restricted to the lower part of the shear zone (Type1 blocks); II, numerous brecciated Fe-Ti-metagabbros scattered in the intermediate to upper levels of the LSZ (Type2 blocks); III, meter-size blocks and decametric-scale slivers of metagabbros showing complex compositional variations and occurrence of breccia layers (Type3 blocks). The latter, wherever preserved, evidence the full transition from intact to highly brecciated rock. In type 2 and 3 blocks the amount of matrix vs clast increases towards the core of breccia layers, associated with reduction in clasts sizes and increasing clasts rotation, likewise representing fault-derived tectonic breccias. The foliation of intact Mg-Al-rich metagabbros (composed of omphacite + rutile ± apatite ± quartz and locally garnet) cut by breccia planes (cement composed of omphacite + garnet ± lawsonite) univocally indicates brecciation at eclogite facies conditions. In the breccias the occurrence of a first omphacite-rich matrix cut by secondary garnet + lawsonite pseudomorphs rich matrix witnesses multiple brittle rupture events, likely driven by different fluid pulses. Field and petrographic data thus demonstrate that brecciation at eclogite-facies conditions have to be considered a constant feature along the LSZ. Presence of different eclogite-facies matrix types in the breccias suggest multiple brittle events driven by successive fluids inputs, potentially associated to intermediate-depth seismicity. Further work is needed to determine the P-T conditions of brecciation and recognize the origin of infiltrating fluids.

THE POLINO CALCIOCARBONATITE IS NOT A CARBONATITE

Lustrino M.*[1], Gaeta M.[1], Palladino D.M.[1], Rossi G.[1] & Stagno V.[1]
[1] Dipartimento di Scienze della Terra, Sapienza Università di Roma, Italy
Corresponding email: michele.lustrino@uniroma1.it

Keywords: carbonatite, limestone, Polino

The Pleistocene (246 ka) Polino monticellite alvikite (volcanic Ca-carbonatite) crops out in a very small area (~ 200 m^2) in central Apennines ~ 100 km NE of Rome. This has been considered as one of the most representative Italian carbonatites by several research groups over the last two decades, and its mineralogy and isotopic composition are considered well established.

The Polino carbonatite is characterized by abundant presence of forsteritic olivine, monticellite and phlogopite, with much rarer Ca-Ti and Ca-Si perovskite and Fe-Ti oxides associated with different generations of calcite.

Several aspects make the classification of this volcanic rock as carbonatite at least questionable. The modal abundance of carbonate minerals is < 50%, rendering the term “carbonatite” inappropriate. In literature the relatively high amount of silicates has been related to the presence of mantle debris in the form of xenocrystic forsterite and phlogopite. However, a mantle origin for these two phases is clearly excluded from a simple petrographic description. Forsterite is often euhedral to subhedral, and without any deformation texture; on the other hand phlogopite is present as tiny elongated euhedral laths, often characterized by inverse zoning with Fe-rich cores and Mg-rich rims. We claim these being characteristics of liquidus phase characteristics rather than mantle fragments occasionally eroded by an upwelling carbonatitic magma. In addition, all the forsterite crystals are characterized by a variable thickness monticellite rim. We interpreted this as a two stage effect: first euhedral forsterite grows in equilibrium from a Mg-rich ultrabasic melt, then monticellite starts forming at the expenses of forsterite around former crystals. Interestingly, monticellite is very commonly found as euhedral groundmass phase.

The late appearance of monticellite can be explained after the interaction of an ultrabasic magma at sub-liquidus conditions with Ca-rich country rock lithologies. These Ca-rich rocks are represented in this view by the very thick Liassic limestone sequence cropping out in Polino area.

In conclusion, our view overturns the classically accepted interpretation, according which monticellite is the reaction product between a carbonatitic magma and mantle xenocrysts. We believe instead that the interaction has occurred between an ultrabasic melt and the sedimentary carbonate wall rocks in a shallow depth magma chamber.

The classification of the Polino volcanic rocks remains of not easy solution. It cannot be defined as alvikite (too low primary carbonate content), basalt (no plagioclase), kamafugite (no kalsilite), melilitite (no melilite), foidite (no foids) or peridotite (not a plutonic/metamorphic rock). It represents a carbonated silicate melt with an ultrabasic (SiO_2 16-25 wt.%) Ca-rich (CaO 34-40 wt.%) alkali-poor (Na_2O+K_2O < 1 wt.%) Al-poor (Al_2O_3 3.8-6.3 wt.%) composition, resulting from the digestion of limestones at shallow crustal depths by a very low volume mafic magma.

THE REDOX BUDGET OF CRUST-DERIVED FLUID PHASES AND IMPLICATIONS FOR THE SLAB-TO-MANTLE ELEMENT TRANSFER

Malaspina N.*[1], Langenhorst F.[2], Tumiati S.[3], Frezzotti M.L.[1] & Poli S.[3]
[1] Dipartimento di Scienze dell'Ambiente, del Territorio e di Scienze della Terra, Università di Milano-Bicocca, Italy
[2] Institut für Geowissenschaften, Friedrich-Schiller Universität Jena, Germany
[3] Dipartimento di Scienze della Terra "A. Desio", Università di Milano, Italy
Corresponding email: nadia.malaspina@unimib.it

Keywords: multiphase inclusions, Fe^{3+} partitioning, subduction

The redox processes taking place in the portion of the mantle on top of the subducting slab is poorly investigated and the oxidising (or reducing) power of crust-derived fluids phases is still unknown.

A case study of supra-subducted mantle affected by metasomatism from crustal fluid phases is represented by garnet orthopyroxenites from the Maowu Ultramafic Complex (China). These rocks are derived from harzburgite precursors metasomatised at ~ 4 GPa and 750°C by a silica- and incompatible trace element-rich fluid phase. The metasomatism produced poikilitic orthopyroxene and inclusion-rich garnet porphyroblasts. Primary multiphase micro-inclusions in garnet display negative crystal shapes and infilling minerals (spinel, amphibole, chlorite, talc, mica) occur with constant volume ratios indicating that they derive from trapped solute-rich aqueous fluids (Malaspina et al., 2006). The epitaxial relationship between spinel and host garnet, and between some hydrous minerals has been demonstrated by single-crystal X-ray diffraction experiments (Malaspina et al., 2015). Epitaxy drives a first-stage nucleation of spinel under near-to-equilibrium conditions, likely promoted by a dissolution and precipitation mechanism between the UHP fluid and the host garnet. A second-stage nucleation involved hydrous phases, which nucleate in a non-registered manner and under far-from-equilibrium conditions. FT-IR and Raman microscopy, together with X-Ray microtomography performed on single inclusions indicate that free water is still preserved in spinel-free inclusions.

To investigate the redox budget of these fluid phases, we measured the Fe^{3+} concentration of the microprecipitates of multiphase inclusions using EELS on a TEM. Results indicate that spinel contains up to 12% of $Fe^{3+}$with respect to total iron, amphibole about 30%, while inclusion phases such as chlorite and phlogopite may contain up to 0.70 of $Fe^{3+}/\Sigma Fe$. The $Fe^{3+}/\Sigma Fe$ of the host garnet has been measured both by Flank Method electron probe microanalyses and EELS and corresponds to 0.10. An oxygen mass balance between crust-derived fluids and the host rock indicates that fluid precipitates appear more oxidised than the host rock. This suggests that even after their interaction with the metasomatic orthopyroxenites, the residual fluid phases could be potentially carriers of oxidised components when escaping the slab-mantle interface.

Malaspina, N., Hermann, J., Scambelluri, M., Compagnoni, R. (2006): Polyphase inclusions in garnet–orthopyroxenite (Dabie Shan, China) as monitors for metasomatism and fluid-related trace ele- ment transfer in subduction zone peridotite. *Earth Planet. Sci. Letters*, **249**, 173-187.

Malaspina, N., Alvaro, M., Campione, M., Wilhelm, H., Nestola, F. (2015): Dynamics of mineral crystallization from precipitated slab-derived fluid phase: first in situ synchrotron X-ray measurements. *Contrib. Mineral. Petrol.*,**169**, 3.

FLUID-ROCK INTERACTIONS IN SERPENTINITES SUBDUCTED TO 60-80 KM DEPTH

Peters D.*[1], John T.[2], Scambelluri M.[3] & Pettke T.[1]
[1] Institut für Geologie, Universität Bern, Switzerland
[2] Fachbereich Geowissenschaften, Freie Universität Berlin, Germany
[3] Dipartimento di Scienze della Terra, dell'Ambiente e della Vita, Università di Genova, Italy
Corresponding email: daniel.peters@geo.unibe.ch

Keywords:

The HP metamorphic serpentinised peridotites of Erro-Tobbio (Italy) offer a unique possibility to study fluid-rock interactions in subducted ultrabasic rocks that reached 550-650°C at 2-2.5 GPa. They contain metamorphic olivine + Ti-clinohumite in both the rock matrix and veins cutting the rock foliation, interpreted to represent partial serpentinite dehydration fluid pathways (Scambelluri et al., 1995; John et al., 2011) being variably retrogressed as, e.g., indicated by chrysotile/lizardite mesh textures in vein olivine in strongly altered samples. This study in progress aims to constraining the origin of fluid(s) and the scale(s) of fluid-rock interaction based on major to trace element systematics including halogens employing detailed bulk rock (nanoparticulate pressed powder pellet LA-ICP-MS (Peters & Pettke, 2016) and ion chromatography / liquid ICP-MS analysis), and *in situ* mineral analysis, with an emphasis on major to trace element data including fluid tracers such as B, As and Sb.

Petrographic observations indicate a multiphase evolution of the HP veins with possibly two generations of diopside growth and different stages of retrograde serpentinisation, whereas serpentinite hosts have remained largely unaffected by retrogression. Bulk serpentinite and vein data reveal prominent increases in Cl, Br, I, and F concentrations relative to primitive mantle, indicating their seawater derivation. Bulk veins are enriched in heavy halogens relative to light ones in comparison to host serpentinites. These patterns indicate either halogen element fractionation upon partial serpentinite dehydration or imperfect equilibration of vein fluids with host rocks upon fluid infiltration, or a combination thereof. *In situ* mineral data shall elucidate which of these processes predominates and how prominently the chemical effect of retrogression affects bulk rock data, when trying to attain original fluid compositions and identify fluid migration pathways.

John, T., Scambelluri, M., Frische, M., Barnes, J.D., Bach, W. (2011): Dehydration of subducting serpentinite: implications for halogen mobility in subduction zones and the deep halogen cycle. *Earth Planet. Sci. Letters*, **308**, 65-76.

Peters, D. & Pettke, T. (2016): Evaluation of major to ultra trace element bulk rock chemical analysis of nanoparticulate pressed powder pellets by LA-ICP-MS. *Geostand. Geoanalyt. Res.* in press.

Scambelluri, M., Müntener, O., Hermann, J., Piccardo, G.B., Trommsdorff, V. (1995): Subduction of water into the mantle: history of an Alpine peridotite. *Geology*, **23**, 459-462.

CARBONATION BY FLUID-ROCK INTERACTIONS AT HIGH-PRESSURE CONDITIONS: IMPLICATIONS FOR CARBON CYCLING IN SUBDUCTION ZONES

Piccoli F.*[1], Vitale Brovarone A.[1], Beyssac O.[1], Martinez I.[2], Ague J.J.[3-4] & Chaduteau C.[2]

[1] Insitut de Minéralogie, Physique des Matériaux et Cosmochimie, Centre National de la Recherche Scientifique, Université Pierre et Marie Curie, Paris, France

[2] Institut de Physique du Globe de Paris, Sorbonne Paris Cité, Université Paris Diderot, Centre National de la Recherche Scientifique, Paris, France

[3] Department of Geology and Geophysics, Yale University, New Haven, CT, USA

[4] Peabody Museum of Natural History, Yale University, New Haven, CT, USA

Corresponding email: francesca.piccoli@gmail.com

Keywords: subduction carbon cycle, carbonation, metasomatism

Carbonate-bearing lithologies are the main carbon carrier into subduction zones. Their evolution during metamorphism largely controls the fate of carbon, regulating its fluxes between shallow and deep reservoirs. Here we report the occurrence of eclogite-facies carbonate-rich rocks (aragonite + omphacite + garnet) within a zone of intense high-pressure fluid-rock interaction and metasomatism in the lawsonite-eclogite San Petrone unit, Alpine Corsica (France). The study outcrops are located along the serpentinite-metasediments contact that experienced a first stage of intense metasomatism during prograde metamorphism, leading to the formation of diopside-lawsonite metasomatic rock. The study carbonate-rich rocks are intimately associated with these metasomatic rocks, and textural, geochemical and isotopic data indicating fluid-mineral reactions are compelling evidence for the precipitation of these carbonate-rich assemblages from COH fluids during high-pressure metamorphism. Cross-cutting relationships indicates that carbonate metasomatism occurred after the diopside-lawsonite metasomatic event. Nevertheless, the paragenes aragonite + omphacite + garnet indicates formation at near peak P-T conditions. We infer that the reactive percolation of COH fluids at ca. 2 GPa and 500°C can spawn high-pressure rock carbonation, by either vein-injection or chemical replacement mechanisms. The discovery of high-pressure rock carbonation brings new insights into the fate of COH fluids produced during subduction. Our results indicate that COH fluids produced in the subducting oceanic crust by decarbonation reactions and carbonate dissolution may not be directly transferred to the mantle wedge, but can interact with mafic/ultramafic slab-forming rocks. Analogue processes can take place in the upper plate, at the slab-mantle wedge interface. High-pressure rock-carbonation by fluid-rock interactions may have an important impact on the global carbon cycle acting as a major carbon sink process in subduction zones and lithospheric mantle reservoirs. Furthermore, high-pressure rock carbonation may modulate the emission of CO_2 at volcanic arcs over geological time scales.

CHANNELIZING REACTIVE POROSITY CONTROLLS FLUID ESCAPE FROM SUBDUCTION ZONES

Plümper O.*[1], John T.[2], Podladchikov Y.[3], Vrijmoed J.C.[4] & Scambelluri M.[5]
[1] Department of Earth Sciences, University of Utrecht, Netherlands
[2] Institut für Geologische Wissenschaften, Freie Universität Berlin, Germany
[3] Institute des Sciences de la Terre, Université de Lausanne, Switzerland
[4] Institut für Geochemie und Petrologie, Eidgenössische Technische Hochschule Zürich, Switzerland
[5] Dipartimento di Scienze della Terra, dell'Ambiente e della Vita, Università di Genova, Italy
Corresponding email: o.plumper@uu.nl

Keywords: subduction zones, serpentinites, dehydration

Within our solar system Earth is the only planet that has both plate tectonics and water. These may not be intuitively linked as the amount of water is extremely small compared to the Earth's entire mass. However, water has an enormous impact on Earth's geodynamics and geochemical cycles at all scales. The most prominent examples of this link between water and plate tectonics are found in subduction zones. In these zones seawater-altered oceanic lithosphere is returned to the mantle, thereby heating up during descent and releasing fluids through hydrous mineral dehydration facilitating global mass transfer. These dehydration reactions, e.g., liberate fluids that trigger mantle melting fueling explosive volcanism and are a source of intermediate-depth seismicity. As the global water input into subduction zones per million years is on the order of the oceans' total water volume efficient, large-scale transport systems need to form to drain the descendent oceanic plates and return subduction zone fluids to the exogenous reservoirs. The fluid escape through these transport systems needs to keep pace with the slab descent velocity of cm/year. Otherwise, even in the presence of other natural outgassing mechanisms the oceans would drain within only a few million years. If fluid escape would be controlled by the low background permeability at the conditions at which dehydration reactions occur (30-300 km, 2-10 GPa), resultant slow, static pervasive fluid flow would be insufficient to drain the descending plates. Thus, a fluid escape mechanism is required that allows fluid flow to organize itself into high flux transport systems. Although globally documented vein systems in high-pressure metamorphic terrains confirm that high fluid fluxes are achieved through fluid flow channelization the rate-limiting microscale mechanism that controls the bottleneck coupling of initial fluid production from a zero-porosity, water-rich rock into a rock characterized by high permeability channels is largely unknown. Here, we show that water release from high-pressure (~ 2.5 GPa) hydrated mantle rocks is controlled by intrinsic chemical heterogeneities that localize dehydration reactions at specific microsites. This results in fluid pressure variations throughout the rock, which force the fluid release to organize itself into a channelized fluid flow network across length scales spanning six-orders of magnitude. We formulate a model that defines the coupling between microscopic fluid release and fluid flow channelization. This is crucial in order to formulating future quantitative models that address spatiotemporal processes, such as the link between fluid release at depth and volcanic eruptions, and the amount of mineral-bound water transferred into the deep Earth. Moreover, our findings shows that mineral dehydration may not cause rock embrittlement, often presumed as the trigger of intermediate-depth subduction zone seismicity. Instead, local decrease in effective viscosity within the ultra-fine grained solid reaction products could trigger thermal runaway shear instabilities and indirectly lead to seismic failure.

STRUCTURAL PROPERTIES OF CARBONATE-SILICATE MELTS: TRACE ELEMENT EXAFS AT HIGH-PRESSURE & TEMPERATURE

Pohlenz J.*[1], Pascarelli S.[2], Mathon O.[2], Rosa A.D.[2], Belin S.[3], Landrot G.[3], Shiryaev A.[4], Murzin V.[5], Veligzhanin A.[6], Wagner J.[1], Künzel D.[1], Irifune T.[7] & Wilke M.[8]

[1] Helmholtz Zentrum Potsdam, GFZ Deutsches GeoForschungsZentrum, Potsdam, Germany

[2] European Synchrotron Radiation Facility, Grenoble, France

[3] Synchrotron SOLEIL, Saint-Aubin, France

[4] Institute of Physical Chemistry and Electrochemistry, Russian Academy of Sciences, Moscow, Russia

[5] Deutsches Elektronen-Synchrotron, Hamburg, Germany

[6] National Research Centre Kurchatov Institute, Moscow, Russia

[7] Geodynamics Research Center, Ehime University, Matsuyama, Japan

[8] Institut für Erd- und Umweltwissenschaften, Universität Potsdam, Germany

Corresponding email: julia.pohlenz@gfz-potsdam.de

Keywords: carbonate melts, melt structure, trace element coordination

Carbonate-rich silicate and carbonate melts play a crucial role in deep Earth magmatic processes, and are controlled by the melt's internal structure. Using extended X-ray absorption fine structure (EXAFS) spectroscopy, we investigate the influence of carbonate concentration on the structural in corporation of yttrium (Y) and lanthanum (La), as representatives for heavy rare earth elements (HREE) and light rare earth elements (LREE) and strontium (Sr), as representative for alkali earths, in silicate-carbonate melts. The melts are synthesised in the system Na_2O-CaO-Al_2O_3-SiO_2-CO_2, resembling compositions as found at Oldoinyo Lengai volcano, TZ. Data of silicate glasses with up to 10 wt.% CO_2 and ~ 5000 ppm Y and Sr, quenched from melts at high pressure/temperature (HP/HT), indicate no effect of CO_2 content on the local structure of Y, whereas we observe an increase in bond length from ~ 2.55 Å to ~ 2.60 Å between Sr and O with increasing CO_2 contents. Water bearing glasses (~ 2 wt.%) also show a slightly increased bond length between Sr and O compared to their water free counterparts. *In situ* measurements on melts (~ 2 GPa, ~ 1000 to 1300°C) as well as on quenched glasses (~ 2 GPa, room temperature) containing either 2 wt.% Y or Sr along the join from silicate-carbonate composition were collected *in-situ* at HP/HT using a Paris Edinburgh-Press. *In situ* experiments reveal longer bond lengths of Y-O and Sr-O (e.g. ~ 2.35 *vs.* ~ 2.28 Å, respectively ~ 2.66 Å *vs.* 2.55 Å for the CO_2-free silicate composition) as well as a more asymmetric pair distribution compared to quenched glasses. Furthermore, there is a minor difference in the Y-O bond lengths between the pure silicate and the carbonate melts of ~ 2.35 *vs.* ~ 2.38 Å, which is even less pronounced for Sr-O bond lengths (~ 2.66 Å *vs.* ~ 2.68 Å). Especially the Y XANES region of the spectra shows distinct differences between *in-situ* and quenched glass data as well as along the join silicate-carbonate, which implies changes in average site symmetry. We will compare these findings to changes in the local structure of La in the same system. We will finalise this study, by comparing our experimental findings with results from molecular dynamic simulations, to derive a structural model for carbonate-silicate melts in order to better understand chemical fractionation processes in carbonate-bearing magmatic systems.

EXPERIMENTAL MODELLING OF DISSOLUTION AND MELTING OF SUBDUCTED PELAGIC CARBONATES

Poli S.*[1]
[1] Dipartimento di Scienze della Terra “A. Desio”, Università di Milano, Italy
Corresponding email: stefano.poli@unimi.it

Keywords: carbonates, calcite, liquids

Despite the utmost importance of calcite in sedimentary materials deposited on the ocean floor and in veined oceanic rocks, hydrothermally altered, the knowledge of high pressure phase relationships on the join $CaCO_3$ - H_2O, and more generally in the system CaO - H_2O - CO_2, is still extremely fragmentary. Calcite and aragonite are expected to undergo dissolution and melting in the presence of H_2O and a continuous transition between a high-density “vapor” and a carbonated hydrous “melt” was suggested to occur close to a second critical endpoint at temperatures as low as 530°C, and pressure higher than 4 GPa (Wyllie & Boettcher, 1969).

Multianvil experiments were performed at 4.2 GPa on bulk compositions in the system CaO-Al_2O_3-SiO_2-H_2O-CO_2, used as a model for impure marbles. Zoisite and/or Al_2SiO_5 saturation is intended to prevent the formation of portlandite and dellaite, experimentally recorded on eutectic melting, but barely found in nature.

Aragonite + kyanite + fluid, and minor lawsonite form at 700°C, replaced by zoisite at 800°C. Between 850 and 900°C, a complex sequence of textural features is observed upon quenching; “chains” and dendrites of $CaCO_3$grow nucleating from liquid-solid interface; they are followed by growth of Si-Al-bearing fibres; spherules of silica precipitate from the residual fluid exsolved from the liquid carbonate phase. At 900°C, both at silica undersaturation and silica saturation, a sharp meniscus bounds the segregated liquid, where the amount of precipitated solids suggests that the liquid approached a hydrous-carbonated “melt”. Estimates of liquid – solid proportions, retrieved by image analysis, at known bulk H_2O content, provide constraints for the composition of the carbonatitic liquids. Chemographic analysis suggets a continuous transition from dissolution to melting at 4.2 GPa, although consistency with the large experimental dataset in the system CaO-Al_2O_3-SiO_2-H_2O remains controversial.

Hydrous liquids enriched in Ca-carbonate potentially generated from a subducting slab at 850-900°C are efficient media for scavenging volatiles from subducted crustal material and for metasomatizing the mantle wedge.

Wyllie, P.J. & Boettcher, A.L. (1969): Liquidus phase relationships in the system CaO-CO_2-H_2O to 40 kilobars pressure with petrological applications. *Am. J. Sci.*, **267A**, 489-508.

DEVELOPMENT OF AN EXAFS SETUP AT THE BEAMLINE BM23 OF THE ESRF OPTIMIZED FOR STUDYING TRACE ELEMENTS *IN-SITU* UNDER EXTREME *P/T* CONDITIONS

Rosa A.D.*[1], Mathon O.[1], Pasternak S.[1], Jacobs J.[1], Cardon H.[2], Krstulovic M.[3], Merkulova M.[4], Louvel M.[5], Tsay A.[6], Ghosh S.[7], Liebske C.[8], Irifune T.[9], Munoz M.[4] & Wilke M.[10]

[1] European Synchrotron Radiation Facilitiy, Grenoble, France

[2] Laboratoire de Géologie, Université de Lyon, France

[3] Helmholtz Zentrum Potsdam, GFZ Deutsches GeoForschungsZentrum, Potsdam, Germany

[4] Institut des Science de la Terre, Université de Grenoble, France

[5] School of Earth Sciences, Univerity of Bristol, United Kingdom

[6] Department of Earth Sciences, University of Toronto, Canada

[7] Indian Institut for Technology, Kharagpur, India

[8] Institut für Geochemie und Petrologie, Eidgenössische Technische Hochschule, Zürich, Switzerland

[9] Geodynamics Research Center, Ehime University, Matsuyama, Japan

[10] Institut für Erd- und Umweltwissenschaften, Universität Potsdam, Germany

Corresponding email: angelika.rosa@esrf.fr

Keywords: *in situ* EXAFS, high P/T diamond anvil cell, trace elements

In situ high *P/T* X-ray absorption spectroscopy (XAS) is of particular importance in geochemistry. This technique provides crucial information on the transport, partitioning and speciation of elements in minerals, melts or fluids under deep Earth's conditions. Here, we present the development of a high *P/T* setup optimized for studying trace elements (*i.e.,* down to concentrations of 1000 ppm) and/or low Z-number elements (i.e., Ni, Fe, Cr) at the EXAFS beamline BM23 of the European Synchrotron radiation facility. The approach is based on a combination of micro X-ray fluorescence emission spectroscopy techniques and a resistively-heated diamond anvil cell (RH-DAC). Experiments are conducted in backscattering geometry using a 4x4 μm^2 focused beam and a single-element fluorescence detector coupled to a polycapillary for background reduction. The high beam stability and energy resolution of BM23, guarantees high-quality XAS data. In addition, a MAR165 detector can be utilized for the collection of X-ray diffraction data in transmission geometry. This complementary system enables the*in situ* characterisation of phase changes under high P/T conditions. The RH-DAC design is based on an optimized heater and gasket composition. The system allows operating *in situ* at stable high *P/T* conditions up to 1300 K and pressures in excess of 20 GPa. For low Z-elements (*K*-edge energies down to 5 k*e*V) and trace elements, optimized diamond anvils are employed consisting of fully perforated single-crystal diamonds and nano-polycrystalline diamond windows.
The potential of the experimental approach is illustrated on preliminary results related to the release and transport of the fluid mobile elements, such as As and Sr, as well as Ni during the *in-situ* formation and breakdown of serpentine at high *P/T* conditions. These new data will allow better constraining the geochemical processes occurring during serpentinization, the physico-chemical properties of subduction zone fluids as well as the global recycling of fluid mobile elements in deep subduction zones.

CARBONATION OF SUBDUCTION-ZONE SERPENTINITE (HIGH-PRESSURE OPHICARBONATE; LIGURIAN WESTERN ALPS) AND IMPLICATIONS FOR THE DEEP CARBON CYCLING

Scambelluri M.[1], Bebout G.E.*[2], Belmonte D.[1], Gilio M.[1], Campomenosi N.[1] & Crispini L.[1]
[1] Dipartimento di Scienze della Terra, dell'Ambiente e della Vita, Università di Genova, Italy
[2] Department of Earth and Environmental Sciences, Lehigh University, Bethlehem, PA, USA
Corresponding email: geb0@lehigh.edu

Keywords: subduction, serpentinite, marble

Much of the long-term carbon cycle in solid earth occurs in subduction zones, where devolatilization, partial melting of carbonated rocks, and dissolution of carbonate minerals lead to the return of CO_2 to the atmosphere via volcanic degassing. Release of COH fluids from hydrous and carbonate minerals influences C recycling and magmatism at subduction zones. Contradictory interpretations exist on the retention/storage of C in subducting plates and in the forearc to subarc mantle. Several lines of evidence indicate mobility of C, of uncertain magnitude, in forearcs. A poorly constrained fraction of the 40-115 Mt/yr of C initially subducted is released into fluids (by decarbonation and/or carbonate dissolution) and 18-43 Mt/yr is returned at arc volcanoes. Current estimates suggest the amount of C released into subduction fluids is greater than that degassed at arc volcanoes: the imbalance could reflect C subduction into the deeper mantle, beyond subarc regions, or storage of C in forearc/subarc reservoirs.

We examine the fate of C in subduction-zone ultramafic rocks via study of fluid–rock evolution of marble and variably carbonated serpentinite in the Ligurian Alps. Based on petrography, major and trace element concentrations, and carbonate C and O isotope compositions, we demonstrate that serpentinite dehydration at 2-2.5 GPa, 550°C released aqueous fluids triggering breakdown of dolomite in nearby marbles, thus releasing C into fluids. Carbonate ± olivine veins document flow of COH fluids and that the interaction of these COH fluids with serpentinite led to the formation of high-*P* carbonated ultramafic-rock domains (high-*P* ophicarbonates). We estimate that this could result in the retention of ~ 0.5-2.0Mt C/yr in such rocks along subduction interfaces. As another means of C storage, 1 to 3 km-thick layers of serpentinized forearc mantle wedge containing 50 modal % dolomite could sequester 1.62 to 4.85 Mt C/yr.

We stress that lithologically complex interfaces could contain sites of both C release and C addition, further confounding estimates of net C loss at forearc and subarc depths. Sites of C retention, also including carbonate veins and graphite as reduced carbonate, could influence the transfer of slab C to at least the depths beneath volcanic fronts.

SUBDUCTION-RELATED ULTRADEPLETED MELTS IN A NASCENT ARC: GEOCHEMICAL AND ISOTOPIC EVIDENCE FROM THE INTRUSIVE SEQUENCE OF THE NEW CALEDONIA OPHIOLITE

Secchiari A.[1-2], Montanini A.*[1], Bosch D.[2], Macera P.[3] & Cluzel D.[4]
[1] Dipartimento di Fisica e Scienze della Terra "Macedonio Melloni", Università di Parma, Italy
[2] Géosciences Montpellier, Université de Montpellier, France
[3] Dipartimento di Scienze della Terra, Università di Pisa, Italy
[4] Pole Pluridisciplinaire de la Matière et de l'Environnement, Université de la Nouvelle Caledonie, Nouméa, New Caledonia
Corresponding email: alessandra.montanini@unipr.it

Keywords: intraoceanic arc, Sr-Nd-Pb isotopes, New Caledonia ophiolite

The obducted sections of intraoceanic arc lithosphere represent a favourable setting to investigate the crust generation in nascent arcs. The New Caledonia ophiolite hosts a mafic-ultramafic igneous sequence overlying harzburgitic rocks that underwent very high degrees of partial melting in a forearc setting (Marchesi et al., 2009; Secchiari, 2016). This sequence has been interpreted as a crust-mantle section in a nascent arc (Pirard et al., 2013). The igneous rocks include dunites, wehrlites and mafic rocks (mainly gabbronorites). Dunites and wehrlites derive from melt/peridotite interactions involving primitive arc tholeiites and boninitic liquids, whereas the mafic rocks are the result of cumulus processes (Marchesi et al., 2009; Pirard et al., 2013). The samples of this study are olivine gabbronorites occurring in the upper part of the sequence as metre-sized sills. Subhedral Ca-rich plagioclase (An = 90-96 mol%) is the dominant phase (50-80 vol%). Mg-rich olivine (5-15 vol%, Fo = 87-89 mol%) occurs as irregularly shaped crystals. Cpx (15-20 vol%) is generally rimmed by interstitial to poikilitic Opx (5-15 vol%). Cpx shows high Mg# (88-92), low Al_2O_3 (1.5-2.4 wt.%) and negligible TiO_2 and Na_2O contents. Bulk rock compositions are characterized by high Mg# (86-93) and very low incompatible trace element contents (e.g., LREE concentrations mostly below 0.1 times chondrite). They show marked LREE depletion, nearly flat and low HREE (Yb_N = 0.2-0.9) and positive Eu anomalies. The highly depleted nature of these rocks is mirrored by Cpx trace element composition. In contrast, fluid-mobile trace elements are relatively enriched and distinct Pb and Sr positive anomalies are observed in both whole rocks and Cpx. The calculated compositions of putative liquids in equilibrium with the most primitive gabbronorites are consistent with melting of a refractory peridotite source in the spinel stability field. The inferred melts have high Mg# of 75-76 and very low REE, Nb, Zr, Hf contents. On the other hand, Ba, Pb and Sr spikes in the calculated liquids argue for the involvment of a subduction-related component. Overall, the liquids show geochemical signatures akin to olivine boninite melts with lower absolute concentrations of LREE and other incompatible trace elements (Ba, Pb, Sr, Zr, Hf). We propose that the New Caledonia gabbronorites reflect injection of primitive, ultradepleted ("boninite-like") magma batches in the lower forearc crust, possibly before aggregation, during the first phases of arc formation. The investigated gabbronorites provide homogeneous initial Nd isotope compositions (ε_{Nd} ranging between +8.2 and +9.4), coupled with high $^{208}Pb/^{207}Pb$ and $^{207}Pb/^{206}Pb$ ratios, falling in a domain intermediate between DMM and Pacific sediments. The heterogeneous Pb isotopic signature of the gabbronorites most likely reflect a subarc asthenospheric mantle source variably modified by subduction-related fluids.

Marchesi, C., Garrido, C.J., Godard, M., Belley, F., Ferré, E. (2009): Migration and accumulation of ultra-depleted subduction-related melts in the Massif du Sud ophiolite (New Caledonia). *Chem. Geol.*, **266**, 171-186.

Pirard, C., Hermann, J., O'Neill, H.S.C. (2013): Petrology and geochemistry of the crust-mantle boundary in a nascent arc, Massif du Sud ophiolite, New Caledonia, SW Pacific. *J. Petrol.*, **54**, 1759-1792.

Secchiari, A. (2016): Geochemical and Sr, Nd, Pb isotope investigation of the New Caledonia ophiolite. PhD Thesis, Univ. of Parma and Univ. of Montpellier, 191 p.

Secchiari, A., Montanini, A., Bosch, D., Macera, P., Cluzel, D. (2016): Melt extraction and enrichment processes in the New Caledonia lherzolites: evidence from geochemical and Sr-Nd isotope data. *Lithos*, in press, DOI: 10.1016/j.lithos.2016.04.030.

ANALYSES OF CO_2 IN FLUIDS FROM PISTON CYLINDER EXPERIMENTS

Sieber M.*[1-2], Yaxley G.M.[1-2] & Hermann J.[1-2]
[1] Research School of Earth Science, Australian National University, Canberra, Australia
[2] Institut für Geologie, Universität Bern, Switzerland
Corresponding email: melanie.sieber@anu.edu.au

Keywords: C-O-H fluids, serpentinite, mantle wedge

Hydrous, carbon bearing fluids released in the fore arc by the breakdown of hydrous minerals during subduction will interact with the overlying (hydrated) peridotites in the mantle wedge. This process is fundamental in assessing the carbon fluxes and budgets in the Earth's mantle as it influences how much carbon is returned in subduction zone related volcanism to the Earth's hydrosphere and atmosphere and how much carbon is stored in the mantle wedge.

We present a high pressure experimental study on the interaction of C-O-H bearing fluids with natural serpentinite. Carbonation of serpentinite is a fast and efficient reaction lowering the CO_2 concentration in the fluid. With progressing carbonation and decreasing CO_2 in the fluid the formation of magnesite+quartz, magnesite+talc, (magnesite+enstatite) and magnesite+antigorite at, e.g., 2 GPa and 600°C was observed. For given pressure and temperature the particular mineral assemblage strongly depends on the modal amount of CO_2 in the fluid. CO_2 concentrations in the experimental fluids have been calculated thermodynamically and analysed by gas chromatography.

In addition, the preferred partitioning of Ca, Sr, Ba and Pb, included in the starting material of the piston cylinder experiments, into the newly formed minerals strongly suggests that the residual fluid is depleted in those elements. The partitioning behaviours indicate that the reaction of a serpentinized mantle wedge with crustal fluids will not only sequester CO_2 in the form of carbonates, but also key incompatible elements such as Sr, Pb and Ba. These elements are highly enriched in arc lavas and thus their transport through the mantle wedge is crucial for understanding element recycling in the subduction-arc system.

NOBLE GASES TRACE EARTH'S SUBDUCTED WATER FLUX

Smye A.*[1], Jackson C.[2], Konrad-Schmolke M.[3], Parman S.[4] & Ballentine C.[5]
[1] Department of Geosciences, Pennsylvania State University, State College, PA, USA
[2] Geophysical Laboratory, Carnegie Institution for Science, Washington, DC, USA
[3] Department of Earth Sciences, University of Göteborg, Sweden
[4] Department of Earth, Environment, and Planetary Sciences, Brown University, Providence, RI, USA
[5] Department of Earth Sciences, University of Oxford, United Kingdom
Corresponding email: smye@psu.edu

Keywords: subduction, noble gases, water

Volatile elements are transported from Earth's surface reservoirs back into the mantle during subduction of oceanic lithosphere (e.g., Schmidt & Poli, 1998). Here, we investigate the degree to which the fate of slab-bound noble gases and water are linked through the subduction process. Both water and noble gases are soluble in ring-structured minerals, such as amphibole, that are common constituents of subducted oceanic lithosphere. Heating and burial during subduction liberates noble gases and water from minerals through a combination of diffusion and dissolution. Combining a kinetic model, parameterized for noble gas fractionation in amphibole (Jackson et al., 2013), with thermodynamic phase equilibria calculations, we quantify the effect of subduction dehydration on the elemental composition of slab-bound noble gases. Results show that post-arc slab water and noble gas fluxes are highly correlated. Hot subduction zones, which likely dominate over geologic history, efficiently remove noble gases and water from the down-going slab; furthermore, kinetic fractionation of noble gases is predicted to occur beneath the forearc. Conversely, hydrated portions of slab mantle in cold subduction zones transport noble gases and water to depths exceeding 200 km. Preservation of seawater-like abundances of Ar, Kr and Xe in the convecting mantle (Holland & Ballentine, 2006) implies that recycling of noble gases and water occurred during cold subduction and that the subduction efficiency of these volatile elements has increased over geological time, driven by secular cooling of the mantle.

Holland, G. & Ballentine, C. (2006): Seawater subduction controls the heavy noble gas composition of the mantle. *Nature*, **441**, 186-191.

Jackson, C.R.M., Parman, S.W., Kelley, S.P., Cooper, R.F. (2013): Noble gas transport into the mantle facilitated by high solubility in amphibole. *Nature Geosci.*, **6**, 562-565.

Schmidt, M. & Poli, S. (1998): Experimentally based water budgets for dehydrating slabs and consequences for arc magma generation. *Earth Planet. Sci. Letters*, **163**, 361-379.

ORIGIN AND GEODYNAMIC SIGNIFICANCE OF POST-COLLISIONAL K-RICH MAFIC MAGMATISM OF THE VARISCAN OROGEN

Soder C.*[1], Romer R.L.[2] & Altherr R.[1]
[1] Institut für Geowissenschaften, Universität Heidelberg, Germany
[2] Helmholtz Zentrum Potsdam, GFZ Deutsches GeoForschungsZentrum, Potsdam, Germany
Corresponding email: Christian.Soder@geow.uni-heidelberg.de

Keywords: continental subduction, mantle metasomatism, lamprophyres

Mantle-derived potassic to ultrapotassic magmatism is a typical feature of collisional orogens. In the Variscides, K-rich magmatic rocks form minor intrusions (lamprophyres) throughout the internal zones of the orogen. The post-collisional dykes are geochemically extremely heterogeneous with crust-like trace element pattern and elevated $^{87}Sr/^{86}Sr$ and $^{207}Pb/^{204}Pb$ and low $^{143}Nd/^{144}Nd$ ratios and with high mantle-compatible element concentrations, which reflects equilibration between the melts and mantle peridotite. This hybrid nature of the lamprophyres requires at least two source components: subducted continental material and mantle peridotite.

Variscan continental collision resulted in subduction of felsic lithologies to mantle depth. These lithologies are potentially responsible for the enrichment of the mantle source. Systematic sampling of dyke rocks across tectonic zones of the Variscan orogen reveal different crustal signatures with distinct isotopic compositions, resembling the local average composition of the upper crust. During thrusting into the mantle, these lithologies were affected by high-degree partial melting due to the breakdown of phengite (and possibly biotite). Whether the crustal trace element signature is transferred unchanged into these melts or not, largely depends on the behaviour of accessory phases that sequester significant amounts of incompatible trace elements, as for instance zircon, rutile or monazite. The crustal melts migrate into the overlying lithospheric mantle, react with peridotite, and freeze to phlogopite-amphibole-pyroxene-rich lithologies. Later remelting during post-collisional extension preferentially mobilizes these metasomes. Most of the observed geochemical variations within individual dyke swarms result from variable contributions of melts from these metasomes and “basaltic” melts from moderately depleted ambient peridotite.

Rare peralkaline minette dykes with affinities to orogenic lamproites are present but are restricted to the suture zone of the former Rheic ocean. These highly trace element-enriched dykes are characterized by low whole-rock Ca and Al, but high Mg/Fe and Ni contents. This suggests the presence of refractory olivine-rich mantle domains, allowing effective mobilization of the metasomes with little dilution by melts from peridotite. The strongly depleted mantle probably resulted from extensive melt-extraction in a supra-subduction zone setting during consumption of oceanic crust along the Rheic suture prior to continental subduction.

HIGH-PRESSURE FLUIDS IN THE MS + COH SYSTEM: AN EXPERIMENTAL STUDY ON FORSTERITE, ENSTATITE AND MAGNESITE SOLUBILITY IN MIXED H_2O–CO_2 FLUIDS AT fO_2 BUFFERED CONDITIONS

Tiraboschi C.*[1], Tumiati S.[2], Ulmer P.[3], Pettke T.[4] & Poli S.[2]

[1] Dipartimento di Scienze dell'Ambiente, del Territorio e di Scienze della Terra, Università di Milano-Bicocca, Italy

[2] Dipartimento di Scienze della Terra "A. Desio", Università di Milano, Italy

[3] Institut für Geochemie und Petrologie, Eidgenössische Technische Hochschule Zürich, Switzerland

[4] Institut für Geologie, Universität Bern, Switzerland

Corresponding email: carla.tiraboschi@unimib.it

Keywords: COH fluids, mantle minerals solubility, piston-cylinder experiments

Fluids effectively transport elements from the subducting lithosphere to the overlying mantle wedge. So far, the amount of solutes mobilized by high-pressure fluids has been mainly investigated in H_2O-only system. However, CO_2 is also thought to be a significant volatile species, as carbon is a relevant component in subduction-related fluids. Nonetheless, the solubility of mantle minerals in mixed H_2O-CO_2 fluids remains experimentally unexplored.

We considered a simplified model mantle-fluid system, the MS + COH, in order to investigate the dissolution of the assemblages forsterite + enstatite and magnesite + enstatite in graphite-saturated COH fluids. Redox conditions were buffered by Ni-NiO-H_2O, employing a double-capsule setting, with an expected X_{CO2} [=CO_2/(H_2O+CO_2)] ranging from 0.5 to 0.8 depending on pressure and temperature. Experiments were performed at pressures from 1 to 1.5 GPa and temperatures from 700 to 1000°C employing a rocking piston cylinder apparatus. Synthetic forsterite and enstatite, nearly pure natural magnesite and glassy carbon spheres were used as starting material in the inner capsule. COH fluids were generated by thermal decomposition of oxalic acid anhydrous ($H_2C_2O_4$). Water (doped with 580 ppm of Cs) has been added in order to constrain the initial X_{CO2} of the fluid to 0.5. A diamond powder layer was employed to trap fluid and solutes, which were analyzed through the "cryogenic" laser ablation ICP-MS technique. With this method the capsule is frozen prior the opening and maintained frozen during the analysis to avoid any precipitation of solutes. The temperature reached by the freezing stage (T = -35°C) is not sufficient to freeze CO_2, which leaves the capsule once is opened. Consequently, the analyzed solute content refers to the remaining aqueous part of the COH fluid and has to be scaled to the bulk X_{CO2} of the COH fluid, retrieved through thermodynamic modeling (Connolly, 1990).

Experimental data show that forsterite + enstatite solubility in COH fluids presents slightly higher SiO_2 solubility (m_{SiO2} = 0.38 mol/kg at P = 1 GPa, T = 700°C) compared to the solubility in the H_2O-only system (Newton & Manning, 2002). Moreover, the presence of CO_2 promotes the formation of Mg-solutes (m_{MgO} = 0.29 mol/kg at P = 1 GPa, T = 700°C), not detected in the MS + H_2O system. The solubility of the assemblage magnesite + enstatite in COH fluids presents lower amounts of solutes, for both SiO_2 (m_{SiO2} = 0.22 mol/kg at P = 1.5 GPa, T = 800°C) and MgO (m_{MgO} = 0.20 mol/kg at P = 1.5 GPa, T = 800°C), compared to the forsterite + enstatite assemblage, suggesting that forsterite represents the major contributor to the COH fluid in terms of solutes. Our results indicate that, differently to what is observed for quartz dissolution in COH fluids (Newton & Manning, 2000), in the MS + COH system CO_2 does not act as an inert diluent, but it promotes the dissolution of Mg-bearing silicates.

Connolly, J.A.D. (1990): Multivariable phase diagrams; an algorithm based on generalized thermodynamics. *Am. J. Sci.*, **290**, 666-718.

Newton, R.C. & Manning, C.E. (2000): Quartz solubility in H_2O-NaCl and H_2O-CO_2 solutions at deep crust-upper mantle pressures and temperatures: 2-15 kbar and 500-900°C. *Geochim. Cosmochim. Acta*, **64**, 2993-3005.

Newton, R.C. & Manning, C.E. (2002): Solubility of enstatite + forsterite in H_2O at deep crust/upper mantle conditions: 4 to 15 kbar and 700 to 900 °C. *Geochim. Cosmochim. Acta*, **66**, 4165-4176.

EXPERIMENTAL CONSTRAINTS ON THE COMPOSITION OF FLUIDS INTERACTING WITH A GRAPHITE-BEARING, CARBONATE-FREE SUBDUCTION MELANGE

Tumiati S.*[1], Miozzi F.[1], Pettke T.[2], Tiraboschi C.[3], Ulmer P.[4] & Poli S.[1]
[1] Dipartimento di Scienze della Terra "A. Desio", Università di Milano, Italy
[2] Institut für Geologie, Universität Bern, Switzerland
[3] Dipartimento di Scienze dell'Ambiente, del Territorio e di Scienze della Terra, Università di Milano-Bicocca, Italy
[4] Eidgenössische Technische Hochschule Zürich, Switzerland
Corresponding email: simone.tumiati@unimi.it

Keywords: volatiles, carbon dioxide, high pressure

CO_2 removal through dissolution of carbonates occurring in altered oceanic lithosphere and its sedimentary cover provides an efficient way to recycle carbon back to the mantle wedge. However, other forms of carbon, such as graphite, are closely associated with silicates in particular in subduction mélanges. Graphite has been considered a refractory sink of carbon in the subduction slab, owing to its lower solubility in aqueous fluids compared to carbonates. However, graphite dissolution mechanisms and solute transport in complex COH fluids at high P are experimentally unconstrained. Estimates of CO_2 in subduction fluids are mainly based on traditional thermodynamic models, relying on a very limited experimental ground. Here we present for the first time experimental constraints on graphite-saturated H_2O-CO_2 fluids, synthesized at 1 GPa and 800°C conditions and redox buffered at fH_2FMQ and fH_2NNO, in equilibrium with i) graphite, ii) graphite + forsterite + enstatite (representative of the mantle component of the mélange), and iii) graphite + quartz (representative of sediments). Experimental fluids were analyzed for volatiles using a capsule-piercing device connected to a quadrupole mass spectrometer. In experiments bearing silicates, dissolved SiO_2 and MgO were measured using a modified version of the "cryogenic technique" by Kessel at al. (2005). At the investigated conditions, the CO_2 content in fluids exceeds the amounts retrieved by traditional thermodynamic models of ternary graphite-saturated COH fluids. Our results suggest that the interaction of deep aqueous fluids with minerals commonly found in subduction mélanges exerts a major role in controlling the volatile composition of the resulting COH fluid, enhancing the CO_2 content towards values unpredicted by thermodynamic models. As a consequence, the deep CO_2 transfer from the slab-mantle interface to the overlying mantle wedge, most favorable in cold subduction zones, where fluids are thought to be stable over melts, needs to be reconsidered.

Kessel, R., Schmidt, M.W., Ulmer, P., Pettke, T. (2005): Trace element signature of subduction-zone fluids, melts and supercritical liquids at 120-180 km depth. *Nature*, **437**, 724-727.

DESERPENTINIZATION PHASES IN SERPENTINITES AS METAMORPHISM INDICATORS: A CASE STUDY OF THE LOWER SILESIA (SW POLAND, CENTRAL EUROPE) VARISCAN OPHIOLITES

Wojtulek P.*[1], Puziewicz J.[1] & Ntaflos T.[2]
[1] Institute of Geological Sciences, University of Wrocław, Poland
[2] Department für Lithosphärenforschung, Universität Wien, Austria
Corresponding email: piotr.wojtulek@ing.uni.wroc.pl

Keywords: Variscan orogen, serpentinite, deserpentinization

The Ślęża, Braszowice-Brzeźnica, Szklary and Nowa Ruda are Variscan ophiolitic mafic-ultramafic massifs occurring in the Fore-Sudetic Block NE margin of the Bohemian Massif in Central Europe). Serpentinites occur in the Ślęża, Braszowice-Brzeźnica and Szklary and have MgO/SiO_2 (0.82-1.20) and Al_2O_3/SiO_2 (~ 0.01) ratios indicating mantle peridotite protolith. As, Pb and Sb are enriched and Rb, Ba, Nb, La, Ce, Sr, Zr, Er and Y depleted relative to primitive mantle. Serpentinites with magnesite veins display Cs enrichment.

Antigorite is a main serpentine phase, chrysotile/lizardite rocks are rare (Dubiñska & Gunia, 1997). The non-pseudomorphic texture developed at expense of pseudomorphic one in Ślęża and Braszowic-Brzeźnica. The Szklary serpentinites do not display clear relationships between serpentine textures.

Serpentinites from Ślęża and Braszowice-Brzeźnica Massifs contain olivine, clinopyroxene and chromite grains interpreted as basaltic melt percolation phases (Wojtulek et al., 2016a, 2016b). Some olivine grains contain magnetite inclusions and display pseudocleavage. The serpentinites contain also microcrystalline olivine-clinopyroxene-magnetite aggregates ("brownish aggregates") with bastite and mesh textures.

Olivine grains with magnetite inclusions have various Fo (86.8-92.7) and NiO contents (0.02-0.55 wt.%). Olivine from "brownish aggregates" has similar Fo, NiO content is 0.20-0.41 wt.%. Both kinds of olivine have elevated MnO contents (up to 0.85 wt.%) relative to olivine interpreted to be a melt-percolation phase by Wojtulek et al. (2016a). Clinopyroxene has low Al_2O_3 and Cr_2O_3 contents (0.00-1.00 wt.% and 0.20-0.60 wt.%, respectively) and high Mg# (96.0-98.1). Spinel grains are zoned: chromite core has Cr# = 49.0-50.3 and is rimmed by Al-poor chromite with Cr# = 69.7-72.7 and magnetite.

Whole rock composition of the Ślęża and Braszowice-Brzeźnica serpentinites is similar to subduction zone serpentinites not affected by later fluid refertilization (cf. Deschamps et al., 2013). The following metamorphic events could be distinguished: (1) low-T serpentinization I forming pseudomorphic lizardite-chrysotile serpentinites, (2) antigorite recrystallization, (3) deserpentinization forming secondary olivine with magnetite inclusions and "brownish structures", (4) high-T serpentinization II forming antigorite intergrowths. Occurrence of deserpentinization antigorite-olivine-diopside suggests temperatures ~ 380-460°C (CMASH phase diagram of Berman et al., 1986).

Similar mineral succession occurs in serpentinites from the Lanzo Massif in Alps (Debret et al., 2013) and in Guatemala (Kodolányi et al., 2012), affected by increasing metamorphic conditions in the subduction zone setting. Secondary antigorite is evidence for decreasing PT conditions, probably due to ophiolite eduction.

Acknowledgements: This study was funded by the National Science Centre of Poland ("Evolution of the serpentinic members of ophiolites from Lower Silesia", DEC-2012/07/N/ST10/03934).

Berman, R.G., Engi, M., Greenwood, H.J., Brown, T.H. (1986): Derivation of internally-consistent thermodynamic data by the technique of mathematical programming: a review with application to the system $MgO\text{-}SiO_2\text{-}H_2O$. *J. Petrol.*, **27**, 1331-1364.

Debret, B., Nicollet, C., Schwartz, S., Andreani, M., Godard, M. (2013): Three steps of serpentinization in an eclogitized oceanic serpentinization front (Lanzo Massif – Western Alps). *J. Metam. Geol.*, **31**, 65-186.

Deschamps, F., Godard, M., Guillot, S., Hattori, K. (2013): Geochemistry of subduction zone serpentinites: A review. *Lithos*, **178**, 96-127.

Dubiñska, E. & Gunia, P. (1997): Sudetic ophiolite: current view on its dynamic model. *Geol. Quart.*, **41**, 1-20.

Kodolányi, J., Pettke, T., Spandler, C., Kamber, B.S., Gméling, K. (2012): Geochemistry of ocean floor and forearc serpentinites: Constraints on the ultramafic input to subduction zones. *J. Petrol.*, **53**, 235-270.

Wojtulek, P.M., Puziewicz, J., Ntaflos, T., Bukała, M. (2016a): Evolution of chromite in chromitites from the Variscan serpentinites of Lower Silesia (SW Poland). *Geol. Quart.*, **60**, 54-64.

Wojtulek, P.M., Puziewicz, J., Ntaflos, T. (2016b): Melt impregnation phases in the mantle section of the Ślęża ophiolite (SW Poland). *Chem. Erde*, in press.

Session S6:

Metamorphism, crustal melting and granite magmas from start to stop and from inclusions to intrusions

Conveners:

Antonio Acosta Vigil (Padova – Italy)

Michael Brown (College Park – USA)

Sergio Rocchi (Pisa – Italy)

Richard White (Mainz – Germany)

THE COMPOSITION OF NANOGRANITOIDS IN MIGMATITES OVERLYING THE RONDA PERIDOTITES (BETIC CORDILLERA, S SPAIN): THE ANATECTIC HISTORY OF A POLYMETAMORPHIC BASEMENT

Acosta-Vigil A.*[1-2], Barich A.[2-3], Bartoli O.[1], Garrido C.J.[2], Cesare B.[1], Remusat L.[4], Poli S.[5] & Raepsaet C.[6]

[1] Dipartimento di Geoscienze, Università di Padova, Italy

[2] Instituto Andaluz de Ciencias de la Tierra, Consejo Superior de Investigaciones Científicas & Universidad de Granada, Spain

[3] Institut für Erd- und Umweltwissenschaften, Universität Potsdam, Germany

[4] Institut de Minéralogie, de Physique des Matériaux, et de Cosmochimie, Centre National de le Recherche Scientifique, Sorbonne Universités, Muséum National d'Histoire Naturelle, Paris, France

[5] Dipartimento di Scienze della Terra "A. Desio", Università di Milano, Italy

[6] Laboratoire d'Etude des Eléments Légers, Institut Rayonnement-Matière de Saclay, Nanosciences et Innovation pour les Matériaux, la Biomédecine et l'Énergie, Gif-sur-Yvette, France

Corresponding email: acostavigil@hotmail.com

Keywords: melt inclusions, granulites, mechanisms of anatexis

The study of the composition of primary melts during anatexis of high-pressure granulitic migmatites is relevant to understand the generation and differentiation of continental crust. Peritectic minerals in migmatites can trap droplets of melt that forms via incongruent melting reactions during crustal anatexis. These melt inclusions commonly crystallize and form *nanogranitoids* upon slow cooling of the anatectic terrane. To obtain the primary compositions of crustal melts recorded in these nanogranitoids, including volatile concentrations and information on fluid regimes, they must be remelted and rehomogenize before analysis. A new occurrence of nanogranitoids was recently reported in garnets of mylonitic metapelitic gneisses (former high pressure granulitic migmatites) at the bottom of the prograde metamorphic sequence of Jubrique, located on top of the Ronda peridotite slab (Betic Cordillera, S Spain). Nanogranitoids within separated chips of cores and rims of large garnets from these former migmatites were remelted at 15 kbar and 850, 825 or 800ºC and dry (without added H_2O), during 24 hours, using a piston cylinder apparatus. Although all experiments show glass (former melt) within melt inclusions, the extent of rehomogenization depends on the experimental temperature. Experiments at 850-825ºC show abundant disequilibrium microstructures, whereas those at 800ºC show a relatively high proportion of rehomogenized nanogranitoids, indicating that anatexis and entrapment of melt inclusions in these rocks likely occurred at pressures ≤1.5 GPa and temperatures close to 800ºC. Electron microprobe and NanoSIMS analyses show that experimental glasses are leucogranitoid and peraluminous, though define two distinct compositional groups. Type I melt inclusions corresponds to K-rich, Ca- and H_2O-poor leucogranitic melts, whereas type II melt inclusions represents K-poor, Ca- and H_2O-rich granodioritic to tonalitic melts. Type I and II melt inclusions are found in most cases at the cores and rims of large garnets porphyroclasts, respectively. We tentatively suggest that these former migmatites underwent two melting events under contrasting fluid regimes, possibly during two different orogenic periods. This study demonstrates the strong potential of melt inclusions studies in migmatites and granulites in order to unravel their anatectic history, particularly in strongly deformed rocks where most of the classical anatectic microstructures and macrostructures have been erased during deformation.

GEOCHRONOLOGY AND PETROGENESIS OF GRANITOID INTRUSIONS RELATED TO THE AKSUG COPPER PORPHYRY DEPOSIT IN THE ALTAI-SAYAN FOLD BELT, RUSSIA

Berzina A.N.*[1], Berzina A.P.[1] & Gimon V.O.[1]

[1] V.S. Sobolev Institute of Geology and Mineralogy, Siberian Branch of the Russian Academy of Sciences, Novosibirsk, Russia

Corresponding email: anitansk@gmail.com

Keywords: Aksug, porphyry copper, petrogenesis

The Altai-Sayan Fold Belt (ASFB) forms the northwestern part of the Central Asian Orogenic Belt (CAOB) with juvenile crust of Vendian-early Paleozoic age. From the Vendian-Cambrian boundary to middle Early Cambrian the accretion of island-arc, back-arc, oceanic and metamorphic complexes took place at this segment of CAOB. Aksug, located in ASFB within Early Paleozoic Khamsara batholith, is a large porphyry Cu deposit, its formation is confined to accretion-collision events related to the interaction of Siberian continent with Paleo-Asian ocean. Porphyry stocks and dikes of predominantly tonalite-plagiogranite composition, emplaced into preceding pluton are associated with major Cu-Mo mineralization. The pluton is composed of diorites, tonalities and plagiogranites with minor gabbroic rocks. Zircon U-Pb geochronology has yielded Middle Cambrian ages for the Aksug intrusions.

In general, rocks of the Aksug deposit possess chemical affinities of subalkaline/tholeiite series. Gabbroic samples show low Rb, Sr, Ba and REE contents, high positive ε_{Nd} (T) value (+6.7 - +7.4), low $(^{87}Sr/^{86}Sr)_i$ ratio (0.7022-0.7029), enrichment in LILEs and LREEs and depletion in HREEs and HFSEs. All these geochemical features suggest that a depleted mantle metasomatized by slab-derived fluids and/or melts was possibly involved in the generation of their precursor magma. High Ba and U contents relative to Th in the Aksug samples support mantle wedge enrichment by slab-derived fluids. Relatively low contents of MgO, Ni and Co in gabbroic samples suggest their petrogenesis via crystal fractionation of mantle-derived melt. Gabbroic rocks have T_{DM} model ages of ~ 0.8 Ga, attributed to the Paleo-Asian Ocean opening and subduction of oceanic plate, followed by metasomatizm of subduction related fluids.

Sr-Nd isotopic characteristics suggest significant contribution of mantle material in the formation of granitoid magmas at Aksug. Mafic and felsic samples show relatively similar geochemical characteristics and overlapping initial Sr and Nd compositions. Lack of correlation between ε_{Nd} and MgO could be interpreted as being due to partial melting/fractional crystallization without high level of contamination/assimilation during generation and evolution of magmas. Felsic samples are depleted in incompatible elements relative to mafic rocks, which is inconsistent with an origin via differentiation of basaltic magma. The Aksug tonalite-plagiogranite rocks have adakite-like geochemical signatures. Relatively high ε_{Nd}(T), ranging from +6.6 to 7.7, low Sr_i (0.7011-0.7029), young T_{DM} (0.6-0.7 Ga) model ages and adakite-like geochemical characterictics in felsic samples suggest that tonalite-plagiogranite magmas may have been generated by partial melting of basaltic lower crustal source formed by underplating of earlier depleted mantle-derived mafic magmas. Similar geochemical signatures and Sr-Nd isotopic compositions for the gabbroic and felsic rocks suggest their derivation from similar sources.

POST-COLLISIONAL LATE VARISCAN GRANITES OF SOUTHERN SARDINIA: EVIDENCES OF CONTRASTING SUITES

Conte A.M.*[1], Naitza S.[2], Oggiano G.[3], Secchi F.[3], Cifelli F.[4], Cuccuru S.[3] & D'Antonio M.[5]
[1] Istituto di Geoscienze e Georisorse, Consiglio Nazionale delle Ricerche, Roma, Italy
[2] Dipartimento di Ingegneria Civile, Ambientale e Architettura, Università di Cagliari, Italy
[3] Dipartimento di Scienze della Natura e del Territorio, Università di Sassari, Italy
[4] Dipartimento di Scienze, Università di Roma Tre, Italy
[5] Dipartimento di Scienze della Terra, dell'Ambiente e delle Risorse, Università Federico II, Napoli, Italy
Corresponding email: aidamaria.conte@uniroma1.it

Keywords: granite rock-suites, Variscan granites, crustal source

The Sardinia portion of the Sardinia-Corsica batholith emplaced mostly during the post collisional evolution of the Variscan chain. The majority of plutons emplaced in about 40 Ma during two phases, the older of which clustered at about 310 Ma, whereas the younger, clustered in the range of 290 Ma.The former is dominated by monzogranitic and granodioritic calc-alkaline plutons, while the latter mostly consists of leucogranites; minor mafic intrusions are more spread in northern Sardinia and preferentially associated to the latter phase. In southern Sardinia, in the frontal part of the orogenic wedge (nappe zone), the younger phase consists of two main rock-suites. The prevalent suite dissects porphyritic granodiorites, is dominated by syderophyllite monzogranites and leucogranites (SGS, syderophyllite granite suite) and, in turn, is crosscut with sharp vertical contacts by Fe-hastingsite granites (HGS, Fe-hastingsite granite suite). Both series are classified as ferroan, F-bearing granites, showing an alkali-calcic character; near liquidus temperatures indicate values in excess of 850°C. Siderophyllitic mica contains ilmenite inclusions and shows in the whole SGS a continuous trend in the Mg-Al plot. Conversely, in the HGS Fe-hastingsite amphibole occurs as early phase hosting magnetite and allanite inclusions.

Magnetic susceptivity data indicate that SGS shows values typical of an ilmenite *series* in the range 20 to $60 \cdot 10^{-6}$ SI unit, whereas HGS plots on the ilmenite/magnetite *series* boundary with values in the range 1.7-$2.8 \cdot 10^{-3}$ SI unit. Different trends displayed by variation diagrams confirm the contrasting behavior between the HGS leucogranites and the SGS monzogranites-leucogranites, the chemical variations of which can be accounted for with crystal/liquid fractionation processes dominated by plagioclase + biotite ± minor amounts of accessory phases.

Field occurrences and petrochemistry indicate a dominant crustal origin for both suites, according to εNd_{290} (–7.47) from Conte *et al*. (2015) and $\delta^{18}O_{S.M.O.W.}$ values (10.5±0.2 – 12.1±0.3) from Boni *et al*. (1992). A Proterozoic age of the involved crustal source may be inferred from the distribution of studied suites in the frontal part of the chain. Constraints on source materials are offered by chemical compositions of our rocks, which meet the liquids experimentally obtained by low degrees of partial melting of a meta-igneous source (Conrad *et al*., 1988). Mass balance calculations indicate for SGS a low degree of partial melting of about 25%. Conversely, the whole data set indicate a different path for the HGS, possibly due to inhomogeneities in the crustal source.

The younger phase of magmatism marks the transition from late- to post-collisional Variscan events in southern Sardinia. Further questions arise from the thermal regimes, which triggered the partial melting, as far modelled by adiabatic decompression during the exhumation of the chain and shear heating (Casini *et al.*, 2015).

Boni, M., Iannace, A., Köppel, V., Früh-Green, G., Hansmann, W. (1992): Late to post-hercynian hydrothermal activity and mineralization in south-west Sardinia (Italy). *Econ. Geol.*, **87**, 2113-2137.

Casini, L., Cuccuru, S., Puccini, A., Oggiano, G., Rossi, P. (2015): Evolution of the Corsica–Sardinia Batholith and late-orogenic shearing of the Variscides. *Tectonophys.*, **646**, 65-78.

Conrad, W.K., Nichols, I.A., Wall, V.J. (1988): Water saturated and undersaturated melting of metaluminous and peraluminous crustal compositions at 10 kbar: evidence for the origin of silicic magmas in the Taupo Volcanic Zone, New Zealand and other occurrences*. J. Petrol.*, **29**, 765-803.

Conte, A.M., Cuccuru, S., Oggiano, G., Naitza, S., Secchi, F., Tecce, F. (2015): Cassiterite veins deposits related to late-variscan ilmenite series in south western Sardinia (Italy): insights for a new tin province. Proc.13th SGA Meeting, **1**, 69-72.

COMPLEX EVOLUTION OF MIXED (NYF + LCT) KRACOVICE PEGMATITE (MOLDANUBIAN ZONE, CZECH REPUBLIC); AN EVIDENCE FROM Li AND REE CONTENTS IN ROCK FORMING MINERALS

Čopjaková R.[1], Škoda R.*[1], Vašinová Galiová M.[2-3] & Novák M.[1]
[1] Department of Geological Sciences, Masaryk University, Brno, Czech Republic
[2] Department of Chemistry, Masaryk University, Brno, Czech Republic
[3] Central European Institute of Technology, Masaryk University, Brno, Czech Republic
Corresponding email: rskoda@sci.muni.cz

Keywords: pegmatite, melt evolution, pegmatite-derived fluids

The Kracovice pegmatite represents the most evolved pegmatite body of NYF pegmatites related to the Třebíč Pluton (Novák et al., 2012). The pegmatite is built from the contact inwards of: a granitic unit (Kfs+Pl+Qz+Bt+Ms), a graphic unit (Kfs+Qz+Tu±Bt) evolving to minor blocky K-feldspar, and an albite unit situated close to a small quartz core. Minor minerals include tourmaline, garnet, topaz and Li-micas, some in several generations. Chemical variations of major (EMP) and trace (REE, Li; LA-ICP-MS) elements in minerals were used for genetic implications and to decipher mineral evolution and replacement processes.

Early magmatic black columnar tourmaline (Tur1; Al-rich schorl) is commonly overgrown by later fluor-elbaite (Tur2) or replaced by fluor-elbaite (TurS). Moreover, fluor-elbaite (TurS) along with with Li-mica partly replaces garnet (Grt1). Al-rich schorl (Tur1) is partly replaced by allanite-(Ce) + chamosite. Early garnet Grt1 ($Sps_{69-56}Alm_{43-30}$) is REE- enriched, whereas later garnet Grt2 is Mn-enriched ($Sps_{86-58}Alm_{41-13}$), REE-poor and F-enriched.

Black Al-rich schorl (Tur1), Grt1 and Bt1 crystallized early from the silicate melt. The presence of magmatic tourmaline and F-rich hambergite indicates a high activity of B in the melt. Lithium contents in early magmatic Fe-Mn silicates are low (100-700 ppm) and in the following order: Bt > Grt > Tur. Magmatic schorl (Tur1) shows the lowest Li contents, even lower than simultaneously crystallizing garnet (Grt1).

The distinct compositional gap between Al-rich schorl (Tur1) and fluor-elbaite (Tur2 and TurS) as well as between Grt1 and Grt2, and Bt1 and Li-rich Bt2 respectively, indicate a crystallisation gap between their formation and significantly distinct conditions of their crystallization. Textural evidences indicate that fluor-elbaite (Tur2) and Grt2 (along with other Li- and F-rich phases e.g. topaz, Li-micas, hambergite) probably started crystallisation before complete solidification of the rock. They probably precipitated from the late magmatic, highly fractionated melt with sodic, alkaline composition, enriched in fluxing components (B, P, F), water, Li, Rb, Cs (resembling boundary layer liquid; see London, 2014) to early hydrothermal conditions. Secondary mineral assemblages fluor-elbaite (TurS) + allanite-(Ce) + chamosite and fluor-elbaite (TurS) + Li-mica, respectively, are likely coeval products of subsolidus reactions of the magmatic Al-rich schorl (Tur1) and garnet (Grt1), respectively, with evolved, REE-poor, Li,F-rich, alkaline pegmatite derived fluids.

The REE patterns in minerals evolve from those without tetrad effect (Tur1, Bt1, Pl in granitic and graphic units) to phases with M-type tetrads (Tur2, TurS, Grt2 > Grt1, Pl in blocky and albite unit, Li-mica, zircon and monazite in blocky unit) and clearly indicate the tetrad effect is not an inherited feature of the pegmatitic magma; however, it gradually evolves during the melt crystallization and subsequent processes.

Acknowledgements: This work was supported by research project GACR P210/14/1347S.

London, D. (2014): A petrologic assessment of internal zonation in granitic pegmatites. *Lithos*,**184**, 74-104.

Novák, M., Škoda, R., Gadas, P., Krmíček, L., Černý, P. (2012): Contrasting origins of the mixed (NYF + LCT) signature in granitic pegmatites, with examples from the Moldanubian Zone, Czech Republic. *Can. Mineral.*, **50**, 1077-1094.

THE CURIOUS CASE OF THE IMPOSTER AMPHIBOLE CUMULATES – IDENTIFYING ZONES OF SIGNIFICANT MASS TRANSFER THROUGH THE LOWER CRUST

Daczko N.*[1], Piazolo S.[1], Meek U.[1], Stuart C.A.[1] & Elliot V.[1]
[1] Department of Earth and Planetary Sciences, Macquarie University, Sydney, Australia
Corresponding email: nathan.daczko@mq.edu.au

Keywords: mass transfer, melt migration, lower crust

Geochemical signatures throughout the layered Earth require significant mass transfer through the lower crust. Though we recognize some geological pathways of magma migration such as dykes and high strain zones, those documented are insufficient to facilitate the volume required for crustal differentiation throughout Earth's history. Ultrabasic rocks such as hornblendite commonly form elongate bodies in exposures of the lower crust and their formation is rarely examined, being most commonly attributed to cumulate processes. Hornblendite bodies (up to 30-40 m thick) hosted within granulite facies gabbroic gneiss of the Pembroke Valley, Fiordland, New Zealand, share many similarities with reported igneous cumulate hornblendite, including a high mode of one or two minerals, unimodal grain size distribution, interlocking euhedral grain shapes, and interstitial minor phases with low dihedral angles. The igneous nature of the hornblendite bodies contrasts with their host gabbroic gneiss which contains a gneissic foliation, evidence of crystal plastic deformation at the grain scale and well-studied metamorphic reaction textures. These two rock types are linked by the progressive modification of structures that can be traced from the host gabbroic gneiss into the hornblendite bodies. The gradual alteration of these structures precludes any interpretation involving cumulate processes in forming the hornblendite; these bodies are imposter cumulates. Instead, we propose that the metasomatic replacement of the host gabbroic gneiss to form hornblendite resulted from channeled high melt-flux through the lower crust. High melt-rock ratios and the chemical interaction between the migrating melt and host rock induced dissolution of plagioclase and pyroxene in the host and growth of mainly hornblende. This reaction-replacement mechanism forms hornblendite bodies delineating significant melt conduits. Accordingly, hornblendite or other basic to ultrabasic bodies in the lower crust may map the “missing” mass transfer zones.

MUSCOVITE DEHYDRATION MELTING: REACTION MECHANISMS, TEXTURES, AND IMPLICATIONS FOR MELT TRANSFER

Dyck B.*[1], Waters D.J.[1-2], St-Onge M.R.[3] & Searle M.P.[1]
[1] Department of Earth Sciences, University of Oxford, United Kingdom
[2] Museum of Natural History, University of Oxford, United Kingdom
[3] Geological Survey of Canada, Ottawa, Canada
Corresponding email: brendan.dyck@earth.ox.ac.uk

Keywords: dehydration melting, anatexis, Himalaya

Dehydration melting of muscovite in metasedimentary sequences is the initial dominant mechanism of granitic melt generation in orogenic hinterlands. In dry (vapour-absent) crust, muscovite dehydrates to produce K-feldspar, sillimanite, and granitic melt. When water vapour is present, sillimanite and melt are the sole products of muscovite dehydration melting, and any K-feldspar produced is as a result of melt crystallisation. Here we identify the reaction mechanisms that control nucleation and growth of K-feldspar, sillimanite, and silicate melt in the metamorphic core of the Himalaya, and outline the textural criteria used to distinguish peritectic K-feldspar from K-feldspar formed during melt crystallisation.

These textural criteria enable a mass-balance of peritectic K-feldspar and sillimanite to constrain the amount of free H_2O present during muscovite dehydration. The resulting modal proportion of K-feldspar in the Himalayan metamorphic core necessitates vapour-absent conditions during anatexis, indicating that the generation of large volumes of (leuco)granitic melt in orogenic belts does not require an external source of fluids.

We have characterised four stages of textural evolution in selected psammitic and pelitic samples that vary primarily in the abundance of protolith muscovite:

1) K-feldspar nucleates epitaxially on plagioclase while intergrowths of fibrolitic sillimanite and the remaining hydrous melt components replace muscovite. These nucleation preferences set up a self-organising system with coupled behaviour between aluminous and quartzofeldspathic domains.

2) K^+ – Na^+ cation exchange between aluminous and quartzofeldspathic domains drives the topotactic replacement of plagioclase by K-feldspar, while melt and intergrowths of sillimanite + quartz form in the aluminous domains.

3) A melt percolation threshold is reached at 7-8 % melt, at which point the system transitions from a closed to open system. Above the melt percolation threshold, the mobility of grain boundaries increases and all solid phases coarsen, resulting in large K-feldspar porphyroblasts.

4) Preferential crystallisation of residual melt on K-feldspar porphyroblasts and coarsened quartz forms an augen gneiss texture with a monzogranitic-tonalitic matrix and an anastomosing network of fibrolitic sillimanite folia.

Melt initially migrates along grain boundaries and micro-fractures. Above the melt percolation threshold, melt migrates along an evolving grain boundary network, eventually accumulating in dilatational domains. The spatial distribution of melt pseudomorph microstructures (cf. Holness & Sawyer, 2008) indicates that melt drainage was most efficient along the network of sillimanite folia. This study demonstrates that coarsened leucocratic domains (i.e., leucosomes) formed from a compositionally layered protolith, preserve a record of textural modification in the presence of melt, but do not strictly represent a volume of crystallised melt.

Holness, M.B. & Sawyer, E. (2008): On the pseudomorphing of melt-filled pores during the crystallisation of migmatites. *J. Petrol.*, **49**, 1343-1363.

MELTING OF GRANITES AT MANTLE DEPTHS: TRACE ELEMENTS GEOCHEMISTRY OF NEAR UHP NANOGRANITES AND THEIR PRESERVED WATER, CHLORINE AND CO_2 CONTENTS

Ferrero S.*[1-2], Wunder B.[3], O´Brien P.[1], Ziemann M.A.[1], Wälle M.[4] & Remusat L.[5]
[1] Institut für Geowissenschaften, Universität Potsdam, Golm, Germany
[2] Museum für Naturkunde, Leibniz-Institut für Evolutions- und Biodiversitätsforschung, Berlin, Germany
[3] Helmholtz Zentrum Potsdam, GFZ Deutsches GeoForschungsZentrum, Potsdam, Germany
[4] Eidgenössische Technische Hochschule, Zürich, Switzerland
[5] Muséum National d'Histoire Naturelle, Institut de Minéralogie, de Physique des Matériaux et de Cosmochimie, Centre National de la Recherche Scientifique, Paris, France
Corresponding email: silv.ferrero@gmail.com

Keywords: partial melting, nanogranites, UHP

High pressure granulites with granitic protolith are a common rock type in the Variscan terrains throughout Europe. One of the most investigated examples is represented by the Orlica-Śnieżnik granulites in the Sudetes, Bohemian Massif. These felsic granulites are characterized by the presence of Ca-rich Grt, Ky and ternary feldspar in a leucocratic matrix with Qz+Kfs+Pl. The garnet has a peritectic origin and contains droplets of crystallized anatectic melt (nanogranites). The petrological investigation of the nanogranites, coupled with re-homogenization experiments, shows that partial melting took place at T ≥ 875°C and 2.7 GPa as result of continental subduction at mantle depth, as also confirmed by geothermobarometric studies. The partial melt has a granitic and metaluminous character. Its water content, estimated via NanoSIMS, is in average 6.34 wt.% (n = 25); previous estimates based on electron microprobe and Raman spectroscopy provided similar values, 6 and 6.5 wt.% respectively. NanoSIMS analyses also show important amounts of chlorine, ~ 1200 ppm. Calcite is also visible as a minor crystallization product of the melt, suggesting that the original melt contained significant CO_2, possibly ≥ 0.60 wt.%.

Composition and volatiles content of the re-homogenized nanogranites are consistent with experimental data, thus suggesting that nanogranites preserve both original chemistry and water content of the deep melt. This is also supported by the finding of relatively rare polymorphs of albite, K-feldspar and quartz - namely kumdykolite, kokchetavite and cristobalite-along with glass in crack-free nanogranites via Raman spectroscopy. The metastable nature of these phases confirms that after formation these natural "pressure vessels" remained completely isolated from the surrounding rock, sheltered by the host garnet. These polymorphs can thus be considered as direct mineralogical criteria to identify preserved melt inclusions in partially melted rocks.

In terms of trace elements, nanogranites show high enrichment in LILE and LREE, with average La_N = 139, much higher than what observed in natural partial melts from metapelites. High enrichment in incompatible elements could be the result of the remelting of a granitic protolith already enriched in LILE and LREE, e.g. because already (partly) anatectic in origin. The enrichment in Ba, Sc, V and Zn of the melt suggests that biotite was involved in the melting reaction, despite the absence of residual biotite as mineral inclusion in garnet.

Our results show how nanogranites preserved in deeply subducted rocks provide crucial information on water budget at depth and fluid speciation, as well as on the melting mechanisms operating in subducted crust.

ORIGIN, TIMING AND ACCRETION MODES OF POST-COLLISIONAL BATHOLITHS: THE MESSAGE FROM GEOCHEMISTRY, ZIRCON OXYGEN ISOTOPES AND U-Pb AGES OF THE CRUST-DERIVED SERRE BATHOLITH (CALABRIA, SOUTHERN ITALY)

Fiannacca P.*[1], Williams I.S.[2] & Cirrincione R.[1]
[1] Dipartimento di Scienze Biologiche, Geologiche e Ambientali, Università di Catania, Italy
[2] Research School of Earth Sciences, Australian National University, Canberra, Australia
Corresponding email: pfianna@unict.it

Keywords: granite petrogenesis, crustal recycling, pluton overaccretion

The late Variscan Serre Batholith forms the middle part of a crustal section continuously exposed from lower-crustal granulites to upper-crustal phyllites. Exposure of both the batholith internal architecture and its potential magma sources offers a rare opportunity to investigate the timescale and mechanisms of batholith construction, as well as the processes of granite petrogenesis. Granitoid bodies were emplaced at depths from ca. 23 to ca. 6 km, with a precise pattern: quartz diorites-tonalites into deep migmatitic metapelites, two-mica granodiorites-granites at intermediate levels and weakly peraluminous granodiorites into shallow paragneisses and phyllites. Geochemical data point to generation of the batholith by assembly of several granitoid bodies derived from different crustal sources. Quartz diorites and tonalites originated from mafic granulites, whereas metagraywackes with different pelitic and mafic contents were the most likely sources of equigranular two-mica granodiorites-granites and biotite granodiorites; the latter could also have been sourced from mafic-intermediate metaigneous rocks. Two-mica porphyritic leucogranites were probably the only rocks crystallised from pure melts, produced by partial melting of mafic pelites. The granitoids have an arc signature inherited from source rocks of magmatic arc derivation, such as magnesian volcanic rocks and sediments produced by rapid erosion of such rocks. All data indicate no direct mantle contribution to the geochemical diversity of the granitoids; magma production was associated solely with recycling of crustal material, suggesting that post-collisional granitoid magmatism is mostly an agent of intracrustal differentiation rather than crustal accretion. SHRIMP U-Pb dating of zircon from the main magma bodies from different crustal levels shows that the batholith was built up in 5.1±4.0 Ma. The oldest granitoid is a 297.3±3.1 Ma quartz diorite from the batholith floor; the youngest a 292.2±2.6 Ma granodiorite from the roof. Three two-mica granites from progressively higher intermediate levels gave ages of 294.9±2.7, 296.1±1.9 and 294.2±2.6 Ma, respectively. These results are consistent with batholith growth by incremental overaccretion, the emplacement level of the new magmas being strongly influenced by the presence of the preexisting granitoid bodies. Lack of mixed zircon populations with contributions from the older granitoids in the younger ones, together with petrographic and geochemical features, suggest trivial magma mixing, consistent with the granitoid bodies being mostly solid at the time of subsequent magma intrusion. The presence in the ca. 296-294 Ma granites of ca. 305-302 Ma anatectic zircon, with distinctive $\delta^{18}O$, places a limit of 8-9 Ma on the time required for effective crustal differentiation, involving recycling of lower crustal components into granites to make up plutonic complexes in the middle-upper crust.

UHT GRANULITES ABOVE A PALAEO-MOHO: THE SRI LANKAN EXAMPLE OF CRUSTAL DIFFERENTIATION

Kriegsman L.M.*[1-2], Dharmapriya P.L.[3] & Malaviarachchi S.P.K.[3]
[1] Taxonomy & Systematics Group, Naturalis Biodiversity Center, Leiden, Netherlands
[2] Department of Earth Sciences, University of Utrecht, Netherlands
[3] Department of Geology, University of Peradeniya, Sri Lanka
Corresponding email: leo.kriegsman@naturalis.nl

Keywords: UHT granulites, Moho, melting

New mapping and petrological analysis (Dharmapriya et al., 2015a, 2015b) reveal that the areal distribution of ultra-high-temperature (UHT) granulites in Sri Lanka is characterized by a NW-SE trending structural high in which the deepest, highest T granulites are exposed. Combining structural data and the occurrences of upper mantle slivers, it is postulated that the UHT granulites represent a relatively thin (several km) lowermost crustal layer above an ultra-hot palaeo-Moho. This layer has been imbricated and intensely refolded with the overlying high-temperature (HT) "ordinary" granulites after peak metamorphism, leading to an apparently thicker package. The UHT granulite layer shows evidence for partial melting of most lithologies and related melt transfer to shallower crustal levels, leading to pervasive volume loss. The resulting lower crust in Sri Lanka is dominated by restitic, felsic assemblages that fit the relamination model of Hacker et al. (2011). The isolated nature of UHT assemblages, partly due to a scarcity of suitable lithologies, is enhanced by retrogression near locally crystallising melts.

The concept of a UHT layer above an ultra-hot palaeo-Moho has some important implications for granulite terrains in general: (i) UHT granulites elsewhere may also represent a thin zone above an ultra-hot palaeo-Moho and overlain by HT granulites, and their spatial relationships may have been complicated by ductile deformation; and (ii) many other granulite terrains may be underlain by a similar zone of UHT granulites, and, if so, new discoveries of UHT domains may be expected. In addition, the patchiness of the geological record due to intense ductile deformation and localised retrogression seems to be a common aspect in the preservation of both UHT and UHP assemblages.

Dharmapriya, P.L, Malaviarachchi, S.P.K., Galli, A., Su, B.-X., Subasinghe, N.D., Dissanayake, C.B. (2015a): Rare evidence for formation of garnet + corundum during isobaric cooling of UHT metapelites: New insights for retrograde P-T trajectory of the Highland Complex, Sri Lanka. *Lithos*, **220**, 300-317.

Dharmapriya, P.L., Malaviarachchi, S.P.K., Santosh, M., Tang, L., Sajeev, K. (2015b): Late-Neoproterozoic ultrahigh temperature metamorphism in the Highland Complex, Sri Lanka. *Precambrian Res.*, **271**, 311-333.

Hacker, B.R., Kelemen, P.B., Behn, M.D. (2011): Differentiation of the continental crust by relamination. *Earth Planet. Sci. Letters*, **307**, 501-516.

THE ULTRA-HIGH TEMPERATURE METAMORPHISM OF THE KHONDALITE BELT, NORTH CHINA CRATON: NEW EVIDENCE FOR A LARGE PARTIALLY MOLTEN OROGENIC CRUST

Lobjoie C.*[1], Wei L.[2], Trap P.[1], Goncalves P.[1] & Marquer D.[1]

[1] Laboratoire Chrono-Environnement, Université de Bourgogne-Franche-Comté, Besançon, France

[2] State Key Laboratory of Lithosphere Evolution, Institute of Geology and Geophysics, Chinese Academy of Sciences, Beijing, China

Corresponding email: cyril.lobjoie@univ-fcomte.fr

Keywords: UHT metamorphism, partial melting, Khondalite Belt

The Khondalite Belt of the North China Craton is a famous Paleoproterozoic high to ultra-high temperature orogenic domain. This domain is mainly constituted of garnet ± spinel ± sapphirine-bearing migmatites, marbles and calc-silicates, S-type granite and a lot of mafic bodies. Petrological study and thermodynamic quantification of P-T conditions by petrogenetic grids and pseudosections were carried out on an olivine-bearing migmatite and on a migmatite bearing sapphirine-granulite relics.

These two migmatites recorded UHT conditions and partial melting events at different crustal levels. The olivine-bearing migmatite shows a complex metamorphic history. Two types of mineralogical assemblages were described within this rock: i) the matrix with micrographic quartz and feldspar with biotite, sillimanite and spinel, and ii) complex symplectites with opx-crd, opx-crd-sp and ol-crd associations. Pseudosection calculation and petrogenetic grid attested for low pressure-UHT metamorphic conditions reaching 0.3-0.35 GPa for 950°C and associated to a clockwise P-T evolution. The partially molten sapphirine-bearing granulite, shows a Sapphirine-Quartz assemblage with a high Ti-content Spinel. Petrogenetic grid and pseudosection calculation constrain P-T metamorphic conditions at around 0.7±0.1 GPa for temperature up to 1050°C. Mineral assemblages and textures observed within the sample also testify to a clockwise P-T path.

In this domain, the beginning of the partial melting was estimated at around 1.93 Ga and probably ending around 1.88-1.89 Ga. New geochronological data on monazite and zircon grains give an age of 1.92-1.91 Ga for the mafic intrusions and the coeval UHT metamorphism for these samples, implying a strong relationship between partial melting at UHT and mafic magmatism.

MAGMATISM FROM THE LOWER CONTINENTAL CRUST: MELTING EXPERIMENTS ON GRANULITE XENOLITHS FROM PASO DE INDIOS, ARGENTINA

Muñoz R.*[1] & Castro A.[1]
[1] Departamento de Geología, Universidad de Huelva, Spain
Corresponding email: rod.mu.cr@gmail.com

Keywords: lower crust melting, cordilleran granitoids, mafic granulites

Xenoliths pulled up by basaltic volcanism are a very valuable way to study the lower crust as, either a source of magmas or residues left after melt extraction. They represent fresh or very weakly altered geochemical and mineralogical samples from unmodified regions of the lower crust. In this study we present whole rock composition (mayor and trace elements) and isotopic signatures (Rb/Sr and Sm/Nd) from six granulite xenoliths from Paso de Indios, Argentina. The granulites have compositions closed to bulk lower continental crust and are depleted in incompatible elements. We used some of the Paso de Indios granulites as starting materials in several piston-cylinder experiments with three main goals: (1) to test the residual character of the lower crust, (2) to test the granite-granulite connection, and (3) to emulate the latest liquid in equilibrium with the granulites in runs with very low melt fractions. Experiments have been performed at 1000, 1050 and 1100°C for 10 kbar and 1100ºC for 15 kbar. The resultant liquids are peraluminous andesites, tonalites and granodiorites, with high contents in CaO (4 to 6 wt.%) and Mg# [molar MgO/(MgO+FeO)] from 0.36 to 0.64. The liquids are andesitic at T > 1000ºC and granitic at 1000ºC with very low melt fractions. The liquids form a linear trend in the MgO-CaO (wt.%) diagram, being slightly more magnesian than typical Patagonian (Cordilleran) granites. The andesitic liquid compositions are more magnesian and have higher alkali contents than the regionally related andesites. On the other hand, the andesitic liquids have compositions similar to vaugnerites in silica (SiO_2 = 53-60 wt.%), magnesium (MgO = 3-4 wt.%) and alkalis (K_2O = 2-4 wt.%). In this way, we argue in favor of a modest contribution by lower crust melting to the generation of Cordilleran granitic batholiths.

FORCE AND MOMENTUM IN GRANITE EMPLACEMENT

Petford N.*[1]
[1] University of Northampton, United Kingdom
Corresponding email: nick.petford@northampton.ac.uk

Keywords: granites, momentum, collision

Four generic stages comprise granite formation on Earth: melt generation, melt segregation, magma ascent and magma emplacement. Moving progressively from deeper to shallower levels, each stage is governed physically by a complex interplay between the equations of momentum and heat transfer. The intrinsic and extrinsic thermodynamics of the problem are understood variably depending upon which stage of the process one chooses to investigate. What is certain is that vertical lengthscales, constrained broadly by the average thickness of the continental lithosphere can be much smaller than horizontal lengthscales characterising granitic domains, for example in Cordilleran arcs a factor of 10 or more. Timescales on the other hand, when defined by total average construction times, may extend over millions of years although the greatest time reflects the summation of intervals between successive intrusive events that are themselves short lived. However, despite the obvious fact that batholithic terrains of different ages exist, implying a repeatable process at work, a system-wide understanding (a grand unified theory if you like) of granite formation remains elusive. One aspect of the ascent and emplacement process that has not been explored in great detail relates to momentum, more precisely granite formation as a problem of both “mass in motion” and “mass at rest”. This talk will explore whether insight can be gained from considering magma emplacement as a collisional event from the perspective of the conservation of momentum and what that may tell us about granite formation more generally.

METAMORPHISM AND MELTING OF METAGRANITOIDS UNDER (U)HP CONDITIONS, EGER CRYSTALLINE COMPLEX (BOHEMIAN MASSIF)

Racek M.*[1], Hasalová P.[2], Závada P.[3], Štípská P.[2], Jeřábek P.[1] & Weinberg R.F.[4]
[1] Institute of Petrology and Structural Geology, Charles University, Prague, Czech Republic
[2] Czech Geological Survey, Prague, Czech Republic
[3] Institute of Geophysics, Czech Academy of Sciences, Prague, Czech Republic
[4] School of Earth, Atmosphere and Environment, Monash University, Clayton, Australia
Corresponding email: martin.racek@natur.cuni.cz

Keywords: UHP metamorphism, melting, Bohemian Massif

The Eger crystalline complex (ECC) is located at the border of the Saxothuringian and Teplá-Barrandian zones of the Bohemian Massif. It consists of high-grade felsic anatectic rocks – orthogneisses, migmatites, and felsic granulites with record of UHP conditions in from of diamond and coesite. Locally is preserved subhorizontal S1 fabric in orthogneisses, as monomineralic banding of alternating Qtz, Ksp, Plg and Bt+Ms+Grt-rich bands. In major part of the complex, S1 foliation is transposed into sub-vertical E-W trending S2 fabric. Within the S2 fabric occur texturally variable rock types, ranging from orthogneiss mylonite to migmatitic orthogneiss together with felsic Ky-bearing granulites. Migmatitic orthogneisses show variable degree of anatexis and continuous transitions from metatexite to diatexite and granite, contemporaneous with the D2 deformation. The mineral assemblage of the banded orthogneiss with S1 fabric is Ksp, Plg, Qtz, Grt, Bt and Ms. The migmatites within the S2 fabric contain higher amount of Ms (up to 15%) and lack Bt in the peak mineral assemblage. Granulites are composed of a “dry” mineral assemblage of Ksp-Plg-Qtz-Grt-Ky. Mineral chemistry shows that the S1 to S2 transformation is accompanied with progressive changes in Ms and Grt compositions. Ms is enriched in Si (from 3.15 to 3.4 Si a.p.f.u.). Grt shows first increase in X_{Fe} from 0.84 in S1 banded orthogneiss to 0.95 in S2 mylonitic orthogneiss, while it generally decreases in the migmatitic rocks (X_{Fe} = 0.85) and the lowest values (X_{Fe} = 0.74) are in the granulite. Results of thermodynamic modeling show that the S2 development is connected with increase of pressure from 10 kbar (S1) to 20 kbar (S2) at temperature of ca. 680°C. Partial melting occurred at HP and probably at higher temperature (> 20 kbar and 750°C). However, the peak pressure is impossible to determine from major element mineral chemistry and was likely significantly higher. This is indicated by garnets present in the S2-related mineral assemblage, which show elevated contents of Na and P (up to 0.05 a.p.f.u.). Substitutions involving Na and P in garnet were described from UHP terrains and are generally interpreted as reflecting very HP conditions. Based on these observations, we suggest that all the texturally variable lithologies in the S2 fabric developed during the same process and in similar P-T conditions and they reflect various degree of hydration and anatexis during the HP metamorphism rather than different P-T conditions. We conclude that the ECC represents a granitic complex subducted into very HP conditions, where it was variably reworked and metamorphosed. The metamorphism was connected with localized hydration and subsequent melting, resulting in heterogeneous modification of the protolith and break-down of the banded texture. Absence of a significant overprint of the observed assemblages in HT – mid-crustal conditions supports the assumed high exhumation rate (1.1-2.5 mm/year) of the complex.

INVESTIGATING MAGMATIC AND TECTONIC PROCESSES FROM 5 TO 30 KM DEPTH IN A THICK CONTINENTAL ARC, ~ 90 Ma MAGMATISM IN THE CASCADES, WASHINGTON, USA

Ratschbacher B.C.*[1], Paterson S.R.[1] & Anderson L.[2]
[1] Department of Earth Sciences, University of Southern California, Los Angeles, CA, USA
[2] Department of Earth Sciences, Boston University, Boston, MA, USA
Corresponding email: barbara.ratschbacher@usc.edu

Keywords: magmatic arc, continental crust formation

The rarity of temporally related continental arc sections exposing deep and shallow parts of the crust make it difficult to test models about the chemical and physical differentiation mechanisms, which operate in the crustal column. The ~ 90 Ma magmatic flare-up event of the Cascades arc exposes a magma plumbing system from ~ 5 to 30 km depth. We focus on temporally related, intrusive complexes, emplaced at shallow to deep mid-crust depths during regional shortening in an exceptionally thick crust (~ 70 km at 90 Ma): the Black Peak intrusion (1-3 kbar; 6400 km^2 exposed area), the Mt. Stuart intrusion (3.5-4 kbar; 5513 km^2 exposed area) and the Tenpeak intrusion (7-10 kbar; 1880 km^2 exposed area). All intrusions are characterized by metaluminous, calc-alkaline compositions. Rare peraluminous compositions at the contact with pelitic rocks are explained by local assimilation. The Tenpeak intrusion is characterized by an incomplete mafic rim facies contemporaneous to its dominant dioritic to tonalitic rocks. Early and late mafic rocks occur in the Mt. Stuart intrusion but tonalitic to granodioritic rocks are dominant. The Black Peak intrusion has an early mafic phase but the main body is dominated by granodiorites. Isotope data show a changing signature from fairly primitive, but more evolved to less evolved with time (0 to +5 εNd_t and 0.705 to 0.7034 Sr_i from ~96 to 87 Ma) independent of emplacement depths. U-Pb geochronology (Matzel et al., 2006; Shea, 2014) shows an incremental construction of each pluton over ~ 3 to 6 million years: nevertheless, high magma addition events, with durations of ~ 200-300 kyr, formed mappable units in each intrusive complex that represent the growth of active magma chambers (1000-6000 km^3) in which in-situ fractionation is supported by isotopic similarity over a wide compositional spectrum (3.2-4.2 εNd over ~46 to 68 wt.% SiO_2). These units record differences in *in-situ* differentiation with depth: amphibole is an early phase in each intrusion and is likely responsile for an increase in the steepness of REE patterns with increasing SiO_2. Abundant titanite and later magmatic epidote in the Tenpeak and pyroxene in the more mafic rocks of the Mt. Stuart accompany it. K-feldspar is only present in the Black Peak intrusion, while biotite is a common late phase independent of depth. An increase in a negative Eu anomaly and decrease in Sr with increase in SiO_2 in the Mt. Stuart and Black Peak intrusions imply plagioclase fractionation. In the Tenpeak these signatures are absent or reversed suggesting plagioclase accumulation.

Preliminary conclusions are: decrease of intrusion size, change in crystallizing phases and accompanied trends in whole rock data with depth. Isotopic data do not change systematically with depth but do with time. Work in progress includes linking mineral chemistry to whole rock data and isotopes, investigating the cause of magma stalling depths and evaluating the interplay between arc tectonism and magmatism.

Matzel, J.E., Bowring, S.A., Miller, R.B. (2006): Time scales of pluton construction at differing crustal levels: Examples from the Mount Stuart and Tenpeak intrusions, North Cascades, Washington. *Geol. Soc. Am. Bull.*, **118**, 1412-1430.

Shea, E.K. (2014): Arc magmatism at different crustal levels, North Cascades, WA. PhD thesis, Massachusetts Institute of Technology, 555 p.

COUPLED THERMO-CHEMICAL PHENOMENA AND GENESIS OF COR FROM LOW-K PSAMMOPELITES DURING SYN-D2 HT-LP HIGH GRADE VARISCAN METAMORPHISM AND HIDROUS MELTING (OSOR COMPLEX, CCR, NE IBERIA)

Reche J.*[1], Martínez F.J.[1] & Traveria M.[1]
[1] Departament de Geologia, Universitat Autònoma de Barcelona, Spain
Corresponding email: joan.reche@uab.cat

Keywords: evolving bulk composition, melting, cordierite-orthoamphibole rocks

The HT-LP Osor Variscan high-grade complex is located in Guilleries massif, N. Catalan Coastal Ranges (CCR, NE of Barcelona). Prograde, HT-LP processes and synchronous D2 compression followed by syn-D-3 extension took place ca. 320-300 Ma (Martínez et. al., 2008). Pelites and psammopelites show evidence of coupling between various thermal, mechanic and chemical phenomena as: ductile deformation, high-T fluid flow, hydrous melting, melt loss/gain and bulk compositional evolution in melts and mesosome domains. All these phenomena toke place during a near isobaric heating-cooling episode followed by a cooling-decompressional stage. High grade rocks and a preliminary model of the large-scale processes involved are described in Reche & Martínez (2002). Focusing on small, m.m. to m. scales, allows a detailed depiction of an evolving sequence of coupling with at least three stages: a) an isobaric (ca. 6 kbar), syn-D2, heating (650-750ºC) with: high-T fluid flow, local hydrous melting of g-bi-sil quartz rich psammopelites (QSP), production of trondhjemitic (T) to granodioritic (Gd) melts and growth of peritectic g and cd. In relation to the melt loss and segregation processes, local Ca/K depleted bulk domains developed in nearby mesosomes giving rise to Fe-Mg amphibole assemblages with: g-bi-sil-cum-oam (ged)-cd and also g-cum-oam-cd (namely cordierite-orthoamphibole or COR rocks). b) In QSP, some q-pl-sill±bi±g±cd±ksp T to Gd leucosomes (Reche et. al., 2015), with extreme sil-rich, mica-absent foliations may represent a compositional evolution trend on the early melts during isobaric cooling (750-650ºC) with still persistent D2 shearing and K-leaching due to fluid flow with an increasingly acidic/magmatic signature. c) The injection and crystallization of abundant late-D2 to inter-kinematic D2-3 leucogranites induced a widespread alkali-metasomatism with extensive blastesis of syn to late D3 mu-pl, probably related with the extensional gravitational instability due to a major change in rheology favoring uplift, exhumation and decompression in the Osor high-grade core of CCR.

Martínez, F.J., Reche, J., Iriondo, A. (2008): U-Pb Shrimp-RG zircon ages of Variscan igneous rocks from the Guilleries massif (NE Iberia pre-Mesozoic basement). Geological implications. *C.R. Geosci.*, **340**, 223-232.

Reche, J. & Martínez, F.J. (2002): Evolution of bulk composition, mineralogy, strain style and fluid flow during HT-LP metamorphic event: sillimanite zone of the Catalan Coastal Ranges Variscan basement, NE Iberia.*Tectonophys*., **348**, 111-134.

Reche, J., Martínez, F.J., Leoz, G. (2015): Prograde PT path, prograde fluid flow, metasomatism and hydrous melting in the Osor high-grade HT-LP complex (CCR, NE Iberia). *Geophys. Res. Abstr.*, **17**, EGU2015-9836.

SLIDING OF THERMALLY WEAKENED PLUTON OVERBURDEN AT CAMPIGLIA MARITTIMA (TUSCANY)

Rocchi S.*[1], Vezzoni S.[1] & Dini A.[2]
[1] Dipartimento di Scienze della Terra, Università di Pisa, Italy
[2] Istituto di Geoscienze e Georisorse, Consiglio Nazionale delle Ricerche, Pisa, Italy
Corresponding email: sergio.rocchi@unipi.it

Keywords: regional extension, pluton emplacement, gravity sliding

Extensional tectonics generates regional-scale structures that often hinders local variations in the overall extensional regime that, if appropriately described and interpreted, could shed light on second-order processes leading to generation of anomalous structures, mass displacement, rock fracturing, and hydrothermal mineralizations.

In the Campiglia Marittima area (Tuscany), a detailed mapping and in abandoned mining tunnels led to the reconstruction of a local deformation history that overlaps with regional extension. This local deformation was triggered at about Miocene-Pliocene boundary by the intrusion of a monzogranitic pluton at the bottom of a thick a carbonatic sedimentary sequence. The emplacement of the pluton gave rise to a perturbation in the local rheological behavior of the carbonate host-rocks leading to the transition from a brittle to ductile regime. The carbonate rocks were thermally weakened and did flow laterally, accumulating downslope of the pluton contact towards the east. As the thermal anomaly was decaying, the brittle-ductile boundary was approaching the pluton, and the ongoing brittle deformation led to the generation of large tension gash-shaped volumes of fractured marble. These fractured volumes were exploited by rising fluids generating the sigmoidal skarn bodies and related Zn-Pb ore shoots. Further decaying of the local, magma-induced deformation is marked by emplacement of small volumes of mafic magma, Fe-Cu ore and felsic dykes. These processes occurred in a corridor bounded by SW-NE fault arrays, that can be defined as transfer zone accommodating different extension rates, generated by concurrence of regional extension and local displacement of the pluton cover.

The Campiglia Marittima case study is a prime example of structural interference among high-angle lithospheric-scale transfer zones, regional shallow crustal extensional structures and local, and low-angle displacement triggered in a transient ductile rheological regime at the top of an intrusive body.

MODELLING THE THERMO-RHEOLOGICAL EVOLUTION OF A GRANITE INTRUSION AND WALL ROCKS: IMPLICATIONS FOR THE LARDERELLO GEOTHERMAL AREA

Rochira F.*[1], Caggianelli A.[1] & de Lorenzo S.[1]
[1] Dipartimento di Scienze della Terra e Geoambientali, Università di Bari, Italy
Corresponding email: f.rochira@studenti.uniba.it

Keywords: thermo-rheological model, magma cooling, brittle-ductile transition

The thermo-rheological evolution of a cooling granitic body and surrounding rocks is presented here. Results of the model can be relevant for the Larderello geothermal area (southern Tuscany, Italy) that since the Early-Middle Miocene has been affected by widespread magmatism and elevated heat flow in a regime of extensional tectonics. The background "long wavelength" heat flow anomaly, mainly due to conductive heat transfer, is in the order of 150-200 mWm^{-2}, far higher than the average value for a continental area (50-60 mWm^{-2}). Another interesting feature of this area regards the so-called "K-horizon", a prominent seismic reflector, regionally located at depths of 8-10 km, and showing an evident culmination in the geothermal areas. The interpretation of this reflector is still controversial. For some authors, it may represent the brittle-ductile transition (Liotta & Ranalli, 1999), for others the roof of a pluton (Bertini et al., 2006). This work aims to provide a contribution to the interpretation of the K-horizon through a thermo-rheological model.

In order to reproduce the observed thermal anomaly, we have set up a model implementing a 2D finite difference code. We have developed a mathematical formulation to model a lenticular symmetrical shape of the pluton, in agreement with the geological cross sections of Bertini et al. (2006) and with mechanisms of pluton accretion (Cruden, 1998). This allows the imposition of the heat flux continuity at the interface between the magma body and the host rock, inside the finite difference scheme. In order to calibrate the size and depth of emplacement of the pluton, we have used a trial and error approach to fit the observed long wavelength heat flow anomaly. Our model estimates of the surface heat flow approach observed values after 200-300 kyr from the emplacement of the magmatic body, having a thickness of ca. 5 km, width in the order of 20 km, and depth of the pluton roof ranging from 3 km (top) to 6 km (lateral vertices).

We set up the rheological model following principles and method described by Ranalli (1995). The temperature field obtained from the thermal model allowed the calculation of the ductile strength of the granite and wall rocks. Brittle strength has been estimated assuming an extensional tectonic regime and a pore fluid factor increasing from the surface to the roof of the pluton. Values of brittle and ductile strength have been used to produce 2D strength profiles of the upper crust with the boundary between the brittle and ductile domains. The cross-sections at different times show the migration of the brittle-ductile transition during magma cooling and an acceptable correspondence with the K-horizon profile after 300 kyr from magma emplacement. It transpires that the interpretation of the K-horizon as the brittle-ductile transition may be compatible with model results.

Bertini, G., Casini, M., Gianelli, G., Pandeli, E. (2006): Geological structure of a long-living geothermal system, Larderello, Italy. *Terra Nova*, **18**, 163-169.

Cruden, A.R. (1998): On the emplacement of tabular granites. *J. Geol. Soc.*, **155**, 853-862.

Liotta, D. & Ranalli, G. (1999): Correlation between seismic reflectivity and rheology in extended lithosphere: southern Tuscany, inner Northern Apennines, Italy. *Tectonophys.*, **315**, 109-122.

Ranalli, G. (1995): Rheology of the Earth. Chapman & Hall, London, 413 p.

DETERMINATION OF MELT FRACTION IN CRYSTAL MUSHES AND TRACE ELEMENT DISTRIBUTION IN HIGHLY CRYSTALLINE DACITIC MAGMAS: EXPERIMENTAL APPROACH USING MELT TRAPS AND LA-ICP-MS ANALYSIS

Schimetzek K.*[1], Parat F.[2], Stechern A.[1] & Holtz F.[1]
[1] Institut für Mineralogie, Leibniz Universität Hannover, Germany
[2] Géosciences Montpellier, Université de Montpellier, France
Corresponding email: kristina.schimetzek@gmx.de

Keywords: crystal mush, crystal/melt ratio, trace element enrichment

In order to understand the evolution of crystal content of silicic magmas during cooling accurate experimental data are needed. A problem in constraining experimentally the crystallization path of magmas lies in the analytics as it is difficult to analyze phases, especially melt, in samples with high crystal content (> 40-50 vol%). In particular melt pools large enough for Laser Ablation or defocused beam microprobe analysis are scarce and crystals are small. Thus, our knowledge on the crystallization history of magmas with high crystal contents is very poor. An important parameter which needs to be determined is the evolution of crystal/melt ratio as a function of temperature at conditions close to the solidus in felsic systems. Mass balance calculations have usually large errors due to the small size of phases which cannot be analyzed accurately. Image analysis of experimental run products is difficult due to the small density differences between phases (e.g., feldspars and melt). In this study we tested a new technique based on mass balance calculation of the concentration of incompatible trace elements after analysis of melt pools that were segregated from the crystal mush. In order to create melt pools that can be easily analyzed by LA-ICP-MS, a trap composed of quartz grains was used to filter the melt from the crystal mush.

The starting material for the experiments was a synthetic dacitic glass powder which was doped with 100 ppm of each of the following elements: U, Ce, Cs, Y, Yb, Nb, P and Zr. A two-step experimental approach was used. The first step was a crystallization experiment in order to produce a highly crystalline sample in which the residual melt was at equilibrium with the solid phases (run duration 20 days). This product placed together with the quartz trap in a capsule for a second step experiment (run duration 3-48 hours). Both steps were conducted at the same P-T conditions in cold-seal pressure vessels (CSPVs). Results from experiments obtained at water-saturated conditions at 200 MPa and in the temperature range 750-675°C are presented.

The phase assemblage of experimental run products is melt, plagioclase, Fe-oxides, amphiboles and/or biotite. Crystal-free melt pools were observed in quartz cavities in run products having initially more than ~ 20 vol% crystals. LA-ICP-MS analysis show in 750°C run product an increase in U from initial 81 (±5) ppm to 114 (±9) ppm, in Nb from initial 107 (±2) ppm to 131 (±16) ppm and in Cs from initial 89 (±3) ppm to 122 (±21) ppm. Amounts of Y, Zr, Ce and Yb at 750°C decrease in the melt due incooperation into amphiboles. Mass balance calculations with initial and enriched values for U, Nb and Cs in combination indicate that the crystal fraction at 750°C is 18-28 vol%. Evaluation of results for experiments at lower temperatures is in progress.

MULTISTAGE MAGMA MIXING AND THE ROLE OF WATER FLUXED MELTING IN AN ANATECTIC TERRANE – KANGAROO ISLAND, SOUTH AUSTRALIA

Schwindinger M.*[1] & Weinberg R.F.[1]
[1] School of Earth, Atmosphere and Environment, Monash University, Clayton, Australia
Corresponding email: martin.schwindinger@monash.edu

Keywords: magma-mixing, water-fluxed melting

Hybridization, such as magma mingling or mixing, is one of the key processes controlling the evolution of granitoid magmas and can happen on a variety of scales and locations. Even though their impact on compositional variety of granites is debated (Clemens & Stevens, 2012), the literature has focused on the interaction between mafic and felsic magmas, with only little research on the interaction between different felsic magmas (e.g. Reichardt et al., 2010).

Here, we report features produced in the ~500 Ma Delamerian Orogeny from the south coast of Kangaroo Island (Foden et al., 2002; Weinberg et al., 2013). This coast exposes turbidites of the Kanmantoo group that have undergone extensive anatexis. We show evidence for hybridization between intrusive granite sheets and *in source* magmas in turbidite migmatites. Muscovite-breakdown assisted by water-fluxed melting of the turbidites resulted in a fine-grained, grey granitic magma, which forms a schollen-rich diatexite. The intrusive granites are more leucocratic, have coarser grain sizes, few or no schollen and schlieren, and are rich in megacrystic K-feldspar. The protolith for both magma is likely to be the Kanmantoo Group (Foden et al., 2002), where the intrusive megacrystic magma is derived from deeper sources. Structures suggest that the megacrystic granite intruded into the diatexite during anatexis, and both were sheared together as magmas. The combination between multiple intrusion events and shearing created opportunities for hybridization, explaining the extreme variability of magmatic rocks types exposed.

We propose that the intrusive magmas were critical for the evolution of the Kangaroo Island migmatites resulting in positive feedback mechanism. Early melting of the migmatites formed a low viscosity trap, impeding the passage of external, intrusive magmas. Thermal and chemical equilibration of water-rich intrusive magmas with their surrounding raised heat and water content and triggered *in-situ* water-fluxed melting, while mixing with locally produced anatectic melts. Further melting made the trap more efficient, reinforcing the process. This process can be extrapolated to other anatectic regions, with magma batches derived from melting of different crustal sources, and resulting from different melting reactions or even to cases where evolved juvenile magmas are involved.

Instead of the classical magma mixing between felsic and mafic magmas, effective magma mixing might be a result of multiple hybridization stages which becomes increasingly more efficient as the magmas involved become increasingly similar as the system evolves. In summary, the outcrops on Kangaroo Island record an analogue to a MASH zone such as envisaged by Hildreth & Moorbath (1988) with the difference that melting, assimilation, storage, and homogenization involves only continental crustal magmas in the middle crust.

Clemens, J.D. & Stevens, G. (2012): What controls chemical variation in granitic magmas? *Lithos*, **134-135**, 317-329.

Foden, J., Elburg, M.A., Turner, S.P., Sandiford, M., O'Callaghan, J., Mitchell, S. (2002): Granite production in the Delamerian Orogen, South Australia. *J. Geol. Soc.*, **159**, 557-575.

Hildreth, W. & Moorbath, S (1988): Crustal contributions to arc magmatism in the Andes of Central Chile: *Contrib. Mineral. Petrol.*, **98**, 455-489.

Reichardt, H., Weinberg, R.F., Andersson, U.B., Fanning, C.M. (2010): Hybridization of granitic magmas in the source: The origin of the Karakoram Batholith, Ladakh, NW India. *Lithos*, **116**, 249-272.

Weinberg, R.F., Hasalová, P., Ward, L.K., Fanning, C.M. (2013): Interaction between deformation and magma extraction in migmatites: Examples from Kangaroo Island, South Australia. *Geol. Soc. Am. Bull.*, **125**, 1282-1300.

HYBRID GRANITIC MAGMA ORIGINATED AT THE ADVANCING FRONT OF BASALTIC UNDERPLATING: INFERENCES FROM THE SESIA MAGMATIC SYSTEM (WESTERN ALPS)

Sinigoi S.*[1], Quick J.E.[2], Demarchi G.[1], Klötzli U.S.[3] & Tavazzani L.[1-2]
[1] Dipartimento di Matematica e Geoscienze, Università di Trieste, Italy
[2] Southern Methodist University, Dallas, TX, USA
[3] Department für Lithosphärenforschung, Universität Wien, Austria
Corresponding email: sinigois@units.it

Keywords: granite, underplating, Ivrea-Verbano

Most rhyolitic and granitic rocks of the large Permo-Carboniferous province of Europe show a restricted range in isotopic compositions, intermediate between mantle and crustal values. We propose an explanation to the relative homogeneity of these hybrid granitic magmas based on geochemistry and field observations of the Sesia Magmatic System, which includes a deep crustal gabbroic complex, upper crustal granite plutons and a volcanic field dominated by rhyolitic caldera fill tuff (Quick et al., 2009). Isotopic compositions of the deep crustal gabbro overlap those of coeval andesitic basalts, whereas coeval granites define a distinct, more radiogenic cluster ($Sr_i \approx 0.708$ and 0.710, respectively). AFC computations starting from the best mafic candidate for a starting melt show that isotopic compositions and trace elements of andesitic basalts may be modelled by assimilation of about 30% of partially depleted crust and about 15-29% fractionation. Trace elements of the deep crustal gabbro cumulates require a further ≈ 60% fractionation of the andesitic basalt and loss of about 40% of silica-rich residual melt (Sinigoi et al., 2016). The composition of the granite pluton is consistent with a mixture of almost equal parts of residual melt delivered from the gabbro and the anatectic melt. Chemical and field evidence lead to infer a conceptual model which links the production of the two granitic components to the evolution of the gabbroic complex. During the growth of the gabbroic complex, progressive incorporation of packages of crustal rocks resulted in a roughly steady-state rate of assimilation. Upwards segregation of anatectic melts delivered from the hot zone above the advancing mafic intrusion facilitates reactive bulk assimilation of the restite by density-driven stoping. At each cycle of mafic intrusion and incorporation of roof layers, residual and anatectic melts are produced in more or less constant proportions, because the amount of anatectic melt produced at the provisional roof is a function of volume and latent heat of crystallization of the intruded mafic melt which in turn produces proportional amounts of hybrid gabbro cumulates and residual melt. Such a process can explain the restricted range in isotopic compositions of most rhyolitic and granitic rocks of the Permo-Carboniferous province of Europe and elsewhere.

Quick, J.E., Sinigoi, S., Peressini, G., Demarchi, G., Wooden, J.L., Sbisà, A. (2009): Magmatic plumbing of a large Permian caldera exposed to a depth of 25 km. *Geology*, **37**, 603-606.

Sinigoi, S., Quick, J.E., Demarchi, G., Klotzli, U. (2016): Production of hybrid granitic magma at the advancing front of basaltic underplating: inferences from the Sesia Magmatic System (south-western Alps, Italy). *Lithos*, **252-253**, 109-122.

EMPLACEMENT AND REJUVENATION OF A GRANITIC BATHOLITH: THE VALLE MOSSO PLUTON (SESIA MAGMATIC SYSTEM)

Tavazzani L.*[1-2], Peres S.[3], Sinigoi S.[1], Demarchi G.[1], Quick J.E.[2] & Klötzli U.S.[4]
[1] Dipartimento di Matematica e Geoscienze, Università di Trieste, Italy
[2] Office of Research and Graduate Studies, Southern Methodist University, Dallas, TX, USA
[3] Dipartimento di Scienze della Terra, Università di Pisa, Italy
[4] Department für Lithosphärenforschung, Universität Wien, Austria
Corresponding email: lorenzo.tavazzani@gmail.com

Keywords: granitic plutons, melt reservoir, rejuvenation

The Lower Permian Valle Mosso pluton (VMP) is a granitic body intruded at upper crustal levels in the rocks of the pre-Alpine basement of the Ivrea-Verbano and Serie dei Laghi units, respectively. The VMP has been recognized as an integral part of a magmatic system termed Sesia magmatic System (Quick et al., 2009), which during the Lower Permian developed through the continental crust up to the surface and caused explosive rhyolitic volcanism that eventually led to the formation of a > 15 km diameter rhyolitic caldera. Fieldwork helped in constraining the VMP internal geometry, with the distinction of several laccolith-shaped intrusive units noticeable for their modal abundances and textural features. Equigranular coarse-grained granite constitutes the bulk of the intrusion, together with subordinate volumes of porphyric granite and numerous small fine-grained two-micas intrusive bodies. A small body (roughly 0.5 by 1 km) of porphyry occurs within the porphyric granite and presents irregular to gradational contacts to its host rock. Major and trace-element and isotopic composition of this porphyry is equal to that of the surrounding granite. However, porphyry matrix and phenocrysts present microtextural features that indicate resorption and undercooling. These features (sieve textures of plagioclase, quartz and biotite resorption) paired with indications from Ti-in-Qz geothermometer on porphyry samples (Wark & Watson, 2006) are descriptive of temperature fluctuations within a crystal mush. Field evidence indicate that the Valle Mosso pluton experienced numerous episodes of mafic melt injections during different stages of its incremental growth. These mafic melts produced significant effects on the thermal budget of the granitic intrusion, rejuvenating and possibly mobilizing batches of the VMP. Based on similar whole-rock composition and reabsorption texture observed in coeval granite porphyry and volcanic products of the Sesia Caldera, a possible link between rejuvenated granitic melts and eruptive products has been postulated. The VMP may provide an insight into the storage and remobilization process that drive the eruption of large amount of melts in caldera-forming volcanic systems.

Quick, J.E., Sinigoi, S., Peressini, G., Demarchi, G., Wooden, J.L., Sbisà, A. (2009): Magmatic plumbing of a large Permian caldera exposed to a depth of 25 km. *Geology*, **37**, 603-606.

Wark, D.A. & Watson, E.B. (2006): TitaniQ: a titanium-in-quartz geothermometer. *Contrib. Mineral. Petrol.*, **152**, 743.754.

STRAIN PARTITIONING, UHT METAMORPHISM, PARTIAL MELTING AND S-TYPE PLUTONISM IN THE DEEP OROGENIC CRUST: THE CASE OF THE KHONDALITE BELT, NORTH CHINA CRATON

Trap P.*[1], Lobjoie C.[1], Wei L.[2], Goncalves P.[1], Marquer D.[1] & Bruguier O.[3]
[1] Laboratoire Chrono-Environnement, Université de Bourgogne-Franche-Comté, Besançon, France
[2] State Key Laboratory of Lithosphere Evolution, Institute of Geology and Geophysics, Chinese Academy of Sciences, Beijing, China
[3] Géosciences Montpellier, Université de Montpellier II, France
Corresponding email: pierre.trap@univ-fcomte.fr

Keywords: UHT metamorphism, crust-mantle interaction, crustal flow

This study reports a detail petro-structural analysis of the Ultra-High Temperature Khondalite Belt (UHTK) and the adjacent High Pressure Granulite (HPG) Belt, in the North China Craton. The UHT Khondalite Belt is constituted of garnet-spinel ± sapphirine-bearing migmatites, garnet-bearing granites and marbles, widely intruded by various scale gabbronoritic bodies. Our petrological study and P-T quantifications performed on migmatites and granulite relics, together with P-T data from literature, indicate that crustal anatexis and UHT metamorphism affected a large part of the orogenic crust, from 15 to 40 km deep. The HPG Belt is mostly composed of high-pressure (~ 15 kbar) mafic granulites hosted in migmatitic gneisses. The geochronological dataset argues for intense partial melting and S-type magmatism over a 100 Ma lasting period, from 1.95 Ga to 1.85 Ga with UHT metamorphism occurring at around 1.92 and 1.88 Ga. The UHTK and HPG Belts represent great parts of hot and partially molten orogenic crust that recorded strong crust-mantle interactions, changes in crustal and mantle-derived melt production and large mass and heat transfers though time and space. In order to understand the structural pattern and highlight how deformation partitioned within this hot crust, we document a set of structural analyses acquired over the UHTK Belt, from the western Wulashan massif to the eastern Jining complex, and the adjacent HPG Belt, in the Huai'an complex. The partially molten rocks recorded two main deformation events, named D1 and D2. The early D1 deformation is underlined by a S1 foliation that is flat-lying or dips weakly toward the South-East. S1 holds a N70E L1 stretching mineral lineation that is sub-horizontal or plunges toward the East. The D1 foliation is reworked by a dextral transpressional D2 deformation responsible for the development of a km-scale system of S2-C2-C'2 shearing structures. The N30E trending S2 foliation is sub-vertical to highly dipping toward the East. Kilometer-scale C2 and C'2 shear zones are sub-vertical and trend N70E and N90-100E, respectively. During ongoing compression of the thickened orogenic root, partial-melting is responsible for a strength drop that enhanced an eastward lateral flow of the deep crust. Structural and petrological observations suggest that the D2 S-C-C' bulk shearing system forms an interconnected network of kilometer scale shear zones that act as pathways for the upward mass-transfer of mafic magmas from the mantle to the upper crust. Interpretation of our results is not in accordance with current models in which the UHTK Belt represents a mobile belt formed in response to collision and exhumation between the Yinshan and Ordos blocks. We rather propose that the UHTK Belt is a continental magmatic arc related to westward subduction between 1.95 and 1.89 Ga and then, involved in the Trans-North China Orogeny due to collision between of the Western and Eastern blocks between 1.89 and 1.83 Ga.

THE ORIGIN OF HIMALAYAN LEUCOGRANITES AND HOW THEY INTERACTED WITH THE OROGEN

Weinberg R.F.*[1]
[1] School of Earth, Atmosphere and Environment, Monash University, Clayton, Australia
Corresponding email: Roberto.Weinberg@monash.edu

Keywords: leucogranites, melting reactions, self-organization

Himalayan leucogranites and migmatites generally share a number of features along the length of the mountain range, such as similar timing and duration of magmatism, common source rocks and clockwise P-T paths. Despite commonalities, most publications emphasize deviations from this general pattern, indicating a fine-tuned local response to the dominant evolution. For example, there are significant differences in P-T-X_{H2O}conditions during anatexis, with melting reactions varying from water-fluxed to biotite-dehydration, instead of being dominated by Ms-dehydration melting, as is commonly suggested.

Zircon and monazite U-Th/Pb ages of anatectic rocks (both migmatites and leucogranites) range between ~ 25 and 15 Ma. Typically, a single sample may have age ranges covering most of this 10 m.yr. period, suggesting recycling of accessory phases from metamorphic rocks and antecrysts. Recent studies linking monazite and zircon ages with their composition have determined the timing of prograde melting and retrograde path, thus constraining the anatectic cycle. In some areas, this cycle youngs systematically down section, towards the leading front of the Himalayas, whereas the opposite is true in other areas**.**

The relative timing of crustal melting and decompression also changes across the belt, leading to a debate about the impact of melting on the evolution of the Himalayas. Melting has been used to explain subsequent decompression, or conversely, decompression has been used to explain subsequent melting. Weakening of the crust due to melting has been used to support channel flow models for extrusion of the Greater Himalayan Sequence, or alternatively, to suggest it triggered a change in its critical taper. Variable relative timing and variable P-T-t paths suggest anatexis resulted from the thermal maturation of the orogeny, and that decompression was controlled by regional, orogen-wide factors, not local geology.

The relationship between granites and movement in the South Tibetan Detachment (STD) is useful in this regard, and reveals that fault motion took place at different times and over different durations, requiring complex internal strain distribution along the Himalayas. Despite differences in rheology at any point in time and sc, and differences in strain, the Himalayan front forms a well-defined arc. Local geology and anatexis probably had only a second-order, local effect in modulating strain distribution, with little effect on the general arc shape of the orogen. This suggests that strain distribution overwhelmed local differences in rheology (e.g., presence or absence of melt) so as to maintain an orogen-wide arc shape. The orogen was most likely evolved as a result of self-organized forward motion of the arc, controlled by the imposed convergence history and energy conservation, balancing accumulation of potential energy and dissipation, and independent of the presence or absence of melt.

PARTIAL MELTING IN ARCHAEAN HIGH-GRADE GNEISS TERRAINS

White R.W.*[1] & Palin R.M.[1]
[1] Institut für Geowissenschaften, Johannes Gutenberg-Universität Mainz, Germany
Corresponding email: rwhite@uni-mainz.de

Keywords: grey gneiss, granulite, amphibolite

Many Archaean terrains are dominantly composed of a range of metabasic to metatonalitic gneisses that have been metamorphosed to amphibolite- to granulite-facies conditions. These terrains include the “grey gneisses” which represent a range of intermediate to felsic rocks dominated by plagioclase and quartz with varying amounts of hornblende, biotite, orthopyroxene and clinopyroxene. Most of these rocks plot in the tonalite, trondhjemite or granodiorite field on a normative an-ab-or triangular plot, but such plots commonly obscure the primary compositional variation present which relates to the silica content and overall maficity which strongly influence the metamorphic assemblages and melt production during high-grade metamorphism.

Phase equilibria calculations on compositions ranging from basaltic to tonalitic show a wide range of metamorphic assemblages, melt ferility and melt composition. For hydrate breakdown melting, rocks of mafic, dioritic and granodioritic composition are moderately fertile with potentially 10's of percent melt produced across the amphibolite-granulite transition. By contrast, leucocratic tonalitic compositions are less fertile because they contain only a small proportion of hydrous ferromagnesian phases such as hornblende and/or biotite. Extensive melting of such rocks would require an external source for H_2O.

Whereas partial melting of metabasic rocks produces primarily tonalitic melt, the intermediate to felsic rocks produce granitic melt and represent a potential source for Archaean granite. Many high-grade Archaean gneiss terrains (e.g. the Lewisian Complex) show extensive evidence for melt formation, segregation and loss, consistent with these being residual. Geochemical studies of such rocks should take into account the loss of a granitic component from such rocks.

TIN DISTRIBUTION BETWEEN MELT AND RESTITE DURING PARTIAL MELTING OF METASEDIMENTARY ROCKS

Wolf M.*[1], Romer R.L.[1] & Franz L.[2]
[1] Helmholtz Zentrum Potsdam, GFZ Deutsches GeoForschungsZentrum, Potsdam, Germany
[2] Institut für Mineralogie und Petrographie, Universität Basel, Switzerland
Corresponding email: mwolf@gfz-potsdam.de

Keywords:

The distribution of ore elements between melt and restite critically influences the potential of a granitic melt to develop granite-bound mineralization. Distribution of Sn between restite and melt during partial melting is largely controlled by the presence of tin sequestering phases such as biotite, muscovite, titanite and magnetite. The stability of these phases controls whether or not Sn is available for dissolution into the melt. Tin released during breakdown of one Sn-bearing phase does not necessarily accumulate in the melt. Released Sn may be retained in restite rather than partition into the melt if there is a tin sequestering phase like biotite.

Modeling using the Theriak/Domino program (De Capitani & Petrakakis 2010) demonstrates that major controlling factors apart from protolith composition are whole rock (WR) water content, water activity ($a(H_2O)$) and oxygen fugacity (fO_2). WR water content controls the modal abundances of OH-bearing minerals and thus influences the position of the solidus and the volume of melt produced during dehydration melting. In terms of biotite stability, WR water content only plays a subordinate role, becoming only important at very low water contents. Oxygen fugacity - ranging between Fe^{2+} and the hematite-magnetite buffer - influences biotite stability, extending it towards higher temperatures at elevated fO_2 values. A decrease in $a(H_2O)$, on the contrary, not only lowers biotite stability towards lower temperatures, but also shifts the solidus towards higher temperatures.

Even though biotite has higher contents of Sn than muscovite, in muscovite-rich rocks a substantial proportion of bulk Sn is hosted by muscovite. Anhydrous melting of such rocks does not necessarily lead to a Sn-rich melt, as large quantities of the released Sn may be redistributed from the melt into restitic biotite. Biotite has a higher thermal stability than muscovite and acts as a tin sequestering phase. Therefore, temperatures of metamorphism need to reach biotite stability limits in order to generate a tin enriched melt. Those conditions are not met by internal heating alone and additional advective heat input is needed in order to reach biotite stability limits. The melt volume produced during biotite dehydration melting is relatively small, but these melts may be markedly enriched in tin, even before further enrichment during magmatic fractionation starts.

De Capitani, C. & Petrakakis, K. (2010): The computation of equilibrium assemblage diagrams with Theriak/Domino software. *Am. Mineral.*, **95**, 1006-1016.

ROLE OF MELT SEGREGATION STYLE ON GRANITE CHEMISTRY AND MULTIPLE MELTING EVENTS IN THE SIERRA DE QUILMES, NW ARGENTINA

Wolfram L.C.*[1], Weinberg R.F.[1] & Becchio R.[2]
[1] School of Earth, Atmosphere and Environment, Monash University, Clayton, Australia
[2] Consejo Nacional de Investigaciones Científicas y Técnicas, Universidad Nacional de Salta, Argentina
Corresponding email: Roberto.Weinberg@monash.edu

Keywords: melt segregation, migmatites, re-melting

The compositional variability of crustal-derived granites has been attributed to a multitude of processes. We describe the relationship between granulite facies migmatites and granites in the Sierra de Quilmes, focussing on the impact of different styles of melt-residuum segregation on granite compositions.

The N–S trending mountains defining the region contain variably metamorphosed turbidites of the Puncoviscana Formation. Early Ordovician subduction on the western Gondwana margin produced widespread high-T, low-P metamorphism of pelites and greywackes during the ~470 Ma Famatinian Orogeny, resulting in extensive anatexis and granite plutonism. The Tolombón complex of the northern Sierra de Quilmes is a tilted metamorphic sequence, providing near-complete exposure from granulite-facies magma source rocks in the southwest, to granite emplacement levels in amphibolite and greenschist facies rocks in the northeast. Anatexis is associated with the fluid-absent incongruent breakdown of biotite, evidenced by peritectic Grt±Crd±Opx in residual assemblages. In the northeast, the Laguna complex is dominated by metatexites where leucosomes feed metre-sized leucogranite bodies and go on to form larger intrusions. The Ovejeria complex in the southwest is dominated by heterogeneous diatexite migmatites with variable contents of schollen, Bt-schlieren and peritectic minerals. These magmas typically remain close to the source, and vary from highly residual diatexites to cleaner, magmas, indicating partial separation between residual solids and melt during diatexite flow.

Geochemistry of these anatectic rocks shows two contrasting trends, which reflect the Laguna and the Ovejeria segregation styles. The Laguna style, where melts were extracted from a coherent partially molten source, is characterized by fractionated melts complementary to residual rocks. The Ovejeria style, reflecting inefficient melt segregation forming dirty diatexites, typically generates granites with compositions close to that of the source rock, indicating whole rock mobilization during melting, followed by melt separation from solids during diatexite flow. Thus, melt segregation styles give rise to two different magmatic suites.

We are particularly interested in evidence for multiple melting events during this orogeny. Here, anatectic granites are commonly overprinted by patch metatexites, where new peritectic garnets in newly formed leucosomes are interpreted to indicate re-melting. As no subsequent major thermal episode followed the Famatinian orogeny, it is likely that this re-melting occurred during the Famatinian event reflecting thermal fluctuations within a relatively short time (~20 Myr).

GENERATION, SEGREGATION AND FRACTIONATION OF ANATECTIC MELT IN THE CONTINENTAL CRUST: INSIGHTS FROM WEST ANTARCTICA

Yakymchuk C.*[1] & Brown M.[2]
[1] Department of Earth & Environmental Sciences, University of Waterloo, Canada
[2] Department of Geology, University of Maryland, College Park, MD, USA
Corresponding email: cyakymchuk@uwaterloo.ca

Keywords: migmatite, granite, granulite

The generation and segregation of granitic melt in the deep crust, followed by extraction, ascent and emplacement into the shallow crust is an important process by which the continents have become differentiated into a depleted lower portion and a complementary enriched upper portion. In the absence of H_2O-rich fluid infiltration, although partial melting commences at the wet solidus, with increasing temperature it is dominated by hydrate-breakdown reactions that vary according to protolith composition. With increasing melt fraction, melt migrates from the initial sites of melt generation to lower pressure sites where it may accumulate (e.g., deformation bands) prior to extraction via ascent conduits that feed plutons at shallower structural levels. Additional evidence of melt drainage from migmatites and granulites includes chemical depletion of these rocks relative to protolith compositions, where the difference is a granitic component, and the preservation of peritectic minerals and absence of extensive retrogression.

The domal Fosdick migmatite-granite complex and surrounding carapace rocks are composed of garnet-bearing migmatitic paragneisses and orthogneisses in the core with a envelope of lower-grade protliths; contemporaneous anatectic granites occur in both units. Inverse phase equilibria modeling of melt-depleted migmatites indicates that the Fosdick complex recorded peak thermal conditions of 850-880°C at 6.5-8.0 kbar. In the migmatites, Lu-Hf garnet ages record peak metamorphism at 116-111 Ma, whereas U-Pb monazite ages range from 106 Ma to 96 Ma (with a peak at ca. 100 Ma), and are interpreted to reflect cooling and melt crystallization from the thermal peak to an elevated solidus over ca. 15 My.

Forward phase equilibria modeling demonstrates that igneous protoliths could have produced 3-17 vol.% melt whereas metasedimentary protoliths would have generated 8-48 vol.% melt at peak thermal conditions. This is generally less than the 43-67 vol.% leucosome observed in outcrop. Therefore, the Fosdick migmatite complex is interpreted to represent both a zone of melt generation and extraction, and a zone of accumulation from melt passing through. Melt extraction from and migration through the Fosdick complex was accomplished *via* a self-organized transport network controlled by the regional stress field and pre-existing heterogeneities inherited from the protoliths (e.g., relict compositional differences and tectonic foliation). Granites within this network have microstructures and compositions consistent with a cumulate origin, and are interpreted to record fractional crystallization during magma ascent. Melt drained from the Fosdick complex was more evolved than primary melt compositions. Thus, melt extracted from migmatite complexes may not be representative of the *in situ* anatectic melt composition but is more likely to represent a variably fractionated derivative relatively enriched in incompatible elements and heat producing elements.

Session S7:

From deep magmatic processes to volcanic eruption

Conveners:

Riccardo Avanzinelli (Firenze – Italy)

Roman Botcharnikov (Hannover – Germany)

Caroline Martel (Orléans – France)

Maxim Portnyagin (Kiel – Germany)

SEQUENCE OF REPETITIVE EXPLOSIVE AND EFFUSIVE ERUPTION PHASES RECORDED IN LAVAS AND EJECTED BOMBS OF SARAY VOLCANO, NW IRAN

Assbichler D.*[1], Asadpour M.[2], Heuss-Assbichler S.[1] & Kunzmann T.[1]
[1] Department für Geo- und Umweltwissenschaften, Ludwig-Maximilians-Universität München, Germany
[2] Department of Geology, Urmia University, Iran
Corresponding email: d.assbichler@lmu.de

Keywords: explosive volcanism, magma recharge, ultrapotassic rocks

The Saray Volcano is located in NW Iran. With about 360 km^2 it is a comparable small volcano with excellent outcrop conditions. Two different lavas and five different magmatic ejecta were investigated. They were classified as trachytic, ultrapotassic rocks and exhibit the same main mineral assemblage: sanidine, pyroxene and phlogopite. These rocks can be assigned as a “one-feldspar-system” because no plagioclase occurs. A genetic link between trachytic lavas and ejecta of the last eruptive phase is evident due to the stratigraphic position of the lava and ejecta. Glassy groundmass in ejecta indicates a rapid cooling of these samples. Therefore it can be expected that the conditions in the magma chamber at the time of eruption are quenched within these samples.

Sanidine phenocrysts may reach a size up to 4 cm. They display a complex zoning pattern caused mainly by varying Ba concentrations up to 6.57 wt.% BaO. Sanidine is the first mineral phase crystallized from the melt. Consequently any change within the magma chamber is expected to affect directly its chemical composition. Two types of phlogopite were identified: Type I phlogopite is cogenetic with sanidine and pyroxene, and is characterized by low contents of Ti and Ba. Type II phlogopite contain higher Ti and Ba concentrations. They are expected to be formed in greater depths and raised up with the magma from upper mantle.

There are clear indications that the eruption was triggered by magma recharge. The detailed petrological observations and the combination of minerals systematics in the different samples enabled the reconstruction of the chronology of the eruption into three phases. Phase I is indicated by the eruption of sanidine rich ejecta followed by the extrusion of a lava dome. Common feature of these rocks is the same crystallization sequence in sanidine. In contrast the sanidine microlites in the groundmass of lava rock are clearly enriched in Ba, Fe and Ti. The decomposition of pyroxene observed in an ejected rock and its replacement by carbonates is a clear sign for extreme CO_2-rich conditions in the melt. The euhedral and almost intact type II phlogopite crystals indicate a fast rise of the magma. Phase II is marked by a second explosive event. In these ejected bombs the effect of interaction with the recharged magma is evident: increase of Ba, Ti and Fe in the chemistry of sanidine, diopside and type I phlogopite, strong attack of type II phlogopite. Sandine nucleations and abundant bubbles in the glass matrix of the ejecta indicate a degassing of the melt. Phase III is represented by late extrusion of a second trachytic lava. Sanidine phenocrysts of this lava are very small compared to the others. They show features of intense dissolution. Sanidine crystals in the groundmass show an alignment in flow direction. They indicate a much slower cooling of the melt compared to lava dome.

EXPERIMENTAL CONSTRAINTS ON THE ORIGIN OF DACITIC VOLCANISM IN ARC SETTINGS

Botcharnikov R.*[1], Holtz F.[1], Stechern A.[1], Almeev R.R.[1] & Sato H.[2]
[1] Institut für Mineralogie, Leibniz Universität Hannover, Germany
[2] Department of Earth and Planetary Sciences, Kobe University, Japan
Corresponding email: r.botcharnikov@mineralogie.uni-hannover.de

Keywords: dacite, experiment, magma evolution

Dacitic volcanism is a ubiquitous phenomenon typically associated with magmas generated in or related to subduction zone magmatism worldwide. The occurrence of dacitic lavas is explained either by polybaric crystal fractionation of mafic magmas during their ascent in the crust or by efficient mixing between mafic- and silicic magma end members in magmatic plumbing systems. Dacitic rocks often exhibit various signatures of magma differentiation such as phenocrysts+microlites assemblages, strong zonation in mineral phases, occurrence of atypical minerals and mafic enclaves and other signs of disequilibrium and complex processes responsible for the formation of dacitic magmas.

Although phase equilibria experiments provide quantitative constraints on the link between abundance, composition of magmatic phases and P-T-fO_2-fH_2O conditions of magma storage and evolution, attention must be paid when the obtained results are applied to natural magmatic systems. Experimentally determined phase equilibria require adaptation to the conditions of local equilibrium in relatively low-temperature highly-viscous magmas following for instance the concept of “reactive subsystem” after Pichavant et al. (2007). However, the definition, localization and extraction of such a “reactive subsystem” from the available natural observations is challenging and alternative or complementary experimental and interpretation approaches are needed.

Here we present experimental data for magmas from several volcanic centers in Central Andes, Japan and Kamchatka focusing not only on the reconstruction of magma storage conditions for dacites but also on the relationship between magma evolution of different end-members involved in the differentiation processes for a given system. Phase equilibria experiments provide results for liquid lines of descent and liquid-solid compositional evolution for each representative member of magmatic sequence from basaltic to rhyolitic end-members as well as for intermediate magmas. Applied as a basis for the interpretation of natural petrological and geochemical trends of magma compositions, these data clearly indicate that magma mixing and hybridization is a predominant process in dacitic volcanic systems. Magma mixing experiments and investigation of mafic enclaves trapped in dacites demonstrate variable time scales of magma interaction before dacitic eruption. Reconstruction of natural pathways of magmatic evolution implies that dacites can be produced either as a hybridization product with a minor abundance in dynamic open systems or as a monotonous and voluminous mixed magma in long-living magmatic systems. The compositions and volumes of erupted dacites are controlled by the efficiency and frequency of periodic replenishment of large silicic magma chambers by injections of mafic magmas and by the buffering capacity of silicic crystal mushes.

Pichavant, M., Costa, F., Burgisser, A., Scaillet, B., Martel, C., Poussineau, S. (2007): Equilibration scales in silicic to intermediate magmas - Implications for experimental studies. *J. Petrol.*, **48**, 1955-1972.

THE INFLUENCE OF EXPERIMENTAL CONDITIONS ON THE DYNAMICS OF STARTING GAS-PARTICLE JETS

Cigala V.*[1], Kueppers U.[1], Pena Fernandez J.J.[2], Sesterhenn J.[2] & Dingwell D.B.[1]
[1] Department für Geo- und Umweltwissenschaften, Ludwig-Maximilians-Universität München, Germany
[2] Institut für Strömungsmechanik und Technische Akustik, Technische Universität Berlin, Germany
Corresponding email: valeria.cigala@min.uni-muenchen.de

Keywords: explosive eruption, jet dynamics, shock-tube

The first stage of an explosive volcanic eruption commonly shows characteristics of a starting gas-particle jet. The dynamics of this gas-thrust region exert a role in determining the subsequent evolution of the eruptive column and, therefore, important hazard assessment implications for both the near- and far-field. Direct observation of eruptive events is possible but often insufficient for complete characterization due to hazard and/or accessibility issues. Important complementary data can be achieved using repeatable laboratory experiments where the parameters of influence can be controlled and their dynamic evolution measured.

Loose natural (basaltic) particles were ejected from a shock-tube via rapid decompression while controlling a) temperature (25 and 500°C), b) overpressure (15 MPa), c) starting grain size distribution (1-2 mm, 0.5-1 mm and 0.125-0.250 mm), d) gas-particle ratio, and e) shock-tube length and vent geometry (nozzle, cylinder, funnel). The velocity of individual particles and the jet spreading angle as well as their dynamic evolution were quantified through image analysis of high speed videos.

The measured initial velocity is ranging from 130 to 300 $m \cdot s^{-1}$, the max gas spreading angle was found to range between 20 and 40° while the max particle spreading angle ranged between 0 and 30°. Moreover, the temporal evolution of velocity and spreading angle displays a clear non-linear behavior.

These experiments mechanistically mimic the process of pyroclast acceleration and ejection during explosive volcanic eruptions. Such controlled and repeatable experiments are capable of constraining the effect of boundary conditions. Therefore, the results should greatly enhance the ability of numerically model explosive ejecta in nature.

WATER-ENHANCED DIFFUSION OF MAJOR ELEMENTS IN NATURAL MELTS: INSIGHTS FROM DIFFUSION COUPLE EXPERIMENTS

González-García D.*[1], Behrens H.[2], Petrelli M.[1], Vetere F.P.[1], Zezza A.[1], Morgavi D.[1] & Perugini D.[1]
[1] Dipartimento di Fisica e Geologia, Università di Perugia, Italy
[2] Institut für Mineralogie, Leibniz Universität Hannover, Germany
Corresponding email: diego.gonzalez@studenti.unipg.it

Keywords: diffusion, shoshonite, rhyolite

Chemical diffusion is a parameter of key importance to understand a wide variety of processes in magmatic systems, from mineral growth/dissolution to compositional modulation in magma mixing processes. Moreover, magma mixing is recognized as potential trigger of highly explosive volcanic eruptions, and as a time-dependent process, diffusion has the potential to shed light on the timescales involved in such mixing processes before and during an eruption. One of the main parameters controlling the diffusivity of elements in a melt is its dissolved water content, which is known to accelerate diffusion.

Here we use the diffusion couple experimental setup to quantify the influence of water content in the diffusive exchange of major elements between two natural end-members: a shoshonite and a rhyolite from the Vulcano system (Aeolian Islands, Italy). Experiments using two glass cylinders derived from each end-member with the same added water content (nominally dry, 1 wt.% and 2 wt.%, respectively) are run for 4 h in an Internally heated pressure vessel (IHPV) at 1200°C and pressures of 0.5, 1 and 3 kbar, finishing with a rapid-quench. Thin sections of run products are analyzed by FTIR and EPMA by measuring concentration-distance profiles extending 2 mm across the interface.

Experiment products are always crystal-free glasses, and only the lower P experiments show bubble formation. The analysis of water content along the profiles shows a uniform water distribution close to the nominal value. Major element concentration-distance profiles have asymmetric shapes extending deeper into the shoshonite than the rhyolite side of the couple, corresponding to a different diffusivity in each end-member, and analysis of the profiles result in systematically higher diffusivity (0.4 to 0.8 log units) in the mafic end-member for all elements. Al (in shoshonite) and Ti are the slowest diffusing components in both melts, while Mg, Ca and K are the fastest. The dispersion in diffusion coefficient values is also higher in the mafic compositions. H_2O content in the melt has the biggest influence in the diffusivity of major elements: a difference of up to one order of magnitude is observed between nominally dry and 2 wt.% H_2O bearing glasses. In the investigated range, a linear correlation can be established between log(D) and water content. In conclusion, our results indicate that even a small variation in water content in melts can produce a significant increase in diffusivity for all components.

BROTHERS SUBMARINE CALDERA VOLCANO, KERMADEC ARC, NEW ZEALAND: A GEOCHEMICAL AND PETROLOGICAL EVOLUTION

Gubbay-Nemes L.J.*[1], Graham I.T.[1], de Ronde C.E.J.[2] & Timm C.[2]
[1] School of Biological Earth & Environmental Sciences, University of New South Wales, Sydney, Australia
[2] GNS Science, Lower Hutt, New Zealand
Corresponding email: leeora.gn@gmail.com

Keywords: magmatism, petrology, geochemistry

The Kermadec Arc is the most hydrothermally-active segment of an intra-oceanic arc in the world. Hosting at least three volcanogenic massive sulfide (VMS) deposits, it is seen as a critical region for understanding the formation of modern VMS systems (de Ronde et al., 2001, 2007, 2011). The arc comprises a chain of 30 major submarine volcanoes that marks the southernmost section of the Pacific Ring of Fire in the Western Pacific region (de Ronde et al., 2012).

Brothers Submarine Caldera Volcano, situated 1.5 km below sea level, is the most hydrothermally-active volcano along the arc extent and hence hosts the largest accumulation of VMS mineralisation, rich in Cu-Au-Ag (up to 90 ppm Au; de Ronde et al., 2001). Although it is arguably the best-studied submarine arc volcano in the world, there is a great paucity of geochemical and petrological data in the published literature.

In this study, the largest sample set to date has been used for geochemical and petrographic analysis, including an array of samples collected over the past two decades and new samples from sites around the caldera, cones and two intersecting dyke ridges. This has established a solid understanding of magmatic evolution and genesis, and the relationship between the newly-discovered dykes and potential for metal and volatile supply for VMS mineralisation at Brothers volcano.

Brothers lavas are dacitic and typically crystal-poor (< 15%). Matrix glass melts however range from dacitic compositions along the caldera to more evolved rhyolitic compositions at the resurgent cone sites. Two basaltic dykes potentially provide the elevated trace metals (copper, cobalt, and zinc) found in the lavas, as well as the source of volatiles and heat necessary to form the VMS mineralisation at Brothers Volcano. These dykes are also host to the most primitive olivine (up to Mg# 93.3) that have been found along the entire arc extent (1200 km), indicating the presence of a deep seated magma source beneath Brothers Volcano.

In 2018 Brothers Volcano will be drilled (up to 800 m below the surface) in a $30 million International Ocean Discovery Program, which will essentially provide the missing link in the understanding of mineral deposit formation along arcs. This geochemical and petrologic study largely constitutes the foundation for the drilling stage of research.

de Ronde, C.E., Baker, E.T., Massoth, G.J., Lupton, J.E., Wright, I.C., Feely, R.A., Greene, R.R. (2001): Intra-oceanic subduction-related hydrothermal venting, Kermadec volcanic arc, New Zealand. *Earth Planet. Sci. Letters*, **193**, 359-369.

de Ronde, C.E., Baker, E.T., Massoth, G.J., Lupton, J.E., Wright, I.C., Sparks, R.J., Bannister, S.C., Reyners, M.E., Walker, S.L., Greene, R.R., Ishibashi, J., Faure, K., Resing, J.A., Lebon, G.T. (2007): Submarine hydrothermal activity along the mid-Kermadec Arc, New Zealand: Large-scale effects on venting. *Geochem. Geophys. Geosyst.*, **8**, Q07007.

de Ronde, C.E., Massoth, G.J., Butterfield, D.A., Christenson, B.W., Ishibashi, J., Ditchburn, R.G., Graham, I.J. (2011): Submarine hydrothermal activity and gold-rich mineralization at Brothers Volcano, Kermadec Arc, New Zealand. *Mineral. Dep.*, **46**, 541-584.

de Ronde, C.E.J., Butterfield, D.A., Leybourne, M.I. (2012): Metallogenesis and mineralization of intraoceanic arcs I: Kermadec arc - introduction. *Econ. Geol.*, **107**, 1521-1525.

INFLUENCE OF OXYGEN FUGACITY ON THE BEHAVIOUR OF SELENIUM AND TELLURIUM IN A BASALTIC MAGMA

Just T.*[1], Parat F.[2], Botcharnikov R.[1], Stechern A.[1], Holtz F.[1] & Alard O.[2]
[1] Institut für Mineralogie, Leibniz Universität Hannover, Germany
[2] Géosciences Montpellier, Université de Montpellier, France
Corresponding email: t.just@stud.uni-hannover.de

Keywords: selenium & tellurium, partition coefficients, oxygen fugacity

Selenium (Se) and tellurium (Te) belong, like sulfur (S), to the Group VIA elements. They are considered to be volatile, siderophile elements in geochemical nomenclature. Se and Te have not been the target of many studies yet, as they are about three orders of magnitude less abundant than S and, therefore, difficult to analyze. Selenium does not degas from all magmas under redox conditions where sulfur is lost, allowing to make use of it as a proxy for the original S content, as well as redox conditions before degassing by assumed S/Se ratios. Nevertheless, only a few Se and Te concentrations are available for mantle peridotites and only little quantitative information is available for the behavior of those elements in crustal magmatic systems.

This study focuses on the influence of oxygen fugacity on the solubility and partitioning of Se and Te in basaltic magmas as a potential redox proxy. Partition coefficients of Se and Te between sulfide minerals and the silicate melt and/or a sulfide melt (if present) as a function of redox conditions are investigated in experiments using natural Etna basalt. The basaltic system is doped with Se and/or Te oxides ± FeS as pyrrhotite seeds. Experiments have been conducted at a pressure of 4 kbar and T = 1030°C at water-saturated conditions in an internally-heated gas pressure vessel (IHPV) at oxygen conditions corresponding to log f_{O2} = QFM-1 to QFM+3.3 (at x_{H2O} = 1). Temperature cycling was implied to ensure large crystals in the run products. Experimental run products were analyzed with microprobe and LA-ICP-MS for Se, Te and S concentrations.

At oxidizing conditions (~ QFM+3,3), the phase assemblage is composed of glass, magnetite and clinopyroxene. An addition of up to 1 wt.% Se or 1 wt.% Te does not lead to the formation of any selenides or tellurides, and no immiscible melt is observed. In samples where sulfur was added, no clinopyroxene was found. At such oxidizing conditions, pyrrhotite is not a stable phase, favoring the crystallization of magnetite around sites where pyrrhotite seeds were dissolved. Preliminary results will be presented focusing on the saturation of magmas with Se- or Te-rich phases as well as on the partitioning of Se and Te between magmatic phases.

EARLY EXPERIMENTAL RESULTS ON THE MAGMATIC ASSIMILATION OF ANHYDRITIC ROCKS

Mandolini T.*[1], Ridolfi F.[2], Mollo S.[3], Renzulli A.[1] & Perugini D.[4]
[1] Dipartimento di Scienze Pure e Applicate, Università "Carlo Bo", Urbino, Italy
[2] Via Galileo Galilei 11, 61122 Pesaro (PU), Italy
[3] Dipartimento di Scienze della Terra, Sapienza Università di Roma, Italy
[4] Dipartimento di Fisica e Geologia, Università di Perugia, Italy
Corresponding email: tommi.redlespaul@gmail.com

Keywords: experimental petrology, trachybasalt, sulphate-carbonate assimilation

Magmatism in complex orogenic contexts set in relatively narrow space-time intervals are often characterized by elevated geochemical variability. A noteworthy example of this is represented by the Tuscan and Roman magmatic provinces. Both are characterized by a broad range of intermediate-basic igneous products of the high potassium calc-alkaline, shoshonitic, potassic and ultrapotassic series (e.g., Lustrino et al., 2011; Ridolfi et al., 2016).

Recently, various experimental petrology studies have shown that magmatic assimilation of $CaCO_3$ results in the formation of a gaseous CO_2-rich phase and a residual melt enriched in alkalies and undersaturated in silica (nepheline-normative) due to abundant crystallization of calcium-rich clinopyroxene (e.g., Dallai et al., 2004; Freda et al., 2008; Iacono-Marziano et al., 2008; Mollo et al., 2010). Although Triassic evaporites are often found in association with, and interbedded with, carbonates throughout the circum-Mediterranean area (e.g. Anidriti di Burano Formation), no experimental studies on the magmatic assimilation of sulphate-carbonate rocks can be found in literature.

The experiments performed in this work simulate what may hypothetically occur when a trachybasaltic magma interacts with evaporitic rocks of the "Anidriti di Burano" Formation ($CaSO_4$ = 79 wt.%; $CaCO_3$ = 21 wt.%) at 1 atm of CO-CO_2-SO_2 and temperatures of 1100-1200°C during its ascent through the upper crust.

The results indicate that magmatic assimilation controls the degree of crystallization, which increases with the percentage of the assimilated anhydrite. Among the mineralogical phases, calcium-rich clinopyroxene (mainly diopside) is ubiquitous in the experimental products, and its abundance reflects the degree of crystallization. Leucite crystallizes mainly at lower temperatures and its abundance increases approximately with the degree of assimilation. Åkermanite (melilite group) is only stable at high degrees of assimilation and at the lowest temperatures. Magmatic assimilation produces residual liquids showing an overall decrease in SiO_2 (desilication of the silicate melt) and total alkali contents that decrease with temperature. At 1100°C and 15-20 wt.% of anhydrite assimilation, the residual liquid is characterized by foiditic compositions (nepheline and leucite normative over 40 wt.%).

Therefore, foiditic rocks containing clinopyroxene, leucite and melilite, typical of some volcanoes of the Roman Magmatic Province, can be generated through the assimilation of high contents of the "Anidriti di Burano" type evaporites by a trachybasaltic magma.

Dallai, L., Freda, C., Gaeta, M. (2004): Oxygen isotope geochemistry of pyroclastic clinopyroxene monitors carbonate contributions to Roman-type ultrapotassic magmas. *Contrib. Mineral. Petrol.*, **148**, 247-263.

Freda, C., Gaeta, M., Misiti, V., Mollo, S., Dolfi, D., Scarlato, P. (2008): Magma–carbonate interaction: an experimental study on ultrapotassic rocks from Alban Hills (Central Italy). *Lithos*, **101**, 397-415.

Iacono Marziano, G., Gaillard, F., Pichavant, M. (2008): Limestone assimilation by basaltic magmas: an experimental re-assessment and application to Italian volcanoes. *Contrib. Mineral. Petrol.*, **155**, 719-738.

Lustrino, M., Duggen, S., Rosenberg, C.L. (2011): The Central-Western Mediterranean: anomalous igneous activity in an anomalous collisional tectonic setting. *Earth-Science Reviews*, **104**, 1-40.

Mollo, S., Gaeta, M., Freda, C., Di Rocco, T., Misiti, V., Scarlato, P. (2010): Carbonate assimilation in magmas: a reappraisal based on experimental petrology. *Lithos*, **114**, 503-514.

Ridolfi, F., Renzulli, A., Perugini, D., Cesare, B., Braga, R., Del Moro, S. (2016): Unravelling the complex interaction between mantle and crustal magmas encoded in the lavas of San Vincenzo (Tuscany, Italy). Part II: Geochemical overview and modelling. *Lithos*, **244**, 233-249.

MAGMA ASCENT BENEATH CONTINENTAL ARC VOLCANOES – INSIGHTS FROM CHEMICALLY AND ISOTOPICALLY ZONED OLIVINES FROM IRAZÚ VOLCANO (COSTA RICA)

Oeser M.*[1], Ruprecht P.[2-3] & Weyer S.[1]
[1] Institut für Mineralogie, Leibniz Universität Hannover, Germany
[2] Department of Geological Sciences, University of Nevada, Reno, NV, USA
[3] Lamont-Doherty Earth Observatory, Columbia University, New York, NY, USA
Corresponding email: m.oeser@mineralogie.uni-hannover.de

Keywords: Fe-Mg isotopic zoning, LA-ICP-MS, diffusion modelling

Recent studies have shown that investigation of Fe-Mg isotopic variations in olivine provides an effective means to reliably trace Fe-Mg inter-diffusion occurring on the mineral scale during magma evolution (Sio et al., 2013; Oeser et al., 2015), because diffusion results in strong kinetic isotope fractionation even at magmatic temperatures (Richter et al., 2003). Modeling of distinctly diffusion-generated zoning in olivine yields constraints on the time scales of magma differentiation processes, leading to a better understanding of volcanic eruptions. Here we investigate the magmatic events prior to the 1963-65 eruption of Irazú volcano, the highest and one of the most active volcanoes in Costa Rica, with recurring explosive andesitic eruptions potentially endangering ~1.6 million people living within 30 km of this volcano. A study by Ruprecht & Plank (2013) showed that mantle-derived magmas can transit the crust and recharge crustal magma chambers beneath Irazú volcano within < 2 years based on preserved Ni zoning in primitive magnesian olivines. Our current study focuses on complexly zoned (in terms of Mg#) olivines, which share the normal zoning history of the rims of the magnesian olivines (~ Fo_{87-88} to Fo_{80-84}), but have high Ni and reversely zoned ferrous cores (Fo_{80}) indicating two episodes of crystal growth. Thus, these olivines appear to have mixed with the magma carrying the primitive magnesian olivines probably at middle to lower crustal depth and erupted together with the mantle-derived olivines in the 1963-1965 eruption. We performed high-precision *in situ* Fe-Mg isotope analyses by femtosecond-LA-MC-ICP-MS (Oeser et al., 2014) on the complexly zoned olivines in order to investigate the origin of this zoning (growth, diffusion, or a combination of both processes) and thus establish the basis for appropriate diffusion modeling. This should then provide reliable mixing-to-eruption time scales for these crustal olivines and constrain further the complex assembly of the erupted magmas. The results of our *in situ* Fe-Mg isotope analyses reveal that chemical and isotopic zoning in the crystals' interior are strongly coupled indicating that the zoning was generated by intra-mineral Fe-Mg inter-diffusion due to the formation of a Mg-rich rim domain. Detailed diffusion modeling of both chemical and isotopic zoning will unravel whether diffusive re-equilibration occurred mainly after the second episode of crystal growth or contemporaneously with the growth of the Mg-rich rim. Furthermore, some olivines appear to be affected by diffusive exchange of Fe-Mg between crystal and melt shortly before eruption, as implied by the narrow normal chemical zoning and enrichments of light Fe and heavy Mg isotopes near the crystal-melt boundary. Thus, the obtained Fe-Mg isotopic profiles can provide a more detailed picture of the complex growth and diffusion history of these crystals, leading to a better understanding of the magmatic processes beneath Irazú volcano.

Oeser, M., Weyer, S., Horn, I., Schuth, S. (2014): High-precision Fe and Mg isotope ratios of silicate reference glasses determined *in situ* by femtosecond LA-MC-ICP-MS and by solution nebulisation MC-ICP-MS. *Geostand. Geoanalyt. Res.*, **38**, 311-328.

Oeser, M., Dohmen, R., Horn, I., Schuth, S., Weyer, S. (2015): Processes and time scales of magmatic evolution as revealed by Fe-Mg chemical and isotopic zoning in natural olivines. *Geochim. Cosmochim. Acta*, **154**, 130-150.

Richter, F.M., Davis, A.M., DePaolo, D.J., Watson, E.B. (2003): Isotope fractionation by chemical diffusion between molten basalt and rhyolite. *Geochim. Cosmochim. Acta*, **67**, 3905-3923.

Ruprecht, P. & Plank, T. (2013): Feeding andesitic eruptions with a high-speed connection from the mantle. *Nature*, **500**, 68-72.

Sio, C.K.I., Dauphas, N., Teng, F.-Z., Chaussidon, M., Helz, R.T., Roskosz, M. (2013): Discerning crystal growth from diffusion profiles in zoned olivine by in situ Mg-Fe isotopic analyses. *Geochim. Cosmochim. Acta*, **123**, 302-321.

EXPERIMENTAL MODELLING OF THE DEEP FEEDING SYSTEM OF BASALTIC VOLCANOES

Pichavant M.*[1]

[1] Institut des Sciences de la Terre d'Orléans, Centre National de la Recherche Scientifique, Université d'Orléans, France

Corresponding email: pichavan@cnrs-orleans.fr

Keywords: experiments, feeding systems, basalt

Basaltic volcanoes are often considered to supply primary melts directly from their mantle source. Yet, recent progress in experimental simulations demonstrates that deep feeding systems are the site of a complex evolution. Understanding deep-seated processes at basaltic volcanoes is important to (1) better interpret the chemistry of basaltic magmas, (2) identify fractionation mechanisms responsible for the generation of differentiated rocks, and (3) develop comprehensive models of volcanic activity for eruption forecasting. During the last 15 years, active basaltic volcanoes from various geodynamic settings (arc: St Vincent, Stromboli, Vesuvius, Vulcano; oceanic island: Piton de la Fournaise) have been investigated experimentally combining methodological and analytical advances on synthetic charges with studies of eruption products (glass inclusions, phenocrysts). Near-liquidus fluid saturation (L-V experiments) have investigated the solubility of volatiles (H_2O, CO_2, S species, halogens) in mafic melts and contributed to the calibration of fluid-melt saturation thermodynamic models. Phase equilibrium results (L-Ctx experiments) have led to the precise determination of key parameters such as T and H_2O melt, and of the fO_2 when adequately controlled and measured experimentally. Residual liquid compositions have been measured in sub-liquidus experiments and models of primitive magma fractionation have developed. Methodologies for the simulation of open-system processes such as magma wall-rock interactions have been introduced. Forcing melt saturation with respect to near-liquidus phases such as Ol or Cpx has allowed to go "uphill" the differentiation sequence and to explore the significance of magma and glass inclusion compositions. These various experimental approaches have yielded results of fundamental significance. It is clear that, for primitive/primary mantle melts entering the crust, the deep feeding system of basaltic volcanoes is a reactive "lower crustal filter" rather than a closed-system high pressure crystallization level. Open-system processes involving interaction between incoming primitive magma and deep-seated wall-rocks, either igneous (Stromboli, Vulcano) or sedimentary (Vesuvius), have been documented. Ultra-calcic melts from arc settings, which were long considered as originated in the mantle, can form at crustal conditions. Reactive assimilation of carbonate rocks can have a profound effect on magma differentiation. More practically, the experimental approach has enabled the internal structure of basaltic volcanoes to be much better constrained and depths of magma accumulation zones to be precisely determined. The complexity and diversity of deep basaltic feeding systems offers perspectives for volcano monitoring but this requires that experimental simulations are better integrated with the other monitoring tools.

REFINEMENT AND APPLICATION OF CALCIC AMPHIBOLE THERMOBAROMETRY FOR IGNEOUS ROCKS: AMP-TBX.XLSX

Ridolfi F.*[1], Renzulli A.[2] & Perugini D.[3]
[1] Via Galileo Galilei 11, 61122 Pesaro, Italy
[2] Dipartimento di Scienze Pure e Applicate, Università "Carlo Bo", Urbino, Italy
[3] Dipartimento di Fisica e Geologia, Università di Perugia, Italy
Corresponding email: filippo.ridolfi@uniurb.it

Keywords: amphibole crystallization, magma systems, P-T-fO_2-X conditions

Amphibole crystal chemistry is controlled by a network of mutual relationships between the composition of the system and physico-chemical parameters such as P, T, fH_2O, fO_2 (Hawthorne et al., 2007; Ridolfi & Renzulli, 2012). Because of a large variety of possible substitution mechanisms, amphibole has many applications in the Earth Sciences. One of its most common applications is in geothermobarometry, especially for volcanic systems. Recently, there has been a growing demand from the geoscience community for the thermobarometric models for Mg-rich calcic amphiboles in equilibrium with calcalkaline or alkaline melts developed by Ridolfi et al. (Ridolfi et al., 2010; Ridolfi & Renzulli, 2012) because of their capability of defining the physico-chemical conditions of magma crystallization in a wide P-T range (up to ~ 2.2 GPa and ~ 1130°C) with low errors (e.g., P ±12%; T ±23°C). Amphibole thermobarometry of Ridolfi & Renzulli (2012) is a single-phase application relying on an empirical procedure to estimate the best pressure result among those of a series of barometric equations obtained through multivariate linear regression of literature experimental data. Amphibole composition (±P) is then used to obtain estimates of T, fO_2 and melt composition by other equations.

In this work we present a refinement of this procedure obtained using a selection of recent published experimental data with low uncertainties (Almeev et al., 2013; Krawczynski et al., 2012; Blatter et al., 2013), and a new thermobarometric spreadsheet (Amp-TBX.xlsx), which can be safely used whenever amphibole crystallization occurs at steady-state magmatic ("perfect" equilibrium) conditions. By contrast, the application of this program to experimental amphiboles crystallized at 150 MPa at cooling rates ($\Delta T/\Delta t$) of 2.3-4.7 °C/h (Shea & Hammer, 2013) results in pressure overestimations of ~ 100-200%. This effect is due to the fact that these experimental amphiboles show disequilibrium textures such as acicular and hopper morphologies and highlights the issue of poorly investigated effect of crystallization kinetics on texture and crystal chemistry of amphibole at dynamic P-T conditions. However, at $\Delta T/\Delta t$ of 0 °C/h, amphibole Al_2O_3 contents are similar to those of the "perfect" equilibrium experiments obtained at about the same pressure (i.e., Ridolfi & Renzulli, 2012) confirming the reliability of Amp-TBX.xls.

Hence, we present suggestions and methods for avoiding, as much as possible, amphiboles crystallized at disequilibrium conditions and maximizing the results obtained by Amp-TBX.xlsx on multiple and profile EMP analyses. Finally, we demonstrate that whenever these suggestions are followed, Amp-TBX.xlsx gives amphibole crystallization pressures (and magma storage depths) which have been verified using other thermobarometric applications (e.g., Ridolfi et al., 2016) and independent methodologies for locating magma chambers, such as seismic tomography and pre-eruptive seismicity.

Almeev, R.R, Holtz, F., Ariskin, A.A., Limura, J.-I. (2013): Storage conditions of Bezymianny Volcano parental magmas: results of phase equilibria experiments at 100 and 700 MPa. *Contrib. Mineral. Petrol.*, **166**, 1389-1414.

Blatter, D.L., Sisson, T.W., Hankins, W.B. (2013): Crystallization of oxidized, moderately hydrous arc basalt at mid to lower-crustal pressures: implications for andesite genesis. *Contrib. Mineral. Petrol.*, **166**, 861-886.

Hawthorne, F.C., Oberti, R., Della Ventura, G., Mottana, A. (2007): Amphibole: crystal chemistry, occurrence, and health issues. *Rev. Mineral. Geochem.*, **67**, 545 p.

Krawczynski, M.J., Grove, T.L., Behrens, H. (2012): Amphibole stability in primitive arc magmas: effects of temperature, H_2O content, and oxygen fugacity. *Contrib. Mineral. Petrol.*, **164**, 317-339.

Ridolfi, F. & Renzulli, A. (2012): Calcic amphiboles in calc-alkaline and alkaline magmas: thermobarometric and chemometric empirical equations valid up to 1,130°C and 2.2 GPa. *Contrib. Mineral. Petrol.*, **163**, 877-895.

Ridolfi, F., Renzulli, A., Puerini, M. (2010): Stability and chemical equilibrium of amphibole in calc-alkaline magmas: an overview, new thermobarometric formulations and application to subduction-related volcanoes. *Contrib. Mineral. Petrol.*, **160**, 45-66.

Ridolfi, F., Braga, R., Cesare, B., Renzulli, A., Perugini, D., Del Moro, S. (2016): Unravelling the complex interaction between mantle and crustal magmas encoded in the lavas of San Vincenzo (Tuscany, Italy). Part I: Petrography and Thermobarometry. *Lithos*, **244**, 218-232.

Shea, T. & Hammer, J.E. (2013): Kinetics of cooling- and decompression-induced crystallization in hydrous mafic-intermediate magmas. *J. Volcanol. Geotherm. Res.*, **260**, 127-145.

CHAOTIC MIXING EXPERIMENTS BETWEEN RHYOLITIC AND SHOSHONITIC MAGMAS FROM AEOLIAN ISLANDS (ITALY)

Rossi S.*[1], Morgavi D.[1], Petrelli M.[1], Vetere F.P.[1] & Perugini D.[1]
[1] Gruppo di Petro-Vulcanologia Sperimentale, Dipartimento di Fisica e Geologia, Università di Perugia, Italy
Corresponding email: stefano.rossi1@studenti.unipg.it

Keywords: magma mixing, chaotic dynamics, time series experiments

In this work we present a set of chaotic mixing experiments using natural melts from Vulcano island (Aeolian Islands, Italy). Vulcano is the southernmost island of the Aeolian Archipelago; its magmatic activity dates back to about 120 ky and last eruption occurred in 1888-1890. We use the chaotic magma mixing apparatus (COMMA; see Morgavi et al., 2016, for detailed description) to trigger chaotic mixing.

The experimental device allows following in space and time the evolution of the mixing process and the associated modulation of chemical composition between end-members. The variation of major and trace elements is studied in detail by electron microprobe (EMPA) and Laser Ablation ICP-MS (LA-ICP-MS) respectively. The experiments were performed at 1200°C, with shoshonitic and rhyolitic melts, resulting in a viscosity ratio, at experimental conditions, of more than three orders of magnitude. The experimental protocol (the duration of each experiment) was chosen to ensure the occurrence of chaotic dynamics in the system and the run duration was progressively increased (e.g. 10.5 h, 21 h, 42 h).

The efficiency of the mixing process is estimated by calculating the decrease of concentration variance in time. The variance of both major and trace elements decays exponentially. Our results confirm and quantify how different chemical elements homogenize in the melt at differing rates. We also show that the mixing structures generated during the experiments are topologically identical to those observed in natural volcanic rocks.

Morgavi, D., Petrelli, M., Vetere, F.P., Gonzalez-Garcìa, D., Perugini, D. (2015). High-temperature apparatus for chaotic mixing of natural silicate melts. *Rev. Sci. Instrum.*, **86**, 105108.

CARBON DIOXIDE SOLUBILITY MODIFED BY CUMULATE ASSIMILATION AT MOUNT ETNA, ITALY

Salem L.[1], Edmonds M.*[1], Maclennan J.[1] & Corsaro R.[2]
[1] Earth Sciences Department, University of Cambridge, United Kingdom
[2] Istituto Nazionale di Geofisica e Vulcanologia, Catania, Italy
Corresponding email: me201@cam.ac.uk

Keywords: melt inclusions, volatiles, assimilation

Reconstructing the loci and rates of melt differentiation and volatile outgassing through the crust is a first order problem in volcano-petrology. Melt inclusions are an important tool in studies that seek to understand the geochemical history of melts, the assimilation of crustal rocks, fractionation and vapor-saturation of mantle-derived magmas as they transit the crust during their ascent and eruption at the surface of the Earth. Melt inclusion volatile records of volatiles, however, are often ambiguous and scattered. It is not clear whether using melt inclusion H_2O-CO_2 as a barometer is satisfactory or robust, given recent studies highlighting the sequestration of CO_2 into bubbles (enhanced by post-entrapment crystallization) and the diffusive loss of H+ through the crystal. Here we present olivine-hosted melt inclusion data from the voluminous 1669 eruption of Mount Etna, Italy, measured by SIMS and electron microprobe. Mount Etna is one of the most prolific convergent margin volcanic outgassers in the world (Allard et al., 1991), supplying almost 10% of the global volcanic output of CO_2 (Burton et al., 2013). Primitive melt inclusions supplying Etna are heterogeneous with respect to their trace element compositions (Kamenetsky et al., 2007), implying not only different degrees of melting, but also a highly enriched mantle source influenced by subduction fluid circulation.

The melts preserved inside olivines show a diverse range of compositions, from LREE-enriched, CO_2-poor to LREE-depleted, Sr-, S- and CO_2-rich. The Sr anomaly in the melt inclusions correlates strongly with CO_2 and with S concentrations; and CO_2 and S correlate negatively with LREE and with Nb. We propose that this mixing array was generated by mixing melts that have assimilated plagioclase cumulates in the crust (thereby enhancing Sr and depleting LREE) and melts that have not (with enriched LREE and no Sr enrichment). The solubility of CO_2 is dependent on melt composition as well as on pressure. The effect of assimilating plagioclase cumulates is to enhance the CaO contents of the melts, thereby enhancing the solubility of CO_2 in them by up to four times at a pressure of 200 MPa. Sulfur fluid-melt partitioning is also suppressed as the mole fraction of Ca and Al in the melt increases (Zajacz, 2015), explaining the strong correlation between CO_2 and S, which is not consistent with degassing. We use the compositions of 1669 melts in combination with an array of primitive melts published by Kamenetsky et al. (2007) to show that the range in CO_2 concentrations are largely controlled by the heterogeneity in melt composition inherited from the interaction between primitive melts and plagioclase cumulates in the crust beneath Mount Etna. Around 70% fractionation of olivine (and some clinopyroxene and plagioclase) must have taken place before the melts mixed to produce the mixed array of compositions. We propose that much of the scatter in melt inclusion CO_2 concentrations in Mount Etna melt inclusion data, which we have shown is also accompanied by systematic trace element variability, may be caused by heterogeneity in melt composition and this reduces the need to invoke other processes such as gas fluxing.

Kamenetsky, V.S., Pompilio, M., Métrich, N., Sobolev, A.V., Kuzmin, D.V., Thomas, R. (2007): Arrival of extremely volatile-rich high-Mg magmas changes explosivity of Mount Etna. *Geology*, **35**, 255-258.

Shishkina, T.A., Botcharnikov, R.E., Holtz, F., Almeev, R.R., Jazwa, A.M., Jakubiak, A.A. (2014): Compositional and pressure effects on the solubility of H_2O and CO_2 in mafic melts. *Chem. Geol.*, **388**, 112-129.

Zajacz, Z. (2015): The effect of melt composition on the partitioning of oxidized sulfur between silicate melts and magmatic volatiles. *Geochim. Cosmochim. Acta*, **158**, 223-244.

EFFECT OF TEMPERATURE AND COMPOSITION ON WATER SOLUBILITY IN PANTELLERITES TO 250 MPa

Stabile P.*[1], Behrens H.[2], Cestelli M.[3], Radica F.[1], Bello M.[1], Carroll M.R.[1], Paris E.[1] & Giuli G.[1]
[1] Scuola di Scienze e Tecnologie - Sezione di Geologia, Università di Camerino, Italy
[2] Institut für Mineralogie, Leibniz Universität, Hannover, Germany
[3] Laboratori Nazionali di Frascati, Istituto Nazionale di Fisica Nucleare, Frascati (RM), Italy
Corresponding email: paola.stabile@unicam.it

Keywords: alkalis effect, temperature dependence, magma degassing

H_2O solubility has been experimentally investigated in pantelleritic glasses in the range 50- 250 MPa and 800-900°C. Using a synthetic glass anlog of pantelleritic magma of Kenya Rift Valley (Ebu-1 in Scaillet & Macdonald, 2006) as starting composition, the molar Na/(Na+K) ratio was varied from 0 (Ebu-C) to 0.74 (Ebu-B) and 1 (Ebu-N) at constant total alkali content.

The compositional dependence of water solubility as a function of Na/(Na+K) was mainly investigated at 840°C in the pressure interval 50-150 MPa. H_2O solubility in rhyolitic systems is strongly dependent on the Na/(Na+K) ratio (Holtz et al., 1995; Vetere et al., 2014) and such dependence for pantellerites is still poorly constrained. Results here reported suggest that Na favors H_2O solubility (determined by FTIR spectroscopy) on equimolar basis. It is worth to remark that this alkali effect has important implications for the chemical and physical properties of rhyolitic melts such as viscosity (Stabile, 2015).

Moreover, considering also the iron redox influence on water solubility as a melt compositional effect, Ebu-B glasses have been further investigated at 850°C and 150 MPa and oxygen fugacity (fO_2) ranging from NNO-4.8 to NNO+4.8 buffer conditions (oxygen fugacity in $\log_{10}$ units realtive to the Ni-NiO buffer). However, the results suggest that fO_2, and in turn Fe^{2+}/Fe^{3+} ratio, do not affect sensibly the H_2O solubility in these glasses.

A nearly linear positive correlation has been found between water solubility and pressure between 50 and 150 MPa at 840°C and between 50 and 250 MPa at 800°C. The temperature influence on water solubility has been often documented as a negative dependence below 400 MPa (Tuttle & Bowen, 1958; Hotlz et al., 1995) but it is not straightforward. The temperature effect reported in this study has been investigated in a small range (800-900°C), chosen to follow water-saturated liquidus of the starting composition Ebu-B. Water solubility increases from 4.80±0.10 wt.% to 7±0.13 wt.% with decreasing temperature at 150 MPa through temperature independence at approximately 50 MPa.

These data will be useful in order to implement existing predictive models of solubility over a wider range of silicate melt compositions and to better understand magma degassing processes.

Holtz, F., Behrens, H., Dingwell, B.D., Johannes, W. (1995): H_2O solubility in haplogranitic melts: Compositional, pressure and temperature dependence. *Am. Mineral.*, **80**, 94-108.

Scaillet, B. & Macdonald, R. (2006): Experimental and thermodynamic constraints on the sulphur yield of peralkaline and metaluminous silicic flood eruptions. *J. Petrol.*, **47**, 1413-1437.

Stabile, P. (2015): Pantelleritic magmas: experimental study on the effect of [Na/(Na+K)] ration and fO_2 on iron redox and viscosity. PhD dissertation, University of Camerino.

Tuttle, O.F. & Bowen, N.L. (1958): Origin of granitic in the light of experimental studies in the system $NaAlSi_3O_8$-$KAlSi_3O_8$-SiO_2-H_2O. *Geol. Soc. Am. Mem.*, **74**, 153 p.

Vetere, F., Holtz, F., Behrens, H., Bocharnikov, R.E., Fanara, S. (2014): The effect of alkalis and polymerization on the solubility of H_2O and CO_2 in alkali-rich silicate melts. *Contrib. Mineral. Petrol.*, **67**, 1014-1031.

HOW IRON ISOTOPES RECORD INTERACTIONS OF CARBONATITE AND SILICATE MAGMAS

Stuff M.*[1-2], Schuessler J.A.[1], Rocholl A.[1] & Wilke M.[2]
[1] Helmholtz Zentrum Potsdam, GFZ Deutsches GeoForschungsZentrum, Potsdam, Germany
[2] Institut für Erd- und Umweltwissenschaften, Universität Potsdam, Germany
Corresponding email: maria.stuff@gfz-potsdam.de

Keywords: experimental, high temperature, immiscible melts

Iron stable isotopes are a promising tracer for magmatic processes in the mantle, particularly because their fractionation is controlled by oxidation state and bonding environment. Iron isotope data from carbonatite rocks show the largest variability found to date in igneous rocks, both on the whole rock and mineral scale (Johnson et al., 2010). Moreover, our own in-situ iron isotope measurements on olivine and magnetite crystals in a melilitite bomb from the Salt Lake Crater at Honolulu complement previous data sets and reveal significant iron isotope inter-mineral variations. These findings indicate the fidelity of iron isotopes as a tracer of carbonatite interactions in the Earth's mantle. However, the application of this tracer is still hampered by the lack of knowledge on the detailed mechanisms causing iron isotope fractionation in carbonatite systems. Hence, to interpret the data from natural rocks, experimentally determined iron isotope fractionation factors are needed.

Here, we present results from kinetic and equilibration experiments in natrocarbonatite systems between immiscible silicate and carbonate melts, performed at 900 to 1200°C and 0.7 GPa in an internally heated gas pressure vessel at intrinsic redox conditions. The iron isotope compositions of coexisting silicate melt (sil.m.) and carbonate melt (carb.m.) were analysed by solution MC-ICP-MS.

The kinetic experiments, in which we used a Fe-58 spiked starting material, show that isotopic equilibrium is obtained after 48 hours. Our data indicate a fractionation of $\delta^{56}Fe_{sil.m.-carb.m.}$ = 0.10±0.07 ‰ in equilibrium at 1200°C. Additionally, $\delta^{56}Fe_{sil.m.-carb.m.}$ changes with bulk chemical composition, likely reflecting the differences between the studied systems in terms of Fe^{3+}/Fe^{2+}-ratios in the two immiscible liquids. Our findings provide experimental support for a carbonatite genesis model, in which negative $\delta^{56}Fe$ values in carbonatites result from differentiation processes, such as liquid immiscibility (Johnson et al., 2010). Their sensitivity to chemical and redox composition makes iron isotopes a potential tool for constraining the original compositions of carbonatite magmas.

Johnson, C.M., Bell, K., Beard, B.L., Shultis, A.I. (2010): Iron isotope compositions of carbonatites record melt generation, crystallization, and late-stage volatile-transport processes. *Mineral. Petrol.*, **98**, 91-110.

GEOLOGY OF THE KEKEM DYKE SWARMS (CAMEROON CENTRAL SHEAR ZONE): AN INSIGHT INTO PALEZOIC AND MESOZOIC MAGMATISMS AND GEODYNAMIC IMPLICATION FOR THE WEST GONDWANA IN CAMEROON

Tchaptchet Tchato D.*[1], Simeni Wambo N.A.[2], Keutchafo Kouamo N.A.[1] & Tchouankoue J.P.[1]
[1] Department of Earth Sciences, University of Yaoundé I, Cameroon
[2] Department of Earth Sciences, University of Ngaoundéré, Cameroon
Corresponding email: bevetteacqua@yahoo.it

Keywords: basalt dykes, Cameroon, West Gondwana breakup

Recent studies have documented Early Paleozoic and Mesozoic magmatisms within the PanAfrican Cameroon Central Shear Zone in Cameroon, which is poorly known so far. To provide additional constrain on the issue, brittle deformation, petrographical and geochemical studies were carry out on the Kekem dyke swarm. SRTM and Landsat 08 Satellite imageries analysis complemented with field study were used for brittle deformation study. It reveals that N70°E and N90°E trends as major fractures and N110-120°E as minor trends. These main fractures trends, which is similar to those reported in the central northern Cretaceous sedimentary basin in Cameroon, suggest that the brittle deformation was of regional extension and post PanAfrican. The petrographical analysis of related basalts show that are made up of olivine, pyroxene, plagioclase and oxide. Geochemical studies reveal that they display a tholeiitic affinity with low SiO_2 contents (44-59 wt.%) and high MgO contents (7.3-12.4 wt.%). Their trace elements patterns shows a moderately enrichment in LREE with respect to HREE (La_N/Yb_N = 5.3-8.2) with a nearly flat HREE profile (Dy_N/Yb_N = 1.3-1.5). They are within intraplate basalt originated from EMI end member mantle source. The above features is similar to those which yielded an emplacement age ranging from 420-164 Ma in the Cameroon central shear zone, which suggest that they likely belong to the same magmatic event. On the contrary, their comparison with Cenozoic alkaline basalt of the Cameroon line and post Neoproterozoic gabbro rocks does not show any similarities and therefore, precludes any relationship in term of magma source region. This, rather, reinforces the existence of Early Paleozoic and Mesozoic magmatism, which could likely represent a forerunner of a crustal extension of the West Gondwana supercontinent. This crustal extension culminated in rifting during cretaceous, which is associated with sedimentation and alkaline magmatism. A correlation of the Mesozoic dyke swarms with those from the South America show similarities, which implies that both areas experienced a similar post PanAfrican evolution marked by Gondwana break up. However, the Paleozoic magmatism in Cameroon likely could suggest that the rifting might have started earlier in Paleozoic time than Jurassic time as previously suggested, and then culminated in Cretaceous time during the opening of the South Atlantic Ocean.

Session S8:

Diffusion, mineral reaction and deformation mechanisms from low to high temperatures: flow and brittle processes of the Earth s interior

Conveners:

Sylvie Demouchy (Montpellier – France)

Katharina Marquardt (Bayreuth – Germany)

DOLOMITE AND MICA MINERAL REACTIONS AND MICROSTRUCTURES FORMED DURING THE SEISMIC CYCLE OF THE ALHAMA DE MURCIA FAULT

Abad I.*[1], Sanchez C.[1], Jimenez-Millan J.[1], Faulkner D.R.[2], Nieto F.[3] & Velilla N.[3]

[1] Departamento de Geología y Centro de Estudios Avanzados en Ciencias de la Tierra, Unidad Asociada al Instituto Andaluz de Ciencias de la Tierra, Universidad de Jaén, Spain

[2] Rock Deformation Laboratory, Department of Earth and Oceanic Sciences, University of Liverpool, United Kingdom

[3] Departamento de Mineralogía y Petrología & Instituto Andaluz de Ciencias de la Tierra, Universidad de Granada, Spain

Corresponding email: miabad@ujaen.es

Keywords:

The Alhama de Murcia Fault is a strike-slip fault located in the eastern Betic Cordillera (SE Spain), cutting rocks from their internal zone. The fault is trending NE-SW and runs along 100 km. The studied samples were collected within the Lorca-Totana segment, directly from the fault plane, including a trench uncovered after the 2011 earthquake. The 5.1-magnitude Lorca Earthquake caused significant localized damage in the Murcia region leaving a total of nine deaths and an estimated four hundred injured. The aim of this study is to carry out a petrographic characterization of rocks from the core and slip zone of this fault in order to recognize particular microstructures and mineral reactions formed during its seismic cycle. X-ray diffraction shows that, as a common feature, all samples contain high amounts of K- and Na-dioctahedral micas and small amounts of quartz, carbonates, chlorite and hematite. There were no significant changes after ethylene glycol solvation, indicating the absence of expandable clays like smectite. However, kaolinite is present in all the XRD profiles. Polished thin sections were studied by a Merlin Carl Zeiss Scanning Electron Microscopy, showing that some rocks from the core-fault are made of:

a) Foliated bands more than 100 µm thick rich in well crystallized muscovite, paragonite and quartz including Fe-rich dolomite and hematite crystals frequently > 20 µm size. In some cases, dolomite grains exhibit intact cores but rims with localized disaggregation, holes and Fe-oxide crystallization.

b) Thin ultrafine-grained bands (around 20 µm thick) made of an apparently poorly crystalline material characterized by the presence of numerous holes and vesicles. Compositionally, this material is made of patches with mica bulk composition and areas of Fe-rich dolomite composition. These patches are hosting a network of dolomite skeletal crystals and dispersed crystals of Fe-oxide and ferropericlase.

c) Patches of kaolinite made of randomly oriented crystals ranging in size from 40 µm to < 2 µm and usually filling gaps in the rock structure. Kaolinite can also be observed in foliated bands associated with K- and Na-micas, following their same orientation.

Poorly crystalline materials from the ultrafine-grained bands show petrographic evidence of mineral reactions and microstructures probably formed during the seismic cycle of the fault. The presence of numerous vesicles and the skeletal habit of dolomite crystals could reveal frictional heating processes that induced dolomite decarbonation and later neo-crystallization of dolomite under rapid cooling. This thermally activated processes during earthquake slip could also promote mica amorphization during the temperature rise induced by earthquake slip.

The production of ultra-fine-grained decomposition products such as those described in the Alhama de Murcia fault can have weakening effects in the slip zone that have been correlated with a dramatic reduction in frictional strength.

THERMOCHRONOLOGY OF FAULT ACTIVITY BY CHARACTERIZATIONS OF CLAY MINERALS (EXAMPLE OF PIC DE PORT VIEUX THRUST, PYRENEES, SPAIN)

Abd Elmola A.*[1], Buatier M.[1], Monié P.[2], Charpentier D.[1], Lanari P.[3], Trincal V.[1] & Labaume P.[2]
[1] Laboratoire Chrono-Environnement, Université de Franche-Comté, Besançon, France
[2] Géosciences Montpellier, Université de Montpellier, France
[3] Institut für Geologie, Universität Bern, Switzerland
Corresponding email: abd_elmola.ahmed@yahoo.com

Keywords:

Clay minerals such as illite/mica and chlorite have been commonly used to quantify diagenetic and low-grade metamorphic conditions. Moreover, they can play a major role in the fault mechanical behavior and chemical transfers. Their chemical and isotopic compositions can record the PT-t conditions during deformation and fluid/rock interaction in fault zones. The focus of the present study is the Pic-de-Port-Vieux thrust, a second-order thrust related to the major Gavarnie thrust in the Axial Zone of the Pyrenees. The thrust footwall comprises a ten-meters thick layer of Upper Cretaceous dolomitic limestone progressively transformed into mylonitic limestones near the fault contact, while the hanging-wall consists of Lower Triassic red pelites and sandstone. In the hanging wall, the core zone of the fault is composed of a 0.6 m-thick layer of intensely foliated green pelites and the damage zone features numerous fractures affecting several meters thick of red pelites. A fault-normal transect in the hanging-wall was investigated to characterize the clay mineralogy and geochemical changes induced by deformation and attributed to the fault activity. In the present study we focus on synkinematic newly formed clay minerals to date and understand the fault activity.

The XRD results on the bulk powder indicate similar mineralogical compositions in the green and red pelites, with mainly muscovite, quartz, chlorite, calcite, minor rutile and apatite. The only difference is hematite which was detected only in the red pelites. XRD patterns of air dried and after EG saturation for oriented preparations of < 2 µm fraction confirm the presence of chlorite and muscovite with no expandable layer. Diagnostic reflections for mica polytypes indicate that muscovite $2M_1$ is the major polytype with relatively small amount of 1*M*. The Kübler index suggests high anchizone metamorphic conditions.

Petrographic observations by optical microscopy and SEM demonstrate that green pelites have been highly deformed compared to the red pelites. Indeed, the green pelites have a well-defined cleavage marked by the preferential orientation of muscovite which display smaller grain size toward the fault contact. Newly formed chlorites preferentially formed in veins at around 300°C according to their chemical composition. The elongated shape of the quartz grains and their smaller size in green pelites matrix compared to the red ones are the result of pressure solution mechanism. Scanning electron microscope images show that the, newly formed synkinematic micas occur with higher proportion close to the fault contact.

Five fractions from each of the two samples were dated using $^{40}Ar/^{39}Ar$ step-heating method. Each fraction has been encapsulated in a quartz tube prior to irradiation. The ^{39}Ar lost by recoil was measured before step heating experiments. All the fractions for sample 12-05 (located at the fault contact) have younger ages compared to the sample 12-07 (located 2 meters away from the fault contact). The age of the finest fraction derived using total gas data is 37.39±0.24 Ma with a plateau-like segment, whereas the coarser fractions produced a staircase shaped spectrum that reaches a maximum age of 305.80±1.47 Ma. These ages will be discussed with respect to the different muscovite phases identified in the two studied samples.

FLUID-ROCK INTERACTIONS AND DEFORMATION CONDITIONS REGISTRATED BY PHYLLOSILICATES IN A MAJOR THRUST (GAVARNIE THRUST AT "PIC DE PORT VIEUX", PYRENEES)

Abd Elmola A.[1], Charpentier D.[1], Lanari P.[2], Trincal V.[1] & Buatier M.*[1]
[1] Laboratoire Chrono-Environnement, Université Bourgogne-Franche Comté, Besançon, France
[2] Institut für Geologie, Universität Bern, Switzerland
Corresponding email: martine.buatier@univ-fcomte.fr

Keywords: phyllosilicates, fault, fluid-rock interactions

The Pic de Port Vieux thrust, a second-order thrust related to major Gavarnie thrust in the Axial Zone of the Pyrenees, juxtaposes Triassic pelites in the hanging-wall and Cretaceous limestone in the footwall. In order to investigate the mineralogical and geochemical changes induced by deformation and subsequent fluid flow, sampling of host rock was conducted along a complete transect in the pelites and also on synkinematic quartz-chlorite veins.

In the hanging wall, deformation and fluid-rock interactions are mainly characterized by a color change from red to green pelites observed up to one meter perpendicularly to the main thrust. Quantitative bulk mineralogy combining XRD, chemical analyses and Mossbauer spectroscopy suggests that both red and green pelites are composed mainly of quartz, calcite and phyllosilicates (chlorite and mica). The color changes are mainly related to hematite dissolution in the green pelites.

The microtextural observations by optical microscopy and scanning electron microscope indicate increase of deformation associated to thrusting toward the fault contact with shear structures markers such as S-C type, shear and extension quartz/calcite-chlorites veins. A decrease in the grain size of phyllosilicates and elongation of quartz grains along the well-defined cleavage is observed in the green pelites. Synckimatic phyllosilicates are more abundant close to the fault contact compared to the red pelites and they formed mainly by fluid-rock interactions and recrystallization of inherited phyllosilicates. Newly formed chlorite preferentially formed in veins.

Chlorite composition from the red and green pelites are located between Sudoite, Amesite and Clinochlore-Daphnite end–members. There is iron-magnesium substitution with a small di-trioctahedral substitution in both red and green pelites chlorite. The only observed difference is that chlorite from green pelite close to the fault contact is Fe-rich compared to newly formed chlorite formed far from the major thrust contact. The mica compositions are closed to muscovite end-members with Tschermak substitution toward celadonite end-member. The red pelites micas display larger dispersions in composition with more Na in the interlayer compared to the green pelites micas which have homogeneous compositions. Temperature estimation using the chlorite thermometer of Vidal et al. (2005, 2006) and Lanari (2014) for 2 samples one at fault contact and the other 1.2 meters away from the fault contact are 311±50°C and 269±50°C respectively.

The thermodynamical modelling of fluid-sediment interactions using the geochemical reaction modelling code PhreeqC have been carried on. Hypothesis concerning the dissolution of hematite have been tested. For this modelisation, we used the mineralogical composition of the sediment and pore water composition in equilibrium with this lithology, and using the estimated temperature for chlorite precipitation, we determine the redox condition favoring hematite dissolution and Fe-rich chlorite precipitation.

Lanari, P., Wagner, T., Vidal, O. (2014): A thermodynamic model for di-trioctahedral chlorite from experimental and natural data in the system $MgO–FeO–Al_2O_3–SiO_2–H_2O$: applications to P–T sections and geothermometry. *Contrib. Mineral. Petrol.*, **167**, 1-19.

Vidal, O., Parra, T., Vieillard, P. (2005): Thermodynamic properties of the Tschermak solid solution in Fe-chlorite: Application to natural examples and possible role of oxidation. *Am. Mineral.*, **90**, 347-358.

Vidal, O., De Andrade, V., Lewin, E., Muñoz, M., Parra, T., Pascarelli, S. (2006) P-T-deformation-Fe^{3+}/Fe^{2+} mapping at the thin section scale and comparison with XANES mapping: application to a garnet-bearing metapelite from the Sambagawa metamorphic belt (Japan). *J. Metam. Geol.*, **24**, 669-683.

GRAIN BOUNDARIES IN FORSTERITE: HOW DO THEY MOVE TO PRODUCE SHEAR?

Bollinger C.*[1], Farla R.[1] & Marquardt K.[1]
[1] Bayerisches GeoInstitut, Universität Bayreuth, Germany
Corresponding email: caroline.bollinger@uni-bayreuth.de

Keywords: grain boundaries, forsterite

The plasticity of the upper mantle is fundamental to understand how mantle convection couples with plate tectonics. As olivine comprises 60% of the upper mantle with a strong elastic and plastic anisotropy, one needs to characterize the rheology in olivine aggregates at mantle conditions. Many experiments at high pressure and high temperature have been performed. However, olivine rheology at lithospheric conditions is still poorly understood. As the pressure-temperature conditions increase from the shallower to the deeper parts of the mantle, plasticity of olivine appears to evolve, leading to fabric transitions which can potentially weaken anisotropy. Hence, knowledge of the type and strength of fabric produced by plastic deformation of olivine polycrystals is required in order to link seismic anisotropy with mantle convection.

Plastic deformation of olivine polycrystals results from the motion of defects. Point (vacancies, interstitials), line (dislocations) and plane (grain boundaries – GB – and stacking faults), “defects” drive diffusion creep, dislocation creep and grain boundary migration, respectively. The development of different textures in olivine assemblages has been to date largely interpreted in term of changes in the dominant slip system activity inside grains in response to changes in P-T conditions and loading, but our present understanding of dislocation creep mechanisms is not sufficient to explain some fabric changes. Recently, it has been proposed that GB sliding may also produce fabric in olivine in response of differential rotation of the grains. This contribution is not taken into account in any micromechanical model currently available (Finite element models, Visco Plastic Self Consistent Models…). GB activity may consequently influence the viscosity of the mantle and control the Earth’s plate tectonic processes.

GB displacement is at the heart of the plastic properties of polycrystals. However, it represents one of the least known parameters in GB physics. We address the question of the GB mobility in polycrystalline olivine under stress and to quantify its contribution to the plasticity of olivine. The aim of this project is to constrain how a GB will respond to a deviatoric stress.

Olivine polycrystals are deformed in multianvils press in different conditions, the displacement of the GBs is measured by scanning electron microscopy done before and after the experiments. A method for measuring the grain boundary mobility is to probe strain distribution in a diametral plane of the sample where the strain markers will consist in a FIB-engraved grid. After deformation, grain boundary migration inducing shear is shown by the deflection of the lines. Those measured data are required in micromechanical models to incorporate the contribution of GB to the plasticity of olivine and ultimately for the viscosity of the mantle.

THE BIVALENCE AND ANOMALIES OF ANTIGORITE IN THRUST FAULT MECHANICS

Campione M.*[1]

[1] Dipartimento di Scienze dell'Ambiente, del Territorio e di Scienze della Terra, Università di Milano-Bicocca, Italy

Corresponding email: marcello.campione@unimib.it

Keywords: antigorite, frictional anisotropy, crystal preferred orientation

Antigorite, the high-temperature, high pressure polymorph of serpentine, is the most abundant hydrous phase within the upper mantle. It is responsible for the seismic shear-wave anisotropy measured in many subduction systems which is attributed to strain-induced lattice preferred orientation. This orientation phenomenon occurs in accordance to two mechanisms, depending on many factors among which we mention strain rate and fluid concentration. Both mechanisms drive the orientation of the antigorite (001) plane parallel to the shear plane (fault plane). However, one mechanism brings about a concentration of the a-axis subparallel to the shear direction, whereas the other mechanism brings about a concentration of the a-axis orthogonal to the shear direction (Katayama et al., 2009).

By an experimental analysis based on scanning force microscopy performed on (001) oriented antigorite single crystals (Campione & Capitani, 2013), we show that the basal surface of this mineral is characterized by a strong frictional anisotropy, reaching levels as high as 100%. Friction is observed to be higher along the a-axis and lower orthogonal to it, displaying an overall orthotropic symmetry in the sliding plane. By virtue of the aforementioned crystal preferred orientation, the shear interface of thrust faults, depending on the orientation mechanism, might be subjected to a hardening process or to a weakening process. The final result is that the fault might evolve as seismic or aseismic, respectively.

This seismic bivalence is not the only peculiarity stemming from the frictional anisotropy of antigorite. We show also that, in the framework of the said hardening process, slip trajectories might be substantially declined from the plate convergence direction.

Campione, M. & Capitani, G.C. (2013): Subduction-zone earthquake complexity related to frictional anisotropy in antigorite. *Nature Geosci.*, **6**, 847-851.

Katayama, I., Hirauchi, K., Michibayashi, K., Ando, J. (2009): Trench-parallel anisotropy produced by serpentine deformation in the hydrated mantle wedge. *Nature*, **461**, 1114-1117.

PRESERVATION OF COMPOSITIONAL ZONING OF ECLOGITE FACIES GARNET WITH GRANULITE FACIES OVERPRINT; HOW FAST THE METAMORPHIC PROCESSES DURING COLLISION OROGENY ARE?

Faryad S.W.*[1], Jedlicka R.[1], Jezek J.[2] & Hauzenberger C.[3]
[1] Institute of Petrology and Structural Geology, Charles University, Prague, Czech Republic
[2] Institute of Applied Mathematics and Information Technologies, Charles University, Prague, Czech Republic
[3] Institut für Erdwissenschaften, Mineralogie & Petrologie, Karl-Franzens Universität, Graz, Austria
Corresponding email: faryad@natur.cuni.cz

Keywords: garnet, diffusion, granulite

Major and trace element distribution in garnet crystals from felsic (quartzo-feldspathic) granulites from Moldanubian Zone in the Bohemian Massif provides evidence of two metamorphic events. The first event is related to continental subduction to ultrahigh pressure (UHP) conditions. The second granulite facies overprint occurred in the mid- to lower crustal levels. Based on the presence of ternary feldspar, the rocks reached ultrahigh-temperature conditions during the second event. The felsic granulites contain lenses and boudins of mantle-derived garnet peridotite, garnet pyroxenite and eclogite. UHP conditions for the host granulite were confirmed by the presence of micro-diamond and coesite inclusions in garnet and zircon. The striking feature of these granulite is the preservation of prograde compositional zoning, that is indicated by rimward decrease of Mn and Ca, but increase of Mg or X_{Mg}. Garnets with strong major component zoning profiles were treated for deciphering trace element variations. The results showed high yttrium and heavy rare earth elements (Y+HREE) concentrations in the garnet core with annuli near rim parts of garnet grains. Formation of the core garnet is related to the low- to medium temperature stage of HP-UHP metamorphism. The new garnet with high Y+HREE in the annuli was formed during the granulite facies event. The multicomponent diffusion modelling was applied to analyse the time-scale at which the rocks with prograde zoning garnet were subject of granulite facies overprint. Preservation of the prograde major component zoning in garnet is explained by syn-convergent exhumation of HP-UHP rocks at relatively low-temperatures in the subduction channel. This process led to partial resorption of garnet and trace element release into the matrix. After the HP-UHP rocks were exhumed to crustal levels within the accretionary complex, they were shortly heated in granulite facies conditions. The new garnet with Y+HREE annuli was formed due to its stabilization at high temperature conditions and availability of elements compatible in garnet. The process of granulite facies heating was caused by slab break-off that results in mantle upwelling and gabbro-norite intrusions into the accretionary complex together with bodies of HP-UHP rocks.

FAULT STRENGTH, EARTHQUAKE NUCLEATION, AND RUPTURE PROPAGATION IN CLAY-RICH FAULT ZONES

Faulkner D.R.*[1]
[1] Department of Earth, Ocean and Ecological Sciences - Rock Deformation Laboratory, University of Liverpool, United Kingdom
Corresponding email: faulkner@liv.ac.uk

Keywords: faults, friction, earthquakes

Many fault zones consist of a fault core that contains a high proportion of clay. The fault core accommodates the large majority of a fault's displacement and therefore is of interest for understanding fault strength, stability and permeability. Clay is known to have low frictional strength and the link between the clay mineralogy and strength is an area of active interest. High-pressure shearing experiments conducted with synthetic clay-rich gouges composed of pure, single phase clays using both water and argon as the pore fluid have helped to understand this link. The frictional strength appears to be related to two factors: (1) the strength of the interlayer bonds of the clay, and (2) the surface charge that influences the capacity to adsorb cations with their hydration shells. Absorption of water onto the mineral surfaces lowers the intergranular friction.

Clay-rich fault gouges also display velocity-strengthening frictional characteristics that imply that earthquake nucleation is not possible and stable fault creep is the most likely mode of failure over earthquake slip. Unstable slip requires the fault to weaken with slip at a rate greater than the rate of elastic unloading. In contrast to the evidence pointing away from earthquake nucleation, recent earthquakes, such as the 1999 M_w 7.6 Chi-Chi earthquake in Taiwan and the 2011 M_w 9.0 Tohoku-Oki earthquake in Japan suggest that rupture propagation through clay-rich faults is possible. Moreover, it may be enhanced for particularly energetic earthquakes, leading to large slip displacements. Results from experiments and modelling indicate that during rapid slip, physical processes such as thermal pressurization can overcome the constitutive frictional properties and weaken the fault such that instabilities can propagate. The low permeability of clay-rich gouges is a key factor as it can enhance the effect of thermal pressurization during rapid slip, leading to slip weakening. It appears that, although earthquake nucleation is not possible on clay-rich patches of faults, ruptures that propagate into these regions after nucleation elsewhere may be able to continue.

FLOW PROCESSES IN DEFORMATION BANDS DEVELOPED ON PLIO-PLEISTOCENE SOFT-ROCKS IN THE BAZA FAULT ZONE (S SPAIN)

García-Tortosa F.J.[1], Jimenez-Millan J.*[1], Abad I.[1], Faulkner D.R.[2], Martin-Rojas I.[3] & Alfaro P.[3]

[1] Departamento de Geología y Centro de Estudios Avanzados en Ciencias de la Tierra, Unidad Asociada al Instituto Andaluz de Ciencias de la Tierra, Universidad de Jaén, Spain

[2] Rock Deformation Laboratory, Department of Earth and Oceanic Sciences, University of Liverpool, United Kingdom

[3] Departamento de Ciencias de la Tierra y del Medio Ambiente, Universidad de Alicante, Spain

Corresponding email: jmillan@ujaen.es

Keywords: deformation bands, active faults, clay smearing

Deformation microstructures in m to cm-scale displacement faults offsetting soft-rocks sequences of interbedded carbonate, marls, sands, silts, gypsum and clays from an excavated trench in the Baza fault (Spain) have been examined. The Baza Fault lies in the Guadix-Baza Basin (Betic Cordillera). This 37-km long structure is a E-dipping active normal fault with a variable strike with N-S and NNW-SSE segments. The fault has associated instrumental and historical seismicity, the most important of which is the 1531 Baza earthquake, with more than 400 fatalities. The aim of this study is to carry out a petrographic characterization of the soft-rocks of the fault zone exposed in a trench in order to recognize particular microstructures and deformation mechanisms ocurring during seismic deformation. X-ray diffraction show that samples contain quartz, calcite, dolomite, feldspars, muscovite, paragonite, illite, smectite and gypsum. Polished blocks were studied by a Merlin Carl Zeiss Scanning Electron Microscopy. Three types of deformation bands were identified:

a) Disaggregation bands. At the coarser grain sized (50-200 µm) sediments made of quartz, calcite, dolomite and feldspars, bands up to 300 µm thick are characterised by granular flow processes such as grain rolling and grain boundary sliding. Grain scale mixing with silt sediments also occurs along discrete bands. Local grain cracking, increasing grain angularity and decreasing grain size, were also observed.

b) Phyllosilicate bands. Shear-induced rotation in sediments rich in coarse muscovite, paragonite and chlorite grains (up to 100 µm long) produce phyllosilicate alignment to form local fabric that can be considered as a particular type of disaggregation band where platy minerals promote frictional grain boundary sliding within the bands.

c) Clay smearing. Deformation of clay-rich sediments (illite, smectite) produces bands with reorientation, flow, and extrusion of clay minerals. Striations and slip surfaces are also sometimes observed. Many of these deformation bands show subsequent precipitation of gypsum.

Textural analysis suggests predominance of ductile deformation mechanisms in the studied fault soft-rocks. Petrograhic data revealed that shearing of sands and silt sediments could involve granular flow or local proto-cataclasis of grains. Phyllosilicate rich-sediments always present ductile deformation. The dominant deformation mechanism may be controlled by the mineral composition of the shear band and the water content. Incorporation of clays and water-rich sediments along shear bands may reduce shear strength.

MODELING [100] DISLOCATION GLIDE IN $MgSiO_3$ POST-PEROVSKITE UNDER D'' CONDITIONS

Goryaeva A.M.*[1], Carrez P.[1] & Cordier P.[1]
[1] Unité Matériaux et Transformations, Université Lille 1, Villeneuve d'Ascq, France
Corresponding email: alex.goryaeva@gmail.com

Keywords: post-perovskite, dislocations, D'' layer

Dislocation motion in crystalline materials represents one of the most efficient mechanisms to produce plastic shear, the key mechanism for CPO development. In case of $MgSiO_3$ post-perovskite (ppv) phase, stable at the core-mantle boundary (CMB) with P-T conditions in excess of 120 GPa and 2000 K, experimental observations of CPO produced in the diamond anvil cell are extremely challenging to perform. Alternatively, theoretical modeling of the ppv plasticity opens new perspectives to understand rheology of the deep mantle.

Atomistic simulations show $MgSiO_3$ ppv to be characterized by remarkably low lattice friction of 1 GPa opposed to the glide of straight [100] screw dislocations in (010), while glide in (001) requires almost 18 times larger stress values. In order to have an idea about real processes at the CMB, the effect of temperature should be taken into account. At finite temperature, dislocation glide occurs through nucleation and propagation of kink-pairs, i.e. dislocation does not move as a straight line, but partly bows out over the Peierls potential. This process is characterized by the kink-pair formation enthalpy ΔH_k which consists of three main contributions: positive increase in elastic energy ΔE_{el} (caused by increase in length of the dislocation line); positive contribution of the Peierls energy ΔW_P (resulting from the fact that a part of the dislocation line lies above the Peierls valley) and, finally, the negative contribution due to the work of the applied stress W_σ. Together, the last two terms contribute to the substrate enthalpy ΔH_P:

$$\Delta H_k = \Delta E_{el} + \Delta W_P - W_\sigma = \Delta E_{el} + \Delta H_P$$

We propose a theoretical study of a kink-pair formation mechanism for [100] screw dislocations in $MgSiO_3$ post-perovskite employing the line tension (LT) model (Seeger, 1984) in conjunction with atomistic modeling, i.e. both ΔE_{el} and ΔH_P terms are computed at atomic scale while combining *ab-initio* and pairwise potential simulation techniques. Within the LT model, a dislocation is considered as an elastic string on a periodic substrate and change in its elastic energy ΔE_{el} during the kink-pair formation is computed as the energy cost associated with the dislocation bowing out. The substrate enthalpy ΔH_P is calculated using Nudged Elastic Band (NEB) method (Henkelman et al., 2000) based on searching the minimum enthalpy path (MEP) between initial and final stable configurations.

The estimated ΔH_k gives an access to evolution of CRSS with temperature. Our results clearly demonstrate that at the lower mantle conditions ppv deforms in the athermal regime in contrast to the high-lattice friction bridgmanite deformed by climb only.

Henkelman, G, Uberuaga, B.P., Jónsson, H. (2000): A climbing image nudged elastic band method for finding saddle points and minimum energy paths. *J. Chem. Phys.*, **113**, 9901-9904.

Seeger, A. (1984): Structure and diffusion of kinks in monoatomic crystals. *in* "Dislocations", P. Veyssiere, L. Kubin & J. Castaing, eds., CNRS, Paris, 141-178.

ASSESSING THE MACROSCOPIC OLIVINE GRAIN GROWTH THROUGH THE MICROSCOPIC PHYSICAL PROPERTIES OF THE INTERGRANULAR MEDIUM

Hashim L.*[1], Gardés E.[2], Sifré D.[1], Morales L.F.G.[3], Précigout J.[1] & Gaillard F.[1]

[1] Institut des Sciences de la Terre d'Orléans, Centre National de la Recherche Scientifique, Orléans, France

[2] Centre de Recherche sur les Ions, les Matériaux et la Photonique, Grand Accélérateur National d'Ions Lourds, Caen, France

[3] Helmholtz Zentrum Potsdam, GFZ Deutsches GeoForschungsZentrum, Potsdam, Germany

Corresponding email: leila.hashim@univ-orleans.fr

Keywords: olivine grain growth, wetness, HP-HT experiments

Grain size in the Earth's mantle is a fundamental parameter that has crucial implications on large-scale processes, such as seismic wave propagation, the permeability and the rheology of rocks. However, grain size is constantly evolving with time, where static grain growth implies an increase of the average grain size whereas dynamic recrystallization contributes to its decrease. Static grain growth is most dominant in grain size-sensitive deformation regimes (i.e., diffusion creep and grain boundary sliding) and is classically defined by an Arrhenius equation of the form:

$$r_f^n - r_i^n = t \cdot k_0 \cdot \exp(-\{E_a\}/\{RT\})$$

with r_f and r_i, the final and initial grain radii, n the grain size exponent, t the experimental duration, k_0 a material-dependent factor and E_a the empirical activation energy for grain growth. These growth parameters are highly dependent on the value of the grain size exponent, which has considerable implications when extrapolating from laboratory to geological length and time scales. Here, we will show that there is no clear grain size exponent value that can be extracted from grain growth experiments and that this value must be fixed based on the appropriate theoretical background. We have therefore investigated static grain growth of olivine-rich mantle aggregates in an intergranular medium being dry, melt-bearing and water- oversaturated. Grain growth experiments were performed and modeled by considering different growth mechanisms (i.e., diffusion-limited and interface reaction-limited). We have established the dry olivine grain growth law from previously published experimental grain growth data at 1-atmosphere and high- temperature conditions. Grain growth rates for these samples are limited by silicon diffusion at grain boundaries through an effective width of 30 nm, which is a factor 30 larger than the structural grain boundary width. Grain growth experiments performed on melt- and water-bearing aggregates show, however, that they are significantly faster than for dry samples. They also indicate that they are comparable regardless of the liquid fraction (i.e. > 0%). This result implies that liquid-bearing olivine grain growth is limited by precipitation reactions at the crystal/liquid interface rather by diffusion through the liquid phase. We propose a general grain growth law, which takes into account dry grain boundaries as well as wetted grain- grain interfaces, through the contiguity and wetness parameters. We show that our unified grain growth law considerably deviates from classical empirically-derived Arrhenius laws, with critical differences at geological time scales. We expect that our law will help unravel physical properties that are dependent on processes happening at the grain boundary scale, such as rheology, diffusion or permeability.

IN SITU DEFORMATION OF OLIVINE IN THE TRANSMISSION ELECTRON MICROSCOPE: FROM DISLOCATION VELOCITY MEASUREMENTS TO STRESS-STRAIN CURVES

Idrissi H.[1], Bollinger C.[2], Cordier P.*[3] & Boioli F.[3]
[1] Electron Microscopy for Materials Science, Department of Physics, University of Antwerp, Belgium
[2] Bayerisches GeoInstitut, Universität Bayreuth, Germany
[3] Unité Matériaux et Transformations, Centre National de la Recherche Scientifique, Université de Lille 1, Villeneuve d'Ascq, France
Corresponding email: patrick.cordier@univ-lille1.fr

Keywords: dislocation, velocity, Transmission Electron Microscopy

There is a growing consensus to recognize that rheological law established for olivine at high-temperature (ca. > 1000°C) fail when extrapolated to low temperatures relevant for the lithospheric mantle. Hence it appears necessary to fit rheological laws against data at low temperatures where olivine tends to become more and more brittle. The usual approach consists in applying confining pressure to inhibit brittleness. Here we propose an innovative approach based on the use of very small samples and numerical modeling.

New commercial *in situ* TEM nanotensile testing equipment recently developed by Hysitron.Inc is combined with weak-beam dark-field TEM diffraction contrast imaging in order to obtain information on the elementary mechanisms controlling the plasticity of olivine: namely glide of [001] screw dislocations. The olivine tensile beams dedicated for *in situ* TEM nanomechanical testing were produced using microfabrication techniques based on MEMS-type procedures. The testing geometry was designed as to induce maximum resolved shear stresses on the [001](110) slip system. Under tensile loads between 2 and 3 GPa, ductile behaviour was reached with the development and propagation of dislocation loops across the sample allowing to measure the velocity of screw and non-screw dislocations as a function of stress. This information is introduced into a numerical model involving Dislocation Dynamics in order to obtain the stress-strain curves describing the mechanical response of olivine single crystals deformed in tension at room temperature.

XANES DETERMINATION OF EQUILIBRIUM AND DIFFUSIVE BEHAVIOUR OF Cr^{2+} AND Cr^{3+} IN SYNTHETIC FORSTERITE AND NATURAL OLIVINE AT 1400°C

Jollands M.C.*[1-2], O'Neill H.S.C.[1], Van Orman J.[3], Berry A.J.[1], Hermann J.[1-4], Newville M.[5] & Lanzirotti A.[5]
[1] Research School of Earth Sciences, Australian National University, Canberra, Australia
[2] Institute des Sciences de la Terre, Université de Lausanne, Switzerland
[3] Department of Geological Sciences, Case Western Reserve University, Cleveland, OH, USA
[4] Institut für Geologie, Universität Bern, Switzerland
[5] Center for Advanced Radiation Sources, University of Chicago, IL, USA
Corresponding email: michael.jollands@unil.ch

Keywords: diffusion, olivine, oxygen fugacity

The rate and mechanisms of Cr diffusion in olivine were studied at 1400°C as a function of fO_2 (over ~16 log units, buffered by CO-CO_2 gas mixes or air), chemical activity (using three-phase powder Cr sources of forsterite-protoenstatite-magnesiochromite or forsterite-periclase-magnesiochromite), crystallographic orientation (three principal axes) and olivine composition (both synthetic forsterite and natural San Carlos olivine). Elemental diffusion profiles were measured using laser ablation inductively coupled plasma mass spectrometry (LA-ICP-MS) and electron probe microanalysis (EPMA), with the valence state changes of Cr determined along some diffusion profiles using X-ray absorption near edge structure (XANES) spectroscopy.

Cr diffusion is highly anisotropic (fastest along the *c*-axis), and considerably faster in the presence of protoenstatite (high $aSiO_2$) than when periclase is present (low $aSiO_2$). Cr diffusion is faster as lower fO_2, whereas diffusive anisotropy is more extreme at higher fO_2. Diffusion of Cr is 1-2 orders of magnitude faster than Fe-Mg inter-diffusion in olivine under similar conditions. The concentration of Cr at the interface is higher at high $aSiO_2$ and low fO_2.

The valence state ratio of chromium ($Cr^{2+}/\Sigma Cr$, where $\Sigma Cr = Cr^{2+}+Cr^{3+}$) is not constant along diffusion profiles in pure forsterite; Cr is either oxidised or reduced during the diffusive process when buffered at low or high oxygen fugacity (fO_2), respectively. Therefore, the external fO_2 is not fully imposed on the crystal interior, the crystal effectively maintains an intrinsic fO_2. Natural olivine shows no such valence state change along experimental profiles, electron transfer is facilitated by Fe^{2+}/Fe^{3+} and therefore the Cr valence state ratio is always in equilibrium with the external fO_2.

Cr^{3+} always substitutes onto an octahedral site. At high silica activity ($aSiO_2$) Cr^{3+} uses M site vacancies for charge balance, whereas at low $aSiO_2$ the mechanism is "spinel-type", potentially charge balanced by Mg^{2+} on the tetrahedral site. Cr^{2+} substitutes directly for Mg^{2+}, forming defects. Several independent methods have been used to verify that the crystal-powder interfaces are at equilibrium: both the $Cr^{2+}/\Sigma Cr$ values at the crystal rims and absolute concentrations of Cr^{2+} and Cr^{3+} as a function of fO_2 support this assumption.

The geometry of Cr^{3+} profiles changes as a function of fO_2 from near 'error function' at high fO_2 to near linear at low fO_2, interpreted as a change in cation-vacancy binding energy.

PERMEABILITY CONTROL OF TRANSIENT SLIP WEAKENING DURING GYPSUM DEHYDRATION AND IMPLICATIONS ON SUBDUCTION ZONES

Leclère H.*[1], Faulkner D.R.[1], Wheeler J.[1] & Mariani E.[1]
[1] School of Environmental Sciences, University of Liverpool, United Kingdom
Corresponding email: henri.leclere@liverpool.ac.uk

Keywords: dehydration reaction, friction, permeability

The understanding of the influence of pore-fluid pressure and friction on stability of fault zones is of first order importance to unravel earthquake triggering. Here, the effects of dehydration reactions on hydraulic and mechanical properties of rock are analysed to better understand the conditions required to trigger earthquakes. Triaxial experiments are conducted using gypsum and a direct shear sample assembly allowing to maintain the normal stress constant and to measure permeability during sliding. The evolutions of shear stress, pore-fluid pressure and permeability are continuously measured throughout the experiment until dehydration reaction reached completion. Tests are conducted with temperature ramp from 70 to 150°C and with different effective confining pressures (50, 100 and 150 MPa) and velocities (0.1 and 0.4 $\mu m \cdot s^{-1}$). Results show that gypsum dehydration induces transient stable slip weakening that is controlled by pore-fluid pressure and permeability evolutions followed by unstable slip on fully dehydrated product. Microstructural analysis shows clear evidence of dehydrated product preferentially localized along Riedel shear structures. A conceptual model is then proposed to explain transient slip weakening during dehydration reactions incorporating the key role played by permeability, and to provide a framework to define the conditions required to trigger unstable events during dehydration reactions.

ELECTRON TOMOGRAPHY STUDY OF DISLOCATIONS IN OLIVINE SINGLE CRYSTALS

Mussi A.*[1], Cordier P.[1], Nzogang B.C.[1] & Demouchy S.[2]

[1] Unité Matériaux et Transformations, Centre National de la Recherche Scientifique, Université de Lille 1, Villeneuve d'Ascq, France

[2] Géoscience Montpellier, Centre National de la Recherche Scientifique, Université de Montpellier 2, France

Corresponding email: alexandre.mussi@univ-lille1.fr

Keywords: olivine, dislocations, electron tomography

The plastic deformation mechanisms of olivine under uppermost mantle conditions are still poorly known. This study will focus on the deformation mechanisms of olivine single crystals deformed around 1000°C and under a hydrostatic pressure of 300MPa. Two olivine single crystals have been deformed with the same orientation and strain rate conditions (Demouchy et al., 2013), but with different temperatures (PoEM9 at 806°C and PoEM8 at 1090°C). Below 1000°C (PoEM9), there are only [001] rectilinear dislocations with a screw nature (Mussi et al., 2014, 2015). Above 1000°C (PoEM8), [100] and [001] dislocations are present in the microstructure. Dislocations are curved and most of them exhibit complex 3D shape. In order to perform precise dislocation and interaction analyses, we need to get the 3D microstructure of dislocations. For that reason, we have conducted transmission electron tomography of dislocations (Barnard et al., 2006). The difficulty of this technique is to keep the dislocation contrast during all the acquisition. To do so, the diffraction vector which images the dislocations, must be perfectly aligned with the sample holder principal axis. The second difficulty is to get a homogeneous dislocation contrast during the tilted series acquisitions. The use of a small precession of the electron beam considerably reduces the contrast heterogeneity (Rebled et al., 2011). Electron tomography enables us to identify, in PoEM9, the [001]{110} and [001](100) slip systems and few collinear interactions between [001] dislocations. We have characterized, in PoEM8, the same slip systems than in PoEM9 for [001] and the [100](001) slip system. Collinear interactions between [001], collinear interactions between [100], and [10±1] junctions are noticed. Numerous dislocation segments are sessile.

Barnard, J.S., Sharp, J., Tong, J.R., Midgley, P.A. (2006): High-resolution three-dimensional imaging of dislocations. *Science*, **313**, 319.

Demouchy, S., Tommasi, A., Boffa Ballaran, T., Cordier, P. (2013): Low strength of Earth's uppermost mantle inferred from tri-axial deformation experiments on dry olivine crystals. *Phys. Earth Planet. Int.*, **220**, 37-49.

Mussi, A., Cordier, P., Demouchy, S., Vanmansart, C. (2014): Characterization of the glide planes of the [001] screw dislocations in olivine using electron tomography. *Phys. Chem. Minerals*, **41**, 537-545.

Mussi, A., Nafi, M., Demouchy, S., Cordier, P. (2015): On the deformation mechanism of olivine single crystals at lithospheric temperatures: an electron tomography study. *Eur. J. Mineral.*, **27**, 707-715.

Rebled, J.M., Yedra, L., Estrade, S., Portillo, J., Peiro, F. (2011): A new approach for 3D reconstruction from bright field TEM imaging: Beam precession assisted electron tomography. *Ultramicroscopy*, **111**, 1504-1511.

ATOMS ON THE MOVE: DEFORMATION-INDUCED TRACE ELEMENT REDISTRIBUTION IN ZIRCON REVEALED USING ATOM PROBE TOMOGRAPHY

Piazolo S.*[1], La Fontaine A.[2], Trimby P.[2], Harley S.[3], Yang L.[2], Armstrong R.[4] & Cairney J.M.[2]
[1] Centre of Excellence for Core to Crust Fluid Systems, Centre for Geochemical Evolution and Metallogeny of Continents & Department of Earth and Planetary Sciences, Macquarie University, Sydney, Australia
[2] Australian Centre for Microscopy & Microanalysis, University of Sydney, Australia
[3] School of Geosciences, University of Edinburgh, United Kingdom
[4] Research School of Earth Sciences, Australian National University, Canberra, Australia
Corresponding email: sandra.piazolo@mq.edu.au

Keywords: crystal-plastic deformation, atomprobe tomography, zircon

One of the fundamental assumptions when using mineral chemistry signatures to decipher geological processes is that trace elements diffuse negligible distances through the pristine crystal lattice in minerals. For example, the reliable use of the mineral zircon ($ZrSiO_4$) as a U-Th-Pb geochronometer and trace element monitor requires minimal radiogenic isotope and trace element mobility. Here, using atom probe tomography, we document the effects of crystal-plastic deformation on atomic-scale elemental distributions in a number of zircons deformed at a range of geological conditions. In all cases, zircons reveal trace element distributions that are significantly influenced by element mobility at the sub-micron to micron scale. Dislocations that move through the lattice accumulate U and other trace elements where the effectiveness of accumulation is element dependent. Pipe diffusion along dislocation arrays connected to a chemical or structural sink results in continuous removal of selected elements (e.g., Pb), even after deformation has ceased. However, in disconnected dislocations trace elements remain locked. As a result, not only absolute elemental content but also element ratios can be markedly changed by crystal-plastic deformation. Our findings have important implications for the use of zircon as a geochronometer, and highlight the importance of deformation and deformation structures on trace element redistribution in minerals and engineering materials.

Relevant publication: Piazolo, S., La Fontaine, A., Trimby, P., Harley, S., Yang, L., Armstrong, R., Cairney, J.M. (2016): Deformation-induced trace element redistribution in zircon revealed using atom probe tomography. *Nature Commun.*, **7**, 10490, DOI: 10.1038/ncomms10490.

NANOSCALE TRANSIENT POROSITY CONTROLS LARGE-SCALE METAMORPHIC FLUID FLOW

Plümper O.*[1], Botan A.[2], Los C.[3], Malthe-Sørenssen A.[2] & Jamtveit B.[2]
[1] Department of Earth Sciences, University of Utrecht, Netherlands
[2] Department of Physics - Physics of Geological Processes, University of Oslo, Norway
[3] Fachbereich Geowissenschaften, Universität Bremen, Germany
Corresponding email: o.plumper@uu.nl

Keywords: metamorphism, fluid flow, porosity

The reaction of fluids with rocks is fundamental for Earth's dynamics as they facilitate heat/mass transfer and induce volume changes, weaknesses and instabilities in rock masses that localize deformation enabling tectonic responses to plate motion. During these fluid-rock interactions it is the ability of a rock to transmit fluid, its permeability, that controls the rates of metamorphic reactions. However, although some geological environments (e.g., sediments) are open to fluids, the majority of solid rocks (e.g., granites, eclogites, peridotites, etc.) are nearly impermeable. Surprisingly though, even in rocks that are nominally impermeable widespread fluid-rock interactions are observed leading to the question: How can fluids migrate through vast amounts of nominally impermeable rocks? Here we investigate one of the most wide-spread fluid-mediated metamorphic processes in the Earth's crust, the albitization of feldspatic rocks. We show that fluid flow and element mobilization during albitization is controlled by an interaction between grain boundary diffusion and reaction front migration through an interface-coupled dissolution-precipitation process. Using a combination of focused ion beam scanning electron microscopy (FIB-SEM)-assisted nanotomography combined with transmission electron microscopy (TEM) reveals that the porosity is dictated by pore channels with a pore diameter ranging between 10 to 100 nm. Three-dimensional visualization of the feldspar pore network reveals that the pore channels must have been connected during the replacement reaction. Analysis of the pore aspect ratios suggests that a Rayleigh-Taylor-type instability associated to surface energy minimization caused the disconnection of the pore channels. Fluid transport in nanometer-sized objects with at least one characteristic dimension below 100 nm enables the occurrence of physical phenomena that are impossible at bigger length scales. Thus, on the basis of our microstructural investigations we used non-equilibrium thermodynamics and molecular dynamics simulations to investigate the influence of nanoscale pore transport phenomena on metamorphic mineral replacement reactions. Our findings suggest that fluid transport through nanoscale transient pore networks may control regional-scale metamorphism and metasomatism.

THERMODYNAMIC MODELLING OF SEPIOLITE: IMPLICATIONS FOR MECHANICAL BEHAVIOUR OF CRUSTAL FAULTS

Sánchez-Roa C.*[1], Vidal O.[2], Jiménez-Millán J.[1], Nieto F.[3] & Faukner D.R.[4]

[1] Departamento de Geología y Centro de Estudios Avanzados en Ciencias de la Tierra, Instituto Andaluz de Ciencias de la Tierra, Universidad de Jaén, Spain

[2] Laboratoire de Géodynamique des Chaînes Alpines, Université Joseph Fourier Grenoble, Centre National de la Recherche Scientifique, Grenoble, France

[3] Departamento de Mineralogía y Petrología, Instituto Andaluz de Ciencias de la Tierra, Universidad de Granada, Spain

[4] Rock Deformation Laboratory, Department of Earth and Ocean Sciences, University of Liverpool, United Kingdom

Corresponding email: catasroa@ujaen.es

Keywords: sepiolite, thermodynamic modelling, fault mechanics

A new thermodynamic model for sepiolite was developed and used to calculate its P-T stability conditions and water content for different bulk rock compositions. The standard state thermodynamic properties, entropy (S°) and enthalpy ($\Delta_f H^0$), were calculated according to the oxide summation method described in Holland (1989) for the S°, and Chermak & Rimstidt (1989) for $\Delta_f H^0$. The starting model was based on synchrotron XRD-data of sepiolite dehydration presented by Post et al. (2007). Their Rietveld refinement results show a dehydration following a step function that allowed us to define four end members in a theoretical sepiolite solid solution with decreasing water contents in their structure. Moreover, the model accounts for the different entropic and enthalpic contributions of three types of water present in the sepiolite structure: zeolitic water (water in the channels); bound water (water molecules completing the coordination of the Mg^{2+} atoms in the edges of the discontinuous octahedral layers) and the structural OH groups.

At high temperature, the stability field of sepiolite is limited by the reaction sepiolite → talc + quartz + H_2O, which occurs at about 325°C at 1 to 500 MPa. The large stability field of this mineral suggests that it could control the mechanical behaviour of crustal faults at depths depending on the geothermal gradient. The dehydration of sepiolite at temperatures lower than 300°C is modest compared to that occurring during its breakdown at 325°C, where 2 out of the 3.4 moles of water leave the structure to form the association talc + quartz; notably, the reaction of sepiolite breakdown involves a reduction of ~ 30% of the original volume. The interaction of the water released and the new porosity opened as a consequence of the volume decrease could have important implications on the stability of clay-bearing fault planes.

Chermak, J.A. & Rimstidt, J.D. (1989): Estimating the thermodynamic properties (ΔG^0_f o and ΔH^0_f) of silicate minerals at 298 K from the polyhedral contributions. *Am. Mineral.*, **74**, 1023-1031.

Holland, T.J.B. (1989): Dependance of entropy on volume forsilicates and oxyde minerals: a review and a predictive model. *Am. Mineral.*, **74**, 5-13.

Post, J.E., Bish, D.L., Heaney, P.J. (2007): Synchrotron powder X-ray diffraction study of the structure and dehydration behavior of sepiolite. *Am. Mineral.*, **92**, 91-97.

INTERPLAY BETWEEN CHEMICAL DIFFUSION AND DEFORMATION

Tajčmanová L.*[1], Moulas E.[1], Vrijmoed J.C.[1] & Zhong X.[1]
[1] Departement Erdwissenschaften, Eidgenössische Technische Hochschule, Zürich, Switzerland
Corresponding email: lucataj@gmail.com

Keywords: diffusion, deformation, coupling

Chemical zoning in minerals reflects variations in pressure (*P*), temperature (*T*) and chemical composition (*X*) along the path which the rock experienced. Therefore, it is important to correctly interpret and quantify such zoning. The extent of intra-granular diffusion is generally controlled by temperature, time and grain-size. However, since many crustal processes occur on a million-year timescale it is very unlikely to preserve chemical zoning at high temperatures given currently available data on diffusion rates.

In the classical view of metamorphic zoning, fast viscous relaxation (and therefore constant pressure) is assumed, with diffusion being the limiting factor in equilibration. Recently, we have focused on the other possible scenario – fast diffusion and slow viscous relaxation – and brings an alternative interpretation of chemical zoning found in high-grade rocks. The aim has been to provide insight into the role of mechanically maintained pressure variations on multi-component chemical zoning in minerals.

We found an inspiration in several specialized analyses of species segregation in biotechnology, chemical engineering and for deep-oil reservoirs that use an equilibrium formulation for calculating compositional gradients either under external forces such as gravity which may be responsible for the maintenance of a pressure gradient or due to an osmotic pressure difference through a semipermeable membrane. In these analyses, the principles of energy, momentum and mass conservation are followed. A geologically relevant application of the aforementioned approach is the calculation of mineral equilibria under mechanically-imposed grain-scale pressure variations.

Furthermore, a coupled model for chemical diffusion and mechanical deformation has been developed and applied to the chemically zoned binary plagioclase. The theory of coupling these two processes is developed in analogy to the studies of poroelasticity and thermoelasticity by applying the conservation of mass, momentum and energy and the constitutive relations derived from fundamental thermodynamic relations. The numerical results suggest two dominant mechanisms that account for the maintained chemical zoning, namely the diffusion-controlled, and mechanically-controlled mechanisms. The dominant mechanisms are controlled by a dimensionless number, the Deborah number, which is characterized by the ratio of the Maxwell characteristic time to the characteristic time of chemical diffusion.

DEFORMATION IN SERPENTINE-RICH SHEAR ZONES: FIELD OBSERVATIONS AND FRICTION OF MINERALOGICALLY-CONTROLLED SERPENTINES

Tesei T.*[1], Viti C.[2] & Collettini C.[3]
[1] Istituto Nazionale di Geofisica e Vulcanologia, Roma, Italy
[2] Dipartimento di Scienze Fisiche, della Terra e dell'Ambiente, Università di Siena, Italy
[3] Department of Scienze della Terra, Sapienza Università di Roma, Italy
Corresponding email: telemaco.tesei@ingv.it

Keywords: serpentines, friction, Elba Island

Serpentines are important constituents of tectonic mélanges associated to major faults, including subduction and strike-slip settings, ophiolites and oceanic core-complex detachments. Despite their abundance it is still unclear the role of serpentines in controlling fault zone structure and evolution, friction and seismogenesis.

Here we present field and microstructural investigation from the Monte Fico Ophiolitic shear zone (MFSZ) coupled with friction experiments on mineralogically controlled serpentines sampled from the same location, which has been identified with extensive optical and TEM investigation.

The compressive structures of MFSZ due to the obduction are characterized by a pervasive S/C fabric, in which the foliation is coated by well-developed slickenfibres of serpentine, suggesting a dominant deformation by dissolution-recrystallization creep and slow strain rates. The compressive shear zone is then cross-cut by normal faults accompanied by extensive brittle fracturing and localization, potentially associated with fast deformation.

Friction experiments were performed on almost monomineralic powdered samples of lizardite, antigorite, chrysotile + polygonal serpentine (from slickenfibres veins), and on powders of massive pseudomorphic serpentinites (mostly liz + chr) and massive interpenetrating serpentinite (atg) for comparison. Our data show that lizardite and chrysotile from the slickenfibres have very low friction ($\mu < 0.2$), lower than antigorite ($\mu \sim 0.5$). Consistently, mixtures of liz + chr from massive serpentinites are also weak ($\mu \sim 0.3$) with respect to atg-bearing serpentinites. Microstructural evidence suggests that the weakness of liz, chr and polygonal serpentine slickenfibre veins could be further enhanced due to preferred orientation of fibres and (001) lamellae, with possible frictional sliding along basal planes.

Our data suggest that the specific serpentine mineralogy and preferred crystal orientation control the strength of natural serpentinites and inherent weakness of serpentinite-bearing faults that can explain the apparent weakness of some major tectonic features such as the San Andreas fault and OCC detachments.

EXPERIMENTAL DUCTILE DEFORMATION OF POLYCRYSTALLINE OLIVINE AT 1000°C

Thieme M.*[1], Demouchy S.[1], Mainprice D.[1] & Barou F.[1]
[1] Geosciences Montpellier, Université de Montpellier & Centre National de la Recherche Scientifique, France
Corresponding email: Manuel.Thieme@gm.univ-montp2.fr

Keywords: experimental deformation, olivine, creep

As the major constituent of Earth's upper mantle, olivine significantly influences its physical and chemical properties. Therefore, to understand the coupling between Earth's brittle crust and the uppermost solid mantle (e.g. during movement of tectonic plates), one has to understand the plasticity of olivine. Since it is often unclear under which conditions natural samples of olivine-rich rock were deformed and since developed microstructure undergoes changes during rock uplift, it is vital to first examine the deformation of olivine in well-constrained laboratory experiments. In the past, deformation experiments were usually run until maximum finite strain and sample failure, leading to a sound understanding of olivine plasticity during steady-state deformation at high temperatures (> 1200°C). For the first time, we deform polycrystalline olivine for predefined values of finite strain (maximum 10%) to look at the microstructure evolution prior to reaching steady state.

Experiments were performed in axial compression in an internally heated gas-medium deformation apparatus (Paterson's press). Deformation was carried out at a temperature of 1000°C, a confining pressure of 300 MPa (±10 MPa) and a constant strain rate of $10^{-5}s^{-1}$, using sample sizes of more than 1.2 cm^3. Samples were subsequently characterized by high-resolution (submicron) electron backscatter diffraction (EBSD). Deformation of olivine at 1000°C is supposed to mostly activate [001] (*hk*0) slip systems. For each value of finite strain, we are planning to determine the density of dislocations, in which plane dislocations are gliding in and how they interact with each other (e.g. [100], [001] and entanglement). We will also investigate the role of disclinations in early microstructure evolution.

We have already performed two deformation experiments with finite strains of 1.5 and 2.6%, showing almost linear increase in applied stress and well reproducible stress-strain curves. Stress rises to 300 MPa at 1.6% of strain and 450 MPa at 2.6% of strain. Compared to previous data (2014; 900°C, 300 MPa, $10^{-5}s^{-1}$), initial stresses are similar, but stress increases more slowly due to a higher temperature of deformation.

We are planning to run more deformation experiments at 1000C and 1200°C, reaching finite strains of 1, 2.5, 5, 7.5 and 10%. Furthermore, we could use obtained data on dislocation densities to calibrate the KAM (kernel average misorientation) data filter available in the MTEX toolbox, allowing to infer dislocation densities directly from EBSD measurements of experimentally deformed polycrystalline olivine.

Session S9:

Inclusions in minerals as record of geological processes: new analysis methods and applications

Conveners:

Matteo Alvaro (Pavia – Italy)

Ross Angel (Padova – Italy)

Silvio Ferrero (Potsdam – Germany)

ORIENTATION RELATIONS OF Fe-Ti-OXIDE MICRO-INCLUSIONS AND THEIR HOSTS IN THE OCEANIC GABBRO

Ageeva O.*[1-2], Habler G.[1], Pertsev A.[2] & Abart R.[1]
[1] Department für Lithosphärenforschung, Universität Wien, Austria
[2] Institute of Geology of Ore Deposits, Petrography, Mineralogy & Geochemistry, Russian Academy of Sciences, Moscow, Russia
Corresponding email: olga.ageeva@univie.ac.at

Keywords: oceanic gabbro, Fe-Ti-oxide micro-inclusions, orientation relations

The shape and crystallographic orientation relations (CORs) of Fe-Ti-oxide micro-inclusions in plagioclase (Pl), clinopyroxene (Cpx) and amphibole (Am) host crystals in gabbro from the Vema lithospheric section of the Mid Atlanic Ridge were studied using electron backscatter diffraction (EBSD). Four types of inclusions are distinguished. The first three represent needle-shaped inclusions in Pl and Cpx. Type 1 is represented by an intergrowth of magnetite (Mt) and ulvospinel (Usp) with identical crystallographic orientation and with Usp-Mt phase boundaries parallel to the traces of {100}Usp and {100}Mt. Type 2 inclusions involve ilmenite (Ilm) besides Mt and Usp showing a rather complex microstructure with very fine lamellae of Ilm and Mt with up to vol. 10% porosity. Small-scale Ilm-Mt lamellae occur within transition zones between coarser grained Mt and Usp type 1 inclusions. Mt and Ilm of type 2 inclusions have phase boundaries parallel to {111}Mt, whereas in areas close to Usp the boundaries are oriented parallel to {100}Mt, and {100} of the adjoining Usp. The thin Mt lamellae have the same crystallographic orientation as the coarser grained Mt and Usp crystals. Type 3 inclusions consist of Ilm-Mt intergrowths with similar CORs as type 2 inclusions. The type 3 inclusions are, however, more coarse grained, and have lower porosity. Type 4 inclusions are single crystal Ilm plates, which are present as inclusions in Pl and Cpx and are the only Fe-Ti-oxide phase in Cpx-hosted amphibole lamellae.

Mt inclusions in Cpx show {110}Mt//(010)Cpx, and {111}Mt//(100)Cpx as well as subparallel to (-101)Cpx. The Mt needles are elongated in the direction perpendicular to (-101). Single crystal Ilm plates form inclusions with (100)Ilm//(010)Cpx and the pole of a (110)Ilm//[001]Cpx. Ilm inside of the Cpx-hosted amphibole lamellae in Cpx shows (100)Ilm//(010)Am, and (001)Ilm//(100)Am, where the latter coincides with the elongation of the Ilm plates.

The CORs between the inclusions and Pl are less strong. Most (80 %) of the Mt inclusions are oriented with (111)Mt//(1-50)Pl and corresponding (110)Mt//[001]Pl, which is also the direction of the Mt needle elongation. No systematic CORs between Ilm plates and Pl host have been observed.

The internal microstructure of type 1 inclusions is ascribed to exsolution of titanomagnetite. The other types may have resulted from the evolution of type 1 inclusions during subsequent events, supposedly due to high-temperature hydrothermal alteration (Pertsev at al., 2015). Ilm plates in amphibole lamellae within Cpx may have formed during redistribution of Ti during Cpx formation or alteration.

The observed microstructural and textural features indicate a complex, polyphase evolution of the Fe-Ti-oxide inclusions. An early stage of unmixing of Mt and Usp was probably related to cooling. Subsequent stages appear to be related to water-rock interaction leading to chemical alteration of the Fe-Ti-oxides and the surrounding host minerals.

Pertsev, A.N., Aranovich, L.Y., Prokofiev, V.Y., Bortnikov, N.S., Cipriani, A., Simakin, S.S., Borisovskiy, S.E. (2015): Signatures of residual melts, magmatic and seawater-derived fluids in oceanic lower-crust gabbro from the Vema lithospheric section, Central Atlantic. *J. Petrol.*, DOI: 10.1093/petrology/egv028

NANOGRANITOID INCLUSIONS IN HIGH-GRADE METAMORPHIC ROCKS

Bartoli O.*[1], Acosta-Vigil A.[1], Ferrero S.[2-3] & Cesare B.[1]
[1] Dipartimento di Geoscienze, Università di Padova, Italy
[2] Institut fur Geowissenschaften, Universitat Potsdam, Germany
[3] Museum fur Naturkunde, Leibniz-Institut fur Evolutions- und Biodiversitatsforschung, Berlin, Germany
Corresponding email: omar.bartoli@unipd.it

Keywords: nanogranitoids, peritectic mineral, crustal melting

Although melt inclusions (MI) are well known to igneous petrologists and have been extensively studied in intrusive and extrusive rocks, MI in crustal rocks that have undergone anatexis (migmatites and granulites) are a novel subject of research. They are generally trapped along the heating path by peritectic phases produced by incongruent melting reactions. Primary MI in high-grade metamorphic rocks are small, commonly 5-10 μm in diameter, and their most common mineral host is peritectic garnet. In most cases inclusions have crystallized into a cryptocrystalline aggregate and contain a granitoid phase assemblage (*nanogranitoid inclusions*) with quartz, K-feldspar, plagioclase and one mica or two depending on the particular circumstances. After their experimental remelting under high confining pressure, nanogranitoid MI can be analyzed combining several techniques (EMP, LA-ICP-MS, NanoSIMS, Raman). Up to now, the compositions of the trapped melt are granitic and metaluminous to peraluminous, and sometimes granodioritic, tonalitic and trondhjemitic, in agreement with the different P-T-a_{H2O} conditions of melting and protolith composition, and overlap those of experimental glasses produced at similar conditions. Being trapped along the up-temperature trajectory – as opposed to classic MI in igneous rocks formed during down-temperature magma crystallization – the fundamental information provided by nanogranitoid MI is the pristine composition of the natural primary anatectic melt for the specific rock under investigation. So far ≈ 600 nanogranitoid MI, coming from several occurrences from different geologic and geodynamic settings and ages, have been characterized. Although the compiled MI database should be expanded to other potential sources of crustal magmas, MI data collected so far can be already used as natural “starting-point” compositions to track the processes involved in formation and evolution of granitoid magmas.

MELT AND FLUID INCLUSIONS IN MANTLE XENOLITHS BENEATH THE RIFT SHOULDER (ADAM'S DIGGINGS) OF RIO GRANDE RIFT: EVIDENCES FOR METASOMATISM

Berkesi M.*[1], Park M.[1-2], Szabó C.[2], Jung H.[1] & Kil Y.[3]
[1] Lithosphere Fluid Research Lab, Eötvös Loránd University, Budapest, Hungary
[2] School of Earth and Environmental Sciences, Seoul National University, Seoul, Korea
[3] Department of Energy and Resources Engineering, Chonnam National University, Gwangju, Korea
Corresponding email: marta.berkesi@gmail.com

Keywords: Rio Grande Rift, mantle metasomatism, inclusion

The Rio Grande Rift (RGR) has been the subject of numerous studies in the last decades. Many papers focused on better understanding the metasomatic processes in the lithospheric mantle mainly based on the geochemical data on the rock-forming minerals. This work, however, aims to describe the melt and fluid generation that might have migrated at mantle depth and interacted with the peridotitic material causing metasomatism beneath Adam's Diggins area (AD). Five xenoliths, the richest in inclusions hosted by the orthopyroxene porphyroclasts, have been selected in this study. Core of the orthopyroxenes can be characterized with clinopyroxene and spinel lamellae as original exsolution phases together with high density CO_2-N_2 (0.98-1.12 g/cm^3) fluid inclusions that might have been present during the formation of lamellae. Exsolution lamellae are interpreted as having formed prior to xenolith ascent to the surface indicating a cooling event in the mantle beneath AD region. An evidence of the infiltration of an alkali and H_2O-bearing silicate-rich melt during this cooling event is documented by silicate melt inclusions (SMI) occurring along some part of the lamellae. We suggest that cooling could have been a rapid process as the presence of kumdykolite (metastable orthorhombic polymorph of albite) has been detected by Raman spectroscopy in the SMI. Volume percentages of the clinopyroxene and spinel lamellae in orthopyroxene were determined and, thus, paleo-temperatures (prior to the formation of the lamellae) and neo-temperatures (after the lamellae formation) were calculated. The difference between the two temperatures became to be ~ 130°C, which is in a good accordance with cooling history of the RGR by apatite fission track data (Ricketts et al., 2015).

Amphibole is also present as reaction product between the clinopyroxene and a silicate melt which melt is represented by the SMI. Furthermore, phases such as talc, amphibole, anhydrite, glass and phlogopite were also identified in the SMI by Raman spectroscopy and FIB-SEM. Major element composition of the latter phase in the SMI and in the rock is very close to one another indicating that the modal metasomatism in the mantle, resulted in the phlogopite formation, was caused by an alkai and H_2O-bearing high silica melt during decompression. A more evolved stage of the alkali-bearing high silica melt might have been entrapped in inclusions that crosscuts both the SMI and the lamellae and is rather fluid-rich. With this study we give a better insight into the characteristic of the possible metasomatic agents in the lithospheric mantle beneath AD region.

Ricketts, J.W., Kelley, S.A., Karlstrom, K.E., Schmandt, B., Donahue, M.S., van Wijk, J. (2015): Synchronous opening of the Rio Grande rift along its entire length at 25–10 Ma supported by apatite (U-Th)/He and fission-track thermochronology, and evaluation of possible driving mechanisms. *Geol. Soc. A. Bull.*, DOI: 10.1130/B31223.1

GENESIS AND EVOLUTION OF THE LATE MIOCENE MAGHREBIAN GRANITOIDS UNRAVELED THROUGH THE NANOGRANITES OF LA GALITE ARCHIPELAGO (TUNISIA)

Braga R.*[1], Ferrero S.[2-3], Wälle M.[4] & Remusat L.[5]

[1] Dipartimento di Scienze Biologiche, Geologiche e Ambientali, Universita di Bologna, Italy

[2] Institut für Geowissenschaften, Universität Potsdam, Golm, Germany

[3] Museum für Naturkunde, Leibniz-Institut für Evolutions- und Biodiversitätsforschung, Berlin, Germany

[4] Eidgenössische Technische Hochschule, Zürich, Switzerland

[5] Muséum National d'Histoire Naturelle, Institut de Minéralogie, de Physique des Matériaux et de Cosmochimie, Centre National de la Recherche Scientifique, Paris, France

Corresponding email: r.braga@unibo.it

Keywords: granitoids, crustal melting, fluid-melt immiscibility

The late Miocene granitoids of La Galite archipelago contain peritectic garnets with primary inclusions of granitic melt. Despite having originally trapped the same melt, such melt inclusions (MI) range from crystallized (nanogranites) to glassy. They coexist with COH fluid inclusions, thus suggesting fluid-melt immiscibility during partial melting at 800°C and 0.4-0.5 GPa (Ferrero et al., 2014). This melt is leucogranitic, almost peralkaline and metaluminous, with a protolith most likely magmatic, similarly to what proposed for other case studies of metaluminous nanogranites (see, e.g., Ferrero et al., 2016). Thus the investigation of these melt inclusions provides useful insights into the formation and evolution of the crustal end-member of the Maghrebian granitoids.

La Galite MI show trace element patterns similar to the upper continental crust and to peraluminous magmas found as MI in peritectic garnets from similar enclaves at El Hoyazo, Spain (Acosta-Vigil et al., 2010). These MI are however generally more enriched in some LILE (Cs, Rb), Li, Ta, U, as well as and some of the middle-REE such as Sm and Gd. The investigated melt shows higher Cs, Rb, Ti, V, Sc, Zn, Co than those resulting from muscovite melting (Acosta-Vigil et al., 2010). Such evidence suggests that biotite was the predominant OH-bearing phase consumed during melting, possibly along with a phase rich in Li and B (cordierite?). The involvement of some U-rich accessory phase cannot be ruled out.

Furthermore, NanoSIMS analyses provide an average content of 2 wt.% H_2O (n = 16). Such amount is consistent with the water content of a melt produced at 800°C / 0.4-0.5 GPa in presence of a CO_2-rich fluids, likely to lower the water activity in the melt, and thus this value can be considered as representative of the original water content. This is also supported by the presence in crystallized MI of relatively rare phases such as kumdykolite, kokchetavite and cristobalite - metastable polymorphs of albite, K-feldspar and quartz. Because of their highly metastable nature, any change of the system in which they occur, e.g., inclusion decrepitation, would have promoted their transformation into their thermodynamically stable polymorphs (Ferrero et al., 2016). Their occurrence can be thus considered as a mineralogical indicator of the preserved nature of La Galite nanogranites.

Acosta-Vigil, A., Buick, I., Hermann, J., Cesare, B., Rubatto, D., London, D., Morgan VI, G.B. (2010): Mechanisms of crustal anatexis: a geochemical study of partially melted metapelitic enclaves and host dacite, SE Spain. *J. Petrol.*, **51**, 785-821.

Ferrero, S., Ziemann, M.A., Angel, R.J., O'Brien, P.J., Wunder, P.J. (2016): Kumdykolite, kokchetavite, and cristobalite crystallized in nanogranites from felsic granulites, Orlica-Snieznik Dome (Bohemian Massif): not evidence for ultrahigh-pressure conditions. *Contrib. Mineral. Petrol.*, **171**, 3.

BUBBLE-BEARING MELT ICLUSIONS AS MINI MAGMA CHAMBERS TO STUDY MELT-VOLATILE EVOLUTION

Esposito R.*[1-2], Lamadrid H.M.[3], Redi D.[4], Steele-MacInnis M.[5], Bodnar R.J.[3], Manning C.E.[1], De Vivo B.[2], Cannatelli C.[2-6] & Lima A.[2]

[1] Department of Earth, Planetary, and Space Sciences, University of California, Los Angeles, CA, USA

[2] Dipartimento di Scienze della Terra, dell'Ambiente e delle Risorse, Università Federico II, Napoli, Italy

[3] Department of Geosciences, Virginia Tech, Blacksburg, VA, USA

[4] Dipartimento di Scienze Biologiche, Geologiche ed Ambientali, Università di Bologna, Italy

[5] Department of Geosciences, University of Arizona, Tucson, AZ, USA

[6] Department of Geology and Andean Geothermal Center of Excellence, Universidad de Chile, Santiago, Chile

Corresponding email: r.esposito@epss.ucla.edu

Keywords: magma degassing, Vesuvius, melt and fluid inclusions

Natural mafic melts emplaced in the Earth's crust exsolve dominantly CO_2-H_2O ± S fluids. Melt inclusions (MI) are aliquots of melts trapped in phenocrysts growing in the magma reservoir. Thus, MI provide the only direct method to analyze volatile contents of undegassed or partially degassed melts trapped at crustal depths. Melt inclusions often contain a bubble vapor when observed at ambient conditions. Bubble-bearing MI represent a natural lab to investigate the type of magmatic fluid that can directly exsolve from a silicate melt. Several studies (e.g., Esposito et al., 2011) reported CO_2 vapor in bubbles of mafic MI at room temperature (T) using Raman spectroscopy. Other recent studies (e.g., Moore et al., 2015) determined that most of the CO_2 in bubble-bearing MI hosted in mafic minerals is stored in the vapor bubble. Despite the detection of CO_2 in bubbles, the expected accompanying H_2O has not been found.

Recently, Esposito et al. (2016) reheated olivine-hosted MI from various eruptions at Mt. Somma-Vesuvius (Italy) spanning a range of time and eruptive style. We quenched bubble-bearing MI from high T (1143-1238°C) to produce a bubble-bearing glass at room T. Using Raman spectroscopy, we detected liquid H_2O at room T and vapor H_2O at 150°C in the vapor bubbles of reheated MI, in addition to CO_2. We speculate that the missing H_2O in bubbles in naturally quenched mafic MI was lost to the adjacent glass during local, sub-micron-scale devitrification prior to sample collection. Thus, we hypothesized that one is less likely to detect H_2O in the bubble of "older" MI. During MI heating experiments, the H_2O is redissolved into the melt and then exsolves from the melt into the vapor bubble, where it remains after quenching, at least on the relatively short time scales of our observations.

Our results suggest that a significant amount of H_2O may be stored in vapor bubbles of bubble-bearing MI. In most MI, the H_2O will be hosted in sub-micron scale hydrous phases at the interface between the bubble and the glass and will not be detected during routine analysis. In addition, we calculated that the composition of magmatic fluids directly exsolving from mafic melts associated the Mt. Somma-Vesuvius may contain up to 29 wt.% H_2O.

Esposito, R., Bodnar, R.J., Danyushevsky, L., De Vivo, B., Fedele, L., Hunter, J., Lima, A., Shimizu, N. (2011): Volatile evolution of magma associated with the Solchiaro eruption in the Phlegrean Volcanic District (Italy). *J. Petrol.*, **52**, 2431-2460.

Esposito, R., La Madrid, H., Redi, D., Steele-MacInnis, M.J., Bodnar, R.J., Manning, C.E., De Vivo, B., Cannatelli, C., Lima, A. (2016): Detection of liquid H_2O in vapor bubbles of reheated melt inclusions: implications for magamatic fluid composition and volatile budgets of magmas? Am. Mineral., in press.

Moore, L., Gazel, E., Tuohy, R., Lloyd, A., Esposito, R., Steele-MacInnis, M.J., Hauri, E.H., Wallace, P., Plank, T., Bodnar, R.J. (2015): Bubbles matter: An assessment of the contribution of vapor bubbles to melt inclusion volatile budgets. *Am. Mineral.*, **100**, 806-823.

MELT INCLUSIONS REVEAL IMMISCIBILITY IN THE UPPER ZONE OF THE BUSHVELD COMPLEX

Fischer L.A.*[1-2], Charlier B.[1-3], Namur O.[1], Roberts J.[4] & Holtz F.[1]
[1] Institut für Mineralogie, Leibniz Universität Hannover, Germany
[2] School of Physical Sciences, University of Tasmania, Hobart, Australia
[3] Départment de Géologie, Université de Liège, Belgium
[4] Department of Geology, University of Pretoria, South Africa
Corresponding email: l.fischer@mineralogie.uni-hannover.de

Keywords: immiscibility, layered intrusion, melt inclusion

The debate is ongoing regarding the formation of immiscible silicate liquids in the Upper Zone of the Bushveld Complex (South Africa), with different parties arguing that immiscibility either never occurred or occurred on a large-scale, with separation of iron- and silica-rich melts at the hundreds of meters scale.

We studied samples from the Bierkraal drill-cores 1 and 3, which cover the entire Upper Zone of the western limb in the Bushveld Complex. Apatite appears rhythmically over the 2 km-thick cumulate sequence in gabbros, troctolites and nelsonites. This mineral commonly contains various types of inclusions, with polycrystalline assemblages containing daughter phases (plagioclase, pyroxenes, amphiboles). Such inclusions are commonly interpreted to represent crystallized equilibrium melts trapped during the growth of apatite. Thus, they have the potential to record the composition of stable melts and therefore the immiscibility process.

In this study we investigated the petrography of polycrystalline inclusions and performed re-homogenization experiments of the inclusions for two selected Fe-Ti-oxide-bearing gabbros. Apatite grains were separated and re-equilibrated at 100 MPa in the temperature range 1060-1100°C using an internally heated pressure vessel. Analyses of major elements were performed with an electron microprobe. Elemental maps of unheated inclusions were obtained with an FE-SEM and used for petrographic description.

Re-homogenized quenched melts cover a wide range of compositions with two presumable end-members that are iron-rich (~35 wt.% FeO; ~28 wt.% SiO_2) and silica-rich (~5 wt.% FeO; ~65 wt.% SiO_2). The compositional range of melt inclusions is typical for immiscible products expected in ferrobasalts and support unmixing of iron- and silica-rich liquids during the crystallization of the Upper Zone of the Bushveld Complex. Immiscible melts from a single stratigraphic location display a range of compositions suggesting that immiscible melts were trapped in apatite at different temperatures along the binodal surface during cooling. Our results indicate that the immiscible process occurred most likely at the scale of layers (50-200 m). Sorting of immiscible melt droplets in the crystal mush possibly resulted in the formation of Fe-Ti-P-rich layers within the Upper Zone (Fischer et al., 2016) but there is no evidence for a perfect separation between mafic and felsic end members at a larger scale.

Fischer, L.A., Wang, M., Charlier, B., Namur, O., Roberts, R.J., Veksler, I.V., Cawthorn, R.G., Holtz, F. (2016): Immiscible iron-and silica-rich liquids in the Upper Zone of the Bushveld Complex. *Earth Planet. Sci. Letters*, **443**, 108-117.

DIAMONDS-BEARING FLUID INCLUSIONS REVEAL CARBON SPECIATION AND SOLUBILITY IN SUBDUCTION ZONE FLUIDS

Frezzotti M.L.*[1]

[1] Dipartimento di Scienze dell'Ambiente, del Territorio e di Scienze della Terra, Università di Milano-Bicocca, Italy

Corresponding email: maria.frezzotti@unimib.it

Keywords: fluid inclusions, carbon, diamond

Fluid inclusions in nodules and boudinaged layers of Mn-rich garnetites from Lago di Cignana tectonic Unit, in Western Alps, preserve a C-saturated (i.e., diamond) oxidized C-O-H fluid phase released during deep oceanic subduction at P ≥ 3.2 GPa, and T of about 600°C (Frezzotti et al., 2011). Since fluid inclusions were formed in metasediments rich in carbonates, their investigation is relevant to studies of carbon in slab fluids in equilibrium with diamonds. Primary fluid inclusions in garnet are dominantly aqueous, and contain Mg-calcite/calcite, quartz, rutile, paragonite, ± diamond, ± dawsonite, ± rhodocrosite, ± hydrous Mg-carbonate and sulfate daughter phases, which all together represent remnants of an oxidizing fluid after diamond crystallization. Dissolved carbon species in H_2O include bicarbonate carbonate, sulfate, ions, and H_4SiO_4 monomers. Concentrations are calculated greater than 0.016 for HCO^{3-}, 0.002 for SO_4^{2-}, and 0.006 for CO_3^{2-} in mol/kg H_2O, respectively, at laboratory conditions. In contrast, CO_2 gas molecules are not a major species in aqueous fluids. Since fluid inclusions contain significant amounts of dissolved silica, it is possible that subduction fluids might have been at conditions above the second critical endpoint. Carbon precipitation by excess concentration from rock-buffered C-O-H oxidized fluids appears as the relevant mechanism for diamond formation, since an origin by graphite conversion would be impeded by the high kinetic barrier necessary to break sp^2 bonds and to fix sp^3 C symmetry at the considered P-T conditions. Metamorphic fluids trapped as inclusions indicate that carbon can be efficiently transferred to the mantle by oxidized subduction fluids throw dissolution reactions at high pressure along a cold subduction geotherm.

Frezzotti, M.L., Selverstone, J., Sharp, Z.D., Compagnoni, R. (2011): Carbonate dissolution during subduction revealed by diamond-bearing rocks from the Alps. *Nature Geosci.*, **4**, 703-706.

Frezzotti, M.L., Huizenga, J.M., Compagnoni, R., Selverstone, J. (2014): Diamond formation by carbon saturation in C-O-H fluids during cold subduction of oceanic lithosphere. *Geochim. Cosmochim. Acta*, **143**, 68-86.

USING HOST-INCLUSION CRYSTALLOGRAPHIC ORIENTATION RELATIONSHIPS TO EXTRACT PETROLOGICAL INFORMATION: NEW INSIGHTS FROM LARGE EBSD DATASETS

Griffiths T.A.*[1], Habler G.[1] & Abart R.[1]
[1] Department für Lithosphärenforschung, Universität Wien, Austria
Corresponding email: th.griffiths@univie.ac.at

Keywords: inclusions, EBSD, crystallographic orientation relationships

Crystallographic orientation relationships (CORs) between crystalline inclusions and their hosts are commonly used to help decipher inclusion origins. To reliably interpret host-inclusion CORs it is essential to first obtain a representative picture of inclusion crystallographic orientations relative to the host. Electron backscatter diffraction (EBSD) allows acquisition of much larger COR data sets from larger sample domains than transmission electron microscopy while retaining the ability to tie orientation information to individual inclusions.

We present data from inclusion-rich metapegmatite garnets from the Koralpe region of the eastern Alps, Austria (Griffiths et al., 2016). Using this dataset of rutile (N = 250), corundum (N = 180) and ilmenite (N = 100) inclusions as an example, we show that small datasets likely obscure the true nature and variety of CORs present in a system. Furthermore, this and other EBSD studies of host and inclusion orientations (e.g., Proyer et al., 2013; Xu et al., 2015) reveal that the concept of CORs as always being "specific" (i.e., requiring host and inclusion orientations to be completely fixed relative to each other) is inadequate to describe the full variety of CORs that can exist. We introduce the concept of "statistical" CORs to describe situations where inclusion orientations have one or two orientational degrees of freedom relative to the host, but nonetheless reflect host crystal symmetry. Statistical CORs have two end member characteristics: "rotation" and "dispersion".

The recognition of multiple specific and statistical CORs developed between the same pair of phases in one sample provides several new COR characteristics that can be compared. These include the relative frequency of particular CORs and the amount of rotation and/or dispersion of statistical CORs. A survey of literature data (including our new results) for rutile inclusions in garnet shows that differences in these parameters exist for samples with different P-T histories and inferred formation mechanisms. If the mechanisms responsible for these differences can be understood, EBSD measurements of host-inclusion CORs could potentially deliver detailed information about inclusion origins and the P-T history of host-inclusion systems.

Griffiths, T.A., Habler, G., Abart, R. (2016): Crystallographic orientation relationships in host–inclusion systems: New insights from large EBSD data sets. *Am. Mineral.*, **101**, 690-705.

Proyer, A., Habler, G., Abart, R., Wirth, R., Krenn, K., Hoinkes, G. (2013): TiO_2 exsolution from garnet by open-system precipitation: evidence from crystallographic and shape preferred orientation of rutile inclusions. *Contrib. Mineral. Petrol.*, **166**, 211-234.

Xu, H., Zhang, J., Zong, K., Liu, L. (2015): Quartz exsolution topotaxy in clinopyroxene from the UHP eclogite of Weihai, China. *Lithos*, **226**, 17-30.

MULTIPHASE SOLID INCLUSIONS IN DIAMOND-BEARING GNEISSES DOCUMENT DIFFERENT STYLES OF MELTING DURING SUBDUCTION AND EXHUMATION

Hermann J.*[1] & Stepanov A.S.[2]
[1] Institut für Geologie, Universität Bern, Switzerland
[2] Centre of Excellence in Ore Deposits, Australian Research Council, University of Tasmania, Hobart, Australia
Corresponding email: joerg.hermann@geo.unibe.ch

Keywords: subduction, melting, UHP metamorphism

Multiphase solid inclusions were found in garnet from a migmatitic, gneiss of the Kokchetav massif (Kazakhstan) that displays the peak metamorphic assemblage of garnet, coesite, phengite, zircon and rutile and was metamorphosed at ultrahigh pressure (UHP) conditions of 5 GPa and 1000°C. A first generation of inclusions occurs at the centre of large garnet in the melanosome of the gneiss. A second generation of inclusions was found in garnet within the leucosome of the sample. Inclusions display negative crystal shapes and are filled by a large variety of major and accessory minerals that don't display any equilibrium textures. Major and trace element concentrations obtained by analysing the entire inclusions by LA-ICP-MS displayed enormous scatter due to the irregular distribution of trace element-rich accessory phases.

In order to homogenise the multiphase solid inclusions, piston cylinder experiments were conducted, where separated garnets were placed in a hydrous kyanite-quartz matrix and heated to 1000°C at 2 GPa for half an hour. The smallest inclusions melted to clean glass. The composition of these glasses was different from matrix glass that developed outside the garnets, providing evidence that the inclusions remained isolated during the homogenisation process. The glass of the homogenised inclusions was analysed by electron microprobe and LA-ICP-MS. Care is required in the interpretation of these analyses because of garnet-glass interactions. Only elements with low concentrations in the host mineral, such as LREE, Th, U, K, Rb, Cs, Ba, Sr and Nb in the case of garnet, can be preserved in the high temperature melt inclusions.

Inclusions trapped in melanosome garnet are characterised by high concentrations of LREE, Th and U, indicating complete dissolution of monazite at peak conditions of T ≈ 1000°C, P ≈ 5 GPa. Extraction of these melts resulted in a pronounced depletion of the Kokchetav gneisses in those elements. Large ion lithophile elements (LILE) are only moderately enriched in the melt and a significant portion is retained in residual phengite. Nb concentration in melts (27 ppm) is about double than in the restite (15 ppm), indicating slightly incompatible behaviour during UHP anatexis despite the presence of residual accessory rutile and phengite. Inclusions in garnet from the leucocratic part of the rock are characterised by low LREE, Nb and high U and represent late melts formed during exhumation at 650-750°C and crustal pressures.

The composition of UHP melts with moderate enrichment in LILE, no depletion in Nb and extreme enrichment in LREE and Th is remarkably different from the trace element signature of arc basalts arguing against involvement of melting subducted continental crust in the generation of arc magmas. The trace element patterns of melts from UHP anatexis as observed in the Kokchetav massif resemble most shoshonitic alkaline igneous rocks, which are common in collisional settings.

MICRODIAMONDS AND PIEZOBAROMETRY: POLYCRYSTALLINE AND MULTIPHASE INCLUSIONS REVEALED BY FIB-TEM

Jakubová P.*[1], Kotková J.[1-2] & Wirth R.[3]
[1] Institute of Geosciences, Masaryk University, Brno, Czech Republic
[2] Czech Geological Survey, Prague, Czech Republic
[3] Chemie und Physik der Geomaterialien, Helmholtz Zentrum Potsdam, GFZ Deutsches GeoForschungsZentrum, Potsdam, Germany
Corresponding email: petra.jakubova13@gmail.com

Keywords: microdiamond, FIB-TEM, piezobarometry

North Bohemian microdiamonds first documented by Kotková et al. (2011) and reaching 10-30 microns in size appear to be well preserved, without any graphite associated. The diamonds have been examined using FIB-TEM in order to characterize on micro to nano-scale their morphology, internal structure, growth/dissolution features, and last, but not least diamond-host interface, and also composition of diamond-forming media potentially preserved in inclusions and interstitial spaces.

Octahedral diamond enclosed in kyanite in the acid rock, and diamond of cuboid shape within garnet and zircon in the intermediate rock have been studied. Diamonds in kyanite are single grains with closed and straight boundaries and only several steps interpreted as growth feature. Both cavities and resorption features are very rare. On the other hand, the outstanding feature of Dia in Grt and Zrn is their polycrystalline character and close association with other phases such as quartz and rutile, which altogether create a grain which was supposed to be one and only diamond grain. Irregular but straight boundaries towards host phase, cavities or gaps are characteristic of the diamond-zircon and diamond-garnet interface. Zig-zag boundary of polycrystalline diamonds both in garnet and zircon as well as interstitial spaces contain an amorphous quenched fluid/melt with composition similar in both of the rock types. We interpret this interface, delimited by {111} crystal faces, as a result of diamond resorption by residual fluids. Moreover, a very thin layer of both ordered and disordered graphite has been detected at diamond-host interfaces of each Dia type.

“Overpressure” in Dia in Grt and Ky and “underpressure” in Dia in Zrn have been revealed by micro-Raman. The excess pressure in Dia enclosed in softer garnet and kyanite can be attributed to elastic resetting at high T and lower P (Angel et al., 2015). This is a plausible explanation for preservation of residual pressure in diamond in our rocks as they were exhumed along a “hot”, adiabatic P-T path (Haifler & Kotková, 2016).

Inclusion piezobarometry for cubic, i.e., elastically isotropic Dia in Grt is a reliable method to determine possible entrapment pressure and temperature from the combination of the equations of state of the two phases with measurement of the residual stress in the inclusion (Angel et al., 2015). However, this method works for single grains of one phase, which does not have to be the case. Our study shows, that attention to the character of the enclosed phases has to be paid.

Angel, R.J., Nimis, P, Mazzucchelli, M.L., Alvaro, M., Nestola, F. (2015): How large are departures from lithostatic pressure? Constraints from host-inclusion elasticity. *J. Metam. Geol.*, **33**, 801-813.

Haifler, J. & Kotková, J. (2016): UHP-UHT peak conditions and near-adiabatic exhumation path of diamond-bearing garnet-clinopyroxene rocks from the Eger Crystalline Complex, North Bohemian Massif. *Lithos*, **248-251**, 366-381.

Kotková, J., O’Brien, P.J., Ziemann, M.A. (2011): Diamond and coesite discovered in Saxony-type granulite: solution to the Variscan garnet peridotite enigma. *Geology*, **39**, 667-670.

PETROGRAPHIC AND FLUID INCLUSION STUDY OF BADENIAN SALT ROCKS FROM THE TRANSYLVANIAN BASIN (ROMANIA)

Kátai O.R.*[1], Tóth A.[1-2], Káldos R.[1] & Szabó C.[1]

[1] Lithosphere Fluid Research Lab, Department of Petrology and Geochemistry, Eötvös Loránd University, Budapest, Hungary

[2] Environmental Science Department, Sapientia Hungarian University of Transylvania, Cluj-Napoca, Romania

Corresponding email: kataiorsolya@yahoo.com

Keywords: salt, microstructure, fluid inclusion

The evaporites in the Transylvanian Basin had formed during the event known as the Badenian Salinity Crisis (BSC), which started 13.82 Ma (Peryt et al., 2006). In the shallower parts of the basin gypsum was deposited, whereas in deeper parts salt deposits formed. Primarily the salt thickness was around 300 meters, the present dimensions in diapirs (e.g., 1.2 x 1.4 x > 2 km in the Praid Basin) is due to the salt tectonics (Krézsek & Bally, 2006). In this study we selected the Praid (part of the Eastern Diapiric Belt) and Dej (part of the Western Diapiric Belt) diapirs to provide a comprehensive petrographic description of the salt rock and a detailed fluid inclusion studies in order to insight into the evolution history of the salt formations in the Transylvanian Basin.

According to petrographic study of salt rock by considering the grain size and morphology of the grain boundaries of halite crystals, four types of textures can be distinguished: primary euhedral, oriented euhedral, inequigranular sutured mosaic and inequigranular polygonal mosaic. In halite grains randomly distributed solid (crystal) inclusions (e.g., dolomite, anhydrite, pyrite, quartz, albite and mica) were identified by Raman spectroscopy. Beside crystal inclusions, large number of fluid inclusions trapped in halite were identified. Based on petrographic observations, two fluid inclusion associations can be distinguished: 1) negative crystal shaped, one phase (i.e. liquid, at room temperature) fluid inclusions appearing in growth zones (forming chevron structures) or randomly distributed in halite that are considered as primary fluid inclusions entrapped during crystallization of the halite, and 2) negative crystal, spherical or irregular shaped fluid inclusions, usually containing two-phases (i.e. liquid+vapor, at room temperature) and situated along healed cracks are considered as secondary ones. High-resolution (HR) Raman spectroscopic measurements were performed to study the fluid compositions. Primary, one phase (liquid) inclusions are aqueous fluid inclusions with high salinity (32-40 wt. % NaCl eq.). Secondary two-phase (liquid+vapor) fluid inclusions are also aqueous fluid inclusions however, their vapor phase contain CH_4, N_2 and CO_2. Based on microthermometric measurements, the liquid phase of the secondary fluid inclusions contain Mg^{2+} and Ca^{2+} ions besides Na^{+}.

The salt textures together with the fluid inclusion petrography show a complex deformation history of the salt deposits. The presence of the CH_4, CO_2 and N_2 only in the secondary fluid inclusions indicates that these components were added to the system during deformation event(s) after the salt formation. Further study of these salt samples extended to other sampling sites can be an important tool in the study of salt formation and the diapir forming processes in the Transylvanian Basin.

Krézsek, C. & Bally, A.W. (2006): The Transylvanian Basin (Romania) and its relation to the Carpathian fold and thrust belt: Insights in gravitational salt tectonics. *Marine Petrol. Geol.*, **23**, 405-442.

Peryt, M.T. (2006): The beginning, development and termination of the Middle Miocene Badenian salinity crisis in Central Paratethys. *Sediment. Geol.*, **188-189**, 379-396.

HIGHLY OXIDISED MAJORITIC INCLUSIONS IN DIAMOND

Kiseeva E.S.*[1], Vasiukov D.M.[2-3], Wood B.[1], Stachel T.[4], McCammon C.A.[2], Chumakov A.[5], Harris J.W.[6] & Dubrovinsky L.[2]

[1] Department of Earth Sciences, University of Oxford, United Kindgom
[2] Bayerisches Geoinstitut, Universität Bayreuth, Germany
[3] Lehrstuhl für Kristallographie, Universität Bayreuth, Germany
[4] Department of Earth and Atmospheric Sciences, University of Alberta, Edmonton, Canada
[5] European Synchrotron Radiation Facility, Grenoble, France
[6] School of Geographical and Earth Sciences, University of Glasgow, United Kingdom
Corresponding email: kate.kiseeva@earth.ox.ac.uk

Keywords: majoritic inclusions in diamonds, Synchrotron Mössbauer source, ferric/ferrous ratios

Inclusions in diamond from the mantle transition zone (410-660 km) provide a window into processes in the deeper parts of the upper mantle. Majoritic garnet is a rare inclusion (to date only ~ 150-200 crystals have been reported) but its Si content is indicative of its depth of re-equilibration and it therefore has the potential to provide a depth profile of composition and properties such as oxidation state in the transition zone. Majorites are complex in composition containing a range of minor elements (Na, Ti, Mn, Cr, K) that could be used to characterise the composition and, more importantly, the origin of the source material from which garnet has crystallised. For example, Kiseeva et al. (2013, 2016) showed that the compositions of a large fraction of majoritic inclusions are consistent with derivation from pyroxenite lithologies rather than from volumetrially dominant peridotitic or eclogitic source rocks. They suggested that these unusual compositions are related to the diamond-forming process. Tappert et al. (2005) showed that diamonds enclosing majorites in the Jagersfontein kimberlite (South Africa) had likely inherited their negative $d^{13}C$ isotopic compositions from organic matter present in a subducting slab.

In this study, we have determined the ferric-ferrous ratios of five small (30 to 100 micrometers in diameter) majoritic inclusions in diamonds from Jagersfontein by using a new technique – the Synchrotron Mössbauer Source (SMS) (beamline ID18 at ESRF). These inclusions were initially analysed using X-ray diffraction at the Extreme Conditions Beamline (ECB), P02.2, at PETRA III and confirmed as single crystals. This observation rules out any contamination by Fe^{3+} from another phase(s). The Fe^{3+} content of the majoritic garnets is substantially higher than values observed in upper mantle garnets and ranges between 15 and over 40% of ferric iron relative to total iron.

The Fe^{3+}/Fe^{2+} ratio of mantle minerals has been commonly used to determine the oxidation state of the mantle. According to experimental data and thermodynamic calculations, with increasing depth, fO_2 should decrease at constant Fe^{3+}/Fe^{2+} ratio (Wood et al., 1990), driving carbonate into the diamond stability field. Carbonate would therefore be unstable and should oxidise Fe^{2+} into Fe^{3+}, with the latter dissolving into garnet according to reactions such as:

$$4\ Fe_2SiO_4 + 2\ FeSiO_3 + CO_2 = 2\ Fe_3^{2+} + Fe_2^{3+}Si_3O_{12} + C$$

This reaction implies that garnet in equilibrium with carbon (in the form of diamond) should have elevated Fe^{3+}/Fe^{2+} ratios, consistent with our new observations. To our knowledge, these are the first data bearing on the oxidation state of majoritic garnets derived from the mantle transition zone.

Our results show that the mantle transition zone is highly heterogeneous and that the diamond-forming process is intimately linked with the oxidation state of garnet according to the reaction proposed above.

Kiseeva, E.S., Yaxley, G.M., Stepanov, A.S., Tkalčić, H., Litasov, K.D., Kamenetsky, V.S. (2013): Metapyroxenite in the mantle transition zone revealed from majorite inclusions in diamonds. *Geology*, **41**, 883-886.

Kiseeva, E.S., Wood, B.J., Ghosh, S., Stachel, T. (2016): The pyroxenite-diamond connection. *Geochem. Persp. Letters*, **2**, 1-9.

Tappert, R., Stachel, T., Harris, J.W., Muehlenbachs, K., Ludwig, T., Brey, G.P. (2005): Diamonds from Jagersfontein (South Africa): messengers from the sublithospheric mantle. *Contrib. Mineral. Petrol.*, **150**, 505-522.

Wood, B.J., Bryndzia, L.T., Johnson, K.E. (1990): Mantle oxidation state and its relationship to tectonic environment and fluid speciation. *Science*, **248**, 337-345.

MICRO-NANOMINERAL ENSEMBLES – INDICATORS OF FORMATION AND DIRECT EVIDENCES OF VARIOUS TYPES OF GOLD ORES (UZBEKISTAN)

Koneyev R.*[1]

[1] Department of Geochemistry, Mineralogy and Petrography, National University of Uzbekistan, Tashkent, Uzbekistan

Corresponding email: ri.koneev@gmail.com

Keywords: nanoensembles, gold, indicators

All minerals endure a nanostate at the crystallization stage and many of them remain “dwarfs”. This applies particularly to the elements, the average content of which constitutes to ppm-ppb (Au, Ag, Pt, Pd, Te, Se, Bi, Sb and others) in the earth's crust and industrial ores. Small size (n-0.0n μm) results the appearance of size effects associated with the increase of the specific surface energy. The temperature of phase transitions and interphase distribution of elements fluctuate. Due to this, micro-nanominerals are constantly non-stoichiometric, and solid solutions become unstable. They usually allocate in the matrix-minerals – pyrite, arsenopyrite, galena etc. (Koneyev, 2006).

Long-term studies of ores of epithermal and orogenic gold deposits in Uzbekistan has shown that each type of mineral is characterized by certain nanomineral ensembles and gold compounds (Koneyev et al., 2011):

Au-As, pyrite-arsenopyrite: (FeAuAsS), cobaltite, nickeline, loellingite, gersdorffite.

Au-Bi-Te, bismuth-telluride: maldonite, pilsenite, hedleyite, tellurobismuthite, joseite, ingodite, tetradymite.

Au-Ag-Te, gold-silver-telluride: calaverite, petzite, sylvanite, altaite, tellurantimony, coloradoite.

Au-Ag-Se, silver-selenide-sulfosalt: electrum, kustelite, petrovskaite, fishesserite, dyscrasite, polybasite, pyrargyrite, stephanite, freibergite, naumannite, aguilarite.

Au-Ag-Sb, antimonite-sulfoantimonite: aurostibite, boulangerite, bournonite, zinkenite, gudmundite, owyheeite, semseyite, chalcostibite.

Au-Hg, orpiment-cinnabar: amalgam Au, kongsbergite, schwatzite.

All types are usually combined in ores, but there are 2-4 types, including pyrite-arsenopyrite, determine the industrial resource. Some of the types correspond to the standard range of vertical geochemical and mineral zonation of mineral deposits, associations and micro-nanoensembles, therefore they apply to a natural disposition (Shneyderhen, 1952). Such information can be used in research and evaluation of hidden gold mineralization.

Acknowledgements: The research was supported by F8-17 grant and “Center of High Technologies”, Uzbekistan.

Koneyev, R.I. (2006): Nanomineralogy of gold epithermal deposits in the Chatcal-Kurama region (Uzbekistan). Delta, Sankt-Petersburg, 218 p.

Koneyev, R.I., Khalmatov, R.A., Mun, Y.S. (2011): Nanomineralogy and nanochemistry of ores from gold deposits of Uzbekistan. *Geol. Ore Dep.*, **52**, 755-766.

Shneyderhen, G. (1952): Ore deposits. IL, M., 501 p.

KINOSHITALITE-BEARING MULTIPHASE INCLUSIONS – CRUSTAL CONTAMINATION OF THE MANTLE

Kotková J.*[1-2] & Čopjaková R.[1-2]
[1] Laboratory of Mineralogy and Special Methods, Czech Geological Survey, Prague, Czech Republic
[2] Department of Geological Sciences, Masaryk University, Brno, Czech Republic
Corresponding email: jana.kotkova@geology.cz

Keywords: kinoshitalite, multiphase solid inclusions, peridotite

Garnet peridotites are commonly associated with high-pressure (HP) granulites of the European Variscan belt. Discovery of microdiamond enclosed in garnet, kyanite and zircon in crustal rocks with HP granulite-facies mineral assemblage (garnet-kyanite or garnet-clinopyroxene + feldspar + quartz) suggests that the mantle rocks were incorporated in the crustal ones during the deep continental subduction (Kotková et al., 2011). The peak P-T conditions of both the ultrahigh-pressure metamorphic rocks (UHPM) and garnet peridotites are comparable (Haifler & Kotková, 2016; Medaris et al., 2015). Isotope composition of carbon in diamond and Hf and O in zircon from the UHPM rocks reflects internal, crustal source of the media from which they formed (Kotková et al., 2016). In contrast, presence of primary kinoshitalite-bearing multiphase inclusions (MSI) in garnet in lherzolite and harzburgite from T7 borehole in the Saxothuringian basement, north Bohemian Massif, may reflect interaction with crustal-derived fluids/melts.

The MSI are polygonal, equant to elongated, 10-40 μm in diameter, and contain dolomite, magnesite, kinoshitalite (Ba-rich mica), amphibole, graphite, minor tiny spinel to magnesiochromite, thorianite, Cl-apatite and pentlandite. Compositions of the phases and bulk composition of the MSI were determined by combined EMPA, SEM, image analysis and micro-Raman spectroscopy.

Kinoshitalite is enriched in Cl (0.04-0.34 apfu) relative to F (≤0.03 apfu). Its Ba contents (0.24 - 0.62 apfu) and X_{Mg} (0.85-0.95) well correlate with whole-rock parameters. Amphibole is pargasite with Si = 6.08-6.27 apfu, ^{VI}Al = 0.80-1.30 apfu, Ca =1.36-1.82 apfu, Na = 1.03-1.43 apfu and X_{Mg} ~ 0.93. It is enriched in Cl (~ 0.1 apfu) compared to F (0.03-0.07 apfu). Apatite is chlorapatite containing up to ~ 0.6 apfu Cl with a high Cl/F ratio (~10). Moreover, minerals in MSI (Ba-rich mica, dolomite, chlorapatite) commonly contain minor Sr. Analysed MSI in a lherzolite sample show similar bulk composition as for X_{Mg}, MgO/FeO, MgO/SiO_2 and SiO_2/Al_2O_3 ratios, but variable CaO content: this is also reflected in different proportion of carbonates. Although X_{Mg} of all the bulk MSI is comparable to the host lherzolite, and also kinoshitalite and pargasite, they are strongly enriched in Ca, Al, and also in P_2O_5, BaO, Na_2O, K_2O and Cr_2O_3, and depleted in SiO_2.

The MSI occur at the margin of a chemically homogeneous, Mg-rich garnet core, which suggests their entrapment close to peak conditions, i.e. > 1100°C and 4.5 GPa: these conditions are above the dry solidus for crustal lithologies and above/close to hydrous and/or carbonated lherzolite solidus. Similarly high X_{Mg} of the bulk MSI, kinoshitalite and pargasite, along with enrichment of MSI in CaO, volatiles (H_2O, CO_2, Cl > F) and LILE (Ba, K, Sr, Th) likely reflects melting of a mantle source metasomatized by slab-derived fluids/melts, with high Cl contents possibly indicating an earlier serpentinization of the mantle.

Haifler, J. & Kotková, J. (2016): UHP-UHT peak conditions and near-adiabatic exhumation path of diamond-bearing garnet-clinopyroxene rocks from the Eger Crystalline Complex, North Bohemian Massif. *Lithos*, **248-251**, 366-381.

Kotková, J., O'Brien, P.J., Ziemann, M.A. (2011): Diamond and coesite discovered in Saxony-type granulite: solution to the Variscan garnet peridotite enigma. *Geology*, **39**, 667-670.

Kotková, J. & Janák, M. (2015): UHP kyaniteeclogite associated with garnet peridotite and diamond-bearing granulite, northern Bohemian Massif. *Lithos*, **226**, 255-264.

Kotková, J., Whitehouse, M., Schaltegger, U., D'Abzac, F.-X. (2016): The fate of zircon during UHT-UHP metamorphism: isotopic (U/Pb, δ^{18}O, Hf) and trace element constraints. *J. Metam. Geol.*, in press.

Medaris, G., Ackerman, L., Jelínek, E., Michels, Z., Erban, V., Kotková, J. (2015): Depletion, cryptic metasomatism, and modal mesatomatism (refertilization) of Variscan lithospheric mantle: Evidence from major elements, trace elements, and Sr-Nd-Os isotopes in a Saxothuringian garnet peridotite. *Lithos*, **226**, 81-97.

ELASTIC GEOBAROMETRY: UNCERTAINTIES ARISING FROM THE SHAPE OF THE INCLUSION

Mazzucchelli M.L.*[1], Burnley P.[2], Angel R.J.[3], Domeneghetti M.C.[1], Nestola F.[3] & Alvaro M.[1]

[1] Dipartimento di Scienze della Terra e dell'Ambiente, Università di Pavia, Italy

[2] Department of Geosciences and High Pressure Science and Engineering Center, University of Nevada, Las Vegas, NV, USA

[3] Dipartimento di Geoscienze, Università di Padova, Italy

Corresponding email: mattialuca.mazzucchelli01@universitadipavia.it

Keywords: elastic geobarometry, host-inclusion systems, Finite Element Modeling (FEM)

Conventional thermobarometry is severely challenged in ultra-high-pressure metamorphic (UHPM) rocks, but these are the only rocks that can provide insights into the detailed processes of subduction, especially deep and ultra-deep subduction. Minerals trapped as inclusions within other host minerals develop residual pressure (P_{inc}) on exhumation as a result of the differences between the thermo-elastic properties of the host and the inclusion. Their elastic behavior therefore provides an alternative and complementary method to conventional geobarometry that is independent of chemistry and chemical equilibria. To provide an accurate interpretation of inclusion pressures, non-linear elasticity has been recently incorporated into the classic host-inclusion elasticity solutions (Angel et al., 2014a; Angel et al., 2015) and is now available in the EoSFit7c software (Angel et al., 2014b).

However, this state-of-the-art analytical solution for elastic barometry makes use of two fundamental classes of assumptions concerning (i) the host-inclusion elastic behavior (i.e. both phases are elastically isotropic), and (ii) the geometry of the system (i.e. the inclusion is spherical and located at the center of an infinite host). At this stage, we maintained the assumption of isotropic elasticity, but we extended the analysis beyond the geometrical assumptions. We used Finite Element Modeling (FEM) to test different geometrical cases within the same boundary conditions. We carried out all of the calculations using the elastic properties of a quartz inclusion entrapped in a diamond host with a hydrostatic and homogeneous stress applied on the exterior of the host. Since in most real cases the host cannot be considered infinite with respect to the inclusion, in our first test we quantified the changes in the mean normal stress (P_{inc}) with respect to the analytical solution arising from the size and the proximity of the inclusion to the host surface. With respect to the analytical solution, the calculated P_{inc} increases by only 2% if the inclusion radius is about 1/3 of that of the host; whereas the increase in pressure is even smaller (0.4%) if the distance between the host-inclusion interface and the exterior is greater than 3 inclusion radii. In the second test the effect of the inclusion shape has been investigated by comparing the results from ellipsoidal inclusions to spherical ones. For all of our ellipsoid models the stress in the inclusion is homogeneous but not hydrostatic. The P_{inc} increases for all ellipsoids relative to the spherical inclusion, up to 45% for a 1:5:5 oblate ellipsoid. The contribution to modifying the final P_{inc} given by the edges and corners, evaluated through cylindrical, cubic and prismatic models, is smaller (less than 10%). This analysis has allowed us to evaluate the uncertainties of the entrapment pressures calculated with the classical isotropic model that arise from the deviation of the shapes of real inclusions from sphere shapes.

Acknowledgements: This work is supported by MIUR-SIR grant “MILE DEEp” (RBSI140351) to M. Alvaro, and ERC starting grant 307322 to F. Nestola.

Angel, R.J., Mazzucchelli, M.L., Alvaro, M., Nimis, P., Nestola, F. (2014a): Geobarometry from host-inclusion systems: The role of elastic relaxation. *Am. Mineral.*, **99**, 2146-2149.

Angel, R.J., Alvaro, M., Gonzalez-Platas, J. (2014b): EosFit7c and a Fortran module (library) for equation of state calculations. *Z. Kristallogr.*, **229**, 405-419.

Angel, R.J., Nimis, P., Mazzucchelli, M.L., Alvaro, M., Nestola, F. (2015): How large are departures from lithostatic pressure? Constraints from host–inclusion elasticity. *J. Metam. Geol.*, **33**, 801-813.

FIRST *IN-SITU* MEASUREMENTS OF Fe^{3+}/Fe_{tot} FOR OXIDES AND SILICATES INCLUDED IN NATURAL DIAMONDS WITH SYNCHROTRON MÖSSBAUER SOURCE

Milani S.*[1], Nestola F.[1], Cerantola V.[2], Anzolini C.[1], McCammon C.[3], Novella D.[4], Kupenko I.[2-5], Chumakov A.[2], Rüffer R.[2] & Harris J.W.[6]

[1] Dipartimento di Geoscienze, Università di Padova, Italy
[2] European Synchrotron Radiation Facility, Grenoble, France
[3] Bayerisches Geoinstitut, Universität Bayreuth, Germany
[4] Lawrence Livermore National Laboratory, University of California, Livermore, CA, USA
[5] Institut für Mineralogie, Universiät Münster, Germany
[6] School of Geographical and Earth Sciences, University of Glasgow, United Kingdom
Corresponding email: sula.milani@unipd.it

Keywords: synchrotron Mössbauer, diamond inclusions, ferric iron

Diamond is the paramount phase to understand the evolution and the physico-chemical condition of the deep portions of the Earth's mantle, mainly because: (i) it is the stable phase through which carbon is stored in the deep mantle for long geologic time; (ii) it does contain and preserve different types of inclusions (fluid, mineral, etc.); (iii) it is the only material sampling the mantle to depths of 800 km (e.g., Harte, 2010), although the majority of the mined diamonds worldwide derive from shallower depth (150 to 250 km). The study of mineral inclusions trapped in diamonds allows the retrieval of different pieces of information about the Earth's interior and its active geodynamics, providing important clues on the initiation of subduction processes (Shirey & Richardson, 2011; Smart et al., 2016), tracking the transfer of material through the mantle transition zone (Stachel et al., 2005; Walter et al., 2011), recording the timing of ingress of fluids to the continental lithosphere (e.g., Shirey et al., 2004), preserving carbonatitic fluid that trigger deep mantle melting (e.g., Schrauder & Navon, 1994; Kopylova et al., 2010), providing samples of primordial noble gases (e.g., Ozima & Igarashi, 2000), and capturing the redox state of the mantle (e.g., Rohrbach & Schmidt, 2011).

Unfortunately the majority of the techniques used so far to study the mineral inclusions are destructive. It is only in the last decade that the studies on inclusions in diamond have started to use non-destructive techniques, providing new information which would otherwise be lost using earlier destructive techniques. Such an example is the rim fluids around inclusions in diamonds. In this study we present details of the experimental setup on the determination of Fe^{3+}/Fe_{tot} ratios of mineral inclusions whilst still within the diamonds by a non-destructive approach using the Synchrotron Mössbauer Source (SMS; Potapkin et al., 2012) at the Nuclear Resonance beamline ID18 (Rüffer & Chumakov, 1996), European Synchrotron Radiation Facility (ESRF), Grenoble. The extremely small X-ray spot size (10×15 μm^2) is perfectly suited for our purposes as some inclusions are smaller than 30-50 µm and the Fe^{3+}/Fe_{tot} variation over the same inclusion cannot be performed by using standard laboratory radioactive sources because of the larger beam size. The average collection time for thicker inclusions (~ 200 µm) was 2 hours per spectrum, whilst the smallest inclusion (~ 30×30×30 μm^3) required a collection time of approximately 10-12 hours in order to get a spectrum with nicely distinguishable features and a high signal-to-noise ratio. In general, application to a suite of silicate and oxide inclusions in diamonds produced comparable results with respect to those obtained using conventional Mössbauer sources (e.g., McCammon et al., 2004).

Harte, B. (2010): Diamond formation in the deep mantle; the record of mineral inclusions and their distribution in relation to mantle dehydration zones. *Mineral. Mag*., **74**, 189-215.

Kopylova, M., Navon, O., Dubrovinsky, L., Khachatryan, G. (2010): Carbonatitic mineralogy of natural diamond forming fluids. *Earth Planet. Sci. Letters*, **291**, 126-137.

McCammon, C.A., Stachel, T., Harris, J.W. (2004): Iron oxidation state in lower mantle mineral assemblages: II. Inclusions in diamonds from Kankan, Guinea. *Earth Planet. Sci. Letters*, **222**, 423-434.

Ozima, M. & Igarashi, G. (2000): The primordial noble gases in the Earth; a key constraint on Earth evolution models. *Earth Planet. Sci. Letters*, **176**, 219-232.

Potapkin, V., Chumakov, A.I., Smirnov, G.V., Celse, J.P., Rüffer, R., McCammon, C.. Dubrovinsky, L. (2012): The ^{57}Fe synchrotron Mössbauer source at the ESRF. *J. Synchr. Rad.*, **19**, 559-569.

Rohrbach, A. & Schmidt, M.W. (2011): Redox freezing and melting in the Earth's deep mantle resulting from carboniron redox coupling. *Nature*, **472**, 209-214.

Rüffer, R. & Chumakov, A.I. (1996): Nuclear-resonance beamline at ESRF. *Hyperfine Inter.*, **97**, 589-604.

Schrauder, M. & Navon, O. (1994): Hydrous and carbonatitic mantle fluids in fibrous diamonds from Jwaneng, Botswana. *Geochim. Cosmochim. Acta*, **58**, 761-771.

Shirey, S.B. & Richardson, S.H. (2011): Start of the Wilson cycle at 3 Ga shown by diamonds from subcontinental mantle. *Science*, **333**, 434-436.

Shirey, S.B., Richardson, S.H., Harris, J.W. (2004): Integrated models of diamond formation and craton evolution. *Lithos*, **77**, 923-944.

Smart, K.A., Tappe, S., Stern, R.A., Webb, S., Ashwal, L.D. (2016): Early Archaean tectonics and mantle redox recorded in Witwatersrand diamonds. *Nature Geosci.*, **9**, 255-259.

Stachel, T., Brey, G.P., Harris, J.W. (2005): Inclusions in sub-lithospheric diamonds: glimpses of deep earth. *Elements*, **1**, 73-87.

Walter, M.J., Kohn, S.C., Araujo, D., Bulanova, G.P., Smith, C.B., Gaillou, E., Wang, J., Steele, A., Shirey, S.B. (2011): Deep mantle cycling of oceanic crust; evidence from diamonds and their mineral inclusions. *Science*, **334**, 54-57.

PHASE TRANSITIONS IN NUMERICAL MODELS

Moulas E.*[1], Podladchikov Y.[2] & Tajčmanová L.[1]
[1] Departement Erdwissenschaften, Eidgenössische Technische Hochschule Zürich, Switzerland
[2] Institut des Sciences de la Terre, Université de Lausanne, Switzerland
Corresponding email: evangelos.moulas@erdw.ethz.ch

Keywords: reactions, volumetric deformation, coupling

During lithospheric deformation rocks experience a large range of pressure and temperature (P-T) conditions. Within this P-T range, metamorphic rocks recrystallize and this leads to significant changes in their physical properties. Incorporating phase transitions in numerical geodynamic models is then required in order to investigate the effect that phase transitions have in lithospheric processes. Many numerical models utilize the Boussinesq approximation, i.e., the assumption that the divergence of velocity is zero and the materials are incompressible. Although these models predict accurately large-scale geodynamic phenomena, their application to crustal processes may be misleading. This could be particularly the case if volumetric changes (such as for coesite-quartz transition) are taken into account. Density changes in crustal systems can vary significantly over a limited range of conditions. In this work, we develop a non-Boussinesq approach to investigate geodynamic scenarios where phase transitions are important. We afterwards compare our findings with results calculated using a standard incompressible approach and demonstrate that solid bodies that experience heating in the order of 100 K may experience pressure buildup of the order of several hundred MPa. This effect is a result from constraints imposed by the mechanical configuration of the system and it is consistent with local thermodynamic equilibrium. In addition, we show that, if the rocks experience a reaction with large volumetric change (e.g., a phase transition) then, the related pressure build up is in the order of GPa. Our findings suggest that the assumption that mineral reactions occur at near-isobaric conditions may be an oversimplification.

RAMAN BASED QUARTZ GEOBAROMETRY OF K-BEARING TOURMALINE

Musiyachenko K.A.*[1-2] & Korsakov A.V.[1-2]
[1] Novosibirsk State University, Russia
[2] V.S. Sobolev Institute of Geology and Mineralogy, Siberian Branch, Russian Academy of Sciences, Novosibirsk, Russia
Corresponding email: kmusiyachenko@gmail.com

Keywords: K-bearing tourmaline, UHPM rocks, Raman spectroscopy

The discovery of K-bearing tourmaline from Kokchetav UHPM rocks has given rise to disputes about its origin (Shimizu & Ogasawara, 2005, 2013; Ota et al., 2008; Korsakov et al., 2009; Marschall et al., 2009). There are two major models of P-T conditions of high-K-Tour formation: the UHP origin (Tour crystallized in the diamond stability field from a silicate melt interacting with B fluid; 1000ºC, 6 GPa) and a low-P-formation (Tour formed from B-fluids at mid-crustal levels < 2.5 GPa).

We have investigated Tour-bearing samples from Kokchetav Massif (Northern Kazakhstan), which include Tour-Qtz rocks with graphite, garnet, and K-feldspar. Tourmalines occur as subhedral or euhedral crystals with color and composition zonation. K-content of Tour in our samples varies from 1.58 to 0 wt.% of K_2O. Common patterns in distribution of K in the Tour zones were identified by SEM and microprobe studies. There are grains with clear core-to-rim zonation: K-content decreases from core to rim. The crystals with low-K core, K-rich mantle and low-K rim were observed in the same samples. Microdiamond inclusions were found in all rock-forming minerals excluding Tour. Inclusions in K-bearing Tour are represented by Qtz, Kfs, graphite, and fluid inclusions. Qtz and Kfs inclusions occur in the high-K mantles and cores (K_2O content up to 1.5 wt.%). Particularly Qtz grains, trapped into the tour, were analyzed by Raman spectroscopy. There is no measurable upshift for main quartz Raman bands, implying lack of any residual stress inside these inclusions. Furthermore all quartz inclusions, occurring in the K-bearing tourmaline, are monocrystalline. Lack of palisade texture, typical for quartz pseudomorphs after coesite, and lack of the residual "overpressure" for the monocrystalline quartz inclusions testify for their origin within the quartz stability field. Estimated P_0-T_0 conditions of entrapment of the quartz inclusions, obtained from Zhang's elastic model (Zhang, 1998), are as high as P < 1.5 GPa and T < 900°C.

Experimental study of Hermann & Spandler (2008) reveals, that in the presence of H_2O-bearing fluid (which is prerequisite for Tour origin) the Kfs is stable under 2.5 GPa. Thus presence of Kfs and Qtz probably could be an evidence of low-P-formation. It is also worth noting, that some samples, which do not contain garnet within the bulk composition, contain it as inclusions in zircon, also there are findings of coesite inclusions in Zrn. But no Tour inclusion was found in Zrn or other UHP minerals so far. Therefore it is likely that crystallization of the K-bearing tourmaline (with K_2O up to 1.6 wt.%) occurs during retrograde stage at P < 2.5 GPa. Furthermore chemical composition of phengitic mica in diamond-bearing tourmaline, displayed on a Ti-Si plot (Shimizu & Ogasawara, 2013), indicates the formation conditions under 3 GPa (Hermann, 2003), while the suggested P-T conditions were 1000ºC and 6 GPa (Shimizu & Ogasawara, 2013).

Acknowledgements: This study was supported by RSF 15-17-30012.

Hermann, J. (2003): Experimental evidence for diamond-facies metamorphism in the Dora-Maira massif. *Lithos*, **70**, 163-182.

Hermann, J. & Spandler, C.J. (2008): Sediment melts at sub-arc depths: an experimental study. *J. Petrol.*, **49**, 717-740.

Korsakov, A.V., Travin, A., Yudin, D.S., Marschall, H.R. (2009): $^{40}Ar/^{39}Ar$ dating of tourmaline from metamorphic rocks of the Kokchetav massif, Kazakhstan. *Doklady Earth Sci.*, **424**, 168-170.

Marschall, H.R., Korsakov, A.V., Luvizotto, G.L., Nasdala, L., Ludwig, T. (2009): On the occurrence and boron isotopic composition of tourmaline in (ultra) high-pressure metamorphic rocks. *J. Geol. Soc. London*, **166**, 811-823.

Ota, T., Kobayashi, K., Kunihiro, T., Nakamura, E. (2008): Boron cycling by subducted lithosphere; insights from diamondiferous tourmaline from the Kokchetav ultrahigh-pressure metamorphic belt. *Geochim. Cosmochim. Acta*, **72**, 3531-3541.

Shimizu, R. & Ogasawara, Y. (2005): Discovery of K-tourmaline in diamond-bearing quartz-rich rock from the Kokchetav Massif, Kazakhstan. *Mitt. Österr. Mineral.Gesell.*, **150**, 141.

Shimizu, R. & Ogasawara, Y. (2013): Diversity of potassium-bearing tourmalines in diamondiferous Kokchetav UHP metamorphic rocks: A geochemical recorder from peak to retrograde metamorphic stages. *J. Asian Earth Sci.*, **63**, 39-55.

Zhang, Y. (1998): Mechanical and phase equilibria in inclusion-host systems. *Earth Planet. Sci. Letters*, **157**, 209-222.

POLYPHASE INCLUSIONS IN ALPINE HIGH-PRESSURE PERIDOTITE MONITOR SUBDUCTION-ZONE DEHYDRATION OF SERPENTINIZED MANTLE (CIMA DI GAGNONE, SWISS ALPS)

Scambelluri M.*[1], Pettke T.[2] & Cannaò E.[1]
[1] Dipartimento di Scienze della Terra, dell'Ambiente e della Vita, Università di Genova, Italy
[2] Institut für Geologie, Universität Bern, Switzerland
Corresponding email: marco.scambelluri@dipteris.unige.it

Keywords: serpentinized mantle, high-pressure meta-peridotite, polyphase inclusions

Serpentinites release at sub-arc depths volatiles and fluid-mobile trace elements found in arc magmas. Constraining element uptake in these rocks and defining the trace element composition of fluids released upon serpentinite dehydration improves our understanding of mass transfer across subduction zones and to volcanic arcs. The eclogite-facies garnet metaperidotite and chlorite harzburgite bodies embedded in paragneiss of the subduction melange from Cima di Gagnone derive from serpentinized peridotite protoliths and are unique examples of ultramafic rocks that experienced subduction metasomatism and devolatilization. In these rocks, metamorphic olivine and garnet trap polyphase inclusions representing the fluid released during high-pressure breakdown of antigorite and chlorite. Combining major element mapping and laser-ablation ICP-MS bulk inclusion analysis, we characterize the mineral content of polyphase inclusions and quantify the fluid composition. Silicates, Cl-bearing phases, sulphides, carbonates, and oxides document post-entrapment mineral growth in the inclusions starting immediately after fluid entrapment.

Compositional data reveal the presence of two different fluid types. The first (type A) records a fluid prominently enriched in fluid-mobile elements, with Cl, Cs, Pb, As, Sb concentrations up to 10^3PM (primitive mantle), ~ 10^2PM Tl, Ba, while Rb, B, Sr, Li, U concentrations are of the order of 10^1PM, and alkalis are about 2PM. The second fluid (type B) has considerably lower fluid-mobile element enrichments, but its enrichment patterns are comparable to type A fluid.

Our data reveal multistage fluid uptake in these peridotite bodies, including selective element enrichment during seafloor alteration, followed by fluid-rock interaction along with subduction metamorphism in the plate interface melange. Here, infiltration of sediment-equilibrated fluid produced significant enrichment of the serpentinites in As, Sb, B, Pb, an enriched trace element pattern that was then transferred to the fluid released at greater depth upon serpentine dehydration (type A fluid). The type B fluid hosted by garnet may record the composition of the chlorite breakdown fluid released at even greater depth.

The Gagnone study-case demonstrates that serpentinized peridotites acquire water and fluid-mobile elements during ocean floor hydration and through exchange with sediment-equilibrated fluids in the early subduction stages. Subsequent antigorite devolatilization at subarc depths delivers aqueous fluids to the mantle wedge that can be prominently enriched in sediment-derived components, potentially triggering arc magmatism without need of concomitant dehydration/melting of metasediments or altered oceanic crust.

RAMAN GEOBAROMETRY OF SOLID AND FLUID INCLUSIONS IN MINERALS FROM THE KOKCHETAV DIAMONDIFEROUS KYANITE GNEISSES

Shchepetova O.*[1-2], Korsakov A.V.[1], Mikhailenko D.[1] & Mikhno A.[1]

[1] V.S. Sobolev Institute of Geology and Mineralogy, Siberian Branch of the Russian Academy of Sciences, Novosibirsk, Russia

[2] Novosibirsk State University, Russia

Corresponding email: olgashchepetova27@gmail.com

Keywords: UHPM rocks, fluid inclusions, Raman geobarometry

Solid and fluid inclusions (SI and FI) are very useful for PT-history reconstruction. Here we present the results of Raman spectroscopy study for SI and FI that were found in kyanite porphyroblasts from diamondiferous gneisses (Kokchetav massif). These gneisses consist of large kyanite (Ky) and garnet (Grt) porphyroblasts, quartz (Qtz), biotite, phengite, K-feldspar, graphite (Gr), accessory rutile, monazite, apatite, zircon and UHP relics – diamond (Dia) and coesite (Coe). Ky porphyroblasts have a zonal distribution of SiO_2 and C polymorphs: there is (i) a Gr-rich core with Qtz inclusions, and (ii) clean overgrowth zone with cuboctahedral diamond crystals. There are two types of SiO_2 inclusions in Gr-rich core: (i) monocrystalline Qtz, and (ii) Qtz with Coe relics. The residual pressures, estimated by shift of Raman bands, vary from 0 to 1 GPa for monocrystalline Qtz, from 0.08 to 0.8 GPa and 0.034 to 1.5 GPa for Qtz and Coe relicts, respectively. The variations of residual pressures can be explained by different factors, such as (i) local heterogeneities in rheological properties within the host mineral, (ii) different amount of fluid, that was entrapped near the peak of metamorphic conditions and (iii) various distances between the inclusions (if the distance between the inclusions is less than 3 of their radius, they could not be considered as isolated inclusions; Zhang, 1998). To estimate the evolution of fluid composition in Ky gneisses, different FI were studied. FI in these rocks were subdivided into 3 groups: (i) FI in Ky and Grt porphyroblasts, (ii) FI in matrix Qtz, (iii) FI in Qtz inclusions in Grt. FI are generally quite small (up to 8 mm). Raman spectroscopy study reveals that most of the FI contain CO_2, N_2, CH_4 and liquid H_2O and that the composition of FI is independent from host mineral. But in different minerals FI have various CO_2 densities. In Ky the CO_2 density is 0.99-1.19 g/cm^3, in Grt ~ 0.79 g/cm^3, in matrix Qtz ~ 0.59-0.99 g/cm^3, in Qtz inclusions in Grt ~ 0.99-1.19 g/cm^3. Pressure values estimated from CO_2 PT-diagram (Yamamoto, 1998) for room temperature vary from 0.02 to 0.2 GPa, which are significantly lower than pressure values estimated for SI. The variations of pressure for FI take place due to different rheological properties of the host mineral and the FI bulk composition. Our study reveals that solid inclusions in Ky porphyroblast have higher residual pressures than fluid inclusions. It can be explained by the different behavior of these inclusions during exhumation stage: the decrepitation significantly reduces the residual "pressures" of fluid inclusions, rather than of solid inclusions.

Acknowledgements: This study was supported by a grant from the Russian Science Foundation (RSF 15-17-30012).

Yamamoto, J., Kagi, H., Kaneoka, I., Lai, Y., Prikhod'ko, V.S., Arai, S. (2002): Fossil pressures of fluid inclusions in mantle xenoliths exhibiting rheology of mantle minerals: implications for the geobarometry of mantle minerals using micro-Raman spectroscopy. *Earth Planet. Sci. Letters*, **198**, 511-519.

Zhang, Y. (1998): Mechanical and phase equilibria in inclusion–host systems. *Earth Planet. Sci. Letters*, **157**, 209-222.

EXPERIMENTAL CALIBRATION AND IMPLICATIONS OF OLIVINE-MELT VANADIUM OXYBAROMETRY FOR HYDROUS MAGMAS FROM MUTNOVSKY VOLCANO (KAMCHATKA)

Shishkina T.*[1-2], Portnyagin M.[1-3], Botcharnikov R.[2], Almeev R.[2] & Holtz F.[2]
[1] Vernadsky Institute of Geochemistry and Analytical Chemistry, Russian Academy of Sciences, Moscow, Russia
[2] Institut für Mineralogie, Leibniz Universität Hannover, Germany
[3] GEOMAR - Helmholtz-Zentrum für Ozeanforschung, Christian-Albrechts-Universität Kiel, Germany
Corresponding email: t.shishkina@geokhi.ru

Keywords: redox conditions, partition experiments, island arc volcanoes

A promising method for the quantification of the redox conditions (oxygen fugacity, fO_2) in basaltic systems, which might be applied to quenched melt inclusions in olivine, exploits the partitioning of vanadium between olivine and coexisting silicate melt (D_V^{Ol-M}). Strong correlation of D_V^{Ol-M} with fO_2 was investigated in a number of experimental works on dry mafic and ultramafic melts in a wide range of fO_2 conditions at pressures of 1 atm and 0.5-2 GPa, temperature range of 1150–1530°C (e.g., Canil & Fedortchouk, 2001; Mallmann & O'Neill, 2009, 2013). Only a few melt compositions equilibrated with olivine at T ≤ 1250°C were studied so far. Although it was shown that melt composition, pressure and temperature have small effect on D_V^{Ol-M}, more data are required to extend the calibration of the V oxybarometry to hydrous low-temperature basalts representing island arc magmas.

This study presents new data on D_V^{Ol-M} gained from crystallization experiments performed with an high-Al basalt from Mutnovsky volcano (Kamchatka) at various aH_2O, 0.1 and 0.3 GPa, 1025-1150°C and ΔQFM = -0.5 to +3.2 at the Institute of Mineralogy in Leibniz University of Hannover. Concentrations of vanadium in experimental and natural glasses and olivines were analyzed at the Institute of Geosciences at the University of Kiel by LA-ICP-MS (Agilent 7500s, 193nm GEOLAS Pro). The determined D_V^{Ol-M} in run products varies between 0.007 and 0.079 and $\log D_V^{Ol-M}$ shows a strong linear correlation with $\lg fO_2$ in the experiments.

For calibration of the V oxybarometer for low temperature hydrous basaltic magmas we used 7 experiments from this study together with 26 experiments performed at T ≤ 1250°C in fO_2 range of -2.0 < ΔQFM < 3.2 with melts containing less than 12 wt.% MgO and less than 4 wt.% Na_2O from previously published data. The resulting linear correlation between D_V^{Ol-M} and ΔQFM can be described with an equation: $\Delta QFM = -3.51 \cdot \lg D_V^{Ol-M} - 4.20$ ($R^2 = 0.96$). This equation reproduces experimental ΔQFM conditions within ±0.35log units for 70% of the experiments.

This equation was applied to estimate redox conditions for Mutnovsky volcano magmas using compositions of melt inclusions in olivine from basaltic tephras. Vanadium concentrations vary in the range of 266-382 ppm in glassy inclusions and of 4.2-6.1 ppm in their host olivines. This corresponds to D_V^{Ol-M} = 0.0152-0.0185. The calculated ΔQFM values vary between +1.8 to +2.2 which is similar to the calculations using the equation from Canil and Fedortchouk (2001) and is about 1 log unit of fO_2 below the value calculated with the oxybarometer proposed by Mallmann & O'Neill (2013). The determined redox conditions for Mutnovsky are in a good agreement with redox estimates using independent methods and confirm relatively oxidizing nature of island-arc basaltic magmatism.

Canil, D. & Fedortchouk, Y. (2001): Olivine-liquid partitioning of vanadium and other trace elements, with applications to modern and ancient picrites. *Can. Mineral.*, **39**, 319-330.

Mallmann, G. & O'Neill, H.S.C. (2009): The crystal/melt partitioning of V during mantle melting as a function of oxygen fugacity compared with some other elements (Al, P, Ca, Sc, Ti, Cr, Fe, Ga, Y, Zr and Nb). *J. Petrol.*, **50**, 1765-1794.

Mallmann, G. & O'Neill, H.S.C. (2013): Calibration of an empirical thermometer and oxybarometer based on the partitioning of Sc, Y and V between olivine and silicate melt. *J. Petrol.*, **54**, 933-949.

A COUPLED MODEL ON CHEMICAL DIFFUSION AND MECHANICAL DEFORMATION WITH APPLICATION TO AN INCLUSION-HOST SYSTEM

Zhong X.*[1], Moulas E.[1], Vrijmoed J.C.[1] & Tajčmanová L.[1]
[1] Departement Erdwissenschaften, Eidgenössische Technische Hochschule, Zürich, Switzerland
Corresponding email: xinzhong0708@gmail.com

Keywords: coupling, diffusion, deformation

Chemically zoned minerals such as garnet, plagioclase, and olivine contain important information that helps us to decipher the pressure, temperature, time, and deformation (*P-T-t-D*) history of a metamorphic rock. Numerical simulations of chemical diffusion in zoned minerals have been mostly used for quantification of duration of metamorphic processes. Apart from chemical diffusion, mechanical deformation has been recognized as an important process in metamorphic rocks. Both chemical diffusion and mechanical deformation are conventionally treated as separate processes. In this study, we build a theoretical model to couple these two processes in order to investigate the generation and preservation of chemical zonation in a kyanite inclusion-plagioclase host system.

The theory of coupling the diffusion-deformation processes is analogous to the classical theories of poroelasticity and thermoelasticity in terms of governing equations. The constitutive relations are derived from fundamental thermodynamic relations to provide cross-coefficients to couple the evolutions of chemical concentration and pressure. Our model uses an elastic rheology for volumetric deformation, and a Maxwell viscoelastic rheology with a non-Newtonian viscosity for shear deformation. Nondimensionalization of the governing equations suggests that the system is controlled by a dimensionless number, the Deborah number (*De*), which is the ratio between the characteristic pressure relaxation time and the characteristic chemical diffusion time.

The numerical model is built in a 1-D radially symmetric coordinate frame considering a kyanite inclusion at higher pressure embedded by a chemically homogeneous plagioclase host at lower pressure. The numerical solutions are benchmarked without coupled effect using two analytical solutions for different rheology in the host: pure elastic and non-linear viscous (Zhang, 1998; Dabrowski et al., 2015). When coupled effect is considered, we observe that: 1) The viscous pressure relaxation in the kyanite inclusion is accompanied by a concomitant generation of pressure gradient in the plagioclase host next to the interface. This pressure gradient is generated due to the necessity to maintain force balance and the applied non-Newtonian viscosity. 2) The pressure gradient in the plagioclase host can potentially trigger a chemical concentration gradient if *De* is larger than 1 to allow relatively faster chemical diffusion. 3) Parameterization using experimental flow laws and diffusion coefficient suggests that *De* number is bigger than one in the plagioclase host at the modeled physical conditions implying that the observed chemical zonation can be potentially maintained by slower mechanical deformation at geological time scale.

Dabrowski, M., Powell, R., Podladchikov, Y. (2015): Viscous relaxation of grain-scale pressure variations. *J Metam. Geol.*, **33**, 859-868.

Zhang, Y. (1998): Mechanical and phase equilibria in inclusion-host systems. *Earth Planet. Sci. Letters*, **157**, 209-222.

Session S10:

Mineral reaction kinetics: microstructures, textures, chemical and isotopic signatures

Conveners:

Rainer Abart (Wien – Austria)

Wilhelm Heinrich (Potsdam – Germany)

Encarnación Ruiz Agudo (Granada – Spain)

THERMOBAROMETRIC EVOLUTION OF REACTION MICROSTRUCTURES IN "ARCLOGITE" – A CASE STUDY FROM THE SITTAMPUNDI LAYERED ANORTHOSITE COMPLEX, INDIA

Bandyopadhyay D.*[1], Ghosh B.[1-2], Nandy S.[3] & Palin R.M.[4]
[1] Department of Geology, University of Calcutta, India
[2] School of Natural System, Kanazawa University, Japan
[3] Central Headquarters, Geological Survey of India, Kolkata, India
[4] Institut für Geowissenschaften, Johannes Gutenberg-Universität Mainz, Germany
Corresponding email: debaditya.b2r@gmail.com

Keywords: arclogite, kelyphite, melting

The term "arclogite" was first coined by Anderson (2005) to refer to eclogite related rock types (e.g., garnet pyroxenite) that formed in arc-related tectonic settings (i.e., arc-eclogite). Recently, using the Sierra Nevada batholith as a case study, a geodynamic model for cyclical arc magmatism, the production of arclogites and silicic melt (continental crust), and delamination of pyroxenitic residua back into the mantle was proposed by Lee & Anderson (2015). Here, we present detailed microstructural observations from an arclogite (retrogressed garnet websterite) from the Sittampundi Layered Anorthosite Complex (SLAC), India, that constrain its thermobarometric evolution, which is compared to other pressure–temperature (*P-T*) data for this poly-metamorphosed terrane (Brandt et al., 2014). We have performed focussed investigation into (1) kelyphite – a fine-grained vermicular intergrowth around garnet (Grt) composed of orthopyroxene (Opx), plagioclase (Pl), and spinel (Sp), ± amphibole (Amph); and (2) different modes of Amph formation within and around clinopyroxene (Cpx), either as alteration along cleavage planes, coronae, or in symplectites.

Mineral proportions in kelyphite shells exhibit distinct characteristics depending on the mineral(s) that they replace. At Grt–Opx contacts, Opx+Sp dominated symplectite (adjacent to Opx) transitions to Opx+Pl±Sp symplectite (adjacent to Grt). Similar structures occur at Grt–Grt contacts, with a thick Opx+Sp symplectite in kelyphite centers (furthest away from Grt) with a transition to Opx+Pl±Sp symplectite adjacent to each Grt grain. In each case (Grt–Opx and Grt–Grt), Sp grains pseudomorph previous euhedral Grt rims. Kelyphites formed at Grt–Cpx contacts lack Sp-pseudomorphism and contain much higher proportions of Amph than the other kelyhphite types. The *P-T* conditions of the major kelyphite microstructure [Type II after Obata (2011)] formation have been constrained using pseudosection modelling (Connolly, 2009). Preliminary results indicate they were generated during near-isothermal decompression from over 10 kbar to ~ 7 kbar at T > 1000 °C, which agrees with estimations for the tectonothermal history of the region (Sajeev et al., 2009). Previous studies have indicated that partial melting could have directly influenced kelyphite formation (Špaček et al., 2013), which agrees with our preliminary pseudosection analysis that predicts decompression having occurred at suprasolidus *P-T*conditions for this bulk-rock composition. Variations in Amph chemistry according to spatial location (and other microstructures) may provide evidence for partial melting and subsequent crystallization during cooling. The microstructures described herein provide a valuable record of the petrological evolution of the SLAC arclogite. Future work will involve detailed characterization of kelyphite morphologies via cutting-edge EBSD and 3DXRCT techniques in order to better understand reaction kinetics and their growth history.

Anderson, D.L. (2005): Large igneous provinces, delamination, and fertile mantle. *Elements.*, **1**, 271-275.

Brandt, S., Raith, M.M., Schenk, V., Sengupta, P., Srikantappa, C., Gerdes, A. (2014): Crustal evolution of the Southern Granulite Terrane, south India: New geochronological and geochemical data for felsic orthogneisses and granites. *Precambrian. Res*., **246**, 91-122.

Connolly, J.A.D. (2009): The geodynamic equation of state: what and how. *Geochem. Geophys. Geosyst.*, **10**. Q10014.

Lee, C.T.A. & Anderson, D.L. (2015): Continental crust formation at arcs, the arclogite "delamination" cycle, and one origin for fertile melting anomalies in the mantle. *Chinese. Sci. Bull*., **60**, 1141-1156.

Obata, M. (2011): Kelyphite and symplectite: textural and mineralogical diversities and universality, and a new dynamic view of their structural formation. *in* "New frontiers in tectonic research - General problems, sedimentary basins and island arcs", E. Sharkov, ed., InTech, Rijeka, 93-122.

Sajeev, K., Windley, B.F., Connolly, J.A.D., Kon, Y. (2009): Retrogressed eclogite (20 kbar, 1020˚C) from the Neoproterozoic Palghat-Cauvery suture zone, southern India. *Precambrian. Res*., **171**, 23-36.

Špaček, P., Ackerman, L., Habler, G., Abart, R., Ulrych, J. (2013): Garnet breakdown, symplectite formation and melting in basanite-hosted peridotite xenoliths from Zinst (Bavaria, Bohemian Massif). *J. Petrol*., **54**, 1691-1723.

THE USE OF CITRATE TO TUNE CALCIUM OXALATE PRECIPITATES ON CALCITE

Burgos-Cara A.*[1-2], Ruiz-Agudo E.[1] & Putnis C.V.[2-3]
[1] Departamento de Mineralogía y Petrología, Universidad de Granada, Spain
[2] Institut für Mineralogie, Universität Münster, Germany
[3] Nanochemistry Research Institute, Curtin University, Perth, Australia
Corresponding email: aburgoscara@ugr.es

Keywords: calcium oxalate, citrate, calcite

Calcium oxalate ($CaC_2O_4 \cdot xH_2O$) minerals are naturally occurring minerals found in fossils, plants, kidney stones and is a by-product in some processes such as paper, food and beverage production (Demadis & Öner, 2009; Chutipongtanate et al., 2012). In particular, calcium oxalate monohydrate phase (COM), also known as whewellite ($CaC_2O_4 \cdot H_2O$), is the most frequently reported mineral phase found in urinary and kidney stones together with phosphates. Also, oxalate patinas are commonly found on calcareous stone in historic buildings (Sabbioni & Zappia, 1991). In the processes above, there is frequently a Ca-bearing mineral which is replaced by calcium-oxalate and that induces its crystallization by heterogeneous nucleation. Organic additives are well known to play a key role in the formation of minerals in both biotic and abiotic systems, either facilitating their precipitation or hindering it. In this regard, recent studies have provided direct evidence demonstrating that citrate species could enhance dissolution of COM and inhibit their precipitation (Masár et al., 2003; Weaver et al., 2007). However, little is known on the effect of organics on the replacement of calcite by calcium oxalate. The present work aims at evaluate the influence of *p*H, citrate and oxalic acid concentrations in calcium oxalate precipitation onto calcite surfaces (Island Spar, Chihuahua, Mexico), through in-situ nanoscale observations performed using atomic force microscopy (AFM, Multimode, Bruker) in flow-through experiments. Significant changes in the morphology of the precipitated whewellite crystals were observed depending on the *p*H of the precipitating solution. We suggest that this is related to changes in citrate speciation with *p*H, as different citrate species seem to preferentially adsorb on different whewellite faces. The results of this study may help in the design of effective treatments for the protection of calcareous stone based on the natural process occurring in monuments, as well as to better understand the process of unwanted oxalate precipitate formation and its inhibition by organic compounds.

Chutipongtanate, S., Chaiyarit, S., Thongboonkerd, V. (2012): Citrate, not phosphate, can dissolve calcium oxalate monohydrate crystals and detach these crystals from renal tubular cells. *Eur. J. Pharmacol.*, **689**, 219-225.

Demadis. K.D. & Öner, M. (2009): Inhibitory effects of “green” additives on the crystal growth of sparingly soluble salts. *in* ”Green chemistry research trends”, J.T. Pearlman, ed., Nova Science, New York, 265-287.

Masár, M., Žúborová, M., Kaniansky, D., Stanislawski, B. (2003): Determination of oxalate in beer by zone electrophoresis on a chip with conductivity detection. *J. Sep. Sci.*, **26**, 647-652.

Sabbioni, C. & Zappia, G. (1991): Oxalate patinas on ancient monuments: the biological hypothesis. *Aerobiologia*, **7**, 31-37.

Weaver, M.L., Qiu, S.R., Hoyer, J.R., Casey, W.H., Nancollas, G.H., De Yoreo, J.J. (2007): Inhibition of calcium oxalate monohydrate growth by citrate and the effect of the background electrolyte. *J. Cryst. Growth*, **306**, 135-145.

TEXTURES AND TRACE-ELEMENT DISTRIBUTION IN ARSENOPYRITE RECORDING POST-CRYSTALLIZATION PROCESSES IN CORCOESTO OROGENIC GOLD DEPOSIT (NW OF SPAIN)

Cepedal A.*[1], Gayol R.[1], Martínez-Abad I.[1], Fuertes-Fuente M.[1], Martin-Izard A.[1] & Boixet L.[2]
[1] Departamento de Geología, Universidad de Oviedo, Spain
[2] Mineira do Corcoesto, Spain
Corresponding email: mcepedal@geol.uniovi.es

Keywords: arsenopyrite, gold, LA-ICP-MS

The timing of Au-deposition in orogenic gold deposits can be difficult to resolve because later stages of superimposed deformation cause Au to be released from As-pyrite or arsenopyrite (Large et al., 2011). Some authors (e.g., Morey et al., 2008, Cook et al., 2013) have shown that correlation between invisible gold and ore textures carries implications for understanding the sequence of events during ore genesis and the mechanisms of incorporation or release of Au. Corcoesto is an orogenic gold deposit located in the Malpica Gold Belt (Spiering et al., 2000), NW of Spain. Gold mineralization mainly occurs in quartz-arsenopyrite veins related to a N30E regional dextral-shear zone (Boixet et al., 2007). In this work we present a mineralogical and geochemical study carried out on mineralized samples. The research includes a petrographic description using optical and electronic microscopy, and microanalyses by electron microprobe, SEM-EDS, and LA-ICP-MS, performed at Oviedo University, Spain. The goal is to recognize different mineralization processes, on basis of textures and trace-element content of arsenopyrite crystals, and to detect the occurrence of refractory gold.

Arsenopyrite occurs as heterometric crystals, isolated or in aggregates, frequently fractured and crosscut by chlorite ± carbonate ± quartz veinlets. Micron to sub-micron inclusions of other metallic minerals are frequent. Under crossed nicols, arsenopyrite crystals appear heterogeneous, especially around fractures, grain boundaries and mineral inclusions. BSE images reveal areas with high micron-scale porosity in fractured crystals, in addition to rims of a new generation of arsenopyrite (Apy-2). Microprobe analyses show a negative correlation between As and S contents. The As values range from 31.4 to 35 at.%, the lowest values (31.3-32.8 at.%) corresponding to Apy-2. The main trace-element is Sb (up to 1354 ppm), followed by Te, which is mainly detected in Apy-2 rims. Ni (up to 1705 ppm) and Co (up to 343 ppm) were sometimes detected, whereas Au was below the detection limit (184-254 ppm).

For the LA-ICP-MS analyses, the MASS-1 y NIST-610 standards were used in order to correct the time-dependent drift of sensitivity and mass discrimination. The analysed elements were Au, Ag, Bi, Cu, Zn, Pb, Te, Co, and Ni. Fe was also monitored and used as the internal standard for quantitative calibration. Data were acquired with a laser-repetition rate of 10 Hz and 7 mJ/pulse, from line-raster (up to 250 µm in length) of 30 µm in diameter and a raster speed of 4 µm/s. The results confirm Sb as the main trace, and the Te-enrichment in the Apy-2 rims. Moreover, the analyses also showed a distinct zoning with respect to Co and Ni, generally in antithetic relationship with Sb. Measured Au concentrations of below 4 ppm in non-porous inner areas of arsenopyrite crystals were considered as refractory, whereas anomalous high concentrations are related to micro-scale inclusions.

Boixet, L., Gleeson, C.F., García-Nieto, J. (2007): The Corcoesto gold deposit. 3rd Int. Applied Geochem. Symp., Oviedo, abstr., 85.

Cook, N.J., Ciobanu, C.J., Meria, D., Silcock, D., Wade, B. (2013): Arsenopyrite-pyrite association in an orogenic gold ore: tracing mineralization history from texture and trace elements. *Econ. Geol.* **108**, 1273-1283.

Large, R.R., Bull, S.W., Maslennikov, V.V. (2011): A carbonaceous sedimentary source-rock model for Carlin-type and orogenic gold deposits. *Econ. Geol.*, **106**, 331-358.

Morey, A.A., Tomkins, A.G., Bierlein, F.P., Weinberg, R.F., Davidson, G.J. (2008): Bimodal distribution of Gold in pyrite and arsenopyrite: examples from the Archean Boorara and Bardoc shear systems, Yilgarn Craton, western Australia. *Econ. Geol.*, **103**, 599-614.

Spiering, E.D., Pevida, L.R., Maldonado, C., González, S., García, J., Varela, A., Arias, D., Martín-Izard, A. (2000): The gold belts of western Asturias and Galicia (NW of Spain). *J. Geochem. Explor.*, **71**, 89-111.

CARBONATION OF GYPSUM AND ANHYDRITE: INFLUENCE OF THE CARBONATE BEARING SOLUTION CONCENTRATION ON ITS REACTION PATWAYS AND POROSITY

Cuesta-Mayorga I.*[1-4], Astilleros J.M.[1-2], Roncal-Herrero T.[3], Grattoni C.A.[4], Fernández-Díaz L.[1-2] & Benning L.G.[4-5]

[1] Departamento de Cristalografía y Mineralogía, Universidad Complutense, Madrid, Spain

[2] Institute of Geosciences, Consejo Superior de Investigaciones Científicas, Universidad Complutense, Madrid, Spain

[3] Department of Physics, University of York, United Kingdom

[4] School of Earth and Environment, University of Leeds, United Kingdom

[5] Helmholtz Zentrum Potsdam, GFZ Deutsches GeoForschungsZentrum, Potsdam, Germany

Corresponding email: iriscuesta@ucm.es

Keywords: carbonation, pseudomorphism, porosity

Gypsum ($CaSO_4 \cdot 2H_2O$) and anhydrite ($CaSO_4$) are among the most abundant non-silicates minerals in the Earth crust. Their interaction with carbonate-bearing solutions has led to the formation of large volumes of diagenetic carbonate deposits. This process involves the dissolution of the primary sulfates and their pseudomorphic transformation into $CaCO_3$ polymorphs. This occurs via a dissolution and reprecipitation mechanism, yet the resulting carbonate polymorphs are different for each sulfate precursor phase. We have previously shown that reacting 0.5M Na_2CO_3 solutions with anhydrite leads to the precipitation of mostly calcite with traces of vaterite. However, the same reaction but in the presence of gypsum occurs via the sequential formation and transformation of amorphous calcium carbonate (ACC), vaterite and calcite (Fernández-Díaz, 2009). These initial data suggested that such carbonation reactions of gypsum and anhydrite result in both cases in the generation of high amounts of porosity, accompanied by wide, prominent gaps between the parent sulfate and the product carbonates in the case of the carbonation of gypsum. However, a quantitative and time resolved assessment of the reactions was lacking.

In this work we present the results of an experimental study where we addressed the effect of initial aqueous carbonate concentration (0.5, 0.25 and 0.05M Na_2CO_3) on the carbonation of calcium sulfate phases. Our aims were to quantify in a time resolved (over 12 days) manner (i) any changes in reaction pathways and (ii) the generation and evolution of porosity during both anhydrite and gypsum carbonation reactions. We have characterized the changes in $CaCO_3$ polymorphs by combining scanning electron microscopy (SEM), glancing X-ray diffraction and Raman and Fourier transform infrared spectroscopy (FTIR) analyses. The generation and evolution of porosity was quantified over time using mercury porosimetry, computed tomography (CT), BET-surface area and nuclear magnetic resonance (NMR). The results reveal that when reacted with low concentration carbonate solutions (0.05M) both gypsum and anhydrite transform to mixtures of aragonite and calcite, and not as shown above to mainly calcite. Furthermore, the total porosity is inversely proportional to the carbonate concentration. Interestingly, in the case of anhydrite this higher porosity includes the development of a gap, similar to that previously observed for gypsum. Regardless of the initial carbonate concentration and for both calcium sulfates, the sizes of the newly-formed pores rapidly increase at the beginning of the process, but steadily decrease over the 12 days of reaction. These observations indicate that the reactant concentration plays a crucial role in the carbonation of gypsum and anhydrite. This factor may have influenced the porosity features of many diagenetic limestones and could have important consequences for industrial applications such as oil recovery and CO_2 sequestration.

Fernández-Díaz, L., Pina, C.M., Astilleros, J.M., Sánchez-Pastor, N. (2009): The carbonatation of gypsum: Pathways and pseudomorph formation. *Am. Mineral.*, **94**, 1223-1234.

IMPACT OF THE ISOMORPHIC SUBSTITUTION (As ↔ P) ON THE STRUCTURE OF COPPER PHOSPHATE MINERALS DETERMINED BY CHEMICAL AND STRUCTURAL INVESTIGATIONS

Dulski M.*[1], Janeczek J.[2], Ciesielczuk J.[2] & Krzykawski T.[2]
[1] Institute of Material Sciences, University of Silesia, Chorzów, Poland
[2] Faculty of Earth Sciences, University of Silesia, Sosnowiec, Poland
Corresponding email: mateusz.dulski@smcebi.edu.pl

Keywords: chemical substitution, microstructure changes due to isomorphic substitution, Raman

Introduction: It is well known that base metal arsenates and phosphates in the oxide zone of ore deposits often form solid solutions due to similar size and charge of $[AsO_4]^{3-}$ (248 pm) and $[PO_4]^{3-}$ (238 pm) tetrahedra. Moreover, in some copper solid solutions are observed substitution between Zn and Cu content. Hence, the general chemical formula of solid solution stands for: $^{[4]}(Zn,Cu)^{[6]}Cu_5(P_{1-x}As_xO_4)_2(OH)_6 \cdot H_2O$. Isomorphic substitution As ↔ P and/or Zn ↔ Cu causes point defects and local structural distortion within structural units. Moreover, degree of the phosphate tetrahedra distortion depends on the number of As atoms substituting for P. Introduction of As into the phosphates structure or Zn into the copper position is reflected in Raman spectra by the appearance of new bands as well as by increase in intensity of arsenate(zinc)-related bands. In addition, depends on the As and/or Zn content it is observed the changes of the unit cell parameters by the X-ray diffraction measurements.

Geological background and analytical methods: Minerals of the cornwallite-pseudomalachite and kipushite-philipsburgite series from Miedzianka in the Sudety Mountains, SW Poland were investigated by electron probe microanalysis (EPMA), X-ray diffraction and Raman spectroscopy.

Results and discussion: EPMA data revealed extended solid solution between both end-members resulted from anionic substitutions: P ↔ As. Hence, the strongest Raman bands related to the arsenate ion vibration are up-shifted with respect to the literature data. The upshift is attributed to the local distortion of tetrahedra caused by shortening As-O bonds and adjustment angles between bonds to accommodate large As ions in the pseudomalachite or kipushite structure. With decreasing content of As ions the As-band is shifted towards lower wavenumber and the reduction in number of Raman bands is observed. 3D Raman imaging data shown a linear correlation between arsenate content and both Raman band positions and full width and half maximum (FWHM). X-ray diffraction analysis revealed a reduction of unit cell parameters with decreasing of the arsenate content in the structure confirming Raman outcomes. In addition, Gibbs diagram was applied to show correlation between Raman band intensity and chemical composition (As, P, OH) of the investigated solid solutions. Hence, the Raman outcomes provide an quantitative data on minerals forming solid solutions. Finally, EPMA data for kipushite-philipsburgite solid solution resulted from cationic substitutions: Cu ↔ Zn in octahedral sites. However, the Zn deficiency observed in samples from Miedzianka suggests that some Cu positions are fourfold coordinated. As a result, Raman spectrum at low-wavenumber range below 400 cm^{-1} is strongly complicated with bands associated with the OCuO and OZnO vibrations. The local structural distortion have only a small impact on the unit cell parameters of both end-members.

PRECIPITATION AND AGING OF CALCIUM CARBONATES IN THE PRESENCE OF COBALT (II)

Fernández-González A.*[1], González-López J.[1] & Jiménez A.[1]
[1] Departamento de Geología, Universidad de Oviedo, Spain
Corresponding email: mafernan@geol.uniovi.es

Keywords: calcium carbonate, cobalt, precipitation-aging

Numerous studies have demonstrated that some toxic elements can be removed from aqueous solutions by its incorporation in the crystal structure of certain minerals. In particular, the incorporation of divalent cations into the crystal structure of different calcium carbonates has been proposed as a valuable solution to remove or reduce the concentration some heavy metal in polluted water.

Cobalt is a toxic metal that can accumulate in some specific areas on the Earth surface due to natural or anthropogenic factors. It is known that the presence of Co^{2+} in water solution avoids the precipitation of calcite and promotes the precipitation of aragonite and amorphous phases of calcium carbonate. However, the evolution of these phases and the polymorphic transformations that could occur after precipitation remain unknown. In this experimental work we have precipitated calcium carbonate in the presence of different amounts of Co^{2+} at room temperature. After precipitation, the solid phases were aged in the remaining aqueous solution for two months. The aging process was monitored by analysing both the aqueous solution and the aged solids at specific periods of time.

The evolution of the precipitated phases was followed by X-ray Powder Diffraction analysis, Scanning and Transmission Electron Microscopy and EDS analysis. The evolution of the remaining water was also followed by measuring *p*H, alkalinity and Co^{2+} concentration for the entire aging time.

In all the experiments the initial solutions were supersaturated for calcite, aragonite, vaterite, monohydrocalcite and sphaerocobaltite. However, it was observed that the first precipitate is a hydrated amorphous cobalt and calcium carbonate. After precipitation, the evolution is complex and depends on the initial Ca/Co proportion. In general, the amorphous phase evolves to a mixture of monohydrocalcite and amorphous hydrated cobalt carbonate. Later, the newly formed monohydrocalcite is also dissolved and aragonite precipitates. Aragonite and the amorphous phase coexisted in the aqueous solution at least after 30 days of aging. Finally, after 60 days, the crystalline phase $Co_2CO_3(OH)_2$ was identified in the solid together with aragonite.

A NEW PATHWAY TO PREDICT WATER-ROCK REACTION RATES

Fischer C.*[1] & Luttge A.[1-2]
[1] Zentrum für Marine Umweltwissenschaften & Fachbereich Geowissenschaften, Universität Bremen, Germany
[2] Department of Earth Science, Rice University, Houston, TX, USA
Corresponding email: cornelius.fischer@uni-bremen.de

Keywords: dissolution, precipitation, rate spectra

Water-rock interaction drives chemical material fluxes caused by dissolution and precipitation processes. Both, the reconstruction of material fluxes in the Earth's history and the prediction of future geochemical and environmental changes depend on our fundamental understanding of the reaction rates. The conventional approach of rate analysis and prediction was based on the application of simple mean rates. However, surface-sensitive methods and resulting information about heterogeneous surface reactivity illustrated quantitatively the inherent rate variability of even single minerals. Thus, the use of simple mean rates for the prediction of material fluxes and resulting porosity evolution is often misleading.

Building on this insight, we have developed the rate spectra concept in order to statistically analyze the heterogeneous surface rates (Fischer et al., 2012; Luttge et al., 2013). First applications illustrated the identification of rate components. Important examples include weathering reactions (Emmanuel and Levenson, 2014) and the corrosion of potential nuclear waste forms (Fischer et al., 2015).

In this study, we demonstrate how the superimposition of multiple rate contributions and the analysis of those individual rate contributors provide mechanistic insight into heterogeneous fluid-rock reactions. We apply long-term experiments and use AFM and interferometry surface data for the analysis of rate modes. In a second step, we apply such information for the parameterization of kinetic Monte Carlo simulation codes. By using this technique, we get information about initial pattern of porosity formation. Both, the heterogeneity of reaction rates and the heterogeneous evolution of porosity are valuable input parameters for reactive transport models. These input parameters have the potential to provide the important link to upscale microscopic information about mineral reactivity to macroscopic predictions about material flux.

Emmanuel, S. & Levenson, Y. (2014): Limestone weathering rates accelerated by micron-scale grain detachment. *Geology*, **42**, 751-754.

Fischer, C., Arvidson, R.S., Luttge, A. (2012): How predictable are dissolution rates of crystalline material? *Geochim. Cosmochim. Acta*, **98**, 177-185.

Fischer, C., Finkeldei, S., Brandt, F., Bosbach, D., Luttge, A. (2015): Direct measurement of surface dissolution rates in potential nuclear waste forms: The example of pyrochlore. *Am. Chem. Soc. - Appl. Mater. Interf.*, **7**, 17857-17865.

Luttge, A., Arvidson, R.S., Fischer, C. (2013): A stochastic treatment of crystal dissolution kinetics. *Elements*, **9**, 183-188.

LINKING EXPERIMENTAL AND NATURAL STUDIES OF DIFFUSION: CURRENT UNDERSTANDING AND FUTURE CHALLENGES

Jollands M.C.*[1]
[1] Institut des Sciences de la Terre, Université de Lausanne, Switzerland
Corresponding email: Michael.Jollands@unil.ch

Keywords:

Understanding the rates and mechanisms of diffusion in geological materials has the capability to allow timescales of geological processes to be determined, regardless of when they happened. However, this requires experimentally determined diffusion coefficients that are 1) reliable (experimentally and analytically robust), and 2) relevant (comparable to natural systems). This talk will address the second point, with reference to several salient points: Use of unrealistic compositions: Experimental studies often make use of synthetic or end member crystals and synthetic, highly doped diffusant sources. In some cases, this may affect diffusivity (e.g., Cr-Al in orthopyroxene, Fe-Mg in olivine, Li in quartz) whereas in other cases, the diffusivity is relatively insensitive to such changes (H and Be in olivine). How can we ensure a reliable comparison between experimental data and natural systems? Disparate analytical methods: One species may have several different diffusion mechanisms (e.g., Ti in olivine). Where experimental studies primarily use step-profiling techniques such as electron microprobe and laser ablation ICP-MS, there is an intrinsic bias towards measuring the fastest diffusion mechanism. If depth profiling methods are used, measurements may be biased towards slower, higher concentration diffusion mechanisms. Experimentally, both methods are correct, but how can we tell which is more relevant to natural systems? Unbuffered or partially-buffered experiments: Chemical activities (silica activity, oxygen fugacity) in rocks are, in general, relatively well buffered. In order to be comparable, experiments need to be conducted in the same, or similar chemical activity conditions. How can we assess whether this could affect timescales determined through diffusion modelling? To demonstrate these points, I shall draw on a series of experimental and 'natural' studies of diffusion. Studying diffusion in geological settings is non-trivial, but with an understanding of natural and experimental systems it can be a powerful and reliable tool.

A COMPUTATIONAL STUDY OF CARBONATE DISSOLUTION KINETICS: HOW TO DEAL WITH THE SYSTEM'S COMPLEXITY?

Kurganskaya I.*[1], Fischer C.[2], Arvidson R.S.[2], Luttge A.[2-4] & Churakov S.[1-5]
[1] Institut für Geologie, Universität Bern, Switzerland
[2] Fachbereich Geowissenschaften & Zentrum für Marine Umweltwissenschaften, Universität Bremen, Germany
[3] Earth Science Department, Rice University, Houston, TX, USA
[4] Chemistry Department, Rice University, Houston, TX, USA
[5] Laboratory for Waste Management, Paul Scherrer Institute, Villigen, Switzerland
Corresponding email: inna.kurganskaya@geo.unibe.ch

Keywords: Monte Carlo, carbonates, surface charge

Carbonate-water systems attract a significant interest from the scientific community with regard to the problems of diagenesis, geochemical carbon cycle, sequestering of CO_2 and toxic metals. The complex interplay between carbonate mineral dissolution, precipitation, and solvent composition governs the evolution of the rock-fluid system. The reliable prediction of this complex system's behaviour requires a fundamental understanding of the dominant processes and their interaction over a wide range of spatial and temporal scales.

We are developing a comprehensive multi-scale model describing dissolution/abiogenic growth kinetics of carbonate minerals at various environmental conditions. The kinetics of carbonate dissolution and growth as a function of both water and crystal chemical composition has been extensively studied using experimental techniques. However, the direct upscaling of microscopic rate data is complicated by the intrinsic reaction rate variability (Arvidson et al., 2003; Fischer et al., 2012; Lüttge et al., 2013).

We investigate the spatio-temporal rate variance using the Kinetic Monte Carlo (KMC) method on nanometer to micrometer scales (Kurganskaya & Luttge, 2016). The model requires an accurate description of relevant elementary surface reactions taking place at selected surface sites, as well as their individual rates. Reactions of protonation/deprotonation at the mineral surface are responsible for the pH-dependence of dissolution rates. The presence of ions may influence these reactions as well as the dissolution rates at specific surface sites via inhibition or catalysis. We employ the Grand Canonical Monte Carlo (GCMC) simulations to access the distribution of aqueous ions near the mineral-water interface and the surface speciation (e.g., surface charge distribution) for a given bulk fluid composition (Churakov et al., 2014). Specifically, we investigate the impact of surface geometry on ion adsorption and charge distribution. The resulting data are then used as input for the KMC model, simulating dissolution at different *p*H conditions and ionic concentrations. We also discuss the estimation of molecular detachment/attachment rates at the large variety of reactive sites affected by the charge and ionic presence. The existing data obtained from atomistic studies of the mechanism and thermochemistry of surface reactions provide us with important model parameters, although the entire parameter set is as yet incomplete. In order to solve this problem, we use a "trial-and-error" approach to estimate missing parameters. Integrating all the relevant data, we test the predictive capability of the new modelling approach on published experimental datasets.

Arvidson, R.S., Ertan, I.E., Amonette, J.E., Luttge, A. (2003): Variation in calcite dissolution rates: A fundamental problem? *Geochim. Cosmochim. Acta*, **67**, 1623-1634.

Churakov, S.V., Labbez, C., Pegado, L., Sulpizi, M. (2014): Intrinsic acidity of surface sites in calcium silicate hydrates and its implication to their electrokinetic properties. *J. Phys. Chem. C*, **118**, 11752-11762.

Fischer, C., Arvidson, R.S., Lüttge, A. (2012): How predictable are dissolution rates of crystalline material? *Geochim. Cosmochim. Acta*, **98**, 177-185.

Kurganskaya, I. & Luttge, A. (2016): Kinetic Monte Carlo approach to study carbonate dissolution. *J. Phys. Chem. C*, **120**, 6482-6492.

Lüttge, A., Arvidson, R.S., Fischer, C. (2013): A Stochastic Treatment of crystal dissolution kinetics. *Elements*, **9**, 183-188.

TRANSFORMATION OF CERUSSITE $PbCO_3$ TO PHOSPHATE PHASES AT WIDE RANGE OF *p*H

Kwaśniak-Kominek M.*[1], Okniñska J.[1] & Manecki M.[1]
[1] Department of Mineralogy, Petrography and Geochemistry, University of Science and Technology, Kraków, Poland
Corresponding email: kwasniak@geol.agh.edu.pl

Keywords: cerussite, pyromorphite, mineral-water interaction

The mechanism of transformation of cerussite $PbCO_3$ into lead phases are partly analogues to the processes of calcite conversion into calcium hydroxylapatite. This analogy does not lead for Cl^- rich system because formation of Ca-chlorapatite is limited. Therefore, the aim of proposed study is to identify the mechanisms of transformation of cerussite in the reaction with phosphate-containing solutions into minerals which belong to apatites and other lead phosphate phases in dependence of *p*H and Cl ions.

The parameters of the experiments include *p*H and presence or absence of the chlorine ions. Cerussite crystals were placed in 2M $(NH_4)H_2PO_4$ or a mixture of 2M $(NH_4)H_2PO_4$ and 0.7M NH_4Cl, at *p*H = 3.0, 5.0, and 7.0. X-ray powder diffraction and Raman spectroscopy were used to identify the reaction products. Microstructural relationship between phases and their chemical composition were determined by electron microprobe (EMP) and scanning electron microscopy (SEM-EDS).

In each case, surface of cerussite crystal was covered by polycrystaline lead phases. In the presence of Cl at wide range of *p*H a layer of pyromorphite replaces thin surface layer of cerussite. Elongated crystals 1-2 μm in size are roughly parallel to each other and perpendicular to the surface. These results show that in presence of Cl ions pyromorphite crystallize as the most stable phase. In the absence of chlorides the reaction products are more complex and their formation depend strongly on *p*H. At *p*H = 3.0 reaction is fast, dissolving cerussite is replaced by a layer of polycrystalline $PbHPO_4$ (P-shultenite) composed of plate crystals 25 μm in size. The main product at *p*H = 5 is well crystalline (up to 100 μm in size) $PbHPO_4$, probably associated with small amount of $Pb_3(PO_4)_2$ under the cover of $PbHPO_4$ layer. At this conditions the porosity of the new phase is apparent the most, particularly within the products grains. This explains why whole cerussite grains are replaced and the reaction is the most advanced. At *p*H = 7 only hydroxylpyromorphite crystallizes in the form of typical hexagonal needles up to 5 μm in size.

The results indicate that local conditions at mineral-water interface directly at the reaction front affect the formation of particular product. This include *p*H and concentration of ions which are strongly affected by limited porosity of newly formed layer of secondary phases.

In the case of cerussite, the *p*H is probably elevated at the front of the reaction (by dissolving carbonates) while Cl ions concentration is limited by already formed layer of pyromorphite. As a result, at certain conditions, hydroxylpyromorphite can form in Cl^- rich solutions against the thermodynamics of the competing reactions.

Acknowledgements: This project is supported by Polish NCN grant No 2014/01/M/ST10/00355.

THE IMPACT OF INTRINSIC MICRO-PROPERTIES OF SERPENTINE MINERALS ON REACTION KINETICS AND Mg EXTRACTION EFFICIENCY IN THE CONTEXT OF ACID-TREATMENT FOR CARBON CAPTURE AND STORAGE

Lacinska A.M.*[1-2-3], Styles M.T.[1], Bateman K.[1], Wagner D.[1], Hall M.R.[2-3], Gowing C.[1] & Brown P.D.[2]
[1] Environmental Science Centre, British Geological Survey, Nottingham, United Kingdom
[2] University of Nottingham, United Kingdom
[3] GeoEnergy Research Centre, University of Nottingham, United Kingdom
Corresponding email: alci@bgs.ac.uk

Keywords: serpentine minerals, micro-properties, reaction kinetics

Serpentine minerals are Mg-rich silicates that serve as a Mg donor in carbon capture and storage by mineralisation (CCSM). The Mg is released via a combination of pre-treatment processes, all of which ultimately lead to accelerated break-up of the crystal structure. The degree of structural break-up, and hence the quantity of metal cations released, controls the extent of subsequent carbonation and thus the overall efficiency of this technological reaction. We present the results of acid-treatment (70°C, P_{amb} and *p*H < 1) of nine comprehensively-examined serpentine polymorphs and polytypes, and the subsequent microanalysis of their post-test residues. The microanalysis highlighted several aspects of great importance to the choice of the optimal feed material for CCSM. It was recognised that the reaction kinetics and the Mg extraction efficiency (Mg^{EE}) of the serpentine minerals depended greatly on the intrinsic properties of crystal structure, chemistry and rock microtexture. Accordingly, the following order of increasing Mg^{EE} was established: Al-bearing polygonal serpentine (<5%) ≤ Al-bearing lizardite 1*T* (≈5%) < antigorite (24-29%) < well-ordered lizardite $2H_1$ (≈65%) ≤ Al-poor lizardite 1*T* (≈68%) < chrysotile (≈70%) < poorly-ordered lizardite $2H_1$ (≈80%) < nanotubular chrysotile (≈85%). On this basis, antigorite and Al-bearing, well-ordered lizardite were rejected as potential feedstock material whereas any chrysotile, non-aluminous, widely spaced lizardite and/or disordered serpentine were recommended. The microanalysis also revealed the presence of a peripheral siliceous layer, up to tens of microns thick, in two samples only, and it was concluded that its formation is not universal and depends greatly upon the intrinsic microtexture of the leached particles. The siliceous layer has a potential to limit the extent of Mg extraction from the serpentines, therefore a comprehensive understanding of their formation and distribution has an important impact on the design of CCSM technology.

This study provides the first comprehensive investigation of nine, carefully-selected serpentine minerals under the same experimental conditions. We focused on material characterisation and the identification of the intrinsic micro-properties of the minerals that affect particle's reactivity. It can therefore serve as a generic basis for any acid-based CCSM pre-treatment.

VARIABILITY OF DISSOLUTION RATES OF SMECTITES AS A FUNCTION OF AMMONIUM ION CONCENTRATION AT CIRCUMNEUTRAL CONDITIONS

Lamarca-Irisarri D.*[1], Sánchez-Encinar A.[1], Van Driessche A.E.S.[2] & Huertas F.J.[1]

[1] Instituto Andaluz de Ciencias de la Tierra, Consejo Superior de Investigaciones Científicas, Universidad de Granada, Spain

[2] Institut des Sciences de la Terre, Centre National de la Recherche Scientifique, Université Grenoble-Alpes, France

Corresponding email: dlamarca82@gmail.com

Keywords: smectite, dissolution, ammonium

The mechanisms of smectite dissolution have been extensively studied, and the effect of *p*H, temperature, catalysts and inhibitors on the reaction (e.g., organic ligands, phosphates, etc.) have been analysed (e.g., Zysset & Schindler, 1996; Bauer & Berger, 1998; Cama et al., 2000; Huertas et al., 2001; Rozalén et al., 2008, 2009). In particular, the behaviour of the dissolution rate of smectite as a function of pH can summarized as follows: the rate increases with decreasing pH, reaching a minimum at near neutral *p*H, and increases again for alkaline conditions. The effect of the solution *p*H is related to the adsorption of protons on the hydroxyl groups of the reactive surface sites. The proton transfer from solution to the mineral surface occurs through the hydronium ions. Our proposal is that in near neutral conditions, other substances in sufficient concentration, such as the ammonium ion, could act as proton donors and promote dissolution.

In a geological context, the main source of ammonium is the maturation of organic matter during diagenesis in sedimentary basins (Williams et al., 1992). Hence, in such an environment the interactions between ammonium and smectites can be expected. Therefore, this study is focused on characterizing these interactions. We conducted experiments for a broad range of ammonium concentrations, from 0.0001 up to 0.5 M in stirred flow-through cells (46 mL) where the solid/solution ratio was 2 g/L (0.09 g of smectite). This range of ammonium concentrations is based on those reported in the literature for natural media. Montmorillonite from the “Cortijo de Archidona” deposit (Cabo de Gata, Almería, SE Spain) was used as smectite source. The flow-through cells were immersed in a thermostatic bath to keep the temperature constant at three different values (25, 50 and 70±1°C). The input solution was led from the reservoir to the cell by a peristaltic pump at a constant pumping rate of 0.02 mL/min and the output solutions were sampled every 48-72 hours.

In general, during the first 1000 hours of experimentation, relatively high Si concentrations are observed. This behaviour is associated with the hydrolysis of soluble silica phases. The concentrations of Al have a reverse behaviour; they are very low during early stages and increase according experimental time increases. This is interpreted as smectite dissolution and Al sorption. To evaluate ammonium effects on smectite dissolution rate, Si-derived dissolution rates under-steady state conditions were plotted versus ammonium concentration. At 25 and 50ºC, the smectite dissolution rate significantly increases with increasing ammonium concentration in solution. At 70ºC, however, the trend is less clear, probably due to silica precipitation and Al sorption at the crystal edges, which reduces the effective smectite reactive surface area. Our results indicate that ammonium act as a catalyst of the dissolution/transformation of smectite under diagenetic conditions.

Bauer, A. & Berger, G. (1998): Kaolinite and smectite dissolution rate in high molar KOH solutions at 35° and 80°C. *Appl. Geochem.*, **13**, 905-916.

Cama, J., Ganor, J., Ayora, C., Lasaga, C.A. (2000): Smectite dissolution kinetics at 80°C and *p*H 8.8. *Geochim. Cosmochim. Acta*, **64**, 2701-2717.

Huertas, F.J., Caballero, E., Jiménez De Cisneros, C., Huertas, F., Linares, J. (2001): Kinetics of montmorillonite dissolution in granitic solutions. *Appl. Geochem.*, **16**, 397-407.

Metz, V., Amram, K., Ganor, J. (2005): Stoichiometry of smectite dissolution reaction. *Geochim. Cosmochim. Acta*, **69**, 1755-1772.

Rozalén, M.L., Huertas, F.J., Brady, P.V., Cama, J., Garcia-Palma, S., Linares, J. (2008): Experimental study of the effect of *p*H on the kinetics of montmorillonite dissolution at 25°C. *Geochim. Cosmochim. Acta*, **72**, 4224-4253.

Rozalén, M., Huertas, F.J., Brady, P.V. (2009): Experimental study of the effect of pH and temperature on the kinetics of montmorillonite dissolution. *Geochim. Cosmochim. Acta*, **73**, 3752-3766.

Williams, L.B., Wilcoxon, B.R., Ferrell, R.E., Sassen, R. (1992): Diagenesis of ammonium during hydrocarbon maturation and migration, Wilcox Group, Louisiana, U.S.A. *Appl. Geochem.*, **7**, 123-134.

Zysset, M. & Schindler, P.W. (1996): The proton promoted dissolution kinetics of K-montmorillonite. *Geochim. Cosmochim. Acta*, **60**, 921-931.

CRYSTAL CHEMISTRY OF TOURMALINES FROM THE ERONGO MOUNTAINS, NAMIBIA, STUDIED BY RAMAN SPECTROSCOPY

Lensing-Burgdorf M.*[1], Watenphul A.[1], Schlüter J.[2] & Mihailova B.[1]
[1] Fachbereich Geowissenschaften, Universität Hamburg, Germany
[2] Centrum für Naturkunde, Mineralogisches Museum, Universität Hamburg, Germany
Corresponding email: martina@burgdorf.at

Keywords: tourmaline, Raman spectroscopy, Erongo

The crystal chemistry of eight black tourmaline samples from miarolitic cavities in granites of the Erongo mountains, Namibia, were studied by Raman spectroscopy and complementary electron microprobe analysis. Tourmalines from that locality usually correspond to the sodium iron end member schorl, $NaFe^{2+}_3Al_6(Si_6O_{18})(BO_3)_3(OH)_3(OH)$. Unusual morphologies caused by dissolution or overgrowth processes suggest that other tourmaline species may occur, including the rare sodium-free iron end member foitite, $(Fe^{2+}_2Al)Al_6(Si_6O_{18})(BO_3)_3(OH)_3(OH)$.

Different tourmaline species can be distinguished by their Raman scattering, especially in the range between 3300-3800 cm^{-1} generated by the ^{V}OH and ^{W}OH stretching modes. Recently a method to calculate the crystal chemistry of tourmalines via Raman peak intensities and positions has been developed (Watenphul et al., 2016). Thus we applied Raman spectroscopy as a fast, preparation-free, and non-destructive technique to different spatial areas of samples with different morphology in order to check for the existence of foitite. Indeed, foitite can be found at the very edge of small needle-like crystals growing on top of the main crystal body. Chemical zonation was detected in both the needle-like crystals and the main body, showing a composition ranging from schorl to foitite. Raman data also indicate the presence of Mg or Li as secondary elements in some samples.

Thin sections of two tourmaline specimens exhibiting different shape reveal optically distinguishable lateral and/or transverse zonation. The core of both crystals is dominated by schorl, outer parts of the crystals tend to be chemically close to the schorl-foitite join.

The ^{V}OH- and ^{W}OH peaks in the Raman spectra were assigned to the most possible occupation of the YZZ-YZZ-YZZ species and YYY species respectively following the peak assignment model developed by Watenphul et al. (2016). The content of ^{Y}(Fe+Mn), ^{Y}Al and ^{Y}Li was calculated from the integrated intensities of the V-site OH-stretching peaks. The X-site occupancy was calculated from the equation $\omega = (41\pm3)x_{(Na+Ca)} + (3467\pm2)$ using the peak position of the V-site OH peak corresponding to the YZZ-YZZ-YZZ species with the highest content of Al. The element contents calculated from the Raman data match well the compositions determined by electron microprobe analysis.

Watenphul, A., Burgdorf, M., Schlüter, J., Horn, I., Malcherek, T., Mihailova, B. (2016): Exploring the potential of Raman spectroscopy for crystallochemical analyses of complex hydrous silicates: II. Tourmalines. *Am. Mineral.*,***101***, 970-985.

INTERFACE MIGRATION MECHANISM ON CORUNDUM/SPINEL/PERICLASE: ATOMIC STUDY *VIA* SCANNING TRANSMISSION ELECTRON MICROSCOPY

Li C.*[1], Griffiths T.A.[1], Pennycook T.J.[2], Mangler C.[2], Götze L.C.[3], Jeřábek P.[4], Meyer J.[2], Habler G.[1] & Abart R.[1]

[1] Department für Lithosphärenforschung, Universität Wien, Austria
[2] Fakultät für Physik, Universität Wien, Austria
[3] Institut für Geologische Wissenschaften, Freie Universität Berlin, Germany
[4] Institute of Petrology and Structural Geology, Charles University, Prague, Czech Republic
Corresponding email: chen.li@univie.ac.at

Keywords: interface reaction, misfit dislocation, diffusion

In nature it is common that a new mineral grows at the contact between two minerals due to the inter-diffusion of elements. Understanding its growth mechanism is critical for reconstructing conditions and rates of mineral formation. The growth of the new phase is controlled by the coupling of *interface reaction* and *long-range diffusion*. To understand the *interface reaction*, it is essential to figure out the atomic structure of the interfaces.

In this research, spinel ($MgAl_2O_4$, Spl) has been grown between periclase (MgO, Per) and corundum (Al_2O_3, Crn) via pulsed laser deposition (Götze et al., 2014) and uniaxial stress methods (Jeřábek et al., 2014) in order to study the initial and progressive growth stages, respectively. Electron Backscatter Diffraction (EBSD) has been used to study the interfacial orientation relationship on both Per/Spl and Spl/Crn reaction interfaces. The EBSD results show that the Spl layer splits into two different sections: a thinner part in topotaxic orientation relationship with Per, and a thicker part topotaxic with Crn. Then Focused Ion Beam (FIB) was used to extract samples from the interface areas with representative orientation relationships, and the atomic structure has been studied by aberration-corrected Scanning Transmission Electron Microscopy (STEM).

The atomic resolution STEM images of the Spl/Crn interface show that the interface is located where the (001) lattice plane of Crn coincides with the (111) lattice plane of Spl, which are both occupied by Al atoms exclusively. On the other side, the Per/Spl interface shows a periodic configuration, consisting of curved segments (convex towards Per). The STEM images reveal regularly spaced misfit dislocations at the positions of “cusps”, occurring every ~ 4.5 nm. A similar configuration is observed at another equivalent interface area with a 90° rotation of the structure. These results reveal the 3D configuration of the interface, which has a grid of convex protrusions of spinel into periclase with a misfit dislocation at each minimum. The structure reveals the mechanism of the interface migration, where climb of the misfit dislocations is the rate-limiting factor and therefore leads to this scalloped geometry. Furthermore, the extra atoms required for dislocation climb leave behind vacancies that eventually form pores at the interface, which provides additional resistance to interface motion and leads to doming of the interface on the scale of individual grains. These results also show that a fundamental understanding of the interface reaction and migration on the atomic scale is the key to understanding the interface migration on the larger scale.

Acknowledgement: This research was funded by the EU’s Horizon 2020 Marie Curie grants No. 656378–Interfacial Reactions (CL) and the Austrian Science Fund (FWF): I1704-N19 in the framework of FOR741-DACH (GH).

Götze, L.C., Abart, R., Milke, R., Schorr, S., Zizak, I., Dohmen, R., Wirth, R. (2014): Growth of magnesio-aluminate spinel in thin-film geometry: in situ monitoring using synchrotron X-ray diffraction and thermodynamic model. *Phys. Chem. Minerals*, **41**, 681-693.

Jeřábek, P., Abart, R., Rybacki, E., Habler, G. (2014): Microstructure and texture evolution during growth of magnesio-aluminate spinel at corundum-periclase interfaces under uniaxial load: The effect of stress concentration on reaction progress. *Am. J. Sci.*, **314**, 940-965.

CRYSTAL GROWTH KINETICS IN THE Ba-Mg-CO_3 SYSTEM: NEW INSIGHTS INTO LOW-TEMPERATURE Mg-CARBONATE GROWTH AND THE DOLOMITE PROBLEM

Lindner M.*[1], Saldi G.D.[2], Schott J.[2] & Jordan G.[1]

[1] Department für Geo- und Umweltwissenschaften, Ludwig-Maximilians-Universität München, Germany

[2] Géosciences Environnement Toulouse, Centre National de la Recherche Scientifique, Université Paul Sabatier, Observatoire Midi-Pyrénées, Toulouse, France

Corresponding email: michael.lindner@lrz.uni-muenchen.de

Keywords: carbonate growth kinetics, mixed-flow reactor, norsethite

Norsethite ($BaMg(CO_3)_2$) is perceived as an analogue mineral to dolomite ($CaMg(CO_3)_2$) because of their structural and chemical similarities (Lippmann, 1973). But in contrast to dolomite, norsethite grows from aqueous solutions at ambient temperatures within few days. This is of special interest as the dehydration barrier of Mg^{2+} is a likely cause of the inhibition of low temperature dolomite precipitation. The relative ease with which norsethite can overcome this barrier shows that the problem of dolomite formation is more complex. In order to attain a comprehensive understanding of the processes, not only growth of norsethite as the intermediate phase in the Ba-Mg carbonate system needs to be investigated but also the growth of the two endmembers (magnesite and witherite) in the presence of the respective other cation.

In this study, mixed-flow reactor experiments were conducted to investigate the growth of Ba-Mg-carbonate minerals at steady-state conditions from aqueous solutions. Experiments on witherite seeds were performed at 50°C, *p*H ~ 7.6 and an ionic strength of 0.1 M in mixed-flow PTFE reactors, whereas experiments on synthetic magnesite seeds were performed at 100°C, *p*H ~ 7.7 and at 0.1 M ionic strength in hydrothermal mixed-flow titanium reactors.

While at Mg^{2+}:Ba^{2+} ratios in solution of 1:10, no effect on growth of witherite could be detected, higher ratios (10:1) led to dissolution of witherite seed material and to precipitation of norsethite. During the experimental run of 10 days, 90 % of the seed material had been transformed to norsethite. Growth experiments on magnesite seeds with Mg^{2+}:Ba^{2+} ratios in solution of 15:1 to 100:1 showed both norsethite precipitation and a continued growth of the magnesite seeds with no apparent influence on magnesite growth rates. Therefore, large parts of the Ba-Mg-carbonate system are dominated by the occurrence of norsethite and even Mg^{2+}:Ba^{2+} ratios in solution as small as 10:1 are sufficient to yield norsethite, whereas Mg^{2+}:Ca^{2+} ratios of 10:1 lead to calcite with only few mol % Mg^{2+} rather than to ordered dolomite (Mucci & Morse, 1983).

The measured growth rates of norsethite provide a lower limit for the growth kinetics of an anhydrous magnesium carbonate at ambient temperatures. With optimized parameters, higher rates at even lower temperatures might be expected. The dehydration barrier of Mg^{2+}, therefore, cannot be the only cause for the lack of low temperature dolomite growth (as pointed out by Xu et al., 2013).

We speculate that the preferential formation of ordered norsethite over a solid solution is facilitated by the large difference in Mg and Ba ionic radii. Due to the presumably very high free energy of formation of the solid solution, ordering into distinct Ba- and Mg-layers is the only way to combine both cations within one phase. This behavior is in great contrast to the Ca-Mg system at low temperatures where all Mg^{2+}:Ca^{2+} ratios in solution fail to precipitate ordered dolomite.

Lippmann, F. (1973): Sedimentary carbonate minerals. Springer, Berlin, 228 p.

Mucci, A. & Morse, J.W. (1983): The incorporation of Mg*2*+ and Sr*2*+ into calcite overgrowths: influences of growth rate and solution composition. *Geochim. Cosmochim. Acta*, **47**, 217-233.

Xu, J., Yan, C., Zhang, F., Konishi, H., Xu, H., Teng, H.H. (2013): Testing the cation-hydration effect on the crystallization of Ca-Mg-CO_3 systems. *Proc. Nat. Acad. Sci. USA*, **110**, 17750-17755.

QUANTIFYING DIFFUSION OF TITANIUM IN OLIVINE

Petrishcheva E.*[1], Jollands M.C.[2-3] & Abart R.[1]
[1] Department für Lithosphärenforschung, Universität Wien, Austria
[2] Research School of Earth Sciences, Australian National University, Canberra, Australia
[3] Institute des sciences de la Terre, Université de Lausanne, Switzerland
Corresponding email: elena.petrishcheva@univie.ac.at

Keywords: Ti-diffusion, olivine, inverse modelling

The behaviour of trace elements in mantle minerals is of key importance in geochemistry and mantle petrology. We consider diffusion of titanium in olivine; experimental observations and invers modelling are presented. The diffusion of titanium along the [001] direction of synthetic forsterite was quantified based on concentration-distance data obtained from in- diffusion experiments done at 1400°C and ambient pressure. Two different oxygen fugacities were applied. In addition, the effect of component activities in the system MgO-SiO_2-TiO_2 as defined by four different buffer assemblages used as a Ti source was studied. To this end, titanium was deposited on the surface of oriented olivine single crystals in the form of the different buffer assemblages using polyethylene glue.

The measured Ti-concentration profiles have complex shapes, which vary with oxygen fugacity and buffer assemblage. The volume distribution of titanium is far from being described by a standard solution of a linear diffusion equation. Relatively high initial concentrations of titanium at the crystal surface associated with high silica activity and low oxygen fugacity conditions result in pronouncedly nonlinear diffusion suggesting a dependence of the diffusivity of titanium on concentration. This is ascribed to the introduction of vacancies during in-diffusion of trivalent or tetravalent titanium on the octahedral sub-lattice. The vacancies are required for charge balancing substitution of tetra- and trivalent titanium for divalent magnesium. The dependence of Ti-diffusivity on Ti-concentration was quantified using a proper modification of the Boltzmann-Matano analysis. Moreover, the Ti-diffusion profiles show a sudden jump from larger to lower concentrations far inside the crystal. This behaviour is ascribed to trapping of tetravalent titanium on the tetrahedrally coordinated site, which is related to the presence of trace amounts of aluminium in the olivine crystal. The Ti trapped on tetrahedral sites becomes “inactive” in terms of diffusion, but it is detected in chemical analysis. The jump occurs at a position where free traps are still available, which coincides with an opposite jump in the background concentration of aluminium. The diffusion of trace amounts of Ti in the 10's to 100's wt. ppm concentration range provides an interesting example of pronouncedly non-linear diffusion, which cannot be treated in the framework of standard error-function solution of the diffusion equation.

CHROMIUM ISOTOPE FRACTIONATION DURING COPRECIPITATION WITH CALCITE USING CO_2-DIFFUSION TECHNIQUE

Rodler A.S.*[1-2], Baldermann A.[3], Dietzel M.[3] & Frei R.[1-2]

[1] Department of Geosciences and Natural Resource Management - Section of Geology, University of Copenhagen, Denmark

[2] Nordic Center for Earth Evolution, Odense, Denmark

[3] Institut für Angewandte Geowissenschaften, Technische Universität Graz, Austria

Corresponding email: alexandra.rodler@reflex.at

Keywords: Cr isotope composition, marine carbonates, paleo seawater

The chromium (Cr) isotope signature of ancient carbonate minerals can provide valuable information about the oxygenation history and redox state of contemporaneous seawater and by extension of the continents (e.g., Frei *et al.*, 2011). However, before the Cr isotope composition of ancient chemical sediments can be fully interpreted, it is essential to properly ascertain the Earth's Cr cycle. Modern marine non-skeletal carbonates appear to faithfully preserve the Cr isotope signal of the ambient seawater, with an offset (≤ 0.2 to ≤ 0.3 ‰; Bonnand *et al.*, 2013) consistent with previous experiments that investigated Cr isotope fractionation upon coprecipitation with calcium carbonate in instantaneous mixing and silica hydrogel experiments (Rodler *et al.*, 2015). However, modern marine biogenic calcium carbonates (corals) show a rather heterogeneous Cr isotope composition and a tendency towards isotopically lower values compared to ambient seawater (Pereira *et al.*, 2015). We employed CO_2 diffusion experiments (e.g., Dietzel *et al.*, 2004) to precipitate calcium carbonate in the presence of aqueous chromate to further study the Cr isotope composition of solid and liquid phases. Final precipitates of these experiments were confirmed as calcite by XRD patterns, ATR-FTIR spectra and SEM images. No significant difference between solid samples that were precipitated at different initial solution Cr concentrations (~ 0.6 to ~ 60 µg g^{-1}) and/or precipitation rates were detected. These experiments further reveal an enrichment of Cr in the precipitates (K_d* of up to ~ 6.5), consistent with previous reports of increased Cr concentrations in chemical sediments compared to seawater. Further, our results for calcite precipitated in the presence of Cr(VI) using a CO_2 diffusion technique, show a preferential incorporation of light Cr isotopes in the final precipitates (relative isotope difference between precipitate and initial solution, $\delta^{53}Cr_{[p\text{-}is]}$, of ~ -0.8 to ~ -2.7‰), particularly pronounced at lower initial solution chromate concentrations. The enrichment of the light Cr isotopes in the precipitates vs. the dissolved Cr is possibly due to reductive processes on the mineral surface during adsorption and incorporation of Cr, which would consequently enrich the solution in heavy Cr isotopes. This would indicate a possible under-estimation of past seawater Cr isotopic signals when using Cr isotope data recorded in ancient marine carbonates, similar to the Cr isotope offset observed for modern corals compared to ambient seawater.

Bonnand, P., James, R.H., Parkinson, I.J., Connelly, D.P., Fairchild, I.J. (2013): The chromium isotopic composition of seawater and marine carbonates. *Earth Planet. Sci. Letters*, **382**, 10-20.

Dietzel, M., Gussone, N., Eisenhauer, A. (2004): Co-precipitation of Sr^{2+} and Ba^{2+} with aragonite by membrane diffusion of CO_2 between 10 and 50°C. *Chem. Geol.*, **203**, 139-151.

Frei, R., Gaucher, C., Døssing, L.N., Sial, A.N. (2011): Chromium isotopes in carbonates - A tracer for climate change and for reconstructing the redox state of ancient seawater. *Earth Planet. Sci. Letters*, **312**, 114-125.

Pereira, N., Voegelin, A.R., Paulukat, C., Sial, A.N., Ferreira, V.P., Frei, R. (2015): Chromium isotope signatures in scleractinian corals from the Rocas Atoll, Tropical South Atlantic. *Geobiol.*, **14**, 54-67.

Rodler, A., Sánchez-Pastor, N., Fernández-Díaz, L., Frei, R. (2015): Fractionation behavior of chromium isotopes during coprecipitation with calcium carbonate: implications for their use as paleoclimatic proxy. *Geochim. Cosmochim. Acta*, **164**, 221-235.

REPLACEMENT PROCESSES IN EVAPORITES: GYPSUM TO BARITE REACTIONS

Ruiz-Agudo C.*[1], Ruiz-Agudo E.[2], Putnis C.V.[1-3] & Putnis A.[4]
[1] Institut für Mineralogie, Universität Münster, Germany
[2] Departamento de Mineralogía y Petrología, Universidad de Granada, Spain
[3] Nanochemistry Research Institute, Department of Chemistry, Curtin University, Perth, Australia
[4] Institute for Geoscience Research, Curtin University, Perth, Australia
Corresponding email: c_ruiz02@uni-muenster.de

Keywords: barite, gypsum, replacement

Mineral replacement reactions are critical in most geochemical processes, including diagenesis, the redistribution of elements in the Earth's crust and hence the formation of secondary mineral and ore deposits. When a mineral surface is in contact with an aqueous fluid, replacement reactions may occur via interface-coupled dissolution-precipitation, resulting in the formation of a new phase (Putnis, 2002, 2009; Putnis & Putnis, 2007; Ruiz-Agudo et al., 2014). In these processes, dissolution of the parent phase occurs and consequently the solution at the mineral-fluid interface becomes supersaturated with respect to a new mineral phase that can nucleate at the surface of the parent mineral (Ruiz-Agudo et al., 2014, and references therein). In the present study, we provide experimental evidence suggesting that during the interaction of gypsum ($CaSO_4 \cdot 2H_2O$) cleavage surfaces with Ba-bearing solutions, gypsum is pseudomorphically replaced by barite ($BaSO_4$). A homogenous micron-sized layer of barite is formed on gypsum cleavage surfaces within some hours of exposure to Ba-bearing solutions. This occurs most likely via an interface-coupled dissolution-precipitation mechanism. Interestingly, our observations show a certain degree of crystallographic control on the product layer by the structure of the parent substrate. Our results support previous work which suggests that barite structures and textures found in Archean deposits in Western Australia and South Africa are probably the result of the pseudomorphic replacement of original evaporitic gypsum deposits (Lamert et al., 1978). In addition, our observations suggest that the pseudomorphic replacement of gypsum by barite could be used as a conservation procedure for gypsum sculptures and plasterworks, increasing their resistance against water and humidity while preserving the surface features of the original mineral substrate.

Lambert, I.B., Donnelly, T.H., Dunlop, J.S.R., Groves, D.I. (1978): Stable isotopic compositions of early Archaean sulphate deposits of probable evaporitic and volcanogenic origins. *Nature*, **276**, 808-811.

Putnis, A. (2002): Mineral replacement reactions: from macroscopic observations to microscopic mechanisms. *Mineral. Mag.*, **66**, 689-708.

Putnis, A. (2009): Mineral replacement reactions. In thermodynamics and kinetics of water-rock interactions. *Rev. Mineral. Geochem.*, **30**, 87-124.

Putnis, A. & Putnis, C.V. (2007): The mechanism of reequilibration of solids in the presence of a fluid phase. *J. Solid St. Chem.*, **180**, 1783-1786.

Ruiz-Agudo, E., Putnis, C.V., Putnis, A. (2014): Coupled dissolution and precipitation at mineral–fluid interfaces. *Chem. Geol.*, **383**, 132-146.

AN EXPERIMENTAL STUDY OF SURFACE ALTERED LAYER FORMATION DURING CHEMICAL WEATHERING OF SILICATE MINERALS: THE ROLE OF ADDITIVES

Ruiz-Agudo E.*[1], Ruiz-Agudo C.[2] & Rodriguez-Navarro C.V.[1]
[1] Departamento de Mineralogía y Petrología, Universidad de Granada, Spain
[2] Institut für Mineralogie, Universität Münster, Germany
Corresponding email: encaruiz@ugr.es

Keywords: surface altered layers, wollastonite, chemical weathering

The chemical weathering and carbonation of primary Ca and Mg silicates (e.g., pyroxenes and olivine) takes place naturally when rocks containing these minerals are exposed to the physical-chemical conditions of the Earth surface. Their weathering takes place by means of the so-called "Urey Reaction": $MSiO_3 + H_2O + CO_2 = MCO_3 + SiO_2 \cdot nH_2O$ (where M is a divalent metal, like Ca^{2+} or Mg^{2+}), which is responsible for the long-term regulation of CO_2 concentration in the atmosphere and of the evolution of T and climate on the Earth surface (on geologic time scales, > 10^6 years). An imbalance in the atmospheric CO_2 concentration can trigger a glaciation, or a global warming event, because CO_2 is an effective greenhouse gas. It has become evident that the increasing CO_2 concentrations associated with massive fossil fuel burning, from preindustrial values (~ 280 ppmv) to the present ones (~ 400 ppmv) are causing a global warming, whose consequences, if CO_2 emissions continue growing at the present rate, can be catastrophic. In addition to cut/reduce emissions, there is an urgent need to capture and store atmospheric CO_2, ideally as stable minerals (carbonates). Such process mimics, at the laboratory or industrial scales, the natural weathering and carbonation of Ca and Mg silicates. Nevertheless, the current lack of knowledge on the exact dissolution mechanism of primary silicates prevent the optimization of this process and its large-scale application. Here we study in detail the mechanism of wollastonite dissolution ($CaSiO_3$) and formation of passivating amorphous silica surface altered layers (SALs) in the presence of inorganic (fluor-containing salts) and organic additives (carboxilic acid derivatives). We provide experimental evidence that demonstrate that these layers form by an interface-coupled dissolution-precipitation mechanism, and show how the presence of the tested additives prevents/limits their formation, thereby speeding-up silicate dissolution and aiding to solve one of the greatest handicaps for the effective use of silicates in the capture and storage of CO_2. Moreover, the results of this study provide information for a better prediction of weathering rates and climate evolution, and for the improvement and optimization of mineral CO_2 capture.

INTRACONTINENTAL OROGENY, CENTRAL AUSTRALIA: SHEAR ZONE PATTERNS AND THE ROLE OF FLUIDS IN LITHOSPHERIC WEAKENING

Silva D.*[1], Daczko N.[1], Piazolo S.[1], Raimondo T.[2] & Putnis A.[3]
[1] Department of Earth and Planetary Sciences, Macquarie University, Sydney, Australia
[2] School of Natural and Built Environments, University of South Australia, Adelaide, Australia
[3] Institute for Geoscience Research, Curtin University, Perth, Australia.
Corresponding email: david.barbosa-da-silva@hdr.mq.edu.au

Keywords: Strangways Range, anastomosing shear zones, fluid interaction

Central Australia, in particular the Arunta Region and the Musgrave Province, has undergone a complex geological history spanning from the Proterozoic to Paleozoic. The Neoproterozoic and Early Paleozoic interval involved intracontinental compression related to tectonic stress that produced crustal thickening and deep exhumation of basement rocks far from active plate boundaries. This peculiar process of intracontinental mountain building was facilitated by an extensive regional network of anastomosing shear zones and thrust faults during the Petermann (600-530 Ma) and Alice Springs (450-300 Ma) Orogenies. In recent years, the role of fluids has been increasingly recognised as one of the key features promoting crustal deformation in these orogenic systems, complementing earlier studies of structural geometry and thermal anomalies.

In this study, we explore the possibility that fluid infiltration into a metastable, stressed crust provides an important mechanism for mechanical weakening and energy dissipation through metamorphism and deformation. We present data from Alice Springs-aged shear zone networks in the eastern Arunta Region, across a field gradient of increasing structural depths from the Reynolds Range to the Strangways Range. We combine GIS-based shear zone pattern analysis and detailed field mapping of longitudinal structural relationships with meso- to microchemical characterisation of shear zones and their adjacent wall rocks. We explore the first-order control that rock type has on shear zone localisation and evolution, contrasting the anastomosing shear zone patterns and character of deformation in lower grade (Reynolds Range) versus higher grade (Strangways Range) shear zones. Finally, we investigate the likely character of the fluids implicated in facilitating intracontinental orogeny: water versus melt or both?

PRELIMINARY MAJOR- AND TRACE-ELEMENT DATA OF WÖHLERITE FROM MIASKITIC AND MILDLY AGPAITIC PEGMATITES OF THE LARVIK PLUTONIC COMPLEX, OSLO REGION, NORWAY

Sunde Ø.*[1], Friis H.[1], Andersen T.[2] & Selbekk R.S.[1]
[1] Natural History Museum, University of Oslo, Norway
[2] Department of Geosciences, University of Oslo, Norway
Corresponding email: oyvind.geologi@gmail.com

Keywords: pegmatite, nepheline syenite, wöhlerite

The Larvik Plutonic Complex (LPC) in the Oslo Rift (Norway) contains pegmatites of both miaskitic (i.e., nepheline syenites with simple minerals such as zircon, titanite, ilmenite) and mildly agpaitic mineralogy (i.e., nepheline syenites with complex Na-Zr silicates, e.g., eudialyte; Sørensen, 1997). The LPC is a composite ring-structured pluton consisting of larvikite, which change in composition from quartz- to nepheline-bearing monzonites with increasing fractionation towards the west. The trend is observed in pegmatite mineralogy with mildly agpaitic assemblages confined to the western margin and currently thought to be related with late nepheline syenites intruding the larvikite, but the petrogenetic association of the pegmatite-forming melt with internal fractionation of the larvikite or late nepheline syenite intrusions is poorly understood.

Wöhlerite, ideally $Na_2Ca_4(Zr,Nb)_2(Si_2O_7)_2(O,OH,F)_4$, is not a characteristic mineral for agpaitic rocks, but it is common in the pegmatites within the LPC. It crystallized as an early magmatic phase in up to 6 cm tabular crystals together with the mafic silicate minerals amphibole, pyroxene, and magnetite. Pegmatites carrying wöhlerite also contain late stage alteration zones associated with a late fluid phase, which is commonly observed as extensive zeolitization of the feltspathoids. Wöhlerites in the alteration zone typically show remobilization of high field strength elements (e.g., Nb^{5+}, Zr^{4+}) resulting in the formation of secondary minerals such as pyrochlore, zircon, and hiortdahlite.

The crystal structure of wöhlerite consists of four octahedral wide walls sharing edges and linked by disilicate groups (e.g., Merlino & Perchiazzi, 1988; Biagioni *et al*., 2012). Cations with different charge and size (e.g., Ca^{2+}, Zr^{4+}) average over the different octahedral sites, and thus imply possible compositional variability in respect to trace elements.

The study investigates the use of wöhlerite as an indicator mineral of the source of pegmatite forming melts, and if contrasting compositional trends record changes in magma composition. A large set of specimens from different localities have been analyzed and quantitative EDS analyses and backscatter images did not reveal either zoning or major chemical variations in the samples. Detailed chemical analyses revealed minor variations in the major elements whereas larger variations were observed for the trace-elements. In particular, wöhlerite from different ring sections show different chondritic normalized REE profiles in respect to the relative proportions of LREE and HREE.

Biagioni, C., Merlino, S., Parodi, G.C., Perchiazzi, N. (2012): Crystal chemistry of minerals of the wöhlerite group from the Los Archipelago, Guinea. *Can. Mineral*., **50**, 593-609.

Merlino, S. & Perchiazzi, N. (1988): Modular mineralogy in the cuspidine group of minerals. *Can. Mineral*., **26**, 933-943.

Sørensen, H. (1997): The agpaitic rocks – an overview. *Mineral. Mag*., **61**, 485-498.

Session S11:

Reading and understanding metamorphic rocks

Conveners:

Lukas Baumgartner (Lausanne – Switzerland)

Pavel Pitra (Rennes – France)

Dave Waters (Oxford – United Kingdom)

NEW CONSTRAINTS ON PT EVOLUTION OF METAMORPHIC ROCKS FROM SINGLE INCLUSION PIEZOBAROMETRY

Alvaro M.*[1], Angel R.J.[2], Mazzucchelli M.L.[2] & Nestola F.[2]
[1] Dipartimento di Scienza della Terra e dell'Ambiente, Università di Pavia, Italy
[2] Dipartimento di Geoscienze, Università di Padova, Italy
Corresponding email: matteo.alvaro@unipv.it

Keywords: elastic geobarometry, mineral inclusion, entrapment pressure

Conventional thermobarometric methods are normally based on chemical equilibria between two or more phases, although the composition and states of order in some minerals can also act as single-mineral thermobarometers (e.g., Nimis & Taylor, 2000). The identification and chemistry of inclusions trapped in host minerals during growth of the host phase has also been used to constrain P-T paths, but for simple stoichiometric phases such as quartz, coesite or diamond, the observation of such phases only provides broad constraints on the P and T of entrapment. The determination of the remnant pressure on the inclusion, measured by X-ray diffractometry, birefringence analysis or Raman spectroscopy, provides an alternative and/or complementary method of barometry using elasticity theory. A remnant pressure in an inclusion is developed because the inclusion and the host have different thermal expansion and compressibilities, and the inclusion does not expand in response to P and T as would a free crystal in air. Instead it is restricted to expand only as much as the host mineral allows, and this constriction in volume can result in inclusions exhibiting over-pressures when the pair is studied at room conditions (Angel et al., 2015). This concept has been known for a long time, but satisfactory quantitative modelling of inclusion-host systems based on non-linear elasticity theory and precise thermal-pressure equations of state has only recently come available, even though it is still restricted to elastically isotropic minerals (Angel et al., 2014).

No mineral is elastically isotropic, but we will describe how the principles of the current theory of host-inclusion elasticity can provide qualitative constraints on P-T paths of metamorphic rocks, such as whether entrapment occurred during burial or exhumation (Angel et al., 2015), and whether the elastic signal from the inclusion has been reset by plastic flow in the host, which would indicate substantial residence times at high temperatures. In this sense, inclusion piezobarometry is very complimentary to conventional chemical geobarometry; the elastic signal may be over-written at high temperatures where chemical equilibrium is easily established, but it can preserve evidence for low-temperature entrapment conditions where chemical equilibrium may not have been attained.

Acknowledgements: This work was supported by ERC starting grant 307322 to Fabrizio Nestola and by the MIUR-SIR grant “MILE DEEp” (RBSI140351) to M. Alvaro.

Angel, R.J., Mazzucchelli, M.L., Alvaro, M., Nimis, P., Nestola, F. (2014): Geobarometry from host-inclusion systems: The role of elastic relaxation. *Am. Mineral.*, **99**, 2146-2149.

Angel, R.J., Nimis, P., Mazzucchelli, M.L., Alvaro, M., Nestola, F. (2015): How large are departures from lithostatic pressure? Constraints from host-inclusion elasticity. *J. Metam. Geol.*, **33**, 801-813.

Nimis P. & Taylor, W.R. (2000): Single clinopyroxene thermobarometry for garnet peridotites. Part I. Calibration and testing of a Cr-in-Cpx barometer and an enstatite-in-Cpx thermometer. *Contrib. Mineral. Petrol.*, **139**, 541-554.

THE LAWSONITE+GLAUCOPHANE METAGABBROS FROM THE ELBA ISLAND (ITALY): NEW INSIGHTS INTO THE INNER NORTHERN APENNINES

Bianco C.[1], Godard G.*[2], Brogi A.[1], Caggianelli A.[1] & Liotta D.[1]
[1] Dipartimento di Scienze della Terra e Geoambientali, Università di Bari, Italy
[2] Institut de Physique du Globe de Paris, Université Paris-Diderot, France
Corresponding email: godard@ipgp.fr

Keywords: HP-LT metamorphism, metagabbro; Tuscan Archipelago

The inner Northern Apennine belt (i.e., northern Tyrrhenian Sea and Tuscany) is an Alpine chain affected by high-P metamorphic conditions during its evolution. Although Elba Island is structurally located close to the Adria-Europe suture zone, for several authors it represents a sector of the orogen affected by low-P metamorphism. The first clear evidence of high-P and low-T metamorphism has been found in metabasite rocks embedded in Cretaceous calcschists of eastern Elba Island (Bianco et al., 2015).

The current work presents a detailed study of the metabasite HP mineral assemblage in order to better understand the metamorphic history of the rocks. It provides detailed petrological, textural and mineralogical data, as well as a thermodynamic modelling that allowed estimating peak P–T conditions and tracing the P–T trajectory during exhumation.

The observed microstructures, together with the mineral composition, show that the highest pressure paragenesis consists of lawsonite+glaucophane+omphacite and thus points to lawsonite-blueschist subfacies. The presence of former lawsonite is evidenced by the occurrence of pseudomorphs of fine-grained epidote + muscovite ± albite ± quartz, displaying the typical rectangular or rhombic shapes of lawsonite. A clear textural evidence, reinforcing this interpretation, is shown by the muscovite lamellae that are parallel to one diagonal alone of the former lawsonite rhombic basal sections, like the (010) clivage of sillimanite, indicating that the two diagonals were not crystallographically equivalent; this implies that the protocrystals were orthorhombic prisms with {110} faces, which is eventually the case of lawsonite. Another line of evidence comes from the different compositions of white mica and epidote in the matrix (phengite and Fe^{3+}-rich epidote) relative to those in the lawsonite pseudomorphs (muscovite and Fe^{3+}-poor clinozoisite), indicating that the protomineral was devoid of Fe^{2+}, Mg and Fe^{3+}.

The thermodynamic modelling using the THERMOCALC software and database has confirmed these observations and suggests that the metabasites have experienced a clockwise P–T path with three main stages of metamorphism represented by lawsonite-blueschist subfacies, epidote-blueschist subfacies and greenschist facies. The estimated peak pressure conditions are 1.5-1.7 GPa, 430-460°C.

Finally, our results allow reconciling Elba Island with the tectonic and metamorphic evolution of the neighbouring localities (Tuscan Archipelago and Southern Tuscany) where HP-LT blueschist-facies metamorphic conditions have also been documented.

Acknowledgements: This research has received funding from the European Union's 7th Framework Programme (agreement No. 608553; Project IMAGE).

Bianco, C., Brogi, A., Caggianelli, A., Giorgetti, G., Liotta, D., Meccheri, M. (2015): HP-LT metamorphism in Elba Island: Implications for the geodynamic evolution of the inner Northern Apennines (Italy). *J. Geodyn.*, **91**, 13-25.

READING AND UNDERSTANDING THE PRECAMBRIAN METAMORPHIC RECORD

Brown M.*[1]
[1] Department of Geology, University of Maryland, College Park, MD, USA
Corresponding email: mbrown@umd.edu

Keywords: paired metamorphism, secular cooling, subduction

In history, we use all available records – from documents to artifacts – to understand past events in the context of their time. Similarly, although the evolution of our planet can be constrained by the rock record, it can only be understood if this evidence is set in the context of Earth's thermal history. Other considerations in reading and understanding the metamorphic record include the role of preservation, the effect of sampling bias and the reliability of data gaps.

Plate tectonics is characterized by one-sided subduction, but how is the first imprint of this asymmetry registered in the rock record? How do we weigh global (commonly younger) *vs* local (commonly older) datasets or distinguish initiation of subduction from episodic or continuous (local or global) subduction? Did a hotter mantle and higher heat production preclude globally linked subduction and plate tectonics, only allowing local and/or episodic subduction? Here I posit that global changes in geodynamics are documented in the apparent thermal gradient(s) of metamorphism preserved in the lithosphere.

Based on a new dataset of age, *T*, *P* and *T*/*P* for Eoarchean to Cenozoic metamorphic rocks, two types of metamorphism, medium d*T*/d*P*, with apparent thermal gradients of 350-775^{o}C/GPa (for the interval 2.8-1.5 Ga, mean of 603±111 (1s)), and high d*T*/d*P*, with apparent thermal gradients of 775-2000^{o}C/GPa (for the interval 2.8-1.5 Ga, mean of 1110±227 (1s)), appear widely in the rock record beginning at *ca.* 2.8 Ga. This emergence of paired metamorphism is interpreted to register the onset of globally linked one-sided subduction, which introduced an asymmetric thermal structure at newly created convergent plate margins, with lower d*T*/d*P* associated with the subducting slab and higher d*T*/d*P* the overriding plate (Brown, 2014). By contrast, prior to 2.8 Ga the crust registers intermediate apparent thermal gradients in both "high-grade" gneiss terranes and "low-grade" greenstone belts, with only sporadic high d*T*/d*P* metamorphism and rare medium d*T*/d*P* metamorphism (although reliable quantitative data are limited). This pattern may reflect a stagnant lid regime (Johnson et al., 2014) in which occurrences of medium d*T*/d*P* metamorphism record episodes of local subduction (Sizova et al., 2015). The change in regime relates to secular cooling since the Mesoarchean, which facilitated the transition to global subduction registered by the widespread appearance of paired metamorphism in the Neoarchean. Ages of metamorphism between the late Mesoarchean and the early Mesoproterozoic define two clusters, similar to zircon ages peaks for the crust, that correlate with supercraton assembly (2.8-2.4 Ga) and formation of the first supercontinent (Columbia/Nuna; 2.0-1.6 Ga), separated by a data gap – a cycle related to plate tectonics. Subsequently, continued secular cooling caused a change to deeper slab breakoff and colder subduction, which is registered in the record of metamorphism by the first appearance of blueschists and UHPM in the Neoproterozoic (Sizova et al., 2014).

Brown, M. (2014): The contribution of metamorphic petrology to understanding lithosphere evolution and geodynamics. *Geosci. Frontiers*, **5**, 553-569.

Johnson, T.E., Brown, M., Kaus, B., VanTongeren, J.A. (2014): Delamination and recycling of Archaean crust caused by gravitational instabilities. *Nature Geosci.*, **7**, 47-52.

Sizova, E., Gerya, T., Brown, M. (2014): Contrasting styles of Phanerozoic and Precambrian continental collision. *Gondwana Res*., **25**, 522-545.

Sizova, E., Gerya, T., Stüwe, K., Brown, M. (2015): Generation of felsic crust in the Archean: a geodynamic modeling perspective. *Precambrian Res*., **271**, 198-224.

POLYMETAMORPHIC GARNET PORPHYROBLASTS IN ECLOGITE-FACIES GARNET-PHENGITE SCHISTS FROM THE ZERMATT AREA, CENTRAL ALPS

Bucher K.*[1] & Weisenberger T.B.[2]
[1] Mineralogie und Petrologie, Universität Freiburg, Germany
[2] Iceland GeoSurvey, Reykjavík, Iceland
Corresponding email: bucher@uni-freiburg.de

Keywords: garnet, polymetamorphism, high-P metapelites

The garnet-phengite schists of the Theodul-Glacier-Unit (TGU) belong to a slab of continental basement rocks tectonically emplaced in the eclogite-facies Zermatt-Saas meta-ophiolite nappe. The cm-sized garnets show a complex texture of granulite-facies garnet fragments in the core healed and overgrown by a younger generation of grossular-rich garnet. The early granulite-facies garnet developed by low-pressure high-temperature metamorphism during a pre-alpine orogenic phase. The late garnet is typical of high-pressure-low-temperature (HPLT) metamorphism and can be related to alpine subduction of the ZSZ.

Thus the garnets of the garnet-phengite schists are polymetamorphic. The detailed compositional and textural features suggest that fragmentation occurred during alpine subduction. The garnet composition patterns indicate that the contacts between the granulite-facies fragments and healing HPLT garnet have been modified by diffusion. The profile suggests that Ca did not exchange at the garnet contacts at the scale of 1 µm, whereas Fe and Mg does efficiently diffuse at the derived temperature of 510˚C for the TGU at the scale of some µm.

Metapelitic granulites are well preserved in the Dent Blanche (DB) nappe of continental origin overriding the Zermatt-Saas ophiolites. Given this geological context, the TGU slab may represent DB material incorporated into the Zermatt-Saas Zone (ZSZ) by a process such as subduction erosion.

The HPLT assemblage of the garnet-phengite schist indicates that the TGU slab has been subducted together with the ZSZ. However, the TGU slab did not follow the ZSZ to the greatest recorded subduction depth. A maximum pressure of 1.8 GPa has been derived for the TGU, whereas the ZSZ reached 2.6 GPa or more). Thus the TGU slab may have been detached from the DB nappe first, subducted with the ZSZ until it reached 1.8 GPa and then detached from the down going ZSZ ophiolites.

JADEITE AND NEPHELINE IN THE GRAN PARADISO MASSIF, W. ALPS: DECIPHERING THE HIGH-PRESSURE EVOLUTION OF CONTINENTAL CRUST

Chopin C.*[1], Guillot F.[2] & Lanari P.[3]
[1] Laboratoire de Géologie, Ecole normale supérieure & Centre National de la Recherche Scientifique, Paris, France
[2] Laboratoire d'Océanologie et de Géosciences, Université de Lille, France
[3] Institut für Geologie, Universität Bern, Switzerland
Corresponding email: chopin@geologie.ens.fr

Keywords: high-pressure metamorphism, continental crust, reaction kinetics

The formation and eventual preservation of high-pressure (HP) mineral assemblages in subducted continental crust are a long-standing issue with kinetic aspects and important geophysical implications. The issue is especially acute in metagranite-dominated terranes, in which the dominant rock-type hardly bears evidence for high-pressure transformation whereas subordinate rock types clearly point to high or very high pressure conditions. How should we read and interpret these messages? Cofacial evolution but heavy kinetic controls? Distinct tectono-metamorphic units with contrasted P-T paths? Effects of mechanical heterogeneity? The internal crystalline massifs of the Western Alps (Monte Rosa, Gran Paradiso and Dora-Maira) are a prime example in this respect. Mineral assemblages in subordinate metapelite, metabasite and magnesian schist ("silvery micaschist") point to HP or ultra-HP conditions there, whereas evidence for HP conditions in metagranite is tenuous and rests on the presence of high-Si phengite and grossular-almandine garnet in orthogneiss (e.g., Le Goff & Ballèvre, 1990; Massonne, 2015; Manzotti et al., 2015). Indeed, the lack of relict jadeite in the HP metagranites of all three massifs has remained like a petrological vexation and the hint for a peculiar behaviour of the granitic system at HP (e.g., Proyer, 2003; Gabudianu Radulescu et al., 2011).

The recent discovery by one of us (FG) of well-preserved jadeite-bearing rocks in orthogneiss of the western Gran Paradiso massif revives this questioning. These rocks occur at the contact of K-feldspar-porphyritic albitite dykes with country-rock augen gneiss and lenses of "silvery micaschist". They contain uncommon mineral assemblages involving i) jadeite, phengite, nepheline, albite, biotite, ii) jadeite, quartz, glaucophane, garnet, chloritoid, paragonite, preiswerkite as well as a new sodic trioctahedral mica. Their paragenetic interpretation is the opportunity to address local Na-metasomatism and their bearing on jadeite formation and preservation in felsic rocks.

Gabudianu Radulescu, I., Compagnoni, R., Lombardo, B. (2011): Polymetamorphic history of a relict Permian hornfels from the central Gran Paradiso Massif (Western Alps, Italy): a microstructural and thermodynamic modelling study. *J. Metam. Geol*., **29**, 851-874.

Le Goff, E. & Ballèvre, M. (1990): Geothermobarometry in albite-garnet orthogneisses: a case study from the Gran Paradiso nappe (Western Alps). *Lithos*, **25**, 261-280.

Manzotti, P., Pitra, P., Langlade, J., Ballèvre, M. (2015): Constraining P-T conditions during thrusting of a higher pressure unit over a lower pressure one (Gran Paradiso, Western Alps). *J. Metam. Geol*., **33**, 981-1002.

Massonne, H.-J. (2015): Derivation of P-T paths from high-pressure metagranites – examples from the Gran Paradiso Massif, western Alps. *Lithos*, **226**, 265-279.

Proyer, A. (2003): The preservation of high-pressure rocks during exhumation: metagranites and metapelites. *Lithos*, **70**, 183-194.

THE EFFECT OF COMPOSITION ON MINOR AND TRACE ELEMENTS IN SPINELS: INSIGHTS FROM EXSOLVED CHROMITE

Colás V.*[1], Tassara C.S.[2], Padrón-Navarta J.A.[3], González-Jiménez J.M.[2], Griffin W.L.[4], Fanlo I.[5], O'Reilly S.Y.[4], Gervilla F.[6], Proenza J.A.[7], Pearson N.J.[4], Camprubí A.[1] & Escayola M.[8]

[1] Instituto de Geología, Universidad Autónoma de México, Mexico

[2] Department of Geology and Andean Geothermal Center of Excellence, Universidad de Chile, Santiago, Chile

[3] Géosciences Montpellier, Centre National de la Recherche Scientifique & Université de Montpellier, France

[4] Centre of Excellence for Core to Crust Fluid Systems & Geochemical Evolution and Metallogeny of Continents, Department of Earth and Planetary Sciences, Macquarie University, Sydney, Australia

[5] Departamento de Ciencias de la Tierra, Universidad de Zaragoza, Spain

[6] Departamento de Mineralogía y Petrología & Instituto Andaluz de Ciencias de la Tierra, Universidad de Granada, Consejo Superior de Investigaciones Científicas, Granada, Spain

[7] Departament de Cristal·lografia, Mineralogia i Dipòsits Minerals, Universitat de Barcelona, Spain

[8] Departamento de Ciencias Geológicas, Universidad de Buenos Aires, Argentina

Corresponding email: vcolas86@gmail.com

Keywords: spinel-magnetite exsolution, partition coefficient, hydrous metamorphism

Chromite grains from ophiolitic chromitite bodies in the metamorphosed ultramafic massifs of Los Congos and Los Guanacos in the Eastern Pampean Ranges of Córdoba (Argentinian Central Andes) shows homogenous and exsolution textures. The major element composition of the exsolved phases in chromite approaches to spinel ($MgAl_2O_4$) and magnetite ($Fe^{2+}Fe^{3+}{}_2O_4$) that define the corners of the spinel prism, at relatively constant Cr^{3+}/R^{3+} ratio (R^{3+} = Cr+Al+Fe^{3+}). The exsolution of spinel-rich and magnetite-rich phases from a precursor chromite have accounted at ≥ 600°C (Sack & Ghiorso, 1991), matching with the amphibolite-granulite facies metamorphism (590-730°C) inferred for the studied ultramafic massifs (Rapela et al., 1998; Martino et al., 2010). The large size of the exsolved phases in chromite (up to 200 µm) provided us, for the first time, LA-ICP-MS analysis for a suite of minor and trace elements to constrain their crystal-crystal partition coefficients between the spinel-rich and magnetite-rich phases ($D_i^{Spl/Mag}$). Minor and trace elements are listed in increasing order of compatibility with the spinel-rich phase: Ti, Sc, Ni, V, Ge, Mn, Cu, Sn, Co, Ga and Zn. Our calculated crystal-crystal partition coefficients reflect the effect that crystal-chemistry of the exsolved phases from chromite imposes on Zn, Ga, Co, Ni, Ti and Sc (and only slightly for Mn). The preferential partitioning of Ti and Sc into the magnetite-rich phase is consistent with high-temperature chromite/melt experiments (e.g., Horn et al., 1994; Nielsen et al., 1994; Wijbrans et al., 2015) and suggests a significant dependence on Fe^{3+} substitution in the spinel structure. However, any clear relationship between the partitioning of Ni into magnetite-rich phase and variations in major element components are revealed from chromite/melt partitioning experiments (Righter et al., 2006; Wijbrans et al., 2015). A compositional effect of major elements on Ga, Co, and Zn is observed in the spinel-rich phase but not in the experiments (Horn et al., 1994; Righter et al., 2006; Wijbrans et al., 2015), because crystal-chemistry differences along the spinel-magnetite exchange vector are poorly covered experimentally. The influence of mayor element composition in the partitioning of Ga, Co and Zn is supported by the strong covariance of these elements in chromite grains from layered intrusions, where this exchange vector is important. An increase of Zn and Co coupled with a decrease of Ga showed in chromite grains from hydrous metamorphosed chromitite bodies cannot be explained exclusively by compositional changes of major elements in this chromite (which is enriched in the magnetite). The most likely explanation is that the content of minor and trace elements in chromite affected by hydrous metamorphism are controlled by the chemistry of metamorphic fluids, which produce the formation of chlorite in equilibrium with metamorphosed chromite.

Horn, I., Foley, S.F., Jackson, S.E., Jenner, G.A. (1994): Experimentally determined partitioning of high field strength-and selected transition elements between spinel and basaltic melt. *Chem. Geol.*, **117**, 193-218.

Martino, R.D., Guereschi, A.B., Anzil, P.A. (2010): Metamorphic and tectonic evolution at 31° 36′ S across a deep crustal zone from the Sierra Chica of Córdoba, Sierras Pampeanas, Argentina. *J. South Am. Earth Sci.*, **30**, 12-28.

Nielsen, R.L., Forsythe, L.M., Gallahan, W.E., Fisk, M.R. (1994): Major-and trace element magnetite-melt equilibria. *Chem. Geol.*, **117**, 167-191.

Rapela, C., Pankhurst, R., Casquet, C., Baldo, E., Saavedra, J., Galindo, C., Fanning, C. (1998) The Pampean Orogeny of the southern proto-Andes: Cambrian continental collision in the Sierras de Córdoba. *Geol. Soc. London Spec. Publ.*, **142**, 181-217.

Righter, K., Leeman, W., Hervig, R. (2006): Partitioning of Ni, Co and V between spinel-structured oxides and silicate melts: Importance of spinel composition. *Chem. Geol.*, **227**, 1-25.

Sack, R.O. & Ghiorso, M.S. (1991): Chromian spinel as petrogenetic indicators: Thermodynamics and petrological applications. *Am. Mineral.*, **76**, 827-847.

Wijbrans, C., Klemme, S., Berndt, J., Vollmer, C. (2015): Experimental determination of trace element partition coefficients between spinel and silicate melt: the influence of chemical composition and oxygen fugacity. *Contrib. Mineral. Petrol.*, **169**, 1-3.

APPLICATION OF Ti-IN-QUARTZ, Ti-IN-ZIRCON AND Zr-IN-RUTILE THERMOMETERS TO METAPELITIC GRANULITES FROM JUBRIQUE SEQUENCE (BETIC CORDILLERA, S SPAIN)

Crivellaro M.*[1], Bartoli O.[1], Cesare B.[1], Acosta-Vigil A.[1-2], Petrelli M.[3] & Garrido C.J.[2]

[1] Dipartimento di Geoscienze, Università di Padova, Italy

[2] Instituto Andaluz de Ciencias de la Tierra, Consejo Superior de Investigaciones Científicas, Universidad de Granada, Spain

[3] Dipartimento di Fisica e Geologia, Università di Perugia, Italy

Corresponding email: marco.crivellaro.6@studenti.unipd.it

Keywords: trace-element geothermometry, migmatite, Betic Cordillera

Constraining the P-T conditions in high-grade metamorphic terranes is crucial for a better understanding of high-temperature metamorphism and crustal anatexis. Recently, new trace-element geothermometers (Ti-in-quartz, Zr-in-rutile and Ti-in-zircon) have been developed and successfully used to estimate the peak and post-peak temperatures of polymetamorphic rocks. In this study we apply these geothermometers to the mylonitic gneisses from the anatectic sequence of Jubrique, which is located on the top of the Ronda peridotite slab (Betic Cordillera, S Spain). This sequence constitutes a strongly thinned crustal section. The rocks studied are granulite-facies migmatitic gneisses made up of Grt, Qtz, Kfs, Pl, Ky, Sil, Crd, Bt and accessory Rt, Ilm, Zrn, Mnz, Spl, Gr, Ap and Py.

The 5 studied samples show the simultaneous presence of all three minerals required for the application of the thermometers and offer the opportunity to compare the results with those obtained in previous studies, through phase equilibria modeling and conventional thermobarometry. Several quartz, zircon and rutile crystals, both included in garnet porphyroclasts and present in the rock matrix, were investigated. Zircon was imaged by cathodoluminescence in order to reveal its internal structure: most zircons show a complex core and an irregular, homogeneous or weakly zoned, rim. Rutile and zircon were analyzed by LA-ICP-MS, giving contents of 1000-2800 ppm Zr and 7-25 ppm Ti, respectively. Ti in quartz (TitaniQ) was measured by EMP, resulting in 100-260 ppm. Pressure values used for calculations are 13 kbar for minerals included in garnet, 5 kbar for matrix quartz and zircon, 9 kbar for matrix rutile.

We recognized two types of quartz included in garnet: 1) large (≈800 μm) irregularly shaped inclusions, both at the rim and at the core of garnet, yielding an average TitaniQ temperature of 878±65°C; 2) small (< 50 μm) single-crystal inclusions, at the garnet core only, yielding an average temperature of 906±36°C. Matrix quartz gave temperatures of 692±44°C (in melanosome) and 665±24°C (in leucosome). Crystallization temperatures calculated for rutile are 847±50°C (rutile in garnet) and 810±25°C (matrix rutile). Average Ti-in-zircon temperatures for zircon included in garnet are 747±34°C (rim) and 750±55°C (core), whereas for matrix zircon the average temperatures are 766±38°C (rim) and 759±46°C (core).

Quartz and rutile included in garnet seem to record peak metamorphic temperatures, in agreement with those published in the literature. Lower Ti-in-zircon temperatures probably record growth or re-equilibration of zircon during cooling from peak temperatures. Lower temperatures calculated for matrix quartz probably record recrystallization under retrograde conditions and deformation. These temperatures are much lower than those obtained through phase equilibria modeling.

P-T CONDITIONS OF THE GARNET-KYANITE GRANULITIC GNEISS FROM TARCU, SOUTH-EAST CORSICA

Cruciani G.*[1], Franceschelli M.[1], Massonne H.-J.[2] & Musumeci G.[3]
[1] Dipartimento di Scienze Chimiche e Geologiche, Università di Cagliari, Italy
[2] Institut für Mineralogie und Kristallchemie, Universität Stuttgart, Germany
[3] Dipartimento di Scienze della Terra, Università di Pisa, Italy
Corresponding email: gcrucian@unica.it

Keywords: granulitic gneiss, P-T conditions, Variscan

In south-eastern Corsica the Variscan Solenzara-Fautea series is mainly composed of garnet-kyanite granulitic gneiss with pyroxenite and pyrigarnite boudins (Faure et al., 2014, and references therein). The granulitic gneiss at the seashore of Tarcu is a foliated rock characterized by an irregular alternation of quartz-feldspathic layers and biotite-garnet-rich dark layers. This rock consists of quartz, perthitic K-feldspar, plagioclase, kyanite, garnet, biotite, some late muscovite and accessory zircon, apatite, monazite, and rutile. Garnet occurs as crystals being up to half a millimeter in diameter or small crystals in the rock matrix or included in kyanite. In the former garnet type, inclusions of rounded quartz and plagioclase occur. Its composition is Alm_{60-80}, Prp_{8-16}, Grs_{4-25}, $Sps_{0.8-3.3}$ with an asymmetric compositional zoning. A Ca-rich core is surrounded by a rim enriched in Fe and Mn. Kyanite is partially replaced by white mica or totally pseudomorphosed to a fine-grained white mica aggregate. Plagioclase, with composition Ab_{77-85}, occurs in crystals of variable size, with the bigger ones strongly altered and surrounded by a very thin rim of albite (Ab_{92}). Plagioclase sometimes contains antiperthite exsolution and, when in contact with K-feldspar, shows myrmekitic texture. Plagioclase also occurs as rounded, anhedral inclusions in garnet with oligoclase to andesine composition. Sporadically, calcic plagioclase with Ab_{67} is associated with garnet. K-feldspar occurs in fine-grained and medium- to coarse-grained crystals in the rock matrix. The coarse-grained crystals often show perthite exsolutions and albite-pericline twinning typical of microcline. K-feldspar also occurs in coarse-grained aggregates with lenticular shape. Biotite from the matrix has X_{Mg} = 0.36-0.44 and Ti = 0.1-0.4 a.p.f.u.. Biotite growing on garnet has lower Ti (0.03 a.p.f.u.). Pressure (P) - temperature (T) peak conditions have been determined using the P-T pseudosection approach for the average composition of three selected samples (SiO_2 72.74 wt.%; Al_2O_3 13.51, Fe_2O_3tot 3.27, MgO 0.92, CaO 1.08, Na_2O 2.39, K_2O 4.18). The quartz + plagioclase + K-feldspar + kyanite + biotite + garnet assemblage of the granulitic gneiss would have formed at $0.9 < P < 1.2$ GPa and $740 < T < 790$°C. Garnet-biotite geothermometer and GASP geobarometer, using different calibrations, yielded temperatures in the range 720-800°C and pressure in the range 1.1-1.3 GPa.

Faure, M., Rossi, P., Gaché, J., Melleton, J., Frei, D., Li, X., Lin, W. (2014): Variscan orogeny in Corsica: new structural and geochronological insights, and its place in the Variscan geodynamic framework. *Int. J. Earth Sci.*,**103**,1533-1551.

NAPPE STACKING AND METAMORPHIC EVOLUTION IN THE WESTERN TAUREN WINDOW

Da Mommio A.*[1], Zanchetta S.[2], Poli S.[1] & Zanchi A.[2]
[1] Dipartimento di Scienze della Terra "A. Desio", Università di Milano, Italy
[2] Dipartimento di Scienze dell'Ambiente, del Territorio e di Scienze della Terra, Università di Milano-Bicocca, Italy
Corresponding email: alessandro.damommio@unimi.it

Keywords: Tauren window, metamorphic evolution, Eastern Alps

The western Tauern Window is a key area for the reconstruction of the tectonic evolution of the Eastern Alps. Here basement units derived from the European margin are stacked together with their parautochthonous post-Variscan cover in a south-vergent crustal scale duplex that also involves the Glockner nappe (calcschists and ophiolites derived from the Penninic ocean).

The major lithostratigraphic units comprise: i) a polymetamorphic basement consisting of mainly amphibolites, migmatites, orthogneisses, and locally pre-Mesozoic ultramafic to mafic bodies; ii) the Tux and Zillertal orthogneiss (part of the "Zentralgneiss Auct.") that intruded unit (i) during early Permian times; iii) the parautochthonous metasedimentary cover including meta-conglomerates, calcitic and dolomitic marbles, calcareous micaschists, quartzites, and subordinate greenschists. iv) the Glockner Nappe, it consists of km-thick sequences of calcschists with interbeddings of prasinites, amphibolites and ultramafic bodies. Along the tectonic contact between the northern and southern duplex antiforms a slice (about 1 km-thick, wedging out westward) of graphite-rich garnet micaschists with minor quartzites and calcschists ("Greiner schists" Auct.) occurs.

The main deformation stages resulted in isoclinal folding and development of the regional foliation in post-Variscan metasedimentary cover and in the Glockner nappe. An amphibolite facies metamorphic stage characterized by static recrystallization of micas, garnet and amphibole ("Garbenschiefer" Auct.) postdates the regional foliation development in the post-Variscan metasedimentary units whereas its occurrence remains controversial in the Glockner nappe.

The complexity of the structural evolution combined with the scarce availability of petrological data have hindered until now a generally accepted definition of boundaries and P-T trajectories of the tectonometamorphic units in the western end of the Tauern Window.

The goal of this work is to provide structural and petrological constraints for identifying boundaries among units and unravel earlier stages of metamorphic history. Our investigation focuses on a transect from the culmination of the Tux antiform to the north and the western end of the Zillertal dome to the south.

Electron microprobe analysis on garnet, micas, staurolite, feldspar and carbonates reveal distinct zoning patterns for the different lithological units. As an example, garnets grown in micaschists synchronous to regional foliation in the Glockner nappe show Ca-Mg rich rims to a relatively Ca-Mg-poor core. On the contrary, in the metasedimentary rocks the Ca content in the garnet tends to increase from rim to core, whereas Mg tends to decrease.

Thermodynamic forward modelling by means of pseudosections analysis on several samples with known bulk composition, supports different metamorphic evolution of the several units before their tectonic coupling and later exhumation.

TRACE ELEMENTS IN METAPELITES: PARTITIONING, IMAGING AND USE FOR THERMOBAROMETRY

Dubacq B.*[1], De Andrade V.[2] & Plunder A.[1-3]

[1] Institut des Sciences de la Terre de Paris, Sorbonne Université, Université Pierre et Marie Curie, Centre National de la Recherche Scientifique, Paris, France

[2] Advanced Photon Source, Argonne National Laboratory, Lemont, IL, USA

[3] Department of Earth Sciences, University of Utrecht, Netherlands

Corresponding email: Benoit.Dubacq@upmc.fr

Keywords: trace element partitioning, equilibrium, metapelite

Building pressure-temperature paths from metamorphic rocks relies on the identification of equilibrium, whether the observed mineral assemblage is used with empirical thermobarometers, multi-equilibrium thermobarometry or compared to pseudosections.

Confidently identifying equilibrium is no trivial task when minerals are zoned and when several paragenesis are found in thin section, which is typical in metapelites, especially for retrograde assemblages.

In this contribution we show how trace and minor elements can be used to better understand the crystallization history of metapelites, providing constraints independently from thermodynamical models based on major elements. To do so, we have used a combination of techniques, starting with a theoretical study of trace element incorporation with atomistic modelling to estimate partition coefficients between crystals. These estimates have been tested on natural metamorphic rocks with well-constrained crystallization history, using point analysis (EPMA and LA-ICP-MS) together with elemental mapping (EPMA and synchrotron µ-XRF), resulting in 1) good agreement between calculated and measured partitioning, 2) identification of mineral assemblages at equilibrium in agreement with thermodynamic modelling, 3) identification of trace elements showing disequilibrium features in otherwise co-stable mineral assemblages. This last point highlights the control of diffusion in fluids on the equilibrium length scale.

A COUPLED ANALYTICAL AND THEORETICAL INVESTIGATION OF ROCK FULGURITES

Elmi C.[1], Chen J.[1], Goldsby D.[1] & Gieré R.*[1]
[1] Department of Earth and Environmental Science, University of Pennsylvania, Philadelphia, PA, USA
Corresponding email: giere@sas.upenn.edu

Keywords: lightning, rock fulgurites, pyrometamorphism

Fulgurite (Latin: *fulgur*, lightning) is a naturally occurring glass formed when lightning strikes sand, rock, or soil. This study seeks to link analytical data for fulgurite-bearing rocks (in this case, a pink granite collected near Baveno, Italy, comprised of quartz, plagioclase ($Ab_{98}An_1Or_1$), orthoclase, and micas) with a physical model of fulgurite formation. The fulgurite occurs as a thin glassy to fine-grained porous layer coating the granite, as identified by enviromental scanning electron microscopy (ESEM). XRPD analyses of the fulgurite identified an amorphous phase, quartz, and cristobalite. The amorphous phase was identified by EMPA as a glass composed mainly of SiO_2 and Al_2O_3, and was heterogeneous owing to the presence of pores. The deficiency of Na, Ca, and K in the glass suggests that alkalis were liberated from feldspars during heating. The presence of the glass indicates that the abrupt electrical (Joule) heating of the rock surface yielded high temperatures, producing a thin melt layer on the surface which then cooled adiabatically. The observed presence of cristobalite would indicate temperatures were ≤ ~ 1700ºC and pressure remained near atmospheric if thermodynamic equilibrium were obtained, which may not have been achieved over the short times of the lightning strike. The brown-to-black color of the fulgurite is due to carbon (up to 7 wt.% as determined by Elemental Analyzer) from lichen, plant residues, and microorganisms present on the weathered surface of the granite prior to the strike. Water vapor and CO_2 are produced from organic matter when it begins to volatilize at ~ 300ºC. The quantity of organic matter in the glass, obtained via Elemental Analyzer, suggests that rapid quenching of the melt traps NO_x, C, and CO_2 gases produced during heating.

To better understand these processes, we developed idealized physical models to simulate the effects of Joule heating and subsequent thermal conduction during and after the lightning strike. The rock was modeled as a semi-infinite half space, and the thermal and electrical conductivities were assumed to decrease with depth near the surface to simulate a high-conductivity weathered skin. The effects of the shock wave, which results from the sudden release of energy of the lightning, were neglected. The modeling reveals that while the lightning strike only lasts about 30 μs, the high electrical current, up to 10 kA, easily generates enough heat to burn the surficial organic matter. Conduction of heat away from the hitpoint after the strike also contributes to the volatilization of organic matter within a proscribed radius. Our simulations indicate that the high-conductivity weathering skin confines the highest temperatures to regions close to the rock surface. Calculations using nominal values of thermodynamic and materials parameters suggest that carbon from burnt organic matter should occur within a ~10 cm radius of the hit point, consistent with observations of the samples. These results provide physical constraints for future study of the chemical reactions that occur during the lightning strike.

NANOGRANITOID INCLUSIONS IN ULTRAMAFIC HIGH-PRESSURE GRANULITES FROM DRONNING MAUD LAND, ANTARCTICA

Ferrero S.[1-2], Palmeri R.[3], Godard G.[4], Wunder B.[5] & Cesare B.*[6]
[1] Institut für Geowissenschaften, Universität Potsdam, Golm, Germany
[2] Museum für Naturkunde, Leibniz-Institut für Evolutions- und Biodiversitätsforschung, Berlin, Germany
[3] Museo Nazionale dell'Antartide, Università di Siena, Italy
[4] Institut de Physique du Globe de Paris, France
[5] Helmholtz Zentrum Potsdam, GFZ Deutsches GeoForschungsZentrum, Potsdam, Germany
[6] Dipartimento di Geoscienze, Università di Padova, Italy
Corresponding email: bernardo.cesare@unipd.it

Keywords: crustal melting, mafic granulites, melt inclusions

Crystallized melt inclusions (MI) occur in boudins of ultramafic granulites hosted in felsic orthogneisses of the Dronning Maud Land, Antarctica. The granulites show a main assemblage consisting of Grt-Cam-Opx-Cpx, formed at ca. 900°C and 12 kbar and retrogressed under 7 kbar with growth of amphibole and Spl-Pl-Opx±Ol symplectites around garnet.

Garnet forms porphyroblasts up to 2 cm in size and contains two generations of MI. The first generation (type 1) is primary and occurs in the inner part of the garnet porphyroblasts. Type 1 MI are generally <10 mm in diameter and isolated, and only in few cases form clusters. They have generally a well-developed negative crystal shape, although some clusters contain abundant tubular inclusions, <40 mm in length. Regardless their shape, the inclusions contain a constant assemblage of kumdykolite (Kml), kokchetavite (Kok) and phlogopite, with quartz/cristobalite and zoisite as minor phases. Occasionally residual glass can be identified via Raman spectroscopy. Kml and Kok are highly metastable polymorphs of albite and K-feldspar respectively, whose presence suggests that the nanogranitoids are undisturbed portions of crystallized melt. The second generation (type 2) is represented by larger (up to 30 mm), pseudosecondary MI. Their assemblage mainly consists of amphibole, feldspar, zoisite, minor magnesite, halite and Opx. A CO_2-rich fluid, with minor amounts of N_2 and CH_4, may be present in type 2 MI.

Fragments of garnet containing MI were heated at 950°C, 22-24 kbar for 24 h. The inclusions were re-homogenized and subsequently analyzed by electron microprobe. Type 1 MI contain a melt of trachytic composition with K/Na = 3.55 and $H_2O \approx 2.5$ wt.%, while type 2 MI is a dacitic melt with K/Na = 0.56 and $H_2O \approx 12$ wt.%.

The presence of primary MI in garnet indicates that melt was present during garnet growth under peak conditions. By analogy with previous case studies of nanogranitoids, this would suggest that both melt and garnet [GG1] are products of the partial melting of the ultramafic boudins, most likely through amphibole dehydration melting. However, while high-silica melts as products of amphibolite have been already observed experimentally, the K-rich character of the investigated melt is unexpected. Such feature may be explained by the participation of biotite as reactant in the melting reaction [GG2]. Alternatively, it may result from the percolation of K-rich melts formed in the adjacent orthogneisses during garnet growth (if the boudins behaved as an open system). An exotic origin is even more likely in the case of the type 2 MI, which are clearly located within microfractures crosscutting garnet.

Despite the uncertainty on the petrogenetic significance of the melt preserved in the MI, this study is important because it documents for the first time the occurrence of MI in metamorphosed (ultra)mafic protoliths.

RATES AND MECHANISMS OF PORPHYROBLAST CRYSTALLISATION: INSIGHTS FROM A GARNET-GRADE SCHIST OF THE LESSER HIMALAYA

George F.R.*[1] & Gaidies F. [1]
[1] Department of Earth Sciences, Carleton University, Ottawa, Canada
Corresponding email: freya.george@carleton.ca

Keywords: equilibration, nucleation, porphyroblast growth

The spatial extent and degree to which a system is chemically equilibrated during a metamorphic mineral reaction directly impacts the size distribution and chemical composition of product porphyroblasts. Consequently, methods that couple the observed textural record with microprobe analysis and phase equilibria and diffusion modelling permit a detailed view of the nucleation and growth history of metamorphic minerals. In this study we comprehensively characterise the three-dimensional distribution and compositional variation of a garnet population within a garnet-grade pelitic schist of the Lesser Himalayan Sequence (LHS) from the Sikkim Himalaya. This permits assessment of the extent of chemical equilibration associated with garnet crystallisation in the sample, and investigation of both the rates and kinetic controls of porphyroblastic garnet crystallisation.

Compositional profiles were collected through centrally-sectioned chemically zoned garnets representative of the observed crystal size distribution, as characterised using a high-resolution µ-computed tomography scanner. The data indicate strong correlations between garnet crystal size and core composition with respect to major end-member components, independent of spatial position in the sample. Systematic steepening of compositional gradients from large to small grains is interpreted as a progressive decrease in the growth rate of relatively late-nucleated garnet. This is inferred to reflect an increase in the interfacial energies during progressive garnet crystallisation.

Numerical simulations of garnet growth indicate that the sample underwent rapid *P-T-t* evolution, with rates of heating and cooling during metamorphism in excess of 100°C/Ma. As a consequence, even the smallest analysed garnet has undergone negligible intracrystalline diffusion with respect to all of its major end-member components. Therefore, the garnet population contains an unparalleled compositional record of the full history of crystallisation over an interval of less than 1 Ma, from incipient nucleation at 518°C and 4.5 kbar to cessation of growth at peak metamorphic conditions at 564°C and 5.6 kbar. Equilibrium forward-modeling of the suite of documented compositions suggests that between these *P-T* bounds, compositional variation within the garnet population is a result of progressive garnet nucleation within a changing effective bulk composition at a succession of near-equilibrium states. Consequently, the departure from equilibrium associated with garnet crystallisation is concluded to be negligible, despite particularly fast rates of metamorphism. This sustained maintenance of an equilibrated matrix leads to the inference that the rate of long-range diffusion in the intergranular medium was fast, relative to interfacial processes operating during garnet crystallisation.

INTERPRETATION(S) OF GARNET DISTRIBUTION AND CHEMICAL ZONING: INSIGHTS FROM MAJOR AND TRACE ELEMENT LA-ICPMS MAPPING. AN EXAMPLE FROM PELITIC MIGMATITES OF SALVADOR DA BAHIA (BRAZIL)

Goncalves P.*[1], Raimondo T.[2] & Santos de Souza J.[3]

[1] Laboratoire Chrono-Environnement, Université de Franche-Comté, Besançon, France

[2] School of Natural and Built Environments, University of South Australia, Adelaide, Australia

[3] Centro de Pesquisa em Geofísica e Geologia, Universidade Federal da Bahia, Salvador da Bahia, Brasil

Corresponding email: philippe.goncalves@univ-fcomte.fr

Keywords: garnet zoning, LA-ICPMS trace element mapping, migmatites

Metamorphic petrologists rely on garnet because of its ubiquity in high grade rocks, its occurrence in many assemblages of interest for thermobarometry, and mostly to its ability to preserve chemical growth zoning. Making the assumption of equilibrium thermodynamics, the P-T evolution of metamorphic rocks can be inferred using phase diagrams. However, this requires first to interpret properly chemical zoning. Growth zoning reflects crystallisation coeval with changes in P-T conditions or bulk composition. This type of zoning is therefore particularly useful to unravel the P-T-X evolution and determine the growth mechanisms involved. However, growth zoning in major divalent cations is commonly altered by post-growth diffusional modifications at high temperatures and information that relates to the environmental conditions of garnet growth are either totally or partially obliterated. The challenge is to interpret correctly the new “altered” zoning and determine or retrieved the least modified garnet composition for thermobarometry.

To minimise the impact of this post-growth diffusional modification and interpret accurately zoning and the growth or consumption processes, trace elements are more appropriate because of their lower diffusion coefficients compared to major elements. In this study, the distribution of trace elements in garnet has been imaged using an emerging LA-ICP-MS mapping technique. This is achieved by rastering of the focused laser beam in linear transects, which are then stitched together by post-acquisition processing to form a quantified image of the trace element distribution, with excellent detection limits (ppb) over a wide isotopic range (^{7}Li to ^{238}U).

This technique has been applied to pelitic migmatite from the Paleoproterozoic Itabuna-Salvador-Curaça belt (adjacent to the Farol da Bara, Salvador da Bahia, Brazil). Garnet shows a consistent evolution depending on its location and distance from leucosomes. Garnet grain size decreases and the number of garnet grains increases in the melanosome away from the leucosome, suggesting a local change in the nucleation/growth process and/or the existence of local temperature gradient due to crystallisation latent heat. Major and trace element chemical zoning varies significantly with the distance from the leucosome. Large garnets in contact with the leucosome preserve bell-shape zonation in REE and grossular (core 0.12, rim 0.03), reassembling those produced by rayleigh fractionation during growth along a decompression-heating path. In contrast, garnets further away from the leucosome, show a distinct depletion of Ca in the core (down to 0.03) that also correlates with the occurrence of large polyphased inclusions of plagioclase and quartz. Trace element mapping revealed that the Ca depletion is not related to a growth zoning but rather to a post-growth intra-diffusional modification. While HREE and Y preserve bell-shape profile, MREE (Dy, Ho, Tb) and “LREE” (Gd, Sm) show a distinct flattening and depletion in the core. This distribution is similar to the calcium distribution and is interpreted as a post-growth modification during a protracted residence at high temperature and the infiltration of fluids, as suggested by the presence of a 3D network of sealed micro-cracks, revealed by the Li map and micro-tomography, that connects the core of the garnet to the matrix. Consequently, the grossular content of the garnet cores cannot be used to retrieve the P-T conditions of the early stage of garnet nucleation.

PLAGIOCLASE CORONAS AROUND GARNETS: IMPLICATIONS FOR PRESSURE-TEMPERATURE PATHS IN ALUMINOUS GNEISSES AND SCHISTS

Hoffmann T.[1], Dutrow B.*[1] & Foster C.T.[2]
[1] Department of Geology and Geophysics, Louisiana State University, Baton Rouge, LA, USA
[2] Department of Geosciences, University of Iowa, Iowa City, IA, USA
Corresponding email: dutrow@lsu.edu

Keywords: metamorphic textures, coronas, gneisses

Textures found in metamorphic rocks provide insight into the metamorphic and tectonic history of the region. One such texture is plagioclase coronas that surround partially resorbed garnets. These corona textures are prevalent in a series of aluminous gneisses from the Sawtooth Metamorphic Complex, Idaho, USA. Here five corona textures, studied in detail, reach 1 cm in size, consist dominantly of anhedral plagioclase (pl) + quartz (qtz) + biotite (bt) with minor sillimanite (sil) surrounding embayed garnets (grt), and are easily distinguished from the biotite-sillimanite rich matrix by different grain sizes and modes. Gneissic samples contain the overall mineral assemblage of bt + sil + grt + pl + qtz with traces of alkali fsp + ilm + mzn + xnt + apa + zrc + gr. Peak pressure (P) - temperature (T) conditions calculated for the samples are near 7 kbar and 750-800°C based on classical geothermobarometry and mineral assemblage diagrams.

To evaluate the formation of the plagioclase coronas, irreversible thermodynamic modeling of grain boundary diffusion was used in combination with phase equilibrium modeling. Irreversible thermodynamic models of material transport between reaction sites of the dissolving garnet and the matrix assuming grain boundary diffusion and local equilibrium conditions was done for a wide range of relative diffusion coefficients and shows that the dissolving garnet produces a series of mantles with a much higher abundance of biotite than actually observed in the rocks. This lack of distinct mantles and abundant biotite adjacent to the garnet interface suggests that the haloes are not simply the result of grain boundary diffusion transport. Phase equilibrium modeling for these P-T conditions indicates that melt is formed by garnet dissolution reactions. Calculations over a P range of about 3 kb suggest that the coronas form during decompression by interaction with the melt. The amount of melt formed and garnet dissolved is proportional to the P change required to produce the observed modes. Additional indications of former melt are: that the original boundary of the garnet is not obvious whereas with solid-state replacement reactions a change in mode, but not assemblage, would mark the original garnet boundary; and that the textures of the garnet at the plagioclase + quartz + biotite interface have cusps and thin peninsulas that suggest a melt interface. Thus, in these aluminous gneisses, plagioclase coronas are likely related to local melts forming in regions with garnets during decompression rather than solid state reactions. Such coronas provide an indication of the amount of P decrease that resulted in melting.

THE BEAUTY AND COMPLEXITY OF PARTIALLY MELTED ALUMINOUS ROCKS: DISEQUILIBRIUM RECORDED BY TI-IN-QUARTZ

Kendrick J.*[1] & Indares A.[1]
[1] Department of Earth Sciences, Memorial University of Newfoundland, St. John's, Canada
Corresponding email: jkendrick@mun.ca

Keywords: Ti-in-quartz, partial melting, microstructures

Since the formulation of the Ti-in-quartz thermobarometer, or "TitaniQ" (Wark & Watson, 2006; Thomas et al., 2010), Ti-in-quartz thermobarometry has been applied to rocks from a wide variety of settings. Trace Ti has also been shown to be correlated with cathodoluminescence (CL) in quartz (Müller et al., 2002; Rusk et al., 2008; Leeman et al., 2012), allowing textures such as growth zonation to be identified in individual crystals. Combined, these techniques are a potentially powerful tool for interpreting the complex histories of rocks. Partially melted metamorphic rocks represent an intriguing, yet largely unexplored, application of the Ti-in-quartz technique (e.g., Spear & Wark, 2009; Zhang et al., 2014). Quartz is produced upon crystallization of partial melt and commonly coexists with rutile; this association is generally considered to ensure that quartz grew in a Ti-saturated environment. Titanium signatures in quartz interpreted using Ti-in-quartz thermobarometry and CL imaging could be used to constrain the retrograde P-T path of migmatites independently from or supplementary to phase equilibria models. Testing this hypothesis requires a critical assessment of the Ti-in-quartz technique in the context of partial melt crystallization, and an investigation of the behaviour of quartz during this process. Thorough imaging of textures is essential, and this study combines wavelength-specific CL maps of quartz with high resolution, false colour, thin section-scale mineralogical maps collected by scanning electron microscope mineral liberation analysis (SEM MLA) software to interpret microstructures not obvious by optical examination. The aluminous migmatites investigated are from the mid pressure and high pressure crustal segments of the central Grenville Province, with P-T paths previously constrained from phase equilibria models (Indares et al., 2008; Lasalle & Indares, 2014). Quartz unequivocally crystallized from partial melt has been identified, for instance as sequences of quartz crystals with different CL signatures filling interstitial former melt sites between feldspars. Titanium contents measured by electron microprobe (EPMA) using multiple spectrometers (10 ppm detection limit, ± 4 ppm precision) are generally too low for melt crystallization temperatures; the last quartz growths contain negligible Ti. Despite the presence of abundant, stable rutile in all samples, quartz in interstitial former melt sites was clearly not capable of equilibrating with rutile. Titanium diffusion was inefficient, resulting in isolated melt pockets of greatly varying Ti activity. These results highlight the dynamic nature of partial melt crystallization and the challenges inherent to interpreting the products of a system in disequilibrium.

Indares, A., White, R.W., Powell, R. (2008): Phase equilibria modelling of kyanite-bearing anatectic paragneisses from the central Grenville Province. *J. Metam. Geol.*, **26**, 815-836.

Lasalle, S. & Indares, A. (2014): Anatectic record and contrasting P–T paths of aluminous gneisses from the central Grenville Province. *J. Metam. Geol.*, **32**, 627-646.

Leeman, W.P., MacRae, C.M., Wilson, N.C., Torpy, A., Lee, C.A., Student, J.J., Thomas, J.B., Vicenzi, E.P. (2012): A study of cathodoluminescence and trace element compositional zoning in natural quartz from volcanic rocks: mapping titanium content in quartz. *Microsc. Microanal.*, **18**, 1322-1341.

Müller, A., Lennox, P., Trzebski, R. (2002): Cathodoluminescence and micro-structural evidence for crystallisation and deformation processes of granites in the Eastern Lachlan Fold Belt (SE Australia). *Contrib. Mineral. Petrol.*, **143**, 510-524.

Rusk, B.G., Lowers, H.A., Reed, M.H. (2008): Trace elements in hydrothermal quartz: relationships to cathodoluminescent textures and insights into vein formation. *Geology*, **36**, 547-550.

Spear, F.S. & Wark, D.A. (2009): Cathodoluminescence imaging and titanium thermometry in metamorphic quartz. *J. Metam. Geol.*, **27**, 187-205.

Thomas, J.B., Watson, E.B., Spear, F.S., Shemella, P.T., Nayak, S.K., Lanzirotti, A. (2010): TitaniQ under pressure: the effect of pressure and temperature on the solubility of Ti in quartz. *Contrib. Mineral. Petrol.*, **160**, 743-759.

Wark, D.A. & Watson, E.B. (2006): TitaniQ: a titanium-in-quartz geothermometer. *Contrib. Mineral. Petrol.*, **152**, 743-754.

Zhang, C., Holtz, F., Koepke, J., Berndt, J., Ma, C. (2014): Decompressional anatexis in the migmatite core complex of northern Dabie orogen, eastern China: petrological evidence and Ti-in-quartz thermobarometry. *Lithos*, **202-203**, 227-236.

COUNTERCLOCKWISE P-T EVOLUTION AT ~1.75 Ga RECORDED FROM Fe- AND Al-RICH ULTRAHIGH-TEMPERATURE METAPELITIC GRANULITES (YENISEI RIDGE): IMPLICATION FOR PROTEROZOIC SUPERCONTINENT TECTONICS

Likhanov I.I.*[1] & Nozhkin A.D.[1]

[1] Sobolev Institute of Geology and Mineralogy, Siberian Branch of the Russian Academy of Sciences, Novosibirsk, Russia

Corresponding email: likh@igm.nsc.ru

Keywords: UHT granulites, counterclockwise P-T path, mantle plume

An ultrahigh-temperature (UHT) granulite assemblage consisting of Grt–Opx–Sil–Crd–Bt–Sp–Pl–Qz–Kfs has been found in Al- and Fe-rich metapelites of the Yenisei Ridge (Likhanov et al., 2015a). Petrography, textural relations, mineral compositions and P-T estimates, indicate three generations of mineral assemblages: (1) pre-peak prograde stage (M1) consisting of a Sp–Opx–Crd–Pl-bearing inclusion assemblage, with low-Al_2O_3contents (3.6-4.4 wt.%) in Opx and P-T conditions of 5.7-7.1 kbar and 800-900°C, (2) peak UHT stage (M2) comprising a coarse-grained Grt–Opx–Sil–Crd-bearing mineral assemblage, with high-Al_2O_3 contents (6.3-6.5 wt.%) in Opx and peak conditions of 7-9 kbar and 920-1000°C, and (3) post-peak retrograde stage (M3) containing an oriented and fine-grained Opx–Crd–Sp-bearing and Sil–Bt–Kfs-bearing assemblage in matrix, with moderate amounts of Al_2O_3 (4.2-4.9 wt.%) in *Opx* and P-T conditions of 5.6-7.5 kbar / 770-900°C. The three discrete stages define a counterclockwise P-T path with a high metamorphic field gradient of dT/dP = 100-200°C/kbar involving initial prograde heating and post-peak retrograde decompression followed by near isobaric cooling. It suggests that UHT metamorphism likely occurred in an overall extensional tectonic setting with associated underplating of mantle-derived mafic magma (Likhanov et al., 2015b). *In situ* U–Th–Pb monazite and zircon dating of a UHT granulite yielded a concordant age of 1744±26 Ma, indicating that UHT metamorphism occurred at Late Proterozoic. This event occurred synchronously with mafic giant radial dyke swarm in the Aldan and Anabar shields and Baikal uplift (~1750 Ma) related to a mantle plume centered in Vilyui River area (Gladkochub et al., 2010). Thus, the Late Proterozoic UHT metamorphism at the western margin of Siberian craton is likely associated with underplating and heating of mantle-derived mafic magma as a result of the Vilyui mantle plume. Synchronous succession and similar style of the tectonometamorphic events within Siberian, Laurentia and Baltica cratons supports their spatial proximity during Proterozoic times (Likhanov et al., 2014), as indicated by the paleocontinental reconstructions of the Nuna supercontinent configuration.

Gladkochub, D.P., Pisarevsky, S.A., Donskaya, T.V., Ernst, R.E., Wingate, M.T.D., Söderlund, U., Mazukabzov, A.M., Sklyarov, E.V., Hamilton, M.A., Hanes, J.A. (2010): Proterozoic mafic magmatism in Siberian craton: An overview and implications for paleocontinental reconstruction. *Precambrian Res.*, **183**, 660-668.

Likhanov, I.I., Nozhkin, A.D., Reverdatto, V.V., Kozlov, P.S. (2014): Grenville tectonic events and evolution of the Yenisei Ridge at the western margin of the Siberian craton. *Geotectonics*, **48**, 371-389.

Likhanov, I.I., Nozhkin, A.D., Reverdatto, V.V., Kozlov, P.S., Khiller, V.V. (2015a): P-T evolution of ultrahigh temperature metamorphism: evidence for a late Paleoproterozoic intraplate extension at the southwestern margin of the Siberian Craton. *Dokl. Earth Sci.*, **465**, 1139-1142.

Likhanov, I.I., Reverdatto, V.V., Kozlov, P.S., Khiller, V.V., Sukhorukov, V.P. (2015b): P-T-t constraints on polymetamorphic complexes of the Yenisey Ridge, East Siberia: implications for Neoproterozoic paleocontinental reconstructions. *J. Asian Earth Sci.*, **113**, 391-410.

CORDIERITE PSEUDOMORPHS IN A PERALUMINOUS GRANITE: AN UNEXPECTED EVIDENCE OF HIGH PRESSURE METAMORPHISM

Lotout C.*[1], Pitra P.[1] & Van Den Driessche J.[1]
[1] Géosciences Rennes, Université Rennes1, France
Corresponding email: caroline.lotout@univ-rennes1.fr

Keywords: eclogitic granite, cordierite pseudomorph, Thermocalc modelling

Granitic rocks constitute the major part of the continental crust, but are known to poorly record metamorphism. Furthermore, late stages tend to erase the record of the early metamorphic history. Pseudomorphs are among the features that may help to unravel this early history of metamorphic rocks, even in the “hostile” granitic lithologies.

In the Lévézou Massif (southern French Massif Central), elongated bodies of peraluminous granitic orthogneisses are parallel to a major regional amphibolite band containing abundant lenses of eclogite. These intrusions have been initially interpreted as syntectonic with the Variscan collision, but we have shown that their emplacement is early ordovician (ca. 470 Ma). These granitic orthogneisses display a variable pattern of deformation, from undeformed porphyritic to ultramylonitic facies. The dominant foliation developed under amphibolite-facies conditions and is parallel to that of the amphibolite band. The undeformed porphyritic facies displays, however, numerous interesting metamorphic textures, as tiny garnet coronae surrounding magmatic biotite, rutile aggregates pseudomorphing ilmenite or rare rectangular clusters dominated by phengite, kyanite, garnet and quartz. The shape and the bulk composition of the latter suggest that they are pseudomorphs after cordierite. Phase diagrams modelling (THERMOCALC) performed on the whole rock composition does not explain these observations but allows to constrain the emplacement conditions of the granite at ca. 2 kbar and 670°C. Nevertheless, pseudosections calculated for the local bulk composition of the cordierite pseudomorphs suggest that they developed at 16-17 kbar and 650-670°C, i.e. under eclogite-facies conditions. Calculations further suggest that despite the H_2O-depleted character of a crystallised granite, the pseudomorphs were saturated in aqueous fluid. This was a possible consequence of early alteration that also enhanced the recrystallisation of the cordierite crystals. The inferred PT conditions are similar to those obtained from the eclogite lenses of the neighbouring amphibolite band, implying that both the granites and the mafic rocks have experienced the same high-pressure event, during the early Variscan subduction. The amphibolite-facies deformation can be related to a common exhumation stage occurring at ca. 350-340 Ma. These rocks are therefore a rare witness of the subduction of the continental crust during the early stages of the Variscan orogen.

CRYSTAL CHEMISTRY AND THERMODYNAMICS OF Fe-CHLORITE: SPECIATION AND SITE OCCUPANCY OF IRON

Masci L.*[1], Dubacq B.[1], Verlaguet A.[1], Chopin C.[2], De Andrade V.[3], Siebert J.[4] & Wehr N.[4]
[1] Sorbonne Universités, Université Pierre et Marie Curie, Université Paris 06, Centre National de la Recherche Scientifique, Institut des Sciences de la Terre de Paris, France
[2] Laboratoire de Géologie, Ecole Normale Supérieure & Centre National de la Recherche Scientifique, Paris, France
[3] Advanced Photon Source, Argonne National Laboratory, Lemont, IL, USA
[4] Institut de Physique du Globe de Paris, Sorbonne Paris Cité, Université Paris Diderot, France
Corresponding email: lorella.masci@upmc.fr

Keywords: Fe-chlorite, iron speciation, site occupancy

Chlorites are found in a wide range of geological environments, from low- to medium-grade metamorphic rocks, with important application fields including thermobarometry and anthropogenic waste storage. The speciation and site distribution of iron in chlorite are highly variable and poorly known, with implications for the thermodynamic status of iron-bearing chlorites. In particular, the absence of thermodynamic data for ferric end-members in chlorite solid solution models limits the applicability of thermometers and petrological tools for mineral assemblages containing iron-rich chlorites, which are common in metamorphic rocks. Iron speciation is linked to the distribution of atoms in Fe^{2+} or Fe^{3+} form in the crystal structure: alternating layers of tetrahedral (T) and octahedral (O) crystallographic sites create the chlorite structure, defining a TOT-O pattern with 14 Å basal spacing. Iron atoms are mainly located in octahedral sites where they substitute for Mg^{2+} and Al^{3+} cations.

This work aims at investigating the thermodynamic properties of iron-rich chlorites. The project development relies on building a chlorite collection gathering crystal-chemical and thermodynamic data on natural and synthetic samples. Natural crystals were chosen to illustrate a variety of solid solution compositions in between chlorite end-members. Syntheses were carried out in a piston-cylinder device under buffered oxygen fugacity. Both natural and synthetic chlorites are analysed with classical tools (XRD, SEM, EPMA) combined with XANES spectroscopy and single-crystal XRD, in order to determine the oxidation state of iron and its site occupancy.

Most of the studied chlorites are trioctahedral (low vacancy content). Combined results on synthetic and natural chlorites show that iron speciation strongly depends on total iron content and dismiss the presence of iron in tetrahedral position. Some synthesis experiments have led to “aluminous serpentine” (7 Å) crystallisation along the daphnite (14 Å) – Fe-amesite (7 Å) join, including experiments close to daphnite bulk composition. This questions the stability of Fe-chlorite along the Tschermak exchange from daphnite to Fe-amesite and its dependency on the redox state of iron.

PRESSURE-TEMPERATURE-TIME EVOLUTION OF METAPELITES FROM THE PORTO VECCHIO REGION, VARISCAN CORSICA

Massonne H.-J.*[1], Cruciani G.[2], Franceschelli M.[2] & Musumeci G.[3]
[1] Institut für Mineralogie und Kristallchemie, Universität Stuttgart, Germany
[2] Dipartimento di Scienze Chimiche e Geologiche, Università di Cagliari, Italy
[3] Dipartimento di Scienze della Terra, Università di Pisa, Italy
Corresponding email: h-j.massonne@mineralogie.uni-stuttgart.de

Keywords: Variscan metamorphism, micaschist, Corsica

The exposed Variscan crust in Corsica and Sardinia is characterized by abundant granitoids and little medium- to high-grade metamorphic rocks. In spite of the rarity of the latter rocks, important conclusions were drawn from petrological studies in regard to geodynamic settings (Rossi et al., 2009; Faure et al., 2014). For instance, the crust in northeastern Sardinia was subjected to high-pressure (HP ≥ 1 GPa) metamorphism around 340 Ma ago (Cruciani et al., 2013). Metamorphic rocks are also exposed north of NE Sardinia in the Porto Vecchio region of Corsica. In this region, we found garnet-bearing micaschists, which were sampled 3 km east and 15 km northeast of Porto Vecchio. In order to decipher the pressure (P) - temperature (T) - time (t) evolution of these rocks, we conducted the following studies in the order given: (1) petrological study of minerals and textures, (2) careful investigation of the chemical compositions of minerals, especially zoned garnet and potassic white mica, with the electron microprobe (EMP), (3) U-Th-Pb dating of monazite with the EMP, (4) calculation of P-T pseudosections for the bulk-rock compositions, determined with X-ray fluorescence spectrometry, and contouring of these pseudosections with relevant isopleths such as those of molar fractions of grossular and pyrope in garnet and the modal content of this mineral, (5) determination of P-T conditions based on intersections of such isopleths.

The micaschists from both localities yielded virtual identical P-T-t data. Maximum pressures were 0.7 GPa at temperatures rising from 580 to 630°C, which are compatible with the lack of indications for melting. Ages of monazite with high Y contents, which probably have formed before garnet, are in the range 350-370 Ma. The metamorphism at peak P-T conditions happened around 340 Ma based on low Y monazite.

We conclude that the studied micaschists belong to the same unit, which extends over the Porto Vecchio region. This unit had experienced peak pressures which are lower than those determined for metamorphic rocks, such as micaschist and gneiss, from northeastern Sardinia. At present, we favour a continent-continent collisional scenario with the studied unit buried during the collisional event but remained part of the upper plate. The HP metamorphic rocks from NE Sardinia could have been part of the interface between the colliding plates and of the upper portion of the lower plate.

Cruciani, G., Franceschelli, M., Massonne, H.-J., Carosi, R., Montomoli, C. (2013): Pressure-temperature and deformational evolution of high-pressure metapelites from Variscan NE Sardinia, Italy. *Lithos*, **175-176**, 272-284.

Faure, M., Rossi, P., Gaché, J., Melleton, J., Frei, D., Li, X., Lin, W. (2014): Variscan orogeny in Corsica: new structural and geochronological insights, and its place in the Variscan geodynamic framework. *Int. J. Earth Sci.*,**103**, 1533-1551.

Rossi, P., Oggiano, G., Cocherie, C. (2009): A restored section of the “southern Variscan realm” across the Corsica-Sardinia microcontinent. *Tectonics*, **341**, 224-238.

UNRAVELLING THE P-T-t EVOLUTION OF THE GRUF COMPLEX BY *IN SITU* ACCESSORY MINERAL DATING AND THERMOMETRY COMBINED WITH P-T MODELING OF MICRODOMAINS

Oalmann J.[1], Möller A.*[1] & Bousquet R.[2]
[1] Department of Geology, University of Kansas, Lawrence, KS, USA
[2] Institut für Geowissenschaften, Christian-Albrechts-Universität Kiel, Germany
Corresponding email: amoller@ku.edu

Keywords: UHT petrochronology, zircon, rutile

Constraining the pressure-temperature-time (P-T-t) evolution of ultra-high temperature (UHT) metamorphic rocks is challenging but crucial to understanding the geodynamic processes of the tectonic settings in which they occur. Equilibration does not generally occur at the scale of a hand sample in UHT rocks. Therefore, it is necessary to study major and accessory mineral reactions in microtextural domains to elucidate their P-T-t history. We present texturally-controlled rutile and zircon U-Pb dating and trace element thermometry combined with thermodynamic modeling of microtextural domains to investigate the P-T-t history of sapphirine-bearing granulites from the Gruf Complex in the Central Alps.

Pressure-temperature modeling of microtextural domains using Theriak-Domino indicates that garnet broke down to sapphirine-bearing assemblages at 900-960°C and 8-10 kbar. The youngest zircon rims, which overgrow resorbed Permian and Jurassic cores have a weighted mean $^{206}Pb/^{238}U$ age of 32.5±0.5 Ma. Titanium-in-zircon temperatures of these rims or any other domains do not exceed 800°C, indicating that zircon was not stable at UHT conditions, but grew during the early retrograde history. We interpret the resorption of the Permian and Jurassic domains to indicate that UHT metamorphism occurred slightly before the young rims crystallized from melt. The $^{206}Pb/^{238}U$ dates of rutile grains are decoupled from texture and range from 30-19 Ma. We interpret these dates to represent 11 m.y. of cooling between ca. 650 and 450°C (the closure temperature range for Pb diffusion in rutile; Mezger et al., 1989; Cherniak, 2000; Kooijman et al., 2010). In contrast, Zr-in-rutile temperatures are strongly coupled with textures and constrain the temperatures of prograde (500-890°C), peak (840-1000°C), and retrograde (650-850°C) metamorphism. Sub-peak temperatures were obtained from rutile in anhydrous, sapphirine-bearing assemblages (e.g., embayments in garnet). We interpret these low temperatures to be the result of limited Zr availability.

Based on these results we present the following model for the evolution of the Gruf Complex: 1) Prograde metamorphism (garnet growth) occurred at temperatures between 500 and 890°C and a maximum pressure of ca. 12 kbar. The timing of this stage is not well constrained and may or may not have been continuous with UHT metamorphism. 2) UHT conditions (900-960°C and 8-10 kbar) were reached during decompression (garnet breakdown) slightly before ca. 32.5 Ma. At ca. 34 Ma (Beltrando et al., 2010), lithospheric thinning in the Central Alps, associated with slab breakoff or roll back, resulted in asthenospheric upwelling, which provided heat for UHT metamorphism. 3) By ca. 30 Ma, the UHT rocks were juxtaposed against upper amphibolite facies migmatites and underwent partial retrograde metamorphism at 650-750°C and ≤ 7.5 kbar. 4) The composite Gruf Complex cooled to below ca. 450°C by ca. 19 Ma.

Beltrando, M., Lister, G.S., Rosenbaum, G., Richards, S., Forster, M.A. (2010): Recognizing lithospheric thinning along a convergent plate margin: the example of the Early Oligocene Alps. *Earth-Sci. Rev.*, **103**, 81-98.

Cherniak, D.J. (2000): Pb diffusion in rutile. *Contrib. Mineral. Petrol.*, **139**, 198-207.

Kooijman, E., Mezger, K., Berndt, J. (2010): Constraints on the U-Pb systematics of metamorphic rutile from in situ LA-ICP-MS analysis. *Earth Planet. Sci. Letters*, **293**, 321-330.

Mezger, K., Hanson, G.N., Bohlen, S.R. (1989): High-precision U-Pb ages of metamorphic rutile: application to the cooling history of high-grade terranes. *Earth Planet. Sci. Letters*, **96**, 106-118.

THERMODYNAMIC MODELLING AND QUANTITATIVE PETROLOGICAL ANALYSIS OF METAMORPHIC ROCKS: AN ESSENTIAL INTEGRATED TOOL TO INVESTIGATE THE PTX EVOLUTION OF OROGENIC PROCESS

Ortolano G.*[1], Cirrincione R.[1], Visalli R.[1] & Godard G.[2]

[1] Dipartimento di Scienze Biologiche, Geologiche e Ambientali, Università di Catania, Italy

[2] Institut de Physique du Globe de Paris, Centre National de la Recherche Scientifique, Université Paris Diderot, Paris, France

Corresponding email: ortolano@unict.it

Keywords: geomatics, effective reactant volume, metamorphic petrology

Thermodynamic modelling of metamorphic rocks, nowadays routinely integrated by several analytical techniques (e.g., SEM and EPMA microanalysis, *in situ* isotopic and geochronological investigations), became in the last years the most efficient tool to quantify the PTXt evolution of the orogenic processes. This is true thanks to the advent of ever more efficient and user-friendly phase diagram computing systems (e.g., Perplex – Connolly, 2005; Connolly & Petrini; 2002; or Thermocalc – Holland & Powell, 1998), stepwise controlled by the calculation of the effective bulk rocks chemistries (Stüwe, 1997; Evans, 2004).

This last parameter is at the base for the quantification of the robustness of the thermodynamically modelled systems in the way to highlight the relation to the real petrogenetic processes. These depend indeed, by the "objective" interpretation of textural equilibria, indispensable to verify the level of the reaction-scale equilibration (e.g., Fiannacca et al., 2012; Ortolano et al., 2014a).

In this view, the use of multivariate statistical analysis applied to EDS or WDS X-Ray maps can be used to extrapolate several parameter of petrological interest, such as the calculation of mineral mode as well as the extraction of Boolean images per original X-ray maps array, each of them representative for the single recognised mineral phase (Ortolano et al., 2014b).

The subsequent calibration of these last images, using some control spot analysis via a multi-linear regression technique, allowing obtaining new image arrays, each of them representative for the elemental concentration within a single phase. These further outputs have been then used to construct maps of the end members via map algebra operation, allowing visualizing the potential zoning patterns of solid solution mineral phases, quantifying at the same time the progressive change of the end-members composition, often sensitive to the PT variation of the investigated metamorphic systems.

Calibration and end-members map extraction have been here implemented in a new semi-automatized GIS-based workflow, which permitted to derive for instance, maps of the real textural equilibria, consequently defining the "objective" effective reactant volumes of the single metamorphic evolutionary stages.

This kind of analytical approach can be lead to a potential huge data extraction, making indispensable lay the groundwork also for the development of a careful data-management, useful to permit a functional and possible interoperable data-interaction.

Yielded results highlight as this new GIS-based workflow can be usefully applied in order to obtain an assisted semi-automated sequential image processing procedure, applicable in all the fields of petrological investigations, with particular focussing in the resolution of metamorphic petrology questions, minimising for instance, the subjectivity of the petrologists in the definition of the scale and composition of textural equilibria.

Connolly, J.A.D. (2005): Computation of phase equilibria by linear programming: a tool for geodynamic modeling and its application to subduction zone decarbonation. *Earth Planet. Sci. Letters*, **236**, 524-541.

Connolly, J.A.D. & Petrini, K. (2002): An automated strategy for calculation of phase diagram sections and retrieval of rock properties as a function of physical conditions. *J. Metam. Geol.*, **20**, 697-708.

Evans, T.P. (2004): A method for calculating effective bulk composition modification due to crystal fractionation in garnet-bearing schists: implications for isopleths thermobarometry. *J. Metam. Geol.*, **22**, 547-557.

Fiannacca, P., Lo Po', D., Ortolano, G., Cirrincione, R., Pezzino, A. (2012): Thermodynamic modelling assisted by multivariate statistical image analysis as a tool for unraveling metamorphic P T-d evolution: an example from ilmenite-garnet-bearing metapelite of the Peloritani Mountains, Southern Italy. *Mineral. Petrol.*, **106**, 151-171.

Holland, T.J.B. & Powell, R. (1998): An internally consistent thermodynamic data set for phases of petrological interest. *J. Metam. Geol.*, **16**, 309-343.

Ortolano, G., Visalli, R., Cirrincione, R., Rebay, G. (2014a): PT-path reconstruction via unraveling of peculiar zoning pattern in atoll shaped garnets via image assisted analysis: an example from the Santa Lucia del Mela garnet micaschists (Northeastern Sicily-Italy). *Per. Mineral.*, **83**, 257-297.

Ortolano, G., Zappalà, L., Mazzoleni, P. (2014b): X-Ray Map Analyzer: a new ArcGIS® based tool for the quantitative statistical data handling of X-ray maps (Geo- and material-science applications). *Comput. Geosci.*, **72**, 49-64.

Stüwe, K. (1997): Effective bulk composition changes due to cooling: a model of predicting complexities in retrograde reaction textures. *Contrib. Mineral. Petrol.*, **129**, 43-52.

A NEW TOOL TO DISPLAY COMPOSITIONAL CHANGES WITHIN METAMORPHIC ZONED MINERALS DUE TO THE DIFFUSION PHENOMENA: THE CASE OF MAMMOLA PARAGNEISS COMPLEX (SERRE MASSIF-SOUTHERN CALABRIA, ITALY)

Ortolano G.[1], Visalli R.*[1], Cirrincione R.[1] & Godard G.[2]

[1] Dipartimento di Scienze Biologiche, Geologiche e Ambientali, Università di Catania, Italy

[2] Institut de Physique du Globe de Paris, Centre National de la Recherche Scientifique, Université Paris Diderot, Paris, France

Corresponding email: rvisalli@unict.it

Keywords: diffusion processes, image analysis, Variscan metamorphism

In recent years, the use of semi-automated image processing techniques integrated with common Geographic Information Systems for the interpretation of many geo-petrological processes has become increasingly widespread (e.g., Ortolano et al., 2014a, Ortolano et al., 2014b). Such techniques, based on multivariate statistical analysis of X-ray maps, are useful in deciphering quantitative structural and modal parameters from selected thin section micro-domains, contributing to minimize the subjectivity of the operator.

In this perspective, this work explore the possibility of treating the diffusion phenomena affecting zoned metamorphic minerals through image analysis, by deriving images for each input parameter (i.e., concentration, temperature, pressure, diffusion coefficient) necessary to the resolution of Fick's diffusion laws. In this way, it is possible to obtain an array of virtual images representing the compositional changes that may occur over time due to the triggering of the diffusion phenomena. Diffusion modeling of the major elemental compositional zonings is a valuable tool to know how long a zoned mineral can resist in chemical disequilibrium with the surrounding matrix at high temperature before the pre-existing composition is modified by diffusion. It allows to derive the timescales of metamorphic processes such as heating and cooling rates, providing information about the burial and exhumation history if mineral diffusion properties, crystal size and temperature are known.

We have investigated millimeter almandine-rich garnet crystals from garnet-micaschists of the Mammola Paragneiss Complex (Serre Massif-Southern Calabria: Angì et al., 2010), highlighting a multistage metamorphic evolution consisting of an orogenic cycle partly overprinted by a thermal one, both of them ascribable to the Variscan orogenesis. In particular, the authors recognize a prograde low amphibolite facies evolution (P = 5.9-7.5 kbar; T = 500-550°C) followed by a retrograde *quasi*-adiabatic decompression (P = 4 kbar; T = 500°C), evolving toward a retrograde deep seated shearing stage (P = 3 kbar; T = 470°C). The subsequent post-tectonic progressive emplacement of huge masses of granitoid bodies gave rise then to a gradually distributed thermal metamorphic overprint (P = 3 kbar; T = 685°C), followed by a low pressure cooling path (P = 1.5 kbar; T = 500°C) consistent with the final unroofing stage of the former crystalline basement complex.

Preliminary results of diffusion modeling obtained by Ortolano et al. (2015) show a timescale of relaxation of the growth zoning around 1-3 My, suggesting prograde and exhumation events to be relatively rapid in this portion of the dismembered southern Variscan European Belt. Taking into account of those results, we have obtained a set of images showing, step-by-step, the compositional variation that occurred during this time period and those that would occur if the diffusion process had continued to act.

Angì, G., Cirrincione, R., Fazio, E., Fiannacca, P., Ortolano, G., Pezzino, A. (2010): Metamorphic evolution of preserved Hercynian crustal section in the Serre Massif (Calabria-Peloritani Orogen, southern Italy). *Lithos*, **115**, 237-262.

Ortolano, G., Zappalà, L., Mazzoleni, P. (2014a): X-Ray Map Analyzer: a new ArcGIS® based tool for the quantitative statistical data handling of X-ray maps (Geo- and material-science applications). *Comput Geosci.*, **72**, 49-64.

Ortolano, G., Visalli, R., Cirrincione, R., Rebay, G. (2014b): PT-path reconstruction via unraveling of peculiar zoning pattern in atoll shaped garnets via image assisted analysis: an example from the Santa Lucia del Mela garnet micaschists (Northeastern Sicily-Italy). *Per. Mineral.*, **83**, 257-297.

Ortolano, G., Visalli, R., Cirrincione, R. (2015): Timescale of relaxation of garnet growth zoning via multi-component diffusion modeling: the example of Mammola Paragneiss Complex (Serre Massif-Southern Calabria). *Rend. Online Soc. Geol. It.*, **35**, 134.

PANAFRICAN(?) HP RELICS IN MAFIC-ULTRAMAFIC ROCKS FROM DRONNING MAUD LAND (ANTARCTICA)

Palmeri R.*[1], Di Vincenzo G.[2], Godard G.[3], Sandroni S.[1] & Talarico F.M.[1-4]
[1] Museo Nazionale dell'Antartide, Università di Siena, Italy
[2] Istituto di Geoscienze e Georisorse, Consiglio Nazionale delle Ricerche, Pisa, Italy
[3] Institut de Physique du Globe de Paris, Université Paris-Diderot, France
[4] Dipartimento di Scienze Fisiche, della Terra e dell'Ambiente, Università di Siena, Italy
Corresponding email: rosaria.palmeri@unisi.it

Keywords: Antarctica, mafic/ultramafic rocks, HP-HT metamorphism

Antarctica is a collage of various terranes that accreted onto old Archaean nuclei in the course of several collisional orogenies, such as the Grenvillian (~ 1300-900 Ma) and Panafrican (~ 600-500 Ma) orogens, as well as during the subduction-accretion orogenies that took place more recently along the palaeo-Pacific margin of Gondwana/Antarctica from the Cambro-Ordovician (Ross-Delamerian orogen) to the Cretaceous-Cainozoic (Andean orogen). These orogenies induced diffuse HP-HT and scarcer HP/UHP metamorphism (see Pauly et al., 2016, and Godard & Palmeri, 2013, respectively).

The Dronning Maud Land (DML) is a key area for the study of the Grenvillian (1.3-0.9 Ga) and/or Panafrican (600-500 Ma) orogenies that have led to the assembly of Rodinia and Gondwana supercontinents, respectively. Central DML occupies a key area of the potential southern continuation of the Mozambique Belt, generally interpreted as the result of collision and amalgamation of East and West Gondwana during the Panafrican time. Several major lithological units were distinguished and mapped in the metamorphic basement of central DML (Colombo & Talarico, 2004). They include meta-igneous and meta-sedimentary units, and syn- to post-metamorphic plutons and dykes.

We report new petrological results on mafic-ultramafic rocks from the Conrad-gebirge, a ridge located in the central DML and consisting of orthogneisses derived from volcanic and plutonic protoliths with minor metasedimentary rocks. Mafic-ultramafic boudins consist of garnet/pyroxene-bearing amphibolites and spinel±garnet±olivine-bearing pyroxenitic-amphibolitic fels. They occur as boudins either isolated or, more often, arranged as trails in highly strained and strongly migmatized zones with Opx-bearing leucosomes. Mafic rocks exhibit various geochemical affinities including IAB, E-MORB to OIB/lamprophyric origins. At least three main metamorphic stages are suggested by the microtextures and P-T modelling: a HP-HT granulite-facies event (Grenvillian or Panafrican) represented by Grt + Opx + Cpx ± Pl ± Cam relics followed by a nearly isothermal decompression to HT and medium P granulite-facies conditions (Opx + Pl + Spl ± Ol symplectite around garnet) and the development of amphibole at lower P-T conditions. The metamorphic evolution of the DML rocks during the Panafrican orogeny is characterized by a clockwise P-T path and a peak at HP granulite-facies conditions witness the continent-continent collision.

Colombo, F. & Talarico, F.M. (2004): Regional metamorphism in the High-grade basement of Central Dronning Maud Land, East Antarctica. *in* "International GeoMaud Expedition of BGR to Central Dronning Maud Land in 1995/96", H.J. Paech, ed., *Geol. Jahrb.*, **B96**, 7-47.

Godard, G. & Palmeri, R. (2013): High-pressure metamorphism in Antarctica from the Proterozoic to the Cenozoic: a review and geodynamic implications. *Gondwana Res.*, **23**, 844-864.

Pauly, J., Marschall, H.R., Meyer, H.P., Chatterjee, N., Monteleone, B. (2016): Prolonged Ediacaran-Cambrian metamorphic history and short-lived high-pressure granulite-facies metamorphism in the H.U. Sverdrupfjiella, Dronning Maud Land (East Antarctica): evidence for continental collision during Gondwana assembly. *J. Petrol.*, **57**, 185-228.

STAUROLITE+KYANITE-BEARING PSEUDOMORPHS AFTER ANDALUSITE (CAP DE CREUS, SPAIN)

Pitra P.*[1] & Martínez F.J.[2]
[1] Géosciences Rennes, Université de Rennes 1, France
[2] Departament de Geologia, Universitat Autònoma de Barcelona, Spain
Corresponding email: pavel.pitra@univ-rennes1.fr

Keywords: kyanite, andalusite pseudomorph, pseudosection modelling

Metapelitic rocks from Cap de Creus (Eastern Pyrenees, Spain) have developed andalusite ± cordierite-bearing assemblages during the Variscan low-pressure high-temperature metamorphism. Andalusite crystals are commonly transformed to very fine-grained assemblages containing staurolite and kyanite (± chloritoid) together with white micas and biotite. The hydrous character of the replacement minerals (pseudomorphing anhydrous andalusite) and the fact that transformation locally occurs along fractures, suggests that it was enhanced by fluid circulation.

Using calculated phase diagrams (pseudosections), the equilibration of the main andalusite-bearing assemblage is constrained at < 4 kbar and 550-600°C. Various types of phase diagrams are combined with a detailed analysis of the crystallisation sequence of the replacement minerals, in order to investigate the conditions of formation of the staurolite + kyanite(±chloritoid)-bearing pseudomorphs. Finally, it is discussed whether the pseudomorphs reflect a “simple” retrograde alteration, a retrogression associated with a pressure increase, or a prograde overprint during another (Pyrenean) orogenic cycle.

SYMPLECTITE FORMATION IN THE PRESENCE OF A REACTIVE FLUID: INSIGHTS FROM HYDROTHERMAL EXPERIMENTS

Spruzeniece L.*[1], Piazolo S.[1], Putnis A.[2-3], Daczko N.[1] & Kilburn M.R.[4]
[1] Department of Earth and Planetary Sciences, Macquarie University, Sydney, Australia
[2] Institute for Geoscience Research, Curtin University, Perth, Australia
[3] Institut für Mineralogie, Universität Münster, Germany
[4] Centre for Microscopy, Characterisation and Analysis, University of Western Australia, Perth, Australia
Corresponding email: liene.spr@gmail.com

Keywords: fluid-rock interaction, hydrothermal experiments, microstructure

This study describes the microstructural and chemical development of symplectites, obtained in hydrothermal mineral replacement experiments. During the experiments polymineralic feldspar-rich samples were exposed to sodium-silicate-H_2O solutions at 600°C and 2 kbar confining pressures for durations of 12 hr to 20 days. Fluid-rock interaction resulted in highly complex reaction rims involving two varieties of kelyphitic symplectite-resembling microstructures consisting of a nanometre-scale intergrowth of gehlenite-zeolite and grossular-zeolite grains. The experimental use of ^{18}O-doped fluids reveals not only that the reactions involved exchange of oxygen isotopes between the rock and fluid, suggesting fluid mediated dissolution-precipitation as the main reaction mechanism, but also the relative sequence of phase growth. Based on the progressive microstructural and chemical evolution of symplectite structures, observed in the performed experiments, a conceptual model for their formation is proposed. We suggest that the combination of fluid mediated open-system mass exchange, reaction generated porosity and ultra-local chemical variations of the interface fluid composition plays a significant role in controlling the formation of symplectite in the presence of a reactive fluid phase.

Our results may have important implications for understanding the fundamental processes involved in symplectite formation in nature and the interpretation of the geological history of mineral assemblages that exhibit symplectite microstructures.

TRACKING THE P–T PATH OF PRECAMBRIAN ECLOGITE USING PSEUDOSECTION, Ti-IN-QUARTZ AND Zr-IN-RUTILE THERMOBAROMETRY

Tual L.*[1], Möller C.[1], Pitra P.[2] & Whitehouse M.[3]
[1] Department of Geology, Lund University, Sweden
[2] Géosciences Rennes, Université de Rennes 1, France
[3] Swedish Museum of Natural History, Stockholm, Sweden
Corresponding email: lorraine.tual@gmail.com

Keywords: thermometry, eclogite, Sveconorwegian orogen

Sveconorwegian eclogite occur as a nappe within the high-grade metamorphic region in southern Sweden, which constitutes a window into the deepest part of this Precambrian mountain belt. Distinct microstructural domains (i.e., garnet core, garnet rim, and matrix) in a Fe-Ti-rich eclogite variety contain abundant quartz, rutile and zircon.

A pseudosection approach was first applied and compared to results from a combination of Zr-in-rutile and Ti-in-quartz. The pressure input used for both thermometers was first deduced for each microstructural domain from the pseudosection. For the *garnet core*, Zr-in-rutile yields temperatures of 700-715°C and Ti-in-quartz ~ 635°C at 7 kbar. For the *garnet rim*, temperatures of 760-790°C (Zr-in-rutile) and 740-890°C (Ti-in-quartz) at 12-18 kbar were calculated. *Matrix* rutile recorded temperatures of ~ 810°C, while quartz recorded temperatures up to ~ 890°C. Additionally, direct combination of Ti content in quartz and Zr content in rutile isopleths (i.e., independent from the pseudosection) yield a prograde path in nearly perfect agreement with the one deduced from the pseudosection.

The pseudosection shows that rutile was produced by continuous breakdown of ilmenite during the early stages of prograde metamorphism, a reaction that ran to completion at ~ 730°C. Most rutile grains in garnet rim and matrix are interpreted to subsequently form by recrystallization of smaller matrix grains. However, they generally do not record the peak-P temperatures and instead range mostly between 775 and 815°C, interpreted as a result of more efficient recrystallization during a dehydration reaction (progressive replacement of hornblende by clinopyroxene).

This study illustrates that both Zr-in-rutile and Ti-in-quartz thermometry cannot only robustly constrain a prograde evolution, but when combined with a pseudosection model can also yield information on recrystallization processes. In fact, the combination of these three methods provides an unrivalled tool for petrologic interpretation.

The variation in Ti concentration in quartz is small regardless of crystal size. This *P–T* path reach very high temperatures (up to 875°C) with a high d*P*/d*T* ratio, both during prograde and retrograde histories. The steep *P–T* path, together with preservation of garnet growth zoning, symplectitic textures and the lack of significant Ti diffusion in quartz is consistent with a short residence time at high-temperature, implying unusual fast burial and exhumation of the eclogite-bearing nappe.

INCLUSION SUITES IN ECLOGITE GARNETS: UNRELIABLE WITNESSES OF PROGRADE METAMORPHIC HISTORY

Waters D.J.*[1-2] & Utting J.[1]
[1] Department of Earth Sciences, University of Oxford, United Kingdom
[2] Museum of Natural History, University of Oxford, United Kingdom
Corresponding email: dave.waters@earth.ox.ac.uk

Keywords: garnet zoning, amphibole, disequilibrium

Mineral inclusions in garnet, if preserved intact from the time of entrapment, are potentially important indicators of metamorphic conditions before and during garnet growth. In contrast, this study indicates that inclusion suites in garnet from UHP eclogite in the Tso Morari Complex, NW Himalayas have been significantly modified by post-entrapment processes involving fracturing and fluid-assisted mass transfer, while leaving the prograde zoning patterns of garnet largely intact.

The studied sample comes from the mafic eclogite body also investigated by St-Onge et al. (2013) and Wilke et al. (2015). The rock contains abundant garnet (up to 1.8 mm diameter) in a matrix of omphacite and amphibole with minor clinozoisite, carbonate, paragonite, phengite and talc. An FEI Quanta 600 SEM with Oxford Instruments EDS detector was used for compositional mapping of garnets and their inclusions, concentrating on amphibole chemistry.

Garnet cores contain abundant and varied mineral inclusions, and show patchy composition variation at low Mg content. Sharply bounded rim zones have few inclusions: an inner rim has low Ca with increasing Mg; the outer rim shows maximum Mg with intermediate Ca. All these garnet compositions fall on plausible prograde zoning trajectories (cf. St-Onge et al., 2013), and reflect evolving mechanisms of (episodic?) growth from core to rim. Superimposed on this zonation, traversing the inner rim and core zones, are narrow linear or network-forming features marked by increase in Mg at the expense of Fe. These link inclusions, merge with the outer rim composition, and are interpreted as marking healed fractures that allowed fluid access to garnet interiors.

Amphibole composition trends were monitored in terms of "gl" = Na^{M4}, "ed" = Na^{A}, "ts" = Al^{IV}-Na^{A} and Mg# = Mg/(Mg+Fe). Cores of larger zoned inclusions are Mg-rich winchites equivalent to matrix amphiboles formed at ~ 2 GPa on the retrograde path (Palin et al., 2014). Most amphiboles form a continuous array of increasing "ed" and "ts", decreasing "gl" and Mg# from winchite through barroisite, taramite and pargasite, terminating at an Al-rich ferropargasite identical to narrow external rims on garnet. A parallel hornblende to ferropargasite trend at lower "gl" is found in composite, albite-bearing inclusions.

Mineral inclusions expected from modelling the prograde path are absent, and instead the compositions and zoning patterns of amphibole inclusions are consistent with retrograde processes. The patterns are best explained by modification of existing inclusions by matrix-derived fluid supplied along now-healed fractures over the P range 2-1 GPa, coupled with growth by consumption of host garnet without re-equilibration of the garnet itself. This therefore represents a situation transitional to the formation of atoll garnets, where in this case the effects of post-peak alteration and replacement involving garnet inclusions are severe, and yet not obvious from the macroscopic texture.

Palin, R.M., St-Onge, M.R., Waters, D.J., Searle, M.P., Dyck, B. (2014): Phase equilibria modelling of retrograde amphibole and clinozoisite in mafic eclogite from the Tso Morari massif, northwest India: constraining the *P–T–M*(H_2O) conditions of exhumation. *J. Metam. Geol.*, **32**, 675-693.

St-Onge, M.R., Rayner, N., Palin, R.M, Searle, M.P., Waters, D.J. (2013): Integrated pressure-temperature-time constraints for the Tso Morari dome (Northwest India): Implications for the burial and exhumation path of UHP units in the western Himalaya. *J. Metam. Geol.*, **31**, 469-504.

Wilke, F.D.H., O'Brien, P.J., Schmidt, A., Ziemann, M.A. (2015): Subduction, peak and multi-stage exhumation metamorphism: Traces from one coesite-bearing eclogite, Tso Morari, western Himalaya. *Lithos*, **231**, 77-91.

HIGH-P ECLOGITE IN THE TRANS-HUDSON OROGEN, CANADA: MODERN-DAY PLATE TECTONIC PROCESSES IN THE PALEOPROTEROZOIC

Weller O.M.*[1] & St-Onge M.R.[1]
[1] Geological Survey of Canada, Ottawa, Canada
Corresponding email: owenmweller@gmail.com

Keywords: high-P eclogite, Trans-Hudson Orogen, plate tectonics

The Trans-Hudson Orogen (THO) is a continental collisional belt that extends from north-eastern to south-central North America, which formed during convergence between the lower Superior and upper Churchill plates from 1.92 to 1.80 Ga (Hoffman, 1988). It has been suggested that the THO represents a middle Paleoproterozoic analogue to the Cenozoic Himalaya-Karakoram-Tibet Orogen (HKTO), due to similarities in length scales of deformation, and time scales of magmatism and metamorphism (St-Onge et al., 2006). A notable discrepancy in this correlation has been the absence of high-pressure rocks in the THO compared with the HKTO, and it was unclear whether this represented a secular tectonic change, or a problem of exposure/preservation.

In this contribution we document a new discovery of eclogite from the THO, which fills in the high-pressure gap in the comparative record between the two orogenies. The eclogite was sampled from a mafic boudin associated with metavolcaniclastic schist and hosted by Archean basement orthogneiss in the Kovik tectonic window of northern Quebec. Both boudin and schist are located in a structurally equivalent setting to the Tso Morari eclogite locality in the western Himalaya. Petrographic analysis of the eclogite reveals that it was characterised by the assemblage garnet–omphacite–kyanite–rutile–biotite–zoisite at high pressures, prior to retrograde symplectite growth. The metavolcanic schist also contains evidence of an early kyanite-grade history, prior to retrograde growth of plagioclase–gedrite–cordierite coronas around garnet.

Phase equilibria modelling of assemblage changes in both eclogite and schist reveals a multi-stage, approximately isothermal, decompression history from ~26 to 7 kbar at 700°C. This pressure–temperature (*P-T)* history overlaps within error with derived *P-T* paths for the Himalayan Tso Morari eclogite (St-Onge et al., 2013). *In situ* Sensitive High Resolution Ion Microprobe U-Pb dating of monazite from the metavolcanic schist indicates that it experienced prograde metamorphism at ca. 1830 Ma, which provides an upper age limit for the timing of peak eclogite-facies metamorphism. Notably this age coincides with the onset of terminal Superior–Churchill collision in the eastern THO, which is analogous with the relative timing of eclogite-facies metamorphism in the Himalaya.

Overall, the exceptional structural, thermobarometric and temporal similarities of the THO eclogite with eclogitic units in the Himalaya suggest that modern-day plate tectonic processes are applicable to at least the middle Paleoproterozoic. Furthermore, the results indicate that a part of the north-eastern THO comprises a previously unrecognised high-pressure domain, which, to the best of our knowledge, exposes the oldest high-pressure eclogite in the world.

Hoffman, P. (1988): United plates of America: Early Proterozoic assembly and growth of Laurentia. *Ann. Rev. Earth Planet. Sci.*, **16**, 543-603.

St-Onge, M.R., Searle, M.P., Wodicka, N. (2006): Trans-Hudson orogen of North America and Himalaya-Karakoram-Tibetan Orogen of Asia: Structural and thermal characteristics of the lower and upper plates. *Tectonics*, **25**, 1-22.

St-Onge, M.R., Rayner, N., Palin, R.M., Searle, M.P., Waters, D.J. (2013): Integrated pressure–temperature–time constraints for the Tso Morari dome (Northwest India): implications for the burial and exhumation path of UHP units in the western Himalaya. *J. Metam. Geol.*, **31**, 1-36.

Session S12:

Clays, zeolites and nanostructured minerals: from mineralogy to applications in industry and environment

Conveners:

Emilia García Romero (Madrid – Spain)

Annalisa Martucci (Ferrara – Italy)

Mercedes Suárez (Salamanca – Spain)

BIODIESEL PRODUCTION USING ZEOLITE CATALYSTS PREPARED FROM SHALE ROCK

Ahmed Z.T.[1], Abbas A.S.[1], Albayati T.M.[2] & Doyle A.M.*[3]
[1] Department of Chemical Engineering, University of Baghdad, Iraq
[2] Department of Chemical Engineering, University of Technology, Baghdad, Iraq
[3] Division of Chemistry and Environmental Science, Manchester Metropolitan University, United Kingdom
Corresponding email: a.m.doyle@mmu.ac.uk

Keywords: zeolite, biodiesel, catalysis

Zeolites occur in nature and have been known for almost 250 years as aluminosilicate minerals. Examples are faujasite, mordenite, offretite, and ferrierite, Today, these and other zeolite structures are of great interest in catalysis, yet their naturally occurring forms are of limited value, because (i) they almost always contain undesired impurity phases, (ii) their chemical composition varies from one deposit to another and even from one stratum to another in the same deposit, and (iii) their properties are not naturally optimised for catalytic applications (Weitkamp, 2000). For these reasons we synthesis faujasite zeolite from inexpensive raw materials. Zeolites are considered one of the most important heterogeneous catalysts, for example it is the active component in catalysts for fluid catalytic cracking and many other processes (von Ballmoos et al., 1997).

Y zeolite was prepared and catalytically active metals were added via aqueous impregnation from various precursor salts. In order to obtain catalysts with a final metals loading of 1 wt.%, the desired amount of metal precursor was dissolved in a volume of 0.1N HCl equal to the pore volume of catalyst support. Subsequent drying of the zeolite achieved a high metal dispersion of metal nanoparticles by inhibiting agglomeration of the salt during the vaporization (Albayati & Doyle, 2013).

Biodiesel is an alternative diesel fuel that is produced from natural sources such as vegetable oils and animal fats. Vegetable oils were first used as a fuel over a century ago by Rudolf Diesel but this source of fuel has been replaced with cheap petroleum oil fractions that are reformed to diesel using heterogeneous catalysts. Despite the continuing widespread use of fossil fuels, and recent technologies that allow increasing amounts of extraction from previously unavailable sources, the total amount of petroleum oil that is available is limited and will some day expire. Vegetable oils are extracted from plants and are therefore an almost limitless means of storing solar energy. However, natural oils typically comprise mostly glycerides/triglycerides and suffer from high viscosity and inappropriate burning rate (cetane number), both of which render them less than ideal as a fuel for transportation. The (trans) esterification of natural oils using heterogeneous catalysis overcomes these problems by generating alkyl esters that are much more suited to use as fuels, and is therefore the focus of much present day research.

It is well known that fly ash may be used to successfully prepare faujasite zeolite. Here we investigate the use of ash derived from a variety of fuel types (coal, timber and peat), following their combustion in a domestic solid fuel stove, as a reagent to prepare zeolite catalysts. The fuels used in this study originate from different geographical locations and the ash residing from their combustion is thus expected to exhibit distinct mineralogical properties. Attempts are also being made to prepare zeolite using naturally occurring shale as an aluminosilica source. Results will be presented showing the elemental composition and crystal structure (where relevant) of the ash and shale samples following varying degrees of thermal pre-treatment. The zeolites prepared will be fully characterised and their activity tested in the transesterification of vegetable oil and the esterification of oleic acid (a simulated free fatty acid found in waste cooking oil). A full set of results showing catalytic testing of all prepared catalysts will be presented at the conference.

Albayati, T.M. & Doyle, A.M. (2013): Hydroisomerisation and hydrocracking of n-heptane over nanoporous trimetallic (Pt-Ni-Co/SBA-15 Catalyst). *Eng. Technol. J.*, **31A**, 18.

von Ballmoos, R., Harris, D.H., Magee, J.S. (1997): Catalytic cracking. *in* "Handbook of Heterogeneous Catalysis, Vol. 4", G. Ertl, H. Knbzinger, J. Weitkamp, eds., Wiley, Weinheim, 1955-1986.

Weitkamp, J. (2000): Zeolites and catalysis. *Solid St. Ionics*, **131**, 175-188.

HIGH PRESSURE-INDUCED SUPRAMOLECULAR ORGANIZATION OF WATER AND ETHANOL IN ALL-SILICA FERRIERITE: A POTENTIAL ROUTE FOR A CHALLENGING SEPARATION PROBLEM

Arletti R.[1], Fois E.[2], Tabacchi G.[2], Vezzalini G.*[3] & Quartieri S.[4]

[1] Dipartimento di Scienze della Terra, Università di Torino, Italy

[2] Dipartimento di Scienze e Alta Tecnologia, Università dell'Insubria & Consorzio Interuniversitario Nazionale per la Scienza e Tecnologia dei Materiali, Como, Italy

[3] Dipartimento di Scienze Chimiche e Geologiche, Università di Modena e Reggio Emilia, Modena, Italy

[4] Dipartimento di Scienze Matematiche e Informatiche, Scienze Fisiche e Scienze della Terra, Università di Messina, Italy

Corresponding email: mariagiovanna.vezzalini@unimore.it

Keywords: Si-ferrierite, high-pressure synchrotron X-ray powder diffraction, water-ethanol separation

Ethanol produced from plant matter is a sustainable option for combustion engines. However, due to its high hygroscopicity, the ethanol-gasoline mixtures (biofuels) are easily contaminated by water, leading to drivability problems (French et al., 2005). Separating ethanol from its aqueous solution currently relies on energy intensive distillation.

Zeolites can play an important role as separation membranes, but their performance strictly depends on the framework structure and composition. All-silica zeolites were proposed in biofuel production for the removal of ethanol from aqueous solutions where ethanol is the minority component (Zhang et al., 2012). By themselves, they are very hydrophobic, but the adsorption of ethanol can promote water co-adsorption through hydrogen bond formation and lower the selectivity (Bai et al., 2012). For this application, the desired zeolite possesses a pore/channel system that accommodates ethanol molecules but disfavors hydrogen bonding with water molecules.

It was demonstrated that the penetration behavior of aqueous and electrolytic solutions in porous materials can be influenced by applying a moderate pressure to the system (see, e.g., Tzanis et al., 2011; Khay et al., 2014.). Very recently, FER topology has been proposed as a top-ranked structure for the separation of ethanol and water (Bai et al., 2015). However, to our knowledge, very few detailed structural data are available in literature on the site location of alcohol and water molecules in Si-FER (Arletti et al., 2014; Lotti et al., 2015).

Hence, to interpret and confirm the predicted outstanding performance of Si-FER in separating ethanol and water, we have further investigated the system at both ambient conditions and under pressure, using a multi-technique approach based on the use of synchrotron X-ray powder diffraction and first-principles modeling.

The *in-situ* HP experiments were performed at SNBL1 (BM01a) beamline at ESRF, using as pressure-transmitting media (PTM) the following two mixtures: m.e.w. (methanol : ethanol : water = 16 : 3 : 1) and e.w. (ethanol : water = 1 : 3).

Our studies show that: 1) during compression of Si-FER in m.e.w. at 0.2 GPa, 15 H_2O molecules penetrate the zeolite pores forming H_2O clusters. Interestingly, no methanol or ethanol penetration was observed; 2) upon compressing in e.w., at about the same P, both components of the PTM penetrate the zeolite cavities, but, remarkably, they are segregated in different cages, leading thus to a supramolecular organization of the organic-water system inside Si-FER. 3) the penetration and segregation phenomena are irreversible upon pressure release. The structure and the stability of the Si-FER/EtOH/H_2O system was studied by a first-principles approach (see Gigli et al., 2014) that confirmed the EtOH segregation in the FER pores.

Arletti, R., Vezzalini, G., Quartieri, S., Di Renzo, F., Dmitriev, V. (2014): Pressure-induced water intrusion in FER-type zeolites and the influence of extraframework species on structural deformations. *Microp. Mesop. Mater.*, **191**, 27–37.

Bai, P., Tsapatsis, M., Siepmann, J.I. (2012): Multicomponent adsorption of alcohols onto silicalite-1 from aqueous solution: Isotherms, structural analysis, and assessment of ideal adsorbed solution theory. *Langmuir*, **28**, 15566-15576.

Bai, P., Jeon, M.Y., Ren, L., Knight, C., Deem, M.W., Tsapatsis, M., Siepmann, J.I. (2015): Discovery of optimal zeolites for challenging separations and chemical transformations using predictive materials modeling. *Nature Commun.*, **6**, 5912.

French, R. & Malone, P. (2005): Phase equilibria of ethanol fuel blends. *Fluid Phase Equilib.*, **228**, 27-40.

Gigli, L., Arletti, R., Tabacchi, G., Fois, E., Vitillo, J.G., Martra, G., Agostini, G., Quartieri, S., Vezzalini, G. (2014): Close-packed dye molecules in zeolite channels self-assemble into supramolecular nanoladders. *J. Phys. Chem. C*, **118**, 15732-15743.

Khay, I., Daou, T.J., Nouali, H., Ryzhikov, A., Rigolet, S., Patarin, J. (2014): High pressure intrusion–extrusion of LiCl aqueous solutions in silicalite-1 zeolite: Influence on energetic performances. *J. Phys. Chem. C*, **118**, 3935-3941.

Lotti, P., Arletti, R., Gatta, G.D., Quartieri, S., Vezzalini, G., Merlini, M., Dmitriev, V., Hanfland, M. (2015): Compressibility and crystal-fluid interactions in all-silica ferrierite at high pressure. *Microp. Mesop. Mater.*, **218**, 42-54.

Tzanis, L., Trzpit, M., Soulard, M., Patarin, J. (2011): High pressure water intrusion investigation of pure silica 1D channel AFI, MTW and TON-type zeolites. *Microp. Mesop. Mater.*, **146**, 119-126.

Zhang, K., Lively, R.P., Noel, J.D., Dose, M.E., McCool, B.A., Chance, R.R., Koros, W.J. (2012): Adsorption of water and ethanol in MFI-type zeolites. *Langmuir*, **28**, 8664-8673

MICROTEXTURE AND GENESIS OF KAOLIN MINERALS IN SEDIMENTARY ENVIRONMENTS OF THE LOWER CRETACEOUS IN NE SPAIN

Bauluz B.*[1], Mayayo M.J.[1] & Yuste A.[1]

[1] Instituto Universitario de Ciencias Ambientales, Departamento de Ciencias de la Tierra, Universidad de Zaragoza, Spain

Corresponding email: bauluz@unizar.es

Keywords: kaolinite, halloysite, electron microscopy

The high contents in kaolin minerals in the Albian sedimentary deposits of the Southern Iberian Range (Spain), their low iron and titanium contents and the lack of carbonates made them appropriated to be nowadays actively mined to manufacture ceramic and refractories (Bauluz et al., 2008). The geological environment of these clay deposits correspond to a typical deltaic and mudflat environment. The clays have greyish and blackish colors because of the organic matter and significant interbedded coal levels.

The clay minerals in these deposits are mainly kaolinite, illite and minor halloysite. XRD patterns show that the 7Å reflection corresponding to kaolinite has an expandable behavior with the etilenglycol treatment, indicating the presence of smectite layers in the kaolin minerals.

Under scanning electron microscopy, kaolinite consists of subeuhedral to euhedral nanometer sized plates, whereas halloysite has tubular morphologies with sizes of approximately 600 x 80 nm. The halloysite tubes are covered by kaolinite plates. In contrast, illite has anhedral morphologies typical of detrital phases.

Transmission electron microscopy (TEM) images indicate that the clay packets have no preferred orientation. It has been observed 20 to 50 nm sized packets of illite and kaolinite, and packets that consist of intergrowths of kaolinite layers (7Å), illite layers (10Å), partially collapse smectite layers (12Å) and partially collapse illite/smectite mixed layers (22Å). Lateral transitions from 10Å to 7Å have been also observed. The TEM images also show that in some areas of the samples the clay packets have diffuse edges. In occasions, the layers in illite packets are split and separated indicating alteration processes. Chemical analyses (TEM) of kaolinite and halloysite indicate that they do not contain iron in their structure.

Microtexture and morphology of the kaolin minerals suggest that kaolinite and halloysite were formed *in situ* probably from the alteration of other clays such as illite. This would explain the presence of intergrowths of the different types of clays (7Å, 10Å, 12Å and 22Å) and the altered textures in illites. The development of the swampy environment in these areas of the sedimentary basin, rich in organic matter and, therefore, with acidic pH, probably promotes the alteration of the detrital silicates and the formation of the kaolin clays. The crystallization of tubular halloysite in low Fe environments has been previously described in literature (Hart et al., 2002); its formation was likely previous to that of the kaolinite in more hydrated conditions.

Bauluz, B., Mayayo, M.J., Yuste, A., González López, J.M. (2008): Genesis of kaolinite from Albian sedimentary deposits of the Iberian Range (NE Spain): analysis by XRD, SEM and TEM. *Clay Miner.*, **43**, 459-475.

Hart, R.D., Gilkes, R.J., Siradz, S., Singh, B. (2002): The nature of soil kaolins from Indonesia and Western Australia. *Clays Clay Miner.*, **50**, 198-207.

DESORPTION OF CHLOROBENZENE CONFINED IN Y ZEOLITE: A COMBINED *IN SITU* SYNCHROTRON X-RAY POWDER DIFFRACTION AND CHROMATOGRAPHIC STUDY

Beltrami G.*[1], Rodeghero E.[1], Martucci A.[1], Cruciani G.[1], Sarti E.[2], Pasti L.[2] & Ardit M.[1]
[1] Dipartimento di Fisica e Scienze della Terra, Università di Ferrara, Italy
[2] Dipartimento di Chimica, Università di Ferrara, Italy
Corresponding email: giada.beltrami@student.unife.it

Keywords: VOCs, Y-zeolite, regeneration

Volatile organic compounds (VOCs) such as chlorobenzene are common pollutants present in groundwater. Because of their human and ecosystems toxicity and their tendency to persist in water the removal of these contaminants it is in the public interest. Recently, the state of the art highlighted that hydrophobic zeolites are environmentally friendly materials, efficient as contaminants adsorbents and perfectly regenerable without changing their initial adsorption capacity (Pasti et al., 2012; Martucci et al., 2015a, 2015b; Leardini et al., 2015; Rodeghero et al., 2016). Structural and kinetic dynamic data are required to full understanding the behaviour of zeolites during the fuel-based compounds desorption process. Actually no *in situ* structural investigation of the VOCs kinetics desorption has been performed on Y zeolite. The challenge of this work is understanding the structural modifications undergoing on this hydrophobic material (HSZ-390HUA, SiO_2/Al_2O_3 = 200, Tosoh Corporation) loaded with chlorobenzene (Cl-B) upon thermal treatment. To obtain this goal the study was carried out with two approaches. Firstly adsorption isotherm from distilled water was performed on zeolites in batches at RT and the concentration of contaminants in aqueous solution was obtained by gas chromatography and mass spectrometry. Then the *in situ* heating allowed us to simulate the regeneration process, which is usually subjected exhausted zeolites after adsorption of hydrocarbons. The desorption process was continuously monitored at the ID22 beamline (ESRF-Grenoble) as a function of temperature (heating rate 20°C/min) from room temperature up to 600°C. The results obtained with Rietveld method indicate that after thermal treatment zeolite does not show any significant crystallinity loss and when all the organic have been ejected (about 300°C), non-equilibrium distortions in the framework are relaxed and channel apertures become more circular. Achieving the reactivation of these materials and its reuse as pollutants adsorbent would expand their capabilities in environmental applications. Additionally, understanding this process can help in optimizing and the design the water remediation technologies (e.g. Permeable Reactive Barriers) and using zeolites as “molecular sieves” to remove fuels-based pollutants from water.

Leardini, L., Quartieri, S., Vezzalini, G., Arletti, R. (2015): Thermal behaviour of siliceous faujasite: Further structural interpretation of negative thermal expansion. *Microp. Mesop. Mater.*, **202**, 226-233.

Martucci, A., Braschi, I., Bisio, C., Sarti, E., Rodeghero, E., Bagatin, R., Pasti, L. (2015a): Influence of water on the retention of methyl tertiary-butyl ether by high silica ZSM-5 and Y zeolites: a multidisciplinary study on the adsorption from liquid and gas phase. *RSC Adv.*, **106**, 86997-87006.

Martucci, A., Rodeghero, E., Pasti, L., Bosi, V., Cruciani, G. (2015b): Adsorption of 1,2-dichloroethane on ZSM-5 and desorption dynamics by *in situ* synchrotron powder X-ray diffraction. *Microp. Mesop. Mater.*, **215**, 175-182.

Pasti, L., Martucci, A., Nassi, M., Cavazzini, A., Alberti, A., Bagatin, R. (2012): The role of water in DCE adsorption from aqueous solutions onto hydrophobic zeolites. *Micropor. Mesopor. Mater.*, **160**, 182-193.

Rodeghero, E., Martucci, A., Cruciani, G., Bagatin, R., Sarti, E., Bosi, V., Pasti, L. (2016): Kinetics and dynamic behaviour of toluene desorption from ZSM-5 using *in situ* high-temperature synchrotron powder X-ray diffraction and chromatographic techniques. *Catalysis Today*, in press.

FLY ASH AS RAW MATERIAL FOR THE SYNTHESIS OF ZEOLITE-ENCAPSULATED TETRAPYRROLES (PORPHYRAZINE AND METALLO PORPHYRAZINE – PORPHYRIN)

Belviso C.*[1], Belviso S.[2], Cavalcante C.[1], Lettino A.[1] & Ragone P.[1]
[1] Istituto di Metodologie per l'Analisi Ambientale, Consiglio Nazionale delle Ricerche, Tito Scalo (PZ), Italy
[2] Dipartimento di Scienze, Università della Basilicata, Potenza, Italy
Corresponding email: claudia.belviso@imaa.cnr.it

Keywords: fly ash, zeolite-encapsulated tetrapyrrole; metallo-porphyrazine/porphyrine

Zeolites are tectosilicates characterised by a three-dimensional network of tetrahedral units that form a system of interconnected pores. Due to their structure and their excellent ion exchange and sorption properties, zeolites are notably useful in a number of applications ranging from environment to enzymatic model and catalysis.

Porphyrins and porphyrazines are organic compounds widely used for different application such as sensors, phototherapeutics, catalysis, optics and photosensitizers due to their photo-physical and electrochemical properties. The adsorption of porphyrins and metallo-porphyrins onto zeolite is quite well documented as well as the influence of these organic compounds on the chemical, electronic and optical properties of guest component. The process of phthalocyanines entrapped within the supercages of zeolite is also discussed in literature. However, a very few papers display the direct synthesis of zeolite-encapsulated tetrapyrrole.

Fly ash is a by-product of thermal power plants partially used in concrete and cement manufacturing. The huge production of fly ash is extremely worrying because of its large disposal in landfill and several investigations have been carried out in order to try to exploit it. In the last few years, much research has been focused on its use for zeolite synthesis (Belviso et al., 2010).

In this study, the synthesis of zeolite around porphyrazine (H_2[OASPz]-Zeo), Cu- porphyrazine (Cu[OASPz]-Zeo) and Cu- porphyrine (P-Zeo) using fly ash as raw material was performed. Zeolite-included tetrapyrroles were characterized by XRD, SEM, TG/DTA, FT-IR and UV-vis.

The results indicate that new composite materials characterized by both zeolite and organic compound formed by hydrothermal method at low incubation temperature (45°C and 60°C) according to the mechanism of "ship-in-a-bottle complexes" (Balkus et al., 1994; Bedioui, 1995). In detail, huge amount of A-type zeolite, and sodalite form in H_2[OASPz]-Zeo sample whereas the main presence of sodalite characterizes both Cu[OASPz]-Zeo and P-Zeo materials.

Due to the electrochemical properties, the final products can be used for new catalyst development.

Balkus, K.J. Jr, Gabrielov, A.G., Bell, S.L., Bedioui, F., Roué, L., Devynck, J. (1994): Zeolite encapsulated cobalt(II) and copper(II) perfluorophthalocyanines. Synthesis and characterization. *Inorg. Chem.*, **34**, 67-72.

Bedioui, F. (1995): Zeolite-encapsulated and clay-intercalated metal porphyrin, phthalocyanine and Schiff-base complexes as models for biomimetic oxidation catalysts: an overview. *Coordin. Chem. Rev.*, **144**, 36-68.

Belviso, C., Cavalcante, F., Fiore, S. (2010): Synthesis of zeolite from Italian coal fly ash: Differences in crystallization temperature using seawater instead of distilled water. *Waste Manag.*, **30**, 839-847.

NEW INSIGHTS ON THE RESPONSE TO HEATING OF METAVARISCITE: AN I*N SITU* SYNCHROTRON POWDER DIFFRACTION STUDY

Berton D.[1], Cruciani G.*[1], Rodeghero E.[1] & Martucci A.[1]
[1] Dipartimento di Fisica e Scienze della Terra, Università di Ferrara, Italy
Corresponding email: cru@unife.it

Keywords: aluminophosphate, metavariscite, *in situ* synchrotron powder diffraction

One of the most remarkable properties of zeolites and zeolite-like aluminophospate materials is their thermal behaviour (i.e., stability, phase transformations, rate, temperature and number of dehydration/ rehydration cycles) which is of crucial importance in the wide industrial applications of these materials (e.g. adsorbers, catalysts, molecular sieves). A number of factors contribute to the macroscopically observable thermal effects such as evolution of H_2O and encapsulated organic species, variation in unit-cell volume and structural breakdown or modification (Cruciani, 2006; Alberti & Martucci, 2011). These effects, which modify the pore and channel geometry, affect the adsorption and diffusion of molecules in zeolites and microporous $AlPO_4$ frameworks, and consequently the adsorption, molecular sieving and catalytic properties of these materials. However, for many zeolite-type materials, detailed and accurate information on their response to heating is still missing and sometimes, even when available, controversial or unreliable. The present investigation strikes to give an exhaustive picture of the structural modifications upon removal of water in metavariscite ($AlPO_4 \cdot 2H_2O$), by means of an *in situ* temperature-resolved powder diffraction study using synchrotron radiation. This Al-phosphate commonly occurs as a weathering product of phosphatic rocks as well as concretions due to phosphatization of kaolin during weathering. It bears a great importance for soil science, since its formation strongly reduces the effectiveness of phosphate fertilizers. The metavariscite structure consists of a three-dimensional framework in which the tetrahedral units link to one another by shared corner-oxygen atoms, and their formulae are designated as T(1)T(2)O4, where T(1) represents the trivalent atom and T(2) is P. We have performed time-resolved dehydration experiments on metavariscite powders at the ID22 beamline (ESRF, Grenoble), using a fixed X-ray wavelength of 0.400031(1) Å. X-ray diffraction patterns were recorded in the 0.5-19.5 2θ range and the crystal structure evolution was continuously monitored through 30 Rietveld structure refinements from 30 to 800°C. TG/DTA curves on a fraction of the same sample contained in an open alumina crucible were measured in air using a Netzsch STA 409 simultaneous TG/DTA thermoanalyser. Temperature range and heating rate were from room temperature (RT) to 900°C and 10°/min, respectively.

The results of the above studies indicate that: (i) from room temperature to 150°C metavariscite (monoclinic dimorph of $AlPO_4 \cdot 2H_2O$) appears as the main phase, (ii) in the range of 170-250°C metavariscite starts to disappear giving rise to α-berlinite (trigonal form of $AlPO_4$) that is the stable phase up to about 610°C, and (iii) above the latter temperature the structure adopts the more stable configuration of the tetragonal β-berlinite polymorph. The occurrence of a transient metastable phase has been also detected.

Alberti, A. & Martucci, A. (2011): Reconstructive phase transitions in microporous materials: Rules and factors affecting them. *Microp. Mesop. Mater*., **141**, 192-198.

Cruciani, G. (2006): Zeolites upon heating: Factors governing their thermal stability and structural changes. *J. Phys. Chem. Solids*, **67**, 1973-1994.

PHILLIPSITE AT HIGH PRESSURE: A SINGLE-CRYSTAL X-RAY SYNCHROTRON DIFFRACTION STUDY

Comboni D.*[1], Gatta G.D.[1], Lotti P.[2], Merlini M.[1] & Liermann H.-P.[3]
[1] Dipartimento di Scienze della Terra "A. Desio", Università di Milano, Italy
[2] Elettra Sincrotrone Trieste, Italy
[3] Deutsches Elektronen-Synchrotron, Photon Science, Petra III Hamburg, Germany
Corresponding email: davide.comboni@unimi.it

Keywords: phillipsite, high pressure, compressibility

Phillipsite is a low Si/Al natural zeolite, often found as autogenic mineral in both "close" and "open" hydrologic system or in vugs of basalt, as an alteration product of volcanic glass. Along with laumontite, it is one of the most common zeolites found in oceanic basalts. In order to investigate the high-pressure behavior of phillipsite and its structural evolution at the atomic scale, we performed an *in situ* single-crystal synchrotron X-ray diffraction experiment up to 10 GPa with a diamond anvil cell, using a nominally penetrating pressure-transmitting fluid (methanol:ethanol:H_2O = 16:3:1 mix) (Gatta, 2010). The unit-cell parameters and the structure refinements within the *P*-range investigated show that: 1) phillipsite does not adsorb further H_2O molecules from the penetrating-transmitting fluid within the *P*-range investigated; 2) the configuration of the extra-framework population changes with pressure (between 2 and 3 GPa), affecting the elastic behavior of the mineral. More in details, two distinct compressional regimes have been observed, in which the bulk moduli differs drastically (i.e., K_V = 89(8) GPa between 0 and 2 GPa, K_V = 18.8(7) GPa between 3 and 9 GPa); 3) phillipsite is crystalline at least up to 10 GPa, and this is surprising if we consider its microporous nature; 4) all the *P*-induced effects are completely reversible in decompression. The structural refinements allowed us to describe the mechanisms, at the atomic scale, that govern its elastic behavior, which are mainly governed by inter-tetrahedral tilting. The relatively low compressibility of phillipsite at room-*P* and its relatively wide *P*-stability shown in this experiment suggests that this zeolite is a potential H_2O carrier during the first phase of the oceanic crust subduction or, toward the industrial front, its potential use in systems for the mechanical energy storage/dissipation (Eroshenko et al., 2001; Soulard et al., 2004).

Acknowledgements: The author acknowledges the Italian Ministry of Education, MIUR-Project: "Futuro in Ricerca 2012 - ImPACT- RBFR12CLQD".

Eroshenko, V., Regis, R.C., Soulard, M., Patarin, J. (2001): Energetics: A new field of applications for hydrophobic zeolites. *J. Chem. Soc.*, **123**, 8129-8130.

Gatta, G.D. (2010): Extreme deformation mechanisms in open-framework silicates at high-pressure: Evidence of anomalous inter-tetrahedral angles. *Microp. Mesop. Mater.*, **128**, 78-84.

Gatta, G.D., Cappelletti, P., Rotiroti, N., Slebodnick, C., Rinaldi, R. (2009): New insights into the crystal structure and crystal chemistry of the zeolite phillipsite. *Am. Mineral.*, **94**, 190-199.

Soulard, M., Patarin, J., Eroshenko, V., Regis, R. (2004): Molecular spring or bumper: A new application for hydrophobic zeolitic materials. *Studies Surf. Sci. Catal.*, **154**, 1830-1837.

STUDY OF NATURAL AND SYNTHETIC WOODWARDITE AS POTENTIAL REEs RECOVERY

Consani S.*[1], Giuli G.[2], Balić-Žunić T.[3], Carbone C.[1], Trapananti A.[4], Cardinale A.[5], Salviulo G.[6] & Lucchetti G.[1]

[1] Dipartimento di Scienze della Terra, dell'Ambiente e della Vita, Università di Genova, Italy
[2] Scuola di Scienze e Tecnologie - Sezione di Geologia, Università di Camerino, Italy
[3] Natural History Museum, University of Copenhagen, Denmark
[4] Istituto Officina Dei Materiali, Consiglio Nazionale delle Ricerche, Perugia, Italy
[5] Dipartimento di Chimica e Chimica Industriale, Università di Genova, Italy
[6] Dipartimento di Geoscienze, Università di Padova, Italy
Corresponding email: sirio.consani@edu.unige.it

Keywords: woodwardite, REEs recovery, XAS

Secondary minerals in mining impacted areas are crucial for the dispersion of elements of environmental concern in the surrounding ecosystems, and their disposal is a issue of great interest (Macías et al., 2012). Many efforts by the researchers were devoted to develop strategies for the recovery of elements of economic interest from secondary minerals (Guezennec et al., 2015). In the neutral mine drainage (*p*H ≈ 7) of Cu mines, the most common secondary phase is woodwardite, $(Cu_{1-x}Al_x)(OH)_2(SO_4)_{x/2}\cdot nH_2O$, a Layered Double Hydroxide with brucite-type layers and sulphate in the interlayer. In the abandoned Libiola Cu mine, woodwardite-rich precipitates (formed at 6.6-1 of Y and 200 mg kg^{-1} of Ce and Nd), making this mineral a potential source of these elements. In order to develop an easy and economic process of recovering REEs from woodwardite, the role of REEs in the crystal structure has to be understood. Trivalent REEs could be incorporated in the crystal structure of woodwardite substituting Al or Cu or could be incorporated as oxyanion inside the interlayer, making REEs easier to be recovered. The aims of this work were to a) characterise the natural samples; b) synthesise woodwardite crystals and c) dope the synthetic woodwardite with Y, La, and Ce to understand their role inside this phase.

The synthesis of woodwardite and of Y, Ce^{3+}, and La doped woodwardite was performed modifying the method of Reichle (1986) that gave as a result nanoscopic woodwardite crystals with a mean size of 4,8 nm. In order to study the effect of pH, the experiment was repeated at *p*H value of 8.1 and 10.1. La was not incorporated in the mineral structure as judged from coprecipitated phases. The cell parameters and the XANES and EXAFS data of natural of Y and Ce synthetic samples (Y *K*-edge and Ce L_3-edge collected at the LISA beamline, ESRF) were used to characterise the role of REEs in woodwardite. The optimal *p*H for the incorporation of REEs has proven to be 8.1, as at higher *p*H a partial oxidation to Ce^{4+} led to the precipitation of CeO_2, thus preventing Ce to be incorporated in woodwardite. The results showed that woodwardite-rich precipitates are promising for REEs recovery, and further study will be done to evaluate the possibility to use woodwardite to recover REEs from other industrial wastes.

Guezennec, A., Bru, K., Jacob, J., d'Hugues, P. (2015): Co-processing of sulfidic mining wastes and metal-rich post-consumer wastes by biohydrometallurgy. *Miner. Eng.*, **75**, 45-53.

Macías, F., Caraballo, M.A., Nieto, J.M. (2012): Environmental assessment and management of metal-rich wastes generated in acid mine drainage passive remediation systems. *J. Hazard. Mater.*, **229-230**, 107-114.

Reichle, W. (1986): Synthesis of anionic clay minerals (mixed metals hydroxides, hydrotalcite). *Solid St. Ionics*, **22**, 135-141.

GUEST GASES AND PHASE TRANSITIONS IN MELANOPHLOGITE (TYPE I CLATHRATE)

D'Alessio D.*[1], Tribaudino M.[1], Mezzadri F.[2], Milanese C.[3], Mantovani L.[1], Pontiroli D.[1] & Riccò M.[1]

[1] Dipartimento di Fisica e Scienze della Terra "Macedonio Melloni", Università di Parma, Italy

[2] Dipartimento di Chimica, Università di Parma, Italy

[3] Laboratorio Idrogeno, Dipartimento di Chimica - Sezione di Chimica Fisica, Università di Pavia, Italy

Corresponding email: daniela.dalessio@studenti.unipr.it

Keywords: melanophlogite, phase transitions, X–ray diffraction

Melanophlogite (MEP) is a tectosilicate, belonging to clathrate group. Clathrates are zeolite–like materials with microporous framework, made up of corner–sharing [SiO_4] tetrahedra, which form pentagonododecahedral [5^{12}] and tetrakaidecahedral [$5^{12}6^2$] isolated cages. Guest gases fill the voids and can act as templates for mineral crystallization (Gunawardane et al., 1987). MEP, potentially interesting for gas storage, occurs in a few sites in the world and each of them has peculiar guest gases.

In this work, we report the preliminary results of a multi–analytical study (DSC and TGA, Raman spectroscopy, SCXRD and XRPD) of MEP from Fortullino (Livorno), Racalmuto (Agrigento) and Varano Marchesi (Parma).

Fortullino MEP includes only CO_2 in structural cages. It is microcrystalline and pseudomorphic in opal. XRPD analyses, carried out between 90 and 500 K, revealed two phase transitions: one from a high temperature cubic to a low temperature orthorhombic (very close to tetragonal) symmetry at 350 K and another to a monoclinic one at 150 K. Throughout phase transitions, most remarkable changes are observed for *b* cell axis, whereas *a* and*c* cell axes retain similar values. High temperature phase transition is hardly constrained, since it happens together with a fast CO_2 loss, which influences cell parameters. TG analyses are conducted on Fortullino MEP between 300 and 1373 K to understand release mechanisms of guest CO_2 and preliminary results have shown a continuous CO_2 loss up to 1273 K, which matches that calculated assuming a complete CO_2 desorption. CO_2 escapes at higher rates between 298 and 500 K and between 700 and 800 K, suggesting different degassing kinetics during heating.

Varano Marchesi MEP, mainly containing CH_4 in structural voids, exhibits cubic shaped crystals, often growing on opal seeds and transformed in pseudomorphic quartz. Analyses of intensity statistics and refined cell parameters from SCXRD measurements, performed between 140 and 300 K, did not identify any phase transition.

The ordering pattern of the guest gases at low temperature could play a crucial factor on mineral structural stability: CO_2 is a linear molecule and its positioning may promote anisotropic configurations; on the contrary, CH_4has an isotropic molecular arrangement and ordering is not likely to promote symmetry breaking, which comes about due to framework deformation (Tribaudino et al., 2010; Gatta et al., 2014). It appears phase transitions occur due to ordering process of the guest gases within a little modified framework.

Attempts to synthesize MEP are still in progress, employing methylamine as guest gases source, tetraethyl orthosilicate as crosslinking agent and water as medium (Gunawardane et al., 1987).

Gatta, G.D., Bersani, D., Lottici, P.P., Tribaudino, M. (2014): High–pressure Raman study of CH_4 in melanophlogite (type I clathrate). *Mineral. Mag.*, **78**, 1661-1669.

Gunawardane, R.P., Gies, H., Liebau, F. (1987): The effect of "help gases" on the formation and stability of clathrasils. *Z. Anorg. Allg. Chem.*, **546**, 189-198.

Tribaudino, M., Gatta, G.D., Lee, Y. (2010): A high–pressure cubic-to-tetragonal phase-transition in melanophlogite, a SiO_2 clathrate phase. *Microp. Mesop. Mater.*, **129**, 267-273.

ZEOLITES FOR SUSTAINABLE AGRICOLTURE: FURFURAL ENCAPSULATION AND CONTROLLED RELEASE IN ZSM-5

Digiacomo F.*[1], Braschi I.[2], Rodeghero E.[1], Blasioli S.[2] & Martucci A.[1]
[1] Dipartimento di Fisica e Scienze della Terra, Università di Ferrara, Italy
[2] Dipartimento di Scienze Agrarie, Università di Bologna, Italy
Corresponding email: flavia.digiacomo@student.unife.it

Keywords: nematicide, furfural, sustainable agricultural

Widespread application of synthetic nematicide on the crops aimed to fight nematode parasite could be a threat to human health and overall environmental quality. Most of synthetic nematicides have been withdrawn from the market, due to their toxicity. This had led to looking for a non-chemical alternative which must be equally effective and eco-friendly, derived from natural materials, aiming to reduce synthetic pesticide input. Recently, it has been proved that an aldehyde, namely furfural, is effective against *Meloidogyne sp.* (a dangerous specie of nematode) (Ntalli et al., 2010). This latter biomolecule can be easily extracted from Melia azedarach fruits, a tree growing in tropical and subtropical areas.

This work is part of a wider multidisciplinary project, which aims to develop an innovative, easy to produce, and eco-sustainable nematicidal formulate by combining a botanical extract of known nematicidal activity with environmentally friendly porous materials. Specifically, an aldehyde - namely, furfural and salicylaldehyde, which is known for its occurrence in Melia azedarach (MA) tree and mainly responsible for the plant defense ability against nematodes - wase encapsulated into microporous alumina-silicate matrices (zeolites) to obtain a nematicidal formulate with a controlled release of the bioactive aldehyde. From a structural point of view, the project is focused on the study of interactions that take place between the guest nematicidal molecule and the host zeolite carrier in order to elucidate, at an atomistic level, the mechanisms that control the adsorption (encapsulation) and desorption (controlled release) properties. The first part of the project was addressed to define the zeolite with the highest encapsulation capacity and that was capable to prolong the bioactivity of the embedded products (encapsulated aldehyde). With this purpose, several zeolites (zeolite Y, mordenite, ferrierite, beta and ZSM-5) with different silica/alumina ratio (from ~ 10 up to 500), pore architecture and type/position of adsorbing sites were tested. In this study the furfural encapsulation into microporous alumina-silicate ZSM-5 (SiO_2/Al_2O_3 = 500) zeolite will be discussed. Furfural was encapsulated into zeolite via adsorption from water and adsorption equilibrium was monitored by adsorption kinetics. Adsorption isotherms were determined in order to define the affinity and maximal adsorption capacity and selectivity of tested zeolite for the selected nematicide. The monitoring was done by liquid chromatographic analysis (HPLC) of equilibrium solutions performed via Jasco 880-PU Intelligent and thermogravimetric analysis (25-900°C, heating rate 10°C/min) of loaded zeolite samples. Electronic nose data were collected on AIRSENSE PEN3. After adsorption, the zeolite samples were structurally characterized with X-ray diffraction (XRD) technique (Bruker D8 Advance diffractometer equipped with SOL-X detector) - coupled with Rietveld refinements of the diffraction patterns. Structural analysis was used to prove the embedding of the aldehydes inside the zeolite pores and to define the interaction distance between the porous framework and each molecule. This combined diffractometric, chromatographic and thermogravimetric study allowed us to: 1) evaluate the maximum adsorption capacity of hydrophobic zeolite against furfural molecules ; 2) localise the biomolecules in the zeolite channel system; 3) probe the interaction between the adsorbate and the zeolite framework; 4) evaluate the release kinetics of the encapsulated molecules in gas phase.

Our results highlighted that ZSM-5 can be useful tool for nematode pest management, and may help improving environmental protection while minimizing risk to overall health.

Ntalli, N.G., Cottiglia, F, Bueno, C.A., Alché, L.E., Leonti, M., Vargiu, S., Bifulco, E., Menkissoglu-Spiroudi, U., Caboni, P. (2010): Cytotoxic tirucullane triterpenoids from Melia azedarach fruits. *Molecules*, **15**, 5866-5877.

MODIFIED CLAYS AS ADSORBENT IN FILTER SYSTEM FOR MEDIUM OR SMALL SCALE WATER DEPURATION

Durán E.*[1], Bueno S.[2], Cornejo J.[1], Gamiz B.[1] & Hermosín M.C.[1]

[1] Instituto de Recursos Naturales y Agrobiología de Sevilla, Consejo Superior de Investigaciones Científicas, Sevilla, Spain

[2] Centro Tecnológico Innovarcilla, Bailén, Spain

Corresponding email: esperanza.duran@irnas.csic.es

Keywords: contamination, pelletization, pesticides

The pesticide contamination of water is increasing as a result of intensive farming (Hermosin et al., 2013) and it makes necessary to develop low-cost systems for water purification, as to be used at farm houses and small agroindustries. Clays are good adsorbents for pesticides. Due to their small size, expansive properties reactive surfaces and modification or "tunning" ability (Hermosin & Cornejo, 1992; Socias-Viciana et al., 1998; Cruz-Guzmán et al., 2005; Gámiz et al., 2015) and thus they have been proposed for water treatment (Beall 2003). In this work we assay and propose clays as adsorbent component in a filter to remove pesticides from water.

The modified clays were prepared from a low value clay (CTI, smectite content, 30%) located in Bailén (Jaen, Spain) by saturation with Fe^{3+} (CTI-FE) and hexadecyltrimethyllammonium (CTI-HDTMA). A commercial organo-clay, Cloisite 10A (Clo, from BKG) was also used for comparison. The pesticides tested were those used in olive crops, as terbuthylazine, tebuconazole and MCPA (Hermosin et al., 2013). The clays were granulated to pellets with carnauba wax (car) as binder through a ram extruder. Powder clay and car were mixed (30% wt car) at 90ºC. Anthracite (Antra 170, AstralPool) was mixed at rate of 40% with the clay pellets as filtering bed in the tank with artificially contaminated water, Antracite helps to avoid clay swelling and to increase the bed porosity and improve the conditions of the water flow. Experiment set-up has a minimum flow of 30 ml/min to obtain pressures of 1 bar. The adsorption tests were carried out using a solution containing the three pesticides at initial concentration of 1 ppm in 40 liters of water. The adsorption kinetics was measured at selected times (15 min, 30 min, 1 h, 2 h, 4 h, 6 h, 8 h, 24 h).

This work reveals that the pelletization process did not affect significantly the pesticide sorption capacity of clays (37-96%) and the pellets were not altered in terms of size showing an excellent water resistance at the end of the experiment. We obtained a high adsorption of the three pesticides tested for the cases of the commercial clay (Clo10) and for CTI-HDTMA, removing from 40-100% of pesticide from water after 24 h of treatment in the filter system. In contrast, the CTI-Fe sample did not perform as a good adsorbent, removing only between 15-42% of the herbicides from water after 24 h of treatment in the filter. CTI-HDTMA reveals as a very promising adsorbent derived from a low cost material to be used in filter systems for removing pesticides from contaminated waters. Hence the development of a small company devoted to the processing of low value clay sample would have to be considered.

Acknowledgments: Projects P11-AGR-7400, RECUPERA 2020, AGL2014-51897-R and Research Group AGR-264 all cofinanced with EU FEDER/FSE Program 2013-19.

Beall, G.W. (2003): The use of organo-clays in water treatment. *Appl. Clay Sci.*, **24**, 11-20.

Cruz-Gúzman, M., Celis, R., Hermosín, M.C., Koskinen, W.C., Cornejo, J. (2005): Adsorption of pesticides from water by functionalized organobentonites. *J. Agr. Food Chem.*, **53**, 7502-7511.

Gámiz, B., Hermosín, M.C., Cornejo, J. (2015): Hexadimethrine-montmorillonite nanocompo-site: Characterization and application as a pesticide adsorbent. *Appl. Surf. Sci*., **332**, 606-613.

Hermosín, M.C. & Cornejo, J. (1992): Removing 2.4-D from water by organo-clays. *Chemosphere*, **24**, 1493-1503.

Hermosín, M.C., Calderón, M.J., Real, M., Cornejo, J. (2013): Impact of herbicides used in olive groves on waters of the Guadalquivir river basin (southern Spain). *Agr. Ecosyst. Environ*., **164**, 229-243.

Socías Viciana, M.M., Hermosín, M.C., Cornejo, J. (1998): Removing prometrone from water by clays and organic clays. *Chemosphere*, **37**, 283-300.

CENOZOIC CLIMATE CHANGES IN THE RUSSIAN EASTERN ARCTIC (KOTEL'NY ISLAND, NEW SIBERIAN ISLANDS ARCHIPELAGO): EVIDENCE FROM PALENOLOGICAL AND CLAY ASSEMBLAGE DATA

Ershova V.B.*[1], Vereshchagin O.S.[1], Prokopiev A.V.[2] & Alexandrova G.N.[3]
[1] Department of Regional Geology, Institute of the Earth Sciences, Saint Petersburg State University, Russia
[2] Diamond and Precious Metal Geology Institute, Siberian Branch of the Russian Academy of Sciences, Yakutsk, Russia
[3] Geological Institute, Russian Academy of Sciences, Moscow, Russia
Corresponding email: ershovavictoria@gmail.com

Keywords: Arctic, climate, clay minerals

The sedimentary basin of the Laptev Sea is a promising hydrocarbon resource base. No deep wells have been drilled offshore on the Laptev Sea in, hence geological studies here are limited to the islands which are represent localized snapshots of the sedimentary successions which give an only information to prediction offshore sedimentary succession (Franke & Hinz, 2009). This work is dedicated to estimation of Cenozoic climatic changes in the Eastern Arctic based on the complex study of the Cenozoic sediments of Kotelny Island (New Siberian Islands).

We have studied the 5 outcrops, located in the northwestern part of the island, 15 samples of which were studied. Pollen studies conducted in the Paleofloristics laboratory GIN RAS according to standard procedures. The study of clay minerals was carried out in the "X-ray diffraction studies" Resource Centre of St. Petersburg State University.

According to palynological data in the Early Eocene sedimentation took place in warm and humid climate, close to subtropical, and the presence of dinoflagellate cysts pointing on shallow marine to brackish water lagoon environments at that time across the sturdy area. For early Pliocene coniferous and small-leaved forests vegetation is reconstructed. Pleistocene palynocomplex indicates the distribution of tundra vegetation, which existed in a relatively warm subarctic climate.

X-ray studies of the clay fraction of Cenozoic sediments formed in different climatic conditions in the period from the early Eocene to the Pleistocene showed a gradual decline in the proportion of kaolinite and increase of chlorite and minerals of the smectite group due to cooling and transition from subtropical (100% kaolinite) to moderate (~ 70% kaolinite, ~ 30% chlorite) and further to the subarctic (~ 50-60% kaolinite, ~ 20-40% chlorite, ~ 10-30% smectite) climate.

Studies have shown a good correlation between the two paleoclimatic indicators - the mineralogical composition of the clay fraction and palynological complexes. Changes in the composition of clay minerals and palynocomplex from the Eocene to the Pleistocene indicates a gradual climate change from subtropical to subarctic in the study region. Thus, it is shown that within the study region there was a significant influence of paleoclimate on the composition of clay minerals in weathering crusts and the products of their redeposition.

Acknowledgements: This work was supported by RFBR grant 15-35-2059.

Franke, D. & Hinz, K. (2009): Geology of the Shelves surrounding the New Siberian Islands, Russian Arctic. *Stephan Mueller Spec. Publ. Ser.*, **4**, 35-44.

EXPLOITING CLINOPTILOLITE AGAINST *HELICOBACTER PYLORI*: POSSIBILITY OR UTOPIA?

Farina M.[1], Cerri G.*[1], Brundu A.[1], Juliano C.[2], Giunchedi P.[2], Rassu G.[2], Bonferoni M.C.[3] & Gavini E.[2]
[1] Dipartimento di Scienze della Natura e del Territorio, Università di Sassari, Italy
[2] Dipartimento di Chimica e Farmacia, Università di Sassari, Italy
[3] Dipartimento di Scienze del Farmaco, Università di Pavia, Italy
Corresponding email: gcerri@uniss.it

Keywords: Helicobacter pylori, cation exchange capacity, zeolite

Helicobacter pylori is a bacterium present in the stomach of about half of the world's population. Infection with *H. pylori* causes 95% of duodenal ulcers and 70% of gastric ones (Stewart & Ackroyd, 2011). Urease, a surface protein component of *H. pylori*, enables ammonia production from the urea of the host. This process is important for the survival of the bacterium in the stomach, because NH_3 is protonated in NH_4^+, which results in a local raise of *p*H (Stewart & Ackroyd, 2011). Clinoptilolite is a natural zeolite that combines cation exchange capacity, high selectivity toward ammonium ion and good stability in acid media, and is having a growing interest in studies for biomedical applications (Milić et al., 2014). A clinoptilolite-based material, specifically prepared for the development of pharmaceuticals (Cerri et al., 2016), has been used to study if this zeolite, due to the properties above reported, is able to develop an antagonistic activity against *H. pylori* growth and infection.

In-vitro tests, performed with a reference strain of *H. pylori* (ATCC®43504™), have shown that clinoptilolite prepared in sodium form is able to inhibit bacterial growth (Minimum Inhibitory Concentration = 0.5 mg/ml); conversely, the same material, but in ammonium form used as control, has not determined effect on *H. pylori* growth up to the highest concentration used (15 mg/ml), meaning that inducing NH_4^+ decrease in the micro-environment of the bacterium can be a good strategy in supporting the fight against *H. pylori*. On the other hand, a set of tests, carried out with solutions of NaCl and in absence of zeolite, have shown that the bacteria also replicate in presence of high Na^+ concentration. These results demonstrate that the bacterial growth has been inhibited by the ability of Na-clinoptilolite to subtract ammonium ions by cation exchange.

A set of experiments have been carried out to evaluate if Na-clinoptilolite is able to develop a synergistic action with amoxicillin, an antibiotic currently used in the eradication therapy of *H. pylori*. Tests have been performed by comparing the extent of inhibition halos observed in plates containing i) amoxicillin ii) amoxicillin and Na-clinoptilolite. Zeolite concentrations of 0.125 and 0.250 mg/ml have determined an increase in the diameter of inhibition halos of, respectively, 24±3 and 73±1% compared with the drug alone, demonstrating the existence of a synergy between amoxicillin and Na-clinoptilolite in the inhibition of *H. pylori* growth.

The stability at 20°C of a formulation [⅓ amoxicillin + ⅔ Na-clinoptilolite] has been studied on three samples stored at 20, 50 and 80% of relative humidity, and compared with that of pure amoxicillin kept at the same conditions. After 18 months, the degradation of the antibiotic has been always < 4%, regardless of zeolite presence, demonstrating that clinoptilolite does not affect amoxicillin stability.

Acknowledgements: Research supported by MIUR PRIN 2010MKHT9B_008 granted to G. Cerri.

Cerri, G., Farina, M., Brundu, A., Daković, A., Giunchedi, P., Gavini, E., Rassu, G. (2016): Natural zeolites for pharmaceutical formulations: Preparation and evaluation of a clinoptilolite-based material. *Microp. Mesop. Mater.*, **223**, 58-67.

Milić, J., Daković, A., Krajišnik, D., Rottinghaus, G.E. (2014): Modified Natural Zeolites - Functional Characterization and Biomedical Application. *in* "Advanced healthcare materials", A. Tiwari, ed., Wiley., Hoboken, 361-403.

Stewart, D.J. & Ackroyd, R. (2011): Peptic ulcers and their complications. *Surgery*, **29**, 568-574.

STRUCTURAL CHARACTERIZATION OF INJECTION MOLDED SEPIOLITE/POLYAMIDE6,6 NANOCOMPOSITES BY MEANS OF STATIC AND DYNAMIC THERMAL METHODS

Fernandez-Barranco C.[1-2], Koziol A.E.[3], Drewniak M.[3] & Yebra-Rodriguez A.*[1-2]
[1] Departamento de Geología, Universidad de Jaén, Spain
[2] Centro de Estudios Avanzados en Ciencias de la Tierra, Universidad de Jaén, Spain
[3] Department of Crystallography, Faculty of Chemistry, Maria Curie-Sklodowska University, Lublin, Poland
Corresponding email: ayebra@ujaen.es

Keywords: sepiolite, nanocomposites, thermal ageing

Clay/polymer nanocomposites (CPN) are suitable industrial materials since the hybrid shows improved technical characteristics with respect to the counterpart (Okada & Usuki, 2006). Polyamide6,6 (PA66) is one of the most widely thermoplastic polymers used as matrix in CPN. The so-called α structure (triclinic) is the most common polymorph of PA66, which undergo into the γ structure (pseudohexagonal) in a solid-to-solid transition when exposed to high temperatures. In recent years, the fibrous clay sepiolite has been used as reinforcing agent in polymer matrix as it enhances thermal properties of the CPN without modification in the hydrogen bonds between PA66 chains. In this work we provide information about the structural changes occurring in the neat polyamide and the nanocomposite before and after the degradation process through a thermo-dynamic study combined with X-Ray diffraction methods. For that purpose CPN pellets were obtained and injected as described elsewhere (Fernández-Barranco et al., 2015). The thermal ageing on static conditions was carried out at 110 and 150°C as described in Yebra-Rodríguez et al. (2014). The powder diffraction data were collected on an X-ray Empyrean diffractometer with the PIXcel-3D detector (PANalytical, The Netherlands), using Cu*K*α radiation, 40 kV and 35 mA, in a 2θ range between 3-35° 2θ. The temperature of the sample was controlled in a XRK 900 reactor chamber (Anton Paar). The starting and aged samples of pure PA66 and sepiolite/PA66 CPN (sep/PA66) were heated dynamically in the range 30-230°C. The diffraction patterns of the samples after cooling were also collected. The PA66...sepiolite contact promotes the occurrence of the C-H...O hydrogen bonds. In injection molded sep/PA66 nanocomposites the clay fibres locate between the polymer lamellae in a sloping suitable position, without involving large distortions in the lattice of PA66.

Acknowledgements: This research was supported by Research Grants 2014/00113/001 (CEACTierra, University of Jaen, Spain) and IEG-0617-0120-35 (Instituto de Estudios Giennenses, Jaen, Spain) and Research Group RNM-325 (CICE, Junta de Andalucia, Spain).

Fernández-Barranco, C., Yebra-Rodríguez, A., La Rubia-García, M.D., Navas-Martos, F.J., Álvarez-Lloret, P. (2015): Mechanical and crystallographic properties of injection-molded polyamide 66 / sepiolite nanocomposites with different clay loading. *Polym. Composite*, **36**, 2326-2333.

Okada, A. & Usuki, A. (2006): Twenty years of polymer-clay nanocomposites. *Macromol. Mater. Eng.*, **291**, 1449-1476.

Yebra-Rodríguez, A., Fernández-Barranco, C., La Rubia, M.D., Yebra A., Rodríguez-Navarro, A.B., Jiménez-Millán, J. (2014): Thermooxidative degradation of injection-moulded sepiolite / polyamide 66 nanocomposites, *Mineral. Mag.*, **78**, 1227-1239.

NEW INSIGHTS ON THE EFFECTS OF DIFFERENT ZEOLITE AMENDMENTS ON PLANTS C-N ISOTOPIC COMPOSITION

Ferretti G.*[1], Natali C.[1], Faccini B.[1], Di Giuseppe D.[1], Bianchini G.[1] & Coltorti M.[1]
[1] Dipartimento di Fisica e Scienze della Terra, Università di Ferrara, Italy
Corresponding email: frrgcm@unife.it

Keywords: natural zeolites, NH_4-enriched zeolites, amendments

The application of inorganic amendments has been recognized as a valuable technique for increasing soil physic-chemical properties (Colombani et al., 2014). Among them, zeolites are known to be well suitable in a wide range of agricultural applications because of their high cation exchange capacity that allow a controlled retention/release of water and nutrients (e.g. NH_4^+) (Reháková et al., 2004).

The main aims of this study were to verify if natural zeolites amendments can increase the uptake of N from chemical fertilizers and if the N transfer from NH_4-enriched zeolites to plants really occurs. The elemental and isotopic composition of plants grown with no zeolite addition (UA) and plants grown on soils amended with natural (NZ) and NH_4-enriched zeolites (CZ) (the latter obtained after mixing with pig-slurry) were compared for two cultivation cycles. It is well known that plants $\delta^{15}N$ can reflect with a good approximation the $\delta^{15}N$ of the main N source in the soil, thus, plants grown under conventional farming (using chemical fertilizers) and plants grown under organic farming (using animal slurry) can be often easily discriminated (Choi et al., 2003).

The experimentation was carried out during 2014 (Maize) and 2015 (Wheat) cultivation cycles in the ZeoLIFE experimental field (Codigoro, Ferrara, Italy). Plants were sampled before the harvest, subdivided in stems and grains and analyzed by EA-IRMS in order to determine the $\delta^{15}N$ and $\delta^{13}C$.

Plants grown on NZ had significantly lower $\delta^{15}N$ with respect to UA plants. Considering that the employed chemical fertilizers have a slight negative $\delta^{15}N$, it is highly possible that natural zeolites have adsorbed part of NH_4^+ ions formed after chemical fertilizers hydrolysis allowing plants to uptake higher amounts of N from this specific source, resulting in a lower tissues $\delta^{15}N$.

On the other hand, both maize and wheat plants grown on CZ registered a significantly higher $\delta^{15}N$, approaching that of the pig slurry employed for enriching the zeolites, confirming that this material can constitute a N pool for plants at least for two cultivation cycles.

The distinct agricultural practices seem to be reflected in the plant physiology, as recorded by the carbon discrimination factor ($\Delta^{13}C$), which generally increases in plots amended with natural zeolites indicating better water/nutrient conditions.

Choi, W.J., Ro, H.M., Hobbie, E.A. (2003): Patterns of natural 15N in soils and plants from chemically and organically fertilized uplands. *Soil Biol. Biochem.*, **35**, 1493-1500.

Colombani, N., Mastrocicco, M., Di Giuseppe, D., Faccini, B., Coltorti, M. (2014): Variation of the hydraulic properties and solute transportmechanisms in a silty-clay soil amended with natural zeolites. *Catena*, **123**, 195-204.

Reháková, M., Čuvanová, S., Dzivák, M., Rimár, J., Gaval'ová, Z. (2004): Agricultural and agrochemical uses of natural zeolite of the clinoptilolite type. Curr. Opin. *Solid St. Mater. Sci.*, **8**, 397-404.

GEOCHEMISTRY AND BIOMARKER ANALYSIS OF THE BENTONITES FROM ESQUIVIAS (MADRID)

García-Rivas J.*[1-2], Torres T.[3], Ortiz J.E.[3], Sánchez-Palencia Y.[3], García-Romero E.[2-4] & Suárez M.[1]

[1] Departamento de Geología, Universidad de Salamanca, Spain

[2] Instituto de Geociencias, Universidad Complutense, Madrid & Consejo Superior de Investigaciones Científicas, Madrid, Spain

[3] Laboratorio de Estratigrafía Biomolecular, Universidad Politécnica de Madrid, Spain

[4] Departamento de Cristalografía y Mineralogía, Universidad Complutense, Madrid, Spain

Corresponding email: javiergr_89@hotmail.com

Keywords: bentonite, geochemistry, biomarker analysis

The Tagus basin, located in the central part of the Iberian Peninsula, presents one of the most important deposits of magnesic clays in the world, with sepiolite and bentonite (saponite) mining. Although it has been studied by several authors both from the sedimentological and mineralogical point of view, the genesis of the Mg-phyllosilicates has been not fully explained. This paper aims to deepen the knowledge of bentonites and, more specifically, pink clays and green clays.

In this work, we collected 31 samples from a quarry in the proximity of Esquivias (Toledo). These samples represent a vertical succession including lutitic levels containing mainly phyllosilicates (pink-clays and green-clays), carbonates and sands. They were characterized and semiquantified by using X-Ray Diffraction. Bulk geochemical analysis were performed by ICP-MS, obtaining major and trace elements (REE, TTE, HSFE, LILE and others). Organic analysis of n-alkanes and n-alkanoic acids were performed by GC-MS. SPSS was used for the statistical analysis.

The XRD treatment of the samples allowed us to catalogue them in 4 different groups: bentonitic, illitic, carbonatic and sandy levels. The bentonitic levels are identified at the outcrop as pink and green clays, both formed mainly by saponite. However, in green clays the presence of quartz and other phyllosilicates (illite and kaolinite) as impurities was higher than in pink clays in which, in addition, the saponite crystallinity was lower. The mineralogical composition of the four groups was compared with the geochemical data using bivariate correlations and multivariate clustering. We observed clear and logical correlations between the chemical composition and the mineralogy, allowing the separation of 3 groups of samples. We observed that the bentonitic samples were likely to have an authigenic origin; in contrast, illitic and sandy samples were more likely to have a detrital origin. Carbonates had different correlations than the previously mentioned samples. The preliminary data of the organic analysis showed some differences in the bentonitic levels, with episodes involving an input of terrestrial vegetation, alternating with others in which algae or a mixed input occurred.

In conclusion, the combination of XRD, geochemistry and biogeochemistry allowed a better differentiation of the sedimentary environments in which the materials were deposited.

INFLUENCE OF INTERLAMINAR Mg IN THE CLASSIFICATION OF SMECTITES

García-Romero E.*[1-2] & Suárez M.[3]
[1] Departamento de Geología, Universidad de Salamanca, Spain
[2] Department de Cristalografía y Mineralogía, Universidad Complutense, Madrid, Spain
[3] Instituto de Geociencias, Universidad Complutense, Consejo Superior de Investigaciones Científicas, Madrid, Spain
Corresponding email: mromero@ucm.es

Keywords: structural formula, exchangeable cations, smectites

As it is well known, the smectites are phyllosilicates whose layers have numerous isomorphic substitutions both in tetrahedral (mainly Si^{4+} replaced by Al^{3+}) and in octahedral positions which originates charge in the layers. The charge is compensated by solvated with water cations in the interlayer (Mg, Ca, K, Na, …). As their name said, the exchange cations are exchangeable by others hydrated cations depending on the medium conditions. Many times the Mg^{2+} is one or the most abundant exchangeable cation, especially when they are magnesic clays, but not only.

The Mg usually appears in most smectites, although it could be in minor quantities, and after a chemical analysis, when the structural formulae are fitted, it is generally allocated in the octahedral position. This can lead to errors since the Mg can be both in the octahedral position and in the interlayer as exchangeable cation. If the amount of exchangeable Mg is high, the mistakes fitting formulae are not trivial. When we fit Mg as octahedral cation, as the first option, we can put a part of the interlayer Mg as octahedral cation and, as a consequence, the fitted mineral will have lower layer charge than it actually has. To be sure which is the Mg correct position, that is to say the real amount of octahedral Mg, it is necessary working with homoionic samples in which the interlayer cations have been changed by other cation different to the Mg. If Mg is in the interlayer, the layer charge and the di/tri octahedral character in the structural formulae change when compare the formula fitted in natural state (with interlayer Mg) and after homoionization. The change can be so significant that affect to the smectite classification.

In this work the chemical composition of individual particles was obtained using analytical electron microscopy (AEM) with TEM, using a JEOL 3000 FX Field Emission Microscope (voltage of 300 kV) whit an OXFORD ISIS EDX spectrometer. The samples were homoinized with a KCl solution.

We show three examples of samples from different geological origins where the homoionization of the smectites lead very significant changes: i) sedimentary smectites that appear as very low charge stevensite, near to talcum, and *change* to saponite after their homoionization, ii) smectites which come from the alteration of basalts in which classification does not change too much after their homoionization, but the physic-chemical properties correlate only with the structural data of the homoionic samples, and iii) smectites derived from ultrabasic rocks.

The present work highlights the need for the samples homoionization as an inevitable routine to avoid mistakes, especially when crystal chemistry data are related to physic-chemistry and application properties.

INFLUENCE OF THE IMPURITIES AND STRUCTURE ON ELECTROMAGNETIC PROPERTIES OF NATURAL NANOSTRUCTURED CARBON MATERIALS

Golubev E.A.*[1]

[1] Laboratory of Structural Crystallography, Institute of Geology, Komi Scientific Center of the Russian Academy of Science, Syktyvkar, Russia

Corresponding email: yevgenygolubev74@mail.ru

Keywords: natural carbonaceous materials, electromagnetic properties, microscopy

Nanostructured carbonaceous materials with high conductivity similar to glassy carbon are interesting for application in electronics and shielding of electromagnetic radiation. Among such natural materials, a large amount of research was devoted to the carbon from shungite rocks from Karelia, Russia (Melezhik et al., 2004). Furthermore, many carbonaceous geomaterials have an interplanar distance in graphite-like domains, a chemical composition, and key physico-chemical properties like the shungites. Such materials differ from glassy carbon by the presence of various impurities (usually less than 5 at.%). This stimulates a detailed study of influence of impurities on the electrical properties of natural carbonaceous materials.

The samples were collected from large deposits of carbonaceous material in Karelia, Novaya Zemlya islands, Subpolar Ural, Kazakhstan, and Siberia. The local electrophysical properties were examined by scanning spreading resistance microscopy and electric force spectroscopy using an Integra Prima atomic force microscope (NT-MDT). Raman spectroscopy was carried out with a LabRam HR800 instrument (Horiba, Jobin Yvon). SEM Tescan Vega LMH with X-ray EDS was used to investigate the chemical composition. The nanostructure of some samples was examined in a FEI CM300UT FEG transmission electron microscope.

It was determined that for almost pure natural carbon materials, type of conductivity is essentially determined by the presence of impurity elements at the boundaries of the graphene layers and, to a lesser degree, by the nanostructured features (Golubev, 2013). Therefore for model of electrical conductivity of natural high-carbonized materials it should be consider the influence of impurity atoms, mainly hydrogen and heteroelements, which block a part of current paths at the boundaries of graphene stacks. Our results of the thermal transformation of bitumens of a medium degree of metamorphism (nonconductive) in oxidizing atmosphere and in vacuum confirm this conclusion. It was shown that hydrocarbon component removal is more important for occurrence of conductivity than graphitization of structure.

Influence of micromineral inclusions on the electromagnetic properties of carbonaceous materials is well detected in the microwave range, which is widely used in radio engineering and communications. Analysis of the spectra of reflection and transmission of electromagnetic waves has shown that the samples with a graphite-like structure can be divided into three groups according to carbon content (more than 60%, 60 to 30% and less than 30%) with different electromagnetic properties. Aggregates of conductive and non-conductive domains can be represented by a simplified equivalent electrical circuit consisting of capacitors, resistors and inductors.

Acknowledgements: This work was supported by RFBR (grant 15-05-04369).

Golubev, E.A. (2013): Electrophysical properties and structural features of shungite (natural nanostructured carbon). *Phys. Solid St.*, **55**, 1078-1086.

Melezhik, V.A., Filippov, M.M., Romashkin, A.E. (2004): A giant Palaeoproterozoic deposit of shungite in NW Russia: genesis and practical applications. *Ore Geol. Rev.*, **24**, 135-154.

ANIONIC CLAY AND CATIONIC ORGANOCLAY AS NANOCARRIERS IN SMART DELIVERY SYSTEMS OF THE HERBICIDE IMAZAMOX

Khatem R.[1], Bakthi A.[1], Celis R.[2] & Hermosín M.C.*[2]

[1] Laboratoire de Biodiversité et Conservation des Eaux et des Sols, Université "Abdelhamid Ibn Badis", Mostaganem, Algeria

[2] Instituto de Recursos Naturales y Agrobiología de Sevilla, Consejo Superior de Investigaciones Científicas, Sevilla, Spain

Corresponding email: mchermosin@irnase.csic.es

Keywords: nanoformulation, pesticide, release

The interest in the use of clays to control environmental pollution has increased considerably, because their abundance in nature, nanocrystalline expansible sheet structure, and low cost make them particularly attractive for pesticide, pharmaceutical and cosmetic industries (Ruiz-Hitzky et al., 2010). The development of new formulations based on clays as smart delivery systems for crop protection is receiving an updated interest (Perez-de-Luque & Hermosín, 2013; Cabrera et al., 2016), being especially attractive for systemic active ingredients (Cabrera et al., 2016). The objective of the present work was to assess the potential of a commercial organoclay and a Mg/Al layered double hydroxide (LDH) as matrices in controlled release formulations of the herbicide Imazamox (Imz), to reduce the free herbicide concentration in soil and hence its potential risk to reach ground water.

The commercial clay used was Cloisite 10A (Clo10, BYK Additives & Instruments) and the Clo10-Imz complexes (20% w/w) were prepared in three ways: (i) ground mixing (GM); (ii) weak complex (WC), and iii) strong complex (SC). The LDH-Imz complexes were prepared by direct synthesis (DS) and by regeneration (RE) of calcined (500ºC) LDH. The Imz content in the LDH nanoformulations was determined by dissolving the formulations in concentrated HCl, and then quantifying the released herbicide by HPLC. The content of Imz in the samples was 35% (w/w) for DS and 10% (w/w) for RE. The stability of the Imz-LDH complexes was monitored for two months. The rate of release of Imz from the nanoformulations into water was evaluated using a batch method. Soil movement of Imz was studied by leaching experiments in glass columns.

The results of the Imz-clay stability test showed no degradation along two months. The water release experiment showed that Imz-Clo10 (GM, WC and SC) and Imz-LDH (DS and RE) formulations performed in a similar way, typical of controlled release formulations, with a final level of Imz release of 97, 79 and 90, and 78 and 95%, respectively. Cumulative soil column leaching profiles displayed similar shapes, with Imz-LDH RE and Imz-Clo10 GM and WC showing the lower concentrations in the initial leachates, but with different final leached percentages for Imz: 78, 67 and 77% for Imz-Clo10 GM, WC and SC, respectively, and 81 and 83% for Imz-LDH RE and DS. In the same conditions, technical and commercial Imz reached final leached percentages of 98 and 90%, respectively. The characterization of the complexes by XRD, SEM and IR spectroscopy help to interpret the slight differences among the behavior of the diverse complexes. The Imz-clay complexes prepared and assayed in this work showed a potential as smart delivery systems or nanoformulations to minimize the groundwater contamination risk associated with the use of Imz, with possibilities for a located application at plant root level.

Acknowledgments: Projects P11-AGR-7400, RECUPERA 2020, AGL2014-51897-R and Research Group AGR-264.

Cabrera, A., Celis, R., Hermosín, M.C. (2016): Imazamox-clay complexes with chitosan- and iron(III)- modified smectites and their use in nanoformulations. *Pest Manag. Sci*., **72**, DOI: 10.1002/ps.4106

Perez-de-Luque, A. & Hermosín, M.C. (2013): Nanotechnology and its use in agriculture. *in* "Bio-nanotechnology. A revolution in food, biomedical and health sciences, part 3", D. Bagachi, ed., Wiley-Blackwell, Chiechester, 383-398.

Ruiz-Hitzky, E., Aranda, P., Darder, M., Rythwo, G. (2010): Hybrids materials based on clays for environmental and biomedical applications. *J. Mater. Chem*., **20**, 9306-9321.

EFFICIENT AND SELECTIVE REMOVAL OF ORGANIC VOLATILE SULPHUR DERIVATIVES USING MONTMORILLONITE INTERCALATED WITH Fe^{3+}-PHENANTHROLINE COMPLEX

Malferrari D.*[1], Bernini F.[1], Borsari M.[1], Brigatti M.F.[1], Castellini E.[1] & Cástro R.G.[2]
[1] Dipartimento di Scienze Chimiche e Geologiche, Università di Modena e Reggio Emilia, Modena, Italy
[2] European Synchtron Radiation Facility - Spanish CRG Beamline, Grenoble, France
Corresponding email: daniele.malferrari@unimore.it

Keywords: montmorillonite, gas adsorption, heptanethiol

In the last twenty years numerous researchers have worked to prepare adsorption materials and catalyzers based on surface modified clays. However, most of the efforts have been directed to the definition of the interactions with carbon dioxide, hydrocarbons (methane in particular), and hydrogen sulfide (De Paolo et al. 2013; Nguyen-Thanh & Bandosz, 2003; Nguyen-Thanh et al., 2005; Bineesh et al., 2011; Kadoura et al. 2016). On the other hand, to our knowledge nothing can be found about interactions between (layered) minerals and volatile thiols and mercaptans. In our view, this gap may be due to the known hydrophobic character of thiols and mercaptans that makes these molecules little suited to interact with the hydrophilic clay and, therefore, representing a deterring factor to undertake researches in this area. Of course, direct sorption of thiols or mercaptans on natural clay surface is not possible. It is then necessary to transform the hydrophilic surface of clay in an hydrophobic media. However, in order to maintain the swelling behavior of clay that allows large molecules hosting in the interlayer, pillaring and any other thermal treatment that drives to a deep structural modification must be avoided.

We prepared a Fe(III)-phenanthroline (Fe(III)Phen) intercalated montmorillonite (MtFe(III)Phen), whose features are detailed in Bernini et al.(2015), that is able to adsorb volatile heptanethiol (CH_3-$(CH_2)_6$-SH) at the solid/gas interface at room pressure and temperature conditions. The interaction between heptanethiol and MtFe(III)Phen is not electrostatic, but occurs through a redox reaction between sulphur and iron of the intercalated Fe(III)Phen complex, as clearly demonstrated through the recognition of specific differences between the X-ray absorption spectra (near edge structure measured at the Fe *K*-edge) of heptanethiol exposed and not exposed MtFe(III)Phen. It should be remarked that IR and UV-Vis spectroscopies measurements on the same samples have driven to the same conclusions. The immobilization mechanism can be summarized as follows:

$$[\text{PhenFe(III)-O-Fe(III)Phen}]^{4+} + 2\ CH_3\text{-RSH} \rightarrow 2\ [\text{PhenFe(II)}]^{2+} + CH_3\text{-RS-SR-}CH_3 + H_2O$$
$$[\text{PhenFe(II)}]^{2+} + CH_3\text{-RSH} \rightarrow [\text{PhenFe(II)SR-}CH_3]^{+} + H^{+}$$
$$[\text{PhenFe(II)-SR-}CH_3]^{+} + CH_3\text{-RSH} \rightarrow [\text{PhenFe(II)(SR-}CH_3)_2] + H^{+}$$

Maximum heptanethiol adsorption (1.99 mol/Kg) has been calculated measuring sulphur and carbon content via elemental analyses. Thermogravimetric measurements coupled with evolved gasses mass spectrometry confirmed previous calculation, and were employed to check the thermal desorption behavior of captured heptanethiol. We demonstrated also the reversibility of the reaction via thermal treatment in oxidizing environment at temperature lower than 240°C, highlighting that the absorbent can be reused several times before exhaustion, thus enhancing promising applicative potentialities ranging from industrial to more wide environmental applications.

Bernini, F., Castellini, E., Malferrari, D., Borsari, M., Brigatti M.F. (2015): Stepwise structuring of the adsorbed layer modulates the physic-chemical properties of hybrid materials from phyllosilicates interacting with the m-oxo Fe^{+3} phenanthroline complex. *Microp. Mesop. Mater.*, **211**, 19-29.

De Paolo, D.J., Cole, D.R., Navrotsky, A., Bourg, I.C. (2013): Geochemistry of geologic CO_2 sequestration. *Rev. Mineral Geochem.*, **77**, 539 p.

Kadoura, A., Kumar, A., Nair, N., Sun, S. (2016) Adsorption of carbon dioxide, methane, and their mixture by montmorillonite in the presence of water. *Microp. Mesop. Mater.*, **225**, 331-341.

Bineesh, K.V., Kim, D.K., Kim, M.I., Selvaraj, M., Park, D.W. (2011): Design, synthesis and characterization of vanadia-doped iron-oxide pillared montmorillonite clay for the selective catalytic oxidation of H_2S. *Dalton Trans.*, **40**, 3938-3945.

Nguyen-Thanh, D. & Bandosz, T.J. (2003): Effect of transition-metal cations on the adsorption of H_2S in modified pillared clays. *J. Phys. Chem. B*, **107**, 5812-5817.

Nguyen-Thanh, D., Block, K., Bandosz, T.J. (2005): Adsorption of hydrogen sulfide on montmorillonites modified with iron. *Chemosphere*, **59**, 343-353.

CAPTURE OF CO_2 BY CONSTRUCTION WASTE

Martín D.*[1], Aparicio P.[1] & Galán E.[1]
[1] Departamento de Cristalografía, Mineralogía y Química Agrícola, Universidad de Sevilla, Spain
Corresponding email: dmartin5@us.es

Keywords: CO_2, carbon capture sequestration, construction waste

Since the Industrial Revolution the CO_2 concentration in the atmosphere was constantly growing, contributing to the increase in average global temperature. One of the options for reducing that CO_2 from the atmosphere is the carbon capture by mineral carbonation. The results of this process of fixing are the safest long term, but the main obstacle to mineral carbonation is to do it economically in terms of both money and energy cost.

This research explores the possibilities of CO_2 sequestration on ceramic construction wastes, in order to propose the injection of CO_2 in an exhausted quarry reclaimed with building ceramic wastes.

The construction wastes used in this investigation were rich in Ca-Mg-silicates. The carbonation was carried out at room temperature, low relative humidity, and low pressure in sealed reactors.

Three types of bricks were selected for this research, mainly composed of quartz, feldspar, mica, gehlenite, wollastonite and kilchoanite. CaO ranges between 14 to 20 wt.% and MgO from 2 to 4 wt.%. The bricks were ground using a jaw crusher, and were classified according to the particle size (> 4 mm, 4-2 mm, 2-1 mm), and using different pressures (10 bar for the smallest and 1 bar for biggest). The relative humidity during the reaction was 20 wt.% and the reaction time ranged from 24 hours to 30 days.

Monitoring of the reaction was followed by XRD, BET, SEM, optical microscopy, a carbon elemental analyzer, Bernard calcimeter and thermogravimetric analysis. Soluble Si, Ca, and Mg produced in the reactions were also analyzed by ICP-EOS.

The results of this study showed that the formation of calcite was accounted for the partial destruction of silicates. The carbonation was proportional to the reaction time and smaller particle size fraction. Also it was detected that the BET-N_2 specific surface area increased with the CO_2 treatment possibly by the destruction of silicates, and those variations were proportional to the reaction time. Layers of carbonates on the silicate surface and crystal growth in pores were observed. As the reaction time increases, soluble Ca reduces and silicon increases. Ca is spent on the calcite formation while Si comes from the destruction of the silicate.

The largest quantities of carbonates were obtained for experiments carried out during 30 days, using the > 4mm fraction, 10 bar of CO_2, 20 wt.% of relative humidity and room temperature.

Acknowledgements: This research was financed by the Andalucía Government (RDCCO2 project, P12-RNM-568).

SPECTROSCOPIC AND MICROSCOPIC EVALUATION OF ORGANIC-CLAY INTERCALATION

Mervat H.*[1], Heba F.[2], Fatma A.[1-3] & El-Herbiny S.[1-3]
[1] Central Metallurgical Research and Development Institute, Cairo, Egypt
[2] National Institute for Standards, Cairo, Egypt
[3] Department of Chemistry, Helwan University, Cairo, Egypt
Corresponding email: hassan_mervat@yahoo.com

Keywords: kaolinite, organic, intercalation

Bulk and < 2 µm size-fractionated kaolinite from Tieh, Egypt has been studied using a combination of X-ray diffraction, electron microscopy and Fourier Transformers Infrared Spectroscopy before and after intercalation with organic. El Tieh sample is disordered, poorly crystalline kaolinite (Hinckley index = 0.55) contains traces of quartz and very sparse mica, calcite and feldspar. Kaolinite K is indicated by its characteristic reflection peaks at 7.14 Å (001) and 3.56 Å (002), quartz (SiO_2) at 3.33 Å, feldspar at 3.23 Å and calcite at 3.03 Å. Mica appears at 10 Å. Anatase (TiO_2) appears at 3.51 Å.

The < 2 µm size-fractionated kaolinite was found to intercalate with Urea, Dimethyl sulphoxide (DMSO), and N-methyl Formamide (NMF) in decreasing order. Upon grinding of kaolinite with urea (1:1) w/w for different times 1, 3 and 5 h, the basal spacing of kaolinite shifted to 7.14, 11.0 and 11.8 Å, respectively. These shifting in 001 basal plane of kaolinite revealed the intercalation of urea into the interlayer sheets of kaolinite. The intercalation ratio (I.R.) increased with the grinding for 1,3 and 5 h from 0, 48.9 and 80%, respectively, and the expansion degree [$\Delta d = d_{001}$ (of the substituted phase) – d_{001} (of kaolinite)] was 0, 3.96 and 4.66 Å respectively. In case of DMSO, intercalation carried out using ultrasonication method the basal space of kaoilinite shifted from 7.14 to 11.04 upon reaction for hours ranged from 1 up to 6 hours. Interlayer expansions (Δd Å) ranges from 0 to 4.04 respectively. The intercalation ratio (I.R.) increased with the time for 1,3 and 6 h from 50, 70 and 70%, respectively. Kaolinite has been intercalated with N-methyl Formamide (NMF) after pretreatment with DMSO that open the interlayer space so that NMF simultaneously penetrate between the layers. the basal spacing of kaolinite shifted from 7.14, up to 11.6 Å. However, the intercalation ratio in this case did not exceeds 60%. The electron microscope study indicated that the kaolinite platelets assumed a tubular morphology similar to halloysite upon intercalation. This appearance is probably due to the reduction of particle size of kaolinite after intercalation with organic during ultraconication and grinding techniques as a result of the intercalation process. During modification of kaolinite, the plates of kaolinite partially exfoliated and shattered into flakes of 500 nm diameter particles.

HYDROCARBONS IN PHLOGOPITES FROM KASENYI KAMAFUGITIC ROCKS (SW UGANDA): CROSS-CORRELATED AFM, CONFOCAL MICROSCOPY AND RAMAM IMAGING

Mesto E.*[1], Lacalamita M.[1], Scordari F.[1], Moro D.[2], Valdrè G.[2], Della Ventura G.[3], Bellatreccia F.[3], Scirè S.[4] & Schingaro E.[1]

[1] Dipartimento di Scienze della Terra e Geoambientali, Università di Bari, Italy

[2] Dipartimento di Scienze Biologiche, Geologiche e Ambientali, Università di Bologna, Italy

[3] Dipartimento di Scienze, Università di Roma Tre, Italy

[4] Dipartimento di Scienze Chimiche, Università di Catania, Italy

Corresponding email: ernesto.mesto@uniba.it

Keywords: phlogopite, atomic force and Raman microscopy, hydrocarbon inclusions

Hydrocarbon fluid inclusions (HCFI) can occur in fractures and microcracks of rocks and veins within forming minerals, e.g. quartz, calcite and pyroxene, and may consist of hydrocarbon oil, H_2O, gases such as CO_2 and CH_4 or solids entrapped along with/or precipitated from the liquid phase at later times (Orange et al., 1996; Mathez et al., 1998). The analysis of the HCFI may be performed on the bulk rock by crushing of the sample or on single inclusions by means of micro-spectroscopy (e.g., optical, infrared, Raman and fluorescence spectroscopy). On the other hand, the amount and location of carbon in Earth is a question of paramount importance in geochemistry, with implications for deep carbon storage systems and their fate in the dynamic of the Earth (Hazen & Schiffries, 2013).

This study presents a cross-correlated surface and near surface investigation of 1*M* and $2M_1$ phlogopite polytypes from Kasenyi kamafugitic rocks (SW Uganda) by means of advanced Atomic Force Microscopy (AFM), confocal microscopy and Raman micro-spectroscopy. Crystallography and crystal chemistry of these micas are reported elsewhere (Lacalamita et al., 2012). AFM revealed comparable nanomorphology and electrostatic surface potential for the two mica polytypes. The widespread presence of protrusions located on the mica flake surface was also observed in both polytypes; confocal microscopy showed these features to range from few nanometers to several micrometers in dimension, and shapes from perfectly circular to ellipsoidic also strongly elongated. An aspect ratio (maximum height/maximum width) from 0.01 to 0.09 was generally observed. Raman spectra collected across the bubbles showed an intense and convolute absorption in the range 3000-2800 cm^{-1}, associated with weaker bands at 1655, 1438 and 1297 cm^{-1}, indicating the presence of fluid inclusions consisting of aliphatic hydrocarbons. High-resolution Raman images provided evidence that these hydrocarbons are confined within the bubbles. To the best of the authors knowledge, HCFI have never been reported in phlogopites.

Hazen, R.M. & Schiffries, C.M. (2013): Why deep carbon? *Rev. Mineral. Geochem.*, **75**, 1-6.

Lacalamita, M., Mesto, E., Scordari, F., Schingaro, E. (2012): Chemical and structural study of 1*M*- and $2M_1$-phlogopites coexisting in the same Kasenyi kamafugitic rock (SW Uganda). *Phys. Chem. Minerals*, **39**, 601-611.

Mathez, E.A. & Mogk, D.M. (1998): Characterization of carbon compound on a pyroxene surface from a gabbro xenoliths in basalt by time-of-flight secondary ion mass spectrometry. *Am. Mineral.*, **83**, 918-924.

Orange, D., Knittle, E., Farber D., Williams, Q. (1996): Raman spectroscopy of crude oils and hydrocarbon fluid inclusions: A feasibility study. *Mineral. Spectr.*, **5**, 65-81.

GREEN RUST: THE FIRST DISCOVERIES IN AUSTRALIA, DNA, AND INDUSTRIAL USES

Mills S.J.*[1], Génin J.-M.R.[2] & Christy A.G.[3]
[1] Geosciences, Museum Victoria, Melbourne, Australia
[2] Institut Jean Barriol, Centre National de la Recherche Scientifique, Université de Lorraine, École Supérieure des Sciences et Technologies de l'Ingénieur de Nancy, Vandoeuvre-Lès-Nancy, France
[3] Centre for Advanced Microscopy, Australian National University, Canberra, Australia
Corresponding email: smills@museum.vic.gov.au

Keywords: green rust, hydrotalcite, layered double hydroxide

The mixed-valence Fe^{2+}-Fe^{3+} compounds commonly called "green rusts" are observed during the aqueous oxidation of iron, and their study since the 1980s has allowed us to explain the domain of corrosion of steels in the E_h-*p*H Pourbaix diagram. They are part of the family of layered double hydroxides (LDH), $M^{2+}_{n-m}M^{3+}_m(OH,O,H_2O)_{2n}X\cdot yH_2O$, where divalent and trivalent cations belong to the same element, iron, and are interconvertible by electron transfer alone, giving them outstanding redox and catalytic properties. The formula of carbonate green rust compounds is $Fe^{2+}_{6(1-x)}Fe^{3+}_{6x}O_{12}H_{2(7-3x)}CO_3\cdot 3H_2O$, and the minerals fougerite (x = 1/3), trébeurdenite (x = 2/3) and mössbauerite (x = 1) all have fixed values of x. In the past, waterlogged gleys at inland localities such as in marshes, lagoons and lakes have been found to be topotactic mixtures of fougerite and trébeurdenite, while marine gleys in intertidal zones are mixtures of trébeurdenite and mössbauerite.

While the majority of our research has been on natural occurrences of green rust in northern France (Brittany and Normandy), we have recently undertaken several field surveys in the Murray–Darling Basin and along the Victorian–South Australian coast, in search of green rust localities. We are able to announce for the first time the occurrence of green rust minerals in both marine and lake settings within SE Australia. DNA analysis of the green rust samples shows a variety of bacteria, some of which are iron-oxidising, and possibly related to green rust formation.

Many countries including France and Australia have major problems with algal contamination of waters. This was extremely evident this summer in Victoria during a major blue-green algal bloom which has been affecting the Murray River since February 2016 (ongoing at the end of April). The bloom is in part caused by excess nitrate (and phosphate) which is dumped into the water by agricultural farming, acting as a food source for the algae. Long term studies by us and other researchers have shown that green rust minerals can catalyse nitrate reduction, thus preventing agricultural runoff from triggering algal blooms. The process involves oxidation of fougèrite/trébeurdenite to mössbauerite with reduction of nitrate to nitrogen gas, and requires bacterial reduction of mössbauerite to regenerate the reduced green rust phases and maintain the cycle. Our interest is now to use this knowledge to create industrial-scale denitrification facilities to prevent large-scale algal blooms which can otherwise cripple local water supplies and economies.

S-BEARING ZEOLITES IN GEOPOLYMERS FROM VOLCANIC KAOLIN

Occhipinti R.*[1], Tarantino S.C.[1-2], Riccardi M.P.[1] & Zema M.[1-2]
[1] Dipartimento di Scienza della Terra e dell'Ambiente, Università di Pavia, Italy
[2] Istituto di Geoscienze e Georisorse, Consiglio Nazionale delle Ricerche, Pavia, Italy
Corresponding email: roberta.occhipinti01@universitadipavia.it

Keywords: alkali activated materials, zeolites, metakaolin

The feasibility of using a volcanogenic sulfate-bearing kaolin derived from rhyolite activated at *T* = 550°C to synthesize geopolymers has been recently assessed. The results are promising, as evidenced by high thermal stability and high compressive strength (ca. 80 MPa) of the synthesized samples. However, the presence of thenardite, $NaSO_4$, deriving from the dissolution of alunite, was observed in these geopolymers (Gasparini et al., 2015).

Aim of the present work is to better identify non soluble sulfate-bearing phases in geopolymers and hence improve sulfate retention.

Geopolymer samples with Si/Al = 1.8 and 2.3 have been prepared starting from a high-quality kaolin, an alunite-bearing kaolin (alunite 13% wt.), as well as from synthetic mixtures of alunite and high-quality kaolinite in different proportions. Leaching tests have been carried out, and chemical analyses performed on leached solution as well as on the resulting leached materials revealed that sulfates are still present inside the sample. In particular, chemical microanalyses have been carried out before and after water leaching and the presence of sulfur-rich particles containing Si and Al has been noticed in all the samples, likely amorphous or nanosized zeolites phases.

To better understand the possibility of sulfate retention into nanocrystalline phases formed in geopolymers, zeolites have been synthesized using the same precursors as starting materials. Silica fume has also been added to the mixture in order to get the same Si/Al ratios used for geopolymers. Syntheses were conducted using a recent method (Belviso et al., 2015) in which kaolinite is pre-treated by fusion with alkalis. Afterwards, samples are incubated in vessels with distilled water at 45°C for one month, in order to promote the growth of zeolites phases.

All resulting samples have been characterized by thermal analysis, X-ray powder diffraction, infrared spectroscopy and scanning electron microscopy. The results demonstrate that different types of zeolites have formed, in different quantities depending on the starting materials. Zeolite Y forms in all samples, whereas zeolite A crystallizes only in samples without alunite. Nosean and cancrinite-type phases are present in all alunite-containing samples and may be responsible for trapping sulfate ions in the early steps of geopolymers formation. More studies are needed in order to improve the sulfate retention inside the zeolite phases, as well as to understand the possible interactions between precipitated nano-crystalline sulfate phases and geopolymer binders for their possible applications.

Belviso, C., Cavalcante, F., Lettino, A., Fiore, S. (2013): A and X-type zeolites synthesised from kaolinite at low temperature. *Appl. Clay Sci.*, **80-81**, 162-168.

Gasparini, E., Tarantino, S.C., Conti, M., Biesuz, R., Ghigna, P., Auricchio, F., Zema, M. (2015): Geopolymers from low-T activated kaolin: implications for the use of alunite-bearing raw materials. *Appl. Clay Sci.*, **114**, 530-539.

STABLE CO_2 HYDRATES IN ZEOLITE Na-Y: STRUCTURAL CHARACTERIZATION BY SYNCHROTRON X-RAY POWDER DIFFRACTION

Quartieri S.*[1], Arletti R.[2], Gigli L.[3] & Di Renzo F.[4]

[1] Dipartimento di Scienze Matematiche e Informatiche, Scienze Fisiche e Scienze della Terra, Università di Messina, Italy

[2] Dipartimento di Scienze della Terra, Università di Torino, Italy

[3] Elettra Sincrotrone Trieste, Italy

[4] Institut Charles Gerhardt, Centre National de la Recherche Scientifique, École Nationale Supérieure de Chimie de Montpellier, France

Corresponding email: squartieri@unime.it

Keywords: CO_2 hydrates, Na-faujasite, synchrotron X-ray powder diffraction

Zeolites are widely used as adsorbents for industrial gas separations. Despite this, there is surprisingly little detailed information available on the CO_2 adsorption properties of most zeolites. The adsorption of CO_2 by zeolites with faujasite structure has been investigated (Bae et al., 2013), being at the basis of several processes of CO_2 capture and storage. In all gas separation processes, regeneration of the adsorbent through an efficient desorption of CO_2 by pressure or temperature swing is a critical step in the economics of the processes. Thermally stable chemisorption of a fraction of CO_2 can hinder the regeneration of the adsorbent and significantly reduce the sorption capacity in successive adsorption-desorption cycles. The most common forms of chemisorbed CO_2 are several carbonate species (named bent CO_2). Another factor severely impairing the CO_2 adsorption capacity of molecular sieves is the preferential adsorption of water vapour. The interactions between water and CO_2 have been extensively studied in the blossoming field of gas chlatrates and the stability of CO_2 hydrates has been suggested to increase in the confined environment of smectites (Martos-Villa et al., 2014). However, despite diffraction methods (XRD) have sometimes been applied to the location of adsorbed CO_2in molecular sieves (Hudson et al., 2012; Bae et al., 2013), to our knowledge advanced powder XRD (XRPD) has never been applied to the elucidation of CO_2-water interactions in zeolite cages.

In this work, the adsorption and desorption of CO_2 molecules in the pores of zeolite Na-Y have been monitored by time-resolved synchrotron XRPD experiments at the MCX beamline of the Elettra Synchrotron Light Source (Trieste, Italy), allowing the positions of the CO_2 molecules and their interactions with adsorbed water to be determined.

The structural refinement of the CO_2-saturated diffraction pattern highlighted the formation of tetrameric CO_2 clusters connected by water bridges to the sodium cations of two adjacent faujasite supercages. The CO_2desorption was followed by collecting a series of diffraction patterns upon heating from room temperature up to 350°C. The hydrated CO_2 clusters are completely desorbed between 250 and 350°C. This high thermal stability suggests that the formation of hydrated complexes could represent a potentially important mechanism of retention of CO_2 during the regeneration of CO_2 adsorbents. The absence of “bent” CO_2 in a system in which water coordinate the alkali cations confirms the spectroscopic evidences about the requirement of a direct interaction CO_2-cations for the formation of carbonate species.

Bae, T.H., Hudson, M.R., Mason, J.A., Queen, W.L., Dutton, J.J., Sumida, K., Micklash, K.J., Kaye, S.S., Brown, C.M., Long, J.R. (2013): Evaluation of cation-exchanged zeolite adsorbents for post-combustion carbon dioxide capture. *Energy Environ. Sci.*, **6**, 128-138.

Hudson, M.R., Queen, W.L., Mason, J.A., Field, D.W., Lobo, R.F., Brown, C.M. (2012): Unconventional, highly selective CO_2 adsorption in zeolite SSZ-13. *J. Am. Chem. Soc*., **134**, 1970-1973.

Martos-Villa, R., Mata, M.P., Sainz-Diaz, C.I. (2014): Characterization of CO_2 and mixed methane/CO_2 hydrates intercalated in smectites by means of atomistic calculations. *J. Mol. Graph. Model*., **49**, 80-90.

STRUCTURAL CHARACTERIZATION OF HIGH-SILICA ZEOLITES EXCHANGED WITH REEs ELEMENTS

Rodeghero E.*[1], Guzzinati R.[2], Martucci A.[1] & Pasti L.[2]
[1] Dipartimento di Fisica e Scienze della Terra, Università di Ferrara, Italy
[2] Dipartimento di Chimica, Università di Ferrara, Italy
Corresponding email: rdglse@unife.it

Keywords: REEs contamination, high-silica zeolites, adsorption

In recent years REEs contamination has increased in environmental matrixes, creating problems to humans and ecosystems due to their bioavailability. Despite the vast literature about the research efforts on REE recycling (Meyer & Bras, 2011), less than 1% of the REEs are being recycled. Today there are many conventional methods for the extraction, recovery and separation of Rees, but these methods need a high consumption of reagents and energy also generating waste and secondary pollutants (Tan et al., 2014). Adsorption process is a good ecofriendly and cost effective alternative to the conventional methods due to the possibility of regeneration and reuse of sorption material, for the wide range of applicability and for economic advantages. The properties of sorbent materials like zeolites to capture and concentrate significant quantities of species make them ideal candidates for the development of remediation processes, separation, environmental monitoring and resource recovery processes (Bryce et al., 2012). In this work Na-Y zeolites ion exchanged with rare earth cations from liquid solutions (Nd and Y) were studied by X-ray diffraction in order to locate the rare earth cations in the zeolite framework and the resulting changes in its structural properties. The REEs adsorption capability of zeolites was evaluated by Inductively Coupled Plasma Optical Atomic Emission (ICP-OES). Different adsorption mechanism involves physical and chemical forces such as sorption/desorption, oxidation reduction reaction, surface precipitation or incorporation of the sorbed lanthanides into the solid matrix (Tan et al., 2014). Rietveld refinements revealed that after REEs ion exchange, a systematic decrease in the values of the unit cell parameters a0 is related to the rare earth ionic radius and its coordination to the oxygen framework. Finally, ^{27}Al magic angle spinning NMR measurements indicate a dealumination process strongly depending on the REEs cations adsorbed.

Bryce, E., Johnson, P.H., Santschi, C.Y.C., Shigeyoshi, O. (2012): Collection of lanthanides and actinides from natural waters with conventional and nanoporous sorbents. *Environ. Sci. Technol.*, **46**, 11251-11258.

Meyer, L. & Bras, B. (2011): Rare earth metal recycling. Proc. 2011 IEEE Int. Symp. on Sustainable Systems and Technology, Chicago, 1-6.

Tan, X., Ren, X., Chen, C., Wang, X. (2014): Analytical approaches to the speciation of lanthanides at solid-water interfaces. *Trends Analyt. Chem.*, **61**, 107-132.

INFLUENCE OF MOISTURE AND TEMPERATURE ON THE TENSILE STRENGTH OF BENTONITE BOUNDED MOULDING SAND

Schiebel K.*[1], Jordan G.[1], Kaestner A.[2], Böhnke S.[3] & Schmahl W.W.[1]
[1] Department für Geo- und Umweltwissenschaften, Ludwig-Maximilians-Universität München, Germany
[2] NIAG Group, Paul Scherrer Institut, Villigen, Switzerland
[3] S&B Industrial Minerals GmbH, Oberhausen, Germany
Corresponding email: Korbinian.Schiebel@lrz.uni-muenchen.de

Keywords: tensile strength, neutron radiography, moulding sand

Quartz sand bounded with water and bentonite, so called green sand, is the most common mould material used in foundry industries. Depending on the temperature and moisture content, bentonite plasticises and stabilizes the mould by a number of forces such as van der Walls attraction, electric double layer attraction and repulsion, capillary forces due water bridges, and cementation due solute precipitation. During casting a temperature gradient arises in the sand mould. Water begins to vaporize and to migrate into colder areas, where it condensates. With time, vaporization and condensation advance further into the mould. Water and temperature gradients lower the strength of the mould significantly. Spalling of sand layers at the top of the mould cavity can be the aftermath. The location of fracture is assumed to be located somewhere between the condensation zone and the dehydrated zone (Patterson & Boenisch, 1961; Odom, 1984; Campbell, 2011). The exact location, temperature and moisture of the rupture plane as well as the ultimate cause of rupture are insufficiently explored. However, an improved knowledge of the physical background of the spalling could considerably help to improve the usability of green sand as an environment-friendly mould material. Therefore, aim of this study is to investigate the effects of the water and heat kinematics on the tensile strength of green sands. To unravel the effects, neutron radiography was performed during tensile testing of green sands at the beam line ICON (Paul Scherer Institute, Switzerland). Therefore, a tensile test stand was constructed, that made it possible to heat the sand and to apply neutron radiography during tensile testing. According to norm P38 (Verein Deutscher Giessereifachleute), the sand was heated from above to induce a temperature and moisture gradient before applying tensile stress. The water and heat kinematics were observed by simultaneously conducted neutron radiography and temperature measurements while tensile testing. For the first time, this combination made it possible to map the water and temperature evolution before tensile testing and identification of the sand properties at the moment of fracture. The radiographs were corrected for beam fluctuations, camera noise, multi scattering, and spectral effects by QNI (Hassanein, 2006). Evaluating the radiographs, the preferred fracture position has been pinpointed at the interface between evaporation and condensation zone, were the water starts to vaporize and the water-bridges, connecting the sand grains, collapse. This leads to a strong decrease of tensile strength and refute the common postulations (Patterson & Boenisch, 1961; Odom, 1984; Campbell, 2011), that the fracture occurs in the condensation zone because of the sand oversaturation. Furthermore, the practicality of simple models to calculate the moisture and position of the fracture area was tested and verified.

Campbell, J. (2011): Complete casting handbook. Butterworth, Amsterdam, 1224 p.

Hassanein, R.K. (2006): Correction methods for the quantitative evaluation of thermal neutron tomography. Diss ETH No. 16809, 149 p.

Odom, I.E. (1984): Smectite clay minerals: Properties and uses. *Phil. Trans. R. Soc. London*, **A311**, 391-409.

Patterson, W. & Boenisch, D. (1961): Die Bedeutung der Festigkeit feuchter, tongebundener Formsande insbesondere der Naßzugfestigkeit. *Giesserei*, **13**, 157.

$K_2Ca_2Si_8O_{19}$ – A NEW POTASSIUM CALCIUM DOUBLE-LAYER SILICATE

Schmidmair D.*[1], Kahlenberg V.[1] & Praxmarer A.[1]
[1] Institut für Mineralogie und Petrographie, Universität Innsbruck, Austria
Corresponding email: Daniela.Schmidmair@uibk.ac.at

Keywords: $K_2Ca_2Si_8O_{19}$, double-layer silicate

Within the context of a systematic re-investigation of phase relationships between compounds of the ternary system K_2O-CaO-SiO_2 we succeeded to synthesize a new potassium calcium silicate with the chemical formula $K_2Ca_2Si_8O_{19}$ via solid state reactions as well as the flux method using KCl as a solvent. Based on single-crystal X-ray diffraction data it was possible to determine its crystal structure using direct methods. The new compound crystallizes in space group *P*-1 with unit cell parameters *a* = 7.4231(7), *b* = 10.7649(10), *c* = 12.1252(10) Å, α = 70.193(8), β = 83.914(7), γ = 88.683(7)°.

$K_2Ca_2Si_8O_{19}$ exhibits similar structural features as so-called CAS-1 or $K_2Ca_2Si_8O_{19}\cdot 4H_2O$ (Xue et al., 2002; Jordá et al., 2005; Gao et al., 2009). This material, which has zeolite-like properties, can be considered as a water containing analogue of the title compound. Like CAS-1, $K_2Ca_2Si_8O_{19}$ is built up of an alternating stacking of silicate double-layers and layer-like arranged chains of edge sharing CaO_6-octahedra. In contrast to CAS-1, however, the silicate sheets of $K_2Ca_2Si_8O_{19}$ are composed of 5, 6, 7 and 8 membered rings of slightly distorted SiO_4-tetrahedra. Single silicate sheets are connected in such a way that channel-like cavities are formed, which host half of the potassium cations. All remaining potassium atoms are located between adjacent chains of CaO_6-octahedra.

Differential thermal analysis and high-temperature in-situ powder X-ray diffraction measurements were employed to study the behavior of this new potassium calcium silicate at elevated temperatures. Both methods revealed that $K_2Ca_2Si_8O_{19}$ melts incongruently at 1054°C producing a melt phase and wollastonite ($CaSiO_3$).

Gao, L., Cao, Y., Zhou, S.L., Zhuang, T.T., Wang, Y., Zhu, J.H. (2009): Eliminating carcinogenic pollutants in environment: Reducing the tobacco specific nitrosamines level of smoke by zeolite-like calcosilicate. *J. Hazard. Mater.*, **169**, 1034-1039.

Jordá, J.L., Prokic, S., McCusker, L.B., Baerlocher, C., Xue, C.F., Dong, J.X. (2005): Synthesis and structure analysis of the potassium calcium silicate CAS-1. Application of a texture approach to structure solution using data collected in transmission mode. *C.R. Chimie*, **8**, 331-339.

Xue, C.F., Liu, G.G., Li, J.P., Dong, J.X. (2002): Hydrothermal synthesis and characterization of zeolite-like crystal material CAS-1. *Front. Solid St. Chem.*, 233-240.

Mg-PHYLLOSILICATES CRYSTAL CHEMISTRY OF THE ANDRIĊI SEPIOLITE DEPOSIT (SERBIA)

Suárez M.*[1], García-Romero E.[2-3], Simic V.[4] & Andric N.[4]
[1] Departamento de Geología, Universidad de Salamanca, Spain
[2] Department de Cristalografía y Mineralogía, Universidad Complutense, Madrid, Spain
[3] Instituto de Geociencias, Universidad Complutense, Consejo Superior de Investigaciones Científicas, Madrid, Spain
[4] Faculty of Mining and Geology, University of Belgrade, Serbia
Corresponding email: msuarez@usal.es

Keywords: crystal chemistry, smectites, sepiolite

The sepiolite deposit Andrići is located in the Pranjani Basin, in the western part of Serbia. The studied section of Andrići deposit represents the sepiolite-bearing succession characterized by rhythmic alternation of clay-rich and dolomite-rich intervals. The section started with claystone dominated by detrital material derived from the surrounding paleorelief of ultramafic rocks. In this basal part smectites are inherited but smectites deposited from solution are also present. In dolomicrite marls, sepiolite occurs as interwoven fibres which coat and fill pores between dolomite crystals while, in the clay-rich layers, sepiolite consists of fibres forming planes. The texture in these layers indicates that sepiolite crystallized directly from solution.

The chemical composition of individual particles was obtained using analytical electron microscope (AEM) with TEM, using a JEOL 3000 FX Field Emission Microscope at an acceleration voltage of 300 kV that incorporates an OXFORD ISIS EDX spectrometer. In these materials, different Mg-phyllosilicates have been found and it is remarkable that all these phyllosilicates are rich in Fe.

In the basal detrital material, Fe-rich chrysotile and two types of smectites appear. From the structural formula obtained, the two smectites can be classified as Fe-rich saponite. In the rest of the section, sepiolite is the main mineral and it can occur with trioctahedral smectites, with dolomite, or almost pure. The crystal chemistry of these three groups is slightly different: i) in dolomitic marls sepiolite has the octahedral content close to the ideal, with very low amounts of ^{VI}Al and Fe^{3+} and also small amounts of tetrahedral substitutions. It is remarkable that Fe^{3+} appears as tetrahedral cation in the mean structural formulae in most samples, which is not very common in sepiolite. ii) The sepiolites that appear with smectites are characterized by the high amount of tetrahedral substitution, while the octahedral content is close to the ideal sepiolite. In these samples, as in the dolomitic levels Fe^{3+} is needed to fill the tetrahedral positions indicating the low availability of Al in the sedimentary ambience. iii) Finally, the purest sepiolite level presents a composition relatively close to the ideal sepiolite whit only small amounts of Al as tetrahedral and octahedral cation.

Session S13:

Ores, minerals and geomaterials in industrial processes and human activities

Conveners:

Piergiulio Cappelletti (Napoli – Italy)

Jan Elsen (Leuven – Belgium)

Bernard Grobety (Fribourg – Switzerland)

Jussi Liipo (Oulu – FInland)

THE USE OF AUTOMATED MINERALOGY TO CHARACTERIZE MINERALURGICAL PRODUCTS OF VHMS ORES FROM THE IBERIAN PYRITE BELT: THE CASE OF ALJUSTREL MINE, SOUTH PORTUGAL

Alves P.*[1], Pinto A.M.M.[2] & Pires S.[3]
[1] Drilling Company and Mining Development, S.A., Aljustrel, Portugal
[2] Institute Dom Luis, Faculty of Sciences, University of Lisbon, Portugal
[3] ALMINA - Alentejo Mines, S.A., Aljustrel, Portugal
Corresponding email: pedro.nunoalves@epdm.pt

Keywords: automated mineralogy, Aljustrel, Iberian Pyrite Belt

Mineralogical data focuses on the characterization of ore samples and products of ore dressing with economic interest and/or with environmental concerns is one of the most important technical supports required for the today's mine activity. The challenge for industry is to increase recoveries and raise productivity while maintaining environmental compliance (Pinto et al., 1991; Pinto, 1996). Since the late 1960s several automated mineralogy systems have been developed, MLA (Mineral Liberation Analyzer) and QEMSCAN, both from FEI, are among the most successful and widespread in the geosciences and mining industry. In 2014 the majority (41%) of the MLA were owned by mining companies or working for them and 18% were owned by the state, applied in research for the mining industry (Sandmann, 2015).

The Aljustrel mine is a giant deposit of the Iberian Pyrite Belt (IPB) where polymetallic volcanogenic massive sulphides commonly show an overall metal zoning from a zinc-rich zone near the hanging wall and a cooper-rich zone near the footwall (Bobos et al., 2006). The mineralogical laboratory of EPDM (Empresa de Perfuração e Desenvolvimento Mineiro S.A.) is located in Aljustrel mining complex. The mineralogical and textural complexity of the IPB massive sulphide ores and the fine liberation sizes of their base metal sulphides (less than 8 to 10 µm) render their beneficiation very demanding, making the understanding of ores and beneficiation products at a microscopic level of paramount importance. Combination of MLA's features output with the filters tools, offers virtually unlimited possibilities. However, untreated MLA's data requires both mineralogical and mineralurgical interpretation to produce a tailored report having the important and relevant information. A specific report has been created for the Aljustrel copper concentrator either adapted for the different type of products and containing the required information for a complete and detailed characterization. Significant advances were achieved by establishing different liberation classes shortening to a level where the concentrator can (re)act. Thus, four classes of free and locked particles were created based on chalcopyrite contains (low, medium, high chalcopyrite contain and free chalcopyrite). Data contained within each different particles class is subdivided by locked type particle of chalcopyrite (e.g., chalcopyrite with sphalerite; with pyrite, etc). Data report also contains additional information for each combination (chalcopyrite contents and associated mineral), such as particle size distribution, chalcopyrite grain size distribution, grade, weight distribution and copper distribution. The production of this tailored report and the achieved improvements within ore dressing processes has only been possible as a consequence of a strong and close collaboration and teamwork, putting together process engineers and mineralogists.

Bobos, I., Durães, N., Noronha, F. (2006): Mineralogy and geochemistry of mill tailings impoundments from Algares (Aljustrel), Portugal: Implications for acid sulfate mine waters formation. *J. Geochem. Explor.*, **88**. 1-5.

Gaspar, O. & Pinto, A.M.M. (1991): The ore textures of the Neves Corvo volcanogenic massive sulphide and their implications for ore beneficiation. *Mineral. Mag.*, **55**, 417-422.

Pinto, A.M.M. (1996): Applied mineralogy, a tool control for the beneficiation of the Neves-Corvo ores. 5th International Congress on Applied Mineralogy, Warsaw, Poland.

Sandmann, D. (2015): Method development in automated mineralogy. PhD dissertation, Freiberg, 126 p.

NON-WETTING FLUID INTRUSION IN HYDROPHOBIC MEDIA: STRUCTURAL INTERPRETATION OF THE ENERGETIC PERFORMANCE OF PURE-SILICA FERRIERITE

Arletti R.*[1], Ronchi L.[2], Quartieri S.[3], Vezzalini G.[4], Ryzhikov A.[2], Nouali H.[2], Daou T.J.[2] & Patarin J.[2]

[1] Dipartimento di Scienze della Terra, Università di Torino, Italy

[2] Université de Strasbourg, Université de Haute Alsace, Equipe Matériaux à Porosité Contrôlée, Institut de Science des Matériaux de Mulhouse, France

[3] Dipartimento di Scienze Matematiche e Informatiche, Scienze Fisiche e Scienze della Terra, Università di Messina, Italy

[4] Dipartimento di Scienze Chimiche e Geologiche, Università di Modena e Reggio Emilia, Modena, Italy

Corresponding email: rossella.arletti@unito.it

Keywords: zeolites, powder diffraction, high pressure

The demand for low cost, efficient and sustainable energy is ever increasing. Since fifteen years, absorption or energy storage using pure-silica zeolites (zeosils) has been developed and opened a new field of applications for these exciting microporous solids (Eroshenko et al. 2001, 2002; Soulard et al. 2004). The basic idea focuses on the intrusion of water or aqueous salt solutions (non-wetting liquid) into a hydrophobic porous material. A certain pressure must be applied to penetrate the non-wetting liquid in such microporous matrices. During this forced penetration (intrusion), the mechanical energy can be converted into interfacial one. Depending on various physical parameters of the porous material - such as its pore system, its dimensionality and pore size - when pressure is released (extrusion) the “zeosil-water” system is able to restore, dissipate or absorb the supplied mechanical energy accumulated during the compression step, with a more or less significant hysteresis. As a consequence, it displays a spring, shock-absorber or bumper behavior, respectively. In the present work, the energetic performances of the pure-silica ferrierite (Si-FER) are studied by means of $MgCl_2 \cdot 21H_2O$ aqueous solution intrusion−extrusion.

Experimental intrusion-extrusion isotherms of $MgCl_2 \bullet 21H_2O$ solution were recorded at room temperature on pure silica FER-type zeolite (Si-FER). The intrusion occurs at 195 MPa and the phenomenon is completely reversible with a slight hysteresis. Hence the system behaves like a spring. The material was deeply characterized before and after intrusion-extrusion experiments. The Rietveld refinement of the synchrotron X-ray powder diffraction data, collected *in situ* at 0.3 GPa shows that both ions and water molecules present in the $MgCl_2$ aqueous solution are intruded in the porosities. However, the solvation degree of the intruded ions differs from the initial solution, revealing a partial desolvation of both magnesium and chloride ions. At a higher pressure (0.68 GPa), a phase transition from the orthorhombic *Pmnn* to the monoclinic $P2_1/n$ s.g. is observed in Si-FER. At 1.47 GPa, the zeolite maintains this monoclinic symmetry, while another phase transition, to the monoclinic $P2_1$ s.g., is argued from the analysis of the pattern of the sample compressed to 2.6 GPa and then collected upon pressure release to ambient conditions.

Eroshenko, V., Regis, R.C., Soulard, M., Patarin, J. (2001): Energetics: A new field of applications for hydrophobic zeolites. *J. Am. Chem. Soc*., **123**, 8129-8130.

Eroshenko, V., Regis, R.C., Soulard, M., Patarin, J. (2002): The heterogeneous systems 'Water-Hydrophobic Zeolites': New molecular Springs. *C. R. Phys*., **3**, 111-119.

Soulard, M., Patarin, J., Eroshenko, V., Regis, R. (2004): Molecular spring or bumper: A new application for hydrophobic zeolitic materials. *in* ”Recent advances in the science and technology of zeolites and related materials: Proceedings of the 14th International Zeolite Conference. Studies in Surface Science and Catalysis”, E. Van Steen, M. Claeys, L.H. Callanan, eds., Elsevier, Amsterdam, 1830-1837.

SILICA CHARACTERIZATION AND BENEFICIATION DESTINED FOR SILICON SOLAR GRADE PRODUCTION

Bobocioiu E.*[1] & Kheloufi A.[2]
[1] Laboratoire de Géologie de Lyon, Ecole Normale Supérieure de Lyon, France
[2] Division Croissance Cristalline des Semi-conducteurs et Procédés Métallurgiques, Centre de Recherche en Technologie des Semi-conducteurs pour l'Energétique, Alger, Algeria
Corresponding email: emabobocioiu@yahoo.fr

Keywords: impurities, silica, leaching

We study the Algerian silica from Tirek and Ain Barda deposits as potential raw material intended to photovoltaic cells production.

The samples are examined with optical microscopy, cathodoluminescence, X-Ray fluorescence (XRF) and Raman spectroscopy. The microscopic investigations show the presence of solid inclusions such as rutile, zircon, micas, amphiboles, tourmaline and Fe-oxides in quartz. The XRF results show 96-97 wt.% SiO_2 and display the following average values of the main oxides: 1.83 wt.% Fe_2O_3, 0.2 wt.% MgO, 0.43 wt.% TiO_2, 0.35 wt.% CaO, 0.38 wt.% Al_2O_3, 0.05 wt.% K_2O, 0.13 wt.% ZrO_2. Raman spectroscopy revealed the presence of aqueous fluid inclusions with CO_2; the aqueous phase can also be a source of contamination of quartz with Ca, Mg, Cl and K.

We employ acid leaching process to remove the mineral impurities from the quartz. As chemical reagent we use H_2SO_4 to increase the porosity of the raw material, and HF to dissolve the metal oxides and silicate minerals. Finally, we use the gravimetric separation to remove the residual impurities from the surface of quartz grains.

The acid leaching treatment and the gravimetric separation increase the content of SiO_2 up to 99.68%. This value is optimal to use the quartz from Tirek and Ain Barda deposits as raw material to produce high purity solar grade silicon.

EFFECTS OF MECHANICAL AND THERMAL ACTIVATION METHODS ON REACTIVITY OF CALCAREOUS CLAYS AS PRECURSORS FOR GEOPOLYMERS

D'Elia A.*[1], Pinto D.[1], Eramo G.[1] & Laviano R.[1]
[1] Dipartimento di Scienze della Terra e Geoambientali, Universita di Bari, Italy
Corresponding email: angela.delia@uniba.it

Keywords: clay activation, carbonate-rich clays, geopolymers

The necessity to provide a greener alternative to low durability and high greenhouse gas emission conventional Portland-based binders is highlighting the importance of geopolymers, whose production offers the possibility to employ a wide range of natural and waste alumino-silicate raw materials, through alkaline activation by low-temperature processes.

The attention towards a more sustainable economy has prompted us to the use of locally available carbonate-rich illitic clays to produce geopolymers, as a less investigated field compared with the most widespread studies conducted on pure clays.

After bulk chemical composition, the SiO_2/Al_2O_3 ratio of about 3:1 makes such carbonate-rich clays suitable for geopolymers, although the complex mineralogical composition put a problem about the processing to achieve the geopolymeric synthesis. Previous studies demonstrated that the molar ratio of soluble SiO_2/Al_2O_3 of raw clays can be increased by mechanical and thermal pre-treatments promoting activation of clays. However, the complete thermal activation of natural clay sediments shows limitations, owing to the incompatibility of different clay mineral activation temperatures.

Therefore, the present study focuses on the influence of mechanical, thermal activation in different red-ox conditions (soaking temperatures between 400 and 900°C) and their combination on the reactivity of calcareous clays from Southern Italy, to form geopolymers. Two series of clay samples from Ripatetta e Lucera (FG) were analysed by XRF, XRPD and the amorphisation of mineral phases induced by both grinding and heating have been estimated by XRPD, SEM, grain size analysis and solubility tests in 10% NaOH solutions.

The obtained results showed the effects of grinding and calcination conditions on the amorphisation of clay minerals and the reactivity of carbonates. In particular, five minutes high energy grinding (30 Hz) brought to almost complete amorphisation of phillosilicates and strong decomposition of calcite, whereas the heating of clays in oxidising atmosphere and in mild reducing conditions did not gave significant differences. Furthermore, the micronisation followed by heating resulted to anticipate the formation of Ca-aluminosilicates at 800°C.

In summary, our pre-treatments pointed to two different scenarios: 1) the micronisation gives amorphisation of clay minerals, without Ca-aluminosilicate formation; 2) the heating or the combination of micronisation-heating treatments gives incomplete amorphisation of phillosilicates and formation of Ca-aluminosilicates. The first scenario should be preferred, since the higher solubility of microcrystalline calcite may enhance the formation of CSH in geopolymers. Otherwise, the formation of Ca-aluminosilicates resulting from the pre-treatments of the second scenario will give less predictable results. The pros and cons of the different pre-treatments will be discussed according to the final characteristics of the geopolymer to produce.

INFLUENCE OF ALTERNATIVE MINERALISERS IN TRADITIONAL CERAMICS

Dapiaggi M.*[1], Pavese A.[1], Pagliari L.[1], Maffioli A.[1], Sciascia L.[2], Merli M.[2], Diella V.[3] & Francescon F.[4]
[1] Dipartimento di Scienze della Terra "A. Desio", Università di Milano, Italy
[2] Dipartimento di Scienze della Terra e del Mare, Università di Palermo, Italy
[3] Istituto per la Dinamica dei Processi Ambientali, Consiglio Nazionale delle Ricerche, Milano, Italy
[4] Ideal Standard International, Trichiana (BL), Italy
Corresponding email: monica.dapiaggi@unimi.it

Keywords: amorphous, mineraliser, ceramics

In traditional ceramics, the starting mixture is made of a plastic component, plus a "hard" component (usually quartz), plus something that may act as a flux (usually feldspars), aiding the melting at high temperature, so that to produce a ceramic material with a low porosity. The use of alternative fluxes (such as NaOH and KOH solutions) has been tested on quartz only, on a mixture of quartz and kaolinite, and on a more traditional mixture encompassing quartz, kaolinite and Na-feldspar. For all the mixtures, quartz with different grain sizes was used (4, 10, and 28 μm).

All the samples were mixed with a fixed amount of a 20%wt solution of NaOH or KOH, in order to produce a paste-like material, treated at 1250°C for 6 hours, and then slowly cooled. The final products were analysed by means of X-ray powder diffraction and the mineralogical composition evaluated with the Rietveld-RIR method, as a non negligible amount of amorphous material was present.

The results showed that, for quartz only, the presence of sodium and potassium cations influence the formation of tridymite and cristobalite, as expected. The novelty of this work stands in the in-situ experiments, which showed that tridymite forms at the expense of cristobalite, which is always the first one to form. This is confirmed by ab initio calculations at HF/DFT level, which showed that cristobalite, in presence of sodium and/or potassium, is energetically favoured (Dapiaggi et al., 2015). In the more complex starting mixtures, the equilibrium mullite/amorphous has been carefully studied, using the results of the quantitative determinations. The results show that there is no significant influence of grain size on the equilibrium, and that Na is more effective than K in reducing the residual quartz. Na and K can effectively be used to control the amount of amorphous material present in the final product.

Dapiaggi, M., Pagliari, L., Pavese, A., Sciascia, L., Merli, M., Francescon, F. (2015): The formation of silica high temperature polymorphs from quartz: Influence of grain size and mineralising agents. *J. Eur. Ceram. Soc.*, **35**, 4547-4555.

ANTHROPOZOIC INITIATED ROCK FORMATION IN TIDAL SAND FLATS

Göttlicher J.*[1], Zuber M.[2], Hamann E.[2], Steininger R.[1] & Baumbach T.[2]
[1] Angstromquelle Karlsruhe, Karlsruhe Institut für Technologie, Germany
[2] Institut für Photonenforschung und Synchrotronstrahlung, Karlsruhe Institut für Technologie, Germany
Corresponding email: joerg.goettlicher@kit.edu

Keywords: Anthropocene, metal waste, concretions

During the last 6 years more than 30 sand concretions have been collected from tidal flats of an East Frisian North Sea island. After sampling under ambient conditions their black color changes to brown within days to months. Some of the concretions remain consolidated, others develop cracks and become brittle. Sizes vary up to several tens of cm. Shapes range from isometric, nodular to laminated. It is assumed that a nucleus is required to form the concretions (Göttlicher & Steininger, 2012a, 2012b). X-ray micro-computer tomography (µ-CT) has been applied prior to cutting to get a 3D image of the inner part and to check for ammunition content because of former military activities nearby the sampling site (Donner, 2014). Almost all of the concretions have a core ranging from irregular shaped metal pieces, sheets, rods to in one case a steel sheath. Two cores were identified as ammunition: A contact fuze and a complete 13 mm cartridge. For the latter the year of production has been reconstructed from the headstamp to (19)38 constraining the max. age of this concretion to ca. 80 y. Both samples had finally to be eliminated by explosive ordnance technicians. Corrosion of metal cores up to complete decomposition is indicated by a lowering of the absorption contrast. The hypothesis is that sea water dissolves ions, mainly Fe from the disposed metal. Fe precipitates depending on *p*H, Eh conditions in different chemical forms serving as cement for sand grains and shell fragments. Concretions may grow as long as core metal is available and diffusion through the increasing mantle thickness maintains, meaning that its max. size is reached when the nucleus is completely "dissolved". A minority of concretions without a core is discussed to be fragments of larger units. Light microscopy and µ-XRF elemental distribution demonstrate the intergrowth of sediment particles by Fe containing cement. Laboratory XRD results in quartz, calcite, aragonite and siderite. Synchrotron µ-XRD enabled to identify akaganeite in brownish cement. Fe *K* XANES data match also with an akaganeite reference, and result for black surface layers in a mixture of Fe^{3+} and Fe^{2+} compounds. S K XANES spectra show sulfate, and in the black layers additionally S^{2-} proving reducing conditions. This study demonstrates that metal waste in tidal flats deposited by human beings act as nuclei for sand concretions, and hence, is an example of anthropozoic initiated rock formation. Such concretions may become part of a sedimentary rock unit when diagenetic processes affect tidal flats on a larger scale. Ongoing work will include other regions of tidal flats in the North Sea and worldwide to get data on distribution and frequency of concretions. 7% of all coastal shelf areas belong to tidal flats (Stutz & Pilkey, 2002) and can in principle be affected if metal waste is present and conditions for corrosion and cement formation are adequate. Further characterization will comprise sample handling under inert atmosphere, test for microbial contributions, chemical analyses of mantle and metal core to get information on origin of nuclei and age of concretions. High resolution µ-CT will be used to determine matrix/sediment grain ratios, volume/mass data of the nuclei and degrees of corrosion to estimate max. size of a concretion that can develop from a given nucleus.

Donner, S. (2014): Vermintes Gewässer. *Natur*, **01-14**, 66-69.

Göttlicher, J. & Steininger, R. (2012a): Characterization of S-containing concretions from the North Sea. Goldschmidt Conference, 24-29 06 2012, Montreal, Canada.

Göttlicher, J. & Steininger, R. (2012b): Iron and sulfur containing sandy aggregates from the North Sea. European Mineralogical Conference, 2-6 09 2012, Frankfurt, Germany.

Stutz, M.L. & Pilkey, O.H. (2002): Global distribution and morphology of deltaic barrier island systems. *J. Coast. Res*., **36**, 694-707.

CORRELATIONS BETWEEN CALCITE MICROSTRUCTURE AND ORDINARY PORTLAND CEMENT CLINKER RAW MEALS BURNABILITY

Galimberti M.*[1], Marinoni N.[1], Della Porta G.[1] & Marchi M.[2]
[1] Dipartimento di Scienze della Terra "A. Desio", Università di Milano, Italy
[2] Italcementi Group S.p.A., Bergamo, Italy
Corresponding email: matteo.galimberti@unimi.it

Keywords: cement clinker, calcite, X-ray powder diffraction

Limestone rock is the main constituent of a standard raw meal for ordinary Portland cement (OPC) clinker production. The OPC manufacturing process has a remarkable environmental impact mainly due to the thermal dissociation of carbonates and the kiln operating temperature (Taylor, 1990; Van Oss & Padovani, 2002); hence, a better comprehension of the whole clinkerization process is essential to save energy, reduce greenhouse gases emissions and increase the kiln output, which are the main aims of modern cement industry. The various aspects of limestones calcination have already been widely investigated; several authors clarified the kinetic mechanisms driving calcination (Lech, 2006; Rodriguez-Navarro et al., 2009), whereas others focused on the thermal decomposition of carbonates used for clinker and lime production, paying particular attention to their petrography (Soltan et al., 2012; Alaabed et al., 2014). Starting from here, the present study aims to go a step forward, by combining petrographic observations and XRPD analyses to investigate how the limestone microfabric and the calcite microstructure affect the progress of the clinkerization. In this light, eight natural limestones from different depositional environments were sampled; preliminarily, a chemical, mineralogical and petrographic characterization by X-ray fluorescence (XRF), X-ray powder diffraction (XRPD) and optical microscopy (OM) was carried out; then, once finely ground below 80 µm, each limestone was dry-mixed with clay minerals and silicon and iron oxides to prepare suitable raw meals for clinker production. These mixtures were moulded into pellets and heated in a laboratory furnace at 1000, 1100, 1200, 1300, 1350, 1400 and 1450°C, respectively, to better observe the evolution of the crystalline phases as a function of temperature (*ex situ* XRPD) and also the final clinker microstructure (Scanning Electron Microscopy). The results attested that the depositional and diagenetic texture of the rock, jointly to the calcite crystals microstructure, affects the raw meal burnability in terms of calcite decomposition temperature, crystalline phases growth and distribution and overall clinker morphology. These findings have significant implications because highlight that it is advisable to also consider the petrography of the limestones during their selection, without focusing only on their bulk chemical composition.

Alaabed, S., Soltan, A.M., Abdelghany, O., Amin, B.E.M., El Tokhi, M., Khaleel, A., Musalim, A. (2014): United Arab Emirates limestones: impact of petrography on thermal behaviour. *Mineral. Petrol.*, **108**, 837-852.

Lech, R. (2006): Thermal decomposition of limestone: Part 3: kinetic curves. *Silic. Industr.*, **71**, 143-148.

Rodriguez-Navarro, C., Ruiz-Agudo, E., Luque, A., Rodriguez-Navarro, A.B., Ortega-Huertas, M. (2009): Thermal decomposition of calcite: Mechanism of formation and textural evolution of CaO nanocrystals. *Am. Mineral.*,**94**, 578-593.

Soltan, A.M., Kahl, W.A., Wendschuh, M., Hazem, M. (2012): Microstructure and reactivity of calcined mud supported limestones. *Miner. Process. Extr. Metall.*, **121**, 5-11.

Taylor, H.F.W. (1990): Cement Chemistry. Academic Press, London, 475 p.

Van Oss, H.G. & Padovani, A.C. (2002): Cement manufacture and the environment: Part I: Chemistry and technology. *J. Ind. Ecol.*, **6**, 89-105.

SYNTHESIS AND CHARACTERIZATION OF SPECIAL CEMENTS WITH REDUCED CO_2-EMISSION BASED ON NEW CLINKER MINERALS USING MINERALIZERS

Galluccio S.*[1] & Pöllmann H.[1]

[1] Fachgebiet Mineralogie-Geochemie, Institut für Geowissenschaften und Geographie, Martin-Luther-Universität Halle-Wittenberg, Germany

Corresponding email: sabrina.galluccio@geo.uni-halle.de

Keywords: special cements, mineralizers, CO_2-reduction

The cement and concrete industry causes approximately 5% of anthropogenic CO_2-emissions of which 70% are due to the used raw materials (Pöllmann, 2015). For the local replacement of the commonly used Portland cement, different special cement types are investigated whose clinker minerals release less CO_2 in their production.

New cement types as belite aluminate cement (Porsal cement: belite, yeélimite, calciumaluminate, mayenite), ferrite cement (Ferrari cement: alite, brownmillerite) and sulfobelite cement (belite, yeélimite, brownmillerite) are produced. By the use of CO_2-free raw materials like secondary raw materials (e.g. laterite), new clinker minerals are synthesized. The new clinker minerals can also be formed at lower temperatures in the presence of mineralizers like calciumsulfate, borate minerals (colemanite) and fluoride minerals (fluorspar).

Fluoride cements as belite fluoroaluminate-, belite fluoroaluminate ferrite and belite fluorosulfoaluminate cement will be synthesized and their properties and phase compositions will be determined. These cements will be formed by the addition of fluorspar to the raw meals. Using additional mineralizers the clinkers can be produced at lower temperatures, the viscosity of the melt is lowered and hydration properties of the clinker are influenced. Besides lower energy consumption, a reduction in CO_2 emissions will be achieved by forming CO_2 reduced phases ($C_{11}A_7 \cdot CaF_2$: 0.34 g CO_2 per g phase, belite: 0.51 g CO_2 per g phase, yeélimite: 0.22 g CO_2per g phase, brownmillerite: 0.32-0.41 g CO_2 per g phase). For this reason the phase relations in the three systems CaO - Al_2O_3 - SiO_2 - CaF_2 (/ $CaBO_{2,5}$/ $CaSO_4$) and the binding of fluoride to the solids at different temperatures will be investigated.

Pöllmann, H. (2015): Mineralogical strategies to reduce CO_2 in the fabrication of alternative cements. IBAUSIL, conference report, **1**, 111-129.

RARE METAL AND REE DEPORTMENT IN ALKALINE GRANITES AND SYENITES: CHANCES AND CHALLENGES FOR GEOMETALLURGY

Gronen L.[1], Sindern S.*[1], Meyer M.[1] & Hellmann A.[1]

[1] Lehrstuhl für Angewandte Mineralogie und Lagerstättenlehre, Rheinisch-Westfälische Technische Hochschule Aachen, Germany

Corresponding email: sindern@rwth-aachen.de

Keywords: geometallurgy, alkaline rocks, rare metals

Alkaline granites and syenites (e.g., Strange Lake/Canada, Amis Complex/Namibia, Khalzan-Burged/Mongolia, Khibina/Russia) host deposits of REE, Y, Nb, Ta, Zr or U, which formed in multiphase processes. Often, significant hydrothermal overprint of magmatic mineral associations and textures can be observed. Consequently, complex and diverse mineral assemblages as well as textural heterogeneity are characteristic features of such deposits. This represents an obstacle to economic mining operations and it would appear that deposits in which a rare metal or REEs are preferentially concentrated in a single mineral phase have a competitive advantage. However, owing to the polymetallic character of these deposits, different commodity targets for the mineral industry are available in a single deposit. In this case mining of a rare metal or REEs as by-product of additional or major metals has a significant price advantage since extraction costs are shared by the bundle of metals mined. Furthermore, mining of polymetallic deposits may allow flexible response to market demands and could lead to enhanced robustness of a mining operation with respect to variable commodity prices.

To become technically and economically viable, beneficiation strategies have to be developed and evaluated, which are optimized for each of the different domains of a polymetallic rare metal and REE deposit. The cross-discipline geometallurgical approach represents a key to successful beneficiation of such granite hosted deposits because it integrates mineralogical, mining engineering and processing knowledge as well as environmental and economic information to define such domains and to define attributes indicative of metal deportment and relevant ore properties in each domain (Lund & Lamberg, 2014; Hunt & Berry, 2015).

In a study on different alkaline granites and syenites conducted at the Klockmann-Laboratory of the Institute of Applied Mineralogy and Mineral Deposits (RWTH Aachen University) quantitative mineralogical parameters are obtained using automated mineralogy (QEMSCAN), XRD, XRF, LA-ICP-MS, electron-microprobe and polarization microscopy. The parameters *host-rock lithology* and *mineral-association* as well as a group of *critical quantitative mineralogical attributes* (e.g., grades of rare metals and REE, grades of ore minerals, concentration of indicator elements Al and F, concentration of potential penalty elements, abundance of magnetic minerals, textural parameters) are evaluated with respect to their geometallurgical relevance for rare metal and REE deposits hosted by alkaline rocks.

Hunt, J. & Berry, R. (2015): Data collection and testing for geometallurgy: Getting more from drill core. Proc. 13th biennial SGA Meeting 2015, 24-27 August, Nancy, France, 1411-1413.

Lund, C. & Lamberg, P. (2014): Geometallurgy – A tool for better resource efficiency. *Eur. Geol.*, **37**, 39-43.

LITHOLOGICAL UNITS AND SN DEPORTMENT OF A COMPOSITIONALLY COMPLEX SKARN ORE (HÄMMERLEIN, ERZGEBIRGE, GERMANY)

Kern M.*[1], Kästner J.[2] & Gutzmer J.[1-2]
[1] Helmholtz-Institut Freiberg für Ressourcentechnologie, Germany
[2] Institut für Mineralogie, Technische Universität Bergakademie Freiberg, Germany
Corresponding email: m.kern@hzdr.de

Keywords: skarn, cassiterite, tin

The Hämmerlein seam is part of the world class Tellerhäuser deposit in the Erzgebirge, Germany, and represents a compositionally complex polymetallic Sn-In-Zn skarn. Current resources amount to 100000 t Sn at a cut-off grade of 0.2 wt. %. In addition, 2100 t of In and 270000 t of Zn have been estimated (Treliver Minerals, 2015). In the late 1970s, 50000 t of ore from the Hämmerlein seam were mined and processed experimentally in a pilot plant, but grade and recovery remained below expectations. Cited reasons for poor recovery the complex mineralogy and variability in grain sizes of valuable minerals (Schuppan & Hiller, 2012). The predicted rise in global Sn consumption and limited availability of high grade deposits (Deutsche Rohstoffagentur, (2014) render the Tellerhäuser deposit an interesting exploration target (Treliver Minerals, 2015).

A consortium of German research institutions currently conducts new beneficiation experiments on the Hämmerlein orebody. Determination of the Sn deportment and the characterization of the different lithological (skarn) units are the first steps in this process. For this purpose, three transects in the central part of the Hämmerlein orebody were mapped and a suite of hand specimen collected to represent all relevant lithotypes within the studied part of the orebody. Thin sections were prepared and analyzed using the Mineral Liberation Analyzer (MLA) to obtain quantitative data about mineralogy, mineral grain sizes, intergrowths, and associations. The remaining material of the hand specimen was crushed to 99% < 250 µm. This granular material was split to produce grain mounts for further mineralogical studies and in order to prepare sample powders for geochemical analysis.

The Hämmerlein skarn orebody can be subdivided into the following three macroscopically distinct lithotypes: 1. magnetite-dominated (40-80 wt.% magnetite), 2. sulphide-dominated (> 20 wt.% sphalerite), and 3. silicate-dominated (> 60 wt.% silicates). In the silicate-dominated unit a gradual transition of different silicate minerals enables further discrimination of a chlorite-rich, an amphibole-chlorite-rich, an epidote-pyroxene-rich and a garnet-rich subunit. The hanging and footwall are best described as mica schist and gneiss, respectively.

The primary host mineral for Sn is cassiterite (SnO_2) with grain sizes between 1 µm and 1 mm. Some of the cassiterite has fibrous crystal habit. Significant amounts (ca. 1.4 wt.%) of coarse-grained (50 µm to 1 mm) cassiterite is present in the chlorite subunit. The amphibole-chlorite subunit contains an average of 0.3 wt.% cassiterite. Samples from other parts of the Hämmerlein orebody indicate significant amounts of cassiterite in the magnetite- and the sulphide-dominated lithotypes as well.

Stokesite ($CaSnSi_3O_9 \cdot 2H_2O$) is the second most abundant Sn mineral. It appears in fine-grained aggregates in the amphibole-chlorite subunit and in the magnetite-dominated ore type reaching concentrations of ca. 0.1 wt.%. Notable Sn concentrations were detected by WDX in some examples of titanite (≤ 17 wt.%), epidote (≤ 3.5 wt.%), amphibole (≤ 1.5 wt.%), garnet (≤ 1.8 wt.%), and iron oxides (≤ 1.8 wt.%).

Our preliminary results illustrate that the Sn mineralisation of the Hämmerlein skarn is indeed very complex. Cassiterite dominates, but other minerals (most notably stokesite) do contribute significantly to the deportment. Further studies will aim to quantify the variability of deportment and other resource characteristics, in order to guide mineral processing test work.

Deutsche Rohstoffagentur (2014): Zinn – Angebot und Nachfrage bis 2020. DERA Rohstoffinformationen 20.

Schuppan, W. & Hiller, A. (2012): Die Komplexlagerstätten Tellerhäuser und Hämmerlein. Oberbergamt Sachsen, Bergbaumonografie, 17, 157 p.

Treliver Minerals (2015): Press Release. Tellerhäuser Project Resource Statement. http://www.anglosaxony.com/assets/file/Press%20Release%20Mar%202015.pdf (last visit: 2016-05-09)

HIGH-*P* BEHAVIOR OF ZEOLITES IN "PENETRATING" FLUIDS: RECENT INSIGHTS AND NEW OPPORTUNITIES FROM *XPRESS*, THE HIGH-*P* DEDICATED DIFFRACTION BEAMLINE AT ELETTRA

Lotti P.*[1-2], Joseph B.[1], Gatta G.D.[2], Comboni D.[2], Lausi A.[1], Merlini M.[2] & Pastero L.[3]
[1] Elettra Sincrotrone Trieste, Italy
[2] Dipartimento di Scienze della Terra "A. Desio", Università di Milano, Italy
[3] Dipartimento di Scienze della Terra, Università di Torino, Italy
Corresponding email: paolo.lotti@elettra.eu

Keywords: zeolites, synchrotron, high pressure

The high-pressure behavior of zeolites when compressed in potentially "penetrating" fluids, i.e. those whose molecules can be intruded into the zeolitic structural micropores, has recently been a subject of growing research interest. Pressure-mediated intrusion of molecules can induce changes in the physical and chemical properties of zeolites, thus offering an excellent tool for the tailoring of the properties of these industrially relevant materials. *In situ* experiments on SiO_2-ferrierite (FER; Lotti et al., 2015) and $AlPO_4$-5 (AFI; Lotti et al., 2016) zeolites, conducted in diamond anvil cells (DACs) using "penetrating" pressure-transmitting fluids, showed that the*P*-induced intrusion of molecules can be readily recognized from the synchrotron single-crystal and powder diffraction data. In case of FER, the complex patterns of phase-transitions at increasing pressure reveal the intrusion, whereas for AFI, the drastically different compressibilities provide evidence of this process. In this scenario, recently commissioned dedicated high-pressure diffraction beamline *Xpress*, at the Elettra synchrotron light-source (Trieste, Italy), represents a new facility for high-pressure investigations in the field of geomaterials, using X-ray diffraction. *Xpress* is part of a scientific partnership between Italy and India (Indian Institute of Science, Bangalore). At *Xpress*, a liquid nitrogen cooled silicon single crystal, cut along the [111] direction, intercepts the beam from multipole superconducting wiggler source and deflects it at a fixed energy of 25 k*e*V. The beam is focused using a toroidal mirror of 1.4 m length and 2.9 mrad grazing angle. The mirror is Pt coated to achieve 80% reflectivity at 25 k*e*V. Focused beam from the mirror is further optimized by collimators (ranging from 30 to 200 micrometer in diameter), in order to have intense and well defined monochromatic beam for the HP-XRD experiments. On-line pressure monitoring is achieved through a ruby fluorescence microscope. The present experimental stage is equipped to host different kinds of DACs, in order to permit room-temperature - high-pressure experiments in the pressure range 0-50 GPa. An image plate MAR345 with a controllable linear movement along the beam direction is available for the collection of the diffraction pattern. The setup for hosting *in-situ* high-*P* single-crystal X-ray diffraction experiments is under development and will be available for users in the near future.

Lotti, P., Arletti, R., Gatta, G.D., Quartieri, S., Vezzalini, G., Merlini, M., Dmitriev, V., Hanfland, M. (2015): Compressibility and crystal-fluid interactions in all-silica ferrierite at high pressure. *Microp. Mesop. Mater.*, **218**, 42-54.

Lotti, P., Gatta, G.D., Comboni, D., Merlini, M., Pastero, L., Hanfland, M. (2016): $AlPO_4$-5 zeolite at high pressure: Crystal-fluid interaction and elastic behavior. *Microp. Mesop. Mater.*, **228**, 158-167.

PLATY LIMESTONE AS CHARACTERISTIC NATURAL AND CULTURAL HERITAGE ALONG THE ADRIATIC KARSTIC COAST

Novak M.*[1], Jež J.[1], Šolc U.[1] & Bavec M.[1]
[1] Geological Survey of Slovenia, Ljubljana, Slovenia
Corresponding email: matevz.novak@geo-zs.si

Keywords: platy limestone, cultural landscape, RoofOfRock project

In the Adriatic area, Cretaceous limestone as the primary building material has played a crucial role in constructing a common human history. One of limestone types in particular, the platy limestone, is one of the most recognizable linking elements of the cultural landscape along the Adriatic karstic coast. It has been used as roof tiling, for construction of dry walls, shepherd cottages and similar objects. Besides being an important element of cultural heritage, it is also important as natural heritage, with often rich and diverse fossil fauna and in particular rare, but well-preserved vertebrate fossils.

For centuries it was excavated in backyards or in small delves in the near vicinity of the villages. Today, there are a number of reasons why this cannot be done in the same way. Natural preservation and conservation have gained importance, as have safety standards and other regulations related to mining and extraction. Even those who in good faith and with the best intentions want to renovate or build a house in the traditional manner, lack knowledge on how to proceed and have no information available, no legal basis, nor building material legally accessible.

Solving the conflict between use of platy limestone for maintenance of cultural heritage and its preservation as natural heritage has been the objective of the RoofOfRock Project (Novak et al., 2015; www.roofofrock.eu). It was implemented under the Adriatic IPA CBC Programme. Its goal was to establish joint platform for platy limestone sustainable use, preservation and promotion, to create the relevant guidelines and to upgrade capacities in preserving such common natural and cultural heritage along the karstic coast of the Adriatic Sea.

Interdisciplinary research of appearance, geological characteristics, use and preservation of platy limestone over the area between Trieste and Dubrovnik has been carried out. The basis for the study was the overview of all important types of limestone used, list of the most important limestone quarries and geological map (1:250,000) of building limestone with estimated exploitation potential. The detailed geological investigation was conducted resulting in a map of occurrence of platy limestones at a scale of 1:50,000 and definition and classification of platy limestones according to their sedimentary, stratigraphic and paleontological characteristics. Estimation of their quality, quantity and exploitation potential was prepared as well (Korbar et al., 2015). 25 selected showcase objects were studied in detail. For each a geological census of all types of limestones used for various architectural elements was made. Emphasis was put on platy limestones, for which source areas were studied. Findings indicate that along the Adriatic karstic coast highly diverse platy limestone types were used. They differ in origin and lithological characteristics as well as in quality and possibility for extraction of plates of different sizes and thicknesses.

Korbar, T., Jež, J., Glamuzina, G., Fuček, L., Jurkovšek, B., Matičec, D., Barudžija, U., Krivic, M., Kurtanjek, N. (2015): Platy limestones in the Adriatic belt of the Dinaric karst region. *in "*Book of abstracts", M. Horvat, L. Wacha, eds., Hrvatski Geološki Institut, Zagreb, 132 (in Croatian).

Novak, M., Biolchi, S., Čebron Lipovec, N., Jež, J., Peternelj, K., Šolc, U. (2015): Roof of rock. Geological Survey of Slovenia, Ljubljana and Neretva Regional Development Agency DUNEA LLC, Dubrovnik, 183 p.

DETERMINATION OF RESISTANCE TO BENDING OF DIMENSION STONES: FIRST RESULTS OF AN EXPERIMENTAL STUDY ON A TECHNOLOGICAL AND TESTS SPECIMENS WITH JOB DIMENSIONS FOR PAVING

Signori G.*[1] & Prodomi A.[1]
[1] Centro Servizi Marmo – Laboratorio Prove, Volargne (VR), Italy
Corresponding email: grazia.signori@gmail.com

Keywords: technical properties, flexural strength, job size specimens

Among the technical properties of dimension stones, the flexural strength is one of the most important characteristics to be determined for the preliminary assessment of the compatibility of a litho-type to the specific intended use (e.g., Wittke, 1990; Winkler, 1994; Siegesmund & Snethlage, 2014).

The current test method, according to standard EN 12372 (2006), provides for the execution of the test in the laboratory for the determination of the flexural strength of specimens from 25 to 100 mm thick according to two “modes”: the identification mode and the technological “mode”, i.e., with specimens with the job finish but not with the real job sizes.

This means that it is not considered as a discriminating step the test of the true elements for vehicular paving. As such an intended use implies considerable loads, fatigue cycles and stress of both the stone elements and the system/stratigraphy once in place, provided bedding was correctly designed, the durability of the pavement may depend on the correct sizing of the elements.

What and how preliminary experimental tests on job specimens can be performed in laboratory?

This preliminary experimental study shows that the execution of tests on job specimens is essential to experimentally measuring the proper operating thickness of the stone elements thus avoid inappropriate choices of shape and thickness.

EN 12372 (2006): Natural stone test methods. Determination of flexural strength.
Siegesmund, S. & Snethlage, R. (2014): Stone in architecture. Springer, Berlin, 552 p.
Winkler, E.M. (1994): Stone in architecture. Springer, Berlin, 315 p.
Wittke, W. (1990): Rock mechanics. Springer, Berlin, 900 p.

QUANTITATIVE ANALYSIS OF CRYSTAL/GRAIN SIZES AND THEIR DISTRIBUTIONS IN 2D AND 3D AIMED TO PREDICTING TECHNICAL PROPERTIES OF DIMENSION STONES

Signori G.*[1], Zucali M.[2], Migliazza R.[2], Lucchelli A.[2] & Sturaro E.[2]
[1] Centro Servizi Marmo – Laboratorio Prove, Volargne (VR), Italy
[2] Dipartimento di Scienze della Terra "A. Desio", Università di Milano, Italy
Corresponding email: grazia.signori@gmail.com

Keywords: fabric orientation, technical properties, "unconventional" fabric

Correlations between technical properties and anisotropy of rocks as dimension stones are well known (e.g., Wittke, 1990; Winkler, 1994; Siegesmund & Snethlage, 2014). Fabric and microstructure are main keys for rock characterization and their study and analyses can lead to the identification and quantification of important commercial parameters, such as mechanical strength, manufacturing behavior and weathering resistance.

Nevertheless either European harmonized product standards and ASTM standards call for a petrographic description according to test method EN 12440 (2007) and ASTM C 1721 (2015), which both require a traditional, brief and concise petrographic analysis.

This contribution proposes to combine the common petrographic study of dimension stones with some further analyses, which are simple but "unconventional" for either the manufacturers or standard test methods (both EN and ASTM) such as:

- Microstructural analysis by optical microscopy;
- 2D and 3D fabric analyses by optical microscopy;
- Anisotropy analyses compared with mechanical properties from image analysis;
- Minero-chemical and crystallographic analyses;
- Determination of Knoop hardness;

with the objective to identify the analyses predictive of the technical characteristics of the several dimension stones types.

Such predictive methods could be very useful, especially for dimension stones recently placed on the market, for which a very few information is available relevant to their physical and mechanical characteristics, manufacturing properties, durability and behaviors after application.

What's more, the listed "unconventional" analyses, especially 2D and 3D fabric analyses revealed that some apparently isotropic rocks at meso- and micro-scale observation, turned out to be faintly oriented, thus likely explaining some peculiar behaviors and properties.

ASTM C 1721 (2015): Standard guide for petrographic examination of dimension stone.
EN 12407 (2007): Natural stone test methods. Petrographic examination.
Siegesmund, S. & Snethlage, R. (2014): Stone in architecture. Springer, Berlin, 552 p.
Winkler, E.M. (1994): Stone in architecture. Springer, Berlin, 315 p.
Wittke, W. (1990): Rock mechanics. Springer, Berlin, 900 p.

INVESTIGATION AND PREDICTION OF LIME AGGLOMERATION, STICKING TENDENCY, AND BLOCKS FORMATION IN VERTICAL DOUBLE SHAFT REGENERATIVE KILNS FOR THE PRODUCTION OF HIGH-CALCIUM OR MAGNESIUM-RICH QUICKLIME

Vola G.*[1-2], Cruciani G.[2], Rodeghero E.[2], Natali C.[2], Bianchini G.[2] & Brignoli G.[3]
[1] Cimprogetti SRL Lime Technologies, Dalmine (BG), Italy
[2] Dipartimento di Fisica e Scienze della Terra, Università di Ferrara, Italy
[3] Assing SpA, Monterotondo (RM), Italy
Corresponding email: gabriele.vola@gmail.com

Keywords: quicklime production, sticking tendency, overburning test

This contribution reports preliminary results on the research activity performed on 25 carbonate rocks, including mud-supported, and grain-supported limestones, diagenetic dolomites, and granoblastic marbles, to evaluate their sticking tendency, and occasional melting at 1300°C, which could occur during the calcination process in vertical double shaft regenerative kilns for the industrial production of high calcium or magnesium-rich quicklime. Samples, made available to Cimprogetti by different worldwide lime producers, have been characterized by means of a complete set of physical (MIP), chemical (WD-XRF), mineralogical (QPA-XRD), petrographic (OM), and thermal analyses (TG-DTG) performed either on powdered rocks, with the only exception of petrographic and porosimetric analyses, or on their insoluble rests. A particular attention was paid to the extraction of the insoluble rest by means of a weak acid attack at high temperature, followed by a centrifugation in deionized water using a spin-dryer device for purifying the sample. This procedure, specifically designed for clay minerals and organic matter analysis, permitted to concentrate some grams of insoluble rest from very pure carbonate samples. Moreover the so-called "overburning test" at 1300°C, according to the internal test method invented by Cimprogetti, has been performed to simulate and predict the lime agglomeration at the highest temperature of the kiln (Vola & Sarandrea, 2014). The quantitative phase analysis (XRD-QPA) according to the Rietveld method on lime blocks obtained from the overburning test, pointed out the formation of predominant lime (CaO), associated with significant content (3-6%) of tricalcium silicate (Ca_3SiO_5 or alite), and dicalcium silicate (Ca_2SiO_4 or belite). More rarely, tricalcium magnesium silicate ($Ca_3Mg(SiO_4)_2$ or merwinite) has been observed too. The presence of such accessorial calcium silicates indicates that chemical reaction between the lime and clay minerals took place, pointing out an early stage of incomplete clinkerization process. Anyway, some blocks of burnt lime with a high sticking tendency (> 40%) do not present accessorial silicates, suggesting the lime agglomeration must be also related to other apparently not so obvious chemical or physical factors. Ongoing analyses, including the screening of the organic carbon (Cwt.%, $\delta^{13}C‰$), ultralight elements (lithium, boron), and halogens (fluorine, chlorine) by means of isotope ratio mass spectrometry (IRMS), inductively coupled plasma mass spectrometry (ICP-MS), and wet chemistry titration, will help to further clarify the key factor for understanding and predicting the lime agglomeration and blocks formation at the highest temperature of the kiln, as suggested by previous authors (Elsen et al., 2011).

Elsen, J., Mertens, G., Snellings, R. (2011): Portland cement and other calcareous hydraulic binders: history, production and mineralogy. *EMU Notes Mineral.*, **9**, 452-457.

Vola, G.. & Sarandrea, L. (2014): Investigating and predicting blockages. World Cement, October 2014, 85-92.

THE EFFECT OF ENVIRONMENTAL INFLUENCES AND CUSTOMARY CLEANSERS ON NATURAL STONES

Welling M.[1], Giehl C.[1], Kögler R.[2], Beermann O.[1] & Duesterhoeft E.*[1]
[1] Institut für Geowissenschaften, Christian-Albrechts-Universität Kiel, Germany
[2] Deutsches Naturstein-Archiv, Wunsiedel, Germany
Corresponding email: ed@min.uni-kiel.de

Keywords: natural stone, customary cleanser

Natural stones are aesthetic rocks that are widely used, e.g., as floor tile, facades or interior decoration. Hence, flaws or damages due to weathering (Siegesmund et al., 2002) or by treatment with corrosive cleansers provoke pecuniary losses. In co-operation with the German Natural Stone Archive in Wunsiedel, which owns the world's largest collection of natural stones, alteration of 22 selected stones upon exposure to UV-light, water, and customary cleansers were investigated. Samples span a wide range, i.e., magmatic and metamorphic rocks (felsic to ultramafic), and sedimentary rocks (silicic to calcareous). Within the present study, exposure to UV light up to 72 h did not detectably alter the rocks, while one-week exposure to rain and distilled water results in minor macroscopic flaws. Dramatic flaws were observed after 24 h using acid cleansers.

Static solution (cleanser or water)-rock interaction experiments were performed at constant solution-to-rock-mass ratio (20:1) for up to 168 h. Uniform 2x2x1 cm rock pieces were exposed to distilled water (*p*H ~ 5.6), rain water (*p*H ~ 6.1), acid- (*p*H ~ 0.4) and alkaline basic-cleanser (*p*H ~ 11.1), nitrate remover (*p*H ~ 0), rust remover (*p*H ~ 8.6), headstone cleaner (*p*H ~ 12.0), and solvent-based oil stain remover. During the experiments, *p*H-values (25°C) periodically monitored served as an indicator for the extent of solution-rock cation-exchange reactions. After experiments the rock pieces were studied using polarization microscopy.

As expected calcitic rocks strongly dissolved into acid cleansers as confirmed by rock mass loss (up to 50% after 24 h) and by increasing solution *p*H-values. However, treatment of serpentinites and foid-bearing rocks causes a similar rise in solution *p*H but only slight rock mass losses. Alkaline cleanser intensified blue color of the "Azul Bahia" sodalite-foyaite, whereas application of the colorant-bearing nitrate remover results in dissolution of sodalite and discoloration (yellow). Strong changes in color, i.e. bleaching of "Kashmir White" granulite to yellow, and staining of "Marron Monichque" foyaite to red, were also observed using the colorant-bearing nitrate remover. Serpentinization of magnesium-rich olivine by acid cleansers resulted in bleaching of the formerly dark rocks. Additionally, our experiments show that in particular SiO_2-undersaturated rocks react with the alkaline rust remover, while manufacturers only declare for careful usage with iron-bearing rocks. Obviously, cleanser additives may also induce undesirable reactions affecting the aesthetics.

The commonly misleading trade names of natural stones (i.e., granite for all rocks with magmatic texture) bear fatal misapplication of customary cleansers. Consequently, appropriate application requires knowledge of experts on paragenesis, mineral composition (e.g., anorthite component of plagioclase, due to different dissolution rates of feldspar endmembers; Franke, 2009) and their individual response to cleanser treatment.

Franke, W.A. (2009): The durability of rocks – Developing a test of rock resistance to chemical weathering. *Am. J. Sci.*, **309**, 711-730.

Siegesmund, S., Weiss, T., Vollbrecht, A. (2002): Natural stones, weathering phenomena, conservation strategies, and case studies. *Geol. Soc. London*, *Spec. Publ.*, **205**, 498 p.

INVESTIGATION ON THE STABILITY FIELD OF FCAM-I, AN ISO-STRUCTURE TO SFCA-I

Zöll K.*[1], Kahlenberg V.[1] & Tropper P.[1]
[1] Institut für Mineralogie und Petrographie, Universität Innsbruck, Austria
Corresponding email: Klaus.Zoell@uibk.ac.at

Keywords: stability of FCAM-I (SFCA-I), iron ore sinters, buffered and unbuffered experiments

So-called SFCA-phases are an important constituent of iron ore sinters, which are the preferred feedstock in most of the European blast furnaces (Matsui et al., 2003). In about 70% of the world's steel production sintering is an important step for the initial treatment of the iron ores and SFCA (silicoferrite of calcium and alumina) represents the main bonding phase between the relict ore particles. According to Kalenga & Garbers-Craig (2010), the physico-chemical properties of iron ore sinters depend noticeably on the MgO content, which is due to the addition of Mg-containing fluxes such as dolomite or fused MgO. The MgO concentration, for example, is positively correlated with the abrasion and tumble indices as well as the coke rate.

Based on these results, our own investigations focused on the influence of MgO on the formation of SFCA starting with the synthesis of pure silicon-free SFCA-I with a magnesium substitution of one atom per formula unit (so-called FCAM-I, an iso-structure to SFCA-I). Preparation of FCAM-I was based on solid-state reactions. In a first test series, the pellets were sintered *in air* in the temperature region between 1200 and 1400°C. The mixtures consisted of 55.2% of Fe_2O_3, 21.2% Al_2O_3, 2.8% MgO and 20.8% of $CaCO_3$ (mol%) corresponding to a hypothetical composition of $Ca_3MgFe_{10}Al_6O_{28}$. The obtained samples were characterized by EMPA, single-crystal and powder X-ray diffraction.

The evaluation of secondary electron images as well as wavelength dispersive analysis proofed the success of the synthesis. Already in the 1200°C experiment pure polycrystalline FCAM-I with crystallite sizes up to 10 mm were formed. A Lebail fit of the observed X-ray powder diffraction data compared well with the unit cell parameters determined for FCAM-I from a single-crystal diffraction study (Manninger & Kahlenberg, 2015).

The stability field of the FCAM phases is not only controlled by temperature and the bulk composition of the system, but is also influenced by oxygen fugacity. Actually, the Fe^{2+}- content is also important factor for the stability of the FCAM-phases. The increase of Fe^{2+} in FCAM-I is almost directly proportional to increasing temperature. The investigations disclosed that iron(III) oxide starts to reduce to iron(II) oxide at temperatures between 1200 and 1400°C. Concurrently, at 1300°C the FCAM-I phase breaks down forming a complex assemblage of new phases that has to be studied in more detail. Finally, the FCAM-I phase disappear completely at temperature above 1400°C.

Furthermore, a series of experiments was made using a platinum capsule-in-capsule geometry with a controlled oxygen fugacity via the hematite-magnetite buffer. A higher oxygen fugacity favours the stability of FCAM-I and shifts the breakdown of this phase to significant higher temperatures. In comparison with the experiments in air, the FCAM-I phase is totally stable up to 1300°C. The calculated Fe^{2+} content of the FCAM-phase is buffered in all experiments to a constant level. Moreover, the rate of crystal growth rises significantly.

Kalenga, M.K., & Garbers-Craig, A.M. (2010): Investigation into how the magnesia, silica, and alumina contents of iron ore sinter influence its mineralogy and properties.*J. South Afr. Inst. Mining Metall.*, **110**, 447-456.

Manninger, T. & Kahlenberg, V. (2015): Structural investigations on a Si-free Mg-containing SFCA-phase with compositions $Ca_3MgFe_{10}Al_6O_{28}$. *Mitt. Österr. Mineral. Gesell.*, **161**, 82 (abstr).

Matsui, Y., Sato, A., Oyama, T., Matsuo, T., Kitayama, S., Ono, R. (2003): All pellets operation in Kobe No. 3 blast furnace under intensive coal injection. *Iron Steel Inst. Japan Int.*, **43**, 166-174.

SUSTAINABLE PORTLAND CLINKERS: NANO-MATERIALS ADDITION TO RAW MIXTURES

Zucchini A.[1], Comodi P.[1], Di Michele A.[1], Vivani R.[2], Brizzi E.*[1], Casagrande S.[1], Santarelli G.[1], Gentili S.[1], Santinelli F.[3] & Neri A.[3]

[1] Dipartimento di Fisica e Geologia, Università di Perugia, Italy

[2] Dipartimento di Scienze Farmaceutiche, Università di Perugia, Italy

[3] Colacem S.p.A, Gubbio (PG), Italy

Corresponding email: memole146@inwind.it

Keywords: Portland clinker, nano-materials, sustainability

The improving of industrial processes sustainability is one of the most attractive topics of the last decades, since the high CO_2 emitted (i.e. more than 8% of the total antropogenic emitted CO_2 comes from cement industry) coming from the requested energy for the rotary kilns and the carbonates decarbonation during firing. The present work tests a new technology to improve the clinker cooking efficiency whit a decrease of the clinker burning temperature (*T*) and, thus, of the emitted CO_2. The project was inspired by considering the CaO diffusion as the driving force for clinker minerals formation during firing and that nano-materials are known to have a lower diffusion *T* than micron-sized materials. The new idea was to add nano-$Ca(OH)_2$ to the raw mixture for clinker production.

The nano-$Ca(OH)_2$ was prepared by sonochemical synthesis starting from $CaCl_2$ and NaOH. The nano-$Ca(OH)_2$ suspension was then spray dried and characterized by means of Field Emission - Scanning Electron Microscopy (FE-SEM), Dynamic Light Scattering, X-ray Powder Diffraction (XRPD) and BET analysis. Results confirmed the nanometric dimension of the synthesized $Ca(OH)_2$.

Two raw mixtures were prepared by mixing carbonates, silicates and nano-sized additives in appropriate proportions: the standard Portland clinker (PC) and the Portland clinker added with a 5 wt.% of nano-$Ca(OH)_2$ (nPC). Three burning *T* were set at 1250, 1350 and 1450°C to analyse the evolution of clinker phases as alite (C3S) and belite (C2S) as well as free lime (CaO) whose concentration decreases as the cooking efficiency increases.

Products were analysed by means of XRPD and collected data were treated by means of the Rietveld method as implemented in TOPAS Academic software. Moreover, high resolution FE-SEM image analysis allowed to analyse the clinker porosity.

The most important result from XRPD analysis is that the free lime concentration decreases in nPC with respect to PC at each burning *T*, confirming an increase of the nano-added raw mixtures cooking efficiency. By this observation we can speculate that the nano-CaO addition to the raw mixture might reflect in a decrease of the clinker burning temperature. The CO_2 emissions are then expected to decrease together with an improvement of the plant productivity.

Additional results show that nPC contains more C2S and minor C3S than PC [e.g., for 1450°C fired samples, C3S = 56.7(7) wt.% and C2S = 8.5(2) wt.% for PC and C3S = 48.7(5) wt.% and C2S = 10.8(2) wt.% for nPC]. This behaviour might be due to the higher reactivity of nPC than PC early in the firing process, when belite formation is the dominant mineralogical reaction. As regards image analysis, the nano-$Ca(OH)_2$ addition was found to decrease the clinker porosity being 35(2)% for PC and 26(3)% for nPC fired at 1450°C. The last observations need to be tested by further experiments to fully understand their cause. Further experiments are also in progress to check for the nano-$Ca(OH)_2$ optimum addition.

Session S14:

Advances in computational and experimental mineralogy: A journey from the surface to the deep Earth and beyond

Conveners:

Paola Comodi (Perugia – Italy)

Catherine A. McCammon (Bayreuth – Germany)

Mainak Mookherjee (Tallahassee – USA)

Azzurra Zucchini (Perugia – Italy)

NEW FEATURES IN EoSFit: FITTING ELASTIC MODULI AND PHASE TRANSITIONS

Angel R.J.*[1], Alvaro M.[2], Gonzalez-Platas J.[3] & Nestola F.[1]
[1] Dipartimento di Geoscienze, Università di Padova, Italy
[2] Dipartimento di Scienze della Terra e dell'Ambiente, Università di Pavia, Italy
[3] Departamento de Física, Universidad de La Laguna, Spain
Corresponding email: rossjohnangel@gmail.com

Keywords: equations of state, bulk modulus, elasticity

Equations of state (EoS) are used to describe the elastic properties of minerals over the pressure and temperature ranges from the surface of the Earth to its core, and beyond. The first release of the EosFit7 suite of programs and subroutine library (Angel et al., 2014) provided facilities for performing calculations with P-V and P-V-T EoS and for fitting EoS parameters to P-V, T-V and P-V-T data, and to linear data such as unit-cell parameters. This allows the variation of the elastic compressibility tensor of a mineral to be determined as a function of P and T. The EosFit7 GUI program is designed as a tool for rapid data analysis and for teaching EoS theory. EosFit7c is a console program with more advanced features, and remains the research and development platform. Both programs are available for MAC-OS, Linux and Windows from www.rossangel.net. We now report two significant new developments to the EosFit7c program and underlying subroutine library.

For common minerals there is now a wealth of direct measurements of their elastic moduli as a function of temperature and pressure, in addition to measurements of their unit-cell parameters. EosFit7c has now been modified so that it can now perform weighted fits of bulk modulus and volume data separately or simultaneously, so as to provide better constraints on EoS parameters. The extension of simultaneous fitting to linear data for non-cubic materials requires some assumptions to be made about the thermo-elastic behaviour of minerals, and these will be described.

Structural phase transitions, such as the alpha-beta transition in quartz, can give rise to very large non-linear variations in the volume and density with temperature and pressure. We have therefore developed a fully self-consistent simplified description of the equation of state of minerals in the neighbourhood of structural phase transitions based on a purely phenomenological adaptation of Landau theory. The resulting P-T-V EoS includes the description of the elastic softening in *both* phases with the minimum number of parameters, and has been incorporated in to the EosFit7c program. The program allows the parameters to be determined by simultaneous fitting of both volume and elastic data, and all types of equation of state calculations to be performed for EoS with phase transitions.

Angel, R.J., Gonzalez-Platas, J., Alvaro, M. (2014): EosFit-7c and a Fortran module (library) for equation of state calculations. *Z. Kristallogr.*, **229**, 405-419.

CAN WE PREDICT MELTING BEHAVIOUR OF MINERALS AT DEEP MANTLE CONDITIONS?

Belmonte D.*[1]
[1] Dipartimento di Scienze della Terra, dell'Ambiente e della Vita, Università di Genova, Italy
Corresponding email: donato.belmonte@unige.it

Keywords: melting, thermodynamics, first principles

Despite the outstanding progress in computer technology and experimental facilities, understanding melting phase relations of solids in the deep mantle is still an open challenge. As a matter of fact, even the most advanced methods to investigate melting currently display some limitations. Laboratory measurements at HP-HT conditions (like *in-situ* LH-DAC or shock-wave experiments) can be applied to complex compositions but they are usually affected by large uncertainties and, nonetheless, the *heat-until-it-melts* approach rarely predict the nature of melting. Theoretical calculations based on molecular dynamics (either semi-empirical or first-principles) provide useful insights on structural change induced by P-T effects in solid and liquid phases but often give quite contrasting results even for non-exotic minerals. Furthermore, MD is often unable to simulate melting in multi-component systems due to the huge computational cost required. Other empirical methods (e.g. the Lindemann melting criterion) are, in general, not adequate to describe the high-pressure melting behaviour of minerals as they do not have a predictive power.

In this work a novel computational scheme to predict melting phase relations of deep mantle minerals at HP-HT conditions by a combination of first principles DFT calculations, polymer chemistry and equilibrium thermodynamics is presented and discussed. The adopted theoretical framework is thermodynamically-consistent and allows to compute multi-component phase diagrams relevant to Earth's deep interior in a broad range of P-T conditions by Gibbs free energy minimisation algorithm. The calculated phase diagrams are in turn used as a source of information to gain some insights on the P-T-X evolution of magmas in the deep mantle, providing also a thermodynamic constraint to both early Earth and present-day melting processes (e.g. generation, differentiation and crystallization history of basaltic magmas and deep magma oceans in the Earth's interior). Specific focus will be devoted to those mineral phases (like majorite-pyrope garnet and phase Anhydrous B), which are often disregarded in modelling melting processes of mantle assemblages due to poor knowledge of their thermodynamic and thermo-physical properties. This against the experimental evidence that they are stable phases at solidus or liquidus conditions in a broad range of bulk compositions (e.g., dry and hydrous CMAS-pyrolite, KLB-1 peridotite). Application of the above method to simulate melting relations in the simplified, but representative, MgO-Al_2O_3-SiO_2 (MAS) system highlights as pressure effects are not only able to change the nature of melting of some minerals (like olivine and pyroxene), but also produce an oversimplification of melting relations in the MAS system by drastically reducing the number of phases with a primary phase field at HP-HT.

CRYSTAL-CHEMICAL AND ISOTOPIC PROPERTIES OF MINERALS BY COMBINING COMPUTATIONAL AND SPECTROSCOPIC TECHNIQUES

Blanchard M.*[1]

[1] Institut de Minéralogie, de Physique des Matériaux, et de Cosmochimie, Université Paris 06, Centre National de la Recherche Scientifique, France

Corresponding email: marc.blanchard@impmc.upmc.fr

Keywords: first-principles calculations, nuclear magnetic resonance, nuclear resonant inelastic X-ray scattering

The presentation will expose two examples where the combined use of spectroscopic and computational techniques contribute significantly to improve our understanding of the crystal-chemical and isotopic properties of minerals. In both cases, in addition to providing a series of atomic-scale information, first-principles methods are used to calculate the spectroscopic properties measured, allowing a direct comparison and thus a thorough analysis of the experimental results.

The first example is a theoretical study of boron incorporation in carbonate minerals. Indeed, the isotopic composition of boron traces in biogenic calcium carbonates is widely used as a proxy for paleo-oceanic acidity and past levels of atmospheric CO_2, based on the assumption that only borate anions are incorporated during crystal growth. However, the actual location of boron in carbonate minerals is poorly known. We determine here from first-principles the stable geometry of boron species in calcium carbonates and compare their theoretical NMR spectroscopic properties to previously published experimental data. It is thus possible to identify and to validate atomic-scale models of the dominant forms of boron in calcite and aragonite, bringing fundamental information on the crystal-chemical mechanisms sustaining the proxy.

The second example deals with the determination of the equilibrium fractionation factors of iron isotopes. Among the non-traditional isotopes, iron isotopes are probably the most investigated. The interpretation of isotopic compositions in natural samples rely however on the knowledge of equilibrium fractionation factors. For this Mössbauer-active element, equilibrium fractionation factors can be determined independently from isotope exchange experiments using Mössbauer spectroscopy and nuclear resonant inelastic X-ray scattering (NRIXS), which are closely related techniques that probe the vibrational properties of the target element. We will present a comparison of vibrational and isotopic properties obtained by first-principles calculations, NRIXS and Mössbauer spectroscopies, on oxide and sulfide minerals (Blanchard et al., 2015). We will show that by combining spectroscopic and theoretical techniques, this work provides reliable isotope fractionation factors.

Blanchard, M., Dauphas, N., Hu, M.Y., Roskosz, M., Alp, E.E., Golden, D.C., Sio, C.K., Tissot, F.L.H., Zhao, J., Gao, L., Morris, R.V., Fornace, M., Floris, A., Lazzeri, M., Balan, E. (2015): Reduced partition function ratios of iron and oxygen in goethite. *Geochim. Cosmochim. Acta*, **151**, 19-33.

INTERNALLY CONSISTENT SINGLE-CRYSTAL ELASTICITY OF IRON-BEARING WADSLEYITE AT HIGH PRESSURES AND HIGH TEMPERATURES

Buchen J.*[1], Marquardt H.[1], Kurnosov A.[1], Speziale S.[2], Kawazoe T.[1] & Boffa Ballaran T.[1]
[1] Bayerisches Geoinstitut, Universität Bayreuth, Germany
[2] Helmholtz Zentrum Potsdam, GFZ Deutsches GeoForschungsZentrum, Potsdam, Germany
Corresponding email: johannes.buchen@uni-bayreuth.de

Keywords: transition zone, wadsleyite, elasticity

As apparent from the selective fate of subducted lithospheric slabs, the transition zone intercedes between the dynamics of Earth's upper and lower mantle. At depths of 410 km and 660 km, changes in mineral assemblages of typical mantle rocks give rise to major discontinuities in seismic velocities making the transition zone seismically visible. The interpretation of these and other seismological observables requires a detailed understanding of the elastic behavior of candidate minerals at relevant pressure and temperature conditions. Wadsleyite, a high-pressure polymorph of $(Mg,Fe)_2SiO_4$, is expected to be a major mineral phase in any peridotitic mantle rock at depths of the upper transition zone. In addition to its high inferred volume fraction, wadsleyite features a remarkable water storage capacity of several weight percent H_2O (Inoue et al., 1995) and bears the potential to cause seismic anisotropy (Kawazoe et al., 2013).

We will present the first internally consistent measurements of single-crystal elastic constants of wadsleyite with a relevant chemical composition (Fe/(Mg+Fe) = 0.11, 0.2 wt.% H_2O) at high pressures and high temperatures. Segments of tailored dimensions were cut from oriented single-crystal sections using a focused ion beam (Marquardt & Marquardt, 2012). To ensure internal consistency, two segments of complementary crystallographic orientations were loaded together into the same pressure chamber of resistively heated diamond anvil cells. Combining Brillouin spectroscopy with single-crystal X-ray diffraction, the complete elasticity tensors were determined under uniform conditions. From the emerging pairs of unit cell volumes and bulk moduli, absolute pressures can be computed.

Our room temperature experiments confirm a small effect of iron on the bulk modulus of wadsleyite (K_S = 171(2) GPa) but indicate a linear reduction of the shear modulus upon substitution of iron for magnesium (G = 106(1) GPa). This suggests a potential mechanism to decouple the seismic signatures of iron and temperature. The multi-sample approach is to be extended for a comparative study addressed to the impact of hydrogen incorporation on the elastic properties of wadsleyite.

Inoue, T., Yurimoto, H., Kudoh, Y. (1995): Hydrous modified spinel, $Mg_{1.75}SiH_{0.5}O_4$: A new water reservoir in the mantle transition region. *Geophys. Res. Letters*, **22**, 117-120.

Kawazoe, T., Ohuchi, T., Nishihara, Y., Nishiyama, N., Fujino, K., Irifune, T. (2013): Seismic anisotropy in the mantle transition zone induced by shear deformation of wadsleyite. *Phys. Earth Planet. Int.*, **216**, 91-98.

Marquardt, H. & Marquardt, K. (2012): Focused ion beam preparation and characterization of single-crystal samples for high-pressure experiments in the diamond-anvil cell. *Am. Mineral.*, **97**, 299-304.

THE WURM PROJECT: COMPUTATIONAL MINERAL PHYSICS, RAMAN SPECTRA, AND A WINDOW TO NEW LOW-TEMPERATURE MINERALOGY

Caracas R.*[1] & Bobocioiu E.[1]

[1] Laboratoire de Géologie, Centre National de la Recherche Scientifique, École Normale Supérieure de Lyon, France

Corresponding email: razvan.caracas@gmail.com

Keywords: Raman, WURM, database

The WURM project aims to build a database of physical properties for minerals (Caracas & Bobocioiu, 2011). We work on natural phases, but also analogues and synthetic compounds. We use the density-functional theory in the ABINIT implementation (Gonze et al., 2009) to determine the theoretical structures of minerals; then we compute the dielectric and dynamic properties. We report the entire vibrational spectrum in the zone-centre. We show the Raman spectra with peak position and intensity, for ideal powders and for single crystals. The WURM project is active since 2008. Over this time we reached 450 computed spectra for more than 300 minerals.

Apart from the direct identification tool based on the Raman spectra, WURM offers a particular chance for mineral hunters. As usual with the density-functional theory the calculations are performed at zero temperature (0 K). But the initial structures we work on are those of minerals found at ambient conditions of temperature. Over this temperature difference, some minerals may exhibit phase transitions, typically order-disorder. Because these transitions are coded in unstable phonon modes, they become visible and fully predictable in our simulations. Such spectra with instabilities are reported on the WURM website, waiting for experimentalists to search and confirm the corresponding phase transitions towards new stable low-temperature minerals.

Caracas, R. & Bobocioiu, E. (2011): The WURM project – a freely available web-based repository of computed physical data for minerals. *Am. Mineral.*, **96**, 437-444.

Gonze, X., Amadon, B., Anglade, P.-M., Beuken, J.-M., Bottin, F., Boulanger, P., Bruneval, F., Caliste, D., Caracas, R., Côté, M., Deutsch, T., Genovese, L., Ghosez, P., Giantomassi, M., Goedecker, S., Hamann, D.R., Hermet, P., Jollet, F., Jomard, G., Leroux, S., Mancini, M., Mazevet, S., Oliveira, M.J.T., Onida, G., Pouillon, Y., Rangel, T., Rignanese, G.-M., Sangalli, D., Shaltaf, R., Torrent, M., Verstraete, M.J., Zerah, G., Zwanzigerf, J.W. (2009): ABINIT: First-principles approach to material and nanosystem properties. *Comput. Phys. Comm.*, **180**, 2582-2615.

HIGH PRESSURE BEHAVIOUR OF CHALCOSTIBITE

Comodi P.*[1], Nazzareni S.[1], Guidoni F.[1], Balić-Žunić T.[2] & Prakapenka V.[3]
[1] Dipartimento di Fisica e Geologia, Università di Perugia, Italy
[2] Natural Hystory Museum of Denmark, Copenaghen, Denmark
[3] Advanced Photon Source, Argonne National Laboratory, Argonne, IL, USA
Corresponding email: paola.comodi@unipg.it

Keywords: sulphosalts, high pressure, synchrotron radiation

The sulfosalts are a class of minerals belonging to the group of sulfides, their general formula is $A_mB_nS_p$ where A is a metal that can be commonly Ag, Cu, Fe and Pb (Me^+, Me^{2+}); B is a semi-metal such as Bi, Sb, As and Te; and S is S and rarely Se and Te.

They present modular structures of variable complexity with octahedral and higher-number coordination and are interesting low P analogue for high P silicate phases of deep mantle: for example the post-perovskite phase of $MgSiO_3$ belongs to the same homologous series as Lillianite ($Pb_3Bi_2S_6$) (Olsen et al., 2008). They can have interesting semiconducting and ion-conducting properties because of the nature of the metalloid–sulfur bond, a complex atom substitution and the presence of the s^2 Lone Electron Pair of metalloids which imply a potential use of sulfosalts in photovoltaic applications (thin film solar cells). Some of them showed interesting phase transition at high P (e.g., Olsen et al., 2011) which could involve dramatic change in semiconducting gap.

Here we present HP data collected *in situ* by single-crystal diffraction experiments at GSECARS-BM13 beamline, Advanced Photon Source (USA) at different P up to 12 GPa. An ETH-type DAC (600 μm diamond culet and a pre-indented rhenium gasket with a 250 μm hole) was charged with a ruby chip and gold crystal as P internal calibrant, Neon as P transmitting medium and the sample. Experiments were carried out using a fixed wavelength of 0.3344 Å, diffraction data were collected with a Mar165 detector, after a calibration for sample-to detector distance, tilting and distortion by using the powder diffraction pattern of CeO_2. Data were collected with the DAC rotated 50° along the ω-axis (from -25 to +25°) with an angular step of 0.5° and time of 1 s per step. The cell parameters and diffraction intensities were extracted using Dioptas and PX^2 softwares.

The bulk modulus determined fitting the volume data, up to about 11 GPa, with a second order Birch-Murnaghan equation of state was 58.6(8) GPa. The calculated compressibility on lattice parameters are: β_a = 4.9 10^{-3}GPa^{-1}, β_b = 3.510^{-3} GPa, β_c = 4.2 10^{-3} GPa^{-1}, with a limited anisotropic behaviour: $\beta_a : \beta_b : \beta_c$ = 1.4 : 1 : 1.2, where *b* parameter is less compressible than *a* and *c*.

The comparison of single crystal refinements performed with data collected at different pressures allow to study the evolution of Sb-S distances and of Lone Electron Pairs up to 12 GPa. At higher pressure a strong variation was observed on the lattice parameters and on the diffraction pattern suggesting that a phase transition occurs, in agreement with data recently observed by Baker et al. (2015) with powder diffraction data and with VIS-spectroscopic measurements by Guidoni et al. (2015).

Baker, J., Kumar, R.S., Sneed, D., Connolly, A., Zhang, Y., Velisavljevic, N., Paladugu, Y., Pravica, M., Chen, C., Cornelius, A., Zhao, Y. (2015): Pressure induced structural transition in $CuSbS_2$ and $CuSbSe_2$ thermoelectric compounds. *J. Alloys Comp.*, **643**, 186-194.

Guidoni, F., Comodi, P., Balić-Žunić, T., Nazzareni, S., Bini, R., Fanetti, S., Brizzi, E. (2015): Structural and photoelectric properties of chalcostibite at high pressure. Congresso SIMP-SGI-SoGei-AIV, Firenze, 2-5 September, abstr.

Olsen, L., Balić-Žunić, T., Makovicky, E. (2008): High-pressure anisotropic distortion of $Pb_3Bi_2S_6$: a pressure-induced, reversible phase transition with migration of chemical bonds. *Inorg. Chem*., **47**, 6756-6762.

Olsen, L., Friese, K., Makovicky, E., Balić-Žunić, T., Morgenroth, W., Grzechnik, A. (2011) : Pressure induced phase transition in $Pb_6Bi_2S_9$. *Phys. Chem. Minerals*, **38**, 1-10.

CHARACTERIZING THE DISTORTIONS AND BOND TOPOLOGY OF TETRAHEDRAL AND OCTAHEDRAL GROUPS IN MINERAL CRYSTAL STRUCTURES

Evans R.J.*[1] & Groat L.A.[1]
[1] Department of Earth, Ocean and Atmospheric Sciences, University of British Columbia, Vancouver, Canada
Corresponding email: rjamesevans@gmail.com

Keywords: crystal structures, structure topology, site distortions

A conception of mineral crystal structures of frequent use to mineralogists is that of three-dimensional networks of cation-centred coordination polyhedra whose shared vertices correspond to anions (usually oxygen, fluorine, chlorine, or sulfur). Almost all minerals contain cation sites that are either four- or six-coordinated. A very large number of mineral structures are classified according to the topology of tetrahedra such as silicate, phosphate, or sulfate groups. Essential metallic earth elements such as magnesium, tin, and the transition metals occur predominantly in octahedral coordination. Aluminum occurs commonly in both octahedral and tetrahedral coordination. Tetrahedra and octahedra in crystal structures generally do not have the highest possible point group symmetry of their coordination, and for many applications it is desirable to characterize the polyhedron's distortion from an ideal shape. Polyhedral distortions, for example, can be correlated with chemical substitutions at the cation site. They can also affect local electronic properties, such as electric field gradients and isomer shifts measurable by nuclear magnetic resonance or Mössbauer spectroscopy.

Many parameters have been proposed to characterize the distortions of octahedra and tetrahedra, quantifying bond lengths, bond angles, edge lengths, polyhedral volumes, and other indicators of overall “shape.” One challenge in examining the limits of distortion of six-fold coordination polyhedra, for example, is in precisely defining what is meant by “an octahedron” in a way that is both mathematically consistent and useful to crystallographers. Here we discuss the calculation and application of some commonly-used octahedral and tetrahedral distortion parameters, their variation with specific types of distortion, and their utility in characterizing mineral crystal structures, as well as offer definitions of four- and six-coordination polyhedra that hold up under mathematical scrutiny. We also discuss the roles octahedra and tetrahedra play in the overall bond topology of mineral structures.

THE EFFECT OF CATIONS ORDER/DISORDER ON THE ELASTIC PROPERTIES OF DOLOMITE

Gentili S.[1], Speziale S.*[2], Zucchini A.[1], Comodi P.[1], Reichmann H.J.[2] & Wunder B.[2]
[1] Dipartimento di Fisica e Geologia, Universita di Perugia, Italy
[2] Helmholtz Zentrum Potsdam, GFZ Deutsches GeoForschungsZentrum, Potsdam, Germany
Corresponding email: speziale@gfz-potsdam.de

Keywords: dolomite, order/disorder, Brillouin spectroscopy

Carbonates are key phases in the chemistry and dynamic of our planet, playing a fundamental role as important carbon carriers to the deep Earth interior. High pressure – high temperature (H*P*-H*T)* experiments as well as direct observation in diamonds have demonstrated that carbonates are stable at deep mantle level, confirming their presence in the deep Earth (Brenker et al., 2007; Litasov & Othani, 2009). Despite the compressibility of simple and binary carbonates is a key parameter for thermodynamic modelling at H*P* conditions, experimental studies of the carbonates elastic properties are extremely limited. In particular, the elastic tensor of dolomite [$CaMg(CO_3)_2$] was determined only in two studies, with results in clear disagreement (Humbert & Plicque, 1972; Chen et al., 2006). In order to give a comprehensive interpretation of the elastic behaviour of dolomite, we have determined the full elastic tensor of a natural dolomite single-crystal by Brillouin scattering, sampling a larger range of crystal orientations than the previous studies. We have prepared two platelets with orientations (-8 -2 10) and (9 -10 2) from a natural crystal from the Eugui metamorphic complex (Spain). The stoichiometry and homogeneity of the used sample have been previously analysed by Reeder & Wenk (1983). We have determined 114 individual acoustic wave velocities in 72 different crystallographic directions. We have then fitted the 7 independent coefficients (C_{ij}) of the elastic tensor and calculated linear axial compressibilities along *a*and *c* axes ($ß_a$, $ß_c$) and the aggregate bulk and shear moduli (*K*, *G*). *K* and *G* are 84 ± 1 and 39 ± 1 GPa, respectively; $ß_a$ and $ß_c$ are $2.52 \pm 0.05 \times 10^{-3}$ and $6.85 \pm 0.05 \times 10^{-3}$ GPa^{-1}, respectively. *G* is in excellent agreement with the previous elasticity studies, while *K*, $ß_a$ and $ß_c$ are only marginally consistent, confirming the need of a large dataset of velocities. Both $ß_a$ and $ß_c$ determined in our Brillouin scattering study are larger than those determined by X-ray diffraction study of single crystals of Eugui dolomite ($1.71\pm0.03 \times 10^{-3}$ and $5.21\pm0.05 \times 10^{-3}$ GPa^{-1}) by Zucchini et al. (2014), probably due to choice of the second order Birch-Murnaghan equation to fit the X-ray diffraction data and the strong correlation between elastic moduli and their pressure derivative in this form of the equation of state. Zucchini et al. (2014) also analysed the baric behaviour of a disordered dolomite structure, and a change of $ß_a$ and $ß_c$, associated to cations disordering, was documented. In order to determine the full elastic tensor of disordered dolomite we have disordered our sample by thermal treatment with an internal heated piston cylinder at 1500 K and 3 GPa. We have then measured Brillouin scattering of the recovered material. Our first and partial results show that the effect of cations disordering is negligible for the constantsC_{11}, C_{12} and C_{44} while constants C_{33} and C_{13} stiffen.

Brenker, F.E., Vollmer, C., Vincze, L., Vekemans, B., Szymanski, A., Janssens, J., Szaloki, I., Nasdala, L., Joswig, W., Kaminsky, F. (2007): Carbonates from the lower part of transition zone or even the lower mantle. *Earth Planet. Sci. Letters*, **260**, 1-9.

Chen, P., Chiao, L., Huang, P., Yang, Y, Liu, L. (2006): Elasticity of magnesite and dolomite from a genetic algorithm for inverting Brillouin spectroscopy measurements. *Phys. Earth Planet. Int.*, **155**, 73-86.

Humbert, P. & Plicque, F. (1972): Propriétés élastiques de carbonates rhombohédriques monocristallines: calcite, magnésite, dolomite. *C. R. Acad. Sci. Paris*, *Ser. B*, **275**, 391-394.

Litasov, K.D. & Othani, E. (2009): Solidus and phase relations of carbonated peridotite in the system CaO-Al_2O_3-MgO-SiO_2-Na_2O-CO_2 to the lower mantle depths. *Phys. Earth Planet. Int.*, **177**, 46-58.

Reeder, R.J. & Wenk, H.R. (1983): Structure refinement of some thermally disordered dolomites. *Am. Mineral.*, **68**, 769-777.

Zucchini, A., Comodi, P., Nazzareni, S., Hanfland, M. (2014): The effect of cation ordering and temperature on the high-pressure behaviour of dolomite. *Phys. Chem. Minerals*, **41**, 783-793.

MODELING THE CREEP PROPERTIES OF OLIVINE IN THE LITHOSPHERIC MANTLE FROM DISLOCATION DYNAMICS MODELS

Gouriet K.*[1], Boioli F.[2], Devincre B.[3], Carrez P.[1] & Cordier P.[1]

[1] Unité Matériaux et Transformations, Université Lille 1, Centre National de la Recherche Scientifique, Villeneuve d'Ascq, France

[2] Institut Lumière Matière, Université Lyon 1, Centre National de la Recherche Scientifique, Villeurbanne, France

[3] Laboratoire d'Etude des Microstructures, Centre National de la Recherche Scientifique - Office National d'Etudes et de Recherches Aérospatiales, Châtillon, France

Corresponding email: karine.gouriet@univ-lille1.fr

Keywords: dislocation dynamics, olivine, creep

Large scale flow in the Earth's mantle involves plastic deformations of rocks and their constitutive minerals. Due to the extremely slow strain rate conditions in the Earth's mantle, it is very challenging to identify the fundamental mechanisms controlling such process. Thus, the development of a multi-scale approach linking the atomic scale properties and the microscopic elementary mechanisms to the macroscopic behavior is needed (Cordier et al., 2012). One of the key steps in this approach is the description of dislocation-based intra-crystalline plasticity. Within this framework, we present a model to investigate the creep of olivine, one of the main constituent of the Earth's mantle, at the mesoscopic scale. In particular, we employ 2.5-Dimensional (2.5-D) dislocation dynamics simulations to investigate the interplay between thermally activated glide and climb (Boioli et al., 2015a, 2015b) motion and to study the effect of climb on olivine creep strain rates.

In this study, we performed simulations in steady state creep conditions on the temperature between 800 and 1700 K, and we applied creep stresses between 10 and 100 MPa. In these ranges of temperature and applied stresses, we investigate the role in plastic behavior of both slip system [100](001) and [001](100) and the evolution of flow law.

Boioli, F., Devincre, B., Marquille, M., Carrez, P., Cordier, P. (2015a): Modeling the creep properties of olivine by 2.5-dimensional dislocation dynamics simulations. *Phys. Rev. B*, **92**, 014115.

Boioli, F., Tommasi, A., Cordier, P., Demouchy, S., Mussi, A. (2015b): Low steady-state stresses in the cold lithospheric mantle inferred from dislocation dynamics models of dislocation creep in olivine. *Earth Planet. Sci. Letters*, **432**, 232-242.

Cordier, P. Amodeo, J., Carrez, P. (2012): Modelling the rheology of MgO under Earth's mantle pressure, temperature and strain rates. *Nature*, **481**, 177-180.

ENERGETICS AND COMPRESSIBILITY OF $2M_1$ MUSCOVITE-PHLOGOPITE SOLID-SOLUTION SERIES TO 9 GPa

Hernández-Laguna A.*[1], Sainz-Díaz C.I.[1], Hernández-Haro N.[1-3], Muñoz-Santiburcio D.[1], Pérez Del Valle C.[2], Ortega-Castro J.[3] & Mookherjee M.[4]

[1] Instituto Andaluz de Ciencias de la Tierra, Consejo Superior de Investigaciones Científicas, Universidad de Granada, Armilla, Spain

[2] Département de Chimie Moléculaire, Université Grenoble Alpes, France

[3] Departament de Química, Institut d'Investigació en Ciències de la Salut, Universitat de les Illes Balears, Palma de Mallorca, Spain

[4] Department of Earth, Ocean and Atmospheric Sciences, Florida State University, Tallahassee, Fl, USA

Corresponding email: alfonso.hernandez@iact.ugr-csic.es

Keywords: density functional theory, muscovite, phlogopite

Layered hydrous silicates are important minerals and are quite ubiquitous in igneous, metamorphic, and sedimentary rocks. They are typically formed as alteration products and helps in transporting significant amount of water into the Earths' interior via subduction. In this study, we have explored energetics and high pressure behavior of micaceous minerals along the phlogopite (Phl) and muscovite (Mus) join. We have used Density Functional Theory (DFT) as implemented in the Siesta code. We have used periodic boundary conditions to explore the Ms-Phl solid solution series. In addition we have used the Generalized Gradient Approximation (GGA) with the PBE (Perdew Bruke Ernzerhof) correlation-exchange functionals. We used a Energy cut-off of 500 Ry and 15 *k*-points in the Monkhorst Pack grid. Our calculations used numerical atomic orbitals and double-z plus polarization basis sets. We also used Troullier-Martins norm-conserving pseudopotentials. Five distinct, compositions along the solid solutions, i.e., Ms, $Ms_{75}Phl25$, $Ms_{50}Phl_{50}$, $Ms_{25}Phl_{75}$, and Phl, where Ms_xPhl_y refers to the solid solution composition with x and y representing the atomic fractions of trivalent aluminum and divalent magnesium ion substitutions in the octahedral sheets. All the compositions considered here have a $2M_1$polytype and a monoclinic spacegroup symmetry. All calculations were performed by fixing the desired pressure and then optimizing cell parameters and atomic positions in the same run to reach convergence thresholds of forces and stresses (0.005 *e*V/Å and 0.002 GPa, respectively). The applied pressures ranged from 0 to 9 GPa in increments of 0.25 GPa to 1 GPa, 2, 3, 6, and 9 GPa. The bulk modulus moduli, K_0 and K_{0i}, was obtained by a finite strain Birch-Murnhagan (BM) equation of state. We have used EOSFIT5.2 to fit the pressure-volume results from DFT. K_0 values were calculated from a BM3 fitting.

Equation of state parameters, bulk modulus, K_0 and cell parameters of Ms predicted using DFT agree nicely with experimental results (Hernández-Haro et al., 2016). K_0 of Phl is 55.4 GPa and also agrees with experimental values (Scordari et al., 2012). Ms shows a K_0 of 60.0 GPa (Hernández-Haro et al., 2016). The values in the series follow a sigmoidal behavior from Phl to Ms, a slow increasing from Phl to $Ms_{25}Phl_{75}$, with values from 55.4 to 55.9 GPa, a linear behavior from $Ms_{25}Phl_{75}$ to $Ms_{75}Phl_{25}$ (K_0 = 59.3 GPa) and a new slow increasing to Ms. The values of K_0' are constant (7.9) from Ms to $Ms_{75}Phl_{25}$ and increase to 8.7 at $Ms_{50}Phl_{50}$ keeping a constant value to Phl. Preliminary results indicate that with the cation substitutions of $Mg^{2+}{}_3$ by $Al^{3+}{}_2$-vac (where vac = vacancy), there is initially a gradual changes in the physical properties towards the intermediate member and then there is a more rapid change in the physical property.

Hernández-Haro, N., Muñoz-Santiburcio, D., Pérez Del Valle, C., Ortega-Castro, J., Sainz-Díaz, C.I., Garrido, C.J., Hernández-Laguna, A. (2016): Compressibility of $2M_1$ muscovite-paragonite series minerals: A computational study to 6 GPa. *Am. Mineral.*, *1***0***1*, 1207-1216.

Scordari, F., Schingaro, E., Mesto, E., Lacalamita, M. (2012): $2M_1$-phlogopite from Black Hills (South Australia): The first case of configurational polytype in micas. *Am. Mineral.*, **97**, 2016-2013.

PHASE BEHAVIOR AND VIBRATIONAL PROPERTIES OF CALCITE-DERIVED $CaCO_3$ POLYMORPHS UP TO 30 GPa: A COMBINED COMPUTATIONAL AND EXPERIMENTAL STUDY

Jahn S.*[1] & Koch-Müller M.[2]
[1] Institut für Geologie und Mineralogie, Universität Köln, Germany
[2] Helmholtz Zentrum Potsdam, GFZ Deutsches GeoForschungsZentrum, Potsdam, Germany
Corresponding email: s.jahn@uni-koeln.de

Keywords: carbonate, density-functional theory, high pressure

High-pressure phase transitions in $CaCO_3$ related to the calcite structure have been investigated in a number of studies using various experimental techniques. The transformations of calcite to calcite-II and further to calcite-III have been known for a long time. However, only recently Merlini et al. (2012) solved the structure of calcite-III using single crystal X-ray diffraction. Above 15 GPa, they observed another high-pressure phase called calcite-VI. Furthermore, calcite-III was shown to be present in two slightly different triclinic structures named calcite-III and calcite-IIIb. Here, we use first-principles calculations in the framework of density-functional theory to study the thermodynamic stability and the vibrational properties of the different calcite-related high-pressure polymorphs. The simulations are complemented by *in-situ* Raman and IR spectroscopy (Koch-Müller et al., 2016). Interestingly, calcite-IIIb seems to have two distinct (meta-)stability fields, whereas calcite-III is stable in between. The reentrant of calcite-IIIb can be explained by a change in compression mechanism and a density-crossover with respect to calcite-III. Theoretical Raman and IR-spectra are broadly consistent with experimental data. The calculations indicate that all calcite-related high-pressure polymorphs are metastable with respect to aragonite. This also seems to be true for calcite-VI, which is denser than aragonite and has been discussed as a possible stable high-pressure phase.

Koch-Müller, M., Jahn, S., Birkholz, N., Ritter, E., Schade, U. (2016): Phase transitions in the system $CaCO_3$ at high P and T determined by in-situ vibrational spectroscopy in diamond-anvil cells and first-principles simulations. *Phys. Chem. Minerals*, in press.

Merlini, M., Hanfland, M., Crichton, W.A. (2012): $CaCO_3$-III and $CaCO_3$-VI, high-pressure polymorphs of calcite: Possible host structures for carbon in the Earth's mantle. *Earth Planet. Sci. Letters*, **333-334**, 265-271.

COMBINED *AB INITIO* AND EXAFS SPECTROSCOPY STUDY ON THE CHARACTERISTICS OF IRON UPTAKE BY CLAY MINERALS

Kéri A.*[1-2], Dähn R.[1], Krack M.[1] & Churakov S.[1-2]
[1] Paul Scherrer Institut, Villigen, Switzerland
[2] Institut für Geologie, Universität Bern, Switzerland
Corresponding email: annamaria.keri@psi.ch

Keywords: atomistic simulation, EXAFS spectroscopy, clay minerals

Clay minerals can bind metals under mildly acidic to basic *p*H conditions. Their ability to retain radionuclides is extensively used in various concepts for the geological disposal of high level radioactive waste (HLW). In the Swiss concept for HLW, spent fuel and vitrified high level waste will be encapsulated in thick walled steel containers (0.25 m) surrounded by compacted bentonite which consist of ~ 75 wt.% montmorillonite. It is expected that due to the resaturation of the bentonite buffer and the corrosion of the steel container under anoxic conditions, radionuclides will be released after the first 10'000 years of the post-closure period. The migration of radionuclides can be retarded by choosing appropriate engineered and geological barriers. Therefore a comprehensive knowledge of the processes at the clay-water interface is required (NAGRA, 2014). The molecular level understanding of the radionuclides binding mechanisms is indispensable to comprehend the competing uptake mechanism of the relevant transition metal ions. It has been demonstrated that the combination of wet chemistry experiments, spectroscopic and atomistic simulations is the most promising approach to investigate highly heterogeneous environmental systems on the molecular level (Churakov & Dähn, 2012). The data analysis of EXAFS spectra allow in the best cases determining the nature of the surface complexes formed at clay mineral edge sites. Molecular simulations based on density functional theory are suitable to ascertain the preferential occupation sites of the clay particles and to serve as the basis for the interpretation of EXAFS data analysis (Churakov & Dähn, 2012). In this study, the Fe sorption mechanism at clay minerals were investigated to understand the oxidative sorption of iron ($Fe(II)_{aq}$ -> $/Fe(III)_{surf}$) that has an influence on the experimentally observed sorption competition with other transition metals (e.g., Ni, Co, Zn) (Dähn et al., 2011; Soltermann et al., 2013). The analysis of the experimental data and the simulation results suggest that Fe(II)/Fe(III) valence interchange (electron transfer) occurs between the Fe atoms absorbed on the surface and incorporated structurally into the bulk.

Churakov, S.V. & Dähn, R. (2012): Zinc adsorption on clays inferred from atomistic simulations and EXAFS spectroscopy. *Environ. Sci. Technol.*, **46**, 5713-5719.

Dähn, R., Baeyens, B., Bradbury, M.H. (2011): Investigation of the different binding edge sites for Zn on montmorillonite using P-EXAFS – the strong/weak site concept in the 2SPNE SC/CE sorption model. *Geochim. Cosmochim. Acta*, **75**, 5154-5168.

NAGRA (2014): Redox properties of iron bearing clays and MX-80 bentonite? Electrochemical and spectroscopy characterization. Nagra Technical Report 13-03, Dübendorf, Switzerland

Soltermann, D., Marques, M.F., Baeyens, B., Brendlé, J.M., Dähn, R. (2013): Competitive Fe(II)-Zn(II) uptake on a synthetic montmorillonite. *Environ. Sci. Technol.*, **48**, 190-198.

RELIABLE AND EFFICIENT *AB INITIO* SIMULATIONS OF COMPUTATIONALLY CHALLENGING MATERIALS

Kowalski P.M.*[1], Beridze G.[1], Ji Y.[1] & Li Y.[1]
[1] Energie- und Klimaforschung, Forschungszentrum Jülich, Germany
Corresponding email: p.kowalski@fz-juelich.de

Keywords:

Having access to efficient supercomputing resources and variety of computational software *ab initio* atomistic modeling has become popular investigation tool in various fields of science and technology, including mineralogy (Jahn & Kowalski, 2014). However, certain minerals represent challenge to the computational methods. For instance, density functional theory (DFT) can even dramatically fail for *f*-elements bearing materials producing highly inaccurate results. On the other hand, in experimentally challenging fields such as nuclear waste management the computer simulations give often the only possibility for investigation of properties of materials of interest. We will discuss the improvements of the DFT obtained with the DFT+*U* method, with the Hubbard *U* parameter derived *ab initio,* for the simulation of the lanthanide- and actinide- bearing materials. We will discuss performance of this method on large sets of lanthanide and actinde-bearing compounds (Beridze & Kowalski, 2014; Blanca-Romero et al., 2014) and subsequent application of *ab initio* techniques in complementary experimental and computational investigation of various materials, including monazite and pyrochlore as ceramic waste forms (Blanca-Romero et al., 2014; Li et al., 2014, 2015; Kowalski et al., 2015; Kowalski & Li, 2016) and various Th and U-bearing minerals (Wu et al., 2014; Xiao et al., 2016). We will demonstrate that complementary experimental and atomistic modeling studies result in superior characterization of these materials.

Beridze, G. & Kowalski, P.M. (2014): Benchmarking the DFT+U method for thermochemical calculations of uranium molecular compounds and solids. *J. Phys. Chem. A*, **118**, 11797.

Blanca-Romero, A., Kowalski, P.M., Beridze, G., Schlenz, H., Bosbach, D. (2014): DFT+U studies of monazite-type ceramics: predicting structural and thermodynamic parameters. *J. Comput. Chem.*, **35**, 1339-1346.

Jahn, S. & Kowalski, P.M. (2014): Theoretical approaches to structure and spectroscopy of Earth materials. *Rev. Mineral. Geochem.*, **78**, 691-743.

Kowalski, P.M. & Li, Y. (2016): Relationship between the thermodynamic excess properties of mixing and the elastic moduli in the monazite-type solid ceramics. *J. Eur. Ceram. Soc.*, **36**, 2093-2096.

Kowalski, P.M., Beridze, G., Vinograd, V., Bosbach, D. (2015): Heat capacities of lanthanide and actinide monazite-type ceramics. *J. Nuclear Mater.*, **464**, 147.154.

Li, Y., Kowalski, P.M., Blanca-Romero, A., Vinograd, V., Bosbach, D. (2014): Ab initio calculation ofexcesspropertiesof $La_{1-x}(Ln,An)_xPO_4$ solid solutions. *J. Solid St. Chem.*, **220**, 137-141.

Li, Y., Kowalski, P.M., Beridze, G., Birnie, A.P., Finkeldei, S., Bosbach, D. (2015): Defect formation energies in $A_2B_2O_7$ pyrochlores. *Scripta Mater*., **107**, 18-21.

Wu, S., Kowalski, P.M., Yu, N., Malcherek, T., Depmeier, W., Bosbach, D., Wang, S., Suleimanov, E.V., Albrecht-Schmitt, T.E., Alekseev, E.V. (2014): Highly distorted uranyl ion coordination and 1D-2D structural relationship in the $Ba_2[UO_2(TO_4)_2]$ (T = P, As) system: An experimental and computational study. *Inorg. Chem.*, **53**, 7650-7660.

Xiao, B., Gesing, T.M., Robben, L., Blanca-Romero, A., Kowalski, P.M., Li, Y., Kegler, P., Klepov, V., Bosbach, D., Alekseev, E.V. (2016): Giant volume change and topological gaps in temperature - and pressure - induced phase transitions: Experimental and computational study of $ThMo_2O_8$. *Chem. - Eur. J.*, **22**, 946-958..

INSIGHTS INTO THE NATURE OF EARTH'S MANTLE FROM ELASTICITY AND RHEOLOGY MEASUREMENTS AT HIGH-PRESSURE/HIGH-TEMPERATURE

Marquardt H.*[1], Kurnosov A.[1], Boffa Ballaran T.[1], Marquardt K.[1], Frost D.[1], Liermann H.-P.[2], Speziale S.[3], Miyagi L.[4], Merkel S.[5], Immoor J.[1], Buchen J.[1] & Schulze K.[1]

[1] Bayerisches Geoinstitut, Universität Bayreuth, Germany

[2] Photon Science, Deutsches Elektronen-Synchrotron, Hamburg, Germany

[3] Helmholtz Zentrum Potsdam, GFZ Deutsches GeoForschungsZentrum, Potsdam, Germany

[4] Department of Geology and Geophysics, University of Utah, Salt Lake City, UT, USA

[5] Unité Matériaux et Transformations, Ecole Nationale Supérieure de Chimie de Lille, Centre National de la Recherche Scientifique, Université de Lille 1, Villeneuve d'Ascq, France

Corresponding email: Hauke.Marquardt@uni-bayreuth.de

Keywords: Earth mantle, elasticity, rheology

Knowledge of the elastic behavior of Earth mantle materials at relevant pressure and temperature conditions is key to constrain the current structure and composition of the mantle through forward modelling of seismic observables. An understanding of the rheological properties is, on the other hand, crucial to construct realistic large scale models that capture Earth's dynamics over time. In this contribution, we present new experimental results on the (1) elastic and (2) rheological properties of mantle minerals at high-pressure and high-temperature and discuss potential implications for our understanding of Earth's mantle.

(1) We will present single-crystal elasticity measurements of bridgmanite and ringwoodite carried out using the combined Brillouin scattering and X-ray diffraction (XRD) system at BGI Bayreuth. Multiple single-crystals, focused ion beam (FIB)-tailored in size and shape (Marquardt & Marquardt, 2012), were loaded together in the sample chambers of resistively-heated diamond-anvil cells (DAC). Such a multi-sample approach allows for internally consistent determinations of all nine independent elastic constants from orthorhombic bridgmanite samples by Brillouin spectroscopy and X-ray diffraction measurements. Furthermore, the multi-sample approach facilitates direct quantification of the effects of chemical variability on the elasticity of cubic ringwoodite at non-ambient conditions. Our experimental approach eliminates uncertainties arising from the combination of data collected under (potentially) different conditions in separate DAC runs, in different laboratories and/or from using different pressure-temperature sensors. We will use our recent results together with seismological observables to discuss the average composition of the mantle as well as chemical variabilities within the mantle.

(2) We will revise the current status of the radial XRD setup at the Extreme Conditions Beamline (P02.2) at PETRA III of the German synchrotron facility DESY (Liermann et al., 2015) that allows for high-temperature deformation experiments at pressures of the lower mantle. We will show results of the experimental high-pressure deformation of lower mantle minerals and mixtures of them at temperatures of up to 1500 K and will outline their possible impact on our picture of Earth's lower mantle (e.g., Marquardt & Miyagi, 2015).

Liermann, H.-P., Konopkova, Z., Morgenroth, W., Glazyrin, K., Bednarcik, J., McBride, E.E., Petitgirard, S., Delitz, J.T., Wendt, M., Bican, Y., Ehnes, A., Schwark, I., Rothkirch, A., Tischer, M., Heuer, J., Schulte-Schrepping, H., Kracht, T., Franz, H. (2015): The extreme conditions beamline P02.2 and the extreme conditions science infrastructure at PETRA III. *J. Synchr. Rad.*, **22**, 908-924.

Marquardt, H. & Marquardt, K. (2012): Focused Ion Beam preparation and characterization of single-crystal samples for high-pressure experiments in the diamond-anvil cell. *Am. Mineral.*, **97**, 299-304.

Marquardt, H. & Miyagi, L. (2015): Slab stagnation in the shallow lower mantle linked to an increase in mantle viscosity. *Nature Geosci.*, **8**, 311-314.

A NUCLEAR INELASTIC SCATTERING WINDOW TO THE DEEP EARTH

McCammon C.A.*[1], Chariton S.[1], Cerantola V.[1-2], Kupenko I.[2-3], Vasiukov D.M.[1-4], Aprilis G.[1-4], Chumakov A.[2] & Dubrovinsky L.[1]

[1] Bayerisches Geoinstitut, Universität Bayreuth, Germany
[2] European Synchrotron Radiation Facility, Grenoble, France
[3] Institut für Mineralogie, Universität Münster, Germany
[4] Lehrstuhl für Kristallographie, Universität Bayreuth, Germany
Corresponding email: catherine.mccammon@uni-bayreuth.de

Keywords: iron carbonate, shear wave velocity, nuclear resonance

Comparison of laboratory measurements of elastic wave velocities of mantle minerals with seismic data constitutes one of the foundations upon which knowledge of the Earth's interior is based. *In situ* measurements are important, because some transitions (for example, spin transitions) are not quenchable, and may influence the elastic properties of iron-containing minerals. In the laboratory setting, techniques such as ultrasonics, Brillouin scattering, and impulsive stimulated scattering offer attractive possibilities to measure sound velocities directly, but stumble when faced with the challenge of iron-containing phases at pressures and temperatures of the deep Earth's interior. Technical developments in the past decade involving third generation synchrotron sources as well as methods for laser heating in the diamond anvil cell have opened new possibilities for such measurements, notably nuclear inelastic scattering where sound velocities of iron-containing minerals can be determined through direct measurement of the partial density of states.

Current models predict the occurrence of carbonates in subducting slabs, yet their presence may be challenging to detect using geophysical methods due to their low abundance relative to other phases. One of the important parameters in deciphering seismic data is the elastic properties of iron-bearing carbonates at high pressure and temperature, particularly the anisotropy and the effect of the high-spin to low-spin transition reported in the literature to occur in Fe^{2+} around 50 GPa. Up to now, however, elastic wave velocities of iron-bearing carbonates have not been measured through the spin transition. To address this problem, we undertook a diamond anvil cell study of iron-bearing carbonates on the Nuclear Resonance beamline (ID18) at the European Synchrotron Radiation Facility in Grenoble, France. Elastic wave velocities were derived from nuclear inelastic scattering data, and results show a substantial increase in shear wave velocity through the spin transition. We will present our latest results and discuss implications for the detectability of carbonate in the deep Earth.

H*P*-H*T* (Mg,Fe)O SUB-SOLIDUS REACTION MODELLING: IMPLICATIONS FOR LOWER MANTLE GEOCHEMICAL HETEROGENEITIES

Merli M.[1], Bonadiman C.[2], Diella V.[3], Sciascia L.[1] & Pavese A.*[4]
[1] Dipartimento di Scienze della Terra e del Mare, Università di Palermo, Italy
[2] Dipartmento di Fisica e Scienze della Terra, Università di Ferrara, Italy
[3] Istituto per la Dinamica dei Processi Ambientali, Consiglio Nazionale delle Ricerche, Milano, Italy
[4] Dipartmento di Scienze della Terra "A. Desio", Università di Milano, Italy
Corresponding email: alessandro.pavese@unimi.it

Keywords: sub-solidus MgO-FeO binary, lower mantle geochemical heterogeneities, sub-solidus reaction modelling

Equilibrium reactions over the sub-solidus MgO-FeO binary, i.e., periclase-like structure (Mg,Fe)O phases, were modelled in the frame of pyrolitic Earth lower mantle *via* (Mg,Fe)O mixing Gibbs energy as a function of composition, *P* and *T*, using quantum mechanical calculations (Hartree-Fock/DFT hybrid scheme), cluster expansion techniques, statistical thermodynamics and chemical equilibrium formalism. We aim to explore how the equilibrium reaction (Mg,Fe)O-products are a source for lower mantle geochemical heterogeneities (e.g., variability of the phases' compositions, phase proportions and density). Iron in Fe-periclase was modelled in both low-spin (LS) and high-spin (HS) state, separately, and the sub-solidus (Mg,Fe)O-system was treated as an open system that exchanges Mg and Fe with the lower mantle, considered as a reservoir. On the basis of our results, LS is the main booster of equilibrium phase changes in the sub-solidus (Mg,Fe)O-system over the lower mantle. The model indicates that the sub-solidus (Mg,Fe)O-system is able to continuously incorporate iron from the reservoir forming equilibrium phases with compositions and proportions that vary over the *P-T* range 24/1920-80/2530 GPa/K. At higher pressure and temperature, up to 128/3150 GPa/K, the sub-solidus (Mg,Fe)O-system stabilizes a *quasi*-invariant iron-rich composition [$(Mg_{0.50}Fe_{0.50})O$], predominant in terms of phase proportions, and two iron-poor compositions given by $(Mg_{0.10}Fe_{0.90})O$ and $(Mg_{0.175}Fe_{0.825})O$. These theoretical results are in agreement with the compositional variance observed in the lower mantle Fe-periclase from diamond inclusions and are consistent with the frequency of occurrence revealed for the compositions of the natural specimens. The density differences among the equilibrium (Mg,Fe)O-phases increase up to ~1 0%, between 24 and 128 GPa. The calculated bulk Fe/Mg partitioning coefficient between perovskite (here used as a chemical approximation of the reservoir) and Fe-periclase is 0.64 at 24 GPa, then drops to 0.19 at 80 GPa, and becomes *quasi*-invariant (0.18-0.16) in the lowermost portion of the Earth mantle (~ 80-128 GPa). These values are consistent with those experimentally determined. Altogether our results suggest that Fe-periclase does cause geochemical heterogeneities over the range 24-80 GPa, but it does not give rise to any sharp discontinuity, so that the deepest lower mantle seismic anomalies (i.e., D''-region) do not seem primarily ascribable to the mixing reactivity of the sub-solidus (Mg,Fe)O-system.

CANDIDATE CARBONATE PHASES IN THE EARTH

Merlini M.*[1], Lotti P.[1-2], Gatta G.D.[1], Crichton W.[3], Hanfland M.[3], Plaisier J.R.[2] & Lausi A.[2]
[1] Dipartimento di Scienze della Terra "A. Desio", Università di Milano, Italy
[2] Elettra Sincrotrone Trieste, Italy
[3] European Synchrotron Radiation Facility, Grenoble, France
Corresponding email: marco.merlini@unimi.it

Keywords:

With the current state of art of experimental facilities, we conducted studies on carbonates at the variable pressures and temperatures existing from the Earth's crust to the mantle/core region conditions. The quality of the diffraction data (single crystal and powder) allow full structural analysis for all the phases encountered. We present an updated overview of all the possible candidate carbonate phases in the inner Earth, based on model carbonate system and on most-likely composition in the ternary diagram $CaCO_3$-$MgCO_3$-$FeCO_3$. The model $BaCO_3$ studied at high temperatures and high pressures present the sequence of transition from aragonite-type phase to disorder-calcite phase and finally NaCl structure. At high pressure, the aragonite-type transform into the post-aragonite above 8 GPa. A similar scenario is observed in $CaCO_3$, but new high-pressure polymorphs denser than aragonite are present above 15 GPa. Dolomite, previously considered unstable at mantle conditions, is demonstrated to be stable above 30 GPa at the high pressures and temperatures existing in the Earth's interior up to the mantle/core boundary. It transforms to dense polymorphs based on distorted calcite-type structure at intermediate pressures, and, above the Mbar, transforms into new polymorphs featuring ring-carbonate C_3O_9 groups. This structure is likely the candidate phase for carbon storage in a carbonate in the Earth's mantle, and may form complete solid solution with $CaCO_3$ and $MgCO_3$. Fe-magnesite, stabilized at high pressures and temperatures, undergoes complex red-ox reactions, with the formation of Fe^{3+} bearing carbonates with stoichiometry different from ABO_3.

HIGH-PRESSURE ELASTICITY OF PHASE-Pi, $Al_3Si_2O_7(OH)_3$

Mookherjee M.*[1], Hermann A.[2] & Wunder B.[3]
[1] Department of Earth, Ocean, and Atmospheric Science, Florida State University, Tallahassee, FL, USA
[2] School of Physics and Astronomy, University of Edinburgh, United Kingdom
[3] Helmholtz Zentrum Potsdam, GFZ Deutsches GeoForschungsZentrum, Potsdam, Germany
Corresponding email: mmookherjee@fsu.edu

Keywords: first principles, elasticity, high-pressure

The mineralogy of subducted sediments can be modeled within the ternary system with Al_2O_3-SiO_2-H_2O (ASH) as end member components. Several hydrous and anhydrous phases belong to the ASH ternary system, including polymorphs of silica, i.e., quartz, coesite, stishovite (SiO_2), corundum (Al_2O_3), aluminosilicate polymorphs, kyanite, andalusite (Al_2SiO_5), gibbsite ($Al(OH)_3$), diaspore (AlOOH), kaolinite ($Al_2Si_2O_5(OH)_4$), topaz-OH ($Al_2SiO_4(OH)_2$), phase-Pi (**(**$Al_3Si_2O_7(OH)_3$), and phase Egg ($AlSiO_3(OH)$). Among these various phases, almost nothing is known about the high-pressure behavior of phase-Pi. High-pressure phase relations have shown that phase-Pi is stable between 2 and 7 GPa (Wunder et al., 1993). In this work we report the equation of state and full elastic stiffness tensor as a function of pressure. We find that the pressure volume results from the first principles simulation could be described by a finite strain fit with V_0, K_0 and K_0' as 310.3 $Å^3$, 133 GPa, and 3.6 respectively. At zero pressure, the full elastic stiffness tensor shows significant anisotropy with the diagonal principal components C_{11}, C_{22}, and C_{33} being 235, 292, 266 GPa respectively, the diagonal shear C_{44}, C_{55}, and C_{66} being 86, 93, and 87 GPa respectively, and the off-diagonal stiffness C_{12}, C_{13}, C_{23}, C_{14}, C_{15}, C_{16}, C_{24}, C_{25}, C_{26}, C_{34}, C_{35}, C_{36}, C_{45}, C_{46}, and C_{56} being 73, 78, 61, 6, -29, 15, 17, 2, 1, -13, -15, 5, 3, 1, and 3 GPa respectively.

Wunder, B., Medenbach, O., Krause, W., Schreyer, W. (1993): Synthesis, properties and stability of $Al_3Si_2O_7(OH)_3$ (phase Pi), a hydrous high-pressure phase in the system Al_2O_3-SiO_2-H_2O (ASH). *Eur. J. Mineral.*, **5**, 637-649.

DATA RECONCILIATION BETWEEN XRD AND CHEMICAL COMPOSITION DATA FOR QUANTITATIVE ANALYSIS BY LINEAR PROGRAMMING

Ohmann S.*[1], Ufer K.[1], Dohrmann R.[1] & Kaufhold S.[1]

[1] Fachbereich Geophysikalische Erkundung und Technische Mineralogie, Bundesanstalt für Geowissenschaften und Rohstoffe, Hannover, Germany

Corresponding email: svenohmann@web.de

Keywords: Rietveld method, linear programming, quantitative phase analysis

In order to understand geological or industrial processes, it is essential not only to measure the chemical composition or the qualitative phase content of the whole rock sample. Instead, it is important to quantify the individual phases based on the best technique available. Rietveld refinement technique is a proved useful method for quantitative analysis also in clay mineralogy, although the degree of precision varies considerably depending on errors caused by the relative complexity of the mineral assemblage (Ufer et al. 2008). The degree of accuracy in quantitative analysis of sedimentary samples can be improved, if chemical data from XRF are used together with the parameters obtained by XRD. We propose a method of linear programming techniques with the goal to minimize the function $f(x_i) = \Sigma \mid x_i - x_{ir} \mid$, where x_i are the whole amount of chemical components of the minerals determined by calculation from Rietveld quantitative analysis, and x_{ir} the components of the bulk obtained by XRF-experiments. The chosen method has got two advantages: 1) In opposite to least squares solutions it does not suffer from the disadvantage that they may lead to negative values which have no physical meaning. 2) The linear programming algorithm is stable and rarely leads to local minima. However, the accuracy of the method is strongly connected to the knowledge of the crystal-chemical composition of those mineral phases that might have a broad compositional variation (Lopez Galindo et al., 1996). In the case of feldspars the composition of the end members can be used in the formulation of the problem instead of using empirical compositions. The weight fraction of the mineral solution is then the sum of the weight fractions of the individual end members. In the case of infeasibility to express compositions of minerals as mixtures of end members a variation of components in the mass balance equations can improve the results of the quantitative analysis data by the Rietveld method.

A mixture of 30.0% quartz, 30.0% labradorite 10.0% calcite and 30.0% muscovite (all mass %) was quantified using the Rietveld method. The results were relatively poor with 26.0% quartz, 26.7% labradorite, 38.5% muscovite, and 7.5% calcite. Obviously this was caused by partly extreme preferred orientation of the crystals in the XRD specimen. Using the proposed linear programming technique calculations lead to quantitative phase contents of 31.0% quartz, 32.8% labradorite, 28.0% muscovite and 9.8% calcite by end member modelling with the end members albite and anorthite (to explain labradorite) and a variation of the amount of Al_2O_3 in muscovite between 0.10 and 0.40 in the oxide formula. These results came much closer to the true composition of the test mixture.

López-Galindo, A., Torres-Ruiz, J., Gonzalez-López, J.M. (1996): Mineral quantification in sepiolite palygorskite deposits using X-ray diffraction and chemical data. *Clay Miner.*, **31**, 217-224.

Ufer, K., Stanjek, H., Roth, G., Dohrmann, R., Kleeberg, R., Kaufhold, S. (2008): Quantitative phase analysis of bentonites by the Rietveld method. *Clays Clay Miner.*, **56**, 272-282.

SEPIOLITE AND PALYGORSKITE INTERACTION WITH CARBON DIOXIDE: EXPERIMENTAL EVIDENCE AND MOLECULAR DYNAMICS SIMULATION

Pedone A.[1], Muniz-Miranda F.[1], Lodesani F.[1], Malferrari D.*[1] & Brigatti M.F.[1]
[1] Dipartimento di Scienze Chimiche e Geologiche, Università di Modena e Reggio Emilia, Modena, Italy
Corresponding email: brigatti@unimore.it

Keywords: carbon dioxide, palygorskite, sepiolite

Global warming resulted from the emission of greenhouse gases has received widespread attention, and numerous reports indicate that more than half of global warming is caused by CO_2 gas alone. Several solid adsorbents have been widely investigated for CO_2 capture, such as clays, zeolites, activated carbon, porous silica, metal oxides, polymer-based adsorbents, ion-exchange resins, metal organic frameworks, among others.

Naturally occurring 2:1 layer silicates are recognized to be effective in carbon dioxide sequestration in sedimentary basins (De Paolo et. al., 2013). Despite relevant recent literature concerning interactions between $CO_2$and 2:1 layer silicates (Giesting et al., 2012; Rao & Leng, 2016) little can be found on modulated layer silicates, with nanotube-like structure such as sepiolite and palygorskite. This gap can be partly attributed to the crystal structure of these materials that is extremely difficult to characterize, thus requiring a combined experimental and theoretical approach.

Ambient CO_2 uptake by both modulated clays has been studied as a function of time at standard ambient temperature and pressure. The results of the experimental work show that natural sepiolite and palygorskite has significant sorption capacity to CO_2 that can be trapped into structural channels and can be easily removed increasing temperature.

These results have been confirmed by molecular dynamics simulations, which has also allowed us to determine the structural and dynamical properties of CO_2 confined in the nanotube-like structures of both sepiolite and palygorskite minerals.

De Paolo, D.J., Cole, D.R., Navrotsky, A., Bourg, I.C. (2013): Geochemistry of geologic CO_2 sequestration. *Rev. Mineral Geochem.*, **77**, 539 p.

Giesting, P., Guggenheim, S., Koster van Groos, A.F., Busch, A. (2012): Interaction of carbon dioxide with Na-exchanged montmorillonite at pressures to 640 bars: Implications for CO_2 sequestration. *Int. J. Greenhouse Gas Control*, **8**, 73-81.

Rao, Q. & Leng, Y. (2016): Molecular understanding of CO_2 and H_2O in a montmorillonite clay interlayer under CO_2 geological sequestration conditions. *J. Phys. Chem. C*, **120**, 2642-2654.

MODELING PLASTICITY OF MgO AT THE MESOSCALE USING 2.5D DISLOCATION DYNAMICS

Reali R.*[1], Boioli F.[2], Gouriet K.[1], Carrez P.[1] & Cordier P.[1]

[1] Unité Matériaux et Transformations, Université Lille 1, Centre National de la Recherche Scientifique, Villeneuve d'Ascq, France

[2] Institut Lumière Matière, Université Claude Bernard Lyon 1, Centre National de la Recherche Scientifique, Villeurbanne, France

Corresponding email: ricreali9@gmail.com

Keywords: MgO, 2.5D dislocation dynamics, rheology

In the lower mantle, viscosity results from the rheological behavior of its two main constituent minerals, namely (Mg,Fe)SiO_3 bridgmanite and (Mg,Fe)O ferropericlase. Understanding how these phases deform is thus of primary importance in geophysics. This is also a very challenging task, since the extreme conditions to which this lower mantle aggregate is subjected are barely reachable in laboratory experiments.

In this study, the contribution of dislocations to the deformation of periclase at the mesoscale is investigated by Dislocation Dynamics (DD) simulations, a modeling tool which considers the collective motion and interactions of dislocations. To model their behavior a so-called 2.5D DD approach is employed. Within this method, dislocations are considered as straight segments perpendicular to a 2D reference plane and local rules are added to mimic 3D behavior (Boioli et al., 2015). In this framework, both the glide and climb mechanisms can be taken into account (Gómez-García et al., 2006).

Before simulating the deformation of MgO under P, T and strain rate conditions of the lower mantle, it is necessary to benchmark the model at ambient pressure, in order to compare the simulated behavior with experiments performed in the same conditions.

At high temperatures (1500-1800 K) the observed creep strain rates are controlled by the competition between dislocation glide and climb mechanisms, the former being responsible for strain production and the latter being the rate-limiting factor.

Results are found in agreement with previous experimental data, confirming that the underlying physical processes are well described and permitting further investigations of MgO plasticity in the Earth's interior environment. We present the results obtained from simulations run at different temperatures and pressures within the lower mantle range of conditions. The possibility to constrain deformation with respect to time allows a characterization of the relationship between stresses and strain rates, a feature that was not previously numerically investigated, which possibly can suggest new inputs for broader scale simulation techniques.

Boioli, F., Carrez, P., Cordier, P., Devincre, B., Marquille, M. (2015): Modeling the creep properties of olivine by 2.5-dimensional dislocation dynamics simulations. *Phys. Rev. B*, **92**, 014115.

Gómez-García, D., Devincre, B., Kubin, L.P. (2006): Dislocation patterns and the similitude principle: 2.5D mesoscale simulations. *Phys. Rev. Letters*, **96**, 125503.

AMFORM.XLSX - A NEW MODEL FOR AMPHIBOLE FORMULA CALCULATION FROM EMP ANALYSES

Ridolfi F.[1], Oberti R.[2], Zanetti A.[2], Renzulli A.*[3] & Perugini D.[4]
[1] Via Galileo Galilei 11, 61122 Pesaro, Italy
[2] Istituto di Geoscienze e Georisorse, Consiglio Nazionale delle Ricerche, Pavia, Italy
[3] Dipartimento di Scienze Pure e Applicate, Università "Carlo Bo", Urbino, Italy
[4] Dipartimento di Fisica e Geologia, Università di Perugia, Italy
Corresponding email: alberto.renzulli@uniurb.it

Keywords: amphibole supergroup, mineral chemistry, user-friendly spreadsheet

Amphiboles are a supergroup of silicate minerals with the general formula $AB_2C_5T_8O_{22}W_2$ containing (at the major- and trace-element levels) many elements of geological/geochemical relevance (Hawthorne et al., 2007; 2012). Their crystal chemistry has drawn the attention of many scientists over the years because of its complexity (indeed, the term amphibole derives from the Greek "αμφιβολος", which means ambiguous; Réné J. Haüy 1743 – 1822; Hawthorne et al., 2007) and ability to record a wide range of geochemical and petrological processes due to mutual relationships between cation ordering, chemical composition of the surrounding environment and P-T-$f$$H_2O$-$f$$O_2$ conditions of crystallization (Holland & Blundy, 1994; Oberti et al., 2000; Ridolfi & Renzulli, 2012). Because of this complexity, deciphering the effects of geological processes is often difficult, and the proper selection of amphibole compositions suitable for development of thermobarometric application is crucial (e.g., Ridolfi & Renzulli, 2012). In particular, routine calculations of amphibole formulae from EMP data may be seriously affected by inappropriate normalization procedures and/or the lack of accurate information on the oxidation state of iron and the contents of hydrogen and lithium (Hawthorne et al., 2012).

We have studied the relationships between element oxide percentages and the unit-formulas of the most abundant amphibole species in the Earth's crust and upper mantle using accurately selected high-quality data of Li-free monoclinic amphiboles belonging to the calcium and sodium-calcium subgroups (a total of 116 EMP+SREF±SIMS analyses of natural and synthetic amphiboles), and Li-free *C*2/*m* end-members (75 ideal composition-formula pairs) and their oxo equivalents. It is worth noting that the high-quality amphibole analyses span a wide compositional range [$Mg/(Mg+Fe^{2+})$ = 0.2-1.0; Fe^{3+}/Fe_{tot} = 0-1] and their group-site cations include A = Na + K ± Ca ± □, B = Ca ± Na ± Mn^{2+} ± Fe^{2+} ± Mg, C = Mg + Ti^{4+} ± Fe^{2+} ± Mn^{2+} ± Cr ± Ni ± Zn ± Al ± Fe^{3+}, T = Si + Al ± Ti, and W = OH ± F ± Cl ± O (where Mn, Cr, Ni, Zn and Cl are ≤ 0.2 apfu).

Theoretical observation and linear regression analysis of these data allowed us to obtain four "mass-based" equations, which are included in an user-friendly spreadsheet (AMFORM.xlsx) allowing to (i) calculate the unit-formula from EMP data with a precision 2-4 times higher than that of recently proposed methods (Hawthorne et al. 2012; Locock, 2014), (ii) discard unreliable analyses, and (iii) estimate $^{W}O^{2-}$ and $^{C}Fe^{3+}$ contents of Li-free (and Cl-poor) *C*2/*m* amphiboles not affected by post-crystallization oxidation/dehydrogenation processes (i.e., with $2\ ^{C}Ti \geq\ ^{W}O^{2-}$).

Hawthorne, F.C., Oberti, R., Della Ventura, G., Mottana, A. (2007): Amphibole: Crystal chemistry, occurrence, and health issues. *Rev. Mineral. Geochem.*, **67**, 545 p.

Hawthorne, F.C., Oberti, R., Harlow, G.E., Maresch, W.V., Martin, R.F., Schumacher, J.C., Welch, M.D. (2012): IMA Report - Nomenclature of the amphibole supergroup. *Am. Mineral.*, **97**, 2031-2048.

Holland, T.J.B. & Blundy, J.D. (1994): Non-ideal interactions in calcic amphiboles and their bearing on amphibole-plagioclase thermometry. *Contrib. Mineral. Petrol.*, **116**, 433-447.

Locock, A.J. (2014): An Excel spreadsheet to classify chemical analyses of amphiboles following the IMA 2012 recommendations. *Comput. Geosci.*, **62**, 1-11.

Oberti, R., Vannucci, R., Zanetti, A., Tiepolo, M., Brumm, R.C. (2000): A crystal chemical re-evaluation of amphibole/melt and amphibole/clinopyroxene D_{Ti} values in petrogenetic studies. *Am. Mineral.*, **85**, 407-419.

Ridolfi, F. & Renzulli, A. (2012): Calcic amphiboles in calc-alkaline and alkaline magmas: thermobarometric and chemometric empirical equations valid up to 1,130°C and 2.2 GPa. *Contrib. Mineral. Petrol.*, **163**, 877-895.

Ridolfi, F., Renzulli, A., Puerini, M. (2010): Stability and chemical equilibrium of amphibole in calc-alkaline magmas: an overview, new thermobarometric formulations and application to subduction-related volcanoes. *Contrib. Mineral. Petrol.*, **160**, 45-66.

INFLUENCE OF PRESSURE ON DISCLINATION STRUCTURES AND GRAIN-BOUNDARY MIGRATION OF A {310}/[001] BOUNDARY IN MgO

Sun X.-Y.[1], Cordier P.*[1], Taupin V.[2], Fressengeas C.[2] & Karki B.B.[3-4]

[1] Unité Materiaux et Transformations, Centre National de la Recherche Scientifique, Université de Lille 1, Villeneuve d'Ascq, France

[2] Laboratoire d'Etude des Microstructures et de Mecanique des Materiaux, Universite de Lorraine, Centre National de la Recherche Scientifique, Metz, France

[3] Department of Computer Science, Louisiana State University, Baton Rouge, LA, USA

[4] Department of Geology and Geophysics, Louisiana State University, Baton Rouge, LA, USA

Corresponding email: xiaoyu.sun@univ-lille1.fr

Keywords: disclination, grain-boundary migration, high pressure

Due to the gravitational self-compression, the pressures in the Earth's mantle are usually thousands or millions of times atmospheric pressure. The high pressure has a great influence to the mechanical and physical behaviors of the Earth materials such as rheology. Here we focus on how pressure may influence the contribution of grain boundaries to the rheology of a crystalline aggregate. We focus on the grain-boundary migration of a MgO {310}/[001] boundary described through its disclination structures. At first, the displacement, strain, rotation and curvature fields in the boundary area at different pressures are obtained using the discrete atomistic positions generated by first-principles calculation. The discontinuties of displacement and rotation fields are described by dislocation and disclination density fields, respectively. Then, the disclination/dislocation model is used as the initial conditions in continuum mechanics simulations to study the pressure-induced boundary migration of tilt boundaries. The present study may provide better understanding of the structure, dynamics of the Earth materials.

HIGH P-T STABILITY OF Fe_5O_6 AND ITS COEXISTENCE WITH OTHER Fe-OXIDES

Woodland A.B.*[1], Uenver-Thiele L.[1] & Boffa Ballaran T.[2]
[1] Institut für Geowissenschaften, Goethe-Universität Frankfurt am Main, Germany
[2] Bayerisches Geoinstitut, Universität Bayreuth, Germany
Corresponding email: woodland@em.uni-frankfurt.de

Keywords: Fe_5O_6, Fe-oxide, high pressure

The recently reported synthesis of Fe_5O_6 (Lavina & Meng, 2015; Woodland et al., 2015) makes the high pressure and temperature phase relations in the Fe-O system even more complicated than suggested just a few years ago when Fe_4O_5 was first discovered (Lavina et al., 2011; Woodland et al., 2012).

A series of multi-anvil experiments have been performed over a large range of pressure and temperature using magnetite and metallic Fe as starting materials.

Fe_5O_6 has a substantial P-T stability field with the low-P phase boundary lying between 8 (here a mixture of magnetite and wüstite is present) and 10 GPa and it remains stable up to at least 23 GPa. This phase was synthesised over a range of temperature from 1100-1600°C. Under these conditions, the assemblages Fe_4O_5 + Fe_5O_6 and Fe_5O_6 + wüstite are stable depending on bulk oxidation state. Under even more oxidizing compositions hematite + Fe_4O_5 is the stable paragenesis. These assemblages are consistent with the model calculations of Myhill et al. (2016). Considering the rather reduced redox conditions expected in the mantle, assemblages involving Fe_5O_6 should be the most relevant for the Earth. Under the conditions so far explored, Fe_6O_7 was not found to be stable. However, X-ray powder diffraction data reveal an additional phase in several experiments that appears to be consistent with a monoclinic Fe_9O_{11} phase. This new phase has a Fe^{3+}/Fe_{tot} = 0.44, which places it between Fe_5O_6 and Fe_4O_5 in terms of oxidation state.

Single-crystal X-ray diffraction confirms that Fe_5O_6 belongs to the *Cmcm* space group, making it structurally related to Fe_4O_5 and a member of the $CaFe_{2+n}O_{4+n}$ series. At ambient conditions, the cell parameters are a = 2.88 Å, b = 9.94 Å, c = 15.37 Å, with small variations depending on the synthesis pressure. The molar volume of Fe_5O_6 decreases slightly with increasing synthesis pressure, suggesting variable cation distributions may play a role in stabilizing this phase, like that observed for spinel. Unpolarized Raman spectra of Fe_5O_6 and Fe_4O_5 are very similar, with one major broad peak at ~ 665 cm^{-1}. This peak is only slightly shifted relative to that of magnetite (671 cm^{-1}). However, additional peaks in the magnetite spectrum should allow it to be distinguished from the other two new Fe-oxides.

Lavina, B. & Meng, Y. (2015): Unraveling the complexity of iron oxides at high pressure and temperature: synthesis of Fe_5O_6. *Sci. Adv.*, **1**, e1400260.

Lavina, B., Dera, P., Kim, E., Meng, Y., Downs, R.T., Weck, P.F., Sutton, S.R., Zhao, Y. (2011): Discovery of the recoverable high-pressure iron oxide Fe_4O_5. *Proc. Nat. Acad. Sci.*, **108**, 17281-17285.

Myhill, R., Ojwang, D.O., Ziberna, L., Frost, D.J., Boffa Ballaran, T., Miyajima, N. (2016) On the P-T-fO_2 stability of Fe_4O_5, Fe_5O_6 and Fe_4O_5-rich solid solutions. *Contrib Mineral Petrol.*, **171**, 51.

Woodland, A.B., Frost, D.J., Trots, D.M., Klimm, K., Mezouar, M. (2012): In situ observation of the breakdown of magnetite (Fe_3O_4) to Fe_4O_5 and hematite at high pressures and temperatures. *Am. Mineral.*, **97**, 1808-1811.

Woodland, A.B., Uenver-Thiele, L., Boffa Ballaran, T. (2015): Synthesis of Fe_5O_6 and the high-pressure stability of Fe^{2+}-Fe^{3+}-oxides related to Fe_4O_5. Goldschmidt Conference, Prague, August 2015. Nr. 3446.

DOLOMITE TO DOLOMITE-II: A HIGH PRESSURE *AB-INITIO* STUDY

Zucchini A.*[1], Prencipe M.[2], Belmonte D.[3] & Comodi P.[1]
[1] Dipartimento di Fisica e Geologia, Università di Perugia, Italy
[2] Dipartimento di Scienze della Terra, Università di Torino, Italy
[3] Dipartimento di Scienze della Terra, dell'Ambiente e della Vita, Università di Genova, Italy
Corresponding email: azzurra.zucchini@unipg.it

Keywords: dolomite, cation disorder, high pressure

Carbonates are referred to as key phases in the Earth carbon cycle being the most important carbon-bearing minerals. Many works are addressed to study the carbonate stability at high pressure (H*P*) conditions and the driving force for phase transitions (e.g., Merrill & Basset, 1975; Ross & Reeder, 1992; Santillàn et al., 2003; Ungureanu et al., 2010; Hammouda et al., 2011; Merlini et al., 2012; Zucchini et al., 2014). Two H*P* phase transitions were observed for dolomite: (i) at approximately 17 GPa to dolomite-II (ex. Santillán et al., 2003; Merlini et al., 2012; Zucchini et al., 2014), and (ii) at approximately 35 GPa to dolomite-III (Merlini et al., 2012). The phase transition occurrence in dolomite seems to be influenced by cation disordering (Zucchini et al., 2014).

The present study is aimed to analyse by *ab-initio* calculations, on the one hand, the driving force for dolomite to dolomite-II phase transition and, on the other hand, the behaviour and stability at H*P* of ordered and disordered dolomites and dolomite-II.

Ab-initio calculations were carried out by means of CRYSTAL09 program (Dovesi et al., 2005). The disordered geometry was taken from Zucchini et al. (2012) and optimised at different pressures up to approximately 26 GPa.

In order to evaluate temperature effects on the phase transition in the range of validity of a fully ordered structural model, thermodynamic calculations were performed on the two dolomite polymorphs.

A soft mode, whose frequency becomes imaginary at *P* higher than approximately 17 GPa, was located at the F point of the rhombohedral Brillouin zone as the driving force for dolomite to dolomite-II phase transition. As regards the baric behaviour, dolomite-II polyhedra distortion was found to decrease with *P* becoming almost regular at ~17 GPa (phase transition). At $P < 17$ GPa the distortion of the dolomite-II like crystal structure increases again to values comparable with the low pressure dolomite. The compressibility analysis shows changes on the dolomite-II like structure deformation style before and after the phase transition [*i.e.* $K_0 = 95.4(5)$ GPa and $K' = 4.26(8)$ at low *P* and $K' = 3.44(3)$, fixing V_0 and K_0, at H*P* after the phase transition].

As regards disordering, it was not shown to significantly influence the dolomite bulk compressibility. However, the disordered dolomite was found not to undergo phase transition in the 0 to 26 GPa *P* range. Thus, the the strong influence of cation disordering on dolomite stability at H*P* is confirmed.

Thermodynamic calculations show that the dolomite to dolomite-II phase transition boundary is located at $P = 16.75$ GPa and $T = 300$ K confirming data from static calculations and soft-mode analysis.

Further calculations, including vibrational analysis, are needed to check for the disordered dolomite stability at H*P*. Additionally, the present study is in progress looking at the dolomite-III crystal structure.

Dovesi, R., Orlando, R., Civalleri, B., Roetti, C., Saunders, V.R., Zicovich-Wilson, C.M. (2005): CRYSTAL: a computational tool for the *ab initio* study of the electronic properties of crystals. *Z. Kristallogr.*, **220**, 571-573.

Hammouda, T., Andrault, D., Koga, K., Katsura, T., Martin, A.M. (2011): Ordering in double carbonates and implications for processes at subduction zones. *Contrib. Mineral. Petrol.*, **161**, 439-450.

Merlini, M., Crichton, W.A., Hanfland, M., Gemmi, M., Müller, H., Kupenko, I., Dubrovinsky, L. (2012): Structures of dolomite at ultrahigh pressure and their influence on the deep carbon cycle. *Proc. Nat. Acad. Sci.*, **109**, 13509-13514.

Merril, L. & Basset, W.A. (1975): The structure of $CaCO_3$(II), a high-pressure metastable phase of calcium carbonate. *Acta Crystallogr.*, **B21**, 343-349.

Ross, N.L. & Reeder, R.J. (1992): High-pressure structural study of dolomite and ankerite. *Am. Mineral.*, **77**, 412-421.

Santillán, J., Williams, Q., Knittle, E. (2003): Dolomite-II: A high-pressure polymorph of $CaMg(CO_3)_2$. *Geophys. Res. Letters*, **30**, 1054.

Ungureanu, C.G., Prencipe, M., Cossio, R. (2010): Ab initio quantum-mechanical calculation of $CaCO_3$ aragonite at high pressure: thermodynamic properties and comparison with experimental data. *Eur. J. Mineral.*, **22**, 693-701.

Zucchini, A., Prencipe, M., Comodi, P., Frondini, F. (2012): Ab initio study of cation disorder in dolomite. *Calphad*, **38**, 177-184.

Zucchini, A., Comodi, P., Nazzareni, N., Hanfland, M. (2014): The effect of cation ordering and temperature on the high-pressure behaviour of dolomite. *Phys. Chem. Minerals*, **41**, 783-793.

Session S15:

Structural behavior and energetic properties of minerals

Conveners:

Matteo Ardit (Ferrara – Italy)

Charles A. Geiger (Salzburg – Austria)

Alan Woodland (Canberra – Australia)

EXPERIMENTAL STUDY OF THE INFLUENCE OF CRYSTALLIZATION CONDITIONS ON CAPTURE AND DISTRIBUTION OF GERMANIUM IN QUARTZ CRYSTALS AND THEIR CHARACTERISTIC

Balitsky D.V.[1], Balitsky V.S.*[1], Balitskaya L.V.[1], Setkova T.V.[1] & Nekrasov A.N.[1]
[1] Institute of Experimental Mineralogy, Russian Academy of Sciences, Chernogolovka, Russia
Corresponding email: balvlad@iem.ac.ru

Keywords: quartz, germanium oxide, hydrothermal crystal growth

The report provides new data on the growth conditions of homogeneous high germanium quartz (HGQ) crystals, and the investigation of their crystal-chemical and piezoelectric characteristics. In contrast to previous studies (Balitsky et al. 2004, 2005), the reproducible growth conditions of HGQ with GeO_2 10-14 wt.% have been determined. These crystals were grown in the heat-resistant autoclaves in solutions of NH_4F on seeds parallel faces trigonal dipyramid {s}, trigonal prism {x} and Y-rods at temperatures above 530°C and pressures above 70 MPa. The growth rate of HGQ crystals under these conditions reaches the first tenths of mm/day. The temperature and growth rate of crystals maximum influences on germanium content in quartz. In the temperature range from 400 to 700°C the GeO_2 content in quartz is changed from 3.6 to 30.06 wt.%. The maximum content of germanium are marked in growth, and sectors, and minimum – in sector. The <+s>, <+x> and <-x> sectors have an intermediate position. Parasitic sectors of growth and zones with various (to several wt.%) content of germanium inside of the sectors is often observed. The most equal distribution of germanium is observed in the and sectors which are not subjected to twining and degeneration. In the sector «striated» character of germanium distribution is observed. It is connects with the regeneration mechanism of crystal growth.

The values of *a* and *c* unit cell parameters equal to 4.9131 and 5.4050 Å accordingly for synthetic quartz and they increase to the values 4.9233 and 5.4240 Å for the quartz containing 24 wt.% of GeO_2. It proves structural position of germanium in quartz structure. The IR-spectra of HGQ show two new absorption bands with maximums close to 1010 and 930 cm^{-1}, and two absorption bands with maximums at 695 and 513 cm^{-1} are disappeared. The Raman spectra of the crystals contained more than 12 wt.% of GeO_2 show that the almost all absorption bands are displaced on 10-15 cm^{-1} in area of the short-wave vibration.

Piezoelectric characteristics of the HGQ crystals are near to gallium orthophosphate, $\alpha \rightarrow \beta$ transition is increased to 900°C and it rises more at increasing of germanium content. The elements prepared from HGQ crystals are greatly increasing the temperature limits of equipment operability. The electromechanical coupling coefficient of HGQ is also near to gallium orthophosphate. Dielectric loss tangent of HGQ crystals in two to three orders of magnitude lower than that of natural and standard synthetic quartz.

Balitsky, V.S., Balitsky, D.V., Nekrasov, A.N., Balitskaya, L.V., Bondarenko, G.V., Samokhvalova, O.L. (2004): Growth, structural-morphological features, and some properties of quartz-germanium oxide solid solution. *Dokl. Earth Sci.*, **396**, 500-503.

Balitsky, V.S., Balitsky, D.V., Nekrasov, A.N., Balitskaya, L.V. (2005): Growth and characterization of $Si_xGe_{1-x}O$ solid solution single crystals. *J. Cryst. Growth*, **275**, 807-811.

MECHANICAL PROPERTIES OF RADIATION DAMAGED ZIRCON AND TITANITE

Beirau T.*[1], Nix W.D.[2], Ewing R.C.[3], Schneider G.A.[4], Boatner L.A.[5], Groat L.A.[6] & Bismayer U.[1]
[1] Fachbereich Geowissenschaften, Universität Hamburg, Germany
[2] Department of Materials Science and Engineering, Stanford University, CA, USA.
[3] Department of Geological Sciences, Stanford University, CA, USA
[4] Institut für Keramische Hochleistungswerkstoffe, Technische Universität Hamburg, Germany
[5] Materials Science and Technology Division, Oak Ridge National Laboratory, TN, USA
[6] Department of Earth, Ocean and Atmospheric Sciences, University of British Columbia, Vancouver, Canada
Corresponding email: tobias.beirau@uni-hamburg.de

Keywords: radiation damage, mechanical properties, zircon

The presented results provide new insights into the relationship between radiation dose dependent structural damage due to natural U and Th impurities and the anisotropic mechanical properties (Poisson's ratio, elastic modulus and hardness) of zircon. Natural zircon samples from Sri Lanka (see Muarakami et al., 1991) and synthetic samples, covering a dose range of zero up to 6.8×10^{18} α-decays/g, have been studied by nanoindentation. Measurements and calculations, based on elastic stiffness constants determined by Özkan (1976), revealed a general radiation-induced decrease in stiffness and hardness and an increase of the Poisson's ratio with increasing dose. Additionally new results of the thermally induced structural reorganization and the macroscopic mechanical properties of radiation-damaged titanite will be presented (Beirau et al., 2016). The thermally induced recrystallization is accompanied by massive dehydration leading to considerable stiffening and hardening.

Beirau, T., Nix, W.D., Ewing, R.C., Schneider, G.A., Groat, L.A., Bismayer, U. (2016): Mechanical properties of natural radiation-damaged titanite and temperature induced structural reorganization: A nanoindentation and Raman spectroscopic study. *Am. Mineral.*, **101**, 399-406.

Murakami, T., Chakoumakos, B.C., Ewing, R.C., Lumpkin, G.R., Weber, W.J. (1991): Alpha-decay event damage in zircon. *Am. Mineral.*, **76**, 1510-1532.

Özkan, H. (1976): Effect of nuclear radiation on the elastic moduli of zircon. *J. Appl. Phys.*, **47**, 4772-4779.

As^{5+} STRUCTURALLY INCORPORATED INTO PHOSPHOSIDERITE ($FePO_4 \cdot 2H_2O$) – AN EXAFS STUDY

Bolanz R.M.*[1], Wierzbicka-Wieczorek M.[1], Giester G.[2], Göttlicher J.[3] & Steininger R.[3]
[1] Institut für Geowissenschaften, Friedrich-Schiller-Universität Jena, Germany
[2] Institut für Mineralogie und Kristallographie, Universität Wien, Austria
[3] Angstromquelle Karlsruhe, Karlsruher Institut für Technologie, Eggenstein-Leopoldshafen, Germany
Corresponding email: ralph.bolanz@uni-jena.de

Keywords: arsenic, As^{5+}, substitution

Monoclinic ($P2_1/n$) phosphosiderite ($FePO_4 \cdot 2H_2O$) is the polymorph of orthorhombic strengite (*Pbca*), which is isostructural to scorodite ($FeAsO_4 \cdot 2H_2O$). While arsenic can be structurally incorporated into strengite by a fractional miscibility between strengite and scorodite, the incorporation of As^{5+} into phosphosiderite and its dehydration product $FePO_4$ ($P2_1/n$) has never been investigated and is the subject of this study. Phosphosiderite was synthesized under hydrothermal conditions at 200°C in the presence of arsenic and incorporated 0.044±0.001, 0.084±0.001, 0.165±0.002, 0.425±0.004 and 0.844±0.014 wt.% As at initial molar As/Fe solution ratios of 0.05, 0.1, 0.2, 0.5 an 1, respectively. At initial molar As/Fe solution ratios of 0.2, 0.5 and 1, the P concentration in phosphosiderite decreases by 1.02, 1.58 and 1.25 P atoms for each incorporated As, respectively. Crystals of As-bearing phosphosiderite display grains sizes up to 60 µm and no significant size or morphology change with increasing As content. The unit-cell parameters of phosphosiderite increase from 5.326(6) Å (*a*), 9.793(8) Å (*b*), 8.709(3) Å (*c*) and 90.54(0)° (β), grown in the absence of As, to 5.329(0) Å (*a*), 9.797(5) Å (*b*), 8.713(7) Å (*c*) and 90.56(7)° (β), for phosphosiderite synthesized at an initial molar As/Fe solution ratio of 1. X-ray absorption spectroscopy displays only arsenic in pentavalent state (As^{5+}), which resides on the P position in phosphosiderite in a local structure similar to strengite and scorodite. Single crystal X-ray diffraction indicates As on the P position of phosphosiderite and decreasing (P/As)–O–Fe bonding angles, which further supports the idea of changes in local coordination.
We propose the structural incorporation of As^{5+} into phosphosiderite by a homovalent substitution of P^{5+} in a strengite/scorodite-like arrangement, in contrast to the dehydration product of phosphosiderite, $FePO_4$, which shows no significant changes in unit-cell parameters with increasing As content and the local coordination of As^{5+} in $FePO_4$ suggests a homovalent substitution of P^{5+} by As^{5+} without substantial structural change.

CRYSTAL STRUCTURE AND PHASE TRANSITION IN NOELBENSONITE $BaMn^{3+}_2[Si_2O_7](OH)_2 \cdot H_2O$

Cametti G.*[1] & Armbruster T.[1]
[1] Mineralogische Kristallographie, Institut für Geologie, Universität Bern, Switzerland
Corresponding email: georgia.cametti@krist.unibe.ch

Keywords: noelbensonite, structure, phase transition

Noelbensonite $BaMn^{3+}_2[Si_2O_7](OH)_2 \cdot H_2O$ is a member of the lawsonite group and the barium analogue of hennomartinite $SrMn^{+3}_2[Si_2O_7](OH)_2 \cdot H_2O$. In this study we investigated a natural sample from the Cerchiara mine, north Appennines, Italy (Lucchetti et al., 1988) by single-crystal X-ray diffraction in order to determine the structure at room temperature (RT) and to evaluate possible temperature dependent phase transitions described for lawsonite and hennomartinite. The structure of the latter minerals exhibits different temperature dependent systems of hydrogen bonds causing the symmetry evolution $P2_1cn \rightarrow Pmcn \rightarrow Cmcm$. X-ray data for noelbensonite were collected at RT, 100, 150, 200, 275 and 325°C.

In contrast to previous assumptions (Kawachi et al., 1996), diffraction data of noelbensonite at RT display the acentric space group $P2_1cn$, a = 6.31303(2), b = 9.0977(3), c = 13.5820(4) Å, V = 779.73(4) Å^3 and the refinement converged to $R1$ = 0.0280. This space group is suggested by the occurrence of several C-centering forbidden reflections (hkl, with $h + k = 2n + 1$).

The structure of noelbensonite determined at RT corresponds to the low temperature (-100°C) structure of lawsonite (Libowitzky & Armbruster, 1995) and to the phase of hennomartinite between 25 and 95°C (Libowitzky & Armbruster, 1996). In contrast to hennomartinite, the noelbensonite $P2_1cn$ structure does not exhibit inversion twinning. Hydrogen positions refined for noelbensonite correspond to those of the $P2_1cn$ hennomartinite phase.

Up to 200°C the structure preserved the $P2_1cn$ symmetry. However, with increase of temperature the weak reflections characteristic of the P Bravais lattice were no longer detectable and strong correlations arose among refined parameters from the approaching C-centered lattice. Such correlations were mastered by imposing constraints on coordinates and displacement parameters. At 275°C the structure changed to space group $Cmcm$. The intermediate $Pmcn$ phase detected in lawsonite (Libowitzky & Armbruster, 1995) was not found for noelbensonite. The $Cmcm$ structure refinement of noelbensonite at 275°C ($R1$ = 0.0310) allowed determination of the hydrogen-bond net. In general, the C-centered structure corresponds to those of hennomartinite at 245°C and of lawsonite above 0°C.

An additional data collection was carried out at RT after heating excursion to 325°C. The diffraction pattern was characterized by reoccurring of weak C-forbidden reflections and the refinement was successful in space group $P2_1cn$ ($R1$ = 0.0286). However, different from the original RT data set, the crystal exhibited inversion twinning (refined twin components 0.71(2)/0.29(2)) indicating that after heating excursion and transformation to the centrosymmetric $Cmcm$ phase, the final low temperature $P2_1cn$ structure preserved features of a center of symmetry displayed as twinning. This may indicate that the natural sample crystallized in space group $P2_1cn$.

Kawachi, Y., Coombs, D.S., Miura, H. (1996): Noélbensonite, a new BaMn silicate of the lawsonite structure type, from Woods mine, New South Wales, Australia. *Mineral. Mag*, **60**, 369-374.

Libowitzky, E. & Armbruster, T.M. (1995): Low-temperature phase transitions and the role of hydrogen bonds in lawsonite. *Am. Mineral*., **80**, 1277-1285.

Libowitzky, E. & Armbruster, T.M. (1996): Lawsonite-type phase transitions in hennomartinite, $SrMn_2[Si_2O_7](OH)_2 \cdot H_2O$. *Am. Mineral*. **81**, 9-18.

Lucchetti, G., Cortesogno, L., Palenzona, A. (1988): Low-temperature metamorphic mineral assemblages in Mn-Fe ores from Cerchiara mine (northern Apennine, Italy). *N. Jb. Miner. Mh.*, **1988**, 367-383.

QUANTIFICATION OF RADIATION EFFECTS IN ZIRCON: FOCUSED-ION BEAM PREPARATION OF THIN LAMELLAE FOR ION-IRRADIATION EXPERIMENTS

Chanmuang C.*[1], Habler G.[2], Lenz C.[1-3], Nasdala L.[1] & Váczi T.[4]
[1] Institut für Mineralogie und Kristallographie, Universität Wien, Austria
[2] Department für Lithosphärenforschung, Universität Wien, Austria
[3] Institute of Materials Engineering, Australian Nuclear Science and Technology Organisation, Lucas Heights, Australia
[4] Department of Mineralogy, Eötvös Loránd University, Budapest, Hungary
Corresponding email: chutimun.chanmuang@univie.ac.at

Keywords: FIB, ion irradiation, Raman spectroscopy

Radiation effects in natural minerals or their synthetic analogs can be very well studied by performing ion-irradiation experiments in the laboratory. Compared to the investigation of U- and/or Th-containing minerals, which have experienced self-irradiation over geologic periods of time, this approach has the advantage that no uncertain thermal history (and hence perhaps damage annealing) needs to be considered in interpreting the results.

To avoid biased conclusions, however, two aspects need to be addressed carefully. First, only analytical techniques should be chosen whose volume resolution is better than the lateral extension of sample volumes affected by ion-irradiation damage. For instance, it has been discussed critically (Nasdala, 2009) that the irradiation damage in zircon created by irradiation with 280 keV Pb ions, which is restricted to a ca. 100 nm thin near-surface layer, cannot be studied readily by means of conventional reflectance infrared absorption spectroscopy (Zhang et al., 2008). This is because the depth resolution of latter technique exceeds the thickness of the sample volume irradiated by more than one order of magnitude. A similar example is found in the study of Picot et al. (2008) who attempted to analyze damaged layers of ca. 1.5 mm thickness by Raman spectroscopy. The spectra of Picot et al. (2008) however were dominated by the Raman signal of the undamaged host behind the thin damaged layer (Nasdala et al., 2009). For the investigation of shallow damage layers, the application of high-resolution techniques such as Rutherford backscattering spectrometry (Grambole et al., 2007) or transmission electron microscopy (Lian et al., 2002) hence appears more worthwhile.

Second, it also needs to be taken into consideration that the creation of a surficial irradiation-damaged layer causes complex stress patterns. The damaged layer is affected by volume expansion, which is partially hindered by the underlying host; this results in compressive strain in the damaged layer. The expansion of the damaged layer, in turn, must result in dilative strain in the neighboring host. Both strain fields are likely to affect Raman spectroscopic results.

We therefore prepare samples to be irradiated as thin lamellae by means of focused-ion-beam cutting (Wirth, 2004). Thicknesses are chosen to correspond to irradiation depths of the ions irradiated: For instance 1.5 mm foils are produced for the irradiation of zircon with 10 MeV Au ions. This approach virtually allows one to remove, prior to the irradiation experiment, the host behind the irradiated volume. Compressive/dilative strain fields can thus be avoided. Also, careful adjustment of sample thicknesses allows us to predict, using SRIM (Ziegler et al., 2010) results, the fraction of irradiation damage created. Aspects of FIB foil preparation are discussed, and first results are presented.

Acknowledgements: Financial support was provided by Austrian Science Fund (FWF) through project P24448 to L.N.

Grambole, D., Herrmann, F., Heera, V., Meijer, J. (2007): Study of crystal damage by ion implantation using micro RBS/Channeling. *Nucl. Instrum. Meth. B*, **260**, 276-280.

Lian, J., Zu, X.T., Kutty, K.V.G., Chen, J., Wang, L.M., Ewing, R.C. (2002): Ion-irradiation-induced amorphization of $La_2Zr_2O_7$ pyrochlore. *Phys. Rev. B*, **66**, 054108.

Nasdala, L. (2009): Pb^+ irradiation of synthetic zircon ($ZrSiO_4$): Infrared spectroscopic investigation – Discussion. *Am. Mineral.*, **94**, 853-855.

Nasdala, L., Grötzschel, R., Probst, S., Bleisteiner, B. (2010): Irradiation damage in monazite ($CePO_4$): An example to establish the limits of Raman confocality and depth resolution. *Can. Mineral.*, **48**, 351-359.

Picot, V., Deschanels, X., Peuget, S., Glorieux, B., Seydoux-Guillaume, A.M., Wirth, R. (2008): Ion beam radiation effects in monazite. *J. Nucl. Mater.*, **381**, 290-296.

Wirth, R. (2004): Focused Ion Beam (FIB): A novel technology for advanced application of micro- and nanoanalysis in geosciences and applied mineralogy. *Eur. J. Mineral.*, **16**, 863-876.

Zhang, M., Boatner, L., Salje, E.K.H., Ewing, R.C., Daniel, P., Weber, W.J., Zhang, Y., Farnan, I. (2008): Micro-Raman and micro-infrared spectroscopic studies of Pb- and Au-irradiated $ZrSiO_4$: Optical properties, structural damage, and amorphization. *Phys. Rev. B*, **77**, 144110.

Ziegler, J.F., Biersack, J.P., Littmark, U. (2010): SRIM – The stopping and range of ions in matter (2010). *Nucl. Instrum. Meth. B*, **268**, 1818-1823.

STRUCTURAL LOCAL DEFECTS AND MODIFICATION OF THE POLAR BEHAVIOUR IN A SYNTHETIC PEROVSKITE

Confalonieri G.*[1], Capitani G.[2], Buscaglia V.[3], Rotiroti N.[1] & Dapiaggi M.[1]
[1] Dipartimento di Scienze della Terra "A. Desio", Università di Milano, Italy
[2] Dipartimento di Scienze dell'Ambiente, del Territorio e di Scienze della Terra, Università di Milano-Bicocca, Italy
[3] Istituto per l'Energetica e le Interfasi, Consiglio Nazionale delle Ricerche, Genova, Italy
Corresponding email: giorgia.confalonieri@unimi.it

Keywords: TEM, synthetic perovskite, structural disorder

$BaTiO_3$ is widely studied material in different research fields. From the geological point of view, this perovskite is often employed to simulate lower mantle deformation in atmospheric pressure by the dislocation-controlled creep mechanisms (Cheng et al., 2006). On the other hand, during the last years, the scientific community has paid great attention on free-lead ferroelectrics and $BaTiO_3$ has become the most widely used functional ceramic material in electronics, finding wide applications in devices as microphones, ultrasonic and underwater transducers, multilayer ceramic capacitors and spark generators (Yasmin et al., 2011). Furthermore, in order to tailor its properties for specific uses, this synthetic perovskite is easily and usually doped to improve the material performance, for example modifying the long-range order and consequently the ferroelectric and dielectric properties. In this work the case of $BaTi_{0.8}Ce_{0.2}O_3$ ceramic perovskite is presented. The incorporation of this amount of cerium in the structure allows to change the features of the pure barium titanate from a conventional ferroelectric to a non-ergotic relaxor (Shvartsman & Lupascu, 2012). This evolution in the polar behaviour depends obviously by the dopant type and amounts, but a clear and satisfying explanation is not yet available. In order to understand the structural modification linked to the Ce-Ti substitution, we undertaken a study of the local structure. Total scattering powder diffraction and TEM exploration have been coupled to study local deviations caused by the cerium introduction. Pair Distribution Function analyses has revealed a considerable local structural disorder, which cannot be described by conventional crystallographic models. Moreover, TEM investigations have demonstrated a chemical homogeneity of the sample and a perfect equilibrium crystallization, but also a very large dislocation density. This kind of defects contributes largely to the local disorder and could play an important role on the polar properties of this material.

Cheng, S.Y., Ho, N.J., Lu, H.Y (2006): Dissocation of the <001> dislocation and their interaction with dislocation loops in tetragonal $BaTiO_3$. *J. Am. Ceram. Soc.*, **89**, 1659-1667.

Shvartsman, V.V. & Lupascu, D.C. (2012): Lead-free relaxor ferroelectrics. *Am. Ceram. Soc.*, **95**, 1-26.

Yasmin, S., Choudhur, S., Hakim, M.A., Bhuiyan, A.H., Rahman, M.J (2011): Effect of cerium doping on microstructure and dielectric properties of $BaTiO_3$ ceramics. *J. Mater. Sci. Technol.*, **27**, 759-763.

A THERMODYNAMIC STUDY OF END-MEMBER ANDRADITE AND ANDRADITE ($Ca_3Fe_2Si_3O_{12}$) – GROSSULAR ($Ca_3Al_2Si_3O_{12}$) SOLID SOLUTIONS

Geiger C.A.*[1] & Dachs E.[1]
[1] Fachbereich Chemie und Physik der Materialien, Universität Salzburg, Austria
Corresponding email: ca.geiger@sbg.ac.at

Keywords: thermodynamics, solid solutions, garnet

Garnet is a key rock-forming mineral whose geological occurrence is widespread. Various petrologic, geochemical and geophysical processes can be best interpreted if garnet's thermodynamic properties are understood. In terms of macroscopic thermodynamic properties, there has been considerable work done over the years investigating garnet solid solutions, but much still needs to be done before a full quantitative understanding is at hand. We have been investigating both natural and synthetic end-member andradite (An) and grossular (Gr) garnets as well as $Ca_3Fe_2Si_3O_{12}$–$Ca_3Al_2Si_3O_{12}$, solid solutions. Volume, heat capacity, and entropy are three fundamental thermodynamic properties and they have been determined for both end members. The mixing properties for each of these functions have been determined for the An-Gr binary.

$Ca_3Fe_2Si_3O_{12}$–$Ca_3Al_2Si_3O_{12}$ garnets were synthesized at high pressures in a piston-cylinder device and, in addition, a number of natural gem-quality single crystals of closely binary composition were obtained. The synthetic samples were carefully characterized by optical microscopy, X-ray diffraction and ^{57}Fe Mössbauer spectroscopy and microprobe analysis in the case of the natural crystals.

The heat capacity, C_p, of synthetic and natural andradite was measured between 2 and 350 K using relaxation calorimetry and from 280 to 800 K using DSC methods. It shows a paramagnetic to antiferromagnetic l-transition related to an ordering of the electron spins of the Fe^{3+} cations with a peak at 11.5 K and extending down to at least 2 K. This l-anomaly moves to lower temperature, weakens and broadens with increasing grossular component in the garnet.

The third-law entropy, $S°$(298.15 K), of the different end-member andradite samples was calculated from the low-temperature C_p data and slight variations in $S°$ were found with preliminary values lying between about 317 and 324 J/(mol·K). Robie et al. (1987) gave a value of 316.4±2.0 J/(mol.K) for synthetic andradite studied with adiabatic calorimetry between 10 and 366 K. However, a full and precise determination of the magnetic phase transition in this latter work was not correct and, thus, their $S°$ value is not quantitative.

Earlier work of ours showed small differences in $S°$ between synthetic and natural grossular crystals (Dachs et al., 2012). In the case of andradite, the slight variations in $S°$ may be due, in part, to small differences in OH contents. Single-crystal IR spectra were recorded on natural and synthetic andradite crystals and minor differences in OH contents were observed. The vibrational entropy of mixing behavior for the $Ca_3Fe_2Si_3O_{12}$–$Ca_3Al_2Si_3O_{12}$ binary was determined to be ideal or nearly so, i.e., $\Delta S^{mix}_{298K} \approx 0$. In contrast to previously published results, the volume of mixing appears to be close to ideal in behavior, $\Delta V^{mix}_{298K} \approx 0$.

Dachs, E., Geiger, C.A., Benisek, A., Grevel, K-D. (2012): Grossular: A crystal-chemical, calorimetric, and thermodynamic study. *Am. Mineral.*,. **97**, 1299-1313.

Robie, R.A., Bin, Z., Hemingway, B.S., Barton, M.D. (1987): Heat capacity and thermodynamic properties of andradite garnet, $Ca_3Fe_2Si_3O_{12}$, between 10 and 1000 K and revised values for $D_fG°_m$ (298.15 K) of hedenbergite and wollastonite. *Geochim. Cosmochim. Acta*, **51**, 2219-2224.

STRUCTURAL INVESTIGATION OF Nd INCORPORATION IN $CaSnO_3$ PEROVSKITE

Goethals J.*[1], Tarrida M.[1], Fourdrin C.[1], Bedidi A.[1], Madon M.[1] & Rossano S.[1]
[1] Laboratoire Géomatériaux et Environnement, Université Paris-Est, Marne-la-Vallée, France
Corresponding email: jules.goethals@u-pem.fr

Keywords: perovskite, Rietveld refinement, Raman spectroscopy

The perovskite structure type ABO_3, which is adopted by a large variety of materials of geological and technological interest, has been extensively investigated in the past decades. Among the interesting compounds the $CaSnO_3$ perovskite has received increasing attention either for its use as analogue for the mantle material (Redfern et al., 2011) or for its wide range of potential applications such as dielectric bodies, gas sensors and anode materials for Li-ion batteries (Cheng & Lu, 2008). When doped with a trivalent rare earth element (REE^{3+}), the $CaSnO_3$ perovskite exhibits promising luminescence properties (Lu et al., 2005 ; Orsi Gordo et al., 2015). Although it could yield better insights on these luminescence properties, the exact distribution of the REE^{3+} between the two potential substitution sites is yet not completely understood. This study thus focuses on the determination of the Nd^{3+} distribution in the $CaSnO_3$ perovskite.

Ceramics have been sintered at high temperature (1550°C) for a wide range of composition (1-x) $CaSnO_3$ - x Nd_2O_3 (with $0 \leq x \leq 0.7$). X-ray patterns were measured in the 2θ range 10-110°. Rietveld refinements of the structures have been performed using Fullprof. Raman spectra were acquired using a 477 nm laser in order to reduce the presence of a fluorescence signal. It is shown that $CaSnO_3$ can incorporate a large amount (up to $x \approx 0.5$) of Nd, at the difference with $CaZrO_3$ that can only accommodate up to $x \approx 0.35$ in the system (1-x) $CaZrO_3$ - x Nd_2O_3 (Larguem, 2006). For $x \leq 0.5$, the unit cell parameters were obtained using the Treor software, and the space groups were determined in an orthorhombic system using Checkcell. It is observed that the unit cell parameters increase linearly with the amount of incorporated Nd. Below x = 0.3, the X-ray patterns are indexed in the orthorhombic *Pbnm* space group. Over this value, the appearance of new reflections leads to a lowering of the symmetry to the *Pmmn* space group. This result suggests a phase transition induced by the Nd incorporation. On the whole range of compositions, Raman vibration modes are strongly affected by the Nd incorporation. An important broadening of almost all the vibrational bands and a shift of some of them are observed. Substitutions of divalent and tetravalent cations on A and B sites have produced similar effects on Raman spectra of the solid solution systems $(Sr_xCa_{1-x})ZrO_3$, $Ca(Zr_ySn_{1-y})O_3$ (Tarrida et al., 2009). Combining Rietveld refinement on the different samples and Raman spectra analysis, the modifications of the $CaSnO_3$ structure in presence of Nd^{3+} are consistent with a majority of Nd^{3+} substituting Ca^{2+} in the A site. A slight proportion of Nd^{3+} however substitutes Sn^{4+} in the B site.

The data obtained in this study complement the existing literature on the substitution of trivalent cations in the perovskite structure especially by evidencing a phase transition, although a linear evolution of the unit cell parameters is observed.

Cheng, H. & Lu, Z. (2008): Synthesis and gas-sensing properties of $CaSnO_3$ microcubes. *Solid St. Sci.*, **10**,1042-1048.

Larguem, H. (2006): Évolution structurale et réactivité chimique hors et sous irradiation de céramiques oxydes envisagées pour le confinement spécifique de radionucléides à vie longue. Thesis, Univ. de Marne La Vallée, 275 p.

Lu, Z., Chen, L., Tang, Y., Li, Y. (2005): Preparation and luminescence properties of Eu^{3+}-doped $MSnO_3$ (M = Ca, Sr and Ba) perovskite materials. *J. All. Comp.*, **387**, 1-4.

Orsi Gordo, V., Tuncer Arslanli, Y., Canimoglu, A., Ayvacikli, M., Galvão Gobato, Y., Henini, M., Can, N. (2015): Visible to infrared low temperature luminescence of Er^{3+}, Nd^{3+} and Sm^{3+} in $CaSnO_3$ phosphors. *Appl. Rad. Isot.*, **99**, 69-76.

Redfern, S.A.T., Chen, C.-J., Kung, J., Chaix-Pluchery, O., Kreisel, J., Salje, E.K.H. (2011): Raman spectroscopy of $CaSnO_3$ at high temperature: a highly quasi-harmonic perovskite. *J. Phys. Cond. Matter*, **23**, 425401.

Tarrida, M., Larguem, H., Madon, M. (2009): Structural investigations of $(Ca,Sr)ZrO_3$ and $Ca(Sn,Zr)O_3$ perovskite compounds. *Phys. Chem. Minerals*, **36**, 403-413.

CERAMIC AND MAGNETIC PROPERTIES OF SYNTHETIC COBALT-DOPED DIOPSIDE

Gori C.*[1], Tribaudino M.[1], Mantovani L.[1], Skogby H.[2], Hålenius U.[2], Dondi M.[3], Delmonte D.[4], Gilioli E.[4], Mezzadri F.[5] & Calestani G.[5]

[1] Dipartimento di Fisica e Scienze della Terra "Macedonio Melloni", Università di Parma, Italy

[2] Department of Geosciences, Swedish Museum of Natural History, Stockholm, Sweden

[3] Istituto di Scienza e Tecnologia dei Materiali Ceramici, Consiglio Nazionale delle Ricerche, Faenza, Italy

[4] Istituto dei Materiali per l'Elettronica ed il Magnetismo, Consiglio Nazionale delle Ricerche, Parma, Italy

[5] Dipartimento di Chimica, Università di Parma, Italy

Corresponding email: claudia.gori@studenti.unipr.it

Keywords: pyroxene, cobalt, pigment

The pyroxene structure can be used as a crystalline host for Co-based pink pigment (Mantovani et al., 2015). Here we present the effects on the coloring and ceramic performances of the chemical and structural modifications induced by the substitution of a smaller cation (Mg^{2+}) by a larger one (Co^{2+}) at the M1 site of the calcium-magnesium pyroxene lattice ($CaCo_xMg_{1-x}Si_2O_6$). The series was synthesized by quenching from melts at T = 1500°C and subsequent annealing at T = 1250°C. The crystals obtained are monophasic with monoclinic structure (space group *C*2/*c*), free of impurities and pink in color. The main structural feature detected is a large increase of the cell volume with the addition of Co^{2+} in the calcium-magnesium pyroxene lattice. Optical absorption and near infrared spectra are dominated by strong absorption bands due to Co^{2+} in octahedral coordination (Dondi et al., 2014). The technological behavior of Co-doped diopside as a ceramic pigment was assessed by simulating the industrial processing of ceramic tiles. Finely ground powders and single crystals were added to the glazes and then pressed to obtain button-shaped pellets. Only a portion of the grounded powders was used in order to obtain a concentration of about 5% by weight of pigment into the glazes. Pulverized pyroxenes were tested in two different glazes, each annealed at its maturing temperature. Co-diopside powder behaves like a dye, dissolving in the melted glazes and imparting a blue-pale violet color due to the diffusion of Co^{2+} into the glassy matrix. Single crystals sized up to 400 µm were tested in two different glazes and heated at 1100°C, following two different kinetic paths. Interface layers and diffusion phenomena between cobalt-pyroxene crystals and glazes in which crystals are dispersed, are revealed by SEM-EDS analysis. Colorimetric data (CIE *L*a*b**) of the glazes containing Co-diopside powders show that a blue coloration (*b** > 25) is obtained even with the occurrence of lower cobalt content in the pyroxene structure (x = 0.2). In the case of glazes tested with Co-diopside powder with x = 0.6, the color coordinates (*L**, *a** and *b**) are very close to those of glazes colored with Co-spinel (Mantovani et al., 2015). Additional investigations were performed on the magnetic properties of Co-doped pyroxenes series. Measurements show a long-range magnetic interaction from a paramagnetic state at the M1 site (filled by Mg and Co clusters) as the Co^{2+} content is increased. With a cobalt concentration around x = 0.8 the magnetic susceptibility (emu/g·Oe) follows the Curie-Weiss law between 150-300 K, but at lower temperatures, the mass magnetization (emu/g) shows the typical cusp expected for a material with global antiferromagnetic interactions (the Néel temperature is T_N = 10 K). The magnetic phase transition disappears with lower Co contents.

Dondi, M., Ardit, M., Cruciani, G., Zanelli, C. (2014): Tetrahedrally coordinated Co^{2+} in oxides and silicates: Effect of local environment on optical properties. *Am. Mineral.*, **99**, 1736-1745.

Mantovani, L., Tribaudino, M., Dondi, M., Zanelli, C. (2015): Synthesis and color performance of $CaCoSi_2O_6$ pyroxene, a new ceramic colorant. *Dyes Pigm.*, **120**, 118-125.

THE ENTHALPY OF FORMATION OF MAGNESIOCARPHOLITE ($MgAl_2[Si_2O_6](OH)_4$)

Grevel K.-D.*[1-2], Nowak W.[1], Majzlan J.[1], Fockenberg T.[2] & Theye T.[3]
[1] Institut für Geowissenschaften, Friedrich-Schiller-Universität Jena, Germany
[2] Institut für Geologie, Mineralogie & Geophysik, Ruhr-Universität Bochum, Germany
[3] Institut für Mineralogie und Kristallchemie, Universität Stuttgart, Germany
Corresponding email: klaus-dieter.grevel@rub.de

Keywords: magnesiocarpholite, calorimetry, enthalpy of formation

Carpholite ($(Mg,Fe)Al_2[Si_2O_6](OH)_4$) with compositions varying from the Fe- to the Mg-endmember and also Mg-rich chloritoid ($(Mg,Fe)Al_2O[SiO_4](OH)_2$) are considered to be two index minerals for low-temperature, high-pressure metamorphic conditions in pelitic rocks (Chopin & Schreyer, 1983). For the derivation of phase diagrams reliable thermodynamic data for these phases are needed. Bertoldi et al. (2006) measured low- and high-temperature heat capacities of natural ferrocarpholite and magnesiocarpholite whereas Grevel et al. (2005) reported *P-V-T* data and the enthalpy of formation of magnesiochloritoid. In this study we derived the enthalpy of formation for synthetic magnesiocarpholite which was synthesized from a gel in a piston cylinder apparatus at 2.5 GPa and 550°C. Seeds of synthetic magnesiocarpholite (Theye, 2000) were used to improve the crystallization process. Purity and composition where checked by XRD and electron microprobe analysis. The enthalpy of drop solution of the sample was then measured at the calorimetry laboratory at Jena university by high-temperature oxide melt calorimetry using lead borate ($2\ PbO \cdot B_2O_3$) at 700°C as solvent (cf. Grevel et al., 2005). The resulting values were used to calculate the enthalpy of formation from the elements, –4754.3±4.0 kJ mol^{-1}. Consistency of the thermodynamic data obtained for magnesiocarpholite with phase equilibrium data reported in the literature (Chopin & Schreyer, 1983, Theye, 2000) was checked by mathematical programming analysis.

Bertoldi, C., Dachs, E., Theye, T. (2006): Calorimetric data for naturally occurring magnesiocarpholite and ferrocarpholite. *Am. Mineral.*, **91**, 441-445.

Chopin, C. & Schreyer, W. (1983): Magnesiocarpholite and magnesiochloritoid: two index minerals of pelitic blueschists and their preliminary phase relations in the model system MgO-Al_2O_3-SiO_2-H_2O. *Am. J. Sci.*, **283-A**, 72-96.

Grevel, K.-D., Kahl, W.-A., Majzlan, J., Navrotsky, A., Lathe, C., Fockenberg, T. (2005): Thermodynamic properties of magnesiochloritoid. *Eur. J. Mineral.*, **17**, 587-598.

Theye, T. (2000): New experimental high pressure data on chloritoid and carpholite. *Eur. J. Mineral.*, *Beiheft No. 1*, **12**, 212.

SYSTEMATIC BEHAVIOR OF K-Na MIXING ENTHALPIES WITH Al-Si ORDER IN ALKALI FELDSPARS AND IMPLICATIONS FOR PHASE EQUILIBRIA

Hovis G.L.*[1]

[1] Department of Geology and Environmental Geosciences, Lafayette College, Easton, PA, USA

Corresponding email: hovisguy@lafayette.edu

Keywords: alkali feldspars, enthalpies of K-Na mixing, Al-Si order-disorder

Because this solution calorimetry laboratory soon will close its doors, we have returned to the alkali feldspar system to measure the enthalpies of solution of a large number of samples in order to achieve the highest possible precision for the heats of K-Na mixing (Hovis, 1986 & 1988). We report on updated investigations of (1) a highly Al-Si ordered low albite - microcline series, (2) a highly disordered analbite - sanidine series, as well as (3) a never-before-studied ion-exchange series based on the Laacher See (Eifel, Germany) “low sanidine”. In all, we have measured the heats of solution of fifty-five new samples, each dissolution in 20.1 wt.% HF at 50°C under isoperibolic conditions. Along with previous measurements on two additional topochemically monoclinic alkali feldspar series, one based on a Madagascar orthoclase specimen and the other on a Swiss adularia, we now have data covering a wide range of alkali feldspar Al-Si distributions. Collectively, data for these five ion-exchange series show clearly that the maximum enthalpies of K-Na mixing systematically increase in magnitude as Al-Si order increases, a (nonlinear) relationship easily expressed in equation form. For four of the series, consistent with the critical compositions of alkali feldspar solvi determined from phase equilibrium studies (e.g., Bachinski & Müller, 1971; Smith & Parsons, 1974), maximum enthalpies of K-Na mixing are achieved in the sodic part of the compositional range at mole fraction potassium between 0.38 and 0.42. The highly disordered analbite - sanidine series, however, displays enthalpies of K-Na mixing that are close to symmetric with respect to composition, this based on highly precise data for a 20-member series. The main variation in enthalpy behavior occurs at the sodic ends of the five series, where solution calorimetric data reflect that higher degrees of Al-Si order make it increasingly difficult, in an energetic sense, to substitute K for Na ions in Na-rich feldspars. With increased Al-Si disorder, and the accompanying volume expansion, K ions find it energetically “easier” to enter the Na-feldspar structure. The nearly symmetric heats of K-Na mixing for analbite - sanidine evidence that K-for-Na and Na-for-K substitution near end-member compositions are about equal energetically for an alkali feldspar structure that is highly expanded by Al-Si disorder. Overall, the systematic behavior observed for enthalpy of K-Na mixing implies that the critical composition for the solvus of highly disordered alkali feldspars occurs closer to the K-Na compositional midpoint than is the case for more ordered feldspars, including the “low sanidine” series. Increased Al-Si order that accompanies feldspar cooling should shift the critical composition of the solvus to more sodic compositions yet at the same time require the limbs of each successive *solvus* to accommodate increasingly higher critical temperatures associated with increasingly greater degrees of order.

Bachinski, S.W. & Müller, G. (1971): Experimental determinations of the microcline - low albite solvus. *J. Petrol.*, **12**, 329-356.

Hovis, G.L. (1986): Behavior of alkali feldspars: Crystallographic properties and characterization of composition and Al-Si distribution. *Am. Mineral.*, **71**, 869-890.

Hovis, G.L. (1988): Enthalpies and volumes related to K-Na mixing and Al-Si order/disorder in alkali feldspars. *J. Petrol.*, **29**, 731-763.

Smith, P. & Parsons, I. (1974): The alkali feldspar solvus at 1 kilobar water-vapour pressure. *Mineral. Mag.*, **39**, 747-767.

CHARACTERISATION OF STRUCTURAL RADIATION DAMAGE BY MEANS OF REE^{3+} MICRO-LUMINESCENCE SPECTROSCOPY – THE EXAMPLE OF ZIRCON AND ZIRCONOLITE

Lenz C.*[1-2], Lumpkin G.R.[1], Thorogood G.J.[1], Ionescu M.[1] & Nasdala L.[2]
[1] Australian Nuclear Science and Technology Organisation, Lucas Heights, Sydney, Australia
[2] Institut für Mineralogie und Kristallographie, Universität Wien, Austria
Corresponding email: christoph.lenz@univie.ac.at

Keywords: heavy ion irradiation, REE photoluminescence spectroscopy, structural disorder

The investigation of radiation-damaged or metamict minerals and their synthetic analogues has increased appreciably over the past two decades, stimulated by the potential use of mineral-like ceramics as waste forms for the immobilisation of reprocessed spent nuclear fuel and other radioactive waste (e.g., Lumpkin, 2006). In this research field, however, a fast and inexpensive technique operating in the micrometre range may open up new opportunities in the characterisation of radiation damage.

Recently, confocal photoluminescence spectroscopy of Rare-earth elements (REE^{3+}) in zircon has been used as structural probe for the characterisation of radiation damage due to self-irradiation by trace U and Th (Lenz et al., 2015a). For zircon or xenotime, Raman spectral parameters are used successfully to estimate the degree of radiation damage on a microscale (e.g., Nasdala et al., 1995; Švecová et al., 2016), whereas this technique cannot be applied to some other mineral phases because of the lack of suitable Raman bands to interpret (e.g., titanite; Kennedy et al., 2010). Here a luminescence-based characterisation may be the most promising alternative, as laser-induced luminescence features of REE^{3+} are common analytical artefacts in Raman spectroscopy of accessory minerals (Lenz et al., 2015b). Additional advantages of using luminescence spectroscopy comprise the opportunity to use further techniques to excite REE^{3+} emissions, e.g., cathodoluminescence spectroscopy coupled to electron-probe techniques (EPMA/SEM).

One major challenge for using spectroscopic techniques is the quantitative calibration of radiation effects (i.e., accumulation of amorphous fraction with certain doses) with their impact on spectral parameters (i.e., spectral band widths). Attempted calibrations based on the study of naturally radiation-damaged minerals, however, are often biased. This is because of insufficient knowledge about their thermal and, hence, annealing history. This problem may be overcome by studying minerals that were artificially ion-irradiated in the laboratory. Here, we present first results of a heavy-ion (Au) irradiation-study of the two important nuclear waste-form matrices zircon ($ZrSiO_4$) and zirconolite ($CaZrTi_2O_7$). Bulk, mono-phase, poly-crystalline ceramics were irradiated with accelerated heavy ions (Au) of variable doses with energies up to 35 MeV. Comparably high heavy-ion energies are chosen to ensure irradiation penetration-depths of 4-5 µm accessible to the spatial resolution of optical confocal spectrometers. We use surface-sensitive, grazing-incident X-ray diffraction of irradiated bulk ceramic pellets for the estimation of the amorphous fraction produced.

Acknowledgements: The presenting author gratefully acknowledge the use of instrumentation funded through honorary associate agreement with the ARC CFSS/GEMOC at Macquarie University, Sydney. Financial support was provided by Austrian Science Fund (FWF) through projects J3662-N19 to C.L. and P24448 to L.N.

Kennedy, A.K., Kamo, S.L., Nasdala, L., Timms, N.E. (2010): Grenville skarn titanite: potential reference material for SIMS U–Th–Pb analysis. *Can. Mineral.*, **48**, 1423-1443.

Lenz, C. & Nasdala, L. (2015a): A photoluminescence study of REE^{3+} emissions in radiation-damaged zircon. *Am. Mineral.*, **100**, 1123-1133.

Lenz, C., Nasdala, L., Talla, D., Hauzenberger, C., Seitz, R., Kolitsch, U. (2015b): Laser-induced REE^{3+} photoluminescence of selected accessory minerals – An "advantageous artefact" in Raman spectroscopy. *Chem. Geol.*, **415**, 1-16.

Lumpkin, G R. (2006): Ceramic waste forms for actinides. *Elements*, **2**, 365-372.

Nasdala, L., Irmer, G., Wolf, D. (1995): The degree of metamictization in zircon: a Raman spectroscopic study. *Eur. J. Mineral.*, **7**, 471-478.

Švecová, E., Čopjaková, R., Losos, Z., Škoda, R., Nasdala, L., Cícha, J. (2016): Multi-stage evolution of xenotime–(Y) from Písek pegmatites, Czech Republic: an electron probe micro-analysis and Raman spectroscopy study. *Miner. Petrol.*, in press, DOI: 10.1007/s00710-016-0442-6.

HYDROGROSSULAR, $Ca_3Al_2(SiO_4)_{3-X}(H_4O_4)_X$: AN A*B INITIO* INVESTIGATION OF ITS STRUCTURAL AND ENERGETIC PROPERTIES

Mahmoud A.*[1], Lacivita V.[2-3], Erba A.[1], D'Arco P.[3] & Mustapha S.[4]

[1] Dipartimento di Chimica & Centro Interdipartimentale "Nanostructured Interfaces and Surfaces", Università di Torino, Italy

[2] Institut du Calculet de la Simulation, Université Pierre et Marie Curie, Paris, France

[3] Institut des Sciences de la Terre, Université Pierre et Marie Curie, Paris, France

[4] Institut de Mathématiques de Jussieu, Université Pierre et Marie Curie, Paris, France

Corresponding email: agnes.mahmoud@unimi.it

Keywords: hydrogarnet, *ab initio*, CRYSTAL code

Silicate garnets are nominally anhydrous minerals (NAMs) with stoichiometry $X_3Y_2(SiO_4)_3$, which, nonetheless, have been found to commonly contain hydrous components. When a Si ion in the SiO_4 tetrahedron is substituted by a $(OH)_4$ defect give rise to the hydrogarnet substitution. In the present study the structural and energetic properties of the grossular-hydrogrossular binary system is investigated with a full *ab initio* quantum chemical approach, considering a set of intermediate compositions. We monitored the incorporation of hydrous components into NAMs within the primitive cell of cubic garnet. Each intermediate term is represented by a number of independent atomic configurations that were efficiently selected via symmetry-adapted Monte-Carlo sampling (Mustapha, 2013; D'Arco, 2013). All configurations have been structurally optimized by means of the CRYSTAL code, the relaxed geometries being characterized by pseudo-cubic cells. At the present level of approximation, the most stable configurations constitute by far the largest contributions to the system properties. Considering only the most stable configurations, average geometrical features of the actual solid solution are closely approximated. The excess volume displays a highly non-ideal behavior that is favorably compared with carefully analyzed and selected experimental data. The excess enthalpy deviates from the regular model; it draws an asymmetric function of composition with two minima that can be associated to structures or compositions observed in nature. Geometrical variations and distribution of the tetrahedra are analyzed. Calculations provide independent support to the use of a split-atom model for experimental refinements on these compounds. The asymmetry of the enthalpy of mixing can be associated with two distinct distribution patterns of the tetrahedra. Hydrogen interactions also contribute to the asymmetry of the excess enthalpy, as it turns out by comparison between compositions close to fully hydrated katoite and those close to grossular.

D'Arco, P., Mustapha, S., Ferrabone, M., Noël, Y., De La Pierre, M., Dovesi, R. (2013): Symmetry and random sampling of symmetry independent configurations for the simulation of disordered solids. *J. Phys.*, *Cond. Matt.*, **25**, 355401.

Mustapha, S., D'Arco, P., De La Pierre, M., Noël, Y., Ferrabone, M., Dovesi, R. (2013): On the use of symmetry in configurational analysis for the simulation of disordered solids. *J. Phys.*, *Cond. Matt.*, **25**, 105401.

THERMODYNAMICS AND CRYSTAL CHEMISTRY OF RHOMBOCLASE, $(H_5O_2)Fe(SO_4)\cdot 2H_2O$, AND THE PHASE $(H_3O)Fe(SO_4)_2$

Majzlan J.*[1], Grevel K.-D.[1], Kiefer B.[2], Dachs E.[3], Benisek A.[3], Grube E.[4] & Nielsen U.G.[4]
[1] Institut für Geowissenschaften, Friedrich-Schiller-Universität Jena, Germany
[2] Department of Physics, New Mexico State University, Las Cruces, NM, USA
[3] Fachbereich Materialforschung & Physik - Abteilung Mineralogie, Universität Salzburg, Austria
[4] Department of Physics, Chemistry, and Pharmacy, University of Southern Denmark, Odense, Denmark
Corresponding email: Juraj.Majzlan@uni-jena.de

Keywords: ferric sulfates, thermodynamics, acid mine drainage

Rhomboclase is a phase typical for very acidic, evolving acid-mine drainage systems. Its thermodynamic properties could be used for modeling the path along which such systems arrive at the precipitation of rhomboclase or other, companion phases. Rhomboclase and related phases are also proton conductors, thus interesting for materials science. In this contribution, we investigated thermodynamics and crystal chemistry of rhomboclase and the related phase $(H_3O)Fe(SO_4)_2$.

Thermodynamic properties of rhomboclase and the phase $(H_3O)Fe(SO_4)_2$ were measured by a combination of acid-solution calorimetry (enthalpy of formation) and relaxation calorimetry (heat capacity and entropy). The data were further refined by mathematical optimization analysis, using the temperature-humidity brackets reported by Xu et al. (2009). The algorithm found a solution, verifying that the brackets and the measured thermodynamic data are consistent and the thermodynamic properties for the transformation reaction between rhomboclase and $(H_3O)Fe(SO_4)_2$ are accurate. The agreement is worse when solubility data at 25ºC (this work) are confronted with the Pitzer model for concentrated $Fe_2(SO_4)_3$-H_2O solutions (Tosca et al., 2007). The reason for this discrepancy is not clear, could possibly lie in the too complex aqueous interactions in such solutions which the model cannot fully capture.

Ab-initio molecular dynamics of the phase $(H_3O)Fe(SO_4)_2$ show that the (H_3O) groups in this phase are in a perpetual motion, including rotations and "umbrella" flipping. The rotational motion, however, is not unconstrained, but performed with an energetic barrier. The simulation, performed for 25ºC for 4.5 ps document well the dynamics of the motion but do not prove hydrogen mobility; for such observations, longer simulations times may be perhaps needed. Solid state ^2H MAS NMR spectroscopy on rhomboclase showed two types local hydrogen environments assigned to of the H_2O groups coordinated to iron and the interlayer $H_5O_2^+$ ion based on the paramagnetic shifts. The water molecules perform rapid rotation around the Fe-O bond at room temperature, whereas the $H_5O_2^+$ ion in the interlayer performs a more complex motions, which further reduces the ^2H quadrupole interaction.

Tosca, N.J., Smirnov, A., McLennan, S.M. (2007): Application of the Pitzer ion interaction model to isopiestic data for the $Fe_2(SO_4)_3$-H_2SO_4-H_2O system at 298.15 and 323.15 K. *Geochim. Cosmochim. Acta*, **71**, 2680-2698.

Xu, W.Q., Tosca, N.J., McLennan, S.M., Parise, J.B. (2009): Humidity-induced phase transitions of ferric sulfate minerals studied by *in situ* and *ex situ* X-ray diffraction. *Am. Mineral.*, **94**, 1629-1637.

IRREGULAR PVT BEHAVIOUR OF APATITE – A RAMAN AND ULTRA-SONIC STUDY BETWEEN -200 AND 300°C

Mirwald P.W.*[1-2], Stalder R.[1], Paulini P.[2] & Tappert R.[1]
[1] Institut für Mineralogie und Petrographie, Universität Innsbruck, Austria
[2] Arbeitsbereich Materialtechnologie, Universität Innsbruck, Austria
Corresponding email: peter.mirwald@uibk.ac.at

Keywords: apatite, irregular PVT properties, low-temperature

Apatite, characterized by its important end members $Ca_{10}(PO_4)_6(OH, F, Cl)_2$, is geochemically the main compound of phosphorus on Earth. Its complex, approximately hexagonal closed packed PO_4^{3-}-ion structure is characterised by a remarkable chemical variability and a considerable P-T stability.

We studied the PVT behaviour a fluor-rich apatite crystal (F : Cl : OH = 0.95 : 0.04 : 0.01) by Raman spectroscopy between -200 and +300°C (Labram HR800/ Horiba Jobin-Y, Nd-YAG laser: 532.2 nm emission line; heating/freezing stage: Linkam THMS 600; T-accuracy: ±5°C). The results were compared with ultrasonic (us)-measurements taken on the same material encased in a small piston cylinder device at low pressure (0.01 MPa) between -220 and 80°C. Methodically the us-measurements rely on the determination of the relative time shift of the zero-crossing positions of the wave train. In addition, the ultrasonic measurements were checked volumetrically by a transducer device that monitored the piston displacement.

The most prominent Raman band of apatite at 965 cm^{-1} reveals a temperature behaviour marked by small irregular changes in peak-position as well as in the full width at half maximum (FWHM) at -160, -90, -40, 0, 40, 100 and 220°C. Similar holds true for the us- measurements in the studied temperature range up to 80°C where irregular changes in the wave velocity are observed at -160, -90, -40, 0, 40°C. The irregularities of both types of data indicate no severe structural changes which might be associated with a phase transformation. These phenomena also seem to extend into the pressure dimension as indicated by own and previous (Bridgman, 1949), piloting compression measurements. The findings in our Raman and us-data obtained in dependence of temperature are supported by analysis of Cp- and thermal expansion data reported in the literature (Dachs et al., 2010; Miyazaki et al., 2009; Hovis et al., 2014).

Taking into account that apatite shows no structural transition, we interpret the temperature dependent irregular variations of the Raman-data and of the ultra-sonic results as subtle but distinct irregularities in the volume-temperature characteristic of the lattice vibrations of the apatite structure. Recently, similar observations have also been made on quartz, calcite and periclase (Mirwald et al., 2014; 2015). Generally, our observations indicate that homogenous crystal phases may show irregular changes in the thermal expansion (and compression) behaviour assumed to be related to not uniformly changing lattice vibrations.

Bridgman, P.W. (1949): Linear compression to 30,000 kg/cm^2 including relatively incompressible substances. *Proc. Am. Acad. Arts Sci.*, **77**, 187-234.

Dachs, E., Harlov, D., Benisek, A.(2010): Excess heat capacity and entropy of mixing along the chlorapatite-fluorapatite binary join. *Phys. Chem. Minerals*, **37**, 665-676.

Hovis, G.L., Scott, B.T., Altomare, C.M., Leaman, A.R., Morris, M.D., Tomaino, G.P., McCubbin, F.M. (2014): Thermal expansion of fluorapatite-hydroxylapatite crystalline solutions. *Mineralogist*, **90**, 2171-2175.

Mirwald, P.W., Tappert, R., Stalder, R. (2014): Anomalous thermal expansion behaviour of quartz and calcite. 21th Gen. Meeting IMA, 1-5-Sept. 2014, Johannesburg, abstr.,.2145.

Mirwald, P.W., Paulini, P., Tappert, R., Stalder, R. (2015): Anomalous PVT behaviour of periclase – an ultra-sonic and Raman study between -200 and +100°C. 25th Goldschmidt Conference 2015, Prague, abstr., 342.

Miyazaki, H., Ushiroda, I., Itomura, D., Hirashita, T., Adachi, N., Ota, T. (2009): Thermal expansion of hydroxyapatite between -100°C and 50°C. *Mat. Sci. Engin. C*, **29**, 1463-1466.

SINGLE-CRYSTAL X-RAY DIFFRACTION STUDY OF $SrGe_2O_5$: A NEW HIGH-PRESSURE STRONTIUM GERMANATE

Nakatsuka A.*[1], Sugiyama K.[2], Ohkawa M.[3], Ohtaka O.[4], Fujiwara K.[1] & Yoshiasa A.[5]
[1] Graduate School of Sciences and Technology for Innovation, Yamaguchi University, Japan
[2] Institute for Materials Research, Tohoku University, Japan
[3] Graduate School of Science, Hiroshima University, Japan
[4] Graduate School of Science, Osaka University, Japan
[5] Graduate School of Science and Technology, Kumamoto University, Japan
Corresponding email: tuka@yamaguchi-u.ac.jp

Keywords: new strontium germanate, high-pressure phase, crystal structure

Germanates have extensively been investigated for various industrial applications as represented in germanate glasses. Meanwhile, germanates have frequently been employed as model substances for the corresponding silicates because they exhibit similar phase-transformations to silicates at lower pressures. Phase and structural studies of germinates have thus provided important insights into phase transformations of silicate minerals in the Earth's interior. However, some germanate systems have not yet been fully examined. The system Sr-Ge-O is one of such examples, although it is a potentially good low-pressure analog of the system Ca-Si-O, one of the major components in the constituent minerals of Earth's crust and mantle. To our knowledge, the four forms of $SrGeO_3$, $SrGe_4O_9$, Sr_2GeO_4 and Sr_3GeO_5 have only been known in the system Sr-Ge-O. However, we recently discovered a new high-pressure strontium germanate $SrGe_2O_5$. We here report the crystal structure of this new phase and its structural features.

Single crystals of $SrGe_2O_5$ crystallized as a coexistent phase with $SrGeO_3$ perovskite single-crystals, in the sample recovered in the high-pressure experiment of $SrGeO_3$ pseudowollastonite conducted at 6 GPa and 1223 K. Single-crystal X-ray diffraction technique was used for the determination and refinement of the crystal structure.

The resulting crystallographic data are as follows: orthorhombic; space group *Cmca*; a = 5.4653(6), b = 9.7379(9), c = 13.7710(12) Å and V = 732.90(13) $Å^3$; Z = 8; D_x = 5.670 g/cm^3. The crystal structure consists of germanium-oxygen framework layers stacked along [001] with Sr atoms located at 12-fold coordinated cuboctahedral site; the layers are formed by the corner-linkages between GeO_6 octahedra and between GeO_6octahedra and GeO_4 tetrahedra. This is isostructural with the high-pressure phases of $SrSi_2O_5$ and $BaGe_2O_5$. From comparison of the present $SrGe_2O_5$ structure with the reported $SrSi_2O_5$ and $BaGe_2O_5$ structures, the effect of cation size on the crystal structure will be discussed in terms of chemical bonding nature.

SYNTHESIS AND CHARACTERIZATION OF A $[Li_{0+X}Mg_{2-2X}Al_{1+X}(OH)_6][Cl \cdot MH_2O]$ (X = 0-1) SOLID SOLUTION

Niksch A.*[1] & Pöllmann H.[1]

[1] Fachgebiet Mineralogie-Geochemie, Institut für Geowissenschaften und Geographie, Martin-Luther-Universität Halle-Wittenberg, Germany

Corresponding email: anton.niksch@geo.uni-halle.de

Keywords: LDH solid solution

Layered double hydroxides (LDHs) consist of alternate positively charged mixed metal hydroxide layers and negative charged interlayer anions. The stoichiometry of these materials can be formulated as $[M^{z+}_{1-x}M^{3+}_{x}(OH)_2]^{p+}[(A^{n-})_{p/n} \cdot mH_2O]$ with z = 2 or 1, M = mono-, bi- and trivalent metallic elements, A = organic or inorganic anion and m = amount of interlayer H_2O depending on the temperature, relative humidity and hydration level (Williams et al., 2011). These layered materials are able to intercalate different types of neutral molecules or exchange the interlayer anion with organic or inorganic anions of different sizes or charges. The positively charged main layer remains stable and is not capable of ion exchange. Due to a similar ion radius between Li and Mg and the chemical similarities, there is a possibility to produce a new solid solution, containing Al^{3+}, Li^+ and Mg^{2+} in the positively charged main layer.

The syntheses were done by mixing solutions of LiCl, $MgCl_2 \cdot 6H_2O$ and $AlCl_3 \cdot 6H_2O$, adding NaOH until a *p*H of 9,5 was reached and heating it up to 100, 120,140 and 160°C in an autoclave for 10h. The products were filtered, washed and dried (RH 35%). Starting with the pure $[Mg_2Al(OH)_6][Cl \cdot 0.55H_2O]$ the amount of Li^+ was raised and the amount of Mg^{2+} was reduced in 10 mol% steps until 100 mol% Li^+ and the the pure $[LiAl_2(OH)_6][Cl \cdot mH_2O]$ LDH was reached. XRD investigations showed two different coexisting mineral phases in the area of 10 mol% - 80 mol% Li^+. The synthesis with 90 mol% Li^+ showed a single mineral phase and a different lattice parameter (*a*) (5.11 Å) compared to the pure $[LiAl_2(OH)_6][Cl \cdot 0.51H_2O]$ LDH (5,08 Å). This difference matched with calculated theoretical lattice parameter (*a*) (5.11 Å) for a Li^+ and Mg^{2+} containing LDH with 10 mol% Mg^{2+}. Syntheses between 90 mol% and 100 mol% Li showed a straight increasing lattice parameter (*a*) from 5.08 to 5.11 Å like calculated. The lattice parameter (*c*) remains nearly constant for all products independent of the Li^+/Mg^{2+} ratio. Analysis by ICP-OES showed that all Mg^{2+} was bound to the solid solution. Calculations suggest that the Mg^{2+} ions occupy both structural positions with 5 % on the Li^+ and 5 % on the Al^{3+} position. The amount of interlayer water was investigated by TGA and is 0.5 mole. Synthesis with temperatures of 100, 120 and 140°C produced nearly similar solid solutions while using higher temperatures than 140°C resulted in a formation of AlO(OH). The solid solution with the highest Mg content and the chemical formula $[Li_{0.9}Mg_{0.2}Al_{1.9}\ (OH)_6]Cl \cdot 0{,}5H_2O$ was produced at 120°C, 10 h synthesis time, *p*H 9,5 and a s/w ratio of 1/15.

Williams, G.R., Morrhouse, S.J., Prior, T.J., Fogg, A.M., Rees, N.H., O'Hare, D. (2011): New insights into the intercalation chemistry of $Al(OH)_3$. *Dalton Trans.*, **40**, 6012-6022.

THERMODYNAMIC DATA OF MAGNESIO- AND ALUMINOCOPIAPITE

Nowak W.*[1], Majzlan J.[1], Dachs E.[2] & Benisek A.[2]
[1] Institut für Geowissenschaften, Friedrich-Schiller-Universität Jena, Germany
[2] Fachbereich Chemie und Physik der Materialien, Universität Salzburg, Austria
Corresponding email: wiebke.nowak@uni-jena.de

Keywords: copiapite-group, enthalpy of formation, standard entropy

Magnesiocopiapite ($MgFe_4(SO_4)_6(OH)_2 \cdot 20H_2O$) and aluminocopiapite ($Al_{2/3}Fe_4(SO_4)_6(OH)_2 \cdot 20H_2O$) are end-members of the copiapite group and are commonly associated with acid mine drainage environments. To gain insights into the development and stability of copiapite-group minerals, a complete and consistent set of thermodynamic data is desired but not existing.

To provide such a data set, both copiapite phases were synthesized and characterized by powder X-ray diffraction and wet-chemical analyses. We measured enthalpies of formation of magnesio- and aluminocopiapite by acid solution calorimetry at T = 298.15 K. The enthalpy of formation from the elements in their standard state ($\Delta_f H^0_{298}$) of magnesiocopiapite is -12198.9±8.2 $kJ \cdot mol^{-1}$ and of aluminocopiapite -12053.9±7.8 $kJ \cdot mol^{-1}$.

From low-temperature heat capacity measurements (using a PPMS instrument), the standard entropy of magnesiocopiapite was calculated by integrating the C_p/T function and is S^0_{298} (magnesiocopiapite) = 1466.6±10.3 $J \cdot K^{-1} \cdot mol^{-1}$. The standard entropy of aluminocopiapite will be acquired soon.

SHORT-RANGE ORDER/DISORDER IN ROCK-FORMING MINERALS: INVESTIGATIONS BY NUCLEAR MAGNETIC RESONANCE AND OTHER SPECTROSCOPIC TECHNIQUES

Palke A.C.*[1] & Geiger C.A.[2]
[1] Gemological Institute of America, Carlsbad, CA, USA
[2] Fachbereich Materialforschung und Physik - Abteilung Mineralogie, Universität Salzburg, Austria
Corresponding email: aaronpalke@gmail.com

Keywords: NMR spectroscopy, short-range order, spectroscopy

Most rock-forming silicates and oxides are multi-component substitutional solid solutions. Therefore, thermodynamic models used in petrological studies involving such solid solutions must consider configurational entropy which is derived from contributions from both long- and short-range order/disorder. The absence of any short-range order is typically assumed in a first approximation. However, several thermodynamic studies of such rock-forming minerals have assumed the presence of short-range order to fit thermodynamic models with experimental data. Nonetheless, in many cases experimental verification of such short-range order is lacking if not nonexistent. Information concerning short-range order/disorder is inaccessible using traditional diffraction techniques which are, however, employed to describe long-range order. To fully describe the order/disorder state of such solid solutions, researchers must turn to spectroscopic techniques that provide small-scale atomic-level structural information.

Fourier-Transform InfraRed (FTIR) spectroscopy has been used to elucidate short-range order in some mineral groups with much success. Additionally, Nuclear Magnetic Resonance (NMR) spectroscopy has the advantage of providing atom-scale structural information while also being an inherently quantitative technique. Thus, if the peaks found in NMR spectra can be confidently assigned to specific atomic configurations, measurement of peak areas can allow for comparison to predictions based on ordered or disordered arrays of substitutional species. A particularly promising development in this field is the use of paramagnetic interactions in NMR spectroscopy. The presence of transition metal or rare earth element ions with unpaired electron spins can produce so-called paramagnetically shifted NMR peaks which can often produce more resolution between specific atomic configurations and can provide local atomic information at a longer length scale than “ordinary” NMR experiments (i.e., up to 4 bonds or up to 5-6 Å away from the NMR nuclide). The results of such experiments will be discussed while also reviewing the state of knowledge concerning short-range order in rock-forming minerals and suggesting directions for future work. The use of paramagnetic interactions in NMR spectroscopy has the potential to provide short-range structural information complementary to long-range picture gleaned from traditional diffraction experiments.

PRESSURE-INDUCED STRUCTURAL ALTERATION IN METAMICT ZIRCON

Pina Binvignat F.A.[1], Malcherek T.[1], Paulmann C.[1], Schlüter J.[2], Angel R.J.[3] & Mihailova B.*[1]
[1] Fachbereich Geowissenschaften, Universität Hamburg, Germany
[2] Centrum für Naturkunde, Mineralogisches Museum, Universität Hamburg, Germany
[3] Dipartimento di Geoscienze, Universita di Padova, Italy
Corresponding email: boriana.mihailova@uni-hamburg.de

Keywords: Zircon, metamict, high pressure

Metamict minerals are characterized by a high degree of structural disorder consisting of coexistence of defect-rich crystalline and amorphous nanoregions caused by the radioactive α-decay of the structurally incorporated actinides (mainly U and Th). In this regard, metamict minerals are ideal model systems for studying the behaviour of actinide-waste-form phases in specific geochemical environments over a geological time-scale period. Thus the analysis of the structural response to pressure of metamict minerals is vital for the better understanding of the long-term elastic stability of the matrix in which actinide-bearing radioactive waste is captured. Metamict zircon has been extensively studied by various methods because it is one of the oldest minerals found in the Earth crust. However, high-pressure structural studies of metamict zircon remain scarce. We have applied complementary polarized Raman spectroscopy and synchrotron single-crystal X-ray diffraction (XRD) to three representative zircon samples exhibiting a low, moderate, and high degree of metamictization in order to analyze the pressure-induced structural changes up to 10 GPa. The XRD data indicate a larger volume compressibility for heavily metamict zircon as compared to the other two samples within the entire pressure range as well as a reduced mosaic spread of the crystallites above 6 GPa. Raman spectroscopy allowed the response of the crystalline and amorphous regions to elastic stress to be distinguished. As expected, the amorphous fraction increases with the radiation dose but within uncertainties, it does not change with pressure. The compressibility of the crystalline fraction increases with the radiation dose, whereas the compressibility of the amorphous fraction is independent of the degree of metamictization. Although all studied samples were chemically homogeneous, the moderately and heavily metamict zircon samples showed two possible pathways for the structure to accommodate pressure: (i) by distorting the SiO_4 tetrahedra and partially changing the Si coordination in the amorphous regions, or (ii) by structural alteration in both the crystalline and amorphous regions. In either case the overall average structure softens between 3 and 6 GPa, as a result of weakening of the Si-O bonds in the amorphous nanoregions and damping of the SiO_4 stretching in the crystalline nanoregions.

ARE THERE POINT DEFECTS IN THE CRYSTALLINE PORTION OF SELF-IRRADIATED MINERALS?

Váczi T.*[1]
[1] Department of Mineralogy, Eötvös Loránd University, Budapest, Hungary
Corresponding email: vaczitamas@caesar.elte.hu

Keywords: radiation damage, point defects, coherence lengths

Radiation damage is found in most actinide-containing minerals (self-irradiation) and in their neighbouring phases (radiation haloes). In the case of self-irradiation, most of the damage is caused by the recoil of heavy daughter nuclei produced in alpha decay events. The recoil damage clusters are disruptions of translational order that effectively limit any coherence-related phenomenon (diffraction, phonon propagation etc.).

Crystalline and amorphous are defined in different ways in diverse analytical methods. In a geometric model, the interfaces are treated as sharp “amorphous”-to-”crystalline” boundaries in a continuum, disregarding scattered defects (Ketcham et al., 2013). Atomistic simulations are able to reveal all permanently displaced atoms but are limited by the size of the simulation box (Devanathan et al., 2006). Monte Carlo (MC) methods are able to predict the statistical distributions of knock-on atomic displacements and, less precisely, the number of displacements per energetic ions (Ziegler et al., 2010). The amorphous fraction may be estimated using ^{29}Si NMR (Farnan & Salje, 2001) or X-ray diffraction (Ríos et al., 2000). Raman spectroscopy, on the other hand, uses a signal from the crystalline fraction (e.g., Nasdala et al., 2001).

A geometric model (Ketcham et al., 2013) suggests that undamaged domain sizes decrease very rapidly with increasing alpha recoil dose (e.g., a mean domain size of a few nanometres were inferred at intermediate alpha doses of 2-3×10^{18} α/g). The defect density in the remaining crystalline domains is unknown, but it is possible to gain insight using experimental Raman data obtained from He-ion irradiated materials (Nasdala et al., 2011) and MC simulations. A careful evaluation of available information suggests that for alpha-particle damage in a crystalline medium (i) the overall damage level may be fairly low (ca. 0.0035 dpa at 1×10^{18} α/g), (ii) the knock-on displacements are most probably not scattered as isolated point defects but show clustering, and (iii) the estimated defect-free domain sizes (or coherence lengths) may be even an order of magnitude larger than the typical space between recoil clusters (e.g., 50-100 nm *vs.* 5-10 nm, respectively, at a dose of 1×10^{18} ion/g). Consequently, the coherence lengths appear to be limited by the distances between recoil clusters (i.e., alpha dose), whereas the contribution of alpha-particle-induced defects or clusters in the ordered lattice, or lattice fragments, may be negligible. The contribution will attempt to demonstrate that in a self-irradiated mineral, at any alpha dose, the translationally ordered domains between recoil clusters may be essentially defect-free. Possible explanations are also offered for the observed lattice swelling in radiation-damaged materials in the lack of a high density of point defects (e.g., Diehm et al., 2012).

Devanathan, R., Corrales, L.R., Weber, W.J., Chartier, A., Meis, C. (2006): Molecular dynamics simulation of energetic uranium recoil damage in zircon. *Mol. Simul.*, **32**,1069-1077.

Diehm, P.M., Ágoston, P., Albe, K. (2012): Size-dependent lattice expansion in nanoparticles: Reality or anomaly? *ChemPhysChem*, **13**, 2443-2454.

Farnan, I. & Salje, E.K.H. (2001): The degree and nature of radiation damage in zircon observed by ^{29}Si nuclear magnetic resonance. *J. Appl. Phys.*, **89**, 2084-2090.

Ketcham, R.A., Guenthner, W.R., Reiners, P.W. (2013): Geometric analysis of radiation damage connectivity in zircon, and its implications for helium diffusion. *Am. Mineral.*, **98**, 350-360.

Nasdala, L., Wenzel, M., Vavra, G., Irmer, G., Wenzel, T., Kober, B. (2001): Metamictisation of natural zircon: accumulation versus thermal annealing of radioactivity-induced damage. *Contrib. Mineral. Petrol.*, **141**, 125-144.

Nasdala, L., Grambole, D., Götze, J., Kempe, U., Váczi, T. (2011): Helium irradiation study on zircon. *Contrib. Mineral. Petrol.*, **161**, 777-789.

Ríos, S., Salje, E.K.H., Zhang, M., Ewing, R.C. (2000): Amorphization in zircon: evidence for direct impact damage. *J. Phys. Cond. Matt.*, **12**, 2401-2412.

Ziegler, J.F., Biersack, J.P., Littmark, U. (2010): SRIM – The stopping and range of ions in matter (2010). *Nucl. Instrum. Meth. B*, **268**, 1818-1823.

TEMPERATURE AND PRESSURE EVOLUTION OF PHONON VIBRATIONS OF DIFFERENT TOURMALINE SPECIES

Watenphul A.*[1], Lensing-Burgdorf M.[1], Schlüter J.[2] & Mihailova B.[1]
[1] Fachbereich Geowissenschaften, Universität Hamburg, Germany
[2] Centrum für Naturkunde, Mineralogisches Museum, Universität Hamburg, Germany
Corresponding email: anke.watenphul@uni-hamburg.de

Keywords: tourmaline, Raman spectroscopy, temperature dependency

Tourmalines, $XY_3Z_6T_6O_{18}(BO_3)V_3W$, are textbook polar crystals with no ferroic phase transition in the entire temperature range of crystal stability and therefore can serve as a model system to follow the influence of composition on macroscopic properties (Pandey & Schreuer, 2012), including heat capacity, thermal expansion, compression, and pyroelectricity. On the other hand, properties are derivatives of the corresponding thermodynamic potential and their behavior is governed by the collectivized atomic vibrations (phonons). Hence, it is important to study how phonons depend on the main thermodynamic variables: composition (x), temperature (T), and pressure (p). Recently relationships between the OH stretching vibrations and the composition of the Y and Z sites as well as of the X site have been established (Watenphul et al., 2016). Our further study also showed correlations between the framework phonons and the Fe^{3+} content as well as the Y-/Z-site occupancy disorder of Mg and Al. Thus by analyzing the T/P evolutions of Raman peaks one can gain information about the local thermal expansions ($\partial\omega/\partial T$) and local pressure compressions ($\partial\omega/\partial P$) of the corresponding chemical species.

In this contribution the phonon temperature dependencies of 5 natural tourmaline species: buergerite, schorl, Fe^{2+}-bearing elbaite, dravite, and uvite are analyzed. All samples are studied by polarized Raman spectroscopy at ambient pressure in the temperature range 80 to 873 K. The majority of phonon modes show the trivial decrease in wavenumber upon heating. Only the lowest-energy lattice vibration as well as the ^{V}OH-stretching modes related to overcharged YZZ-YZZ-YZZ species exhibits unusual positive $\partial\omega/\partial T$. The latter might point to a stronger interaction of ^{V}H with the bridging oxygen atoms of the SiO_4 tetrahedra. The local thermal expansions of the YZZ-YZZ-YZZ and YYY species as derived from framework and OH-stretching vibrations show a clear dependency on the charge of the octahedrally coordinated cations. Strong influence of the X-site occupancy on the local thermal expansion is deduced from the behavior of ^{V}OH. A clear difference is observed in the $\partial\omega/\partial T$ values of ^{V}OH species associated with vacant and occupied X sites. By comparing the trends for dravite and uvite, the effect of the dominant type of X-site cations can be evaluated.

High-pressure Raman scattering experiments are currently being conducted on the same tourmaline samples and the analysis of the data is expected to further contribute to our understanding of the relation chemistry - phonons - properties.

Pandey C.S. & Schreuer, J. (2012): Elastic and piezoelectric constants of tourmaline single crystals at non-ambient temperatures determined by resonant ultrasound spectroscopy. *J. Appl. Phys.*, **111**, 013516.

Watenphul, A., Burgdorf, M., Schlüter, J., Horn, I., Malcherek, T., Mihailova, B. (2016): Exploring the potential of Raman spectroscopy for crystallochemical analyses of complex hydrous silicates: II. Tourmalines. *Am. Mineral.*,**101**, 970-985.

ANNEALING OF RADIATION DAMAGED TITANITE

Zietlow P.[1], Beirau T.[1], Mihailova B.[1], Paulmann C.[1], Malcherek T.[1], Groat L.A.[2] & Bismayer U.*[1]
[1] Mineralogisch-Petrographisches Institut, Universität Hamburg, Germany
[2] Department of Earth and Ocean Sciences, University of British Columbia, Vancouver, Canada
Corresponding email: ubis@uni-hamburg.de

Keywords: Metamict, radiation damage, annealing

The structural damage of metamict minerals is caused by natural α-radiation. The result of the irradiation over geological times is a heterogeneous, amorphous to quasi-amorphous matrix which may contain crystalline clusters. Metamict minerals are metastable and their properties deviate considerably from those of long range ordered structures. Thermal treatment leads to the reorganisation of such metastable structures and depending on its initial state, nucleation and recrystallization processes occur simultaneously in the material. Our study provides information about metamict minerals with focus on titanite, which reorganises its long range order on annealing (Beirau et al., 2012).

Beirau, T., Mihailova, B., Matveeva, G., Kolb, U., Malcherek, T., Groat, L.A., Bisayer, U. (2012): Structural anisotropy and annealing-induced nanoscale atomic rearrangements in metamict titanite. *Am. Mineral.*, **97**,1354-1365.

Session S16:

New minerals, modular structures and mineral groups

Conveners:

Luca Bindi (Firenze – Italy)

Stuart J. Mills (Melbourne – Australia)

Marco Pasero (Pisa – Italy)

Igor V. Pekov (Moscow – Russia)

JORDANITE HOMOLOGUES FROM THE POLLONE MINE (APUAN ALPS, ITALY): THE GEOCRONITE-JORDANITE ISOTYPIC PAIR AND THE NEW N = 3.5 HOMOLOGUE MARCOBALDIITE

Biagioni C.*[1], Dini A.[2], Merlino S.[1], Moëlo Y.[3], Orlandi P.[2], Paar W.H.[4], Pasero M.[1] & Zaccarini F.[5]

[1] Dipartimento di Scienze della Terra, Università di Pisa, Italy

[2] Istituto di Geoscienze e Georisorse, Consiglio Nazionale delle Ricerche, Pisa, Italy

[3] Institut des Matériaux Jean Rouxel, Centre National de la Recherche Scientifique, Université de Nantes, France

[4] Fachbereich Chemie und Physik der Materialien, Universität Salzburg, Austria

[5] Department Angewandte Geowissenschaften und Geophysik, Universität Leoben, Austria

Corresponding email: biagioni@dst.unipi.it

Keywords: marcobaldiite, jordanite homologous series, lead sulfosalts

The jordanite homologous series has the general formula $Pb_{4N-2}Me^{3+}{}_6S_{4N+7}$ (Makovicky et al., 2006). The minerals belonging to this series are characterized by the stacking, along **b**, of trigonal prismatic layers with *N*-octahedra-thick layers. The *N* = 4 homologue is represented by the most common members of this series, jordanite, ideally $Pb_{14}As_6S_{23}$, and geocronite, $Pb_{14}Sb_6S_{23}$, whereas the *N* = 3 member, kirkiite, $Pb_{10}(As_3Bi_3)S_{19}$, is exceptional. These structural differences are reflected in the unit-cell parameters. Both *N* = 3 and *N* = 4 homologues are characterized by two short unit-cell axes of ≈ 8.5 and 8.9 Å, whereas the third long axis increases from 26 to 32 Å from kirkiite to the jordanite-geocronite pair.

One of the classic localities for the occurrence of geocronite is represented by the Pollone mine, Valdicastello Carducci (Apuan Alps, Tuscany, Italy), where it has been known since XIX Century (Kerndt, 1845). During our study of the baryte - pyrite - iron oxide ore deposits from southern Apuan Alps, historical as well as new specimens of geocronite from this locality were rexamined using single-crystal X-ray diffraction coupled with electron-microprobe analysis. The chemistry of the studied samples ranges between As-bearing geocronite, $Pb_{14}Sb_{3.8}As_{2.2}S_{23}$, and Sb-bearing jordanite, $Pb_{14}As_{3.4}Sb_{2.6}S_{23}$. The crystal structure of grains representative of the different compositions have been refined, allowing a better understanding of the pnictogen partitioning within the different structural sites of the jordanite-geocronite pair (Biagioni et al., 2016).

Surprisingly, one of the studied specimens, together with the two short unit-cell parameters typical of the jordanite series, revealed for the third one a value of 29.4 Å, intermediate between those of the *N* = 3 and *N* = 4 homologues. Consequently, it was hypothesized that it could be the first *N* = 3.5 homologue. The crystal structure solution confirmed this hypothesis, allowing the definition of the new mineral marcobaldiite, ideally $Pb_{12}(Sb,As,Bi)_6S_{21}$ (IMA 2015-109). It was found in a quartz vein as a black prismatic crystal associated with tennantite. Marcobaldiite is triclinic, *P*-1, with unit-cell parameters *a* = 8.9248(9), *b* = 29.414(3), *c* = 8.5301(8) Å, α = 98.336(5), β = 118.175(5), γ = 90.856(5)°, *V* = 1944.1(3) Å^3, *Z* = 2. Electron microprobe analysis gave (in wt.%): Pb 64.05, Bi 4.24, Sb 9.10, As 4.51, S 17.24, total 99.14. It corresponds to the chemical formula (on the basis of 18 cations per formula unit) $Pb_{11.98}(Sb_{2.90}As_{2.33}Bi_{0.79})_{\Sigma 6.02}S_{20.80}$. The crystal structure of marcobaldiite (R1 = 0.0682) can be described as formed by the 1:1 alternation of two different layers of distorted octahedra, one three-octahedra thick (kirkiite-type slab) and the other four-octahedra thick (jordanite-type slab). Layers are connected by one atomic layer of three bicapped triangular prismatic Pb atoms and one triangular pyramidal As.

Biagioni, C., Dini, A., Orlandi, P., Moëlo, Y., Pasero, M., Zaccarini, F. (2016): Lead-antimony sulfosalts from Tuscany (Italy). XX. Members of the jordanite-geocronite series from the Pollone mine, Valdicastello Carducci: Occurrence and crystal structures. *Minerals*, **6**, 15.

Kerndt, T. (1845): Über die Krystallform und die chemische Zusammensetzung des Geo-Kronits von Val di Castello. *Ann. Phys.*, **141**, 302-307.

Makovicky, E., Balić-Žunić, T., Karanović, L., Poleti, D. (2006): The crystal structure of kirkiite, $Pb_{10}Bi_3As_3S_{19}$. *Can. Mineral.*, **44**, 177-188.

CRYSTAL STRUCTURE OF TURNEAUREITE AND CRYSTAL-CHEMICAL RELATIONSHIPS AMONG THE MINERALS OF THE SVABITE SUBGROUP (APATITE SUPERGROUP)

Biagioni C.[1], Bosi F.[2], Hålenius U.[3] & Pasero M.*[1]
[1] Dipartimento di Scienze della Terra, Università di Pisa, Italy
[2] Dipartimento di Scienze della Terra, Sapienza Università di Roma, Italy
[3] Department of Geosciences, Swedish Museum of Natural History, Stockholm, Sweden
Corresponding email: marco.pasero@unipi.it

Keywords: turneaureite, apatite supergroup, crystal structure

Minerals of the apatite supergroup have the general formula $M1_2M2_3(TO_4)_3X$. Within the apatite supergroup, the triad svabite – johnbaumite – turneaureite represents one of the rare cases in which three natural end-members are known corresponding to three different X^- anions, i.e., svabite, $Ca_5(AsO_4)_3F$, johnbaumite, $Ca_5(AsO_4)_3(OH)$, and turneaureite, $Ca_5(AsO_4)_3Cl$. The only other known case is represented by the eponymous series of calcium phospates fluorapatite – hydroxylapatite – chlorapatite (Pasero et al., 2010). We present here the results of a combined chemical (electron microprobe) and structural (single crystal X-ray diffraction) study of turneaureite, which follows similar studies carried out on johnbaumite (Biagioni & Pasero, 2013) and svabite (Biagioni et al., 2016). This allows us to make a comparative analysis of the crystal-chemical features of the three calcium arsenate minerals with the apatite structure.

The studied sample of turneaureite comes from Nordmark, Värmland, Sweden. Electron microprobe analyses resulted in the following empirical formula: $(Ca_{4.82}Mn_{0.17}Ba_{0.02}Sr_{0.01})(As_{2.94}P_{0.02}S_{0.02}Si_{0.01})O_{12}[Cl_{0.47}(OH)_{0.42}F_{0.11}]$. The crystal structure of turneaureite was refined in the space group $P6_3/m$ to R1 = 0.0180, wR2 = 0.0475 for 716 independent reflections, with a = 9.9218(3), c = 6.8638(2) Å.

The crystal structure of turneaureite was compared with those of johbaumite (sample from the Jakobsberg mine) and of svabite (sample from the Harstigen mine). The samples of all three minerals originate from three neighbouring Långban-type deposits in the county of Värmland.

The geometry of the coordination polyhedra is similar in these three minerals of the savbite subgroup. ^{M1}Ca atoms are nine-fold coordinated in tri-augmented trigonal prisms, ^{M2}Ca2 atoms are seven-fold coordinated in pentagonal bipyramids, and ^{T}As atoms are tetrahedrally coordinated. Also average bond distances are quite similar in the three structures (johnbaumite, svabite, turneaureite, in Å: <M1-O> = 2.586, 2.586, 2.579; <M2-O> = 2.480, 2.485, 2.529; <T-O> = 1.671, 1.674, 1.678). There is, however, a relevant difference in the z fractional coordinate of X^- anionic position (0, 0, z). In turneaureite chlorine lies at z = 0.319, with an additional mixed-occupancy (OH/F/Cl) site at z = 1/4. In johnbaunite the hydroxyl group lies at z = 0.216, with no additional site. In svabite fluorine lies at z = 1/4, with an additional, mixed-occupancy (F/OH) site at z = 0.195. This results in different Ca2–X bond distances in the three minerals, in keeping with the variable nature of the X^- anion.

Biagioni, C. & Pasero, M. (2013): The crystal structure of johnbaumite, $Ca_5(AsO_4)_3OH$, the arsenate analogue of hydroxylapatite. *m. Mineral.*, **98**, 1580-1584.

Biagioni, C., Bosi, F., Hålenius, U., Pasero, M. (2016): The crystal structure of svabite, $Ca_5(AsO_4)_3F$, an arsenate member of the apatite supergroup. *Am. Mineral.*, **101**, in press, DOI: 10.2138/am-2016-5636.

Pasero, M., Kampf, A.R., Ferraris, C., Pekov, I.V., Rakovan, J., White, T.J. (2010): Nomenclature of the apatite supergroup minerals. *Eur. J. Mineral.*, **22**, 163-179.

WENKITE, A REVISED STRUCTURE

Bonaccorsi E.*[1]
[1] Dipartimento di Scienze della Terra, Università di Pisa, Italy
Corresponding email: elena.bonaccorsi@unipi.it

Keywords: Wenkite, crystal structure, superstructure

Wenkite was found in the marbles of Candoglia (Ivrea zone, Alps, Italy), by Papageorgakis (1959, 1962), who studied its physical and optical properties, determined its hexagonal lattice constants and proposed the chemical formula: $Ba_{4.5}Ca_{4.5}Al_9Si_{12}O_{42}(OH)_5(SO_4)_2$. Wenk (1966) refined the lattice constants, obtaining a = 13.511(1), c = 7.462(1) Å, and determined P-62m as the most probable space group. Merlino (1973) and Wenk (1973) independently solved and refined the crystal structure of wenkite, which showed a disordered distribution of Si and Al within the tetrahedral sites, a positional disorder of the sulfate groups and additional disorder in the extraframework cations. Merlino (1973) obtained the crystal chemical formula $(Ba,K)_4(Ca,Na)_6(Si,Al)_{20}O_{41}(OH)_2(SO_4)_3$, and discussed the structural relationships between wenkite and offretite. These two phases have very similar unit cell parameters and both structures are characterized by columns of polyhedral cages [4665], with point-group symmetry -62m. However, they show different structures, related to the different positions of the mirror planes in offretite (space group P-6m2) and in wenkite (space group P-62m). A new data collection was carried out on a crystal of wenkite, which resulted in a better refinement of the disordered structure. Moreover, the X-ray data collections revealed a superstructure corresponding to a hexagonal unit cell with a = 23.400(3) Å, c = 14.903(2) Å. This supercell is different from that described by Lee (1976), who observed in transmission electron microscopy additional superstructure reflections which doubled both the a and the c parameters. A possible model for the superstructure of wenkite is proposed.

Lee, F. (1976): The submicroscopis structure of wenkite. *in* "Electron microscopy in mineralogy", H.R. Wenk, ed., Springer, Heidelberg, 361-370.

Merlino, S. (1973): The crystal structure of wenkite. *Acta Crystallogr.*, **B30**, 1262-1266.

Papageorgakis, J. (1959): Ein neues Bariummineral des Marmors von Candoglia in der unteren Val d'Ossola. *Schweiz. Mineral. Petrog. Mitt.*, **39**, 333-335.

Papageorgakis, J. (1962): Wenkit, ein neues Mineral von Candoglia. *Schweiz. Mineral. Petrog. Mitt.*, **42**, 269-274.

Wenk, H.R. (1966): New X-ray data for wenkite. *Schweiz. Mineral. Petrog. Mitt.*, **46**, 85-88.

Wenk, H.R. (1973): The structure of wenkite. *Z. Kristallogr.*, **137**, 113-126.

POLYTYPISM, TOPOLOGICAL AND CRYSTALCHEMICAL RELATIONS AMONG NATROCHALCITE GROUP AND BRACKEBUSCHITE GROUP MINERALS

Cámara F.*[1] & Ciriotti M.E.[2]
[1] Dipartimento di Scienze della Terra, Università di Torino, Italy
[2] Associazione Micromineralogica Italiana, Devesi-Cirié (TO), Italy
Corresponding email: fernando.camaraartigas@unito.it

Keywords: polytype, brackebuschite, natrochalcite

Natrochalcite group (NG) and brackebuschite group (BG) minerals have the general formulas $AM_2TO_4X_2$ and A_2MTO_4X, respectively (where $A = R^{+}$ and R^{2+} cations in 7-8 fold coordination; $M = R^{2+}$, R^{3+} cations in 6-fold coordination; $T = R^{4+}$, R^{5+}, R^{6+} cations in 4 fold coordination; X = O, OH, H_2O). From a structural point of view, NG minerals have MO_4X_2 octahedra sharing edges forming infinite chains that run parallel to [010], which are linked, forming layers, by TO_4 isolated tetrahedra and very strong hydrogen bonding by the (OH) or H_2O groups at the X sites; these layers are linked by A atoms and weak hydrogen bonds. BG minerals differ in the formula by a $A_1(MX)_{-1}$ substitution that can be a combination of different heterovalent exchanges. From a topological point of view, the replacement of M cations and X groups by an A cation occurs in chains of octahedra alternating within the layers. This relation has been already described by Hofmeister & Tillmanns (1978). Apart from this change, the rest of the topological relations remains in a broad sense unchanged. This implies that both groups of minerals are structurally related and could be regrouped. Different lattices and symmetries are observed in both groups of minerals (including triclinic and monoclinic metrics with eventual doubling of cell parameters), which are related to cation and proton ordering and can be explained as different combination of the same reduced triclinic cell (see Effenberger *et al*., 2000, and Fanfani & Zanazzi, 1967, for a description of the cell relations in NG and BG, respectively). Recent work on BG group minerals from Valletta Mine (Italy) allowed us to observe a new polytype that represents a novelty in this group of minerals. The structure of the polytype and its relation with NG and BG minerals will be presented.

Effenberger, H., Krause, W. Bernhardt, H.-J., Martin, M. (2000): On the symmetry of tsumcorite group minerals based on the new species rappoldite and zincgartrellite. *Mineral. Mag*., **64**, 1109-1126.

Fanfani, L. & Zanazzi, P.F. (1967): Structural similarities of some secondary lead minerals. *Mineral. Mag.*, **36**, 522-529.

Hofmeister, W. & Tillmanns, E. (1978): Strukturelle Untersuchungen an Arsenbrackebuschit. *Tschermaks Mineral. Petrogr. Mitt.*, **25**, 153-163.

MODULAR STRUCTURE AND TOPOLOGY OF $CsNaCu(P_2O_7)$ AND $CsNaCo(P_2O_7)$, AND THEIR COMPARISON WITH WOOLDRIDGEITE

Chernyatieva A.P.*[1], Mannasova A.Z.[1], Filatova A.A.[1] & Krivovichev S.V.[1]
[1] Department of Crystallography, Institute of Earth Science, Saint Petersburg State University, Russia
Corresponding email: chernyatieva@mail.ru

Keywords: structural topology, fundamental building block, pyrophosphate

There are three known natural pyrophosphates: canaphite, $Na_2Ca(P_2O_7)\cdot 4H_2O$, arnhemite, $(K,Na)_4Mg_2(P_2O_7)_2\cdot 5H_2O$, and wooldridgeite, $Na_2CaCu_2(P_2O_7)_2\cdot 10H_2O$, and only the latter contains a transitional metal cation as a structure-forming element. In contrast, the number of synthetic pyrophosphates is by far exceeds seven hundred compounds. However, the basic principles of structure formation of transitional metal pyrophosphates are quite similar for both natural and synthetic materials. Herein we describe results of our study of $CsNaCu(P_2O_7)$ and $CsNaCo(P_2O_7)$, two new transitional metal pyrophosphates prepared using high-temperature solid-state reactions.

$CsNaCu(P_2O_7)$ (1) is orthorhombic, $Pmn2_1$, a = 5.147(8), b = 15.126(2), c = 9.717(2) Å, V = 756.20 Å^3, R_1 = 0.066. $CsNaCo(P_2O_7)$ (2) is monoclinic, $P2_1/n$, a = 7.425(2), b = 7.648(2), c = 12.931(3) Å, β = 90.72(2)°, V = 734.2(3) Å^3, R_1 = 0.040.

The structure of (1) contains two Cu sites coordinated by four oxygen atoms each arranged at the vertices of distorted squares (Cu–O = 1.952–1.973 Å). Each CuO_4 square is complemented by an apical O atom (Cu–O = 2.074 Å), forming a $[CuO_5]$ tetragonal pyramid. Each CuO_5 pyramid shares two its vertices with one adjacent P_2O_7 group to form $[Cu(P_2O_7)]^{2-}$ fundamental building blocks (FBB) that has a shape of 3-membered Cu-P-P ring. Adjacent FBBs are linked into chains and the adjacent chains are further linked by longer Cu-O bonds into 2-dimensional layers.

The FBB in the structure of (2) is again a 3-membered Co-P-P ring, but formed by the CoO_4 tetrahedron. The FBBs are linked by sharing common O atoms to form a three-dimensional $[Co(P_2O_7)]^{2-}$ framework with cavities occupied by the Cs^+ and Na^+ cations. The framework topology is of the *srs* type, if each FBB is considered as a single node. Therefore, the copper pyrophosphate network in (2) can be identified as an augmented *srs* net.

It is of interest that the crystal structure of wooldridgeite contains similar 3-membered Cu-P-P rings as in the structure of (1) but linked into one-dimensional chains (Cooper & Hawthorne, 1999). Another related structure is that of $Cs_2CuP_2O_7$, where FBBs are linked to form a three-dimensional framework with an augmented ***dia*** net as an underlying network (Mannasova et al., 2016).

Acknowledgements: This work was supported for by the Russian Foundation for Basic Research (grants 14-05-00910 and 16-35-00182). X-ray diffraction measurements have been performed at the SPbSU X-ray Diffraction Resource Centre.

Cooper, M.A. & Hawthorne, F.C. (1999): The crystal structure of wooldridgeite, $Na_2CaCu^{2+}{}_2(P_2O_7)_2\cdot 10H_2O$, a novel copper pyrophosphate mineral. *Can. Mineral*., **37**, 73-81.

Mannasova, A.A., Chernyatieva, A.P., Krivovichev, S.V. (2016): $Cs_2CuP_2O_7$, a novel low-density open-framework structure based upon an augmented diamond net. *Z. Kristallogr.*, **231**, 65-70.

MINERALS DESCRIPTIONS AND HUMAN CIVILIZATION

Ciriotti M.E.*[1] & Cámara F.[2]
[1] Associazione Micromineralogica Italiana, Devesi-Cirié (TO), Italy
[2] Dipartimento di Scienze della Terra, Università di Torino, Italy
Corresponding email: m.ciriotti@tin.it

Keywords: mineral description, history

Minerals have been given names since the beginning of history, a knowledge that was recorded through different documents and treatises on mineral classifications and mineral commodities. The great diversity of chemical composition, physical properties, crystal forms and occurrences have challenged taxonomic efforts for centuries: an objective description of minerals requires a statement of specific characteristics related to a mineral (*s.l.*) and a reference object (holotype) must be accessible for research. Rules should avoid proliferation of multiple description of equivalent items. A concerted effort on an international basis to regulate mineral description and naming was carried out only in the last half century. The foundation of the International Mineralogical Association (IMA, Madrid 1958) and the Commission on New Minerals and Mineral Names (CNMMN), this latter in 1959, has certainly promoted a large number of mineral descriptions in literature since then: 3666 mineral species, tripling the number of type descriptions from 1800 to 1960, while only 59 type descriptions had been produced until 1800 (data from the Mineralogical Database by Ciriotti, 2016), even if the number of known mineral species was confidently larger (> 3x). Nonetheless, IMA-CNMMN is certainly not the only cause of the proliferation of mineral descriptions in recent times: the cited period coincides with the "*technological mineralogy*" (Tomalino, 2011) when accurate chemical determination of microvolumes became available along with the boosting of structure determination by development of direct methods for structure solving. At the same time, there has been a substantial growth of activity by amateur mineralogists and collectors and of their collaboration with academic community. The previous period comprises the "*crystallographic mineralogy*" and "*structural mineralogy*" (Tomalino, 2011), in which mineral descriptions were certainly boosted by the need of mineral commodities by the industrial revolution and the strong advancement of physics at the beginning of the twentieth century.

Ciriotti, M.E. (2016): Database mineralogico sistematico: quando, dove, come e perché. *Micro*, **14**, 2-20.
Tomalino, M.U. (2011): Una storia della mineralogia. Geda, Nichelino, 389 p.

HEXANIOBATES, A NEW GROUP OF MINERALS

Friis H.*[1]
[1] Natural History Museum, University of Oslo, Norway
Corresponding email: henrik.friis@nhm.uio.no

Keywords: hexaniobates, new minerals, molecular mineralogy

Peterandresenite, $Mn_4Nb_6O_{19}\cdot 14H_2O$, was the first naturally occurring hexaniobate described (Friis et al., 2014). Since peterandresenite two more hexaniobates have been discovered namely melcherite, $(Ba,K)_2(Na,Ca)_2MgNb_6O_{19}\cdot 6H_2O$, and hansesmarkite, $Ca_2Mn_2Nb_6O_{19}\cdot 20H_2O$ (Andrade et al., 2015; Friis et al., 2016). The central feature of all hexaniobates is the $[Nb_6O_{19}]^{8-}$ ion, known as the Lindqvist ion (Lindqvist, 1953). The Lindqvist ion consists of six edge-sharing Nb-octahedra creating a super octahedron. The connectivity between the Lindqvist ions creates the three-dimensional structures. The connectivity is achieved through a combination of direct cation bonds, but also through hydrogen bonds.

The three minerals have three different structures and consequently also symmetries. In hansesmarkite (*P*-1), the Lindqvist ions are connected via edge- and corner-sharing with the Mn-octahedron resulting in a rod of Mn-octahedra and Lindqvist ions along [100]. The Ca-site protrudes from the Lindqvist ion into the space between the rods and a three dimensional structure is achieved purely through H-bonds (Friis et al., 2016). In peterandresenite (*C*2/*m*), the Lindqvist ions are also connected *via* edge- and corner-sharing with one of two Mn-octahedra, but create a layer perpendicular to the *c*-axis. The second Mn-octahedron protrudes from the Lindqvist ions into the space between adjacent layers and again the three-dimensional structure is achieved solely through hydrogen bonds (Friis et al., 2014). In melcherite (*R*-3), the Lindqvist ions are directly connected via cation polyhedra into a three-dimensional structure (Andrade et al., 2015). The differences in connectivity in the three minerals result in hansesmarkite and peterandresenite readily disintegrate during heating or in vacuum, whereas melcherite is more stable.

Peterandresenite and hansesmarkite are both among the last minerals to form in the hydrothermal alteration stage of one pegmatite in the AS Granit larvikite quarry, Tvedalen, Norway. They both occur on thin fracture planes in the pegmatite on gonnardite. Furthermore, peterandresenite has been found on the Be-zeolite chiavennite associated with the Nb-mineral fersmite. The origin of the Nb for these late stage minerals is the breakdown of primary pyrochlore in the pegmatite. The presence of secondary Nb-minerals with low thermal stability raises some question into the mobility of high field strength elements in these types of pegmatites.

The current contribution will focus on the structure of this new group of minerals with an emphasis on hansesmarkite and peterandresenite. Furthermore, the mobility of Nb during alteration and the concept of Molecular Mineralogy will be discussed.

Andrade, M.B., Atencio, D., Menezes Filho, L.A.D. (2015): Melcherite, IMA 2015-018, CNMNC Newsletter 25. *Mineral. Mag.*, **79**, 529-535.

Friis, H., Larsen, A.O., Kampf, A.R., Evans, R.J., Selbekk, R.S., Sánchez, A.A., Kihle, J. (2014): Peterandresenite, $Mn_4Nb_6O_{19}\cdot 14H_2O$, a new mineral containing the Lindqvist ion from a syenite pegmatite of the Larvik Plutonic Complex, southern Norway. *Eur. J. Mineral.*, **26**, 567-576.

Friis, H., Weller, M.T., Kampf, A.R. (2016): Hansesmarkite, $Ca_2Mn_2Nb_6O_{19}\cdot 20H_2O$, a new hexaniobate from a syenite pegmatite in the Larvik Plutonic Complex, southern Norway. *Mineral. Mag.*, in press, DOI: 10.1180/minmag.2016.080.109.

Lindqvist, I. (1953): The structure of the hexaniobate ion in $7Na_2O\cdot 6Nb_2O_5\cdot 32H_2O$. *Ark. Kemi*, **5**, 247-250.

POTENTIALLY NEW LATIUMITE GROUP MINERAL, $KCa_3Al_2(SiO_4)(Si_2O_7)(PO_4)$ FROM LEUCITE-BEARING PARALAVA OF THE HATRURIM COMPLEX, NEGEV DESERT, ISRAEL

Galuskin E.V.*[1], Galuskina I.O.[1], Krüger B.[2] & Vapnik Y.A.[3]

[1] Institute of Mineralogy and Petrography, Faculty of Earth Sciences, University of Silesia, Sosnowiec, Poland

[2] Universität Innsbruck, Austria

[3] Department of Geological and Environmental Sciences, Ben-Gurion University of the Negev, Beer-Sheva, Israel

Corresponding email: evgeny.galuskin@us.edu.pl

Keywords: latiumite, tuscanite, P-analog of latiumite

Small bodies of paralavas within the field of development of larnite pseudoconglomerates were found on the west slope of Parsa Mt. in the Negev Desert near Arad town, Israel. Wollastonite, esseneite-diopside, gehlenite, anorthite, andradite-schorlomite, leucite and P-bearing members of the latiumite group are the main minerals of these paralavas. The latiumite group consist of latiumite $(Ca,K)_4(Si,Al)_5O_{11}(SO_4,CO_3)$, and tuscanite $(K, \square)Ca_6(Si,Al)_{10}O_{22}(SO_4,CO_3)_2(OH)\cdot H_2O$ (Tilley & Henry, 1952; Cannillo et al., 1973; Orlandi et al., 1977). The structure of these minerals is represented by tetrahedral hybrid *zweier* double layers of composition $[(Al,Si)_5O_{11}]$. The K occurs in the cavities of this layers, where Ca- atoms, SO_4 and CO_3 groups are located between them. The potentially new minerals of the latiumite group from paralavas crystalize in $P2_1$ space group with cell parameters $a \approx 12.075$, $b \approx 5.101$, $c \approx 10.884$ Å, $\beta \approx 107.06°$. Their common empirical formula is $(K_{0.6}Ca_{0.05\text{-}0.1}\square_{0.3\text{-}0.35})_{\Sigma1}Ca_3Al_2[(SiO_4)_{0.73\text{-}0.9}(AlO_4)_{0.1\text{-}0.27}]_{\Sigma1}(Si_2O_7)[(PO_4)_{0.43\text{-}0.7}(SO_4)_{0.3\text{-}0.57}]_{\Sigma1}$ and they do not contain any CO_3. The P-content increases from the center to the rim of crystals. Low-P phases are related to latiumite, and high-P ones to potentially new minerals with end-member formula: $KCa_3Al_2(SiO_4)(Si_2O_7)(PO_4)$. Substitution $PO_4 \rightarrow SO_4$ can be realized according to the two isomorphic schemes: $(PO_4)^{3-} + (SiO_4)^{4-} \rightarrow (SO_4)^{2-} + (AlO_4)^{5-}$ or $(PO_4)^{3-} + K^{1+} \rightarrow (SO_4)^{2-} + \square$, to which correspond two end-members: $KCa_3Al_2(AlO_4)(Si_2O_7)(SO_4)$ and $\square\ Ca_3Al_2(SiO_4)(Si_2O_7)(SO_4)$, respectively. An empirical formula of latiumite from the type locality is $(K_{0.85}\square_{0.15})Ca_3Al_2[(AlO_4)_{0.85}(SiO_4)_{0.15}](Si_2O_7)[(SO_4)_{0.7}(CO_3)_{0.3}]$ (Cannillo et al., 1973), therefore the end-member formula should be $KCa_3Al_2(AlO_4)(Si_2O_7)(SO_4)$ or $KCa_3Al_3Si_2O_{11}(SO_4)$. Transition from the P-analog of latiumite to tuscanite implies a substitution according to the schemes: $(PO_4)^{3-} \rightarrow (SO_4)^{2-} + (OH)^-$ and $(PO_4)^{3-} + K^{1+} \rightarrow (SO_4)^{2-} + H_2O$. The empirical formula of tuscanite (Orlandi et al., 1977) is: $(K_{0.88}Sr_{0.04}(H_2O)_{1.08})_{\Sigma2}(Ca_{5.25}Na_{0.51}Fe^{3+}_{0.10}Mg_{0.11})_{\Sigma5.97}(Si_{6.34}Al_{3.66})_{\Sigma10}O_{22}[(SO_4)_{1.38}(CO_3OH)_{0.55}(O_4H_4)_{0.11}]_{\Sigma2.04}$.The end-member formula of tuscanite can be represented as $[K(H_2O)]_{S2}Ca_6Si_6Al_4O_{22}(SO_4)_2(OH)$. The positions of OH group and H_2O in the structure of tuscanite were not determined. Therefore, it is possible that tuscanite is an sum of two end-members: $½[KCa_3Al_2(AlO_4)(Si_2O_7)(SO_4)] + ½[\ \square Ca_3Al_2(SiO_4)(Si_2O_7)\ (SO_4)]$. The structural study point out a doubling along the *a* direction of tuscanite unit-cell ($P2_1/a$, $a = 24.036(14)$, $b = 5.110(3)$, $c = 10.888(8)$ Å, $\beta = 106.95°$) in comparison with latiumite ($P2_1$, $a = 12.06$, $b = 5.08$, $c = 10.81$ Å, $\beta = 106°$) (Orlandi et al., 1977), which probably is connected with a substitution of K for H_2O. Taking into consideration that $K < 1$ *apfu* in the empirical formula of tuscanite, its end-member formula on the analogy of latiumite should look as $(H_2O)Ca_3Al_2(SiO_4)(Si_2O_7)(SO_4)$ or $(H_2O)Ca_3Al_2Si_3O_{11}(SO_4)$.

Acknowledgements: Investigations were partially supported by the National Sciences Centre (NCN) of Poland by decision no. 2013/11/B/ST10/00272 (I.G. and E.G.).

Cannillo, E., Dal Negro, A., Rossi, G. (1973): The crystal structure of latiumite, a new type of sheet silicate. *Am. Mineral*., **58**, 466-470.

Orlandi, P., Leoni, L., Mellini, M., Merlino, S. (1977): Tuscanite, a new mineral related to latiumite. *Am. Mineral*., **62**, 1110-1113.

Tilley, C.E. & Henry, N.F.M (1952): Latiumite (sulphatic potassium-calcium-aluminium silicate), a new mineral from Albano, Latium, Italy. *Mineral. Mag*., **30**, 39-45.

ELECTRONIC *D-D* TRANSITIONS AND INTERVALENCE CHARGE TRANSFER PROCESSES IN 3*D*-CATIONS IN CYPRINE AND CHEMICALLY RELATED VESUVIANITE GROUP MINERALS

Hålenius U.*[1], Panikorovskii T.L.[2] & Shilovskikh V.V.[3]
[1] Department of Geosciences, Swedish Museum of Natural History, Stockholm, Sweden
[2] Department of Crystallography, Saint Petersburg State University, Russia
[3] Department of Colloidal Chemistry, Saint Petersburg State University, Russia
Corresponding email: ulf.halenius@nrm.se

Keywords: cyprine, vesuvianite group, optical absorption spectroscopy

The new vesuvianite group mineral cyprine, ideally $Ca_{19}Cu^{2+}(Al_{10}Mg_2)Si_{18}O_{68}(OH)_{10}$, was recently described (Panikorovskii *et al*., 2015) from Wessels Mine, North Cape province, South Africa. The mineral is defined as a member of the vesuvianite group with Cu^{2+} as the dominant cation at the Y1 site. In contrast to the green-coloured Cu-bearing vesuvianite variety from Sauland in Norway named "cyprine" by Berzelius (1821), the Wessels Mine cyprine (*sensu stricto)* shows colours ranging from brownish red to purple. Polarised optical absorption spectra recorded on cyprine single crystals from Wessels Mine display major absorption bands polarised in E||O (*i.e.* E perpendicular to the c-axis) at 24000, 18000, 15600 and 12000 cm^{-1}. The observed range of colours in Wessels Mine cyprine is explained by strong variations in I_{24000}/I_{18000} band ratios. In spectra of purple coloured cyprine the band at 24000 cm^{-1} is virtually absent, while it is a dominant feature in spectra of red and brownish red cyprine. In spectra of Cu-bearing vesuvianite from Sauland only one major absorption band, also E||*O*-polarised, at 15600 cm^{-1} is observed.

The present spectra of Wessels Mine cyprine are similar to those of Cu-free, Mn-rich vesuvianite crystals from Lower Silesia, Poland (Platonov *et al*., 1995). These latter spectra were interpreted by Platonov *et al.* (1995) in terms of electronic *d-d* transitions in Mn^{3+} at the *Y*1 site (~ 24000 cm^{-1} band) and Mn^{3+} at the *Y*3 site or alternatively at a distorted *Y*1 site (18000 cm^{-1}). Based on the crystal chemistry of the Wessels Mine cyprine as determined by microprobe analyses and crystal structure refinement, inclusive cation occupancy determinations, we propose a revised assignment scheme: Electronic *d-d* transitions in Mn^{3+} at the *Y*3 site give rise to the 18000 cm^{-1} band and Cu^{2+} at the *Y*1 site causes the 15600 cm^{-1} band. Charge transfer processes involving Mn^{2+} and Fe^{3+} at the *Y*3 and *Y*2 sites cause the 24000 cm^{-1} absorption band. The assignment of the latter band is in agreement with its polarisation and its intensity changes in spectra of heat treated cyprine. Crystals treated for several hours under reducing atmospheres in the temperature range 600-800°C show continuous decrease in intensity of the 18000 cm^{-1} band. In contrast, the intensity of the 24000 cm^{-1} absorption band is almost unaffected by this treatment. Subsequent treatment under oxidising conditions at elevated temperatures restores the intensity of the 18000 cm^{-1} band, which reflects its relation to a $^{Y3}Mn^{3+}+O^{2-} \leftrightarrow {}^{Y3}Mn^{2+}+OH^-$ redox process.

Berzelius, J.J. (1821): Die Anwendung des Löthrohrs in der Chemie und Mineralogie. Schrag, Nürnberg, 263 p.

Panikorovskii, T.L., Shilovskikh, V.V., Avdontseva, E.Y., Zolotarev, A.A., Pekov, I.V., Britvin, S.N., Krivovichev, S.V. (2015): Cyprine, IMA 2015-044. CNMNC Newsletter No. 27, October 2015, page 1228. *Mineral. Mag.*, **79**, 1229-1236.

Platonov, A.N., Zabinski W., Sachanbinski, M. (1995): Optical absorption spectra of Mn^{3+} ions in vesuvianites from Lower Silesia, Poland. *Eur. J. Mineral.*, **7**, 1345-1352.

NEW CHALLENGES IN MINERAL NOMENCLATURE AND CLASSIFICATION

Hatert F.*[1], Mills S.J.[2], Pasero M.[3] & Hålenius U.[4]
[1] Laboratory of Mineralogy, University of Liège, Belgium
[2] Geosciences, Museum Victoria, Melbourne, Australia
[3] Dipartimento di Scienze della Terra, Università di Pisa, Italy
[4] Swedish Museum of Natural History, Stockholm, Sweden
Corresponding email: fhatert@ulg.ac.be

Keywords: CNMNC, mineral nomenclature, classification

The Commission on New Minerals, Nomenclature and Classification (CNMNC) of the IMA was established in 2006, by merging the Commission on New Minerals and Mineral Names (CNMMN) with the Commission on Classification of Minerals (CCM). The roles of CNMNC are of prime importance for the mineralogical community: validation of new mineral species, validation of mineral names, nomenclature of minerals (redefinitions, discreditations, revalidations, renamings, modifications of chemical formulae, …), group nomenclature, classification issues. However, the guidelines of CNMNC are not always easy to establish, due to the complex crystal-chemistry of minerals, and to the diversity of scientific disciplines involved in Mineralogy. In this talk, we will describe a few examples of challenging nomenclature and classification issues, which were handled by the CNMNC these last years. (i) The first issue concerns the definition of new mineral species (Hatert & Burke, 2008): what is the boundary between two species affected by complex substitution mechanisms? Are you allowed to define a mineral species with two atoms on the same crystallographic site? Or, on the contrary, is it possible to group crystallographic sites together for nomenclature purposes? (ii) The second issue concerns the naming of minerals (Hatert *et al*., 2013): what are the guidelines for the use of chemical prefixes and suffixes? Are you allowed to modify historical mineral names for nomenclature purposes? How to use structural prefixes in mineral names? (iii) The last issue concerns mineral classification (Mills *et al*., 2009): which are the guidelines to classify minerals? Is it possible to establish an official CNMNC-approved classification of minerals? By answering these questions, we hope to clarify some recent CNMNC guidelines and to explain the next steps of mineral nomenclature.

Hatert, F. & Burke, E.A.J. (2008): The IMA-CNMNC dominant-constituent rule revisited and extended. *Can. Mineral.*, **46**, 717-728.

Hatert, F., Mills, S.J., Pasero, M., Williams, P.A. (2013): CNMNC guidelines for the use of suffixes and prefixes in mineral nomenclature, and for the preservation of historical names. *Eur. J. Mineral.*, **25**, 113-115.

Mills, S.J., Hatert, F., Nickel, E.H., Ferraris, G. (2009): The standardisation of mineral group hierarchies: application to recent nomenclature proposals. *Eur. J. Mineral.*, **21**, 1073-1080.

WILANCOOKITE, A NEW BERYLLOPHOSPHATE FROM MINAS GERAIS, BRAZIL

Hatert F.*[1], Philippo S.[2], Ottolini L.[3], Dal Bo F.[1], Scholz R.[4], Chaves M.L.S.C.[5], Yang H.[6], Downs R.T.[6] & Menezes Filho L.A.D.[7]

[1] Laboratoire de Minéralogie, Université de Liège, Belgium

[2] Musée National d'Histoire Naturelle, Luxembourg, Luxembourg

[3] Istituto di Geoscienze e Georisorse, Consiglio Nazionale delle Ricerche, Pavia, Italy

[4] Department of Geology, Federal University of Ouro Preto, Brazil

[5] Institute of Geosciences, Federal University of Minas Gerais, Belo Horizonte, Brazil

[6] Department of Geosciences, University of Arizona, Tucson, AZ, USA

[7] (†) Belo Horizonte, Brazil

Corresponding email: fhatert@ulg.ac.be

Keywords: wilancookite, beryllophosphate, Brazil

Wilancookite, $(Ba,K,Na)_8(Ba,Li,□])_6Be_{24}P_{24}O_{96}.32H_2O$, is a new beryllophosphate discovered in the Lavra Ponte do Piauí granitic pegmatite, Itinga, Jequitinhonha, Minas Gerais, Brazil. The mineral forms tiny colourless dodecahedral {110} crystals reaching 100 µm in diameter, deposited on moraesite fibres. The lustre is vitreous, the streak is white, and the mineral is non-fluorescent either under long or short-wavelength ultraviolet light. No cleavage has been observed, but the mineral is brittle with an irregular fracture. Mohs hardness is 4-5, calculated density is 3.05 g/cm^3. Wilancookite is isotropic, colourless, non-pleochroic, with n = 1.560(2) (measured under λ = 590 nm). Quantitative chemical analyses were performed with a Cameca SX-50 electron microprobe (Ruhr-Universität Bochum, Germany); Be and Li contents were determined with a Cameca IMS 4f ion microprobe (CNR-IGG, Pavia, Italy). The empirical formula of wilancookite, based on 96 anhydrous oxygen atoms per formula unit (*apfu*), is: $(Ba_{7.54}K_{0.32}Na_{0.14})_{\Sigma 8.00}(Ba_{3.04}Li_{1.57}□_{1.39})_{\Sigma 6.00}Be_{24.08}(P_{23.88}Al_{0.38}Si_{0.03})_{\Sigma 24.29}O_{96}\cdot 32H_2O$. The simplified formula is $Ba_8(Ba_3Li_2□)Be_{24}P_{24}O_{96}\cdot 32H_2O$. The Raman spectrum is characterized by peaks at 430 (Be-O), 580 (v_4 PO_4), 1000 (v_1 PO_4), 1050 (v_3 PO_4), 1600 (v_2 H_2O), 3430 and 3680 (v_3 H_2O) cm^{-1}. An X-ray structural study was carried out on a crystal measuring 0.089 x 0.070 x 0.065 mm. A total of 1292 reflections were extracted, corresponding to 805 unique reflections. The unit-cell parameter refined from these reflections, a = 13.5398(2) Å, is in good agreement with that refined from the X-ray powder diffraction data. The crystal structure was refined in space group $I23$, to an R_1 value 0.0458; it is characterized by a framework similar to that of pahasapaite, $(Ca,Li,K,□)_{24}Li_8Be_{24}P_{24}O_{96}.38H_2O$. This framework is based on corner-sharing BeO_4 and PO_4tetrahedra forming a large cavity that contains Ba atoms and water molecules. Three different type of rings are building the cavity: eight-membered rings are parallel to {100} planes, six-membered rings are parallel to {111} planes, and four-membered rings are parallel to {110} planes. The positions of Ba atoms and water molecules are significantly different to those of Ca and Li in pahasapaite; however, the general topology of the framework is preserved. The mineral is named to honour William R. Cook Jr (1927-2006) and his wife Anne, very active mineral collectors. This name was originally given by Luiz A.D. Menezes Filho (1950-2014), when he discovered this species. The mineral species and its name were approved by the IMA-CNMNC under number 2015-034.

TWO NEW CHROMIC POLYSOMES OF BETA-ALUMINA OBSERVED IN SLAGS FROM THE PRODUCTION OF LOW-CARBON FERROCHROMIUM: BETA-ALUMINA-14*H* & BETA-ALUMINA-21*R*: $Na_{2-X}(Al,Mg,Cr)_{17}O_{25}$

Hejny C.*[1], Kahlenberg V.[1], Schmidmair D.[1], Tribus M.[1] & deVilliers J.[2]
[1] Institute für Mineralogie und Petrographie, Universität Innsbruck, Austria
[2] Department of Materials Science and Metallurgical Engineering, University of Pretoria, South Africa
Corresponding email: clivia.hejny@uibk.ac.at

Keywords: beta-alumina, polysomatic series, crystal structure

In the production of stainless steel from ferrochrome and scrap metal, extensive decarburization is necessary to reduce the carbon content to very small amounts (<0.04%) in stainless and low carbon steels. In order to prevent the presence of high amounts of carbon a series of experiments were done to test the feasibility of producing low carbon ferrochrome from chromite using aluminothermic reduction. Since the product of the reduction is alumina with a very high melting point, fluxing agents such as sodium salts are added to produce a liquid slag that can be tapped and to facilitate alloy separation (Bhonde et al., 2007). A mixture of chromite, aluminium and flux raw materials ($NaNO_3$ and $NaClO_3$) was ignited and left to react autogenously, heated by the exothermic reduction reaction. The products were subsequently left to cool in air and the metal and slag were separated once it achieved a temperature that allowed handling.

Examination of the slag revealed the presence of unknown phases that seemed to be related to the beta-alumina phases but additionally containing substantial amounts of chromium. The new phases were analysed by electron microbe and single-crystal diffraction. Two phases of $Na_{2-x}(Al,Mg,Cr)_{17}O_{25}$ composition were found to be composed of an alternating stacking of a spinel-type and a Na-hosting block. Similar structures are known for beta-alumina and beta''-alumina, $NaAl_{11}O_{17}$. However, the spinel-type block in $Na_{2-x}(Al,Mg,Cr)_{17}O_{25}$ is composed of five cation layers whereas the spinel block in beta-alumina contains only three cation layers. This different number of layers in the spinel block explains the different stoichiometry of the new chromic phases in comparison to well-known beta- and beta''-alumina. The two new phases, beta-alumina-14*H*, $P6_3/mmc$, a =5.6467(2), *c* = 31.9111(12) Å, and beta-alumina-21*R*, *R-3m*, *a* = 5.6515(3), *c* = 48.068(3) Å have a 14-layer and 21-layer stacking with a 2 x (*cccccch*) and a 3 x (*ccccccc*) repeat sequence of oxygen layers in cubic and hexagonal close packing, respectively. Beta-alumina-14*H,* beta-alumina-21*R,* beta-alumina and beta''-alumina can very conveniently be described as different members of a polysomatic series according to Veblen (1991), in a similar manner as it has been done for related spinel-, beta-alumina-type-, magnetoplumbite- and högbomite-structures (Beevers & Ross, 1937; Bettmann & Peters, 1969; Peters et al., 1971; Adelsköld, 1938; Armbruster, 2002; Hejny & Armbruster, 2002; Hejny et al., 2002).

Adelsköld, V. (1938): X-ray studies of magnetoplumbite, $Pb_{0.6}Fe_2O_3$, and other substances resembling beta-alumina, $Na_2O.11Al_2O_3$. *Ark. Kemi Mineral.Geol.*, **12A**, 29, 1-9.

Armbruster, T. (2002): Revised nomenclature of högbomite, nigerite, and taaffeite minerals. *Eur. J. Mineral.*, **14**, 389-395.

Beevers, C.A. & Ross, M.A.S. (1937): The crystal structure of beta-alumina, $Na_2O{\cdot}11Al_2O_3$. *Z. Kristallogr.*, **97**, 59-66.

Bettman, M. & Peters, C.R. (1969): Crystal structure of $Na_2O{\cdot}MgO{\cdot}5Al_2O_3$ with reference to $Na_2O{\cdot}MgO{\cdot}5Al_2O_3$ and other isotypal compounds. *J. Phys. Chem.*, **73**, 1774-1780.

Bhonde, P.J., Ghodgaonkar, A.M., Angal, R.D. (2007): Various techniques to produce low carbon ferrochrome. Proc. Infacon XI, New Delhi, India, 18-21 February 2007, 85-89.

Hejny, C. & Armbruster, T. (2002): Polysomatism in högbomite: The crystal structures of 10*T*, 12*H*, 14*T*, and 24*R* polysomes. *Am. Mineral.*, **87**, 277-292.

Hejny, C., Gnos, E., Grobety, B., Armbruster, T. (2002): Crystal chemistry and intergrowth of ferrohögbomite-2*N*2*S*, a well known but newly defined mineral species. *Eur. J. Mineral.*, **14**, 957-967.

Peters, C.R., Bettman, M., Moore, J.W., Glick, M.D. (1971): Refinement of the structure of sodium β-alumina. *Acta Crystallogr.*, **B27**, 1826-1834.

Veblen, D.R. (1991): Polysomatism and polysomatic series: A review and applications. *Am. Mineral.*, **76**, 801-826.

Se-BEARING THAUMASITE FROM PYROMETAMORPHIC ROCKS OF THE HATRURIM COMPLEX IN JORDAN

Juroszek R.*[1], Galuskina I.O.[1], Vapnik Y.A..[2] & Galuskin E.V.[1]
[1] Department of Geochemistry, Mineralogy and Petrography, University of Silesia, Sosnowiec, Poland
[2] Department of Geological and Environmental Sciences, Ben-Gurion University of the Negev, Beer-Sheva, Israel
Corresponding email: rafal0824@op.pl

Keywords: Hatrurim Complex, Se-bearing thaumasite, Raman spectroscopy

Minerals of the thaumasite-ettringite series are widespread as later minerals filling veins and cavities in pyrometamorphic rocks of the Hatrurim Complex distributed in the vicinity of rift zone of the Dead Sea in Israel and Jordan. Thaumasite $Ca_3[(S,Se)O_4][Si(OH)_6](CO_3)\cdot 12H_2O$ containing about 10-12 wt.% SeO_3 was found in cuspidine zones in spurrite rocks at South Siwaqa locality in Jordan. Thaumasite fills small veins together with calcite, potentially new mineral $\{Ca(OH_2)_2\}[Zn_2(OH)_6]$, baryte, ettringite, afwillite and other undiagnosed Ca-hydrosilicates. There are two generation of thaumasite: early, forming hexagonal prismatic crystal up to 1 mm – with low Se contents (SeO_3 < 1 wt.%) and later, forming single crystals up to 10 µm and epitaxial zone on early thaumasite – with high Se contents (SeO_3 > 1 wt.%).

Mineral with high content of selenium has not been described in this group. However, reference on ettringite with small concentrations of Se (640 ppm) was made recently (Sokol et al., 2012).

The Raman spectrum of Se-bearing thaumasite is characterized by several strong bands: 1115 cm^{-1} corresponding to $v_3\,(SO_4)^{2-}$, 1085 cm^{-1} – $v_1\,(CO_3)^{2-}$, 993 and 971 cm^{-1} – $v_1\,(SO_4)^{2-}$, 808 cm^{-1} – $v_1\,(SeO_4)^{2-}$, 655 cm^{-1} – v_1 (SiOHe), 455 cm^{-1} – $v_2\,(SO_4)^{2-}$, 410 cm^{-1} – $v_4\,(SeO_4)^{2-}$ and 325 cm^{-1} – $v_2\,(SeO_4)^{2-}$ (Sankaranarayanan & Krishnan, 1972, Gatta et al., 2012). Se concentration in thaumasite correlates with intensity of band at 808 cm^{-1}. In the OH region there are three main bands: 3500, 3440, 3370 cm^{-1}, characteristic for thaumasite (Gatta et al., 2012).

Minerals of the ettringite group are very important compounds in cement industry. They have a significant potential for immobilization of potentially toxic elements such as Cr, As and Se. So, this group of minerals can be used for environmental protection.

Acknowledgements: Investigations were partially supported by the National Sciences Centre (NCN) of Poland by decision no. 2013/11/B/ST10/00272.

Gatta, G.D., McIntyre, G.J., Swanson, J.G., Jacobsen S.D. (2012): Minerals in cement chemistry: A single-crystal neutron diffraction and Raman spectroscopic study of thaumasite, $Ca_3Si(OH)_6(CO_3)(SO_4)\cdot 12H_2O$, *Am. Mineral.*, **97**, 1060-1069.

Sankaranarayanan, V.N. & Krishnan, R.S. (1972): Raman and infrared spectra of ammonium selenite and lithium ammonium selenite, *Proc. Indian Acad. Sci. A*, **76**, 267-279.

Sokol, E., Kokh, S., Seryotkin, Y., Gaskova, O., Kozmenko, O. (2012): Cr^{+6}, Cr^{+3}, Fe^{+3} and Se in natural ettringite group minerals. EMC2012 - European Mineralogical Conference, Frankfurt, abstr., 143.

TEMPERATURE AND MOISTURE DEPENDENT INVESTIGATIONS ON ALUNOGEN AND THE CRYSTAL STRUCTURE OF META-ALUNOGEN

Kahlenberg V.*[1], Braun D.E.[2], Krüger H.[1], Orlova M.[1] & Schmidmair D.[1]
[1] Institut für Mineralogie und Petrographie, Universität Innsbruck, Austria
[2] Institut für Pharmazie - Pharmazeutische Technologie, Universität Innsbruck, Austria
Corresponding email: volker.kahlenberg@uibk.ac.at

Keywords: alunogen, meta-alunogen, high-temperature

Alunogen, a naturally occurring hydrous aluminum sulfate is usually described as a heptadecahydrate corresponding to the formula $Al_2(SO_4)_3 \cdot 17H_2O$. Notably, the exact water content of alunogen has been a matter of debate for quite a long time and various compositions between 16 and 18 water molecules per formula unit (pfu) have been reported. This variability is a direct consequence of the fact that alunogen crystals, which are exposed to air of low relative humidity at room temperature easily start to dehydrate partially, i.e. alunogen can be considered a non-stoichiometric hydrate (Fang & Robinson 1976).

Starting with a synthetic alunogen sample with composition $Al_2(SO_4)_3 \cdot 16.6H_2O$ the high-temperature and moisture dependent behavior has been studied by DTA/TG measurements, *in-situ* powder X-ray diffraction as well as gravimetric moisture sorption/desorption studies. Heating experiments using the different techniques prove that alunogen undergoes a first dehydration process already starting at temperatures slightly above 30°C. The crystalline product of the temperature induced dehydration corresponds to the synthetic equivalent of meta-alunogen having the following chemical composition: $Al_2(SO_4)_3 \cdot 13.7H_2O$. On the other hand, meta-alunogen can be also obtained at ambient temperatures when stored at relative humidities (RH) lower than 20%. However, a pronounced hysteresis between desorption and sorption isotherms has been observed.

Structural investigations on meta-alunogen were performed using a sample that has been kept at dry conditions (0% RH) over phosphorus pentoxide. Powder diffraction data were acquired on an in-house high-resolution diffractometer in transmission mode using a sealed glass capillary as sample holder. Indexing resulted in a triclinic unit cell with the following lattice parameters: a = 14.347(5), b = 12.483(5), c = 6.090(2) Å, α = 92.654(1), β = 96.663(1), γ = 100.830(1)°. These data correct earlier findings of Náray-Szabó (1969) who suggested an orthorhombic cell. *Ab-initio* structure solution in space group *P*-1 by simulated annealing provided a crystal chemically meaningful model involving sulfate tetrahedra, $Al(H_2O)_6$-octahedra and additional zeolitic water molecules.

Since hydrous aluminum sulfates have been postulated to occur in Martian soils (Golden et al., 2005) our results may help in the identification of meta-alunogen by X-ray diffraction not only on the surface of the Earth but also using the Curiosity Rover's ChemMin instrument.

Fang, J.H. & Robinson, P.D. (1976): Alunogen, $Al_2(H_2O)_{12}(SO_4)_3 \cdot 5H_2O$: Its atomic arrangement and water content. *Am. Mineral.*, **61**, 311-317.

Golden, D.C., Ming, D.W., Morris, R.V., Mertzman, S.A. (2005): Laboratory-simulated acid-sulfate weathering of basaltic materials: implications for formation of sulphates at Meridiani Planum and Gusev crater, Mars. *J. Geophys*. *Res*., **110**, E12S07.

Náray-Szabó, I. (1969): Über die Hydrate des Aluminiumsulfats. *Acta Chim. Acad. Sci. Hungaricae*, **60**, 27-36.

SYNTHESIS AND CRYSTAL STRUCTURE OF $Mn(SeO_4)\cdot 2H_2O$, A NEW MEMBER OF THE VARISCITE FAMILY OF COMPOUNDS

Kovrugin V.M.*[1-2-3], Aliev A.[2], Colmont M.[2], Mentré O.[2] & Krivovichev S.V.[1]

[1] Department of Crystallography, Saint Petersburg State University, Russia

[2] Unité de Catalyse et Chimie du Solide, Centre National de la Recherche Scientifique, Université de Lille 1 - Sciences et Technologies, Villeneuve d'Ascq, France

[3] Laboratoire de Réactivité et Chimie des Solides, Centre National de la Recherche Scientifique, Université de Picardie Jules Verne, Amiens, France

Corresponding email: kovrugin_vm@hotmail.com

Keywords: variscite, crystal structure, synthesis

The crystal structure of new compound $Mn(SeO_4)\cdot 2H_2O$ belongs to the variscite structure type $M(TO_4)\cdot 2H_2O$, where M = Fe^{3+}, Al^{3+}, Ga^{3+}, In^{3+} or Zn^{2+}, and T = P^{5+}, As^{5+} or Se^{6+}. This group of compounds includes such minerals as mansfieldite $Al(AsO_4)\cdot 2H_2O$, scorodite $Fe(AsO_4)\cdot 2H_2O$, yanomamite $In(AsO_4)\cdot 2H_2O$, strengite $Fe(PO_4)\cdot 2H_2O$, and variscite $Al(PO_4)\cdot 2H_2O$ itself. It should to be noted that the title compound is the second example of the variscite-type phase containing metal cations in the 2+ oxidation state.

Several studies of this group of isotypic minerals and synthetic compounds revealed interesting adsorption properties of their microporous 3D frameworks (Xu et al., 1994; Tang et al., 2001).

Evaporation method from aqueous solution of hydrated manganese(II) chloride (2.4 mmol), 40% selenic(VI) acid (4.7 mmol) and distilled water (10 ml) was used for the synthesis of $Mn(SeO_4)\cdot 2H_2O$. The solution was stirred with a magnetic stirrer at 80°C for 3 hours until it became fully homogeneous, then was poured onto a watch glass and left to evaporate in a fume hood at room temperature. Single crystals of $Mn(SeO_4)\cdot 2H_2O$ suitable for X-ray diffraction analysis appeared at the bottom of the watch glass after two days.

The 3D microporous framework of the crystal structure of $Mn(SeO_4)\cdot 2H_2O$ can be described as composed from interlinked heteropolyhedral sheets. The structural topology of the framework can be visualized using a graphical approach (Krivovichev, 2004) in which each manganese octahedron is represented by a black vertex and selenate pyramids are symbolized by white vertices. The resulting black-and-white graph is based upon hexagonal non-planar rings.

Acknowledgements: This work was supported by the Russian Foundation for Basic Research RFBR (grant 16-35-00191).

Krivovichev, S.V. (2004): Combinatorial topology of salts of inorganic oxoacids: zero-, one- and two-dimensional units with corner-sharing between coordination polyhedra. *Crystallogr. Rev.*, **10**, 185-232.

Tang, X., Gentiletti, M.J., Lachgar, A. (2001): Synthesis and crystal structure of indium arsenate and phosphate dihydrates with variscite and metavariscite structure types. *J. Chem. Crystallogr.*, **31**, 45-50.

Xu, Y., Koh, L., An, L., Qiu, S.-L., Yue, Y. (1994): Synthesis and characterization of a novel microporous indiumphosphate. *in* "Studies in surface science and catalysis", J. Weitkamp, H.G. Karge, H. Pfeifer, W. Hölderich, eds., Elsevier, Amsterdam, 2253-2260.

FIRST NATURAL OCCURENCE OF "$KAlSiO_4$-*O*1"

Krüger B.*[1], Krüger H.[1], Tropper P.[1], Tribus M.[1] & Joachim B.[1]
[1] Institut für Mineralogie und Petrographie, Universität Innsbruck, Austria
Corresponding email: biljana.krueger@uibk.ac.at

Keywords: kalsilite, Hatrurim Complex, topology

The first natural crystals of "$KAlSiO_4$-*O*1" have been found in the pyrometamorphic rocks of the Hatrurim Complex, Negev Desert, Israel, associated with schorlomite, melilite, pseudowollastonite, rankinite and sulfate-rich apatite. They have been previously described as Fe-rich kalsilite (Sharygin et al., 2006). Nevertheless, using X-ray single-crystal analysis, they were identified as the known '*O*1' polymorph of kalsilite, which is up to now only known as synthetic compound.

Transparent, irregularly shaped grains of "$KAlSiO_4$-*O*1" (up to 0.5 x 0.5 mm across) crystallize in space group $P2_1$ with cell parameters a = 15.6553(1), b = 9.0384(1), c = 8.5274(2) Å, β = 90.018(1)°, V = 1206.62(3) $Å^3$. As well as the synthesized, natural crystals are affected by inversion, pseudo-orthorhombic and pseudo-hexagonal twinning. However, additional reflections or diffuse scattering was not observed. Pseudosymmetry and twinning made the identification of this phase rather difficult. Therefore, Raman spectra of "$KAlSiO_4$-*O*1" were collected and compared to known spectra of the synthetic crystals.

Several polymorphs of $KAlSiO_4$ are known to exist. The "$KAlSiO_4$-*O*1" phase is structurally closely related to the stuffed derivatives of tridymite, but the topology of the Si/Al-ordered framework is different. In the structure of "$KAlSiO_4$-*O*1" the K^+ cations are situated between sheets of six-membered rings of $(Al,Si)O_4$ tetrahedra. The sequence of the directedness of the tetrahedra within one ring [free apex pointing up (U) or down (D)] is different for trydimite and "$KAlSiO_4$-*O*1". The framework of tridymite exhibits UDUDUD rings. In the framework of the "*O*1"-phase two different types of six-membered rings can be distinguished. The rings with UUDDUD and the UUUDDD configuration are occurring in a ratio of 2:1. A similar arrangement has been found in the structure of megakalsilite ($KAlSiO_4$; Khomyakov et al., 2002) where the same two types of rings appear in a ratio of 1:3.

The crystal structure of the *O*1 phase has been solved from X-ray powder diffraction data and refined using the Rietveld method (Gregorkiewitz et al., 2008) and further confirmed by single-crystal analysis (Kremenovic et al., 2013). The results of structural refinement as well as MAS NMR measurements (Gregorkiewitz et al., 2008) have shown an ordered distribution of Si and Al tetrahedra in the framework.

The synthesis diagram of KAl_2O-SiO_2 with tentative solid solutions limits (Cook et al., 1977) shows potential stability field of this phase between 950 and 1450°C. Upon heating above 1450°C "$KAlSiO_4$-*O*1" transforms to so-called "$KAlSiO_4$-*O*2" phase with a doubled b parameter and an orthorhombic unit cell (a = 15.600, b = 18.110, c = 8.560 Å).

Cook, L.P., Roth, R.S., Parker, H.S., Negas, T. (1977): The system K_2O-Al_2O_3-SiO_2.Part l. Phases on the $KAlSiO_4$-KAlO, join. *Am. Mineral.*, **62**, 180-190.

Gregorkiewitz, M., Li, Y., White, T.J., Withers, R.L., Sobrados, I. (2008): The structure of "orthorhombic" $KAlSiO_4$-*O*1: evidence for Al-Si order from MAS NMR data combined with Rietveld refinement and electron microscopy. *Can. Mineral.*, **46**, 1511-1526.

Khomyakov, A.P., Nechelyustov, G.N., Sokolova, E.V., Bonaccorsi, E., Merlino, S., Pasero, M. (2002): Megakalsilite, a new polymorph of $KAlSiO_4$ from the Khibina alkaline massif, Kola Peninsula, Russia: mineral description and crystal structure. *Can. Mineral.*, **40**, 961-970.

Kremenovic, A., Lazic, B., Krüger, H., Tribus, M., Vulic, P. (2013): Monoclinic structure and nonstoichiometry of '$KAlSiO_4$-*O*1'. *Acta Crystallogr.*, **C69**, 334-336.

Sharygin, V.V., Vapnik, Y., Sokol, E.V., Kamenetsky, V.S., Shagam, R. (2006): Melt inclusions in minerals of schorlomite-rich veins of the Hatrurim Basin, Israel: composition and homogenization temperatures. ACROFI-1 Conference, Nanjing, China, 189-192.

SUPERSTRUCTURE AND DISORDER IN SYNTHETIC SHULAMITITE

Krüger H.*[1], Jaeger F.D.[1] & Konrad B.[1]
[1] Institut für Mineralogie und Petrographie, Universität Innsbruck, Austria
Corresponding email: Hannes.Krueger@uibk.ac.at

Keywords: shulamitite, superstructure, stacking faults

The crystal structure of the mineral shulamitite $Ca_3TiFeAlO_8$ (Sharygin et al., 2013) is related to the the better-known structure of brownmillerite (BM). Structural units in both structures are (1) perovskite-like layers of corner-sharing octahedra (O layers), and (2) layers with parallel *zweier* single-chains of tetrahedra (T layers). In brownmillerite, the layers are stacked alternately (OTOT), whereas in shulamitite the sequence is OOTOOT. Within the T layers, tetrahedral chains may adopt two different configurations, right- or left-handed. This allows different patterns with respect to intra- and interlayer order. For BM-type structures several ordering patterns are described (e.g., D'Hondt et al., 2008). The structural model of shulamitite published by Sharygin et al. (2013) exhibits random disorder of the chains (*Pmma*), whereas the synthetic Fe-analog $Ca_3TiFe_2O_8$ (Rodríguez-Carvajal et al., 1989) was described as acentric with only one type of chain in the whole structure ($Pcm2_1$). However, the structural variations caused by different ordering patterns are rather small and cannot easily distinguished by diffraction methods without paying special attention to very weak features.

We have synthesized crystals of shulamitite and its Fe-analog. Single crystal X-ray diffraction experiments using extraordinary long exposure time, show that both materials exhibit alternating intralayer order of tetrahedral chains. In $Ca_3TiFe_2O_8$, lines of diffuse scattering prove that no correlation between neighbouring T-layers exists (absence of interlayer ordering), whereas synthetic shulamitite shows very weak but sharp superstructure reflections according to perfect intra- and interlayer ordering.

D'Hondt, H., Abakumov, A.M., Hadermann, J., Kalyuzhnaya, A.S., Rozova, M.G., Antipov, E.V., Tendeloo, G.V. (2008): Tetrahedral chain order in the $Sr_2Fe_2O_5$ brownmillerite. *Chem. Mater.*, **20**, 7188-7194.

Rodríguez-Carvajal, J., Vallet-Regí, M., Calbet, J.G. (1989): Perovskite threefold superlattices: A structure determination of the $A_3M_3O_8$ phase. *Mater. Res. Bull.*, **24**, 423-430.

Sharygin, V.V., Lazić, B., Armbruster, T.M., Murashko, M.N., Wirth, R., Galuskina, I.O., Galuskin, E.V., Vapnik, Y., Britvin, S.N., Logvinova, A.M. (2013): Shulamitite $Ca_3TiFe^{3+}AlO_8$ – a new perovskite-related mineral from Hatrurim Basin, Israel. *Eur. J. Mineral.*, **25**, 97-111.

POTENTIAL NEW VANADIUM MINERAL BELONGING TO THE APATITE GROUP FROM HATRURIM COMPLEX, ISRAEL

Krzątała A.*[1], Galuskina I.O.[1], Galuskin E.V.[1] & Vapnik Y.A.[2]
[1] Department of Geochemistry, Mineralogy and Petrography, University of Silesia, Sosnowiec, Poland
[2] Department of Geological and Environmental Sciences, Ben-Gurion University of the Negev, Beer-Sheva, Israel
Corresponding email: arcadius91@gmail.com

Keywords: Hatrurim Complex, vanadium apatite, apatite group

Potentially new mineral species belonging to the apatite supergroup (Pasero et al., 2010) with the end-member crystal chemical formula $Ca_5(VO_4)_3F$ was found at three localities in vein-like bodies of paralavas, hosted by melilite hornfels of the Hatrurim Complex, Israel: Nahal Morag, Zuk Tamrur and Gurim anticline at the Hatrurim Basin. Rankinite, gehlenite, andradite–schorlomite, fluorapatite, fluorellestadite, larnite, wollastonite, pseudowollastonite, aradite, zadovite, barioferrite, magnesioferrite, khesinite, gurimite, delafossite, walstromite and ferrian perovskite are typical mineral association of coarse-grained paralavas.

Small grains of vanadium analogs of apatite are not exceeding 10-15 μm in size. They are generally confined to small enclaves within fine-grained gurimite, walstromite, delafossite, secondary Ca hydrosilicates. Vanadium analogs of apatites crystallized at the later stage from residual melt.

The empirical formula of vanadium analog of fluorapatite (mean of 7 analyses) is $(Ca_{4.75}Sr_{0.11}Ba_{0.09}Na_{0.05})_{\sum 5}[(VO_4)_{2.52}(PO_4)_{0.33}(SO_4)_{0.1}(SiO_4)_{0.05}]_{\sum 3}(F_{0.49}Cl_{0.28}OH_{0.23})_{\sum 1}$. Content of potentially new vanadium end-members rises up to 49% of vanadium analog of fluorapatite.

In the Raman spectra of vanadium apatite and apatite with varying amount of VO_4 and PO_4 bands with changing intensities were observed at ~806 cm^{-1} and ~868 cm^{-1} and at ~960 cm^{-1}. The presence of S and Si in composition of apatite leads to an appearance of additional Raman bands at ~997 cm^{-1} (SO_4) and ~855 cm^{-1} (SiO_4). The presence of OH groups in the channel sites was confirmed by Raman spectroscopy (bands at ~ 3600- 3660 cm^{-1}).

Acknowledgements: Investigations were supported by the National Sciences Centre (NCN) of Poland by decision no. 2013/11/B/ST10/00272.

Pasero, M., Kampf, A., Ferraris, C., Pekov, I., Rakovan, J., White, T. (2010): Nomenclature of the apatite supergroup minerals. *Eur. J. Mineral.*, **22**, 163-179.

NEW MODULAR PRINCIPLES AND STRUCTURES DEFINED FOR THE SARTORITE HOMOLOGOUS SERIES OF Pb-Aa(Sb)-Ag-Tl SULFOSALTS

Makovicky E.*[1], Topa D.[2] & Stroeger B.[3]
[1] Department of Geoscience and Natural Resource Management, University of Copenhagen, Denmark
[2] Naturhistorisches Museum Wien, Austria
[3] Technische Universität Wien, Austria
Corresponding email: emilm@ign.ku.dk

Keywords: Sartorite homologous series, series of omission derivatives, compositionally intermediate structures

The sartorite homologous series, originally defined for the Pb-As sulfosalts with minor Sb, Tl and/or Ag (Makovicky, 1985) is a modular series based on a combination of two types of modules (double-layer ribbons, respectively 3 and 4 cation coordination polyhedra wide), either with only one type of module, or both modules present in the 1:1 and 1:2 ratio. The N = 4 ribbons can either be Ag-free or Ag-containing, forming different structures, with different arrangement of As(Sb)-S crankshaft chains in the ribbons.

New structural and chemical investigations, chiefly by our group, revealed two new mechanisms which enlarge the spectrum of modular phenomena among the sartorite homologues. On the one hand, the known distinction between the Ag(Tl)-free and Ag-containing structures, such as the pair dufrenoysite – rathite has been enriched by a subclass of low-Ag structures, with superstructures which differ from the Ag-free ones: argentobaumhauerite versus baumhauerite, $Ag_{3.5}Pb_{33}As_{55}S_{112}$ versus liveingite, and a low-Ag As-Sb sulfosalt polloneite versus dufrenoysite. In the low-Ag sulfosalts, the gamut of modules is widened by the coexistence of Ag-free and Ag-containing N = 4 modules in one structure (or of As-rich and Sb/Ag-rich modules in polloneite) which leads to a spectacular doubling or tripling of one of the cell parameters.

A different type of modular variability occurs in the pure N = 3 structure of the series, “a sartorite group *sensu stricto*”. In these newly defined minerals, the usual 4.2 Å × 2 parameter of ribbon periodicity is altered to 7-, 9-, 11-, and 13-fold multiples of 4.2 Å along the ribbon stretch. The still hypothetical 5-tuple structure contains a W-shaped module composed of predominantly As coordination polyhedra which alternates with a pair of As polyhedra. The next, heptasartorite structure has one four-member crankshaft chain added along one side of the W-chain, the enneasartorite structure has such chains added on both sides of the W-chain, hendekasartorite has asymmetrically added one and two chains, respectively, whereas the 13-tuple has two and two chains separating the W-chain and the two-As configuration. Each W-module is connected with one S vacancy which is preferably compensated by exchange of one prismatic Pb site by thallium. With the increasing cell parameter of the omission homologue, the frequency of this Tl exchange – S vacancy pair decreases. This exchange competes with the As + Tl for 2 Pb exchange but it still displaces the mineral composition from the ideal N = 3 line in the Pb-(As,Sb)-(Ag,Tl) diagram.

Makovicky, E. (1985): The building principles and classification of sulphosalts based on the SnS archetype. *Fortschr. Mineral.*, **63**, 45-89.

STRUCTURE, POLYTYPISM AND DISORDER OF DENISOVITE, $K_{14}Ca_{42}Na_6Si_{60}O_{162}F_{16}(OH)_4 \cdot 2H_2O$, OBTAINED BY A COMBINATION OF (S)TEM IMAGING, ELECTRON DIFFRACTION TOMOGRAPHY AND X-RAY POWDER DIFFRACTION

Mugnaioli E.*[1-2], Rozhdestvenskaya I.V.[3], Czank M.[4], Depmeier W.[4], Schowalter M.[5], Rosenauer A.[5] & Schmidt M.U.[6]

[1] Dipartimento di Scienze Fisiche, della Terra e dell'Ambiente, Università di Siena, Italy

[2] Centro per l'Innovazione nelle Nanotecnologie, Istituto Italiano di Tecnologia, Pisa, Italy

[3] Department of Crystallography, Saint Petersburg State University, Russia

[4] Institut für Geowissenschaften, Christian-Albrechts-Universität Kiel, Germany

[5] Institut für Festkörperphysik, Universität Bremen, Germany

[6] Institut für Anorganische und Analytische Chemie, Goethe-Universität Frankfurt am Main, Germany

Corresponding email: enrico.mugnaioli@unisi.it

Keywords: order-disorder sequence, transmission electron microscopy, electron diffraction tomography

Denisovite, ideally $K_{14}Ca_{42}Na_6Si_{60}O_{162}F_{16}(OH)_4 \cdot 2H_2O$, is a rare mineral uniquely found in the Khibini and in the Murun massifs, Russia. A comprehensive structural characterization of denisovite was obtained by a combination of aberration-corrected high-angular annular dark-field scanning-transmission electron microscopy (AC-HAADF-STEM), high-resolution transmission electron microscopy (HR-TEM), electron diffraction tomography (EDT) and X-ray powder diffraction (XRPD).

Denisovite crystallizes in asbestos-like fibers of typical diameter of 200-500 nm. Structure investigation is complicated by the fact that all investigated fibers show pronounced diffuseness of diffraction spots along **a*** for *hkl*reflection lines with $l = 2n+1$.

The structure model of denisovite (a = 31.0964(8), b = 19.5701(5), c = 7.21526(12) Å, β = 96.6669(6)°, space group *P*2/*a*) was first deduced on the basis of AC-HAADF-STEM images and later on obtained *ab-initio* by direct methods on the basis of EDT reflection intensities and refined by XRPD Rietveld method. The structure can be visualized as being composed by two types of *dreier* silicate chains: a xonotlite-like dreier double chain $[Si_6O_{17}]^{10-}$ and a tubular loop-branched *dreier* triple chain $[Si_{12}O_{30}]^{12-}$, both extending parallel to **c**. The silicate chains are connected by ribbons of edge-sharing (Ca,Na)-octahedra.

Similarly to the related mineral charoite (Rozhdestvenskaya et al., 2010; Rozhdestvenskaya et al., 2011), the denisovite structure can be described as an order-disorder (OD) sequence consisting of layers with translation vectors **b** and **c**, and a third basic vector **a**/2 along the missing periodicity. Layers have symmetry *P*(*m*)2*m* and are stacked according to screw axes $2_{1/2}$ or $2_{-1/2}$ || **c**. Even if two sequences with a maximum degree of order (MDO) are possible ("$2_{-1/2}$, $2_{-1/2}$ …" and "$2_{-1/2}$, $2_{1/2}$ …"), only the first one was experimentally observed by HR-TEM imaging. In analogy with charoite, this MDO sequence corresponds to the polytype "denisovite-96". Unlike charoite, an ordered "zig-zag" MDO sequence corresponding to the hypothetical polytype "denisovite-90" was never observed.

The denisovite structure is pervasively disordered along **a** and it was never possible to collect an EDT data set without significant diffuse scattering along **a***, even for areas as small as 50 nm in diameter (about 15 cell repetitions along **a**). The pervasive disorder is confirmed by HR-TEM imaging along [010], which typically shows multiple stacking faults and reversals of the stacking angle β in a range of few unit cell repetitions.

At the structural level, the dreier silicate chains constitute a rigid module that can be connected to different sides of the octahedral bands. Neighboring modules can be shifted by +¼**[001]** or -¼**[001]**. Due to the geometrical relation

$$| a \cos(\beta) | = c/2$$

the β reversal can be described both by a (100) nano-lamellae twinning, or by keeping the cell setting constant and changing the space group description to *P*2/*n*.

Rozhdestvenskaya, I., Mugnaioli, E., Czank, M., Depmeier, W., Kolb, U., Reinholdt, A., Weirich, T. (2010): The structure of charoite, $(K,Sr,Ba,Mn)_{15-16}(Ca,Na)_{32}[(Si_{70}(O,OH)_{180})](OH,F)_{4.0} * nH_2O$, solved by conventional and automated electron diffraction. *Mineral. Mag.*, **74**, 159-177.

Rozhdestvenskaya, I., Mugnaioli, E., Czank, M., Depmeier, W., Kolb, U., Merlino, S. (2011): Essential features of the polytypic charoite-96 structure compared to charoite-90. *Mineral. Mag.*, **75**, 2833-2846.

NEW ARSENATE MINERALS IN FUMAROLE EXHALATIONS OF THE TOLBACHIK VOLCANO, KAMCHATKA, RUSSIA

Pekov I.V.*[1], Zubkova N.V.[1], Yapaskurt V.O.[1], Britvin S.N.[2], Belakovskiy D.I.[3], Vigasina M.V.[1], Lykova I.S.[1-3], Turchkova A.G.[1] & Sidorov E.G.[4]

[1] Faculty of Geology, Moscow State University, Russia

[2] Department of Crystallography, Saint Petersburg State University, Russia

[3] Fersman Mineralogical Museum, Moscow, Russia

[4] Institute of Volcanology and Seismology, Far East Branch of the Russian Academy of Sciences, Petropavlovsk-Kamchatsky, Russia

Corresponding email: igorpekov@mail.ru

Keywords: new arsenate mineral, fumarole, Tolbachik volcano

Natural arsenates include almost 350 mineral species. Most of them (295) are H-bearing, with OH^- and/or H_2O, and 50 species are H-free. The majority of H-bearing arsenate minerals occur in the oxidation zone of chalcogenide ores and in hydrothermal deposits. Among H-free natural arsenates, 26 species are known in volcanic fumaroles of the oxidizing type, including 20 minerals endemic for this formation. The richest and most diverse arsenate mineralization of this genetic type occurs in exhalations of active fumaroles located at the Second scoria cone of the Northern Breakthrough of the Great Tolbachik Fissure Eruption (NB GTFE, 1975-1976), Tolbachik volcano, Kamchatka, Russia. Arsenates were first found here in 1980s as rare constituents of oxide-sulfate fumarolic incrustations (Vergasova & Filatov, 1993). Seven new minerals, namely alarsite $Al(AsO_4)$ (1994), coparsite $Cu_4O_2[(As,V)O_4]Cl$ (1999), urusovite, $CuAlO(AsO_4)$ (2000), bradaczekite $NaCu_4(AsO_4)_3$ (2001), filatovite $K[(Al,Zn)_2(As,Si)_2O_8]$ (2004), lammerite-β $Cu_3(AsO_4)_2$ (2012), and hatertite $Na_2(Ca,Na)(Fe^{3+},Cu)_2(AsO_4)_3$ (2013) were discovered here by L.P. Vergasova, S.K. Filatov, G.L. Starova, S.V. Krivovichev and their co-authors, and lammerite, johillerite and nickenichite were found: see overview in Pekov et al. (2014). During fieldworks in 2012, we have uncovered at the Second scoria cone of the NB GTFE an earlier unknown active, hot fumarole with extremely rich arsenate mineralization that caused its name Arsenatnaya. 25 of 26 Tolbachik arsenates (except coparsite) are known in this fumarole, including tilasite, svabite, berzeliite, and durangite first found in this formation and 12 new minerals approved by the IMA CNMNC in 2013-2015 based on our proposals. Besides, more than ten insufficiently studied arsenate phases are determined in Arsenatnaya. All the arsenates were collected from fumarole cameras with temperatures 350-450ºC and are H-free. The new mineral species are ericlaxmanite* $Cu_4O(AsO_4)_2$ (tric.), kozyrevskite* $Cu_4O(AsO_4)_2$ (orth.), popovite** $Cu_5O_2(AsO_4)_2$, shchurovskyite** $K_2CaCu_6O_2(AsO_4)_4$, dmisokolovite** $K_3Cu_5AlO_2(AsO_4)_4$, melanarsite** $K_3Cu_7Fe^{3+}O_4(AsO_4)_4$, arsmirandite** $Na_{18}Cu_{12}Fe^{3+}O_8(AsO_4)_8Cl_5$, vasilseverginite** $Cu_9O_4(AsO_4)_2(SO_4)_2$, yurmarinite* $Na_7(Fe^{3+},Mg,Cu)_4(AsO_4)_6$, pharmazincite $K[ZnAsO_4]$, katiarsite* $KTiO(AsO_4)$, and arsenowagnerite $Mg_2(AsO_4)F$. The arsenate mineralization is uncommon in the crystal chemical aspect: ** - new structure type, * - structure type earlier known only for synthetic compounds. The new arsenates with species-defining Cu^{2+}contain additional anions O^{2-} not bonded with As^{5+} but forming bridges Cu-O-Cu and playing the same role in structures as OH^- or H_2O in copper oxysalts formed at lower temperatures. All 19 arsenates first discovered at Tolbachik are endemics of this volcano that highlights the originality of arsenic mineralization in fumaroles of the oxidizing type.

Acknowledgements: The work was supported by RFBR, grant 14-05-00276.

Pekov, I.V., Zubkova, N.V., Yapaskurt, V.O., Belakovskiy, D.I., Lykova, I.S., Vigasina, M.F., Sidorov, E.G., Pushcharovsky, D.Y. (2014): New arsenate minerals from the Arsenatnaya fumarole, Tolbachik volcano, Kamchatka, Russia. I. Yurmarinite, $Na_7(Fe^{3+},Mg,Cu)_4(AsO_4)_6$. *Mineral. Mag.*, **78**, 905-917.

Vergasova, L.P. & Filatov, S.K. (1993): Minerals of volcanic exhalations – a new genetic group (after the data of Tolbachik volcano eruption in 1975-1976). *Zap. Vser. Miner. Obsh.*, **122(4)**, 68-76 (in Russian).

OXO-CENTERED STRUCTURAL UNITS IN BISMUTH OXYSULFATES FROM VULCANO, AEOLIAN ISLAND, ITALY

Pinto D.*[1] & Garavelli A.[1]
[1] Dipartimento di Scienze della Terra e Geoambientali, Università di Bari, Italy
Corresponding email: daniela.pinto@uniba.it

Keywords: Bi-oxysulfates, oxo-centered polyhedra, crystal structure

Traditional inorganic crystal chemistry and structural mineralogy are based upon the concept of cation-centered polyhedra. However, there is a number of inorganic compounds that can be considered as consisting of strongly bonded structural units formed by anion-centred coordination polyhedra. A general review of inorganic compounds based upon anion-centered tetrahedra has been recently reported in Krivovichev et al. (2013). Such a kind of compounds are formed by "additional" anions, i.e., anions not belonging to oxyanions. In this contribution, we shall consider some examples of new natural Bi compounds with additional oxygen anions (O_a), recently discovered among fumarolic products at La Fossa crater (Vulcano, Aeolian Islands, Italy): balićžunicite (Pinto et al., 2014), leguernite (Garavelli et al., 2014), and two phases with compositions $Bi_{14}O_{16}(SO_4)_5$ and $Bi_{30}O_{33}(SO_4)_9(AsO_4)_2$, hereafter *Phase I* and *Phase II*, respectively (Pinto et al., 2015a). Crystal structures of these compounds are built up by a combination of strongly bonded Bi-O structural units and isolated $(SO_4)^{2-}$ tetrahedra. Owing to the stereoactivity of Bi^{3+} lone electron pairs, coordination environments of Bi atoms are generally distorted and asymmetrical with three or four closest oxygens (distances < 2.5 Å) on one side against farer oxygens on the opposite side. Taking into account the short bonds only, the most usual Bi coordinations in these compounds are trigonal bipyramidal BiO_4e or distorted tetrahedral BiO_3e (*e* = lone electron pair). However, the crystal structures of these compounds can be more suitably described in term of structural units based upon oxo-centred polyhedra. In particular, extended one-dimensional Bi-O units of fluorite-like structure can be observed in the crystal structures of leguernite, *Phase I* and *Phase II*. They are formed by chains of edge-sharing oxo-centred OBi_4 tetrahedra condensed to adjacent chains by sharing edge, so forming ribbons with different section in each structure: 3 x 2 cross section in leguernite, shifted 2 x 4 cross section in *Phase I* and alternation of the latter motif with a 5 x 3 cross section ribbon in *Phase II* (Pinto et al., 2015a). Nearly planar trapezoidal units formed by OBi_3 coordinations are instead observed in baličžunicite (Pinto et al., 2015b). In these structures bonds between O_a and Bi are generally shorter than bonds between sulfate oxygens (O_T) and Bi, and bond-valence sums show expected values if parameters provided by Krivovichev (2012) are used for Bi-O_a bonds. In analogy to OCu_4 tetrahedra in other fumarolic systems, the presence of oxocentered O-Bi units in the structures of these minerals provides indirect evidence for the possible presence of oxocentered O-Bi complexes in volcanic gaseous steam. Due to the general reducing conditions of fumaroles at Vulcano, we suppose that the oxygen involved in the formation of O-Bi complexes could be provided by local processes of atmospheric contamination of volcanic gas phase.

Garavelli A., Pinto D., Mitolo, D., Bindi, L. (2014): Leguernite, $Bi_{12.67}O_{14}(SO_4)_5$, a new Bi-oxysulfate from the fumarole deposit of "La Fossa" crater, Vulcano, Aeolian Islands, Italy. *Mineral. Mag.*, **78**, 1629–1645.

Krivovichev, S.V. (2012): Derivation of bond-valence parameters for some cation-oxygen pairs on the basis of empirical relationship between r_0 and *b*. Z. *Kristallogr.*, **227**, 575-579.

Krivovichev, S.V., Mentré, O., Siidra, O.I., Colmont, M., Filatov, S.K. (2013): Anion-centered tetrahedra in inorganic compounds. *Chem. Rev.*, **113**, 6459−6535.

Pinto, D., Garavelli, A., Mitolo, D. (2014): Baličžunicite, $Bi_2O(SO_4)_2$, a new fumarole mineral from the "La Fossa" crater at Vulcano, Aeolian Islands, Italy. *Mineral. Mag.*, **78**, 1043-1055.

Pinto, D., Garavelli, A., Bindi, L. (2015a): Fluorite-related one-dimensional units in natural bismuth oxysulfates: the crystal structures of $Bi_{14}O_{16}(SO_4)_5$ and $Bi_{30}O_{33}(SO_4)_9(AsO_4)_2$. *Acta Crystallogr.*, **B71**, 514-523.

Pinto, D., Garavelli, A., Balić-Žunić, T. (2015b): The crystal structure of baličžunicite, $Bi_2O(SO_4)_2$, a new natural bismuth oxide sulfate. *Mineral. Mag.*, **79**, 597-611.

HIGH TEMPERATURE X-RAY DIFFRACTION STUDIES OF OXYGEN-DEFICIENT $Ca(Fe,Mn,Ti)O_{3-\delta}$ PEROVSKITES

Schaller A.M.*[1], Stöber S.[1] & Pöllmann H.[1]

[1] Fachgebiet Mineralogie-Geochemie, Institut für Geowissenschaften und Geographie, Martin-Luther-Universität Halle-Wittenberg, Germany

Corresponding email: stefan.stoeber@geo.uni-halle.de

Keywords: perovskite, high-temperaure X-ray diffraction, crystal structure

The aim of this study was to characterize and parametrize the structural development of oxygen-deficient $Ca(Fe,Mn,Ti)O_{3-\delta}$ perovskites as a function of composition and temperature. The phases were synthesized by the Pechini method, Stoichiometric concentrations of Ca-, Fe-, Mn - nitrate stock solutions and tetraisopropylorthotitanate were homogenized with citric acid and ethylene glycol in order to get the precursor after dehydration at 120°C. Finally, the precursor was sintered in an electric furnace at 510°C to release organic matter and at 1250°C to get the perovskite phase.

The coupled substitution $2Fe'_{Ti} + V_o^{\cdot\cdot} <=> Mn^x_{Ti} + Ti^x_{Ti}$ was applied on the orthorhombic $ABO_{3-\delta}$-type perovskite structure with space group *Pnma* (Ross et al., 2004) and solid solutions with the composition $CaFe_x(Mn_{(1-x)/2})Mn_{(1-x)/2})O_{3-\delta}$ (with x ranging from 0.08 to 0.33). Phase purity was determined by ICP/OES and microprobe analysis.

Ambient and high temperature X-ray diffraction (HT-XRD) data were collected with Mo-radiation using an PANalytical Empyrean diffractometer, equipped with an Anton Paar HTK 1200N high temperature oven chamber with capillary extension for transmission measurements and an PANalytical GaliPIX^{3D} detector between 298 to 1273 K. The obtained X-ray diffractograms were analyzed by the LeBail and Rietveld method with TOPAS-Academic (version 4.1).

The HT-XRD measurements of the $Ca(Fe,Mn,Ti)O_{3-\delta}$ perovskites allowed to study the phase transitions and associated modifications as well as the crystal structure, including cell distortions and the octahedra tilt (Glazer, 1972; Aleksandrov, 1976) along certain directions as a function of temperature.

Aleksandrov, K.S. (1976): The sequences of structural phase transitions in perovskites. *Ferroelectrics*, **14**, 801-805.

Glazer, A. (1972): The classification of tilted octahedra in perovskites. *Acta Crystallogr.*, **B28**, 3384-3392.

Ross, N.L., Zhao, J., Angel, R.J. (2004): High-pressure structural behavior of $GdAlO_3$ and $GdFeO_3$ perovskites. *J. Solid St. Chem.*, **177**, 3768-3775.

A NEW K-Nb-CYCLOSILICATE $K_2(Nb,Ti)_2(Si_4O_{12})O(O,F)$ FROM CHUKTUKON CARBONATITE MASSIF, CHADOBETS UPLAND, RUSSIA

Sharygin V.V.*[1-2], Doroshkevich A.G.[1-3], Seryotkin Y.V.[1-2], Karmanov N.S.[1], Belogub E.V.[4-5] & Moroz T.N.[1]

[1] V.S.Sobolev Institute of Geology and Mineralogy, Siberian Branch of the Russian Academy of Sciences, Novosibirsk, Russia

[2] Novosibirsk State University, Russia

[3] Geological Institute, Siberian Branch of the Russian Academy of Sciences, Ulan-Ude, Russia

[4] Institute of Mineralogy, Ural Branch of the Russian Academy of Sciences, Miass, Russia

[5] Faculty of Geology, National Research South Ural State University, Miass, Russia

Corresponding email: sharygin@igm.nsc.ru

Keywords: K-Nb-cyclosilicate, carbonatite, Chadobets upland

The Chuktukon massif is one of intrusions within the Chadobets upland,SW Siberian Platform, Krasnoyarsky krai, Russia (Lapin & Lisitsyn, 2004). The phase $K_2(Nb,Ti)_2(Si_4O_{12})(O,F)_2$ (rippite, IMA 2016-025) was discovered in metasomatically altered calciocarbonatites from boreholes. It was found in primary mineral assemblage, who also includes calcite, fluorcalciopyrochlore, Mg-F-rich mica (tainiolite or yongzhumingite), fluorapatite, fluorite, Nb-rutile, olekminskite, K-feldspar, Fe-Mn-dolomite and quartz-1. Goethite, francolite (Sr-rich carbonate-fluorapatite) and psilomelane (romanèchite ± hollandite) aggregates as well as barite, quartz-2, monazite-(Ce), parisite-(Ce), synchysite-(Ce) and Sr-Ba-hydropyrochlore are related to a stage of metasomatic (hydrothermal) alteration of carbonatites. The calcite-dolomite coexistence assumes crystallization temperature near 837°C for the primary carbonatite paragenesis.

Majority of rippite prismatic crystals are weakly zoned and show Ti-poor composition $K_2(Nb_{1.93}Ti_{0.05}Zr_{0.02})[Si_4O_{12}](O_{1.93}F_{0.07})$. Raman and IR data indicate that it is virtually free in H_2O and (OH)-groups. Rare grains may contain an outermost zone, which is enriched in Ti (+Zr) and F, up to $K_2(Nb_{1.67}Ti_{0.32}Zr_{0.01})[Si_4O_{12}](O_{1.67}F_{0.33})$. It strongly suggests the incorporation of (Ti,Zr) and F in the structure of rippite via the isomorphism $Nb^{5+} + O^{2-} \rightarrow (Ti,Zr)^{4+} + F^{1-}$. The content of a hypothetical end-member $K_2Ti_2[Si_4O_{12}]F_2$ may be up to 17 mole%.

Mineral is tetragonal: *P*4*bm*, a = 8.73885(16), c = 8.1277(2) Å, V = 620.69(2) Å^3, Z = 2. It is closely identical in the structure and cell parameters to synthetic $K_2Nb_2(Si_4O_{12})O_2$ (or $KNbSi_2O_7$) (Crosnier et al., 1992; Foster et al., 1999). Like synthetic phase, rippite has nonlinear properties. Some physical properties for rippite: colorless; hardness - 4-5 (Mohs); cleavage - (001) very perfect, (100) perfect to distinct; density (meas.) = 3.17(2) g/cm^3; density (calc.) = 3.198 g/cm^3.

Rippite belongs to cyclosilicates with the $[Si_4O_{12}]^{8-}$ single rings and seems to be in close structural relation with the labuntsovite-supergroup minerals (Chukanov et al., 2002), namely with vuoriyarvite-(K), $K_2(Nb,Ti)_2(Si_4O_{12})(O,OH)_2 \cdot 4H_2O$. But rippite-related structure seems to be a new structural type among $[Si_4O_{12}]$-cyclosilicates because of different connection of the octahedral chains and $[Si_4O_{12}]^{8-}$ rings in the above minerals.

Chukanov, N.V., Pekov, I.V., Khomyakov, A.P. (2002): Recommended nomenclature for labuntsovite-group minerals. *Eur. J. Mineral.*, **14**, 165-173.

Crosnier, M.P., Guyomard, D., Verbaere, A., Piffard, Y., Tournoux, M. (1992): The potassium niobyl cyclotetrasilicate $K_2(NbO)_2Si_4O_{12}$. *J. Solid St. Chem.*, **98**, 128-132.

Foster, M.C., Arbogast, D.J., Photinos, P., Nielson, R.M., Abrahams, S.C. (1999): $K_2(NbO)_2Si_4O_{12}$: a new ferroelectric. *J. Appl. Crystallogr.*, **32**, 421-425.

Lapin, A.V. & Lisitsyn, D.V. (2004): About mineralogical typomorphism of alkaline ultrabasic magmatites at Chadobets upland. *Otech. Geol.*, **6**, 83-92.

FROM CHEMICAL COMPOSITION TO STRUCTURE TOPOLOGY IN TITANIUM SILICATES (TS-BLOCK MINERALS)

Sokolova E.*[1] & Cámara F.[2]
[1] Department of Geological Sciences, University of Manitoba, Winnipeg, Canada
[2] Dipartimento di Scienze della Terra, Università di Torino, Italy
Corresponding email: elena_sokolova@umanitoba.ca

Keywords: Ti-disilicates, TS-block, quantitative classification

Titanium silicate minerals are common as accessory minerals in alkaline rocks. A prominent feature of such rocks is their extraordinary variety of minerals, many of which are readily soluble in water or are altered under atmospheric conditions. In a group of minerals of fixed structure topology, the relation between structure and chemical composition is well known. However, in a group of minerals of reasonable complexity in which the structure topology is related but not identical, the general relation between structure topology and chemical composition is not known. This problem is of major theoretical significance in terms of the relation between structure and chemical composition. It is simple to go from structure topology to chemical composition. However, what one wants to do is to go in the inverse direction: from chemical composition to structure topology. Here I review (a) a structural hierarchy for titanium disilicate minerals containing the TS (titanium-silicate) block, and (b) the relation between structure topology and chemical composition for those minerals (Sokolova 2006). There are forty titanium disilicate minerals that contain the TS (Titanium-Silicate) block, a central O (Octahedral) sheet and two adjacent H (Heteropolyhedral) sheets of [5-7]-coordinated polyhedra and Si_2O_7 groups. The TS block is characterized by a planar minimal cell based on translation vectors, $\mathbf{t}_1$ and $\mathbf{t}_2$, the lengths of these vectors are $\mathbf{t}_1$ ~ 5.5 and $\mathbf{t}_2$ ~ 7 Å, and $\mathbf{t}_1$ ^ $\mathbf{t}_2$ is close to 90°. The general formula of the TS block is $AP_2BP_2MH_2MO_4(Si_2O_7)_2X_{4+n}$, where MH_2 and MO_4 = cations of the H and O sheets; MH = Ti, Nb, Zr, Y, Mn, Ca + REE, Ca; MO = Ti, Zr, Nb, Fe^{3+}, Fe^{2+}, Mg, Mn, Ca, Na; AP and BP = cations at the peripheral (P) sites = Na, Ca + REE, Ca, Ba, Sr, K; X_{4+n} = anions = O, OH, F, H_2O; n = 0, 1, 1.5, 2, 4. There are three topologically distinct TS blocks based on three types of linkage of H and O sheets. In the crystal structures of TS-block minerals, TS blocks either link directly or alternate with I (intermediate) blocks. The I block consists of alkali and alkaline-earth cations, oxyanions (PO_4), (SO_4) and (CO_3), and H_2O groups. There are four groups of TS-block structures, based on the topology and stereochemistry of the TS block: Groups I, II, III and IV, where Ti (+ Nb + Zr + Fe^{3+} + Mg + Mn) = 1, 2, 3 and 4 apfu, respectively. The relation between structure topology and chemical composition in TS-block minerals allows us to assess the correctness of a TS-block structure. For example, the Ti (+ Nb + Zr + Fe3+ + Mg + Mn) sites must be always fully occupied. Examples will be given. The quantitative classification of TS-block structures into the four Groups is the key issue for prediction of structure topology of the TS block based on the content of Ti (+ Nb + Zr + Fe^{3+} + Mg + Mn) determined from the chemical analysis (Sokolova & Camara, 2013). Examples of TS-block minerals predicted and later found in Nature will be given.

Sokolova, E. (2006): From structure topology to chemical composition. I. Structural hierarchy and stereochemistry in titanium disilicate minerals. *Can. Mineral.*, **44**, 1273-1330.

Sokolova, E. & Cámara, F. (2013): From structure topology to chemical composition. XVI. New developments in the crystal chemistry and prediction of new structure topologies for titanium disilicate minerals with the TS block. *Can. Mineral.*, **51**, 861-891.

RAMAN SPECTROSCOPIC AND STRUCTURAL DATA OF A POTENTIALLY NEW MINERAL "CHLORELLESTADITE"

Środek D.*[1], Galuskina I.O.[1], Galuskin E.V.[1], Dulski M.[2-3], Kusz J.[4], Książek M.[3-4] & Gazeev V.M.[5]

[1] Faculty of Earth Sciences, University of Silesia, Sosnowiec, Poland

[2] Institute of Material Science, University of Silesia, Chorzów, Poland

[3] Silesian Center for Education and Interdisciplinary Research, Institute of Material Science, Chorzów, Poland

[4] Institute of Physics, University of Silesia, Katowice, Poland

[5] Institute of Geology of Ore Deposits, Petrography, Mineralogy and Geochemistry, Russian Academy of Sciences, Moscow, Russia

Corresponding email: srodek.dorota@gmail.com

Keywords: "chlorellestadite", crystal structure, apatite supergroup

"Chlorellestadite" with simplified ideal formula $Ca_5(SiO_4)_{1.5}(SO_4)_{1.5}Cl$, was found in altered xenolith on the north-west slope of the Shadil Khokh volcano belonging to the Kel'sky volcanic plateau in the Greater Caucasus Mountain Range in South Ossetia (Gfeller et al., 2015). It creates small (up to 40 μm), elongated, bright blue crystals in dark green zones composed mainly of Cl-bearing minerals such as chlormayenite, Cl-bearing jasmundite, "albovite" ($Ca_3(SiO_4)Cl_2$) and also spurrite and secondary low-temperature Ca-hydrosilicates. Empirical crystal chemical formula of "chlorellestadite" is the following: $Ca_{4.99}Na_{0.02}(SiO_4)_{1.51}(SO_4)_{1.49}(Cl_{0.63}OH_{0.27}F_{0.10})_{\Sigma 1.}$

The Raman spectrum of "chlorellestadite" is analogical to the others spectra of the ellestadite group minerals. The main bands are at 274 (Ca-O vibrations), 460, 625 (SiO_4^{4-} and SO_4^{2-} bending vibrations), 855, 1007, 1085, 1149 (SiO_4^{4-} and SO_4^{2-} symmetric stretching vibrations). In the 3300-3800 cm^{-1} range very weak (noise level) bands, which are associated with the vibration of hydroxyl groups, are observed.

X-ray studied "chlorellestadite" is hexagonal, space group $P6_3/m$, a = 9.6002(2), c = 6.8692 (2) Å, V = 548.27(3) $Å^3$. The arrangement of Cl, OH and F in anion column is similar as for Cl-OH apatite when Cl > OH (Hughes et al., 2016) and their large value of the anisotropic displacement parameters along c axis indicate that they are disordered in this direction.

Acknowledgements: D.Ś. is grateful for the financial support by the National Science Centre project, Preludium no. 2015/17/N/ST10/03141.

Gfeller, F., Środek, D., Kusz, J., Dulski, M., Gazeev V., Galuskina, I., Galuskin, E., Armbruster, T. (2015): Mayenite supergroup, part IV: Crystal structure and raman investigation of Al-free eltyubyuite from the Shadil-Khokh volcano, Kel' Plateau, Southern Ossetia, Russia. *Eur. J. Mineral.*, **27**, 137-143.

Hughes, J.M., Harlov D., Kelly, S.R., Rakovan, J., Wilke, M. (2016): Solid solution in the apatite OH – Cl binary system: compositional dependence of solid solution mechanisms in calcium phosphate apatites along the Cl – OH binary. *Am. Mineral.*, in press, DOI: 10.2138/am-2016-5674

POTENTIALLY NEW MINERAL $\{Ca(OH_2)_2\}[Zn_2(OH)_6]$ FROM THE HATRURIM COMPLEX, DABA - SIWAQA, JORDAN

Stasiak M.*[1], Galuskin E.V. [1], Kusz J.[2], Galuskina I.O.[1], Krzykawski T.[1], Vapnik Y.A.[3], Murashko M.[4] & Dulski M.[5]

[1] Department of Geochemistry, Mineralogy and Petrography, University of Silesia, Katowice, Poland

[2] Institute of Physics, University of Silesia, Katowice, Poland

[3] Department of Geological and Environmental Sciences, Ben-Gurion University of the Negev, Be'er Sheva, Israel

[4] Faculty of Geology, Saint Petersburg State University, Russia

[5] Silesian Center for Education and Interdisciplinary Research, Institute of Material Science, Chorzów, Poland

Corresponding email: marta.stasiak@gmail.com

Keywords: new mineral, calcium hexahydroxodizincate dehydrate, Jordan

A potentially new mineral, $\{Ca(OH_2)_2\}[Zn_2(OH)_6]$, was found in thin veins in spurrite marbles of the Daba Siwaqa area in the Hatrurim Complex, Central Jordan. It is associated with Se-bearing thaumasite, calcite and awfillite in altered parts of marls, which are surrounded by unaltered spurrite rock containing: calcite, ghelenite and minerals of srebrodolskite-brownmillerite, spinel-magnesioferrite, fluormayenite-fluorkyuygenite, fluorapatite-fluorellestadite series. Lakargiite, vorlanite, larnite, zinkite, monteponite as well as Zn, Fe, Cu and Ni sulphides occur as accessory. The transition zone between altered and unaltered marls is cuspidine enriched and rarely elbrusite and Cu, Ni, Pb selenides were found here. The new mineral forms colourless flat crystals 30-50 μm in size and aggregates up to 300 μm. The empirical formula calculated on the basis of 3 cations and 8 O *apfu* is $Ca_{0.98}Zn_{2.02}(OH)_6 \cdot 2H_2O$, but taking into consideration that H_2O groups form aquametallic complexes with Ca and $Zn(OH_4)$-tetrahedra form pyroxene chains, the following crystal chemical formula is proposed $\{Ca(OH_2)_2\}[Zn_2(OH)_6]$. Unit cell parameters were obtained by X-ray single-crystal diffraction ($P2_1/c$, a = 6.3889(8), b = 10.9692(14), c = 5.7588(8) Å; β = 101.949(14)°, V = 394.84(9)Å^3, Z = 2) and they are close to the unit cell parameters of a synthetic analogue, with the chemical formula usually written as $CaZn_2(OH)_6 \cdot 2H_2O$ (Stahl & Jacobs, 1997; Xavier et al., 2009). In $\{Ca(OH_2)_2\}[Zn_2(OH)_6]$, the Zn^{2+}-tetrahedra form corner sharing chains (pyroxene-like chains = $[Zn_2(OH)_6]^{2-}$), three-dimensionally linked by isolated Ca^{2+}-polyhedra. Ca takes part in the formation of $[Ca(OH)_4(OH_2)_2]$ aqua-complex. Hydrogen bonds in $\{Ca(OH_2)_2\}[Zn_2(OH)_6]$ are strong in aqua-complexes and relatively strong in OH groups of pyroxene-like chains, whereas the remaining OH groups are characterized by weak hydrogen bonds. Also Raman spectroscopy confirms the dual character of hydrogen bonds strength in $\{Ca(OH_2)_2\}[Zn_2(OH)_6]$. Strong bands about 3497 and 3623 cm^{-1} are related to O-H stretching vibrations in OH groups and weaker bands about 2920, 3025, 3190 cm^{-1} are related to O-H stretching vibrations in HOH and a very weak band at 1612 cm^{-1} originated from bending vibrations in HOH. 3497 and 3623 cm^{-1} bands are characteristic for the new mineral (Lin et al.,1995; Kesic et al., 2015). Furthermore the main bands in the Raman spectrum of $\{Ca(OH_2)_2\}[Zn_2(OH)_6]$ are related to vibrations in tetrahedra $Zn(OH)_4^{2-}$ (cm^{-1}): 297, 344 (n_2+n_4); 440, 449, 479 (n_1+n_3); 990 (Zn-O-Zn); 1065 (Zn-O-H) (Lin et al., 1995; Kesic et al., 2015). $\{Ca(OH_2)_2\}[Zn_2(OH)_6]$ is a low-temperature, hydrothermal mineral. Its temperature of formation is not higher than 150-200°C.

Kesic, Z., Lukic, I., Zdujic, M., Jovalekic, C., Liu, H., Skala, D. (2015): Mechanochemical synthesis of $CaO \cdot ZnO \cdot K_2CO_3$ catalyst: characterization and activity for methanolysis of sunflower oil. *Chem. Ind. Chem. Engin. Quart.*,**21**, 1-12.

Lin, T.-C., Mollah, M.Y.A., Vempati, R.K., Cocke, D.K. (1995): Synthesis and characterization of calcium hydroxyzincate using X-ray diffraction, FT-IR spectroscopy, and scanning force microscopy. *Chem. Mater.*, **7**, 1974-1978.

Stahl, R. & Jacobs, H. (1997): Zur Kristallstruktur von $CaZn_2(OH)_6 \square 2H_2O$. *Z. Anorg. Allgem. Chemie*, **623**, 1287-1289.

Xavier, C.S., Sczancoski, J.C., Cavalcante, L.S., Paiva-Santos, C.O., Varela, J.A., Longo, E., Li, M.S. (2009): A new processing method of $CaZn_2(OH)_6 \cdot 2H_2O$ powders: Photoluminescence and growth mechanism. *Solid St. Sci.*, **11**, 2173-2179.

CRYSTAL CHEMISTRY OF 3*D*-ELEMENTS BEARING TOURMALINES: CATION DISTRIBUTION - MAXIMUM CONCENTRATION - CHEMICAL DEFORMATIONS

Vereshchagin O.S.*[1], Rozhdestvenskaya I.V.[1], Frank-Kamenetskaya O.V.[1] & Zolotarev A.A.[1]
[1] Department of Crystallography, Institute of Earth Science, Saint Petersburg State University, Russia
Corresponding email: oleg-vereschagin@yandex.ru

Keywords: tourmaline, cation distribution, structural stability

Crystal chemical features of tourmalines containing trivalent (41 structure) and divalent (46 structures) 3*d* elements were analyzed on the basis of structural X-ray data. The data source was the results of original research of natural and synthetic tourmalines (Vereshchagin et al., 2014), as well as the ICSD and AMCSD databases. We evaluated concentration limits of 3*d* elements in the tourmaline structure, cation distribution over crystallographic positions and chemical deformation associated with their occurrence. It was shown that isomorphic capacity of Mg-Al tourmalines containing trivalent cations of Fe, Cr or V is limited by the ratio of non-equivalent YO_6 and ZO_6 octahedra and does not exceed ~ 7 a.p.f.u. (maximum concentration implemented in povondraite (Grice & Ercit, 1993)). Entering of divalent cations of Mn, Fe, Ni, Co or Cu to Li-Al tourmaline is limited by charge balance and concentration of the cations does not exceed 3 a.p.f.u. Results of the study of synthetic tourmalines revealed that the absence of minerals in tourmaline supergroup in which cations of Co, Cu or Ni are species-specific is not connected with structural restrictions. It was found that cations of 3*d* elements occupy not only YO_6, but ZO_6 octahedra when their concentration increases and achieves the limit (more than 1 and 1.6 a.p.f.u. for trivalent and divalent cations, respectively). The process of disordering of cations is caused by the intention to preserve the stability of the structure. Results of bond valence constrains calculations (Hawthorne, 2002) indicates that the disordering of trivalent cations of 3*d* elements in octahedral positions is due to the fact that the [3*YW*] cluster, and hence the whole structure, becomes less stable with increasing the content of 3*d* elements in the structure. The grade of disordering increases with further increasing of the concentration of 3*d* elements cations. If the content of trivalent cations is about 5-7 a.p.f.u. their distribution becomes close to the statistical. The increasing of the content of 3*d* elements cations, accompanied by their disordering leads to a reduction in the disparity of YO_6 and ZO_6 octahedra and their distortions, and in the case of trivalent cations - also in reducing the corrugation of rings of tetrahedra. The sizes of nonequivalent octahedra become almost equal in case of statistical distribution of trivalent cations 3*d* elements.

Acknowledgements: This work was supported by the SPbSU (grant 3.38.243.2015).

Grice, J.D. & Ercit, T.S. (1993): Ordering of Fe + Mg in the tourmaline crystal structure: the correct formula. *N. Jb. Miner. Abh.*, **165**, 245-266.

Hawthorne, F.C. (2002): Bond valence constraints on the chemical composition of tourmaline. *Can. Mineral.*, **40**, 789-797.

Vereshchagin, O.S., Rozhdestvenskaya, I.V., Frank-Kamenetskaya, O.V., Zolotarev, A.A. (2014): Ion substitutions and structural adjustment in Cr-bearing tourmalines. *Eur. J. Mineral.*, **26**, 309-321.

DESCRIPTION AND REFINEMENT OF ZINCOBOTRYOGEN $ZnFe^{3+}(SO_4)_2(OH)\cdot 7H_2O$, A NEW MINERAL FROM XITIESHAN LEAD-ZINC DEPOSIT, QINGHAI PROVINCE, CHINA

Yang Z.*[1], Giester G.[2], Mao Q.[1], Ma Y.[1], Zhang D.[1] & Li H.[1]
[1] Institute of Geology and Geophysics, Chinese Academy of Sciences, Beijing, China
[2] Institut für Mineralogie und Kristallographie, Universität Wien, Austria
Corresponding email: yangzhm@mail.iggcas.ac.cn

Keywords: zincobotryogen, new mineral, crystal-structure refinement

Zincobotryogen was firstly reported as a variety of botryogen from Xitieshan lead-zinc deposit, Qinghai Province, China (Tu et al., 1964). The crystal structure of zincobotryogen was determined, but without refinement of the (Zn,Mg) site populations and without hydrogen atoms locations (Yang & Fu, 1988). In the present study, using the original zincobotryoge sample the chemical analyses were performed by an electron microprobe analyzer and the crystal structure is reinvestigated. All atoms including hydrogen atoms have been located and the hydrogen bounding system is discussed. The (Zn,Mg) site population has been refined, which confirms that zincobotryogen is deserved as a mineral species. The new mineral species and its name have been approved by the Commission on New Minerals, Nomenclature and Classification, International Mineralogical Association (IMA No. 2015-107).

Zincobotryogen occurs in the oxidation zone of the Xitieshan lead-zinc deposit, Qinghai, China. The mineral is associated with pickeringite, jarosite and quartz. The mineral forms prismatic crystals, which size varies from 0.05 to 2 mm. The mineral is optically positive ($2V_{calc}$ = 54.1º), with Z ≈ *b* and X ∧ *c* = 10º. The elongation is negative. The refractive indices are n_α =1.542, n_β =1.551, n_γ =1.587. The pleochroism scheme is X = colourless, Y = light yellow, Z = yellow. Microprobe analysis gave (in wt.%): SO_3 38.04, Al_2O_3 0.04, Fe_2O_3 18.46, ZnO 13.75, MgO 1.52, MnO 1.23, H_2O 31.06 (by calculation), total 104.10. The simplified formula is $(Zn,Mg)Fe^{3+}(SO_4)_2(OH)\cdot 7H_2O$. The mineral is monoclinic, $P12_1/n1$, *a* = 10.504(2), *b* = 17.801(4), *c* = 7.1263(14) Å, and β = 100.08(3)°, *V* = 1311.9(5) $Å^3$, Z = 4, D_{calc} = 2.277 g/cm^3. The strongest lines in the powder X-ray diffraction pattern are [*d*(I)(*hkl*)]: 8.92(100)(110), 6.32(77)(-101), 5.56(23)(021), 4.08(22)(-221), 3.21(31)(231), 3.03(34)(032), 2.77(22)(042). The crystal structure was refined using 2816 unique reflections to R1(*F*) = 0.0355 and wR2(F^2) = 0.0651. The refined formula is $(Zn_{0.84}Mg_{0.16})Fe^{3+}(SO_4)_2(OH)\cdot 7H_2O$. The atomic arrangement is characterized by chains with composition $[Fe^{3+}(SO_4)_2(OH)(H_2O)]^{2-}$ and ~7 Å repeat distance running parallel to the *c* axis. The chain links to a $[MO(H_2O)_5]$ octahedron and a unshared (H_2O) molecule, and forms a larger chain building module with composition $[M^{2+}Fe^{3+}(SO_4)_2(OH)(H_2O)_6(H_2O)]$. The inter-chain module linkage involves only hydrogen bonding.

According to the chemical composition and site population, the sample of “botryogen” with a formula as $(Zn,Mn,Mg,Fe^{2+})Fe^{3+}(SO_4)_2(OH)\cdot 7H_2O$ (Zemann, 1961) from Rammelsberg mine, Germany, should be redefined as zincobotryogen.

Tu, G., Li, X., Xie, X., Yin, S. (1964): Zincobotryogen and zincocopiapite - two new varieties of sulphate minerals. *Acta Geol. Sinica*, **44**, 99-101.

Yang, H. & Fu, P. (1988): Crystal structure of zincobotryogen. *Acta Mineral. Sinica*, **8**, 1-12 (in Chinese with English abstract).

Zemann, J. (1961): Über den Botryogen vom Rammelsberg. *Fortschr. Mineral.*, **39**, 84.

AN ORDERED ARRANGEMENT FOUND IN LOCAL STRUCTURE OF PEROVSKITE-TYPE $SrCo_{1-X}Mn_XO_3$ SOLID SOLUTION: XAFS ANALYSIS AND SPIN STATE CHANGE OF Co^{4+} IONS

Yoshiasa A.*[1], Nakatsuka A.[2], Okube M.[3], Arima H.[3] & Sugiyama K.[3]
[1] Graduate School of Science and Technology, Kumamoto University, Japan
[2] Graduate School of Science and Engineering, Yamaguchi University, Japan
[3] Department of Institute for material research, Tohoku University, Japan
Corresponding email: yoshiasa@sci.kumamoto-u.ac.jp

Keywords: ordered arrangement, local structure, perovskite-type solid-solution

The octahedra in perovskite-type structure form the framework by sharing six vertexes. Oxide ion is located in the center between two cations occupying the octahedral sites. If the two atoms kind occupying the octahedral sites is different, oxide ion is shifted from the center. Three types of combination, Co-O-Co, Co-O-Mn and Mn-O-Mn, is formed in the cubic perovskite-type $SrCo_{1-x}Mn_xO_3$ solid-solution. Unique ordered arrangement is observed in the solid solution in connection with the spin state of Co^{4+} ion. The unique ordering is an arrangement to avoid the Mn-O-Mn formation as much as possible (Yoshiasa et al., 1990). We will introduce that the local ordered arrangement would occur in order to maintain the three dimensional periodicity.

The cubic perovskite-type oxides stabilize the tetravalent state of the first row transition metal ion. The Co^{4+} ion in $SrCoO_3$ is in the low spin state electron condition. $SrCoO_3$ is a ferromagnet and $SrMnO_3$ is an anti-ferromagnet. $Sr(Co,Mn)O_3$ solid-solutions are obtained by treating the corresponding oxygen-deficient phases under oxygen pressure of 130 Mpa at 573 K for 72 h. The $SrCo_{1-x}Mn_xO_3$ solid-solution is formed over whole composition range with cubic perovskite-type structure. The change from ferromagnetism to anti-ferromagnetism occurred at x = 0.333. The spin state of Co^{4+} ion changes from low to high at x = 0.333 in connection with a peculiar variation of the lattice constants in the range does not follow Vegard's law. The local structure of $SrCo_{1-x}Mn_xO_3$ was investigated in order to study the effect of replacement of Co^{4+} ions with Mn^{4+} ions on the spin state of Co^{4+} ions. XAFS measurements near the Co and Mn K-edges were made with synchrotron radiation at KEK, Japan. The accrual average Co-O or Mn-O distances in the solid-solution are determined by EXAFS method. The mean (Co,Mn)-O distances were obtained by X-ray diffraction (one-half of the lattice constant). The average Mn-O distance decreases with increase of Co^{4+} ion content in the range 0.334+ ion content. On the other hand, the average Co-O distance increases with Mn^{4+} ion content with a break at x = 0.33. The O^{2-} ion moves toward the Mn^{4+} ion and away from the Co^{4+} ion in the Co-O-Mn combination. The strength of the ligand field for the Co^{4+} ion becomes weak gradually with increase of Mn^{4+} ion content. Little change in the Mn-O distances in the range $0.0 < x < 0.33$ can be interpreted by forming little Mn-O-Mn combinations (i.e., the Co-O-Mn and Co-O-Co combinations preferentially exist).

Yoshiasa, A., Inoue, Y., Kanamaru, F., Koto, K. (1990): Local structure and spin state of Co^{4+} ions in the perovskite-type $SrCo_{1-x}Mn_xO_3$ solid-solution. *J. Solid State Chem.*, **86**, 75-81.

HYDROTALCITE-GROUP AND QUINTINITE-GROUP MINERALS: STRUCTURAL CHARACTERIZATION AND IDENTIFICATION FEATURES

Zhitova E.S.*[1-2], Krivovichev S.V.[1-3], Pekov I.V.[4] & Yakovenchuk V.N.[3]

[1] Department of Crystallography, Institute of Earth Sciences, Saint Petersburg State University, Russia

[2] Institute of Volcanology and Seismology, Far East Branch of the Russian Academy of Sciences, Petropavlovsk-Kamchatsky, Russia

[3] Nanomaterials Research Center, Kola Scientific Center of the Russian Academy of Sciences, Apatity, Russia

[4] Faculty of Geology, Moscow State University, Russia

Corresponding email: zhitova_es@mail.ru

Keywords: hydrotalcite, quintinite

The hydrotalcite supergroup (natural layered double hydroxides, LDHs) includes 42 structurally and chemically similar species with the general formula $[M^{2+}_{1-x}M^{3+}_{x}(OH)_2]^{q+}(X^{n-})_{q/n}\cdot yH_2O$, where M^{2+} = Mg, Ni, Mn, Fe, Zn, Cu, Ca; M^{3+} = Al, Fe, Cr Mn, Co; X = CO_3, OH, Cl, SO_4, $Sb(OH)_6$, $Ca(H_2O)_6$, $Na(H_2O)_6$ (Mills et al., 2012). Crystal structures of LDHs consist of edge-sharing octahedral metal hydroxide layers $[M^{2+}_{1-x}M^{3+}_{x}(OH)_2]$ alternated with interlayers formed by anionic groups, water molecules and sometimes cation complexes.

In the course of the present study, a number of minerals of the hydrotalcite (characterized by M^{2+}:M^{3+} = 3:1) and quintinite (characterized by M^{2+}:M^{3+} = 2:1) groups from more than 15 localities were investigated by single-crystal and powder *X*-ray diffraction, electron-microprobe and IR spectroscopy methods. The studied hydrotalcite-group minerals with Mg and Al as major cations were found in two polytypes, 3*R* and 2*H*, both with disordered distribution of M^{2+} and M^{3+} cations within metal-hydroxide layers. On the contrary, quintinite has a strong tendency for the formation of superstructures due to cation ordering (6*R*, 1*M* and 2*T* polytypes), although cation-disordered polytypes 3*R* and 2*H* have also been observed (Krivovichev et al., 2012; Zhitova et al., 2010).

Since hydrotalcite-group and quintinite-group minerals are often very similar in the majority of properties, their unambiguous identification is problematic. On the basis of detailed X-ray diffraction studies and analysis of literature data, we suggest identification features for the Mg-Al carbonate members of the quintinite and hydrotalcite groups on the basis of the difference in the basal *d*-values that are ~7.56 and ~7.80 Å, respectively, whereas intermediate cation ratios ($2 < M^{2+}:M^{3+} < 3$) correspond to the intermediate *d*-values. The difference in the *d*-value is explained by the increasing electrostatic interaction with the increase of the M^{3+} content in brucite-type layers (Zhitova et al., 2016). The strengths of hydrogen bonding is also reflected by the position of bands in the IR spectra.

Krivovichev, S.V., Yakovenchuk, V.N., Zhitova, E.S. (2012): Natural double layered hydroxides: structure, chemistry, and information storage capacity. *in* "Minerals as advanced materials II", S.V.Krivovichev, ed., Springer, Berlin, 87-91.

Mills, S.J., Christy, A.G., Génin, J-M.R., Kameda, T., Colombo, F. (2012): Nomenclature of the hydrotalcite supergroup: natural layered double hydroxides. *Mineral. Mag*., **76**, 1289-1336.

Zhitova, E.S., Yakovenchuk, V.N., Krivovichev, S.V., Zolotarev, A.A., Pakhomovsky, Y.A., Ivanyuk, G.Y. (2010): Crystal chemistry of natural layered double hydroxides. 3. The crystal structure of Mg,Al-disordered quintinite-2*H*. *Mineral. Mag*., **74**, 841-848.

Zhitova, E.S., Krivovichev, S.V., Pekov, I.V., Yakovenchuk, V.N., Pakhomovsky, Y.A. (2016): Correlation between the *d*-value and the M^{2+}:M^{3+} cation ratio in Mg-Al-CO_3 layered double hydroxides. *Appl Clay Sci*., in press.

HIGH-TEMPERATURE BEHAVIOR OF KUPLETSKITE-(Cs)

Zolotarev A.A.*[1], Zhitova E.S.[1], Gabdrakhmanova F.A.[1], Vladykin N.V.[2] & Krivovichev S.V.[1]
[1] Department of Crystallography, Institute of Earth Sciences, Saint Petersburg State University, Russia
[2] Vinogradov Institute of Geochemistry, Siberian Branch of the Russian Academy of Sciences, Irkutsk, Russia
Corresponding email: aazolotarev@gmail.com

Keywords: kupletskite-(Cs), thermal iron oxidation, crystal structure

Kupletskite-(Cs), $(Cs,K)_2Na(Mn,Fe^{2+})_7(Ti,Nb)_2(Si_4O_{12})_2O_2(OH)_4F$, is a member of the kupletskite group of the astrophyllite supergroup (see Sokolova et al., 2016, and references therein). The crystal structures of these minerals are based upon HOH blocks, where the O-layer consists of edge-sharing octahedra (formed by the *C* cations: cation sites M1-4) and H-layers are heteropolyhedral layers constructed from $[Si_4O_{12}]^{8-}$ astrophyllite-type ribbons and *D*-centered octahedra (DO_6). The *A* and *B* cations are located in between the HOH blocks (Woodrow, 1967; Piilonen et al., 2003a, 2003b; Cámara et al., 2010; Sokolova, 2012). Herein we present data on the high-temperature behavior of kupletskite-(Cs) and refinement of the crystal structure of the high-temperature modification (HT) of kupletskite-(Cs) from Darai-i-Pioz glacier, Tien-Shan mountains, northern Tajikistan (Yefimov et al., 1971). It has been shown previously that, upon heating, astrophyllite has a phase transition around 500°C as a result of the Fe^{2+} oxidation (Zhitova et al., 2015). Kupletskite-(Cs) is characterized by the predominance of Mn over Fe^{2+}, which makes it of interest to compare thermal behavior of minerals from the two groups. In general, the observed pattern is similar: in the region from 25 to 500°C the crystal structure is expanding, with the direction of maximal expansion perpendicular to the HOH blocks. In contrast, in the region from 525 to 800°C HT-phase experiences contraction: the *a* and *c* parameters are decreasing. The crystal structures of both initial and calcined kupletskite-(Cs) were studied by means of single-crystal X-ray diffraction. The crystal structure of the initial sample was refined to $R_1 = 0.032$ (*P*-1, *a* = 5.3904(10), *b* = 11.946(2), *c* = 11.799(2) Å, α =113.135(5), β = 94.573(6), γ = 103.115(17)°, *V* = 668.2(2) Å^3, *Z* = 1). The crystal structure of the HT phase was refined to $R_1 = 0.048$ (*P*-1, *a* = 5.312(2), *b* = 11.832(4), *c* = 11.739(5) Å, α = 112.996(10), β = 93.587(10), γ = 104.39(4)°, *V* = 647.3(5) Å^3, *Z* = 1). Analysis of the M-O bond lengths and polyhedral volumes in the HT-phase indicates considerable bond(volume)-shortering for the octahedral M2, M3 and M4 sites, which allows to interpret the observed phase transition as resulting from the oxidation of Fe^{2+} coupled with dehydroxylation that is confirmed by IR spectroscopy. Thus, the thermal behavior of kupletskite-(Cs) is similar to the thermal behavior of astrophyllite, taking into account features of the M-sites population due to the general predominance of Mn over Fe^{2+}.

Acknowledgements: A. Zolotarev is grateful to President Federation Grant for Young Candidates of Sciences (MK-3296.2015.5).

Cámara, F., Sokolova, E., Abdu, Y., Hawthorne, F.C. (2010): The crystal structures of niobophyllite, kupletskite-(Cs) and Sn-rich astrophyllite: revisions to the crystal chemistry of the astrophyllite-group minerals. *Can Mineral.*,**48**, 1-16.

Piilonen, P.C., LaLonde, A.E., McDonald, A.M., Gault, R.A., Larsen, A.O. (2003a): Insights into astrophyllite-group minerals. I. Nomenclature, composition and development of a standardized general formula. *Can Mineral.*,**41**,1-26.

Piilonen, P.C., McDonald, A.M., LaLonde, A.E. (2003b): Insights into astrophyllite-group minerals. II. Crystal chemistry. *Can Mineral.*, **41**, 27-54.

Sokolova, E. (2012): Further developments in the structure topology of the astrophyllite-group minerals. *Mineral Mag.*, **76**, 863-882.

Sokolova, E., Cámara, F., Hawthorne, F.C., Cirotti, M. (2016): The astrophyllite supergroup: nomenclature and classification. *Mineral Mag.*, in press.

Woodrow, P.J. (1967): The crystal structure of astrophyllite. *Acta Crystallogr.*, **22**, 673-678.

Yefimov, A.F., Dusmatov, V.D., Ganzeyev, A.A., Katayeva, Z.T. (1971): Cesium kupletskite, a new mineral. *Dokl. Akad. Nauk SSSR*, **197**, 140-143.

Zhitova, E.S., Krzhizhanovskaya, M.G., Krivovichev, S.V., Hawthorne, F.C., Yakovenchuk, V.N., Ivanyuk, G.U. (2015): High-temperature crystal chemistry of astrophyllite from Kola peninsula, Russia. Proc. 8th European Conference on Mineralogy and Spectroscopy, *Per. Mineral.* (spec. issue), 199-200.

Session S17:

Mineral diversity, complexity and evolution

Conveners:

Edward S. Grew (Orono – USA)

Sergey V. Krivovichev (Saint Petersburg – Russia)

GEOCHEMICAL CHARACTERISTICS OF CARBONATES FROM (Sn)-Ag-Pb-Zn DEPOSITS OF THE VERKHOYANSK FOLD-TRUST BELT (RUSSIA, SAKHA-YAKUTIA)

Anikina E.*[1], Vikent'eva O.[1], Bortnikov N.S.[1] & Gamyanin G.N.[1]

[1] Institute of Geology of Ore Deposits, Petrography, Mineralogy and Geochemistry, Russian Academy of Sciences, Moscow, Russia

Corresponding email: lena-anikina@yandex.ru

Keywords: carbonates, chemical composition, REE

The Verkhoyansk fold-trust belt, which extend along the northeast margin of the ancient Siberian platform, hosts numerous vein (Sn)-Ag-Pb-Zn deposits. The chemical composition, REE distribution and stable isotopes (C, O) in carbonates from several deposits: Kupol'noe, Mangazeyskoe, Menkeche, and Prognoz, have been studied. Multistage ore formation was recognized. Carbonates are major veins mineral and were deposited during different stages. Carbonate veins bear economically valuable minerals such as galena, sphalerite, tetrahedrite, Ag-Pb and Ag antimony sulfosalts.

Early siderite-1 (large-block), late siderite-2 (banded), ankerite and calcite were identified in the deposits. Wide compositional variations in CaO, FeO, MgO, MnO, CO_2 contents in carbonates were revealed by electron probe micro analyses (wt.%): 0-54.2, 0.7-57.2, 0.1-12.6, 0.4-22.3, 37.8-45.0, respectively, in Kupol'noe deposit; 0-29.5, 7.1-60.0, 0.1-16.7, 0.1-7.1, 35.9-45.9, respectively, in Mangazeyskoe; 0-28.4, 0-28.4, 0-28.4, 0.9-35.9, 35.9-45.9, respectively, in Menkeche, 0.0-2.1, 42.0-56.7, 0.2-7.3, 3.0-8.3, 31.5-40.3, respectively, in Prognoz. Generally, the chemical composition of carbonates in deposits studied is similar. An except is Menkeche and Kupol'noe deposits, where higher Mn contents were found. This feature is typical for the southern part of the Verkhoyansk belt.

The $\delta^{13}C$ (V-PDB) and $\delta^{18}O$ (V-SMOW) values vary from -15.0 to -9.2‰ and from +17.4 to +29.2‰, respectively, in Kupol'noe deposit, from -9.1 to -2.9‰ and +13.5 to +19.5‰ in Mangazeyskoe, from -12.5 to -5.1‰ and +13.0 to 28.8‰ in Menkeche, and from -12.1 to -3.2‰ and +9.1 to 29.8‰ in Prognoz.

The REE distribution in carbonates is controlled by crystal chemistry: their contents increase in order: siderite (0.3-13.4 ppm) – ankerite (2-238 ppm) – calcite (3.4-285.5 ppm). A positive Eu anomaly (Eu/Eu* = 1.5-9.4) is recognized in all carbonates.

An increase of the La/Yb ratio from early to late generations is possibly correlated with a *p*H decrease in hydrothermal fluids. The positive Eu anomaly assumes the REE remobilization by high-temperature (> 200°C) fluids depleted CO_3^{2-} and deposition of carbonates at low temperature (< 200°C).

Mineral-forming fluids were predominantly magmatic in the origin. The estimated $\delta^{13}C_{CO2}$ values of the fluid (from -18.4 to -8.5‰) suggest a change carbon isotope composition during the fluid phase separation due to a removal of the gas phase or a depletion of the heavy C isotope resulted from a deposition of carbonates.

Acknowledgements: The study was supported by the Russian Academy of Sciences, Program of Fundamental Research A 72-2.

EVOLUTION OF ORE MINERAL ASSOCIATIONS IN SOME ORE-FORMING SYSTEMS: LOCAL AND GENERAL REGULARITIES, APPLIED QUESTIONS

Avgustinchik I.*[1]

[1] Department of Market Conditions, Central Research Institute of Geological Prospecting for Base and Precious Metals, Moscow, Russia

Corresponding email: iavgust39@mail.ru

Keywords: magmatic ore-forming systems, mineral diversity

Processes and products of mineral evolution in ore-forming systems (OFS) provide new mineralogical information due to input of time parameter in the analysis of data on minerals, their chemical and crystal structure, properties, emergence, location and further transformations on Earth and other planetary bodies. New judgement of changes in mineral variety, structural complexity and their ensembles provides existential system approach to quantitative interpretation of the OFS chemical and mineral associations. This one of the perspective new field of mineralogy draws considerable interest and attention to itself. Specifics of each OFS define several fundamental factors: 1. element diversity and the cation and ligand budget in the local space of system generation; 2. system evolution duration as a developing nonlinear system with its evolution etaps, bifurcations (catastrophes), development peak, recession and death in the generation space and at chamber stage, that defines its opportunities and differentiation results; 3. compatible and incompatible ore-forming element properties in system; the first are spent during early mineral phases crystallization, the second are collected as part of the final products of system evolution. Empirical data have revealed the widest ranks of elements and their minerals in the ore and magmatic systems which have undergone deep differentiation at chamber stages of their development (Cr-Ti-V-Cu-Ni-Co-PGE-Ag-Au, Sn and sulphide-Sn, a.o.) unlike the systems with substance differentiation in the generation space (the most of Au ore systems). Incompatible elements (Sb, Bi, Te, Se, Ge, Ag, Au, et al.) and their mineral associations collect at final stages of “system life” and are clues to system type, scale, life duration and economic potential. These fundamental properties of compatible and incompatible elements reflect in classes, types and structures of ore minerals, which associations consistently form and change or replace to each other in system. The wide range of modern mineralogical and geochemical research methods allows to define the place and role of the majority of these elements and minerals at various time spans (etaps and stages) of OFS development. On examples of some Cr-Ti-V-Cu-Ni-Co-PGE-Ag-Au, Cu-Mo-W-Ag-Au porphyry, Sn and sulphide-cassiterite, Au-Ag, Sb-Bi-Te-Se-Au and actually gold OFS the same of incompatible ore elements and their minerals time evolution is shown. The use of revealed regularities in the applied forecasting purpose is considered.

LIGHT-INDUCED ALTERATION OF ALACRANITE, As_8S_9

Bonazzi P.*[1] & Bindi L.[1]
[1] Dipartimento di Scienze della Terra, Università di Firenze, Italy
Corresponding email: paola.bonazzi@unifi.it

Keywords: arsenic sulfides, light-induced alteration, crystal structure

A new sample coming from the As-sulfide bearing-sandstones of Lăzăreşti, Ciomadu volcanic area, Romania, was found to be rich of alacranite, having a diffraction quality higher than that previously described for that locality (Kristály et al., 2006). Several single crystals were checked by means X-ray single-crystal diffraction: the unit-cell parameters were found to match roughly those of the alacranite from type locality (Bonazzi et al., 2003), with unit-cell volumes ranging from about 849 to 861 Å^3; noteworthy, the smaller the unit-cell volumes the higher was the diffraction quality. Thus, a crystal (A1) suitable for the whole intensity data collection and light exposure experiments was selected on this basis [V = 849(1) Å^3]. The structure refinement (R1 = 8.25%) fully confirmed the model previously obtained for alacranite from Uzon Caldera. In spite of the smaller volume of the unit-cell, all the sulfur positions were found to be fully occupied. It was then supposed that larger volumes could correspond to initial steps of light-induced alteration, which in molecular As-sulfides usually produces an increase of the unit-cell volume due to the replacing of As_4S_4 (r-type) molecules by As_4S_4 (p-type) (Bonazzi et al., 2011; Zoppi et al., 2013) and As_4S_5 (Bonazzi et al., 2006).Thus, the effect of the light exposure on the structure of alacranite, was investigated using either 550 nm or the 440 nm long-wavelength pass filter (LWPF). The action of the light filtered using a 550 nm LWPF did not produce any significant effect on the unit-cell, thus confirming what previously observed for alacranite from the type locality (Bonazzi et al., 2006). On the other hand, employing the 440 nm LWPF, remarkable variations of the unit-cell parameters were observed, producing and increase of the unit-cell volume of 2.7% after 1520 min of lightening. In particular, the *a* and *c* parameters strongly increase, while *b* and the β angle decrease as a function of the light exposure time. After 1520 min, a new diffraction experiment (with a CCD-equipped instrument) indicated that alacranite transformed in an orthorhombic phase (space group *Pccn*), identical to that already obtained by the light-induced alteration of a non-stoichiometric As_4S_{4+x} crystal (Bindi & Bonazzi, 2007). To follow the ongoing of the transformation path, a second crystal [A2; V = 850(8) Å^3] was exposed to the 440 nm LWPF light for 900 min. However, when the crystal was examined by X-ray, it was already completely transformed in the orthorhombic phase. The subsequent structure refinement (R1 = 12.05%) confirmed the model previously obtained (Bindi & Bonazzi, 2007) and led to the chemical formula $As_4S_{4.93}$.

Finally, another crystal was selected [A3; V = 850(7) Å^3] and exposed to the 440 nm LWPF light for 600 min. At this step the unit-cell volume was V = 870(8) Å^3 and the structure refinement (R1 = 9.18%) indicated a $C2/c$ disordered phase wherein different kind of As_4S_n molecules replace each to other.

Bindi, L. & Bonazzi, P. (2007): Light-induced alteration of arsenic sulfides: A new product with an orthorhombic crystal structure. *Am. Mineral.*, **92**, 617-620.

Bonazzi, P., Bindi, L., Popova, V., Pratesi, G., Menchetti, S. (2003): Alacranite, As_8S_9: Structural study of the holotype and re-assignment of the original chemical formula. *Am. Mineral.*, **88**, 1796-1800.

Bonazzi, P., Bindi, L., Pratesi, G., Menchetti, S. (2006): Light-induced changes in molecular arsenic sulfides: state of the art and new evidence by single-crystal X-ray diffraction. *Am. Mineral.*, **91**, 1323-1330.

Bonazzi, P., Bindi, L., Muniz Miranda, M., Chelazzi, L., Rödl, T., Pfitzner, A. (2011): Light-induced molecular change in synthetic $HgI_2 \cdot As_4S_4$: evidence by single-crystal X-ray diffraction and Raman spectroscopy. *Am. Mineral.*, **96**, 646-653.

Kristály, F., Szakáll, S., Bonazzi, P., Bindi, L., Papucs, A. (2006): Neogen volcanism related arsenic sulphide paragenesis from Lazaresti and Bodoc (Ciomadu Area, Harghita Mts.), and Covasna. *Rom. J. Mineral Deposits and Rom. J. Mineral.*, **82**, 192-195.

Zoppi, M., Bindi, L., Rödl, T., Pfitzner, A., Bonazzi, P. (2013): Light-induced structural changes in $(HgBr_2)_3(As_4S_4)_2$: An X-ray single-crystal diffraction, Raman spectroscopy and *ab initio* study. *Solid State Sci.*, **23**, 88-95.

COMPLEXITY OF URANYL MINERALS: A STRUCTURAL HIERARCHY APPROACH

Burns P.C.*[1] & Lussier A.J.[1]
[1] Department of Civil and Environmental Engineering, University of Notre Dame, IN, USA
Corresponding email: pburns@nd.edu

Keywords: uranyl minerals, structural hierarchy

Many new uranyl minerals have been discovered and described over the past decade, mostly owing to the systematic study of samples from previously recognized localities. Uranyl minerals exhibit a vast array of structures. About 20 of these consist of sheet structural units that contain only uranyl bipyramids, with low valence cations and water in the interlayers. Many more also contain sheets that arise from the linkage of uranyl bipyramids with various oxyanions, including silicate, phosphate, arsenate, sulfate, etc. To a lesser extent, uranyl polyhedra also link with oxyanions to form chains, finite clusters, and frameworks in a few cases. Previously structural hierarchies of uranyl minerals have relied upon graphical descriptions and the topological arrangement of anions within sheets. Here we will emphasize the many newly discovered uranyl minerals and how they challenge existing ideas concerning structural hierarchies, with appropriate reference to synthetic materials.

WHAT DO WE MEAN BY "CHALCOPHILICITY" AND "SIDEROPHILICITY" IN THE CRUST?

Christy A.G.*[1]
[1] Research School of Earth Sciences, Australian National University, Canberra, Australia
Corresponding email: andrew.christy@anu.edu.au

Keywords: chalcophile, siderophile, mineral diversity

Goldschmidt (1937) classified elements as "siderophile", "chalcophile" or "lithophile" depending on their distribution within the Earth. These characteristics were defined in the context of planetary formation, to represent partitioning behaviour between metal, sulfide and silicate melts under conditions of high temperature and pressure and a whole-planet bulk composition with high iron but very low oxygen content. Goldschmidt himself pointed out that the geochemical preferences were dependent on pressure, temperature and bulk composition. The vast majority of the Earth's 5000 mineral species form in low-temperature, low-pressure, oxygen-rich conditions near the surface. Hence, while Goldschmidt's terms are often used to describe elements whose primary crustal minerals are intermetallic compounds and alloys ("siderophile"), of the sulfide anion class ("chalcophile"), or oxycompounds ("lithophile"), this is not strictly valid.

The abundances of the chemical elements in the crust of the Earth vary by ten orders of magnitude. One manifestation of this is the number of mineral species in which a given element is an essential component, which varies with atomic abundance in an approximate 0.3 power law relationship. However, it is clear that some elements form considerably more mineral species than predicted; these are all elements which show distinctive stereochemistry, and as a result do not readily enter solid solution in minerals of more abundant elements (Christy, 2015). Their unusual bonding preferences make them generally "incompatible", and readily concentrated from the mantle upward through the crust, resulting in local anomalies of otherwise rare elements that further increase the count of mineral species, as well as being of vital economic importance as ore deposits. The majority of anomalously diverse elements are those classed by Goldschmidt as "chalcophile" or "siderophile".

Observations of mineral occurrence and distribution between anion classes can be used to create an empirical but pedagogically useful "chalcophilicity scale", which makes it evident that the geochemical behaviour of some elements, such as iron, is very different under present crustal conditions from what it was in the differentiating early Earth. A thermodynamic approach can be used to quantify element preferences as coordinates in a two-dimensional parameter space. The coordinates are free energies for model reactions between elements, oxides and sulfides that represent metal nobility under variously oxygen-absent or sulphur-absent conditions, and capture the bulk composition-dependent reordering of native metal stability proposed by Burns & Fyfe (1966). Alternative axes can be chosen that correlate more closely with (i) the empirical crustal "oxyphile"-"metallophile" sequence and (ii) electronegativity or Pearson hardness. Such quantification should ultimately prove useful in refining estimates of numbers and distribution of new mineral species.

Burns, R.G. & Fyfe, W.S. (1966): Distribution of elements in geological processes. *Chem. Geol.*, **1**, 49-56.
Christy, A.G. (2015): Causes of anomalous mineralogical diversity in the Periodic Table. *Mineral. Mag*., **79**, 33-49.
Goldschmidt, V. M.(1937): The principles of distribution of chemical elements in minerals and rocks. *J. Chem. Soc*., **1937**, 655-672.

COMPOSITIONAL EVOLUTION IN PYROXENES OF THE PERALKALINE NEPHELINE SYENITE (KOLA PENINSULA, RUSSIA)

Filina M.*[1] & Kogarko L.[1]
[1] Department of Geochemistry, Vernadsky Institute of Geochemistry and Analytical Chemistry, Russian Academy of Sciences, Moscow, Russia
Corresponding email: makimm@mail.ru

Keywords: evolution of alkaline clinopyroxenes, alkaline magmatism, Kola alkaline province

Pyroxenes from peralkaline nepheline syenites of the Niva intrusion and peralkaline dyke (Akimenko et al., 2014; Arzamastsev et al., 2000) has been investigated. This massif and dyke are located in the northwestern part of the Belomorian mobile belt (Kola Peninsula, Russia). Among the major minerals of the syenites are nepheline (10-15 vol%), orthoclase (15-20 vol%), lamprophyllite group minerals (15-20 vol%), titanian aegirine-augite (10-15 vol%), aenigmatite (10-15 vol%), alkaline amphibole (5-10 vol%), natrolite (5-10 vol%), and astrophyllite (up to 5 vol%).

Pyroxenes, form small (0.5-1.3 mm), needle-like or prismatic crystals, often zoned with green-yellow core and green rim, there is a weak pleochroism. Investigated pyroxenes belong to diopside-hedenbergite-aegirine series, typical for peralkaline rock. The central part of the crystal composition correspond to augite, marginal parts aegirine-augite sometimes almost completely corresponds aegirine composition. Most pyroxene grains are zoned, from the core to the rim increases the contents of sodium, iron and titanium, and a decrease of the content of magnesium and calcium. Pyroxenes contain titanium up to 6.05 wt.% TiO_2 in the marginal parts of the crystal, titanium is present in the pyroxene in the form of $NaTiSiAlO_6$, and partly in the form neptunite $Na_2FeTiSi_4O_{12}$ (Ferguson et al., 1977), the presence of the neptunite molecule can be confirmed Na-Ti apfu positive correlation.

To estimate the evolution of pyroxenes we used Na-Mg parameter Stevenson (Stephenson, 1972), the main trend of the pyroxene evolution is increase Ti-aegirine (Na, Fe^{3+}) component and decrease diopside (Ca, Mg) and hedenbergite (Ca, Fe^{2+}) components. Contents of Al and Mn shows a slight variations. We investigated the distribution of rare earth and trace elements in the pyroxenes by secondary ion mass spectrometer. Investigated pyroxenes are slightly enriched by light rare earths.

Investigated pyroxene are similar in chemical composition to the pyroxene of the Khibiny and Lovozero alkaline massifs (Kogarko et al., 2016; Yakovenchuk et al., 2008), they show a continuous evolution towards aegirine components, while the pyroxene of Ilimaussaq alkaline massif (Larsen, 1976; Marks & Markl, 2001) especially in early evolution stage shows growth hedenbergite component and increase aegirine component at the later stage. We suggest that this difference depends on oxygen fugacity in the alkaline magmatic systems.

Acknowledgements: This study was supported by the grant RSF 15-17-30019.

Akimenko, M.I., Kogarko, L.N., Sorokhtina, N.V., Kononkova, N.N., Mamontov, V.P. (2014): A new occurrence of alkaline magmatism on the Kola peninsula: An agpaitic dyke in the Kandalaksha region. *Dokl. Earth Sci.*, **458**, 1125-1128.

Arzamastsev, A.A., Belyatsky, B.V., Arzamastseva, L.V. (2000): Agpaitic magmatism in northeastern Baltic Shield: A study of the Niva intrusion, Kola Peninsula, Russia. *Lithos*, **51**, 27-46.

Ferguson, A.K. (1977): The natural occurrence of aegirine-neptunite solid solution. *Contrib. Mineral. Petrol.*, **60**, 247-253.

Kogarko, L.N., Williams, C.T., Wooley, A.R. (2006): Compositional evolution and cryptic variation in pyroxenes of the peralkaline Lovozero intrusion, Kola Peninsula, Russia. *Mineral. Mag.*, **70**, 347-359.

Larsen, L.M. (1976): Clinopyroxenes and coexisting mafic minerals from the alkaline Ilimaussaq intrusion, South Greenland. *J. Petrol.*, **17**, 258-290.

Marks, M. & Markl, G. (2001): Fractionation and assimilation processes in the alkaline augite syenite unite of the Ilimaussaq intrusion, South Greenland, as dedused from phase eguilibria. *J. Petrol.*, **10**, 1947-1969.

Stephenson, D. (1972): Alkali clinopyroxenes from nepheline syenites of the South Qoroq Centre, South Greenland. *Lithos*, **5**, 187-201.

Yakovenchuk, V.N., Ivanyuk, G.Y., Pakhomovsky, Y.A., Menshikov, Y.P., Konoplev, N.G., Korczak, Y. (2008): Pyroxenes Khibiny alkaline massif (Kola Peninsula, Russia). *Russian Notes Mineral. Soc.*, **2**, 96-113.

PALEOPROTEROZOIC BUDDINGTONITE FORMATION IN A PSEUDOMORPH AFTER BERYL – AN EXAMPLE OF EARLY ORGANIC-IGNEOUS INTERACTION IN THE EARTH'S HISTORY

Franz G.*[1], Khomenko V.[2], Nissen J.[3], Wirth R.[4] & Vyshnevskyi O.[2]
[1] Fachgebiet Mineralogie-Petrologie, Technische Universität Berlin, Germany
[2] National Academy of Sciences, Kiev, Ukraine
[3] Zentraleinrichtung Elektronenmikroskopie, Technische Universität Berlin, Germany
[4] Chemie und Physik der Geomaterialien, Helmholtz Zentrum Potsdam, GFZ Deutsches GeoForschungsZentrum, Potsdam, Germany
Corresponding email: gerhard.franz@tu-berlin.de

Keywords: buddingtonite, organic matter, Paleoproterozoic

Buddingtonite commonly forms in hydrothermal deposits via interaction of NH_4-bearing fluids of biogenic origin, and therefore most localities are known from Phanerozoic rocks. We investigated a deposit of gem quality topaz, beryl and morion quartz in the Nb-Y-F chamber pegmatites from Volodarsk-Volynskii, Zhytomyr Oblast in NW Ukraine. The pegmatites are genetically and spatially connected with rapakivi-like differentiated granites of the gabbro-anorthosite Korosten pluton with an intrusion age of 1.8-1.76 Ga. To our knowledge this is the oldest reported locality of buddingtonite formation, which occurs in a breccia in a pseudomorph after beryl.

The breccia formation is considered as a late-stage event after cooling of the pegmatite to T ≤ 200°C, possibly due to fluid overpressure of the large miarolitic chambers with a volume of 40 m^3, in extreme cases up to 250 m^3. The pseudomorph after beryl is situated in a matrix of opal-chalcedony with small fragments of albite, alkali-feldspar and quartz, and consists of a rim rich in bertrandite, an inner zone of dominantly buddingtonite + F-bearing muscovite + opal ± betrandite ± euclase ± organic matter ± Ta-oxide ± REE-minerals, with a core of Fe-rich muscovite + smectite ± chlorite. Buddingtonite solid solutions of NH_4-K-H_3O occur as euhedral, platy crystals with typical sector zoning and as fibrous crystals, replacing alkalifeldspar. F-bearing muscovite has a minor tobelite component. Opal has variable H_2O contents as indicated by BSE images, and abundant nm-sized inclusions of Fe-Ba-REE-Th-U-Y-S-P-minerals. FTIR-investigations show that its brown staining is due to C-H-O compounds. Organic matter has a conspicuous pattern in BSE, due to different degrees of condensation. Most-condensed parts have a high content of O, Zr, Si, Y, Sc, U, Th. C (and N, present in small amounts) are negatively correlated with O. Organic matter was also identified in fluid inclusions in healed cracks of gem-quality beryl from Volyn, indicating the infiltration of organic matter into the pegmatite within the stability field of beryl (≥ approximately 250°C), and before formation of the pseudomorph.

Buddingtonite formation requires a high concentration of NH_4 in a fluid and is therefore only possible in Earth history, once enough organic matter is present. We propose a model for the evolution of the pegmatite and the buddingtonite formation, which starts with pegmatite intrusion into a near-surface environment rich in organic matter. Hydrothermal convection cells mobilized organic matter, mixed it with the igneous fluid and incorporated it into the pegmatite, concentrating HFSE and REE in the organic matter, and causing the breakdown of beryl to buddingtonite+bertrandite. During further cooling, the chambers were destroyed, the high amount of Si precipitated as opal, and F-muscovite partly transformed into tobelite. Such a scenario is only possible once significant biogenic activity in the Precambrian occurred, in this case in the late Paleoproterozoic.

TERRESTRIAL MERRILLITE

Galuskina I.O. *[1], Galuskin E.V.[1] & Vapnik Y.A.[2]
[1] Faculty of Earth Sciences, University of Silesia, Sosnowiec, Poland
[2] Department of Geological and Environmental Sciences, Ben-Gurion University of the Negev, Beer-Sheva, Israel
Corresponding email: irina.galuskina@us.edu.pl

Keywords: merrillite, whitlockite, Hatrurim Complex

Altered breccia-like rocks, in which phosphates of the merrillite type were revealed, occurs at locality close to the Ye'elim Mt., Negev Desert, Israel. Rocks which belong to the Hatrurim Complex are represented by angular brick-red and orange fragments 0.1-10 cm in size and hematite balls, which are cemented by white-grey mineral aggregates being a mixture of calcite, barite, zeolites and Ca-hydrosilicates. In orange and brick-red fragments grains of wollastonite, aegirine-diopside, andradite, apatite, plagioclase are identified, embedded in aggregates of secondary Ca-hydrosilicates, hydrogarnets and zeolites. Minerals of the merrillite are confined to brick-red fragments, where forms intergrowths with apatite. Two minerals with similar composition and structure are currently known: extraterrestrial merrillite $NaMgCa_9(PO_4)_7$ and terrestrial whitlockite $MgCa_9(PO_4)_6(PO_3OH)$. Three types of merrillite are described in meteorites and lunar rocks, which *de facto* are different mineral species. All three types were revealed in rocks at the Ye'elim Mt. Merrillite of the I type: $Mg(Y_{0.35}La_{0.14}Nd_{0.13}Ce_{0.09}Pr_{0.03}Sm_{0.02})_{S0.76}Ca_{8.36}[(PO_4)_{6.92}(SiO_4)_{0.04}(SO_4)_{0.04}]_{\Sigma 7}$, was detected as inclusions in apatite. In a Raman spectrum of this merrillite one strong band $v_1(PO_4)$ about 975 cm^{-1} and shoulder near 965 cm^{-1} were noted, what is characteristic for REE-merrillite (Jolliff et al., 2006). Two other types of merrillite: $Na_{0.97}Mg_{0.96}K_{0.03}Sr_{0.02}La_{0.01}Y_{0.04}Ca_{8.95}(PO_4)_{6.97}(SiO_4)_{0.01}(SO_4)_{0.03}$ (II type) and $Na_{0.3}Mg_{1.0}Ca_{9.35}(PO_4)_7$ (III type) form both separate grains and intergrowths with apatite. Their Raman spectra show two strong lines $v_1(PO_4)^{3-}$ vibrations: 961 and 975 cm^{-1} and 957 and 972 cm^{-1}, respectively. Such character of Raman spectra with $v_1(PO_4)^{3-}$ band dublet is typical for merrillite and whitlockite with low concentration of REE (Jolliff et al., 2006). Band near 923 c m^{-1} is characteristic for whitlockite and probably is related to vibrations in $(PO_3OH)^{2-}$ (Jolliff et al., 2006), this band is absent in merrillite spectra from Israel. Empirical formula of I type of merrillite can be simplified to $Mg(Y,REE)_{0.76}Ca_{8.36}(PO_4)_7$, what gives an end-member formula $\square MgYCa_8(PO_4)_7$. Merrillite of II and III types will be answered to the end-member formulae: $NaMgCa_9(PO_4)_7$ and $\square MgCa_{9.5}(PO_4)_7$, respectively. Merrillite from pyrometamorphic rocks of Israel has extraterrestrial analogue: $NaMgCa_9(PO_4)_7$ – Suizhou meteorite (Xie et al., 2015); $\square MgREECa_8(PO_4)_7$ – Apollo 14 lunar rock (Hughes et al., 2006); $\square MgCa_{9.5}(PO_4)_7$ – Angra dos Reis achondrite (Dowty, 1977). Our results point out that considering the problems of mineral diversity in Earth and interplanetary space, it is necessary to take into attention both exploration degree of defined mineralogical objects and formal requirements of distinguishing the mineral species.

Acknowledgements: Investigations were partially supported by the National Sciences Centre (NCN) of Poland by decision no. 2013/11/B/ST10/00272 (I.G. and E.G.).

Dowty, E. (1977): Phosphate in Angra dos Reis: structure and composition of the $Ca_3(PO_4)$ minerals. *Earth Planet. Sci. Letters*, **35**, 347-351.

Hughes, J.M., Jolliff, B.L., Gunter, M.E. (2006): The atomic arrangement of merrillite from the Fra Mauro Formation, Apollo 14 lunar mission: The first structure of merrillite from the Moon. *Am. Mineral*., **91**, 1547-1552.

Jolliff, B.L., Hughes, J.M., Freeman, J.J., Zeigler, R.A. (2006): Crystal chemistry of lunar merrillite and comparison to other meteoritic and planetary suites of whitlockite and merrillite. *Am. Mineral*., **91**, 1583-1595.

Xie, X., Yang, H., Gu, X., Downs, R.T. (2015): Chemical composition and crystal structure of merrillite from the Suizhou meteorite. Am. Mineral.,**100**, 2753-2756.

FLUOR-ELBAITE, LEPIDOLITE AND Ta-Nn OXIDES FROM A PEGMATITE OF THE 3000 Ma SINCENI PLUTON, SWAZILAND: EVIDENCE FOR LITHIUM-CESIUM-TANTALUM (LCT) PEGMATITES IN THE MESOARCHEAN

Grew E.S.*[1], Bosi F.[2], Gunter M.E.[3], Hålenius U.[4], Trumbull R.B.[5] & Yates M.G.[1]
[1] School of Earth and Climate Sciences, University of Maine, Orono, ME, USA
[2] Dipartimento di Scienze della Terra, Sapienza Università di Roma, Italy
[3] Department of Geological Sciences, University of Idaho, Moscow, ID, USA
[4] Department of Geosciences, Swedish Museum of Natural History, Stockholm, Sweden
[5] Helmholtz Zentrum Potsdam, GFZ Deutsches GeoForschungsZentrum, Potsdam, Germany
Corresponding email: esgrew@maine.edu

Keywords: LCT pegmatite, Archean, tourmaline

In their reviews of the temporal distribution of rare-metal pegmatites, Tkachev (2011) and McCauley & Bradley (2014) reported that the oldest pegmatites to contain beryl and minerals of Li, Sn and Ta are found in the Barberton greenstone belt and neighboring Swaziland, and are dated at 2990-3113 Ma. Among these are granitic pegmatites associated with the S-type Sinceni pluton dated at 3074 Ma (Trumbull, 1993; 1995a, 1995b; Maphalala & Kröner, 1993). Many pegmatites in this region contain minor beryl and cassiterite mineralization, but are otherwise not chemically specialized. An exception in the Sinceni field is a Li-rich pegmatite near Zishineni (Trumbull et al., 1993). We present detailed mineralogical data for fluor-elbaite, lepidolite and complex Ta-Nb oxides from this pegmatite and show that it is one of the earliest known examples of the LCT family (Černý & Ercit, 2005). Zishineni elbaite forms green crystals up to 5 cm long. Spindle stage measurements give ω = 1.652(1), ε =1.627(1) (589.3 nm). Optical absorption spectroscopy shows Fe and Mn are divalent; infra-red spectroscopy demonstrates the presence of Li and indicates the presence of (OH) at both the (OH) sites. Electron microprobe analysis of the largest prism, which is zoned in Fe and Ca, and several smaller grains in two analytical sessions gives the following ranges: SiO_2 36.4-37.7, Al_2O_3 37.7-39.4, FeO 1.1-3.3, MnO 3.1-3.9, Na_2O 2.4-2.7, CaO 0.2-1.1, F 1.5-1.9 wt.%. The formula calculated for 6 Si and 9 (*Y*+*Z*) site occupancy from the grand average for one session is: $(Na_{0.77}Ca_{0.13}K_{0.01}\square_{0.09})(Li_{0.94}Fe_{0.33}Mn_{0.49}Al_{1.23}Ti_{0.01})Al_6Si_6O_{18}(BO_3)_3[(OH)_{2.65}O_{0.35})](F_{0.92}OH_{0.08})$. The formula is consistent with infrared evidence for (OH) at two sites. Crystal-structure refinement (*R*1 for 1454 reflections ~ 2%) yields site populations in good agreement with this formula in terms of bond distances and site scatterings. However, the refinement gives a bond valence sum for the O3 site indicating (OH) = 3 apfu. Micas include lepidolite in flakes several millimeters across that are veined and overgrown by fine-grained muscovite. Silica and (FeO+MnO) increase, and Al decreases with F, all giving tight linear fits for both micas taken together, implying both micas can be regarded as mixtures of muscovite and a lithium mica consisting of 55 mole% polylithionite, 35 mole% masutomilite (Fe ≈ Mn) and 10% trilithionite. Muscovite and lepidolite contain 1.1 and 1.5-2.1 wt.% Rb_2O and < 0.2 wt.% and 0.7-2.2 wt.% Cs_2O, respectively. Other minerals include spessartine (e.g., $Sps_{93}Alm_4Grs_3$) in scattered grains up to 0.5 mm across and monazite. Oxides occur sparsely in muscovite, rarely in lepidolite, as grains up to 11 μm long, including fluorcalciomicrolite with Ca > Na and Ta >> Nb, and oxides rich in Mn, Nb and Ta (Nb > Ta); Mn, W, Ta and Nb; or Pb and Ta. The oxides, together with the muscovite, are interpreted to be related to later hydrothermal reworking of the primary lepidolite−fluor-elbaite assemblage.

Černý, P & Ercit, T.S. (2005): The classification of granitic pegmatites revisited. *Can. Mineral*., **43**, 2005-2026.

Maphalala, R.M. & Kröner, A. (1993): Pb-Pb single zircon ages for the younger Archean granitoids of Swaziland, Southern Africa. *in* "16th Colloquium African Geology", R. Maphalala & M. Mabuza, eds., Geol. Survey Mines Dept., Mbabane, abstr., 201-206.

McCauley, A. & Bradley, D.C. (2014): The global age distribution of granitic pegmatites. *Can. Mineral*., **52**, 183-190.

Tkachev, A.V. (2011): Evolution of metallogeny of granitic pegmatites associated with orogens throughout geological time. *in* "Granite-related ore deposits", A.N. Sial, J.S. Bettencourt, C.P. de Campos, P. Ferreira, Valderez, eds., *Geol. Soc. London Spec. Publ.*, **350**, 7-23.

Trumbull, R.B. (1993): A petrological and Rb–Sr isotopic study of an early Archean fertile granite–pegmatite system: the Sinceni Pluton in Swaziland. *Precamb. Res*., **61**, 89-116.

Trumbull, R.B. (1995a): A fluid inclusion study of the Sinceni rare-element pegmatites of Swaziland. *Mineral. Petrol*., **55**, 85-102.

Trumbull, R.B. (1995b): Tin mineralization in the Archean Sinceni rare element pegmatite field, Kaapvaal craton, Swaziland. *Econ. Geol*., **90**, 648-657.

EVOLUTION OF STRUCTURAL TOPOLOGY *VS*. CHEMICAL COMPOSITION IN MIXED URANYL SULFATE-SELENATES

Gurzhiy V.V.*[1], Tyumentseva O.S.[1] & Krivovichev S.V.[1]
[1] Department of Crystallography, Saint Petersburg State University, Russia
Corresponding email: vladgeo17@mail.ru

Keywords: uranyl sulfate, uranyl selenate, crystal structure

Uranium compounds containing oxoanions of hexavalent cations (S, Mo, Cr, Se) are of special importance from the environmental and mineralogical points of view. It is of great interest that natural and synthetic chemistry of these compounds are remarkably different. For instance, uranyl sulfate minerals do not contain any noticeable amounts of Se, and, whereas uranyl sulfates are one of the most widespread natural secondary phases, uranyl selenates are unknown as minerals, though there are seven natural uranyl selenites reported to date. It is noteworthy that there are several isotypic uranyl sulfates and selenates known, which points out to the possibility of Se^{6+} - S^{6+} substitution in minerals and synthetic compounds.

Phase formation in the aqueous systems of uranyl nitrate, sulfuric and selenic acids with addition of monovalent (Na, K, Rb) and divalent (Mg, Mn, Ni) cations has been investigated. During synthetic experiments, a number of phases have been detected, including those with novel structural topologies unprecedented among inorganic oxysalts. Single-crystal X-ray diffraction analysis, topological considerations and information-based complexity calculations (Krivovichev et al., 2014) demonstrated some interesting implications for mineralogy and explorative inorganic chemistry of uranium: the absence of a continuous solid solution in the systems and the absence of isotypic sulfate and selenate phases.

For instance, four different types of crystalline phases with variable S and Se contents were isolated from the system with K^+ cations. The phases obtained are based upon uranyl sulf(selen)ate layers with different topologies. The tetrahedral sites are occupied by both S and Se with pronounced preference of Se for the tridentate TO_4 tetrahedra. The most remarkable is the compound $K_3(H_5O_2)(H_3O)_2[(UO_2)_5(SeO_4)_{5.3}(SO_4)_{2.7}(H_2O)](H_2O)_z$ that contains a novel type of heteropolyhedral layers with the U:T ratio equal to 5:8. The layers are strongly modulated with the large identity period of 57.399 Å. The phase was found in very small amount (as few crystals only) and has an unusually high structural complexity (7.119 bits/atom and 1979.066 bits/cell), which points out at its possible transitional or even metastable character. It has been recently observed that very complex structures with giant periods may form as transitional architectures between phases with relatively small structural information amounts (Aliev et al., 2014). In general, our study reveals a rather complicated evolution of the structure and composition of crystalline phases in the system under consideration depending upon the changing Se:S ratio. There are "stable" regions of phase formation with moderately complex structures that are separated by transitional states with explosive fluctuations of structural complexity measured as a Shannon information.

Acknowledgements: This work was supported by St. Petersburg State University (3.38.136.2014) and President of Russian Federation grant for young scientists (no. MK-6209.2016.5). The XRD studies have been performed at the X-ray Diffraction Centre of St. Petersburg State University.

Aliev, A., Kovrugin, V.M., Colmont, M., Terryn, C., Huvé, M., Krivovichev, S.V., Siidra, O.I., Mentré, O. (2014): Revised bismuth chloroselenite system: evidence of a noncentrosymmmetric structure with a giant unit cell. *Cryst. Growth Des*., **14**, 3026-3034.

Krivovichev, S.V. (2014): Which inorganic structures are the most complex? *Angew. Chem. Int. Ed*., **53**, 654-661.

SILICATE MINERALS AND THE STRUCTURAL HIERARCHY HYPOTHESIS: SHEET SILICATES

Hawthorne F.C.*[1]
[1] Department of Geological Sciences, University of Manitoba, Winnipeg, Canada
Corresponding email: frank_hawthorne@umanitoba.ca

Keywords: structure hierarchy, sheet silicates

The structure hierarchy hypothesis states that crystal structures may be ordered hierarchically according to the polymerization of coordination polyhedra of higher bond valence (Hawthorne, 2014). A mathematical hierarchy is an ordered set of elements where the ordering reflects a natural hierarchical relation between the elements. A structure hierarchy may be defined as "a classification of atomic arrangements arranged (ranked) according to their principal constituent cation-polyhedra and the connectivity of those polyhedra". Structural hierarchies have been developed for sulfates, phosphates, arsenates, borates, beryllates, uranyl minerals, aluminofluorides and oxo-centered structures, but conspicuously absent from this list are the silicate minerals *sensu lato*, presumably because of the sheer number of silicate minerals. Here I will discuss a general approach to this issue and specifically discuss the sheet-silicate minerals. Hawthorne (2015) discussed the structures of sheet silicates in terms of n-connected plane nets ($2 < n \leq 4$) and showed how such nets can be combined with various oikodoméic operations (topological building operations) to generate sheet-silicate (*sensu lato*) structures, the formulae of which are related to the oikodoméic operations used to build the silicate part of the structure. We may build on this approach by arranging sheet-silicate structures into a hierarchy of increasing degree of complication of the constituent nets and their associated oikodoméic operations. The principal divisions within the sheet silicates are the generally accepted single-, double- and triple-sheet structures (Liebau, 1985). Within these groups, we may organize sheet structures in increasing complexity of their parent nets. Structures based on simple 3-connected nets have the stoichiometry $[T_{2n}\Phi_{5n}]$ (Φ = unspecified anion). Oikodoméic operations produce nets with vertices and nets of different connectivity, giving rise to a range of stoichiometries for the silicate sheets. Single sheets range from $[T\Phi_{2.80}]$ to $[T\Phi_{2.33}]$ and double sheets range from $[T\Phi_{2.70}]$ to $[T\Phi_{2.00}]$, with significant stoichiometric overlap with looped chain and ribbon stoichiometries at $[T\Phi_{2.80}]$ to $[T\Phi_{2.50}]$, and complete stoichiometric overlap with frameworks and interrupted frameworks at $[T\Phi]$ to $[T\Phi_{2.00}]$. I will examine the relation between the degree of complication, stoichiometry, complexity of the silicate unit and the complexity of the complete structure, as Bowen's reaction series suggests that a more detailed examination of these parameters as a function of paragenesis may be worthwhile.

Hawthorne, F.C. (2014): The structure hierarchy hypothesis. *Mineral. Mag.*, **78**, 957-1027.

Hawthorne, F.C. (2015): Generating functions for stoichiometry and structure of single-and double-layer sheet-silicates. *Mineral. Mag.*, **79**, 1675-1709.

Liebau, F. (1985): Structural chemistry of silicates. Springer, Berlin, 347 p.

ON THE MINERALOGY OF THE "ANTHROPOCENE EPOCH"

Hazen R.H.*[1], Grew E.S.[2], Origlieri M.[3] & Downs R.T.[3]
[1] Geophysical Laboratory, Carnegie Institution for Science, Washington, DC, USA
[2] School of Earth and Climate Science, University of Maine, Orono, ME, USA
[3] Department of Geosciences, University of Arizona, Tucson, AZ, USA
Corresponding email: rhazen@ciw.edu

Keywords: mineral evolution, urbanization, deforestation

The "Anthropocene Epoch" has been proposed as a new post-Holocene geological time interval – a period characterized by the pervasive impact of human activities on the geological record. Prior to the influence of human technologies, the diversity and distribution of minerals at or near Earth's surface arose through physical, chemical, and/or biological processes. Since the advent of human mining and manufacturing, particularly since the industrial revolution of the mid-eighteenth century, mineral-like compounds have experienced a punctuation event in diversity and distribution, owing to the pervasive impact of human activities. A variety of anthropogenic mineral-like compounds, as well as alterations in mineral distributions in the near-surface environment, are likely to be preserved as distinctive stratigraphic markers far into the future. We review the nature and extent of these impacts and consider their possible influence on Earth's mineral evolution. We focus on two aspects of what might be termed "Anthropocene mineralogy" – the distinctive changes, most notably increases in the diversity and changes in the near-surface distribution of minerals and mineral-like phases, associated with human activities. First, we consider mineral diversity by exploring several different types of human-mediated mineralogy and proposing a taxonomy for these phases. We catalog two broad types of human-mediated mineral-like compounds: (1) phases from the more than 5000 approved IMA mineral species that occur exclusively or predominantly as an inadvertent consequence of human activities, and (2) examples of synthetic mineral-like phases, many of which are not known to occur naturally. Second, we consider how human activities have altered the distribution of naturally occurring minerals in Earth's near-surface environment, most notably through large-scale movements of rocks and sediments as a consequence of mining operations and the construction of cities and roads. We conclude by returning to the important question: if one were to revisit Earth in tens of millions of years, what stratigraphic evidence might be preserved in the form of the modified diversity and distribution of minerals and mineral-like compounds to provide unambiguous markers for Earth's "Anthropocene Epoch"?

RECENT ADVANCES IN MINERAL EVOLUTION AND MINERAL ECOLOGY

Hazen R.M.*[1], Hystad G.[2], Golden J.J.[3], Hummer D.R.[1], Liu C.[1], Downs R.T.[3], Morrison S.M.[3], Grew E.S.[4] & Krivovichev S.V.[5]

[1] Geophysical Laboratory, Carnegie Institution for Science, Washington, DC, USA

[2] Department of Mathematics, Computer Science, and Statistics, Purdue University Calumet, Hammond, IN, USA

[3] Department of Geosciences, University of Arizona, Tucson, AZ, USA

[4] School of Earth and Climate Science, University of Maine, Orono, ME, USA

[5] Department of Crystallography, Saint Petersburg State University, Russia

Corresponding email: rhazen@ciw.edu

Keywords: mineral ecology, mineral evolution, philosophy of mineralogy

Large databases of mineral species (rruff.info/ima) and their localities (e.g., mindat.org) provide resources to investigate the diversity and distribution of mineral species on Earth. Studies in "mineral evolution" examine the expanding repertoire of minerals through 4.5 billion years of planetary history. We find striking correlations of mineralization, structural complexity, and species diversification with tectonic processes, the oxygenation of the atmosphere, the formation of continents, and the rise of the terrestrial biosphere (Hazen et al., 2008, 2012; Golden et al., 2013; Hazen, 2013; Grew & Hazen, 2014; Grew et al., 2016). Different classes of minerals (e.g., carbonates, sulfides, oxide spinels), as well as subsets of minerals incorporating selected chemical elements (e.g., C, Co, Cr, Cu, Hg, Mn, Mo, U), display distinctive episodicity over the past 3 billion years, as well as features that underscore the co-evolution of the geosphere and biosphere.

Mineral evolution research has led to a new approach, called "mineral ecology," that considers the frequency distribution of mineral species on Earth. Mineral frequency distributions are analogous to the occurrence of words in a book: a few words are common, but most words are rare and used only once or twice in a given text. Most mineral species, similarly, are rare, with more than half of the >5100 IMA approved species known from 5 or fewer localities (Hazen & Ausubel 2016). Minerals thus conform to a Large Number of Rare Events (LNRE) distribution – a statistical model that facilitates the determination of "accumulation curves", which are widely used in ecosystem research to estimate total biodiversity (Hystad et al., 2015a, 2015b; Hazen et al., 2015a, 2015b, 2016). We employ LNRE models to estimate total mineral diversity. More than 1500 mineral species exist on Earth but have yet to be discovered and described.

We will present our latest results, with an emphasis on minerals of the first-row transition elements, which play significant roles in biochemistry as well as geochemistry.

Golden, J., McMillan, M., Downs, R.T., Hystad, G., Goldstein, I., Stein, H.J., Zimmerman, A., Sverjensky, D.A., Armstrong, J.T., Hazen, R.M. (2013): Rhenium variations in molybdenite (MoS_2): Evidence for progressive subsurface oxidation. *Earth Planet. Sci. Lett*ers, **366**, 1-5.

Grew, E.S. & Hazen, R.M. (2014): Beryllium mineral evolution. *Am. Mineral*., **99**, 999-1021.

Grew, E.S., Krivovichev, S.V., Hazen, R.M., Hystad, G. (2016): Evolution of structural complexity in boron minerals. *Can. Mineral*., in press.

Hazen, R.M. (2013): Paleomineralogy of the Hadean Eon: A preliminary species list. *Am. J. Sci*., **313**, 807-843.

Hazen, R.M. & Ausubel, J. (2016): On the nature and significance of rarity in mineralogy. *Am. Mineral*., in press, DOI: 10.2138/am-2016-5601.

Hazen, R.M., Papineau, D., Bleeker, W., Downs, R.T., Ferry, J.M., McCoy, T.J., Sverjensky, D.A., Yang, H. (2008): Mineral evolution. *Am. Mineral*., **93**, 1693-1720.

Hazen, R.M., Golden, J., Downs, R.T., Hystad, G., Grew, E.S., Azzolini, D., Sverjensky, D.A. (2012): Mercury (Hg) mineral evolution: A mineralogical record of supercontinent assembly, changing ocean geochemistry, and the emerging terrestrial biosphere. *Am. Mineral*., **97**, 1013-1042.

Hazen, R.M., Grew, E.S., Downs, R.T., Golden, J.J., Hystad, G. (2015a): Mineral ecology: Chance and necessity in the mineral diversity of terrestrial planets. *Can. Mineral*., **53**, 295-323.

Hazen, R.M., Hystad, G., Downs, R.T., Golden, J.J., Pires, A.J., Grew, E.S. (2015b): Earth's "missing" minerals. *Am. Mineral*., **100**, 2344-2347.

Hazen, R.M., Hummer, D.R., Hystad, G., Downs, R.T., Golden, J.J. (2016): Carbon mineral ecology: Predicting the undiscovered minerals of carbon. *Am. Mineral*., **101**, 889-906.

Hystad, G., Downs, R.T., Hazen, R.M. (2015a): Mineral frequency distribution data conform to a LNRE model: Prediction of Earth's "missing" minerals. *Mathem. Geosci.*, **47**, 647-661.

Hystad, G., Downs, R.T., Grew, E.S., Hazen, R.M. (2015b): Statistical analysis of mineral diversity and distribution: Earth's mineralogy is unique. *Earth Planet Sci. Lett*ers, **426**, 154-157

NATURAL MEMBERS OF THE PHOSPHOHEDYPHANE – HEDYPHANE – MIMETITE SERIES

Hochleitner R.*[1], Kaliwoda M.[1] & Rewitzer C.[2]
[1] Mineralogische Staatssammlung München, Staatlichen Naturwissenschaftlichen Sammlungen Bayerns, München, Germany
[2] Furth im Wald, Germany
Corresponding email: rupert.hochleitner@lrz.uni-muenchen.de

Keywords: phosphohedyphane, hedyphane, solid solution

Phosphohedyphane is a special member of the apatite supergroup with the ideal endmember formula $Ca_2Pb_3(PO_4)_3Cl$. The new mineral was described by Kampf et al. (2006) from the Capitana mine, Atacama Province, Chile. Subsequent investigations showed that this mineral is widely distributed in lead bearing oxidation zones. A fluorine dominant phase was described by Kampf and Housley (2011) as fluorphosphohedyphane. Hedyphane is the long known arsenate analog of phosphohedyphane. It was originally described from Långban, Sweden (Breithaupt, 1830).

During the investigation of minerals from the hydrothermally overprinted oxidation zone of the Preguiça mine, Southern Portugal (Will et al., 2014) the authors found with numerous EDS analyses a series of mineral phases which proved to be members of a solid solution series between mimetite, hedyphane and phosphohedyphane.

According to Kampf et al. (2006) the P/(P+As) and the 5xCa/Ca+Pb values were calculated. Phases with 5xCa/Ca+Pb value between 1 and 3 and P/(P+As) values higher than 0.5 are phosphohedyphan or arsenian phosphohedyphan respectively, phases with 5xCa/Ca+Pb value between 1 and 3 and P/(P+As) values lower than 0.5 are hedyphane. If the 5xCa/Ca+Pb value is lower than one, the phases are mimetite and pyromorphite respectively.

The members of the phosphohedyphane-hedyphane solid solution (PHH) are found as hexagonal to needlelike white to yellow to slightly greenish crystals. They are often grown on older cerussite which is corroded and sometimes even disappeared leaving hollow pseudomorphs.

The 5xCa/Ca+Pb values vary between 1.25 and 2.5 for phosphohedyphanes, between 1 and 1.25 for hedyphanes and 0.14 and 1 for mimetites. There is a significant formation path from nearly pure mimetites to hedyphanes to phosphohedyphanes. There is a direct correlation between Ca and P content: a high 5xCa/Ca+Pb value corresponds with a high P/(P+As) and vice versa.

This suggests a formation of the members of the PHH solid solution by calcium and phosphor rich surface generated solutions whereas lead and arsenic are supplied by the earlier grown cerussite and mimetite.

This is supported by the fact that some of the phosphohedyphane crystals are largely zoned with an arsenic rich mimetite core and calcium and phosphor rich outer zones. The EDS analyses show that there is a complete solid solution between hedyphane and phosphohedyphane whereas an extension of this solid solution towards chlorapatite does not exist in nature as already suggested by Kampf et al. (2006).

Breithaupt, A. (1830): Bestimmung neuer Mineral-Specien, 2. Hedyphan. *J. Chem. Phys.*, **60**, 308-316.

Kampf, A.R. & Housley, R.M. (2011): Fluorphosphohedyphane, $Ca_2Pb_3(PO_4)_3F$, the first apatite supergroup mineral with essential Pb and F. *Am. Mineral.*, **96**, 423-429.

Kampf, A.R., Steele, I.M., Jenkins, R.A. (2006): Phosphohedyphane, $Ca_2Pb_3(PO_4)_3Cl$, the phosphate analog of hedyphane: Description and crystal structure. *Am. Mineral.*, **91**, 1909-1917.

Will, P., Friedrich, F., Hochleitner, R., Gilg, A. (2014): Fraipontite in the hydrothermally overprinted oxidation zone of the Preguiça mine, Southern Portugal. Mid-European Clay Conference, Dresden, 16-19 September 2014, abstr.

STRUCTURAL AND CHEMICAL COMPLEXITY OF MINERALS: RELATIONS AND TIME EVOLUTION

Krivovichev S.V.*[1], Krivovichev V.G.[2] & Hazen R.M.[3]
[1] Department of Crystallography, Saint Petersburg State University, Russia
[2] Department of Mineralogy, Saint Petersburg State University, Russia
[3] Geophysical Laboratory, Carnegie Institution for Science, Washington, DC, USA
Corresponding email: s.krivovichev@spbu.ru

Keywords: structural complexity, chemical complexity, Shannon information

The concept of mineral evolution has emerged recently as a new paradigm in mineralogical sciences that reflects evolution of composition and structure of non-living matter at the level of crystalline compounds (Hazen et al., 2008). Yushkin (1982) pointed out the necessity of formulation of quantitative criteria that would describe the state of mineralogical kingdom at certain stages of its time development, and both Petrov (1970) and Yushkin (1977) indicated that Shannon informational (entropy) methods can be employed to measure chemical complexity and diversity of geochemical and mineralogical systems. Krivovichev (2013) proposed to use Shannon information content to describe structural complexity of minerals and inorganic compounds and outlined basic applications of this approach to the understanding of structural evolution of minerals and mineral associations. It was also demonstrated that structural complexity parameters are directly related to configurational entropy of crystalline solids (Krivovichev, 2016).

Indeed, owing to the absence of directed functionality in mineral systems (which distinguishes them from biological forms), both structural and chemical complexity of minerals can be evaluated by means of Shannon-information-based parameters. In this study, we calculated Shannon-information complexity characteristics for all currently known and structurally characterized mineral species (based upon the IMA list of minerals and mineral formulas; only species-forming elements were taken into account).

The database of the complexity parameters for minerals was analysed for the following trends: (1) structural (per atom and per unit cell) and chemical (per atom and per formula unit) complexity *versus* number of species-forming chemical elements; (2) structural complexity *versus* chemical complexity; (3) structural and chemical complexity *versus* time, on the basis of Hazen et al. (2008) and Hazen (2013) lists of minerals for different stages of the evolution of the Universe. The results strongly indicate that: (1) chemical and structural complexity of minerals are closely related, though the relation cannot be described by a linear function; (2) chemical and structural complexity increase with time. This co-variation suggests that the major driving force for the evolution of complexity in the mineral world is the chemical differentiation of matter.

Hazen, R.M. (2013): Paleomineralogy of the Hadean eon: a preliminary species list. *Am. J. Sci*., **313**, 807-843.

Hazen, R.M., Papineau, D., Bleeker, W., Downs, R.T., Ferry, J.M., McCoy, T.J., Sverjensky, D.A., Yang, H. (2008): Mineral evolution. *Am. Mineral*., **93**, 1693-1720.

Krivovichev, S.V. (2013): Structural complexity of minerals: Information storage and processing in the mineral world. *Mineral. Mag*., **77**, 275-326.

Petrov, T.G. (1970): On the measure of complexity of geochemical systems from the viewpoint of the information theory. *Dokl. Akad. Nauk SSSR*, **191**, 924-926 (in Russian).

Yushkin, N.P. (1977): Theory and methods of mineralogy. Selected problems. Nauka, Leningrad, 291 p. (in Russian).

Yushkin, N.P. (1982): Evolutionary ideas in modern mineralogy. *Zap. Vser. Miner. Obsh*., **116**, 432-442 (in Russian).

MINERAL SYSTEM BASED ON THE NUMBER OF SPECIES-DEFINING CHEMICAL ELEMENTS IN MINERALS, THEIR TYPES, DISTRIBUTION AND MINERAL EVOLUTION OF EARTH'S CRUST

Krivovichev V.G.*[1], Charykova M.V.[2] & Krivovichev S.V.[3]
[1] Department of Mineralogy, Saint Petersburg State University, Russia
[2] Department of Geochemistry, Saint Petersburg State University, Russia
[3] Department of Crystallography, Saint Petersburg State University, Russia
Corresponding email: vkrivovi@yandex.ru

Keywords: mineral species, mineral systems, mineral diversity

Recent contributions to the studies of mineral evolution on the Earth (Hazen et al., 2008; Krivovichev, 2013) have attracted considerable attention to the problems of mineral diversity and their evolution through time. In quantitative level mineral diversity can be estimated by using the concept of the mineral systems. Any mineral can be attributed to a particular system, the components of which are the species-defining chemical elements required to construct the crystal structure of the mineral. The main rule of coding of the minerals is to determinate the sequence of chemical element's symbols which are included in their formulas. We are used the so-called "*thermochemical*" sequence of chemical elements. For example, microcline, $K(AlSi_3O_8)$, responds to the system OSiAlK, and muscovite, $KAl_2(AlSi_3O_{10})(OH)_2$, responds to the system OHSiAlK (Krivovichev & Charykova, 2013). Based on sets of essential, species-defining chemical elements in minerals, *n*-componental mineral systems are allocated (where *n* = 1, 2, 3, 4, 5, 6, 7, 8, 9, 10) for all known up to 2015 mineral species (5043). Our approach gives the only ability to correctly organize mineral species using their chemical composition and allows us to arrange the data into coherent frameworks emphasizing changes in mineral diversity and composition with time. The concept of mineral systems can be used to assess the mineral diversity of natural objects.

According to Hazen et al. (2008) we subdivided the mineral evolution of Earth into 4 partially overlapping stages, each of which saw the expansion of mineralogical diversity and/or variation in relative mineral abundances. The starting point of mineral evolution is the "ur-minerals" – the 12 earliest mineral phases to appear in the pre-solar nebulae (I), then different processes produced the chondritic meteorites, which incorporate about 60 primary mineral phases (II), and for the Hadean Eon Hazen (2013) estimated 425 mineral species (III), whereas as post-Hadean processes may be responsible for over 4500 of the more than 5000 approved mineral species (IV).

The mineral diversity can be estimated by the distribution of mineral species among the 8 (I), 24 (II), 38 (III), and 70(IV) essential mineral-forming chemical elements, and by the number of minerals (in parentheses) which depends on the number of elements in the systems (italic and bold), as follows: (I) – ***1***(3), ***2***(5), ***3***(4); (II) – ***1***(7), ***2***(21), ***3***(19), ***4***(10), ***5***(3); (III) –***1***(15), ***2***(77), ***3***(81), ***4***(111), ***5***(82), ***6***(43), ***7***(14), ***8***(2); (IV) – ***1***(44), ***2***(403), ***3***(732),***4***(1357), ***5***(1424), ***6***(643), ***7***(293), ***8***(111), ***9***(28), and ***10***(8). The mean "numbers of elements" were estimated as follows: 2.08±0.45 (I); 2.68±0.13 (II); 3.86±0.07 (III); 4.50±1.47 (IV).

In conclusion it should be emphasized that the proposed mineral systems is convenient in terms of quantitative analysis of mineral diversity.

Acknowledgements: This work was supported by Russian Federation Basic Research (grant no 16-05-00293).

Hazen, R.M. (2013): Paleomineralogy of the Hadean eon: a preliminary species list. *Am. J. Sci.*, **313**, 807-843.

Hazen, R.M., Papineau, D., Bleeker, W., Downs, R.T., Ferry, J.M., McCoy, T.J., Sverjensky, D.A., Yang, H. (2008): Mineral evolution. *Am. Mineral.*, **93**, 1693-1720.

Krivovichev, S.V. (2013): Structural complexity of minerals: information storage and processing in the mineral world. *Mineral. Mag.*, **77**, 275-326.

Krivovichev, V.G. & Charykova, M.V. (2013): Classification of mineral systems. St.-Peterburg Univ. Press, 196 p. (in Russian).

FIRST HIGH-PRESSURE SYNTHESIS OF LITHIUM-RICH TOURMALINE AND EVIDENCE FOR THE INCORPORATION OF Li AT THE *X* SITE

Kutzschbach M.[1-2], Ertl A.*[3-4], Wunder B.[1], Krstulovic M.[5], Trumbull R.B.[1] & Rocholl A.[1]

[1] Chemie und Physik der Geomaterialien, Helmholtz Zentrum Potsdam, GFZ Deutsches GeoForschungsZentrum, Potsdam, Germany

[2] Fachgebiet Mineralogie-Petrologie, Technische Universität Berlin, Germany

[3] Mineralogisch-Petrographische Abteilung, Naturhistorisches Museum, Wien, Austria

[4] Institut für Mineralogie und Kristallographie, Universität Wien, Austria

[5] Institut für Erd- und Umweltwissenschaften, Universität Potsdam, Germany

Corresponding email: andreas.ertl@a1.net

Keywords: tourmaline, crystal structure, Raman spectroscopy

The light lithophile cation lithium (Li^+) can be an important component of tourmaline, especially in chemically evolved granites and pegmatites. In the structure of tourmaline, with the general chemical formula $^{[9]}X^{[6]}Y_3{}^{[6]}Z_6(^{[4]}T_6O_{18})(^{[3]}BO_3)_3V_3W$, the Li^+ ion is assumed to exclusively occupy the large octahedral position Y to a maximum of 2 apfu Li. For the calculation of phase equilibria that involve tourmaline a reliable characterization of chemical and physical properties of end-member tourmaline is a prerequisite. However, as summarized in a review by London (2011), all attempts to synthesise Li-rich tourmaline, which is relevant for pegmatite formation conditions, have been unsuccessful.

Here, we describe the synthesis of Li-rich tourmaline at 40 kbar and 700°C in the system Li_2O-Al_2O_3-SiO_2-B_2O_3-H_2O (LASBH). The solid starting material was seed-free and consisted of a homogenous mixture of Li_2O, γ-Al_2O_3, quartz, and H_3BO_3. The solid run products after 12 days run duration comprise rossmanitic tourmaline (68 wt.%), dumortierite (28 wt.%), such as traces of spodumene (3 wt.%) and coesite (1 wt.%). Tourmaline forms idiomorphic, large prismatic crystals (30 x100 µm), which are inclusion-free and chemically unzoned.

An optimized formula, based on single-crystal X-ray structure refinement (SREF) data, on SIMS data (Li_2O: ~1.3 wt.%) and on EMP data (SiO_2, B_2O_3, Al_2O_3), results in the crystal-chemical formula: $^{X}[\square_{0.85(5)}Li_{0.15(5)}]\ ^{Y}[Al_{2.31(2)}Li_{0.69(2)}]\ ^{Z}Al_{6.00}\ ^{T}[Si_{5.38(3)}B_{0.62(3)}]\ O_{18}\ (BO_3)_3\ ^{V}(OH)_{3.00}\ ^{W}[(OH)_{0.85}O_{0.15}]$.

Remarkably, a significant amount of Li can be assigned to the *X* site. Reliable assignment of the OH-stretching vibrations in a polarized single-crystal Raman spectrum confirms the incorporation of ~0.2 Li apfu at the *X* site. This is in agreement with the SREF data that shows an electron density at the *X* site, which is equal to a similar amount of Li at this site. As derived from the SREF, the average <*X*-O> distance is significantly greater (~2.6 Å), than the <*Y*-O> distance (~2.0 Å). Therefore, Li at the *X* site is likely to have a major effect on the Li isotope fractionation between (natural) tourmaline and fluid, as the light ^{6}Li isotope prefers the longer Li-O bonds (Wunder et al., 2011).

London, D. (2011): Experimental synthesis and stability of tourmaline: a historical overview. *Can. Mineral.*, **49**, 117-136.

Wunder, B., Meixner, A., Romer, R.L., Jahn, S. (2011): Li-isotope fractionation between silicates and fluids: Pressure dependence and influence of the bonding environment. *Eur. J. Mineral.*, **23**, 333-342.

SAKHARJOK ALKALINE MASSIF: A NEW MINERALOGICAL OBJECT ON THE KOLA PENINSULA

Lyalina L.*[1] & Selivanova E.[1-2]
[1] Geological Institute, Kola Scientific Centre of the Russian Academy of Sciences, Apatity, Russia
[2] Nanomaterials Research Centre, Kola Scientific Centre of the Russian Academy of Sciences, Apatity, Russia
Corresponding email: lialina@geoksc.apatity.ru

Keywords: rare element minerals

The Kola Peninsula is notable for several unique mineralogical objects. Khibiny and Lovozero (more than 210 minerals were found here for the first time), Western Keivy alkali granites, Kovdor, Voron'i Tundras and Kolmozero pegmatites are well-known to mineralogists. All localities listed above are large geological objects with mineral deposits and unique mineral assemblage.

Sakharjok massif, located in the Southern part of Western Keivy alkali granites massif can also be included among the unique mineralogical objects. It was discovered and researched by Batieva & Bel'kov (1984). This massif is a fissure type intrusion of a small size – 7 km length and 1.5-2 km width. The Sakharjok intrusion composed of two main types of rock – nepheline syenite and alkaline syenite. Large outcrops of essexite are located within nepheline syenite. Pegmatite with a rich beryllium mineralization is developed on a contact of nepheline syenite and essexite. Complex Zr-Y-REE deposit is related with nepheline syenite.

Mineralogical researches made in the last few years allowed us to study of Sakharjok minerals on a modern day level and to establish new mineral species.

Mineralogical features of zircon - the main ore mineral - demonstrate its long multistage crystallization on magmatic, pegmatitic, postmagmatic/hydrothermal and metamorphic stages of rock formations.

Britholite group minerals are the main concentrators of the REEs in Sakharjok deposit. The wide diversity of minerals – fluorbritholite-(Ce), britholite-(Ce), fluorbritholite-(Y), fluorcalciobritholite, and also not approved species "calciobritholite" are present in rocks. The strong spatial and genetic relation between britholite and apatite with the wide isomorphism and a narrow gap between silicates and phosphates is established.

Two rare beryllium silicates – meliphanite and leucophanite are found in a large pegmatite body developed on a contact of nepheline syenite and essexite and also in micaceous rim of the same pegmatite. Coexistence of meliphanite and leucophanite and especially their intergrowth are observed for the first time. Another very rare beryllium mineral is found in this specified pegmatite – behoite.

Hainite, a rare member of rosenbuschite group minerals was found for the first time in Russia and the fifth time overall. Sakharjok hainite has a high Y content, which is unusual for a mineral and never occurred in other localities before. At the same time, new mineral species - cation-deficient analogue of hainite was found. The mineral is approved by IMA CNMNC under the name of batievaite-(Y).

Mimetite in Sakharjok has a very unusual morphology. It is represented by parallel-fibrous aggregates. The length of individual fibers (up to 1 mm) is much greater than their thickness (~ 1 μm).

Sakharjok alkaline massif is a peculiar mineralogical object, where rare and new mineral species with unusual morphology, internal structure, chemical composition and mineral associations are established.

Batieva, I.D. & Bel'kov, I.V. (1984): The Saharjok alkaline intrusion: rocks and minerals. Kola Branch, USSR. Acad. Sci., Apatity, 133 p. (in Russian).

POSTCRYSTALLIZATION EVOLUTION OF EPISTOLITE-GROUP HETEROPHYLLOSILICATES AND ROLE OF NATURAL ION EXCHANGE IN FORMATION OF NEW MINERAL SPECIES IN THIS GROUP

Lykova I.S.*[1-2], Pekov I.V.[2], Yapaskurt V.O.[2], Zubkova N.V.[2], Zolotarev A.A. Jr[3] & Giester G.[4]
[1] Fersman Mineralogical Museum, Russian Academy of Sciences, Moscow, Russia
[2] Faculty of Geology, Moscow State University, Russia
[3] Institute of Earth Sciences, Saint Petersburg State University, Russia
[4] Institut für Mineralogie und Kristallographie, Universität Wien, Austria
Corresponding email: innalykova@mail.ru

Keywords: heterophyllosilicate mineral, natural ion exchange, peralkaline rock

Natural layered titano- and niobosilicates (heterophyllosilicates) of the bafertisite series belonging to the epistolite group are typical accessory or even rock-forming minerals of some peralkaline rocks and related pegmatites (Lovozero and Khibiny, Russia; Ilìmaussaq, Denmark; Mont Saint-Hilaire, Canada). The Na-richest and H-free members of the group, namely lomonosovite, ideally $Na_{10}Ti_4(Si_2O_7)_2(PO_4)_2O_4$, and vuonnemite, ideally $Na_{11}TiNb_2(Si_2O_7)_2(PO_4)_2O_3F$, crystallize directly in magmatic or pegmatitic hyperagpaitic systems. H-bearing members of the group are products of lomonosovite or vuonnemite alteration under hydrothermal and supergene conditions. Transformations of lomonosovite into murmanite $Na_4Ti_4[Si_2O_7]_2O_4(H_2O)_4$ and vuonnemite into epistolite $Na_4TiNb_2(Si_2O_7)_2O_2(OH)_2(H_2O)_4$ by leaching of Na^+ and PO_4^{3-} ions from the interlayer space and replacing them by H_2O molecules are well known and described in detail (see Khomyakov, 1995, and references therein). The transformation of lomonosovite into betalomonosovite, ideally $Na_6Ti_4(Si_2O_7)_2[PO_3(OH)][PO_2(OH)_2]O_2(OF)$, by partial leaching of Na^+ from the interlayer space was discussed by Ageeva (1999), however the crystal chemical mechanism of this process has remained insufficiently clear due to variable chemical composition of betalomonosovite and discrepant data on its crystal structure. Another important and, until recently, unnoted mechanism of postcrystallization transformation of heterophyllosilicates is natural ion exchange. Two new zinc heterophyllosilicates, vigrishinite $NaZnNb_2Ti[Si_2O_7]_2O(OH,F)_3(H_2O)_{4+x}$ ($x < 1$) and zvyaginite $NaZnNb_2Ti[Si_2O_7]_2O(OH,F)_3(H_2O)_{4+x}$ ($x < 1$) described from a hydrothermally altered peralkaline pegmatite at Mt. Malyi Punkaruaiv (Lovozero), were formed as a result of natural cation exchange reactions of murmanite and epistolite, respectively, with low-alkaline hydrothermal solutions enriched in Zn^{2+}mobilized from dissolved earlier sphalerite. A new mineral; calciomurmanite $(Na,\square)_2Ca(Ti,Mg,Nb)_4[Si_2O_7]_2O_2(OH,O)_2(H_2O)_4$ found at Mt. Flora (Lovozero), was formed as a result of ion exchange of Na^+ for Ca^{2+} in murmanite. Our experimental data, showing that in aqueous solutions epistolite group minerals have strong cation-exchange properties toward a large series of cations, preeminently Ca and chalcophile Zn, Cu^{2+} and Ag, even under low-temperature conditions (< 100ºC), became one of the main arguments confirming ion-exchange origin of the described minerals. Postcrystallization processes may lead to splitting of some sites (P in betalomonosovite) and cation ordering (Zn-Ca in vigrishinite, Zn-Na in zvyaginite and Ca-Na in calciomurmanite) in crystal structures of heterophyllosilicates and/or to change of unit cell configuration (betalomonosovite. vigrishinite and zvyaginite in comparison with their protophases).

Acknowledgements: The work was supported by the Russian Science Foundation, grant no. 14-17-00048. The support by the SPbSU X-Ray Diffraction Resource Centre is acknowledged.

Ageeva, O.A. (1999): Typomorphism of accessory lomonosovite from rocks of the Khibiny massif. *Zap. Vser. Miner. Obsh.*, **2**, 99-104 (in Russian).

Khomyakov, A.P. (1995): Mineralogy of hyperagpaitic alkaline rocks. Clarendon, Oxford, 223 p.

OPPOSING CONCENTRATIONS OF Li AND Be IN CORDIERITE/SEKANINAITE FROM GRANITIC PEGMATITES IN THE MOLDANUBICUM; AN INDICATION OF THE DEPTH OF ANATECTIC PROCESSES?

Novák M.*[1], Gadas P.[1], Hreus S.[1], Kocáb J.[1] & Vašinová Galiová M.[2]
[1] Department of Geological Sciences, Masaryk University, Brno, Czech Republic
[2] Department of Chemistry, Masaryk University, Brno, Czech Republic
Corresponding email: mnovak@sci.muni.cz

Keywords: cordierite, sekaninaite, lithium

Cordierite-group minerals (CGM) have the general formula $^{Ch}(Na,K,Cs)_{0-1}{}^{VI}(Mg,Fe^{2+},Mn,Li)_2{}^{IV}Al_3{}^{IV}Si_5{}^{IV}(Al,Be,Mg,Fe^{2+},Fe^{3+})O_{18} \cdot x^{Ch}(H_2O,CO_2,CH_4,N_2)$ modified from Bertoldi et al. (2004). The homovalent substitution (1) Mg $(Fe^{2+}Mn)_{-1}$ is responsible for main compositional variations, whereas Li and Be are typically incorporated via the exchange vectors (2) $NaLi\,\square_{-1}(R^{2+})_{-1}$ and (3) $NaBe\,\square_{-1}Al_{-1}$ (Bertoldi et al., 2004). CGM enriched in Li and/or Be incorporated via the exchange vectors (2) and (3) are known mainly from Al-rich pegmatites and leucogranites.

CGM are typical accessory minerals in some granitic pegmatites of the Moldanubian Zone (Černý & Povondra, 1967; Černý et al., 1997). Three main paragenetic and compositional types of CGM were recognized: (i) columnar crystals of cordierite in simple anatectic pegmatites typically from migmatized gneisses and granulites (Horní Bory), (ii) small grains to large conic crystals of sekaninaite in zoned Al-rich pegmatites with abundant schorl and andalusite (Dolní Bory), and (iii) graphic intergrowths of CGM with quartz and conic crystals in more evolved beryl or elbaite pegmatites (e.g., Vìžná I). The former two occur exclusively in the territory of the Bory Granulite Massif, whereas the latter type is distributed within the Moldanubian Zone with no evident regional constrain; some pegmatites were contaminated from host serpentinite.

Based on LA-ICP-MS data (in ppm), Li-rich sekaninaite from Dolní Bory (Li = 993-2277, Be = 7-51), and Be-rich cordierite from Vìžná I (Li = 433-708, Be = 3620-5739) represent the most opposing compositions; cordierite from Horní Bory (Li = 270-388, Be = 53-315) is rather poor in both Li and Be. Lithium-enriched sekaninaite from Dolní Bory shows unique composition in CGM where Be is typical minor element and usually Be predominates over Li (see Gadas et al., 2016, for review). Also the absence of Be-bearing minerals and very low concentrations of Be in other minerals (e.g., andalusite, muscovite, tourmaline, cookeite) in the Bory pegmatite district indicates very low contents of Be. Typical feature of the rocks related to the Bory granulite massif is abundant CGM present in several paragenetic, morphological and compositional types not only in various pegmatites but also in their host migmatized gneisses and granulites. Abundance of cordierite along with typical FM minerals garnet and biotite in granulitic rocks is evident and documents significant role of MP to LP processes producing cordierite. London (2008) presents the model for derivation of beryl-bearing pegmatites when magmas are arising within the stability field of the assemblage garnet+sillimanite (beryl is common) or cordierite (beryl is rare or absent). The Bory Granulite Massif fits very well the second one. Hence, concentrations of Li and Be in CGM from granitic pegmatites may reflect melting in a shallow depth although the composition of the protolith (e.g., original Li/Be) may have played a role.

Bertoldi, C., Proyer, A., Garbe-Schönberg, D., Behrens, H., Dachs, E. (2004): Comprehensive chemical analyses of natural cordierites: implication for exchange mechanism. *Lithos*, **78**, 389-409.

Černý, P. & Povondra, P. (1967): Cordierite in West-Moravian desilicated pegmatites. *Acta Univ. Carol.*, *Geol.*, **10**, 203-221.

Černý, P., Chapman, R., Schreyer, W., Ottolini, L., Bottazzi, P., McCammon, C.A. (1997): Lithium in sekaninaite from the type locality, Dolní Bory, Czech Republic. *Can. Mineral.*, **35**, 167-173.

Gadas, P., Novák, M., Szuszkiewicz, A., Szełęg, E., Vašinová Galiová, M. (2016): Manganoan Na,Be,Li-rich sekaninaite from miarolitic pegmatite at Zimnik, Strzegom-Sobótka massif, Sudetes, Poland. *Can. Mineral.*, in press.

London, D. (2008): Pegmatites. *Can. Mineral.*, *Spec. Publ.*, **10**, 347 p.

THE CRYSTAL STRUCTURE OF GINORITE, $Ca_2B_{14}O_{20}(OH)_6(H_2O)_5$, AND THE ANALYSIS OF DIMENSIONAL REDUCTION AND STRUCTURAL COMPLEXITY IN THE CaO-B_2O_3-H_2O SYSTEM

Pankova Y.A.*[1], Krivovichev S.V.[1], Gorelova L.A.[1-2] & Pekov I.V.[3]

[1] Department of Crystallography, Institute of Earth Sciences, Saint Petersburg State University, Russia

[2] Laboratory of Structural Chemistry of Oxides, Institute of Silicate Chemistry, Russian Academy of Sciences, Saint Petersburg, Russia

[3] Department of Mineralogy, Faculty of Geology, Moscow State University, Russia

Corresponding email: y.pankova.spbu@gmail.com

Keywords: calcium borate, ginorite, crystal structure

The crystal structure of ginorite, $Ca_2B_{14}O_{20}(OH)_6(H_2O)_5$, from Chalkar salt dome, Kazakhstan, has been studied by means of single-crystal X-ray diffraction analysis at 293 and 150 K. The structure model developed for strontioginorite, $SrCaB_{14}O_{20}(OH)_6(H_2O)_5$, by Grice et al. (2005) has been used and the structure data for ginorite and strontioginorite have been compared in order to reveal rigid unit modes and "soft points" in the borate polyanion that change its geometrical parameters upon the changing temperature and chemical composition. Ginorite is monoclinic, $P2_1/a$, $Z = 4$. Refined unit-cell parameters are a 12.728(1), b 14.303(1), c 12.755(1) Å, β 101.147(2)°, V 2278.3(4) Å^3 at 293 K and a 12.728(1), b 14.240(1), c 12.750(1) Å, β 101.163(2)°, V 2268.9(4) Å^3 at 150 K. The crystal structure was refined to R indices of 0.035 and 0.034 for 10391 and 8773 unique observed reflections for 293 and 150 K, respectively.

In order to investigate the relations between structural complexity and chemical composition, twenty-seven structurally characterized phases with the general formula $(CaO)_n(B_2O_3)_m(H_2O)_p$ have been analyzed (e.g., ginorite can be described as $(CaO)_2(B_2O_3)_7(H_2O)_8$). Structural complexity parameters have been calculated using Shannon-information-based parameters derived by Krivovichev (2013, 2014). The obtained results have been visualized by constructing ternary CaO-B_2O_3-H_2O compositional diagram with the fourth dimension featuring either dimensionality of borate unit or structural and chemical complexity. The study allowed us to identify compositional regions, where most complex (=information-rich) structures in the system appear.

Grice, J.D. (2005): Strontioginorite: crystal-structure analysis and hydrogen bonding. *Can. Mineral*., **43**, 1019-1026.

Krivovichev, S.V. (2013): Structural complexity of minerals: information storage and processing in the mineral world. *Mineral. Mag*., **77**, 275-326.

Krivovichev, S.V. (2014): Which inorganic structures are the most complex? *Angew. Chem. Int. Ed*., **53**, 654-661.

THE STRUCTURAL COMPLEXITY OF URANYL-OXIDE HYDROXY-HYDRATE MINERALS: IMPLICATIONS FOR THEIR FORMATION AND OCCURRENCE

Plášil J.*[1]
[1] Institute of Physics, Academy of Sciences of the Czech Republic, Prague, Czech Republic
Corresponding email: plasil@fzu.cz

Keywords: uranyl-oxide minerals, structural complexity, mineral evolution

Uranyl-oxide hydroxy-hydrate minerals are important products formed during very initial stages of oxidation-hydration weathering of uraninite under oxidizing conditions (Finch & Ewing, 1992; Finch & Murakami, 1999; Krivovichev & Plášil, 2013; Plášil, 2014). Since they form as a result of reactions between uraninite and aqueous fluids these minerals play a key role in control of amount of U dissolved and released to the environment. Uraninite alteration is of the primary importance because of the analogy between alteration of natural uraninite and an UO_{2+x} in the spent nuclear fuel, SNF (Janeczek et al., 1996). The entire family of uranyl-oxide hydroxy-hydrate minerals is nowadays due to modern mineralogical studies a well-known mineral group (e.g., Krivovichev, 2013). There are intrinsic structural relationships as well as paragenetical relationships among this group of minerals showing apparent trends in evolution of these minerals and some links between their chemical composition, crystal structures and occurrences (e.g., Schindler & Hawthorne, 2004). Current study contributes to the knowledge of these minerals and their formation based on considerations stemming from the evaluation of structural complexities of these minerals and the bond-valence approach calculations.

Among the family of the chemically and structurally related minerals we can discern those that do not contain any mono-, di- or trivalent metal cations in the interstitial and contain only a high portion of molecular H_2O, such as schoepite, $[(UO_2)_8O_2(OH)_{12}](H_2O)_{12}$ (Finch et al., 1996). On the other hand we can found there minerals with a relatively high contents of $Me^{+,2+}$ and a low content of H_2O, as e.g., richetite, $(Fe,Mg)_xPb_{8.57}[(UO_2)_{18}O_{18}(OH)_{12}]_2(H_2O)_{41}$ (Burns, 1998), does have. From the paragenetical observations we can infer the alteration sequence, where the highly hydrated species are related to the very initial stages of alteration, while those containing higher $Me^{+,2+}$ concentrations are relatively younger compared to them. The incorporation of $Me^{+,2+}$ is connected with the rise of structural (as well as chemical) complexity of these minerals, as a record of the "incoming information" – the activity of fluids. The evolution of the uranyl-oxide minerals is in line with preliminary bond-valence calculations, showing an increasing trend in the charge-deficiency per anion (*CDA*) value.

Burns, P.C. (1998): The structure of richetite, a rare lead uranyl oxide hydrate. *Can. Mineral.*, **36**, 187-199.

Finch, R.J. & Ewing, R.C. (1992): The corrosion of uraninite under oxidizing conditions. *J. Nucl. Mater.*, **190**, 133-156.

Finch, R.J. & Murakami, T. (1999): Systematics and paragenesis of uranium minerals. *Rev. Mineral. Geochem.*, **38**, 91-179.

Finch, R.J., Cooper, M.A., Hawthorne, F.C., Ewing, R.C. (1996): The crystal structure of schoepite, $[(UO_2)_8O_2(OH)_{12}](H_2O)_{12}$. *Can. Mineral.*, **34**, 1071-1088.

Janeczek, J., Ewing, R.C., Oversby, V.M., Werme, L.O. (1996): Uraninite and UO_2 in spent nuclear fuel: a comparison. *J. Nucl. Mater.*, **238**, 121-130.

Krivovichev, S.V. (2013): Crystal chemistry of uranium oxides and minerals. *in* "Comprehensive inorganic chemistry II - Vol. 2", J. Reedijk & K. Poeppelmeier, eds., Elsevier, Oxford, 611-640.

Krivovichev, S.V. & Plášil, J. (2013): Mineralogy and crystallography of uranium. *in* "Uranium, from cradle to grave", P.C. Burns & G.E. Sigmon, eds., Mineral. Ass. Canada Short Course 43, Winnipeg, May 2013, 15-119.

Plášil, J. (2014): Oxidation–hydration weathering of uraninite: the current state-of-knowledge. *J. Geosci.*, **59**, 99-114.

Schindler, M. & Hawthorne, F.C. (2004): A bond-valence approach to the uranyl-oxide hydroxy-hydrate minerals: Chemical composition and occurrence. *Can. Mineral.*, **42**, 1601-1627.

CRYSTAL-CHEMICAL PARADIGM OF MODERN MINERALOGY. WHAT IS NEXT? ON THE ONTOGENY PARADIGM

Povarennykh M.Y.*[1]

[1] Vavilov Institute for History of Natural Science and Technology, Russian Academy of Sciences, Moscow, Russia

Corresponding email: mpovarennykh@mail.ru

Keywords: crystal-chemical and ontogenical paradigms of mineralogy

During the recent 50 years, facts and observations have been accumulated in mineralogy that are hardly compatible with the now adopted crystal-chemical paradigm. These include biopyribols, quasicrystals, irregular aperiodic and mixed-layered crystals, the presence of feedback relations between minerals and mineralogenetic environment with the elements of self-organization, the ability of minerals to accummulate, contain and inherit genetic information. The crystal-chemical paradigm cannot explain several long-recognized phenomena such as zonality and sectoriality of mineral grains, their capability to structural, morphological and chemical evolution, non-stoichiometry, metamictness, etc. At present, in mineralogy there is no unified conceptual approach to such objects as opals, coal macerals, solid bitumens (kerites), amber, etc. There has been a number of recent publications on natural carbon nanoclusters and their non-carbon analogues that, due to their dimensions, may be considered as mineral embryos or *protominerals* (Povarennykh & Matvienko, 2014). Using the Urmantsev General System Theory (Urmantsev, 1988), the author has worked out the main principles of the new mineralogical paradigm that includes the crystal-chemical paradigm as its part and suggests the following subkingdoms of the mineral kingdom: *caviclusts* (nanominerals, possessing *one or more* elementary layers), *crystals* (objects possessing *thousands* of elementary layers) and *mineraloids* (possessing one or more elementary layers connected by liquid and/or rather weak hydrogen bonds) (Povarennykh, 1988, 2000; Povarennykh & Onoprienko, 1986; Povarennykh & Matvienko, 2014). In short, we suggest the transition from the paradigm “minerals are essentially crystals or pieces of crystalline space” to the paradigm “minerals are essentially superposition of elementary layers as their surface transposition trajectories”. The idea allows one to return to the following essential notions of mineral “life”: a) “elementary layer” (more primary unit than “unit cell”), b) “growth by surface after surface”, c) “zonal and sectorial inner structure”, d) “evolution” (time axis and crystal lattice cannot be adapted by definition, and the latter does not correspond to three fundamental synergetic natural processes postulates: irreversibility, nonlinearity, and nonequilibrium), as well as including into the Mineral Kingdom subkingdoms of mineraloids and caviclusts (nanominerals) on equal terms with crystals. It will allow mineralogists to change the visual angle at the main object of their science and to come to another mineralogical*gestalt*. Comparison at the time axis of “nodal points” of Matter existence (gaseous nebula à gaseous-dust cloud à planetozimals à planet spheres à planets and evolution of the Universe elemental composition) allows to outline the general features of the “natural” mineral systematics – *Periodic System of Minerals* (Povarennykh, 1988, 2013; Povarennykh & Matvienko, 2014).

Povarennykh, M.Y. (1988): Significance of the “surface” notion while consideration of the main mineralogical object. *in* “Theory of Mineralogy”, 20-22 (in Russian).

Povarennykh, M.Y. (1990): Development of the mineral notion. *in* “The idea of evolution in geology. Matter and structural aspects”, Nauka, Novosibirsk, 92-104 (in Russian).

Povarennykh, M.Y. (1996): Fullerenes as protominerals. *Zap. Vser. Miner. Obsh.*, **5**, 97-103 (in Russian).

Povarennykh, M.Y. (2000): From the protomineral to the periodic system of minerals. System Planet Earth, Moscow State University, 63-72 (in Russian).

Povarennykh, M.Y. & Matvienko, E.N. (2014): Development of a theory of mineralogy and petrography. Theoretical-system basement of the creation of natural classification of minerals and rocks, and Periodic System of Minerals. Lambert, Saarbrucken, 117 p.

Povarennykh, M.Y. & Onoprienko, V.I. (1986): Towards the essence of the “Mineral” notion. *Geol. J.*, **46**, 53-57 (in Russian).

Urmantsev, Y.A. (1988): Evolutionics or general development theory of nature, society and thinking. Puschino, 187 p. (in Russian).

PLOTTING THE WHOLE MINERALOGICAL SYSTEM – THE CONCEPT AND THE RESULTS

Rieder M.*[1]
[1] Nanotechnology Centre, Technical University Ostrava, Czech Republic
Corresponding email: milan_rieder@jhu.edu

Keywords: mineralogical system, information entropy, hydration trend

The mineralogical system can be projected into 2*D*, either to plot physical data along the third dimension, or for the purpose of identification of unknown phases from their chemical composition (Rieder, 2014). Four pairs of variables were considered, one variable (common to all four pairs) is Shannon's (1948) information entropy - a measure of the "complexity" of the formulae. The other four are different functions of the atomic numbers of elements present in the formula. The identification capability of these projections appears promising, and plots of some scalar properties against the 2*D* base have revealed interesting tendencies.

Most of the 4975 end-member mineral formulae used in the project were taken from Ciriotti's (2012) MinData Base, and the physical data come from several sources. Physical properties plotted as a third dimension against the 2*D* base (density, mean refractive index, mean reflectance) all exhibit highest values for minerals that are composed of elements with high atomic numbers and have a simple stoichiometry (low information entropy), and lowest for minerals that are composed of light elements and have a complex stoichiometry.

The availability of atomic fractions of elements in 4975 minerals makes it straightforward to plot two or more elements against each other, across all mineral groups. The H vs. O plot reveals a dominant hydration trend, extending from an-hydrogenous phases towards the mineral ice. This trend may be related to the geological history of mineral formation on Earth. Other element pairs (O *vs*. F; O *vs*. Cl; Al *vs*. Si; O *vs.* S) confirm and/or supplement our current knowledge about their crystal-chemical behavior. The H *vs.* (Al & Si) plot should alert everyone to the possibility that his aluminosilicate mineral contains hydrogen (Rieder, 2016).

Similarly, atomic fractions available were binned to yield histograms showing concentration preferences of individual elements within the mineralogical system. Such histograms reflect all crystal-chemical roles the elements are playing, and their appearances are correspondingly diversified (H, O, S, Si, Ca).

Ciriotti, M.E. (2012): MinDataBase (CLASS & SEARCH), version 1012.01.31.

Rieder, M. (2014): The mineralogical system: 2*D* projections and their potential in mineral identification. *Eur. J. Mineral*., **26**, 703-710.

Rieder, M. (2016): The mineralogical system: Can global plots teach us something new? *Mineral. Mag.*, in press, DOI: 10.180/minmag.2016.080.012.

Shannon, C.E. (1948): A mathematical theory of communication. *Bell Syst. Tech. J*., **27**, 379-423, 623-656.

STRUCTURAL AND TOPOLOGICAL COMPLEXITY OF URANYL SELENATES

Tyumentseva O.S.*[1], Gurzhiy V.V.[1] & Krivovichev S.V.[1]
[1] Department of Crystallography, Saint Petersburg State University, Russia
Corresponding email: o-tyumentseva@mail.ru

Keywords: structural complexity, topological complexity, uranyl selenates

Uranyl selenates display an outstanding structural and chemical diversity with more than 130 pure inorganic or organically templated compounds. Crystal structures of uranyl selenates are based upon a variety of complex mineral-like units formed by polymerization of U and Se coordination polyhedra that could be classified into 40 different topological types. Most of these units are layers due to the specific coordination of U(VI) atoms that favors two-dimensional polymerization of polyhedra.

Recently, several basic principles of uranyl selenate structures formation have been reported. However, it is still not clear why some topologies are quite common, whereas others are not. Thus, it seems to be promising to introduce an additional measure such as complexity, which could shed light and provide a numerical explanation of crystallization tendencies in the uranyl selenate systems.

Herein we report on the investigation of the complexity of uranyl selenates. The aim of this research is to obtain information-based complexity parameters of structural units of particular compounds and their systematic study. The variation of the complexity between different topological groups has been considered.

It is noteworthy that the structural complexity may be higher than the topological complexity, which makes the latter more important. In addition, information-based parameters of structural complexity depend upon correct crystal structure determination, whereas topological-information content is a measure of topological complexity only.

The quantitative characteristics of structural and topological complexity were evaluated as amounts of structural and topological information per atom (I_G) and per unit cell ($I_{G,total}$) according to the formulas derived in Krivovichev (2012, 2013, 2014).

For instance, for the structures of uranyl selenate compounds based upon the $[(UO_2)(SeO_4)_2(H_2O)]^{2-}$ layers with the l1/2b topology, topological complexity parameters are I_G = 3.125 bits/atom and $I_{G,total}$ = 50.000 bits/unit cell; whereas the similar values for real structures are usually higher (e.g., for $Cs_2[(UO_2)(SeO_4)_2(H_2O)](H_2O)$: I_G = 4.000 bits/atom and $I_{G,total}$ = 128.000 bits/unit cell).

In this study, we demonstrate how complexity of uranyl selenates varies from one topology to another. Our investigation allows for a quantitative evaluation of topological and structural complexity and provides a tool to compare complexities of different types of structures. Analysis of topological and structural complexity in the uranyl selenate system indicates that both kinds of information-based complexity parameters behave in a similar fashion: the most topologically and structurally complex compounds appear to be the denser from the structural point of view. The results of the present study shows the utility of topological (ideal) complexity parameters when discussing occurrence and stability of inorganic structure types.

Acknowledgements: This work was supported by St. Petersburg State University (3.38.136.2014) and Russian Foundation for Basic Research (grant no. 16-33-60142). The XRD studies have been performed at the X-ray Diffraction Centre of St. Petersburg State University.

Krivovichev, S.V. (2012): Topological complexity of crystal structures: quantitative approach. *Acta Crystallogr.*, **A68**, 393-398.

Krivovichev, S.V. (2013): Structural complexity of minerals: information storage and processing in the mineral world. *Mineral. Mag.*, **77**, 275-326.

Krivovichev, S.V. (2014): Which inorganic structures are the most complex? *Angew. Chem. Int. Ed.*, **53**, 654-661.

EVOLUTION OF REE MINERALS

Uher P.*[1], Kohút M.[2], Ondrejka M.[1] & Konečný P.
[1] Department of Mineralogy and Petrology, Comenius University, Bratislava, Slovakia
[2] Earth Science Institute, Slovak Academy of Sciences, Bratislava, Slovakia
[3] State Geological Institute of Dionýz Štúr, Bratislava, Slovakia
Corresponding email: puher@fns.uniba.sk

Keywords: evolution of minerals, REE minerals, mineral diversity

Minerals of rare earth elements (REE, La to Lu and Y) belong to typical constituents of Earth lithosphere. They occurs mainly in continental crust, especially in uncommon lithologies, such as nepheline syenites, rare-element granitic pegmatites, some skarns, and also oxidation zone assemblages. Recently, 287 valid mineral species with REE as essential elements have been described, they occupy 5.6% of all known minerals (IMA list of minerals, March 2016). Because of relatively low concentration of REE in bulk Earth rocks and their moderate geochemical mobility, specific geological processes (such a volatile-rich magmatic fractionation) led to concentrations sufficient for their saturation and precipitation as essential REE minerals. Consequently, first REE minerals originated at least 0.6 - 0.8 Ma after accretion of Earth.

Application of the mineral evolution approach (e.g., Hazen et al., 2008; Grew & Hazen 2014) enables to recognize 5 basic stages of mineral evolution and diversification of REE species during Earth history:

(1) Hadean (4.56 to 4.0 Ga) early primitive litosphere with poor differentiation, extensive volcanism and hydrosphere evolution, probably without known essential REE minerals (possible presence of monazite and xenotime ?); REE concentrated in some minerals (e.g., hibonite, apatite, zircon).

(2) Eoarchean to Mesoarchean (4.0 to 3.1 Ga) mildly differentiated lithosphere with increased lithological contrast; first documented essential REE minerals (U-Th-Pb dating): monazite-(Ce), xenotime-(Y); possibly britholite group (?).

(3) Mesoarchean to Paleoproterozoic (3.1 to 1.8 Ga) early plate-tectonic cycles in lithosphere, connected with first production of nepheline syenites and rare-element pegmatites, rise of cyanobacteria and great oxidation event (2.4 to 2.2 Ga); new and complex REE minerals (ca. 50 to 70 species ?).

(4) Paleoproterozoic to Neoproterozoic (1.8 to 0.54 Ga) advanced lithosphere with contrasting lithology and increasing interactions with oxygen-bearing atmosphere and organisms, producing new combinations of REE minerals (e.g., REE carbonates); up to 150 REE mineral species.

(5) Phanerozoic (0.54 Ga to present) complex lithosphere with strong interactions with oxygen-rich atmosphere and biologically mediated mineralogy; main increasing of REE mineral diversity (up to 300 species), including typical oxidation, low-temperature phases (e.g., hydrous REE sulphates and oxalates).

Grew, E.S. & Hazen, R.M. (2013): Beryllium mineral evolution. *Am. Mineral.*, **99**, 999-1021.

Hazen, R.M., Papineau, D., Bleeker W., Downs, R.T., Ferry, J.M., McCoy, T.J., Sverjensky, D.A., Yang, H. (2008): Mineral evolution. *Am. Mineral.*, **93**, 1693-1720.

Session S18:

Planetary materials: from dust to planets and early Earth

Conveners:

Luigi Folco (Pisa – Italy)

Christian Koeberl (Wien – Austria)

Armin Zeh (Karlsruhe – Germany)

TRACES OF FLUIDS-APATITE CRYSTALS INTERACTIONS IN ARCHEAN BARBERTON GREENSTONE BELT

Birski L.*[1], Słaby E.[1], Wirth R.[2], Giera A.[1], Lepland A.[4-5-6] & Schreiber A.[3]
[1] Institute of Geological Sciences, Polish Academy of Sciences, Warsaw, Poland
[2] Chemie und Physik der Geomaterialien, Helmholtz Zentrum Potsdam, GFZ Deutsches GeoForschungsZentrum, Potsdam, Germany
[3] Geomechanik und Rheologie, Helmholtz Zentrum Potsdam, GFZ Deutsches GeoForschungsZentrum, Potsdam, Germany
[4] Geological Survey of Norway, Trondheim, Norway
[5] Institute of Geology, Tallinn University of Technology, Estonia
[6] Center for Arctic Gas Hydrate, Environment and Climate, Arctic University of Norway, Tromsø, Norway
Corresponding email: l.birski@twarda.pan.pl

Keywords: apatite, TEM, Barberton

It has been deduced from nature (Hansen & Harlov, 2007; Harlov et al., 2007) and from experiments (Harlov et al., 2005) that the presence of xenotime and monazite inclusions in apatite, can be treated as trace of metasomatic events in rocks. REEs are metasomatically removed from apatite and can form REE phosphates, e.g., monazite or xenotime. Additionally apatite is highly susceptible to interaction with fluids over a wide range of temperatures, pressures and environments (Harlov, 2015). It makes this mineral ideal for tracing metasomatic processes. We investigated several apatite TEM foils from Archean Barberton Greenstone Belt and Pongola Supergroup. In case of TEM foils of apatite crystals from Pongola Supergroup influence of fluid alteration is hardly visible. Only single inclusions of iron and zinc sulfides were noticed. Furthermore, a zircon inclusion was found, which indicates igneous origin of minerals. Moreover, at the phase boundaries between apatite and quartz, zones of dissolution and recrystallization, filled with amorphous silicate, and the rare mineral berlinite were observed. The occurrence of berlinite indicates rather low (200-300°C) temperature of metasomatic processes (Byrappa & Yoshimura, 2002). Apatite crystals from Barberton GB are of secondary, hydrothermal origin. A wide range of inclusions in apatite were identified in TEM foils. Apatite from carbonaceous metachert contains iron sulfide inclusions that are either elongated, with length up to ca. 500 nm and width approx. 20 nm or nano-size granular with strict orientations. Furthermore, rock porosity was noticed. Bigger pores are partially filled by inclusions, nano-sized pores frequently create pore-rich zones, commonly parallel to inclusions. Apatite from volcanoclastic sandstone does not contain any inclusions, yet micro-size pores with characteristic, connected with cracks, triangle-shape dissolution zones, which indicate the overpressure of fluids deforming semi-plastic material. Additionally, parallel and simply curved, low angle grain boundaries were observed. It might indicate deformation and recrystallization process. TEM foils of apatite from volcanoclastic sandstone apatite revealed xenotime- and monazite-inclusions rich-zones. It might indicate the primal variations of REEs concentrations in apatite. Furthermore, apatite-fluid interaction fronts were investigated. Observation of apatite from silicified tuff has revealed micro-size edge-shaped pores with dissolution zones partially filled by REE-phosphates and iron sulfide inclusions. Nano-size inclusion rich zones and channel-like structures, created by migrating fluids were noticed. Simply curved or locally straight, parallel low-angle grain boundaries are common. We managed to identify numerous inclusions and textures which indicate the conditions of metasomatic alteration. Fluid compositions were variable and fluid-apatite interaction was not equally intense in whole area of Barberton GB.

Acknowledgements: The research was funded by Polish NCN grant no. 2013/11/B/ST10/04753 and supported by the EU COST Action TD1308 “ORIGINS”.

Byrappa, K. & Yoshimura, M. (2001): Hydrothermal growth of some selected crystals. *in* ”Handbook of hydrothermal technology”, K. Byrappa, M. Yoshimura, eds., Noyes, New Jersey,198-314.

Hansen, E.C. & Harlov, D.E. (2007): Whole-rock, phosphate, and silicate compositional trends across an amphibolite- to granulite-facies transition, Tamil Nadu. *India. J. Petrol.*, **48**, 1641-1680.

Harlov, D.E. (2015): Apatite: A fingerprint for metasomatic processes. *Elements*, **11**, 171-176.

Harlov, D.E., Marshall, H.R., Hanel, M. (2007): Fluorapatite-monazite relationships in granulite-facies metapelites, Schwarzwald, southwest Germany. *Mineral. Mag.*, **71**, 223-234.

Harlov, D.E., Wirth, R., Förster, H.J. (2005): An experimental study of dissolution-reprecipitation in fluorapatite: fluid infiltration and the formation of monazite. *Contrib. Mineral. Petrol*., **150**, 268-286.

PRELIMINARY PETROLOGICAL STUDY AND GAMMA-ACTIVITY MEASUREMENTS OF SINNAI METEORITE

Bonadiman C.*[1], Cruciani G.[2], Franceschelli M.[2], Marchi M.[2], Taricco C.[3-4], Colombetti P.[3-4], Bhandari N.[5], Sinha N.[6], Rubinetti S.[3], Romero A.[4], Tassinari R.[1] & Lugari C.[1]

[1] Dipartimento di Fisica e Scienze della Terra, Università di Ferrara, Italy

[2] Dipartimento di Scienze Chimiche e Geologiche, Università di Cagliari, Italy

[3] Dipartimento di Fisica, Università di Torino, Italy

[4] Osservatorio Astrofisico di Torino, Istituto Nazionale di Astrofisica, Torino, Italy

[5] Physical Research Laboratory, Navrangpura, Ahmedabad, India

[6] Wentworth Institute of Technology, Boston, MA, USA

Corresponding email: bdc@unife.it

Keywords: ordinary chondrites, thermometry, cosmic ray activity

We report here the results of mineral and radioactivity analysis performed on Sinnai meteorite which fell near Sinnai Village (39°18' N, 9°12' E), southern Sardinia, on February 19th 1956. The meteorite sample, initially weighing about 2 kg, was crushed by impact on the ground into seven small pieces. The four biggest pieces are retained in the Mineralogical Museum of the University of Cagliari and were made available for our study. Two samples of 350 g and 351 g for measurement of cosmogenic radionuclides and a sample of 80 g for study of bulk and mineral major and trace element composition have been used in this study. As expected in the OC meteorites, the bulk elemental abundances of Sinnai are enriched relative to CI for lithophile and refractory siderophile elements (REE = 1.32 x CI; Ni = 1.38 x CI). The petrographic and mineralogical descriptions, reported by Rossetti & Sitzia (1958), allowed the first classification of the stone as H6 group of ordinary chondrite (OC). The Sinnai stone is characterized by a high abundance of chondrules up to 2 mm in size, most rounded in shape with olivine and sub calcic pyroxenes and rare plagioclase as the main silicates. Matrix abundances (20-25 vol%) is estimated higher than expected for H group of ordinary chondrites. Olivine chondrules occur as granular, skeletal, glassy poorly-devitrified and porphyritic types. The fine-grained matrix consists of olivine and Ca-poor pyroxene, rarer Ca-rich pyroxene, plagioclase, Cl-apatite and merillite. Opaque minerals consist of Fe-sulfurs, Fe-Ni alloys and rarer chromite. Olivine is highly magnesian with fayalite mole fractions in the range of 0.080-0.170; the dominant pyroxene is a low-Ca clinoenstatite to clinohyperstene in which the mole fraction of wollastonite (Wo) and ferrosilite are 0.004-0.014 and 0.142-0.650, respectively.Ca-rich pyroxene is diopside in composition with $Wo_{0.38-0.49}$. Plagioclase is oligoclase-albite ($Ab_{0.83-0.97}$) with little variation from grain to grain. Spinel is extremely variable in compositions: Al_2O_3 ranges from 9 to 50 wt.% and FeO from 11.5 to 29.7 wt.%. Olivine-spinel thermometry (Ballhaus et al., 1991) gives temperatures of 630, 810 and 1050°C; these values could reflect temperatures far from a resolved thermal metamorphism of the parent body. Two-pyroxene geothermometry (Brey & Köhler, 1990) has been applied to Ca-poor pyroxene-diopside pairs which record temperatures in the range 980-1025°C, higher than those assigned to the H6 type metamorphic grade.

The two biggest samples (of about 350 g each) were analysed by gamma-spectrometry at the underground Laboratory of Monte dei Cappuccini (OATo-INAF) in Torino, Italy, in order to reveal the activity of cosmogenic radioisotopes of the samples. The activity of a radioisotope gives information about cosmic ray flux and heliospheric magnetic field intensity roughly over a mean life of the isotope before the meteorite fall on the Earth. The cosmogenic radioisotopes ^{26}Al and ^{44}Ti were detected in both samples; while the first one averages the cosmic ray intensity over a million years and its activity is insensitive to decadal or century scale variations in cosmic ray flux, ^{44}Ti allows to draw information about centennial Gleissberg variation of solar activity. It was possible to detect the very low activity of ^{44}Ti thanks to the high-efficiency and selective gamma-ray spectrometer (HPGe-NaI) we set up at the underground laboratory in Torino (Colombetti et al., 2013). The measurements will allow confirmation of high cosmic ray intensity expected during the early 20th century (Taricco et al., 2006).

Ballhaus, C., Berry, R.F., Green, D.H. (1991) High pressure experimental calibration of the olivine–orthopyroxene–spinel oxygen geobarometer: implications for the oxidation state of the upper mantle. *Contrib. Mineral. Petrol*., **107**, 27-40.

Brey, G.P. & Köhler, T. (1990): Geothermobarometry in four-phase lherzolites II. New thermobarometers, and practical assessment of existing thermobarometers. *J. Petrol*., **31**, 1353-1378.

Colombetti, P., Taricco, C., Bhandari, N., Sinha, N., Di Martino, M., Cora, A., Vivaldo, G. (2013): Low gamma activity measurement of meteorites using HPGe–NaI detector system. *Nucl. Instrum. Meth. Phys. Res. A*, **718**, 140.

Rossetti, V. & Sitzia, R. (1958): Meteorite di Sinnai (Cagliari). *Per. Mineral.*, **1**, 179-199.

Taricco, C., Bhandari, N., Cane, D., Colombetti, P., Verma, N. (2006): Galactic cosmic ray flux decline and periodicities in the interplanetary space during the last 3 centuries revealed by ^{44}Ti in meteorites. *J. Geophys. Res.*, *Space Phys.*, **111**, A08102

VNIR REFLECTANCE OF HEDs: SPECTRAL VARIABILITY FROM POWDERS TO SLABS

Carli C.*[1], Moggi-Cecchi V.[2], Pratesi G.[2-3] & Capaccioni F.[1]
[1] Istituto di Astrofisica e Planetologia Spaziali, Istituto Nazionale di Astrofisica, Roma, Italy
[2] Museo di Storia Naturale, Università di Firenze, Italy
[3] Dipartimento di Scienze della Terra, Università di Firenze, Italy
Corresponding email: cristian.carli@iaps.inaf.it

Keywords: HED, spectroscopy, reflectance

Visible and Near-Infrared (VNIR) reflectance spectroscopy is an important technique to map mineralogy and mineralogical variations across planetary surfaces using remotely sensed data. Laboratory measurements on mineral and rocks are needed to improve the capability to recognize the different minerals. In particular, an important aspect is to understand in multi-mineral aggregates the influence of physical properties (e.g., particle size) that contribute to the spectral shape. This permits also to investigate the heterogeneity of rock samples, at the spatial resolution scale of a set-up, and to study samples, i.e., meteorites, which in several cases cannot be crushed into powders.

Meteorite spectra are used to correlate those materials with their parent bodies, one example is represented by Howardite, Eucrite and Diogenite (HED). HEDs show igneous-like characteristics (e.g. composition, texture) and display VNIR spectra revealing the two dominating pyroxenes absorptions, around 1 and 2 µm (Burns, 1993). The HED spectra are compatible with those of Vesta's asteroid family (e.g., Feierberg & Drake, 1980). Powder spectra of some HED have been measured by different authors and a linear relationship between the position of the two absorptions have been evidenced. This relationship can be qualitatively correlated with the different pyroxene presents from diogenite to eucrite. Anyway, HEDs are composed by a wide range of heterogeneous samples and only few of them can be investigated as powders. The analysis of slab's surfaces can permit to measure a wider range of samples and to investigate the heterogeneity of these samples.

Here we present VNIR spectral characteristics of several HED slabs belonging to the Museo di Storia Naturale dell'Università di Firenze. These samples have been measured using a spectrogoniometer coupled with a FieldspecPro®, with incidence angle 30° and emission angle 0°, and an illuminated spot of circa 6 mm in diameter. We considered the variability in reflectance and absorption parameters of eucrites and diogenites, and comparing these with pyroxene, plagioclase and olivine compositions. In particular, we focused our attention in the analysis of three different eucrites, with an evident variation in reflectance, and an olivine diogenite (NWA6232) characterized by an olivine clast of circa 6 mm. These four samples have been characterized as slabs and powders to deep investigate also the influence of size on spectral shape and on absorption band parameters. Moreover the presence of an olivine clast as large as the illuminated spot has been used to extrapolate the olivine relative abundance respect to the surrounding materials directly from the samples.

Burns, R.G. (1993): Mineralogical applications of crystal field theory. Cambridge Univ. Press, Cambridge, 551 p.

Feierberg, M.A. & Drake, M.J. (1980): The meteorite-asteroid connection: The infrared spectra of eucrites, shergottites, and Vesta. *Science*, **209**, 805-807.

THE METAL-RICH EUCRITE ALH 12073

Di Rocco T.*[1], Nava J.[1], Gemelli M.[1], D'Orazio M.[1], Domeneghetti M.C.[2], Alvaro M.[2], Pack A.[3] & Folco L.[1]
[1] Dipartimento di Scienze della Terra, Università di Pisa, Italy
[2] Dipartimento di Scienze della Terra e dell'Ambiente, Università di Pavia, Italy
[3] Geowissenschaftliches Zentrum, Universität Göttingen, Germany
Corresponding email: tommaso.dirocco@dst.unipi.it

Keywords: eucrites, siderophile elements, impact melt

ALH 12073 is a 500 mg meteorite fragment, partially covered by fresh fusion crust, recovered from the Near Western Allan Hills ice field, during the 2012-2013 campaign of the Italian Programma Nazionale di Ricerche in Antartide (PNRA).

In thin section, ALH 12073 shows unbrecciated, inequigranular, medium- to fine-grained subophitic texture. It maily consists of anhedral plagioclase (46 vol%) and low-Ca pyroxene (34 vol%), plus minor euhedral tridymite (7 vol%), high-Ca pyroxene (4 vol%), Fe,Ni metal (4 vol%), sulfide (3 vol%), phosphates (2 vol%) and traces of chromite.

The low-Ca pyroxene is orthopyroxene ($En_{63.1}$, $Fs_{33.9}$, $Wo_{3.1}$) with a relatively uniform composition, and average Fe/Mn ratio of 26. The plagioclase is anorthite ($An_{92.4}$, $Ab_{7.5}$, $Or_{0.2}$). The high-Ca pyroxene is augite ($En_{43.3}$, $Fs_{16.1}$, $Wo_{40.5}$). The chromite is Mg-rich with an average Mg# of 10%. The Fe, Ni metals are divided in low Ni-phase (kamacite) and high Ni-phase (taenite).

Opx-Cpx pairs provide an average equilibrium crystallization temperatures of T = 961±21°C; the closure temperature of the Fe-Mg cation ordering in three orthopyroxenes (Fs_{36}) determined through the calibration curve by Stimpfl (2005), T_c, are 891±23, 968±22 and 979±27°C.

Triple oxygen isotope composition of ALH 12073 ($\delta^{18}O$ = 4.4±0.15‰; $\delta^{17}O$ = 2.06±0.15‰) is, within uncertainty, in the range described by HED meteorites.

According to its bulk composition ALH 12073 is a sub-alkaline basalt (SiO_2 = 49.44 wt.%; $Na_2O + K_2O$ = 0.16 wt.%). Trace element abundances have been carried out by solution-ICP-MS on a representative aliquot of the sample (105 mg). The REE pattern is flat with relatively unfractionated La/Yb ratio (La/Yb_N = 0.8) and a large positive Eu anomaly (Eu/Eu* = 3.8). The concentration of incompatible lithophile trace elements such as Ba, Sr, Zr, Nb, Hf, Th, U and Rb exhibits striking similarities with cumulate eucrites. In turn, when compared to whole rock literature data, the siderophile elements (bulk Fe, Ni, Co) plot far off the field of HED meteorites, towards higher concentrations.

On the basis of pyroxene Fe/Mn ratio and oxygen isotope composition, the ALH 12073 basalt belongs to the HED family, i.e. eucrite. The relatively high $\delta^{18}O$ value could reflect the high modal plagioclase content of the rock (Wiechert et al., 2004). Pyroxene thermospeedometric data indicate quenching after equilibrium crystallization at temperatures of about 1000°C. Quenching is consistent with the occurrence of tridymite. The high metal and bulk siderophile element content is anomalous for eucrites and needs explanations. Several possibilities can be proposed: 1) introduction of foreign metal by impact (e.g., Kaneda and Warren, 1998). 2) Change of $f(O_2)$ during crystallization. 3) Increase of sulfur partial pressure during heating and subsequent reduction (Palme et al., 1988). 4) Kinship with metal-rich meteorites. All of these options will be discussed.

Kaneda, K. & Warren, P. (1988): Iron-Nichel metal-bearing unique eucrite Elephant Moraine 92023: its petrography, siderophile concentrations and petrogenesis. *Meteorit. Planet. Sci.*, **33**, A81-A82.

Palme, H., Wlotzka, F., Spettel, B, Dreibus, G., Weber, H. (1988): Camel Donga: A eucrite with high metal content. *Meteoritics*, **23**, 49-57.

Stimpfl, M. (2005): The Mn,Mg-intracrystalline exchange reaction in donpeacorite ($Mn_{0.54}Ca_{0.03}Mg_{1.43}Si_2O_6$) and its relation to the fractionation behavior of Mn in Fe, Mg-orthopyroxene. *Am. Mineral.*, **90**, 155-161.

Wiechert, U.H., Halliday, A.N., Palme, H. & Rumble, D. (2004): Oxygen isotope evidence for rapid mixing of the HED meteorite parent body. *Earth. Planet. Sci. Letters*, **221**, 373-382.

Fe-SILICIDE-BEARING METEORITES: FEEDING BODIES FOR REDUCED TERRESTRIAL PLANETS?

Downes H.*[1-2] & Herrin J.S.[3]
[1] Department of Earth and Planetary Sciences, Birkbeck University, London, United Kingdom
[2] Department of Earth Sciences, Natural History Museum, London, United Kingdom
[3] School of Materials Science and Engineering, Nanyang Technological University, Singapore
Corresponding email: h.downes@ucl.ac.uk

Keywords: silicide, meteorites, planets

Some heterogeneous accretion models for Earth (Wade &Wood, 2005) and other terrestrial planets have suggested that the early accreting phases may have been strongly reduced. Ureilites are carbon-rich, reduced, ultramafic achondrite meteorites composed mostly of mafic minerals such as olivine and pyroxenes (Mittlefehldt et al., 1998). They are thought to be residues of partial melting within the mantle of a planetesimal parent body. They occur as brecciated and unbrecciated types. Despite having undergone high temperature processes and relatively high degrees (20-30%) of silicate partial melting, ureilites retain a significant amount of iron metal and relatively high abundances of siderophile elements. Some ureilites (exclusively regolith breccias) also contain phases such as the iron silicides suessite ($(Fe,Ni)_3Si$) and rare hapkeite (Fe_2Si) (Herrin et al., 2008; Ross et al., 2009; Smith et al., 2010).

Suessite contains approximately 15 wt.% Si and 3.5 wt.% Ni. Siderophile elements in suessite are considerably fractionated, with the more compatible siderophiles (Rh, Pt, Ru, Mo, Ir, W, Os and Re) mostly strongly enriched above chondrite by approximately 10x. In contrast, the less compatible siderophile elements (Ge, As, Au, Pd, Ni and Co) are less strongly enriched (approximately 2-5x chondritic abundances). These results are very similar to siderophile element data for metals in monomict ureilites (Goodrich et al., 2013) which have considerably lower Si contents (generally < 4 wt.% Si).

In contrast, Si-free kamacite in polymict ureilites shows flat siderophile element patterns, parallel to chondrite but enriched by 2-10x. There are strong variations in Ni content from 5 to 15 wt.% Ni. This “chondritic” kamacite may not be indigenous to the ureilite parent body but may have been introduced to the regolith by chondritic impactors.

The presence of FeSi minerals and other Fe-X phases (X = S, P, C) in ureilites indicates very low redox conditions. These conditions must have occurred at low pressures, since the ureilite parent asteroid is estimated to have been only ~100 km in radius. Such small bodies at different stages of metal-silicate segregation may have contributed highly reduced phases to the accreting terrestrial planets.

Goodrich, C.A., Ash, R.D., Van Orman, J.A., Domanik, K., McDonough, W.F. (2013): Metallic phases and siderophite elements in main group ureilites: Implications for ureilite petrogenesis. *Geochim. Cosmichim. Acta*, **112**, 340-373.

Herrin, J.S., Mittlefehldt, D.W., Jones, J.H. (2008): Petrogenesis of Fe,Si-metals in brecciated ureilites. *Meteor. Planet. Sci.*, **43** (Suppl.), #5327 (abstr.).

Mittlefehldt, D.W., McCoy, T.J., Goodrich, C.A., Kracher, A. (1998): Non-chondritic meteorites from asteroidal bodies. *Rev. Mineral.*, **36**. 195 p..

Ross, A.J., Downes, H., Smith, C.L., Jones, A.P. (2009): Highly reduced metals and sulfides in ureilites: remnants of the UPB core? *Meteor. Planet. Sci.*, **44** (Suppl.), #5269 (abstr.).

Smith, C.L., Ross, A.J., Downes, H. (2010): Iron silicides in polymict ureilites – recording the complex history of the ureilite parent body. *Meteori. Planet. Sci.*, **45** (Suppl.), #5221 (abstr.).

Wade, J. & Wood, B.J. (2005): Core formation and the oxidation state of the Earth. *Earth Planet. Sci. Letters*, **236**, 78-95.

FROM MEDIUM- TO HIGH-K GRANITOIDS: TOWARDS STABILIZATION OF THE SOUTHERN SÃO FRANCISCO CRATON

Farina F.*[1-2], Albert C.[1], Aguilar C.[1], Moreno J.A.[3], Narduzzi F.[1] & Lana C.[1]
[1] Department of Geology, Federal University of Ouro Preto, Brazil
[2] Section des Sciences de la Terre, Université de Genève, Switzerland
[3] Department of Geology and Natural Resources, University of Campinas, Brazil
Corresponding email: fannak@gmail.com

Keywords: TTG series, high-K granites, Neoarchean

Field observations, whole-rock geochemical data as well as zircon U–Pb ages and Hf isotopes have been carried out for two Archean complexes (i.e., Bação and Bonfim) in the Southern São Francisco Craton in eastern Brazil. The basement of these domes is composed of fine-grained banded gneisses intruded by leucogranitic dikes and weakly foliated granites. Zircon U-Pb ages indicate that these rocks formed during three magmatic events: Rio das Velhas I (2920-2850 Ma), Rio das Velhas II (2800-2760 Ma) and Mamona (2750-2680 Ma). Most of the granites and gneisses have high silica content (> 70 wt.%) and based on their silica *vs*. K_2O composition are subdivided in medium- and high-K granitoids. Medium-K rocks have chemical affinity similar to rocks of the tonalite-trondhjemite-granodiorite series (TTGs); i.e., high Na_2O and Al_2O_3 associated to low contents of heavy-rare earth elements (HREE). Their overall whole-rock chemical features indicate that they formed through mixing between a magma generated by partial melting of metamafic rocks and a component derived by recycling Paleo- and Mesoarchean continental crust. These rocks, which form during the two earlier periods of magmatism, exhibit distinct and variable Hf isotopic ratios (ε_{Hf} from +4 to -4), with this evidence indicating different degree of continental crustal recycling involved in the genesis of individual gneiss samples. High-K granites, whose composition is similar to late-Archean biotite and two-mica granites, were produced between 2750 and 2680 Ma and their emplacement represents the last magmatic event in the craton.

To gain a better understanding on the transition between medium- and high-K granites and thus to shed light on the processes that led toward the stabilization of the craton, we studied three plutons in a well-exposed crustal section in the Bonfim complex. The oldest of these intrusions is the medium-K Samambaia pluton (2770 Ma), which exhibits a large range of major element variability (SiO_2 = 64-75 wt.%), coupled with low contents in HREE, negative Eu anomalies (Eu/Eu* = 0.7), low Sr contents and negative ε_{Hf}. Taken together these data suggest that the Samambaia pluton formed by fractional crystallization of a gabbroic rock with OIB affinity with minor contamination with the continental crust. The Vieira granite (2720 Ma) and the Moeda granite (2680 Ma), are very silica-rich (average SiO_2 = 74 wt.%), high-K rocks. They are characterized by low Sr and Rb contents, marked negative Eu anomalies (Eu/Eu* < 0.5) and negative ε_{Hf} between -2 and -8. The geochemistry of Moeda and Vieira granites suggests that these rocks were formed by partial melting of mature metasedimentary sequences. The relatively sharp transition between medium- and high-K granites tracks the onset of basin deposition during the Neoarchean Rio das Velhas II event followed by melting of these neo-formed basins at depth in a post-collisional setting.

WILD 2 GRAINS CHARACTERIZED COMBINING MIR/FIR/RAMAN MICRO-SPECTROSCOPY AND FE-SEM/EDS ANALYSES

Ferrari M.*[1], Rotundi A.[1-2], Rietmeijer F.J.M.[3], Della Corte V.[1], Baratta G.A.[4], Brunetto R.[5], Dartois E.[5], Djouadi Z.[5], Merouane S.[5], Borg J.[5], Brucato J.R.[6], Le Sergeant d'Hendecourt L.[5], Mennella V.[7], Palumbo M.E.[4] & Palumbo P.[1-2]

[1] Istituto di Astrofisica e Planetologia Spaziali, Istituto Nazionale di Astrofisica, Roma, Italy

[2] Dipartimento di Scienze e Tecnologie, Università "Parthenope", Napoli, Italy

[3] Department of Earth and Planetary Sciences, University of New Mexico, Albuquerque, NM, USA

[4] Osservatorio Astrofisico di Catania, Istituto Nazionale di Astrofisica, Catania, Italy

[5] Institut d'Astrophysique Spatiale, Centre National de la Recherche Scientifique, Université Paris Sud, Orsay, France

[6] Osservatorio Astrofisico di Arcetri, Istituto Nazionale di Astrofisica, Firenze, Italy

[7] Osservatorio Astronomico di Capodimonte, Istituto Nazionale di Astrofisica, Napoli, Italy

Corresponding email: marco.ferrari@iaps.inaf.it

Keywords: stardust, cometary particles, spectroscopy

We present the results of the analyses of two bulk terminal particles (TPs), C2112,7,171,0,0 (TP2) and C2112,9,171,0,0 (TP3), (Rotundi et al., 2014), derived from the Jupiter-Family comet 81P/Wild 2 returned by the NASA Stardust mission (Brownlee et al., 2006). Each particle, embedded in a slab of silica aerogel, was pressed in a diamond cell. Aerogel is usually cause of problems when characterizing the minerals and organic materials present in the embedded particles. We overcame this common issue by means of the combination of FE-SEM/EDS, IR and Raman µ-spectroscopy, three nondestructive analytical techniques, which provided bulk mineralogical and organic information on TP2 and TP3. This approach proved to be a practical solution for preliminary characterization, i.e. scanning particles for chemical and mineralogical heterogeneity.

Using this type of bulk characterization prior to more detailed studies, could be taken into account as a standard procedure to be followed for selecting Stardust particles-of-interest.TP2 and TP3 are dominated by Ca-free and low-Ca, Mg-rich, Mg,Fe-olivine. The presence of melilite in both particles is supported by IR µ-spectroscopy and corroborated by FE-SEM/EDS analyses, but is not confirmed by Raman µ-spectroscopy possibly because the amount of this mineral is too small to be detected. TP2 and TP3 show similar silicate mineral compositions, but Ni-free, low-Ni, sub-sulfur (Fe,Ni)S grains are present only in TP2. TP2 contains indigenous amorphous carbon hot spots, while no indigenous carbon was identified in TP3. These non-chondritic particles probably originated in a differentiated body. The presence of high temperature melilite group minerals in TP2 and TP3 reinforces the notion that collisionally ejected refractory debris from differentiated asteroids may be common in Jupiter-Family comets. This raises the question whether similar debris and other clearly asteroidal particles could be present in Halley-type comets and, if so, which fraction of the dust in these comets is truly represented by non-processed silicates and organic material. The work done for Stardust samples is important to understand the similarities and differences among comets. In fact, the results of this study are relevant also for the ROSETTA mission that encountered the Jupiter-Family (J-F) comet 67P/Churyumov-Gerasimenko in August, 2014. At the time this mission was launched, our ideas of comet dust were biased by the findings of the Halley missions. The Stardust mission showed an unexpected richness of dust that originated from the inner solar system. Rosetta is confirming these results (Rotundi et al., 2015; Della Corte et al., 2015), but also adding information, in particular on the presence of a primitive and unprocessed dust component (Fulle et al., 2015).

Brownlee, D. et al. (2006): Comet 81P/Wild 2 under a microscope. *Science*, **314**, 1711-1716, DOI: 10.1126/science.1135840.

Della Corte, V. et al. (2015): GIADA: shining a light on the monitoring of the comet dust production from the nucleus of 67P/Churyumov-Gerasimenko. *Astron. Astrophys.*, **583**, A13. DOI: 10.1051/0004-6361/201526208.

Fulle, M. et al. (2015): Density and Charge of Pristine Fluffy Particles from Comet 67P/Churyumov-Gerasimenko. *Astrophys. J. Letters*, **802**, L12, DOI: 10.1088/2041-8205/802/1/L12.

Rotundi, A. et al. (2014): Two refractory Wild 2 terminal particles from a carrot-shaped track characterized combining MIR/FIR/Raman microspectroscopy and FE-SEM/EDS analyses. *Meteor. Planet. Sci.*, **49**, 550-575, DOI: 10.1111/maps.12274.

Rotundi, A. et al. (2015): Dust measurements in the coma of comet 67P/Churyumov-Gerasimenko inbound to the Sun. *Science*, **347**, DOI: 10.1126/science.aaa3905.

STRETCHING OUT THE AUSTRALASIAN MICROTEKTITE STREWN FIELD IN VICTORIA LAND TRANSANTARCTIC MOUNTAINS: AN UPDATE

Folco L.*[1], D'Orazio M.[1], Gemelli M.[1], Rochette P.[2], Gattacceca J.[2] & Glass B.P.[3]
[1] Dipartimento di Scienze della Terra, Università di Pisa, Italy
[2] Centre de Recherche et d'Enseignement de Géosciences de l'Environnement, Université d'Aix-Marseille, Centre National de la Recherche Scientifique, Aix-en-Provence, France
[3] Department of Geosciences, University of Delaware, Newark, DE, USA
Corresponding email: luigi.folco@unipi.it

Keywords: Australasian microtektites, impact cratering, Transantarctic Mountains

Regional distribution: Petrographic and geochemical studies of microtektites collected in newly explored summit plateaus of the Transantarctic Mountains (i.e., Schroeder Spur, Killer Nunatak, Miller Butte in the inland catchment of the Rennick Glacier, and Allan Hills, in the inland catchment of the Mackay-David Glaciers) document a regional distribution of Australasian microtektites in Victoria Land.

Projectile contamination(?): A geochemical comparison with Australasian microtektites from deep sea sediments (AUS/DSS, n = 54; Glass et al., 2004; Glass & Koeberl, 2066) at lower latitudes confirms that Transantarctic Mountain microtektites (AUS/TAM; n = 44) are strongly depleted in volatile elements, thereby indicating that they experienced higher thermal regimes. Furthermore, the AUS/TAM are depleted in Ni, Co relative to AUS/DSS. In particular, we observe that Ni and Co contents decrease with distance from the hypothetical source crater location in Indochina, with concentrations of up to Ni = 471 and Co = 42 µg/g in the AUS/DSS, and Ni < 26 and Co < 13 µg/g in the TAM/AUS. The concentrations of these elements in AUS/DSS are significantly higher than in the UCC (Ni = 20 µg/g, Co = 10 µg/g; Taylor & McLennan, 1995), and could be ascribed to meteoritic projectile contamination, as suggested previously (Glass et al., 2004). In this view, we can speculate that projectile contamination decreases with distance from the source crater and eventually becomes negligible (or null) in those microtektites that were thrown at greater distances, as far south as the Antarctic.

Microtektite ejection angle: Ballistic calculations reveal that the extraordinary distance of the Transantarctic Mountain microtektites from the hypothetical impact location in Indochina (~ 11000 km) could be more efficiently attained at relatively low ejection angles (20-40°).

Glacial history of the East Antarctic Ice Sheet: The occurrence of Australasian microtektites (~ 0.8 Ma old) on specific glacial surfaces of the Antarctic bedrock constrains the glacial history of the East Antarctic Ice Sheet in Victoria Land. In particular, data from Allan Hills supports a glaciological scenario envisaging an extremely stable East Antarctic Ice Sheet over at least the last ~1 Ma in the inland catchment of the Mackay/David glaciers. This is consistent with the large accumulation of meteorites in the adjacent blue ice field (Folco et al., 2016).

Acknowledgements: Work supported by *PNRA* (PEA2013 AZ2.04 "Meteoriti Antartiche").

Folco, L., D'Orazio, M., Gemelli, M., Rochette, P. (2016). Stretching out the Australasian microtektite strewn field in Victoria Land Transantarctic Mountains. *Polar Science*, in press, DOI: 10.1016/j.polar.2016.02.004

Glass, B.P. & Koeberl, C. (2006): Australasian microtektites and associated impact ejecta in the South China Sea and the Middle Pleistocene supereruption of Toba. *Meteorit. Planet. Sci.*, **41**, 305-326.

Glass, B.P., Huber, H., Koeberl, C. (2004): Geochemistry of Cenozoic microtektites and clinopyroxene-bearing spherules. *Geochim. Cosmochim. Acta*, **68**, 3971-4006.

Taylor, S.R. & McLennan, S.M. (1995). The geochemical evolution of the continental crust. *Rev. Geophys.*, **32**, 241-265.

I-TYPE COSMIC SPHERULES: AN X-RAY MICRO-CT STUDY

Gemelli M.*[1], Di Rocco T.[1], Iacoviello F.[2], Shearing P.[2] & Folco L.[1]
[1] Dipartimento di Scienze della Terra, Universita di Pisa, Italy
[2] Electrochemical Innovation Laboratory, Department of Chemical Engineering, University College London, United Kingdom
Corresponding email: maurizio.gemelli@unipi.it

Keywords: micrometeorites, X-Ray micro-CT, platinum group elements

Micrometeorites are microscopic particles, collected at the Earth's surface and mainly produced by collisions among solid bodies and by surface evaporation of icy bodies in the Solar System (i.e., Folco & Cordier, 2015). I-type cosmic spherules (CS) are dark, opaque, melted micrometeorites dominated by magnetite (Fe_3O_4) and wüstite (FeO) crystals. I-type CS frequently contain µm-sized Ni-rich Fe,Ni metal blebs (i.e., Rudraswami et al., 2014) as well as µm- and nm-sized platinum-group element (PGE) nuggets (i.e., Rudraswami et al., 2011). The aim of this work is twofold: 1) to study the internal texture of the I-type CS, 2) to characterize the distribution of the metal blebs and PGE nuggets and to estimate their relative volumes. Accordingly, we have selected a large number of I-type CS, collected in loose sediments on the tops of the Transantarctic Mountains (Rochette et al., 2008) during the 2012-13 and 2014-15 Italian Programma Nazionale di Ricerche in Antartide (PNRA) campaign. The selected I-type CS look completely unaltered and provide excellent material for our study. The external morphology of 10 CS has been described by preliminary SEM analyses. Subsequently, non-destructive mapping of I type CS has been carried out by X-ray microcomputed tomography (micro-CT) using a Zeiss Xradia 520 Versa 3D X-ray microscope, at the Electrochemical Innovation Lab, part of the Department of Chemical Engineering of University College London. The microscope was operated at 140 kV with a high energy filter in place (HE1) and an optical magnification of 20x. 3D tomographic reconstructions on 5 CS allowed: 1) Distinction of at least four components, i.e. the voids, the iron oxide domains, the metal blebs and the PGE nuggets; 2) Estimation of the true Total-Volume/Bleb-Volume ratio. This ratio can be used as an oxygen barometer. It is in fact suggested that, during atmospheric entry, the metal separates form the host at low $f(O_2)$. Subsequently, oxidizing conditions lead to the formation of wüstite and magnetite in various proportions (Rudraswami et al., 2014). 3) Characterization of the void distribution. Irregular voids are frequently observed around the metal blebs. They are suggested to be the result of contraction due to quenching after atmospheric entry heating and to be function of mass of the CS, efficiency of metal segregation and cooling rate (Feng et al., 2005). 4) Speculate on the origin of the peculiar web structure of the oxide phases resulting from wüstite domains surrounded by magnetite. More samples are going to be analyzed in the next weeks. Results will be discussed at the Conference.

*Acknowledgements***:** This work is supported by the Italian Programma Nazionale delle Ricerche in Antartide (PNRA) through the PEA2013 AZ2.04 "Meteoriti Antartiche".

Feng, H., Jones, K.W., Tomov, S., Stewart, B., Herzog, G.F., Schnabel, C., Brownlee, D.E. (2005): Internal structure of type I deep-sea spherules by X-ray computed tomography. *Meteor. Planet. Sci.*, **40**, 195-206.

Folco, L. & Cordier, C. (2015): Micrometeorites. *in* "Planetary Mineralogy", M.R. Lee, H. Leroux, eds., *EMU Notes Mineral.*, **15**, 253-297.

Rochette, P., Folco, L., Suavet, C., van Ginneken, M., Gattacceca, J., Perchiazzi, N., Braucher, R., Harvey, R.P (2008): Micrometeorites from the Transantarctic Mountains. *Proc. Nat. Acad. Sci. USA*,**105**, 18206-18211.

Rudraswami, N.G., Parashar, K., Shyam Prasad, M. (2011): Micrometer- and nanometer- sized platinum group nuggets in meicrometeorites from deep-sea sediments of the Indian Ocean. *Meteor. Planet. Sci.*, **46**, 470-491.

Rudraswami, N.G., Shyam Prasad, M., Babu, E.V.S.S.K., Vijia Kumar, T. (2014): Chemistry and petrology of Fe–Ni beads from different types of cosmic spherules: Implication for precursors. *Geochim. Cosmochim. Acta*, **145**, 139-158.

HYDROGEN AND CHLORINE ISOTOPE RATIOS IN EARLY ARCHEAN APATITE CRYSTALS FROM THE ISUA SUPRACRUSTAL BELT, SW GREENLAND – INITIAL RESULTS

Giera A.*[1], Słaby E.[1], Wiedenbeck M.[2], Birski L.[1] & Lepland A.[3]
[1] Institute of Geological Sciences, Polish Academy of Sciences, Warsaw, Poland
[2] Helmholtz Zentrum Potsdam, GFZ Deutsches GeoForschungsZentrum, Potsdam, Germany
[3] Geological Survey of Norway, Trondheim, Norway
Corresponding email: ndgiera@cyf-kr.edu.pl

Keywords: Archean apatite, volatiles, SIMS

The origin of water and other volatiles on the Earth remains a matter of controversy, particularly so in light of this topic's relevance for the emergence of life on our planet. Published research on the origin of water on the Earth has focused on the D/H ratios of various water reservoirs, e.g., comets and meteorites (Pinti, 2005). The most recent research from this field reports evidence for primordial water within Earth's deep mantle, implying that Earth's water probably came from the protosolar nebula and indicating that the isotopic composition of seawater has evolved over time (Hallis et al., 2015). Up until now the oldest terrestrial apatite has never been investigated as a mineralogical tracer of volatile evolution of the early Earth. This study makes use of this unique archive to investigate Archean δD values, suggesting extra-terrestrial sources of volatiles, combined with the examination of $^{37}Cl/^{35}Cl$ ratios, which indicate mantle/crustal origin for this component. The current research includes detailed analyses of apatite crystals from the Isua supracrustal belt (ca. 3.8 Ga) located in southern West Greenland. In previous studies it was shown that the rocks of this succession hold geochemical signature of the Late Heavy Bombardment at 3.9-3.8 Ga (Jørgensen et al., 2009), which may have delivered some amount of water to the Earth. The preliminary results of our research obtained using a Cameca 1280-HR secondary ion mass spectrometer show small, but significant variations in the hydrogen isotopic composition of apatite crystals both from different rock types – banded iron formation (BIF), metachert and metacarbonate – as well as from three independent BIF specimens. δD values for all samples were determined to be isotopically light in comparison to VSMOW, within the range from -87 to -57 ‰. Furthermore, the chlorine isotope compositions ($\delta^{37}Cl$) of apatite crystals from two BIFs and one mafic dyke were found to have values varying from -0.2 to 1.7‰ (relative to Standard Mean Ocean Chloride). Preliminary isotopic data imply that an Archean ocean was deuterium-depleted as compared to its present-day composition, supporting the protosolar nebula theory of the Earth's water origin as suggested by Hallis et al. (2015).

Acknowledgements: We thank T. John (Freie Universität Berlin), F. McCubbin (University of New Mexico), and A. Sarafian (Woods Hole Oceanographic Institution) for providing the reference materials for SIMS analyses. The research was funded by Polish NCN grant no. 2013/11/B/ST10/04753 and supported by the EU COST Action TD1308 "ORIGINS".

Hallis, L.J., Huss, G.R., Nagashima, K., Taylor, G.J., Halldórsson, S.A., Hilton, D.R., Mottl, M.J., Meech, K.J. (2015): Evidence for primordial water in Earth's deep mantle. *Science*, **350**, 795-797.

Jørgensen, U.G., Appel, P.W.U., Hatsukawa, Y., Frei, R., Oshima, M., Toh, Y., Kimura, A. (2009): The Earth–Moon system during the late heavy bombardment period – Geochemical support for impacts dominated by comets.*Icarus*, **204**, 368-380.

Pinti, D.L. (2005): The origin and evolution of the oceans. *in* "Lectures in Astrobiology, Vol. I", M. Gargaud, B. Barbier, H. Martin, J. Reisse, eds., Springer, Berlin-Heidelberg, 83-112.

IRON OXIDATION STATE IN FULGURITE GLASS

Giuli G.*[1], Pratesi G.[2], Paris E.[1] & Cibin G.[3]
[1] Scuola di Scienze e Tecnologie - Sezione di Geologia, Università di Camerino, Italy
[2] Museo di Storia Naturale, Università di Firenze, Italy
[3] Diamond Light Source, Didcot, United Kingdom
Corresponding email: gabriele.giuli@unicam.it

Keywords: fulgurite glass, iron redox, Shock metamorphism

Fulgurites are glasses produced by lightnings striking a rock, soil or sand. They can be found as hollow tubes with thin glass walls, as strong glass cylinders, or as glass droplets. Pevious studies found shocked high pressure minerals within the glass, as well as reduced mineral phases as metallic Si or Fe-Si alloys (Essene & Fisher, 1986; Wasserman et al., 2002).

Here we show preliminary results on the Fe oxidation state two fulgurite glasses: one is a black droplet from Elko County (USA), whereas the second is a glass tube, from Sahara desert, sealed at both ends and containing unmolten sand in its interior.

Peliminary Scanning Electron Microscopy data do not reveal reduced/metallic mineral phases within the glass of the two studied samples. Fe *K*-edge XANES data were collected in order to determine quantitatively the Fe oxidation state by careful analysis of the pre-edge peak. The spectra the both fulgurite samples are consistent with Fe being mostly divalent, similar to tektite glasses (Giuli et al., 2002, 2010a, 2010b). The sand enclosed in the tube fulgurite does not show any sign of reduction, and the pre-edge peak of a sand sample carefully homogenised show Fe to be mostly trivalent.

Essene, E.J. & Fisher, D.C. (1986): Lightning strike fusion: extreme reduction and metal-silicate liquid immiscibility. *Science*, ***234***, 189.193.

Giuli, G., Pratesi, G., Paris, E., Cipriani, C. (2002): Fe local structure in tektites by EXAFS and High resolution XANES spectroscopy. *Geochim. Cosmochim. Acta*, **66**, 4347-4353.

Giuli, G., Eeckhout, S.G., Cicconi, M.R., Koeberl, C., Pratesi, G., Paris, E. (2010a): Iron oxidation state and local structure in North American tektites. *in* "Large meteorite impacts and planetary Evolution", W.U. Reimold, R. Gibson, eds., *Geol. Soc. Am. Spec. Pap.*, **465**, 645-652.

Giuli, G., Pratesi, G., Eeckhout, S.G., Koeberl, C., Paris, E. (2010b): Iron reduction in silicate glass produced during the 1945 nuclear test at the trinity site (Alamogordo, New Mexico, USA). *in* "Large meteorite impacts and planetary Evolution", W.U. Reimold, R. Gibson, eds., *Geol. Soc. Am. Spec. Pap.*, **465**, 653-662.

Wasserman, A.A., Melosh, H.J., Lauretta, D.S. (2002): Fulgurites: a look at transcient high temperature processes in silicates Proc. 33rd Lunar Planet. Sci. Conf., abstr., #1308.

COSMOCHEMISTRY OF NEAR-CRITICAL SILICATE FLUIDS

Green E.C.R.*[1], Artacho E.[2-3-4-5] & Connolly J.A.D.[1]
[1] Institut für Geochemie und Petrologie, Eidgenössiche Technische Hochschule Zürich, Switzerland
[2] CIC nanoGUNE, San Sebastián, Spain
[3] Cavendish Laboratory, University of Cambridge, United Kingdom
[4] Basque Foundation for Science, Bilbao, Spain
[5] Donostia International Physics Center, San Sebastián, Spain
Corresponding email: eleanor.green@erdw.ethz.ch

Keywords: silicate fluid, thermodynamic properties, simulation

The thermodynamic properties of low-density silicate fluids must be estimated in order to model interactions between silicate protoplanetary bodies and their discs. Arguments based on these properties, and the liquid-vapour phase relations to which they give rise, have been used to constrain models of Moon formation (e.g., Genda & Abe, 2003; Pahlevan et al., 2011; Canup et al., 2013; Visscher & Fegley, 2013). Such studies include implicit or explicit assumptions about the critical conditions above which silicate liquid and vapour phases can no longer be distinguished. However, the relevant conditions of high temperature and low pressure are almost inaccessible to experiments. Consequently the material properties of low-density silicate fluids are poorly known, as are their phase relations including the critical conditions.

In an effort to address this problem, we present results of first-principles molecular dynamics simulations on SiO_2 fluid, at low densities of 500-2240 kg/m^3 and temperatures of 4000-6000 K. The simulations provide hitherto unavailable constraints on the equation of state (EoS) of near-critical SiO_2 liquid. Towards lower densities and higher temperatures, O_2 begins to separate from an increasingly Si-enriched liquid, indicating that silica liquid boils incongruently, an observation that places further constraints on the appropriate form of an EoS. Supercritical behaviour at the SiO_2 composition occurs above 5000-6000 K and 0.2-0.6 GPa. Additional sets of simulations, on the bulk compositions $FeSiO_3$ and $MgSiO_3$, are planned or underway, with the aim of calibrating a molecular EoS in the system Mg-Fe-Si-O.

Canup, R.M., Barr, A.C., Crawford, D.A. (2013): Lunar-forming impacts: High-resolution SPH and AMR-CTH simulations. *Icarus*, **222**, 200-219.

Genda, H. & Abe, Y. (2003): Modification of a proto-lunar disk by hydrodynamic escape of silicate vapor. *Earth Planets Space*, **55**, 53-57.

Pahlevan, K., Stevenson, D.J., Eiler, J.M. (2011): Chemical fractionation in the silicate vapor atmosphere of the Earth. *Earth Planet. Sci. Letters*, **301**, 433-443.

Visscher, C. & Fegley, B. (2013): Chemistry of impact-generated silicate melt-vapor debris disks. *Astrophys. J. Letters*, **767**, L12.

DECOMPOSITION AND MELTING OF CARBONATES IN CONTACT WITH SILICATE MELTS IN MEMIN LASER MELTING EXPERIMENTS

Hamann C.*[1-2], Hecht L.[1-2], Schäffer S.[3], Deutsch A.[4] & Lexow B.[3]
[1] Museum für Naturkunde, Leibniz-Institut für Evolutions- und Biodiversitätsforschung Berlin, Germany
[2] Institut für Geologische Wissenschaften, Freie Universität Berlin, Germany
[3] Fraunhofer-Institut für Kurzzeitdynamik, Freiburg, Germany
[4] Institut für Planetologie, Westfälische Wilhelms-Universität Münster, Germany
Corresponding email: christopher.hamann@mfn-berlin.de

Keywords: Impact melting, carbonate decomposition, projectile–target interaction

The reaction of carbonates to meteorite impacts is a topic of lively discussion in the impact community (e.g., Ivanov & Deutsch, 1997; Osinski et al., 2008). Specifically, the question is whether carbonates decompose and liberate CO_2, or simply melt like silicates. However, evidence from terrestrial impact craters is often ambiguous, hence, some authors favor decomposition (e.g., Hörz et al., 2015), while others favor melting (e.g., Osinski et al., 2015). Laboratory experiments with well-defined conditions may help answering this question. Here, we discuss four laser melting experiments involving carbonates in contact with silicates, performed in the Multidisciplinary Experimental and Modeling Impact Research Network (MEMIN).

We used a ytterbium fiber laser at Fraunhofer-Institut für Kurzzeitdynamik, Freiburg, Germany, to simulate *P-T* conditions of impact melt formation during decompression. These experiments combine quasi-instantaneous melting and vaporization during laser irradiation with subsequent quenching in the ambient atmosphere. We irradiated layers of sandstone and basalt attached onto layers of marble and limestone (the laser penetrated through the silicate layer into the carbonate layer below). The experiments were filmed with high speed and infrared cameras and experimental products were studied with optical microscopy, SEM, EMPA, and Raman spectroscopy.

In the sandstone experiments, the laser formed a pool of siliceous melt that quenched within ~ 18 s from > 2100 to 500°C ($dT/dt \approx 89$°C/s) to a transparent to milky glass. The glass is mainly a mixture of SiO_2 and CaO with increasing CaO content towards a carbonate reaction zone that lies below the silicate melt pool. Locally, silicate emulsions formed as the melt passed through a miscibility gap in the system SiO_2–CaO. Moreover, pseudowollastonite, $CaSiO_3$, crystallized close to the carbonate reaction front in the siliceous melt. In the basalt experiments, the laser formed a pool of basaltic melt on top of a carbonate reaction front as well, but penetrated much further into the carbonate layer. The basaltic melt quenched within ~ 36 s from 1900 to 500°C ($dT/dt \approx 29$°C/s) to a brown glass and the carbonate layer cooled within ~ 12 s from > 2100 to 500°C ($dT/dt \approx 133$°C/s). The basaltic melt is thoroughly homogenized and enriched in CaO. At the contact between basaltic melt and carbonate reaction front exists an assemblage of quenched, Ca,Fe,Al-rich silicate melt, idiomorphic, Si,Al-bearing calcite crystallites, lath-shaped, Ca,Si-rich, volatile-bearing quench crystals, and MgO. This resembles quenched immiscible silicate and carbonatite liquids known from quenching experiments (Lee & Wyllie, 1997). Moreover, merwinite, $Ca_3Mg(SiO_4)_2$, crystallized in the basaltic melt close to the carbonate reaction front. In summary, our experiments show that the reaction of carbonates in contact with superheated silicate (impact) melts is complex and possibly involves both melting and decomposition.

Hörz, F., Archer, P.D. Jr, Niles, P.B., Zolensky, M.E., Evans, M. (2015): Devolatilization or melting of carbonates at Meteor Crater, AZ? *Meteorit. Planet. Sci.*, **50**, 1050-1070.

Ivanov, B.A. & Deutsch, A. (2002): The phase diagram of $CaCO_3$ in relation to shock compression and decompression. *Phys. Earth Planet. Int.*, **129**, 131-143.

Lee, W. & Wyllie, P.J. (1997): Liquid immiscibility between nephelinite and carbonatite from 1.0 to 2.5 GPa compared with mantle melt compositions. *Contrib. Mineral. Petrol.*, **127**, 1-16.

Osinski, G.R., Spray, J.G., Grieve, R.A.F. (2008): Impact melting in sedimentary target rocks: an assessment. *In* "The sedimentary record of meteorite impacts. Geological Society of America Special Paper 437", K.R. Evans, J.W. Horton, D.T. King, J.R. Morrow, eds., Geological Society of America, Boulder, 1-17.

Osinski, G.R., Bunch, T.E., Flemming, R.L., Buitenhuis, E., Wittke, J.H. (2015): Impact melt- and projectile-bearing ejecta at Barringer Crater, Arizona. *Earth Planet. Sci. Letters*, **432**, 283-292.

Fe ISOTOPE COMPOSITION OF CHONDRULES FROM THE MURCHISON (CM) CHONDRITE

Hezel D.C.*[1], Wilden J.[1], Frank-Richter S.[2] & Wombacher F.[1]
[1] Institut für Geologie und Mineralogie,Universität Köln, Germany
[2] Institut für Materialphysik im Weltraum, Deutsches Zentrum für Luft- und Raumfahrt, Köln, Germany
Corresponding email: d.hezel@uni-koeln.de

Keywords: chondrules, Fe, isotope

Introduction: Chondrules are a major component in chondritic meteorites (chondrites), and formed during brief high temperature events in the protoplanetary disk prior to planet formation. In CM chondrites, chondrules are dominantly of type I, i.e. Fe-poor and Mg-rich. During formation, chondrules were open systems, i.e. they exchanged material with the surrounding gas (e.g., Friend et al., 2006, and references therein). Such a material exchange might also fractionate stable isotopes. Bouvier et al. (2013) studied Mg isotopes in CM chondrite chondrules and concluded that the observed, variable Mg isotope compositions of the chondrules are best explained by a mixture of parent body and open system nebula processes.

Magnesium is a major element in type I chondrules, whereas Fe is a minor element. Further, if opaques (e.g. sulphide or metal) are present in the chondrule, the bulk chondrule Fe composition will be dominated by the opaque phase. Possible Fe isotope fractionations in chondrules might therefore trace fractionations in opaque phases, should their modal abundances exceed only a few vol.%. Further, Fe isotope fractionations might be used to locate the origin of the fractionation: parent body or nebula. Parent body fractionations might drive Fe isotope compositions of all chondrules in the same direction, while open system nebula processes might drive Fe isotope compositions in both directions. Both processes have been suggested before and for different chondrites (e.g., Mullane et al., 2005; Needham et al., 2009; Hezel et al., 2010, 2015; Moynier et al., 2010).

Results: We currently study the Fe isotope composition of and opaque modal abundances in bulk chondrules from the CM chondrite Murchison. The first set of samples consists of 14 chondrules. We use tomography to determine the opaque modal abundance before measuring the Fe isotope compositions. The opaque abundances range from 0.0 to 6.5 vol.%. The bulk Fe content in most chondrules is dominated by their silicate phases. The δ^{56}Fe compositions (relative to IRMM-014) of the 14 studied chondrules range from -0.21 to +0.24‰. This is a small range for chondrules, when compared to e.g. CV chondrite chondrules (e.g., Mullane et al., 2005; Hezel et al., 2010).

Conclusions: The carrier of the Fe isotope composition of most chondrules are the silicate phases. The negative and positive bulk chondrule Fe isotope compositions relative to the standard indicate open system exchange between the chondrule and the surrounding gas, e.g. evaporation and re-condensation processes. Additional exchange and fractionation on the hydrously altered CM parent body are likely.

Bouvier, A., Wadhwa, M., Simon, S.B., Grossman, L. (2013): Magnesium isotopic fractionation in chondrules from the Murchison and Murray CM2 carbonaceous chondrites. *Meteor. Planet. Sci.*, **48**, 339-353.

Friend, P., Hezel, D.C., Mucerschi, D. (2016): The conditions of chondrule formation, Part II: Open system. *Geochim. Cosmochim. Acta*, **173**, 198-209.

Hezel, D.C., Needham, A.W., Armytage, R., Georg, B., Abel, R., Kurahashi, E., Coles, B.J., Rehkämper, M., Russell, S.S. (2010): A nebula setting as the origin for bulk chondrule Fe isotope variations in CV chondrites. *Earth Planet. Sci. Letters*, **296**, 423-433.

Hezel, D.C., Poole, G., Hoyes, J., Coles, B.J., Unsworth, C., Albrecht, N., Smith, C., Rehkämper, M., Pack, A., Genge, M., Russell, S.S. (2015): Fe and O isotope composition of meteorite fusion crusts: possible natural analogues to chondrule formation? *Meteor. Planet. Sci.*, **50**, 229-242.

Moynier, F., Agranier, A., Hezel, D.C., Bouvier, A. (2010): Sr stable isotope composition of Earth, the Moon, Mars, Vesta and meteorites. *Earth Planet. Sci. Letters*, **300**, 359-366.

Mullane, E., Russell, S.S., Gounelle, M. (2005): Nebular and asteroidal modification of the iron isotope composition. *Earth Planet. Sci. Letters*, **239**, 203-218.

Needham, A.W., Porcelli, D., Russell, S.S. (2009): An Fe isotope study of ordinary chondrites. *Geochim. Cosmochim. Acta*, **73**, 7399-7413.

THE IMPACT BOMBARDMENT HISTORY OF THE EARLY EARTH

Koeberl C.*[1-2]
[1] Naturhistorisches Museum Wien, Austria
[2] Department für Lithosphärenforschung, Universität Wien, Austria
Corresponding email: christian.koeberl@univie.ac.at

Keywords: impact cratering, shock metamorphism, early Earth

Over the past decades, the study of impact craters and their formation has reached a degree of maturity that has led to a reasonably good understanding of the processes involved in their formation, and their importance for the evolution of planetary bodies in the solar system and, especially, on Earth. If a late heavy bombardment during the period from about 3.8 to 4 billion years ago occurred on the Moon, the Earth must have been subjected to an impact flux more intense than that recorded on the Moon. The consequences for the Earth must have been devastating, and may have included partial or total remelting of the crust. So far, no unequivocal record of a late heavy bombardment on the early Earth has been found. The earliest rocks on Earth date back to slightly after the end of the heavy bombardment, although there are relict zircons up to 4.4 Ga old (in which no unambiguous impact-characteristic shock features have yet been found). In terms of evidence for impact on Earth, the first solid evidence exists in the form of various spherule layers found in South Africa and Australia with ages between about 3.2-3.4 and 2.5 Ga; these layers represent several (the exact number is still unknown) large-scale impact events. The oldest documented (and preserved) impact structures on Earth have ages of 2.02 and 1.86 billion years. Thus, the impact record for more than half of the geological history of the Earth is extremely poor, and there is little information about the impact record and its effects during the first 2.5 billion years of Earth history. Impact structures or ejecta are commonly identified from specific characteristics, such as the presence of evidence for shock metamorphism, and/or geochemical indications of the presence of an extraterrestrial component. Only elements that have high abundances in meteorites, but low abundances in terrestrial crustal and mantle-derived rocks are useful for such studies (such as the PGEs). Elevated abundances of siderophile elements in impact melt rocks, breccias, or ejecta, compared to target rock abundances, can be indicative of the presence of either a chondritic or an iron meteoritic component. However, in some cases the PGE interelement abundances can be fractionated. These problems can, in part, be overcome by the use of isotopic tracers, such as Os or Cr isotopes, for extraterrestrial components. The Os isotopic method is very sensitive and can detect sub-percent levels of extraterrestrial component in impact breccias and melt rocks, but it is not possible to determine a meteorite type. In contrast, the Cr isotopic method relies on the fact that all terrestrial rocks have a uniform Cr isotopic composition, whereas different meteorite types have different isotopic anomalies. The Cr isotopic method is selective not only regarding the Cr source (terrestrial vs. extraterrestrial), but also regarding meteorite type. Such studies have recently been performed on the early Archean spherule layers mentioned above.

METAL-SILICATE CHEMICAL AND ISOTOPIC FRACTIONATION OF Zn AND COSMOCHEMICAL ESTIMATION OF THE S CONTENT OF THE EARTH'S CORE

Mahan B.*[1], Siebert J.[1], Pringle E.A.[1] & Moynier F.[1-2]

[1] Institut de Physique du Globe de Paris, Université Paris Diderot, Sorbonne Paris Cité, Centre National de la Recherche Scientifique, France

[2] Institut Universitaire de France, Paris, France

Corresponding email: brandonmmahan@gmail.com

Keywords: Zn partitioning, isotopic fractionation, core formation

The abundance of volatile elements (e.g., H, C, S) controls the rheologic properties of rocks in the Earth's mantle, and therefore is critical to planetary processes such as core/mantle differentiation and mantle convection. Furthermore, the conditions of volatile emplacement on Earth is poorly constrained, and thus our understanding of the chemical processing of terrestrial bodies is limited. Metal-silicate differentiation experiments provide us with experimental access to the conditions of core formation. By investigating the elemental partitioning and isotopic fractionation of volatile and moderately volatile elements in this way, we can further constrain the conditions of core formation and emplacement of volatiles on Earth. Zinc is a moderately volatile element with a 50% condensation temperature of 726 K, similar to that of sulfur (664 K), and has been used to estimate the S content of the bulk Earth (BE). Thus, Zn metal-silicate fractionation provides first order experimental access to the conditions of core formation, as well as providing indirect information into the origin and eventual fate of volatile and siderophile elements on Earth. However, the partitioning of Zn between metal and silicate, as well as Zn metal-silicate isotopic fractionation, is not well known. We have conducted complimentary suites of Zn metal-silicate differentiation experiments to estimate both the elemental partitioning and isotopic fractionation of Zn between metal and silicate as a function of time, temperature, and composition. Experiments were conducted at 2 GPa and temperatures from 1473 to 1973 K in a piston cylinder apparatus and run durations ranged from 5 to 240 minutes for four distinct starting materials. Within the dataset, chemical and isotopic equilibrium was achieved within ten minutes of experimental outset. Zn metal-silicate isotopic fractionation was unresolvable at our level of detection (50 ppm on the $^{66}Zn/^{64}Zn$ ratio) regardless of experiment temperature and composition, indicating that the Zn isotopic composition of silicate phases can be used as a proxy for the overall isotopic signature of bulk telluric bodies. Partitioning results from this study were combined with data from the literature to provide a robust parameterization of Zn metal-silicate partitioning as a function of temperature and pressure. We have calculated new estimates of the Zn content of the Earth's core and the BE as 239±107 ppm and 113±29 ppm (respectively), values that are significantly higher than previous estimates (0 and 24-40 ppm, respectively). By assuming similar volatilities for Zn and S, and a chondritic S/Zn ratio, we have calculated a new cosmochemical estimate for the S content of the Earth's core of 6.3±1.6 wt.%, indicating that S is either a major contributor to the density deficit of the Earth's core, or that S and Zn had differing volatilities prior to or during the formation and differentiation of the Earth, i.e., the S/Zn ratio is non-chondritic.

PRELIMINARY DATA ON TWO NEW RUMURUTI CHONDRITES FROM NORTHWEST AFRICA

Moggi-Cecchi V.*[1], Pratesi G.[1-2], Caporali S.[3] & Carli C.[4]
[1] Museo di Storia Naturale, Università di Firenze, Italy
[2] Dipartimento di Scienze della Terra, Università di Firenze, Italy
[3] Dipartimento di Chimica, Università di Firenze, Italy
[4] Istituto di Astrofisica e Planetologia Spaziali, Istituto Nazionale di Astrofisica, Roma, Italy
Corresponding email: vanni.moggicecchi@unifi.it

Keywords: meteorites, chondrites, Rumuruti

Two stones, weighing 149 and 433 respectively, were purchased in 2016 by Nicola Castellano and Mario Di Martino, respectively, from a Moroccan dealer (field labels C139 and DiMart2015-4). The outer surfaces of both main masses display a partial black fusion crust. The cut surfaces reveal a chondritic texture, with metal spots and chondrules set in a silicate matrix. The type specimens, weighing 20,6 and 38 g, respectively, are at the Museo di Storia Naturale dell'Università di Firenze, while the masses are with owners. SEM analyses have been performed at the Dipartimento di Chimica of the University of Florence by means of a Hitachi SEM, while EMPA-WDS analyses at the Firenze IGG–CNR laboratories with a Jeol microprobe. Both the thin sections show a marked chondritic texture consisting of well-defined, small (up to 0.9 mm) chondrules as well as chondrule and mineral fragments set in a slightly recrystallized matrix of silicates and sulfides. Chondrules account for about 60 % of the section by area and are of various textural types, the most common being PO, POP, and poikilitic pyroxene, while RP are rare. Silicate phases, both in the matrix and among fragments, are mainly represented by olivine, orthopyroxene and diopside. Opaque phases, mainly pentlandite, form globular aggregates about 240 μm in size or continuous rims made of tiny grains around chondrules. Both meteorites appear unbrecciated in the thin sections studied, and the poor matrix-chondrules integration suggests a petrologic type 4. Both shock and weathering features are not marked, pointing to a S1 and W2 for C139 and similar features (S2; W2) for DiMart2015-4. SEM and EMPA analyses show that olivine is slightly inhomogeneous and ranges from $Fa_{19.1}$ mol.% to $Fa_{26.1}$ mol.% (mean $Fa_{24.7}$) for C139 and from $Fa_{22.4}$ mol.% to $Fa_{31.5}$ mol.% (mean Fa_{27}) for DiMart2015-4, while low-Ca pyroxene displays a wide compositional variation, ranging from Fs_{11} mol.% to $Fs_{21.2}$ mol.% (mean $Fs_{14.4}$) for C139 and from $Fs_{13.1}$ mol.% to $Fs_{22.8}$ mol.% (mean $Fs_{19.0}$) for DiMart2015-4. Textural and compositional data (Greenwood et al., 2000) and the similarities with other R chondrites (Schulze et al., 1994; Weisberg et al., 1991) point to a classification of both meteorites as R4.

Greenwood, J.P., Rubin, A.E., Wasson, J.T. (2000): Oxygen isotopes in R-chondrite magnetite and olivine: links between R chondrites and ordinary chondrites. *Geochim. Cosmochim. Acta*, **64**, 3897-3911.

Schulze, H., Bischoff, A., Palme, H., Spettel, B., Dreibus, G., Otto, J. (1994): Mineralogy and chemistry of Rumuruti: The first meteorite fall of the new R chondrite group. *Meteor. Planet. Sci.*, **29**, 275-286.

Weisberg, M.K., Prinz, M., Kojima, H., Yanai, K., Clayton, R.N., Mayeda, T.K. (1991): The Carlisle Lakes-type chondrites - A new grouplet with high $\delta^{17}O$ and evidence for nebular oxidation. *Geochim. Cosmochim. Acta*, **55**, 2657-2669.

PRE-TERRESTRIAL SHOCK METAMORPHISM AND EXPERIMENTAL SHOCK-WAVE LOADING IN THE METEORITE MINERALS

Muftakhetdinova R.*[1], Grokhovsky V.[1] & Petrova E.[1]
[1] Institute of Physics and Technology, Ural Federal University, Yekaterinburg, Russia
Corresponding email: gizrozka91@bk.ru

Keywords: meteoritic minerals, shock, deformation effects

A complete view of the evolution of the Solar system is not possible without an understanding of the impact processes. The meteorites retained traces of the space history in their structure and composition.

This work focuses on the study of physical properties, structures and fracture features of different type extraterrestrial substance both as pre-terrestrial shock events, both as after experimental shock loading. The iron octahedrite Sikhote-Alin (IIAB), ataxite Chinga (IVB), ordinary chondrites Chelyabinsk LL5 and Tsarev L5 before and after shock waves loading were investigated using optical microscope Axiovert 40 MAT and SEM Zeiss SIGMA VP.

The most common extraterrestrial minerals are kamacite, taenite, phosphide, sulfide, olivine, pyroxene, chromite, etc. The shock interaction processes between meteoroids bodies in the space as far as between meteoroids and the atmosphere, and the Earth surface are usually accompanied by the high pressures and temperatures. These processes led to meteorites minerals structure changing. Shock effects in meteorites were observed as: Neumann bands, plastically deformed metal grains, brittle fractures of phosphides, slip lines and fragmented structure. The formation of shock remelting zones, shock veins, darkening of minerals ("shock blackening"), mosaicism and planar deformation structures in olivine and the high-pressure ε-phase were observed at a high intensity shock stages (Axon, 1969; Stoffler et al., 1991; Grokhovsky et al., 2000; Wang et al., 2013).

The unique spherically converging shock waves loading experiments provided the wide range of pressures and temperatures in the sample. Our shock-wave loading experiments on meteorites matter revealed all shock structure changes mentioned above. The sample of the Sikhote-Alin meteorite showed traces of $\alpha \rightarrow \varepsilon \rightarrow \alpha$ transformation after a strong explosion loading with the converging shock waves.

This work was supported in part by RFBR grant No 15-35-21164.

Axon, H.J. (1969): Pre-Terrestrial deformation effects in iron meteorites. *in* "Meteorite research", P.M. Millman, ed., Reidel, Dordrecht, 796-805.

Grokhovsky, V.I., Kozlov, E.A., Kuzina, M.S., Teplov, V.A. (2000): Shock experiment in spherical wales with iron meteorites. *Meteor. Planet. Sci.*, **35**, À66.

Stoffler, D., Keil, K., Scott, E.R.D. (1991): Shock metamorphism of ordinary chondrites. *Geochim. Cosmochim. Acta*, **55**, 3845-3867.

Wang, S.J., Sui, M.L, Chen, Y.T., Lu, Q.H., Ma, E., Pei, X.Y, Li, Q.Z., Hu, H.B. (2013): Microstructural fingerprints of phase transitions in shock-loaded iron. *Sci. Rep.*, **3**, 01086-1- 01086-6.

NEW INSIGHTS ON THEO'S FLOW LAVA USING INTRACRYSTALLINE THERMOMETRY ON AUGITES

Murri M.*[1], Scandolo L.[1], Fioretti A.M.[2], Nestola F.[3], Domeneghetti M.C.[1] & Alvaro M.[1]
[1] Dipartimento di Scienze della Terra e dell'Ambiente, Università di Pavia, Italy
[2] Istituto di Geoscienze e Georisorse, Consiglio Nazionale delle Ricerche, Padova, Italy
[3] Dipartimento di Geoscienze, Università di Padova, Italy
Corresponding email: mara.murri01@universitadipavia.it

Keywords: augite, Fe-Mg exchange reaction, lava flow

Terrestrial analogues are often investigated to get insight into the geologic evolution and magmatic processes of planetary bodies. Theo's flow (Ontario, Canada) is a 120 m thick magmatic unit containing (bottom to top) the following layers: peridotite (up to 9 m), clinopyroxenite (up to 60 m), gabbro (up to 40 m) and hyaloclastite (up to 10 m thick). The pyroxenite is regarded as the best terrestrial analogue of nakhlite, including Miller Range (MIL) 03346 (Domeneghetti et al., 2013; Alvaro et al., 2015; Treiman 2005).

Based on a careful petrological and stratigraphic analysis Lentz et al., (2011) concluded that the lithologic diversity observed in Theo's flow (TS) results from a differentiation processes of a single, thick magma pulse, and was not generated by multiple magmatic injections of distinct composition. Their conclusion is mainly based on the absence of sharp boundaries between adjacent units and on the progressive compositional changes observed in mineral and bulk-rock compositions (Lentz et al., 2011). These authors also observed that the average composition of the whole magmatic pile matches the average composition of the top, quenched hyaloclastite. Given the analogies of the clinopyroxenite with Martian lava flows, the mechanism and timing of differentiation of Theos's flow is of great interest and yet, it is still not fully understood thus deserving further investigation.

Aiming at better understanding magmatic evolution and the cooling history of whole Theo's flow, we use a geothermometric calibration to calculate the equilibrium closure temperature (T_c) of the Fe^{2+}-Mg intracrystalline exchange reaction between M1 and M2 sites in augites separated from four samples collected at the lower (TSC 3.9; TSC 3.12), middle (TSC 3.22) and upper (TSC 3.31) part of the flow. All selected clinopyroxene have Fs composition within the compositional range reported in Murri et al. (2016) calibration.

For each crystal we performed a high-resolution single-crystal X-ray diffraction analysis followed by structural refinement. The resulting T_c, calculated for all investigated clinopyroxenes, are almost identical within error (682°C ± 30) and are also similar to the clinopyroxene T_c previously obtained from TS7 Theo's sample (Domeneghetti et al., (2013) located in lower middle part of the flow. This relatively uniform T_c appears inconsistent with the differential cooling rate expected for samples collected at significantly different height (bottom to top) across a ca. 120 thick lava flow and cannot support a scenario of a single magma unit differentiated *in situ*.

Acknowledgments: MM and MA have been funded by the MILE DEEp project (RBSI140351) to M. Alvaro. MCD has been funded by the PEA13 grant to L. Folco. F.N. has been funded by the INDIMEDEA ERC starting grant (#307322) to F. Nestola. We thank Allan Treiman for kindly supplying Theo's Flow samples. The authors wish to thank the Department of Mineral Sciences, Smithsonian Institution for providing Theo's Flows samples (MMNH7255).

Alvaro, M., Domeneghetti, M.C., Fioretti, A.M., Cámara, F., Marinangeli, L. (2015): Thermal history of nakhlites: a new geothermometer for augites. *Meteor. Planet. Sci.*, **50**, 499-507.

Domeneghetti, M.C., Fioretti, A.M., Cámara, F., McCammon, C., Alvaro, M. (2013):Thermal history of nakhlites: A comparison between MIL 03346 and its terrestrial analogue Theo's flow. *Geochim. Cosmochim. Acta*, **121**, 571-581.

Lentz, R.C.F., McCoy, T.J., Collins, L.E., Corrigan, C.M., Benedix, G.K., Taylor, G.J., Harvey, R.P. (2011): Theo's Flow, Ontario, Canada: A terrestrial analog for the Martian nakhlite meteorites. *in* "Analogs for planetary Exploration" W.B. Garry, J.E. Bleacher, eds., Geological Society of America, 263-277.

Murri, M., Scandolo, L., Fioretti, A.M., Nestola, F., Domeneghetti, M.C., Alvaro, M. (2016): The role of Fe content on the Fe-Mg exchange reaction in augite. *Am.Mineral.*, in press.

Treiman, A.H. (2005): The nakhlite meteorites: Augite-rich igneous rocks from Mars. *Chem. Erde - Geochem.*, **65**, 203-270.

SPECTRAL CLASSIFICATION AND MINERALOGICAL CHARACTERIZATION OF NILI FOSSAE (MARS) FOR A BETTER UNDERSTANDING OF HYDRATED MINERALOGIES

Serventi G.*[1], Carli C.[2], Altieri F.[2], Geminale A.[2], Sgavetti M.[1], Grassi D.[2], Orosei R.[3] & Bellucci G.[2]
[1] Dipartimento di Fisica e Scienze della Terra "Macedonio Melloni", Università di Parma, Italy
[2] Istituto di Astrofisica e Planetologia Spaziali, Istituto Nazionale di Astrofisica, Roma, Italy
[3] Istituto di Radioastronomia, Istituto Nazionale di Astrofisica, Bologna, Italy
Corresponding email: giovanna.serventi@unipr.it

Keywords: mars, reflectance spectroscopy, hydrated minerals

The presence of hydrated minerals on Mars provides a record of water-related processes and, in particular, the identification of phyllosilicates puts constraints on the evolution of Mars (Poulet et al., 2005). Even if data from the Observatoire pour la Minèralogie, l'Eau, les Glaces, et l'Activitè (OMEGA, Bibring et al., 2004) and from the Compact Reconnaissance Imaging Spectrometer for Mars (CRISM, Murchie et al., 2007) showed the presence of different hydrated minerals, on Mars the spectral regions where hydrated minerals absorb are also affected by an atmosphere dominated by CO_2 and H_2O. Among the different methods that have been proposed to separate the atmospheric signature from the surface, we consider the Surface Atmosphere Separation (SAS) method recently proposed by Geminale et al. (2015). This method is based on the principal component analysis and target transformation from the analyzed data set, while in the standard approach (Langevin et al., 2005) the atmosphere is removed by the division of a scaled atmospheric spectrum measured across Olympus Mons.

In this work, we propose a mineralogical interpretation of the Nili Fossae region, considering SAS corrected OMEGA data and we compare results with previous interpretations (e.g., Bibring et al. 2005; Mangold et al. 2007; Mustard et al. 2007). In particular, we first spectrally classify the region using the Spectral Angle Mapping (SAM; Kruse et al., 1993) classification with a spectral library iteratively built from the image. Then, applying the Modified Gaussian Model (MGM; Sunshine et al., 1990), we deeply investigate the electronic and molecular absorptions between 0.7-2.5mm. Mainly, we recognized five spectral regions dominated by: iron-hydroxides, pyroxenes (both orthopyroxene and clinopyroxene), olivine and phyllosilicates. We focused on the hydrated mineralogy: overtone absorptions in the 1.9-2.3 μm are fundamental to recognize different mineralogies, and to discriminate between phyllosilicates characterized by different cations in the octahedral environment. In particular, by MGM deconvolution, we recognize regions where are present montmorillonite (Al-OH), nontronite (Fe^{3+}-OH), chamosite (Fe^{2+}-OH) and their mixtures. These minerals indicate particular environments and formation conditions: for example, montmorillonite and nontronite are typical of alkaline conditions abundant in Ca or Na, but the second is more enriched in Fe (Bishop et al., 2008), probably indicating different bedrocks. On the other hand, the presence of chamosite could be related to hydrothermal alteration of igneous rocks. We also recognized a region characterized by spectra typical of olivine with associated OH modes, probably indicating alteration processes.

Bibring, J.-P., Soufflot, A., Berthé, M., Langevin, Y., Gondet, B., Drossart, P., Bouyé, M., Combes, M., Puget, P., Semery, A., Bellucci, G., Formisano, V., Moroz, V., Kottsov, V., Bonello, G., Erard, S., Forni, O., Gendrin, A., Manaud, N., Poulet, F., Poulleau, G., Encrenaz, T., Fouchet, T., Melchiori, R., Altieri, F., Ignatiev, N., Titov, D., Zasova, L., Coradini, A., Capaccioni, F., Cerroni, P., Fonti, S., Mangold, N., Pinet, P., Schmitt, B., Sotin, C., Hauber, E., Hoffmann, H., Jaumann, R., Keller, U., Arvidson, R., Mustard, J., Forget, F. (2004): OMEGA: Observatoire pour la Minéralogie, l'Eau, les Glaces et l'Activité. *in*: "Mars Express: The scientific payload" A. Wilson, ed., ESA Publications Division, Noordwijk, 37-49.

Bibring, J.-P., Langevin, Y., Gendrin, A., Gondet, B., Poulet, F., Berthé, M., Soufflot, A., Arvidson, R., Mangold, N., Mustard, J., Drossart, P. (2005): Mars surface diversity as revealed by the OMEGA/Mars Express observations. *Science*, **307**, 1576.1581.

Bishop, J.L., Lane, M.D., Dyar, M.D., Brown, A.J. (2008): Reflectance and emission spectroscopy study of four groups of phyllosilicates: Smectites, kaolinite-serpentines, chlorites and micas. *Clay Miner.*, **43**, 35–54.

Geminale, A., Grassi, D., Altieri, F., Serventi, G., Carli, C., Carrozzo, F.G., Sgavetti, M., Orosei, R., D'Aversa, E., Bellucci, G., Frigeri, A. (2015): Removal of atmospheric features in near infrared spectra by means of principal components analysis and target transformation on Mars: I. Method. *Icarus*, **253**, 51-65

Kruse, F.A., Lefkoff, A.B., Boardman, J.W., Heidebrecht, K.B., Shapiro, A.T., Barloon, P.J., Goetz, A.F.H. (1993): The Spectral Image Processing System (SIPS) - Interactive visualization and analysis of imaging spectrometer data. *Remote Sens. Environ.*, **44**, 145-163.

Langevin, Y., Poulet, F., Bibring, J.P., Gondet, B. (2005): Sulfates in the north polar region of Mars detected by OMEGA/Mars Express. *Science*, **307**, 1584-1586.

Mangold, N., Poulet, F., Mustard, J. F., Bibring, J.-P., Gondet, B., Langevin, Y., Ansan, V., Masson, P., Fassett, C., Head III, J.W., Hoffmann, H., Neukum, G. (2007): Mineralogy of the Nili Fossae region with OMEGA/Mars Express data: 2. Aqueous alteration of the crust. *J. Geophys. Res.*, **112**, E8.

Murchie, S., Arvidson, R., Bedini, P., Beisser, K., Bibring, J.-P., Bishop, J. Boldt, J., Cavender, P. Choo, T., Clancy, R.T., Darlington, E.H., Des Marais, D., Espiritu, R., Fort, D., Green, R., Guinness, E., Hayes, J., Hash, C., Heffernan, K., Hemmler, J., Heyler, G., Humm, D., Hutcheson, J., Izenberg, N., Lee, R., Lees, J., Lohr, D., Malaret, E., Martin, T., McGovern, J.A., McGuire, P., Morris, R., Mustard, J., Pelkey, S., Rhodes, E., Robinson, M., Roush, T., Schaefer, S., Seagrave, G., Seelos, F., Silverglate,P., Slavney, S., Smith, M., Shyong, W.-J., Strohbehn, K., Taylor, H., Thompson, P., Tossman, B., Wirzburger, M., Wolff, M. (2007): Compact Reconaissance Imaging Spectrometer for Mars (CRISM) on Mars Reconaissance Orbiter (MRO). *J. Geophys. Res.*, **112**, E5.

Mustard, J.F., Poulet, F., Head, J.W., Mangold, N., Bibring, J.-P., Pelkey, S.M., Fassett, C.I., Langevin, Y., Neukum, G. (2007): Mineralogy of the Nili Fossae region with OMEGA/Mars Express data: 1. Ancient impact melt in the Isidis Basin and implications for the transition from the Noachian to Hesperian. *J. Geophys. Res.*, **112**, E08S03.

Poulet, F., Bibring, J.-P., Mustard. J.F., Gendrin, A., Mangold, N., Langevin, Y., Arvidson, R.E., Gondet, B., Gomez, C., Berthé, M., Erard, S., Forni, O., Gondet, B., Manaud, N., Poulleau, G., Soufflot, A., Combes, M., Drossart, P., Encrenaz, T., Fouchet, T., Melchiorri, R., Bellucci, G., Altieri, F., Formisano, V., Fonti, S., Capaccioni, F., Cerroni, P., Coradini, A., Korablev, O., Kottsov, V., Ignatiev, N., Titov, D., Zasova, L., Pinet, P., Schmitt, B., Sotin, C., Hauber, E., Hoffmann, H., Jaumann, R., Keller, U., Forget, F. (2005): Phyllosilicates on Mars and implications for early martian climate. *Nature*, **438**, 623-627.

Sunshine, J.M., Pieters, C.M., Pratt, S.F. (1990): Deconvolution of mineral absorption bands: an improved approach. *J. Geophys. Res.*, **95**, 6955-6966.

ALKALI FELDSPAR CRYSTALS FROM MORASKO IAB IRON METEORITE: PRODUCT OF MAGMA DIFFERENTIATION, METASOMATISM OR PROJECTILE - TARGET MATERIAL INTERACTION

Słaby E.*[1], Karwowski Ł.[2], Majzner K.[3], Wirth R.[4], Muszyński A.[5], Simon K.[6], Domonik A.[7], Moszumańska I.[1], Schreiber A.[4] & Orłowski R.[1]

[1] Institute of Geological Sciences, Polish Academy of Sciences, Warsaw, Poland
[2] Faculty of Earth Sciences, University of Silesia, Katowice, Poland
[3] Faculty of Chemistry, Raman Imaging Group, Jagiellonian University, Kraków, Poland
[4] Helmholtz Zentrum Potsdam, GFZ Deutsches GeoForschungsZentrum, Potsdam, Germany
[5] Institute of Geology, Adam Mickiewicz University, Poznań, Poland
[6] Abteilung Geochemie, Georg-August-Universität, Göttingen, Germany
[7] Institute of Hydrogeology and Engineering Geology, University of Warsaw, Poland
Corresponding email: e.slaby@twarda.pan.pl

Keywords: alkali feldspar, trace elements, growth texture

Alkali feldspar crystals have been recognized in the troilite-graphite nodules of the Morasko IAB iron meteorite. Their chemical, microtextural and structural properties have been studied with the use of Electron Microprobe Analysis (EMPA), Laser Ablation Inductively Coupled Plasma Mass Spectrometry LA-ICP-MS, Transmission Electron Microscope (TEM) and Raman spectroscopy. The feldspars occur as perthitic or antiperthitic intergrowth, whereas the albite lamellae are perfectly twinned. The structural properties reveal intergrown phases with fairly disordered patterns. The EMP analyses demonstrated that the intergrown phases are mainly rich in sodium or potassium, resulting in near albite or orthoclase compositions. The calculated compositions, on the basis of a segmented perthite-antiperthite image, indicate that the Or-to-Ab proportions in the homogenized crystals were almost 0.3:0.7, thus suggesting anorthoclase crystallizing under high-temperature conditions. Much more extensive information was obtained through an LA-ICP-MS study. Large ion lithophile elements LILEs were chosen (e.g., Ba, Sr, Rb, LREE, Pb, and Ga) to track the origin of the crystals. Their concentrations indicate crystallization from a melt strongly depleted in LILEs.

There is no unique solution for feldspar origin. Alkali feldspar might be a product of a highly differentiated melt. In such a case the progressive evolution of the melt should result in enrichment in LILEs, which is not the case. The melt that crystallized the feldspar cannot be related to impact-induced partial melting of the chondritic material alone. The crystallization product of such a melt should be plagioclase. Assuming that plagioclase is replaced due to high temperature metasomatism, some relics of primary phase are expected. We suppose magmatic origin of alkali feldspar. The derived melt is probably contaminated by silica-rich target material during the IAB projectile – target material interaction and accompanied by metal and sulfide melts that are both immiscible with a silicate melt.

MODELLING OF HT-IR SPECTRA OF FORSTERITE FOR REMOTE SENSING

Stangarone C.*[1], Tribaudino M.[1], Prencipe M.[2], Helbert J.[3], Maturilli A.[3], D'Amore M.[3] & Ferrari S.[4]
[1] Dipartimento di Fisica e Scienze della Terra "Macedonio Melloni", Università di Parma, Italy
[2] Dipartimento di Scienze della Terra, Università di Torino, Italy
[3] Institut für Planetenforschung, Deutschen Zentrums für Luft- und Raumfahrt, Berlin, Germany
[4] Centro di Ateneo di Studi e Attività Spaziali "G. Colombo", Università di Padova, Italy
Corresponding email: claudia.stangarone@studenti.unipr.it

Keywords: forsterite, *ab initio* modelling, IR spectroscopy

Spectral signatures of minerals are intimately related to the crystal structure; therefore, they may represent a remote sensing model to determine surface composition of planetary bodies, analysing their spectral reflectance and emission. For Planetary surfaces, which are influenced by extreme environmental conditions as Mercury, which is the closest planet to the sun, data interpretation must take into account changes in spectral characteristics induced by the high temperatures conditions (Helbert et al., 2013). In this work, we study experimental thermal emissivity spectra with an innovative approach: we calculate IR spectra, with ab initio methods, of the main mineral families that presumably compose the surface of Mercury and we compare them with high temperature laboratory measurements. The goal is to interpret the high temperature infrared (HT-IR) emissivity spectra that will be collected by the Mercury Radiometer and Thermal infrared Imaging Spectrometer (MERTIS), the spectrometer developed by DLR that will be on board of the ESA BepiColombo Mercury Planetary Orbiter (MPO) (Helbert et al., 2010). The approach was firstly used on olivine (Sprague et al., 2009), one of the possible major phases in the surface of Mercury. A natural sample of olivine ($Fo_{\#90}$) has been studied at Planetary Spectroscopy Laboratory (PSL; Maturilli et al., 2016). The emissivity of the sample has been measured at different steps of temperature by means of a planetary simulation chamber that has the unique capability to heat samples to temperatures up to 1000 K. IR reflectance spectra of forsterite has been then simulated using the Hybrid HF/DFT Hamiltonian WC1LYP (Lee et al., 1988; Wu & Cohen, 2006), by means of the CRYSTAL code (Dovesi et al., 2013). IR vibrational frequencies at high temperature are calculated evaluating the vibrational frequencies at the Γ point of first BZ of the unit cell at different volumes corresponding to increasingly higher temperatures. Thus, in order to simulate extreme environmental conditions, IR frequencies and intensity has been calculated for volumes estimated at 0, 300 and 1000 K (taking into account zero point effects). The comparison with the experiment reveals that such computational approach can reliably be used to predict band shifts due to temperature: a significant good agreement between measurements and simulated data is shown, especially within the spectral range 1200-600 cm^{-1}.

Dovesi, R., Saunders, V.R., Roetti, C., Orlando, R., Zicovich-Wilson, C.M., Pascale, F., Civalleri, B., Doll, K., Harrison, N.M., Bush, I.J., D'Arco, P., Llunell, M., Causà, M., Noël, Y. (2014): CRYSTAL14 user's manual. University of Torino, 382 p.

Helbert, J., Hiesinger, H., Walter, I., Säuberlich, T., Maturilli, A., D'Amore, M., Knollenberg J., Lorenz E., Peter G., Arnold, G.E. (2010): MERTIS: understanding Mercury's surface composition from mid-infrared spectroscopy. *in*"SPIE Optical Engineering Applications", International Society for Optics and Photonics, 78080J-78080J.

Helbert, J., Nestola, F., Ferrari, S., Maturilli, A., Massironi, M., Redhammer, G.J., Capria, M.T., Carli, C., Bruno, M. (2013): Olivine thermal emissivity under extreme temperature ranges: Implication for Mercury surface. *Earth Planet. Sci. Letters*, **371**, 252-257.

Lee, C., Yang, W., Parr, R.G. (1988): Development of the Colle-Salvetti correlation-energy formula into a functional of the electron density. *Phys Rev. B*, **37**, 785.

Maturilli, A. & Helbert, J. (2016): The Planetary Spectroscopy Laboratory (PSL): Spectral Measurements of Planetary Analogues from UV to FIR. *Lunar Planet. Sci. Conf.*, **47**, 1986.

Sprague, A.L., Hanna, K.D., Kozlowski, R.W.H., Helbert, J., Maturilli, A., Warell, J.B., Hora, J.L. (2009): Spectral emissivity measurements of Mercury's surface indicate Mg-and Ca-rich mineralogy, K-spar, Na-rich plagioclase, rutile, with possible perovskite, and garnet. *Planet. Space Sci.*, **57**, 364-383.

Wu, Z. & Cohen, R.E. (2006): More accurate generalized gradient approximation for solids. *Phys. Rev. B*, **73**, 235116.

CONDENSATION TEMPERATURES OF VOLATILE ELEMENTS AND THEIR ABUNDANCES IN SILICATE EARTH

Wood B.*[1] & Harrison T.[1]
[1] Department of Earth Sciences, University of Oxford, United Kingdom
Corresponding email: bernie.wood@earth.ox.ac.uk

Keywords: volatility, condensation temperature, thermodynamic data

The temperature of condensation of the elements from a gas of solar composition at low pressure (~ 10^{-4} bar) is commonly used as a guide to understanding their abundances in the silicate Earth. For this exercise the abundance of each element in the Earth is generally normalised to that in CI chondrites in order to remove pre-solar nucleosynthetic differences. Thus we find that silicate Earth has approximately constant abundances (ratioed to CI) of lithophile elements (e.g., Ca, Sc, Al, REE) with condensation temperatures (of 50% of the mass of the element) above ~ 1420 K. There are superimposed depletions in siderophile and chalcophile elements which are predominantly related to core formation. For elements which condense at lower temperatures there is a clear trend of decreasing abundance with decreasing 50% condensation temperature. The Earth is clearly volatile-depleted relative to CI chondrites and considerable energy is expended trying to understand deviations from a smooth volatile depletion pattern. For example, Ag and Cu have similar condensation temperatures (Lodders, 2003) but Ag is 6 times more depleted than Cu in silicate Earth. Indium is anomalously "overabundant" and Zn three times more abundant than Pb despite identical condensation temperatures.

In order to examine the meaningfulness of condensation temperature in the context of elemental abundance we have re-examined the results of Lodders (2003) for 30 elements of differing volatility. This task was complicated by the fact that her software and database are proprietry and the assumptions made in terms of solid solution properties are not explicitly stated in Lodders (2003). Nevertheless we were able to reconstruct and reproduce many of her results. Some important differences help to resolve the anomalies discussed above. For example we obtain a 50% condensation temperature of 1047 K for Cu (Lodders-1037) but only 730 K for Ag (Lodders-996K) thus explaining differences in relative abundance. Pb is found to condense at significantly lower temperature than Zn which is also significant in the terms of abundances. Indium, however, remains stubbornly volatile with a condensation temperature of ~ 530 K.

We think it likely that the high abundance of In in silicate Earth occurs due to its dissolution in silicate melts and crystals rather than in the metals and sulfides assumed in the condensation calculations. Although there are no free energy data for Indium silicates, our parallel experiments (Norris & Wood, 2016) indicate that In is much less volatile in volcanic systems then its condensation temperature would imply.

Lodders, K. (2003): Solar system abundances and condensation temperatures of the elements. *Astrophys. J.*, **591**, 1220-1247.

Norris, C.A. & Wood, B. (2016): Measured volatilities of important trace elements in the Earth. This meeting.

LINEAR Hf ISOTOPE-AGE ARRAYS OF ARCHEAN CRUSTAL ROCKS: WHAT DO THEY REFLECT? AN EXAMPLE FROM THE PIETERSBURG BLOCK (SOUTH AFRICA)

Zeh A.*[1] & Laurent O.[2]
[1] Institut für Angewandte Geowissenschaften, Karlsruhe Institut für Technologie, Germany
[2] Department de Géologie, Université de Liège, Belgium
Corresponding email: armin.zeh@kit.edu

Keywords: Archean, crust differentiation, U-Pb-Hf isotopes

Combined U-Pb and Lu-Hf isotope data from zircon populations are widely used to constrain Hadean-Archean crustal evolution. Linear Hf isotope-age arrays are interpreted to reflect the protracted, internal reworking of crust derived from the (depleted) mantle during a short-lived magmatic event, and related $^{176}Lu/^{177}Hf$ ratios are used to constrain the composition of the reworked crustal reservoir. Results of this study, however, indicate that linear Hf isotope-age arrays can also result from complex geodynamic processes and crust-mantle interactions, as shown by data from geochemically well characterized granitoids of the Pietersburg Block (PB), northern Kaapvaal Craton (South Africa).

Most granitoids (and rare K-rich gabbros) of the PB with ages between 2.94 and 2.05 Ga (n = 32) plot on a linear Hf isotope-age array with very low $^{176}Lu/^{177}Hf$ of 0.0022 (TTG-like), although they show a wide compositional range, were derived from various sources and emplaced successively in different geodynamic settings. The crustal evolution occurred in five successive stages: (I) predominately mafic crust formation in an intra-oceanic environment (3.4-3.0 Ga); (II) voluminous TTG crust formation in an early accretionary orogen (3.0-2.92 Ga); (III) internal TTG crust reworking and subduction of TTG-derived sediments in an Andean-type setting (2.89-2.75 Ga); (IV) (post-)collisional high-K magmatism derived from a metasomatized mantle source (2.71-2.67 Ga); and (V) alkaline magmatism in an intra-cratonic environment (2.05-2.03 Ga).

The linear array results from voluminous TTG crust formation during stage II, and involvement of this crust during all subsequent stages by two different processes: (i) internal crust reworking through both partial melting and assimilation at 2.89–2.75 Ga, leading to the formation of biotite granites coeval with minor TTGs, and (ii) subduction of TTG-derived sediments underneath the PB, causing enrichment of the mantle that subsequently became source for high-K granitoids and mafic rocks at 2.68 and 2.05 Ga. Some scatter along the array might have resulted either from assimilation of ancient crust, intracrustal Lu/Hf fractionation or melting of heterogeneous mantle sources. The results show that without any information about the nature and composition of zircon-hosting granitoids, Hf isotope-age arrays are of limited use to constrain Hadean-Archean magmatogenesis and geodynamics.

Session S19:

Gem materials

Conveners:

Gaston Giuliani (Vandœuvre-lès-Nancy – France)

Lee A. Groat (Vancouver – Canada)

Federico Pezzotta (Milano – Italy)

CHARACTERIZATION OF BLUE BANDED CHALCEDONY (AGATE) FROM YOZGAT PROVINCE, TURKEY

Adamo I.*[1], Zullino A.[1], Lorenzi R.[2], Prosperi L.[1] & Akkas B.[3]
[1] Istituto Gemmologico Italiano, Milano, Italy
[2] Dipartimento di Scienza dei Materiali, Università di Milano-Bicocca, Italy
[3] Izmir, Turkey
Corresponding email: ilaria.adamo@igi.it

Keywords: chalcedony, agate, moganite

Chalcedony is a micro- or crypto-crystalline form of silica that occurs in a wide variety of patterns and colours. The name agate is used for the variety that displays a distinct banding with successive different coloured layers (O'Donoghue, 2006). The different varieties of chalcedony have been used for a long time as gemstones in jewellery and as carving materials for producing ornamental objects. Chalcedony, including agate, occurs in every part of the world, in widespread geological environments. Turkey has been known since ancient times as an important source of various coloured gem quality chalcedony (Hatipoğlu et al., 2013). Purplish blue banded chalcedony (agate) coming from Middle Eocene andesitic volcanic rocks in the Yozgat Province, northeast of central Anatolia, has recently been made available in the gem market.

This study aims to provide a gemmological and mineralogical characterization of the agates from this locality investigating a set of gem-quality cut and rough samples by means of traditional gemmological tests, combined with X-ray powder diffraction (XRPD), confocal micro-Raman spectroscopy, and trace elements determination by means of laser ablation inductively coupled plasma mass spectroscopy (LA-ICP-MS).

The investigated samples show the rolling flow structure typical for agate, with alternating purplish blue and white bands. XRPD and Raman spectroscopy show that the silica phases occurring in agates from this locality are α-quartz and moganite, a recently discovered monoclinic polymorph of SiO_2 (Miehe & Graetsch, 1992), which is commonly intergrown with quartz in chalcedony. The moganite content is heterogeneous across a single sample, showing the maximum XRPD and Raman peaks intensity in correspondence with the blue bands. The variations in the moganite-to-quartz ratio along a section perpendicular to the banding were estimated from the intensity ratios of the main Raman symmetric stretching-bending modes of α-quartz (465 cm^{-1}) and moganite (502 cm^{-1}), according to Kingma & Hemley (1994). The moganite/quartz ratio is not uniform but shows a cyclic pattern that well correlates with the rhythmically banded structure of the agate samples. The cyclic variation of the moganite content in agates is a feature that is connected to the mechanism of agate genesis (Götze et al., 1998). LA-ICP-MS analyses showed that trace elements are present in very low concentrations and with a homogeneous distribution over the section perpendicular to the agate banding. Iron is the only chromophore element exceeding 10 ppm that we found in these agates. The relatively constant iron amount across the different coloured banding makes the understanding of the causes of colour of this blue chalcedony a hard challenge and further investigations are in progress.

Götze, J., Nasdala, L., Kleeberg, R., Wenzel, M. (1998): Occurrence and distribution of "moganite" in agate/chalcedony: a combined micro-Raman, Rietveld, and cathodoluminescence study. *Contrib. Mineral. Petrol.*, **133**, 96-105.

Hatipoğlu, M., Chamberlain, S.C., Kibici, Y. (2013): Characterization of the Sündikendağı deposit of moganite-rich, blue chalcedony nodules, Mayislar-Saricakaya (Eskişehir). *Ore Geol. Rev.*, **54**, 127–137.

Kingma, K.J. & Hemley, R.J. (1994): Raman spectroscopic study of microcrystalline silica. *Am. Mineral.*, **79**, 269-273.

Miehe, G. & Graetsch, H. (1992): Crystal structure of moganite: a new structure type for silica. *Eur. J. Mineral.*, **4**, 693-706.

O'Donoghue, M. (2006): Gems. Butterworth-Heinemann., Oxford, 873 p.

THE GEM ANDRADITE FROM ANTETEZAMBATO, NORTHERN MADAGASCAR: NEW MINERALOGICAL AND GEOCHEMICAL DATA

Andriamamonjy A.*[1], Giuliani G.[2], Razafindratsimba S.N.[1], Fallick A.E.[3] & Chatagnier P.-Y.[4]
[1] Département de Sciences de la Terre et de l'Environnement, Université d'Antananarivo, Madagascar
[2] Centre de Recherches Pétrographiques et Géochimiques, Université de Lorraine, Vandœuvre-lès-Nancy, France
[3] Isotope Geosciences Unit, Scottish Universities Environmental Research Centre, Glasgow, United Kingdom
[4] BOREAL Gemstone Company, Lausanne, Switzerland
Corresponding email: andsalfred@yahoo.com

Keywords: gem andradite, trace elements, oxygen isotopes

The gem garnet deposit occurs in a swampy area of mangroves about 10 km southwest of the village of Antetezambato in the Ambato peninsula (Rondeau et al., 2009). It is a skarn-fracturing type formed by thermal metamorphism due to the intrusion of the Ambato granite and associated volcanic rocks and syenite, in the Liassic sediments of the Isalo Formation. Gem-andradite is found in veinlets, cracks and drusy cavities or as pseudomorphs of coral (Raoul et al., 2015) and ammonite in calcareous and argillaceous sandstone. It is associated with calcite, quartz, chalcedony and zeolite (Pezzotta, 2010).

Two generations of garnet are found: (i) And1 the gem-quality andradite as several mm to 3 cm across crystals; and (ii) And2 microscopic zoned crystals (10 to 300 µm) found either in cavities of dissolution of And1 or in a calcitic gangue at the periphery of And1. And1 contains inclusions of wollastonite, diopside, pyrite and calcite (Pezzotta et al., 2011; this work), and F-apatite with 2 wt.% As_2O_3, F-vesuvianite (up to 2.3 wt.% F) and fluorite (this work). Primary fluid inclusions (FI) in And1 belong to the H_2O-NaCl system (Giuliani et al., 2015). Numerous cavities of dissolution are found in And2 and at the border of And1 crystals.

Trace element contents of both andradites were analyzed by EPMA and ICP-MS with a special focus on the variation of colour from demantoid (green to yellowish green) to topazolite (yellow to brown). And1 is close to pure end-member andradite (99.5 to 90.6 mol. % Adr). Mg and Ti are respectively up to 0.08 and 0.33 wt.%. Ga, Cr, V and Mn are below the detection limit (~ 100 ppm). The Al_2O_3 content increases from 0.11 wt.% for topazolite to 0.51 wt.% for demantoid. ICP-MS data on demantoid and topazolite show an enrichment in light, and depletion in heavy, REE with a positive Eu anomaly as shown by Bocchio et al. (2010). The demantoid and topazolite contain tin (16 < Sn < 89 ppm), arsenic (14 < As < 54) and nickel (14 < Ni < 23). The content of Sn and As decreases from green to brown colour while the reverse is observed for Ni. F content is the same for all colours (0.01 to 0.07 wt.%).

And2 backscattered electron images (BSE) show the strong chemical zoning of the Al-rich crystals with Al_2O_3 contents between 0.4 and 10.5 wt.% (99.8 mol. % Adr to about $Adr_{46}Grs_{54}$). Values of TiO_2, MgO and F are respectively between, 0.01 to 1.47 wt.%, 0.03 to 1.45 wt.%, and 0.08 to 0.57 wt.%. Such inhomogeneous andradite-grossular solid-solution series are characteristic also for andradites related to skarns from Namibia (Bocchio et al., 2010) and Iran (Karimzadeh Somarin, 2004).

The oxygen isotope composition of gem green andradite is between -1.6 and -1.4‰ (VSMOW) (n = 3; mean $\delta^{18}O$ = -1.5±0.1‰). The negative $\delta^{18}O$-values, unusual for garnet, combined with the skarn paragenesis and geometry reflect the probable circulation of low $\delta^{18}O$-meteoric water in the hydrothermal system accompanied with metasomatism and mineral dissolution at shallow depth.

Bocchio, R., Adamo, I., Diella, V. (2010): The profile of trace elements, including the REE, in gem-quality green andradite from classic localities. *Can. Mineral.*, **48**, 1205-1216.

Giuliani, G., Boiron, M.C., Morlot, C., Raoul, J., Chatagnier, P.-Y. (2015): Demantoid garnet with giant fluid inclusion. *Gems Gemol.*, **51**, 446-462.

Karimzadeh Somarin, A. (2004): Garnet composition as an indicator of Cu mineralization: evidence from skarn deposits of NW Iran. *J. Geochem. Explor.*, **81**, 47-57.

Pezzotta, F. (2010): Andradite from Antetezambato, North Madagascar. *Mineral. Rec.*, **41**, 209-229.

Pezzotta, F., Adamo, I., Diella, V. (2011): Demantoid and topazolite from Antetezambato, Northern Madagascar: Review and new data. *Gems Gemol.*, **47**, 2-14.

Raoul, J., Chatagnier, P.-Y., Fritsch, E., Rondeau, B., Segura, O. (2015): Pseudomorphes de fossiles en andradite démantoïde, Antetezamabato, Madagascar. *Règne Minéral*, **123**, 21-26.

Rondeau, B., Mocquet, B., Lulzac, Y., Fritsch, E. (2009): Les nouveaux grenats démantoïdes d'Ambanja, province d'Antsiranana, Madagascar. *Règne Minéral*, **90**, 41-46.

THE CONTRIBUTION OF MAJOR AND TRACE ELEMENTS IN THE EMERALD-DEPOSITS CLASSIFICATION SCHEME: STATISTICAL TREATMENT OF EMPA AND SIMS DATA

Aurisicchio C.[1], Conte A.M.[1], De Vito C.[2], Medeghini L.*[2], Moroz I.[3] & Ottolini L.[4]
[1] Istituto di Geoscienze e Georisorse, Consiglio Nazionale delle Ricerche, Roma
[2] Dipartimento di Scienze della Terra, Sapienza Università di Roma, Italy
[3] Institute of Earth Sciences, Hebrew University of Jerusalem, Israel
[4] Istituto di Geoscienze e Georisorse, Consiglio Nazionale delle Ricerche, Pavia
Corresponding email: laura.medeghini@uniroma1.it

Keywords: emerald deposits, EMP-SIMS-PC analysis

Since ancient times, the mining and exchange of emeralds have been playing an important role in the history of civilizations. The widespread diffusion of this gem very far from the deposits highlights the historical importance of emeralds in the economic and religious structures of ancient cultures. Therefore, studies aimed at connecting each gemstone to its source (i.e., its provenance) continue to be a central topic for archaeologists, historians, geologists, gemologists, and so on.

Today, the scientific community is involved to solve the existing debate about the emerald-deposits genetic classification schemes, which is based on several genetic models (Gavrilenko & Dashevsky, 1998; Dereppe et al., 2000; Schwarz & Giuliani, 2001; Schwarz et al., 2001; Barton & Young, 2002). Some authors classified emerald deposits in two, three, five or more different categories (Gavrilenko & Dashevsky, 1998; Dereppe et al., 2000), or suggested artificial neural networks (ANN, based on 450 electron microprobe analyses) to group the worldwide deposits.

The genetic model for emerald formation involves the interaction of Be-bearing magmatic hydrothermal fluids, related to granitic-pegmatitic complex, with Cr- and V-bearing mafic and ultramafic metamorphic rocks within localized deformation zones. However, Zwaan (2006) noticed that a significant number of emerald deposits cannot be unambiguously classified using the existing schemes, and suggested that a future classification scheme should be based on the trace elements geochemistry of the gemstone.

In order to individuate useful geochemical markers for provenance purpose, we present and discuss for the first time the chemical composition of both major and trace elements of selected emerald samples from some of the most important worldwide deposits. Electron Microprobe (EMP) and Secondary Ion Mass Spectrometry (SIMS) investigations allowed to determine major and trace elements concentrations used for binary and spider diagrams along with statistical analysis, i.e., Principal Component Analysis (PCA). Crossing the different results, we observed that major or trace elements considered separately did not give useful results in term of discrimination; indeed, we were able to discriminate each deposit with high reliability when both groups of elements were considered at once. In particular, PCA results identified different groups on the basis of their content of SiO_2, Al_2O_3, V, Sc, B, Li. Moreover, spider and binary diagrams involving Cs, Rb, B, Li, Cr, V, Sc highlighted peculiar differences inside the emerald deposits, and in particular for those deposits not discriminated by the PCA.

Barton, M.D. & Young, S. (2002): Non-pegmatitic deposits of beryllium: mineralogy, geology, phase equilibria and origin. *in* "Beryllium: Mineralogy, Petrology, and Geochemistry", E.S. Grew, ed., *Rev. Mineral. Geochem.*, **50**, 591-691.

Dereppe, J.M., Moreaux, C., Chauvaux, B., Schwarz, D. (2000): Classification of emeralds by artificial neural networks. *J. Gemm.*, **27**, 93-105.

Gavrilenko, E.V. & Dashevsky, D.M. (1998): Properties of emeralds of different genesis and their diagnostic meaning. *Proc. Russian Mineral. Soc.*, **127**, 45-57.

Schwarz, D. & Giuliani, G. (2001): Emerald deposits – a review. *Aust. Gemmol*., **21**, 17-23.

Schwarz, D., Giuliani, G., Grundmann, G., Glas, M. (2001): Die Entstehung der Smaragde, ein vieldisskutiertes Thema, ExtraLapis. *in* "Smaragd: der kostbarste Beryll, der teuerste Edelstein", D. Schwarz & R. Hochleitner, eds., Weise, München, 68-73.

Zwaan, J.C. (2006): Gemmology, geology and origin of the Sandawana emerald deposits, Zimbabwe. *Scripta Geol.*, **131**, 1-211.

SPECTROSCOPIC CHARACTERIZATION OF Cr AND V AS CHROMOPHORES IN SELECTED GEM MINERALS

Bačík P.*[1], Fridrichová J.[1], Malíčková I.[1], Milovský R.[2], Luptáková J.[2] & Škoda R.[3]
[1] Department of Mineralogy and Petrology, Comenius University, Bratislava, Slovakia
[2] Earth Science Institute, Slovak Academy of Sciences, Bratislava, Slovakia
[3] Department of Geological Sciences, Masaryk University, Brno, Czech Republic
Corresponding email: bacikp@fns.uniba.sk

Keywords: chromium, vanadium, spectroscopy

Gem-quality samples of selected oxides and silicates with Cr and V presumed as chromophores were studied with Raman, optical and X-ray fluorescent spectroscopy. Studied samples included corundum (ruby from Madagascar, Mozambique, India, and Tanzania), spinel (red spinel from Vietnam and Myanmar), chrysoberyl (alexandrite from Tanzania), diopside (chromdiopside from Russia), garnets (demantoid from Slovakia and Madagascar, uvarovite from Russia, tsavorite from Tanzania), zoisite (green zoisite, tanzanite from Tanzania), beryl (emerald from Colombia), and tourmalines (V-rich uvite from Tanzania and Myanmar).

Chromium is dominant chromophore in rubies with the exception of the V-dominant sample from Tanzania, red spinel and chrysoberyl. Similarly, in diopside, Cr prevails over V. From andradites from different locations, the significant increase in Cr was observed only in demantoide from Dobšiná, Slovakia. In uvarovite, Cr is major element. In grossular-tsavorite from Tanzania, V is the main chromophore, similarly to tanzanite. However, in green zoisite from Tanzania which is in association with ruby, Cr is in slight dominance. All samples containing Cr exhibit strong photoluminescence in the red area.

In optical spectra, there were typical two absorption bands observed in the spectra of all samples. However, the wavelengths of absorption band in yellow-to-red region was shifted to longer wavelengths in silicates (diopside – 650 nm, 1.91 *e*V; uvarovite – 620 nm, 2.00 *e*V; uvite and emerald – 610 nm, 2.03 *e*V; unheated tanzanite – 605 nm, 2,05 *e*V) than in oxides (chrysoberyl – 595 nm, 2.08 *e*V; ruby – 560 nm, 2.21 *e*V; spinel – 540 nm, 2.30 *e*V). The absorption spectrum of blue heated tanzanite displayed broad band between 500 and 650 nm indicating oxidation of V.

Moreover, all samples display variably intensive luminescence due to Cr. Location and shape of the luminescent bands depends on the structure of the studied minerals. Ruby have narrow luminescence band with great intensity at around 693 nm. Chrysoberyl has intensive band at 680 nm accompanied with broader and less intensive bands at 675, 690 and 710 nm. Spinels exhibit luminescence bands split into 675, 685, 687, 696, 697, 699, 707, 717 and 722 nm. The wavelength of the sharp band in garnets varies between 660 and 700 nm. In both zoisite spectra, sharp band at 690 nm is accompanied with very intensive sharp band at 715 nm. Spectrum of diopside contains only broad band at 750 nm. Tourmalines display sharp luminescence band at 685 nm and broad band combined from bands at 740 nm. Emerald display very similar combination of sharp band at 685 nm and broad band at 728 nm.

Based on spectroscopic data we presume that absorption and luminescence spectra of studied minerals depend on crystal-chemical properties of minerals, bond strength in Cr- and V-hosting polyhedra and the ligand field which in oxides is stronger than in silicates.

Acknowledgements: This contribution was supported by VEGA 1/0079/15 project.

COLORED GEMS: A REVIEW ON NON DESTRUCTIVE AND NON INVASIVE APPROACHES IN ART AND GEMMOLOGY

Barone G.*[1], Bersani D.[2], Lottici P.P.[2], Mazzoleni P.[1] & Raneri S.[1]
[1] Dipartimento di Scienze Biologiche, Geologiche e Ambientali, Università di Catania, Italy
[2] Dipartimento di Fisica e Scienze della Terra "Macedonio Melloni", Università di Parma, Italy
Corresponding email: gbarone@unict.it

Keywords: gems, jeweler, spectroscopic methods

The possibility to incorporate high technology instruments into the world of gemstone testing requires constant researches finalized to inspect several challenges as efficiency and performance of various methods, development of comprehensive appropriate databases and establishment of analytical protocols (Barone et al., 2015a). In these perspectives, recent literature has focused on advanced applications in gems studies. For example, several works show the large amount of information which is possible to obtain with portable Raman analysis on precious and fashionable faceted loose gems, available in the gem market (such as emeralds, sapphires and rubies) (Barone et al., 2014, 2016a; Bersani et al., 2014). They demonstrate that the method could help and speed up the certification procedures, allowing to distinguish natural and synthetic gems, identify fakes and possible treatments used to improve their appearance. Moreover, they recommend standard micro-Raman equipments fast and easy instrument to support provenance studies, thanks to the analysis of fluid inclusions or of some peculiar spectroscopic regions (as in the case of the OH region in emeralds for the estimation of alkali ions amount). Additionally, these works discuss the combined use of complementary techniques, such as portable X-ray fluorescence (e.g., for the identification of chromophores in colored inorganic gems) or ^{13}C solid state nuclear magnetic resonance (e.g., for the characterization of fossil resins in terms of chemical fingerprint and maturation degree) (Barone et al., 2016b). Even if the aforementioned researches were made on loose gems, they represent a fundamental reference for the identification of gemstones mounted on precious objects or found in unmovable artworks preserved in Museums. In fact, recent measurement campaigns carried out on jewel collections in Sicilian Regional Museum (e.g., "M. Accascina" and "P. Orsi", in Messina and Siracusa, respectively) have emphasized the potential of portable Raman instruments for the identification of gems (Barone et al., 2015b, 2016c). Numerous analyses carried out in a really short time and with different excitation wavelengths on a large number of artifacts (necklaces, earrings, rings, brooches, hair clips, precious belts and loose engraved gems) have permitted the fast classification of precious and semi-precious gemological materials, allowing to identify the composition of interesting gems as well as reveal misclassification. Reviewing the aforementioned applications, this paper intends to be a practical resource for researchers, gemologists, collectors and Museum curators who would like to go deeper inside in the potential of complementary non-invasive and non-destructive spectroscopic methods that could practically help studies of inorganic and organic gemological materials.

Barone, G., Bersani, D., Crupi, V., Longo, F., Longobardo, U., Lottici, P.P., Aliatis, I., Majolino, D., Mazzoleni, P., Raneri, S., Venuti, V. (2014): A portable versus micro-Raman equipment comparison for gemmological purposes: the case of sapphires and their imitations. *J. Raman Spectr.*, **45**, 2014, 1309-1317.

Barone, G., Bersani, D., Jehlička, J., Mazzoleni, P., Raneri, S., Vandenabeele, P. (2015a): Fast on-site identification of minerals by using portable Raman equipment in gemological trade contexts and in collectors exhibitions.*Per. Mineral.*, **208**, 27-28.

Barone, G., Bersani, D., Jehlička, J., Lottici, P.P., Mazzoleni, P., Raneri, S., Vandenabeele, P., Di Giacomo, C., Larinà, G. (2015b): Nondestructive investigation on the 17-18th centuries Sicilian jewelry collection at the Messina regional museum using mobile Raman equipment. *J. Raman Spectr.*, **46**, 989-995.

Barone, G., Bersani, D., Lottici, P.P., Mazzoleni, P., Raneri, S., Longobardo, U. (2016a): Red gemstone characterization by micro-Raman spectroscopy: the case of rubies and their imitations. *J. Raman Spectr.*, DOI 10.1002/jrs.4919

Barone, G., Capitani, D., Mazzoleni, P., Proietti, N., Raneri, S., Longobardo, U., Di Tullio, V. (2016b): ^{13}C solid State NMR and μ-Raman Spectroscopic Characterization of Sicilian Amber. *Appl. Spectr.*, in press.

Barone, G., Mazzoleni, P., Raneri, S., Bersani, D., Jehlička, J., Lottici, P.P., Vandenabeele, P., Lamagna, A., Manenti, A.M. (2016c): Raman investigation on precious jewelry collections preserved in Paolo Orsi Regional Museum (Siracusa, Sicily) by using portable equipment. *Appl. Spectr.*, in press.

Bersani, D., Azzi, G., Lambruschi, E., Barone, G., Mazzoleni, P., Raneri, S., Longobardo, U., Lottici, P.P. (2014): Characterization of emeralds by micro-Raman spectroscopy. *J. Raman Spect.*, **45**, 2014, 1293-1300.

THE PEDOGENETIC MODEL FOR THE FORMATION OF PRECIOUS OPAL DEPOSIT OF WEGEL TENA, ETHIOPIA

Chauviré B.*[1], Rondeau B.[1], Mazzero F.[2], Ayalew D.[3] & Chamard-Bois S.[4]
[1] Laboratoire de Planétologie et Géodynamique de Nantes, Centre National de la Recherche Scientifique, University of Nantes, France
[2] Opalinda, Paris, France
[3] Department of Earth Sciences, Addis Ababa University, Ethiopia
[4] Gemlab-GemTechLab, Genève, Switzerland
Corresponding email: boris.chauvire@univ-nantes.fr

Keywords: opal, Ethiopia, soil formation

Since its discovery in 2008, the opal deposit in the Wegel Tena area (Ethiopia) becomes a major precious opal provider. It is located in an Oligocene ignimbritic trapp 1600 km^2 large. It has been proposed that opal formation resulted from the pedogenesis of a specific ignimbritic stratum (Rondeau et al., 2012). This study brings new field evidences and laboratory results that complete and reinforce the pedogenetic model for gem opal formation.

In the 16 mines visited, we observed that, in contrast with the other strata, the opal-bearing layers are strongly weathered: e.g. volcanic glass turned into montmorillonite. Plant fossils are found in both the host-rock and opals. Examination of these fossils under SEM in opal has revealed a well preserved cellular structure, suggesting a fast mineralization. Petrographic examination of opal-bearing rocks reveals granular microstructure and illuvial clays. These features are typical of pedogenesis processes.

Preliminary measurements of oxygen isotopes composition in opals ranges from $\delta^{18}O$ = +26.2 to +31‰. This is consistent with a low-temperature precipitation (Henderson et al., 1971; Rondeau et al., 2004).

Many rough samples exhibit a strong zonation with a central transparent, orange core surrounded by a translucent, white, more porous rim. This suggests that the opal initially formed under the central state, and was transformed after its precipitation under the influence of a fluid present in the (paleo-) soil. The trivalent iron in opal causes the orange color and oxalic acid is a well-known iron complexor. In addition, this organic acid is common in soils. Therefore, this assumption of late transformation was tested in the lab by attacking orange, transparent opals by oxalic acid at various concentrations. Some samples turned white, translucent and more porous within a few weeks. This reveals the role of soil fluids in the formation and the subsequent transformation of opals.

In the field, most lenticular deposits occur within an unwelded ignimbrite stratum. More, some deposits are superimposed in the sequence, vertically 10 to 20 meters distant and locally separated by a fresh, unweathered, welded ignimbrite. Hence, the “opal story” occurred several times at the same place on the map, separated by an episode of volcanic emission. This suggests a paleo-topographic control on the disposition of the deposits. However, the strata are rather flat at a large scale reading, without any obvious topographic indicators.

In conclusion, the observations are consistent over the 16 mines visited in the Wegel Tena area, all pointing toward the pedogenetic model for precious opal formation. The size of the ignimbrite plateau, together with the repetition of the process in space and time, promises a significant potential for gem opal exploration in the area.

Henderson, J.H., Jackson, M.L., Syers, J.K., Rex, R.W. (1971): Cristobalite authigenic origin in relation to montmorillonite and quartz origin in bentonites. *Clays Clay Miner.*, **19**, 229-238.

Rondeau, B., Fritsch, E., Guiraud, M., Renac, C. (2004): Opals from Slovakia (‘Hungarian’ opals): a re-assessment for the conditions of formation. *Eur. J. Mineral.*, **16**, 789-799.

Rondeau, B., Cenki-Tok, B., Fritsch, E., Mazzero, F., Gauthier, J.-P., Bodeur, Y., Bekele, E., Gaillou, E., Ayalew, D. (2012): Geochemical and petrological characterization of gem opals from Wegel Tena, Wollo, Ethiopia: opal formation in an Oligocene soil. *Geochem. Explor. Environ. Anal.*, **12**, 93-104.

A NEW INSIGHT ON THE GEM-QUALITY PINK EPIDOTE ("CLINOTHULITE") FROM VAL MALENCO, CENTRAL ALPS, ITALY

Diella V.*[1], Adamo I.[2], Bocchio R.[3] & Marinoni N.[3]
[1] Istituto per la Dinamica dei Processi Ambientali, Consiglio Nazionale delle Ricerche, Milano, Italy
[2] Istituto Gemmologico Italiano, Milano, Italy
[3] Dipartimento di Scienze della Terra "A. Desio", Università di Milano, Italy
Corresponding email: valeria.diella@cnr.it

Keywords: clinozoisite, thulite, gemstone

Val Malenco, Central Alps (Sondrio, Italy) is a valley well-known for its variety of minerals, which has attracted the interest of mineralogists and collectors since the end of 19th Century. Some of the stones recovered in Val Malenco have also a significant interest as gemological materials, such as the case of demantoid garnet, nephrite jade, serpentine minerals and rhodonite (Bocchio et al., 2010; Adamo & Bocchio, 2013; Diella et al., 2014; Adamo et al., 2016). Another stone found in Val Malenco, is "clinothulite", a pink colored material, similar to rhodonite as aspect, but fully different from the mineralogical and gemological point of view. This stone was described for the first time in 1934 by Pietro Sigismund, a mineral collector, who labeled it as thulite, i.e. the manganese-bearing variety of zoisite (Dana, 1920), used as gemstone and carving material in the manufacture of jewellery and ornamental objects. More recently, Bianchi et al. (1987) recognized in this stone a monoclinic symmetry and named it "clinothulite" which stands for "monoclinic thulite". The main outcrop of "clinothulite", 70-80 m in length and almost 1 m in thickness, occurs near the locality of Pizzo Tremogge at an altitude of 2920 m and it is enclosed in gneissic rocks and associated to calcium silicate marbles of Paleozoic age. "Clinothulite" is very fine-grained and displays an agreeable pink color, sometimes with white or light green veins, due to the occurrence of a few of accessory minerals such as green epidote, pyroxene, amphibole, calcite, mica and pyrite.

This study aims to provide a review and an update of "clinothulite" from Pizzo Tremogge investigating a suite of gem-quality samples (3 faceted gems and 2 rough pieces) by means of traditional gemological tests, XRPD data, combined with quantitative full-phase analysis using the Rietveld method, and EMPA-WDS measurements.

All the examined samples (7.58-10.77 ct) are opaque, inert to UV radiation and have a refractive index approximately of 1.69. The density ranges from 3.10 to 3.22 g/cm^3, with variations related to the occurrences of the accessory minerals. The cell parameters (a = 8.876, b = 5.595, c = 10.149 Å, β = 115.46°, V = 455.04 Å^3) suggest a monoclinic symmetry and agree with those reported in literature for clinozoisite. The chemical composition compares well with that of thulite samples from literature, both of orthorhombic and monoclinic symmetry, and is very close to the idealized formula of clinozoisite, $Ca_2Al_3[O(OH)(SiO_4)(Si_2O_7)]$, with an almost stoichiometric content of Ca and Si (*Ca* ~ 2.000, Si ~ 3.000 *apfu*). On the contrary, Al is lower than 3.000 *apfu* and shows a well definite negative correlation with Fe (0.116 to 0.559 *apfu*) indicating the substitution between these elements. The samples contain also a minor amount of Ti, Cr, Mg and Mn. In particular, the Mn content is low (0.001 to 0.008 *apfu.*) but it causes the soft pink coloration that makes "clinothulite" an attractive gem material.

Adamo, I. & Bocchio, R. (2013): Nephrite jade from Val Malenco, Italy: Review and update. *Gems Gemol.*, **49**, 98–106.

Adamo, I., Diella, V., Bocchio, R., Rinaudo, C., Marinoni, N. (2016): Gem-quality serpentine from Val Malenco, Central Alps, Italy. *Gems Gemol.*, **52**, 38-49.

Bianchi Potenza, B., Crespi, R., Liborio, G. (1986): Epidoti rosa (clinothuliti) di Valtellina. *La Gemmologia*, **11**, 11-13.

Bocchio, R., Adamo, I., Diella, V. (2010): The profile of trace elements, including the REE, in gem-quality green andradite from classic localities. *Can. Mineral.*, **48**, 1205-1216.

Dana, E.S. (1920): The System of Mineralogy of James Dwight Dana 1837-1868. Descriptive Mineralogy. 6th ed. Wiley, New York, 1134 p.

Diella, V., Adamo, I., Bocchio, R. (2014): Gem-quality rhodonite from Val Malenco (Central Alps, Italy). *Per. Mineral.*, **18**, 207-221.

WHY ARE SOME MINERAL GEM QUALITY? CRYSTAL GROWTH CONSIDERATIONS

Fritsch E.*[1], Rondeau B.[2] & Pinsault L.[2]

[1] Institut des Matériaux Jean Rouxel, Centre National de la Recherche Scientifique & Université de Nantes, France

[2] Laboratoire de Planétologie et Géodynamique de Nantes, Centre National de la Recherche Scientifique & Université de Nantes, France

Corresponding email: emmanuel.fritsch@cnrs-imn.fr

Keywords: gem mineral, crystal growth, spiral growth

Several authors have concentrated on understanding what is causing a crystal to be gem rather than an ordinary part of a rock. Several factors have been put forth (Groat & Laurs, 2009). Undoubtedly, the right chemical ingredients must be present in about the right proportions so that a given gem species or variety can grow. For example, to grow emerald, a variety of green beryl, one needs Si, Al, O, which are common, but especially Be, Cr and/or V, elements less common and rarely encountered together. Also, undesirable elements (often iron) must be in limited concentration.

Other factors of importance have been noted variously: thermodynamic conditions, the presence of space, and a favorable environment for mining. The purpose of this work is to demonstrate that the genesis of a gemstone can be explained by the conjunction of several, complementary, favorable crystal growth factors.

Firstly, one needs to have a few seeds created for a given volume, and not a lot: if too many seeds appear, then there will be many small crystals, instead of one large one, which is desired. This means an inhomogeneous nucleation. This is why many synthetic gems are grown from a seed.

Secondly, the growth must be slow enough to avoid creating many defects in the growing gem. This is achieved in Sunagawa's diagram by a low driving force (Sunagawa, 2005). These conditions correspond to a growth by spiral growth dislocation. This leads to the flat growth hillocks seen on natural or synthetic gems. This also limits the incorporation of fluid inclusions that may alter the transparency of the crystal.

These conditions must be maintained for the time required to grow a suitable crystal, a parameter which is particularly difficult to ascertain, but which is likely small compared to the geological time scale.

In case of no space available, the growing species needs imposing its size or morphology on its immediate environment. This is required in particular for metamorphic and metasomatic gems.

There are no dramatic post-growth events before either the crystal reaches the surface or is mined underground. Tectonic events creating cracks or increasing pressure may result in the mechanical destruction of a potentially gem crystal. Dissolution must be limited as well.

Groat, L.A. & Laurs, B.M. (2009): Gem formation, production, and exploration: why gem deposits are rare and what is being done to find them. *Elements*, **5**, 153-158.

Sunagawa, I. (2005): Crystals: growth, morphology and perfection. Cambridge Univ. Press, 295 p.

PINK AND RED SPINELS IN MARBLE: TRACE ELEMENTS, OXYGEN ISOTOPES AND SOURCES

Giuliani G.*[1-2], Fallick A.E.[3], Boyce A.J.[3], Pardieu V.[4] & Pham V.L.[5]
[1] Géosciences Environnement Toulouse, Université Paul Sabatier, Toulouse, France
[2] Centre de Recherches Pétrographiques et Géochimiques, Université de Lorraine, Vandœuvre-lès-Nancy, France
[3] Isotope Geosciences Unit, Scottish Universities Environmental Research Centre, Glasgow, United Kingdom
[4] Gemological Institute of America, Bangkok, Thailand
[5] Centre for Gems and Gold Research and Identification of Vietnam, Hanoi, Vietnam
Corresponding email: giuliani@crpg.cnrs-nancy.fr

Keywords: gem spinel, trace elements, oxygen isotopes

The combination of V-Cr-Fe-Zn trace elements with oxygen isotope composition of pink and red spinel-bearing marbles is reported for the first time. The O-isotope composition of the worldwide spinels range widely between 5.6 and 24.2‰ (n = 34). Spinels can be classified into three sets of $\delta^{18}O$ values. (1) The first group, in the range 5.6 to 8.6‰ (n = 3; mean $\delta^{18}O$ = 6.8±1.6‰) concerns the historical Kul-i-Lal spinel in a primary deposit mined in Tajikistan. (2) The second $\delta^{18}O$ group, between 12.1 and 18.5‰ (n = 12) corresponds to spinels from Vietnam and Myanmar. In northern Vietnam, it includes the primary and placer deposits of Cong Troi and An Phu, with respectively $\delta^{18}O$ values between 14.8-17.7‰ (n = 3) and 14.3-17‰ (n = 7). In the Namya placer located in northern Myanmar, the $\delta^{18}O$ values are between 15.6 and 17.3‰ (n = 2). (3) Spinels from the third group characterized by the highest $\delta^{18}O$ values ($19 < \delta^{18}O < 24.2$‰, n = 19) are found for primary and placer deposits: (i) primary deposits are those from Pamreso in Kenya ($22 < \delta^{18}O < 22.9$‰, n = 2), Ipanko in Tanzania ($23.1 < \delta^{18}O < 23.3$‰, n = 5) and Paigutan in Nepal ($18.8 < \delta^{18}O < 19.9$, n = 3); (ii) the placers include Kiswila ($20.6 < \delta^{18}O < 21.1$‰, n = 2) and also a piece of the giant 53 kg spinel rough discovered in the eluvial deposit of Ipanko ($\delta^{18}O$ = 23.3‰) in Tanzania. A second population of alluvial spinels from An Phu in Vietnam have $\delta^{18}O$ values in the range 22.5-24.2‰ (n = 5) while those of Mogok in Myanmar have $\delta^{18}O$ values between 21 and 22.8‰.

The trace element contents of pink and red spinels were analyzed by EPMA, excepted for Ga, Co, Ni and Zr. Gem spinel ($MgAl_2O_4$) contains additional significant elements such as Fe, Cr, V and Zn. Ti and Mn are low to very low except for Mogok and Namya spinels (respectively up to 0.27 and 0.20 wt.% TiO_2). Highest concentrations of ZnO have been found for spinels from Ipanko (up to 1 wt.%), An Phu (up to 1.27 wt.%) and Paigutan (up to 0.67 wt.%). FeO is highly variable from An Phu (up to 0.9 wt.%) and Cong Troi (up to 1.4 wt.% FeO) to Mogok (0.02 wt.%). The colour of spinel depends on Cr and V contents with influence of Fe. The Cr content (as Cr_2O_3) varies from 0.005 wt.% for very light pink (Cong Troi) to 5 wt.% for deep red (Namya) spinels. V content (as V_2O_3) varies from values below the detection limit (0.005 wt.%) to 0.93 wt.% (Namya). The triangular diagrams V-Zn-Fe and V-Zn-Cr permit to define contrasted chemical domains for some of the economic deposits. Simple consideration on the V/Cr ratio and Zn content with the oxygen isotopic ranges of spinels permitted the discrimination of the historical Kul-i-Lal deposit and those of Ipanko, Paigutan, Pamreso, Cong Troi, and apparently the distinction between Namya and Mogok spinels. The combination of oxygen isotopes with chemical analysis provides a preliminary database for the identification of almost all the geographic sources of the main worldwide productive areas and occurrences.

UPDATE ON THE HEAT TREATMENT DETECTION OF TANZANITE

Karampelas S.*[1], Hainschwang T.[2] & Notari F.[3]
[1] GRS, Gem Research Swiss AG, Adligenswil, Switzerland
[2] GGTL, Balzers, Liechtenstein
[3] GGTL, Genève, Switzerland
Corresponding email: steka@gemresearch.ch

Keywords: tanzanite, heating, spectroscopy

The blue to bluish-purple variety of zoisite, known as tanzanite, is commonly obtained via heat treatment of zoisite of various – typically brownish – colours. At about 550°C all these “off-colours” turn to attractive blue to purple hues, which define the colour variety named “tanzanite”. All otherwise coloured zoisite should be called “zoisite” with the colour prefix. The distinction of untreated and heat treated tanzanite has been the topic of research since the 1990’s but until today no satisfactory solution has been found. In this study the effects of the heat treatment on zoisite and the possibilities and limitations of its identification are demonstrated. It is shown that today the heat treatment can only be identified under very specific circumstances since the spectroscopic methods described in earlier studies are not always reliable for the detection of the heating of today’s tanzanite production.

PRESSURE-TEMPERATURE-FLUID CONSTRAINTS FOR THE POONA EMERALD DEPOSITS, WESTERN AUSTRALIA: FLUID INCLUSION AND STABLE ISOTOPE STUDIES

Marshall D.*[1], Downes P.[2], Ellis S.[1] & Jones P.[3]
[1] Department of Earth Sciences, Simon Fraser University, Burnaby, Canada
[2] Western Australian Museum, Welshpool, Australia
[3] Department of Earth Sciences, Carleton University, Ottawa, Canada
Corresponding email: marshall@sfu.ca

Keywords: emerald, fluid inclusions, thermometry

Poona is a mining district located approximately 75 km to the northwest of the town of Cue in Western Australia. Emerald was discovered at Poona in 1909 and gem quality emeralds have been produced from the area (Simpson, 1948). Most of the emerald extracted from the Poona district has come from the Aga Khan mine, with total production in the area in excess of 23,000 carats (Franchitto, 1990). The emerald deposits of the Poona region occur in the northern Murchison Domain of the Youanmi Terrane that forms part of the mineral-rich Archean Yilgarn Craton. The northern Murchison Domain contains autochthonous volcano-sedimentary greenstone sequences (2820-2700 Ma) that include intrusive mafic–ultramafic rocks, and extensive suites of granitic rocks (2815-2600 Ma) that accompanied and post-dated greenstone belt volcanism (Van Kranendonk et al., 2013). Generally, the metamorphic grade in this region varies from lower amphibolite facies to lower greenschist and prehnite-pumpellyite facies. The greenstone sequences and some granitic suites have been multiply deformed. This makes the study of these deposits challenging and studies have been carried out by a number of researchers (Grundmann & Morteani, 1998; Graindorge, 1978; Franchitto, 1990).

Emerald from the deposits at Poona show micrometre- to millimetre-scale chemical, optical, and cathodoluminescence zonation. This zonation combined with petrology, mineral chemistry, fluid inclusion and isotope studies indicates early emerald precipitation from a single-phase saline fluid of approximately 12 mass percent NaCl equivalent over the temperature range of 335-525°C and pressures ranging from 70 to 400 MPa. Secondary emerald-hosted fluid inclusions indicate subsequent emerald precipitation from higher salinity fluids. Likewise, the $\delta^{18}O$-δD of channel fluids extracted from Poona emerald are consistent with multiple origins yielding both igneous and metamorphic signatures. The combined multiple generations of emerald precipitation, different fluid compositions, and the presence of both metamorphic and igneous fluids trapped in emerald likely indicate a protracted history of emerald precipitation at Poona conforming to both an igneous and a metamorphic origin at various times throughout the geological history of the region.

Franchitto, A. (1990): Emerald, green- and colourless-beryl mineralization at Poona, Murchison Province, Western Australia. Honours Dissert., Univ. of Western Australia, 208 p.

Graindorge, J.M. (1974): A gemmological study of emerald from Poona, Western Australia. *Austr. Gemmol.*, **12**, 75-80.

Grundmann, G. & Morteani, G. (1998): Alexandrite, emerald, sapphire, ruby and topaz in a biotite-phlogopite fels from the Poona, Cue district, Western Australia. *Austr. Gemmol.*, **20**, 159-167.

Simpson, E.S. (1948): Minerals of Western Australia. Western Australia Government Printer, Perth. 87 p.

Van Kranendonk, M.J., Ivanic, T.J., Wingate, M.T.D., Kirkland, C.L., Wyche, S. (2013): Long-lived, autochthonous development of the Archean Murchison Domain, and implications for Yilgarn Craton tectonics. *Precambr. Res.*, **229**, 49-92.

RECLASSIFICATION OF EMERALD DEPOSIT FORMATIONAL MODELS BASED ON TECTONIC AND METAMORPHIC CONDITIONS

Marshall D.*[1], Giuliani G.[2], Groat L.A.[3], Fallick A.E.[4] & Branquet Y.[5]
[1] Earth Sciences Department, Simon Fraser University, Burnaby, Canada
[2] Centre National de la Recherche Scientifique, Nancy, France
[3] Department of Earth, Ocean and Atmospheric Sciences, University of British Columbia, Vancouver, Canada
[4] Scottish Universities Environmental Research Centre, Glasgow, United Kingdom
[5] Institut des Sciences de la Terre d'Orléans, Orléans, France
Corresponding email: marshall@sfu.ca

Keywords: emerald, gems, economic resources

Although emerald deposits are relatively rare, they can be formed in a few specific geologic settings and their classification system or models used to describe emerald precipitation and predict its occurrence has been too restrictive leading to confusion as to the exact mode of formation for some emerald deposits. Generally speaking emerald is beryl doped with sufficient concentrations of the chromophores chromium and vanadium to result in the green and sometimes bluish green or yellowish green traded as emerald. The limiting factor in the production of emerald is geological conditions resulting in an environment rich in beryllium and chromium or vanadium (Groat et al., 2008).

Historically, emerald deposits have been classified into three broad types (Giuliani et al., 2015). The first and most abundant deposit type, in terms of production, is pegmatite related and formed via the interaction of beryllium-rich pegmatites or similar granitic intrusions into chromium- or vanadium-rich rocks as such as ultramafic and volcanic rocks, or shales derived from those rocks. These are often referred to as magmatic-metasomatic (Ma) emeralds. A second deposit type, accounting for most of the world's gem emerald quality, is the sedimentary (Se) type, generally involving the interaction, along faults and fractures, of upper level crustal brines rich in Be from evaporite interaction with shales and other Cr- and/or V-bearing sedimentary rocks. The third and relatively rare deposit type is the metamorphic-metasomatic (Me) emerald deposit. In this deposit model deeper crustal fluids circulate along faults or shear zones and interact with metamorphosed shales, carbonates and ultramafic rocks. In this model Be and Cr (±V) may either be transported to the deposition site via the fluids or already be present in the host metamorphic rocks intersected by the faults or shear zones. All three emerald deposit models require some level of tectonic activity and commonly continued tectonic activity can result in the metamorphism of an existing Se or Ma type deposit. In the extreme, at deeper crustal levels, high-grade metamorphism can result in the partial melting of metamorphic rocks blurring the distinction between Me and Ma (Grundmann & Morteani, 1989) or potentially even between Me and Se deposits. Likewise, granites and pegmatites are generally emplaced at mid-crustal levels into a dynamic metamorphic environment of faulting, shearing, and metasomatism. In this paper we propose an enhanced classification for emerald deposits based on the classic Me, Ma, and Se models, but also including temperature, tectonic environment, fluid and emerald chemistry.

Giuliani, G., Branquet, Y., Fallick, A., Groat, L., Marshall, D. (2015): Emerald deposits around the world, their similarities and their differences. *InColor*, **57**, 56-69.

Groat, L., Giuliani, G., Marshall, D., Turner, D. (2008): Emerald deposits and occurrences: A review. *Ore Geol. Rev.*, **34**, 87-112.

Grundmann, G. & Morteani, G. (1989): Emerald mineralization during regional metamorphism: the Habachtal (Austria) and Leydsdorp (Transvaal, South Africa) deposits. *Econ. Geol.*, **84**, 1835-1849.

MELT INCLUSIONS IN YOGO SAPPHIRES AS A CLUE TO THEIR ORIGIN

Palke A.C.*[1], Renfro N.D.[1] & Berg R.B.[2]
[1] Gemological Institute of America, Carlsbad, CA, USA
[2] Montana Bureau of Mines and Geology, Montana Tech, Butte, MT, USA
Corresponding email: aaronpalke@gmail.com

Keywords: sapphire, lamprophyre, melt inclusions

Yogo sapphires have been mined from an ultramafic lamprophyre dike in central Montana, USA for more than 100 years. The ultramafic lamprophyre host rock is properly termed a ouachitite and is primarily composed of phlogopite and clinopyroxene. The sapphires have a corroded and etched appearance suggesting they were not in equilibrium with the lamprophyre host, at least at the time of emplacement. This has led many researchers to speculate the sapphires are xenocrysts originating in Al-rich metamorphic rocks sampled by the lamprophyre on its ascent toward the Earth's surface. Other work has suggested the sapphires originated in the parental magma of the lamprophyre or that they formed as a restitic mineral through partial melting of pelitic-type rocks as the lamprophyre pooled at the base of the lithosphere (Dahy, 1991). We report here the analysis of glassy melt inclusions observed in Yogo sapphires and discuss the implications for their genesis.

The glassy melt inclusions occur as small (< 50 mm) negative crystal shaped inclusions with a prominent gas bubble. Larger melt inclusions are observed as well and Raman analysis of these inclusions shows the presence of calcite and analcime. Rapidly cooling these sapphires from 1400°C allows these inclusions to be quenched to a homogeneous glassy phase. These melt inclusions are enriched in Al_2O_3 (19-21 wt.%), relatively low in SiO_2 (50-55 wt.%), with moderate Na_2O and CaO (each about 4-6 wt.%), and low contents of FeO_{total}, MgO, and K_2O (< 2 wt.% each). The melt inclusions generally occur as isolated inclusions removed from the sapphire surfaces or surface-reaching fractures and can therefore be considered to be primary inclusions representing the magmatic medium in which the sapphires grew.

The magma represented by these inclusions is dramatically different in composition from the MgO-, FeO_{total}-, and CaO-enriched, SiO_2- and Al_2O_3-poor host lamprophyre making it unlikely that the Yogo sapphires originated from the same parental magma as the lamprophyre. In fact, the disparate compositions of these two magmas lend credence to the hypothesis that the sapphires represent a restitic component from partial melting of Al-rich lower crustal rocks by the lamprophyre as suggested by Dahy (1991). Finally, the melt inclusions are mineralogically and compositionally similar to Na- and Ca-rich, analcime- and calcite-bearing globular, leucocratic ocelli observed in the Yogo ouachitite. It is possible that the sapphires and other xenoliths represent the restite and the leucocratic ocelli the partial melt created through this process and that both were entrained in the lamprophyre as it began to rise through the lithosphere.

Dahy, J.P. (1991): Geology and igneous rocks of the Yogo sapphire deposit, Little Belt Mountains, Montana. *in* "Guidebook of the Central Montana Alkalic Province", D.W. Baker, R.B. Berg, eds., *Montana Bureau Mines Geol. Spec. Publ.*, **100**, 45-54.

COLOMBIAN EMERALD AND EUCLASE: TRAPICHE *VERSUS* TRAPICHE-LIKE TEXTURES?

Pignatelli I.*[1], Giuliani G.[1-2], Chatagnier P.-Y.[3]
[1] Centre de Recherches Pétrographiques et Géochimiques, Centre National de la Recherche Scientifique, Université de Lorraine, Vandœuvre-lès-Nancy, France
[2] Géosciences Environnement Toulouse, Centre National de la Recherche Scientifique, Université de Toulouse III, Institut de Recherche pour le Développement, Centre National d'Etudes Spatiales, Toulouse, France
[3] BOREAL Gemstone Company Lausanne, Switzerland
Corresponding email: isabella@crpg.cnrs-nancy.fr

Keywords: euclase, emerald, trapiche texture

Schmetzer et al. (2011) distinguished "trapiche" and "trapiche-like" textures. Trapiche textures are characterized by crystallographically equivalent growth sectors separated by more or less sharp boundaries of inclusions. Trapiche textures are typical of minerals with high symmetry and having inclusions of organic matter or graphite (Pignatelli et al., 2015). Otherwise, trapiche-like textures are caused by the distribution either by color-inducing elements or inclusions widespread in alternating portions of the crystal, such as in sapphire, quartz and aquamarine. However, the use of these two terms is still matter of debate. The comparison of Colombian trapiche emeralds and euclase samples with an atypical texture is interesting to elucidate this debate. Trapiche emeralds are found only in the black shales of few mines on the western side of the Eastern Cordillera Basin and their formation is controlled by the structural geology of the emerald deposits, affected by strong fluid pressure variations along faults and thrusts. The control of both geology and crystal symmetry gives rise to the ideal trapiche texture formed by a core, arms and dendrites, sometimes surrounded by an overgrowth. Fluid supersaturation due to local decompression favored the formation of emerald's seeds and the incorporation of black shale matrix as dendrites during the growth of the crystals. The dendrites developed around the core and along the *a*-axis, *i.e*. they separated pinacoidal (core) and prismatic (arms) growth sectors. After the decompression, an overgrowth is formed and it is generally of deep green color reflecting higher amount of Cr and V.

Colombian euclases from Gachala analyzed in this study are characterized by a texture never observed before and described here for the first time. Preliminary optical observations underline the similarity between the textures of euclase and trapiche emerald. The similarities between euclase and emerald do not end here and concern: i) the geological environment, because euclase samples are also found in the Eastern Cordillera Basin, but in the eastern side; ii) chemistry, in fact they have not only the same major elements but also the same chromophore ones (Cr ~ 360 ppm; V ~ 170 ppm in euclase); iii) presence of organic matter and solid inclusions separating the growth sectors. The inclusions (carbonates, micas, feldspaths, F-apatite, tourmaline, thorite, rutile, pyrite, and monazite) suggest the trapping of metasomatised black shale matrix during the euclase's growth as reported for the trapiche emeralds. However, the dendrites in euclase's texture are not developed, indicating that the formation mechanism as well as the local geological conditions during the growth are most likely different from those of trapiche emeralds. This is, thus, emblematic and some questions arise: a trapiche or trapiche-like texture for euclase? How can we unambiguously distinguish these textures when the minerals have common features?

Pignatelli, I., Giuliani, G., Ohnenstetter, D., Agrosì, G., Mathieu, S., Morlot, C., Branquet, Y. (2015): Colombian trapiche emeralds: Recent advances in understanding their formation. *Gems Gemol.*, **51**, 222-259.

Schmetzer, K., Bernhardt, H.J., Hainschwang, T. (2011): Chemical and growth zoning in trapiche tourmaline from Zambia – a re-evaluation. *J. Gemmol.*, **32**, 151-173.

PARADISE BEJEWELED: THE GEMS OF DANTE'S *DIVINE COMEDY*

Pizzorusso A.C.*[1]
[1] Independent Geologist, New York, NY, USA
Corresponding email: tweetingdavinci@gmail.com

Keywords: gems, gemology, Dante

Dante Alighieri, the author of the *Divine Comedy,* was a man of vast knowledge in many fields, including gemology. From a geological point of view, the *Divine Comedy* is a veritable treasure trove, containing pearls, rubies, topazes, emeralds, sapphires and diamonds, as well as crystal, amber and glass. Most of these gemological references can be found in the *Paradiso*, the Canticle of Light, in which Dante makes abundant use of illumination on objects in the form of reflection, refraction and shadow to convey a variety of metaphors and concepts – pearls, the intellectual lustre of the wise; rubies, souls of Christian warriors; diamonds, fortitude and steadfastness; and the sapphire, emblematic of the Virgin Mary, Queen of Heaven.

It is evident that Dante was well aware of the intrinsic physical characteristics of each gemstone and its astrological association as well as the spiritual, metaphysical, and medicinal attributes each was purported to possess. His working knowledge of light's reflection, refraction and dispersion on specific gems is extraordinary as he combines the thought process of a physicist with the words of a bard. All of this in an era in which many rare, faceted precious stones were entering Europe and the principles of gemology, as we know them, lay centuries in the future.

Using gemological passages from the *Divine Comedy*, the author will show how Dante used the physical characteristics of each gem to describe the intrinsic characteristics of humanity, starting with man and proceeding upward toward the souls, angels, saints and finally to the divine – as characterized by a brilliant, spotless diamond.

DIRECT OBSERVATION OF MELTING AND CRYSTALLIZATION IN THE SYSTEM $LiAlSi_4O_{10}$–H_2O: IMPLICATIONS FOR CRYSTAL GROWTH IN GEM-BEARING POCKETS IN MIAROLITIC PEGMATITES

Reid M.G.[1] & Anderson A.J.*[1]
[1] Department of Earth Sciences, St. Francis Xavier University, Antigonish, Canada
Corresponding email: aanderso@stfx.ca

Keywords: pegmatite, crystallization, hydrothermal diamond anvil cell

A series of hydrothermal diamond anvil cell (HDAC) experiments (n = 41) were conducted in order to investigate melting and crystallization in the system $LiAlSi_4O_{10}$–H_2O. Water-saturated petalite melt was held at various pressures and temperatures below the petalite hydrothermal melting curve. *In situ* observation of this undercooled melt afforded measurement of crystal growth rates in real time. Crystallization was observed to occur in the silicate melt, the aqueous fluid, or concurrently in both mediums. Some of the crystals that initially grew in the silicate melt continued to grow beyond the melt-fluid interface by the transfer of melt material in the aqueous fluid. Raman spectroscopic and SEM-EDS analysis of the experimental products indicate that quartz and α-spodumene formed under high pressure conditions, and β-spodumene and virgilite ± lithian mica crystallized at lower pressures. The growth rate of lithium aluminosilicate minerals ranged between 7.52×10^{-8} and 8.52×10^{-6} cm/s and were essentially the same in the melt and aqueous fluid. Hydrothermal etching of crystals commenced at the temperature and pressure of crystallization but only after the silicate melt was totally consumed. These HDAC experiments provide insights into the crystallization of gem-bearing pockets which are generally believed to have formed from a volatile-saturated melt in the late stages of pegmatite crystallization. Our observations are in agreement with the model proposed by Jahns (1982) which contends that pocket minerals form in a low density fluid by rapid diffusion of ions from the residual silicate melt to the growing crystal faces.

Jahns, R.H. (1982): Internal evolution of pegmatite bodies. *in "*Granitic pegmatites in science and industry", P..Černý, ed., *Mineral. Ass.Canada Short Course*, **8**, 293-327.

GEM LAZULITE-BEARING BLUE QUARTZITE FROM ITREMO, MADAGASCAR: A POTENTIAL FOR NEW MINERAL SPECIES

Rondeau B.*[1], Fritsch E.[2], Stéphant N.[2], Boulet C.[1] & Chauviré B.[1]

[1] Laboratoire de Planétologie et Géodynamique de Nantes, Centre National de la Recherche Scientifique, Université de Nantes, France

[2] Institut des Matériaux Jean Rouxel, Centre National de la Recherche Scientifique, Université de Nantes, France

Corresponding email: benjamin.rondeau@univ-nantes.fr

Keywords: phosphates, new mineral species, lazulite

Lazulite-bearing blue quartzite is known at Mount Ibity, Itremo, central Madagascar, and mined for facetted gemstones and decorative tiles. It contains numerous solid inclusions as inframillimetric, euhedral crystals. Many mineral species have been identified among these inclusions, including lazulite that gives the blue color to the quartzite, augelite, trolleite, svanbergite, goyazite, crandallite, berlinite, tourmaline, apatite, celestine, anhydrite, muscovite, dumortierite, hematite, zircon, and many others (Lasnier & Fritsch, 2002; Ackermand et al., 2006). Some of them contain phosphorus, boron, strontium and aluminum, which points toward a specific protolith enriched in these elements. This has been proposed to be a shallow continental shelf sand that has been percolated by B and Sr-rich hydrothermal fluids, and then was metamorphized in the greenschist- to amphibolite facies (Morteani & Ackermand, 2006).

During the systematic investigation of solid phases present in some facetted gemstones, we encountered in one sample several crystals of an undeterminable mineral species. These transparent, very light brown crystals are less than 100 µm long and 60 µm large, and are clearly anisotropic between crossed polars. Their chemical composition was measured using Wavelength Dispersive Spectroscopy and gave $(Mg,Fe)_{2.01}(Ca,Sr)_{1.03}Al_{0.95}(PO_4)_3F_{0.65}$. The composition was remarkably homogeneous through each crystal and from a crystal to another. This composition is not electronically equilibrated and shows a negative imbalance. In order to check positive elements not measured by WDS, we measured boron, beryllium and lithium using LA-ICP-MS, but all of these elements were below the detection limit (26 ppm for B, about 1 ppm for Be and Li).

We measured the Raman scattering properties of these crystal, and again the spectra were remarkably homogeneous among the population. We observed numerous sharp and intense Raman modes below 1200 cm^{-1}. The most intense modes are a doublet at 101 and 123 cm^{-1}, a single peak at 418 cm^{-1} and a triplet at 986, 1028 and 1043 cm^{-1}. Less intense modes are visible at 279, 513, 569, 592, 621, 662, 1063, 1103, 1128 and 1148 cm^{-1}. Among the intense peaks, the most sensitive to anisotropy are those at 101, 123 and 1043 cm^{-1}. No peaks were observed between 1200 and 4000 cm^{-1}, indicating that the mineral does probably not contain OH or H_2O.

The chemical composition and the Raman properties are not those of any known mineral species, hence we consider it as a new mineral species. Its structure is currently under investigation by X-ray diffraction.

Considering the unusual mineral paragenesis that reflects this unusual geological story, we consider that other mineral species may be discovered in these quartzite in the future. This may also strengthen the economic value of the blue quartzite as it may renew its interest toward systematic mineralogy collectors.

Ackermand, D., Morteani, G., Razakamanana, T. (2006): Lazulite-bearing metaquartzite of the Itremo Group (Central Madagascar): scientific significance and economic importance. *in* "Proceedings of the German-Malagasy Research Cooperation in Life and Earth Sciences", C. Schwitzer, S. Brandt, O. Ramilijaona, M. Rakotomalala Razanahoera, D. Ackermand, T. Razakamanana, J.U. Ganzhorn, eds, Concept, Berlin, 1-18.

Lasnier, B. & Fritsch, E. (2002): Quartz bleu gemme de Madagascar, Inclusions et genèse. 19th Réunion des Sciences de la Terre, Nantes, France.

Morteani, G. & Ackermand, D. (2006): Mineralogy, geochemistry and petrology of an amphibolite-facies aluminium-phosphate and borosilicate (APB)-bearing quartzite from the Mesoproterozoic Itremo Group (Central Madagascar). *N. Jb. Mineral. Abh.*, **182**, 123-148.

MULTI-METHODOLOGICAL CHARACTERIZATION OF TURQUOISE FROM ROYAL MINERALOGICAL MUSEUM OF NAPLES

Rossi M.*[1], Rizzi R.[2], Capitelli F.[3], Vergara A.[4] & Ghiara M.R.[1-5]
[1] Dipartimento di Scienze della Terra, dell'Ambiente e delle Risorse, Università Federico II, Napoli, Italy
[2] Istituto di Cristallografia, Consiglio Nazionale delle Ricerche, Bari, Italy
[3] Istituto di Cristallografia, Consiglio Nazionale delle Ricerche, Roma, Italy
[4] Dipartimento di Scienze Chimiche, Università Federico II, Napoli, Italy
[5] Centro Musei delle Scienze Naturali e Fisiche, Università Federico II, Napoli, Italy
Corresponding email: manuela.rossi@unina.it

Keywords: historic sample of turquoise, multi-methodological characterization, turquoise group

Turquoise is a group of minerals (triclinic, space group *P*-1; Foord & Taggart, 1998) with general formula $A_{0-1}B_6(PO_4)_4(OH)_8 \cdot 4H_2O$, where Cu, Fe^{2+}, Zn and (rarely) Ca occupy the A site, and Al^{3+} and Fe^{3+} the B site. The turquoise alteration processes affect the mineralogical and gemological properties, but at the same time provide elements for the identification of the provenance of archaeological artifacts (Hull et al., 2008). The present research is aimed to a detailed characterization of five historic turquoise samples, in function of their provenience. The investigated samples of "turquoise" belong to the collection of the Real Museo Mineralogico, of Università di Napoli Federico II. The provenances of the turquoise samples are: TUR1 Sinai, Egypt; TUR2 Santa Fè, New Mexico; TUR3 Saxony, Germany; TUR4 Montebras Creuse, France; TUR5 Nischapur, Iran. The samples were investigated by means of a multi-methodological approach based on XRPD, EMPA-WDS, BSE, SEM, LA-ICP-MS, FTIR and Raman spectroscopy. The turquoise group minerals found in the samples are: turquoise (TUR1, TUR2, TUR4, TUR5), faustite (TUR1), chalcosiderite (TUR3) and planerite (TUR4, TUR5). The other phosphates, found in the samples associated to "torquoise", are: variscite (TUR2, TUR3, TUR4), goyazite (TUR1), crandallite (TUR5), wavellite (TUR4) and apatite (TUR5). The other minerals fond are: voltaite, adularia, quarzo and magnetite. In particular the turquoise, in the samples TUR1, shows the presence of Ca, Sr, Ba and Si, whereas the faustite shows a ratio Zn/Cu = 1.80 and in some areas the not negligible amount of Si and Ca. In effect the diffractometric data for turquoise, highlight the slight shifts of a few characteristic peaks. The chalcosiderite in TUR3 shows the peculiar amount of Fe^{2+}, Cu and Ca. In this case the diffractometric data highlight considerable shifts of characteristic peaks not reported in literature (Cid-Dresdner & Villarroel, 1972; Giuseppetti et al., 1989). The planerite show the presence of Na in TUR4 and Fe^{3+} in TUR5, even if the diffractometric data are in agreement with those reported in literature. The turquoise studied show trace element values that indicate petrological features of the rocks in which they formed. In particular it highlights the differences in TUR1 between faustite and turquoise for the contents of U; in TUR2, TUR3, TUR4 and TUR5 there are respectively particular concentrations of; As and Ba; As and U; Li and Ta; Li and Ba. The variscite is characterized in TUR2 and TUR3 by the presences of Fe^{3+}. In particular the diffractometric data for TUR3 show the differences to those reported in literature (Onac et al., 2004). The goyazite in TUR1 shows the presence of Ca and Ba. Ba presence in TUR1 is further confirmed by Raman spectroscopy, highlighting also the presence of gorceixite. This study has highlighted the crystal chemistry complexity of turquoise group minerals and that in all samples there are various paragenesis and minerogenetic associations.

Cid-Dresdner, H. (1965): Determination and refinement of the crystal structure of turquoise, $CuAl_6(PO_4)_4(OH)_8(H_2O)_4$. *Z. Kristallogr.*, **121**, 87-113.

Cid-Dresdner, H. & Villarroel, H.S. (1972): Crystallographic study of rashleighite, a member of the turquoise group. *Am. Mineral.*, **57**, 1681-91.

Foord, E.E. & Taggart, J.E. Jr (1998): A reexamination of the turquoise group: the mineral aheylite, planerite (redefined), turquoise and coeruleolactite. *Mineral. Mag.*, **62**, 93-111.

Giuseppetti, G., Mazzi, F., Tadini, C. (1989): The crystal structure of chalcosiderite, $CuFe^{3+}{}_6(PO_4)_4(OH)_8 \cdot 4H_2O$. *N. Jahrb. Mineral. Mh.*, **1989**, 227-239.

Hull, S., Fayek, M., Mathien, F.J., Shelley, P., Roler Durand, K. (2008): A new approach to determining the geological provenance of turquoise artifacts using hydrogen and copper stable isotopes. *J. Archaeol. Sci.*, **35**, 1355-1369.

Onac, B.P., Kearns, J., Breban, R., Pintzaru, S.C. (2004): Variscite ($AlPO_4 \cdot 2H_2O$) from Cioclovina Cave (Sureanu Mountains, Romania): a tale of a missing phosphate. *Studia Univ. Babeş-Bolyai*, *Geol.*, **49**, 3-14.

PHYSICAL, CHEMICAL AND GEMOLOGICAL PROPERTIES OF SOME RHODONITES FROM TANATZ ALP (SWITZERLAND)

Scacchetti M.*[1], Marinoni L.[2], Caucia F.[2] & Scetti I.[2]
[1] Società Reggiana di Scienze Naturali, Reggio Emilia, Italy
[2] Dipartimento di Scienze della Terra e dell'Ambiente, Università di Pavia, Italy
Corresponding email: mauscacchetti@alice.it

Keywords: Tanatz Alp, rhodonite, pyroxmangite

We investigated the chemical, physical and gemological properties of some samples of rhodonite (and Mn-rich deposits that contain them) from Alpe Tanatz near the village of Splügen in Switzerland. Rhodonites and other Mn rich minerals occur inside large black blocks, located on the slope to the west of the switchbacks that climb to the pass (1720 m). Alpe Tanatz lies between the crystalline basement and the sedimentary cover of the nappe of Tambo. Because of the scarce knowledge of the relationships with the surrounding geological formations, the Mn deposits of Alpe Tanatz have been little investigated compared to those in the nearby ores of Fianel and Starlera in Val Ferrera, mined in the last century (Brugger, 1996). Some gems of rhodonites extracted from the samples have been analyzed with physical and optical methods (weight, density, refractive index, color, size, microscopic observations). Samples of Mn deposits have been analysed by X-Ray Powder Diffractometry (XRPD) to determine the mineralogical composition, by Scanning Electron Microscopy (SEM) for the major elements and Laser Ablation - Inductively Coupled Plasma - Mass Spectrometry (LA-ICP-MS) for trace elements. The color of investigated rhodonites vary from pale pink to purplish-pink, they are opaque and impure for the presence of braunite, rhodochrosite and spessartine; the density varies between 3.4 and 3.6 g/cm^3 and average refraction index is 1.72. The mineralogical assemblage of Mn deposits is composed by rhodonite, kutnohorite, spessartine, quartz, ankerite, rhodochrosite, pyroxmangite. Pyroxmangite and rhodonite are two polymorphs formed at different conditions of pressure and temperature. The presence of pyroxmangite was revealed by XRPD patterns and by Ca contents lower than in rhodonite. Both polymorphs usually form through processes of regional or contact metamorphism, and also metasomatism. Pyroxmangite is usually stable at temperatures below about 400°C and pressures < 2 kbar, while rhodonite is stable at higher temperatures (Maresch & Mottana 1976). Pyroxmangite probably represents a relict phase.

We also identified the presence, as accessory phase, of khristovite, that is very interesting for its rarity. Major element analyses on rhodonites showed Mg is between 0.02 and 0.04 a.p.f.u., Ca between 0.08 and 0.10 a.p.f.u. while Fe is absent; Mn and Ca are negatively correlated; trace element are Zn (around 300 ppm) and As (around 100 ppm). The pink color of rhodonites is clearly related to Mn and no other cromophore occur.

Investigated rhodonites are good quality gems because are compact with no fractures; they also show a nice pink color, although not homogeneous for the presence of orange and purple tints, due respectively to spessartine, and rhodochrosite. However since these gems are opaque and microcrystalline, their commercial value is by far lower than that of the Australian transparent gems from Broken Hill or American from Franklin in New Jersey.

Brugger, J. (1996): The Fe, Mn (V, Sb, As, Be, W) deposits of val Ferrara (Graubünden, Switzerland). Unpublished thesis, Basel University, 188 p.

Maresch, W.V. & Mottana A. (1976): The pyroxmangite-rhodonite transformation for the $MnSiO_3$ composition. *Contrib. Mineral. Petrol.*, **55**, 69-80.

ACQUISITIONS BY THE NEW MAINE MINERAL & GEM MUSEUM: RECENT AND HISTORIC GEM PRODUCTION FROM MAINE PEGMATITES

Simmons W.*[1], Falster A.[1], Francis C.[1], Felch M.[1] & Webber K.[1]
[1] Maine Mineral and Gem Museum, Bethel, ME, USA
Corresponding email: wsimmons@uno.edu

Keywords: tourmaline, pegmatite, gems

We are currently building a unique museum that will open with the largest collection and display of Maine minerals, gems and historical mining material ever assembled for this renowned gem pegmatite district. Granitic, Li- and B-rich pegmatites in the Oxford Pegmatite Field have produced gem material for nearly 200 years and are famous for gem tourmaline.

The 1972 discovery of the famous 9x2x2 m gem-tourmaline pocket in the Dunton pegmatite at Newry produced the finest color-zoned teal green and raspberry red crystals with characteristic steep pyramidal terminations found in North America. Numerous noteworthy crystals and cut gems from this historically significant find were among the Museum's first acquisitions. In 1989, the Bennett pegmatite in Buckfield produced the largest morganite crystal from North America and the Museum has acquired a suite of gems from this crystal, including a 158.5 ct. flawless stone. From the purchase of the locally famous Perham store collection, the Museum acquired a suite of aquamarines from the Aldrich pegmatite in Stoneham, including a 124.9 ct. gem that is the second largest from North America. There is also a large suite of amethyst crystals and gems from the Deer Hill pegmatite, including the largest from the locality, a 161.8 ct. gem. Deep purple gem quality apatite from the Pulsifer pegmatite on Mt. Apatite is well known and the Museum has purchased a 22 ct. cut deep purple fluorapatite.

In the last decade, there has been a renaissance in mining Maine pegmatites and the Museum has acquired most of the significant gem tourmaline production from Mt. Marie, a previously little known locality in Paris. Mount Marie produced exceptional vividly colored tourmaline ranging from electric blue to blue-green to intense pink to red and greenish yellow to champagne colors. The Museum bought over 4000 cts. of gem-quality crystals and cutting rough from the Havey pegmatite in East Poland, mined in 2012. This pegmatite produces very consistent light green elbaite, making it very desirable for the gem industry, and also yields minor amounts of pink and blue-green colors.

Overall, gem tourmaline from the Oxford Pegmatite Field is elbaite in composition with very small liddicoatite and dravite components, most with low X-site vacancies, although minor quantities of rossmanite are present at Mt. Mica (Simmons *et al*., 2005; Roda-Robles *et al.,* 2015). The color of the elbaite is related principally to the amount of iron, manganese and, to a lesser extent, titanium present. Green and blue are Fe dominant in the Y-site, whereas pink and red is Mn dominant with low Fe content. Mt. Marie tourmaline is very low in Ti and this may relate to the vivid and pure colors.

Sparked by worldwide interest in new sources of pollucite, local attentiveness resulted in the discovery of some exceptional etched pocket crystals of gem pollucite that yielded flawless gems up to 4 ct.

Roda-Robles, E., Simmons, W.B., Pesquera, A., Gil-Crespo, P.P., Torres-Ruiz, Nizamoff, J., Torres-Ruiz, J. (2015): Tourmaline as a petrogenetic monitor of the origin and evolution of the Berry-Havey pegmatite (Maine, U.S.A.). *Am..Mineral.*, **100**, 95-109.

Simmons, W.B., Laurs, B.M., Falster, A.U., Koivula, J.I., Webber, K.L. (2005): Mt. Mica: A renaissance in Maine's gem tourmaline production. *Gems Gemol.* **41**, 2-15.

EMERALDS AND RED BERYLS INVESTIGATED BY LASER INDUCED BREAKDOWN SPECTROSCOPY (LIBS)

Tempesta G.*[1] & Agrosì G.[1]
[1] Dipartimento di Scienze della Terra e Geoambientali, Universita di Bari, Italy
Corresponding email: gioacchino.tempesta@uniba.it

Keywords: LIBS, emerald, red beryl

Laser Induced Breakdown Spectroscopy (LIBS) is a valuable technique for doing qualitative and quantitative chemical analyses of all elements in one shot, including light elements like Li and Be. LIBS requires no sample preparation and enables detection of all atomic species, even those present in small amounts (as trace elements). Improved instrumentation performance and use of the objective lens of a microscope to focus the laser beam make it possible to obtain high resolution and reduce sample damage to a minimum. Moreover, the use of a double-pulse laser gives an enhanced signal useful for quantitative chemical analyses. Consequently, a considerable improvement in the detection limit of the trace elements can be obtained. This identification is crucial in determining the "origin" of gemstones. Micro-LIBS appears very attractive for gemmological studies because it allows to select the smallest sampling areas, ensuring a low destructivity and a better representativeness of the analyses. Nevertheless, the main problem affecting LIBS is the difficulty of performing quantitative analyses. The recent development of new software means that it is also possible to perform quantitative analyses with or without standards. The latest methods are Calibration-Free LIBS (CF-LIBS) and One-Point Calibration LIBS (OPC-LIBS) (Cavalcanti et al., 2013). Recently, quantitative analyses by LIBS were carried out on synthetic emeralds to distinguish the different synthetic processes by chemical composition (Agrosì et al., 2014). The micro-LIBS analyses were also performed on red beryl samples in order to distinguish them from pezzottaite and quantify the amount of chromophores (Tempesta & Agrosì, 2016). In this study, we use the micro-LIBS prototype coupled with a petrographic microscope to investigate the origin of the red and green colours of some beryls by evaluating the quantitative amount of chromium, vanadium and manganese. It is worth noting that this analytical set-up permits significantly to reduce the laser damage up to 5-10 μm, making this technique particularly suitable to gemmological objectives.

Agrosì, G., Tempesta, G., Scandale, E., Legnaioli, S., Lorenzetti, G., Pagnotta, S., Palleschi, V., Mangone, A., Lezzerini, M. (2014): Application of Laser Induced Breakdown Spectroscopy to the identification of emeralds from different synthetic processes. *Spectrochim. Acta B*, 1**02**, 48-51.

Cavalcanti, G.H., Teixeira, D.V., Legnaioli, S., Lorenzetti, G., Pardini, L., Palleschi, V. (2013): One point calibration for calibration-free laser-induced breakdown spectroscopy quantitative analysis. *Spectrochim. Acta B*, **87**, 51-56.

Tempesta, G. & Agrosì, G. (2016): Micron destructive and standarless chemical analyses of red beryls by means of Laser Induced Breakdown Spectroscopy. *Eur. J. Mineral.*, in press, DOI: 10.1127/ejm/2016/0028-2529.

MINERALOGICAL INSIGHTS FROM NEAR-FIELD HYPERSPECTRAL IMAGING OF SAPPHIRE-BEARING MARBLE AND ITS POTENTIAL FOR EXPLORATION, BAFFIN ISLAND, NUNAVUT, CANADA

Turner D.*[1], Groat L.A.[1], Rivard B.[2] & Belley P.[1]
[1] Department of Earth, Ocean and Atmospheric Sciences, University of British Columbia, Vancouver, Canada
[2] Department of Earth and Atmospheric Sciences, University of Alberta, Edmonton, Canada
Corresponding email: dturner@eos.ubc.ca

Keywords: corundum, marble, hyperspectral

Baffin Island (Nunavut, Canada) is located in the remote arctic where geological exposure is high but terrain is expansive and field seasons are short. It is host to the Meta Incognita microcontinent, which includes the ~ 2.0-1.9 Ga Lake Harbour Group; a package of shelf sediments of high metamorphic grade that are prospective for marble-hosted gemstones (e.g., Beluga and Agpik Sapphire Occurrences, Soper River Lapis Lazuli Occurrence). The small footprint of these occurrences in combination with their unique mineralogical makeup, unusual settings and unfamiliarity to most geoscientists has resulted in very few discoveries in this remote area. These factors combine to make a positive case for mapping and exploration of these targets by high spatial resolution hyperspectral imaging.

Hyperspectral imaging (also known as imaging spectroscopy) is a non-destructive analytical technique that exploits the interaction between electromagnetic energy (i.e., light) and a material's surface. For geological materials, the interactions of interest are generally related to the mineralogy and mineral chemistry of the target. Diagnostic features of spectrally active minerals are expressed as absorption of electromagnetic energy at specific wavelengths, and allow for mapping of these features in two-dimensional space.

Thirty five (35) samples from the Beluga Corundum Occurrence were studied using high spatial (~ 0.25 mm / pixel) and high spectral resolution (VNIR-SWIR, ~ 550 nm to 2500 nm) in a laboratory setting. Hand samples and thin section offcuts were chosen, allowing comparison to previous petrogenetic studies (e.g., Dzikowski, 2013).

Geological investigations (e.g., Gertzbein, 2005) noted the association of corundum occurrences with calc-silicate lenses within the marble. Minerals directly associated with mineralization include plagioclase, clinopyroxene, phlogopite, muscovite, calcite, graphite, nepheline, and scapolite among other rare phases. Both academic and exploration work identified the importance of scapolite, nepheline and phlogopite.

Investigations of the hyperspectral images were able to successfully reproduce mineralogical and textural information relevant to gem mineralization extracted through thin section petrography. Scapolite and phlogopite from these rocks were shown to have distinct spectral responses from the host calcite. Furthermore, spectrally distinct prehnite and thomsonite were readily distinguishable in the hyperspectral images and are also locally associated with corundum mineralization.

This work focused on hand samples of mineralized material and showed that hyperspectral imaging can be useful in understanding mineralogical relationships of marble-hosted corundum. Hyperspectral imaging can also be scaled up to an outcrop or landscape scale, and our results suggest that airborne hyperspectral imaging has good potential for exploration in areas with good exposure, such as in the Canadian North.

Dzikowski, T.J. (2013): A comparative study of the origin of carbonate-hosted gem corundum deposits in Canada. PhD Thesis, University of British Columbia, 278 p.

Gertzbein, P.J. (2005): Geology surrounding the Beluga sapphire occurrence, Kimmirut, Nunavut: A preliminary examination. *Can. Gemmol.*, **26**, 50-57.

Session S20:

High-tech metal minerals in Europe

Conveners:

Erik Jonsson (Uppsala – Sweden)

Krister Sundblad (Turku – Finland)

MINERALOGY AND MINERAL CHEMISTRY OF THE OLSERUM-DJUPEDAL REE DEPOSITS, SOUTHEASTERN SWEDEN

Andersson S.S.*[1], Wagner T.[1] & Jonsson E.[2-3]
[1] Department of Geosciences and Geography, University of Helsinki, Finland
[2] Department of Earth Sciences, Uppsala University, Sweden
[3] Department of Mineral Resources, Geological Survey of Sweden, Uppsala, Sweden
Corresponding email: stefan.andersson@helsinki.fi

Keywords: REE phosphates, hydrothermal, Sweden

The Olserum-Djupedal REE mineralisation in SE Sweden represents an uncommon type of REE deposit, dominated by high-grade REE phosphates and ferromagnesian gangue minerals. The mineralised area is confined to the border between the Palaeoproterozoic metasedimentary unit of the Västervik formation and a younger anatectic granite belonging to the Transscandinavian Igneous Belt (TIB). In the Olserum area, monazite-(Ce), xenotime-(Y) and apatite are the main REE phases and they typically occur as cm-sized, fractured crystals in gangue-dominated biotite + quartz ± magnetite ± gedrite to ferrogedrite ± cordierite ± muscovite ± chlorite ± andalusite ± albite veins within metasedimentary rocks. The Olserum deposit has an indicated resource of 4.5 Mt at 0.6% TREO with 33.9% HREO (Reed, 2013). Further north in the Djupedal area and towards the contact to the granite, the metasedimentary rocks are strongly migmatised and the REE-bearing veins are more irregular and discontinuous. In addition to monazite, xenotime and apatite, younger allanite-(Ce) and REE-fluorocarbonates also occur. Biotite, quartz, cordierite, muscovite, magnetite, tourmaline and anthophyllite are the main gangue minerals in the REE-bearing veins. Accessory minerals in the Olserum-Djupedal deposits include ilmenite, rutile, hematite, pyrite, chalcopyrite, galena, staurolite, epidote-group minerals, ferberite, zircon, uraninite, thorite and unidentified REE-Y-Nb-W-U oxides. Late tourmaline-bearing granitic to pegmatitic veins crosscut the mineralised zone, but the observation that some REE-bearing veins occur within the granite indicates that ore formation was coeval with or post-date granite magmatism. The latest stage of ore formation is manifested by abundant magnetite-monazite intergrowths in biotite-quartz schlieren in the granite. Biotites from the ore zone display the highest K/Rb ratios, and this ratio decreases towards the youngest granite in the area. Li, Mn, Fe, Zn, Tl and Cs show a distinct trend of increasing concentrations with decreasing K/Rb ratios, whereas Mg, Al and Si all decrease. Na is enriched and Ti depleted in the ore relative to biotites from veins in the granite and magmatic biotites. In comparison to other biotites in the Västervik formation, those from the Olserum-Djupedal deposits are enriched in Nb, with concentrations locally reaching 400 ppm. Magnetites from the REE ore are enriched in Al, Mg, V and Ti relative to magnetites associated with the schlieren and veins in the granite and magnetites from the granite. Our working hypothesis is that the Olserum-Djupedal area represents a syn-TIB magmatic-hydrothermal system with multiple pulses of hydrothermal REE mineralisation having formed as a result of granite magmatism. Future work will focus on fluid inclusion chemistry in order to constrain the nature, composition and origin of the REE mineralising fluids.

Reed, G.C. (2013): Amended and restated technical report for Olserum REE deposit, southern Sweden. Tasman Metals, Vancouver, 85 p.

EXTRACTING RARE EARTH ELEMENTS FROM ACID MINE DRAINAGE

Ayora C.*[1], Macías F.[2], Torres E.[1], Lozano A.[1], Pérez-López R.[2] & Nieto J.M.[2]
[1] Instituto de Diagnóstico Ambiental y Estudios del Agua, Consejo Superior de Investigaciones Científicas, Barcelona, Spain
[2] Departamento de Geología, Universidad de Huelva, Spain
Corresponding email: caigeo@idaea.csic.es

Keywords: acid rock leaching, basaluminite, fluorite

Rare Earth Elements and Yttrium (REY) are raw materials of increasing importance for modern technologies, and finding new resources has become a pressing need. Acid Mine Drainage (AMD) is commonly considered as an environmental pollution issue. However, REY concentrations in AMD can be several orders higher than in other waters. With respect to shale standards, the REY distribution pattern in AMD is convex and enriched in intermediate and expensive REY, such as Tb and Dy. Uranium and Th are commonly below detection limits. Traditional AMD passive remediation systems are based on the reaction of AMD with calcite-based permeable substrates followed by settling ponds. There, schwertmannite and basaluminite successively precipitate as the AMD is neutralized by calcite. Column experiments simulating AMD treatment demonstrate that schwertmannite does not incorporate REY which, in turn, are retained in basaluminite. In addition to basaluminite, fluorite may precipitate and accumulate REY. Although REY rates in the treatment residue may be competitive (median of 0.25%), the annual reserves for an entire region, such as the Iberian Pyrite Belt (IPB) are low (100 t) and only comparable to countries with modest production. However, AMD is expected to continue for hundreds of years; therefore, total reserves are unlimited. In that sense, the IPB would function as a regional-scale heap leaching process, where rain and oxygen would act as natural driving forces with no energy investment. Furthermore, because the main objective of AMD passive remediation systems is to remove acidity and pollutants, the benefits for water reserves and ecosystems are obvious. Therefore, recovery from AMD could be considered an environmentally benign and renewable new REY resource.

SPODUMENE PEGMATITES IN SOUTHEAST IRELAND: PETROGENESIS AND ECONOMIC POTENTIAL AS A RESOURCE OF LITHIUM AND RARE METALS

Barros R.*[1], Menuge J.F.[1-2] & Harrop J.[3]
[1] School of Earth Sciences, University College Dublin, Ireland
[2] Irish Centre for Research in Applied Geosciences & Earth Institute, University College Dublin, Ireland
[3] International Lithium Corp., Vancouver, Canada
Corresponding email: renata.barros@ucdconnect.ie

Keywords: spodumene pegmatite, geochemical modelling, Leinster granite

Pegmatites are important resources of Li, Cs and Ta. These unusual rocks might form as residual magma after crystallisation of granite or as separate partial melts of rare element-rich source rocks. We are investigating textural and geochemical data of spodumene pegmatites and associated rocks in southeast Ireland to better understand how they formed and evaluate their economic potential.

The SE irish pegmatite belt consist of mainly NE-SW-striking dykes with varying thickness (< 20 m), both spodumene-bearing and barren pegmatites, which intrude the eastern margin of the Tullow Lowlands pluton (part of the S-type Leinster Granite), minor granitic intrusions and Lower Palaeozoic metasedimentary rocks. The pegmatite dykes are steeply dipping, variably between NW and SE. Emplacement ages for the granite and the pegmatites are around 400 Ma (O'Connor et al., 1989, 1991) and extreme fractional crystallisation of the Leinster Granite has been proposed as the origin of Li-rich pegmatites (Whitworth & Rankin, 1989; O'Connor et al., 1991; Whitworth, 1992).

The mineralised pegmatites consist of spodumene, muscovite, quartz, albite, spessartine and apatite, with accessory sphalerite and cassiterite. Aplitic material replacing the pegmatitic texture is common and is composed of albite, quartz, spessartine, beryl, cassiterite, sphalerite and phosphates. Barren pegmatites consist of K-feldspar, quartz, albite, muscovite and minor garnet and apatite. The **s**podumene pegmatites have sharp and irregular contacts with the granite and the schist, often marked by a contact zone (< 20 cm) with occasional tourmaline crystallisation. Barren pegmatites are only observed within the granite, in places highly frequent, and have both diffuse and sharp contacts.

Whole-rock geochemical data from eight drill cores through the spodumene pegmatite show a mean content of Li (6000 ppm), Rb (600 ppm), Be (150 ppm), Cs (70 ppm), Sn (70 ppm) and Ta (30 ppm), representing 15 to 300 times the bulk continental crust concentrations. Weighted average grades of 1-4% Li_2O suggest the potential for discovering a significant Li resource, with some additional potential for other strategic metals such as Sn and Ta, which motivates exploration. Relative to the pegmatites, the Tullow granodiorite pluton is enriched in Ba, Sr, and incompatible elements such as LREE, Zr, Th, Ti and Y.

Geochemical modelling of *in situ* crystallisation (Langmuir 1989) using average concentrations of Li, Rb, Cs, Ba and Sr considered granodiorite as the initial magma, with different degrees of crystallisation and appropriate partition coefficients for the crystallising assemblage (feldspars-quartz-biotite-muscovite). The range of compositions obtained failed to reach the extreme concentrations of spodumene pegmatites, so it is unlikely that they represent residual granitic magmas as previously suggested. Batch melting modelling (Shaw, 1970) of psammitic rocks indicates that the granodiorite could have been formed from a feldspar-rich source and the pegmatites from a feldspar-poor source.

Langmuir, C.H. (1989): Geochemical consequences of *in situ* crystallization. *Nature*, **340**, 199-205.

O'Connor, P.J., Aftalion, M., Kennan, P.S. (1989): Isotopic U-Pb ages of zircon and monazite from the Leinster Granite, Southeast Ireland. *Geol. Mag.*, **126**, 725-728.

O'Connor, P.J., Gallagher, V., Kennan, P.S. (1991): Genesis of lithium pegmatites from the Leinster Granite margin, southeast Ireland: geochemical constraints. *Geol. J.*, **26**, 295-305.

Shaw, D.M. (1970): Trace element fractionation during anatexis. *Geochim. Cosmochim. Acta*, **34**, 237-243.

Whitworth, M.P. (1992): Petrogenetic implications of garnets associated with lithium pegmatites from SE Ireland. *Mineral. Mag.*, **56**, 75-83.

Whitworth, M.P. & Rankin, A.H. (1989): Evolution of fluid phases associated with lithium pegmatites from SE Ireland. *Mineral. Mag.*, **53**, 271-284.

RARE METAL VEIN-TYPE MINERALIZATIONS IN THE HISTORIC FREIBERG ORE DISTRICT (GERMANY)

Bauer M.E.*[1], Ostendorf J.[1] & Seifert T.[1]
[1] Institut für Mineralogie, Technische Universität Bergakademie Freiberg, Germany
Corresponding email: matthias.bauer@mineral.tu-freiberg.de

Keywords: indium, rare metal, sphalerite

The hydrothermal polymetallic sulfide veins of the historic Freiberg mining district are traditionally subdivided according to their orientation (in general NNE-SSW to N-S and W-E to WNW-ESE) and their mineral associations. The “Stehende” sulfide veins, mineralized in the N-S striking fissure veins of the central Freiberg mining district, show two types of late-Variscan mineralization: (1) a Zn-Sn-Cu polymetallic sulfide association bound by quartz as main gangue mineral, and (2) a Ag-Sb-Pb polymetallic sulfide association dominated by carbonates as gangue minerals (Seifert & Sandmann, 2006). The element indium was discovered in ores of this paragenesis at the Bergakademie Freiberg 150 years ago (Reich & Richter, 1863, 1864). Both associations formed in a post-collisional extensional regime, in which lamprophyre dikes indicate the influence of mantle-derived fluids (Seifert, 2008). Both types of mineralization have recently been dated to ca. 280 Ma (Rb-Sr method on sphalerite) (Ostendorf et al., 2015), refuting the previous thinking that the Ag-Sb-Pb association could be 80 Ma younger (Romer et al., 2010). The W-E to WNW-ESE striking sulfide veins of the fluorite-barite association (“Spatgänge”) are, on the contrary, as old as previously thought and tend to host higher concentrations of germanium and gallium in sphalerite, compared to veins of the Zn-Sn-Cu polymetallic sulfide association.

Here, we present new data on the mineral chemistry of indium-, germanium- and gallium-bearing sphalerites from various depths and vein systems in the ore district. Further, we discuss fluid inclusion data recorded by quartz and sphalerite linked to the indium mineralization (samples of the Zn-Sn-Cu association) in the hydrothermal system. Large vein quartz samples (up to 10 cm in size) show well-developed growth zoning with fluid inclusion assemblages and cogenetic indium-bearing sphalerites (500 – 2000 ppm In) trapped in several major growth zones. Homogenization temperatures are in the range of 360 to 250°C. We observed very low-salinity (0-3 wt.% $NaCl_{eq}$) and high-salinity fluids (19-22 wt.% $NaCl_{eq}$), showing, besides a general long-term cooling trend, a process of mixing of fluids from two sources.

Ostendorf, J., Henjes-Kunst, F., Seifert, T., Gutzmer, J. (2015): Rb-Sr dating of sphalerite from polymetallic sulfide veins of the Freiberg ore district, Erzgebirge (Germany). Goldschmidt Conf, Prague, abstr., 2362.

Reich, F. & Richter, T. (1863): Vorläufige Notiz Über ein neues Metall. *J. Prakt. Chem.*, **89**, 441-448.

Reich, F. & Richter, T. (1864): Ueber das Indium (Fortsetzung). *J. Prakt. Chem.*, **92**, 480-485.

Romer, R.L., Schneider, J., Linnemann, U. (2010): Post-Variscan deformation and hydrothermal mineralization in Saxo-Thuringia and beyond: a geochronological review. *in* ”Pre-Mesozoic geology of Saxo-Thuringia: From the Cadomian active margin to the Variscan orogen”, U. Linnemann, R.L. Romer, eds. Schweizerbart, Stuttgart, 347–360.

Seifert, T. (2008): Metallogeny and petrogenesis of lampophyres in the Mid-European Variscides. Post-collosional magmatism and its relationship to late-Variscan ore forming processes in the Erzgebirge (Bohemian Massif). IOS, Rotterdam, 304 p.

Seifert, T. & Sandmann, D. (2006): Mineralogy and geochemistry of indium-bearing polymetallic vein-type deposits: Implications for host minerals from the Freiberg district, Eastern Erzgebirge, Germany. *Ore Geol. Rev.*, **28**, 1-31.

DEPOSITION CONDITIONS FOR THE INDIUM-BEARING POLYMETALLIC QUARTZ VEINS AT SARVLAXVIKEN, SOUTH-EASTERN FINLAND

Broman C.*[1], Sundblad K.[2-3], Valkama M.[2] & Villar A.[2]
[1] Department of Geological Sciences, Stockholm University, Sweden
[2] Department of Geography and Geology, University of Turku, Finland
[3] Department of Earth Sciences, Saint Petersburg State University, Russia
Corresponding email: curt.broman@geo.su.se

Keywords: fluid inclusions, In-mineralization, Rapakivi granites

In-bearing polymetallic undeformed and unmetamorphosed quartz veins occur in the 1.64 Ga anorogenic Wiborg Rapakivi Batholith (Cook et al., 2011) and adjacent 1.90 Ga Svecofennian crust (Villar et al., 2016) in SE Finland. A three-stage model (generations 1, 2a and 2b) has been proposed for the veins in the Wiborg Rapakivi Batholith based on field relations (Valkama et al., 2016) but the genetic and temporal relation to the veins in the Svecofennian crust has remained uncertain. Although distinct metal associations are recognized, the metal distribution does not show any clear zonation pattern.

Primary fluid inclusions in quartz vein generations 1, 2a and 2b appear with variable aqueous liquid and vapour proportions (5 to 90 vol.% vapour). Microthermometry yield homogenization temperatures from 100 to 500°C (to liquid and vapour) and salinities of 0 to 16 eq. mass % NaCl. Inclusions with low salinities dominate, but higher salinities are often recorded in metal-rich parts of the veins. There is no evidence for boiling or post-entrapment modifications but the spread in fluid inclusion data may be explained by processes involving condensation and cooling of an initially low-salinity (< 3 mass % NaCl) vapour during its ascent through the fractured granite. The vapour probably had a high temperature (500-600°C) and was released from a crystallizing late-stage magma. Cooling and condensation of the vapour resulted in a turbulent flow with complex geometry and temperature-salinity pattern indicated by the fluid inclusions. In response to the rapid cooling, the rapakivi-hosted veins were deposited. The quartz veins in the Svecofennian crust were also formed from late-stage rapakivi igneous activity but at the very last stage of vein formation (thus considered to represent a generation 3) from a cool (< 100°C) and low-salinity (< 1 mass % NaCl) aqueous fluid.

Cook, N.J., Sundblad, K., Valkama, M., Nygård, R., Ciobanu, C.L., Danyushevsky, L. (2011): Indium mineralization in A-type granites in southeastern Finland: insights into mineralogy and partitioning between coexisting minerals. *Chem. Geol.*, **284**, 62-73.

Valkama, M., Sundblad, K., Nygård, R., Cook, N.J. (2016): Mineralogy and geochemistry of indium-bearing polymetallic veins in the Sarvlaxviken area, Lovisa, Finland. *Ore Geol. Rev.*, **75**, 206-219.

Villar, A., Sundblad, K., Lokhov, K. (2016): Thermal and hydrothermal influence of rapakivi igneous activity on Late Svecofennian granites in SE Finland. Bull. Geol. Soc. Finland, 32th Nordic Geol. Winter Meeting, Helsinki, abstr., 114.

INDIUM-ENRICHED POLYMETALLIC MINERALISATIONS IN SVECOFENNIAN LITHOLOGIES, BERGSLAGEN, SWEDEN

Högdahl K.*[1-2], Jonsson E.[2-3] & Kritikos A.[2]
[1] Department of Geology and Mineralogy, Åbo Akademi University, Finland
[2] Department of Geosciences, Uppsala University, Sweden
[3] Department of Mineral Resources, Geological Survey of Sweden, Uppsala, Sweden
Corresponding email: karin.hogdahl@geo.uu.se

Keywords: indium, Svecofennian, Sweden

The Filipstad district in the westernmost part of the 1.92-1.79 Ga Svecokarelian orogen in Bergslagen, south-central Sweden is known to be enriched in indium (Burke & Kieft, 1980; Kieft & Damman, 1990; Jonsson et al., 2013; Sundblad, 2016), particularly in mineralisations occurring in the vicinity of the post-Svecokarelian Gåsborn granite. The main In carriers are Cu sulphides and sphalerite, but also rare roquesite and possibly sakuraiite.

LA-ICP-MS analyses were performed on sphalerites from 19 polymetallic mineralisations hosted by ca. 1.9 Ga Svecofennian lithologies (mainly skarn hosted by marbles in felsic metavolcanic rocks) in westernmost Bergslagen. We have thus identified new occurrences with elevated In contents (> 30 ppm) in westernmost Bergslagen, and enlarge the In-anomalous area (Nordmark to the west and Hasselhöjden to the southeast of the known occurrences). Sphalerites from all but one (Nordmark) of the mineralisations located along and within the extensive 1.8 Ga Filipstad granite are In barren. In Nordmark, massive, early sphalerite exhibits an In content of > 200 ppm, whereas later-formed, vein-hosted sphalerite from the same mineralisation exhibits < 1 ppm In.

Applying the diagrams of Ye et al. (2013), in order to tentatively discriminate between sphalerite from VMS and exoskarn deposits, In-enriched sphalerites from westernmost Bergslagen plot within or close to the fields of their VMS deposits, indicating a link between In mineralisation and Svecofennian volcanic-hydrothermal processes. Furthermore, bulk geochemical data of sulphide assemblages in three Svecofennian-hosted mineralisations (Stollberg, Tomtebogruvorna and Kalvbäcken) 100-150 km to the NE of the Filipstad district exhibit elevated In contents (30-40 ppm), which shows that In-anomalous mineralisations in the Svecofennian of central Sweden are more widespread than hitherto known, and also located outside of areas featuring major intrusions of younger granites.

Burke, E.A.J. & Kieft, C. (1980): Roquesite and Cu-In-bearing sphalerite from Långban, Bergslagen, Sweden. *Can. Mineral*., **18**, 361-363.

Jonsson, E., Högdahl, K., Majka, J., Lindeberg, T. (2013): Roquesite and associated indium-bearing sulfides from a Paleoproterozoic carbonate-hosted mineralization: Lindbom's prospect, Bergslagen, Sweden. *Can. Mineral*., **51**, 629-641.

Kieft, C. & Damman, A.H. (1990): Indium-bearing chalcopyrite and sphalerite from the Gåsborn area, western Bergslagen, central Sweden. *Mineral. Mag*., **54**, 109-112.

Sundblad, K. (2016): 300 million years of indium-forming processes in A-type igenous environments in the Fennoscandian Shield. *Bull. Geol. Soc. Finland*, Special Volume, 111-112 (abstr.).

Ye, L., Cook, N., Ciobanu, C.L., Yunping, L., Quian, Z., Tiegeng, L., Wei, G., Yulong, Y., Danyushevskiy, L. (2011): Trace and minor elements in sphalerite from base metals deposits in South China: A LA-ICPMS study. *Ore Geol. Rev.*, **39**, 188-217.

REE IN APATITE-IRON OXIDE ORES: THE CASE OF THE PALAEOPROTEROZOIC BERGSLAGEN PROVINCE, SWEDEN

Jonsson E.*[1-2], Majka J.[2], Högdahl K.[2-3], Harlov D.[4] & Persson-Nilsson K.[1]
[1] Department of Mineral Resources, Geological Survey of Sweden, Uppsala, Sweden
[2] Department of Earth Sciences, Uppsala University, Sweden
[3] Department of Geology and Mineralogy, Åbo Akademi University, Finland
[4] Helmholtz Zentrum Potsdam, GFZ Deutsches GeoForschungsZentrum, Potsdam, Germany
Corresponding email: erik.jonsson@sgu.se

Keywords: REE, apatite, Kiruna-type deposit

The apatite-iron oxide (AIO) deposits of the Grängesberg-Blötberget-Idkerberget-Kopslahyttan mining districts are located in the northwestern part of the Palaeoproterozoic Bergslagen ore province in south central Sweden. Besides being the largest concentration of iron oxide ore in this province, these deposits also represent a potential source of REE (e.g., Goodenough et al., 2016). The AIO deposits have been extensively debated as to their origin, particularly whether they formed from hydrothermal processes, or whether they formed directly from high-temperature iron oxide melts (cf. Jonsson et al., 2013, and references therein). Overall in these deposits, the REE were originally hosted by the abundant fluorapatite, but are also present in monazite-(Ce), allanite-(Ce), xenotime-(Y), and epidote, as well as in REE-fluorocarbonate(s). Within the altered immediate host rocks, REE are concentrated in allanite-(Ce), fluorapatite and monazite-(Ce).

The formation of small, often but not always, epitaxially oriented, platy inclusions of monazite-(Ce) in fluorapatite through a fluid-mediated dissolution-reprecipitation process is suggested in the Grängesberg district ores (Jonsson et al., 2016), which is also comparable to other Kiruna-type deposits (e.g., Harlov et al. 2002). Thus, for all of these deposits, the original main host for REE is likely to have been fluorapatite. This was later (post-primary crystallisation) overprinted by a fluid phase, leading to partial dissolution and subsequent re-precipitation of monazite (± xenotime-(Y)) within the fluorapatite grains, and partial remobilization to crystallise e.g. allanite-(Ce) in cracks and along contacts external to the fluorapatite grains. To what extent this fluid was related to a process of fluid expulsion during the crystallization of the apatite-iron oxide melt, or to later, e.g. syn-regional metamorphic fluids, is presently unclear.

Acknowledgements: The presentation is based on results from SGU-funded work on the Grängesberg district, as well as on-going research within the EURARE and StartGeoDelineation (ERA-MIN) projects.

Goodenough, K.M., Schilling, J., Jonsson, E., Kalvig, P., Charles, N., Tuduri, J., Deady, E.A., Sadeghi, M., Schiellerup, H., Müller, A., Bertrand, G., Arvanitidis, N., Eliopoulos, D.G., Shaw, R.A, Thrane, K., Keulen, N. (2016): Europe's rare earth element resource potential: an overview of metallogenetic provinces and their geodynamic setting. *Ore Geol. Rev*., **72**, 838-856.

Harlov, D., Andersson, U.B., Nyström, J.O., Förster, H.-J., Broman, C., Dulski, P. (2002): Apatite-monazite relations in the Kiirunavaara magnetite-apatite ore, northern Sweden. *Chem. Geol*., **191**, 47-72.

Jonsson, E., Troll, V.R., Högdahl, K., Harris, C., Weis, F., Nilsson, K.P., Skelton, A. (2013): Magmatic origin of giant central Swedish "Kiruna-type" apatite-iron oxide ores. *Sci. Rep*., **3**, 1644.

Jonsson, E., Harlov, D., Majka, J., Högdahl, K., Persson-Nilsson, K. (2016): Fluorapatite-monazite-allanite relations in the Grängesberg apatite-iron oxide ore district, Bergslagen, Sweden. *Am. Mineral.*, in press.

THE OTANMÄKI REE MINERALIZATION (FINLAND) – A POTENTIAL SOURCE OF CRITICAL ELEMENTS IN EUROPE

Kärenlampi K.*[1], Paulick H.[1], Hanski E.[1], Kontinen A.[2] & Jylänki J.[3]
[1] Oulu Mining School, University of Oulu, Finland
[2] Geological Survey of Finland, Kuopio, Finland
[3] Otanmäki Mine Oy, Oulu, Finland
Corresponding email: kimmo.karenlampi@oulu.fi

Keywords: REE deposit, critical elements, Fennoscandia

The Otanmäki area in central Finland contains promising rare earth element and niobium mineralization. Although discovered already in 1982, the genesis of the mineralization remains poorly understood. A PhD project on the deposit started at the University of Oulu in January 2016 with the aims to generate a geological and mineralogical characterization of the deposit in order to elucidate the mineralization processes and to study the beneficiation properties of the REE minerals. Here we report results from on-going studies on drill cores and outcrops.

The bedrock of the Otanmäki area is dominated by ca. 2.05 Ga, fine- to coarse-grained, peralkaline to peraluminous A-type granites (the Otanmäki Granite Suite; OGS). It is bordered by Archaean TTG-gneisses to the north, south and west. To the east, it is in contact with the metasedimentary rocks of the Paleoproterozoic Kainuu Schist Belt and is also intruded by ca.1.80 Ga granite-pegmatite dykes. The OGS forms a 65-km-long and 1- to 8-km-wide, boomerang-shaped body showing a moderate to strong deformation related to the ca. 1.8-1.9 Ga Svecofennian orogeny.

The Nb-REE mineralization is located in the western part of the OGS, where alkali-amphibole±alkali-pyroxene bearing granites are dominant. The immediate wall rock suite to the Nb-REE mineralization consists of quartz-feldspar gneisses and associated interlayers of amphibolites and mica-schists. During the drilling campaigns in 1981-1985, two separate mineralizations were outlined: Katajakangas (Ka) and Kontioaho (Ko). Both form shallow dipping, concordant layers with sharp contacts to the quartz-feldspar gneisses that reach several hundreds of meters in strike length and extend to depths of at least 150-200 m. These layers are 0.2-1.4 m (Ka) and 7-12 m (Ko) thick and contain the following REE minerals: allanite-(Ce) [$(Ce,Ca,Y)_2(Al,Fe^{3+})_3(SiO_4)_3(OH)$], bastnäsite-(Y) [$(Y,Ce)CO_3F$], a columbite-group mineral [$(Fe,Mn)(Nb,Ta)_2O_6$], and fergusonite-(Y) [$Y(Nb,Ta)O_4$], together with zircon [$ZrSiO_4$] and thorite [$(Th,U)SiO_4$]. Representative sections show 1.0-2.5 wt.% ZrO_2, 0.1-1.0 wt.% Nb_2O_5, and 0.5-3.6 wt.% TREO at Katajakangas, and 1.4-6.3 wt.% ZrO_2, 0.05-0.3 wt.% Nb_2O_5, 0.3-2.1 wt.% TREO at Kontioaho.

During the PhD project, geological data from field and drill core investigations will be integrated with detailed mineralogical, geochemical and isotope data, in order to evaluate the genetic relationship between the Otanmäki Nb-REE mineralization and the peralkaline OGS, and the role of later thermal and tectonic events. Furthermore, the suite of quartz-feldspar gneisses associated with the mineralization will be dated (U-Pb *in-situ* zircon) in order to determine the temporal and genetic relationships to the 2.05 Ga OGS. The ultimate goal of the project is to assess the possibilities of economic utilization of the Nb-REE mineralization and to enhance the potential to discover new similar occurrences, and hence to strengthen the high-tech metal self-sufficiency of Finland and Europe.

PRIMARY *VS* SECONDARY BERYLLIUM-MINERALS IN PROTEROZOIC GRANITIC PEGMATITES IN SWEDEN

Langhof J.*[1], Jonsson E.[2-3] & Gustafsson L.[4]
[1] Department of Earth Sciences, Swedish Museum of Natural History, Sweden
[2] Department of Mineral Resources, Geological Survey of Sweden, Sweden
[3] Department of Earth Sciences, Uppsala University, Sweden
[4] Skarpnäck, Sweden
Corresponding email: jorgen.langhof@nrm.se

Keywords: beryllium, granitic pegmatite, Fennoscandian Shield

Overall, the economic potential of beryllium in certain deposits in granites as well as in rare Be-enriched volcanic rocks and metasomatites is significant. Yet, the most wide-spread host of this high-tech metal in the upper continental crust is represented by moderately evolved, beryl-bearing granitic pegmatites.

In the Swedish part of the Fennoscandian shield, the occurrence of beryl in pegmatites has been known for a long time, and was locally also test-mined on a modest scale in the 1950s and 60s. The occurrences known at the time were summarized by Brotzen (1959), and a more modern review of overall rare-metal enriched pegmatite districts in Sweden was given by Smeds (1990). Besides the common Be host in these systems, the ring-silicate beryl, a number of often secondary, or late-stage, Be-bearing minerals may also occur. Mårtensson (1960) was the first to observe this and described such an assemblage cross-cutting and partly replacing a beryl-rich zone in the Kolsva pegmatite (south central Sweden). Subsequent to this, a number of related assemblage types and minerals were identified from an array of pegmatites in the Proterozoic of Sweden (Jonsson & Langhof, 1996). Additional discoveries have been made later, and presently, some 75 discrete granitic pegmatites in Swedish bedrock are known to contain beryl. Of these, 33 also contain late-stage or secondary Be minerals. These mainly comprise silicates, such as bavenite, euclase, milarite and phenakite, with bertrandite [$Be_4Si_2O_7(OH)_2$] being the by far most common. More rarely, in somewhat higher-fractionated and phosphate-rich systems, late-stage Be phosphates, such as hurlbutite [$CaBe_2(PO_4)_2$] may also occur. In total, 13 different late-stage Be-rich species are presently known in these systems. In every studied case, primary magmatic beryl served as the source of Be for the late-stage minerals. These formed either through fluid-mediated dissolution-reprecipitation reactions in beryl, essentially *in situ*, or through dissolution followed by Be remobilization and precipitation distal to the beryl. In some cases, both processes were active simultaneously. The formation, abundance and distribution of the late-stage Be minerals clearly represents important information relevant to potential future exploitation of such deposits, as well as clues to the late and post-magmatic evolution of the pegmatites and their host rocks.

Brotzen, O. (1959): Mineral association in granitic pegmatites. A statistical study. *Geol. För. Stockholm Förh.*, **81**, 231-296.

Jonsson, E. & Langhof, J. (1996): Late-stage beryllium silicates in Proterozoic Swedish pegmatites – an overview. 22nd Nordic Geological Winter meeting, Turku Åbo, abstr., 81.

Mårtensson, C. (1960): Euklas und Bertrandit aus dem Feldspatpegmatit von Kolsva in Schweden. *N. Jb. Miner. Abh.*, **94**, 1248-1252.

Smeds, S.-A. (1990): Regional trends in mineral assemblages of Swedish Proterozoic granitic pegmatites and their geological significance. *Geol. För. Stockholm Förh.*, **112**, 227-242.

HIGH-TECH METALS IN THE LAGOA SALGADA DEPOSIT

Lima A.*[1], Leal S.[1] & Barros J.[2]
[1] Institute of Earth Sciences, Department of Geosciences, Environment and Spatial Planning, University of Porto, Portugal
[2] Redcorp Lda, Braga, Portugal
Corresponding email: allima@fc.up.pt

Keywords: selenium, indium, VMS

The increasing consumption of indium (In) and selenium (Se) has significantly stimulated their extraction output, adding economic interest to critical metal resources that a few years ago were either unknown, or unconsidered (Pinto *et al*., 2014).

The Iberian Pyrite Belt is one of the most outstanding European ore provinces, hosting one of the largest concentrations of massive sulphides in the Earth's Crust. The Lagoa Salgada ore body, the most northerly of the Iberian Pyrite Belt, is a small massive sulphide deposit with an inferred mineral resource of 3.7 Mt. The ore body is composed of a central stockwork zone – a more than 700 m thick volcanosedimentary complex – and a massive sulphide lens in the northwest. It is covered by more than one hundred meters of sediments of the Sado Tertiary basin (Lima *et al*., 2013).

The ore mineralization is mainly composed of pyrite with minor sphalerite, chalcopyrite, galena, tetrahedrite-tennantite, arsenopyrite, stannite, cassiterite, and supergene minerals**,** which occur in different amounts throughout the basic textural domains.

Lima et al. (2013) studied massive sulphide ore samples by electron-probe microanalysis (EMPA) and identified a sphalerite generation occurring as 20 µm sized inclusions in recrystallized arsenopyrite, with 23000 ppm In. This In content is three times higher than the most indium-rich sphalerite elsewhere in the same ore body (Oliveira et al., 2011).

This discovery has encouraged the exploration concession holder Redcorp to increase the efforts to find more detailed information on high-tech metals in the Lagoa Salgada Deposit as possible by-products of copper-lead-zinc ores. Recently, new samples were collected to test the presence of Se and In in areas not studied before, e.g., the Central Stockwork (Borehole LS28 and LS26). One 1.5 m thick breccia sample, with 1.01% Cu, 4,46% Pb and 5.23% Zn, has 194 ppm Se. The average Se grade of three samples with 4 m in borehole LS28 is 99 ppm, and the **a**djacent borehole LS26 has a 3 m sequence with on average 101 ppm Se. Oliveira et al. (2011) reported Se contents up to 146 ppm elsewhere in the ore body (borehole LS5). The metallographic study is being developed and no Se-bearing phases such as junoite were found until now, but the strong association with Pb and Zn must be related to the presence of Se **i**n galena and sphalerite as in Neves-Corvo (Pinto et al., 2014).

The complexity of this deposit highlights the need of prospecting new areas inside the ore body with focus on the already two identified high-tech metals that can possibly become important by-products.

On-going work on the Lagoa Salgada (new drilling, re-logging, ore microscopy and whole rock geochemistry, etc) would define the feasibility of the principal Cu-Zn-Pb ores, but also by-products as Au and Ag, and now In and Se.

Lima, A.M.C., Rodrigues, B.C., Oliveira, A., Guimarães, F. (2013): Recent research on indium from the Lagoa Salgada orebody, Iberian Pyrite Belt, Portugal. *Mineral. Mag.*, **77**, 1610.

Oliveira, D.P., Matos, J.X., Rosa, D.R.N., Rosa, C.J.P., Figueiredo, M.O., Silva, T.P., Guimarães, F., Carvalho, J., Pinto, A., Relvas, J., Reiser, F. (2011) The Lagoa Salgada orebody, Iberian Pyrite Belt, Portugal. *Econ. Geol.*,**106**, 1111-1128.

Pinto, A.M.M., Relvas. J.M.R.S., Carvalho, J.R.S., Liu, Y., Pacheco, N., Pinto, F., Fonseca, R. (2014): High-tech metals in the zinc-rich massive ores of the Neves Corvo deposit. *Comun. Geol.*, **101**, 825-828.

LITHIUM EXPLORATION IN PORTUGAL: RESULTS FROM STREAM SEDIMENT ANALYSIS IN THE BARROSO-ALVÃO AREA

Lima A.*[1], Leal S.[1], Dias C.[1], Dias F.[1] & Noronha F.[1]

[1] Institute of Earth Sciences, Department of Geosciences, Environment and Spatial Planning, University of Porto, Portugal

Corresponding email: allima@fc.up.pt

Keywords: lithium, spodumene, stream sediments

The Barroso-Alvão (BA) district, northern Portugal, contains a large population of several dozens of aplite–pegmatite dykes. These bodies are hosted by medium-grade metasedimentary rocks of Silurian age belonging to the Galicia Tras-os-Montes geotectonic zone. Two types of aplite-pegmatite dykes, both crosscutting the metasediments, are encountered in the BA district. The first type is represented by countless, thin (on average meter-size), mainly aplitic dykes and veins, which contain low-grade (< 3 kg/t) Sn-Li mineralization (in cassiterite and petalite). The second type is composed of larger aplite–pegmatite dykes, which are very poor in cassiterite and with spodumene as Li silicate. All pegmatite dykes display irregular patterns: the spodumene rich pegmatites are usually flat-lying, while the others are steeply dipping. A large majority of these dykes exhibits a systematic tectonic control, which may indicate the ascent of the pegmatite-forming magma along dilation zones or preferential structural planes in the enclosing schists during, and after the peak of orogenic metamorphism (Charoy et al., 2001; Lima et al., 2007).

After the discovery of Li pegmatites in the BA district (Noronha, 1987), the Geological Survey of Portugal (IGM) did a stream sediments campaign including 665 stream sediment samples and 223 alluvial samples (Pires, 1995). The samples were analyzed for Li, Sn, W, Nb, Ta and U and the results were presented as tenor isolines.

The stream sediments results were used to identify spodumene-bearing and petalite-bearing pegmatites (Lima et al., 1999) and veins (Lima et al., 2007).

The importance of recognizing if a Li mineralization consists of spodumene or petalite as the principal Li mineral is very important for the Industry. In the case of Li carbonate production, it is only feasible if it is produced from spodumene concentrates. That is the reason why the use of crossed chemical analytical results is also crucial for this study. One of the problems was the contamination caused by historical tin mining. To have a better control on that and not miss spodumene bearing veins a GIS project that supports implementation of catchment basin analysis of stream sediment anomalies was applied in the terms of Carranza (2009): (a) creating polygons representing sample catchment basins, (b) estimating areal proportions of lithologic units in sample catchment basins, (c) estimating local background uni-element concentrations attributable to lithologic units, (d) correcting uni-element residuals for downstream dilution, and (e) classifying geochemical anomalies based on dilution-corrected uni-element residuals.

This methodology allowed approximately 5 dozens of spodumene and 2 dozens of petalite bearing veins to be recognized.

Carranza, E. (2009): Handbook of exploration and environmental geochemistry. Geochemical Anomaly and Mineral Prospectivity Mapping. GIS Volume 11, 351 p.

Lima, A.M.C., Noronha, F., Charoy, B., Farinha, J. (1999): Exploration for lithium deposits in the Barroso-Alvao area, Northern Portugal. 5th Biennial Meeting of the Society for Geology Applied to Mineral Deposits / 10th Quadrennial Symposium of the International-Association-on-the-Genesis-of-Ore-Deposits, London, 1113-1116.

Lima, A.M.C., Vieira, R.C., Martins, T., Noronha, F., Da Silva, F. (2007): The use of geochemistry exploration to identify lithium bearing pegmatite-aplite veins in Northern Portugal. 9th Biennial SGA Meeting, Dublin.

London, D. (1984): Experimental phase equilibria in the system $LiAlSiO_4$-SiO_2-H_2O: a petrogenetic grid for lithium-rich pegmatites. *Am. Mineral.*, **69**, 995-1004.

Noronha, F. (1987): Nota sobre a ocorrência de filões com espodumena na folha de Dornelas.Portuguese Geological Survey internal report.

Pires, M. (1995): Prospecção Geológica e Geoquímica. Relatório interno da Prospecção de Jazidas Litiníferas e de Metais Associados entre as Serras de Barroso e Alvão – Ribeira de Pena. Internal report of the Portuguese Geological Survey, IGM, Lisboa, 46 p.

Stewart, D.B. (1978): Petrogenesis of lithium-rich pegmatites. *Am. Mineral.*, **63**, 970-980.

RØDBERGITE – A POTENTIAL SOURCE FOR REE WITHIN THE FEN COMPLEX, NORWAY

Marien C.*[1], Dijkstra A.[1] & Wilkins C.[1]
[1] School of Geography, Earth and Environmental Science, Plymouth University, United Kingdom
Corresponding email: christian.marien@plymouth.ac.uk

Keywords: carbonatite, Fen complex, rare earth elements

Rare Earth Elements (REE) are crucial for a variety of high-technology applications e.g. wind turbines, catalysts, hybrid vehicles, rechargeable batteries and wind turbines. The secure supply of REE as a strategic resource is important for the further development of the high-tech industry in the EU.

A potential source region of REE within the EU is the carbonatite-peralkaline Fen Complex in Norway. Carbonatites exhibit the highest REE contents amongst all magmatic rocks and are therefore especially promising regarding REE-mineralisations. A key part of this research project is to understand the formation of rødbergite – a red, fine-grained carbonate rock – as an alteration product of, e.g., carbonatites, and the implications of the alteration on the REE content and REE-mineral species.

Rødbergite samples were taken from a variety of different locations focusing on the transition between carbonatite and rødbergite. Especially the Bjørndallen transect gives a unique insight in the alteration from carbonatite into rødbergite. Detailed mineralogical studies on the samples of the Bjørndallen transect, combining SEM-EDS analysis with large area EDS-mapping, made it possible to identify the main REE mineral species as well as the general distribution of the REE minerals. Furthermore, the samples were analysed for trace element compositions to evaluate their economic potential.

The mineralogical investigation of the Bjørndallen transect shows a clear dominance of REE-fluorocarbonates amongst the REE minerals in the carbonatite adjacent to the rødbergite. The beginning alteration of carbonatite to rødbergite causes the breakdown of the primary minerals. REE minerals in rødbergite are dominated by monazite. Additionally the REE concentration increases from 0.16 wt.% TREO in the adjacent unaltered carbonatite up to 1.35 wt.% in rødbergite. Preliminary results suggest an uneven distribution of REE within the rødbergite, creating a separation between HREE and LREE. Apatite aggregates within the rødbergite were identified to play a role as a trapping mechanism for REE bearing fluids and therefore influence the distribution of REE in the samples. Additionally the chondrite-normalized REE concentrations display a significant variation among different rødbergite samples. This could be the result of separate fluid pulses each with a different REE signature.

These results indicate that the formation of rødbergite is clearly associated with the enrichment of REE. The moderate separation of REE into HREE and LREE, as described for the Bjørndallen transect, might also be the case for other rødbergite localities and is still subject of ongoing research. The Fen complex has at least to be considered a strategic REE source for the EU and may even be economically exploitable.

FERROMANGANESE CRUSTS FROM CANARY ISLAND SEAMOUNT PROVINCE AS SOURCE OF HIGH TECH METALS

Marino E.*[1-2], González F.J.[1], Lunar R.[2], Somoza L.[1], Ortega L.[2], Reyes J.[1] & Bellido E.[1]
[1] Instituto Geológico y Minero de España, Madrid, Spain
[2] Departamento de Cristalografía y Mineralogía, Universidad Complutense, Madrid, Spain
Corresponding email: emarino@ucm.es

Keywords: ferromanganese crusts, Atlantic ocean, hydrogenetic

Ferromanganese crusts that cover seamounts and seabed plateaus of the oceans have been studied since the 1980s for their high contents of strategic elements and High Tech Metals. These specifics ores can grow by three different genetic models: hydrothermal, hydrogenetic and diagenetic. Most important for strategic metal contents are hydrogenetic crusts that have a low growth rate (0.5 to 10 mm/Ma) that**,** in addition to its structure**,**allow high concentrations of valuable metals like Co, V, Ni, Cu, REEs and PGEs to form (Hein et al., 2013; González et al., 2012, 2016).

This work presents the results of 15 representative samples of thick Fe-Mn crusts from four Cretaceous seamounts (The Paps, Tropic, Echo and Drago) at the southern Canary Island Seamount Province (CISP) in the NE Central Atlantic. The studied seamounts, the oldest of the CISP (ranging from 91 to 119 Ma), are located on the southern side of CISP within the Spanish EEZ and extended Continental Shelf submitted by Spain on the 14th December, 2014 to UNCLOS. Fe-Mn crusts were recovered along flanks and summits of these seamounts from 1700 to 3000 m depth by the rock dredge method. The growth of thick crust in CISP is related to the presence of a very thick oxygen minimum zone (OMZ) in the NE Central Atlantic Ocean, reaching thickness up to 250 mm at 2400 m. Mineralogical and chemical studies indicate a hydrogenetic origin with a high abundance of Fe-Mn oxyhydroxides. The main Mn minerals are vernadite with interlayered todorokite and asbolane-buserite. Fe oxides are essentially feroxhyte and goethite. These oxides compose about 75-90% of the crusts, the remainder being composed of detritic quartz (aeolian), feldspars, authigenic and detritic calcite, authigenic phosphates and calcareous bioclasts (foraminiphera and/or coccoliths) that can be included in the lamination during their growth.

The crusts show high average contents in Fe (23 wt.%), Mn (16 wt.%), and trace elements like Co (4700 µg/g), Ni (2800 µg/g), V (2400 µg/g) and Pb (1600 µg/g). The contents of rare earth elements plus yttrium (REY) is 2800 µg/g with high proportions of Ce (1600 µg/g) while the contents of the platinum group elements (PGEs) are 230 ng/g and enrichment in Pt (182 ng/g). The crusts show two main types of growing layers: 1) dense lamination of oxides with high contents in Mn+Co+Ni associated with vernadite and Cu+Ni+Zn related to todorokite; 2) botryoidal layers with high contents in Fe+Ti+V and REEs conjoint with goethite. The Fe-Mn crusts from the CISP region show higher contents of Fe, V, Pb and REEs but lower contents of Mn, Co, Ni and PGEs than in samples of Pacific or Indian oceanic seamounts. The Fe enrichment is related to Sahara eolian dust and to submarine volcanic plumes of the CISP hotspot. This Fe enrichment with the action of upwelling currents and biological productivity support a substantial OMZ development and slow growth rates in crusts (1-2 mm/Ma) that allow the enrichment of strategic metals in CISP crusts similar to other Spanish Atlantic seamounts (González et al., 2016).

González, F.J., Somoza, L., León, R., Medialdea, T., de Torres, T., Ortiz, J.E., Lunar, R., Martínez-Frías, J., Merinero, R. (2012): Ferromanganese nodules and micro-hardgrounds associated with the Cadiz Contourite Channel (NE Atlantic): Palaeoenvironmental records of fluid venting and bottom currents. *Chem. Geol.*, **310-311**, 56-78.

González, F.J., Somoza, L., Hein, J.R., Medialdea, T., León, R., Urgorri, V., Reyes, J., Martín-Rubí, J.A. (2016): Phosphorites, Co-rich Mn nodules, and Fe-Mn crusts from Galicia Bank, NE Atlantic: Reflections of Cenozoic tectonics and paleoceanography. *Geochem. Geophys. Geosyst.*, **17**, 346-374.

Hein, J.R., Mizell, K., Koschinsky, A., Conrad, T.A. (2013): Deep-ocean mineral deposits as a source of critical metals for high- and green-technology applications: Comparison with land-based resources. *Ore Geol. Rev.*, **51**, 1-14.

RARE EARTH ELEMENTS EXPLORATION OF FELSIC IGNEOUS ROCKS AND THEIR WHEATHERING PROFILES ON GRAN CANARIA ISLAND, SPAIN

Menéndez I.*[1], Mangas J.[1], Quevedo-González L.Á.[1], Tauler E.[2] & Méndez-Ramos J.[3]
[1] Instituto de Oceanografia y Cambio Global, Universidad de Las Palmas de Gran Canaria, Spain
[2] Departament de Cristal·lografia, Mineralogia i Dipòsits Minerals, Universitat de Barcelona, Spain
[3] Departamento de Física, Universidad de La Laguna, Spain
Corresponding email: inmaculada.menendez@ulpgc.es

Keywords: rare earth elements (REE), wheathering profiles, Mn-oxides

Gran Canaria Island, a hotspot-derived intraplate oceanic island, holds a variety of felsic igneous rocks (i.e., syenites, phonolites, trachytes and rhyolites) consisting of lava and pyroclastic flows, dykes and domes, subsequently leading to the development of weathering paleosoil profiles, comprising both preserved B and C (saprolite) horizons. The felsic rock types are associated with magmatic Miocene activity of the Tejeda caldera (14.1 - 7.3 Ma) and Pliocene stratovolcano formation of Roque Nublo (5.5 - 2.9 Ma). A set of 45 samples was collected and analysed for geochemistry (FUS-ICP, FUS-MS, TD-ICP, INAA) in order to assess both the concentration and distribution of major, minor, and trace elements, focusing on Rare-Earth Elements (REE) which underpin a broad range of emerging technologies in green energy and electronic industries, as efficiency enhancement of solar cells and artificial photosynthesis H_2 generation (Méndez Ramos et al., 2013), in line with EU Raw Materials Initiative in H2020*.

In regards to resulting data sets, the concentration of REE in Miocene alkaline bedrocks varies for syenites (474-590 ppm), trachytes (588-601 ppm), phonolites (828-1036 ppm) and rhyolites (446-577 ppm); whereas lower contents are found in Pliocene trachytic lavas (446 ppm) and phonolitic domes (333-577 ppm). REE-enriched saprolites and B-horizon range 471-1584 ppm and 429-1329 ppm, respectively. In general, LREE values are one order of magnitude higher than HREE and chondrite-normalised REE plots showed the same trend. The percentage change of REE in B-horizon and saprolites, in relation to the bedrock, indicate an increase of up to 20% of LREE in B-horizons and around 10% of HREE in saprolites. The REE enrichment involves an increment of around 11% in value for saprolite and 24% for B-horizon after different weathering index calculations (WIP, V, PIA, CIA, CIW, R, STI) using bedrock levels as a baseline. Furthermore, the “loss on ignition” (LOI) contents increase around 114% and 415% in saprolite and B-horizon, respectively. Spearman correlation matrix of geochemical values was performed on every type of sample. Firstly, the REE contents in the bedrock are positively correlated with major (i.e., MnO, SiO_2) and trace elements (i.e., Ge, Hf, In, Nb, Sn, Ta, Y, W); positively for HREE with Na_2O, Ga and Zn; and negatively for REE with Al_2O_3, CaO, Ba, Sc and V. Secondly, the REE contents in saprolites are positively correlated with trace elements (i.e., Be, In, Nb, Pb, Sn, Th, Y, Zn); positively for HREE with MnO; and negatively for REE with Al_2O_3. Thirdly, the REE contents in B-horizons are positively correlated with Pb and Y; positively for HREE with MnO, Cs, Hf, Nb, Sn and Zn; and negatively for HREE with TiO_2, Ba, Cu and Sr. Hence, a positive correlation was detected in each case between REE and MnO, so the REE mobility in the bedrock and wheathering profiles may be determined by Mn leaching and the precipitation of Mn-bearing minerals as Mn-oxides, frequently observed on the studied materials with granular habits and dendritic textures.

Méndez-Ramos, J., Acosta-Mora, P., Ruiz-Morales, J.C., Hernández, T., Borges, M.E., Esparza, P. (2013): Turning into the blue: materials for enhancing TiO_2 photocatalysis by up-conversion photonics. *RSC Advances* **3**, 23028.

* EU Raw Materials Initiative in Horizon 2020, and “EIT (European Institute of Innovation and Technology) Raw Materials” action (http://ec.europa.eu/DocsRoom/documents/10010/ and http://eitrawmaterials.eu/index.php); ambitious vision of turning the challenge of raw materials dependence into a strategic strength for Europe.

HIGH-TECH METAL CONTENT OF SPHALERITE FROM EASTERN ALPINE PALEOZOIC SEDIMENT-HOSTED LEAD-ZINC DEPOSITS

Onuk P.*[1] & Melcher F.[1]
[1] Department Angewandte Geowissenschaften und Geophysik, Universität Leoben, Austria
Corresponding email: peter.onuk@unileoben.ac.at

Keywords: LA-ICP-MS, Pb-Zn deposits, critical metals

Silver-bearing Pb-Zn mineralization hosted within Paleozoic units of the Eastern Alps is known since Medieval times. Mining stopped due to the small sizes of the deposits and the economic situation after the Second World War. The renewed interest in these Pb-Zn deposits is driven by the incorporation of critical metals like Ge, Ga and In into the sphalerite lattice. Because these metals are extensively used in the electronics industry, some of the deposits may become economically interesting in the future.

In the Austroalpine nappe system, SEDEX-type deposits are known from the Graz Paleozoic and the Gurktal nappe. The Pb-Zn-Ba ores located in the Graz Paleozoic (Styria) formed in the Lower Devonian in an euxinic basin structure associated with submarine alkaline volcanism (Weber, 1990). In a sphalerite concentrate from the Arzberg-Haufenreith deposit, 10 ppm Ge, 11 ppm Ga, 1800 ppm Cd, 29 ppm In, and 5 ppm Tl have been reported (Cerny & Schroll, 1995). *In situ* LA-ICP-MS measurements of sphalerite grains, collected from five ancient mining sites and one exploration adit reveal a large variation of trace element concentrations with median values of 4.67 wt.% Fe, 1832 ppm Cd, 138 ppm Co, 18 ppm Ag, 9 ppm Ga, 0.36 ppm Ge, 1 ppm In, 1 ppm Sn and 5 ppm Sb. Maximum values reach 220 ppm for Ge, 399 ppm for Ag and 83 ppm for In.

Pb-Zn-mineralization at Meiselding located in the Gurktal Nappe (Carinthia) is classified as a metamorphically overprinted SEDEX-type deposit. The Pb-Zn mineralisation of Vellach-Metnitz in the same tectonic unit shows vein-like NW-SE striking tectonic structures (Weber, 1997). At Meiselding, sphalerite carries up to 1900 ppm In, 250 ppm Ge, 65ppm Ga, 282 ppm Co and 2.9 wt.% Cd. From Metnitz, sphalerite carries up to 65 ppm In, 924 ppm Ge, 381ppm Ga, 679 ppm Co and 4380 ppm Cd.

The Zn-Cu-Pb veins next to Koprein (Paleozoic of the Karawanken Range, Carinthia), with high indium concentrations (Cerny & Schroll, 1995), may also represent a vein-type deposit of unknown age. LA-ICP-MS data of sphalerite from Koprein show up to 373 ppm In, 2 ppm Ge, 177 ppm Ga and 457 ppm Co; Cd ranges from 1495-3180 ppm, and Fe from 1.1-7.7 wt.%.

The Eastern Alps host a variety of small to medium-sized copper and pyrite mineralizations, which are located in the Penninic and Austroalpine nappe systems. Major deposits have been mined in the Subpenninic Habach Group, the Penninic Bündnerschiefer Group, the Austroalpine Ennstal quartz phyllite zone and the Austroalpine Greywacke Zone. Literature and recent LA-ICP-MS data indicate elevated concentrations of In, Sn and Cu also in these sphalerites.

Cerny, I. & Schroll, E. (1995): Heimische Vorräte an Spezialmetallen (Ga, In, Tl, Ge, Se, Te und Cd) in Blei-Zink- und anderen Erzen. *Archiv Lagerstättenforsch. Geol. Bundes.*, **18**, 5-33.

Weber, L. (1990): Die Blei-Zinkerzlagerstätten des Grazer Paläozoikums und ihr geologischer Rahmen. *Archiv Lagerstättenforsch. Geol. Bundes.*, **12**, 289 p.

Weber, L. (1997): Handbuch der Lagerstätten der Erze, Industrieminerale und Energierohstoffe Österreichs. Erläuterungen zur Metallogenetischen Karte von Österreich 1:500.000. *Archiv Lagerstättenforsch. Geol. Bundes.*,**19**, 607 p.

Re-BEARING Cu-(Mo)-PORPHYRY DEPOSITS OF THE URALS: LINKS TO TECTONIC EVOLUTION

Plotinskaya O.Y.*[1], Grabezhev A.I.[2] & Seltmann R.[3]

[1] Institute of Geology of Ore Deposits, Petrography, Mineralogy, and Geochemistry, Russian Academy of Sciences, Moscow, Russia

[2] Institute of Geology and Geochemistry, Ural Branch of the Russian Academy of Sciences, Yekaterinburg, Russia

[3] Centre for Russian and Central EurAsian Mineral Studies, Department of Earth Sciences, Natural History Museum, London, United Kingdom

Corresponding email: plotin@igem.ru

Keywords: porphyry, rhenium, Urals

Most of the porphyry Cu (±Mo,Au) deposits of the Urals can be subdivided into several groups according to subduction zones of different ages (Puchkov, 2016):

(1) Deposits related to Silurian intra-oceanic subduction: porphyry Cu deposits of the Birgilda-Tomino ore cluster (Birgilda, Tomino, and Kalinovskoe) and the Zeleny Dol porphyry Cu deposit. These deposits are associated with Na-K calc-alkaline diorites with moderate LREE to HREE enrichment (La_n/Yb_n = 6.50).

(2) Deposits linked to the Magnitogorsk intra-oceanic arc which was active from Early Devonian (Emsian) and collided to the East European plate in the Late Devonian (Famennian). Porphyry-style mineralization of the Magnitogorsk megaterrane shows an evolving relationship from gabbro-diorite-quartz diorite in the Middle Devonian (Salavat and Voznesenskoe porphyry Cu deposits) to granodiorite-plagiogranodiorite (Yubileinoe porphyry Au deposit) and syenite (Verkhneuralskoe porphyry Mo occurrence) in the Late Devonian with an increase in the mean La_n/Yb_n ratio (2.97 to 14.29).

(3) Deposits located in the Trans-Uralian megaterrane and linked to the Late-Devonian to Carboniferous subduction. This includes the Late Devonian to Early Carboniferous Mikheevskoe porphyry Cu deposit linked to an intra-oceanic arc, Late Carboniferous deposits of the Alexandrov volcanic arc terrane (Bataly porphyry Cu deposit) and Early Carboniferous deposits formed due to eastward Andean-type subduction under the Kazakh continent (Benkala porphyry Cu deposit). The REE patterns of the Mikheevskoe (La_n/Yb_n = 3.10). Benkala and Bataly deposits have significant LREE enrichment (La_n/Yb_n = 11.01 and 17.01 respectively).

(4) Continent-continent collision of the East European plate and the Kazakh continent in the Late Carboniferous produced the Talitsa porphyry Mo deposit located in the East Uralian megaterrane. It is related to sub-alkaline granodiorite to granite and establishes the highest LREE to HREE enrichment (La_n/Yb_n = 42.01).

Porphyry Cu deposits linked to intra-oceanic arcs have high Cu/Mo (600 to 115-120) and low Mo/Re ratios (< 1000 ppm) and exhibit high Re contents in molybdenite (Grabezhev, 2013). The Re content in molybdenite mineral fractions in the Mikheevskoe deposit ranges, e.g., from 289 to 3025 ppm but in single EMPA analyses it reaches 1.09 wt.% (Plotinskaya et al., 2015). In the Tomino deposit, the Re contents in molybdenite are 440 to 3140 ppm and in single EMPA analyses up to 0.49 wt.% in the Tomino deposit and up to 0.95 wt.% in the Kalinovskoe deposit.

The Re contents in molybdenite in porphyry Cu deposits**,** linked to active continental margin, are much lower, e.g., 40 to 210 ppm in Benkala deposit. The same is evident for collision-related porphyry Mo deposits, e.g., 187 ppm in the Talitsa deposit (Grabezhev, 2013).

Acknowledgements: This study was supported by the PRAS program #4, RFBR # 14-05-00725, 16-05-00622, NHM (CERCAMS program). It is a contribution to IGCP-592 sponsored by UNESCO-IUGS.

Grabezhev, A.I. (2013): Rhenium in porphyry copper deposits of the Urals. *Geol. Ore Dep.*, **55**, 13-26.

Plotinskaya, O.Y., Grabezhev, A.I., Seltmann, R. (2015): Rhenium in ores of the Mikheevskoe Mo-Cu porphyry deposit, South Urals. *Geol. Ore Dep.*, **57**, 118-132.

Puchkov, V.N. (2016): General features relating to the occurrence of mineral deposits in the Urals: what, where, when and why. *Ore Geol. Rev.*, DOI: 10.1016/j.oregeorev.2016.01.005.

GEOCHEMICAL CONSTRAINTS ON RARE-EARTH ELEMENT DISTRIBUTION OF SEAMOUNT-DERIVED DEPOSITS FROM AMANAY, BANQUETE AND CONCEPTION BANK (CANARY ISLANDS)

Quevedo-González L.Á.*[1], Mangas J.[1], Menéndez I.[1], Tauler E.[2] & Méndez-Ramos J.[3]
[1] Instituto de Oceanografía y Cambio Global, Universidad de Las Palmas de Gran Canaria, Spain
[2] Departament de Cristal·lografia, Mineralogia i Dipòsits Minerals, Universitat de Barcelona, Spain
[3] Departamento de Física, Universidad de La Laguna, Spain
Corresponding email: luisquevedo.master@gmail.com

Keywords: seamounts, rare-earth elements, Fe-Mn oxyhydroxides

Seamounts are scattered undersea features with increasing scientific and economic interest. Indeed, they are broadly recognized as a potential source of raw materials. Rare-Earth Elements (REE) currently emerge as critical raw elements in the "EU Raw Materials Initiative" in Horizon 2020 (European Commission, 2014) for high-tech industries, especially in renewable energy related to increasing efficiencies in photovoltaic solar cells and H_2 generation by water-splitting and artificial photosynthesis (Méndez-Ramos et al., 2013). In the vicinity of 28-30°N latitudes (NW Africa), three Canarian seamounts (Amanay, Banquete and Conception Bank) occur within an oceanic, hotspot-derived intraplate setting, featuring a Paleocene-age chain of volcanic islands and banks. A set of 65 seamount-related samples (igneous rocks, sedimentary rocks and sediments) were analysed for petrography (SEM), mineralogy (XRD) and geochemistry (FUS-ICP, FUS-MS, TD-ICP, INAA) characterization.

Major oxides (%) and REE (ppm) are delimited for each group of samples. Firstly, a subset of 35 igneous rocks of mainly high-alkali, ultramafic-mafic lavas (SiO_2 = 42.83±5.77; MgO = 7.77±2.93; Na_2O + K_2O = 4.07±1.45) shows REE totals of 272.93±161.03 ppm (including an ultramafic rock sample exceeding 1000 ppm). Secondly, a subset of 10 sediment samples (bioclastic silty-clayey sands) with variable amounts of clay minerals, feldspar and quartz (SiO_2 = 8.25±4.59; CaO = 44.44±3.60) shows REE totals of 40.28±15.97 ppm. Thirdly, a subset of 20 sedimentary rocks with diverse major oxide proportions: Ca-rich (CaO = 39.34±7.98), P-rich (P_2O_5 = 12.81±1.05), Fe-rich (Fe_2O_3 = 38.27±17.83), Fe-Mn-rich (Fe_2O_3 = 25.07±6.77; MnO = 14.70±2.64) and detrital rocks (SiO_2 = 41.24±2.38; Al_2O_3 = 13.62±0.46) shows REE totals from tens (Ca-rich rocks) and hundreds (detrital rocks) to thousands of ppm (Fe-Mn crusts; total REE of 1956.16±512.47 ppm up to 2500 ppm).

Spearman correlation matrices were computed to infer geochemical patterns for REE enrichments. Thus, REE in igneous rocks are positively correlated with major (K, P, Ti) and trace elements (Ba, Ga, Hf, Nb, Sr, Ta, Th, Y, Zn, Zr). Also, REE in sediments are positively correlated with major (Al, Fe, K, Mn, Si, Ti) and trace elements (Ba, Nb, Sc, Ta, Th, V, Zr) but inversely with Ca, Sr and LOI, and thus, the REE contents increase for low-carbonated, mineralized, mud-rich sands. Lastly, REE in sedimentary rocks are positively correlated with depth, major (Fe, Mn, Ti) and trace elements (Ba, Nb, Sc, Ta, Th, V, Zr); whereas negative with Ca. Since REE minerals are unlikely in the REE-enriched sedimentary rocks (Co-Ni-rich Fe-Mn crusts; REE contents up to 2500 ppm) are more likely to occur through ionic substitutions in Fe-Mn oxyhydroxides in Mn-bearing (e.g., todorokite) and Fe-bearing (e.g., goethite) minerals (Muiños et al., 2013).

European Commission (2014): Report on critical raw materials for the EU. Report of the Ad hoc Working Group on defining critical raw materials (http://ec.europa.eu/DocsRoom/documents/10010)

Méndez-Ramos, J., Acosta-Mora, P., Ruiz-Morales, J.C., Hernández, T., Borges, M.E., Esparza, P. (2013): Turning into the blue: materials for enhancing TiO_2 photocatalysis by up-conversion photonics. *RSC Adv.*, **3**, 23028-23034.

Muiños, S.B., Hein, J.R., Frank, M., Monteiro, J.H., Gaspar, L., Conrad, T., Garcia-Pereira, H., Abrantes, F. (2013): Deep-sea Fe-Mn crusts from the Northeast Atlantic Ocean: Composition and resource considerations. *Mar. Geores. Geotech*., **31**, 40-70.

HIDDEN SKARN-HOSTED TUNGSTEN MINERALIZATION IN CENTRAL GERMANY – UNCOVERING A PREVIOUSLY UNKNOWN ORE TYPE

Rödel T.*[1] & Borg G.[1]

[1] Fachgruppe Petrologie und Lagerstättenforschung, Martin Luther Universität Halle-Wittenberg, Germany

Corresponding email: tim.roedel@geo.uni-halle.de

Keywords: tungsten, skarn, supergene deposit

The Delitzsch tungsten occurrence in Central Germany was discovered during an exploration drilling campaign by the former state-owned SDAG Wismut in 1971-1973. It was further explored only until 1990, as a continuation was not pursued due to economic reasons (Schenke, 1995).

Nonetheless recent developments on the world market and linked geopolitical considerations justify a re-evaluation of historic sample material of the blind ore body. Previously unknown mineralogical features have been discovered and documented during a first pilot survey of selected samples from several drill cores. Indicators for a progressive evolution of the mineralized fluids were identified, including zonation patterns exhibited by andraditic garnets and scheelite as the main ore mineral. Additionally, the geochemical classification of the predominantly SiO_2-rich high K-calc-alkaline to shoshonitic granodioritic and aplitic rocks of the Delitzsch intrusive complex was verified and extended. The post-Variscian plutonic rocks fit geotectonic discriminations for volcanic arc to syn-collisional granites. Normalized REE-spectra confirm an increasing fractionation from dioritic to granodioritic and aplitic rocks.

In the current study, a previously unknown ore type has been investigated. Historical reports indicated that up to one quarter of the tungsten reserve in the deposit is bound to altered, corroded and disintegrated garnet skarns in the upper portions of the ore body. This was interpreted to be an effect of Paleogene tropical weathering of the exposed pre-Tertiary rocks. Iron hydroxides and oxides have been identified as hosts to elevated anomalous tungsten concentrations of up to 3 %. Scheelite as a classic ore mineral of the deposit does only occur as micro-grains, which could be an indication for a minor late-stage supergene re-precipitation of $(WO_4)^{2-}$.

Supergene enrichment blankets are well-studied for other commodities but are exotic with regard to tungsten. The enriched oxidized zone of the tungsten skarn occurrence at Delitzsch can be regarded as a previously unknown source for this strategic metal.

Schenke, G. (1995): Über das Wolfram-Molybdän-Erzvorkommen von Delitzsch. *Z. Geol. Wissensch.*, **23**, 27-35.

ANALYSIS OF LITHIUM BEARING PEGMATITES BY LASER-INDUCED BREAKDOWN SPECTROSCOPY (LIBS)

Romppanen S.*[1], Kaski S.[1], Järvinen J.[1] & Häkkänen H.[2]
[1] Department of Chemistry, University of Jyväskylä, Finland
[2] Department of Biological and Environmental Science, University of Jyväskylä, Finland
Corresponding email: sari.m.romppanen@jyu.fi

Keywords: LIBS, Li-pegmatites, lithium

Laser-induced breakdown spectroscopy (LIBS) is a powerful tool for the rapid analysis of solid materials. In the LIBS technique, a high power laser pulse is focused on a sample to create a plasma. Emission from the atoms and ions in the plasma is collected via fiber optics and analysed by using a spectrograph and a gated CCD-detector for time-delayed detection. High resolution atomic emission spectra from a few laser pulses can be recorded in a fraction of a second**,** allowing very reliable qualitative identification of material. Characteristic emission spectra can be measured directly from the sample surface and no sample preparation is necessarily needed. LIBS, unlike, e.g., XRF, is able to detect all elements in the periodic table, including light and non-conductive elements. LIBS is a very sensitive method for detecting lithium. Concentrations as low as 5 ppm have been measured in samples of granitic pegmatites (Fabre et al., 2002).

We have investigated spodumene and adjacent minerals from the Li-pegmatites of the Länttä deposit in Kokkola in western Finland by LIBS. Representative maps of relative distributions of several elements have been constructed from the high resolution atomic emission spectra. As an example, lithium and beryllium distribution maps are presented. Differences in relative lithium concentrations can also be detected inside the spodumene grains.

Based on the high resolution LIBS spectra, a mineral classification of the Länttä pegmatite samples has been conducted using multivariate statistics. As a result, mineral species like spodumene, feldspar, quartz and muscovite have been recognized. Our group has previously used a similar approach to identify sulphide minerals (Kaski et al., 2003).

By adding the data of elemental distributions to mineralogical information, a holistic picture of the investigated rock sample can be constructed. For example, the observed slightly lower lithium and respectively higher beryllium contents seem to indicate minerals representing chemical alteration. The combination of elemental distributions and mineral classification can, for example, be used to estimate mineralized areas in drill cores. In addition, LIBS data can be used to interpret the occurrence of photoluminescence in spodumene according to the content of possible activator or quencher elements.

Fabre, C., Boiron, M.-C., Dubessy, J., Chabiron, A., Charoy, B., Martin Crespo, T. (2002): Advances in lithium analysis in solids by means of laser-induced breakdown spectroscopy: an exploratory study, *Geochim. Cosmochim. Acta*, **66**, 1401-1407.

Kaski, S., Häkkänen, H., Korppi-Tommola, J. (2003): Sulfide mineral identification using laser-induced plasma spectroscopy. *Minerals Engin*., **16**, 1239-1243.

INDIUM-BEARING POLYMETALLIC MINERALIZATION ASSOCIATED WITH 1.52-1.85 Ga A-TYPE GRANITES IN THE FENNOSCANDIAN SHIELD

Sundblad K.*[1-2], Valkama M.[1], Cook N.J.[3], Nygård R.[4], Lokhov K.[2] & Ivashchenko V.[5]
[1] Department of Geography and Geology, University of Turku, Finland
[2] Institute of Earth Sciences, Saint Petersburg State University, Russia
[3] School of Chemical Engineering, University of Adelaide, Australia
[4] Ödemarksvägen 107, Broby, Finland
[5] Institute of Geology, Karelian Scientific Center of the Russian Academy of Sciences, Petrozavodsk, Russia
Corresponding email: krisun@utu.fi

Keywords: Fennoscandian Shield, indium mineralization

Indium has an increasing demand for liquid crystal displays, high-definition televisions and other products of modern electronic industry. Most of the indium on the global market is a by-product of zinc mining from a number of ore types. However, even if many mines in Sweden and Finland currently are major Zn producers, they are not significant In producers. Instead, since the first indium discovery in the Fennoscandian Shield (Pitkäranta, Ladoga region, in 1910), almost all recent indium discoveries in the Precambrian of Finland and Sweden were made in veins and skarn mineralizations, in close association with 1.85-1.52 Ga anorogenic granites, none of them in current production.

Moderate grades (up to 83 ppm In) have been recorded in greisen veins in A-type granites of various ages in the *Transscandinavian Igneous Belt*: 1.85 Ga (Gillerdrågen and Tyfors) and 1.67-1.70 Ga (Van and Norra Hålen), all located NW of Bergslagen. 1.85 Ga anorgenic granites are also responsible for the metal supply to the polymetallic ores in Svecofennian supracrustal formations in westernmost Bergslagen (Getön, Hällefors, Gruvåsen and Långban), where up to 100 ppm In has been recorded.

A number of In-bearing polymetallic mineralizations occur in the western parts of the 1.64 Ga *Wiborg batholith*, SE Finland. High grades are recorded for the Zn-Pb-Ag-rich vein at Jungfrubergen (up to 600 ppm In) and the Cu-As-Sn-rich Korsvik veins (up to 1500 ppm), the latter with In in roquesite, sphalerite and chalcopyrite (Cook et al., 2011). Indium also occurs with grades of ca. 40 ppm in compact magnetite-sphalerite bodies at Getmossmalmen and Pahasaari.

Polymetallic veins associated with the 1.57 Ga *Eurajoki stock*, SW Finland, contain up to 570 ppm In.

Indium is abundant (up to 600 ppm) in the Zn-rich skarn ores at Pitkäranta, along the western margin of the 1.54 Ga *Salmi batholith*, where < 1 km^2 1.52 Ga late-stage granite plutons were the metal sources for the ore-forming fluids. Indium is usually sphalerite-hosted but tiny roquesite grains occur in the Hopunvaara deposit (Valkama et al., 2016).

Cook, N.J., Sundblad, K., Valkama, M., Nygård, R., Ciobanu, C.L., Danyushevsky, L. (2011): Indium mineralization in A-type granites in southeastern Finland: insights into mineralogy and partitioning between coexisting minerals. *Chem. Geol.*, **284**, 62-73.

Valkama, M., Sundblad, K., Nygård, R., Cook, N.J. (2016): Mineralogy and geochemistry of indium-bearing polymetallic veins in the Sarvlaxviken area, Lovisa, Finland. *Ore Geol. Rev.*, **75**, 206-219.

INDIUM–BEARING POLYMETALLIC VEINS IN THE SARVLAXVIKEN AREA, SE FINLAND

Valkama M.*[1], Sundblad K.[1-2], Nygård R.[3] & Cook N.J.[4]
[1] Department of Geography and Geology, University of Turku, Finland
[2] Department of Earth Sciences, Saint Petersburg State University, Russia
[3] Ödemarksvägen 107, Broby, Finland
[4] School of Chemical Engineering, University of Adelaide, Australia
Corresponding email: mmvalk@utu.fi

Keywords: In-mineralization, mineralogy, geochemistry

A number of polymetallic vein mineralizations of different styles and metal associations, including base, alloy, noble and critical metals, have been discovered around the Sarvlaxviken bay in the westernmost parts of the Mesoproterozoic Wiborg Batholith, south-eastern Finland. The veins occur in two rapakivi granite varieties: coarse-grained wiborgite; and medium-grained Marviken granite. The veins are divided into five groups based on the dominant metal associations. The Li–As–W–Zn–Mn, Pb–Zn and Cu–As–In associations are hosted by wiborgite, and are strongly controlled by a NNW-trending tectonic pattern that evolved in two main stages. The Li–As–W–Zn–Mn association (generation 1) formed in a typical greisen environment with Li-bearing mica in significant alteration halos around a narrow quartz vein. This greisenization was accompanied by silicification, followed by sericitization and chloritization. The Pb–Zn association occurs in a similar vein type but without typical high-temperature minerals and is considered to have formed at a higher crustal level. Generations 2a and 2b formed under more brittle conditions leading to fracturing, quartz veining and metal precipitation of ore minerals. This metal association is characterized by very high contents of Cu, As and up to 1490 ppm In but with ≤ 0.4% Zn, which leads to very high In/Zn ratios (up to 8400) enabling formation of abundant roquesite. The As–Sn–Cu and Mo–Bi–Be associations are hosted by alteration zones without hydrothermal quartz in the Marviken granite. Mineralization with moderately high contents of As, Sn and Cu is associated with greisenization while mineralization with spectacular contents of Be as well as high contents of Mo and Bi is associated with sericitization, chloritization and berylification. The internal age relations between the wiborgite-hosted, NNW-trending veins show a clear evolution from a typical greisen type environment (the Li–As–W–Zn–Mn and Pb–Zn associations of generation 1) to cooler and more brittle conditions governing quartz veining and precipitation of ore minerals belonging to the Cu–As–In association (generations 2a and 2b). The age relations between these wiborgite-hosted veins and the veins in the Marviken granite are more uncertain but the presence of a NS-trending granitic dyke on the eastern side of the Sarvlaxviken bay, with similar ore-fertile geochemical composition as the Marviken granite, indicates that the tectonically controlled veins formed simultaneously with the emplacement of the Marviken granite and associated hydrothermal activity.

Session S21:

Mineralogy, geochemistry and valorization of industrial and mining wastes

Conveners:

Salvador Morales Ruano (Granada – Spain)

José Miguel Nieto (Huelva – Spain)

Rafael Pérez López (Huelva – Spain)

MIGRATION OF ARSENIC AND CADMIUM FROM ZINC OXIDE EMITTED FROM A SINTERING MACHINE IN PYROMETALLURGICAL PROCESS OF Zn AND Pb PRODUCTION

Adamczyk Z.[1] & Nowińska K.*[1]
[1] Institute of Applied Geology, Faculty of Mining and Geology, Silesian University of Technology, Gliwice, Poland
Corresponding email: katarzyna.nowinska@polsl.pl

Keywords: zinc, lead, pyrometallurgy

Zinc oxide is one of the main entities present in the dust discharged from the stack of the Sintering Machine at the Miasteczko Śląskie Zinc Smelting Plant (Poland). Along with zinc oxide, trace elements are discharged into the environment, among them As and Cd, in amounts of 0.0148 Mg/year and 0.0049 Mg/year, respectively, and 0.0182 g/(m^2 x year) As and 0.0076 g/(m^2 x year) Cd in fallen dust.

In a hypergenic environment zinc oxide is unstable and will decompose into ionic form Zn^{2+} over the whole pH range, and thereby trace elements As and Cd contained in zinc oxide will be released to the environment as a potential pollutant. However, under specific conditions, Zn may form hydrozincite and smithsonite. Hydrozincite is the more environmentally stable form, as its stability region has a wider range of *p*H and Eh than that of the less stable smithsonite. Smithsonite forms only at temperatures close to 10°C and within a narrow range of relatively high *p*H values of 11.0 to 11.5.

The plotted Eh and *p*H diagrams indicate that in the *p*H range of 4.5 to 7.5, and at temperatures of -5 to +30°C, which is characteristic of the soil and water environment of the area under study, arsenic will occur in the solid form, whereas slight changes in Eh will cause transformation of solid As into the ionic form $HAsO^{3-}$, followed by H_2AsO^{4-} (at *p*H < 7), and $HAsO_4^{2-}$ (at *p*H > 7).

Cadmium, on the other hand, will occur in its mobile ionic form Cd^{2+} over the entire *p*H and Eh range prevailing in the area under study.

Analysis of the results leads to the conclusion that both arsenic and cadmium contained in the zinc oxide from the sintering machine used in the ISP process, due to the high mobility of these elements in the soil and water environment of the smelting plant, pose a potential threat to that environment.

MINERAL CARBONATION OF INDUSTRIAL WASTES

Aparicio P.*[1], Galán E.[1] & Martín D.[1]
[1] Departamento de Cristalografía, Mineralogía y Química Agrícola, Universidad de Sevilla, Spain
Corresponding email: paparicio@us.es

Keywords: industrial wastes, carbon sequestration, CO_2

Since the Industrial Revolution the CO_2 concentration and other greenhouse gases (GHG) have increased due to the use of fossil fuels as the main source of energy. Currently there are several studies that used industrial waste as raw material for the capture of CO_2 by mineral carbonation processes. The biggest advantage of mineral carbonation is that CO_2 is caught after reacting with the appropriate material to be stabilized as a "green" mineral. However, two weak points of mineral carbonation are the low speed of reaction and the cost of the process. In this sense, the use of industrial waste rich in alkaline elements, as Ca and Mg, contribute to reducing costs. Industrial products suitable for mineral carbonation include slag, cements, ashes, etc.

In the present study an industrial waste was used as a source of Ca/Mg for the capture and its transformation into a carbonate of Ca/Mg. This waste comes from the Cu-metallurgy, which produces large amount of this residue. The chemical composition is mainly 70 wt.% CaO, 28 wt.% LOI, with minor SO_3, MgO and Fe_2O_3 (less than 1 wt.%). The main crystalline phases are portlandite (80 wt.%) and calcite (20 wt.%).

The study was focused on the control of the variables involved in the process (temperature, pressure, solid-liquid ratio, agitation speed and time of reaction) to achieve the maximum carbonation with the lowest possible cost.

Reactions were obtained in two sealed reactors of different volume: 0.3l and 5l, respectively, in atmosphere of CO_2, working with pressure of 10 bars in the smaller and 1 bar in the bigger. The amounts of dry residue introduced were 10 and 100 g, according to their volume. In both case the reactions ran at room temperature. Monitoring of carbonated products was followed by XRD, elemental analysis, calcimetry (Bernard's method) and thermogravimetry (TG). The mineralogical composition was quantified using a Rietveld procedure. The reaction was also controlled *in-situ* using a X-ray diffractometer equipped with a reaction chamber.

The residue carbonation occurred rapidly in contact with CO_2. After 15 minutes of reaction, calcite formed reached up 60wt.%, and after 30 minutes of reaction the proportion of calcite reached up 91 wt.%, working with around 40% humidity. Agitation favors the carbonation, reducing the reaction time required to complete the reaction. Reaction was completed with agitation in 15 minutes at 60% humidity, and 5 minutes at 90%. It was also found that the starting residue amount has not significant influence on the carbonation process under the same working conditions, i.e., the reaction time per gram was independent of the material subjected to the experiment.

Acknowledgements: This research was financed by the Andalucía Government (RDCCO2 project, P12-RNM-568).

INDUCING THE PRECIPITATION OF LAYERED DOUBLE HYDROXIDES TO REMOVE DIVALENT METALS FROM MINE-WASTE DRAINAGES (IGLESIAS, ITALY)

Atzori R.*[1], Ardau C.[1], Podda F.[1], Agrosì G.[2] & Frau F.[1]
[1] Dipartimento di Scienze Chimiche e Geologiche, Università di Cagliari, Italy
[2] Dipartimento di Scienze della Terra e Geoambientali, Università di Bari, Italy
Corresponding email: roberta.atzori@unica.it

Keywords: mine drainages, metal contamination, waste-water treatment

The removal of toxic metals from waste waters is one of the most important problems in mining environments. Various technologies to reduce the release of toxic metals to the environment have been developed. Layered double hydroxides (LDH) are a series of lamellar compounds with general formula $[M^{2+}_{1-x}M^{3+}_{x}(OH)_2]$ $(A^{n-})_{x/n}\cdot mH_2O$ widely studied for the removal of anionic pollutants from water (Ardau et al., 2011, 2012, 2013). Since LDH precipitation presupposes the presence of a divalent metal and a trivalent metal in adequate ratios, our idea was to use M^{3+}-poor drainages from the impoundment of "Red Muds" from the Monteponi mine area (Iglesias, Sardinia, Italy) as a reagent for the precipitation of LDH and the consequent removal of metals. These drainages are characterised by neutral pH and high levels of SO_4 (~ 4000 mg/L), Mg (~ 600 mg/L), Zn (~ 200 mg/L) and other metals (Pb, Mn, Cd), but very low concentrations of trivalent metals (Fe^{3+} and Al^{3+}). The precipitation of LDH was tested through different batch experiments by adding to water an adequate amount of a salt of Al $[Al_2(SO_4)_3\cdot 18H_2O]$ and NaOH to maintain a neutral *p*H. The main parameter controlling the type of precipitates and the associated removal of metals seems to be the *p*H. XRD analysis of precipitates and chemical analysis of water (before and after the experiments) and precipitates showed either the formation of poor crystalline LDH combined with complete removal of dissolved Zn (98%), as well as removal of significant amounts of Mn, Cd, Pb and Ni, or the formation of more crystalline LDH combined with significantly lower removal of Zn (63%), Mn, Cd, Pb and Ni. In all experiments, Al added to the drainage was not detected in the final solution, indicating a complete precipitation. The precipitates have been also analyzed by HRTEM-EDS-SAED; it was possible to characterize the amorphous Al-sulphate forming at acidic *p*H as a precursor of the poor crystalline LDH forming as *p*H is increased and removal of metals is more efficient. These results encourage further investigations on the removal of metals from mine waters by inducing the precipitation of LDH as a simple and effective waste-water treatment method.

Acknowledgements: This study was financially supported by the Consorzio AUSI (Consorzio per la Promozione delle Attività Universitarie del Sulcis-Iglesiente).

Ardau, C., Cannas, C., Fantauzzi, M., Rossi A., Fanfani, L. (2011): Arsenic removal from surface waters by hydrotalcite-like sulphate minerals: field evidences from an old mine in Sardinia, Italy. *N. Jb. Miner. Abh.*, **188**, 49-63.

Ardau, C., Frau, F., Dore, E., Lattanzi, P. (2012): Molybdate sorption by Zn-Al sulphate layered double hydroxides. *Appl. Clay Sci.*., **65-66**, 128-133.

Ardau, C., Frau, F., Lattanzi, P. (2013): New data on arsenic sorption properties of Zn-Al sulphate layered double hydroxides: Influence of competition with other anions. *Appl. Clay Sci.*, **80-81**, 1-9.

CHEMICAL AND PETROLOGICAL CHARACTERIZATION OF MUNICIPAL SOLID WASTE BOTTOM ASH: A COMPARISON WITH VOLCANICS PRODUCTS

Bello M.*[1] & Carroll M.R.[1]
[1] Scuola di Scienze e Tecnologie - Sezione di Geologia, Università di Camerino, Italy
Corresponding email: marco.bello@unicam.it

Keywords: bottom ash, volatile metals, volcanic products

A petrological study was conducted on municipal solid waste (MSW) bottom ash, products of incinerators combustion.

The preliminary investigation was carried out under atmospheric pressure at 1000, 1050, 1100 and 1200°C and different melting times from 1 to 72 h. The aim was to better constraint the equilibrium reaction time for such compositions, with particular interest in the behavior of Cl and volatile metals such as Pb and Zn. Further experiments were performed in the cold seal pressure vessels at 25, 50, 75, 500 and 1000 bars.

The waste products were found to be mainly composed of rock-like fragments, glass, silicate minerals and various waste metals. In order to characterize and model the bottom ash petrogenesis, all the MSW were mineralogically and chemically studied by using X-ray diffractometer analyses, optical microscopy and electron microprobe analyses.

The samples here investigated are similar to trachy-basalt but with a quite complex heterogeneous glass chemistry. Moreover, many volatile metals, e.g. zinc and lead, result to be incorporated in salts and silicates, as well as in silicate glasses, and their speciation in melts and crystals in MSW products are still widely unknown.

For this reason, the present study is important to compare the MSW products with natural rock systems and, more specifically, to high-temperature volcanic products, and to provide a more complete understanding of the complex conditions of combustion, melting and crystallization (Eusden et al., 1999). Furtheremore, it is essential to infer the same results in analogue natural volcanic products and to improve their comprehension.

Eusden, J.D., Eighmy, T.T., Hockert, K., Holland, E., Marsella, K. (1999): Petrogenesis of municipal solid waste combustion bottom ash. *Appl. Geochem.*, **14**, 1073-1091.

CHANGES IN COMPOSITION AND MINERALOGY OF ENERGY-FROM WASTE AIR POLLUTION CONTROL RESIDUES DUE TO WATER WASHING

Bogush A.A.*[1], Stegemann J.A.[1] & Roy A.[2]

[1] Centre for Resource Efficiency & the Environment, Department of Civil, Environmental & Geomatic Engineering, University College London, United Kingdom

[2] J. Bennett Johnston, Sr., Center for Advanced Microstructures & Devices, Louisiana State University, Baton Rouge, LA, USA

Corresponding email: annakhol@gmail.com

Keywords: APC residue, waste characterisation, element speciation

The generation of energy from waste (EfW) in highly engineered and controlled facilities is an effective way to recover value from municipal solid waste (MSW). Air pollution control residues (APCR) are generated in the flue gas cleaning process and can include fly ash and the solid material captured downstream from the acid gas treatment units and before the gases are released into the atmosphere (Quina et al., 2008). APCRs are classified as hazardous wastes because they are alkaline and contain high concentrations of heavy metals and soluble salts (Amutha Rani et al., 2008; Astrup et al., 2005; Bogush et al., 2015; Chandler et al., 1997; Quina et al., 2008). Commonly, APCRs are landfilled as hazardous waste (Quina et al., 2008).

The main goal of this work was characterisation and comparison of raw and washed APCRs from a UK EfW facility. A thorough analysis of these residues is necessary to enable development of the best options for APCR management.

Both raw and washed APCRs are highly complex materials, comprised mainly of Ca, Si, Al, and S, with high Na, K and Cl in raw APCRs removed by washing. Ca (up to 34%) is significantly enriched in APCRs because excess $Ca(OH)_2$ is used to scrub acid flue gases. The concentration of Cl (6.7%) in the APCR is high because municipal solid waste usually contains a significant amount of polyvinyl chloride. Concentrations of most other elements, including Mg, Fe and potential pollutants (e.g., Zn, Pb, Cr, Cu) increase when the APC residue is washed, due to dissolution of the soluble salts (~ 16%).

The main mineral phases in raw APCRs, determined by PXRD, are calcite ($CaCO_3$), anhydrite ($CaSO_4$), sylvite (KCl), halite (NaCl), calcium chloride hydroxide (CaClOH), lime (CaO), and quartz (SiO_2). The soluble salts such as KCl, NaCl, CaClOH, and CaO dissolved, while $Ca(OH)_2$ was formed as a secondary mineral, in washing.

The local composition and micromorphology of the investigated samples were examined by SEM-EDS and reflect the overall complex composition. Both raw and washed APCRs contain aggregates, spherical particles, glassy and fine phases. After water washing, the percentage of fine particles (< 10 µm) increased significantly, but the percentage of bigger particles (100-500 µm) decreased, which may indicate that these particles were originally agglomerated by soluble salts. Some phases were found to be enriched in potential pollutants (Zn and Pb); for example, a spherical particle of Ca-Zn-silicate and a shapeless particle of Pb chloride.

Metal speciation in the raw and washed APCRs were examined using XANES and EXAFS spectroscopy. As an example, XANES identified changes in Zn speciation resulting from washing.

Characterisation of APCRs with and without washing is significant for our further research on the relationship between metal uptake in cement clinker and paste minerals and the properties of wastes used in co-processing or blended cements.

Acknowledgements: This work was conducted with funding from the Environment Agency and EPSRC.

Amutha Rani, D., Boccacchini, A.R., Deegan, D., Cheeseman, C.R. (2008): Air pollution control residues from waste incineration: current UK situation and assessment of alternative technologies. *Waste Manag.*, **28**, 2279-2292.

Astrup, T., Rosenblad, C., Trapp, S., Christensen, T.H. (2005): Chromium release from waste incineration air-pollution-control residues. *Environ. Sci. Technol.*, **39**, 3321-3329.

Bogush, A.A., Stegemann, J.A., Wood, I., Roy, A. (2015): Element composition and mineralogical characterisation of air pollution control residue from UK energy-from-waste facilities. *Waste Manag.*, **36**, 119-129.

Chandler, A.J., Eighmy, T.T., Hartlen, J., Hjelmar, O., Kosson, D.S., Sawell, S.E., Van der Sloot, H.A., Vehlow, J. (1997): Municipal solid waste incinerator residues. Elsevier, Amsterdam, 973 p.

Quina, M.J., Bordado, J.C., Quinta-Ferreira, R.M. (2008): Treatment and use of air pollution control residues from MSW incineration: an overview. *Waste Manag.*, **28**, 2097-2121.

FIRST STEPS FOR RARE EARTH ELEMENTS RECOVERY FROM WASTES GENERATED IN A FERTILIZER INDUSTRY

Cánovas C.R.*[1], Pellet-Rostaing S.[2], Chapron S.[2] & Macías F.[1]
[1] Departamento de Geología, Universidad de Huelva, Spain
[2] Laboratoire du Tri-ionique par les Systèmes Moléculaires auto-assemblés (LTSM), Institute de Chimie Séparative de Marcoule, Bagnols sur Cèze, France
Corresponding email: carlos.ruiz@dgeo.uhu.es

Keywords: phosphogypsum, leaching experiments, waste valorization

Europe is facing that its mineral richness has been actively mined over many centuries, so accessible mineral deposits are mostly exhausted. Although raw materials are essential for the economy of countries worldwide, their availability is increasingly under pressure. This is especially significant for rare earth elements (REE) which at least 85% of the annual global supply is provided by China (USGS. 2016). The strong dependence of countries with absence of primary REE deposits has encouraged to seek alternative REE resources. One potential source of these metals are industrial landfilled stocks such as phosphogypsum (PG) piles generated by the fertilizer industry. About 5 tons of PG are generated for every ton of phosphoric acid produced, with an annual generation between 100 and 280 Mt (Parreira et al., 2003). The PG stacks generated (100 Mt) after 40 years of operation by a fertilizer plant in SW Spain have been studied in order to estimate its potential valorization as source of REE.

Results obtained from an extensive sampling of PG samples (n = 49) yielded an average content in heavy- and light-REE of 123 mg/kg and 160 mg/kg, respectively. However, a high variability is observed along the stacks with minimum and maximum values of 20 and 647 mg/kg, respectively. The economic feasibility of a mining exploitation is strongly dependent on the mineral cut-off grade. Considering average values, the PG stacks have a REE oxide grade of 0.034%, a value one or two orders of magnitude lower than conventional REE deposits worldwide such as carbonatites, deposits associated with alkaline igneous rocks or lateritic deposits (Orris & Grauch, 2002). However, the huge volume of PG generated, i.e. around 100 Mt, yields a total reserve of 12300 and 16000 tons of heavy- and light-REE subject to potential valorization.

The extractability of REE in PG was addressed by using different acid solutions (i.e., 0.5M H_2SO_4 and 3M HNO_3) as preliminary step for selective recovery of these metals. The best REE leaching performance was obtained using a solution 3M HNO_3,above 80% of REE was released, while caused a dissolution of 63% of gypsum originally present. The use of 0.5M H_2SO_4 provided lower efficiencies; between 46 and 58% of REE contained in PG was released, dissolving less than 6% of gypsum. The higher rate of gypsum dissolution by HNO_3 contributed to a higher level of impurities in the acid liquor. This information could be of paramount importance in subsequent steps to recover the REE contained in these wastes.

Orris, G.J. & Grauch, R.I. (2002): Rare earth eement mines, deposits and occurrences. U.S Geological Survey Open File Report 02-189. U.S Geological Survey, Tucson, AZ.

Parreira, A.B., Kobayashi, A.R.K. Jr, Silvestre, O.B. (2003): Influence of Portland cement type on unconfined compressive strength and linear expansion of cement-stabilized phosphogypsum. *J. Environ. Eng.*, **129**, 956-960.

USGS (2016): Mineral commodities summaries 2016. U.S. Geological Survey, 202 p., DOI: 10.3133/70140094

REEY WATER SCAVENGING AND ENRICHMENT BY POORLY CRYSTALLINE ALUMINUM HYDROXYSULFATES: ALPINE NATURAL STREAMS *VS* AMD PASSIVE TREATMENT SYSTEMS

Caraballo M.A.*[1-2-5], Hochella M.F. Jr[2], Wanty R.B.[3], Verplanck P.L.[3], Ayora C.[4], Macías F.[5] & Nieto J.M.[5]

[1] Departamento de Ingeniería de Minas, Universidad de Chile, Santiago, Chile

[2] Department of Geosciences, Virginia Polytechnic and State University, Blacksburg, VA, USA

[3] U.S. Geological Survey, Denver Federal Center, Denver, CO, USA

[4] Instituto de Diagnóstico Ambiental y Estudios del Agua, Consejo Superior de Investigaciones Científicas, Barcelona, Spain

[5] Departamento de Geología, Universidad de Huelva, Spain

Corresponding email: mcaraballo@ing.uchile.cl

Keywords: REEY, hydrobasaluminite, acid mine drainage

Rare Earth Elements and yttrium (REEY) are critical raw materials for modern technological applications. In 2011, global demand was 105 kt of REEY oxides and is expected to grow up to 160 kt in 2016 (Hatch, 2012). Due to the almost complete control exercised by China on the production of these strategic elements, many other major economies around the world are searching for new sources of REE that could offer some flexibility and independence in the REEY market.

REEY contents recorded in waters affected by acid mine drainage (AMD, ranging between 4,000 and 80,000 pmol/L) are several orders of magnitude higher that medians values reported for non-polluted natural waters. Additionally, the geochemistry of these elements in AMD solutions is strongly linked to *p*H, and therefore to AMD neutralization processes. Verplanck (2013) report that REEs behave conservatively at *p*H values below 5 and partition into colloidal phases and precipitates at water *p*H above 5.

The present study investigates the presence, partitioning and possible enrichment of REEY in two samples of pure hydrobasaluminite ($Al_4SO_4OH_{10}\cdot 12\text{-}36H_2O$) precipitated in an alpine polluted river (Paradise Portal, Rocky Mountains, USA) and in an AMD passive treatment system (Mina Esperanza, Iberian Pyrite Belt, SW Spain).

Geochemically, NASC-normalized REE patterns in both AMDs show a typical convex curvature, indicating enrichment in Medium REE with respect to Light REE and Heavy REE. REE/NASC normalized values in Mina Esperanza´s passive treatment waters and precipitates show no water/solid fractionation (parallel curves showing the same tendencies). However, REE/NASC normalized values in Paradise Portal waters and precipitates show some water/solid fractionation for Medium and Heavy REE.

Concerning REE scavenging and enrichment in hydrobasaluminite, the high ability of this mineral to accumulate REEY was confirmed. It was observed that despite Mina Esperanza's water having half the cumulative REEY concentration than Paradise Portal's water, the existence of an alkaline treatment at Mina Esperanza induced the generation of hydrobasaluminite precipitates with more than 2,000 mg/Kg of REEY (almost 30 times higher than the concentration observed in Paradise Portal´s hydrobasaluminite).

The significant REEY enrichment observed in hydrobasaluminite, the ubiquity of AMD around the world, the rising environmental awareness leading to the implementation of more and more AMD treatment facilities, and the compelling need of new and alternative REEY sources, offer a unique opportunity to explore the economical feasibility of “environmentally mining” REEY from AMDs.

Hatch, G.P. (2012): Dynamics in the global market for rare earths. *Elements*, **8**, 341-346.

Verplanck, P.L. (2013): Partitioning of rare earth elements between dissolved and colloidal phases. *Procedia Earth Planet. Sci.*, **7**, 867-870.

THE CASE OF STOPPANI SPA (GE), AN EXTREME POLLUTED CR(VI) SITE: MINERALOGICAL AND GEOCHEMICAL CHARACTERIZATION OF WASTE, SOILS, AND WATER. EFFICIENCY OF PECULIAR MAGHEMITE NANOPARTICLES FOR CR(VI) REMOVAL FROM POLLUTED WATERS

Carbone C.*[1], Salviulo G.[2], Vianello F.[3-4], Baratella D.[3], Magro M.[3-4], Molinari S.[1], Canepa M.[5], Belmonte D.[1], Dinelli E.[5] & Brescianini C.[5]

[1] Dipartimento di Scienze della Terra, dell'Ambiente e della Vita, Università di Genova, Italy

[2] Dipartimento di Geoscienze, Università di Padova, Italy

[3] Dipartimento di Biomedicina Comparata e Alimentazione, Università di Padova, Legnaro, Italy

[4] Regional Centre of Advanced Technologies and Materials, Palacki University, Olomouc, Czech Republic

[5] Dipartimento di Scienze Biologiche, Geologiche e Ambientali, Università di Bologna, Italy

Corresponding email: carbone@dipteris.unige.it

Keywords: Cr(VI), environmental mineralogy, maghemite nanoparticles

Heavy metal pollution has become a severe problem in industrialization and urbanization process at regional scale. Among the toxic heavy metals, Cr(VI) is considered as a priority pollutant, as it is widely used in metal processing, electroplating, leather tanning and pigment industry. The Stoppani S.p.A. industry, located in the Cogoleto and Arenzano Area (Genova, Italy), transformed Cr(III) of chromite mineral ($FeCr_2O_4$) taken from local ophiolitic rocks to Cr(VI). It ceased the activity at the beginning of 2003, and since 2001, the Stoppani S.p.A. has been included, with DM n.468, into the national program of environmental remediation and restoration. In the 1918-1982 period, it discharged up to 1 million tons of post-treatment mud on the neighboring beaches. Thus, groundwater resulted heavily polluted by hexavalent Cr (maximum over than 1000000 µg/L).

The aim of this work is: a) geochemical characterization of pumping wells water and percolating water from wastes, b) mineralogical characterization of soils and waste materials, c) test the efficiency of peculiar maghemite nanoparticles, called Surface Active Maghemite Nanoparticles, (SAMNs) (Magro et al., 2010) for Cr(VI) removal from polluted waters.

The samples object of this study are representative of soils, and waste deposits and polluted waters. The results of solid fractions indicate that soil and waste deposits are characterized by high concentrations of soluble Cr(VI) (12553 µg/L); total Cr(VI) (20420 µg/L) and total Cr (89615 µg/L) and are composed by the presence of residual roasting chromite and roasting product such as: trona, dawsonite, gypsum, ettringite, thenardite and brownmillerite. The chromate ions in these materials could be related either to the substitution of sulfate ions in ettringite or to the presence of microporosity of waste materials. The water samples object of this work are representative of 3 pumping wells distinguished on the basis of the Cr(VI)-content: sample W1 (527 < Cr(VI) < 11700 µg/L); W6 (83800 < Cr(VI) < 146000 µg/L); W9 (10500 < Cr(VI) < 232000 µg/L) and two samples of leached waters (about 4000µg/L). The application of peculiar magnetic nanoparticles (SAMNs, 1 g L^{-1}) on three water samples removed 75-80 % of Cr(VI), while, if the same treatment was accomplished at *p*H 3.0, Cr(VI) removal was about 95 % with respect the initial concentration. Temperature, in the 4-25°C range, did not influence Cr(VI) removal by SAMNs. A second treatment with SAMNs on the same water samples increased Cr(VI) removal efficiency up to 98%, leading to a final Cr(VI) concentration below the limits stated by Italian law. SAMNs represent efficient candidates for the magnetic removal of Cr(VI) from aqueous polluted environments, greatly reducing operational costs, while improving stability of spent residuals. Further experiments are in progress in order to validate the efficiency of SAMNs on large scale magnetic cleanup of real industrial effluents.

Magro, M., Valle, G. Russo, U., Nodari, L., Vianello, F. (2010): Maghemite nanoparticles and method for preparing thereof. International Patent Application WO/2012/010200.

BASALUMINITE AS SCAVENGER OF CONTAMINANTS

Carrero S.*[1], Fernández-Martínez A.[2], Pérez-López R.[1] & Nieto J.M.[1]
[1] Departamento de Geología, Universidad de Huelva, Spain
[2] Institut des Sciences de la Terre, Université Grenoble Alpes, Gières, France
Corresponding email: sergio.carrero@dgeo.uhu.es

Keywords: basaluminite, EXAFS, PDF

Basaluminite is a poorly crystalline Al-hydroxysulfate mineral which has been described as the most typical mineral in Al-SO_4-bearing systems (Nordstrom, 1982). This mineral precipitates in aquatic environment with high Al and sulfate concentration in solution and low *p*H (4.5-5), such as streams, lakes and sediments affected by acid mine drainage (AMD), acid sulfate soils (ASS) and acid hydrothermal activity. Basaluminite has been described as scavenger of trace elements from de solution, such as Cu and Si (Bigham & Nordstrom, 2000), however previous precipitation of Fe-phases in natural streams remove potential toxic elements (e.g., arsenic and selenium), masking basaluminite affinity for them (Carrero et al., 2015). Several laboratory experiments have reported that Fe-phases common in streams affected by AMD (e.g., schwertmannite) shown high capacity to uptake As and Se oxyanions from the solution, holding these molecules with combination of inner and outer-sphere binding surface complexes (Waychunas et al., 1995). To our knowledge, there are no published studies on As and Se-basaluminite interaction, and nothing is known about the structural coordination of these element. This study examines sorption of As and Se onto synthetic basaluminite. Adsorption capacity was calculated throughout batch sorption experiment where the solid phase was exposed to solution with As or Se loading range between $3 \cdot 10^{-5}$ to $1 \cdot 10^{-2}$ mol L^{-1}. After to reach the equilibrium, the solid resulted was examined using synchrotron light source technics (i.e., differential pair distribution function, d-PDF; and extended X-ray absorption fine structure, EXAFS). Synthetic basaluminite showed high sulfate content in its chemical composition, which played a crucial role in sorption processes. Oxyanion exchange between structural sulfate with arsenate and selenate in solution was the mechanism which took place during the adsorption experiment. Arsenate sorption capacity by basaluminite was three times higher than selenate, where the exchange ratio was 1:2 and 1:1 sulfate with respect to arsenate and selenate, respectively. EXAFS experiment at the S *K*-edge in basaluminite showed that outer-sphere was the most probably sulfate structural coordination, where this molecule seen to be located in the interlayer space. On the other hand, d-PDF of As and Se onto basaluminite, indicated that arsenate was coordinate in bidentate inner-sphere position, whereas sulfate were replaced with selenate in outer-sphere position. The present study is relevant because it is the first work which quantifies the sorption retention capacity of trace element onto basaluminite, describing the binding mechanisms of these oxyanion. The results brought in this experiment are relevant in the understanding of trace elements behaviour in environment affected by AMD and ASS, opening a new research lines focused on natural recovery and treatment systems.

Bigham, J.M. & Nordstrom, D.K. (2000): Iron and aluminum hydroxysulfates from acid sulfate waters. *Rev. Mineral. Geochem.*, **40**, 351-403.

Carrero, S., Pérez-López, R., Fernandez-Martinez, A., Cruz-Hernández, P., Ayora, C., Poulain, A. (2015): The potential role of aluminium hydroxysulphates in the removal of contaminants in acid mine drainage. *Chem. Geol.*, **417**, 414-423.

Nordstrom, D.K. (1982): The effect of sulfate on aluminum concentrations in natural waters: some stability relations in the system Al_2O_3-SO_3-H_2O at 298 K. *Geochim. Cosmochim. Acta*, **46**, 681-692.

Waychunas, G.A., Xu, N., Fuller, C.C., Davis, J.A., Bigham, J.M. (1995): XAS study of AsO_4^{3-} and SeO_4^{2-} substituted schwertmannites. *Physica B*, **209**, 481-483.

COMBINING SEM-EDS AND OPTICAL-MICROSCOPE METHODS IN INVESTIGATIONS OF THE CO-OCCURRENCE OF MINERAL- AND ORGANIC MATTER IN COAL WASTES

Ciesielczuk J.*[1-2], Misz-Kennan M.[1] & Fabiańska M.[1]
[1] Faculty of Earth Sciences, University of Silesia, Katowice, Poland
[2] Centre for Polar Studies KNOW (Leading National Research Centre), University of Silesia, Katowice, Poland
Corresponding email: justyna.ciesielczuk@us.edu.pl

Keywords: coal wastes, SEM-EDS, reflected light optical microscope

Coal wastes are typically composed of mudstones, sandstones, and clays forming layers of varying thicknesses. Dispersed organic matter occurs in all. The fact that both mineral- and organic matter is usually of very small grain size makes insightful investigation difficult.

Coal-waste investigations require the use of various methods for mineral- and organic-matter identification. Basic methods are: Scanning Electron Microscopy combined with EDS (to give rough chemical compositions and preliminary identifications of mineral phases); X-Ray diffraction (to identify mineral phases); Reflected Light Optical Microscopy (for identification of organic matter and reflectance measurements). The detection limits and minimum analytical grain sizes for the individual methods are different. SEM-EDS and RLOM can investigate objects of sizes ranging from ca. 1-10 mm whereas the X-ray micro-diffraction technique allows identification of objects of ca. 100 mm in minimum diameter. As XRD is a destructive method, it should be used at the end of the identification process. RLOM and SEM samples can be prepared in the same way. The best are polished blocks or thin sections but, for reflected optical microscopy, they must be covered with immersion - a procedure incompatible with SEM. Furthermore, the same objects observed with SEM and RLOM look so different that, without some indication, they can be difficult to find.

Knowing all the difficulties in combining these methods, we propose the following procedure for the investigation of mineral- and organic matter. (1) Stick a piece(s) of aluminium tape of known shape(s) to polished section. (2) Draw or photograph the sample. (3) Examine the sample using SEM in known/marked places. (4) Find objects using RLOM in marked places. (5) Use binocular microscope to find objects already investigated by SEM-EDS and RLOM and, where larger than 100 mm, powder for X-ray micro-diffraction.

Acknowledgements: The project has been financed from the funds of the Leading National Research Centre (KNOW) received by the Centre for Polar Studies for the period 2014-2018 and statutory research of Faculty of Earth Sciences, University of Silesia.

HYDROTHERMAL ALTERATION OF STEEL SLAGS: A NOVEL VALORIZATION ROUTE

Crouzet C.*[1], Brunet F.[1], Recham N.[2], Ferrasse J.-H.[3] & Goffé B.[4]

[1] Institut des Sciences de la Terre, Centre National de la Recherche Scientifique, Université Grenoble Alpes, Grenoble, France

[2] Laboratoire de Réactivité et Chimie des Solides, Centre National de la Recherche Scientifique, Université de Picardie Jules Verne, Amiens, France

[3] Laboratoire de Mécanique, Modélisation et Procédés Propre, Centre National de la Recherche Scientifique, Université Aix-Marseille, Aix-en-Provence, France

[4] Centre Européen de Recherche et d'Enseignement de Géosciences de l'Environnement, Centre National de la Recherche Scientifique, Université Aix-Marseille, Aix-en-Provence, France

Corresponding email: camille.crouzet@ujf-grenoble.fr

Keywords: steel slag valorization, hydrogen production, hydrothermal experiments

According to the World Steel Association (2015), more than 1.4 billion tons of steel were annually produced since 2010 in the world. Production of steel generates steel slags which represent 10 to 15% by weight of steel output (Van Oss, 2013), being 140 to 220 Mt each year. Their valorization is partial and limited to the production of secondary aggregates for civil engineering applications. A significant part of steel slags are currently not enhanced and simply stored on site. Mainly composed of Ca, Fe and Si, many investigations were performed to develop new valorization paths. Thus, steel slags were well known for their ability to store carbon under mineral forms due to their high content in free Ca. Valorization as cement was also studied due to the close mineralogical composition between Portland cement and steel slag. However, particular interests were always focused on Ca – Si phases but only few studies were dedicated on iron.

The new valorization process of steel slag developed here was initiated by Malvoisin et al. (2013) and was inspired from the serpentinization process observed in mid-oceanic ridge settings (Charlou, 2002). Under specific hydrothermal conditions, a redox reaction occurs between olivine iron (II) content and water under high pressure and temperature. Iron (II), FeO equivalent, is partially oxidized into magnetite, Fe_3O_4, and water is reduced into dihydrogen, H_2, according to reaction (1). With a FeO content equivalent to 15-20% in weight, up to 10 NL of high-purity H_2 may be produced per kg of steel slag. Steel slags are excellent candidates to export this process to an industrial and large scale production of H_2.

$$3\ FeO_{(s)} + H_2O_{(l)} = Fe_3O_{4(s)} + H_{2(g)} \quad (1)$$

Hydrothermal experiments were conducted in the liquid domain of water from 150 to 350°C under 200 bars. Reaction kinetics were monitored from hydrogen production and aqueous speciation thanks to a sampling autoclave. Influence of experimental parameters, such as temperature or crushing, on hydrogen production yield were investigated. Moreover, a specific study was conducted in parallel on commercial FeO to identify the oxidation mechanisms and the effect of acidic conditions.

Mineralogical characterizations were performed on solid samples before and after oxidation by XRPD, SEM, and TEM. Hydrogen production was quantified by gas chromatography and solution compositions were analyzed by ICP-AES and complexation – spectrophotometry method. SUPCRT thermodynamic database and Phreeqc software were used to predict mineral transformations and multiphasic equilibriums.

Acknowledgements: This work is supported by CNRS through the “Mission Interdisciplinaire: Défi Transition Energétique: Ressources, Société, Environnement – ENRS” program.

Charlou, J-L., Donval, J-P., Fouquet, Y., Jean-Baptiste, P., Holm, N. (2002): Geochemistry of high H_2 and CH_4 vent fluids issuing from ultramafic rocks at the Rainbow hydrothermal field (36°14’N, MAR), *Chem. Geol.*, **191**, 345-359.

Malvoisin, B., Brunet, F., Carlut, J., Montes-Hernandez, G., Findling, N., Lanson, M., Vidal, O., Bottero, J-Y., Goffé, B. (2013): High-purity hydrogen gas from the reaction between BOF steel slag and water in the 473-673 K range, *Int. J. Hydrogen Energy*, **38**, 7382-7393.

Van Oss, H.G. (2013): Slag, iron and steel: U.S. Geological Survey. *2011 Minerals Yearb.*, **1**, 69.1-69.9.

World Steel Association (2015): Steel statistical Yearbook 2015. Worldsteel Committee on Economic Studies, 122 p.

TRACE ELEMENTS MOBILITY DURING IRON-PRECIPITATES DIAGENESIS

Cruz-Hernández P.*[1], Pérez-López R.[1] & Nieto J.M.[1]
[1] Departamento de Geologia, Universidad de Huelva, Spain
Corresponding email: pablo.cruz@dgeo.uhu.es

Keywords: arsenic, aging, goethite

Arsenic (As) is a potentially toxic element for the human beings. This toxic is often associated with massive sulfide ore deposits. Sulfide oxidation in meteoric conditions releases acidity and high concentrations of sulfate and metal(oid)s such as Fe, As, Cd, Cu, Zn, Pb. The leachate from oxidation of sulfide-rich wastes derived from the mining activity is known as Acid Mine Drainage (AMD). Schwertmannite ($Fe_8O_8(OH)_{5.5}(SO_4)_{1.25}$) usually precipitates as a poorly-crystalline mineral from AMD solutions (Bigham et al., 1996). Schwertmannite is a good scavenger of trace elements from the solution, showing predilection by As (Acero et al., 2006). However, schwertmannite transforms into goethite (FeOOH) in natural conditions in some weeks (Acero et al., 2006) and into hematite (Fe_2O_3) over centuries (Pérez-López et al., 2011).

The present study deals with the behavior of As(V) during the mineralogical transformation of the AMD precipitates. To this end, the precursor phase, schwertmannite, was synthesized in presence of different As(V) concentrations at 60°C. Batch experiments were carried out by heating solutions of $Fe_2(SO_4)_3$ (5 M) in presence of different contents of Na_2HAsO_4 (0, 0.05, 0.0125, 0.25, 0.5 and 1 mM of As(V)) during different time periods, whereupon the water was filtered and analyzed and the precipitates were characterized by X-ray diffraction (XRD). Also structural changes were analyzed with differential pair diffraction (PDF).

Iron concentration in solution reveals three stages: (I) a first sharp decrease due to massive homogeneous nucleation, (2) a slight decrease linked to cluster growth, and (3) a steady-state that denotes equilibrium solution-mineral. The first stage and part of the second correspond to schwertmannite precipitation, which is concomitant with the decrease of SO_4 concentrations. After that, SO_4 is released due to the transformation of schwertmannite into goethite. Similar to the behaviour of SO4, As is depleted from the solution by schwertmannite precipitation at the onset of the experiment and then it is slightly released to solution during the long-term transformation into goethite. This fact indicates that removal As capacity in more crystalline phases is lower than in their poorly-crystalline precursors.

Spontaneous precipitation rate of schwertmannite was obtained by linear regression of the change in $[Fe]_{precipitated}$ with the time in the first stage. It was observed that increase of $[As]_{initial}$ in solution decreases the precipitation rate. Moreover, in the experiment of 1 mM of As(V), an amorphous phase seems to occur according to XRD instead of schwertmannite. Pseudo-first order transformation rates of schwertmannite into goethite can be calculated using the natural logarithm of $[SO_4]_{precipitated}$ / $[SO_4]_{initial}$ during the transformation period, as proposed by Ford (2002). Accordingly, it was observed that the increase of $[As]_{initial}$ in solution also decreases the transformation rate of schwertmannite into goethite.

Acero, P., Ayora, C., Torrentó, C., Nieto, J.M. (2006): The behavior of trace elements during schwertmannite precipitation and subsequent transformation into goethite and jarosite. *Geochim. Cosmochim. Acta*, **70**, 4130-4139.

Bigham, J.M., Schwertmann, U., Traina, S.J., Winland, R.L., Wolf, M. (1996): Schwertmannite and the chemical modeling of iron in acid sulfate waters. *Geochim. Cosmochim. Acta*, **60**, 2111-2121.

Ford, R.G. (2002): Rates of hydrous ferric oxide crystallization and the influence on coprecipitated arsenate. *Environ. Sci. Technol.*, **36**, 2459-2463.

Pérez-López, R., Asta, M.P., Román-Ross, G., Nieto, J.M., Ayora, C., Tucoulou, R. (2011): Synchrotron-based X-ray study of iron oxide transformations in terraces from the Tinto-Odiel river system: Influence on arsenic mobility. *Chem. Geol.*, **280**, 336-343.

ELEMENT MOBILIZATION IN WATER FROM COAL, MINING AND COMBUSTION WASTES, EAST MARITSA LIGNITE BASIN, BULGARIA

Dimitrova D.*[1] & Yossifova M.[1]
[1] Geological Institute, Bulgarian Academy of Sciences, Sofia, Bulgaria
Corresponding email: didi@geology.bas.bg

Keywords: lignites, dry residues, element migration

Phase-mineral and chemical composition of dry residues, resulting of evaporation of rain- and distilled waters interacting with coal, mining (black clay) and combustion waste (fly and bottom ash), may provide information about initial element migration.

Dry residues of four surface water samples, collected from the Maritza East coal basin and six distilled water leachates of coal, clay and combustion wastes were studied by XRD and SEM-EDS. Dry residues are produced as follows: 1) evaporation of 400 ml of each surface water sample in drying furnace at 70ºC; 2) soaking of 100 g of coal for briquettes (from outcrop), fuel for thermo-electric power stations (TEPSs), black clay and combustion waste into 400 ml ultra pure water for 96 hours, filtering and evaporation at 70ºC.

The *p*H and electric conductivity (EC) of waters were measured in the laboratory. The *p*H of surface waters is mostly acidic (2.8-3.9), as one with *p*H 7.52, while pH of laboratory produced leachates is predominantly neutral (6.9-7.6), except for leachates from coal/fuel (5.5/3.7). Concentrations of Zn (1.75-2.59 mg/l) and Cu (0.046-0.256 mg/l) were measured in surface water samples by ICP-AES.

Powder X-ray diffraction revealed three major minerals formed in dry residues from surface waters: gypsum (15-54%), hexahydrite (11-44%), löweite (7-41%), ferrinatrite (1.4-17%), rhomboclase (0.6-0.8%), sideronatrite (8 %) and boussingaultite (17%). SEM-EDS study detected other minor (Na-Ca, Na-Al, Na, Al unidentified sulfate and Si-S phases) and accessory (celestine, barite, halite, sylvite, Fe oxide/hydroxide, Cr-Mn-Ni-Au phase (?)) minerals. The phases formed in laboratory dry residues are as follows: 1) from combustion wastes - gypsum (68-92%), hexahydrite (8.4-31%), calcite, celestine, halite and sylvite; 2) from coal/fuel for TEPS - gypsum (70-76%), löweite (20-27%), hexahydrite, calcite, halite, fibroferrite, celestine, barite, ferrinatrite, Fe-Mg sulfate with P, Ca-Mg-Fe, Na, Ba-Sr sulfate; 3) from black clay - gypsum (40%), thenardite (49%), halite, glauberite, eugsterite, Bi-S and Fe-Cr-S phase. These phases occur as euhedral crystals, crusts, cryptocrystalline granular and amorphous masses.

The composition of dry residues from surface waters is mainly represented by S, Ca, Na, Mg, Fe and to lesser extent Al, Mn, K, Si, Sr and Cl. The migration of these elements is also confirmed by composition of laboratory dry residues. The presence of Fe is limited to sulfates in residues from coal/fuel. Sources of S, Ca, Na, Mg, Fe are authigenic minerals in coals (gypsum, pyrite, calcite), clays, organic matter and acids, rain waters and phases formed during coal combustion.

Waters in the mining area are sulfate rich, with acidic *p*H tendency, which assist in mobilization of many elements (S, Ca, Na, Mg, Fe, Al, Mn, K, Si, Sr, Ba, P, Cl, Cr, Ni, Cu and Zn) and their redistribution to the environment - surface and underground waters, soil and vegetation.

INTERACTION OF Cu-BEARING SOLUTIONS WITH CALCITE, ARAGONITE AND GYPSUM: A COMPARATIVE STUDY

Jiménez A.*[1], Astilleros J.M.[2], Fernández-Díaz L.[2-3], Fernández-González A.[1], Pérez-Garrido C.[4], Cubillas P.[5] & Prieto M.[1]

[1] Departamento de Geología, Universidad de Oviedo, Spain

[2] Departamento de Cristalografía y Mineralogía, Universidad Complutense, Madrid, Spain

[3] Instituto de Geociencias, Consejo Superior de Investigaciones Científicas, Universidad Complutense, Madrid, Spain

[4] Centro Nacional de Investigación sobre la Evolución Humana, Burgos, Spain

[5] Department of Earth Sciences, University of Durham, United Kingdom.

Corresponding email: amjimenez@uniovi.es

Keywords: copper, remediation, calcareous minerals

Copper is present in igneous and sedimentary rocks in minor to trace amounts. Copper participates in numerous essential to life biological processes and is considered a strategic element for a variety of industrial and agricultural applications. Copper can be released to the environments as a component of wastewaters, which can increase its concentration in natural waters to reach values considered toxic for the health of organisms. Previous works have demonstrated that the surfaces of abundant calcium bearing rock-forming minerals like calcite, aragonite and gypsum are efficient uptakers of dissolved metals. Understanding the mechanism involved in the interaction between these minerals and waters bearing metals should help to develop improved strategies for the treatment of mining wastes. In this work, we focus on waters bearing copper and study their interaction with calcite, aragonite and gypsum combining microscopic and nanoscopic observations. We aim to obtain information on their relative effectiveness as copper uptakers, for which we have conducted series of batch type and AFM experiments at room temperature. The batch type sorption experiments involved the reaction of ~ 1 g of 1.0-1.5 mm sized fragments of the corresponding calcium bearing mineral with $CuNO_3$ (1.0, 5.0 and 10mM) in thermostat closed polypropylene vessels during increasing reaction times (between 1 and 12 days). Chemical analyses of the aqueous solution after different elapsed times evidence that the interaction with any of the three calcium-bearing minerals results in the removal of dissolved copper. The characterization of the interacted mineral fragments by scanning electron microscopy (SEM) and conventional powder glancing X-ray diffraction (XRD) shows the development of rough surfaces on the minerals accompanied by the formation of randomly distributed malachite ($Cu_2CO_3(OH)_2$) spherulites. The reaction mechanisms involve the continuous dissolution of the primary phase followed by the precipitation of malachite regardless the calcium-bearing primary phase. The rate of dissolution directly relates to the initial concentration of copper in the aqueous solution in all three cases. However, the degree of surface coverage by malachite precipitates significantly differs depending on the substrate. Thus, while precipitates cover wide areas of aragonite surfaces, they form isolated patches on specific areas of the surfaces of calcite and gypsum. AFM observations confirm the strong interaction between all solid and copper-bearing aqueous solutions, with etch pits rapidly forming and coalescing and a new, epitactic-related phase immediately forming on the substrate. Our results once again evidence the relevance of mineral-water interactions in controlling the fate of pollutants and the suitability of mineral/water interaction-based strategies to control and remedy mining-related contamination.

FLY ASH FROM MUNICIPAL SEWAGE SLUDGE INCINERATION – A SOURCE OF PHOSPHOROUS

Kasina M.*[1], Kowalski P.R.[1] & Michalik M.[1]
[1] Institute of Geological Sciences, Jagiellonian University, Kraków, Poland
Corresponding email: monika.kasina@uj.edu.pl

Keywords: municipal sewage sludge, fly ash, phosphorous

International Fertilizer Industry Association (2005) estimated that phosphorus supply will disappear in the next few decades therefore a sustainable use of phosphorous is one of the target for management of this limited, non-renewable resource. Recycling of phosphorus from municipal sewage sludge (MSS) is an option to fulfil a demand for this compound. Depending on the MSS composition there are different possibilities of phosphorus recovery (bioleaching, electro-kinetic process or chemical extraction). MSS rich in phosphorus could be used directly as a fertilizer however it is not possible due to high content of metals, harmful elements, toxic organic substances and biological components. Currently the most reasonable method for MSS utilization is its incineration what causes reduction of the amount of waste with simultaneous sanitization/detoxification. As a result of MSS incineration fly ash (FA) and air pollution control (APC) residues are produced. FA can contain a high phosphorus content (8 wt.%), which indicates a potential as phosphorus resource. The goal of our study was to characterize phosphorous rich phases in FA produced in fluidized bed incinerator in one of Polish MSS thermal treatment plant and FA potential for phosphorus recovery.

Chemical composition of MSS and FA was determined using ICP-OES and MS methods. To characterize phosphorous rich phases scanning electron microscope (SEM) with energy dispersive spectrometer (EDS) was used whereas a main mineral composition was determined using X-Ray diffraction (XRD).

FA was reddish, fine material, where 30 wt.% of grains were 0.25-0.63 mm in size. It was a Si-P-Ca-Fe-Al dominated material containing 18 wt.% of P_2O_5. The content of P_2O_5 in MSS was 7 wt.%. It means that incineration of MSS caused concentration of phosphorous in FA. High content of Ca and Fe in FA may promote Ca-, and Fe-phosphate precipitation. This assumption was confirmed by XRD and EDS analyses where apart from quartz and hematite apatite and Fe-rich phosphates were detected. Ca-phosphates were usually fibre-like or rounded, up to few µm in diameter, Fe-rich phosphates occurred as porous fragments up to few µm in size, often with dispersed inclusions of Fe-oxides. The content of potentially hazardous elements (Ni, Cr, Zn, Cu, As, Pb, Sn, Hg, Sb) determined using the ICP-MS method was low. In total the concentration of these elements did not exceed 0.5 wt.%.

The studied FA due to high phosphorus content and low share of hazardous elements can be considered as fertilizer without toxic metals elimination.

Acknowledgments: The study was supported by Polish National Science Centre NCN grant No UMO-2014/15/B/ST10/04171.

International Fertilizer Industry Association (2005): Medium-term outlook for global fertilizer demand, supply and trade. June 2005.

ALUMINUM RICH PHASES IN MUNICIPAL SOLID WASTE INCINERATION (MSWI) BOTTOM ASH

Kowalski P.R.*[1], Kasina M.[1] & Michalik M.[1]
[1] Institute of Geological Sciences, Jagiellonian University, Kraków, Poland
Corresponding email: p.kowalski@uj.edu.pl

Keywords: Al-rich phases, MSWI bottom ash, metallic fragments

Bottom ash is a waste incineration residue produced in the largest quantities. It is a multi-component material where non-combustible fraction of waste is concentrated. Usually bottom ash contains over ten percent of metallic elements. Among them Al and Fe are dominating and constitutes ~ 10 wt.% of the average ash composition. In MSWI incinerator the temperature used is usually in the range of 950-1100°C what allows for Al melting (pure Al melts at 660°C) and its interaction with produced silicate melt and other waste components thermally affected in the furnace. Despite the fact that recovery of Al is not economically reasonable due to its high secondary production from recycling, Al-rich phases in MSWI bottom ash are studied and for example were reported as possible resource in the process of hydrogen production (Saffarzadeh et al., 2016).

The material used for this study was MSWI bottom ash collected from one of the biggest waste incineration plant in Poland. The investigation was mostly based on chemical analysis of components in thin section using scanning electron microscope (SEM) coupled with energy dispersed spectrometer (EDS). X-Ray diffraction (XRD) method was used for determining mineral composition of samples, whereas ICP-MS, ICP-OES method were applied for chemical analysis of bulk composition of bottom ash.

Studied bottom ash was multi-component material with domination of the amorphous phase (~ 50 wt.%), which mostly forms grains in matrix and cement in aggregates. It was Si-based material with high content of Ca, Fe, Al (4.5 wt.%) and Na. The mineral phase was dominated by silicates and aluminosilicates (melilite group minerals and feldspars). Besides being bond in mineral phases Al was concentrated in metallic fragments which were its main forms of occurrence in the bottom ash. Four main types of metallic fragments were present: separate grains, large fragments in aggregates (mostly fully oxidized), inclusions and occurrences on the marginal zones of grains and pores.

Various forms of metallic fragments were observed and their degree of oxidation as well. It was possible to observe forms from pure Al cores covered only by passivation layer (oxidized rim), through layered grains to fully oxidized Al fragments. Impurity of Al grains increased with the rising content of oxygen. Outer oxidation zones were often composed of several elements with local enrichment in metallic elements (e.g., Zn, Cr, Fe).

High content of Al-rich phases and their forms of occurrence allows to consider studied bottom ash as a resource for hydrogen production, nevertheless further studies on their reactivity are needed.

Acknowledgements: Research was funded by Polish National Science Centre (grant No. UMO-014/15/B/ST10/04171).

Saffarzadeh, A., Arumugam, N., Shimaoka, T. (2016): Aluminum and aluminium alloys in municipal solid waste incineration (MSWI) bottom ash: A potential source for the production of hydrogen gas. *Int. J. Hydrogen Energ.*, **41**, 820-831.

REE MINERALOGY OF WASTES FROM ACID MINE DRAINAGE TREATMENT

Lozano A.*[1], Torres E.[1], Carrero S.[2], Fernández-Martínez A.[3] & Ayora C.[1]

[1] Departament de Geociències, Instituto de Diagnóstico Ambiental y Estudios del Agua, Consejo Superior de Investigaciones Científicas, Universitat de Barcelona, Spain

[2] Departamento de Geología, Universidad de Huelva, Spain

[3] Institut des Sciences de la Terre, Centre National de la Recherche Scientifique & Université Grenoble Alpes, Grenoble, France

Corresponding email: alba.lozano@idaea.csic.es

Keywords: basaluminite, adsorption, fluorite

Acid Mine Drainage (AMD) carries a large amount of Rare Earth Elements and Yttrium (REY). Passive remediation systems essentially consist of AMD neutralization with calcite. As *p*H increases inside these treatments, a sequential precipitation of schwertmannite, basaluminite and gypsum have been described to form (Macías et al., 2012). Column experiments emulating a treatment system were performed with three different AMD as inflow solutions. Chemical analyses performed after months of functioning showed that REY concentration in pore water was not affected by schwertmannite precipitation, but it drastically decreased concomitantly with basaluminite. Not all REY content, however, was removed with basaluminite; a significant amount of up to 50% remains in solution down to a decantation vessel after the columns. Different precipitates were identified under SEM-EDS and XRD: basaluminite, gypsum, Zn-woodwardite $[(Zn,Cu)_2Al(OH)_6(SO_4)_{0.5}\cdot 3H_2O]$, bechererite $(Zn,Cu)_6Zn_2(OH)_{13}[(Si,S)(O,OH)4]_2$, fluorite and cuprite. Two mechanisms for REY retention are proposed: sorption on basaluminite, and co-precipitation with fluorite. The link of REE with Al and F were evidenced by their coexistence in the leachate with mild acids (*p*H 5) under a sequential extraction procedure. However, synchrotron µ-XRF mapping showed that REE was correlated with Al in the basaluminite zone of the columns and uncorrelated downstream and in the decantation vessels. Whilst Al was in solution, fluorine was captured by the strong AlF^{2+} and AlF_2^+ aqueous complexes. After basaluminite precipitated, however, free F^- was released and the solubility product of fluorite was reached. These chemical and spectroscopic analyses show that AMD treatment in passive remediation systems can concentrate REE and Yttrium in different mineral precipitates whose nature depend on the water Al and F concentrations. Further mineralogical studies are on-going to evaluate the potential of AMD as a source of critical rare earths.

Macías, F., Caraballo, M.A., Rötting, T.S., Pérez López, R., Nieto, J.M., Ayora, C. (2012): From highly polluted Zn-rich acid mine drainage to non-metallic waters: Implementation of a multi-step alkaline passive treatment system to remediate metal pollution. *Sci. Total Environ.*, **433**, 323-330.

POTENTIAL VALORIZATION OF SLUDGE FROM EXTREME METAL-POLLUTED ACID MINE DRAINAGE NEUTRALIZATION

Macías F.*[1], Pérez-López R.[1], Caraballo M.A.[2], Cánovas C.R.[1] & Nieto J.M.[1]
[1] Departamento de Geología, Universidad de Huelva, Spain
[2] Departamento de Ingeniería de Minas, Universidad de Chile, Santiago, Chile
Corresponding email: francisco.macias@dgeo.uhu.es

Keywords: mine water neutralization, metal sludge, waste valorization

Acid Mine Drainage (AMD) can be treated by active or passive treatments (Johnson & Hallberg, 2005). Generally, active are applied to working mines because they imply the continuous use of energy and chemicals, whereas passive rely on green energy, so they are most appropriate for abandoned mines (Johnson & Hallberg, 2005). The aim of the neutralization is to remove acidity and metals from the AMD, but implies the generation of sludge that retain acidity and metals. A study of the sludge produced by both technologies at 108 mine sites reported a production of about 9500 tones of dry sludge per year (Zinck & Griffith, 2013). This is indicative of the huge worldwide production of these wastes. Given that mineral production continues to be necessary for economic growth, the recycling and reuse of mining and mineral-processing wastes are important management strategies (Lottermoser, 2011). The sludge of active neutralization of an extreme metal-polluted AMD from the Iberian Pyrite Belt (IPB) has been selected to check the base- and tech-metal contents and evaluate the readily of their extraction by leaching with dilute acids.

The treatment comprises an alkaline dosing followed by an agitation/sedimentation step. The system treats an AMD with 628 mg/L of Al, 398 mg/L of Cu, 2231 mg/L of Fe, 2074 mg/L of Zn, 881 mg/L of Mn, 15 mg/L of Co and 6.7 mg/L of REY (rare earth elements and yttrium). The resulting sludge contains some base metals at high concentrations, such as Zn and Cu with around 43 and 6 g/kg, respectively; in mining terms, ore grades deduced from these values would correspond to 4% for Zn and 0.6% for Cu, which are mineable in current market conditions. Other base metal such as Co (443 mg/kg) could increase the potential value of this waste. Moreover, the sludge contains high contents of technology metals such as REY in remarkable concentrations (200 mg/kg), which could be also considered as valuable by-products. Considering the annual production (4300 tones), it can be deduced the annual output of metals of interest: 186 tones/year for Zn, 26 tones/year for Cu, 1.9 tones/year for Co and 0.9 tones/year for REY.

The metal extractability from the sludge was addressed by dilute acids (HCl and H_2SO_4) at 0.5M concentration. For base metals, the H_2SO_4 leaching is the most efficient extraction solvent, showing recovery percentages higher than 90% for Zn, Cu and Co. The HCl extraction shows also noticeable recoveries, except for Cu in which extraction values were lower than 60%. The REY extraction is also more effective by H_2SO_4 leaching, with recovery values ranging 80-90%, with the exception of Ce (around 60%). The base- and tech-metal content in this sludge from extreme metal-polluted AMD neutralization, the local annual production, and the worldwide annual production of this type of wastes suggest a potentiality for its valorization as metal ores. The readily extraction by dilute acids supports this suggestion.

Johnson, D.B. & Hallberg, K.B. (2005): Acid mine drainage remediation options: a review. *Sci. Total Environ.*, **338**, 3-14.
Lottermoser, B.G. (2011): Mine wastes: Recycling, reuse and rehabilitation of mine wastes. *Elements*, **7**, 405-410.
Zinck, J. & Griffith, W. (2013): Review of mine drainage treatment and sludge management operations. Mining Association of Canada, MEND Report 3.43.1.

KU LEUVEN RESEARCH PROGRAMME ON THE ZERO-WASTE RECYCLING OF MINE TAILINGS

Machiels L.[1], Muchez P.[2], Cappuyns V.[3], Elsen J.*[2], Jones P.T.[4] & Binnemans K.[1]
[1] Department of Chemistry, Catholic University of Leuven, Belgium
[2] Department of Earth and Environmental Sciences, Catholic University of Leuven, Belgium
[3] Center for Economics and Corporate Sustainability, Campus Brussels, Catholic University of Leuven, Belgium
[4] Department of Materials Engineering, Catholic University of Leuven, Belgium
Corresponding email: jan.elsen@ees.kuleuven.be

Keywords:

KU Leuven (Belgium) has a strong active research program on zero-waste recycling of metal-containing industrial waste streams. Examples are metallurgical slags (from ferrous and non-ferrous metallurgy) and metallurgical sludges (bauxite residue from the alumina production and goethite from zinc production) (Binnemans et al., 2015; KU Leuven SIM^2, 2016). KU Leuven is also one the founders of EURELCO, the European consortium of enhanced landfill mining of municipal and industrial landfills.

Currently, KU Leuven is setting-up a research program on the zero-waste recycling of mine tailings. This programme involves several projects on both Flemish and the European level, ranging from fundamental research to competitive industrial development. At this moment, key European partners in academia, industry, civil society and government are being identified.

The research programme aims at creating holistic solutions for economic and sustainable recycling of mining waste throughout Europe. The programme covers geophysical and geochemical exploration, metal mapping and assessment of the exploitation potential using multi-criteria analysis and modelling. Exploitation involves both in-situ and ex-situ mining. In the in-situ mining approach, the deposit is treated *in situ* allowing maximum metal recovery, while the residual mineral fraction – which remains in place - is environmentally cleaned ensuring a safe afterlife. In the ex-situ mining approach, the deposit is excavated/dredged and recycled through dewatering, mineral processing and metallurgical treatment. At KU Leuven, focus is on metallurgical treatment covering the recovery of base, precious and critical metals, using a broad range of metallurgical techniques, ranging from hydro-, solvo-, iono- and pyrometallurgy and using process intensification.

Priority is given to achieve zero-waste solutions, in which a technology is designed for combining recovery of valuable metals with cleaning of the residual mineral fraction from hazardous components, such as As, Hg and Cd. In this way the mineral fraction – most commonly representing > 95% of the waste streams, does not need to be re-landfilled and – when properly engineered – it can even be used in high added value applications, such as cement and novel binder systems, building materials and even as a catalyst or pigment.

A cross-sectoral industrial approach is aimed for, in which the whole value chain ranging from waste producer till final product user, but also societal actors and policy makers, are involved already at the start of a new technological development. In this way, sustainability, economics, legal, policy aspects and business opportunities are assessed with the relevant partners throughout the development process. Additionally, the R&D agenda of universities, industry, societal actors and EU policy makers can be aligned and effective tech transfer routes can be drafted, in which lab inventions are upscaled to industrially feasible processes and eventually commercial successes.

Binnemans, K., Jones, P.T., Blanpain, B., Van Gerven, T., Pontikes, Y. (2015): Towards zero-waste valorisation of rare-earth-containing industrial process residues: a critical review. *J Cleaner Prod.*, **99**, 17-38.

KU Leuven SIM^2 (2016): KU Leuven Sustainable Inorganic Materials Management. http://set.kuleuven.be/mrc/sim2 (Last consulted: 06/05/2016).

HIGHLY POLLUTED ACID MINE DRAINAGE REMEDIATION BY PASSIVE TECHNOLOGY

Nieto J.M.*[1], Macías F.[1] & Ayora C.[2]
[1] Departamento de Geología, Universidad de Huelva, Spain
[2] Consejo Superior de Investigaciones Científicas, Barcelona, Spain
Corresponding email: jmnieto@uhu.es

Keywords: acid mine drainage, passive treatment system, dispersed alkaline substrate

The Odiel River (SW Spain) is highly polluted by Acid Mine Drainage (AMD), representing a worldwide case of fluvial system demoted by metals and acidity. The construction of the Alcolea reservoir, which will store these acidic waters (Olías et al., 2011) and the mandatory of European water regulations (EC decision, 2000) show the need to find solutions to improve the river water quality. Most of the pollution sources in the Odiel River come from orphan sites, therefore technical solutions should be based on passive technologies. Currently, the only passive treatment that has been shown effective treating highly polluted AMD is the Dispersed Alkaline Substrate (DAS) (Ayora et al., 2013). DAS consists of a fine-grained alkaline reagent (limestone sand) mixed with a coarse inert matrix (wood shavings). This final mixture has a porosity of 50% and shows a high reactivity. Preliminary results of the first full-scale DAS plant are summarized here.

The system is carried out by a first pre-treatment (PN), based on a Natural Fe-oxidizing Lagoon (NFOL) (Macías et al., 2012), followed by two DAS reactive tanks serially connected with two decantation ponds. The plant currently treats the whole flow of the abandoned mine of "Mina Esperanza" (1 L/s). This AMD has low *p*H (mean of 2.6), high net acidity (mean of 1910 mg/L as $CaCO_3$ equivalents), and high concentration of metals (596 mg/L of Fe, 112 mg/L of Al, 16 mg/L of Cu, 12 mg/L of Zn, and 0.1-3 mg/L of As, Cr, Cd, Co, Ni and REY (rare earths plus yttrium).

During the first 164 days of full working 9688 m^3 of AMD has been treated. All metals analyzed at the outflow are below detection limits, with the exception of Fe, whose retention ranging 90-97%. Acidity is completely removed, with mean value at the outflow of -195 mg/L as $CaCO_3$ equivalents. The treated water after neutralization is a net alkalinity discharge with mean *p*H value of 6.6. During this time, permeability reduction and/or alkalinity generation decrease has not been detected at the outflows of limestone-DAS tanks. These data are indicative of the high performance of the DAS.

The NFOL pre-treatment during these 164 days has accumulated 732 kg of Fe and 1.5 kg of As. In the first reactive tank 1.1 tons of Al, 3.6 tons of Fe, 150 kg of Cu, 120 kg of Zn and 6 kg of REY has been retained. Despite of the large quantity of metals retained within the tank, loss of permeability has not been observed. This is due to the original porosity of the reactive mixture (50%), and because limestone dissolution generates a secondary porosity (limestone dissolution during the monitoring period has been around 11.5 tons), so the permeability of the reactive mixture is kept along the time. This will allow long times of treatment; only when the limestone grains have been dissolved, they should be replaced by fresh limestone-DAS reactive mixture.

Ayora, C., Caraballo, M.A., Macías, F., Rötting, T.S., Carrera, J., Nieto, J.M. (2013): Acid mine drainage in the Iberian Pyrite Belt: 2. Lessons learned from recent passive remediation experiences. *Environ. Sci. Poll. Res.*, **20**, 7837-7853.

EC Decision (2000) Council Decision 2000/60/EC of 23 October 2000: establishing a communitarian frame of action in the scope of water policy. Official Journal L 327, 22/12/2000, 88 p.

Macías, F., Caraballo, M.A., Nieto, J.M., Rötting, T.S., Ayora, C. (2012): Natural pretreatment and passive remediation of highly polluted acid mine drainage. *J. Environ. Manag.*, **104**, 93-100.

Olías, M., Nieto, J.M., Sarmiento, A.M., Cánovas, C.R., Galván, L. (2011): Water quality in the future Alcolea reservoir (Odiel River, SW Spain): a clear example of the inappropriate management of water resources in Spain. *Water Res. Manag.*, **25**, 201-215.

MUNICIPAL AND INDUSTRIAL GLASSES FOR THE PRODUCTION OF ECOSUSTAINABLE BUILDING MATERIALS

Paris E.[1], Grandinetti V.[2], Stabile P.[1], Radica F.[1], Giuli G.[1], Ansaloni F.[1] & Carroll M.R.*[1]
[1] Scuola di Scienze e Tecnologie - Sezione di Geologia, Università di Camerino, Italy
[2] Grandinetti SRL, S. Severino Marche (MC), Italy
Corresponding email: michael.carroll@unicam.it

Keywords: glass waste, recycling tiles

Glasses recovered from municipal and industrial wastes have been studied in the frame of the LIFE EU project “ECOTILES” with the aim to produce new ecosustainable building materials. By using recycled glass from urban and industrial waste for the production of fully recycled (up to nearly 70%) pre-casted cement-based products (Terrazzo-tiles), the goal of ECOTILES is to reduce by 20% the environmental impact of the industrial production, compared with that of traditional tiles, while achieving the manufacture of high-grade pre-casted products. The products, involving the re-use of glass waste, will contribute to the achievement of EU 2020 goals on Waste and Resource Efficiency by reducing emissions, extraction of raw materials, waste, impacts on human health and the environment.

A set of 40 industrial/municipal glass wastes, have been collected with the purpose of characterizing the materials for demo productions and to investigate the properties of the glasses to predict possible problems arising during the production, like thermal expansion or ASR (Alkali Silica Reaction) in the cement mix. The glasses, characterized by different colors and uses, have been analyzed for chemical composition and water content by EMPA and FTIR spectroscopy.

The glass waste samples can be classified as “soda-lime” glass (SLG). Among the analysed samples, SiO_2, Al_2O_3, MgO, Na_2O, CaO, Fe_2O_3, are the most abundant components, with variable trace amounts of sulphur, manganese, copper and lead, depending on the glass color. Regarding the alkali contents, Na, used as a flux, is always predominant (average Na_2O 11.4±1.8 wt.%) whereas K is invariably present in low amounts (average K_2O 0.99±0.66 wt.%).

Although the chemical composition is rather similar, even small chemical differences can affect the glass physical properties (e.g., density) due to the role of each element as network former or modifier. Moreover, all the glass compositions investigated result to be anhydrous (usually < 500 ppm H_2O), which is essential for the re-use of the waste since water content influences viscosity.

ASSESSING CHLOROMETHANES ABIOTIC REDUCTIVE DECHLORINATION BY PYRITE AND MAGNETITE AT NEUTRAL AND ALKALINE CONDITIONS

Rodríguez-Fernández D.[1], García-Moliner D.[1], Bagaria-Rovira F.[1], Soler A.[1], Rosell M.[1] & Domènech C.*[1]
[1] Grup de Mineralogia Aplicada i Geoquímica de fluids, Departament de Mineralogia, Petrologia i Geologia Aplicada, Universitat de Barcelona, Spain
Corresponding email: cristina.domenech@ub.edu

Keywords: chloromethanes, iron minerals, isotopes

Carbon tetrachloride (CT) and chloroform (CF) are frequent volatile organic groundwater pollutants. In our study site, CT and CF degradation was confirmed by shifts in carbon isotopic composition ($\delta^{13}C$) over time in the aquifer under neutral iron-reducing conditions (Rodríguez-Fernández et al., 2015) as well as under the alkaline conditions (*circa p*H 12) generated in recharge water interception trenches filled with concrete-based construction wastes (Torrentó et al., 2014). Although at *p*H 12 CF degradation was mainly attributed to alkaline hydrolysis, other degradation mechanisms for chloromethanes could be possible.

To ascertain if Fe-bearing minerals in the field had a significant role, the potential abiotic reductive dechlorination of CT and CF by pyrite (Py) and magnetite (Mag) was studied.

Minerals were crushed, 100 µm-sieved and pretreated under anoxic conditions for surface activation following Slater et al. (2002) and dried by lyophilisation. SEM-EDS characterization, surface area determination by BET before and after HCl cleaning and average particle size measures were done. Anoxic rotating batch experiments were performed at room temperature at pH 7 and 12 for CT and CF, separately. Amber glass 42 mL-vials were filled without headspace with 1 g of mineral powder, pH buffered solutions, 1 mM $FeCl_2$ (Elsner et al., 2004) and 1.3 or 1.4 µL of pure CT or CF, respectively. Control vials (Bk) with buffer and $FeCl_2$ but without minerals were prepared. The vials were sacrified by 0.2 µm-filtration (afterwards, samples at *p*H 12 were neutralized with acetic acid), separated in three 12 mL-aliquots and stored at 4°C in darkness. Volatile organic compounds concentration was measured by HS-GC-MS and $\delta^{13}C$, with HS-SPME-GC-IRMS. Remaining volume was used for *p*H measurements.

In CF *p*H 7-experiments, neither carbon isotopic changes nor degradation products were observed along 21 days. In CF *p*H 12-experiments, significant δ^{13}CCF enrichment and dichloromethane production over time was observed in Bk, Py and Mag experiments, probably related to alkaline hydrolysis processes (Torrentó et al., 2014). No enhancing effects of Py and Mag were observed in CF degradation during experiment time. In CT Bk and Mag *p*H 7-experiments, shifts in δ^{13}CCT were not detected after 11 days. By contrast, CT Py *p*H 7-experiments and all CT *p*H 12-experiments underwent concentration decrease, δ^{13}CCT enrichment and CF production. Carbon disulphide was also generated but only in Py presence. Results indicated that Mag, Py and dissolved Fe(II) rapidly activated CT degradation at *p*H 12 in contrast with extremely slow alkaline hydrolysis expected after Jeffers et al. (1989).

This research supports the revalorization of mining and industrial Py wastes for groundwater remediation and the utility of isotopic tools for monitoring, and confirms that Mag coating in zero-valent iron reactive barriers at neutral pH can slow down chloromethanes degradation (Danielsen & Hayes, 2004).

Danielsen, K.M. & Hayes, K.F. (2004): *p*H dependence of carbon tetrachloride reductive dechlorination by magnetite. *Environ. Sci. Technol.*, **38**, 4745-4752.

Elsner, M., Haderlein, S.B., Kellerhals. T., Luzi, S., Zwank, L., Angst, W., Schwarzenbach, R.P. (2004): Mechanisms and products of surface-mediated reductive dehalogenation of carbon tetrachloride by Fe(II) on goethite. *Environ. Sci. Technol.*, **38**, 2058-2066.

Jeffers, P.M., Ward, L.M., Woytowitch, L.M., Lee Wolfe, N. (1989): Homogeneous hydrolysis rate constants for selected chlorinated methanes, ethanes, ethenes and propanes. *Environ. Sci. Technol.*, **23**, 965-969.

Rodríguez-Fernández, D., Rosell, M., Domènech, C., Torrentó, C., Palau, J., Soler, A. (2015): C and Cl-CSIA for elucidating chlorinated methanes biotic and abiotic degradation at a polluted bedrock aquifer. *Procedia Earth Planet. Sci.*, **13**, 120-123.

Slater, G.F., Sherwood Lollar, B., Allen King, R., O'Hannesin, S. (2002): Isotopic fractionation during reductive dechlorination of trichloroethene by zero-valent iron: influence of surface treatment. *Chemosphere*, **49**, 587-596.

Torrentó, C., Audí-Miró, C., Bordeleau, G., Marchesi, M., Rosell, M., Otero, N., Soler, A. (2014): The use of alkaline hydrolysis as a novel strategy for chloroform remediation: feasibility of using urban construction wastes and evaluation of carbon isotopic fractionation. *Environ. Sci. Technol.*, **48**, 1869-1877.

CARBONATION OF KATOITE OBTAINED FROM PHOSPHOGYPSUM DISSOLUTION WITH WASTES OF THE ALUMINIUM INDUSTRY FOR MINERAL CO_2 SEQUESTRATION

Romero-Hermida I.[1], Morales-Flórez V.[2], Esquivias L.[2], Santos A.[3] & Pérez-López R.*[4]
[1] Departamento de Química-Física, Universidad de Cádiz, Spain
[2] Departamento de Físicade la Materia Condensada, Universidad de Sevilla & Consejo Superior de Investigaciones Científicas, Spain
[3] Departamento de Ciencias de la Tierra, Universidad de Cádiz, Spain
[4] Departamento de Ciencias de la Tierra, Universidad de Huelva, Spain
Corresponding email: rafael.perez@dgeo.uhu.es

Keywords: phosphogypsum, aluminium industry, CO_2 sequestration

Phosphogypsum (PG) is a waste resulting from the production of phosphoric acid for phosphate fertilizers. This waste consists mainly of gypsum (> 95%), which contains residual phosphoric acid and, at a lesser extent, other reagents and products from the industrial process such as sulphuric acid. These acid solutions are also loaded with high concentrations of contaminants derived from raw phosphate ore (Lottermoser, 2010).

Around 120 Mt of PG were stockpiled on the Tinto river salt-marshes (Estuary of Huelva, SW Spain). When PG is placed into the stack, the highly-polluted acid solutions migrate as a groundwater flow, which emerges on the edge of the stack forming superficial leakages known as edge outflows. This leaching mechanism is the main vector of contaminants to the Estuary of Huelva (Pérez-López et al., 2015). An inventory of edge outflows in the entire disposal modules of the PG stack has been recently published, involving even some zones that had been previously restored. This fact demonstrates the ineffectiveness of the preliminary restoration actions (Pérez-López et al., 2016). These solutions are characterized by a pH of 1.9 and concentrations of 6000 mg/L for P, 1970 mg/L for S, 100 mg/L for Fe, 10-30 mg/L for Zn, As and U, and 1-10 mg/L for Cr, Cu and Cd, among others.

A solution to manage the problem of the PG stack in Huelva should ideally consider: (1) recycling PG to reduce the amount of stacked waste, (2) minimizing the high mobility of contaminants that impact on the estuarine environment, and (3) obtaining a by-product that is commercial or that may face other environmental problems. With these requirements in mind, PG has been already considered for CO_2 sequestration process under atmospheric conditions (Cárdenas-Escudero et al., 2011). In the current study, a new process has been designed working exclusively with industrial wastes. Firstly, phosphogypsum is transformed into a carbon sequestration agent – katoite - by alkaline dissolution with a liquid Na-Al-rich caustic waste of the aluminium anodizing industry (Eq. 1), and then katoite reacts with aqueous CO_2 and is transformed into calcite (Eq. 2).

$$3\,(CaSO_4 \cdot 2H_2O) + 6\,Na^+_{(aq)} + 12\,OH^-_{(aq)} + 2Al^{3+}_{(aq)} \leftrightarrow 3\,Na_2SO_4 + Ca_3Al_2(OH)_{12} + 6\,H_2O \quad (1)$$

$$Ca_3Al_2(OH)_{12} + 3\,CO_2 \leftrightarrow 3\,CaCO_3 + 2\,Al(OH)_3 + 3\,H_2O \quad (2)$$

Our results demonstrate high efficiencies of katoite precipitation and carbonation. According to the experimental protocol and considering the complete stockpiled phosphogypsum, the system proposed would favour the production of up to 73 Mt of katoite that could capture a total of approx. 20 Mt of CO_2 into 94 Mt of stable calcite. The fate of trace elements contained originally in the phosphogypsum waste was also investigated, and trace impurities were found to be completely transferred and stabilized into the final calcite. The calcite could be used for treatment of acidic contaminated soils/waters or even for diverse civil engineering applications.

Cárdenas-Escudero, C., Morales-Flórez, V., Pérez-López, R., Santos, A., Esquivias, L. (2011): Procedure to use phosphogypsum industrial waste for mineral CO_2 sequestration. *J. Hazard. Mater.*, **196**, 431-435.

Lottermoser, B.G. (2010): Mine wastes: Characterization, treatment and environmental impacts, 3rd ed. Springer, Berlin, 400 p.

Pérez-López, R., Nieto, J.M., de la Rosa, J.D., Bolívar, J.P. (2015): Environmental tracers for elucidating the weathering process in a phosphogypsum disposal site: Implications for restoration. *J. Hydrol.*, **529**, 1313-1323.

Pérez-López, R., Macías, F., Cánovas, C.R., Sarmiento, A.M., Pérez-Moreno, S.M. (2016): Pollutant flows from a phosphogypsum disposal area to an estuarine environment: An insight from geochemical signatures. *Sci. Total Environ.*, **553**, 42-51.

MOBILITY OF POTENTIALLY TOXIC ELEMENTS IN THE ŚWIĘTOCHŁOWICE SLAG HEAP: EVIDENCE FROM MINERAL LIBERATION ANALYZES

Tyszka R.*[1], Pietranik A.[2] & Stankowska S.[2]
[1] Institute of Soil Science and Environmental Protection, Wrocław University of Environmental and Life Sciences, Poland
[2] Institute of Geological Sciences, University of Wrocław, Poland
Corresponding email: tyszkarafal@gmail.com

Keywords: weathered slag, Zn-Pb minerals, element mobility

Slags after Zn-Pb ore smelting were deposited in Świętochłowice as an unconfined heap without any barriers between the slag heap and the environment. The deposition started over a century ago, but several years ago the heap was almost completely removed as a part of remediation works. During removal the inner part of the heap was uncovered and revealed that the heap is mostly composed of weathered, fine grained material (Tyszka et al., 2014). The material had higher contents of potentially toxic elements (PTE) than unweathered slag, but seemed to be preserved in a meta-stable state with PTE being immobilized by secondary phases within the heap.

To further constrain mobility of PTE within the heap we separated heavy minerals from three horizons within the heap: (1) The lowest horizon (LH) comprising fine grained, pinkish, weathered material. The material dominates within the heap and forms its innermost part (Tyszka et al., 2014). (2) The middle horizon (MH) comprising yellowish-brown soil-like material. (3) Greyish uppermost horizon (UH) of unknown origin. Tyszka et al. (2014) analysed composition of these three horizons and showed that the lowest one contained high contents of PTE, whereas the upper two had several times lower concentrations. The initial interpretation was that the upper horizons were composed of foreign material added to the surface as part of remediation works. The analyses of heavy minerals presented in this study partly contradicts this interpretation. The analyses employed both classic study of mineral particles by Secondary Electron Microscope, but also utilized the Mineral Liberation Analyzer system. The general outcome is that both lowermost and uppermost horizons, despite large difference in chemical composition, contain similar heavy mineral phases in similar proportions. In both horizons phases containing Zn and Pb are present as one of dominating phases (LH – 24%, UH – 14%). In contrast, the middle horizon does not have Zn and Pb phases and contains, e.g. ilmenite (11%), which is absent in LH and UH. The implication is that the middle horizon indeed represents foreign material added at one point to the heap as some failed attempt in remediation. On the other hand, LH and UH both represent material from the heap, but PTE were mobilized from the UH after it was deposited on the heap surface. The PTE are still present within LH, but probably after it was also exposed after slag removal, the load of PTE is going to be mobilized posing a serious environmental risk.

Acknowledgements: RT acknowledges National Science Centre (Poland) project no. UMO 2014/13/B/ST10/01120.

Tyszka, R., Kierczak, J., Pietranik, A., Ettler, V., Mihaljevič, M. (2014): Extensive weathering of zinc smelting slag in a heap in Upper Silesia (Poland): Potential environmental risks posed by mechanical disturbance of slag deposits. *Appl. Geochem.*, **40**, 70-81.

CONCENTRATION AND MODE OF OCCURRENCE OF REY, Sc, Th AND U IN MINING AND COMBUSTION WASTE PRODUCTS FROM THE EAST MARITSA LIGNITE, BULGARIA

Yossifova M.*[1] & Dimitrova D.[1]
[1] Geological Institute, Bulgarian Academy of Sciences, Sofia, Bulgaria
Corresponding email: mariana@geology.bas.bg

Keywords: trace elements, coal wastes, LA-ICP-MS

The Maritsa East lignite basin is located in SE Bulgaria as a part of the Zagore Depression of the Upper Thracian tectonic trough. The coal-bearing formation has Miocene age and consists of three lignite seams interbedded by clay rocks. The mining and power producing enterprise Maritsa East (more than 200 km^2) is the biggest unit for lignite mining and thermo-electric power generation in Bulgaria.

Composite samples of coal, coal lithotypes (xylain, vitrain and liptain) and clays (yellow-, blue- and black-colored) from outcrops in the mine, fuel for combustion, fly and bottom ash from the thermo-electric power stations (TEPSs) depots were studied. Samples were ashed and analyzed by wet chemical analysis, XRF, XRD and LA-ICP-MS.

The REY (rare earth elements and yttrium) content (in ppm) in samples is as follows: black clay (538), yellow clay (430), coal (243), blue clay (221), fly and bottom ash (219), fuel for TEPS (206), vitrain (148), liptain (100) and xylain (94). Scandium content is almost equal in all coal and waste samples (22 ppm), excluding lithotypes where is much lower (4.4-9.0 ppm). Thorium content vary in clays from 24.7 to 27.9 ppm, in coal and fuel for TEPSs - 16.6-23.8 ppm, while in lithotypes is from 5.5 to 13.1 ppm. Uranium has highest content in blue clay (17.6 ppm), while in coal/fuel and waste products is up to 9.5 and 13.0 ppm, respectively. Among the studied lithotypes, vitrain is characterized with the highest U content (5.2 ppm, ash basis). The concentrations of REY, Sc, Th and U in coal/fuel for TEPS, fly and bottom ash compared to average values for world brown coals (REY = 390.4 ppm) are lower or equal (only Sc). The concentrations of REY, Sc and Th in different clays compared to values of sedimentary rocks (REY = 175.5 ppm) are higher, outlining trends of distribution with enrichment factor (EF) as follows: highest values are determined in black clay (2.2-5.8), moderate in yellow clays 1.5-3.6, and almost equal to average concentrations in blue clays. Uranium demonstrates opposite behavior, concentrating in blue clay (EF = 5.2), while in yellow and black clays has EF 1.4 and 0.9, respectively. REY correlate well between one another and with Ti, Cs, Rb, Th, K, Si, P and Zn. Thorium correlates well with Al, Cr and Ga. Uranium shows best correlation with Ti, Cr and Sc, less discernible with Si, K, Ga and Rb. This suggests that REY and Th are associated with illite, kaolinite, plagioclase, K-feldspar, muscovite, glass and phosphates (?), while U probably has a mix mode of occurrence (sorbed onto clay minerals, organic matter (?), Ti and U bearing phases).

The average REY contents of Maritsa East lignites and their wastes of combustion are low, but their contents in yellow and especially black clay within the coal bearing formation are ~ 500 ppm. Total thickness of black and yellow clay partings is up to 20 m and 100 m respectively, thus these clays could be considered as possible sources of REY.

THE POTENTIAL RECYCLING OF BORON SLUDGES IN CERAMIC TILES

Zanelli C.*[1], Iglesias C.[2], Domínguez E.[3] & Dondi M.[1]
[1] Istituto di Scienza e Tecnologia dei Materiali Ceramici, Consiglio Nazionale delle Ricerche, Faenza (RA), Italy
[2] Piedra Grande SA, Trelew, Argentina
[3] Departamento de Geología, Universidad Nacional del Sur, Bahia Blanca, Argentina
Corresponding email: chiara.zanelli@istec.cnr.it

Keywords: ceramic tiles, wastes, borate

Residues from beneficiation of borate ores have been extensively investigated in the world in the last decade. The recycling of boron-containing wastes has been assessed in clay bricks, ceramic tiles, as well as ceramic frits and glazes. All these studies agree about the technological feasibility of the utilization of borate residues, though with different amounts depending on the end-use. Such recommended percentages of waste are higher in clay bricks (≤ 30%) than in ceramic tiles (≤ 8%) and glazes (≤ 5%). The clay bricks can tolerate an amount of B_2O_3 widely spanning from around 1 to 5-6%. In the case of glazes, this percentage seems to be ≤ 1%. The objective of this study was aimed at appraising the re-use of boron sludge, coming from Argentinian production factories, in porcelain stoneware tiles, addressing key-points in processing and product performance. The rationale consists in adding different waste amounts (2-5-10% wt), then testing their technological behavior at the laboratory scale and finally characterizing semi-finished and finished products in order to assess technological feasibility. The batches were designed by two different strategies: adding boron waste in replacement of ball clay in an “Argentinian-style formulation” and in replacement of sodic feldspar in an “Italian-style body”. Argentina has an important boron production with a yearly output of 170.000 tn of borax and boric acid compounds. The waste sludge comes from the Tincalayu mine located at the western end of Salar del Hombre Muerto in the Salta province. The waste was taken directly during a routine industrial processing day; it came from the boric acid obtained after a hot water leaching for the borax solubilization. The waste sludge is composed by quartz (~ 20% wt.), plagioclase (~ 50% wt.), boro-muscovite (~ 20% wt.) and borates (~ 10% wt.). The percentage of iron oxide higher (~ 3%) and the relatively low loss an ignition (~ 11%) are the further features peculiar of the boro sludge. While the amount of iron is a limitation for its use in the white firing bodies, the latter is undoubtedly an advantage for its utilization in vitrification tiles. Boron sludge is characterized by a very strong fusibility, witnessed by a melting temperature close to 1100°C, value almost 300°C lower than a most strong ceramic flux and nearly 600°C below than a typical fluxes used in porcelain stoneware tiles. The boro sludge recycling is possible in the ceramic industrial practice only if a careful and controlled industrial deposition is done. During some steps of the conventional technological process such as milling and shaping, a slight reduction of the powder moisture, a fluctuation of expansion after pressing (i.e., 0.3-0.6 cm/m) and improved compaction (bulk density of dry bodies increased for addition over 2% of waste) were detected. Moreover, the waste implies an increase of reactivity: the firing temperature can be reduced according to the amount of waste added.

Session S22:

Platinum group minerals and accessory minerals: development in their characterisation

Conveners:

Oskar Thalhammer (Leoben – Austria)

Anna Vymazalová (Prague – Czech Republic)

Federica Zaccarini (Leoben – Austria)

SYNCHROTRON TTS-μXRD: A POWERFUL TOOL FOR *IN-SITU* MINERALOGICAL IDENTIFICATION OF PGM INCLUDED IN POLISHED THIN SECTION

Aiglsperger T.[1], Villanova-de-Benavent C.*[1], Rius J.[2], Galí S.[1], Font-Bardia M.[1] & Proenza J.A.[1]
[1] Departament de Mineralogia, Petrologia i Geologia Aplicada, Universitat de Barcelona, Spain
[2] Institut de Ciència de Materials de Barcelona, Consejo Superior de Investigaciones Científicas, Spain
Corresponding email: cvillanovadb@ub.edu

Keywords: tts-μXRD, synchrotron, PGM

Platinum group minerals (PGM) are a group of minerals for which at least one of the six platinum group elements (PGE) (i.e., Os, Ir, Ru, Rh, Pt, Pd) is essential to the mineral. They usually occur as micrometre-sized particles/aggregates making their mineralogical identification challenging. As a matter of fact PGM are generally discovered in polished blocks and/or polished thin sections. However, in most cases their small grain sizes limit the possibility to extract crystals from the matrix for subsequent single crystal XRD analysis. Hence, the aim of this contribution is to highlight the potential of the innovative technique of synchrotron through-the-substrate X-ray microdiffraction (tts-μXRD), which allows a precise *in-situ* mineralogical identification of micrometric PGM included in polished thin sections (Rius et al., 2011). The diffraction experiments were performed on the MSPD beamline at the ALBA Synchrotron Facility-CELLS, Cerdanyola del Vallès, Barcelona, 08920, Spain. By way of illustration we present the first-time mineralogical identification of PGM via synchrotron tts-μXRD.

PGM bearing monolayer polished sections were first transformed to polished thin sections (30 μm thick) attached to an approximately < 1 mm thick glass substrate. Subsequently, the X-ray diffraction information was obtained by rotating the thin section with the selected microvolume at the origin (Arndt & Wonacott, 1977) and processed with Bruker software (TOPAS, 2009). Ruthenian hexaferrum was successfully identified and compared with literature data. The tts-μXRD results are coincident with previous analyses carried on an equivalent ruthenian hexaferrum grain using a single crystal diffractometer.

Arndt, U.W. & Wonacott, A.J. (1977): The rotation method in crystallography. Elsevier, Amsterdam, 275 p.

Rius, J., Labrador, A., Crespi, A., Frontera, C., Vallcorba, O., Melgarejo, J.C. (2011): Capabilities of through-the-substrate micro-diffraction: application of Patterson-function direct methods to synchrotron data from polished thin sections. *J. Synchr. Rad.*, **18**, 891-898.

TOPAS (2009): General profile and structure analysis for powder diffraction data, version 4.2. Bruker AXS, Germany.

GEOCHEMICAL EVOLUTION OF PGM-BEARING SULFIDES IN LOW-MINERALIZED ROCKS FROM THE YOKO-DOVYREN LAYERED INTRUSION, RUSSIA

Ariskin A.*[1-2], Danyushevsky L.[3], Nikolaev G.[2], Gilbert S.[3], Fiorentini M.L.[4], Kislov E.[5-6] & Barmina G.[2]

[1] Faculty of Geology, Moscow State University, Russia

[2] Vernadsky Institute of Geochemistry and Analytical Chemistry, Russian Academy of Sciences, Moscow, Russia

[3] Centre for Ore Deposit Research and Earth Sciences, University of Tasmania, Hobart, Australia

[4] Centre for Exploration Targeting, School of Earth and Environment, Australian Research Council, Centre of Excellence for Core to Crust Fluid Systems, University of Western Australia, Perth, Australia

[5] Geological Institute, Siberian Branch of the Russian Academy of Sciences, Ulan-Ude, Russia

[6] Faculty of Chemistry, Buryat State University, Ulan-Ude, Russia

Corresponding email: ariskin@rambler.ru

Keywords: low sulfide PGE mineralization, layered massif

The 728 Ma Yoko-Dovyren massif (YDM) is the largest intrusion of the Synnyr-Dovyren volcano-plutonic complex in Northern Transbaikalia, Russia (Ariskin et al., 2015a). It includes sub-economic deposits of Cu-Ni sulfide ores coupled with PGE-rich sulfide horizons (Kislov et al., 2016). Five different types of low-sulfide mineralization in the YDM include: (1) pyrrhotite-rich sulfide clusters within the lower chilled zone of the YDM; (2) pentlandite-rich sulfides (mss) disseminated in the lowermost dunites; (3) Cu-PGE-rich sulfides occurred as round silicate-sulfide agglomerations in lower troctolites (Ariskin et al., 2015b); (4) sulfide-poor Cu-PGE-rich mineralization in leucogabbro and anorthosites near the transition zone from troctolites to olivine gabbro (the so-called Main 'Reef'; Kislov, 1998); and (5) pyrrhotite-rich PGE-depleted sulfides in gabbronorites near the roof. In addition, sporadic PGE-rich sulfide occurrences took place in leucogabbro situated between the Main Reef and the near-roof sulfide-horizon (Kislov, 1998). Assuming this sulfide succession has to represent a genetic record of the history of sulfide saturation in the Dovyren magma chamber, we performed a detailed study of the sulfide geochemistry. To quantify these characteristics, we combined the mineralogy of base metal sulfides (MLA-derived proportions of Pn, Po, Cpy, and Cub) with results of LA-ICPMS of the sulfide phases, giving rise to the bulk sulfide composition in each particular low-mineralized rock. These studies were carried out at the Central Science Laboratory of the University of Tasmania (Hobart, Australia), using FEI Quanta 600 SEM fitted with EDS for the Mineral Liberation Analysis, and two laser ablation microprobes coupled to an Agilent 7700s quadrupole ICPMS.

Comparisons of the average sulfide compositions from different horizons evidence that PGM-bearing sulfides from the Main Reef are ~10 fold depleted in IPGE (Os-Ir-Ru) and Rh with respect to similar Cu-rich sulfides in lower troctolites. Also, the 'anorthositic' Cu-rich sulfides contain 2-4 times more Pd, Ag, Cd, and 2 times less Se. This observation allow the conclusion that despite close similarity in PGE-mineralogy of the mineralized troctolites and anorthosites (Kislov et al., this volume), geochemistry of Cu-rich sulfides from troctolites provides a record of an earlier stage of the sulfide immiscibility in more primitive intercumulus melts as compared to those originated in the gabbroic part of the YDM. Primitive mantle normalized bulk-rock PGE spectra support for this conclusion.

Acknowledgements: This research was supported by the Russian Science Foundation (RSF) grant No. *16*-17-10129.

Ariskin, A.A., Danyushevsky, L.V., Konnikov, E.G., Maas, R., Kostitsyn, Y.A., McNeill, A.W., Meffre, S., Nikolaev, G.S., Kislov, E.V. (2015a): The Dovyren Intrusive Complex (northern Baikal region, Russia): isotope-geochemical markers of contamination of parental magmas and extreme enrichment of the source. *Russian Geol. Geophys.*, **56**, 411-434.

Ariskin, A.A., Nikolaev, G.S., Danyushevsky, L.V., Kislov, E.V., Malyshev, A., Barmina, G.S. (2015b): New type of low-sulfide PGE mineralization in primitive troctolites from the Yoko-Dovyren layered massif. *in* "Proceedings of XII All-Russian Petrographic Conference", vol. 1, A.I. Golubev, V.V. Shiptsov, eds., Petrozavodsk, 289-291 (in Russian).

Kislov, E.V. (1998): The Yoko-Dovyren layered massif. BNTs RAN, Ulan-Ude, 265 p. (in Russian).

Kislov, E., Ariskin, A., Danyushevsky, L., Goemann, K., Nikolaev, G., Malyshev, A. (2016): PGE-mineralogy of the Main Reef and sulfide-poor troctolite from the Yoko-Dovyren massif (Northern Baikal Region, Russia). This meeting.

UNUSUAL PALLADIUM–THALLIUM MINERALIZATION IN THE ANOMAL'NYI DEPOSIT, KONDYOR RING COMPLEX, NORTHERN KHABAROVSKIY KRAY, RUSSIA

Barkov A.Y.[1], Shvedov G.I.[2], Polonyankin A.A.[3] & Martin R.F.*[4]
[1] Research laboratory of industrial and ore mineralogy, Cherepovets State University, Russia
[2] Noril'skgeologiya OOO, Noril'sk, Russia
[3] Russian Platinum Group, Moscow, Russia
[4] Department of Earth and Planetary Sciences, McGill University, Montreal, Canada
Corresponding email: robert.martin@mcgill.ca

Keywords: Pd–Tl mineralization, new mineral species, Kondyor ring complex

The Kondyor alkaline ultramafic complex, in northern Khabarovskiy kray, at the eastern margin of the Aldan Shield, northeastern Russia, continues to surprise! Here, we describe novel associations involving Pd and Tl from the Anomal'niy Cu–PGE deposit, located in the central area of the annular complex. They are found in vein-type settings associated with bodies of "kosvite" (magnetite-rich clinopyroxenite) in the dunite-(peridotite) core, in pegmatitic and micaceous mafic rocks. The "kosvite" bodies are closely associated with a vein-like system of mineralized rocks. They are highly micaceous, up to ~20 m thick, and coarse-grained to pegmatitic. In addition to being anomalously rich in phlogopite, with a high content of apatite, they also contain diopside rich in aegirine, subordinate orthopyroxene rich in ferrosilite, albite, Ba-bearing potassium feldspar, deuteric clinochlore, chamosite, talc, disseminated titaniferous magnetite, and Sr-bearing fluorapatite. The micaceous veins contain grains of base-metal sulfides (BMS), along with a great variety of ore species, especially those rich in Cu, Pd, and Pt. Juxtaposed assemblages of ore minerals include sulfides of the chalcopyrite – bornite – (secondary chalcocite) association, cubanite, fletcherite, REE-based minerals [allanite-(Ce), monazite-(Ce), bastnäsite-(Ce) and xenotime-(Y)], and various species of platinum-group minerals [isomertieite or arsenopalladinite rich in Sb, mertieite-II, mertieite-I, sobolevskite, kotulskite, merenskyite, zvyagintsevite (?), palarstanide, paolovite, hollingworthite, and unnamed PGM], Au-Ag alloy, along with uncommon bismuthides, selenides, sulfosalt minerals, and native bismuth. Also present are unnamed phases of arsenide – bismuthide – thallide compositions, $Pd_5(As,Tl,Bi)$ and $Pd_5(Tl,As,Bi)$, which are documented here for the first time. The As-dominant composition corresponds to: $Pd_5(As_{0.40}Tl_{0.31}Bi_{0.18}S_{0.11}Te_{0.06})$, or $Pd_5(As,Tl,Bi)$. It is likely a new species of PGM, related to synthetic Pd_5As, which is known in the system Pd–As. The Tl-dominant phase is rich in Bi and As, and corresponds to $Pd_5(Tl_{0.48}As_{0.20}Bi_{0.20}S_{0.11}Te_{0.05})$. The oxides $Pd_4(Bi,Te,Tl)O_6$ and $Pd_4(Tl,Bi,Te)O_6$ seem to have formed *in situ* by oxidation reactions at the expense of the associated PGM intergrowths. An evolved environment, depleted in Cr and Ni, and enriched in Cu, Pd, Bi, Pb and volatile components, is indicated for the vein-type deposit at Anomal'niy. The presence of end-member albite coexisting with Ca-bearing minerals indicates a temperature of 400ºC or less. This deposit contrasts with the Pt-bearing chromitites found in dunite in the central zone of the massif. Note that both types of deposit seem to involve local volatile-enriched environments and associations with low-temperature minerals.

LATEST NEWS FROM THE KHATYRKA METEORITE

Bindi L.*[1], Lin C.[2], Ma C.[3] & Steinhardt P.J.[2]
[1] Dipartimento di Scienze della Terra, Università di Firenze, Italy
[2] Department of Physics, Princeton University, NJ, USA
[3] Division of Geological and Planetary Sciences, California Institute of Technology, Pasadena, CA, USA
Corresponding email: luca.bindi@unifi.it

Keywords: new minerals, alloys, meteorite

Two unnamed phases with simplified formula AlCu and Al_3Fe were found in one of the fragments recovered from an expedition to the Koryak Mountains in far eastern Russia in 2011 (Steinhardt & Bindi, 2012) as a result of a search for samples that would provide information on the origin of the quasicrystal mineral icosahedrite (Bindi et al., 2009, 2011, 2012). The recovered fragments have meteoritic (CV3-like) oxygen isotopic compositions and are identified collectively as coming from the Khatyrka meteorite (MacPherson et al., 2013), which formed 4.5 billion years ago during the earliest stages of the solar system.

The two phases were found in association with icosahedrite and khatyrkite in one polished section. Other minerals identified in this section are forsterite, spinel, hercynite, chromite, magnetite, corundum, iron, taenite, suessite, naquite, xifengite, aluminum, nickel, copper, unnamed Al_7Cu_2Fe, plus glass with various compositions. Associated minerals in other fragments include trevorite, diopside, forsterite, ahrensite, clinoenstatite, nepheline, coesite, stishovite, pentlandite, Cu-bearing troilite, khatyrkite, taenite and Al-bearing taenite, steinhardtite and decagonite (the second natural quasicrystal; Bindi et al., 2015).

Electron microprobe analysis, high-resolution SEM and electron backscatter diffraction have been used to characterize the composition and structure of the two new minerals. The two new minerals correspond to the synthetic β and λ phase of the Al-Cu-Fe system (Zhang & Lück, 2003), usually associated to the icosahedral phase (natural icosahedrite) and the ω phase (natural unnamed Al_7Cu_2Fe).

Bindi, L., Steinhardt, P.J., Yao, N., Lu, P.J. (2009): Natural quasicrystals. *Science*, **324**, 1306-1309.

Bindi, L., Steinhardt, P.J., Yao, N., Lu, P.J. (2011): Icosahedrite, $Al_{63}Cu_{24}Fe_{13}$, the first natural quasicrystal. *Am. Mineral.*, **96**, 928-931.

Bindi, L., Eiler, J., Guan, Y., Hollister, L.S., MacPherson, G.J., Steinhardt, P.J., Yao, N. (2012) Evidence for the extra-terrestrial origin of a natural quasicrystal. *Proc. Nat. Acad. Sci. USA*, **109**, 1396-1401.

Bindi, L., Yao, N., Lin, C., Hollister, L.S., Andronicos, C.L., Distler, V.V., Eddy, M.P., Kostin, A. Kryachko, V., MacPherson, G.J., Steinhardt, W.M., Yudovskaya, M., Steinhardt, P.J. (2015): Natural quasicrystal with decagonal symmetry. *Sci. Rep.*, **5**, 9111.

MacPherson, G.J., Andronicos, C.L., Bindi, L., Distler, V.V., Eddy, M.P., Eiler, J.M., Guan, Y., Hollister, L.S., Kostin, A., Kryachko, V., Steinhardt, W.M., Yudovskaya, M., Steinhardt, P.J. (2013): Khatyrka, a new CV3 find from the Koryak Mountains, Eastern Russia. *Meteor. Planet. Sci.*, **48**, 1499-1514.

Steinhardt, P.J. & Bindi, L. (2012): In search of natural quasicrystals. *Rep. Progr. Phys.*, **75**, 092601-092611.

Zhang, L. & Lück, R. (2003): Phase diagram of the Al-Cu-Fe quasicrystal-forming alloy system. I. Liquidus surface and phase equilibria with liquid. *Z. Metallk.*, **94**, 91-97.

ALTERATION OF PRIMARY PLATINUM-GROUP MINERALS DURING WEATHERING OF THE FREETOWN LAYERED COMPLEX, SIERRA LEONE

Bowles J.F.W.*[1], Suárez S.[2-3], Prichard H.M.[2] & Fisher P.C.[2]
[1] School of Earth, Atmospheric and Environmental Sciences, University of Manchester, United Kingdom
[2] School of Earth and Ocean Sciences, Cardiff University, United Kingdom
[3] Departamento de Mineralogía y Petrología, Universidad del País Vasco, Leioa & Ikerbasque, Bilbao, Spain
Corresponding email: john.bowles@manchester.ac.uk

Keywords: platinum-group minerals, Freetown Intrusion (Sierra Leone), Pt-Pd mobility

Samples of fresh and weathered rocks and saprolite from the platiniferous Horizon B of the Freetown Layered Complex have been studied for their platinum-group mineral (PGM) content. Between outcrops of apparently fresh rock there is saprolite containing residual rock fragments (corestones) to a depth of about 2 m. The fresh rocks contain small PGM ranging from 1-7 µm in size, including cooperite (PtS) and isoferroplatinum (Pt_3Fe), with minor tetraferroplatinum (PtFe), tulameenite (Pt_2FeCu), Os-bearing laurite (RuS_2), and other Pt-Rh-Ir-base metal sulphide-bearing PGM. This conforms to the earlier studies that first found PGM in the Freetown rocks (Bowles et al., 2013).

The weathered rocks contain fewer sulphides and Pt_3Fe than the fresh rocks but they contain some tulameenite and a high proportion of disordered Cu-(±Pd)-bearing Pt-Fe alloys. The Pt- and Pd-bearing saprolite contains scarce, smaller (1-3 µm) ordered PtFe and disordered $PtFe_3$. All the samples are devoid of Pd-rich PGM. The Pt-Fe alloys show a clear sequence during weathering, passing systematically through ordered and disordered phases and becoming increasingly Fe-rich as weathering proceeds. Pt-Fe-oxides appear late in this weathering process. During weathering, copper sulphides hosting the primary PGM and the PtS (containing up to 3% Pd) have been destroyed to provide the minor Cu and Pd found in some of the disordered Pt-Fe alloys. These compositional changes and features such as the transition from euhedral to irregularly-shaped PGM, the presence of reaction fronts, and symplectic textures all demonstrate progressive alteration of the PGM during weathering and breakdown of the rocks. Examples of these alteration textures will be shown during the presentation. Alteration occurred over a long period with a ready supply of organic acids that may have contributed to the leaching and transport of PGE.

The saprolitic profile has retained the original rock fabric and has permitted ground water to seep down slope. The ground water has transported Pt, Pd (and probably Au) derived from weathering of the mineralized rocks into the saprolite cover above unmineralized rocks down slope. The metal movement in solution is marked by changes in the Pt/Pd ratio indicating that these metals have moved independently. Palladium is present in marginally higher concentrations in the deeper saprolite than in either the corestones or the upper saprolite, suggesting there has been some retention of Pd in the deeper saprolite. Platinum and Pd are less concentrated in the upper saprolite than the deeper saprolite indicating that they have both been leached from the upper saprolite.

These observations of the weathering of the PGM of the Freetown Intrusion provide an important link between the PGM of the fresh rocks and the alluvial nuggets found in the streams draining the intrusion. Understanding these processes is critical to the interpretation of geochemical surveys during the search for new deposits.

Bowles, J.F.W., Prichard, H.M., Suárez, S., Fisher, P.C. (2013): The first report of platinum-group minerals in magnetite-bearing gabbro, Freetown Layered Complex, Sierra Leone: occurrences and genesis. *Can. Mineral*., **51**, 455-473.

DISTRIBUTION OF PLATINUM-GROUP ELEMENTS IN THE SAN AGUSTÍN (CHROMITE-Ni ARSENIDE ORES) AND EL GALLEGO (SULPHIDE-GRAPHITE ORES) DEPOSITS, CARRATRACA ULTRAMAFIC MASSIF, SOUTHERN SPAIN

Chatzipanagiotou C.*[1], Gervilla F.[2] & Fontboté L.[1]
[1] Département de Sciences de la Terre, Université de Genève, Switzerland
[2] Departamento de Mineralogía y Petrología, Universidad de Granada, Spain
Corresponding email: christos1990@gmail.com

Keywords: Ronda ultramafic massifs, chromite-Ni arsenides, platinum group elements

The Carratraca massif is one of the several lherzolite massifs outcroping in the Ronda area, southern Spain. They are portions of Earth upper mantle structured in three tectonometamorphic domains (from top to bottom: garnet mylonites to spinel tectonites, granular peridotites, and plagioclase tectonites) emplaced at high temperature in the continental crust. Three mineralisation types occur inside these ultramafic bodies (Gervilla and Leblanc 1990; Gervilla et al., 2002): 1) Chromite ores with minor amounts of olivine, clinopyroxene or orthopyroxe ("Cr ores"), 2) chromite-Ni arsenides ores with with orthopyroxene and/or cordierite ("Cr-Ni ores"), 3) Fe–Ni–Cu sulphides with variable amounts of graphite and minor chromite, having phlogopite and plagioclase as main gangue minerals ("S-G ores").

The San Agustín Cr-Ni deposit is hosted by spinel tectonites (Chatzipanagiotou, 2016). Its primary mineralogical assemblage is chromite and nickelite (NiAs) with cordierite gangue. Nickel diarsenides (rammelsbergite-safflorite-löllingite; $NiAs_2$-$CoAs_2$-FeAs2) and rarely sulpharsenides (gersdorffite-cobaltite; NiAsS-CoAsS) occur as accessory minerals. In addition, sperrylite ($PtAs_2$) and Au-Cu alloys were identified in two samples. El Gallego S-G deposit is located 400 m NW of San Agustín, hosted by garnet mylonites (Chatzipanagiotou, 2016). Its main mineralogical assemblage consists of pyrrhotite, pentlandite, chalcopyrite, cubanite, chromite, and graphite. Nickelite and cobaltite-gersdorffite are accessory minerals.

Both ore occurrences contain relatively high amounts of PGE. The analysed Cr-Ni ore samples from San Agustín have bulk PGE contents between 0.7 and1.6 ppm, approaching the chondritic values and showing chondrite-normalised PGE patterns with smooth, slightly positive slopes from Os to Pd and, one of the two sperrylite-bearing samples, is characterised by a strong, positive anomaly in Pt. Au contents range between 6.7 and 14.5 ppm, well above the chondritic values. The El Gallego S-G ore samples exhibit a wider range in noble metals contents, ranging from 0.2 to 8 ppm PGE and from 0.02 to 10 ppm Au. Their chrondrite-normalised PGE patterns vary from almost flat to slightly positively-sloped. Two of the three analysed samples exhibit strong positive anomalies in Pt and Au, in contrast with previously published geochemical data from the same type of deposits in the Ronda area and in Beni Bousera, which showed negative Pt anomalies. No platinum-group minerals were found at El Gallego despite the high PGE values measured.

The abundance of PGE in San Agustín Cr-Ni ores compared to the amounts measured in El Gallego S-G ores suggests that PGE concentrate preferentially in arsenide-bearing ores, leaving sulfide ores abnormally impoverished in these noble metals. PGE are possibly hidden in solid solution in Ni arsenides except in some samples where sperrylite is found. The measured values in noble metals overlap the fields of other types of magmatic ores (Sudbury, komatiite related deposits) of economic interest. In addition, the strong positive anomalies in Pt and Au overlap the fields of some of the known richest deposits such as those located in the Noril'sk-Talnahk district and in the Bushveld complex.

Chatzipanagiotou, C. (2016): The San Agustín chromite-Ni arsenide and El Gallego Fe-Ni-Cu-sulphide-graphite deposits, Carratraca ultramafic massif, southern Spain: mineralogy and geochemistry. Master Thesis, Univ. of Geneva, Switzerland, 89 p.

Gervilla, F. & Leblanc, M. (1990): Magmatic ores in high-temperature alpine-type lherzolite massifs (Ronda, Spain, and Beni Bousera, Morocco). *Econ. Geol.*, **85**, 112-132.

Gervilla, F., Gutierrez-Narbona, R., Fenoll Hach-Ali, P. (2002): The origin of different types of magmatic mineralizations from small-volume melts in the lherzolite massifs of the Serranía de Ronda (Málaga, Spain). *Bol. Soc. Españ. Mineral.*, **25**, 9-96.

ZIRCON AND MONAZITE REVEAL THE METAMORPHIC EVOLUTION OF THE EASTERN PAMPEAN RANGES, ARGENTINA

Escayola M.*[1], Pimentel M.[2] & Ramos V.A.[1]

[1] Instituto de Estudios Andinos, Universidad de Buenos Aires, Consejo Nacional de Investigaciones Científicas y Técnicas, Buenos Aires, Argentina

[2] Institute of Geosciences, University of Brasilia, Brazil

Corresponding email: mescayola@gl.fcen.uba.ar

Keywords: zircon, U-Pb, Pampean Ranges

The Eastern Pampean Ranges comprise high-grade supracrustal sequences with belts of ophiolite remnants. U-Pb and Nd isotopic data suggest that the tectonic evolution of the Pampean Ranges started ca. 640 Ma in a back-arc basin. To the south of the Ranges there is a body of Kinzigite. Its particular mineral association (Qtz+Grt+Crd+Pl+Bt+Mag+-Ath) and the lack of Kf distinguishes this rock unit from the migmatites around.

One kinzigite sample was selected for zircon and monazite conventional TIMS and SHRIMP U-Pb analyses, as well as for whole-rock, garnet and cordierite Sm-Nd analysis. Monazite grains are euhedral, pale yellow, clear, homogeneous. Zircon crystals are mostly euhedral, prismatic, transparent and fine grained (50 to 150 ìm). Rims of new zircon around older cores are ubiquitous. Cathodoluminiscence images reveal that virtually all zircons contain cores of low luminescence.

Uranium concentrations of the zircon grains vary between 162 and 591 ppm and Th/U ratios are from 0.018 to 1.317. The lowest Th/U ratios are for rims with the age of ca. 510 Ma whereas higher Th/U ratios correspond to cores with ages ranging from ca. 576 to 510 Ma. Both cores and rims possibly originated during a single temperature-progressive high-grade metamorphic event.

Monazite age is of 517±4 Ma and it must have grown concomitantly with the low Th/U ratio zircon rims during the highest temperature metamorphic event.

Zircon ID-TIMS U-Pb method yielded the age of 517±5 Ma for the high-grade metamorphic event. Some grains, however, clearly show an older core surrounded by metamorphic zircon and a few analyses of such grains indicated ages ranging from ca. 622 to 2200 Ma. The pattern is, therefore, compatible with a detrital sedimentary protolith for the kinzigite.

Sm-Nd isotopic analyses indicated high $^{147}Sm/^{144}Nd$ ratio (0.166) and TDM model age of ca. 2.6 Ga. The high value of the Sm/Nd ratio maybe explained because the rock suffered strong LREE depletion during melting and extraction of granitic melts, resulting in some fractionation between Sm and Nd.

Previous studies (Sims et al., 1998; Rapela et al., 1998) U-Pb SHRIMP data on zircon and monazite yielded ages of 530 Ma, and were interpreted as the age of the *in situ* metamorphic peak related to crustal thickening and compression with P-T conditions of 8.6 Kbar and 810°C; culminating in isothermal uplift and low pressure anatexis linked to the generation of peraluminous discordantly emplaced granites (520 Ma, 4-5 kbar, 715°C). Our data reveal that high-grade metamorphism followed collision and medium-grade metamorphism and mark the final stages of evolution of orogen at 517 Ma related to slab break-off.

Rapela, C.W., Pankhurst, R.J., Casquet, C., Baldo, E., Saavedra, J., Galindo, C., Fanning, C.M. (1998): The Pampean orogeny of the southern proto-Andes: Cambrian continental collision in the Sierras de Córdoba. *in* "The Proto-Andean margin of Gondwana", R.J. Pankhurst & C.W. Rapela, eds., *Geol. Soc. London Spec. Publ.*, **142**, 181-217.

Sims, J., Ireland, T.R., Camacho, A., Lyons, P., Pieters, P.E., Skirrow, R., Stuart-Smith, P.G., Miró, R. (1998): U-Pb, Th-Pb, and Ar-Ar geochronology from the Southern Sierras Pampeanas, Argentina: implications for the Paleozoic tectonic evolution of the western Gondwana margin. *in* "The Proto-Andean margin of Gondwana", R.J. Pankhurst & C.W. Rapela, eds., *Geol. Soc. London Spec. Publ.*, **142**, 259-281.

MINERALOGY OF “PLATINA” FROM THE FIRST-MINED PLATINUM DEPOSIT

García-Guinea J.[1] & Gervilla F.*[2]

[1] Museo Nacional de Ciencias Naturales, Consejo Superior de Investigaciones Científicas, Madrid, Spain

[2] Departamento de Mineralogía y Petrología & Instituto Andaluz de Ciencias de la Tierra, Consejo Superior de Investigaciones Científicas, Universidad de Granada, Spain

Corresponding email: gervilla@ugr.es

Keywords: historical samples, platina, platinum-group minerals

The first reference on the platinum element was published by Jorge Juan y Antonio de Ulloa (Ulloa, 1748). The existence of a metal so-called platina by Ulloa was well known by Spanish colonizers living in the Pacific coast of what is now Colombia and Ecuador. Platinum was considered less valuable than silver and hence was probably termed with a diminutive name of silver (“plata” in Spanish), “platina” meaning cheap silver. In those years it had low price and could be used to adulterate gold. The samples carried by Ulloa to Spain gave rise to an increasing scientific interest in the new metal leading to the development of experiments for the refinement of platinum, first in the Laboratories of Vergara and later in the laboratories of the Hortaleza Street in Madrid (in the House of the Platina). The material used in such experiments started with the original samples carried by Ulloa and continued with “Platina” concentrates shipped by the Viceroyalty of New Granada to Madrid between 1748 and 1799.

The Museo Nacional de Ciencias Naturales in Madrid (Spain) keeps a small batch of precious metals which is closely associated with the historical refinement of platinum in Madrid. One of the flask labelled “Platina y Oro del Choco” (“Platina and Gold from Choco”) contains natural heavy mineral grains taken in a rivercourse which mainly are platinum-group minerals, gold and intergrown magnetite and ilmenite with accesory hematite, garnet, augite, apatite, titanite, quartz, calcite shells, plant relicts, etc. The sample is fully compatible with others collected from rivers of the Pacific coast of Colombia-Ecuador and perhaps it is one of the historical flasks handled by Ulloa.

Preliminary SEM-EDS, EPMA and Raman investigations show that the platinum-group minerals assemblage (what was called “platina” in the XVIII century) mainly consist of isoferroplatinum containing some Pd, Ir, Os, Rh and Cu [$(Pt_{2.98}Pd_{0.04}Ir_{0.02}Os_{0.01}Rh_{0.01})_{S=3.06}(Fe_{0.93}Cu_{0.01})_{S=0.94}$], with minor amounts of Ir-Os alloys ($Ir_{0.58}Os_{0.23}Pt_{0.15}Fe_{0.03}Rh_{0.01}$), minute, idiomorphic to subidiomorphic grains of laurite included in isoferroplatinum and tiny grains of what probably correspond to irarsite, associated with laurite. Native gold is quite pure, showing Au contents between 89.70 and 99.84 wt.% and minor silver (0.08-8.74 wt.% Ag), antimony (0.20-0.62 wt.% Sb) and bismuth (0.11-0.30 wt.% Bi).

Ulloa, J.J. y A. de (1748): Relación histórica del viage a la América Meridional, hecho de orden de su Majestad e el Reyno del Perú. Marín, Madrid.

THE ROLE OF ACCESSORY CHLORITE AS PETROGENETIC INDICATOR OF HYDROTHERMAL VMS Fe-Cu-Zn SULFIDE ORE DEPOSITS IN THE NORTHERN APENNINE OPHIOLITES (EASTERN LIGURIA AND EMILIA ROMAGNA, ITALY)

Garuti G.*[1] & Zaccarini F.[1]
[1] Department Angewandte Geowissenschaften und Geophysik, Universität Leoben, Austria
Corresponding email: giorgio.garuti1945@gmail.com

Keywords: chlorite, VMS deposits, Italy

Chlorite is a common product of fluid-rock interaction and is frequently found as a secondary replacement of mafic minerals in low-grade metamorphic rocks and strongly diagenetic sediments. Chlorite is also a typical accessory mineral of hydrothermalites. The VMS Fe-Cu-Zn sulfide deposits associated with the Northern Apennine ophiolites contain chlorite in differnt minerogenetic contexts: type-1) in sulfide-mineralized hydrothermal veins (quartz-carbonate) cutting across mafic-ultramafic rocks, type-2) in mafic-ultramafic rocks (basalt, gabbro, sepentinite) as a result of convective circulation of thermally-modified sea-water below the sub-oceanic floor, and type-3) as detrital sedimentary mineral accumulating on the sea-floor at the venting site of metalliferous brines. Due to its non-stoichiometry and compositional variability, the mineral chemistry of chlorite in the Northern Apennine Fe-Cu-Zn sulfide deposits reflects the different environments of crystallization, being affected by changes in temperature, host-rock composition/mineralogy, and composition of the parent hydrothermal fluids. Type-1 chlorite from quartz-carbonate veins in basalt is dominated by Mg-Fe substitution, at constant ^{VI}Al, and relatively high Mn/Cr ratio, similar to the chlorite of type-2 in basalt and gabbro. Type-1 chlorite from quartz-carbonate veins cutting across serpentinite is characterized by concomitant substitution of Mg for Fe and ^{VI}Al, and high Cr/Mn ratio. Type-3 chlorite, associated with sea-floor, stratiform deposits has relatively high ^{VI}Al composition with variable Fe/Mg depending on the mafic or ultramafic nature of the substratum. The composition of the Northern Apennine chlorites exhibits Fe-Mg-^{VI}Al exchanges in the octahedral site similar to the chlorite from metabasic rocks. The metabasic rocks represent a wide range of metamorphic conditions, whereas the VMS deposits have undergone only weak sub-oceanic metamorphism. The similarity in chlorite composition appears to be essentially due to the similarity between the mafic-ultramafic protoliths that have generated the chlorite in the Northern Apennine deposits and metabasic rocks. Other factors, such as seafloor or sub-seafloor environment of formation, have influenced the temperature of chlorite crystallization, causing an increase of the amount of ^{IV}Al, that substitutes for Si in the tetrahedral site with increasing temperature. Temperatures obtained from type-1 and type-2 chlorites vary in a range of 85-360°C, with more than 90% of data plotting between 200 and 310°C. In contrast, chlorite from sea-floor stratiform ores crystallized at relatively low temperatures, between 50 and 298°C, with 85% of the values clustering in the range of 100-200°C. However, exchanges in the octahedral site of chlorite, involving Fe, Mg, ^{VI}Al, and the other minor elements Cr and Mn appear to be exclusively influenced by the mafic or ultramafic nature of the rocks hosting the VMS deposits.

PLATINUM GROUP MINERALS FROM THE VURUCHUAIVENCH PGE DEPOSIT, MONCHEGORSK IGNEOUS COMPLEX, KOLA PENINSULA, RUSSIA

Grokhovskaya T.*[1], Karimova O.[1] & Magazina L.[1]
[1] Institute of Geology of Ore Deposits, Petrography, Mineralogy and Geochemistry, Russian Academy of Sciences, Moscow, Russia
Corresponding email: tlg@igem.ru

Keywords: platinum group minerals, Vuruchuaivench intrusion

Newly obtained data are reported on a great variety of PGM species in recently discovered Vuruchuaivench PGE deposit. The Vuruchuaivench layered intrusion is part of the Early Paleoproterozoic Monchegorsk Igneous Complex. The reef-type PGE mineralization is hosted by layered sulfide-bearing gabbronorites with intercumulus base metal sulfides (BMS), bearing a large variety of PGM, with BMS and PGM found in close association. Magmatic PGE-bearing BMS consist of the pyrrhotite-chalcopyrite-pentlandite assemblage with variable proportions of minerals. The secondary and minor ore minerals are millerite, bornite, pyrite, cobaltite-gersdorffite, sphalerite, magnetite, electrum and native silver. PGM occur within BMS grains and at the contacts between sulfides and silicates. The most common PGM are sperrylite, menshikovite, palladoarsenide, arsenopalladinite, isomertieite, Pt-Pd-bismuthtellurides, braggite, with minor other PGM species. Sperrylite and braggite usually form individual grains and/or more rare intergrowths with other PGM. Intergrowths of kotulskite, merenskyte, hollingworthite and electrum are sometimes hosted in pentlandite. The Vuruchuaivench deposit is characterized by a relatively little varying set of Pd-Ni-As-(±Sb) droplet-like (oval or spherical) intergrowths, which are variably replaced by Ni-cobaltite, amphiboles and chlorite. Polymineralic intergrowths consist of menshikovite, isomertieite, arsenopalladinite, stibiopalladinite, and palladoarsenide. Kotulskite, sobolevskite and electrum were also identified in these aggregates. These intergrowths are usually hosted in chalcopyrite. Evidence of immiscibility between arsenide and sulfide melts is provided by experiments and observations at some magmatic Cr-Ni arsenide deposits (Gervilla et al., 1996). Experimental studies also show that Pt and Pd are preferably concentrated in arsenide melt and then crystallize as Pt-Pd-(Ni) arsenide minerals (Helmy et al., 2013). Unusual droplet-like Pd-As±Ni±Sb intergrowths hosted by BMS found at the Vuruchuaivench deposit likely suggest that the arsenide and sulfide melts were immiscible when these oval and spherical blebs were formed. The association of certain PGM species with actinolite, hornblende, quartz, apatite, chlorite suggests that volatile components should have participated in the mineralizing processes. The close association of PGM and BMS and the strong correlation between the concentrations of PGE and Cu, Ni and S at the Vuruchuaivench PGE deposit provide evidence that primary PGM were partly derived from sulfide melt and partly produced by immiscibility between sulfide and arsenide melts (spherical blebs). The secondary PGM species and native silver could be formed during remobilization of BMS by magmatic fluids and/or hydrothermal solutions.

Gervilla, F., Leblanc, M., Torres, R.J., Fenoll Hach-Ali, P. (1996): Immiscibility between arsenide and sulfide melts: a mechanism for the concentration of noble metals. *Can. Mineral.*, **34**, 485-502.

Helmy, H.M., Ballhaus, C., Fonseca, R.O.C., Nagel, T.J. (2013): Fractionation of platinum, palladium, nickel, and copper in sulfide–arsenide systems at magmatic temperature. *Contrib. Mineral. Petrol.*, **166**, 1725-1737.

GEOLOGICAL AND METALLOGENIC CHARACTERIZATION OF MASSIVE MAGNETITE IN THE MINING CONCESSION "EMILIO ALBERTO" – CASCAS DISTRICT - REGION LA LIBERTAD (PERU)

Herrera A.*[1], Nazzareni S.[1] & Morales J.[2]
[1] Dipartimento di Fisica e Geologia, Università di Perugia, Italy
[2] Departamento de Ingeniería Geológica, Universidad Nacional de Cajamarca, Peru
Corresponding email: albertherrerav@gmail.com

Keywords: geological-metallogenic studies, economic minerals, skarn

The western part of the Peruvian Andes, has been interested by a strong active tectonics during the past geologic time, in particular magmatic and hydrothermal events occurred during Andina tectonics. In the Cascas district (region La Libertad, Perù) is located the exploration concession "Emilio Alberto", this area is characterised by Upper Jurassic and Lower Cretaceous sedimentary rocks that have been intruded by Paleogene granodioritic bodies. The stratigraphic sequence (from Upper Jurassic to Lower Cretaceous) is characterised by Jurassic limestones of the Chicama formation to Lower Cretaceous sandstones of the Chimu formation and limestone of the Santa formation (Reyes, 1980). The granitic intrusion bodies formed several skarn ore deposits across the region (Chira et al., 2011).

The geological stratigraphy of the "Emilio Alberto" exploration concession is characterised by a thin layer of limestone (around 150 m thick) overlapping a thick sequence of sandstones, on this stratigraphic succession outcrops a granitic body (around 20 square meters on surface) that intruded the limestone-sandstone sequence. Field mining exploration of the area allowed to describe both a thermal metamorphic zone and a metasomatic zone, and limited outcropping areas of hydrothermal alteration.

Preliminary mineralogical analysis detected the presence of andradite garnet, amphibole, and evidences of hydrothermal alteration. Moreover massive pure magnetite and traces of sulphides such as chalcopyrite and pyrite, has been found as ore minerals in the area suggesting the presence of skarn mineralization.

A characterization of the mineralization and alterarion zone will be presented, in particular the concentration of magnetite in the sandstones levels.

A detailed identification of the economic and skarn-related minerals will provide information to understand the geological processes occured in the Cascas district and related to the mineralization, contributing with new data to the geology and metallogeny of the area and likewise evaluating the potential development of a project within the concession Minera "Emilio Alberto".

Chira Fernández, J.E., Vásquez Oliva, R., Vargas Rodríguez, L.E., Palomino Colona, C.G. (2011): Prospecciòn geoquimica regional entre los paralelos 7º y 8º sur - vertiente Pacifica. Boletin Nº 28 Serie B. *Geologìa Economica*, Lima-Peru, 15-41.

Reyes, L. (1980): Geologia de los cuadrangulos de Cajamarca, San Marcos y Cajabamba. Hojas 15-f, Boletín Nº 31 Serie A, Lima-Peru, 15-24.

PLATINUM-GROUP ELEMENTS AND MINERALS IN THE LOWER AND MIDDLE GROUP CHROMITITES OF THE BUSHVELD COMPLEX, SOUTH AFRICA

Junge M.*[1], Oberthür T.[1] & Osbahr I.[2]
[1] Bundesanstalt für Geowissenschaften und Rohstoffe, Hannover, Germany
[2] Helmholtz-Zentrum Dresden-Rossendorf, Helmholtz-Institut Freiberg für Ressourcentechnologie, Germany
Corresponding email: malte.junge@bgr.de

Keywords: Bushveld Complex, platinum-group-minerals, chromitites

The 2,050 Ma old Bushveld Complex in South Africa is the largest layered mafic-ultramafic intrusion on Earth and contains the largest resources of platinum-group elements (PGE) as well as economically important reserves of chromium and vanadium. The correlation between chromite and PGE is remarkably well expressed as even the thinnest chromitite stringers in the Bushveld Complex contain elevated concentrations of PGE. The UG-2 chromitite has been investigated in great detail, however, studies on the distribution of PGE and the mineralogical character of the PGM in the LG and MG chromitites are scarce and the knowledge of the distribution and the mineralogical siting of the PGE in the chromitite seams of the Lower Group (LG) and Middle Group (MG) of the Bushveld Complex is limited.

In the present study, concentrates from the LG-6 and MG-2 chromitites of the Bushveld Complex are studied to determine the distribution of the PGE and the nature of the platinum-group mineral (PGM) in these chromitite seams. Quantitative mineralogical analysis using the Mineral Liberation Analyser (MLA) software was carried out in order to determine the PGM proportions in these concentrates. The dominant PGM are sulfides, namely cooperite-braggite, malanite-cuprorhodosite, and laurite, followed by PGE-sulfarsenides, sperrylite, and Pt-Fe alloys. The additional information of PGM area percentages compared to frequency data obtained by the MLA data, show that in LG and MG chromitites of the western Bushveld Complex laurite grains make up the largest area amount of PGM. The matching sets of PGM present in the LG and MG chromitites of both the western and the eastern Bushveld Complex, and the UG-2 chromitite show far-reaching similarities which support the indication of a characteristic, general chromitite-related PGM assemblage. These PGM in the LG and MHR are mostly associated with silicates (54 and 60% in the LG-6 and MG-2, respectively), followed by sulfides (32 and 37% in the MG-2 and LG-6, respectively). Rarer associations are with chromite (2%) or other PGM (5 to 7%). Palladium and Rh contents in sulfides (mainly pentlandite) may range up to thousands of ppm in ores associated with mafic-ultramafic intrusions (Cabri et al., 1984, Oberthür et al., 1997, Osbahr et al., 2013). Palladium and Rh contents in pentlandite of the LG and MG chromitites of this study are low and erratic although maximum contents of 7731 ppm Pd and 6023 ppm Rh were detected. Rare thiospinels of the polydymite-linnaeite-greigite series achieve PGE contents of 1428 ppm Pt, 5370 ppm Rh and 1460 ppm Pd.

Cabri, L.J., Blank, H., El Goresy, A., Laflamme, J.H.G., Nobiling R., Sizgoric, M.B., Traxel, K. (1984) Quantitative trace-element analyses of sulfides from Sudbury and Stillwater by Proton Microprobe. *Can. Mineral*., **22**, 521-542.

Oberthür, T., Cabri, L.J., Weiser, T., McMahon, G., Müller, P. (1997) Pt, Pd and other trace elements in sulfides of the Main Sulfide Zone, Great Dyke, Zimbabwe – a reconnaissance study. *Can. Mineral*., **35**, 597-609.

Osbahr, I., Klemd, R., Oberthür, T., Brätz, H., Schouwstra, R. (2013) Platinum-group element distribution in base-metal sulfides of the Merensky Reef from the eastern and western Bushveld Complex, South Africa. *Miner. Deposita*, **48**, 211-232.

CRYSTAL STRUCTURE REFINEMENT OF MERTIEITE-II, $Pd_8(Sb,As)_3$

Karimova O.*[1], Zolotarev A.A.[2] & Kojonen K.[3]
[1] Department of Crystal Chemistry of Minerals, Institute of Geology of Ore Deposits, Petrography, Mineralogy and Geochemistry, Russian Academy of Sciences, Moscow, Russia
[2] Department of Earth Science, Saint Petersburg State University, Russia
[3] Geological Survey of Finland, Espoo, Finland
Corresponding email: oxana.karimova@gmail.com

Keywords: mertieite-II, crystal structure, As-Sb ordering

Mineral mertieite, with general formula $Pd_{5+x}(Sb,As)_{2-x}$ was discovered at Goodnews Bay, Alaska (Desborough et. al., 1973). Authors derived two types of composition for mertieite grains: mertieite-I, $(Pd_{5.04}C_{0.4})(Sb_{0.92}As_{0.9})$, and mertieite-II, $(Pd_{5.13}Cu_{0.02})(Sb_{1.53}As_{0.33})$. Later (Cabri et. al., 1975), reexamined mertieites and found that mertieite-II has the composition $Pd_8(Sb,As)_3$, rhombohedral unit cell and cell dimensions: a = 7.55 and c = 43.18 Å.

The crystal structure of synthetic antimony analogy of mertieite-II, Pd_8Sb_3, was determined by Woperson & Shubert (1976) on the base of single crystal X-ray diffraction. The structural model was proposed in non-centrosymmetric space group $R3c$, R = 0.14. Marsh (1994) refined the structure in centrosymmetric space group $R\text{-}3c$, R = 0.126. Current study is devoted to crystal structure analysis of natural arsenic containing mertieite-II, $Pd_8(Sb,As)_3$.

Crystals of mertieite-II from the Kaarrojja River (Inari commune, Polar Finland) were studied by means of single crystal X-ray diffraction. Experimental data were collected on XCalibur diffractometer at the Center of X-ray diffraction studies at St. Petersburg State University. Total numbers of 3548 and 5387 reflections were collected for crystal **I** and **II**, respectively (Mo$K\alpha$ X-radiation). Structure was solved by direct methods and refined to final R factors 0.0226 (**I**) and 0.0242 (**II**) using SHELX program complex (Sheldrick, 2008). Mineral is trigonal, space group is $R\text{-}3ch$, Z = 6. The unit cell parameters are: a = 7.5172(3), c = 43.037(2) Å, V = 2106.1(2) Å^3 (**I**) and a = 7.5135(4), c = 43.003(3) Å, V = 2102.4(3) Å^3 (**II**).

SEM analysis (JEOL JSM-5300+Link ISIS, IGEM RAS) gave composition for mertieite-II crystals (wt.%): Pd 70, Sb 26.6, As 3.5 (**I**), Pd 73.7, Sb 27.1, As 4.4 (**II**). Empirical formulae are $Pd_{7.84}Sb_{2.61}As_{0.55}$ (**I**) and $Pd_{7.87}Sb_{2.53}As_{0.61}$ (**II**), calculated on 11 atoms per unit cell.

Crystal structure of mertieite-II contains four Pd atoms positions. Wyckoff positions are: two 36f (Pd1 and Pd2) and two 12c (Pd3 and Pd4). Coordination numbers (CN) are: 11, 12, 13, 11 - for Pd1, Pd2, Pd3 and Pd4 atoms, respectively. Sb atoms are occupied 18e (CN = 10) and 12c (CN = 9) positions. Arsenic atoms are located in 6b position (CN = 8). The structure of merieite-II is isotypic with the Pd_8Sb_3 structure. The As-for-Sb substitution in the mertieite-II was found to not affect the main structural topology. Crystal structure analysis determined, that As and Sb atoms are separated on different positions in the mertieite-II structure. Crystal chemical formula for mertieite-II is defined as $Pd_{16}Sb_5As$.

Cabri, L.J., Laflamme, J.H.G., Stewart, J.M., Rowland, J.F., Chen, T.T. (1975): New data on some palladium arsenides and antimonides. *Can. Mineral*., **13**, 321-335.

Desborough, G.A., Finney, J.J., Leonard, B.F. (1973): Mertieite, a new palladium mineral from Goodnews Bay, Alaska. *Am. Mineral*., **58**, 1-10.

Marsh, R.E. (1994): The centrosymmetric-noncentrosymmetric ambiguity: some more examples. *Acta Crystallogr*., **A50**, 450-455.

Sheldrick, G.M. (2008): A short history of SHELX. *Acta Crystallogr.*, **A64**, 112-122.

Wopersnow, W. & Schubert, K. (1976): Kristallstruktur von Pd_8Sb_3. *J. Less-Comm. Met.*, **48**, 79-87.

NON-TYPICAL Pt-Pd-Au MINERALIZATION IN DIORITE-GRANODIORITE INTRUSIVES OF KURAMA VOLCANO-PLUTONIC REGION (UZBEKISTAN)

Khalmatov R.*[1] & Koneyev R.[1]
[1] Department of Geochemistry, Mineralogy and Petrography, National University of Uzbekistan, Tashkent, Uzbekistan
Corresponding email: r.khalmatov@yahoo.com

Keywords: PGE, gold, granodiorite

Traditional PGE deposits are associated with mafic-ultrabasic massifs (Norilsk, Bushveld). In Uzbekistan, there is no separate fields, but there are some gold ores and Au-Cu porphyry deposits that are distinguished by high potential of platinum (Turesebekov et al., 2005).

An unusual Pt-Pd-Au mineralization was established during the survey and assessment work for gold in the area of Kandyr diorite-granodiorite intrusion, located between the epithermal deposits Kochbulak and Au-Cu porphyry Kalmakyr in tectonic zones of hydrothermally altered quartz-chlorite-sericite metasomatic rocks.

Mass-spectrometric analysis (ICP-MS) identified Pt in amounts of 0.1 to 1.7 ppm in 22 samples of altered intrusives and metasomatic rocks, atomic absorption analysis from 12 samples determined Pd around 0.3 to 2.44 ppm. Two samples were supervised in the Czech Geological Survey. Recorded content were fully confirmed.

Electron-probe microanalyzer Jeol Superprobe 8800R detected various Pt-Pd, Pt-Pd-Sn phase of intermediate compositions between niggliite (PtSn) and atokite $(Pt,Pd)_3Sn$, and Pd-Pt-Sn, Pd-Pt-Cu-Sn, Pd-Cu-Sn-Ni, and Pd-Ag-Pb phase of intermediate compositions between paolovite (PdSn), cabriite (Pd_2SnCu) (Jusko-Zakharov et al., 1986). Au-Cu-Sn phase with variable ratio of components, admixtures of Ag, Fe and Ni was determined. Above listed compounds were not recorded earlier in the fields of Uzbekistan.

The studies have generated more questions than answers. While it is clear that, the Pt-Pd-Au mineralization, which is characterized by geological conditions of the location and the mineralogical and geochemical features, was established. The deep Dukent-Goshsay fault extending in this area is considered to be a source for ore.

Acknowledgements: The research was supported by A13-16 grants and “Center of High Technologies” Uzbekistan.

Jusko-Zakharova, O.N., Ivanov, V.V., Sobolev, L.N. (1986): Minerals of precious metals. Nedra, Moscow, 272 p.

Turesebekov, A.H., Koneyev, R.I., Ignatikov, Y.N. (2005): PGE in the processing products and ores of deposits of goldbearing Uzbekistan. 10th Int. Platinum Symposium, Oulu, August 8-11, 2005, 596-598.

PGE-MINERALOGY OF THE MAIN REEF AND SULFIDE-POOR TROCTOLITE FROM THE YOKO-DOVYREN MASSIF (NORTHERN BAIKAL REGION)

Kislov E.*[1-2], Ariskin A.[3-4], Danyushevsky L.[5], Goemann K.[6], Nikolaev G.[4] & Malyshev A.[1-2]
[1] Geological Institute, Siberian Branch of the Russian Academy of Sciences, Ulan-Ude, Russia
[2] Faculty of Chemistry, Buryat State University, Ulan-Ude, Russia
[3] Faculty of Geology, Moscow State University, Russia
[4] Vernadsky Institute of Geochemistry and Analytical Chemistry, Russian Academy of Sciences, Moscow, Russia
[5] Centre for Ore Deposit Research and Earth Sciences, University of Tasmania, Hobart, Australia
[6] Central Science Laboratory, University of Tasmania, Hobart, Australia
Corresponding email: evg-kislov@yandex.ru

Keywords: low sulphide PGE mineralization, layered massif

Several types of low-sulfide mineralization in the Yoko-Dovyren massif (YDM) demonstrate a wide diversity of the sulfide compositions, ranging from pyrrhotite- and pentlandite-rich varieties to those containing as much as 70-80% of chalcopyrite and cubanite. The Cu-rich sulfides associate with Pd-rich pentlandite and a number of platinum-group minerals (PGM), mostly Pt-Pd tellurides and bismuthotellurides. There are two major horizons containing the PGE mineralization.

The first one (known as the Main Reef) is located within the transitional zone from the rhythmic layered troctolite to overlying Ol-gabbro and leucogabbro (Distler & Stepin, 1992). This highly heterogeneous zone has a variable thickness (150-200 m) and has been traced along the strike of the Dovyren intrusion for over 20 km (Kislov, 1998). It is composed of concordant veins and lenses of coarse-grained and taxitic troctolites and gabbroic rocks, including sulfide-poor anorthosites. The latter are observed as large schlieren and lens-like bodies commonly surrounded by gabbro-pegmatites. Anorthositic bodies are usually a few cm to 1 m thick and extend for 2 to 5 m along strike of the massif, forming a discontinuous sulfide-poor mineralized zone. PGM-bearing sulfides occur in these anorthosites and hosting leucogabbro as thin layers of intercumulus sulfides, commonly of 0.5 cm wide. Despite, generally, the sulfide-poor character of the Main Reef, the amount of PGE-sulfides in anorthosites may locally reach up to 3-5 vol%.

The second site of the Cu-rich PGE-mineralization was discovered below the Main Reef, in mesocratic troctolites ~200-300 m above the dunite/troctolite boundary (Ariskin et al., 2015). Those poorly-mineralized (mostly unaltered) olivine-plagioclase adcumulates sporadically contain small round silicate-sulfide clusters, several cm to 10-15 cm in diameter. In thin sections these heterogeneous schlieren display typical intercumulus sulfides filling the pore space between olivine and plagioclase crystals, or covering the olivine grains.

In this paper we present results of detailed SEM studies of the PGE mineralogy for several rock mounts that represent both PGM-bearing anorthosites from the Main Reef and PGE-mineralized troctolites. These studies were carried out at the Central Science Laboratory of the University of Tasmania (Hobart, Australia), using a Hitachi SU-70 field emission scanning electron microscope (FE-SEM) equipped with a Oxford XMax80 SDD/Aztec 2.1 energy dispersive x-ray spectrometry (EDS) system. Totally, more than 80 PGM grains were identified in the samples, ranging in size from 1 to 40 microns. A distinctive feature of the PGM assemblages is their original character, which is recorded in primary phase boundaries with hosting orthomagmatic sulfides.

Acknowledgements: This research was supported by the Russian Science Foundation (RSF) grant No. *16-17-10129.*

Ariskin, A.A., Nikolaev, G.S., Danyushevsky, L.V., Kislov, E.V., Malyshev, A., Barmina, G.S. (2015): New type of low-sulfide PGE mineralization in primitive troctolites from the Yoko-Dovyren layered massif. *in* "Proceedings of XII All-Russian Petrographic Conference", vol. 1, A.I. Golubev, V.V. Shiptsov, eds., Petrozavodsk, 289-291 (in Russian).

Distler, V.V. & Stepin, A.G. (1993): Low-sulfide PGE-bearing unit of the Yoko–Dovyren layered ultrabasic-basic intrusion (Northern Baikal region). *Dokl. Akad. Nauk*, **328**, 498-501.

Kislov, E.V. (1998): The Yoko-Dovyren layered massif. BNTs RAN, Ulan-Ude, 265 p. (in Russian).

USING ACCESSORY MINERALS TO SHED LIGHT ON THE EVOLUTION OF ROCKS

Klötzli U.S.*[1]
[1] Department für Lithosphärenforschung, Universität Wien, Austria
Corresponding email: urs.kloetzli@univie.ac.at

Keywords: accessory minerals, petrology, geochronology

Our present knowledge on the mineralogical, geochemical, temporal, pressure-temperature, and deformational evolution of rocks is primarily based on the analysis of minerals. Traditionally, an important part of the this knowledge is gained by the analysis of major and minor minerals, for instance the P-T evolution and deformation history of rocks gained from classical petrological and structural data. On the other hand, a substantial amount of the geochronological data stems from accessory minerals such as zircon, monazite, molybdenite, sphene, rutile, xenotime, galena, apatite, columbite, ...

But despite of the abundance of such geochronological data derived from accessory minerals our understanding of the petrological behaviour of the latter is still very limited, in contrast to what we know from major and minor mineral phases. Thus the relation between absolute age and the host rocks evolution sensu lato remains to be enigmatic. This is a lamentable drawback for the advancement of our understanding of the "system rock".

Only relatively recently have Earth scientists started to investigate the petrological behaviour of accessory minerals more profoundly. Using the accessory mineral composition, petrography, textures and structures the insight into the relation of major/minor and accessory minerals is now rapidly increasing. This development goes hand in hand with the analytical capabilities to accurately and precisely analyse the minerals elemental and isotopic composition in even smaller areas. Petrologic forward modelling is also a tool to gain more profound insights into the stability fields and mineral assemblages and parageneses of accessories.

The presentation will discus the most important new aspects of accessory mineral petrology, their relation to the more abundant mineral phases, and analytical techniques. A number of case studies will be presented to highlight new aspects in our understanding of accessory minerals and their importance for a better comprehension of the evolution of rocks.

MOBILITY OF PLATINUM AND PALLADIUM UNDER SUPERGENE WEATHERING CONDITIONS IN THE PRESENCE OF ORGANIC MATERIAL: FIRST EXPERIMENTAL RESULTS

Kotzé E.*[1], Schuth S.[1], Oppermann L.[1-2], Holtz F.[1], Junge M.[2] & Botcharnikov R.[1]
[1] Institüt für Mineralogie, Leibniz Universität, Hannover, Germany
[2] Bundesanstalt für Geowissenschaften und Rohstoffe, Hannover, Germany
Corresponding email: e.kotze@mineralogie.uni-hannover.de

Keywords: PGE mobility, supergene deposits, organic material

Near-surface platinum group element (PGE) ores have much industry potential; however, knowledge about PGE mobility and interaction with organic matter, which is necessary for beneficiation, is insufficient. The goal of this study is to quantify the solubility of synthetic and natural Pt- and Pd- tellurides and sulphides in aqueous solutions containing organic acids (laboratory synthesized humic acids) under surface weathering conditions (oxidising, 25°C). The PGE-enriched chromite concentrate from the Thaba Mine in the western Bushveld Complex is used as a natural material.

Time-series leaching experiments with Pd and Pt telluride and sulphide powders have been conducted in Teflon containers kept in a shaker at ambient T and P. The powders were subjected to three leaching steps: with distilled water, with 0.1M humic acid sodium salt (HASS) solution and with 0.1M humic acid powder (HAP) solution. To better mimic the weathering conditions, a long-term experiment was set up in stationary (only moved when sampling) beakers with strongly diluted solutions of HAP (0.1, 1, and 10 ppm, which correspond to the natural concentration of humic acids sampled from soil horizons at Thaba Mine). Sample aliquots have been taken after 1 week, 4 weeks and 8 weeks, and will continue until August 2016. After experiments, the solution aliquots have been analysed by SF-ICP-MS (Element XR, Thermo Scientific).

For the $PdTe_2$ powder, Pd concentrations in the solutions are between 2 and 10 ppb and no difference is observed between the three different solutions. Samples with PdTe also have solutions with Pd values between 2 and 10 ppb for the distilled water and HASS solutions, but in the HAP solution, the Pd rises to between 20 and 70 ppb. In contrast the water solution with Pd-sulphide shows very high values of Pd (compared to the rest of the experiment) in the range 1500 to 3000 ppb. The same concentrations of Pt are observed in water solution containing Pt-sulphides. For both Pd and Pt, a downward trend is observed from water to HASS to HAP solutions. Pd values fall between 300 and 600 ppb in HASS, and 60 to 150 ppb in HAP. Platinum falls between 100 and 310 ppb in HASS, and 40 to 150 ppb in HAP.

The chromite concentrate from Thaba Mine shows very low values of Pd and Pt in solution. Palladium has consistently higher values than Pt, reflecting a higher mobility under experimental conditions. Both elements show values below 0.5 ppb in the water solution. In the HASS and HAP solutions, the values of Pd and Pt fall between 0.1 and 22 ppb.

These results suggest (1) that Pd is generally more mobile than Pt under supergene weathering conditions, and (2) that the nature and composition of primary minerals which are exposed to weathering is crucial to understand the mobility of PGEs at supergene conditions. These data are consistent with natural observations indicating that Pd is easily mobilized and strongly depleted in oxidised ores.

GEOCHEMICAL AND TEMPORAL EVOLUTION OF ACCESSORY URANINITE FROM THE PUR-BANERA BASIN, NORTHWESTERN INDIA: EVIDENCE OF HREE+Y-METASOMATISM

Mishra B.*[1], Ozha M.K.[1] & Pal D.C.[2]
[1] Department of Geology and Geophysics, Indian Institute of Technology, Kharagpur, India
[2] Department of Geological Sciences, Jadavpur University, Kolkata, India
Corresponding email: bmgg@iitkgp.ac.in

Keywords: accessory uraninite, EPMA dating, NW India

The mineral uraninite contains highest uranium in its structure (i.e., up to ~88.15 wt.%) amongst all the known U-bearing minerals. Due to auto-oxidation, the mineral rarely preserves its pure form ($U^{4+}O_2$) in nature (Dahlkamp, 1993), resulting non-stoichiometry and defects within the mineral, favouring cationic substitution, which can consequently modify and alter its formula to $(U^{4+}_{1-x-y-z}U^{6+}_{x}REE^{3+}_{y}M^{2+}_{z})O_{2+x-(0.5y)-z}$ (Janeczek & Ewing, 1995). Besides, the mineral can readily exchange elements during subsequent fluid-assisted events, wherein the incorporation of minor (Si, Al, K, Fe, Ca, and Na) and trace (viz., Th, Y, and REEs) elements into its structure is a function of the physico-chemical conditions (temperature, redox condition, and fluid composition) and thereby can act as a tracer of geochemical ambience pertinent to its formation (Pal & Rhede, 2013). Further, dating of uraninite can provide constrains to the timing of its formation and subsequent fluid-mediated alteration, if any (Kempe, 2003; Pal & Rhede, 2013).

The Aravalli-Delhi Fold Belt (ADFB) in Northwestern India comprises the metasedimentary belt of Pur-Banera in its central part, which hosts considerable U-anomalies in the Samarkiya area. Preliminary studies reveal uraninite to be the ubiquitous U-bearing accessory mineral in the area (Shaji et al., 2007). However, the absence of well constrained geochronological data vis-à-vis the age of uraninite and subsequent hydrothermal events hinders any meaningful interpretation of geochemical and temporal evolution of the mineral. This study integrates geochemical characterization and *in situ* U-Th-Pb_{Total} dating of accessory uraninite and aim to decipher the geochemical evolution of uraninite during subsequent hydrothermal events.

Geochemistry and X-ray mapping of uraninite document diverse compositions, in which the pristine and the modified grains respectively preserve the compositions of the earlier and subsequent events. The pristine grains are characterized by insignificant concentration of ΣHREE+Y (≤1 oxide wt. %) elements, while the enrichment (max. ~5.04 oxide wt.%) of the same within the modified grains characterize discrete subsequent event related to HREE+Y-metasomatism. Chemical dating of pristine uraninites reveal an age at ~1.87 Ga, followed by two subsequent events at ~1.20 Ga and ~ 0.96 Ga. On the contrary, following the method of Pal and Rhede (2013), an age at ~1.23 Ga is obtained from the modified uraninite grains, which indicates the maximum age of the pristine uraninite. The oldest age (~1.87 Ga) represents the first stage of uraninite formation in the area, wherein the age is in agreement with previously reported metamorphic ages from the area (Ozha et al., 2016). Further, the second generation of uraninite precipitated during a subsequent hydrothermal event at ~1.23-1.20 Ga, in which the grains underwent modification by HREE+Y metasomatism. The latest event during ~0.96 Ga is inferred as the last hydrothermal event in the area resulting re-precipitation of uraninite, where the age is pervasive throughout the ADFB (Bhowmik et al., 2010; Ozha et al., 2016). Thus, the Samarkiya area witnessed three hydrothermal events related to formation of uraninite. In addition, influx of HREE+Y-bearing aqueous fluid eventually modified the pristine compositions related to the second generation of uraninite.

Bhowmik, S.K., Bernhardt, H.J., Dasgupta, S. (2010): Grenvillian age high-pressure upper amphibolite-granulite metamorphism in the Aravalli-Delhi Mobile Belt, Northwestern India: New evidence from monazite chemical age and its implication. *Precambrian Res*., **178**, 168-184.

Dahlkamp, F.J. (1993): Uranium ore deposits. Springer, Berlin, 460 p.

Janeczek, J. & Ewing, R.C. (1995): Mechanisms of lead release from uraninite in the natural fission reactors in Gabon. *Geochim. Cosmochim. Acta*., **59**, 1917-1931.

Kempe, U. (2003): Precise electron microprobe age determination in altered uraninite: consequences on the intrusion age and the metallogenic significance of the Kirchberg granite (Erzgebirge, Germany). *Contrib Mineral Petrol*., **145**, 107-118.

Ozha, M.K., Mishra, B., Hazarika, P., Jeyagopal, A.V., Yadav, G.S. (2016): EPMA Monazite geochronology of the basement and supracrustal rocks within the Pur-Banera basin, Rajasthan, India: evidence of Columbia breakup. *J. Asian Earth Sci*., **117**, 284-303.

Pal, D.C. & Rhede, D. (2013): Geochemistry and chemical dating of uraninite in the Jaduguda uranium deposit, Singhbhum Shear Zone, India-implications for uranium mineralization and geochemical evolution of uraninite. *Econ Geol*., **108**, 1499-1515.

Shaji, T.S., Desapati, T., Fahmi, S., Yadav, G.S., Pande, A.K. (2007): Occurrence of uraninite and brannerite in the Samarkiya area, Bhilwara district, Rajasthan. *Current Sci*., **92**, 592-594.

EQUILIBRIA OF THE Cu-Sn-S SYSTEM IN ACQUEOUS SOLUTIONS: A NUMERICAL APPROACH

Montegrossi G.*[1], Giaccherini A.[2] & Di Benedetto F.[1-3]
[1] Istituto di Geoscienze e Georisorse, Consiglio Nazionale delle Ricerche, Firenze, Italy
[2] Dipartimento di Chimica, Università di Firenze, Italy
[3] Dipartimento di Scienze della Terra, Università di Firenze, Italy
Corresponding email: montegrossi@igg.cnr.it

Keywords: kuramite, Eh-*p*H diagrams, thermodynamic modeling

A relevant research effort is devoted to the synthesis and characterisation of phases belonging to the ternary system Cu-Sn-S, mainly for their possible applications in semiconductor technology. Among all the phases described in the system, kuramite, Cu_3SnS_4, mohite, Cu_2SnS_3, and $Cu_7Sn_4S_{16}$ have attracted the most relevant interest. In the past, numerous studies were carried out claiming for the description of new phases in the ternary compositional field. In this study we aim to revise the existing literature on this ternary system, with a special focus on the stable phases in a temperature range between 25 and 250°C.

It is noteworthy to mention that the only two ternary phases observed in nature are mohite and kuramite, whose occurrence is described as very rare.

A further step in the comprehension of the stability relationships of the relevant phases of the system, is the numerical model of the stable solid phases in contact with a water solution. This information is crucial to either assess the conditions for the hydrothermal deposition under natural conditions, or to design the laboratory set up for the synthesis of their analogues.

The numerical modelling of the Eh-*p*H diagrams were carried out at 25°C by means of *Phreeqc* program with the *lnll-supcrt* thermodynamic database. Owing to the complexity of this task, the subsystems Cu-O-H, Sn-O-H, Cu-S-O-H and Sn-S-O-H were firstly considered as reference.

Here we report our preliminary results of this numerical modelling, starting from the simplest subsystems.

ACCESSORY RUTILE IN THE CEDROLINA CHROMITITES, BRAZIL: MAGMATIC OR METAMORPHIC IN ORIGIN?

Portella Y. de M.*[1], Zaccarini F.[2], Luvizotto G.L.[1], Garuti G.[2], Angeli N.[1], Bakker R.J.[2] & Thalhammer O.A.R.[2]
[1] Department of Petrology and Metallogeny, São Paulo State University, Rio Claro, Brazil
[2] Department Angewandte Geowissenschaften und Geophysik, Universität Leoben, Austria

Corresponding email: yuri_portella@hotmail.com

Keywords: rutile, chromitite, Brazil

Abundant accessory rutile, representing up to more than 3% of modal composition, from the the Cedrolina chromitite, located in the context of the Pilar de Goiás Greenstone Belt (central Brazil), has been analysed by electron microprobe. The chromitite consists of a tabular, elliptical body (up to 2.4 m thick) that strikes NE-SW, comprising an area of 230 x 100 m, and plunging about 20° to the NW. Mica-talc-chlorite schists that represent the poly-metamorphic product of ultramafic rocks host the chromitite body, which is concordantly emplaced with the main regional foliation. The chromite ore displays a peculiar nodular texture, characterized by rounded and ellipsoidal aggregates (up to 1.5 cm in diameter) often strongly deformed and fractured, immersed in a matrix of altered silicates (mainly Cr-rich chlorite and talc) and minute chromite fragments. Chromite is characterized by high Cr# (0.80-0.86), high Fe^{2+}# (0.70-0.94), and low TiO_2 (av. = 0.18 wt.%) consistent with variation trends of spinels from metamorphic rocks. Rutile occurs as small needles/prisms (less than 5 µm) included in chromite or it forms bigger prismatic to irregular grains, ranging from a few dozens microns up to >100 µm, that can be found dispersed in the matrix (concordantly oriented with the main metamorphic foliation) and, more frequently, located in the chromite-matrix contact. The largest crystals are anhedral and occur in the chromite-matrix interface, or filling fractures inside the chromium spinel. These unusually large crystals occasionally contain micro inclusions of chromite fragments. Using micro analyses data, it was possible to verify that rutile near or included in chromite, as well as dispersed in the matrix, all have similar composition. Compositional evidence shows high Cr_2O_3 content (av. 2.77 wt.%, up to 5.7 wt.%) suggesting that rutile was most likely formed by remobilization of Ti from chromite during later metamorphism. Additionally, Zr-in-rutile trace element data was also applied to geothermic calculations, giving an average crystallization temperature range of 530-590°C (at 0.4 GPa) which is in agreement with the regional greenshist to low amphibolite facies peak metamorphism temperature described in literature for the Central Brazil Greenstone Belts. The summarization of this data leads to the confirmation that rutile did not crystallize at high temperatures synchronously with the host chromitite, but plausibly formed due to Ti remobilization from chromite during the low amphibolite facies main regional metamorphic event, concomitantly or right after deformation, eventually incorporating chromite fragments and filling fractures as a metamorphic overgrowth product.

RESTITIC OR NOT? INSIGHTS FROM TRACE ELEMENT CONTENT OF SPINELS IN MANTLE XENOLITHS

Princivalle F.*[1], Musco M.E.[1-2], Petrelli M.[3], Caldeira R.[4], de Ignacio C.[5], De Min A.[1], Marzoli A.[6], Mata J.[7], Perugini D.[3], Boumehdi M.A.[8], Youbi N.[8] & Lenaz D.[1]

[1] Dipartimento di Matematica e Geoscienze, Università di Trieste, Italy

[2] Istituto Nazionale di Oceanografia e di Geofisica Sperimentale, Trieste, Italy

[3] Dipartimento di Fisica e Geologia, Universià di Perugia, Italy

[4] Geology, Hydrogeology and Coastal Geology Unit, National Laboratory for Energy and Geology, Amadora, Portugal

[5] Departamento de Petrología y Geoquímica, Universidad Complutense, Madrid, Spain

[6] Dipartimento di Geoscienze, Università di Padova & Istituto di Geoscienze e Georisorse, Consiglio Nazionale delle Ricerche, Padova, Italy

[7] Institute Dom Luis, Faculty of Sciences, University of Lisbon, Portugal

[8] Department of Geology, Cadi Ayyad University, Marrakech, Morocco

Corresponding email: princiva@units.it

Keywords: spinel, trace elements, mantle xenoliths

We studied the trace elements composition, determined by LA-ICP-MS, of mantle xenolith spinels from Libya (LB), Morocco (MOR) and Cameroon (CAM). Lenaz et al. (2000) and Kamenetsky et al. (2001) found out that it is possible to distinguish spinels restitic after magma extraction (so-called peridotitic) and spinels crystallized from melts (so-called magmatic) according to their Fe^{2+}/Fe^{3+} ratio and their TiO_2 content. By using these discriminators, spinels from LB have been classified as peridotitic while those from MOR and CAM are considered as magmatic. Moreover, previous studies showed that, according to their structural parameters and cooling history, it is possible to split the peridotitic Libyan spinels in two groups: those with a intracrystalline closure temperature in the range 480-640°C (LB I) and those in the range 680-940°C (LB II).

Among the minor elements, Ni is the most abundant. Its content, expressed in ppm, is in the range 1148-3862 in LB samples, 2950-3920 in CAM, and 2238-3922 in MOR. It is followed by Mn (760-1458 LB; 761-970 CAM; 824-1217 MOR), Zn (742-1580 LB; 414-771 CAM; 463-966 MOR), V (404-1116 LB; 377-519 CAM; 407-907 MOR) and Co (271-372 LB; 202-267 CAM; 229-281 MOR). Gallium (38-89 LB; 65-150 CAM; 65-95 MOR), Cu (1.88-8.13 LB; 1.48-4.91 CAM; 0.48-8.08 MOR) and Sc (0.08-2.67 LB; 0.32-1.39 CAM; 0.22-1.66 MOR) are the less abundant.

When comparing the content of Cr_2O_3 with the minor elements it is possible to recognize a positive correlation with Sc, V, and Mn and a negative one with Ni and, less significantly, with Ga. No trends are recognized between total iron and the elements considered.

It is noticeable that for some elements there is no or only small overlapping between the peridotitic (LB) and magmatic spinels (CAM and MOR). These elements are Zn, which is higher than 742 ppm in all the LB spinels whereas few CAM and MOR spinels exceed this value, and Co, which is higher than 270 ppm in LB spinels with only a few spinels from MOR reaching this value. When considering the other elements two different behaviours can be recognised, with LBII spinels differing from all the others. Thus, LBII spinels are richer in Sc, V and Mn and poorer in Ni and Ga than LBI, CAM and MOR.

Further studies on other mantle xenoliths occurrences will clarify if the observed differences in the above discriminating elements can be used to distinguish between restitic spinels and spinels crystallized from melts or correspond to some kind of “regional” mantle heterogeneity.

Acknowledgements: Funding provided by FRA 2015 project of Trieste university to DL.

Kamenetsky, V.S., Crawford, A.J., Meffre, S. (2001): Factors controlling chemistry of magmatic spinel: an empirical study of associated olivine, Cr-spinel and melt inclusions from primitive rocks. *J. Petrol.*, **42**, 655-671.

Lenaz, D., Kamenetsky, V.S., Crawford, A.J., Princivalle, F. (2000): Melt inclusions in detrital spinel from the Alps (Italy-Slovenia): a new approach to provenance studies of sedimentary basins. *Contrib. Mineral. Petrol.*, **139**, 748-758.

MICRO-, AND NANOSCALE FABRICS OF PGM FROM THE VOLCANIC ANKARAMITE AND Pt-RICH CHROMITITE OF THE URAL-ALASKAN-TYPE ULTRAMAFIC COMPLEXES: SEM AND TEM STUDY

Pushkarev E.*[1], Ballhaus C.[2], Kamenetsky V.[3] & Wirth R.[4]
[1] Institute of Geology and Geochemistry, Ural Branch of the Russian Academy of Sciences, Ekaterinburg, Russia
[2] Steinmann Institut, Universität Bonn, Germany
[3] School of Earth Sciences, University of Tasmania, Hobart, Australia
[4] Helmholtz Zentrum Potsdam, GFZ Deutsches GeoForschungsZentrum, Potsdam, Germany
Corresponding email: pushkarev.1958@mail.ru

Keywords: platinum-group minerals, ankaramite, chromitite

Two different types of platinum-group minerals (PGM) have been studied using scanning and transmission electron microscope technics. The first type belongs to magmatic PGM captured by the Cr-spinel phenocrysts in the Uralian volcanic ankaramite. The second one is typical for the Pt-rich chromitite of the Ural-Alaskan-type intrusions.

A volcanic ankaramite (Kamenetsky et al., 2015) from the Southern Urals (Russia) contains high-Mg phenocrysts of Cr-diopside and Cr-spinel. Cr-spinel comprises rare inclusions of olivine (Fo_{90}) and Cr-diopside, abundant melt inclusions and the PGM represented by Fe-Pt alloys, intergrown with the sulphides of Os, Ru, Rh, Cu, Ni and silicates. TEM study of Pt-Fe magmatic inclusions helped determine an exsolution structure, which is represented by regularly oriented nanoscale lamellas. The compositions of different lamellas are similar. It indicates that spinodal exsolution took place close to the top of solvus. Often in between PGM and chromite occur thing films of silicate glass and (or) clinopyroxene, about 100-150 nm of thickness. The composition of glass has Mg# = 0.8 and $CaO/Al_2O_3 > 1$, that is similar to ankaramite. This study provides additional evidences of PGM crystallization from the ankaramite melt.

The most abundant minerals in the second type are Pt-Fe alloys with addition of Os-Ir alloys and other minerals. They occur in interstitial space between chromite grains together with low temperature silicates – serpentine, glagolevite, phlogopite, calcium garnets. All these minerals have common interface which indicate their co-crystallization. The structural features of serpentine allow assume its primary precipitation from the Si-Mg solution (colloid). Using TEM facilities we have found nanoclusters (1-10 nm) of Pt-Fe alloys within serpentine. Similar nanoclusters have been determined in polycrystalline aggregate forming big grains in serpentine. The nanoclusters have different orientation of atomic chains. Perhaps, such structure was formed due to coalescence of numerous nanoclusters of Pt-Fe within a serpentine colloid. The most obtained SEM and TEM data support the idea about post-magmatic, relatively low temperature precipitation of PGM in chromitite of the Ural-Alaskan-type ultramafic complexes.

Acknowledgements: This study is supported by RFBR, grant 16-05-00508-a.

Kamenetsky, V.S., Park, J.-W., Mungall, J.E., Pushkarev, E.V., Ivanov, A.V:, Kamenetsky, M.B., Yaxley, G.M. (2015): Crystallization of platinum-group minerals from silicate melts: Evidence from Cr-spinel–hosted inclusions in volcanic rocks. *Geology*, **43**, 903-906.

SUBMICRON STRUCTURAL DETERMINATION OF "TOO-SMALL-TO-STUDY" PGM WITH PRECESSION ELECTRON DIFFRACTION: THE EXAMPLE OF ZACCARINIITE (RhNiAs)

Roqué-Rosell J.*[1], Aiglsperger T.[1], Portillo J.[2-3], Plana-Ruiz S.[2], Mendoza J.[2], Trifonov T.[4] & Proenza J.A.[1]

[1] Departament de Mineralogia, Petrologia i Geologia Aplicada, Universitat de Barcelona, Spain

[2] Centres Científics i Tecnològics, Universitat de Barcelona, Spain

[3] Nanomegas SPRL, Forest, Belgium

[4] Centre de Recerca en Nanoenginyeria, Universitat Politècnica de Catalunya, Barcelona, Spain

Corresponding email: josep.roque@ub.edu

Keywords: PGM, PED, zaccariniite

Platinum group minerals (PGM) are a group of minerals for which at least one of the six platinum group elements (PGE) (i.e., Os, Ir, Ru, Rh, Pt, Pd) is essential to the mineral. However, they usually occur as micrometric minerals in nature making their exact mineralogical characterization challenging. Of approx. 120 PGM accepted by the IMA in 2002 only 8 have had their crystal structure directly determined (Cabri, 2002). This implies that for the vast majority of PGM, their crystallography and their ideal chemical formulae are still poorly understood. Hence, the aim of this contribution is to show the great potential of electron crystallographic analysis, and in particular, Precession Electron Diffraction (PED) to determine the submicron structure (Viladot et al., 2013) of "too-small-to-study" PGM by using the example of zaccariniite (RhNiAs). For the first time on a natural occurring zaccariniite from Loma Peguera (Rep. Dominicana), a Focused Ion Beam prepared lamella has been examined in a Transmission Electron Microscope (TEM) at 200 kV to produce a series of PED patterns both along high symmetry zone axis, as well as in tomographic series. The analysis of the data helped to determine the cell parameters resulting in a basic tetragonal lattice. On this basic structure a commensurable modulation of order 3 has been observed, as well as diffuse streaking. The possible Space groups compatible with the visible reflections observed have been studied according to their symmetrization residual. A proposal for the atoms positions will be presented, in accordance to the elemental analysis ratio obtained in the TEM with Energy Dispersive X-ray (EDX) analysis.

Cabri, L.J. (2002): The platinum-group minerals. in "The geology, geochemistry, mineralogy and mineral beneficiation of Platinum-Group Elements". L.J. Cabri, ed., Canadian Institute of Mining, Metallurgy and Petroleum, Special Volume, **54**, 13-129.

Viladot, D., Portillo, J., Gemí, M., Nikolopoulos, S. (2013): Hafnium-silicon precipitate structure setermination in a new heat-resistant ferritic alloy by precession electron diffraction techniques. *Microsc. Microanal.*, **20**, 1-8.

PETROLOGICAL SIGNIFICANCE OF MINERAL INCLUSIONS IN ACCESSORY MINERALS OF HP AND UHP ROCKS: THE PROBLEM OF INCLUSIONS AND "PSEUDO-INCLUSIONS"

Schertl H.-P.*[1], Hertwig A.[2], Maresch W.[1] & Li X.-P.[3]

[1] Institut für Geologie, Mineralogie & Geophysik, Ruhr-Universität Bochum, Germany

[2] Wisconsin Secondary Ion Mass Spectrometer Laboratory, Department of Geoscience, University of Wisconsin, Madison, WI, USA

[3] Shandong Provincial Key Laboratory of Depositional Mineralization & Sedimentary Minerals, Shandong University of Science and Technology, Qingdao, China

Corresponding email: hans-peter.schertl@rub.de

Keywords: inclusions, pseudo-inclusions, accessory minerals

Mineral inclusions in rigid accessory minerals are of considerable petrological importance, particularly in HP and UHP metamorphic rocks. Common accessories such as zircon, monazite and rutile are known to be important container minerals that provide valuable information on the prograde history of a rock.

In the last decade, combined mineral inclusion as well as SHRIMP studies on zircon have become increasingly routine. One key objective is to link the ages of distinct inclusion-bearing zircon domains, made visible using cathodoluminescence techniques, to particular mineral assemblages and thus to the PT-conditions derived for these assemblages. However, host minerals and their inclusions must be very carefully examined, and interpretations treated with caution. More and more often so-called "pseudo-inclusions" have been discovered which do not represent primary mineral inclusions, but are a product of later fluid influx into the host minerals along minute cracks. Thus, the observed inclusion assemblage may not reflect the actual PT-conditions at which that particular domain of the host mineral crystallized. In the case of zircon in UHP pyrope-quartzite rocks from the Dora-Maira Massif, for example, magmatic core domains of zircons (270 Ma) contain metamorphic inclusions of coesite or high-Si phengite formed at about 35 Ma (e.g., Gebauer et al., 1997). Similar examples are known from HP albite-jadeite rocks, jadeitites and their blueschist country rocks in the Rio San Juan Complex (RSJC), Dominican Republic. For instance, detailed studies document that a magmatic domain in zircon from a blueschist formed at about 115 Ma contains a lawsonite inclusion which was presumably formed at about 78 Ma. The zircon domain was characterized using REE and trace-element as well as oxygen-isotope analysis, and was shown to be typical for zircon formed in igneous oceanic crust. Zircons separated from an albite-jadeite rock contain inclusions of calcium amphibole (Hertwig et al., 2016), presumably of primary igneous origin. Nevertheless, the same zircons also contain "pseudo-inclusions" of analcime which are of secondary origin. A number of domains in zircons from a jadeitite of the RSJC contain inclusions of omphacite and jadeite (Schertl et al., 2012), which were initially interpreted to have grown simultaneously with the zircon and, hence, to reflect the PT-conditions during crystallization of these zircon domains at 114 Ma. However, subsequent studies have shown that REE patterns and Th/U ratios indicate that this zircon domain age of 114 Ma must represent the age of protolith formation rather than the age of jadeitite crystallization.

Pyrite is also an important "container mineral" for HP metamorphic minerals, whose value has been underestimated. The jadeite-bearing rocks from the RSJC demonstrate that pyrite crystals can contain jadeite inclusions. Pyrites from a two-mica epidote–plagioclase gneiss from Qianliyan Island in China (Li et al., 2014) contain inclusions of garnet and omphacite, pointing to earlier eclogite-facies conditions. This gneiss underwent intensive low-P recrystallization, and as a result neither garnet nor omphacite was able to survive in the matrix.

We conclude that, while mineral inclusions in accessories are of enormous significance, the interrelationship between the enclosed mineral and its host must be studied very carefully in order to avoid misleading interpretations.

Gebauer, D., Schertl, H.-P., Brix, M., Schreyer, W. (1997): 35 Ma old ultrahigh-pressure metamorphism and evidence for very rapid exhumation in the Dora Maira Massif, Western Alps. *Lithos*, **41**, 5-24.

Hertwig, A., McClelland, W.C., Kitajima, K., Schertl, H.-P., Maresch, W.V., Stanek, K., Valley, J.W., Sergeev, S.A. (2016): Inherited igneous zircons in jadeitite predate high-pressure metamorphism and jadeitite formation in the Jagua Clara serpentinite mélange of the Rio San Juan Complex (Dominican Republic). *Contrib. Mineral. Petrol.*, DOI 10.1007/s00410-016-1256-6.

Li, X.-P., Xu, H., Schertl, H.-P., Kong, F.-M. (2014): Eclogite from the Qianliyan Island in the Yellow Sea: a missing link between the mainland of China and the Korean peninsula. *Eur. J. Mineral.*, **26**, 727-741.

Schertl, H.-P., Maresch, W.V., Stanek, K.P., Hertwig, A., Krebs, M., Baese, R., Sergeev, S.S. (2012): New occurrences of jadeitite, jadeite quartzite and jadeite-lawsonite quartzite in the Dominican Republic, Hispaniola: Petrological and geochronological overview. *Eur. J. Mineral.*, **24**, 199-216.

Pt-Pd MINERALIZATION AND BEHAVIOR OF PGE, Cu, Ni, Au IN DIFFERENT ORE TYPES OF THE MONCHEGORSK PLUTON

Shapovalova M.*[1-2] & Tolstykh N.[2]
[1] Department of Geology and Geophyisics, Novosibirsk State University, Russia
[2] V.S. Sobolev Institute of Geology and Mineralogy, Siberian Branch of the Russian Academy of Sciences, Novosibirsk, Russia
Corresponding email: shipchiki@mail.ru

Keywords: Monchegorsk, PGE, Cu-Ni mineralisation

The Monchegorsk Pluton (Monchepluton) is located in Kola PGE-bearing province of north-eastern part of the Baltic Shield. The Pluton includes the intrusion consisting of two parts: meridional and latitudinal directions. The age of Monchegorsk is 2507±9 Ma (Mitrofanov & Smol'kin, 2004).

The samples with sulfides and platinum group minerals (PGM) from various types of ores (low-sulfide, disseminated and massive) were selected to analyze. The ores are located in pyroxenites, norites and anorthosites. The compositions of base metals sulfide and PGM have been investigated. The relations of Ni/(Ni+Fe) in pentlandite increase from 0.51 to 0.56 so S volatility rises (Kolonin et al., 2000) during fractionation of rocks from pyroxenites to anorthosites. The composition of pyrrhotite changes from a troilite in finely disseminated ores ($Fe_{0.97}S$) to monoclinic pyrrhotite in the densely-disseminated ores ($Fe_{0.85}S$) in this direction.

The following PGM have been found in associations: sperrylite ($PtAs_2$), insizwaite ($PtBi_2$), moncheite ($PtTe_2$), michenerite (PdBiTe), froodite ($PdBi_2$), merenskyite ($PdTe_2$) and maslovite (PtBiTe). The most of them were described previously in this Pluton (Grokhovskaya et al., 2009) excepting maslovite that we have found for the first time. Compositions of the michenerite from the different type of ores are in the field of stability of synthetic compositions on the Pd-Te-Bi diagram. According to Hoffman & MacLean (1976) michenerite enriched in Te is stable up to 501°C and michenerite enriched in Bi is stable up to 489°C. Thus, the michenerite of Monchepluton formed in this interval of temperatures.

Significantly higher concentrations of refractory elements (Os, Ir, Ru) and Rh are observed in disseminated ores in comparison with massive and low-sulfide horizon (20-50 ppm against 3-4 ppm in the sum). Accumulation of refractory PGE occurs at an early stage of ore-forming process. The fusible elements (PPGE) were accumulated at a later stage of the sulfide melt evolution. The PGM paragenesis becomes enriched in Pd relatively to Pt as melanocratic properties of rock species decrease. The contents of Ni, Cu and Au change similar to those of PPGE. The total of absolute concentration of PGE in the low-sulfide horizons and in disseminated ores are much less (587-1643 and 272-1288 ppm, respectively) than in massive ores (9946 ppm). However, PGE concentrations recalculated to 100% sulfide have an inverse relation. The same features are observed in Norilsk ores (Dodin et al., 2009).

Thus there is a tendency of the accumulation of PPGE concentrations from melanocratic rocks (pyroxenite) to a more fractionated rocks (norite and anorthosite), as well as from the dissemenated mineralization to massive ores. Therefore, the volatility of sulfur increases during of evolution of ore-forming system.

Acknowledgements: The work was supported by RFBR (projects no16-05-00581, 16-05-00884), RSF (project no 14-17-00250) and ESB (project no 2-1).

Dodin, D.A., Sluzhenikin, S.F., Mantises, M.A. (2009): Ores and minerals of Norilsk region. "POLE STAR" studio, 230 p.

Grokhovskaya, T.L., Lapina, M.I., Mokhov, A.V. (2009): Association and genesis of minerals of platinum group in sulphidic-poor ores of the deposit Moncha Tundra (The Kola Peninsula, Russia). *Geol.Ore Dep.*, **51**, 520-539.

Hoffman, E. & MacLean, W.H. (1976): Phase relations of michenerite and merenskyite in the Pd-Bi-Te system. *Econ. Geol.*, **71**, 1461-1468.

Kolonin, G.R., Orsoyev, D.A., Sinyakova, E.F., Kislov, E.V. (2000): Use of the relation of Ni:Fe in pentlandite for assessment of sulfur's volatility during forming of sulphidic mineralization with PGE of the Yoko-Dovyren massif.*Rep. Acad. Sci.*, **370**, 87-91.

Mitrofanov, F.P. & Smol'kin, V.F. (2004): Layered intrusions of Monchegorsk ore region: petrology, mineralization, isotopes, and deep structure. KSC-RAS, Apatity, 177 p.

ISOMORPHISM AND PHASE HETEROGENEITY IN MINERALS OF NOBLE METALS IN PGE-Cu-Ni AND PGE ORES OF THE NORILSK REGION

Sluzhenikin S.F.*[1]

[1] Institute of Geology of Ore Deposits, Petrography, Mineralogy and Geochemistry, Russian Academy of Sciences, Moscow, Russia

Corresponding email: sluzh@igem.ru

Keywords: platinum group minerals, Norilsk, noble metals

Most minerals of platinum metals show a wide range of isomorphic substitution between Pt and Pd as well as among Bi, Te, Sn, Sb, As and Pb.

The widest range of isomorphism is found for minerals of the isometric $PtBi_2$-$PtTe_2$-$PtSb_2$-$PdTe_2$-$PdBi_2$ and Pt_3Sn-Pd_3Sn-Pd_3Pb-Pd_3Sb-Pd_3As systems where the continuous isomorphism between Pt and Pd, the wide replacement between Bi and Sb, Bi and Te and the limited substitution between Sb and Te are known for the first while the second system shows the continuous isomorphism between Pb and Sn, Sn and As, Sn and Sb, and limited one – between Pb and Sb, Pb and As.

Hexagonal, trigonal and orthorhombic minerals such as moncheite - merenskyite $PtTe_2$-$PdTe_2$, sobolevskite - kotulskite PdBi-PdTe, polyarite PdPb-PdBi form the continuous Bi-Te and Pb-Bi isomorphic series and the limited Pt-Pd series. There is also minerals with the composition Pd(Bi,Te,Pb) with the wide isomorphism among Bi,Te and Pb.

Minerals of the $(Pd,Cu,Pt)_3(Sn,Sb,Pb)$ system such as stannopalladinite, cabriite, taimyrite and tatyanaite show the wide isomorphism between Pd and Pt. Platinum content varies from 0 to 40 at.%, Cu content from 14 to 36 at.% of the Pd+Pt+Cu atomic sum. Lead content reaches 45 at.% of the Sn+Sb+Pb sum at the limited isomorphism among the elements.

The wide Pt-Pd and limited (Pt,Pd)-Ni isomorphism is found in Pt-Pd-Ni sulfides. The composition of cooperite varies $(Pt_{0.95}Pd_{0.02}Ni_{0.02})_{1.00}S_{1.00}$ - $(Pt_{0.84}Pd_{0.09}Ni_{0.07})_{1.00}S_{1.00}$, the composition of braggite from $(Pt_{0.80}Pd_{0.15}Ni_{0.05})_{1.00}S_{1.00}$ to $(Pd_{0.77}Pt_{0.13}Ni_{0.10})_{1.00}S_{1.00}$, and that of vysotskite from $(Pd_{0.88}Ni_{0.12})_{1.00}S_{1.00}$ to $(Pd_{0.76}Ni_{0.24})_{1.00}S_{1.00}$. The Ni-free varieties of braggite and vysotskite were found.

The significant isomorphism among Pt, Cu, Pb, Ni and Fe with base metals prevailing over Pt exists in kharaelakhite.

The regular changes of mineral compositions were observed. The central part of minerals of the $PtBi_2$-$PtTe_2$-$PtSb_2$-$PdTe_2$-$PdBi_2$ system may be composed of Pt-michenerite with the periphery built of Bi-geversite. In the Pt_3Sn-Pd_3Sn-Pd_3Pb-Pd_3Sb-Pd_3As system, rustenburgite and Pt-rich atokite are replaced by Pt-poor atokite while Sn-rich minerals (atokite) are replaced by Pb-rich and Sb- и As-bearing endmembers which are also enriched with Au. The cores of Pt-Pd-Ni sulfides are commonly rich in Pt whereas the rims are enriched in Pd. The central parts of minerals of the Pd-Cu-Pt-Sn (±Sb,Pb) system are also richer in Pt whereas the marginal parts of the grains are commonly richer in Pb up to 45 at.% of the Sn+Sb+Pb at. sum. The change of the composition is commonly irregular in block-textured intergrowths.

The wide isomorphism of elements in minerals results in the co-existence of minerals with the same compositions but of the different structures.

NOBLE METALS IN SULFIDES AND ARSENIDES FROM ULTRAMAFIC ROCKS WITHIN THE ANDEAN SUBDUCTION FACTORY

Tassara C.S.*[1], Garrido L.[1], Romero R.[1], González-Jiménez J.M.[1], Reich M.[1], Barra F.[1], Morata D.[1], Schilling M.[2] & Plissart G.[2]

[1] Departamento de Geología & Centro de Excelencia en Geotermia de Los Andes, Universidad de Chile, Santiago, Chile

[2] Instituto de Ciencias de la Tierra, Universidad Austral de Chile, Valdivia, Chile

Corresponding email: tassara.carlos.sant@ug.uchile.cl

Keywords: platinum group minerals, xenolith, serpentinite

Xenoliths and exhumed peridotite bodies crop out in the rear and front of the South American Andes cordillera, mainly in Argentina and Chile. These correspond to portions of the subcontinental lithospheric mantle (SCLM) originally present beneath the Andes.

The suite of xenoliths displays variable degree of depletion and/or refertilisation as well as distinct types of modal, stealth and cryptic metasomatism that have affected the distribution of noble metals. Recent published whole-rock data (Mundl et al., 2015) indicates that this portion of the SCLM has variable amounts of PGEs (Os: 0.09-4.81 ppb, Ir: 0.22-5.39 ppb, Ru: 1.99-7.21 ppb, Pt: 0.05-6.2 ppb, Pd: 0.002-2.71 ppb). In these mantle xenoliths the distribution of noble metals is mainly controlled by micrometric base metal sulfides (chalcopyrite, pentlandite and pyrrhotite) and submicrometric platinum-group minerals (Os-Pt alloys and laurite, RuS_2). *In situ* LA-ICP-MS analyses on 9 of these sulfide grains show considerable variation in PGE+Au concentration, consistent with values reported for mantle sulfides elsewhere. The IPGE (Os, Ir, Ru) show the highest and most variable values (Os: 1.83-282 ppm, Ir: 0.13-135.55 ppm, Ru: 0.48-72 ppm), the PPGE (Pt, Pd, Rh) are less concentrated yet also extremely variable (Pt: 0.06-259 ppm, Pd: 0.06-43.41, Rh: 0.22-2113 ppm) while Au contents are between 0.02 and 5.96 ppm.

In addition to mantle xenoliths, slivers of ultramafic rocks, often affected by serpentinization and systematically associated with late Paleozoic metapelitic rocks, have also been described in the fore-arc in Chile. Serpentinite shear zones crosscutting relatively fresh peridotites exhibit higher contents of PGE (Os: 9 ppb, Ir: 9 ppb, Ru: 17 ppb; Pt: 34 ppb, Pd: 49 ppb, Rh: 3 ppb) than the fresh peridotite rocks (Os: 1-4 ppb, Ir: 1-4 ppb, Ru: 6-9 ppb; Pt: 3-7 ppb, Pd: 3-6 ppb, Rh: 1-2 ppb). Interestingly, these shear zones filled by antigorite contain late veins of metamorphic pyroxene intergrowths with Ni-arsenides. An examination of these serpentinite rocks using SEM and EMPA reveals the presence of orcelite ($Ni_{5-x}As_2$) and breithauptite (NiSb) associated or including minute platinum-group minerals such as irarsite (IrAsS), osarsite (OsAsS), laurite (RuS_2), Pt-Sb and Pt-Fe alloys (González-Jiménez et al., 2016).

The data presented here highlights that metasomatic events either in the upper mantle or during exhumation (hydration) of peridotites by metamorphism may produce significant noble metal mobilization in the Andean subduction factory.

González-Jiménez, J.M., Barra, F., Garrido, L.N.F., Reich, M., Satsukawa, T., Romero, R., Salazar, E., Colás, V., Orellana, F., Rabbia, O. (2016): A secondary precious and base metal mineralization in chromitites linked to the development of a Paleozoic Accretionary complex in Central Chile. *Ore Geol. Rev.*, **78**, 14-40.

Mundl, A., Ntaflos, T., Ackerman, L., Bizmis, M., Bjerg, E.A., Wegner, W., Hauzenberger, C.A. (2015): Geochemical and Os-Hf-Nd-Sr isotopic characterization of North Patagonian mantle xenoliths: Implications for extensive melt extraction and percolation processes. *J. Petrol.*, DOI: 10.1093/petrology/egv048.

MELLINIITE, SECOND DISCOVERY OF THIS RARE PHOSPHIDE FROM AN ARGENTINIAN Fe-Ni-METEORITE

Thalhammer O.A.R.*[1], Zaccarini F.[1], Strauss V.[1] & Gallas P.[2]
[1] Department Angewandte Geowissenschaften und Geophysik, Universität Leoben, Austria
[2] Werbung und Promotion GmbH, Tattendorf, Austria
Corresponding email: oskar.thalhammer@unileoben.ac.at

Keywords: melliniite, second discovery, meteorite

Melliniite (first discovery by Pratesi et al., 2006) was found within an Argentinian (Campo de Sielo) Fe-Ni meteorite. The sample was kindly provided from the exhibition centre Amethyst Welt Maissau (Lower Austria). Melliniite forms tiny little inclusions (i.e. 15 to 50 µm in diameter) within Fe-Ni metal alloy (i.e. kamacite) and is mostly surrounded by a Cl-Fe envelope. The largest grain discovered is elongated with a size of around 94 x 11 µm. The chemical composition, analysed *via* wave-length dispersive system of a Jeol JXA 8200 superprobe, equals nicely to a metal/phosphorus ratio of 4:1. The P-contents are very constant ranging from 12.56 and 12.90 wt.%. However, two compositional types of melliniite can be distinguished on the basis of the Fe:Ni ratio. One type is characterised by a Fe:Ni ratio of around 1:0.8, and a second type displays a Fe:Ni ratio of around 1:1.3.

Since the discovery of melliniite (Pratesi et al., 2006), characterised by the highest coordination number for P atoms and highest density values for a Fe-Ni-P compound, there are speculations on the significant importance of this rare mineral for the Earth´s core mineralogy regarding stability, sequestering and derivation of phosphorus. Wu et al. (2011) have shown that melliniite is a stable phase at up to 400 GPa. In this context, it seems interesting that in the present occurrence melliniite is associated with Cl.

Acknowledgements: This contribution is dedicated to Giorgio Garuti and his scientific input into the scientific community!

Pratesi, G., Bindi, L., Moggi-Cecchi, V. (2006): Icosahedral coordination of phosphorus in the crystal structure of melliniite, a new phosphide mineral from the Northwest Africa 1054 acapulcoite. *Am. Mineral*., **91**, 451-454.

Wu, X., Mookherjee, M., Gu, T., Qin, S. (2011): Elasticity and anisotropy of iron-nickel phosphides at high pressures. *Geophys. Res. Letters*, **38**, L20301.

THE PGE: ARE THEY PARTY ANIMALS OR LONE DOGS? A LOOK AT WHAT THEIR MINERALOGY HAS TO SAY

Tredoux M.*[1]
[1] Department of Geology, University of the Free State, Bloemfontein, South Africa
Corresponding email: mtredoux@ufs.ac.za

Keywords: platinum-group elements, nanoparticles, platinum-group minerals

The platinum-group elements (PGE: Pt, Pd, Rh, Ru, Ir, Os) are very rare in crustal rocks: in general their concentrations are at the low $ng.g^{-1}$ levels, and even their ores contain only a few $\mu g.g^{-1}$ (ppm). Traditionally, this meant that only a few types of PGE-containing material (ores and meteorites) could be accurately assessed. The economic geochemists, e.g., Naldrett (1989), Barnes (1993), and Oberthür (2002, and references therein), concluded that the PGE are chalcophile, and occur primarily as constituents of sulphide minerals. The cosmochemists, on the other hand, maintain that the PGE are associated with the Ni-Fe alloys only, i.e., that they are siderophile. This conundrum was addressed for the first time head-on by Tredoux et al. (1995), who suggested that the apparent chalcophile behaviour of the PGE in S-rich systems is in fact underlain by pre-existing nano-nuggets (or clusters) of the PGE with various metallic ligands. The idea was for long treated with scepticism, until analytical techniques developed to a point that made it possible for such nano-features to be demonstrated. In recent years, nano-sized platinum-group minerals (PGMs) have been observed both experimentally (Helmy et al., 2013) and in natural material (Wirth et al., 2013). What has become clear is the importance of ligands, such as As and Sb, to stabilise the PGE through early mineral formation: of the 136 PGMs recognised by the CNMNM of the IMA, only 38 (28%) do not contain any semi-metals. Of these, 7 are inter-PGE alloys, 12 are alloys of PGE with Fe (±Ni), 6 are alloys of PGE with Cu(±Zn), 1 is an alloy between Pd and Si and 1 is an oxide. Only 11 PGMs are actually pure sulphides. Reconsideration of the basics of elemental substitution during crystallisation highlights the difficulties which the PGE would encounter in base metal sulphide crystal lattices and these will be discussed. The author is of the opinion that any association of the PGE with sulphide is a mechanical phenomenon (the "wool-on-velcro™" model) rather than a pure chemical one. In the case of other minerals which seem to concentrate the PGE, such as olivine and chromite, it is pertinent that they are all very early-forming, and may well use PGE nano-clusters as seeds around which to nucleate - once again a mechanical rather than chemical association. The suspected nano-PGMs would be very hard to pinpoint analytically, especially in thin or polished sections; to bring them to light the whole sample should be dissembled with a technique such as hydro-fracturing. Seeing as the PGE, which represent 6.7% of the periodic table, only account for 2.7% of the known minerals, it is possible that there are some interesting discoveries ahead for hard-working PGE mineralogists working along these lines.

Barnes, S.-J. (1993): Partitioning of platinum group elements and gold between silicate and sulphide magmas in the Munni Munni Complex, Western Australia. *Geochim. Cosmochim. Acta*, **57**, 1277-1290.

Helmy, H.M., Ballhaus, C., Fonseca, R.O.C., Wirth, R., Nagel, T., Tredoux, M. (2013): Noble metal nanoclusters and nanoparticles precede mineral formation in magmatic sulphide melts. *Nature Comm*., DOI: 10.1038/ncomms3405.

Kadlag, Y. & Becker, H. (2015): Fractionation of highly siderophile and chalcogen elements in components EH3 chondrites. *Geochim. Cosmochim. Acta*, **161**, 166-187.

Naldrett, A.J. (1989): Stratiform PGE deposits in layered intrusions. *in* "Platinum-group elements: Mineralogy, geology, recovery" L.J. Cabri, ed., Can. Inst. Mining Metall., Spec. Vol. **23**, 197-232.

Oberthür, T. (2002): Platinum-group element mineralization of the Great Dyke, Zimbabwe. in "The geology, geochemistry, mineralogy and mineral beneficiation of platinum-group elements" L.J. Cabri, ed., Can. Inst. Mining Metall., Spec. Vol. **54**, 483-506.

Wirth, R., Reid, D.L., Schreiber, A. (2013): Nanometer-sized platinum-group minerals (PGM) in base metal sulfides: new evidence for an orthomagmatic origin of the Merensky reef PGE ore deposit, Bushveld complex, South Africa. *Can. Mineral.*, **51**, 143-155.

Tredoux, M., Lindsay, N.M., Davies, G., McDonald, I. (1995): The fractionation of the platinum-group elements in magmatic systems, with the suggestion of a novel causal mechanism. *South Afr. J. Geol.*, **98**, 157-167.

Zaccarini, F., Tredoux, M., Miller, D.E., Garuti, G., Aiglsperger, T., Proenza, J.A. (2014): The occurrence of platinum-group and gold minerals in the Bon Accord Ni-oxide body, South Africa. *Am. Mineral.*, **99**, 1774-1782.

THE BON ACCORD NiO BODY, BARBERTON GREENSTONE BELT, SOUTH AFRICA: A SOURCE OF POTENTIAL NEW PHASES IN THE Ni-Sb-As SYSTEM

Tredoux M.*[1], Zaccarini F.[2], Garuti G.[2] & Miller D.E.[1]
[1] Department of Geology, University of the Free State, Bloemfontein, South Africa
[2] Department Angewandte Geowissenschaften und Geophysik, Universität Leoben, Austria
Corresponding email: mtredoux@ufs.ac.za

Keywords: Ni-Sb-As system, Bon Accord, South Africa

Selected samples from the enigmatic oxide-silicate occurrence of Bon Accord, located in the Barberton greenstone belt on the northeastern border of South Africa with Swaziland, have been investigated by reflected-light microscopy and by electron microprobe. The Bon Accord body is well known among the mineralogists because it is the type locality of the following rare, Ni-rich minerals: trevorite, liebenbergite, nichromite, cochromite, willemseite, nimite and bonaccordite. The origin and exact nature of the Bon Accord body is still matter of discussion: It may represent a terrestrial magmatic spinel-olivine precursor which was hydrothermally altered (Tredoux et al., 2014, 2016, and references therein) or a desulfurized NiS deposit (O'Driscoll et al., 2014). The possibility that it may represent a paleometeorite (De Waal, 1978) has been discounted by recent Cr isotopic data (Tredoux et al., 2014). The Bon Accord body contains >40 wt.% NiO whole rock and it shows an enrichment in the platinum-group elements (PGE), gold, arsenic and antimony (Tredoux et al., 1989). The main goal of this study was to characterize the accessory minerals that occur as tiny and randomly distributed grains generally associated with trevorite, liebenbergite and nepouite. Platinum-group minerals (PGM) containing Pd-Sb, Pd-Sb-As, Pd-Cu-Sb, Pt-Sb, Pt-As-S, Ru-As-S, Ru-S along with sperrylite, ruthenium, members of the sobolevskite-kotulskite series and electrum have been identified (Zaccarini et al., 2014). These results are in good agreement with previous analyses of PGE-Au concentrations in the bulk rock. Several minerals that belong to the Ni-Sb-As system have been also analyzed. Some of them, such as breithauptite and orcelite (Bindi et al. 2014) are know minerals. However, most of them cluster around the following stoichiometries: Ni_3Sb–$Ni_3(Sb,As)$–Ni_3As, $Ni_5(Sb,As)_2$, $Ni_7(Sb,As)_3$ and $Ni_{11}(Sb,As)_8$ (Tredoux et al., 2016). These compounds form small grains with a size generally less than 20 µm. Under reflected-light microscope they are all very similar, showing a yellow colour and a relatively high reflectance. Some of these phases have been described in synthetic systems, but up to now not in nature. This observation suggests that most of the analyzed compounds in the Ni-Sb-As system probably represent new minerals and, in particular, the $Ni_{11}(Sb,As)_8$ phase may represent the Sb-equivalent of maucherite. However, their small sizes make it very difficult to obtain X-ray diffraction data to confirm this assumption. Research is currently underway to try to determine the physical properties of the potential new minerals.

Bindi, L., Tredoux, M., Zaccarini, F., Miller, D., Garuti, G. (2014): Non-stoichiometric nickel arsenides in nature: the structure of orcelite, Ni_{5-x} As_2 (x = 0.25), from the Bon Accord oxide body, South Africa. *J. All. Comp*., **601**, 175-178.

De Waal, S.A. (1978): The nickel deposit at Bon Accord, Barberton, South Africa – a proposed paleometeorite. *in "M*ineralisation in metamorphic terranes", W.J. Verwoerd, ed., Geol. Soc. South Afr., Johannesburg, 87-98.

O'Driscoll, B., Clay, P.L., Lenaz, D., Cawthorn, R.G., Adetunji, J., Kronz, A. (2014): Trevorite: Ni-rich spinel formed by metasomatism and desulphurisation processes at Bon Accord, South Africa? *Mineral. Mag*., **78**, 145-163.

Tredoux, M., de Wit, M.J., Hart, R.J., Armstrong, R.A., Lindsay, N.M., Sellschop, J.P.F. (1989): Platinum group elements in a 3.5 Ga nickel-iron occurrence, Possible evidence of a deep mantle origin. *J. Geophys. Res*., **94**, 795-813.

Tredoux, M., Roelofse, F., Shukolyukov, A. (2014): A Cr isotopic study of the Bon Accord NiO body, Barberton greenstone belt, South Africa. *Chem. Geol.*, **390**, 182-190.

Tredoux, M., Zaccarini, F., Garuti, G., Miller, D.E. (2016): An investigation of phases in the Ni-Sb-As system, and associated platinum-group minerals, which occur in the Bon Accord oxide body, Barberton greenstone belt, South Africa. *Mineral. Mag*., **80**, 187-198.

Zaccarini, F., Tredoux, M., Miller, D.E., Garuti, G., Aiglsperger, T., Proenza, J.A. (2014): The occurrence of platinum-group and gold minerals in the Bon Accord Ni-oxide body, South Africa. *Am. Mineral*., **99**, 1774-1782.

SPINEL CHEMISTRY FOR THE CHARACTERISATION OF PERIDOTITES FROM SABAH (BORNEO ISLAND, MALAYSIA)

Tsikouras B.*[1-2], Sharif A.H.[1], Ifandi E.[2], Hamdan H.[1], Tarif R.[1], Sulaiman H.[1] & Teo C.H.[1]
[1] Department of Physical and Geological Sciences, University Brunei Darussalam, Bandar Seri Begawan, Brunei
[2] Department of Geology, University of Patras, Greece
Corresponding email: basilios.tsikouras@ubd.edu.bn

Keywords: spinels, Sabah, Borneo Island

Ultramafic rocks occurring in the area of Sabah (Borneo Island) are dominated by fertile and refertilised lherzolites with minor harzburgites. Variably serpentinised harzburgites occur throughout the ultramafic bodies, too. Replacive bodies of dunite, mostly in the form of dunite channels, provide strong field evidence for melt impregnation. Cumulate and non-cumulate gabbros, a sheeted-dyke complex of dolerites, as well as basalts occur in close association to the peridotites. The fertile lherzolites include two distinct Al-rich spinels: a group-1 with Cr# clustering between 5 and 7 and a group-2 with Cr# varying between 9 and 13. The refertilised lherzolites and harzburgites contain Cr-spinel with Cr# ranging approximately at 30-42. Group-2 Al-spinels show frequent lobate boundaries. This evidence, coupled with the fact that these crystals, as well as Cr-spinels are closely intergrown with chlorite, suggest their formation from variable degrees of modification of former high Al-spinels. Intergrowths of orthopyroxene with Al-spinel are observed in the fertile lherzolites indicating that they have once equilibrated in the garnet stability field. The extremely fertile nature of group-1 Al-spinels suggest that their host peridotites represent subcontinental lithospheric Mantle lherzolites. The group-2 Al spinels and the Cr-spinels are analogous to those occurring in abyssal peridotites. The investigated peridotites have been impregnated by percolating melts at multiple stages of metasomatism, as it is indicated by the presence of unstained olivine, Al- and Na-rich augite and plagioclase. It is proposed that extending continental lithosphere in the NE Borneo ascended similar to orogenic massifs such as Lherz, Lanzo and Ronda peridotites. Rifting and evolution of an oceanic basin is related to the exposure of abyssal peridotites and harzburgites at an environment close to an ocean-continent transition.

PGE OCCURENCES IN THE BOHEMIAN MASSIF: AN OVERVIEW

Vymazalová A.*[1] & Pašava J.[1]
[1] Czech Geological Survey, Prague, Czech Republic
Corresponding email: anna.vymazalova@geology.cz

Keywords: platinum-group elements, platinum-group minerals, Bohemian Massif

There are several occurrences of platinum-group elements (PGE) in various types of mineralization in the Bohemian Massif. The highest values of PGE, in total (ΣPGE) 4.8 ppm (out of which Pt is 4.7 ppm) were identified in ore sample from the Tisová deposit. The Tisová Fe-Cu-As deposit is considered as an example of the Besshi type deposit in Variscan intracontinental setting, located in the Krušné Hory Mountains, the west part of Bohemian Massif. Despite of the high Pt enrichment in studied ore samples the principal PGE carriers were not identified. Anomalous PGE concentrations often accompanied by PGM were found in magmatic types of deposits in the Bohemian Massif: 1) Ransko 2) Kunratice and Rožany 3) Svitavy. The Ransko gabbro-peridotite massif in Eastern Bohemia is a strongly differentiated intrusive complex of Variscan age. The complex hosts low grade Ni-Cu ores mainly developed close to the contact of olivine-rich rocks with gabbros, in troctolites. Anomalous PGE values, in total (ΣPGE) 0.8 ppm were detected in Cu-Ni (532 ppb Pd and 182 ppb Pt) and Ni-Cu (143 ppb Pd) ores from the Jezírka orebody. Among platinum-group minerals (PGM) michenerite, froodite, and sperrylite were described. The Cu-Ni mineralization at Kunratice and Rožany, located in the northern part of the Bohemian Massif, are hosted by gabbroic dykes (dolerites) cross-cutting the granitic Lusatian Granitoid Complex. The highest PGE content, in total (ΣPGE) 0.2 ppm was found in Cu-Ni massive ore sample. The PGM assemblages are characterized by sperrylite, unnamed Pd-Ni-Bi tellurides, melonite, vavřínite, altaite, native gold, and recently observed moncheite and michenerite. PGM are located within base-mertal sulphides and also in matrix silicates. Anomalous concentrations of (PGE), in total (ΣPGE) 0.4 ppm (up to 281 ppb Pd, up to 110 ppb Pt) were detected in low Ni-Cu (Cr) mineralized pyroxenite and serpentinite recovered from the HSV-1 structural borehole at Svitavy. The mafic and ultramafic rocks of the Svitavy anomaly complex, hidden under the platform Upper Cretaceous sediments, are only known from drill holes and can be considered as the continuation of the Letovice ophiolite. PGM like milotaite, chrisstanleyite and Se-bearing merenskyite were also described from the selenide-bearing uranium mineralization from Předbořice, in the central Bohemia. PGE enrichment was also observed in metal-rich black shales of the Barrandian Upper Proterozoic, Kamenec (up to 102 ppb Pd and up to 25 ppb Pt) and Hromnice locality. Recent mineralogical study of heavy fraction from the Holocene pyrope-rich garnet placer deposit Vestřev, located in Krkonoše Piedmont Basin of the Bohemian Massif resulted in identification of several PGM. Pt-Fe alloys and Os-Ir-Ru minerals (native osmium, iridium, ruthenium) were observed.

Session S23:

The future of critical metals: mineralogy, metallogenesis and geometallurgy

Conveners:

John Bowles (Manchester – United Kingdom)

Nigel Cook (Adelaide – Australia)

Hannah Hughes (Johannesburg – South Africa)

Ni LATERITES AS FUTURE UNCONVENTIONAL PGE ORE DEPOSITS

Aiglsperger T.*[1], Proenza J.A.[1] & Longo F.[2]
[1] Departament de Cristal·lografia, Mineralogia i Dipòsits Minerals, Universitat de Barcelona, Spain
[2] Facultad de Ingeniería y Arquitectura, Universidad Catolica Tecnologica del Cibao, La Vega, Dominican Republic
Corresponding email: thomas.aiglsperger@ub.edu

Keywords: Ni laterites, PGE, PGM

Large oxidized deposits associated with near surface modification of ultramafic rocks are considered worthy exploration targets for unconventional PGE (Os, Ir, Ru, Rh, Pt and Pd) ore deposits. In general, total PGE concentrations found in Ni laterites around the world are in the range of less than 100 ppb to up to a few hundred ppb. However, lateritic crust with 2 ppm PGE over the Ora Banda Sill, Western Australia, was reported from Gray et al. (1996) as well as more than 4 ppm PGE from Burundi (Maier et al., 2008). Aim of this contribution is to evaluate the potential of Ni laterites as future nonconventional PGE ore deposits via a detailed geochemical and mineralogical investigation of Ni laterites from the northern Caribbean. Ni laterites from the study area are systematically enriched in the limonite (above Mg-discontinuity) and reach values of up to 0.6 ppm total PGE.

The PGE enrichment is independent of PGE-enriched substratum (e.g. chromitites) and mainly explained by residual accumulation of PGE-bearing mineral phases (e.g. disseminated Cr-spinel). However, results also provide morphological and chemical evidence for *in situ* neoformation of PGM within Ni laterites by bioreduction and/or electrochemical accretion. Indeed, observed accumulations of most likely biogenic mediated *in situ* growth of Pt rich nanoparticles are believed to significantly contribute to Pt anomalies in Ni laterites.

To assess an economic significance of observed PGE enrichment in Ni laterites the final product of an active Ni laterite ore deposit (Falcondo; Dominican Republic) (i.e. ferronickel-cone after pyrometallurgical extraction from hydrous Mg silicates found in saprolite) was sent to Genalysis for PGE determination. The results show PGE concentrations of more than 2 ppm total PGE. We believe that innovative direct extraction technologies such as the carbonyl process recently introduced by Terekhov & Emmanuel (2013), tested by the authors to be capable to produce 1.7 t PGE from a standard 1000000 t limonite Ni ore, as well as ongoing improvements in the metal extraction from oxidized ores by biomining (Johnson & du Plessis, 2015) result in a more diverse supply chain for PGE in the near future.

Gray, J.D., Schorin, K.H, Butt, C.R.M. (1996): Mineral associations of platinum and palladium in lateritic regolith, Ora Banda Sill, Western Australia. *J. Geochem. Explor.*, **57**, 245-255.

Johnson, D.B. & du Plessis, C.A. (2015): Biomining in reverse gear: Using bacteria to extract metals from oxidised ores. *Miner. Eng.*, **75**, 2-5.

Maier, W.D., Barnes, S.-J., Bandyayera, D., Livesey, T., Li, C., Ripley, E. (2008): Early Kibaran rift-related mafic–ultramafic magmatism in western Tanzania and Burundi: Petrogenesis and ore potential of the Kapalagulu and Musongati layered intrusions. *Lithos*, **101**, 24-53.

Terekhov, D.S. & Emmanuel, V.E. (2013): Direct extraction of nickel and iron from laterite ores using carbonyl process. *Miner. Engin.*, **54**, 124-130.

ROLE OF AUTOMATED MINERALOGY IN OPTIMISING MINERAL PROCESSING OF CARBONATITE HOSTED REE AT SONGWE HILL, MALAWI

Al Ali S.*[1], Wall F.[1], Pascoe R.[1], Rollinson G.[1] & Dawes W.[2]
[1] Camborne School of Mines, University of Exeter, United Kingdom
[2] Mkango Resources Ltd, Calgary, Canada
Corresponding email: shaa201@exeter.ac.uk

Keywords: geometallurgy, rare earth minerals, carbonatite

Rare earth element (REE) ore deposits contain a variety of REE and REE-bearing minerals. Hence the beneficiation processes for REE ores can vary widely and it is essential to have a good understanding of the mineralogical characteristics when designing processing routes.

Quantitative automated mineralogy is an important tool in determining the mineralogical characteristics of ore deposits, and in monitoring mineral processing. In this study, eight samples of carbonatite core from eight drill holes, crushed to 1.7 mm, and a composite sample ground to 0.053 and 0.038 mm were selected, to determine the mineral characteristics of the REE carbonatite deposit in Songwe Hill, Malawi.

A species identification protocol (SIP) for RE-minerals was developed for QEMSCAN® with input and validation from analytical electron microscopy (SEM/EDS) and electron probe microanalysis (EPMA).

The QEMSCAN® technique was used to determine modal mineralogy and give quantitative information on mineral associations. Perceptions from geological studies can be misleading for process mineralogy. For example, at Songwe Hill, ankerite veins cut calcite and would be separated in a paragenetic chart. However, many of the ankerite crystals touch host calcite and so the two minerals are in direct association so far as process mineralogy is concerned. Calcite, ankerite, K-feldspar, Fe/Mn oxides, strontianite and baryte are the main gangue minerals. Synchysite-(Ce), apatite and minor florencite-(Ce) are the most common REE /REE-bearing minerals, with some variations in their proportions between samples. Apatite hosts the more valuable mid and heavy REE, and occurs in distinct textural associations compared to synchysite-(Ce). These have been identified and quantified.

A particular challenge is the chemical similarity between the REE, Ca-minerals such as synchysite-(Ce), röntgenite-(Ce) and parisite-(Ce) but when required, it is possible to set up the QEMSCAN® to distinguish these Ca:REE ratios. Bastnäsite-(Ce), with no Ca component, is much easier to distinguish from the other REE fluorcarbonates.

REE fluorcarbonates are also challenging because of their common occurrence either as narrow laths, which is the main textural type at Songwe Hill, or as syntaxial intergrowths with each other. The QEMSCAN® technique can recognise the syntaxial intergrowths on a scale of about > 10 µm but it is more challenging to identify them on a smaller scale.

Spectral overlaps between the REE make subtle changes in proportions of the various REE difficult to detect, and this is a limitation of the technique, as is the high detection limit in the rapidly-acquired spectra used by QEMSCAN®, of about 3 wt.%, for REE in REE-bearing minerals.

With careful set-up, checked by EPMA or SEM/EDS analyses, QEMSCAN® can be applied to complex REE deposits, during the development of the metallurgical flow sheet and to provide a comprehensive method for checking the success of the separation processes.

RARE-ELEMENT MINERALIZATION IN THE Sn-Ta PENOUTA ORE DEPOSIT, NW SPAIN

Alfonso P.*[1], Garcia-Valles M.[2], Hamid S.[1], Tomasa O.[1], Llorens T.[3], Oliva J.[3], Guasch E.[1], Anticoi H.[1] & García-Polonio F.[3]

[1] Departament d'Enginyeria Minera, Industrial i TIC, Universitat Politècnica de Catalunya, Barcelona, Spain

[2] Departament de Cristal·lografia, Mineralogia i Dipòsits Minerals, Universitat de Barcelona, Spain

[3] Strategic Minerals, Salamanca, Spain

Corresponding email: pura@emrn.upc.edu

Keywords: tantalum, rare-metal granite, Nb-Ta oxide minerals

The Penouta Sn-Ta deposit, located in Galicia, northeast of Spain, is a greisenized granitic cupula where Ta occurs as disseminations in a leucogranite stock intruded in Precambrian-Lower Cambian gneisses and mica-schists of the Viana do Bolo series. These rocks are overlain by gneisses of the Ollo de Sapo formation.

The Penouta leucogranite is a medium to fine grained inequigranular rock constituted by quartz, k-feldspar, albite and muscovite. Quartz has "snowball" texture with euhedral poikilitic crystals of about 1 mm in diameter. Accessory minerals are mainly biotite, spessartite, zircon, cassiterite, Nb-Ta oxides, monacite, xenotime, native bismuth and pyrite. The leucogranite has undergone two alteration processes with albitization, muscovitization and kaolinitization. Bulk-rock major and trace element composition was determined. These leucogranites are peraluminous and P-poor, with 0.03-0.07 wt.% P_2O_5. The rare element content is high, with 900-1500 ppm Rb, 30-65 ppm Cs, 120-533 ppm Li, 80-226 ppm Ta, 45-124 ppm Nb and up to 1350 ppm of Sn.

Columbite-group minerals are the most common Ta-bearing phases, but microlite, wodginite or ixiolite and Ta-rich cassiterite also occur. Columbite-group minerals are mainly manganotantalite and manganocolumbite with average size of 80µm. Crystals often are concentrically zoned, with a Nb-rich core surrounded by a Ta-rich rim, with sharply boundary between them. In other cases these minerals exhibit a convoluted zoning or are homogeneous. Many of the columbite-group crystal exhibit dissolution textures that affect to columbite and especially to the tantalite rims. The Mn/(Mn+Fe) ratio is 0.33-0.97 and the Ta/(Ta+Nb) ratio is 0.07-0.93. These values are typical of highly evolved systems. Microprobe analyses reveal variable contents of Sn, and W, being the highest contents in tantalite.

Wodginite, or ixiolite, has between 6 and 27 wt.% of SnO_2 and up to 65 wt.% of Ta_2O_5 The Mn/(Mn+Fe) ratio is 0.60-0.91. Microlite is formed as a late replacement of columbite-group minerals and occurs associated with tantalite and cassiterite, usually in rounded grains of less than 60 µm in diameter. Wodgnite, or ixiolite, is formed replacing tantalite or cassiterite. Usually it is Ca-rich, but uranmicrolite and plumbomicrolite also exist.

Cassiterite occurs as black, subhedral to anhedral, homogeneous crystals usually between 50 and 200 µm in size. At least two generations of cassiterite are recognized, the earlier generation is Nb, Ta-poor but in the late generation Ta content can reach up to more than 9 wt.% of Ta_2O_5 and 1.7 wt.% Nb, being the Ta Ta/(Ta+Nb) ratio from 0.60 to 0.91.

Several stages of crystallization of Nb-Ta minerals can be differentiated; the first stage was columbite-rich and a late stage is responsible of the tantalite rim around columbite and of the replacement of columbite crystals by tantalite. Microlite and wodginite, or ixiolite, formed during the late stage.

A COMPARATIVE STUDY OF Au-Bi-SIDERITE-SULFIDE ARKACHAN AND Ag-Pb-Zn MANGAZEYSKOE DEPOSITS, SAKHA (YAKUTIA), RUSSIA

Anikina E.*[1], Vikent'eva O.[1], Bortnikov N.S.[1], Gamyanin G.N.[1] & Prokof'ev V.Y.[1]
[1] Institute of Geology of Ore Deposits, Petrography, Mineralogy and Geochemistry, Russian Academy of Sciences, Moscow, Russia
Corresponding email: lena-anikina@yandex.ru

Keywords: mineral deposits, fluid inclusions, REE

These deposits are hosted sedimentary rocks of Verkhoyansk fold and thrust belt. They are confined to an intersection of north-north-southern and north-eastern regional strike-slipe faults. A depositional sequence of ores, a composition of vein and ore minerals, fluid inclusions, REE distribution and stable isotopes (C, O, S) in minerals of Arkachan Au-Bi-siderite-sulfide and Mangazeyskoe Ag-Pb-Zn deposit s have been studied.

The Arkachan deposit was formed during 3 ore stages: main gold, silver–polymetallic, and silver–antimony stages. Three types of fluid inclusions (FI) in quartz and carbonates consisted of (I) liquid-rich H_2O + CO_2 ± CH_4 + NaCl, (II) vapour-rich CO_2 ± CH_4, and (III) aqueous-saline solutions, are distinguished. The T_{hom} and salinity of FI-I vary from 385 to 280°C and 18.8 to 26.2 wt.% NaCl equiv, respectively, those in FI-III range from 261 to 324°C and 3.7 to 9.5 wt.% NaCl equiv. The $\delta^{18}O$ of quartz II changes from +13.6 to 16.3‰(SMOW); $\delta^{18}O$ and $\delta^{13}C$ of siderite vary from +13.6 to +17.7‰ (V-SMOW) and from –6.0 to –3.0 (V-PDB), respectively. The range of $\delta^{34}S$ from –5.7 to 16.0‰ (V-CDT) has been obtained for sulfides.

Three types mineralizations are recognized at the Mangazeyskoe deposit: quartz-pyrite-arsenopyrite, quartz-carbonate-sulfide, silver-polymetallic. Fluid inclusions found in quartz and carbonates are subdivided in three types: (I) liquid-rich H_2O + CO_2, (II) vapour-rich CO_2, and (III) aqueous liquid-vapour FI. T_{hom} and salinity are in the range of 367-217°C and 13.8-2.6 wt.% NaCl equiv in FI-I, 336-126°C and 15.4-0.8 wt.% NaCl equiv in FI-III, respectively. The $\delta^{34}S$ values of sulfide change from -7.4 to +7.1‰. The $\delta^{18}O$ and $\delta^{13}C$ values of carbonates vary from -9.1 to -2.9‰ (V-PDB) and from +13.5 to + 19.5‰ (V-SMOW), respectively.

The deposits display common features: (1) three fluid types with a contrasting chemical composition, (2) there is evidence for fluid phase separation and fluid mixing, (3) isotope data suggest an involvement of magmatic fluid.

The $^{40}Ar/^{39}Ar$ age of muscovite from Arkachan is 101.9±1.4 Ma. The U/Pb age of zircon from Mangazeyskoe deposit is 97.8±0.9 Ma. These events are presumably related to the formation of Okhotsk-Chukotka Andean-type active continental margins along the North Asia. An origin of hydrothermal systems is related to intrusions of granitoid stocks and dikes derived from mixed mantle–crustal magma. These processes are favorable for an association Sn, Ag-Pb-Zn and Au-Bi deposits related to granitoid magmatism within the West Verkhoyansk province.

Acknowledgements: The work was supported by by BES, Russian Academy of Sciences (Program N. 2)

Fe,Mn- AND Fe,Mg-CHLORITE: A GENETIC LINKAGE TO W- AND Cu,Mo-METALLIZATION IN THE MAGMATIC-HYDROTHERMAL SYSTEM OF BORRALHA, NORTHERN PORTUGAL

Bobos I.*[1] & Noronha F.[1]

[1] Institute of Earth Sciences, Department of Geosciences, Environment and Land Planning, University of Porto, Portugal

Corresponding email: ibobos@fc.up.pt

Keywords: chlorite, chemistry, thermodynamic model

The W-deposit of Borralha is located at the contact zone between the metasedimentary formations (Silurian) with a porphyritic biotite granite of Borralha (315 Ma), both constituting the main host rocks. The mineralization occurs in quartz veins and two breccia structures, where the fragmented rocks were cemented by quartz. Major ore minerals are wolframite and scheelite associated with sulphide minerals (i.e., chalcopyrite + molybdenite and pyrite, pyrrhotite, sphalerite, galena, bismuthinite, native bismuth, marcasite) and Pb-Bi-Ag sulphosalts. It is assumed that mineralizations are associated with the late orogenic biotite granite of Gerês (290 Ma). The petrogenetic and petrophysical studies of biotite granites reveal that these have risen relatively high in the crust, and settled in upper crustal levels (6-7 km) involving temperature gradients, responsible for contact metamorphism under P-T conditions of 200 MPa and 500-600°C sufficient to promote the conductivity and convection of hot fluids. Previous fluid inclusion studies suggest that W mineralization is related with aqueous-carbonic fluids at a 300ºC.

Chlorite minerals were identified macroscopic and microscopic joined with quartz, feldspars, sulfides (chalcopyrite and molybdenite) and oxides (wolframite and scheelite). Selected chlorite minerals joined to sulfides and oxides were studied by X-ray diffraction (XRD), infrared spectroscopy (FTIR) and electron microprobe analysis (EMPA). XRD shows a trioctahedral structural type of chlorite. Also, FTIR confirmed the trioctahedral structure of chlorite samples by the OH^- stretching bands at 3685 cm^{-1} and by doublet arises from the OH^--stretching vibrations at 3560 and 3420 cm^{-1} of the interlayer hydroxide sheet. EMPA identified two different compositional variation of chlorite corresponding to Mg^{2+} for Mn^{2+} substitution in the brucitic sheet. Crystal chemistry of Fe,Mg-chlorite and Fe,Mn-chlorite is: $(Al_{1.45}Fe_{3.33}Mn_{0.11}Mg_{1.05})_{5.93}(Si_{2.68}Al_{1.32})_4O_{10}(OH)_8$ and $(Al_{1.35}Fe_{3.37}Mn_{0.51}Mg_{0.36})_{5.99}(Si_{2.65}Al_{1.35})_4O_{10}(OH)_8$. Chemistry of both chlorites was plotted at the middle field between clinochlor (daphnite) to amesite in the diagram of R^{2+} *vs.* Si^{4+}. In addition to EMPA results, the oxidation state of Fe^{2+}/Fe^{3+} and $Fe^{3+}/\Sigma Fe$ ratios of chlorite minerals were determined by X-photoelectron spectroscopy. Oxygen isotopes measured on both chlorite-type minerals show values of 6.91 and 9.74‰ (V-SMOW).

A genetic linkage with the W-mineralization (wolframite, scheelite) was found for Fe,Mn-chlorite, whereas the Fe,Mg–chlorite is linked to chalcopyrite and molybdenite mineralization. Chlorite geothermometry (Bourdelle & Cathelineau, 2015) estimated a temperature of 564ºC for Fe,Mn-chlorite (W-mineralization) and 320ºC for Fe,Mg-chlorite (sulfides mineralization).

Bourdelle, F. & Cathelineau, M. (2015): Low-temperature chlorite geothermometry: a graphical representation based on a *T*–R^2–Si diagram. *Eur. J. Mineral.*, **27**, 617-626.

Noronha, F. (1984): Caractéristiques physico-chimiques des fluides associés à la gènése du gisement de tungsténe de Borralha - Nord du Portugal. *Bull. Minéral.*, **107**, 273-284.

Noronha, F., Vindel, E. Lopez, J.A., Doria, A., Garcia E., Boiron, M.C., Cathelineau, M. (1999): Fluids related to tungsten ore deposits in Northern Portugal and Spanish Central System: a comparative study. *Rev. Soc. Geol. España*, **12**, 397-403.

TRACE ELEMENT MAPPING - A POWERFUL TOOL TO ASSESS THE SMALL-SCALE DISTRIBUTION OF CRITICAL METALS

Brodbeck M.*[1], Kleinhanns I.[2], Schönberg R.[2], Wenzel T.[2] & Kamber B.S.[1]
[1] Department of Geology, Trinity College, Dublin, Ireland
[2] Fachbereich Geowissenschaften, Eberhard Karls Universität Tübingen, Germany
Corresponding email: maurice.brodbeck@icrag-centre.org

Keywords: trace element mapping, LA-ICP-MS, Bushveld Complex

Trace element mapping by laser ablation inductively-coupled-plasma mass spectrometry (LA-ICP-MS) has widespread applications in geosciences. The distribution of certain trace elements in rock forming mineral grains can serve as a record for magmatic processes. For example, events of mafic recharge in a magma chamber can be easily recognized by Cr-, Ni-, or Sc-enriched zones in pyroxene crystals (Ubide et al., 2015). In an economic geology context, the supply of new batches of melt is important for sulphide melt formation and oxide crystallisation and recharge reconstruction has potential to contribute to an improved understanding of the genesis of magmatic ore deposits.

Trace element mapping also lends itself to *in situ* measurements of concentrations of critical elements in ore minerals, due to the low detection limits of modern LA-ICP-MS instruments. The distribution of critical metals within base metal sulfides, especially Zn and Cu ores is poorly understood, which limits production and recovery of these important raw materials. In an earlier study, (Ulrich et al., 2009) demonstrated the ability of LA-ICP-MS mapping to visualise the complex distribution of platinum group elements (PGEs) in sulphide inclusions within chromite.

Here we report high-resolution LA-ICP-MS trace element maps (Cr, Ni, V, Y, Th) and major element data of orthopyroxene crystals in cumulate rocks of the Bushveld Igneous Complex, adding to existing Sr-isotope data obtained *in situ* on plagioclase data from (Brodbeck, 2015). Orthopyroxene and plagioclase are the main rock forming mineral phases in the noritic-to melanoritic rocks that bound the chromitite seams of the UG2 unit, a world-class PGE and Cr deposit. The UG2 unit is one of the chromitite layers that are hosted in the Bushveld Igneous Complex.

The Bushveld Igneous Complex comprises the most voluminous mafic layered intrusion (65.000 km^2) on Earth and hosts the world's largest ore reserves of PGEs, Cr and V, but despite substantial research efforts the origin of the magma and the processes that led to mineralisation have remained controversial. In the sampled core (BH8039), the UG2 unit is *ca.* 7 m thick and consists of seven stratigraphically traceable subunits. With the exception of the two chromitite seams, remaining subunits consist of silicates.

The task at hand was to assess if chromite formation took place inside- or outside the magma chamber of the BC. Trace element mapping opened new insights in the magmatic history of the UG2 unit. The model previously developed by (Brodbeck, 2015), which assumes that the two UG2 chromitite seams originated from different processes, could be re-assessed.

Brodbeck, M. (2015): Constraining chromitite formation through *in situ* geochemical analyses - A study of the UG2 unit, Bushveld Complex, South Africa. Master thesis, Univ. Tübingen.

Ubide, T., McKenna, C., Chew, D.M., Kamber, B.S. (2015): High-resolution LA-ICP-MS trace element mapping of igneous minerals: In search of magma histories. *Chem. Geol.*, **409**, 157-168.

Ulrich, T., Kamber, B.S., Jugo, P.J., Tinkham, D.K. (2009): Imaging element-distribution patterns in minerals by laser ablation – inductively coupled plasma – mass spectrometry (LA-ICP-MS). *Can. Mineral.*, **47**, 1001-1012.

INDIUM AND SELENIUM IN THE NEVES-CORVO VHMS DEPOSIT

Carvalho J.R.S.[1], Relvas J.M.R.S.*[1], Pinto A.M.M.[1], Pacheco N.[2], Fonseca R.[2], Santos S.[2], Caetano P.[2], Reis T.[2] & Gonçalves M.[2]

[1] Institute Dom Luis, Faculty of Sciences, University of Lisbon, Portugal

[2] Somincor / Lundin Mining, Neves Corvo mine, Portugal

Corresponding email: jrelvas@fc.ul.pt

Keywords: indium, selenium, Neves-Corvo

High concentrations of indium and selenium have been reported in some massive and stockwork ores of the Neves-Corvo deposit (*e.g*., Gaspar, 2002; Schwarz-Schampera & Herzig, 2002; Serranti et al., 2002; Benzaazoua et al., 2003; Pinto et al., 2014; Carvalho et al.,, 2015; Frenzel et al., 2015). Indium and selenium distribution in Neves-Corvo is complex. It results from the combined effects of early ore-forming processes and zone refining (long lasting hydrothermal re-working), which have been subsequently obscured/enhanced by tectonic-metamorphic remobilization. At the deposit scale, both indium and selenium positively correlate with copper. High average indium and selenium contents occur in the copper-rich ore types, their concentrations being instead very low in the zinc and zinc-lead ores. At smaller scales, however, indium and selenium distributions reflect successive events of chemical redistribution and mineral reallocation. It is clear that most indium in the deposit is allocated to sphalerite, chalcopyrite and stannite, particularly in the copper-rich ores. However, very fine-grained (usually < 10 µm), rare minerals such as roquesite, and other indium-bearing phases (sakuraiite-roquesite?) were recognized by SEM/EDS as well. Other indium-bearing minerals identified include ferroskesterite, kesterite, and tennantite. On average, the indium content in chalcopyrite (660 ppm) is 2-3 times lower than in sphalerite (1400 ppm). Stannite averages 1.3 wt.% indium.

High selenium contents have been detected in galena (~ 2.9 wt.%) and in very minor complex Pb-Bi(-Cu,Ag) sulfosalts. Selenium is mainly contained in galena, arsenopyrite, chalcopyrite, pyrite, tetrahedrite and stannite, and in minor cobaltite, tennantite, glaucodot, kesterite, mawsonite, naumanite, idaite and carrolite. On average, the selenium content in galena is 50 times higher than in chalcopyrite (610 ppm) and sphalerite (590 ppm).

The copper concentrates produced at the mine has significant indium (+ selenium) concentrations, and the high indium content of sphalerite from some copper-zinc ores, or associated to shear structures, might justify a selective exploitation strategy towards the production of an indium-rich zinc concentrate in the future.

The overall positive correlation between the copper and the indium and selenium contents indicates a genetic connection between the copper and the indium-selenium metallogenesis. The exceptional ore geochemistry and unique stable and radiogenic isotope signatures of the Neves-Corvo ores are consistent with a magmatic-hydrothermal model for the deposit (Relvas et al., 2001; 2006). Furthermore, recent Sr, Nd and Pb isotope data from the Lombador orebody highlight the equally relevant role of footwall leaching for the metal budget of the deposit (Carvalho et al., 2015).

Acknowledgements: This is a contribution to ZHINC project (PTDC/CTE-GIX/114208/2009). Acknowledgements are due to S. Scott, Y. Liu, D. Smythe, G. Kretschmann, F. Marques and M. Frenzel.

Benzaazoua, M., Marion, P., Pinto, A.M.M., Migeon, H., Wagner, F.E. (2003): Tin and indium mineralogy within selected samples from the Neves Corvo ore deposit (Portugal): a multidisciplinar study. *Miner. Eng*., **16**, 1291-1302.

Carvalho, J.R.S., Pinto, A.M.M., Relvas, J.M.R.S., Pacheco, N., Fonseca, R., Santos, S., Caetano, P., Reis, R, Gonçalves, M. (2015): On the Indium and Selenium Distribution and Mineral Allocation at the Neves Corvo Deposit, Portugal. Proc. 13th Biennial SGA Meeting, 24-27 August 2015, Nancy, France, 695-698.

Frenzel, M., Bachmann, K., Krause, J., Carvalho, J.R.S., Relvas, J.M.R.S., Pacheco, N., Gutzmer, J. (2015): Mineralogical deportment of indium in the Neves-Corvo deposit - implications for recovery and extraction. SEG 2015 Meeting, World-Class Ore Deposits: Discovery to Recovery, September 27-30, 2015, Hobart, Australia.

Gaspar, O. (2002): Mineralogy and sulphide mineral chemistry of the Neves Corvo ores, Portugal: Insight into their genesis. *Can. Mineral*., **40**, 611-636.

Pinto, A.M.M., Relvas, J.M.R.S., Carvalho, J.R.S., Liu, Y. (2014): High-tech metals in the zinc-rich massive ores of the Neves Corvo deposit. *Comun. Geo*., **1010**, 825-828.

Relvas, J.M.R.S., Tassinari, C.C.G., Munhá, J., Barriga, F.J.A.S. (2001): Multiple sources for ore-forming fluids in the Neves-Corvo VHMS deposit of the Iberian Pyrite Belt (Portugal): strontium, neodymium and lead isotope evidence. *Mineral. Dep.*, **36**, 416-427.

Relvas, J.M.R.S., Barriga, F.J.A.S., Longstaffe, F. (2006): Hydrothermal alteration and mineralization in the Neves-Corvo volcanic-hosted massive sulfide deposit, Portugal: II. Oxygen, hydrogen and carbon isotopes. *Econ. Geol.*, **101**, 791-804.

Schwartz-Shampera, U. & Herzig, P.M. (2002): Indium: geology, mineralogy, and economics. Springer, Heidelberg, 257 p.

Serranti, S., Ferrini, V., Masi, U., Cabri, L.J. (2002): Trace-element distribution in cassiterite and sulfides from rubané and massive ores of the Corvo deposit, Portugal. *Can. Mineral*., **40**, 815-835.

NANOSCALE CHARACTERIZATION OF COMPOSITIONALLY-ZONED SPHALERITE

Ciobanu C.L.*[1], Maunders C.[2], Cook N.J.[1] & Wade B.P.[3]
[1] School of Chemical Engineering, University of Adelaide, Australia
[2] FEI Company, Eindhoven, Netherlands
[3] Adelaide Microscopy, University of Adelaide, Australia
Corresponding email: cristiana.ciobanu@adelaide.edu.au

Keywords: sphalerite, strategic metals, HAADF-STEM transmission electron microscopy

The ZnS polymorphs (sphalerite and wurzite) are important hosts, and currently the dominant source for several strategic metals, including Ga, Ge and In. This necessitates a sound understanding of how these elements are incorporated into the ZnS structures, including lattice-scale constraints, oxidation states of substituting elements, mechanisms of substitution, and the scale of compositional zoning. Questions of how crystal structures are modified or undergo transformation when significant amounts of trace/minor elements are added go to the very fundamentals of solid solution.

This contribution addresses compositionally zoned Cu-In-Fe-Ag-Sn-bearing sphalerite from Toyoha, Japan. Previous studies of the same specimen (Cook et al., 2009; Ciobanu et al., 2011) have shown that highly-substituted sphalerite, up to 9 mol% Cu_2S, 8 mol% In_2S_3 and 9 mol% FeS, occurs as oscillatory zoned grains. Sphalerite still richer in Fe (up to 13 wt.% FeS) occurs as separate domains/grains that are also oscillatory-zoned but depleted in other minor elements. This Fe-richest sphalerite shows abundant crystal-structural defects and particularly twinning along the (111)* axis, where the latter provides an easy mechanism of conversion between sphalerite and ZnS polytypes identified by Transmission Electron Microscopy (TEM).

Here we address the correlation between compositional zoning and crystal-structural modifications for sphalerite with highest Cu-In-Fe substitution (down to 76 mol% ZnS). Synchrotron µ-XRF mapping of a slice cut perpendicular to oscillatory zoning and extracted by *in-situ* Focused Ion Beam-SEM technique reveals detail of the compositional pattern and interestingly, shows an overlap between Cu, In and Fe maps. The fine, µm- to sub-µm scale banding across a zone ~10 µm in width, combines highly-contrasting with gradational trends.

The mapped slice was FIB-thinned and studied using an ultra-high resolution FEI Titan Themis TEM (Adelaide Microscopy), allowing for atomic-scale High-Angular Annular Dark Field Scanning TEM imaging. The specimen was tilted to the $[1\text{-}10]_{ZnS}$ zone axis and imaging reveals that the zonation pattern in Cu-In-rich sphalerite extends down to the nanoscale with band thickness ranging from a few up to hundreds of nm throughout the gradational pattern. High-resolution imaging shows atomic-scale chemical evidence for crystal-structural continuity across domain boundaries with sharp contrast and no crystal defects.

Although the concept of minor elements incorporation in minerals via solid solution, allowing for chemical changes across isomorphic mineral series is long established, atomic-scale evidence of such a model is, to our knowledge, documented here for the first time. Further work should include constraining solid-solution limits between sphalerite and isomorphic sakuraiite, $(Cu,Zn,Fe,In,Sn)_4S_4$ (Kissin & Owen, 1986), as well as the role played by oscillatory zoning in controlling high levels of substitution within crystal structures.

Ciobanu, C.L., Cook, N.J., Utsunomiya, S., Pring, A., Green, L. (2011): Focussed ion beam - transmission electron microscopy applications in ore mineralogy: bridging micron- and nanoscale observations. *Ore Geol. Rev.*,**42**, 6-31.

Cook, N.J., Ciobanu, C.L., Pring, A., Skinner, W., Danyushevsky, L., Shimizu, M., Saini-Eidukat, B., Melcher, F. (2009): Trace and minor elements in sphalerite: a LA-ICP-MS study. *Geochim. Cosmochim. Acta*, **73**, 4761-4791.

Kissin, S.A. & Owens, D.R. (1986): The crystallography of sakuraiite. *Can. Mineral.*, **24**, 679-683.

INTO THE DEPTH OF THE ARBURESE VEIN SYSTEM (SW SARDINIA, ITALY): ARSENIDE-SULFIDE EVOLUTION IN THE Ni-Co ORES

Conte A.M.[1], Cuccuru S.[2], Naitza S.*[3], Oggiano G.[2], Secchi F.[2] & Tocco S.[4]
[1] Istituto di Geoscienze e Georisorse, Consiglio Nazionale delle Ricerche, Roma, Italy
[2] Dipartimento di Scienze della Natura e del Territorio, Università di Sassari, Italy
[3] Dipartimento di Ingegneria Civile, Ambientale e Architettura, Università di Cagliari, Italy
[4] Istituto di Geologia Ambientale e Geoingegneria, Consiglio Nazionale delle Ricerche, Cagliari, Italy
Corresponding email: snaitza@unica.it

Keywords: hydrothermal Ni-Co, two-stage mineralization, mafic magmas

The Arburese region (SW Sardinia) is well-known for a large swarm of mineralized veins hosted in low-grade metamorphic rocks, extending for about 20 km around the Late Variscan (304±1 Ma) Arbus pluton, made up of a core of cordierite-bearing biotite leucogranites and an external shell of granodiorites with subordinate mafic rocks (Cuccuru et al., 2015). The largest veins occur in the northern and western sectors (past Montevecchio district), with a primary mineral association of Pb-Zn (Cu, Ag) sulfides in quartz and siderite. Recent works on the southern branch of the vein system (Naitza et al., 2015) evidenced a more complex metallogeny, with Ni-Co-As-Sb-Bi-Pb-Zn-Cu-Ag ores. New microscopy, SEM-EDS and EPMA data allow to highlight the depositional history of these ores, defining two stages of mineralization. In the *Arsenide stage*, early precipitation of quartz with abundant Ni monoarsenide (nickeline) was followed by growth of Ni antimonide (breithauptite) on nickeline, by Ni, Ni-Co, Co, Fe diarsenides, triarsenides, sulfoarsenides (rammelsbergite, skutterudite, safflorite/löllingite, cobaltite, gersdorffite/ullmannite) and Bi minerals (bismuthinite and native Bi), replacing nickeline and forming rims and inclusions on previously crystallized phases. The *Sulfide stage* was preceded by cataclasis of the ores; initial abundant precipitation of quartz, siderite and sphalerite, cementing the fragments of the arsenide ores, was followed by Pb-Cu-Ag sulfides (galena, chalcopyrite, tetrahedrite/freibergite, bournonite, proustite/pyrargirite, stephanite), and, at last, by ankerite, calcite and pyrite. These sequences of mineralization suggest a relationship with distinct hydrothermal fluids: 1) an earlier fluid, carrying Ni, Co, As and Sb, deposited as arsenides and sulfoarsenides into structurally-controlled traps in response to variations in physicochemical conditions; 2) a late, carbonate and Pb-Zn-Cu-Ag -rich fluid, permeating fractures re-opened after a tectonic phase that involved the previous mineralization, and originating a “Montevecchio-type” mineral association. Depositional histories similar to the *Arsenide stage* have been reported in other hydrothermal Ni-Co deposits worldwide, as in the Bou Azzer district, Morocco (Ahmed et al., 2009). The geochemistry of these ores requires the presence in the geological sequence of a Ni-Co-rich source (e.g., mafic rocks) from which these elements could be leached by acidic and moderately oxidizing hot fluids. Analogous conditions may have been attained in the Arbus pluton, which includes an olivine-bearing end member (Secchi et al., 1991), possible Ni-Co source for fluids of magmatic origin. During the emplacement of the igneous complex, widespread uralitization of pyroxenes in granodiorites point to high fluid/rock interactions; moreover, quartz- Fe-cordierite graphic intergrowths in leucogranites support a late dehydration of magmas.

Ahmed, A.H., Shoji, A., Ikenne, M. (2009): Mineralogy and paragenesis of the Co-Ni arsenide ores of Bou Azzer, Anti-Atlas, Morocco. *Econ. Geol.*, **104**, 249-266.

Cuccuru, S., Naitza, S., Secchi, F., Puccini, A., Casini, L., Pavanetto, P., Linnemann, U., Hofmann, M., Oggiano, G. (2015): Structural and metallogenic map of late Variscan Arbus Pluton (SW Sardinia, Italy). *J. Maps*, DOI: 10.1080/17445647.2015.1091750.

Naitza, S., Cuccuru, S., Oggiano, G., Secchi, F. (2015): New observations on the Ni-Co ores of the southern Arburese Variscan district (SW Sardinia, Italy). *Geoph. Res. Abstr.*, **17**, EGU2015-12659.

Secchi, F.A., Brotzu, P., Callegari, E. (1991): The Arburèse igneous body (SW Sardinia, Italy) - An example of dominant igneous fractionation leading to peraluminous cordierite-bearing leucogranites as residual melts. *Chem. Geol.*, **92**, 213-249.

MULTI-TRACE ELEMENT CONCENTRATION DATA FOR MINERALS: IDENTIFYING POTENTIAL NEW RESOURCES OF CRITICAL ELEMENTS

Cook N.J.*[1] & Ciobanu C.L.[1]
[1] School of Chemical Engineering, University of Adelaide, Australia
Corresponding email: nigel.cook@adelaide.edu.au

Keywords: trace elements, strategic metals, opportunities and challenges

Advancing technologies require a wide range of non-traditional metals, necessitating secure supplies, and, in turn, driving a search for alternative resources and a greater understanding of their mineralogy and distribution in Nature. These strategic metals include Sc, Ga, Ge, In, Hf, PGE and REE, as well as Co, Ta, Nb, V and Sn. The list can be extended to include non-metals (e.g. Te), and commodities with little value today but potentially of major future significance, e.g. Th.

The large volumes of multi-trace element data for specific minerals obtained by, e.g., LA-ICP-MS, provide valuable information on which elements can occur in which minerals, and at what concentrations. Although the likely host minerals for many sought-after elements in any given system are either obvious, or can be accurately predicted from geochemistry, Nature is capable of surprise. Emerging data supports high, and in some cases, economically interesting concentrations of strategic elements within minerals from which they are not traditionally exploited, and in some cases, within gangue minerals in which they are not even expected to occur. REE, for example, are widely dispersed, yet the processes leading to their enrichment in silicates, phosphates and other minerals remain poorly constrained. Further examples include the presence of Sn, In, Mo, various HFSE (and As) in skarn andradite, concentrations of Ga in epidote and other aluminosilicates, or the hundreds or thousands of ppm W and Mo, and other elements like Sc, measured in some Fe-oxides. Although the mineralogy of many rare elements has been extensively explored, data are lacking on how, when, and at what concentrations, Sc or other strategic elements can occur in more abundant, or more easily exploitable minerals.

Although most if not all of the above examples have little economic potential today, an awareness of their mineralogical distribution is increasingly valuable for identification of new opportunities. The concept of that what is today's waste could be tomorrow's ore is key to this new thinking. Well-constrained mineralogical distributions may, for example, impact on decisions on long-term storage of mining or processing waste. The need to recognize ways to add value to a mining project by optimizing by-product recovery (Mudd et al., 2016) may also drive innovation in extractive technology, and especially in techniques such as in-situ leaching. A good example is the possibility of REE recovery from phosphogypsum, a difficult to dispose waste product of phosphate mining and fertilizer production (Shivaramaiah et al., 2016).

Studies of the mineralogical distribution of strategic elements should be as holistic as possible, so as to able to appreciate not only ranges of absolute concentration but also understand how elements of interest partition among co-existing phases. LA-ICP-MS datasets can also provide information on the distribution of deleterious and 'penalty' elements, thus optimizing processing.

Mudd, G.M., Jowitt, S.M., Werner, T.T. (2016): The world's by-product and critical metal resources part I: Uncertainties, current reporting practices, implications and grounds for optimism. *Ore Geol. Rev.*, in press.

Shivaramaiah, R., Lee, W., Navrotsky, A., Yu, D., Kim, P., Wu, H., Hu, Z., Riman, R., Anderko, A. (2016): Location and stability of europium in calcium sulfate and its relevance to Rare Earth recovery from phosphogypsum waste. *Am. Mineral.*, in press, DOI: 10.2138/am-2016-5684.

SUPERGENE GOLD ENRICHMENT IN THE CASTROMIL GOLD DEPOSIT

Cruz C.*[1], Lima A.[1], Santos P.[2] & Noronha F.[1]
[1] Institute of Earth Sciences, Department of Geosciences, Environment and Spatial Planning, University of Porto, Portugal
[2] MedGold Resources Corp, Paredes, Portugal
Corresponding email: claudiacfcruz@gmail.com

Keywords: gossan, supergene gold enrichment

The northwestern part of Portugal is an important Variscan metallogenic province, particularly for gold. These occurrences are mainly hosted by Variscan granites and Paleozoic metasediments (Noronha *et al*., 2000).

Castromil and Serra da Quinta gold deposits are included in Lagares Licence explored by MedGold Resources Corp. These occur in Central-Iberian Zone, on the eastern flank of the Valongo anticline (NW Portugal), at the contact between the Castelo de Paiva biotite granite and Silurian metasediments. Both the host rocks and mineralized structures follow the same trend, N140ºE and are affected by different episodes of deformation (Vallance *et al*., 2002).

The Castromil deposit, similarly to many other Iberian mines, was mined by the Romans as open pit (exploiting a gossan) and surface galleries, and their works are still preserved. The open pit and the outcropping mineralized structures correspond to oxidized sulphides essentially composed by goethite, scorodite and clay minerals (gossan) resulting from weathering. Recent drilling, which has drilled below the oxidation level exhibits hydrothermal alteration, associated with the highest primary gold mineralization grade (Medgold's Channel Sampling Results, 2015).

Metallographic studies were made in twenty polished sections and twenty-nine thick sections, sixteen of those were from gossan supergenic mineralization and thirteen from drill core with primary or hypogene mineralization.

Supergene mineralization is developed on oxide zone, that replace the hypogene mineral association. Primary gold mineralized structures are mainly composed by quartz and sulphides. The most significant sulphides are arsenopyrite, pyrite, chalcopyrite, pyrrhotite, galena, sphalerite and bismuth. Electrum is the principal precious-metal mineral. Native-gold and silver sulphides (acanthite) constitute the minor ones. Different electrum/ gold occurrence modes were observed: hosted in iron oxides, encapsulated in sulphides, included in quartz and in sulphides filling latter fractures or in grain boundaries.

The boxwork structures developed in gossan indicate the pre-existing sulphide mineralogy. Presence of gold in gossan is still quite conspicuous and the values interestingly above 2.07 g/T with an average value of about 4.02 g/T (Medgold's Channel Sampling Results, 2015).

The SEM-EDS and WDS study of gold particles reveal particles with different contents of Ag, which allow to conclude the presence of native-gold and electrum particles. The particles encapsulated in sulphides are poorer in Ag (20.43-25.17%) than particles hosted in sulphide fractures or in grain boundaries (37.46-51.45%). In gossan the referred two main types of particles can be found and are assumed as hypogene in origin, however a supergenic enrichment of these particles can be observed by latter deposition of native-gold (< 16.11% Ag).

Native-gold in gossan is associated with poorly crystallized iron oxides. The supergene gold enrichments formation result from mobilization and re-precipitation of this metal.

Medgold's Channel Sampling Results (2015): Available at: http://www.medgoldresources.com/s/lagares.asp. Accessed in April 2016.

Noronha, F., Cathelineau, M., Boiron, M.C., Banks, D.A., Dória, A., Ribeiro, M.A., Nogueira, P., Guedes, A. (2000): A three stage fluid flow model for Variscan gold metallogenesis in northern Portugal. *J. Geochem. Explor.*, **71**, 209-224.

Vallance, F., Cathelineau, M., Boiron, M.C., Fourcade, S., Shepherd, T.J., Naden, J. (2003): Fluid-rock interactions and the role of late Hercynian aplite intrusion in the genesis of Castromil gold deposit, northern Portugal. *Chem. Geol.*, **194**, 201-224.

ANTIMONY MINERALISATION IN SOUTH WEST ENGLAND: NEW INSIGHTS INTO CRITICAL METAL ORE GENESIS

Deady É.*[1-2], Knight H.[1], Moore K.[1], Gunn A.G.[2], Naden J.[2] & Boyce A.J.[3]
[1] Camborne School of Mines, University of Exeter, United Kingdom
[2] Minerals and Waste, British Geological Survey, Keyworth, United Kingdom
[3] Scottish Universities Environmental Research Centre, Glasgow, United Kingdom
Corresponding email: ed349@exeter.ac.uk

Keywords: antimony, mineral resources, security of supply

The BGS risk list (British Geological Survey, 2015) and the EU criticality study (European Commission, 2014) both identify antimony (Sb) as being at "very high risk" of supply shortage. Antimony is primarily used for the production of antimony trioxide (Schwartz-Schampera, 2014) a key component in flame-retardant material. The demand for this is predicted to grow with increased health and safety regulation in developing nations. The majority of antimony is produced in China, with almost 80% of world production in 2014 (Brown et al., 2016). Research into the formation of Sb deposits at the BGS is contributing to improving global supply security.

The North Herodsfoot deposit in Cornwall, UK, was historically worked for Pb-Ag and other base metals; the mine is also known for its spectacular specimens of "cog-wheel" bournonite ore (Starkey, 2012). New samples from the mine waste tailings at North Herodsfoot have been used to study the multi-phase polymetallic mineralisation. The paragenesis includes galena (± argentiferous galena), bournonite, pyrite, arsenopyrite, chalcopyrite ± sphalerite ± pyrostilpnite-pyragarite. A preliminary paragenetic model of the deposit incorporates previously unidentified Ni-bearing phases (gersdorffite NiAsS), which are associated with pyrite.

The deposit has historically been classified as a Mid-Triassic, low-temperature "crosscourse" deposit based on little more than a shared geometry with other similar, antimony-free, deposits in South West England (Scrivener et al., 1994). A geochemical study of both the fluid inclusions and S isotopes from this deposit has been conducted. The first fluid inclusion data from samples of legacy tailing at the North Herodsfoot Mine reveal that the Herodsfoot lode has strong geochemical similarities with other crosscourse deposits in South West England. Ore fluids comprise high salinity (18-27 wt.% NaCl equiv.) H_2O-NaCl-$CaCl_2$ brines that ingressed at low temperatures (T_h 83-129°C) (Knight et al., 2016). Preliminary S isotope data from the same samples show $\delta^{34}S$ values of -4 to -10 per mil, consistent with a sedimentary source of S. This is similar to S isotopes data from other crosscourses in the regions (Gleeson et al., 2001).

These preliminary mineralogical and isotopic data provide a basis for the development of a robust model for Sb mineralisation in South West England, and possibly also more widely applicable.

British Geological Survey (2015): Risk List 2015.

Brown, T.J., Wrighton, C.E., Idoine, N.E., Raycraft, E.R., Shaw, R.A., Deady, É.A., Rippingdale, J., Bide, T. (2016): World Mineral Production 2010-2014.

European Commission (2014): Report on critical raw materials for the EU. Report of the Ad Hoc Working group on defining critical raw materials. May 2014.

Gleeson, A.A., Wilkinson, J.J., Stuart, F.M., Banks, D.A. (2001): The origin and evolution of base metal mineralising brines and hydrothermal fluids, South Cornwall, UK. *Geochim. Cosmochim. Acta*, **65**, 2067-2079.

Knight, H., Deady, É., Gunn, A.G., Moore, K., Naden, J. (2016): Ore fluid characteristics of antimony deposits in South West England: new insights into ore genesis in Wadebridge-Port Isaac and Herodsfoot. *Appl. Earth Sci.*, *Section B*, in press.

Schwartz-Schampera, U., (2014): Antimony. *in* "Critical metals handbook", A.G. Gunn, ed., Wiley, UK, 70-98.

Scrivener, R.C., Darbyshire, D.P.F., Sheperd, T.J. (1994): Timing and significance of crosscourse mineralisation in SW England. *J. Geol. Soc.*, **151**, 587-590.

Starkey, R.E. (2012): The Herodsfoot Mine, Lanreath, Cornwall, England. *Mineral. Rec.*, **43**, 411-486.

THE RESIDENCE OF THE CRITICAL METAL COBALT IN OXIDE MINERAL DEPOSITS - A SYNTHETIC STUDY

Dressler S.*[1-2], Kirk C.A.[1-2], Norman R.L.[2], Herrington R.J.[2] & Schofield P.F.[2]
[1] Department of Chemistry, Loughborough University, United Kingdom
[2] Department of Earth Sciences, Natural History Museum, London, United Kingdom
Corresponding email: s.dressler@lboro.ac.uk

Keywords: cobalt, iron-oxyhydroxide, synthesis

Goethite (α-FeOOH) is the most common iron-oxyhydroxide in (almost all) soils, ore deposits, and continental and marine sediments, such as deep-sea ferromanganese nodules (Manceau et al., 2000). Due to its small particle size and the resulting high specific surface area (8 to 200 m^2g^{-1}), goethite has a high potential to incorporate other elements and rarely occurs with its ideal formula in naturally occurring deposits (Cornell & Schwertmann, 2003). It often contains adsorbed or substituted cations, which can be either divalent cations, such as Ni, Zn, Cd, trivalent cations, e.g. Al, V, Cr, Mn, Co, or tetravalent cations, such as Si, Ge and Pb (Manceau et al., 2000). Knowledge about elements present and their incorporation into the structure, structurally or surface adsorbed, is essential for the extractive industry. However, many of these non-iron-elements exist in low concentrations (< 2 mol%) in the structure of natural goethite and it is often challenging to determine their presence (Gasser et al., 1996).

One approach to investigate doping is to carry out synthetic studies. This research is focused on cobalt doped iron-oxyhydroxide systems, such as goethite and ferrihydrite, to investigate the effects of time, concentrations of Co starting reagents, *p*H and temperature on the phases produced. Cobalt is not a rare metal, but it is economically exploitable in several countries. For over 2000 years and up to the 20th Century, the main use of cobalt was colouring glasses and ceramics, but now it is one of the most essential key elements in many technologically important materials (Cobalt Development Institute, 2006). Due to its great physical attributes, e.g. high temperature resistance, cobalt is used for producing alloys that maintain their strength at high temperatures. Furthermore, it is a significant element in many clean energy technologies, such as wind and wave generators (Boland & Kropschot, 2011), and pharmaceuticals. Nevertheless, the globally leading and irreplaceable use of cobalt is as a cathode material in Li rechargeable batteries. The synthesis of a set of cobalt doped goethite samples and the preliminary results from characterisation of the phases using X-ray diffraction and IR-spectroscopy will be presented.

Boland, M.A. & Kropschot, S.J. (2011): Cobalt-For Strength and Color. U.S. Geological Survey Fact Sheet 2011-3081, 2 p.

Cobalt Development Institute (2006): Available at http://www.thecdi.com/ [Accessed April 2016].

Cornell, R.M. & Schwertmann, U. (2003): The iron oxides: structure, properties, reactions, occurrences and uses. Wiley, Weinheim, 664 p.

Gasser, U.G., Jeanroy, E., Mustin, C., Barres, O., Nüesch, R., Berthelin, J., Herbillon, A.J. (1996): Properties of synthetic goethites with Co for Fe substitution. *Clay Miner.*, **31**, 465-476.

Manceau, A., Schlegel, M., Musso, M., Sole, V., Gauthier, C., Petit, P., Trolard, F. (2000): Crystal chemistry of trace elements in natural and synthetic goethite. *Geochim. Cosmochim. Acta*, **64**, 3643-3661.

CHEMISTRY OF Nb-Ta OXIDE MINERALS FROM SANTA MARIA DE ITABIRA PEGMATITE DISTRICT, MINAS GERAIS, BRAZIL

Elizetti de Freitas M.[1], Javier Rios F.*[1], Andrade S.[2] & de Moraes R.[2]
[1] Nuclear Technology Development Center, National Nuclear Energy Commission, Belo Horizonte, Brazil
[2] Institute of Geosciences, University of São Paulo, Brazil
Corresponding email: javier@cdtn.br

Keywords: Nb-Ta (REE-U-Th) oxide minerals mineralogy, chemistry, evolutive patterns

The Neoproterozoic pegmatites of Santa Maria de Itabira district, Minas Gerais- Brazil, in the Eastern Brazilian Pegmatite Province, are characterized by the frequent occurrence of high quality gem minerals, mainly aquamarine, and they often occur associated with rare metal minerals, for instance, Nb-Ta oxides. These pegmatites are related to post-tectonic S-type calc-alkaline granitic intrusions during the Brasiliano/Panafrican event. The samples of Nb-Ta oxide minerals were analyzed with EMP and LA-ICPMS in order to make a detailed chemical characterization The Nb-Ta oxide minerals from different groups have the same general characteristic: the concentrations of Nb >> Ta and Fe >> Mn. In the columbite group minerals, ferrocolumbite is predominant and the crystals were usually homogenous. The aeschynite samples were classified as aeschynite-(Y), with Ti predominance in the B-site and Y + REE in the A-site. The fergusonite-(Y) has restrict occurrence, but it is the main Y repository in the region. The composition of samarskite group minerals varies between samarskite and ishikawaite fields, although the U+Th are predominant if compared to Y+REE in the A-site, and they form two distinct groups: 1. richer in Y; 2. richer in REE, mainly Dy, Yb and Er. The REE distribution patterns, mainly the ones obtained by LA-ICPMS, show that all minerals tend to have HREE enrichment and negative Eu anomaly. The aeschynite, which is also rich in LREE, presents an almost flat pattern. The Nb-Ta oxide minerals, in spite of the fact that it belongs to different groups, with varied chemical compositions, are representative and consistent with the mineralogical assemblage of the pegmatite district of Santa Maria de Itabira. Their chemical characteristics indicated several evolutive patterns: 1. the Nb-Ta oxides minerals were formed in the low fractionation conditions, where the most complex oxides occurred in the F-bearing pegmatites; 2. the predominance of beryl as the main accessory mineral and the absence of Li and B minerals in this area, confirms the low fractionation conditions of pegmatites, if compared to the other pegmatite districts of the Eastern Brazilian Pegmatite Province; 3. the REE pattern similarities were interpreted as assign that the different pegmatites of this district were formed in the same conditions; 4. the high concentration of U, Th, Y and REE in these minerals may be related to the presence of the fluxing elements, such as F and P, during formation of the pegmatites; 5. despite the restrict occurrence in these pegmatites, the Nb-Ta oxides minerals are an important repository of Y, REE, U and Th.

MINERAL RESOURCE OF CRITICAL METALS (Te-Ge-Se-In) IN EPITHERMAL DEPOSITS OF "LA CAROLINA" DISTRICT, SAN LUIS (ARGENTINA)

Gallard-Esquivel M.C.[1], Cepedal A.*[2], Fuertes-Fuente M.[2] & Martin-Izard A.[2]

[1] Departamento de Geología, Universidad Nacional de San Luis, Consejo Nacional de Investigaciones Científicas y Técnicas, San Luis, Argentina

[2] Departamento de Geología, Universidad de Oviedo, Spain

Corresponding email: mercedf@geol.uniovi.es

Keywords: argyrodite, indium, San Luis metallogenic belt

La Carolina gold-bearing district is sited at the western end of the metallogenic belt of San Luis (Argentina), which is spatially and genetically related to the mesosilicic volcanism of Mio-Pliocene age. The volcanic arc has migrated eastwards, due to the flattening of the Nazca plate in the 27°-33°S segment, known as the Pampean flat-slab (Ramos et al., 2002). At La Carolina, the volcanic activity, including lavas and pyroclastic rocks (surges and phreatic/phreatomagmatic breccias) of andesitic, dacitic, latitic and trachytic composition, occurred between 8.2 and 6.3 Ma (Urbina & Sruoga, 2009). The district represents a maar-diatreme system disturbed by dome emplacements. Volcanic rocks intruded and overlay a Precambrian to Paleozoic igneous-metamorphic basement.

This work presents the study carried out on ore samples from Puesto La Estancia and Cerro Mogote prospects, located in the southern area of La Carolina district. They are base metal sulfide-rich epithermal deposits combining stockworks and disseminated mineralized zones, spatially related to phreatic breccias. The aim of this work is to characterize the ore and gangue mineral paragenesis (performed by SEM-EDS and electron microprobe at Oviedo University), and emphasis is placed on critical metal-bearing mineralogy.

In the studied samples, mineralization infills veins or occurs as the matrix of volcanic breccias. At least two stages of mineralization were observed. Stage-1 mainly includes pyrite, sphalerite and galena, with quartz and Mn-carbonates as the main gangue minerals. Stage-2 includes pyrite, sphalerite, galena and chalcopyrite, which is locally abundant. Gangue minerals are Mn-Fe-Mg(-Ca) carbonates, with lesser amounts of kaolinite and quartz. The main accessory minerals are tetrahedrite-tennantite, acanthite, hessite, argyrodite (Ag_8GeS_6), polybasite-pearceite [$(Ag,Cu)_{16}(Sb,As)_2S_{11}$] and electrum. They occur as small grains and blebs, isolated or in aggregates, included in pyrite and sphalerite, or attached to the main sulfide grains replacing them. Locally, the mineral paragenesis is enriched in Te±Se. Here, Te-Se-bearing polybasite-pearceite (3.2 to 4.3 wt.% Te; 1.0 to 2.2 wt.% Se) occurs along with the Te-rich member benleonardite [$Ag_8(Sb,As)Te_2S_3$]. Selenium-rich cervelleite (Ag_4TeS, 4.2 to 6.38 wt.% Se) is related to hessite in intergrowth textures. Moreover, alburnite ($Ag_8GeTe_2S_4$), the Te-rich member of the argyrodite group, was also identified. Microprobe analyses of galena also showed Se contents up to 1.75 wt.%. Sphalerite from stage-1 is Fe-poor (< 2 wt.%), whereas sphalerite from stage-2 is Fe-rich (up to 12.5 wt.%), becoming Fe-poor at the end of this stage and rich in indium (up to 0.2 wt.% In). Pyrite can be rich in As (up to 6 wt.%) and has minor amounts of Cu, Ag, Sb, Se and Te. Microprobe X-ray maps showed a complex compositional zoning reflecting changes in the composition of hydrothermal fluids.

Ramos, V.A., Cristallini, E.O., Perez, D.J. (2002): The Pampean flat-slab of the Central Andes. *J. South Am. Earth Sci.*, **15**, 59-78.

Urbina, N.E. & Sruoga, P. (2009): La Faja Metalogenética de San Luis (FMSL), Sierras Pampeanas, Argentina: mineralización y geocronología en el contexto metalogenético regional. *Rev. Soc. Geol. Argent.*, **64**, 635-645.

THE RELATIONSHIP BETWEEN MAGNETITE AND COPPER-SILVER MINERALISATION OF THE KALAHARI COPPERBELT IN CENTRAL-EASTERN NAMIBIA

Gill S.-J.*[1]
[1] Birkbeck College, University of London, United Kingdom
Corresponding email: mordred82@yahoo.com

Keywords: Kalahari Copperbelt, magnetite, ore deposits

The Kalahari Copperbelt (KCB) is composed of a series of late-mid Proterozoic basins which stretch discontinuously for ~ 800 km, roughly NE-SW across Namibia and into north-western Botswana. Exploration along the KCB in Namibia led to the discovery of copper-silver mineralisation within the Tsumis Group meta-sediments of the Sinclair Supergroup, which are lateral equivalents to the *ca.* Mesproterozoic metasedimentary Ghanzi Group in Botswana. Much of the KCB is buried beneath the thick Cenozoic cover of the Kalahari Group sand, calcrete and silcrete. This study was done in collaboration with Eiseb Prospecting and Mining, who are actively exploring for economic concentrations of Cu-Ag mineralisation in this heretofore unexplored portion of the KCB. Early research by the company indicated an association between the mineralisation and magnetite. This study explores that relationship.

The preferred exploration model currently used along the KCB is one of stratiform sediment-hosted mineralisation (SSC) where mineralisation is the result of leaching of 'red bed' sediments by oxidising basinal fluids and precipitation of these minerals when the fluids encounter reductants such as reduced sedimentary horizons, mobile reductants such as organic matter, or reduced fluids. In this study that model challenged.

Petrography evidence from suggests that magnetite and the argentiferous Cu(-Fe) sulfides were coeval with the Pan African orogeny and concomitant deformation. The trace element geochemisty of magnetite suggests an evolving fluid system where enrichment progressed from the basement metavolcanics (bimodal suite) into the overlying sediments via a network of deep-seated faults. The elements V, Cr, Ni, Co and Ti are most useful at illustrating the evolution of the fluid, as are discriminant diagrams. The trace element contents of the basement magnetite samples also shows promise as an indicator for the tectonic environment of the host rock.

THE ÇANAKLI REE PLACER DEPOSIT, TURKEY: AN ALKALINE VOLCANIC SOURCE?

Goodenough K.*[1], Deady É.[1], Lacinska A.[1], Shaw R.A.[1] & Roberts N.M.W.[2]
[1] Minerals and Waste, British Geological Survey, Edinburgh, United Kingdom
[2] National Isotope Geoscience Laboratory, British Geological Survey, Keyworth, United Kingdom
Corresponding email: kmgo@bgs.ac.uk

Keywords: rare earth elements, placer, mineral resources

The Çanakli deposit, a part of the Aksu Diamas project, Turkey, owned by AMR Mineral Metal Inc., has an inferred resource of 494 million tonnes at about 0.07% TREO (total rare earth oxide). This deposit is a potentially important source of European rare earth element (REE) supply.

Phreatoplininan eruptions of Plio-Quaternary age, related to the alkaline Gölcük volcano, located approximately 20 km north-west of the deposit are thought to be the source of the REE mineralisation. The deposit is hosted in Quaternary sediments situated in a topographic low in Mesozoic limestones. REE-bearing heavy minerals occur in lenses and are disseminated within channelised debris flows. The source of the REE is being investigated by the British Geological Survey through the EU-funded FP7 project EURARE (www.eurare.eu).

Preliminary scanning electron microscopy analysis of heavy mineral concentrates confirms the presence of REE-bearing minerals such as allanite and chevkinite (Deady et al., 2016). Allanite was also found in the samples from pyroclastic flows from the Gölcük alkaline volcano. LA-ICP-MS will be used to chemically fingerprint the REE-bearing minerals both in the placer and the ash fall deposits. This will be used clarify if the source of the REE was the Gölcük magma. The mineralogical analysis will be followed by U/Pb dating of zircons from both the placer and volcanic ash horizons to determine the age of the deposit. The intense H_2O variations in the magma (Platveot et al., 2014) were responsible for the explosive nature of the eruptions at Gölcük and the extensive development of ash clouds, from which REE-bearing minerals are considered to have been deposited.

If the Çanakli REE deposit resulted solely from the accumulation of air-fall tuff-borne minerals in a topographic depression, with no additional concentration processes, then this is a new type of deposit. Improved understanding of the origin of this deposit could help to identify additional REE resources in similar settings globally, including those at Monte Vulture, Italy.

Acknowledgements: The research leading to these results has received funding from the European Community's Seventh Framework Programme ([FP7/2007–2013]) under Grant Agreement no. 309373. This publication reflects only the author's views, exempting the Community from any liability.

Deady, É., Goodenough, K., Lacinska, A., Hardy, L.R. Shaw, R.A. (2016): Rare earth element placer deposits and alkaline volcanics: a case study from Aksu Diamas, Çanakli, Turkey. *Applied Earth Sci.*, *Section B*, in press.

Platevoet, B., Elitok, Ö., Guillou, H., Bardintzeff, J-M., Yagmurlu, F., Nomade, S., Poisson, A., Deniel, C., Özgür, N. (2014): Petrology of Quaternary volcanic rocks and related plutonic xenoliths from Gölcük volcano, Isparta Angle, Turkey: Origin and evolution of the high-k alkaline series. *J. Asian Earth Sci.*, **92**, 53-76.

RARE EARTH POTENTIAL OF APATITE IN THE SCHIEL COMPLEX, SOUTH AFRICA

Graupner T.*[1], Henjes-Kunst F.[1], Klemd R.[2], Gerdes A.[3], Dohrmann R.[1] & Kaufhold S.[1]
[1] Bundesanstalt für Geowissenschaften und Rohstoffe, Hannover, Germany
[2] GeoZentrum Nordbayern, Friedrich-Alexander Universität Erlangen-Nürnberg, Erlangen, Germany
[3] Institut für Geowissenschaften - Geochemie und Petrologie, Goethe-Universität Frankfurt am Main, Germany
Corresponding email: torsten.graupner@bgr.de

Keywords: Schiel Complex, apatite, rare earth elements

The Proterozoic Schiel Complex, located in the eastern part of the Southern Marginal Zone of the Limpopo Belt, intruded the Goodplaats Gneiss close to the Kudus River Lineament (Verwoerd & du Toit, 2006). The studied horseshoe shaped eastern intrusion is mainly composed of granite, syenite and quartz syenite, but also contains phoscorite bodies and veins of carbonatite (not exposed). New U-Pb LA ICP-MS zircon ages vary between 2060±3 Ma (two phoscorite samples) and 2050±10 Ma (syenite) and hint on a contemporaneous formation of the Schiel Complex and the Phalaborwa intrusion, as dated at 2060.6±0.5 Ma (Reischmann, 1995; cf. Bushveld Complex igneous event (2050-2060 Ma)). Previous exploration activities at Schiel examined the apatite-vermiculite-magnetite mineralisation in the eastern intrusion (central valley); however, activities ceased with negative results (Viljoen, 1966; Prins et al., 1981). The present investigation of apatite-mineralised rocks at Schiel focuses on their potential for rare earth element (REE) extraction in addition to a mining for phosphate. Apatite from various types of magmatic rocks was characterised using light microscopy, electron-probe microanalysis, isotopic investigation and hot-cathode cathodoluminescence (CL) microscopy. Soil overlying the hidden ore bodies and extracted apatite crystals from soil were investigated using X-ray fluorescence analysis and CL microscopy. Furthermore, a determination of the exchangeable cations was carried out for two soil samples. Total REE (+ Y) concentrations range from <100 ppm to 6000 ppm in rocks at Schiel (80 samples; mean: 980 ppm) and from 1050 ppm to 3950 ppm in the soils on top of ore bodies (56 samples; mean: 2120 ppm). The major REE carriers in syenitic rocks are apatite, titanite and allanite and in phoscorite predominantly apatite. Small grains of monazite-group minerals are scarce in most rocks and are commonly arranged adjacent to apatite crystals or are intergrown with thorium silicate aggregates. Apatite in all rocks is clearly of primary magmatic origin according to textural and isotopic (Sm-Nd data) evidences. At least two types of apatite are distinguished based on their CL properties: (i) coarse grained euhedral apatite with high to moderate REE concentrations shows dark to brighter shades of bluish CL colours, and (ii) low-REE apatite, either forming overgrowth on the first type or forming fine grained aggregates, has greenish CL colours. First results indicate that REE in the Fe-rich smectite- and kaolinite-bearing soils are commonly hosted by apatite with bluish CL colours, whereas the fraction of metals on ion exchange positions was low. Rare earth element concentrations in apatite from Schiel vary strongly between different host rocks; importantly, they are sometimes significantly higher than REE concentrations in apatite from pyroxenite and carbonatite from Phalaborwa (cf. Dawson & Hinton, 2003; Graupner et al., 2014).

Dawson, J.B. & Hinton, R.W. (2003): Trace-element content and partitioning in calcite, dolomite and apatite in carbonatite, Phalaborwa, South Africa. *Mineral. Mag.*, **67**, 921-930.

Graupner, T., Opperman, R., Tongu, E.L. (2014): Rare-earth elements. *in "*Investor's and Procurement Guide South Africa, Part 1: Heavy Minerals, Rare Earth Elements, Antimony", P. Buchholz, ed., DERA, Berlin, 73-116.

Prins, D., van Graan, S.J., du Rand, H.G.J., Oberholzer, J.W. (1981): Schiel - Phosphate deposit: An order of magnitude feasibility study - March 1981. TECHNOCOM Mineral Development Sevices (PTY) Ltd, 42 p.

Reischmann, T. (1995): Precise U/Pb age determination with baddeleyite (ZrO_2), a case study from the Phalaborwa Igneous Complex, South Africa. *South Afr. J. Geol.*, **98**, 1-4.

Verwoerd, W.J. & du Toit, M.C. (2006): The Phalaborwa and Schiel complexes. *in "*The geology of South Africa", M.R. Johnson et al., eds., Geological Society of South Africa, Johannesburg, 291-299.

Viljoen, V.E. (1966): Volledige geologiese verslag op die Schiel Fosfaat Voorkoms. Geologiese Opname, Pretoria, 38 p.

MINERAL ASSEMBLAGES IN THE TIN (-INDIUM) SANTA FE MINING DISTRICT, BOLIVIA

Jiménez-Franco A.*[1], Alfonso P.[1], Canet C.[2], Trujillo E.[3] & Garcia-Valles M.[4]
[1] Departament d'Enginyeria Minera, Industrial i TIC, Universitat Politècnica de Catalunya, Barcelona, Spain
[2] Instituto de Geofísica, Universidad Nacional Autónoma de México, Mexico
[3] Facultad Nacional de Ingeniería, Universidad Técnica de Oruro, Bolivia
[4] Departament de Cristal·lografia, Mineralogia i Dipòsits Minerals, Universitat de Barcelona, Spain
Corresponding email: abigail@emrn.upc.edu

Keywords: stannite, sakuraiite, indium

The Santa Fe Mining District (SFD) is located in the Bolivian portion of the Central Andean Belt, which is an important tin province that hosts abundant world-class deposits, some of them with high indium content. In this work, we studied the mineralizations of Japo, Santa Fe and Morococala, in the SFD, in order to understand the mineralizing processes with focus in mineral chemistry and mineralogical assemblages.

The SFD consists of a turbiditic Ordovician metasedimentary basement overlaid by a continuous sedimentary Silurian sequence represented by the Cacañiri, Llallagua and Uncia Fm. This sequence was folded and thrusted by an intense tectonic activity and is unconformably covered by the volcanic complex of the Morococala Fm., constituted by calc-alkaline lavas and tuffs of Miocene age (Grant et al., 1979). The ore mineralization is associated to felsic magmatism, represented by several generations of dykes and the San Pablo stock, of Oligocene-Miocene age (Grant et al., 1979).

Ore mineralization occurs as veins and disseminations and consists of cassiterite, sulphides and sulfosalts. A wide shear zone and two fracture systems are developed: (1) N°40, dipping 60°W, with Sn-Zn, and (2) N°40, dipping 75°E, with Zn-Pb-Ag.

Mineralogy was characterized by X-ray diffraction, scanning electron microscopy and electron probe micro-analyzer (EPMA). Mineral assemblages in the district are rather uniform but the relative contents among ore minerals vary from one deposit to another. Two main stages of mineralization are distinguished: (1) An early Sn mineralization represented by cassiterite; and (2) a late Sn and Zn-Pb-Ag mineralization, represented by sphalerite, galena, stannite group and sulfosalts.

In Japo and Morococala cassiterite and sulphides as stannite, stannoidite, sakuraiite and këwhile predominate. EPMA analyses indicate that in these mines indium content ranges between 0.12 and 0.25 wt.% in cassiterite, reaches up to 0.9 wt.% in stannite, and attains the highest concentration in sakuraiite, with up to 2 wt.%. On the other hand, in the Santa Fe mine galena, sphalerite and Ag-sulfosalts predominate. Galena shows an average silver content of 0.30 wt.% and sphalerite has indium contents up to 0.24 wt.%. Several sulphides and sulfosalts with Se, Bi and Ag contents as ourayite, gustavite, matildite, jamesonite, jaskólskiite and bismuthinite also were found.

Mineral deposition occurred in a multistage event: (1) Magmatic stage and injection of hydrothermal fluids rich in Sn; (2) metasomatism producing the alteration of metasedimentary sequences, synchronous to late magmatic stage; (3) late hydrothermal stage with sulphide deposition; and (4) supergene alteration rich in phosphates (mainly plumbogummite and crandallite).

Grant, J., Halls, C., Sheppard, S., Avila, W., Snelling, N. (1979): K-Ar ages of igneous rocks and mineralization in part of the Bolivian Tin Belt. *Econ. Geol.*, **74**, 838-851.

PGE DEPOSITS: IT'S NOT JUST ABOUT THE GRADE

Kinnaird J.A.[1], Yudovskaya M.[1], Chikwiri F.[1-2] & Hughes H.S.R.*[1]
[1] Economic Geology Research Institute, Department of Geosciences, University of the Witwatersrand, Johannesburg, South Africa
[2] Mimosa Mining, Zvishavane, Zimbabwe
Corresponding email: hannah.hughes@wits.ac.za

Keywords: platinum minerals

There is a tendency in exploration companies to assay for certain elements and to define an ore body based on results without necessarily checking the mineralogy to determine whether the element of interest can be extracted cost effectively. Without involving process mineralogy, a project may be doomed to failure. For platinum deposits, valuable lessons can be learned from the Platreef of the northern limb of the Bushveld Complex and the Great Dyke in Zimbabwe, where specific zones are not economic to process.

In the Platreef, platinum-group minerals (PGMs), are dominated by Pd-bearing tellurides, antimonides, bismuthides, bismutho-antimonides and complex bismuthotellurides (Hutchinson & Kinnaird, 2005). PGMs occur in rims around orthopyroxenes, as discrete grains within secondary silicates and as grains adjacent to, or along the margins of, composite sulphides and rarely as inclusions in sulphides. This mineral assemblage results in good PGE recovery during processing. Immiscible sulphide droplets in the magma, which scavenged platinum group elements, were later modified by the incorporation of crustally-derived S, As, Te, Bi and Sb. Felsic melts redistributed some of the sulphides and PGMs as they percolated through the Platreef. Late-stage metasomatic fluids altered the primary silicates further and remobilised the PGEs to form PGMs disseminated within tremolite, talc and serpentine. This final stage may account for the decoupling of Cu and Ni from Pt and Pd and for the distribution of very small (< 5 mm) lower temperature PGM within a meshwork of serpentine, tremolite and talc fibres (Hutchinson & Kinnaird, 2005). These small silicate-hosted PGM report to the tailings during beneficiation, so serpentinised zones are deleterious to recovery of PGE.

Where platinum deposits have oxidized zones at surface, the platinum group elements may be distributed in a completely different spectrum of minerals. For example, in the Great Dyke primary ores are sperrylite ($PtAs_2$), braggite-cooperite, RhIrPt sulpharsenides and Pt-Pd bismutho-tellurides plus gold, an assemblage of minerals that results in a good recovery of PGE. In contrast, the mineralogy of the oxidized material is very complex and PGE recovery is poor (Locmelis et al., 2010; Chikwiri, 2013), yet Prendergast (1988) estimated a resource of 389 Mt of oxidised ore for the Great Dyke. MLA studies show that relict primary PGM such as sperrylite, cooperite and braggite may remain, but there is a significant loss in PGE bismuthotellurides (particularly kotulskite) in the oxide ore and a gain in the relative proportion of electrum and secondary PGE alloys such as ferroplatinum (Chikwiri, 2013). PGE remain in solid solution in relict pentlandite (Obertur & Melcher, 2005). In addition PGE oxides and hydroxides may replace primary PGM, or be incorporated into iron or manganese oxides and hydroxides (Obertur & Melcher, 2005) resulting in an assemblage of ores that it is currently uneconomic to process.

Chikwiri, F. (2013): Comparison between the mineralogy and geochemistry of the pristine sulphide ore and oxide ore at Mimosa Mine, Zimbabwe. Honours thesis, Univ. of the Witwatersrand, 118 p.

Hutchinson, D. & Kinnaird, J.A. (2005): Complex multistage genesis for the Ni-Cu-PGE mineralisation in the southern region of the Platreef, Bushveld Complex, South Africa. *Trans. Inst. Min. Metall.*, **114**, 208-224.

Locmelis, M., Melcher, F., Oberthur, T. (2010): Platinum-group element distribution in the oxidised Main Sulfide Zone, Great Dyke, Zimbabwe. *Mineral. Dep.*, **45**, 93-109.

Oberthur, T. & Melcher, F. (2005): PGE and PGM in the supergene environment: a case study of persistence and redistribution in the Main Sulphide Zone of the Great Dyke, Zimbabwe. *in* "Exploration for platinum-group element deposits", E.J. Mungall, ed., Mineralogical Association of Canada, **35**, 97-112.

Prendergast, M.D. (1998): 8th International Platinum Symposium. Pre-symposium excursion to the Great Dyke of Zimbabwe.

RARE EARTH ELEMENT REMOBILISATION IN FELDSPARS: EXAMPLES FROM IOCG SYSTEMS IN THE OLYMPIC Cu-Au PROVINCE

Kontonikas-Charos A.*[1], Ciobanu C.L.[2], Cook N.J.[2], Ehrig K.[3] & Krneta S.[1]
[1] School of Physical Sciences, University of Adelaide, Australia
[2] School of Chemical Engineering, University of Adelaide, Australia
[3] BHP Billiton Olympic Dam, Adelaide, Australia
Corresponding email: alkiviadis.kontonikas-charos@adelaide.edu.au

Keywords: trace elements, feldspars, remobilisation

Feldspars hosted by rocks that form part of, or are associated with, Fe-oxide Cu-Au systems in the Olympic Cu-Au Province, South Australia, contain significant concentrations of trace element, either within the feldspar lattice (REE, Ga), or as sub-microscopic-scale inclusions (Fe). Observed textures imply a strong link between fluid/rock interaction and remobilisation of trace elements within individual feldspar grains, or away from the feldspar entirely. Reactions such as albitisation (replacement of initial feldspar by albite) and deuteric coarsening (recrystallisation of igneous alkali feldspars through interaction with deuteric fluids) are well constrained in terms of major element exchange. The behaviour of trace elements during fluid/rock interaction requires further constraints, however, in order to track their redistribution in the context of a mineralizing system.

Study of the Roxby Downs Granite (RDG), proximal to, and within, the Olympic Dam (OD) orebody, shows concentrations of ~ 1.5 wt.% Fe within red-stained K-feldspar from altered RDG. These concentrations are attributed to disseminated µm-sized hematite inclusions within this K-feldspar, however LA-ICP-MS spot analyses on inclusion-free areas gave similar concentrations, suggestive of Fe within the feldspar lattice. The red-stained K-feldspar is overprinted by a complex fine-grained bastnäsite-synchysite-molybdenite intergrowth and sericite. Importantly, the K-feldspar grain outline is retained, implying pseudomorphic replacement resulting from coupled dissolution-reprecipitation reactions (CDRR). Moreover, there is a decrease in ΣREE in feldspars with proximity to the orebody, thus hinting at release and remobilisation of REE from feldspars during fluid/rock interaction and CDRR.

A study on rocks from the Moonta-Wallaroo region (Kontonikas-Charos et al., 2014) supports the applicability of REE-fractionation trends in feldspars as geochemical tracers of hydrothermal alteration. Similar to trends observed at OD, measured ΣREE in feldspars from non-mineralized host rocks were greater than those from mineralized host rocks. REE mobility is further supported by spot analyses from an albite-biotite schist which reveal (hydrothermal) albite contains up to ~ 200 ppm ΣREE. Nanoscale investigations found no sign of inclusions within the albite; REE are thus interpreted to be sited in the feldspar lattice. Whole-rock ΣREE concentrations were ~ 200 ppm, indicating that albite accounts for the majority of REE. This appears to contradict the initial trend observed in mineralized host rocks, however when considering that albite formed at high fluid/rock ratios and not via CDRR, as well as the lack of REE-accessories, it is expected that albite would be the main repository. Moreover, hundreds of ppm Ga were found within K-feldspars. Nanoscale studies can constrain trace element redistribution in minerals and track their behavior from host to newly-formed phases. Considering the crustal abundance of feldspars, their role in re-concentrating critical metals such as REE and Ga cannot be ignored.

Kontonikas-Charos, A., Ciobanu, C.L., Cook, N.J. (2014): Albitization and redistribution of REE and Y in IOCG systems: Insights from Moonta-Wallaroo, Yorke Peninsula, South Australia. *Lithos*, **208–209**, 178-201.

CHEMICAL AND ISOTOPIC CHARACTERIZATION OF THE HÄMMERLEIN TIN-SKARN DEPOSIT, WESTERN ERZGEBIRGE, GERMANY

Lefebvre M.*[1], Romer R.L.[1] & Roscher M.[2]
[1] Helmholtz Zentrum Potsdam, GFZ Deutsches GeoForschungsZentrum, Potsdam, Germany
[2] Saxore Bergbau GmbH, Freiberg, Germany
Corresponding email: lefebvre@gfz-potsdam.de

Keywords: tin-skarn, indium, Erzgebirge

The Hämmerlein Sn-skarn deposit of the Western Erzgebirge is associated with schists and gneisses that reached peak metamorphic conditions at 340 Ma. The skarns formed around 320-325 Ma, when the Eibenstock granite was emplaced and magmatic fluids migrating along the contacts of different lithological units induced decarbonation of the marble layers, resulting in the development of a series of contrasting skarn types. The different units of the deposit are magnetite skarn, garnet skarn, pyroxene skarn, sulphide skarn and amphibole skarn with intercalated layers of gneiss and schist. Cassiterite is the major ore mineral. In the schists, it typically forms coarse grains (up to 1 mm) and in the various skarns ranging from fine-grained (< 100 µm) and fine disseminated to coarse > 1 mm grains and agglomerates. Relatively high content of In has been found in exsolutions of Cu-Zn-Fe sulfides in chalcopyrite patches within the magnetite skarn and in the Fe-rich sphalerite layer beneath the magnetite skarn.

Fluids inducing the skarn-forming reactions enriched the rocks in Sn, W, In, Cd, Sb and F. The enhanced contents of As, Bi, and U in the skarn, however, are likely to be related to later events, as there is important *ca.* 180 Ma old U mineralization in the region and this U mineralization typically shows multiple later redistributions with addition of As and Bi. REE seem to have been largely immobile and to be inherited from the protoliths, as indicated by the REE pattern and the Nd isotopic composition. All skarns are characterized by similar flat UCC-normalized REE pattern with a positive Eu anomaly, whereas, the schists and gneisses do not have a positive Eu anomaly and their patterns show slightly higher LREE contents. The REE pattern of cassiterite-bearing schists is the same as the one of unmineralized schists. The εNd values of skarns and schists overlaps correspond to those of the unmetamorphosed sediments and are markedly lower than those of the granite. The distribution of Sn and In within different skarn units is heterogeneous, indicating that mineralization is not controlled by fluid-flow alone, but also by precipitation at reaction fronts with selective mineralogically controlled scavenging of ore elements and the reaction history of the fluid, in particular whether the fluid had lost its metal content during earlier fluid-induced reactions.

PRELIMINARY FINDINGS ON THE DISTRIBUTION AND ENRICHMENT OF TELLURIUM (Te) AND SELENIUM (Se) IN HYDROTHERMAL ORE DEPOSITS OF THE TROODOS OPHIOLITE, CYPRUS

Martin A.J.*[1], McDonald I.[1], Prichard H.M.[1] & MacLeod C.J.[1]
[1] School of Earth and Ocean Sciences, Cardiff University, United Kingdom
Corresponding email: MartinAJ4@cardiff.ac.uk

Keywords: Troodos, hydrothermal, tellurium

Tellurium and selenium are identified as critical elements in low carbon energy technologies under the European Union's Strategic Energy Technology Plan (SET-Plan) (Moss et al., 2013). The use of Te and Se within photovoltaic cells (CdTe and CIGS) underpins their strategic importance within the EU and rest of the World. The criticality of these metals stems from the potential for significant growth in demand due to a transition to low carbon, solar dominated energy production (38 GW in 2010 to 630 GW in 2030- Moss et al., 2013), their low crustal abundance (0.002 mg/kg Te and 0.05 mg/kg Se; Perkins, 2011) and their secondary (by-product) nature of production through the refining of copper (approximately 90%; Lu et al., 2015). Global Te production in 2010 was 0.50 Kt and projections by Moss et al. (2013) suggest that by 2030 the EU will consume over 50% of global Te production.

The future economic importance and significance of Te and Se in emerging technologies is paralleled by a poor understanding of the source, mobilisation and concentration of Te and Se within hydrothermal ore deposits. Te and Se have been of little interest in the recent past as production from copper refining has kept pace with global demand, and it is evident this will not suffice in the future with demand set to significantly outstrip supply.

This study aims to locate and understand the processes that concentrate Te and Se in Cu-rich VMS systems (historically important sources of these critical elements).and the classic VMS deposits associated with the Troodos ophiolite have been chosen as a test case. Troodos is widely accepted to represent a suprasubduction oceanic spreading environment (Gass, 1980) and hosts numerous Cyprus type Cu rich VMS deposits (see Adamides, 2010a, 2010b). This Study will utilise high resolution (ICP-MS) soil sample data collected from the whole of the southern part of Cyprus (Cohen et al., 2012) to investigate Te and Se in rocks underlying soil anomalies.

Te and Se have never before been investigated within the Troodos ophiolite hydrothermal system. The results presented here aim to provide initial evidence on the distribution of Te and Se within both "on and off axis" hydrothermal systems, specifically the Au-Te system. Silicification occurs within umbers (chemical sediments) and many VMS deposits (e.g., Agrokipia and Mathiati) and has been shown to be responsible for ppm level Au mineralisation (Prichard & Maliotis, 1998). The implications of secondary silicification and fluid flow post VMS deposit formation have never been investigated for Te and Se. The current portion of this study presents preliminary findings from the 2016 field season on the concentration and distribution of Te and Se within both on-axis VMS type mineralisation and silicificied deposits located off-axis.

Adamides, N. (2010a): Mafic-dominated volcanogenic sulphide deposits in the Troodos ophiolite, Cyprus. Part 1- The deopsits of the Solea graben. *Appl. Earth Sci.*, **119**, 65-77.

Adamides, N. (2010b): Mafic-dominated volcanogenic sulphide deposits in the Troodos ophiolite, Cyprus. Part 2- A review of genetic models and guides for exploration. *Appl. Earth Sci.*, **119**, 193-204.

Cohen, D.R, Rutherford, N.E, Morisseau, E., Zissimos, A.M. (2011): Geochemical atlas of Cyprus. University of New South Wales Press, Sydney, 144 p.

Gass, I.G. (1980): The Troodos massif: Its role in the unravelling of the ophiolite problem and its significance in the understanding of constructive plate margin processes. *in* "Ophiolites - Proceedings: International Ophiolite Symposium, Cyprus 1979", Geological Survey Department, Ministry of Agriculture and Natural Resources, Nicosia, Cyprus, 23-35.

Lu, D., Chang, Y., Yang, H., Xie, F. (2015): Sequential removal of selenium and tellurium from copper anode slime with high nickel content. *Trans. Nonferrous Met. Soc. China*, **25**, 1307-1314.

Moss, R.L., Tzimas, E., Kara, H., Willis, P., Kooroshy, J. (2013): The potential risks from metals bottlenecks to the deployment of Strategic Energy Technologies. *Energy Pol.*, **55**, 556-564.

Perkins, W.T. (2011): Extreme selenium and tellurium contamination in soils – An eighty year-old industrial legacy surrounding a Ni refinery in the Swansea Valley. *Sci. Total Environ.*, **412-413**, 162-169.

Prichard, H.M. & Maliotis, G. (1998): Gold mineralization associated with low-temperature, off-axis, fluid activity in the Troodos ophiolite, Cyprus. *J. Geol. Soc.*, **155**, 223-231.

FORMATION CONDITIONS OF TWO PHOSPHORITE OCCURRENCES FROM THE TRANSDANUBIAN MOUNTAIN RANGE (HUNGARY)

Molnár Z.*[1], Kiss G.B.[1], Zaccarini F.[2], Dunkl I.[3] & Dódony I.[1]
[1] Department of Mineralogy, Eötvös Loránd University, Budapest, Hungary
[2] Department Angewandte Geowissenschaften und Geophysik, Universität Leoben, Austria
[3] Geowissenschaftlichen Zentrum, Universität Göttingen, Germany
Corresponding email: molnarzsuzsa89@gmail.com

Keywords: U and REEs, anoxic

The carbonate-dominated Mesozoic sequence of the Transdanubian Mountain Range contains layered phosphorite in Triassic (near Pécsely) and nodular phosphorite in Cretaceous (near Tata) strata. Uranium enrichment has been already proven in the Triassic phosphorite layers (Kiss & Virágh, 1958), in contrast, the detailed chemical composition of the Cretaceous one (Fülöp, 1975) has not been studied, yet. The study of these formations is necessary because they may contain critical elements (REEs).

The LA-ICP-MS U-Pb age is 237±11 Ma of the Triassic phosphorite, which coincides well with the stratigraphic age of the host limestone. The main mineral is carbonate-fluorapatite, however calcite and rarely hematite also occur. According to EPMA analyses, the U enrichment in the phosphorite layer is most likely related to the carbonate-fluorapatite, as it contains 0.023-0.3 mass% U. Based on ICP-MS and ICP-OES studies a total REE+Y content of 116-158 ppm was proven.

The Cretaceous nodular phosphorite occurs at the basis of the Aptian grey, crinoid-bearing limestone. The main minerals of the crust around the bio- and siliciclasts are apatite, calcite, quartz, glauconite and Fe-oxide-hydroxides. According to EPMA studies, it contains a small amount of U (< 0.041 mass%), and based on ICP-MS and ICP-OES analyses a total REE+Y content of 1055 ppm was proven.

According to the whole rock geochemical analyses, many similarities and differences can also be observed. The patterns of the REE distribution diagrams are very similar; however some differences appear when the data are normalised to the North Atlantic Shale Composite (NASC). The Triassic phosphorite is slightly depleted relative to the NASC, in contrast the Cretaceous phosphorite shows strong enrichment. The Triassic samples indicate negative Ce and Eu anomaly, whereas the Cretaceous ones show positive anomaly. Based on the redox-sensitive proxies defined by Morford & Emerson (1999), such as Th/U, V/Sc ratios and REEs, both phosphorite occurrences formed in anoxic environment, however the Cretaceous was closer to the suboxic conditions.

The structure and texture of the Cretaceous phosphorite strongly differ from the Triassic one, indicating principal differences in their formation. The phosphorite from Pécsely formed with prolonged bathing of seamounts in oxygen-minimum zone water and the formation mechanism was direct, inorganic precipitation. The Cretaceous occurrence formed as a direct result of concentrionary growth from cold, ascending (upwelled) seawater in continental margin environment. The described models are supported by the known geological background also.

Fülöp, J. (1975): Tatai Mezozóos alaphegységrögök. *Geol. Hung.*, **16**, 1-225.

Kiss, J. & Virágh, K. (1958): An uranium-bearing phosphatic rock in the Triassic of the Balaton Uplands around Pécsely. *Bull. Hung. Geol. Soc.*, **89**, 85-97.

Morford, J.L. & Emerson, S. (1999): The geochemistry of redox sensitive trace metals in sediments. *Geochim. Cosmochim. Acta*, **63**, 1735-1750.

CRITICAL ELEMENTS IN NONSULFIDE ZINC DEPOSITS

Mondillo N.*[1-2], Herrington R.J.[2], Boni M.[1] & Arfé G.[1]
[1] Dipartimento di Scienze della Terra, dell'Ambiente e delle Risorse, Università Federico II, Napoli, Italy
[2] Department of Earth Sciences, Natural History Museum, London, United Kingdom
Corresponding email: nicola.mondillo@unina.it

Keywords: nonsulfide Zn deposits, critical elements, germanium

Nonsulfide zinc ore is a very general term, describing a group of supergene and hypogene deposits mainly consisting of Zn-oxidized minerals (Hitzman et al., 2003). Sulfide deposits that commonly are progenitors of nonsulfide mineralization contain sphalerite, which is a known host for gallium, germanium and indium. The aim of the present study is to understand the mobility of the critical element Ge during sulfide oxidation and the formation of secondary nonsulfide ores. Germanium has geochemical affinity to both Si^{4+} and Fe^{3+}, and this can produce a concentration of this element in both silicates and Fe-oxy-hydroxides. It has been shown that supergene alteration has increased the Ge grade in the Tsumeb-type deposits, where primary germanite and renierite are altered to secondary Ge-minerals (Höll et al., 2007). Economic Ge grades have been also measured in hydrothermal minerals like willemite (Tres Marias mine, Mexico; Saini-Eidukat et al., 2009).

To determine the mineral residence of Ge in nonsulfide Zn deposits we conducted a focused program of sampling and analysis on specimens from the Natural History Museum (NHM) collections in London, and on material we collected personally in selected mines and prospects.

The most relevant results were obtained on a batch of Kabwe (Kamona & Friedrich, 2007) specimens from the NHM Ores collection, and on drillcore samples of the Rio Cristal (Bongará) prospect in Peru. Kabwe (Broken Hill, Zambia) is a carbonate-hosted sulfide Zn-Pb deposit, where sphalerite, galena, pyrite, chalcopyrite and accessory Ge-sulfides are patchily replaced by the hydrothermal Zn-silicate willemite. The entire assemblage is overprinted by minerals typical of the supergene environment: smithsonite, cerussite, hemimorphite, sauconite, pyromorphite, Pb-vanadates and Fe-oxy-hydroxides.

The Rio Cristal prospect (Bongarà, Peru) is a typical smithsonite-rich nonsulfide deposit, deriving from a deep weathering process of an original MVT sphalerite-bearing orebody. In the analyzed drillcores, several gossanous samples contain enhanced amounts of goethite and hemimorphite.

Whole rock chemical analyses and laser ablation on Zn silicates and Fe-oxy-hydroxides from the two deposits have shown that at Kabwe Ge is only hosted in willemite, not in typical supergene phases; at Rio Crystal, instead, the highest Ge amounts are associated with hemimorphite and goethite.

From the present dataset, it seems that the abundance of willemite at Kabwe prevents any Ge-concentration in supergene hemimorphite and goethite. Being the first sulfide-replacing mineral, willemite incorporated most of Ge previously contained in Zn- and Ge-sulfides, not favoring a Ge-enrichment in any other supergene phase. It follows that the absence of willemite in the Rio Crystal ores may be critical for Ge-behaviour in other supergene minerals, and Fe-oxy-hydroxides and hemimorphite probably acted almost exclusively as adsorption agents for remobilized Ge.

Hitzman, M.W., Reynolds, N.A., Sangster, D.F., Allen, C.R., Carman, C.E. (2003): Classification, genesis, and exploration guides for nonsulphide Zinc deposits. *Econ. Geol.*, **98**, 685-714.

Höll, R., Kling, M., Schroll, E. (2007): Metallogenesis of germanium – A review. *Ore Geol. Rev.*, **30**, 145-180.

Kamona, A.F. & Friedrich, G.H. (2007): Geology, mineralogy and stable isotope geochemistry of the Kabwe carbonate-hosted Pb-Zn deposit, Central Zambia. *Ore Geol. Rev.*, **30**, 217-243.

Saini-Eidukat, B., Melcher, F., Lodziak, J. (2009): Zinc-germanium ores of the Tres Marias Mine, Chihuahua, Mexico. *Mineral. Dep.*, **44**, 363-370.

GOLD MINERALIZATION IN THE NEVES-CORVO VHMS DEPOSIT

Pinto A.M.M.*[1], Relvas J.M.R.S.[1], Barriga F.J.A.S.[1], Carvalho J.R.S.[1], Liu Y.[2], Pacheco N.[3], Fonseca R.[3], Santos S.[3], Caetano P.[3], Reis T.[3] & Gonçalves M.[3]

[1] Institute Dom Luis, Faculty of Sciences, University of Lisbon, Portugal

[2] Department of Earth Sciences, University of Toronto, Canada

[3] Somincor / Lundin Mining, Neves Corvo Mine, Portugal

Corresponding email: alvaro.pinto@fc.ul.pt

Keywords: gold, Neves-Corvo, Iberian pyrite belt

The Neves-Corvo deposit locates in the Iberian Pyrite Belt and embraces seven massive sulphide orebodies, as follows: Neves, Corvo, Graça, Lombador, Zambujal, Semblana and Monte Branco. Since 1988, the deposit has been a significant copper producer worldwide, and the larger base metal-mining operation in EU. After 15 years of operation for tin (1990-2005), the production of cassiterite concentrates was interrupted. Since 2006, Neves-Corvo operates for copper and zinc, having lead and silver as economic by-products. Indium and selenium, although recognized in the deposit, do not add value to the mining operation.

In Neves-Corvo, gold occurs mostly associated with the copper-rich ores. Significant gold contents and high maximum gold grades (up to 95 ppm) have been found in the stockwork and at the base of the copper-rich ores of the Lombador and Neves North orebodies (Pinto et al., 1994; Ferreira et al., 1997). Gold is distributed in two different types of stringer mineralization: the barren stockworks and the copper-rich stockwork ores. In the first case, gold occurs as micro-inclusions in arsenopyrite. However, in restricted domains of the Neves North orebody, gold occurs in the bornite-rich ores, a complex metal suite with high-sulphidation mineralogy, very rich copper grade and high Sn, Sb, Se and In (Pinto et al., 1998, 2005).

The Lombador oreboby has the highest potential for economic gold mineralization. Recent research at this orebody has investigated the gold contents of its copper (up to 3,36 ppm Au), zinc (up to 3,02 ppm Au) and copper-zinc (up to 1,25 ppm Au) massive ores, and of two different types of copper-rich stockwork ores (5,46 and 22,6 ppm Au, respectively). The mineral carriers for gold include native gold, electrum, chalcopyrite (up to 900 ppm Au), sphalerite (up to 1100 ppm Au) and pyrite (up to 175 ppm Au). Native gold and electrum have only been found in the stringer copper ores. Native gold occurs as inclusions in alloclasite and/or as small grains distributed along the alloclasite-arsenopyrite contacts. Two generations of Se- and Ge-bearing alloclasite were identified, both containing nickel. Late alloclasite has up to 0,4% Ni, whereas the early alloclasite, which nickel content goes up to 3,5%, contains some gold inclusions and adsorption droplets.

Gold, as electrum, occurs with chalcopyrite, fahlore and sphalerite. Moreover, gold occurs with native bismuth and bismuth minerals. Native bismuth in the deeper parts of the stockworks indicates prevalence of low sulphur activity. Upward increase of sulphur activity and gradual, solubility-controlled availability of other metals, accounted for replacement of bismuth by lead and copper to form galenobismutite and late Cu-Pb-Bi-sulphosalts, such as lindstromite, nufieldite, giessenite and junoite.

Full understanding of gold mineralization at Neves-Corvo remains an open issue.

Acknowledgements: This is a contribution to ZHINC project (PTDC/CTE-GIX/114208/2009). S. Scott is gratefully acknowledged.

Ferreira, A., Pinto, A.M.M., Bowles, J.F.W. (1997): The occurrence of gold in the Neves Corvo ore deposit, Portugal. Neves Corvo Field Conference Abstracts, Society of Economic Geologists, Lisbon.

Pinto, A.M.M., Bowles, J.F.W., Gaspar, O.C. (1994): The mineral chemistry and textures of wittichenite, miharaite, carrolite, mawsonite and In-Bi-Hg tennantite from Neves Corvo, Portugal. XVI General Meeting of IMA, Pisa, Italy, abstr.

Pinto, A.M.M., Marion, P., Ferreira, A. (1998): Caracterização do ouro invisível em “minérios” FE da massa de Neves Norte do Jazigo de Neves Corvo. V Congresso Nacional de Geologia, Lisboa.

Pinto, A.M.M., Bowles, J.F.W., Benzaazoua, M., Marion, P., Ferreira, A., Barriga, F.J.A.S. (2004): Gold Mineralization at the Neves Corvo Ore Deposit, Portugal. 32nd International Geological Congress, Florence.

Pinto, A.M.M., Relvas, J.M.R.S., Barriga, F.J.A.S., Munhá, J., Pacheco, N., Scott, S.D. (2005): Gold mineralization in recent and ancient volcanic-hosted massive sulfides: the PACMANUS field and the Neves Corvo deposit. *in* “Mineral Deposit Research: Meeting the Global Challenge, Vol. 1”, J. Mao, F.P. Bierleing, Eds., Springer, Berlin-Heidelberg, 683-686.

MALAYAITE AND OTHER TIN-BEARING MINERALS IN THE TUNGSTEN SKARN OF TABUAÇO, NORTHERN PORTUGAL

Ramos V.*[1], Guedes A.[1-2] & Noronha F.[1-2]
[1] Institute of Earth Sciences, University of Porto, Portugal
[2] Department of Geosciences, Environment and Spatial Planning, University of Porto, Portugal
Corresponding email: violetaramos@fc.up.pt

Keywords: malayaite, W-skarn, Portugal

Tabuaço W-skarn is located in Northern Portugal. Recent exploration works revealed the presence of a series with two main skarn horizons with scheelite mineralization: the "Upper Horizon" or "Main Horizon"; and the "Lower Horizon" (Colt, 2016). Both are separated by schists and are below an important carbonate rich barren horizon the "Upper Carbonate Horizon" that corresponds to an impure limestone, and above black schists. This series belongs to the "Douro Supergroup", Upper Precambrian in age, in the contact with a Variscan peraluminous granite. The skarns are composed by vesuvianite, fluorite, scheelite, calcite, apatite, quartz, plagioclase, K-feldspar, epidote group minerals, pyroxene, sericite, garnet and amphibole. Besides scheelite, scarce Sn minerals and rare sulphides (sphalerite and arsenopyrite) are also present. Currently, the Tabuaço W deposit is one of the European sites investigated under the scope of project FAME (Flexible and Mobile Economic Processing Technologies) that focuses on improving processing technologies and to recover valuable materials from low grade and/or complex feedstock's ore. This contribution focus on the occurrence of malayaite, stokesite and cassiterite association that has never been described in Portuguese deposits. Several analytical techniques were used for their identification, namely, optical microscopy, scanning electron microscopy, Raman microspectroscopy and electron microprobe. Combining the structure of the skarn and how W and Sn minerals occur, three main types of mineralized skarns are considered: M Type **–** layered to massif, whitish to light greyish, medium to coarse-grained with coarse scheelite (> 500 mm); L Type **–** layered with light greenish and pinkish zones, fine to medium-grained; and F Type **–** fine grained scarcely layered to massif, brownish with fine scheelite (< 250 mm). Malayaite ($CaSnSiO_5$), characterized by a greenish yellow fluorescence colour under short UV light, occurs typically with a bipyramidal shape included in vesuvianite. It is more abundant near late fractures, cutting F-type skarn. Malayaite is replaced by cassiterite, fluorite, quartz and calcite. Furthermore, WDS analysis confirmed the existence of a solid solution between malayaite and titanite, which presents Al, Fe and Ti in its structure. Stokesite ($CaSnSi_3O_9 \cdot 2H_2O$) is present in microcracks cutting vesuvianite. It is suggested that there were at least two episodes of Sn-mineralization: an earlier one, corresponding to the crystallization of malayaite and a later one responsible for stokesite and cassiterite deposition. Malayaite is regarded as stable at relatively high temperature (400-500°C), alkaline conditions, but can also form at low temperature if the system is sufficiently poor in CO_2 and HF. Stokesite is stable in more basic conditions and lower temperatures than malayaite, while cassiterite occurs at low temperature (300-400°C) and acid conditions (rich in CO_2 and HF) (Burt, 1978; Plimer, 1984; Zhiji, 1984).

Burt, D.M. (1978): Tin silicate-borate-oxide equilibria in skarns and greisens – the system CaO-SnO_2-SiO_2-H_2O-B_2O_3-CO_2-F_2O_{-1}. *Econ. Geol.*, **73**, 269-282.

Colt (2016). http://coltresources.com/tabuaco/ (accessed on 3rd May, 2016).

Plimer, I.R. (1984): Malayaite and tin-bearing silicates from a skarn at Doradilla via Bourke, New South Wales. *Austr. J. Earth. Sci.*, **31**, 147-153.

Zhiji, R. (1984): Geochemical characteristics of tin-bearing magnetite-skarns. *Chinese J. Geochem.*, **3**, 115-127.

MINERALOGY OF SMELTER- AND MINING-DERIVED PARTICULATES DEPOSITED IN SEMI-ARID SOILS

Tuhý M.*[1], Ettler V.[1] & Mihaljeviè M.[1]
[1] Institute of Geochemistry, Mineralogy and Mineral Resources, Charles University, Prague, Czech Republic
Corresponding email: tuhymar@gmail.com

Keywords: mining, smelting, semiarid soils

This paper is focused on contaminated semiarid area near an operating copper smelter and old mine-tailing disposal sites in Tsumeb in the northern Namibia, where copper, lead, zinc and to lesser extent silver and germanium were historically mined. It has already been demonstrated that soils and plants from this area are highly polluted by dust particles originating from mining and mineral processing activities (Kribek et al. 2016; Mihaljeviè et al. 2015). In this paper, we focus on the mineralogy of mining and smelter-derived particulates extracted from topsoils (litter, n = 4) and biomass samples (n = 2) collected in this area (litter from marula and acacia trees, grass samples).

The soil and biomass samples were digested in mineral acids and analysed by ICP-MS. High levels of inorganic contaminants were found: up to 5800 mg Cu kg^{-1}, 1920 mg As kg^{-1}, 4880 mg Pb kg^{-1}, 3310 mg Zn kg^{-1}. Highest levels of contaminants occurred especially in the fined-grained fractions (<2 mm). Moreover, main part of contaminants was bound in the mineral samples (soils) in contrast to organic carbon-rich biomass samples.

Scanning electron microscopy coupled with energy dispersion spectrometry (SEM/EDS) and electron probe microanalysis (EPMA) were used for the identification of the metal(loid)-bearing phases in heavy mineral fraction of the soil and biomass samples. Spherical particles, which originate from the smelting process were observed. Secondly angular shaped grains were probably transported directly by wind during the ore processing or from nearby mine-tailing disposal sites.

Bushfires can be responsible for transformation and remobilization of particles from the polluted topsoils and biomass. We plan to perform thermal soil/biomass burning experiment to understand the extent of such transformation processes under conditions simulating bushfires in this area.

Acknowledgements: This study was supported by the Czech Science Foundation (GAÈR 13-17501S).

Køíbek, B., Majer, V., Knésl, I., Keder, J., Mapani, B., Kamona, F., Mihaljevic, M., Ettler, V., Penížek, V., Vanìk, A., Sracek, O. (2016): Contamination of soil and grass in the Tsumeb smelter area, Namibia: Modeling of contaminants dispersion and ground geochemical verification. *Appl. Geochem.*, **64**, 75-91.

Mihaljeviè, M., Ettler, V., Vanìk A., Penížek, V., Svoboda, M., Køíbek, B., Sracek, O., Mapani, B., Kamona, A. (2015): Trace elements and the lead isotopic record in Marula (Sclerocarya Birrea) tree rings and soils near the Tsumeb Smelter, Namibia. *Water Air Soil Pollut.*, **226**, 177.

CRITICAL METALS IN THE ORES OF THE SVETLINSK Au-Te DEPOSIT, SOUTHERN URALS

Vikent'eva O.*[1], Vikentyev I.[1] & Bortnikov N.S.[1]

[1] Institute of Geology of Ore Deposits, Petrography, Mineralogy, and Geochemistry, Russian Academy of Sciences, Moscow, Russia

Corresponding email: ovikenteva@rambler.ru

Keywords: critical metals, gold deposit, LA-ICP-MS

The large Svetlinsk gold-telluride deposit occurs within the volcano-sedimentary rocks (metabasite, terrigenious/volcanoclastic sediments and marble) metamorphosed up to amphibolitic facies. The gold-sulfide-telluride-quartz veins and veinlets are superimposed onto the disseminated pyrite-pyrrhotite mineralization. The bulk analyses revealed that gold ores contained (in ppm) 5-17 Sb, 4-7.3 Te and 2.5-4 Se. This communication describes the minerals that are the carriers of the critical metals.

Two groups of critical minerals were found. The critical metals such as Te, Sb, Co, and Ni are those that are the major constituents of minerals. Some metals are the isomorphic admixture in the second group of minerals.

Tellurides are typical minerals for this deposit. Melonite $NiTe_2$, frohbergite FeTe, altaite PbTe, tsumoite BiTe, tellurantimony Sb_2Te_3, Au-Ag tellurides (calaverite $AuTe_2$, sylvanite $AuAgTe_4$, krennerite $(Au,Ag)Te_2$, petzite $AuAg_3Te_2$, hessite Ag_2Te, γ-hessite $Ag_{1,9}Te$, χ-phase $Ag_{3.3\text{-}3.4}Au_{0.5\text{-}0.6}Te_{1.9\text{-}2.0}$), as well as volynskite $AgBiTe_2$ and tetradymite Bi_2Te_2S occur in ores.

Tetrahedrite is a main Sb mineral is, whereas the tellurantimony, ullmannite (NiSbS), bournonite ($CuPbSbS_3$) are occasionally found. Two generations of tetrahedrite were discovered. Early Zn-tetrahedrite ($Cu_{9.6\text{-}9.8}Zn_{1.5\text{-}1.8}Fe_{0.2\text{-}0.5}Sb_{3.9\text{-}4.4}S_{12.7\text{-}13.2}$) is associated with chalcopyrite and Co-Ni arsenides ($Fe_{0.17\text{-}0.19}Ni_{0.34\text{-}0.36}Co_{0.45\text{-}0.47}As_{0.94\text{-}0.95}S_{1.04\text{-}1.07}$ and $Fe_{0.30}Ni_{0.64}As_{0.95}S_{1.06}$), ullmannite and bournonite. Late Ag-rich tetrahedrite ($Cu_{9.43\text{-}9.81}Ag_{0.29\text{-}0.71}Zn_{0.78\text{-}1.14}Fe_{0.83\text{-}1.14}Cd_{0.01\text{-}0.04}Pb_{0.01}Sb_{3.49\text{-}3.62}As_{0.14\text{-}0.26}Bi_{0.01\text{-}0.04}S_{12.92\text{-}13.25}Se_{0\text{-}0.02}$) is closely associated with tellurides (hessite, tsumoite, petzite) and native gold.

Unnamed mineral phases AuSbTe, $SbBi_2Te_4$, $SbBiTe_3$ and Au_3Sb_2 have been found in the gold ores.

First laser ablation-inductively coupled plasma-mass spectrometry (LA-ICP-MS, LabMaTer at the Université du Québec à Chicoutimi) data have been obtained for pyrites from the disseminated pyrite-pyrrhotite mineralization (Py I) and from the gold-sulfide-telluride-quartz veins (Py II). Py I contains (in ppm) Te 4.6-192, Sb 0.1-50.8, Co 11.7-6088, Ni 2.5-2382, Ga 0.1-47, Ge 0.1-5.3, V 1.3-102, Cr 0.1-27, Se 2.2-71, In up to 4.2; while Py II bears Te 1.9-26.5, Sb 0-8.7, Co 38-331, Ni 115-587, Ga up to 3.4, Ge 0.2-0.5, V 0.1-95, Cr up to 13.6, Se 3.5-15, In below the detection limit. Both early and late pyrites in some probes contain Pd (up to 0.1 ppm). The positive correlation between the contents of Au, Ag and Te was found in Py I and Py II. Sb content correlates with Au in Py II. This may indicate the presence of nanoscale inclusions of petzite Ag_3AuTe_2, hessite Ag_2Te and aurostibite $AuSb_2$ in pyrite. Cu-rich pyrite (I and II) and Ni-rich Py II contain detectable value of Pd.

The data obtained should be considered for the improvement of the processing of primary gold ores.

Acknowledgements: This work was supported by Rus. Sci. Found. (14-17-00693) & Prog.4 of Presidium of RAS.

OCCURRENCES OF PLATINUM GROUP MINERALS (PGM) AND OTHER RARE ACCESSORY PHASES IN ITALY: WHERE AND WHY

Zaccarini F. *[1] & Garuti G.[1]
[1] Department Angewandte Geowissenschaften und Geophysik, Universität Leoben, Austria
Corresponding email: federica.zaccarini@unileoben.ac.at

Keywords: platinum group minerals, Ivrea-Verbano zone, Italy

Platinum group minerals (PGM) have been described in the Ivrea-Verbano zone, western Alps, Italy. The Ivrea-Verbano Zone consists of mantle-derived magmas (the basic complex) underplated beneath - or intruded into - the lower crust of the Adria continent composed of amphibolite to granulite grade metasediments and metavolcanics (the kinzigitic series). This regional magmatic event was driven by thinning of the continental crust with associated uplift of a mantle plume, whose relicts are the Finero, Balmuccia, and Baldissero mantle massifs. The PGM occur as tiny, generally less than 10 microns, and accessory phases in two different types of ore deposits: magmatic Ni-Cu-Fe sulphides and chromitite. The Ni-Cu-Fe sulphides had been mined for Ni in the last century and they can be divided in three distinct groups of mineralizations: 1) layers in the peridotite-pyroxenite-gabbro-anorthosite basic complex, 2) ultramafic sill intruding metasediments, 3) ultramafic discordant pipes in gabbros and metasediments. The ore minerals mainly consist of base metals sulphides (BMS) such as pyrrhotite, pentlandite and chalcopyrite. The most abundant PGM are tellurides of Pt and Pd that belong to the merenskyite-moncheite-melonite series, accompanied by minor sperrylite and irarsite. Also a Re sulphide, probably rheniite, molybdenite, hessite, electrum and cobaltite were analyzed. PGM and rheniite occur associated with the BMS. Trace amounts of platinum group elements (PGE) have been detected in the BMS. These observations suggest that PGE and chalcogenides were initially collected by an immiscible sulphide liquid. After, they were exsolved together with Te and As to form discrete PGM. Rheniite probably formed because a reaction between the mafic-ultramafic magma and the host metasediments. Small pods and schlieren of chromitites have been reported in peridotites from the subcontinental metasomatic mantle of the Finero complex. They have been only prospected but never mined. The PGM recognized in Finero form small grains generally included in chromite. They consist of laurite and thiospinels of the cuproiridsite-cuprohodsite-malanite series. Rare specific phases of Rh, that probably represent new minerals species, have been also analyzed. Other accessory minerals described in the Finero chromitites are uraninite, thorianite or huttonite, baddeleyite, zircon and zirconolite. The Finero PGM crystallized at high temperature during the magmatic stage and under relatively high S fugacity. The presence of Zr-Th-U minerals suggests the presence of a carbonatitic metasomatic agent. The accessory minerals described in the magmatic Ni-Cu-Fe sulphides and chromitite of the Ivrea-Verbano zone indicate that their host deposits may represent an uncommon type of mineralization formed in an extensional regime during an underplating event occurred in the deep crust.

Session S24:

The petrology-geochronology connection

Conveners:

Robert Anczіewicz (London – United Kingdom)

Daniela Rubatto (Bern – Switzerland)

Igor Villa (Milano – Italy)

DETECTION OF DISTINCT CRUSTAL DOMAINS IN THE SOUTHERN GRANULITE TERRANE (SOUTH INDIA) BY LA-ICP-MS ZIRCON DATING, AND IMPLICATIONS FOR THE GONDWANA FORMATION

Brandt S.*[1], Raith M.M.[2], Schenk V.[3], Sengupta P.[4], Srikantappa C.[5] & Gerdes A.[6]
[1] GeoZentrum Nordbayern, Universität Erlangen-Nürnberg, Erlangen, Germany
[2] Steinmann-Institut für Geologie, Mineralogie und Paläontologie, Universität Bonn, Germany
[3] Institut für Geowissenschaften, Christian-Albrechts-Universität Kiel, Germany
[4] Department of Geological Sciences, Jadavpur University, Kolkata, India
[5] Department of Geology, University of Mysore, India
[6] Institut für Geowissenschaften, Goethe-Universität Frankfurt am Main, Germany
Corresponding email: soenkesoeren.brandt@web.de

Keywords: Southern Granulite Terrane, U-Pb zircon dating, Gondwana

The Southern Granulite Terrane of India is a key area for reconstructing the evolution of the late-Neoproterozoic supercontinent Gondwana. Based on LA-ICPMS U-Pb zircon dating for felsic orthogneisses, meta-anorthosites and granites we have identified two distinct crustal domains in the Madurai Province, the major part of the Southern Granulite Terrane. The Western Madurai Domain is largely composed of a late-Neoarchaean (2.53-2.46 Ga) subduction-related, magnesian granitoids, which were reworked during early-Palaeoproterozoic (2.47-2.43 Ga) granulite facies metamorphism and partial melting. The Eastern Madurai Domain is dominated by a vast supracrustal sequence, which was deposited on a mid- to late-Palaeoproterozoic (2.05-1.62 Ga) basement of magnesian felsic orthogneisses. Both domains of the Madurai Province were intruded by voluminous mid-Neoproterozoic (0.83-0.79 Ga) A-type granites during a major phase of extensional rifting. A-type granite magmatism was coeval with the emplacement (0.795 Ga) of the massif-type Kadavur Gabbro Anorthosite Complex. Regional mid-Neoproterozoic (0.82-0.74 Ga) metamorphism is temporally and spatially related to the anorthosite and A-type granite magmatism. Convergence of the two domains in the late-Neoproterozoic (ca. 0.55 Ga) culminated in their collision along a SSW-NNE-trending belt of ultrahigh-temperature metamorphic rocks, the Kambam-*UHT*-Belt, and was associated with the intrusion of leucogranites (0.56-0.53 Ga). Accretion of the Madurai Province to the Archaean Dharwar Craton occurred in the earliest Palaeoproterozoic along the Moyar-Bhavani-Cauvery Suture, a distinct crustal domain characterized by late-Neoarchaean (2.50 Ga) subduction-related, magnesian felsic orthogneisses. These resemble the age and composition of the Western Madurai Domain orthogneisses, and intruded Mesoarchaean felsic orthogneisses (2.85 Ga) and (ultra)basic complexes, which represent remnants of oceanic crust. The suture zone was, coeval with the Western Madurai Domain, affected by early-Palaeoproterozoic (2.49-2.45 Ga) *HP*-granulite facies metamorphism and only locally affected by an early-Cambrian overprint (0.54 Ga). The inferred early-Palaeoproterozoic accretion of the Madurai Province to the Dharwar Craton and the extension-related origin of the voluminous mid-Neoproterozoic A-type granites are at variance with the recently proposed concept of a Neoproterozoic subduction zone and suture separating the craton from the Madurai Province (e.g., Santosh et al., 2012; Collins et al., 2013). In a Gondwanan palaeogeographic model we link the dominantly Neoarchaean Western Madurai Domain with the Antananarivo Domain of central Madagascar and the widely Paleoproterozoic Eastern Madurai Domain with the Trivandrum and Nagercoil Blocks of southern India, the Anosyen-Androyan domain of southern Madagascar and the Wanni Complex of Sri Lanka.

Collins, A.S., Clark, C., Plavsa, D. (2013): Peninsula India in Gondwana: The tectonothermal evolution of the Southern Granulite Terrane and its Gondwanan counterparts. *Gondwana Res.*, **25**, 190-203.

Santosh, M., Xiao, W.J., Tsunogae, T., Chetty, T.R.K., Yellapa, T. (2012): The Neoproterozoic subduction complex southern India: SIMS zircon U-Pb ages and implications for Gondwana assembly. *Precambrian Res.*, **192-195**, 190-208.

15 MILLION YEARS OF ULTRA-HIGH-PRESSURE METAMORPHISM IN WESTERN NORWAY: INSIGHTS FROM U-Pb ZIRCON GEOCHRONOLOGY, NORDØYANE DOMAIN

Butler J.P.[1], Jamieson R.A.*[2], Robinson P.[3], Dunning G.R.[4] & Pecha M.[5]
[1] Department of Oceanography, Dalhousie University, Halifax, Canada
[2] Department of Earth Sciences, Dalhousie University, Halifax, Canada
[3] Geological Survey of Norway, Trondheim, Norway
[4] Department of Earth Sciences, Memorial University, St. John's, Canada
[5] Arizona LaserChron Centre, Department of Geosciences, University of Arizona, Tucson, AZ, USA
Corresponding email: beckyj@dal.ca

Keywords: geochronology, petrology, tectonics

The Western Gneiss Region (WGR) of Norway is a giant ultra-high-pressure (UHP) terrane formed during Silurian–Devonian subduction of the Baltican continental margin beneath Laurentia, with subsequent exhumation attributed to regional extension. Recent tectonic models have proposed that the WGR was formed and exhumed from UHP conditions either as a strong, coherent body of crust driven by plate extension (e.g., Butler et al., 2015), or alternatively as a weak, partially-molten plume driven by buoyancy forces (Labrousse et al., 2015). Evaluating these hypotheses requires detailed constraints on the time and duration of UHP metamorphism, partial melting, and exhumation, with dates that can be linked to the mineral assemblages formed at each stage. Here we present the results of a combined ID-TIMS and LA-ICP-MS U-Pb (zircon) geochronology study of eclogites and associated rocks from the island of Harøya, in the Nordøyane UHP domain. The eclogite zircons exhibit a "soccerball" morphology, and are generally zoned, with Proterozoic cores and thin overgrowths that range in age from 413-397 Ma. A recently discovered coesite-bearing eclogite contains sparse, very small, unzoned zircons that yielded an age of ca. 407 Ma. Samples analysed for REE compositions show HREE depletion indicative of coeval garnet growth, and together with petrographic relationships support zircon formation at eclogite-facies conditions. Zircons from the surrounding migmatitic gneisses exhibit Proterozoic cores with euhedral overgrowths that yielded ages of ca. 394-392 Ma, interpreted as the time of crystallization from melt. Zircons from a syn-extension pegmatite produced an age of ca. 388 Ma. The broad age range from a small area is consistent with suggestions that the WGR underwent protracted residence at (U)HP conditions (Kylander-Clark et al., 2009), beginning ca. 415 Ma, followed by relatively slow exhumation to amphibolite facies conditions by 388 Ma. The ca. 15 Myr duration implies that the WGR was strong enough to resist buoyancy-driven detachment and exhumation. However, the youngest eclogite ages overlap (within uncertainty) with zircon rim ages from leucosomes, which may support previous suggestions that melting began at or near UHP conditions. The textural complexity of both the zircons and their host rocks in this small part of the WGR demonstrates the need for both high analytical and spatial resolution for U-Pb age determinations, and complementary methods to link ages to corresponding metamorphic assemblages, in order to test and refine models for the formation and exhumation of UHP terranes.

Butler, J.P., Beaumont, C., Jamieson, R.A. (2015): Paradigm lost: Buoyancy thwarted by the strength of the Western Gneiss Region (ultra)high-pressure terrane, Norway. *Lithosphere*, DOI: 10.1130/L426.1

Kylander-Clark, A.R.C., Hacker, B.R., Johnson, C.M., Beard, B.L., Mahlen, N.J. (2009): Slow subduction of a thick ultrahigh-pressure terrane, *Tectonics*, **28**, TC2003.

Labrousse, L., Duretz, T., Gerya, T. (2015): H_2O-fluid-saturated melting of subducted continental crust facilitates exhumation of ultrahigh-pressure rocks in continental subduction zones. *Earth Planet. Sci. Letters*, **428**, 151-161.

THE ORIGIN OF BADDELEYITE, SRILANKITE, HÖGBOMITE AND ZIRCON CORONAS IN Ti-Fe ORES FROM THE MARISCAL-SOCONUSCO MASSIF-TYPE ANORTHOSITE COMPLEX, SOUTHEASTERN MEXICO

Cisneros de León A.*[1], Schmitt A.K.[1] & Weber B.[2]
[1] Institut für Geowissenschaften, Universität Heidelberg, Germany
[2] Departamento de Geología, Centro de Investigación Científica y de Educación Superior, Ensenada, Mexico
Corresponding email: alejandro.cisneros@geow.uni-heidelberg.de

Keywords: baddeleyite, zircon, rutile

In southeastern Mexico (Chiapas Massif Complex), rutile-bearing ilmenitite is a member of the newly discovered Mariscal-Soconusco massif-type anorthosite complex which is located at the southeastern North American plate boundary. Detailed petrographical and backscattered electron microscopy of ilmenitite exhibits ubiquitous evidence of baddeleyite as a precursor phase of zircon and srilankite ($ZrTi_2O_6$). Specifically, metamorphic zircon occurs in a wide variety of textural relationships such as (1) discontinuous zircon coronas around rutile, (2) trails along ilmenite grain boundaries in contact with chlorite, (3) accumulations of up to 100 zircon grains hosted in biotite + chlorite lenses, (4) rims around srilankite, and (5) within or along the grain boundaries of högbomite ($[Mg,Fe]_2[Al,Ti]_5O_{10}$). *In situ* cathodoluminescence imaging revealed complex zoning in all zircon textures, suggesting m ultiple generations of zircon overgrowths. The evidence of spinel transforming into högbomite, baddeleyite into srilankite, and the formation of rutile, are interpreted to be the outcome of reactions involving Ti from the ilmenite matrix during high-grade metamorphic conditions. Zr is an important trace component in the Ti-bearing phases participating in these reactions, as chemical microanalyses suggest (högbomite, Zr = 300 ppm on average, n = 5; rutile, Zr = 830 ppm on average, n = 8). We interpret baddeleyite as the result of Zr exsolution from magmatic ilmenite as described by Bingen et al. (2001), as well as from metamorphic rutile and högbomite at different stages of the rock evolution, most likely during cooling. The transformation of baddeleyite (and srilankite) into zircon most likely occurred during subsequent metamorphic events where excess silica was present (Bingen et al., 2001). This suggests a multi-episodic exsolution of baddeleyite from Zr-rich phases and subsequent growth of metamorphic zircon during the evolution of the rutile-bearing ilmenitite, which is compatible with a polymetamorphic evolution of the Chiapas Massif Complex (Cisneros de León, 2015). The understanding of textural relationships of metamorphic zircon with precursor mineral phases is of paramount importance in order to further constrain timing and metamorphic conditions involved in its genesis.

Bingen, B., Austrheim, H., Whitehouse, M. (2001): Ilmenite as a source for zirconium during high-grade metamorphism? Textural evidence from the Caledonides of Western Norway and implications for zircon geochronology. *J Petrol.*, **42**, 355-375.

Cisneros de León, A. (2015): Petrogénesis del complejo anortositico Mariscal-Soconusco y rocas asociadas en el complejo Macizo de Chiapas. Master Thesis, Instituto de Geología, Universidad Nacional Autónoma de México, 180 p.

DETRITAL-ZIRCON GEOCHRONOLOGY AND SEDIMENTARY PROVENANCE OF THE SÃO FRANCISCO CRATON COVERS

Dias A.N.C.*[1], Chemale F. Jr[2], Martins-Ferreira M.A.C.[3], Lana C.[4] & Pereira A.A.[1]
[1] Department of Physics, Chemistry and Mathematics, Center of Sciences and Technology for Sustainability, Federal University of São Carlos, Brazil
[2] Centre for Exact and Technological Sciences, University of the Rio dos Sinos Valley, São Leopoldo, Brazil
[3] Institute of Geosciences, University of Brasília, Brazil
[4] Department of Geology, Federal University of Ouro Preto, Brazil
Corresponding email: diasanc@hotmail.com

Keywords: Lu-Hf and U-Pb zircon dating, São Francisco Craton cover, Proterozoic basins

Lu-Hf and U-Pb zircon data were used to distinguish the provenance and main unconformities of sedimentary cover formed from Statherian to Cambrian in the São Francisco Craton. Three main sedimentary basins has been worked, the incratonic Espinhaço Basin (1.8-0.9 Ga), passive margin deposits (< 0.9 Ga to > 0.63 Ga) and red-bed foreland deposits (Ediacaran to Cambrian) of the São Francisco Group. Our U-Pb data allow distinct detrital zircon age distribution and recognize the following major unconformities: at base of Paleo-Mesoproterozoic Espinhaço Supergroup is recognized Paleoproterozoic and Archean contributions; whereas at the top of Espinhaço Supergroup occurs dominant Paleoproterozoic and subordinate Mesoproterozoic contribution. In Neoproterozoic to Cambrian basins (Supergroup San Francisco), there are two main units: at the base (Jequitaí Formation; lower Sete Lagoas Formation) with age distribution of Paleoproterozoic and Mesoproterozoic, suggesting the same source of Upper Supergroup Espinhaço. At the top (TM = Três Marias Formation) we find strong contribution of Brasiliano zircons and something of Meso and Paleoproterozoic ones. Lu-Hf of same detrital zircon grains of upper part of the EsS and of the SFG suggest distinct sources for the studied material, where those zircons of Paleoproterozoic age in the Espinhaço units are mostly of juvenile to slightly reworked crustal signature and those zircons grains of the SFG show strong epsilon Hf negative values with Mesoarchean model ages. The present data suggest first regional unconformity between the lower section and upper section of the Espinhaço Group units with the strong input of Mesoproterozoic zircon grains (as younger as 1.3 Ga) in the upper section. The unconformity between passive margin and foreland deposits is marked by the changing of cratonic derived zircon input (Archean to Mesoporterozoic ages) to strong Ediacaran contribution associated with the Neoproterozoic Brasiliano Orogeny.

CORES FROM ICDP PALEOVAN LINK FELDSPAR TEXTURES TO $^{40}Ar/^{39}Ar$ RESULTS TAKING A LIMNOLOGIC AGE-MODEL INTO ACCOUNT

Engelhardt J.*[1], Sudo M.[1], Stockhecke M.[2] & Oberhänsli R.[1]
[1] Institut für Erd- und Umweltwissenschaften, Universität Potsdam, Germany
[2] Large Lakes Observatory, University of Minnesota, Duluth, MN, USA
Corresponding email: jonsen@geo.uni-potsdam.de

Keywords: feldspar, $^{40}Ar/^{39}Ar$ method, zoning patterns

Volcaniclastic falls in ICDP PALEOVAN cores from Lake Van, Turkey, contain sodium-rich sanidine and anorthoclase showing major and trace element zoning. Stockhecke et al. (2014) defined an age-model recording the lake's 600 kyr lasting history based on climato-stratigraphic correlations, tephrostratigraphy, paleomagnetics and $^{40}Ar/^{39}Ar$ analytics. Thirteen total-fusion (TF) and two stepwise heating (SWH) inverse isochron $^{40}Ar/^{39}Ar$ ages from volcaniclastic feldspars of this study agree within two σ uncertainties with the age-model. Additional five inverse isochron ages from TF analyses and one from a SWH analysis are significantly older than the age-model. Ternary feldspars in deviating samples show chemical zoning that indicates complex growth histories and transparent melt inclusions. The chemical zoning is visible in cathodoluminescence (CL) or back-scattered electron (BSE) images and can be subdivided following the definition by Ginibre et al. (2004). Pseudo-oscillatory (PO-type) zoning has the potential to record resorption processes mostly due to a sensitive alternation of Fe contents and is visible in CL images. Compositional (C-type) zoning reflects anticorrelated anorthite (An) and orthoclase contents. Samples being dominated by C-type zoning feldspar reflect variations of the feldspars' An components in ratios of calcium-derived $^{37}Ar_{Ca}$ relative to potassium-derived $^{39}Ar_K$. TF analyses that resulted in highest values for $^{37}Ar_{Ca}/^{39}Ar_K$ also resulted in scattering radiogenic ^{40}Ar ($^{40}Ar^*$) contents relative to $^{39}Ar_K$. One overlapping and two deviating samples are rich in C-type ternary feldspars that show An-rich components as resorbed subdomains that are overgrown by an An-poorer component. These samples indicate that subdomains are of a xenocrystic character that possibly have been degassed to varying degrees, but result in statistically robust inverse isochron ages. Blank-, potassium- and atmosphere-corrected intensities for ^{38}Ar are commonly interpreted to be derived from chlorine (Kelley, 2002). As chlorine is not incorporated in the feldspar structure, ^{38}Ar can indicate the contribution of mixed phases to the samples' argon release. Three deviating isochron ages reveal highest ratios of $^{38}Ar_{Cl}/^{39}Ar_K$ relative to scattering $^{40}Ar^*/^{39}Ar_K$ signals, but minute or no indications of extraneous ^{40}Ar in initial $^{40}Ar/^{36}Ar$ ratios. Calcium-derived isotopic evidence and their corresponding textural compositions possibly explain ages that are older than suggested by the lacustrine age-model. Inverse isochron ages having robust parameters for the goodness of fit appear to adulterate erroneous analyses into isotopically reliable ages. ICDP Lake Van cores monitor the effect of inherited ^{40}Ar that is derived from older material whose age contrast is radiometrically small and goes undetected in inverse isochron age calculations.

Ginibre, C., Wörner, G., Kronz, A. (2004): Structure and dynamics of the Laacher See magma chamber (Eifel, Germany) from major and trace element zoning in sanidine: A cathodoluminescence and electron microprobe study. *J. Petrol.*, **45**, 2197-2223.

Kelley, S. (2002): Excess argon in K-Ar and Ar-Ar geochronology. *Chem. Geol.*, **188**, 1-22.

Stockhecke, M., Kwiecien, O., Vigliotti, L., Anselmetti, F.S., Beer, J., Çağatay, M.N., Channell, J.E.T., Kipfer, R., Lachner, J., Litt, T., Pickarski, N., Sturm, M. (2014): Chronostratigraphy of the 600,000 year old continental record of Lake Van (Turkey). *Quatern. Sci. Rev.*, **104**, 8-17.

HOW MANY OCEAN FLOORS? GEOCHEMICAL AND GEOCHRONOLOGICAL STUDY OF AMPHIBOLITES FROM THE WESTERN TATRA MOUNTAINS (CENTRAL WESTERN CARPATHIANS)

Gawęda A.*[1], Burda J.[1], Klötzli U.S.[2], Golonka J.[3] & Szopa K.[1]
[1] Faculty of Earth Sciences, University of Silesia, Katowice, Poland
[2] Department für Lithosphärenforschung, Universität Wien, Austria
[3] AGH University of Mining and Metallurgy, Kraków, Poland
Corresponding email: aleksandra.gaweda@us.edu.pl

Keywords: Tatra Mts., amphibolite, U-Pb zircon dating

The ocean floor is represented mostly by mafic rocks of basaltic composition in a broad sense. The geochemistry and dating of oceanic rift-related mafic complexes bring the information about the time frames and geotectonic development of the ocean floor.

Western Tatra Mountains metamorphic cover, exposed on the northern and southern parts of the Tatra granitoid intrusion, represents the Early Paleozoic sequence of metapelites intercalated with amphibolites. The protolith of amphibolites were subalkaline basalts of MORB affinity, intruding basin floored by the attenuated continental crust (Gawęda et al., 2000). U-Pb zircon dating revealed the three group of protolith ages. Amphibolites from southern metamorphic cover show the protolith age of 499±5 Ma, overgrown by rims dated at 351±3 Ma. Amphibolites from the northern metamorphic cover show the protolith age (magmatic cores) of 560±9 Ma, with metamorphic rims dated at 359±7 Ma. Detrital cores dated at 1487 Ma and 605 Ma are present. Amphibolites from Goryczkowa Unit show the 560±5.7 Ma magmatic ages, while the metamorphic overgrowths are dated at 512 Ma, 447±14 Ma and 339 Ma. Detrital cores are dated at: 3166 Ma, 2627 Ma and 602 Ma. All zircon cores show the oxygen isotope composition corresponding to the mantle character of the protolith magma, with $\delta^{18}O_{VSMOW}$ = 4.8-6.9‰, while rims show the high $\delta^{18}O_{VSMOW}$ values in the range of 7.3-9.5‰, typical of crustal melts.

All three investigated amphibolite suites represents two different geological histories. Amphibolites from the southern metamorphic cover are the consequence of the Rheic Ocen opening (at ca. 500 Ma) and its closure (at ca. 350 Ma). Amphibolites from the northern metamorphic cover and Goryczkowa Unit are the result of the eastern Iapetus formation (ca. 560 Ma). But their further history was different: Basin represented by Goryczkowa Unit underwent multistep closure (512 Ma and 447 Ma) with final Variscan metamorphic episode at ca. 340 Ma, imprinted in zircon rims. Basin represented by Western Tatra closed during initial Variscan episodes at 360 Ma, coeval with migmatization stage and partial melting of the accretionary prism. The presented results underline the metamorphic envelope to the Tatra granite represent different ocean units and different terranes, subsequently derived from Gondwana and collided to Baltica/Laurussia during Caledonian and Variscan events.

Acknowledgements: This study was financially supported by NCN grant No 012/07/B/ST10/04366 (given to AG).

Gawęda, A., Winchester, J.A., Kozłowski, K., Narębski, W., Holland, G. (2000): Geochemistry and paleotectonic setting of the amphibolites from the Western Tatra Mountains. *Geol. J.*, **35**, 69-85.

U-Pb SIMS ANALYSIS OF JADEITE-BEARING ORTHOGNEISS AT TAVAGNASCO, SESIA ZONE, WESTERN ALPS, ITALY

Gilotti J.A.*[1], McClelland W.C.[1], Coble M.A.[2] & Compagnoni R.[3]
[1] Department of Earth & Environmental Sciences, University of Iowa, Iowa City, IA, USA
[2] Dipartimento di Scienze della Terra, Università di Torino, Italy
[3] Department of Geological & Environmental Sciences, Stanford University, Stanford, CA, USA
Corresponding email: jane-gilotti@uiowa.edu

Keywords: Sesia zone, zircon, jadeite orthogneiss

Orthogneiss within the Eclogitic Micaschist Complex of the Sesia Zone was collected from a quarry west of Tavagnasco in the Aosta Valley for U/Pb analysis to refine the protolith and metamorphic age of pre-Variscan intrusions. The granitic orthogneiss has an eclogite facies assemblage of jadeite, quartz, K-feldspar, phengite and rare garnet. Liermann et al. (2002) determined upper and lower intercept ages of 396±21 and 68±7 Ma, respectively, from TIMS (thermal ionization mass spectrometry) analysis of 7 single zircon grains; similar intercept ages of 435±8 and 52±17 Ma were determined for a sample of the same orthogneiss unit above Montestrutto. Zircons separated for this study display oscillatory zoned cores that are embayed and overgrown by oscillatory zoned rims in cathodoluminescence (CL) images. SIMS (secondary ion mass spectrometry) U/Pb-trace element analysis targeted specific CL domains. Four concordant analyses from the cores give a weighted mean $^{206}Pb/^{238}U$ age of 457±5 Ma. The cores have Th/U = 0.1 and negative Eu anomalies (Eu/Eu* = 0.01) typical of igneous zircon. The grains give Ti-in-zircon T estimates of ca 780°C. An Ordovician crystallization age is inferred for the granitic protolith. The rim analyses define a range of ^{207}Pb-corrected $^{206}Pb/^{238}U$ ages from 74 to 86 Ma. Four concordant analyses define a weighted mean $^{206}Pb/^{238}U$ age of 78±2 Ma. The rims have lower Th/U (0.01), less negative Eu anomalies (Eu/Eu* = 0.1-0.2) and steeper HREE (Yb/Gd = 112-157), trends consistent with metamorphic zircon rim growth at eclogite facies conditions. Ti-in-zircon T estimates for the rims are ca. 600°C. The rim ages are consistent with the timing of the initial HP eclogite facies metamorphism documented in the Sesia zone (Rubatto et al., 2011; Regis et al., 2014). We have not yet identified evidence for multiple periods of rim growth and the zircons examined lack evidence for pre-Alpine metamorphism.

Liermann, H.-P., Isachsen, C., Altenberger, U., Oberhänsli, R. (2002): Behavior of zircon during high-pressure, low-temperature metamorphism: Case study from the Internal Unit of the Sesia Zone (Western Italian Alps). *Eur. J. Mineral.*, **14**, 61-71.

Regis, D., Rubatto, D., Darling, J., Cenki-Tok, B., Zucali, M., Engi, M. (2014): Multiple metamorphic stages within an eclogite-facies terrane (Sesia Zone, Western Alps) revealed by U/Th-Pb petrochronology. *J. Petrol.*, **55**, 1429-1456.

Rubatto, D., Regis, D., Hermann, J., Boston, K., Engi, M., Beltrando, M., McAlpine, S.R.B. (2011): Yo-Yo subduction recorded by accessory minerals in the Italian Western Alps. *Nature Geosci.*, **4**, 338-342.

THE LARGE LAYERED GOIAS COMPLEXES: NEW U-Pb AND PRELIMINARY Lu-Hf *IN SITU* ZIRCON ANALYSES FROM BARRO ALTO AND CANA BRAVA

Giovanardi T.*[1], Lugli F.[2], Girardi V.A.V.[1], Correia C.T.[1], Tassinari C.C.G.[1], Sinigoi S.[3], Cipriani A.[2] & Mazzucchelli M.[2]

[1] Institute of Geosciences, University of São Paulo, Brazil

[2] Dipartimento di Scienze Chimiche e Geologiche, Università di Modena e Reggio Emilia, Modena, Italy

[3] Dipartimento di Matematica e Geoscienze, Università di Trieste, Italy

Corresponding email: tommaso.giovanardi@gmail.com

Keywords: zircon, Lu-Hf, U-Pb

The large layered Goiás complexes are three mafic-ultramafic layered intrusions which outcrop in a ~350 km, NNE-trend belt within the Brasilia Belt (central Brazil). Fom N to S, they are: Cana Brava, Niquelândia and Barro Alto. The intrusion age and geological hystory of these intrusions is still presently debated.

New U-Pb SHRIMP-II zircon analyses were performed in samples from Cana Brava and Barro Alto, the two poorest-known complexes among them, providing for a coeval Neoproterozoic intrusion age at ~790 Ma of both complexes, consistent with literature ages for the Niquelândia complex.

Inherited zircons with Mesoproterozoic ages are consistent with the formation age of the metavolcanic-metasedimentary sequences in magmatic contact with these three complexes and suggest some degree of contamination of the complexes. This contamination in Niquelândia and Cana Brava is well known in the literature as revealed by bulk-rock Rb-Sr and Sm-Nd systematics. The two complexes show enrichment of the contamination in their gabbroic sequence with local enrichment where the crustal xenoliths are more abundant. Conversely, the upper part of Niquelândia, mainly formed by anorthosite, is almost or totally uncontaminated.

The Lu-Hf analyses on zircons from the Goiás complexes were performed during the instrument calibration of the Lu-Hf methodology at the laboratories of Centro Interdipartimentale Grandi Strumenti at the Università di Modena e Reggio Emilia. The measurements were carried out using a Neptune MC-ICPMS coupled with a New Wave UP-213 laser ablation. The instrument was firstly calibrated on a standard solution and successively *in situ* analyses on complexes zircons were carried out together with CZ3 and TEMORA2 zircon standards. Mass bias and isobaric interference were corrected offline using the IsotopeMaker free software of Zhang et al. (2015).

Preliminary Lu-Hf *in situ* zircon data show negative εHf(t) values which are consistent with crustal contamination of the Barro Alto and Cana Brava parental melts as show by Rb-Sr and Sm-Nd in Cana Brava. The new Lu-Hf data, togheter with a review of literature data, show, for Barro Alto, a contamination similar to Niquelândia for the Rb-Sr and Sm-Nd systematics: zircons from the gabbroic sequence are contaminated, while zircons from the upper anorthosites are poorly contaminated. Inherited zircons commonly show positive εHf(t) values, which suggest mantle-derived melts for the magmatism of the metavolcanic-metasedimentary sequence.

Acknowledgements: We want to thank the Research Support Foundation of the State of São Paulo (FAPESP), in the frame of project 2013/19519-6 for financial support and the Programma Giovani Ricercatori Rita Levi Montalcini to A.C.

Zhang, L., Ren, Z.-Y., Xia, X.-P., Li, J. Zhang, Z.-F. (2015): IsotopeMaker: A Matlab program for isotopic data reduction. *Int. J. Mass. Spectrom.*, **392**, 118-124.

LA-ICP-MS U-Pb DETRITAL AND MAGMATIC ZIRCON AGES OF THE LATE ORDOVICIAN GLACIAL DIAMICTITES AND PEBBLES, TAURIDES AND SOUTHEAST ANATOLIAN AUTOCHTHONE BELT, TURKEY: PROVENANCE OF THE NORTHEASTERN GONDWANA (EGYPT-SINAI PENINSULA)

Gürsu S.*[1-2], Möller A.[2], Usta D.[3], Köksal S.[4], Ates S.[5], Sunkari E.D.[1] & Göncüoğlu M.C.[6]
[1] Muğla Sitki Koçman University, Muğla, Turkey
[2] Department of Geology, University of Kansas, Lawrence, KS, USA
[3] Mineral Research and Exploration, General Directorate, Adana Division, Adana, Turkey
[4] Central Laboratory, Middle East Technical University, Ankara, Turkey
[5] Mineral Research and Exploration, General Directorate, Department of Geological Research, Ankara University, Turkey
[6] Department of Geological Engineering, Middle East Technical University, Ankara, Turkey
Corresponding email: semihgursu@mu.edu.tr

Keywords: Late Ordovician, glacial successions, provenance

Late Ordovician (Hirnantian) glacial deposits observed at the northern margin of Gondwana (Africa and Arabia) and the southern margin of the European continent are one of the most extensive glacial deposits despite the duration of the glacial episode shorter than 1 million years (Ghienne, 2003). The outcrops of the Late Ordovician (Hirnantian) glacial deposits in the southern part of Turkey are mainly located in Bedinan-Yurtyeri-Kiziltepe area of the South Anatolian Autochthone Belt-SAAB, Sariz-Kayseri, Tufanbeyli-Adana, Feke-Adana, Kozan-Adana in the Eastern Taurides-ET and at Ovacik-Silifke-Mersin in the Central Taurides-CT of the Taurides-Anatolite Platform-TAP representing Gondwanan origin. The glacial successions in the central and eastern Taurides and SAAB are mainly composed of diamictites, conglomeratic sandstones, pebble-bearing sandstones, sandy diamictites, rounded-subrounded granitic pebbles (dropstone), rounded-subrounded lonestones, fine-grained sandstones, and sandy/muddy diamictites. The rounded/sub-rounded granitic pebbles (dropstone) are only observed in the central Taurides and eastern Taurides of the TAP. LA-ICP-MS U-Pb zircon ages of the granitic pebbles within the matrix of the diamictites are dated as 576.5±3.3 Ma, 576.7±5.7 Ma, 598.4±7.5 Ma, 717.5±8.0 Ma, 789.5±3.7 Ma, and 964.6±4.6 Ma, respectively. The oldest age (964.6±4.6 Ma) of the dated granitic pebbles clearly indicate the Kibaran age basement rocks that transported either from Mozambique Belt or Arabian-Nubian Shield (Sinai, Egypt). But the long prismatic subhedral / sub-rounded morphologies of the Kibaran age zircons in the samples are not consistent with a long-distance transportation from Mozambique Belt. Recent studies indicated that the Arabian-Nubian Shield has Kibaran-age basement rocks located in the Sinai Peninsula (Egypt) (Be'eri-Shlevin et al., 2012; Eyal et al., 2014). The geochemical signatures and dated granitic pebbles in the CT and ET are interpreted to have been derived from the Late Neoproterozoic granitoids/meta-granitic rocks of the Arabian-Nubian Shield (ANS; the Sinai Peninsula and the Eastern Desert of Egypt). Three diamictite samples from CT, ET and SAAB and two rounded-subrounded lonestone samples were analyzed to determine their provenance by using U-Pb zircon geochronology. The distribution of the zircon populations in both of the diamictites and lonestone display more enrichment in the Ediacaran and Cryogenian with significant Tonian and less pronounced Mesoproterozoic, Paleoproterozoic and Neoarchean ages. The youngest $^{206}Pb/^{238}U$ ages in the diamictites (499.1±4.2 in the SAAB, 530.5±5.3 in the ET, 562.5±5.4 Ma in the CT) and in the lonestones (528.2±4.5 in the CT and 530.8±5.2 Ma in the ET) indicate that detrital zircons were directly transported from the northern margin of Gondwana and/or Arabia than peri-Gondwanan parts of the European margin during the Late Ordovician. In addition, the sub-rounded, long prismatic to rounded and short prismatic morphologies of the xenocrsyts in the diamictites and lonestone pebbles show that these were not directly transported from the Saharan craton or Kibaran basement rocks observed in the Mozambique Belt to the Ordovician basins. The morphologies of the Kibaran age detrital zircons in the diamictites and lonestone pebbles in the CT and ET representing TAP is not consistent with long-distance transportation from the Mozambique Belt. Kernel/probability density diagrams of zircon ages from the lonestone pebbles with in the diamictites in the ET and CT are interpreted as evidence that they were derived from Late/Middle Cambrian siliciclastic rocks in the Israelean part of the Sinai Peninsula. Abundant Late Neoproterozoic detrital zircons with high percentages of Cryogenian ages in the CT indicate that the CT may have been closer to the juvenile basement of the ANS than its counterparts in the ET and SAAB. The provenance of detrital zircon populations in the diamictites in the CT and ET is directly correlated with magmatic activity of the Elat-Feiran island arc, Sa'al island arc and the post-collisional magmatic suites in the Sinai Peninsula. The distinctive age pattern between 1.00-1.05 Ga with significant peaks at 995.4±4.3, 1050±10 Ma, and a limited number of Middle Paleoproterozoic - Neoarchean zircon ages and rounded / sub-rounded Kibaran-age zircon

populations indicates that glacial successions in the SAAB have different paleogeographic position than their equivalent units in the CT and ET during deposition of the Late Ordovician glacial units and is interpreted to be derived from the Ha'il / Afif terranes of the eastern Arabian shield as their provenance during the Late Ordovician glaciation.

Be'eri-Shlevin, Y., Eyal, M., Eyal, Y., Whitehouse, M.J., Litvinovsky, B. (2012): The Sa'al volcano-sedimentary complex (Sinai, Egypt): a latest Mesoproterozoic volcanic arc in the northern Arabian Nubian Shield. *Geology*, **40**, 403-406.

Eyal, M., Be'eri-Shlevin, Y., Eyal, Y., Whitehouse, M.J., Litvinovsky, B. (2014): Three successive Proterozoic island arcs in the Northern Arabian-Nubian Shield: Evidence from SIMS U-Pb dating of zircon. *Gondwana Res.*, **25**, 338-357.

Ghienne, J.F., Deynoux, M., Manatschal, G., Rubino, J.L. (2003): Palaeovalleys and fault-controlled depocentres in the Late-Ordovician glacial record of the Murzuq Basin (central Libya). *C. R. Geosci.*, **335**, 1091-1100.

TIMESCALE OF PERVASIVE MELT MIGRATION IN THE CRUST

Hasalová P.*[1], Schaltegger U.[2], Schulmann K.[1-3], Weinberg R.F.[4], Štípská P.[1-3], Kylander-Clark A.R.C.[5], Holder R.[5] & Sergeev S.[6]

[1] Centre for Lithospheric Research, Czech Geological Survey, Prague, Czech Republic
[2] Département de Sciences de la Terre, Université de Genève, Switzerland
[3] Institut de Physique du Globe de Strasbourg, Université de Strasbourg, France
[4] School of Earth, Atmosphere and the Environment, Monash University, Clayton, Australia
[5] Department of Earth Science, University of California, Santa Barbara, CA, USA
[6] A.P. Karpinsky Russian Geological Research Institute, Saint Petersburg, Russia
Corresponding email: pavlina.hasalova@geology.cz

Keywords: melt migration, crust, monazite geochronology

Movement of a large volume of granitic melt is an important factor in the compositional differentiation of the continental crust and the presence of melt in rocks profoundly influences their rheology. Different mechanisms controlling melt migration through crust were proposed. We suggest that pervasive melt flow, analogous to reactive porous melt flow in mantle, could be possibly one of them. It is generally accepted that migration of felsic melts in continental crust starts with short distance pervasive microscopic flow into segregation veins which extract melt. However, we show that pervasive melt flow may be a regional mode of melt migration in continental crust. In such scenario, melt driven by deformation passes pervasively along grain boundaries through the whole rock volume. And the term pervasive melt flow is used for grain-scale, diffuse, porous and reactive flow of felsic silicate melt through rocks. This is effectively an open-system process that thoroughly reworks the resident rock mass. Through-flow of melt destroys pre-existing fabrics and the original chemical and isotopic nature of the protolith. Melt segregation is inefficient and protolith become isotropic granite-like, with partly preserved relics of the original, without ever containing more than a few melt percent at any time. This mode is favored by rocks of low strength and low mechanical anisotropy, as well as homogeneous deformation and low melt pore pressure, which inhibit melt segregation. In our view, pervasive melt migration may be a common though cryptic mechanism, capable of obliterating the original character of pre-existing rocks giving rise to isotropic granites. The fabric and geochemical nature of these granites encapsulates the complex history of hybridization. The porous flow of silicate melts in continental crust is a process which can operate over a long time and impacts on the rheology of the crust during orogeny. Pervasive melt flow is slow and possibly sustained over millions of year, as exemplified by the Bohemian Massif where this process lasted up to10 m.yr. In order to demonstrate the extensive timescale of such pervasive melt migration we present precise U-Pb monazite ID-TIMS (isotope dilution thermal ionization mass spectrometry) and U-Pb monazite Laser Ablation Split Stream (LASS) geochronology in combination with monazite chemistry as well as U-Pb zircon SHRIMP geochronology.

THE AGE OF HYDROTHERMAL SULFIDIC VEIN MINERALIZATIONS IN VARISCAN BASEMENT ROCKS OF THE NÍZKE TATRY MOUNTAINS (SLOVAKIA)

Kiefer S.*[1], Majzlan J.[1], Gerdes A.[2] & Chovan M.[3]
[1] Institut für Geowissenschaften, Friedrich-Schiller-Universität Jena, Germany
[2] Institut für Geowissenschaften, Goethe-Universität Frankfurt am Main, Germany
[3] Department of Mineralogy and Petrology, Comenius University, Bratislava, Slovakia
Corresponding email: Stefan.Kiefer@uni-jena.de

Keywords: sulfidic-vein-mineralizations, U/Pb-ages

The hydrothermal ore mineralizations in the Nízke Tatry Mountains belong to the most important metallogenic camps in Western Carpathians. The ore veins occur in Variscan granitoid and high-grade metamorphic rocks which were overprinted by the Alpine orogeny. The age and the origin of ore mineralizations, however, are largely unknown. Here, we present preliminary results of a detailed study of the ore mineralizations in the Low Tatra Mountains including optical, geochemical and isotopic data. The mineralization can be subdivided into three stages: 1. quartz with arsenopyrite and pyrite; 2. Fe-rich dolomite with Pb-Sb-sulfosalts, sphalerite and pyrite; 3. calcite and dolomite with tetrahedrite (Chovan et al., 1996). The gangue minerals show low Pb and U concentrations and have been dated with the U/Pb method using LA-ICP-MS. Minerals used for dating were mostly hydrothermal carbonates with U concentrations of about 2 ppm, but we also used intergrowths of hydrothermal clays and monazite, possible also zircon, for the dating. One sample gave Variscan age (320 Ma) that most likely represents the age of the country rocks. Furthermore, it was possible to obtain two groups of ages: 1. A group with ages of around 22-23 Ma and 2. a group with ages of around 130-140 Ma. The older ages may correspond to the Early Cretaceous compression, folding and thrusting of the Variscan basement (Hurai et al., 2015). These authors dated monazite from ore veins in the Gemeric unit in the Western Carpathians and obtained an age of 139 Ma. Although our results are still preliminary and we will establish more data in the future, we are planning to interpret both age groups in terms of the known geological evolution of the Western Carparthians. Furthermore, we will link the ages to specific types of mineralization or remobilization events.

Chovan, M., Slavkay, M., Michálek, J. (1996): Ore mineralizations of the Dumbierske Tatry Mts. (Western Carpathians, Slovakia). *Geol. Carpath.*, **47**, 371-382.

Hurai, V., Paquette, J.L., Lexa, O., Konečný, P., Dianiška, I. (2015): U-Pb-Th geochronology of monazite and zircon in albitite metasomatites of the Rožňava-Nadabula ore field (Western Carpathians, Slovakia): implications for the origin of hydrothermal polymetallic siderite veins. *Mineral. Petrol.*, **109**, 519-530.

ZONING IN GARNETS AND ZIRCONS FROM LOWER CRUSTAL XENOLITHS FROM NW RUSSIA

Koreshkova M.*[1] & Downes H.[2]
[1] Institute of Earth Sciences, Saint Petersburg State University, Russia
[2] Department of Earth and Planetary Sciences, Birkbeck University, London, United Kingdom
Corresponding email: mk6456@mail.ru

Keywords: garnet, zircon, lower crust

We have studied major and trace elements compositions of minerals constituting Grt-granulites and plagioclase-free xenoliths from lamprophyres and kimberlites of NW Russia. The data are combined with the results of U-Pb zircon dating. Samples come from two localities: alkaline dikes and pipes of Kandalaksha (southern part of the Kola Peninsula) and the Arkhangelsk kimberlite, which cut through the Archean Belomorian Mobile Belt.

Garnets show some increase in CaO content and decrease in Mg# from grain cores to rims. The profiles are convex-upward for Mg# and trough-like for Ca, with flat central zone. We suggest that the zoning was due to diffusional exchange during final cooling and was superimposed onto more homogeneous grains. At the same time, garnets have significant zoning in RE and HFS elements. In Arkhangelsk samples, garnets show strong decreases in HREE and Y, comparable in magnitude to the zoning in Zr and Hf, whereas garnets from Kola xenoliths exhibit significant zoning only in Zr and Hf. Garnets from Arkhangelsk Grt-granulites retained the growth zoning due to Rayleigh distillation. We suggest that garnets from Kola samples were re-equilibrated under relatively high temperature so that they have lost initial growth zoning in Y and HREE but partially preserved zoning in Zr and Hf contents due to the difference in diffusivities of REE and Hf (Bloch et al., 2015) and the expected similar behavior of Zr.

Zircons mostly have complex textural and compositional zoning that reflects stages and modes of its formation. The results of dating can be ascribed to the inferred zircon generations. In Arkhangelsk samples and two Grt-granulites from Kola, the final zircon generations co-existed with garnets present in the rocks (using $D^{zrn/grt}$ of REE and Y from Rubatto & Hermann, 2007). However, there are a few samples where zircon is suggested to be formed in equilibrium with garnet having much lower HREE contents than in present garnet composition. Such garnets could have existed in these rocks but underwent later homogenization of zoning in HREE and Y due to slow cooling or a superimposed event. Generally, zoning in Zr, Hf, Y, HREE, Ca and Mg# in garnets from lower crustal xenoliths reflects different stages of its existence: growth, homogenization and diffusional exchange during final cooling. Zircon retains information about the metamorphic pre-history of lower crustal rocks and can be out of equilibrium with the final mineral association.

Bloch, E., Ganguly, J., Hervig, R.,·Cheng, W. (2015): ^{176}Lu-^{176}Hf geochronology of garnet I: experimental determination of the diffusion kinetics of Lu^{3+} and Hf^{4+} in garnet, closure temperatures and geochronological implications. *Contrib. Mineral. Petrol.*, **169**, 12.

Rubatto, D. & Hermann, J. (2007): Experimental zircon/melt and zircon/garnet trace element partitioning and implications for the geochronology of crustal rocks. *Chem. Geol.*, **241**, 38-61.

LASER-ABLATION SPLIT-STREAM PETROCHRONOLOGY

Kylander-Clark A.R.C.*[1]
[1] Department of Earth Science, University of California, Santa Barbara, CA, USA
Corresponding email: kylander@geol.ucsb.edu

Keywords: geochronology, trace elements, laser ablation

One of the biggest challenges in assessing the timing and rates of geologic processes is having the ability to match the age of a dated mineral to the conditions at which that mineral grew. This is especially challenging for high-temperature chronometers that can grow and remain stable over a wide range of pressures and temperatures. The development of the laser-ablation split-stream method has afforded the ability to rapidly aquire chemical and chronologic data that are directly linked; as such, timing and rates of processes are better constrained than before. Several examples are given within:

1) Zircon and monazite from a single, coesite-bearing sample from the Western Gneiss Region in western Norway record the entire 30+ Myr history of metamorphism during Caledonian orogenesis, from intial burial, through ultrahigh-pressure (UHP) conditions, and back to crustal levels. Early monazite (~ 425 Ma) contains low concentrations of Sr and HREE, consistent with plagioclase and garnet stability during prograde metamorphism. 420-400 Ma ages from monazite (high Sr, increased Eu/Eu*, low HREE) and zircon (increased Eu/Eu*, low HREE) indicate the timing of HP conditions, and monazite with low Sr and high HREE indicates the breakdown of omphacite and garnet at 390 Ma.

2) Titanite is becoming more widely used as chronometer, primarly because laser ablation has made analysis more feasible. Nevertheless, dates produced from titanite can be difficult to interpret because titanite may alter more easily than zircon and monazite. LASS analyses of titanite, combined with X-ray maps and backscattered electron images provide insight into processes involved in growth, recrystallization and dissolution/reprecipitation, and allow us to better interpret ages and the geologic process that they represent. This study presents recrystallized titanite from metamorphic terranes as well as oscillatory-zoned titanite from igneous rocks, and suggests some possible processes that explain the TE/age trends.

3) Detrital zircons have long been used to investigate the location and geology of landforms in the past. By adding chemical information to the age data, a clearer history can be produced. Recent LASS data from Mesozoic sedimentary rocks indicate changes in chemistry of the Sierra Nevada–Peninsular Ranges batholith, as well and the exposure and erosion of distinct units (e.g., ophiolites) over discrete time periods.

DATING THE ONSET OF A LOWER CRUSTAL SHEAR ZONE: A (LUCKY) CASE FROM THE NORTHERN SECTOR OF THE IVREA-VERBANO ZONE (VAL CANNOBINA, ITALY)

Langone A.*[1], Zanetti A.[1], Tiepolo M.[2] & Mazzucchelli M.[3]
[1] Dipartimento di Scienze della Terra e dell'Ambiente, Università di Pavia, Italy
[2] Dipartimento di Scienze della Terra "A. Desio", Università di Milano, Italy
[3] Dipartimento di Chimica e Scienze della Terra, Università di Modena and Reggio Emilia, Modena, Italy
Corresponding email: langone@crystal.unipv.it

Keywords: zircon, shear zone, Ivrea-Verbano zone

A detailed textural and U-Pb geochronological investigation has been performed on zircons from a ductile shear zone established in lower crustal mafic intrusives. The investigated shear zone is hosted in the Finero mafic-ultramafic complex of the northeastern sector of the Ivrea-Verbano Zone, Southern Alps. It developed at the base of the lower to middle continental crust section, where mafic to ultramafic rocks intruded into a sequence of metapelites and metabasites (i.e., Kinzigite Formation) constituting the polymetamorphic basement of the Adria plate. The shear zone forms a braided belt that can be followed for several km, from the Cannobino River to the Mt. Gridone, and developed entirely within gabbroic/dioritic rocks, partly intruded during Triassic time (~ 232 Ma; Zanetti et al., 2013). The shear zone is characterized by a well-developed foliation, a lineation, and a compositional banding, where amphibole, clinopyroxene and garnet occur as large rounded to elliptical porphyroclasts, resulting embedded in a fine grained matrix mainly consisting of plagioclase, amphibole, pyroxenes and ilmenite. The shear zone was active during uplift and cooling of the wall rock, and recorded retrograde metamorphic conditions ranging from 650 to 500°C at 0.6-0.4 GPa (Kenkmann, 2000). The mylonitic deformation is generally placed no earlier than 230 Ma, lasting until about 170 Ma at the latest (e.g., Handy & Zingg, 1991).

Numerous zircon grains were obtained from the mineral separation of one (~ 2 kg weight) sample collected in the Cannobino River (northern Ivrea-Verbano Zone, Southern Alps). Zircon grains were examined also directly on petrographic thin sections of samples collected throughout the (ultra)mylonitic belt. According to petrographic and microstructural analyses zircon occurs as rounded grains within the mylonitic matrix, easily recognisable due to their dimensions up to 110 µm.

Cathodoluminescence (CL) study at the SEM revealed a well developed systematic zoning of zircon grains with dark cores surrounded by brighter domains, locally asymmetric, and with a thickness up to 30 µm. The dark inner core can show zoning features suggesting magmatic growth.

Preliminary LA-ICP-MS U-Pb results from zircon separates yielded mainly late Triassic concordant ages of about 235 Ma for the dark CL cores and about 204 Ma for the brighter CL (mylonitic) overgrowths.

The sizes, distributions, shapes and CL features of zircon grains provide strong evidence of a metamorphic response of zircon during ductile deformation. The observed features can be interpreted as evidence of dissolution/recrystallization in response to fluid influx during high-temperature shearing.

Further microstructural investigations, mineral chemistry and trace element characterization of different zircon domains are in progress and will provide more evidence for the petrochronological evolution of such a lower crustal shear zone.

Handy, M.R. & Zingg, A. (1991): The tectonic and rheological evolution of an attenuated cross section of the continental crust, Ivrea crustal section, southern Alps, northwestern Italy and southern Switzerland. *Bull. Geol. Soc. Am.*, **103**, 236-253.

Kenkmann, T. (2000): Processes controlling the shrinkage of porphyroclasts in gabbroic shear zones. *J. Struct. Geol.*, **22**, 471.487.

Zanetti, A., Mazzucchelli, M., Sinigoi, S., Giovanardi, T., Peressini, G., Fanning, M. (2013): SHRIMP U-Pb zircon Triassic intrusion age of the Finero Mafic Complex (Ivrea-Verbano Zone, Western Alps) and its geodynamic implications. *J. Petrol.*, **54**, 2235-2265

PRELIMINARY U-Pb LA-ICPMS ZIRCON ANALYSES FROM THE GOIAS COMPLEXES: SHRIMP COMPARISON AND INTRUSION AGE

Lugli F.[1], Giovanardi T.[2], Girardi V.A.V.[2], Correia C.T.[2], Tassinari C.C.G.[2], Sinigoi S.[3], Cipriani A.[1] & Mazzucchelli M.*[1]

[1] Dipartimento di Scienze Chimiche e Geologiche, Università di Modena e Reggio Emilia, Modena, Italia

[2] Institute of Geosciences, University of São Paulo, Brazil

[3] Dipartimento di Matematica e Geoscienze, Università di Trieste, Italia

Corresponding email: maurizio.mazzucchelli@unimore.it

Keywords: zircon, U-Pb, LA-ICPMS

Cana Brava, Niquelândia and Barro Alto are three mafic-ultramafic layered intrusions (from N to S) which form a ~ 350 km, NNE-trend belt within the Brasilia Belt (Goiás state, Brazil). Presently, their intrusion ages and geological evolution are still debated.

The Niquelândia and Barro Alto complexes are formed by two main sequences: the upper sequence and the lower one. Some authors suggest that the two sequences represent two separate intrusions: the upper sequence would be a Mesoproterozoic intrusion at ~ 1.3 Ga, whereas the lower sequence a Neoproterozic one at ~ 790 Ma. According to this interpretation, the two sequences were re-crystallized by Neoproterozoic metamorphism and exhumed and juxtaposed during the Brazilian event of formation of the Gondwana continent.

Another model suggests that the two sequences are part of the same intrusion, which occurred during the Neoproterozoic and was exhumed during the Brazilian event.

New U-Pb SHRIMP-II zircon analyses were performed at the Universidade de São Paulo from samples from Cana Brava and Barro Alto, the two least-known complexes in order to clarify the sequence of events that led to their formation.

Analyses were then replicated at the CIGS of the Università di Modena e Reggio Emilia using a X Series^{II} quadrupole ICP-MS coupled with a New Wave UP-213 Nd:YAG laser ablation system. Zircons were sampled through a 40 µm spot (static mode), using a He flux of 0.6 l/min, with an energy density of ~ 6 J/cm^2. Daily instrument calibration was performed with the NIST 610 standard, monitoring also the oxide production rate ($^{232}Th^{16}O/^{232}Th$ << 0.01%). Laser-induced elemental fractionation was corrected by repeated analyses of the standard zircon TEMORA2 (Black et al., 2004). A secondary reference material (zircon CZ3) was used to check the precision and accuracy of the corrections. Our LA-ICP-MS data are preliminary, but very promising being the accuracy of the measured ratio within the SHRIMP variability. We are currently working to improve the precision of our methodology, which however is now comparable with literature LA-ICP-MS data (propagated 2SE ~ 2-6%; Horstwood et al., 2008).

Overall, the isotopic data of Cana Brava and Barro Alto complexes provide for a coeval Neoproterozoic intrusion age at ~ 790 Ma. These ages are consistent with those reported in literature for Niquelândia.

Mesoproterozoic ages, consistent with the formation age of the metavolcanic-metasedimentary sequence in magmatic contact with the complexes, were found in inherited zircon cores.

Our data clearly show that the Goiás complexes are formed by single bodies intruded during the Neoproterozoic at ~790 Ma and that the hypothesis of two separate intrusions juxtaposed by tectonic must be discarded.

Acknowledgements: We want to thank the Research Support Foundation of the State of São Paulo (FAPESP), in the frame of project 2013/19519-6 for financial support and the Programma Giovani Ricercatori Rita Levi Montalcini to A.C.

Black, L.P., Kamo, S.L., Allen, C.M., Davis, D.W., Aleinikoff, J.N., Valley, J.W., Mundil, R., Campbell, I.H., Korsch, R.J., Williams, I.S., Foudoulis, C. (2004): Improved $^{206}Pb/^{238}U$ microprobe geochronology by the monitoring of a trace-element-related matrix effect; SHRIMP, ID-TIMS, ELA-ICP-MS and oxygen isotope documentation for a series of zircon standards. *Chem. Geol.*, **205**, 115–140.

Horstwood, M.S.A., Evans, J.A., Montgomery, J. (2008): Determination of Sr isotopes in calcium phosphates using laser ablation inductively coupled plasma mass spectrometry and their application to archaeological tooth enamel. *Geochim. Cosmochim. Acta*, **72**, 5659–5674.

DETRITAL ZIRCON GEOCHRONOLOGY OF PARAGNEISS ADJACENT TO JADEITE-BEARING ORTHOGNEISS AT TAVAGNASCO, SESIA ZONE, ITALY

McClelland W.C.*[1], Gilotti J.A.[1] & Compagnoni R.[2]
[1] Department of Earth & Environmental Sciences, University of Iowa, Iowa City, IA, USA
[2] Dipartimento di Scienze della Terra, Università di Torino, Italy
Corresponding email: bill-mcclelland@uiowa.edu

Keywords: detrital zircon, Sesia Zone, western Alps

Paragneiss adjacent to jadeite-bearing orthogneiss within the Eclogitic Micaschist Complex of the Sesia Zone was collected near a quarry west of Tavagnasco in the Aosta Valley for U/Pb detrital zircon analysis to evaluate the provenance, protolith and metamorphic ages for metaclastic rocks in this portion of the Sesia Zone. The paragneiss displays compositional layering interpreted as a vestige of primary layering that has been transposed and penetratively polydeformed during Alpine orogenesis. The unit contains an eclogite-facies assemblage of quartz, feldspar, phengite, garnet, jadeite and rutile. The paragneiss hosts orthogneiss with a protolith age of 457±5 Ma determined by U/Pb SIMS zircon analysis. The sample yielded a large population of zircon grains that are texturally complex in cathodoluminescence (CL) images. Core domains are elongate to equant, euhedral to rounded but often embayed, and typically display well developed oscillatory zoning. The cores are overgrown by 1- to 30-micron-thick rims that are oscillatory zoned and impart a subrounded external morphology to the grains. Many of the grains appear to record multiple periods of rim growth based on variation in observed CL textures. A total of 35 out of 115 grains analyzed by laser ablation inductively coupled plasma mass spectrometry (LA-ICP-MS) at the Arizona LaserChron Center pass acceptance criteria of <10% discordance. The observed ages range from ca. 550 Ma to ca. 2610 Ma (using 1000 Ma as the cutoff between use of $^{206}Pb/^{238}U$ *versus* $^{206}Pb/^{207}Pb$ ages) but define major peaks at 575-600 Ma, 655 Ma and 765 Ma with minor peaks at 1055, 1870, 2000 and 2605 Ma. Strongly discordant analyses define linear arrays with $^{207}Pb/^{206}Pb$ ages as old as 3.2 Ga. The youngest group of mutually overlapping concordant grains (n = 4) defines a weighted mean $^{206}Pb/^{238}U$ age of 569 ± 9 Ma which is interpreted as the maximum depositional age for the paragneiss protolith. Discordant analyses are interpreted to reflect the combined effects of Pb-loss in the original detrital grains and analysis of mixed metamorphic and detrital domains. Two concordant analyses at ca 78 Ma are consistent with an age of 78±2 Ma determined on HP metamorphic rims on zircon in the adjacent orthogneiss by the SIMS method. The prominent Neoproterozoic detrital zircon population and Ediacaran maximum depositional age is consistent with derivation from the Gondwana margin (e.g., Schaltegger & Gebauer, 1999). Future refinement of detrital zircon age and chemical characteristics for paragneiss units in the Eclogitic Micaschist Complex may help refine tectonic boundaries between various tectonometamorphic slices proposed for the Sesia Zone (e.g., Regis et al. 2014).

Regis, D., Rubatto, D., Darling, J., Cenki-Tok, B., Zucali, M., Engi, M. (2014): Multiple metamorphic stages within an eclogite-facies terrane (Sesia Zone, Western Alps) revealed by U/Th-Pb petrochronology. *J. Petrol.*, **55**, 1429-1456.

Schaltegger, U. & Gebauer, D. (1999): Pre-Alpine geochronology of the Central, Western and Southern Alps. *Schweiz. Mineral. Petrogr. Mitt.*, **79**, 79-87.

ERUPTION CHRONOLOGY OF A LONG DORMANT VOLCANIC SYSTEM IN THE EASTERN CARPATHIANS

Molnár K.*[1], Harangi S.[1-2], Dunkl I.[3], Lukács R.[2], Kiss B.[2], Seghedi I.[4] & Schmitt A.K.[5]

[1] Department of Petrology and Geochemistry, Eötvös Loránd University, Budapest, Hungary

[2] Volcanology Research Group, Eötvös Loránd University, Budapest, Hungary

[3] Abteilung Sedimentologie und Umweltgeologie, Geowissenschaftliches Zentrum, Georg-August Universität, Göttingen, Germany

[4] Institute of Geodynamics, Romanian Academy, Bucharest, Romania

[5] Department of Earth, Planetary and Space Sciences, University of California, Los Angeles, CA, USA

Corresponding email: mkata90@gmail.com

Keywords: zircon, (U-Th)/He dating, eruption chronology

During the last decade, the zircon (U-Th)/He geochronology has become a promising method for dating eruption histories even in case of very young (Quaternary) volcanic products. It is proved to be particularly applicable when other dating methods such as radiocarbon, K/Ar, and $^{40}Ar/^{39}Ar$ techniques encounter analytical or interpretational difficulties often caused by a lack of appropriate materials for dating. Zircon (U-Th)/He method can be used to infer the date of the rapid cooling of the erupted magma, i.e., the eruption age. However, when the crystals formed less than ~ 350 ka, correction for U-series disequilibrium is necessary. The effect of the secular disequilibrium can be corrected by the U-Th zircon dates, which provides additional information also about the timescale of the magma storage.

Here, we provide a detailed zircon (U-Th)/He dating approach to refine the eruption chronology of the Ciomadul dacite volcanic complex, found at the East Carpathians, eastern-central Europe. It is characterized by an intermittent precursor lava dome activity with extrusion of 0.1-0.6 km^3 dacitic magma, followed by the build-up of a massive lava dome complex with two explosion craters. The erupted products are fairly homogeneous dacite with similar mineral cargo. During the field campaigns we focused on the volcanic products of the Ciomadul lava dome complex and sampled all the known localities to cover the whole volcanic period and avoid sampling bias. According to the new (U-Th)/He results the precursor lava domes were formed between ~ 1000 and 300 ka, during several intermittent eruption events which were separated by long repose times: Bába Laposa: 950±50 ka, Delaul Mare: 840±12 ka, Puturosul: 710±50 ka, Bálványos: 580±20 ka and Turnul Apor: 330±40 ka. After another long quiescence, volcanic activity renewed at about 200 ka and became more productive. Numerous lava domes were developed between ca. 160 and 100 ka, which form the 10-12 km^3 central lava dome edifice. Following a ca. 40 ka lull of volcanism, a more explosive phases with minor dome building activity occurred between ~ 56 and 32 ka. Since 32 ka, the volcano has been again in a dormant state. However, geophysical data still suggest melt-bearing magma body beneath the volcano. The zircon U-Th crystallization ages imply that a silicic crystal mush could have been present for several 100's ka before the eruptions and this was rapidly remobilized by uprising hot basaltic magmas.

This new geochronological data set yields an unique insight into the temporal evolution of a dacitic volcanic complex and provides clear evidences for long (several 10's and even 100's kyr) repose times between the eruption periods that have to be considered in the volcanic hazard assessments of long dormant volcanic systems.

Acknowledgements: This research is supported by the OTKA K116528 project.

ATOM PROBE ANALYSIS OF DISCORDANT ZIRCON REVEALS PRESERVATION OF $^{207}Pb/^{206}Pb$ CRYSTALLISATION AGES IN NANOSCALE DISLOCATION LOOPS

Reddy S.M.*[1-2], Peterman E.M.[3], Saxey D.W.[1-4], Rickard W.D.A.[1-4], Fougerouse D.[1-2], Snoeyenbos D.R.[5] & Kylander-Clark A.R.C.[6]

[1] Geoscience Atom Probe, Advanced Resource Characterisation Facility, John de Laeter Centre, Curtin University, Perth, Australia

[2] Department of Applied Geology, Western Australian School of Mines, Curtin University, Perth, Australia

[3] Department of Earth and Oceanographic Science, Bowdoin College, Brunswick, ME, USA

[4] Department of Physics and Astronomy, Curtin University, Perth, Australia

[5] Department of Geosciences, University of Massachusetts, Amherst, MA, USA

[6] Department of Earth Science, University of California, Santa Barbara, CA, USA

Corresponding email: s.reddy@curtin.edu.au

Keywords: geochronology, zircon, nanoscale

Geochronologic analysis of zircon is often compromised by isotopic discordance associated with mobilization and loss of radiogenic Pb during metamorphism, deformation and/or metasomatism. Multiple analyses of single zircon grains by secondary ion mass spectrometry (SIMS) and/or laser ablation inductively coupled plasma mass spectrometry (LA-ICP-MS) indicate that isotopic discordance can be heterogeneous at length scales down to at least 10 µm, but the processes underpinning this remain unclear. Understanding the controls on the distribution of Pb, the nature of different Pb reservoirs, and the mechanisms of Pb retention have the potential to enhance our ability to extract meaningful geological dates from discordant zircon but this requires nanoscale isotopic analyses.

Here, we present atom probe data from an undeformed zircon from a kyanite-garnet metapelite (> 4.5 GPa, ca. 800°C) of the Rhodope Metamorphic Complex, Greece. The zircon grain has a discordant inherited detrital core rimmed by concordant metamorphic rim dated by LA-ICP-MS at ~ 150 Ma. The upper intercept of the zircon core, extrapolated from peak metamorphism at 150 Ma, is 2144±33 Ma; consistent with published detrital core ages from the region. Four atom probe specimens prepared from the zircon core show homogeneous distributions of Zr, Si, O, and Hf, but Pb is heterogeneously distributed in clusters measuring up to 20 nm in diameter. The cluster sizes and their relative spacing differ among the four specimens, but all have a similar toroidal morphology, consistent with the shape and size of dislocation loops. The clusters also differ in Pb concentration (~ 3.5 -5.0 at.%), but all clusters indicate local Pb enrichment despite overall Pb loss from the zircon core. Minor enrichment in Y and Al (~ 1 at.%), but not in U, is also present in the clusters. $^{207}Pb/^{206}Pb$ ratios measured from eight clusters are equivalent (within error), and yield a mean $^{207}Pb/^{206}Pb$ age of 2258±88 Ma that is slightly older than the crystallisation age inferred from LA-ICP-MS data. The $^{207}Pb/^{206}Pb$ date calculated with reference to the 150 Ma metamorphic event is 2186±93 Ma, which is consistent with the crystallisation age.

The observed trace element enrichment, toroidal cluster morphology and similar $^{207}Pb/^{206}Pb$ ratios are consistent with the clusters arising from dislocation loops that formed and entrapped diffusing radiogenic Pb during the 150 Ma metamorphic event. Differences in size, number and distribution of Pb-rich nanoclusters among the analysed specimens thus provide an explanation for variations in zircon discordance at the µm-scale. Measured isotopic ratios from these specimens indicate the timing of Pb migration in response to a high-temperature metamorphic event and the preservation of the original crystallization age. These data demonstrate that geologically meaningful dates can be recovered by atomic-scale isotopic tomography, even from discordant zircon.

PROTACTINIUM PARTITIONING IN SYNTHETIC AND NATURAL ZIRCON

Schmitt A.K.*[1], Cisneros de León A.[1] & Trail D.[2]
[1] Institut für Geowissenschaften, Universität Heidelberg, Germany
[2] Department of Earth & Environmental Sciences, University of Rochester, NY, USA
Corresponding email: axel.schmitt@geow.uni-heidelberg.de

Keywords: geochronology, accessory minerals, uranium series

Protactinium (^{231}Pa) is the longest-lived intermediate daughter isotope in the ^{235}U decay chain, and its partitioning into zircon during crystallization has a non-negligible control on the total accumulation of radiogenic ^{207}Pb over time. High-precision zircon geochronology critically depends on accurate corrections for initial disequilibrium, but because the initial abundance of ^{231}Pa in secular equilibrium zircon is unknown, model zircon-melt partitioning coefficient (D) ratios D_{Pa}/D_U are required for correction. Some previous efforts to establish D_{Pa}/D_U have used indirect constrains (e.g., Rioux et al., 2015) where D_{Th}/D_U and D_{Pa}/D_U is manipulated to reach concordance between ^{206}Pb/^{238}U and ^{207}Pb/^{235}U ages. The draw-back of this approach is that D_{Th}/D_U is not directly measured by conventional thermal ionization mass spectrometry (TIMS), and therefore D_{Pa}/D_U will also depend on the model assumptions for D_{Th}/D_U. Direct analysis of ^{231}Pa in zircon has so far been the domain of high-sensitivity and high-resolution ion microprobes (or secondary ionization mass spectrometry; SIMS). Here, we report initial results from a two-pronged approach to constrain Pa partitioning by targeting experimentally synthesized and natural zircon. Both types of zircon were analyzed on the Heidelberg University CAMECA ims 1280-HR. Experiments are based on synthesis of zircon with natural uraninite in secular equilibrium in the melt charge, which circumvents the handling of radioactive and difficult to obtain ^{231}Pa. Zircons were synthesized in a silicate melt at 1000°C and 1 GPa, with the oxygen fugacity buffered at the fayalite-quartz-magnetite equilibrium. Experimental zircons show a correlation between D_{Th}/D_U and D_{Pa}/D_U. We also report new data for natural zircon from El Chichón (Mexico) trachyandesite which erupted in 1982. Zircon rim ages predate the eruption by 10^3 to 10^5 ka. Age-corrected D_{Pa}/D_U for El Chichón zircon calculated for published whole-rock Pa/U (Pickett & Murrell, 1997) average 1.7±0.2 (n = 12; MSWD = 1.16). This value is in agreement with previous zircon D_{Pa}/D_U data for high-silica rhyolite (Schmitt, 2007, 2011). Additional experiments and investigation of natural zircon will address if Pa partitioning can be linked to other trace element proxies. This would permit more reliable corrections of ^{207}Pb-based ages than currently possible.

Pickett, D.A. & Murrell, M.T. (1997): Observations of ^{231}Pa/^{235}U disequilibrium in volcanic rocks. *Earth Planet. Sci. Letters*, **148**, 259-271.

Rioux, M., Bowring, S., Cheadle, M., John, B. (2015): Evidence for initial excess ^{231}Pa in mid-ocean ridge zircons. *Chem. Geol.*, **397**, 143-156.

Schmitt, A.K. (2007): Letter: Ion microprobe analysis of (^{231}Pa)/(^{235}U) and an appraisal of protactinium partitioning in igneous zircon. *Am. Mineral.*, **92**, 691-694.

Schmitt, A.K. (2011): Uranium series accessory crystal dating of magmatic processes. *Ann. Rev. Earth Planet. Sci.*, **39**, 321-349.

SOURCE OF THE RARE-METAL MINERALIZATION OF THE ELET'OZERO MASSIVE, NORTH KARELIA

Sorokhtina N.V.*[1], Belyatsky B.V.[2], Antonov A.V.[2], Kononkova N.N.[1] & Lepekhina E.N.[2]
[1] Department of Geochemistry, Vernadsky Institute, Moscow, Russia
[2] Center of Isotopic Research, A.P. Karpinsky Russian Geological Research Institute, Saint Petersburg, Russia
Corresponding email: nat_sor@rambler.ru

Keywords: alkaline magmatism, pyrochlore, geochronology

The alkaline–gabbro Elet'ozero massif occurs within the Karelian megablock in the eastern part of the Baltic Shield (Sharkov et al., 2015). This Proterozoic massif is one of the largest (~ 100 km^2) within the Kola-Karelian Alkaline Province. The massif forms lopolite-like concentric zoned body and consists of the different rocks (from older to younger): gabbro and pyroxenite (~ 90% of the area), diabase, spessartite, nepheline syenite (~ 10% of the area). All rocks were largely transformed by CO_2-rich alkaline fluids of the later derivatives of the alkaline magmas.

The rare-metal ore deposits are confined to alkaline nepheline syenite pegmatites. The alkaline pegmatites are composed of plagioclase and nepheline mainly, minor amphibole, pyroxene, micas, fluorapatite, titanite, magnetite, pyrochlore group minerals, zircon and others.

Zircon, fluorite, Ca-, Sr- and REE-carbonates, sulfides and barite inclusions are often found in the central zones of the pyrochlore crystals. While pyrochlore is replaced by allanite-(Ce), fersmite, columbite and mongolite along fracture zones and margins. The central zones of unaltered pyrochlore usually consist of hydroxycalciopyrochlore (Atencio et al., 2010). Na_2O, BaO, SrO, UO_2 and ThO_2 average content is up to 3 wt.%, Pb enrichment of the core parts is determined by galena microinclusions (1-2 mkm). The pyrochlore rims are "hydropyrochlore" or "kenopyrochlore" and characterized by a cation deficiency. The *A*-site total of "hydropyrochlore" (up to 0.29 apfu) is significantly lower than the hydroxycalciopyrochlore, F and K_2O contents are as low as a limits of detection, SiO_2 is up to 4.82 wt.%. The evolution trends of pyrochlore-group minerals composition are directed to decreasing of Ti, Nb, Ta, Ca and Na and accompanied by an increase of REE and Fe according to isomorphic substitution: $Ti^{4+} + Ca^{2+} \leftrightarrow (Nb,Ta)^{5+} + Na^{+}$; $(Nb,Ta)^{5+} \leftrightarrow Fe^{3+} + Ca^{2+}$; $2Ca^{2+} \leftrightarrow Na^{+} + REE^{3+}$.

SHRIMP-II U-Pb zircon dating of the Elet'ozero gabbro has shown that the time of the intrusion was 2040-2010 Ma. The alkaline pegmatites were injected about 1900 Ma significantly disturbing U-Pb isotopic system of gabbro zircons (Sharkov et al., 2015). The duration of the magmatic massif formation may be estimated only as 40-60 Ma. Rare-metal mineralization according to mineralogical and isotope-geochemical pyrochlore data was a polystage process complicated by secondary enrichment and recrystallization of ore deposits at 1740, 1680-1660 and 400 m.y. ago. Sm-Nd and U-Pb isotope systems of pyrochlore single grains reflect tectonothermal massif evolution, which was followed by structural and chemical mineral changes including cation-ion exchange with postmagmatic fluids, recrystallization of pyrochlore accompanied by component redistribution inside the grain during its formation (closed geochemical system) or component redistribution and exchange with the surrounding minerals (open system).

Acknowledgements: The study was supported by RSF 15-17-30019.

Atencio, D., Andrade, M.B., Christy, A.G., Gieré, R., Kartashov, P.M. (2010): The pyrochlore supergroup of minerals: nomenclature. *Can. Mineral.*, **48**, 673-698.

Sharkov, E.V., Belyatsky, B.V., Bogina, M.M., Chistyakov, A.V., Shchiptsov, V.V., Antonov, A.V., Lepekhina, E.N. (2015): Genesis and age of zircon from alkali and mafic rocks of the Elet'ozero Complex, North Karelia. *Petrology*, **23**, 259-280.

MESOARCHAEAN POLYMETAMORPHISM OF THE DWALILE SUPRACRUSTAL SUITE OF THE ANCIENT GNEISS COMPLEX, SWAZILAND

van Schijndel V.*[1], Stevens G.[1], Frei D.[1] & Lana C.[2]
[1] Department of Earth Sciences, Stellenbosch University, South Africa
[2] Department of Geology, Federal University of Ouro Preto, Brazil
Corresponding email: valby@sun.ac.za

Keywords: Greenstone Belt, geochronology, pseudosection modelling

The Archaean greenstone remnants of the Dwalile Supracrustal Suite (DSS) are infolded within the gneisses of the Ancient Gneiss Complex (AGC) in Swaziland (Hunter et al., 1978). The greenstone rocks are complex and are affected by multiple processes. The detrital zircons show a very limited spread of ages between 3550 and 3360 Ma and display characteristic oscillatory zoning. In addition, some samples contain zircon and monazite that record younger metamorphic ages. A combined study of geochronology and pseudosection modelling is used to distinguish between the different phases of metamorphism.

Amphibolite facies schists with a St + Grt + Bt + Ms + Qtz-assemblage equilibrated under syn-tectonic peak metamorphic conditions of 550 to 625°C and 4 to 6.5 kbar. This event is dated at ca. 3150 Ma by U-Pb in monazite in a variety of samples. Two hbl-bearing schists recorded new growth of zircon at ca. 3150 Ma. In these samples, the zircons show sector zoning but are irregular in shape and have low Th/U ratios of <0.06 and <0.21, respectively, which is distinctive of metamorphic zircon grown in the amphibolite facies (Vavra et al., 1999).

A younger but higher grade metamorphic event is recorded in two peraluminous samples that contain secondary euhedral zircons with distinctive fir-tree sector zoning and monazite. This metamorphic event reached peak conditions at ca. 2990 Ma. One sample is a Pl + Opx + Crd + Bt + Hc + Qtz- bearing rock and another sample contains Grt + Qtz + Hc + Sericite (likely after Crd and Pl). The garnet-free sample contains opx + cdr + pl pseudomorphs of garnet with fine grained opx + crd symplectite produced in pressure shadows around former garnet. The symplectite is aligned with the stretching direction and Mg# in the symplectite crystals is similar to the opx and crd in the matrix. Pseudosection modelling of garnet stability in this rock, as well as the microstructural and mineral chemical evidence suggests decompression prior to the attainment of peak temperature. Phase relations indicate minimum temperatures of 800°C and pressures below 4 kbar. Elevated $^{176}Hf/^{177}Hf$ ratios, but almost unchanged $^{176}Lu/^{177}Hf$ ratios in zircon argue for the presence of melt (Xia et al., 2014). This is in agreement with the presence of melt inclusions in hercynite.

The 3150 Ma metamorphic event pre-dates the intrusion of the 3140 Ma Pigg's Peak Batholith (Schoene & Bowring, 2007). It most likely records a renewed NW-ward subduction starting at ca. 3180–3160 Ma as is proposed by Taylor et al. (2012) for the high-grade Luboya-Kubuta terrane, south-central Swaziland.

The geodynamic context of the ca. 2990 Ma granulites is somewhat more certain. These rocks record crustal thinning by rifting and heating due to mantle upwelling, partial melting and the intrusion of mantle melts into the crust. This is documented by the ca. 2995 Ma mafic to intermediate Usushwana Complex (Gumsley et al., 2015), which intrudes the DSS to the southwest.

Gumsley, A., Olsson, J., Söderlund, U., de Kock, M., Hofmann, A., Klausen, M. (2015): Precise U-Pb baddeleyite age dating of the Usushwana Complex, southern Africa–Implications for the Mesoarchaean magmatic and sedimentological evolution of the Pongola Supergroup, Kaapvaal Craton. *Precambrian Res*., **267**, 174-185.

Hunter, D.R., Barker, F., Millard, H.T. Jr (1978): The geochemical nature of the Archean Ancient Gneiss Complex and Granodiorite Suite, Swaziland: a prelinary study. *Precambrian Res.*, **24**, 131-155.

Schoene, B. & Bowring, S.A. (2007): Determining accurate temperature–time paths from U–Pb thermochronology: An example from the Kaapvaal craton, southern Africa. *Geochim. Cosmochim. Acta*, **71**, 165-185.

Taylor, J., Stevens, G., Buick, I.S., Lana, C. (2012): Successive midcrustal, high-grade metamorphic events provide insight into Mid-Archean mountain-building along the SE margin of the proto–Kaapvaal craton. *Geol. Soc. Am. Bull.*, **124**, 1191-1211.

Vavra, G., Schmid, R., Gebauer, D. (1999): Internal morphology, habit and U-Th-Pb microanalysis of amphibolite-to-granulite facies zircons: geochronology of the Ivrea Zone (Southern Alps). *Contrib. Mineral Petrol.*, **134**, 380-404.

Xia, Q.-X., Zheng, Y.-F., Yan, H., Wu, F.-Y. (2014): Contrasting Lu-Hf andU-Th-Pb isotope systematics between metamorphic growth and recrystallization of zircon from eclogite-facies metagranites in the Dabie orogen, China. *Lithos*, **112**, 477-496.

Session S25:

Biogeochemical interfaces and environmental (bio)mineralogy

Conveners:

Giovanni De Giudici (Cagliari – Italy)

Jonathan Lloyd (Manchester – United Kindgom)

Caroline Peacock (Leeds – United Kingdom

REDUCTIVE DISSOLUTION OF IRON(OXYHYDR-)OXIDES AS ASSESSED BY MEDIATED ELECTROCHEMICAL ANALYSIS

Aeppli M.*[1-2], Brown A.R.[2], Voegelin A.[1-2], Hofstetter T.B.[1-2] & Sander M.[1]

[1] Institut für Biogeochemie und Schadstoffdynamik, Eidgenössische Technische Hochschule Zürich, Switzerland

[2] Eidgenössische Anstalt für Wasserversorgung, Abwasserreinigung und Gewässerschutz, Dübendorf, Switzerland

Corresponding email: meret.aeppli@usys.ethz.ch

Keywords: Fe oxides, electrochemistry, thermodynamics

Iron (oxyhydr-)oxides are redox-active geochemical phases that are ubiquitous in natural and engineered systems. By undergoing electron transfer reactions with abiotic and biotic reaction partners, these minerals play key roles in the biogeochemical cycling of major and minor elements as well as in the redox transformations of organic and inorganic pollutants. Electron transfer to iron oxides is most commonly studied in batch systems by reacting the oxides with chemical bulk reductants or by incubating them with iron reducing bacteria, followed by quantification of the reductant consumed or the Fe(II) formed. In this work, we demonstrate the applicability of a novel electrochemical approach, mediated electrochemical reduction, to assess the kinetics and thermodynamics of iron oxide reduction. This approach relies on the use of a dissolved electron transfer mediator to facilitate electron transfer between the working electrode of an electrochemical cell and iron oxides that are added to the cell. It allows for a direct and highly sensitive quantification of the number of electrons that are transferred to the oxide over time and an independent control of *p*H and reduction potential during reduction (Sander et al., 2015). Using mediated electrochemical reduction, we systematically studied the rates and extents of electron transfer to three iron oxides 6-line ferrihydrite, goethite and hematite at *p*H 5.0 to 8.0 and at an applied reduction potential of -350 mV *vs.* SHE. We found that both the rates and extents of electron transfers to the oxides decreased when increasing the *p*H of the suspension from 5.0 to 8.0. While the decrease in reduction rate and extent was relatively small for 6-line ferrihydrite, it was more pronounced for goethite and hematite and occurred over a relatively narrow *p*H range of *p*H 6.5 to 8.0. The reactivity differences between the minerals were consistent with the lower thermodynamic stability of 6-line ferrihydrite as compared to goethite and hematite. We ascribe the decreases in reactivity with increasing *p*H to concomitant decreases in the differences between the calculated potentials of the oxides and the potential applied to the working electrode in the electrochemical cell. Consistent with the expectations, the addition of Fe(II) to the electrochemical cell decreased the oxide reduction rates and extents while the addition of phenanthroline, a strong ligand for Fe(II), had the opposite effect (presumably due to lowering resp. increasing the reduction potentials of the oxide systems). This work is the first to show that mediated electrochemistry can be employed to study reductive dissolution dynamics of Fe oxides and lays the ground for more comprehensive investigations of thermodynamic properties of Fe oxides.

Sander, M., Hofstetter, T. B., Gorski, C.A. (2015): Electrochemical analyses of redox-active iron minerals: a review of nonmediated and mediated approaches. *Environ. Sci. Technol.*, **49**, 5862-5878.

THE NONCLASSICAL QUATARON CONCEPT OF CRYSTAL GROWTH

Askhabov A.*[1]
[1] Institute of Geology, Komi Scientific Center of the Russian Academy of Sciences, Syktyvkar, Russia
Corresponding email: xmin@geo.komisc.ru

Keywords: crystal growth, clusters, quatarons

As is known, in the 20th Century two concepts were developed in parallel in the theory of growth of crystals. According to the first connected with the names of Kossel, Stransky, Kaishev, etc., growth units are separate atoms or ions. The second concept originating with Fedorov and more connected with the name of Balarev assumes growth of crystals by joining of ready crystal blocks. At various times there were suggestions about participation in growth of crystals of intermediate formations (molecular complexes, associates, clusters, etc.). However on this basis it was not possible to develop the alternative concept of crystal growth because of arising contradictions with the classical theory of nucleation and crystal growth.

The situation with relatively stable existence of prenucleation clusters in crystal-forming media after long enough discussions of last years has considerably changed (Gebauer et al., 2014). It is already recognized that formation of nuclei occurs through such clusters (the so-called two-step (Vekilov, 2010) or quataron mechanism of nucleation (Askhabov, 2004). However till now that fact that growth of crystals also occurs by means of such clusters (the quataron model of growth of crystals) is practically ignored.

Quatarons (special pre-crystallization clusters), thanks to their unique properties, are ideal units for crystals growth (Askhabov, 2015). Their joining to a crystal is facilitated by that they topologically are close to structural modules of a crystal. These modules are already potentially “contained” in quatarons. Complete adaptation of quataron structure to a crystal structure occurs on a growing face. As a result the two-dimensional nucleus is formed on the face and by that the problem of formation of a source of steps at layered crystal growth is solved.

On the whole, the following variants of crystals growth with participation of quatarons are possible: transformation of quatarons into two-dimensional nuclei on a growing face of crystals (2D mechanism of crystal growth); decay of quatarons on a growing face into separate atoms (atomic Kossel growth of crystals); crystallization of quatarons in medium and their transport to a growing face (3D growth of crystals). The limiting case of the 3D growth is the block mechanism (oriented aggregation (agglomeration) of crystalline particles).

Acknowledgements: This work is supported by RFBR (14-05-00592/16) and Program of Basic Researches of RAS (15-18-5-45).

Askhabov, A.M. (2004): Cluster (quataron) self-organization of matter at nanolevel and formation of crystalline and non-crystalline materials. *Zap. Vser. Miner. Obshch.*, **133**, 108-123 (in Russian).

Askhabov, A.M. (2011): The quataron concept: main ideas and some applications. *Proc. Komi Sci. Centre*, *Ural Branch*, *Russian Acad. Sci.*, **3**, 70-77 (in Russian).

Askhabov, A.M. (2015): Quataron nature of the nonclassical mechanism of crystal nucleation and growth. *Vestnik Inst. Geol. Komi Sci. Centre*, *Ural Branch*, *Russian Acad. Sci.*, **4**, 3-7.

Gebauer, D., Kellermeier, M., Gale, J.D., Bergström, L., Cölfen, H. (2014): Pre-nucleation clusters as solute precursors in crystallization. *Chem. Soc. Rev.*, 43, 2348-2371.

Vekilov, P. (2010): The two-step mechanism of nucleation of crystals in solution. *Nanoscale*, **2**, 2346-2357.

CONSIDERATION ON THE MOUNT ETNA FINE ASH RAISES CONCERNS FOR THE HEALTH DUE TO THE CHEMICAL RELEASE AND THE IRON BEHAVIOR

Bardelli F.[1], Barone G.[2], Costagliola P.[3], D'Acapito F.[4], De Giudici G.[5], Di Benedetto F.[3], Giuffrida A.[2], Mazzoleni P.*[2], Montegrossi G.[6] & Podda F.[3]

[1] Istituto di Nanotecnologia, Consiglio Nazionale delle Ricerche, Roma, Italy

[2] Dipartimento di Scienze Biologiche, Geologiche e Ambientali, Università di Catania, Italy

[3] Dipartimento di Scienze della Terra, Università di Firenze, Italy

[4] Istituto Officina dei Materiali, Consiglio Nazionale delle Ricerche, c/o ESRF, Grenoble, France

[5] Dipartimento di Scienze Chimiche e Geologiche, Università di Cagliari, Italy

[6] Istituto di Geoscienze e Georisorse, Consiglio Nazionale delle Ricerche, Firenze, Italy

Corresponding email: pmazzol@unict.it

Keywords: Mt. Etna ashes, health, Gamble solution

Mount Etna is the most active and largest volcano in Mediterranean area and is located on eastern Sicily (Italy). The recent activity of the volcano is characterized by paroxysmal events from the South-East Crater (Andronico et al., 2011) consisting in lava fountains associated to lava flows emission and the formation of ash-plumes. The dispersion of the erupted ashes on densely populated area periodically causes a lot of damages to the environment and to the infrastructure and raises concerns for the health of the inhabitants. This latter has been frequently overlooked because the lack of free silica phases with the exception of rare cristobalite xenocrystals. However, Barone et al. (2016) showed the mineralogical and chemical surface modification of glass particles emitted by Mt Etna as function of gas interaction during the explosive activity. In this communication we present preliminary data regarding the possible respiratory health effects of the fine ashes. In particular we investigate the release of dangerous element in lung due to fine volcanic ash particles and the possible risk due to the formation of free radicals on the surface of particles caused by the behavior of iron (Horwell et al., 2013).

The first topic was investigated using Gamble solution leaching experiments according the recently proposed protocols (Stewart et al., 2013). They evidenced the presence of S, Si, Li, Ni, Cu and Tl in the leachate above detection limit only for some selected grain size fraction (<38 micron). Zn, Ba, Fe and Al were found in meaningful amounts for all the samples. Notice that As was found for only one sample.

The iron behavior was studied by means of Electron Paramagnetic Resonance (EPR), high field high frequency EPR (HFEPR) and X-ray Absorption Spectroscopy (XAS), this latter performed at the Fe *K* edge. The preliminary results highlight, from the analysis of the pre-edge and XANES regions, the coexistence of Fe(II) and Fe(III) species in an almost constant ratio at a given particle granulometry. Conversely, Fe(III)/Fe(II) ratio increases with decreasing the particle granulometry, suggesting that the oxidation layer is almost constant in thickness. Fe(III) is found distributed over at least two different phases, most of it being included in the volcanic glass, and the remaining hosted in an own, magnetic, phase, probably an Fe oxide. Finally, important for the goal of this communication is the absence of iron-induced hydroxyl radical.

Andronico, D. & Corsaro, R.A. (2011): Lava fountains during the episodic eruption of South-East Crater (Mt. Etna), 2000: insights into magma-gas dynamics within the shallow volcano plumbing system. *Bull. Volcanol*., **73**, 1165-1178.

Barone, G., Mazzoleni, P., Corsaro, R.A., Costagliola, P., Di Benedetto, F., Ciliberto, E., Gimeno, D., Bongiorno, C., Spinella, C. (2016): Nanoscale surface modification of Mt. Etna volcanic ashes. *Geochim. Cosmochim. Acta*, **174**, 70-84.

Barone, G., Ciliberto, E., Costagliola, P., Mazzoleni, P. (2014): X-ray photoelectron spectroscopy of Mt. Etna volcanic ashes. *Surf. Interface Anal*., **46**, 847-850.

Horwell, C.J., Fenoglio, I., Fubini, B. (2007): Iron-induced hydroxyl radical generation from basaltic volcanic ash. *Earth Planet. Sci. Letters*, **261**, 662-669.

Stewart, C., Horwell, C., Plumlee, G., Cronin, S., Delmelle, P., Baxter, P., Calkins, J., Damby, D., Morman, S., Oppenheimer, C. (2013): Protocol for analysis of volcanic ash samples for assessment of hazards from leachable elements. Int. Volcanic Health Hazards Network Publ., 22 p.

ELECTROCHEMICAL CHARACTERISATION OF MICROBIAL FE(III) REDUCTION

Brown A.R.*[1], Aeppli M.[2], Voegelin A.[1], Sander M.[2] & Hofstetter T.B.[1]
[1] Eidgenössische Anstalt für Wasserversorgung, Abwasserreinigung und Gewässerschutz, Dübendorf, Switzerland
[2] Institut für Biogeochemie und Schadstoffdynamik, Eidgenössische Technische Hochschule Zürich, Switzerland
Corresponding email: ashley.brown@eawag.ch

Keywords: Fe(III) reduction, *Shewanella*, electrochemistry

Dissimilatory Fe(III)-reducing bacteria, such as *Shewanella oneidensis*, may impart significant controls on the availability, mobility and toxicity of bulk and trace elements, via both direct enzymatic and indirect (e.g., *via*biogenic Fe(II)-mediated) processes. Mineral dissolution and secondary (bio)mineralization reactions often accompany the reduction of solid phase Fe(III) and these processes may subsequently alter system thermodynamics (i.e., redox potentials) that defines the pool of reactive and/or bioavailable Fe. There is therefore a clear requirement to assess rates and extents of Fe(III) reduction and relate these observations to thermodynamic parameters. Conventional quantification of formed Fe(II) commonly relies on the ferrozine and 1,10-phenanthroline colorimetric assays. However, both these assays have limitations, including: (i) the ability to only assess Fe(II), with the addition of a reductant required to quantify total Fe; (ii) the requirement for a time-consuming acid digest step, to achieve complete mineral dissolution; (iii) overestimation of Fe(II) by ferrozine due to photochemical reduction of the Fe(III)-ferrozine complex, and (iv) overestimation of Fe(II) by phenanthroline due to interference from the Fe(III)-phenanthroline complex. Alternatively, mediated electrochemical reduction and oxidation (MER/MEO) and mediated potentiometric measurements, two complementary amperometric and potentiometeric techniques, offer to directly quantify both the electron accepting and donating capacities of a given Fe-containing sample (and thus the total amounts of Fe(III) and Fe(II), respectively) as well as the reduction potential of the system (Sander et al., 2015). MER and MEO have previously been successfully applied to the abiotic redox cycling of Fe-bearing phyllosilicates (Gorski et al., 2013) and the microbial reduction of dissolved humic substances, which act as terminal electron acceptors in anaerobic respiration (Klüpfel et al., 2014). Here we demonstrate that mediated electrochemical techniques can also be used to quantify the extracellular electron transfer to solid phase Fe(III) (oxyhydr-)oxides, such as 6-line ferrihydrite by *S. oneidensis*, allowing the direct and highly sensitive quantification of both Fe(II) and Fe(III) and precluding any requirement for sample preparation or acid digest steps. The contribution will also show how the electrochemical analyses can be complemented by TEM and spectroscopic analyses (e.g., XRD and XAS) to link biological and mineralogical limits to Fe(III)-reduction to thermodynamic constraints. The presented work will lay the foundation for a more comprehensive and systematic analysis of the thermodynamic controls on microbial Fe(III) reduction for a range of poorly soluble Fe-bearing mineral phases, including Fe oxides and Fe(III)-bearing phyllosilicates.

Gorski, C.A., Klüpfel, L.E., Voegelin, A., Sander, M., Hofstetter, T.B. (2013): Redox properties of structural Fe in clay minerals: 3. Relationships between smectite redox and structural properties. *Environ. Sci. Technol.*, **47**, 13477-13485.

Klüpfel, L., Piepenbrock, A., Kappler, A., Sander, M. (2014): Humic substances as fully regenerable electron acceptors in recurrently anoxic environments. *Nature Geosci.*, **7**, 195-200.

Sander, M., Hofstetter, T.B., Gorski, C.A. (2015): Electrochemical analyses of redox-active iron minerals: a review of nonmediated and mediated approaches. *Environ. Sci. Technol.*, **49**, 5862-5878.

MICROORGANISMS IN AMD PROCESSES AND THEIR ROLE IN METALS FATE: THE CASE OF LIBIOLA Fe-Cu MINE AND GROMOLO STREAM FLOW (EASTERN LIGURIA, ITALY)

Carbone C.[1], Consani S.*[1], Zotti M.[1], Giovine M.[1], Tolotti R.[1], Cutroneo L.[1], Capello M.[1] & Lucchetti G.[1]
[1] Dipartimento di Scienze della Terra, dell'Ambiente e della Vita, Università di Genova, Italy
Corresponding email: lucchett@dipteris.unige.it

Keywords: AMD, microorganisms, metals

Abandoned sulphide mine sites, due to sulphide oxidation and lack of infrastructures maintenance, often cause an enrichment in heavy metals and metalloids of environmental concern in the surrounding ecosystems. Acid Mine Drainage (AMD) process can remobilise high loads of ecotoxic elements jeopardising the quality of aquatic and terrestrial systems. AMD waters are extremophile environments, but many microorganisms, such as microbes, algae, and fungi, are able to survive to metals and acid stresses (Das et al., 2009), deeply influencing the mobility of elements. Bacteria can dramatically fasten the dissolution rate of sulphides, while fungi and algae can accumulate or absorb metals onto their cellular walls or EPS (Extracellular Polymeric Substances). The abandoned Libiola Fe-Cu mine (Eastern Liguria, Italy) is a well known AMD impacted area (Carbone et al., 2013), where acidic and metal polluted waters flow into the Gromolo stream flow, the main watercourse of the area. The aims of this work are: a) characterise the microorganisms living in AMD precipitates and in the AMD impacted Gromolo stream flow; b) evaluate their role in the release or uptake of metals.

In acid waters ochreous precipitates the presence of acidophilic or estremophile diatom genera (*Achnantidium*, *Fragilaria*, and *Pinnularia*) and bacteria were recognised. In particular, many S and Fe oxidising bacteria (genera *Thiomonas*, *Leptospirillum*, *Acidithiobacillus*, and *Acidimicrobium*) were found. In near-neutral greenish-blue precipitates, fungal strains belonging to different genera (*Penicillium*, *Cladosporium*, and *Thricoderma)*were isolated and tested for Cu and Zn bioaccumulation capacity. The results showed that the isolated strains, especially *Penicillium*, are able to uptake a high concentration of metals in their biomass (up to 13600 and 1520 mg kg^{-1} for Cu and Zn, respectively).

In the Gromolo stream flow, a significant difference between the diatom assemblage before and after the confluence of AMD water was observed, as biodiversity dropped and many acidophilic species appeared. Moreover, teratological forms, mainly of *Fragilaria* and *Achnantidium*, indicate that metals are bioavailable and accumulated, as confirmed by DTG (Diffusion Gradient in Thin film) data (34 and 52 µg l^{-1} for Zn and Cu, respectively) collected in the same sampling point.

The results show that bacteria facilitate metals release caused by AMD, while algae and fungi can, at least temporarily, accumulate and scavenge metals from solution.

Carbone, C., Dinelli, E., Marescotti, P., Gasparotto, G., Lucchetti, G. (2013): The role of AMD secondary minerals in controlling environmental pollution: Indications from bulk leaching tests. *J. Geochem. Explor.*, **132**, 188-200.

Das, B.K., Roy, A., Koschorreck, M., Mandal, S.M., Wendt-Potthoff, K., Bhattacharya, J. (2009): Occurrence and role of algae and fungi in acid mine drainage environment with special reference to metals and sulphate immobilization. *Water Res*., **43**, 883-894.

BIOMONITORING OF AIRBORNE Hg BY *PINUS NIGRA* BARKS: AN EXAMPLE FROM THE Mt. AMIATA AREA, SOUTHERN TUSCANY, ITALY

Chiarantini L.[1], Rimondi V.[1], Benvenuti M.[2], Beutel M.W.[3], Costagliola P.[2] & Lattanzi P.*[1]
[1] Istituto di Geoscienze e Georisorse, Consiglio Nazionale delle Ricerche, Firenze, Italy
[2] Dipartimento di Scienze della Terra, Università di Firenze, Italy
[3] School of Engineering, University of California, Merced, CA, USA
Corresponding email: pierfrancolattanzi@gmail.com

Keywords: mercury, tree barks, air quality monitoring

Although tree barks are not routinely employed for biomonitoring purposes, they offer some potential advantages, such as a year-round and almost ubiquitous availability, and easy identification and sampling. Tree barks appear particularly suited for biomonitoring of airborne mercury, because: 1) some experimental studies suggest an affinity between this metal and barks; 2) mercury reaches tree wood and bark mostly through leaves rather than through roots, i.e. the systemic uptake from soils can be considered marginal.

To test the application of this potential tool, we sampled *Pinus nigra* barks from the Mt. Amiata region, which was until 1980 the third largest Hg producing region of the world. *Pinus nigra* was selected because of its wide diffusion in the investigated area, and because of its multilayered barks, that may allow to investigate the distribution of Hg across its thickness.

Barks and related soils were collected in different sites, including: the Abbadia San Salvatore mining area; two sites close to geothermal power plants (presently exploited for electricity production), and two sites (Bagni S. Filippo and Vivo D'Orcia) which should provide a local background value. In addition, we choose another area which should be unaffected by Hg contamination (Monte Morello near Florence). Bark samples were sliced at least in three portions (external, middle and internal), and analyzed separately by means of Direct Mercury Analyzer (Milestone DMA-80). Mercury concentrations were then corrected for water loss.

The maximum Hg contents (up to 8.7 mg/kg) were displayed in barks collected in close proximity of the Abbadia mining/retorting facilities, representing the highest Hg concentrations ever recorded in barks. All barks display a general decrease of Hg concentration from the surface inwards, suggesting Hg deposition (and in-depth penetration) from the atmosphere, with no significant systemic intake of Hg from soil. Lower, but still high Hg (hundreds of microg/kg) contents were recorded also in the background areas at Bagni San Filippo, where a positive anomaly of Hg in air was recently reported. Mercury contents in tree barks around the two geothermal plants are the lowest recorded in the Mt. Amiata region, including the "background" sites.

Speciation of mercury in the analyzed barks was investigated by X-ray absorption spectroscopy in a recent experiment carried out at ESRF, Grenoble; the results should be available for presentation at the Conference.

Mercury concentration in lichens grown on Hg-polluted soils in the area is of same order of magnitude as the analyzed barks, suggesting that barks are possibly as reliable as lichens in recording regional differences of Hg pollution.

CHEMICAL PROCESSES AND POSSIBLE BIOLOGICAL CONTRIBUTION DURING WEATHERING OF TETRAHEDRITE, $(Cu,Ag)_2(Fe,Zn,Hg)_{10}(Sb,As)_4S_{13}$

Chovan M.*[1], Števko M.[1], Majzlan J.[2], Radková A.[3], Jamieson H.[3] & Lalinská-Voleková B.[1]
[1] Department of Mineralogy and Petrology, Comenius University, Bratislava, Slovakia
[2] Institut für Geowissenschaften, Friedrich-Schiller-Universität Jena, Germany
[3] Department of Geological Sciences and Geological Engineering, Queen's University, Kingston, Canada
Corresponding email: sawe76@web.de

Keywords: tetrahedrite, trombolite, tripuhyite

Tetrahedrite is a complex solid solution of composition $(Cu,Ag)_2(Fe,Zn,Hg)_{10}(Sb,As)_4S_{13}$. The number of elements that fit in the structure of this mineral is rather high. Weathering of such complex matrix provides a unique opportunity to trace the mobility and behavior of a number of metals and metalloids in the near-surface environment. In this work, we have investigated weathering of tetrahedrite in an environment where carbonates and pyrite are essentially lacking and tetrahedrite is the major ore mineral dispersed in Permian arkoses at a site Piesky near Špania Dolina (central Slovakia). In the tetrahedrite studied, Sb/(Sb+As) is always > 0.5 and Zn/(Zn+Fe) is also > 0.5. The Ag content is moderate, Hg is not present. Missing pyrite and carbonates imply missing acidity-generation potential and acidity-buffering potential, respectively.

The initial weathering product of tetrahedrite is an X-ray amorphous olive-green mass, referred to as *trombolite* in old literature (Zepharovich, 1873). We used optical and electron microscopy to distinguish several components and define the variable chemical composition. Elements present in original tetrahedrite fractionate into the Cu-As rich remnants, rimmed by Fe- and Sb-dominating veinlets. Ag is retained in secondary acanthite, Zn and S are washed out. The earliest stage of weathering are marked by aggregates and crystals of chalcocite and covellite that grow directly on tetrahedrite and later give way to the oxide weathering products. Synchrotron X-ray diffraction identified tripuhyite- and stibiconite-like phase in the Fe-Sb material; the Cu-As material is X-ray amorphous.

In the later stages, Cu is the most mobile metal and As is a mobile metalloid. A number of supergene minerals can be found in the outcrops, old mines, and the historical dumps. The top of the profiles through the oxidation zone contains mostly malachite and azurite; an isotopic study of carbon in these minerals is underway. Malachite is also being formed currently in some buried dumps. Below, a rich association of Cu arsenates/phosphates is observed, including chalcophyllite, clinoclase, cornwallite-pseudomalachite, olivenite-libethenite, tangdanite, and bariopharmacosiderite, and camérolaite. Jarosite is also present on the dumps. Abundant colorless, clear barite crystals that grow on Cu carbonates witness Ba mobility in the oxidation zone. The preliminary measurements of the Cu isotopic composition ($\delta^{65}Cu$) of selected secondary Cu minerals shows great variations (from –4 to +4‰). More measurements will be done soon to characterize the variations and help to understand this unusually large isotopic range for a heavy metal.

Mining activities in the studied area modified water flow and irreversibly altered the weathering processes. The manifestation of these changes is an overprint of the supergene minerals by a paragenesis of Cu sulfates including antlerite, brochantite and jarosite. Langite, devilline, and posnjakite precipitate inside the dumps, along with some of the brochantite and malachite. Water samples will be analyzed for a number of elements, including those found in tetrahedrite, to define mobility of these elements, given the geological and mineralogical background that is well known at the site studied.

Zepharovich, V.V. (1873): Mineralogisches Lexikon für das Kaiserthum Österreich, II. Band. Braumüller, Wien, 436 p.

ENHANCED *IN-SITU* MICROBIAL TREATMENT OF STRONTIUM IN SEDIMENT SYSTEMS BY STIMULATION WITH GLYCEROL PHOSPHATE

Cleary A.*[1], Newsome L.[1], Lloyd J.R.[1], Shaw S.[1], Boshoff G.[2], Trivedi D.[2], Atherton N.[3] & Morris K.[1]

[1] Research Centre for Radwaste Disposal &Williamson Research Centre for Molecular Environmental Science, School of Earth, Atmospheric and Environmental Sciences, University of Manchester, United Kingdom

[2] National Nuclear Laboratory, Warrington, United Kingdom

[3] Sellafield Ltd. Land Quality, Sellafield, United Kingdom

Corresponding email: adrian.cleary@manchester.ac.uk

Keywords: bioreduction, phosphate, radionuclides

Nuclear fuel cycle operations over the last 60 years have led to a legacy of radioactively contaminated land at sites such as Sellafield and Dounreay in the UK and Hanford and Oak Ridge in the USA. ^{90}Sr is often considered one of the priority mobile radionuclides present at elevated concentrations in groundwater within these sites but may also be present with other contaminants in groundwaters. *In situ* bioremediation treatments are capable of immobilising several radioactive contaminants within the subsurface, including U, ^{99}Tc and ^{90}Sr. It is important that the products of remediation are resilient to environmental perturbations and also that these remediation strategies consider treatment of likely co-contaminants present at nuclear licensed sites.

The dominant control on ^{90}Sr mobility in the environment is sorption as the Sr^{2+} ion although Sr removal to solids may be increased through addition of sorbent materials such as hydroxylapatite, or by increasing the *p*H through nitrate bioreduction. The co-precipitation of Sr into stable mineral phases is also another pathway which has the potential to ensure the long term removal of ^{90}Sr from groundwater.

The focus of this study is co-precipitation of Sr with stable phosphate minerals using an in-situ biomineralisation treatment previously shown to treat soluble uranium (Newsome *et al*., 2015a). In the current work, a pure culture biomineralisation experiment with soluble Sr^{2+} was conducted anaerobically using glycerol phosphate as the electron donor to stimulate growth of a *Serratia isolate* (Newsome *et al*., 2015b*)* and in a synthetic freshwater minimal media containing Sr^{2+} and Ca^{2+} (0.7 and 16 mM). Following the biodegradation of glycerol phosphate, inorganic phosphate was released to solution and a decrease in Ca^{2+} and Sr^{2+} concentrations was observed. These data will be discussed in terms of aqueous and solid phase analyses.

Additionally, a series of sediment microcosms were stimulated with glycerol phosphate under anaerobic conditions to examine the impact of this on Sr behaviour. Here, results show that sediments treated with glycerol phosphate removed 90±2% Sr from solution compared to only 44±1.2% removal from untreated sediments. Ongoing work is examining the nature and stability of strontium phases that are responsible for the enhanced removal using a range of direct and sequential extraction processes. Overall, these data suggest that enhanced removal of Sr from solution during biostimulation by glycerol phosphate may occur through the formation of phosphate biominerals. This opens up new routes for the co-treatment of strontium and other redox active radionuclides such as technetium and uranium. The latter has been shown to be reduced in sediment systems in the presence of glycerol phosphate to form a recalcitrant U(IV)-phosphate (Newsome *et al*., 2015a).

Newsome, L., Morris, K., Trivedi, D., Bewsher, A., Lloyd, J.R. (2015a): Biostimulation by glycerol phosphate to precipitate pecalcitrant pranium(IV) phosphate. *Environ. Sci. Technol*., **49**, 11070-11078.

Newsome, L., Morris, K., Lloyd, J.R. (2015b): Uranium biominerals precipitated by an environmental isolate of *Serratia* under anaerobic conditions. *PLoS One*, **10**, e0132392.

MICROBIAL PROCESSES WITHIN BENTONITE BARRIER MATERIALS

Haynes H.*[1], Pearce C.[2-3-4], Morris K.[1], Pattrick R.[1], Pimblott S.[2-3] & Lloyd J.R.[1]
[1] Williamson Research Centre for Molecular Environmental Science & Research Centre for Radwaste Disposal, School of Earth, Atmospheric, and Environmental Sciences, University of Manchester, United Kingdom
[2] School of Chemistry, University of Manchester, United Kingdom
[3] Dalton Cumbrian Facility, University of Manchester, Cumbria, United Kingdom
[4] Geosciences Group, Pacific Northwest Laboratory, Richland, WA, USA
Corresponding email: haydn.haynes@postgrad.manchester.ac.uk

Keywords: bentonite, microbiology, mineralogy

The United Kingdom has been generating nuclear waste since the 1940's. Radioactive Waste Management is responsible for implementing geological disposal of the UK's radioactive waste. Wastes are to be disposed of in a future Geological Disposal Facility (GDF), and will include higher activity wastes, and potentially, other nuclear materials, as defined in the White Paper on implementing geological disposal (DECC, 2014). High heat generating wastes (HHGW) consist mostly of spent fuel (SF) from current/future power stations, and high level waste from SF reprocessing.

Bentonite is a clay-based barrier material considered for use in many HHGW disposal concepts. Bentonite delivers several safety functions including long-term low permeability, a chemical environment favouring disposal canister integrity, attenuation of the migration of radionuclides released from the waste, limiting the transfer of soluble corroding agents to the container, and minimizing microbial activity. This project aims to extend the UK's current knowledge base concerning microbial processes within bentonite, by exploring the following objectives:

1. Demonstrate the effect of bentonite density/swelling pressure on microbial activity, in relation to microbial colonization, as well as on microbial Fe(III) reduction.

2. Understand the impact of stresses including gamma irradiation on aforementioned processes, including the impact on *in situ* processes, and the mineralogical structure of bentonite.

3. Consider the influence of temperature and evolving resaturation on the microbial population within the bentonite buffer and their interaction with bentonite, using samples from the FEBEX *in-situ* experiment (ENRESA, 2000) at the Grimsel Test Site.

DECC (2014): Department of Energy and Climate Change - Implementing Geological Disposal. Report URN 14D/235.
ENRESA (2000): National Radioactive Waste Company - FEBEX project: full-scale engineered barriers experiment for a deep geological repository for high level radioactive waste in crystalline host rock. Report 01/2000.

HIERARCHICAL DOMAIN STRUCTURE OF CALCIUM CARBONATES IN *PINCTADA MARTENSII* SHELLS

He J.*[1-2], Zhao S.[2] & Bismayer U.[1]
[1] Mineralogisch-Petrographisches Institut, Universität Hamburg, Germany
[2] School of Earth Sciences, China University of Geosciences, Wuhan, China
Corresponding email: jianhan.he@uni-hamburg.de

Keywords: biominerals, aragonite, domain structure

Aragonite formed in biomaterials such as shells of bivalves has excellent mechanical properties because of its hierarchical structure and complex topology. In this study, polarized microscopy shows complex ordering features in the nacreous layer; X-ray diffraction and Raman spectroscopy show that there are two calcium carbonate polymorphs in different parts of the shells; Electron Backscatter Diffraction was applied to obtain the local crystal orientation of nacre. The results show that the c-axes of the majority of the aragonite nano-particles is oriented perpendicular to the shell body, a and b-axes are organized in a two level domain structure. In the primary domain structure, there occurs a ca. 64° misorientation of the *a*-axes between different domains. In the secondary domain structure, misorientation angles of two different aragonite sheets are around 10° or 20°. This kind of domain structure is relevant for the growth mechanism of aragonite in nacre.

ON THE FORMATION OF AGGREGATION AND CRYSTALLIZATION STRUCTURES OF HUMAN OXALATE RENAL STONES

Izatulina A.R.*[1], Punin Y.O.[1], Shtukenberg A.G.[1], Kalkura S.N.[2] & Frank-Kamenetskaya O.V.[1]
[1] Department of Crystallography, Saint Petersburg State University, Russia
[2] Crystal Growth Centre, Anna University, Chennai, India
Corresponding email: alina.izatulina@mail.ru

Keywords: oxalate renal stones, aggregation structure, crystallization structure

Herein we report on the oxalate renal stones internal structure (whewellite spherulitic aggregates, correlation between whewellite and weddellite, thin rhythmic zoning of whewellite renal stones after the organic substance impurity, weddellite dendrite structures) investigations along with the calcium oxalates crystallization modeling experiments in terms of temperature and concentrations of inorganic and organic components of the solution variations. For all the diversity of the internal structure of renal stones, there are two distinctly different types of genetic structures of these pathological entities - crystallization and aggregation (sedimentation) structures. Among the calcium oxalate stones both types of structures are found, although crystallization structures are more common. The results of calcium oxalate renal stones internal structure analysis show the essentially nonstationary processes of calcium oxalate phases crystallizations. Repeated nucleation acts of whewellite spherulites, periodic alternation of whewellite and weddellite phases reflect changes in the composition of physiological solution caused by external factors related to the activity of the organism. Intensive aggregation of crystals during deposition indicates the decrease of volume concentration on the background of increasing the crystals size, based on crystal size distribution graphs analysis. At the initial stages of crystallization fine particles are mainly captured by larger ones in the form of substance deposition on the initiating centers: organic blobs, dead cells, and so on. During the crystallization the effect of the dominant growth of large aggregates increases; the process develops autocatalytically; fine particles disappear more rapidly than large ones, and the crystal size distribution compresses simultaneously with an increase in the average particle size. The investigation showed that the inhibition of the nucleation and growth of calcium oxalate monohydrate crystals in normal physiological solution occurs at normal amino acid composition, due to adsorption on the stone surface. Whewellite crystallize with the oxalate ions concentration is up to oxalatourea disease value. An addition of organic substance (ovalbuminum, gelatin, protein-containing environ) or microorganisms (bacteria and viruses) in oxaluria disease condition contributes whewellite crystallization and leads to formation of weddellite with variable amount of water that results in a different stability.

Acknowledgements: This work was supported by St. Petersburg State University (no. 3.38.243.2015). The XRD studies have been performed at the X-ray Diffraction Centre of St. Petersburg State University.

THE APPLICATION OF SUBSURFACE METAL-REDUCING BACTERIA FOR THE PRODUCTION OF COPPER NANOPARTICLES

Kimber R.L.*[1], Pattrick R.[1], Figueroa-Garcia A.[2] & Lloyd J.R.[1]
[1] School of Earth, Atmospheric and Environmental Sciences, University of Manchester, United Kingdom
[2] Magnetic Spectroscopy Group, Diamond Light Source, Didcot, United Kingdom
Corresponding email: richard.kimber@manchester.ac.uk

Keywords: copper nanoparticles, biosynthesis, XAS

Metal nanoparticle production and application has received considerable global attention over the past two decades due to their unusual and useful properties which differ from bulk materials. The excellent conductivity, catalytic activity and relatively low cost of copper has generated much recent interest in the production of Cu nanoparticles (Cu-NPs) for diverse uses including catalysis, anti-microbial applications, and magnetic storage media. Current synthesis methods involve the use of non-aqueous solvents under highly controlled conditions or toxic chemicals in aqueous conditions. Therefore, a simple, cost-effective, and environmentally friendly synthesis route is highly desired. Previous work on Cu-NP biosynthesis has focussed largely on microbial detoxification mechanisms. Here we report the biosynthesis of Cu-NPs using subsurface metal-reducing bacteria. Characterization of biosynthesized Cu-NPs and mechanistic information regarding their production are discussed.

Cu-NPs were synthesized from an aqueous Cu^{2+} solution using the metal-reducing bacterium *Shewanella oneidensis.* To investigate potential reduction mechanisms during Cu-NP formation, deletion mutants lacking either*mtr* c-type cytochromes of the outer membrane (OM) or all cytochromes beyond the cytoplasmic membrane bound *cymA* were used in addition to the wild type strain. ICP-AES data indicates reduction of > 90% and > 95 % of 50 µM Cu by all *S. oneidensis* strains after 24 and 96 hours, respectively. At a higher Cu concentration of 200 µM, the wild type strain was able to reduce up to 3.5 times more Cu^{2+} than the mutants. This suggests that the *mtr*OM cytochromes play an important role in cell defence against Cu toxicity, with OM reduction limiting cellular uptake of Cu^{2+}. TEM imaging confirmed the presence of crystalline Cu-NPs ranging from individual particles of 5nm to aggregates up to 400nm. The majority of these particles are associated with the cells and are present as both extra-cellular and intra-cellular particles. Electron microscopy imaging is ongoing to determine better the extent of intra- and extra-cellular particles. HR-TEM FFT images and lattice spacings correspond well with the 111 and 222 planes of metallic Cu. XANES data collected at the Cu *K*- and Cu-$L_{2,3}$ edges confirmed the oxidation state of the biosynthesised nanoparticles is Cu^0. EXAFS analysis is ongoing and will also be presented.

This work demonstrates the green synthesis of Cu-NPs using metal-reducing bacteria. Due to the anti-microbial properties of Cu, little information exists on bacterial reduction mechanisms which this work addresses through the use of cytochrome targeted deletion mutants. HR-TEM and XAS analysis provide detailed characterisation of the synthesised Cu-NPs. The ability of metal-reducing bacteria to produce nanoparticles from Cu-bearing solutions offers the potential to use these bacteria to produce useful nanomaterials from Cu-bearing waste streams which we are currently exploring.

MICROBIAL MECHANISMS IN BIOMINERALIZATION

Kothe E.*[1], Klose M.[1], Meier A.[1] & Schütze E.[1]
[1] Institut für Mikrobiologie, Friedrich-Schiller-Universität Jena, Germany
Corresponding email: erika.kothe@uni-jena.de

Keywords: biomineralization, microorganisms, metal resistance

Activities of microorganisms can lead to formation of biominerals. This biomineralization has been described to be either 'microbially controlled' or “microbially induced”. The distinction is easily established, when intracellular formation of biominerals is seen, like with magnetotactic bacteria *versus* mere changes of environment followed by classical mineral formation. However, evidence is accumulating for intermediate processes with specific proteins inducing different crystalloid (macro)morphology. This includes specific microscopic or nanoscale lattice structures provided by the protein backbone, but also the supply of mineral components (e.g., phosphate, reduced nitrogen compounds, etc.) through microbial exudation. Especially with respect to metal resistance mechanisms, this is an active process, costly to the cells. Hence, the concept of biomineralization should be re-visited and a more detailed classification of biomineralization processes is needed including formation of a stable backbone determining the macromorphology of biominerals even at distance from cell surfaces.

Here, examples of microbial biomineralization processes in metal rich environments on a former heap site is discussed. The formation of manganese hydroxides, like birnessite, leading to massive hardpan formation, is one of the examples derived from the former uranium mining site in Thuringia, Germany. Other examples with different macromorphologies include carbonates, (magnesium) calcite or vaterite, formed under laboratory conditions with strains of streptomycetes in dependence of excreted amphipathic surface proteins of the bacteria. And as a third example, the formation of (nickel) struvite, switzerite and nickel phosphate formation on soil from the former mining site under laboratory conditions will be discussed.

From the original research, a new concept for microbially aided, extracellular biomineral formation is developed. The concept thus extends the previous distinction of biomineralization on the part of the “microbially induced” formation in a process oriented way including microbial physiology and secondary metabolism into a unified concept of biomineralization.

THE REMOVAL OF HEAVY METAL AND RADIONUCLIDE COMPLEXES *VIA* THE BIODEGRADATION OF ISOSACCHARINIC ACID IN NUCLEAR WASTE DISPOSAL

Kuippers G.*[1], Bryan N.[2], Bagshaw H.[1], Morris K.[1] & Lloyd J.R.[1]

[1] Research Centre for Radwaste and Decommissioning & Williamson Research Centre for Molecular Environmental Science, School of Earth, Atmospheric and Environmental Sciences, University of Manchester, United Kingdom

[2] National Nuclear Laboratory, Warrington, United Kingdom

Corresponding email: gina.kuippers@manchester.ac.uk

Keywords: isosaccharinic acid, biodegradation, radionuclide

It is UK Government policy to dispose of higher activity radioactive waste through geological disposal into an engineered deep underground geological disposal facility (GDF). Low-level (LLW) and intermediate-level (ILW) radioactive wastes are very heterogeneous, containing significant amounts of cellulosic material. After closure of the GDF, eventual resaturation with groundwater will result in the development of a highly alkaline environment within the cementitious backfill. Under these high pH conditions, cellulose is unstable and will be degraded chemically, forming a range of water-soluble degradation products, including isosaccharinic acid (ISA). As ISA is known to form stable, soluble complexes with a range of radionuclides, in particular Am(III), Eu(III), Np(IV), U(VI) and U(IV) and other metals, such as Ni(II), the impact of microbial metabolism on this organic substrate was investigated, to help determine the role of microorganisms in moderating the transport of radionuclides and metals from a cementitious GDF.

In this study we focused on circumneutral conditions representative of the geosphere surrounding a GDF. Here we report the fate of ISA in circumneutral microcosms poised under anaerobic conditions; the latter with nitrate, Fe(III) or sulfate added as electron acceptors for microbial metabolism. Data are presented confirming the fermentation of ISA and to acetate, propionate and butyrate prior to utilization of these acids during Fe(III) and sulfate reduction thereby also reducing methanogenic gas production. Also presented are the microbial communities associated with these processes that were characterized using 16S rRNA gene pyrosequencing.

Data will also be presented on ISA complex formation and breakdown under Fe(III)- and sulfate-reducing conditions poised with nickel(II) and uranium(VI), both of which are forming complexes with ISA. Uranium(VI) is a major constituent of nuclear waste with the isotopes ^{235}U and ^{238}U of greatest significance due to their substantially long half-lives. Nickel(II) is an important component of the metal alloys used in reactor components. Two radioactive isotopes of concern, ^{59}Ni and ^{63}Ni, are produced by neutron activation of these metal components. Transmission electron microscopy (TEM) and environmental scanning electron microscopy (ESEM) were applied to obtain insight into the impact of biomineral formation in controling the fate of the metals. With X-ray absorption spectroscopy (XAS) changes in metal speciation during ISA metabolism were identified. Based on this outcome, the impact of ISA degradation on metal and radionuclide solubility, and hence mobility, will be also assessed in future experiments.

MINERALOGICAL CHARACTERISTICS OF IRON-MANGANESE CUTANS IN A AND B HORIZON OF SUBTROPICAL SOILS IN CHINA

Li Y.*[1], Li Y.[1], Xu X.[1], Lu A.[1], Yang X.[1], Wang H.[1] & Ding C.[1]

[1] Key Laboratory of Orogenic Belts and Crustal Evolution, School of Earth and Space Sciences, Beijing University, China

Corresponding email: 1201110579@pku.edu.cn

Keywords: subtropic soils, cutan, iron and manganese oxides

The morphology, mineral phase and chemical compositions of iron-manganese cutans in A (0-20 cm) and B horizon (20-50 cm) of subtropical soils in Changsha, China, were investigated by OM, ESEM, EDX, XRD and HRTEM. An observed by OM and ESEM, 180-500 μm wide iron-manganese cutans in B horizon contain layering patterns, characterized by an outer layer rich in manganese & iron (~ 20 wt.% MnO_2, ~ 10 wt.% Fe_2O_3) and an inner layer rich in iron (~ 12 wt.% Fe_2O_3). The results of XRD and HRTEM indicate that the manganese & iron layers are composed of multi phases including quartz, muscovite, kaolinite, and nanoscaled manganese & iron minerals such as hollandite, goethite, birnessite, feitknechtite and vernadite; while, the iron layers are mainly composed of quartz, muscovite, goethite and kaolinite. As compared to B horizon, no stratification was observed in A horizon, where the thickness of the iron-manganese cutans are only 10-15 μm. In the cutans of A horizon, the content of Fe_2O_3 is ~ 10 wt.%. The main mineral phases were quartz, clay minerals and nanoscaled Fe- (oxy) hydroxide minerals including goethite, hematite and ferrihydrite. While, both crystallized and amorphous manganese oxides were rarely found in the cutans of A horizon. In conclusion, iron and manganese oxides in the cutans of A and B horizon are nanoparticles and exhibit diverse morphological features. The improved understanding of iron and manganese oxides provided a detailed look at the complex and varied iron oxide and manganese oxide mineralogy in cutans and would help to better understand how cutans affect the soil quality and the ecological environment.

SEMICONDUCTING PROPERTY OF Fe/Mn OXIDES ON EARTH SURFACE

Li Y.[1], Lu A.*[1] & Ding H.[1]
[1] Key Laboratory of Orogenic Belts and Crustal Evolution, School of Earth and Space Sciences, Beijing University, China
Corresponding email: liyan-pku@pku.edu.cn

Keywords: semiconducting mineral, Fe/Mn oxides, photocatalysis

Fe and Mn oxides [e.g., hematite (Fe_2O_3), goethite (FeOOH), birnessite (MnO_2)], which are semiconducting minerals, exist in almost all terrestrial weathering environments. In addition to the well-known photosynthesis, it should be noted that photocatalysis of semiconducting minerals on Earth surface is another vital process for inorganic world to utilize solar energy. In this study, we investigate the semiconducting property of some common Fe/Mn oxides by using first principle theory calculation, synchrotron soft X-ray emission and absorption spectroscopy and photoelectrochemical methods. The first principle theory calculation results for Fe oxides (goethite and hematite) and Mn oxides (birnessite) show that the top of the valence band is a hybrid bonding between the electronic states of O 2*p* and Fe or Mn 3*d*; while the bottom of the conduction band is mainly contributed by Fe or Mn 3*d* states, with the participation of electronic states of O 2*p*. According to the oxygen *K*-edge adsortion and emission spectra, the bandgap of nature goethite, hemetatite, hex-birnessite, mon-birnessite, δ-MnO_2 and cryptomelane are determined to be 2.30 *e*V, 2.10 *e*V, 2.32 *e*V, 1.77 *e*V, 1.36 *e*V and 1.23 *e*V, respectively, all of which are visible light-responsive semiconductors. In terms of Fe oxides, the substituting atom of Al participate in the formation of valence band and shift the band edge to a higher energy level, therefore resulting in the reduced bandgap as compared to their synthetic “pure” counterpart. In terms of Mn oxides (hex-birnessite, mon-birnessite, δ-MnO_2 and cryptomelane), the potentials of the conduction band edges are: -0.32 V, 0.09 V, 0.39 V, 0.46 V, and valence band edges are: 2.00 V, 1.86 V, 1.75 V, 1.69 V, respectively at *p*H 6. As compared to the redox potential of humic acid in surrounding environment, the Mn oxides possess enough capability to oxidize it. Besides, both the photoelectrochemical and photocatalytic experiments indicate the photocatalytic activity of layered Mn oxides (hex-birnessite, mon-birnessite, δ-MnO_2) are higher than tunnel structure Mn oxides (cryptomelane). The time-current curves of natural soil cutans, which are rich in Fe/Mn oxides, show obvious increase of current in simulated solar light irradiation. Whereas, the photocurrent of the cutans sharply reduced to a very low value when the Fe/Mn oxides are removed by acid washing. This is the direct evidence for natural Fe/Mn oxides photocatalysis. Our results suggest that the photocatalysis of Fe/Mn oxides is an important driving force for natural geochemistry processes.

PHOTOELECTRONS TRANSFER BETWEEN MINERALS AND MICROORGANISMS TOWARDS CARBON DIOXIDE FIXATION

Lu A.*[1], Li Y.[1], Ding H.[1] & Wang C.[1]
[1] School of Earth and Space Sciences, Beijing University, China
Corresponding email: ahlu@pku.edu.cn

Keywords:

Solar energy is the ultimate energy source on Earth, and almost all life depends on it, either directly or indirectly. Due to the deficiency of intracellular photosensitive components, chemotrophic microorganisms could not utilized solar energy directly. Nevertheless, photosensitive components are not necessary for microorganisms to utilize solar energy. Lu et al. (2012) presented evidence demonstrating solar energy mediated by semiconducting mineral photocatalysis, acting as energy source, promoted the growth of some non-photosynthetic bacteria. In most cases, the band gap of a natural semiconducting mineral is narrower than its synthetic "pure" counterpart, which makes it more vulnerable to excitation by photons when exposed to visible light. When sunlight falls on the Earth surface, photons with proper wavelengths excite the semiconducting minerals to generate photoelectron–hole pairs. The potentials of surrounding species such as humic acid, ascorbic acid, as well as other reductive chemicals are negative enough to scavenge photoholes, leaving photoelectrons as potential electron sources. In this pathway, the semiconducting minerals play a role similar to that of photosystems in photosynthesis, increasing the electron energy. This energy yielding pathway for non-phototrophic bacteria is an ongoing process all over the surface of the Earth. In natural environment, bacterial extracellular electrons yielding pathways are complex and these pathways are possible to participate in microbial-mineral electrons transfer mechanisms. We discuss here the major mechanisms of electron transfer between minerals and microorganisms based on an assessment of the results from recent studies. Considering physiological flexibility of microorganisms and energy availability of semiconducting minerals, there is high probability of finding alternative energy transfer pathways linking semiconducting minerals and microbes. The transport of semiconducting mineral photoelectrons occurs across several key interfaces as semiconducting minerals, organic/inorganic substances and microorganisms. The essence of semiconducting mineral photocatalysis and microbial community interactions is the energy transform and transport among solar energy, chemical energy, electric energy and bioenergy on different interfaces. This pathway would aid carbon dioxide to be fixed in forms of organics or carbonate minerals. On one hand, as chemoautotrophic bacteria utilize carbon dioxide as solo carbon source, the photoelectrophy pathway promotes the bacterial growth and the dissimilation of carbon dioxide into organics. On the other hand, the photoelectrophy pathway for chemoheterotrophic bacteria also stimulate the bacterial growth and metabolism. This process improve the degradation efficiency of organics into carbon dioxide, and simultaneously increase the solubility of carbon dioxide in water, which help to form carbonate minerals.

Lu, A., Li, Y., Jin, S., Wang, X., Wu, X.-L., Zeng, C., Li, Y., Ding, H., Hao, R., Lv, M., Wang, C., Tang, Y., Dong, H. (2012): Growth of non-phototrophic microorganisms using solar energy through mineral photocatalysis. *Nature Commun.*, **3**, 768-775.

MICROFUNGI-MINERAL INTERACTIONS IN SULPHIDE-RICH HARDPANS

Marescotti P.*[1], Cecchi G.[1-2], Di Piazza S.[1-2], Lucchetti G.[1], Mariotti M.G.[1] & Zotti M.[1-2]
[1] Dipartimento di Scienze della Terra, dell'Ambiente e della Vita, Università di Genova, Italy
[2] Dipartimento di Scienze della Terra, dell'Ambiente e della Vita - Laboratorio di Micologia, Università di Genova, Italy
Corresponding email: marescot@dipteris.unige.it

Keywords: microfungi, waste-rocks, sulphides

Recent studies on contaminated waste rock-dumps from abandoned sulphide mines have highlighted the presence of a larger number of microfungi playing an active role on the biogeochemical cycles of metals and metalloids (Marescotti et al., 2013; Zotti et al., 2014).

This work aims to study the bioweathering and biomineralization potential of *Trichoderma harzianum* Rifai by evaluating the interactions among sulphide-bearing hardpans and a native microfungal strain isolated from an abandoned sulphide mine (Libiola mine, NW Italy). Decimetric-thick hardpands are widespread at the surface of the waste-rock dumps from Libiola Mine. They consist in mixtures of mine-waste material with high percentage of non-economic sulphides. Minerals and rock fragments are strongly cemented by Fe-oxides and -oxyhydroxides which precipitate within porosity from iron-rich acid solutions.

Five hardpan samples were collected from the surface of a barren waste-rock dump located close to a mine adit. The hardpan samples were manually disaggregated, homogenized, and sieved and subdivided in four identical aliquotes for the chemical and mineralogical analyses and for the realization of the experimental protocol. Four replicated mesocosm tests were realized pouring 5 g of disaggregated and homogenized hardpan into four 100 ml flasks, together with 20 ml of liquid medium MEA (Malt Extract Agar). The flasks were autoclaved for 20 min at 120° C. A *T. harzianum* Rifai (ML 8-12) solution was prepared diluting fungal conidia in a semisolid suspension of Tween 80 (polysorbitan 80). Every flask was inoculated with 5 ml of the fungal solution, and stored in the dark at 24°C for two months. At the end of the incubation period, all the samples (mesocosm and control samples) were collected and analyzed by stereomicroscopy, and ESEM-EDS.

T. harzianum was able to grow on all autoclaved samples, covering and interacting with hardpan clasts, in particular with those characterized by the presence of disseminated sulphides exposed on the surface. ESEM analyses evidenced that the whole surface of the fungal hyphae became rough and enveloped with new formed idiomorphic gypsum crystals, thus indicating that the fungal hyphae were providing nucleation sites for the genesis of these minerals and, presumably, indirectly favored sulphide alteration.

These results allowed to speculate that the new formed gypsum crystals may be mineralized by *T. harzianum*. In particular, they might be the consequence of an active, direct, and controlled fungal mineralization, or might be the effect of a biologically-induced mineralization, where the fungus modified the local microenvironment creating the condition that favored extracellular chemical precipitation of gypsum.

Marescotti, P., Roccotiello, E., Zotti, M., De Capitani, L., Carbone, C., Azzali, E., Mariotti, M.G., Lucchetti, G. (2013): Influence of soil mineralogy and chemistry on fungi and plants in a waste-rock dump from the Libiola mine (eastern Liguria, Italy). *Per. Mineral.*, **82**, 141-162.

Zotti, M., Di Piazza, S., Roccotiello, E., Lucchetti, G., Mariotti, M.G., Marescotti, P. (2014): Microfungi in highly copper-contaminated soils from an abandoned Fe-Cu sulphide mine: growth responses, tolerance and bioaccumulation. *Chemosphere*, **117**, 471-476.

ZINC BEHAVIOUR AT THE MINERAL-ROOT INTERFACE: PLANT RESPONSE TO ZINC EXTREME ENVIRONMENTS

Medas D.[1]*, De Giudici G.[1], Meneghini C.[2] & Lattanzi P.[1]
[1] Dipartimento di Scienze Chimiche e Geologiche, Università di Cagliari, Italy
[2] Dipartimento di Fisica, Università di Roma Tre, Italy
Corresponding email: dmedas@unica.it

Keywords: plant roots, mineral evolution, zinc

Plants growing on polluted soils need to control the bioavailability of pollutants to reduce their toxicity. The functions of biomineralizations in plants can have multiple functions such as Ca-regulation, defence against predators, detoxifying aluminium and heavy metals, alleviating water, salt, and temperature stress, detoxifying oxalic acid (He et al., 2014).

Reactions occurring at the mineral-root interface represent a potential tool for mitigating metal dispersion because of their influence on the bio-geochemical cycle of elements and metals mobility. Biomineralization at the mineral-root interface leads to the immobilization of contaminants through accumulation by roots or precipitation at the rhizosphere and seems to be the only sustainable type of phytostabilization (McCutcheon & Schnoor, 2003). These processes reduce the mobility of the contaminants and prevents their migration to the groundwater or air, and also reduce bioavailability for entry into the food chain (Prasad & de Oliveira Freitas, 2003).

In order to unravel the microscopic processes occurring at the mineral-root interface two plant species were selected, *Euphorbia pithyusa* L. and *Pistacia lentiscus* L., from different highly Zn-contaminated tailings in Sardinia (Italy). Thin slices of *E. pithyusa* and *P. lentiscus* roots were investigated by micro-X-ray fluorescence mapping, and roots and rhizosphere materials were examined by X-ray absorption spectroscopy at the Zn *K*-edge, X-ray diffraction, and scanning electron microscopy. Results indicate: i) in the rhizosphere, Zn occurs in different phases; ii) both *Euphorbia pithyusa* L. and *Pistacia lentiscus* L. are able to extract Si, Al and Zn from the soil minerals to build a Zn-silicate biomineralization at the root epidermis; iii) Zn is stored in the root epidermis, and does not appear to be bound with organic molecules but the ZnO5 polyhedra form a short range order structure with Si atoms.

Investigated plants use Si and Al extracted by soil minerals to build a biomineralization rim, which is able to capture Zn. These Zn-silicate biomineralizations have relevant implication for phytoremediation techniques and for further biotechnology development. Future research aims to investigate other plant species, and Zn isotope fractionation during its accumulation and translocation.

He, H., Veneklaas, E.J., Kuo, J., Lambers, H. (2014): Physiological and ecological significance of biomineralization in plants. *Trends Plant Sci.*, **19**, 166-174.

McCutcheon, S.C. & Schnoor, J.L. (2004): Overview of Phytotransformation and Control of Wastes. *in* "Phytoremediation: Transformation and control of contaminants", S.C. McCutcheon, J.L. Schnoor, eds., Wiley, Hoboken, 3-58.

Prasad, M. & de Oliveira Freitas, H. (2003): Metal hyperaccumulation in plants - Biodiversity prospecting for phytoremediation technology. *Electr. J. Biotechnol.*, **6**, 285-321.

THE IMPACT OF MICROBIAL PROCESSES ON TECHNETIUM, URANIUM AND NEPTUNIUM SPECIATION AND FATE – REDOX CYCLING, BIOMINERALS AND STABILITY OF REACTION PRODUCTS

Morris K.*[1], Law G.[2], Lloyd J.R.[1], Livens F.[1-2], Mosselmans F.[1-3], Pattrick R.[1], Shaw S.[1], Brookshaw D.[1], Newsome L.[1], Rizoulis A.[1], Masters Waage N.[1-2], Williamson A.[1] & Bots P.[1]

[1] Research Centre for Radwaste Disposal & Williamson Research Centre, School of Earth, Atmospheric and Environmental Sciences, University of Manchester, United Kingdom

[2] Centre for Radiochemistry Research, School of Chemistry, University of Manchester, United Kingdom

[3] Diamond Light Source Ltd, Didcot, United Kingdom

Corresponding email: katherine.morris@manchester.ac.uk

Keywords: molecular environmental science, biogeochemistry, radionuclides

Globally, there is a significant legacy of defunct nuclear plant and facilities and associated contaminated ground; these represent some of the most hazardous sites in the world and their decommissioning and management is of critical concern. Additionally, the common route identified by Government for management of the wastes generated from the nuclear fuel cycle is via deep geological disposal. Finally, many countries see new nuclear power as a critical part of their long term decarbonisation energy mix. These factors have resulted in a new focus on environmental radioactivity over the past few years. Our work has applied synchrotron based techniques coupled to radiochemistry, biogeochemistry, electron microscopy and geochemistry approaches to gain new insights into radionuclide behaviour in complex environmental systems. These approaches have highlighted that biogeochemical processes can have a profound effect on the mobility of radionuclides in natural and engineered environments and have revealed a surprising specificity for bioreduction pathways between different radionuclides and diversity of reduction products in a range of systems. I will present data demonstrating our molecular environmental science understanding of the speciation, fate and biogeochemical cycling of radionuclides in systems relevant to radioactive waste disposal and radioactively contaminated land and demonstrate how these processes will help in underpinning the safe management and disposal of our nuclear legacy. Specific examples will include tailored bioreduction and biomineralisation approaches to cleaning-up mobile U(VI) contamination in groundwaters, examining the effects of multiple cycles of biogeochemically driven redox cycling of Tc in sediment systems, understanding the influence of microbes on sheet silicates in the context of reductive precipitation of U, Tc and Np of relevance to geological disposal, high pH biogeochemistry and its influence on radionuclide behaviour, and examining the mechanisms of reduction, and fate of reduction products in pure culture experiments to underpin mechanisms of bioreduction in environmental systems (Brookshaw et al., 2015; Newsome et al., 2015; Rizoulis et al., 2012; Williamson et al., 2014).

Brookshaw, D.R., Pattrick, R.A., Bots, P., Law, G.T., Lloyd, J.R., Mosselmans, J.F.W., Vaughan, D.J., Dardenne, K., Morris, K. (2015): Redox interactions of Tc (VII), U (VI), and Np (V) with microbially reduced biotite and chlorite. *Environ. Sci. Technol.*, **49**, 13139-13148.

Newsome, L., Morris, K., Trivedi, D., Bewsher, A., Lloyd, J.R. (2015): Biostimulation by glycerol phosphate to precipitate recalcitrant uranium(IV) phosphate. *Environ. Sci. Technol.*, **49**, 11070-11078.

Rizoulis, A., Steele, H.M., Morris, K., Lloyd, J.R. (2012): The potential impact of anaerobic microbial metabolism during the geological disposal of intermediate-level wast. *Mineral. Mag.*, **76**, 3261-3270.

Williamson, A.J., Morris, K., Law, G.T.W., Rizoulis, A., Charnock, J.M., Lloyd, J.R. (2014): Microbial reduction of U(VI) under alkaline conditions: Implications for radioactive waste geodisposal. *Environ. Sci. Technol.*, **48**, 13549-13556.

MICROBIAL IRON REDUCTION IN EXTREME ENVIRONMENTS

Nixon S.L.*[1], Cockell C.S.[2] & Lloyd J.R.[1]
[1] School of Earth, Atmospheric and Environmental Sciences, University of Manchester, United Kingdom
[2] School of Physics and Astronomy, University of Edinburgh, United Kingdom
Corresponding email: sophie.nixon@manchester.ac.uk

Keywords: geomicrobiology, habitabilit, extremophiles

Microbial iron reduction is a widespread microbial metabolism, and plays an important role in the biogeochemical cycling on iron and carbon (Lovley, 2013). It also represents a compelling metabolism to operate on Mars, past and present (Nixon *et al*., 2012). Iron-reducing microorganisms are capable of drawing upon a wide range of organic electron donors and inorganic electron acceptors (Lloyd, 2003). Accordingly, these microorganisms are often employed in bioremediation of hydrocarbon- and metal/radionuclide-contaminated land (e.g., Anderson et al., 1998). Furthermore, the ability of these microorganisms to pass electrons across biofilms renders them well suited for use in microbial fuel cells (Nevin et al., 2008). Iron-reducing microorganisms applied in these scenarios typically grow best at mesophilic and neutrophilic conditions. However, with the exceptions of hydrothermal vents and acid mine drainage environments, relatively little is known about this metabolism in more extreme temperature and *p*H conditions.

Here we compile data published on temperature and pH growth optima conditions of all characterised iron-reducing microorganisms to date. Only microorganisms known to conserve energy from iron reduction are considered. Data from enrichment studies are also considered.

The data show that most characterised iron-reducing microorganisms grow best at moderate *p*H and temperatures. However, this most likely reflects a sampling bias away from more extreme and hence difficult to sample environments. Furthermore, adaptation to extreme temperatures is evident only at neutrophilic *p*H, and vice versa. Data appears to be lacking on the presence of viable iron-reducing microorganisms in environments hosting a combination of extreme temperature and *p*H conditions.

Not only does studying microbial iron reduction at extreme environments shed light on the limits to microbial habitability on Earth and beyond, it also widens the potential for its application in bioremediation, bio-mining and a number of other anthropogenic environmental interventions.

Anderson, R.T., Rooney-Varga, J.N., Gaw, C.V., Lovley, D.R. (1998): Anaerobic benzene oxidation in the Fe(III) reduction zone of petroleum-contaminated aquifers. *Environ. Sci.Technol.*, **32**, 1222-1229.

Lloyd, J.R. (2003): Microbial reduction of metals and radionuclides. *FEMS Microbiol. Rev.*, **27**, 411-425.

Lovley, D.R. (2013): Dissimilatory Fe(III)- ad Mn(IV)-reducing prokaryotes. *in* "The prokaryotes: prokaryotic physiology and piochemistry", E. Rosenberg, E.F. DeLon, S. Lory, E. Stackenbrandt, F. Thompson, eds., 4th ed. Springer, Berlin-Heidelberg, 287-308.

Nevin, K.P., Richter, H., Covalla, S.F., Johnson, J.P., Woodard, T.L., Orloff, A.L., Jia, H., Zhang, M., Lovley, D.R. (2008): Power output and columbic efficiencies from biofilms of *Geobacter sulfurreducens* comparable to mixed community microbial fuel cells. *Environ. Microbiol.*, **10**, 2505-2514.

Nixon, S.L., Cockell, C.S., Tranter, M. (2012): Limitations to a microbial iron cycle on Mars. *Planet. Space Sci.*, **72**, 116-128.

BIOGEOCHEMICAL INTERFACES IN THE HYPORHEIC ZONE OF SAN GIORGIO RIVER (SARDINIA SW, ITALY)

Pusceddu C.*[1], Medas D.[1], De Giudici G.[1], Meneghini C.[2] & Giannoncelli A.[3]
[1] Dipartimento di Scienze Chimiche e Geologiche, Università di Cagliari, Italy
[2] Dipartimento di Fisica, Università di Roma Tre, Italy
[3] Elettra Sincrotrone Trieste, Italy
Corresponding email: clau.pux@libero.it

Keywords: biomineralization, biogeochemical Interfaces, synchrotron

Rio San Giorgio is a mine-polluted stream located in the past Pb-Zn mining district of Sulcis Iglesiente (Sardinia SW, Italy). It is characterized by widespread occurrence of vegetation that dominates the stream bed morphology, erosional processes and water velocity. The dominant plant species are *Phragmites australis* and *Juncus acutus*, which are both known to accumulate Zn in high concentrations (Rycewicz-Borecki et al., 2016; Mateos-Naranjo et al., 2014).

In this study, water, sediments and plants were investigated by several techniques to depict biogeochemical interfaces at the hyporheic zone (Byrne et al., 2010).

Core samples were collected along the stream bed to sample plant roots and sediments. Mineralogical analysis of cores sampled along the river indicate that some relevant biogeochemical processes take place. Particularly, SEM imaging with EDS microanalysis allowed us to recognize framboidal pyrite on the surfaces of *Phragmites australis* and *Juncus acutus* roots. Additionally, nanoparticles of zinc sulphide were found on filaments of organic matter. This indicates that redox interface associated to sulphur reducing bacteria dominates in the river hyporheic zone.

Root samples were investigated by synchrotron techniques (Medas et al., 2015). STXM images indicates that the Zn, Fe, Si and Al are concentrated in the outer part of the roots. XANES indicates that iron oxides dominates iron speciation in the *Phragmites australis* roots. The redox biogeochemical interface and the rhizosphere processes are likely limiting the heavy-metal mobility. Ongoing research is aimed to better understand the biosphere-geosphere interaction processes and their effect in Rio San Giorgio.

Byrne, P., Reid, I. Wood, P.J. (2010): Sediment geochemistry of streams draining abandoned lead/zinc mines in central Wales: the AfonTwymyn. *J. Soil Sedim*., **10**, 683-697.

Mateos-Naranjo, E., Castellanos, E.M, Perez-Martin, A. (2014): Zinc tolerance and accumulation in the halophytic species Juncus acutus- *Environ. Exper. Botany*, **100**, 114-121.

Medas, D., De Giudici, G., Casu, M.A., Musu, E., Gianoncelli, A., Iadecola, A. Meneghini,C., Tamburini, E., Sprocati, A.R., Turnau, K., Lattanzi, P. (2015): Microscopic processes ruling the bioavailability of Zn to roots of Euphorbia pithyusa L. Pioneer. *Plant Environ. Sci. Technol*., **49**, 1400-1408.

Rycewicz-Borecki, M., McLean, J.E., Dupont, R.R. (2016): Bioaccumulation of copper, lead, and zinc in six macrophyte species grown in simulated storm water bioretention systems. *J. Environ. Manag.*, **166**, 267-275.

PROMOTION OF MICROBIAL EXTRACELLULAR ELECTRON TRANSFER BY NATURE HEMATITE

Ren G.[1], Ding H.[1], Li Y.[1] & Lu A.*[1]

[1] Key Laboratory of Orogenic Belts and Crustal Evolution, School of Earth and Space Sciences, Beijing University, China

Corresponding email: renguiping@pku.edu.cn

Keywords: red soil, hematite, microbial

Red soil are rich in Fe oxides such as hematite, goethite, magnetite, etc., and also abundant in microorganisms. Considering the ubiquitous interactions between microorganisms and minerals, red soil can be employed as a proper niche for investigating the flexible interacting pathway between Fe oxides and microorganisms. For this reason, we designed a dual-chambered reactor, where soil microorganisms were inoculated into the anode chamber and nature hematite-coated graphite was used as the cathode. The results showed that, as compared to the air cathode, the open circuit voltage of the electrochemical reactor with a hematite cathode increased from 414.64 to 511.46 mV, and the maximum output power increased from 171.0 to 260.2 mW/m^3. Raman spectra showed the half-peak width of almost all spectra belonging to hematite doubly increased, which indicated the crystalline degree of the mineral decreased. However, no soluble iron ions were detected in the cathode chamber, indicating either the hematite acted as a semiconductor to mediate the cathodic electrons transfer, or the iron ions released from the decomposition of hematite quickly formed new mineral phase at the cathode. Furthermore, a typical three-electrode electrochemical cell was used to analyze the promotion mechanism of hematite in extracellular electron transfer process. Cyclic voltammetry curves showed that with the hematite, the system current increased and a pronounced cathodic and anodic peak was observed at 0.43 and 0.55 V (vs. SCE), respectively, implying the hematite introduced a new redox reaction. Electrochemical impedance spectroscopy (EIS) results showed that the hematite-coated FTO electrode exhibited a notable decreased polarization resistance (*Rp*) from 44840 Ω to 1665 Ω, as compared to the bare FTO electrode. The results indicated the cathodic electron transfer dynamics was significantly improved by using hematite to lower the overpotential of the cathode. Therefore, we conclude that natural iron oxide in red soil not only effectively participate in but also significantly promote the process of extracellular electron transfer.

PATHWAYS AND KINETICS OF BIOGEOCHEMICAL REDOX REACTIONS AT THE MOLECULAR SCALE

Rosso K.M.*[1]
[1] Pacific Northwest National Laboratory, Richland, WA, USA
Corresponding email: kevin.rosso@pnnl.gov

Keywords: electron transfer, iron oxide, cytochrome

Redox reactions are the most fundamental and versatile reactions in nature. Transfer of electrons from one species to another is the simplest means of chemical transformation. On Earth, iron is the most abundant redox-active element. The thermodynamics and kinetics of the oxidation state change between ferric and ferrous iron lie at the heart of iron mineralogy and distribution at the Earth's near-surface, and the ubiquitous evolutionary incorporation of this redox couple within living systems. Despite its essentiality, predicting rates of iron or iron-mediated redox reactions in geochemical and geomicrobiological systems, which span 12 orders of magnitude, remains a challenge. This presentation addresses elementary aspects of this problem using mineralogic and geomicrobiologic illustrations, demonstrates the necessity of theory and computational molecular simulation for understanding electron transfer rates, and outlines the methodological state-of-the-art for this purpose. As one example, at the Earth's near-surface, the juxtaposition of aqueous ferrous iron and solid-phase ferric iron oxides and oxyhydroxides is a common and dynamic redox interface. Here, Fe(II)-Fe(III) electron transfer underpins reductive recrystallization of these minerals, yielding atom exchange that impacts their stable isotopic signatures. Using a combined experiment and molecular simulation approach, the mechanism and kinetics of complete iron atom exchange between an aqueous Fe(II) pool and well-defined goethite (FeOOH) crystallites, observed to occur without change in mineralogy, crystallinity, crystal size or shape, will be explained in terms of linked nanosecond ferrous-ferric valence interchange reactions within surfaces of goethite crystallites. In Earth's geomicrobiology, enzymatic electron transfer to extracellular Fe(III)-bearing minerals by metal-reducing bacteria is a process optimized by evolution to catalytic perfection using iron-based multiheme cytochromes. To shed light into how and why individual electron transfer steps in bacterial multi-heme cytochromes combine to form an overall biomolecular function, and how fast they can occur, extensive computer simulations of step-wise electron transfer along heme "wires" within the recently crystallized decaheme cytochrome MtrF will be presented. Because the individual hemes are not easily distinguished spectroscopically in such proteins, the determined individual and overall electron conductance rates to be discussed are experimentally inaccessible. Lines of molecular-level research such as these are collectively converging on a picture of achievable predictability and understanding of rates of natural redox reactions at the macroscopic scale, for iron and also other redox-active elements, across a broad range of geochemically and biogeochemically complex Earth systems.

A NEW MULTI-ANALYTICAL APPROACH IN THE STUDY OF SYNOVIAL FLUID CRYSTALS: A COMBINED INVESTIGATION OF ELECTRON MICROSCOPY, MICRO-RAMAN SPECTROSCOPY AND X-RAY MICRO-DIFFRACTION

Vettorello A.*[1], Frallonardo P.[2], Nestola F.[1], Oliviero F.[2], Peruzzo L.[3] & Scanu A.[2]
[1] Dipartimento di Geoscienze, Università di Padova, Italy
[2] Unità di Reumatologia, Dipartimento di Medicina, Università di Padova, Italy
[3] Istituto di Geoscienze e Georisorse, Consiglio Nazionale delle Ricerche, Padova, Italy
Corresponding email: arianna.vettorello@studenti.unipd.it

Keywords: multi-analytical approach, calcium pyrophosphate, basic calcium phosphate

The presence of particles and crystals in synovial fluid, easily recognizable under optical microscope, is a common feature in patients with various types of rheumatic disorders. Some crystals, such as monosodium urate (MSU), calcium pyrophosphate dihydrate (CPPD) and basic calcium phosphate (BCP), are certainly linked to specific disease, as gout, chondrocalcinosis and inflammatory osteoarthritis (Yavorskyy et al., 2008).

In clinical practice, crystals identification is based on synovial fluid analysis made by optical microscopy in transmitted polarized light, which represents an effective outpatient procedure, relatively simple and cheap (Pascual & Jovani, 2005; Oliviero et al., 2005). The main disadvantages of this technique are the lack of specificity and the presence of other crystals or particles of different nature, that can create difficulties of interpretation.

Almost all synovial fluid samples studied during this project was extracted from knee joint by arthrocentesis. Then, all samples were diluted and centrifuged in order to obtain a small amount of crystals from the liquid, that was fixed on a suitable holder. The next step consisted in synovial fluid crystals analysis by analytical techniques commonly used by geologists in the mineralogical, petrological and crystallographic fields, in order to understand their specific role in the development of the rheumatic diseases. The samples were analyzed by optical microscopy in transmitted polarized light (OM), scanning electron microscopy (SEM) equipped with EDS (chemical analysis), micro-Raman spectroscopy, X-ray powder diffraction (XRPD) and X-ray micro-diffraction (XRSC).

The multi-analytical approach applied during this project represents a new analytical tool that will become useful to study in a very specific way crystals involved in rheumatic disorders.

Oliviero, F., Pascual, E., Punzi, L. (2005): Detection and identification of crystals in synovial fluid. *Reumatismo*, **57**, 208-211.

Pascual, E. & Jovanì, V. (2005): Synovial fluid analysis. *Clin. Rheumatol.*, **19**, 371-386.

Yavorskyy, A., Hernandez-Santana, A., McCarthy, G., McMahon, G. (2008): Detection of calcium phosphate crystals in the joint fluid of patients with osteoarthritis – analytical approaches and challenges. *Analyst*, **133**, 302-318.

Session S26:

Mineral-hazards. The environmental and human health problem represented by raw and man-processed mineral phases

Conveners:

Alessandro F. Gualtieri (Modena – Italy)

Mickey Gunter (Moscow – USA)

Marisa Rozalen (Granada – Spain)

TOPOCHEMISTRY OF IRON AND SURFACE REACTIVITY OF CROCIDOLITE AND TREMOLITE AMPHIBOLE ASBESTOS: A COMPARATIVE CASE STUDY

Andreozzi G.B.*[1], Pacella A.[1] & Turci F.[2-3]

[1] Dipartimento di Scienze della Terra, Sapienza Università di Roma, Italy

[2] Dipartimento di Chimica, Università di Torino, Italy

[3] Centro Interdipartimentale per lo Studio degli Amianti e di altri Particolati Novici "G. Scansetti", Università di Torino, Italy

Corresponding email: gianni.andreozzi@uniroma1.it

Keywords: amphibole asbestos, iron, free radicals

Non-occupational, environmental and unintentional exposure to naturally occurring asbestos (NOA) represents a potentially important source of risk for human health in several parts of the world. One of the most significant physico-chemical properties relevant to asbestos toxicity is chemical reactivity of fibre surfaces, which is commonly associated to bulk iron content and oxidation state. However, scarce information is still available about dependence on surface iron topochemistry, which is the basis for defining relationships between chemical structure and biologic activity, i.e., structure-activity relationships (SARs).

Two tremolite samples, from Italy (Castelluccio, Basilicata) and USA (Maryland), and one crocidolite (UICC standard) were thoroughly characterized prior and after incubation in an oxidative solution (H_2O_2 buffered at *p*H 7.4) from 1 hour to 1 month. Fibres dissolution, structure modification, surface chemistry, iron topochemistry and surface reactivity in terms of free-radical production were monitored. Two conventional target molecules ($H_2O_2$and $HCOO^-$) and the DMPO spin-trapping/EPR technique were used to measure radical activity. The two tremolites have similar composition but different surface area (~10 and 3 m^2g^{-1} for Castelluccio and Maryland, respectively). UICC crocidolite has surface area comparable to Castelluccio tremolite (~9 m^2g^{-1}), but bulk Fe content 20 times greater than tremolite. The higher surface area of Castelluccio tremolite and UICC crocidolite likely accounts for a faster leaching process during incubation. However, normalizing dissolution rates to surface area, crocidolite dissolves faster than tremolite, with a lifetime 2.5 times shorter.

During the dissolution process, Fe is progressively oxidised and its surface nuclearity increases, from single ion to dinuclear or oligonuclear oxo-iron complexes up to Fe-rich oxi-hydroxide nanoparticles, as revealed by both XPS and HR-TEM. Chemical reactivity tests performed on both pristine and incubated samples evidenced that surface alteration and iron topochemistry significantly affect the capability of producing free-radicals. Direct comparison between UICC crocidolite and Castelluccio tremolite showed that $HO^{\cdot}$ production, which is activated by both Fe(II) and Fe(III), was similar for pristine samples, but diverged after the shortest incubation time. An opposite trend was observed for each sample by monitoring $COO^{-\cdot}$ production, which is only activated by Fe(II). Such a behaviour is due to formation of a thick fibre coating enriched in Fe(III) oxi-hydroxides in crocidolite, and to surface Fe active sites much more dispersed in tremolite. The present findings, together with previous studies on iron speciation at asbestos surfaces (Pacella et al., 2014, 2015), allow the formulation for the first time of a general reactivity paradigm that correlates the modification of iron state at fibre surfaces with the potency of asbestos to generate free radicals in solution.

Pacella, A., Fantauzzi, M., Turci, F., Cremisini, C., Montereali, M.R., Nardi, E., Atzei, D., Rossi, A., Andreozzi, G.B. (2014): Surface modifications and dissolution reactions of UICC crocidolite in buffered solutions at physiological *p*H: a combined ICP-OES, XPS and TEM investigation. *Geochim. Cosmochim. Acta*, **127**, 221-232.

Pacella, A., Fantauzzi, M., Turci, F., Cremisini, C., Montereali, M.R., Nardi, E., Atzei, D., Rossi, A., Andreozzi, G.B. (2015): Surface alteration mechanism and topochemistry of iron in tremolite asbestos: a step toward understanding the potential hazard of amphibole asbestos. *Chem. Geol.*, **405**, 28-38.

ANALYSIS OF RESPIRED AMPHIBOLE FIBERS (ASBESTOS AND NON-ASBESTOS CLASSIFIED): DISCRIMINATION BETWEEN NATURAL AND ANTHROPOGENIC SOURCES USING SENTINEL ANIMALS

Belluso E.*[1-2-3], Fornero E.[4] & Capella S.[1-3]

[1] Dipartimento di Scienze della Terra, Università di Torino, Italy

[2] Istituto di Geoscienze e Georisorse, Consiglio Nazionale delle Ricerche, Torino, Italy

[3] Centro Interdipartimentale per lo Studio degli Amianti e di altri Particolati Nocivi "G. Scansetti", Università di Torino, Italy

[4] Dipartimento di Scienze e Innovazione Tecnologica, Università del Piemonte Orientale, Alessandria, Italy

Corresponding email: elena.belluso@unito.it

Keywords: amphibole fibers, sentinel animals, SEM-EDS

Five species of amphiboles are classified as asbestos when they occur with length > 5 µm, width < 3 µm, aspect ratio > 3:1 (World Health Organization, 1977) and named tremolite asbestos, actinolite asbestos, grunerite asbestos (or amosite), anthophyllite asbestos, crocidolite.

Because of their peculiar properties the three last were industrially used and constitute several asbestos containing materials that represent anthropogenical sources of asbestos (ASA).

Tremolite asbestos and actinolite asbestos occur naturally (NOA) in certain types of rocks worldwide mined for ornamental stones and railway ballast. They are particularly abundant in serpentinites where they can occur as main mineral in rock veins or as accessory minerals. Therefore, owing their natural presence in rocks, they are geographically widespread even where asbestos have been banned.

Both natural events (i.e. weathering) as well as human activity (such as building or road construction) may cause the release of these fibers from NOA and ASA into the atmosphere and increase their background levels in the environment.

Owing to their size, these fibers can enter into the respiratory system. If respired in large amounts for a long period they can have toxic effects (Dodson, 2003). Correlation between high dose exposures (as in occupational or para-occupational exposure) and specific asbestos-related diseases has been known for many years. At present it is not possible to define a lowest exposure threshold below which an increased risk of some deleterious health effects would not occur (Hillerdal, 1999) and no measurements concerning the relative amounts of asbestos (and amphiboles asbestos in particular) released by anthropogenic versus natural processes are available.

Our aim was to evaluate the degree of exposure to respirable fibrous amphibole (asbestos and not asbestos classified) investigating their burden in the lungs of sentinel animals lived in 6 different areas in Piedmont Region (NW Italy) where both NOA sources and ASA exist and are well known.

Fiber identification and quantification were performed using a scanning electron microscope (SEM) with an energy dispersive spectrometer (EDS).

We detect different kinds of amphibole fibers dispersed both from NOA (tremolite/actinolite and edenite) and ASA (crocidolite and amosite). The fibres lung burden, interpreted in light of the lithological data and human activity for the examined area, reflects overall a qualitative correlation with presence of both natural and human activity dispersion sources.

Dodson, R.F., Atkinson, M.A., Levin, J.L. (2003): Asbestos fiber length as related to potential pathogenicity: a critical review. *Am. J. Ind. Med.*, **44**, 291-297.

Hillerdal, G. (1999): Mesothelioma: cases associated with non-occupational and low dose exposure. *Occup. Environ. Med*., **56**, 505-513.

World Health Organization (1997): Asbestos and other natural mineral fibres. International Programme for Chemical Safety. *in* "Environmental Health Criteria", Geneva, Switzerland.

PRELIMINARY XAS AND ESE INVESTIGATIONS ON CRYSTALLINE SILICA CONTAINED IN LUNG TISSUES

Belluso E.[1], Capella S.[1], Di Benedetto F.*[2], Bardelli F.[3], Giaccherini A.[4], Montegrossi G.[5], Romanelli M.[2], Zoleo A.[6] & D'Acapito F.[7]

[1] Dipartimento di Scienze della Terra, Università di Torino, Italy

[2] Dipartimento di Scienze della Terra, Università di Firenze, Italy

[3] istituto di Nanotecnologia, Consiglio Nazionale delle Ricerche, Roma, Italy

[4] Dipartimento di Chimica, Università di Firenze, Italy

[5] Istituto di Geoscienze e Georisorse, Consiglio Nazionale delle Ricerche, Firenze, Italy

[6] Dipartimento di Scienze Chimiche, Università di Padova, Italy

[7] Istituto Officina dei Materiali, Consiglio Nazionale delle Ricerche, c/o ESRF, Grenoble, France

Corresponding email: francesco.dibenedetto@unifi.it

Keywords: health effects, silica, XAS

Numerous studies point to the relevant role of specific features of each industrial material (e.g. occurrence of fresh surfaces, chemical composition of silica surface, including the heteroions, presence and type of associated mineralogical phases, thermal or chemical activation/passivation of the pristine surfaces) in modulating the reactivity of silica particles in contact with the lung tissues.

To achieve deeper understanding of the health effects of crystalline silica, and namely of their variability in different industrial settings, we recently started a characterisation of bulk and breathable silica particles of industrial origin using advanced techniques.

In particular, this study aims at revealing the population of inorganic radicals and the Fe speciation when crystalline silica are breathed, two relevant parameters for assessing their health effects. Spectroscopic characterisation of an autoptic specimen of human lung through Electron Spin Echo Spectroscopy (ESE) and X-ray Absorption Spectroscopy (XAS) at the Fe *K* edge have been carried out at the Department of Chemical Sciences and at the LISA beamline at the ESRF (Grenoble, France), respectively. Two different samples were considered: a section of the lung tissue and a filter containing the dusts recovered from the tissue after digestion.

Preliminary ESE investigations suggest the presence of Fe, Cu and radical signals: while the former are relatively obvious while investigating a biological tissue, the latter deserves a further research. Its signal is anisotropic and it can be safely attributed to an inorganic species. The same evidence characterises the filter containing the respirable dusts. XAS investigations evidenced the presence of Fe in the form of ferrihydrite and hematite. Ferrihydrite, in particular, can originate from ferritin, an iron-storage protein in the human body. This finding was also confirmed by the analysis of the dusts extracted from the tissue. These results will be discussed in light of the existing information in industrial materials.

TRACE ELEMENTS IN HAZARDOUS MINERAL FIBERS

Bloise A.*[1], Barca D.[1], Gualtieri A.F.[2], Pollastri S.[2] & Belluso E.[3-4]

[1] Dipartimento di Biologia, Ecologia e Scienze della Terra, Università della Calabria, Arcavacata di Rende (CS), Italy

[2] Dipartimento di Scienze Chimiche e Geologiche, Università di Modena e Reggio Emilia, Modena, Italy

[3] Dipartimento di Scienze della Terra, Università di Torino, Italy

[4] Centro Interdipartimentale per lo studio degli amianti e di altri particolati nocivi "G. Scansetti", Università di Torino, Italy

Corresponding email: andrea.bloise@unical.it

Keywords: mineral fibers, asbestos, trace elements

The aim of the present study was to investigate the concentration levels of trace elements in various type of fibrous-asbestiform minerals (Pollastri et al., 2014; Bloise et al., 2016a), using Inductively Coupled Plasma mass spectrometry (ICP-MS), in order to understand their possible contribution to the health problems. Indeed, there are both epidemiological and experimental indications that trace elements such as trace metals are carcinogenic for the human lungs (e.g., Nemery, 1990), and some researchers claimed that asbestos fibers may play a passive role in producing diseases as carriers of trace elements (Dixon et al., 1970). This issue represents a relevant problem especially in areas with outcrops of ophiolitic rocks (e.g., Bloise et al., 2016b) or sedimentary rocks in the case of erionite and where asbestos minerals were used in the manufacturing industry (Gualtieri, 2012). Mineral fibers of social, health, economic and industrial importance were selected for this study: Three chrysotiles of different origin, four amphibole asbestos minerals (crocidolite UICC, tremolite, amosite UICC and anthophyllite UICC) and the fibrous zeolite erionite. For the first time, we reported a systematic and comparative investigation of the levels of trace elements in these mineral fibers. In all samples, the following trace elements have been investigated: Li, Be, Sc, V, Cr, Mn, Co, Ni, Cu, Zn, As, Rb, Sr, Y, Sb, Cs, Ba, La, Pb, Ce, Pr, Nd, Sm, Eu, Gd, Tb, Dy, Ho, Er, Tm, Yb, Lu, Th, U; their distribution in the various mineral species was also discussed. The obtained results indicate that the amount of trace metals such as Mn, Cr, Co, Ni, Cu and Zn is higher in anthophyllite and chrysotile samples whereas the amount of rare earth elements (REE) is higher in erionite and tremolite samples. The role of REE concerning the asbestos-related health effects, was also discussed. High As, Be and Pb were detected in fibrous erionite. Since there is a convincing evidence of a relationship between lung cancer mortality and cumulative As, Be, and Pb exposure, the toxicity of fibrous erionite could be also related to the synergetic effect of these contaminants. Considering that both asbestos minerals and fibrous erionite are used for *in-vitro* studies as standard reference to test their cytotoxicity, the determination of their trace element content may be crucial as such contaminants could adversely affect the experimental results. In addition, the knowledge emerging from this work could have a significant impact in the frame of understanding the mineral fibers-related lung diseases.

Bloise, A., Catalano, M., Barrese, E., Gualtieri, A.F., Gandolfi, N.B., Capella, S., Belluso, E. (2016a): TG/DSC study of the thermal behaviour of hazardous mineral fibers. *J. Therm. Anal. Calorim*., **123**, 2225-2239.

Bloise, A., Punturo, R., Catalano, M., Miriello, D., Cirrincione, R. (2016b): Naturally occurring asbestos (NOA) in rock and soil and relation with human activities: the monitoring example of selected sites in Calabria (southern Italy). *Ital. J. Geosci*., **135**, 268-279.

Gualtieri, A.F. (2012): Mineral fiber-based building materials and their health hazards. *in* "Toxicity of building materials", F. Pacheco-Torgal, S. Jalali, A. Fucic, ed., Sawston, Cambridge, 166-195.

Nemery, B. (1990): Metal toxicity and the respiratory tract. *Eur. Resp. J.*, **3**, 202-219.

Pollastri, S., Gualtieri, A.F., Lassinantti Gualtieri, M., Hanuskova, M., Cavallo, A., Gaudino, G. (2014): The zeta potential of mineral fibers. *J. Hazard. Mater.*, **276**, 469-479.

HIGH RESOLUTION TEM INVESTIGATION OF MINERAL FIBRES IN CONTACT WITH ORGANIC MEDIA

Bursi Gandolfi N.*[1], Pollastri S.[1], Gualtieri A.F.[1], Langenhorst F.[2], Belpoggi F.[3] & Vigliaturo R.[4]
[1] Dipartimento di Scienze Chimiche e Geologiche, Università di Modena e Reggio Emilia, Modena, Italy
[2] Institut für Geowissenschaften, Friedrich-Schiller-Universität Jena, Germany
[3] Centro di Ricerca sul Cancro, Fondazione Europea di Oncologia e Scienze Ambientali "B. Ramazzini", Bologna, Italy
[4] School of Chemistry and Physics, University of KwaZulu-Natal, Durban, South Africa
Corresponding email: nicola.bursigandolfi@unimore.it

Keywords: TEM, mineral fibres, mesothelioma

Mineral fibres like fibrous amphiboles and erionite are among the most feared minerals worldwide because they may provoke fatal lung diseases, such as mesothelioma, through inhalation. The close relationship between inhaled fibres and respiratory diseases have been demonstrated by many scientific works (Davis, 1989) but the mechanisms of cyto- and geno-toxicity are not completely understood. In fact, it is difficult to draw a conclusive model to explain the biochemical activity of these fibres because a number of parameters act a synergetic role, such as fibre size, crystal habit, morphology, presence of iron and biopersistence (Donaldson et al., 2010 and references therein).

In a long term project conducted since 2011, a systematic characterization of mineral fibres of social and economic importance has been combined with *in vitro* and *in vivo* tests to assess their toxicity potential. The mineral fibres selected for the research project are three chrysotiles (UICC, Canada; Balangero and Val Malenco, Italy), four fibrous amphiboles (amosite UICC, anthophyllite UICC, crocidolite UICC and tremolite from Val d'Ala, Italy), and fibrous erionite (Jersey, Nevada, USA). The representative samples of chrysotile UICC, crocidolite and erionite are exactly the same used for an *in vivo* testing performed in the '80s on Sprague–Dawley rats by the Ramazzini Cancer Research Institute (Maltoni and Minardi, 1989). Fibres within histological organs of these rats were fully characterized through FEG-SEM investigations (Bursi et al., 2015). These samples were also treated with human cell cultures for different contact times and then characterized using *in situ* synchrotron radiation. On all samples, dissolution experiments at acidic *p*H in contact with simulated lung fluid (SLF) solutions are in progress to test their effective biodurability *in vitro.* To draw a conclusive model out of all the experimental data collected during the last 5 years, some specific issues need to be clarified. For example, the presence of iron in erionite only in the form of oxide-like nanoparticles on the surface of the fibres (Pollastri et al., 2015) needs further experimental evidences. The results of the *in vitro* and i*n vivo* experiments confirm that chrysotile have a low biodurability compared to amphiboles, but also that when in contact with organic media, it leads to amorphization of the fibres; the nature as well as the chemical composition of this silica-rich pseudo-morph needs to be better investigated. Similarly, although crocidolite and erionite seems to be very stable in contact with the organic media, there could be a release of chemical elements before the dissolution *s.s.* of the fibres, eventually followed by partial amorphization. All these issues may be clarified with a high resolution TEM study and for this reason, a collaboration with the University of Jena has been activated. The outcome of this study will be fully described in this contribution.

Davis, J.M.G. (1989): Mineral fibre carcinogenesis: experimental data relating to the importance of fiber types, size, deposition, dissolution and migration. *in* "Non-occupational exposure to mineral fibres", J. Bignon, J. Peto, R. Saracci, eds., IARC Sci. Publ., **90**, 33-45.

Bursi Gandolfi, N., Gualtieri, A.F., Pollastri, S., Tibaldi, E., Belpoggi, F. (2016): Assessment of asbestos body formation by high resolution FEG–SEM after exposure of Sprague–Dawley rats to chrysotile, crocidolite, or erionite. *J. Hazard. Mater.*, **306**, 95-104.

Donaldson, K., Murphy, F.A., Duffin, R., Poland, C.A. (2010): Asbestos, carbon nanotubes and the pleural mesothelium: a review of the hypothesis regarding the role of long fibre retention in the parietal pleura, inflammation and mesothelioma. *Part. Fibre Toxicol.*, **7**, 1.

Maltoni, C. & Minardi, F. (1989): Recent results of carcinogenicity bioassays of fibres and other particulate materials. Non-occupational exposure to mineral fibers. *in* "Non-occupational exposure to mineral fibres", J. Bignon, J. Peto, R. Saracci, eds., IARC Sci. Publ., **90**, 46-53.

Pollastri, S., D'Acapito, F., Trapananti, A., Colantoni, I., Andreozzi, G.B., Gualtieri, A.F. (2015): The chemical environment of iron in mineral fibres. A combined X-ray absorption and Mössbauer spectroscopic study. *J. Hazard. Mater.*, **298**, 282-293.

RECENT EXPOSURE TO INORGANIC FIBERS AIRBORNE: EVALUATION BY URINE SAMPLES

Capella S.*[1-3] & Belluso E.[1-2-3]

[1] Dipartimento di Scienze della Terra, Università di Torino, Italy

[2] Istituto di Geoscienze e Georisorse, Consiglio Nazionale delle Ricerche, Torino, Italy

[3] Centro Interdipartimentale per lo Studio degli Amianti e di altri Particolati Nocivi "G. Scansetti", Università di Torino, Italy

Corresponding email: silvana.capella@unito.it

Keywords: inorganic fibres, urine, SEM-EDS

Urinary asbestos presence was evaluated as indicator of occupational exposure to chrysotile asbestos already in 1985 (Finn & Hallenbeck, 1985). Detection of asbestos in the urine represents the first step in developing a biological indicator of recent exposure.

Airborne inorganic fibres (as asbestos) reaching lung alveoli undergo different processes. A fate involves migration of inorganic fibres across the alveolar membrane into the interstitial lung tissue. They can either remain there or pass into the blood circulation and thus reach other organs of the body.

In subjects with occupational or domestic environmental exposure to asbestos, a long list of studies (Auerbach, 1980; Huang, 1988; Molinini, 1997) document the presence of asbestos fibers in various organs in the digestive tract, urinary tract and in other body parts. Fiber deposition was found relevant in the liver and in the kidney.

In the present study we aimed to investigate the presence of inorganic fibers (asbestos and non asbestos classified) in urine of subjects from different areas of Piedmont Region (NW Italy) and Biancavilla (S Italy) for mapping environmental recent exposure to mineral fibres.

After chemical digestion, scanning electron microscopy (SEM) equipped with an energy dispersive spectrometry (EDS) was selected as the most suitable technique for qualitative as well as quantitative evaluation of urinary inorganic fibers. Inorganic fibers detected were identified and then quantified as fibres for 10 cc of urine (ff/10cc).

Our results showed that inorganic fibers investigation in the urine can be a good method for qualitative assessment of recent exposure to airborne mineral fibers dispersed from natural or anthropogenic sources, when the characteristics of the area are known.

This investigation can therefore be useful to assess possible situations of pollution in the recent past which the subjects have been exposed.

Auerbach, O., Conston, A.S, Garfinkel, L., Parks, V.R., Kaslow, H.D., Hammond, EC. (1980): Presence of asbestos bodies in organs other than the lung. *Chest*, **77**,133-137.

Finn, M.B. & Hallenbeck, W.H. (1985): Detection of chrysotile asbestos in workers' urine. *Am. Ind. Hyg. Assoc. J.*, **46**, 162-169.

Huang, J., Hisanaga, N., Sakai, K., Iwata, M., Ono, Y., Shibata, E., Takeuchi, Y. (1988): Asbestos fibers in human pulmonary and extrapulmonary tissues. *Am. J. Ind. Med.*, **14**, 331-339.

Molinini, R., Paoletti, L., Batisti, D., Gentile, A., Mera, E., Strada, L., Zanframundo, N., Pollice, L. (1997): Individuazione di fibre di asbesto in tessuti extrapolmonari. Risultati preliminari. *in* "L'amianto: dall'ambiente di lavoro all'ambiente di vita. Nuovi indicatori per futuri effetti" C. Minoia, G. Scansetti, G. Piolatto, A. Massola, eds., Pi-Me, Pavia, 289-293.

THALLIUM ACCUMULATION INSIDE PIPELINES OF DRINKABLE WATER DISTRIBUTION SYSTEMS: THE CASE OF THE SOUTHERN APUAN ALPS ABANDONED MINING SITES

D'Orazio M.*[1], Biagioni C.[1], Vezzoni S.[1] & Petrini R.[1]
[1] Dipartimento di Scienze della Terra, Università di Pisa, Italy
Corresponding email: massimo.dorazio@unipi.it

Keywords: thallium, drinkable water, pyrite

At the beginning of September 2014, some of the authors (MD, RP) documented a severe thallium (Tl) contamination of the drinkable water distributed by the public aqueduct of Valdicastello Carducci-Pietrasanta (Lucca Province, Tuscany, Italy). The contaminated water originated from a spring outflowing within a dismissed mining area in the Baccatoio stream catchment (Pollone and Monte Arsiccio mines) where baryte, thallium-bearing pyrite and iron oxides were mined up to 1989. The spring has a Tl content variable from about 5 to 35 µg/L, above the maximum admissible content (2 µg/L) set by the Italian and Comunitary regulations for groundwaters, and an average discharge rate of about 40 L/s. Despite the spring was removed from the drinking water system, the Tl contamination in drinkable waters of Valdicastello persisted or worse. This anomalous behavior prompted a study of the steel pipeline interior. We found that the abundant iron oxyhydroxides (magnetite, goethite, low-crystallinity phases) encrustations lining the internal surface of the pipelines are peppered by micro- and nano-spherules of thallium oxide, identified through X-ray powder diffraction as avicennite, $Tl(III)_2O_3$. Bulk analysis of the encrustations revealed a Tl content of about 1.5 wt.%. Interestingly, the segment of pipeline from the spring to the water filtering and disinfection plant of Valdicastello was found free of Tl oxide spherules. Inside the water treatment plant was active a chlorination system. The oxidative reaction between Tl^+ (the most likely Tl species dissolved in the water from the spring according to thermodynamic data) and chlorine is energetically feasible at standard conditions, and it is likely the cause of the precipitation of $Tl(III)_2O_3$ particles, even if additional studies are necessary. Leaching experiments performed on the pipeline encrustations suggest that Tl occurs not only as $Tl(III)_2O_3$ particles but also as more mobile forms.

The present study contributes to gain insights into the mechanisms of oxidation and the complex nature of reactions involving thallium redox cycles in drinking water systems.

CHROMIUM AND NICKEL IN SERPENTINITIC SOILS AND ROCKS IN OPHIOLITE FROM DIFFERENT OROGENIC SETTINGS (LIGURIA, ITALY)

Fornasaro S.*[1], Marescotti P.[1], Crispini L.[1], Comodi P.[2], Malerba G.[1] & Lercari M.[1]
[1] Dipartimento di Scienze della Terra, dell'Ambiente e della Vita, Università di Genova, Italy
[2] Dipartimento di Fisica e Geologia, Università di Perugia, Italy
Corresponding email: silvia.fornasaro@gmail.com

Keywords: serpentinitic soils, ecotoxic metals

Serpentinitic soil is a generic term used to describe any soil formed from ultramafic (peridotite and pyroxenite) or serpentinitic bedrocks (Oze, 2004). These soils are generally characterized by low contents of essential elements (P, K, and N), high contents of ecotoxic metals (Cr, Co, Ni), and low Ca/Mg ratios.

In this study, we have determined the concentration and distribution of Cr and Ni in serpentinitic rocks and soils from the high pressure-low temperature metaophiolite of the Voltri Massif (VM - Western Alps) and from the low grade ophiolite of the Bracco-Val Graveglia Unit (BG - Northern Apennines).

Trace element concentrations were assessed *in situ* by means of Field Portable X-Ray Fluorescence spectrometer (FP-EDXRF) and in laboratory by ICP-MS. The mineralogy and the mineral chemistry were determined by optical microscopy, scanning electron microscopy (SEM-EDS), and electron microprobe analyses (WDS). Soil color and granulometry were also assessed.

In the parent rocks, Ni was generally higher in the Apennine than in the Alpine Domain (BG: mean = 2409 ppm, median = 2548 ppm; VM: 1933 ppm, median = 2004 ppm) whereas Cr showed an opposite behavior (BG: mean = 1844 ppm, median = 2123 ppm; VM: 2239 ppm, median = 2301 ppm). Cr and Ni in soils significantly varied from site to site either in the Alpine and Apennine domain. The bulk chemistry of the soil profiles evidenced a conservative behavior of Cr with quite homogeneous concentrations along the soil profiles and a good correlation with the Cr content of the parent rocks. Conversely, the Ni distribution evidenced a high variability and a general increase in the upper horizons (up to a factor of 2) due to the weathering of the primary Ni-bearing minerals (mainly olivine and serpentine minerals) and to deposition of the authigenic secondary minerals (mainly Fe-oxyhydroxides and clay minerals).

The mineral -chemistry results showed that within bedrocks and soil profiles most of the Cr was contained within primary Fe-oxides and spinel group minerals (mainly magnetite and chromite). It is worth to note that rocks and soils from Apennine domain evidenced much higher spinel contents and a significant enrichment in Fe-Ni sulphides than those from Voltri massif. The main Ni-bearing minerals were olivine and serpentine group minerals, though non-trascurable Ni concentration were also detected in primary and authigenic Fe-oxides.

Most of the detected Cr- and Ni-bearing primary minerals resulted partially altered or completely unaltered either in rocks and soils evidencing their tendency to remain as stable residual minerals. Cr- and Ni-bearing secondary authigenic minerals were mainly represented by Fe-oxides and -oxyhydroxides and, subordinately, by clay minerals and iddingsitic mixtures.

Oze, C., Fendorf, S., Bird, D.K., Coleman, R.G. (2004): Chromium geochemistry of serpentine soil. *Int. Geol. Rev.*, **46**, 97-126.

ENVIRONMENTAL RELEVANCE OF SOLID BY-PRODUCTS FROM MUNICIPAL SOLID WASTE INCINERATION ASSESSED BY COMBINING MAGNETIC AND MINERALOGICAL ANALYSIS

Funari V.*[1], Mantovani L.[2], Tribaudino M.[2], Vigliotti L.[3], Braga R.[1] & Dinelli E.[1]
[1] Dipartimento di Scienze Biologiche, Geologiche e Ambientali, Università di Bologna, Italy
[2] Dipartimento di Fisica e Scienze della Terra "Macedonio Melloni", Università di Parma, Italy
[3] Instituto di Scienze Marine, Consiglio Nazionale delle Ricerche, Bologna, Italy
Corresponding email: valerio.funari@unibo.it

Keywords: industrial waste, magnetic mineralogy, superparamagnetic grains

Bottom (BA) and Fly Ashes (FA) from Municipal Solid Waste Incineration (MSWI) represent huge amounts of solid by-products that still pose environmental and health problems. Some routes for MSWI ashes management/reuse have been proposed (e.g., inertization, landfilling, reuse as filler, geopolymers), but not all of BA and FA hazardous components are fully understood. Precise identification of minerals from BA and FA is challenging due to several factors: high number of phases, MSWI combustion temperature, and variable chemical composition of feedstock materials. In addition, (trans)formation of magnetic iron oxides, which have been correlated with heavy metals pollution and the presence of toxic ultrafine superparamagnetic (SP) grains in a range of materials, occurs during incineration and quenching.

We have undertaken the study of BA and FA samples from Italian MSWI plants by combining magnetic and mineralogical analysis for probing mineralogy and the extent of SP grains. The BA and FA samples are characterized by narrow hysteresis curves and low coercivity (Bc, 7.2-14.1 mT), suggesting significant reversible component of magnetization. Also, the analysis of thermomagnetic properties shows that both BA and FA gain magnetization during cooling. The Low temperature remanent curves by Magnetic Properties Measurement System (MPMS) show magnetite-like shapes for most of samples, but the Vervey transition in FA samples is not clear probably due to the presence of oxidized/impure magnetite or unblocking of SP grains. Measurements of AC susceptibility by MPMS might support the fact of a significant contribution of SP grains in FA (FA show larger frequency dependence than BA).

We performed XRD analysis on FA and BA samples, including different magnetic extracts of BA in order to shed some light on iron oxides phases. The main mineralogical phases found in BA are quartz, calcite-vaterite, melilite group minerals and plagioclase; FA contain Ca-aluminosilicates and more sulphates and chlorides with respect to the BA. Iron oxides such as wurstite, hematite, and the magnetic spinel-type iron oxides are noted both in BA and FA. The XRD pattern on BA magnetic extracts confirms that magnetite or impure spinel-type iron oxides (e.g., Mg-magnetite, Ti-magnetite, and maghemite) are in charge of their strong magnetic response. However, on the basis of previously obtained chemical analysis, the presence of impure magnetite containing Cr, Zn, Mn, and Cu cannot be ruled out neither in BA nor in FA. Rietveld refinement to assess the extent of minor metals substitution is ongoing.

These preliminary observations emphasise the metastable nature of MSWI ashes and might lead to a better assessment of the environmental impact related to iron oxides.

Acknowledgment: V.F. acknowledges a Visiting Fellow at the Institute for Rock Magnetism (IRM). The IRM is a US National Multi-user Facility supported through the Instrumentation and Facilities program of the National Science Foundation, Earth Sciences Division, and by funding from the University of Minnesota.

THE EFFECT OF VOLCANIC ASH COMPOSITION AND GLASS CONTENT ON JET ENGINE SAFETY

Giehl C.*[1-2], Brooker R.A.[1-3], Marxer H.[1] & Nowak M.[1]
[1] Fachbereich Geowissenschaften, Eberhard Karls Universität Tübingen, Germany
[2] Institut für Geowissenschaften, Christian-Albrechts-Universität Kiel, Germany
[3] School of Earth Sciences, University of Bristol, United Kingdom
Corresponding email: christopher.giehl@min.uni-kiel.de

Keywords: turbine blades, thermal barrier coating, wetting behaviour

The grounding of commercial aircraft throughout Europe due to the long lasting Eyjafjallajökull volcanic eruption in Iceland April 2010, has focused public attention on the potential dangers of flying jet engines through ash clouds. One of the most serious issues is related to the melting of volcanic ash in the combustion chamber to form a deposit of silicate material on hot turbine parts behind the combustor or the clogging of the air-flow holes that cool the blade. This results in blade damage, restricts cooling efficiency and ultimately causes the engine to stall. In this study, we highlight both the influence of volcanic ash composition and glass vs. crystal ratio on the interaction of ash particles with hot turbine parts.

We have simulated melting for a range of typical volcanic compositions in a combustion flame and deposition on nickel superalloy, a material commonly used for hot turbine sections with vanes and blades. For the experiments, partly crystalline basaltic, andesitic, dacitic and rhyolitic rock powders, and their remelted and quenched glass analogues, were used. The wetting of the surface with melt and the adhesion properties of the deposit when cooled, as well as the importance of melting rate of ash particles during entrainment in the combustion flame were investigated.

Four types of deposition behaviour on the alloy blade were identified: (1) particles bouncing off, (2) continuous accumulation of partly molten particles to form a cindery layer, (3) development of a melt pool directly on the blade or on top of partly molten particles, and (4) formation of melt bath with a very low wetting angle. As we can show experimentally, bulk chemical composition, crystal/glass ratio and resulting initial particle contact and deposit formation exert strong controls on the wetting of turbine blades. When considering safety limits for flying, the nature of the “ash” might be as important as ash concentration (200 mg/m^3; Clarkson et al., 2016).

Initial ash deposits allow a subsequent rapid accumulation of more material until a catastrophic build-up and clogging of vane and blade air-film cooling systems occurs. The nature of the initial coating (completely molten pool or partly molten particles) dictates the ease of removal by ‘in flight cooling’ that involves closing down the engines, allowing the melt to solidify and then relying on thermal shock to dislodge the material from the turbine vanes.

Clarkson, R.J., Majewicz, E.J.E., Mack, P. (2016): A re-evaluation of the 2010 quantitative understanding of the effects volcanic ash has on gas turbine engines. *J. Aerosp. Engin.*, DOI: 10.1177/0954410015623372.

POTENTIALLY CARCINOGENIC ERIONITE IN ITALY: GEOLOGICAL OCCURRENCE AND RISK ASSESSMENT

Giordani M.*[1], Mattioli M.[1], Valentini L.[2] & Ballirano P.[3]
[1] Dipartimento di Scienze Pure e Applicate, Università "Carlo Bo", Urbino, Italy
[2] Dipartimento di Scienze Biomolecolari, Università "Carlo Bo", Urbino, Italy
[3] Dipartimento di Scienze della Terra, Sapienza Università di Roma, Italy
Corresponding email: matteo.giordani@uniurb.it

Keywords: erionite, zeolite, Italy

Erionite is a fibrous mineral of the zeolite group mainly occurring as hydrothermal alteration product. The exposure of humans to erionite fibres has been unambiguously linked to malignant mesothelioma cases (Baris et al., 1978), and in vivo studies have demonstrated that erionite is significantly more tumorigenic than asbestos (Coffin et al., 1992). Recently, a growing concern has developed regarding the potential risks for environmental and occupational exposures to erionite in Turkey (Carbone et al., 2011), in the United States (Saini-Eidukat & Triplett, 2014), in Mexico (Ortega-Guerrero & Carrasco-Nùñez, 2014) and possibly in Iran (Ilgren et al., 2015). Newly researches on the identification of segregation of Fe(II) provide very important information for the understanding of the molecular mechanism/s inducing its strong carcinogenicity (Ballirano et al., 2015). Notwithstanding this, the relationships among mineralogical features and biological activity of erionite have not yet been fully understood and there are no systematic studies on the distribution of erionite or other similar fibrous zeolites in the environment.

In Italy, erionite was reported in Sardinia and Veneto (Passaglia & Galli, 1974; Mattioli et al., 2016). Nevertheless, a systematic mapping of its distribution, the quantification of its presence in rocks and data about airborne fibers are still missing. Here we present mineralogical data of new erionite occurrences from Northern Italy, with a state of the art on the occurrence of erionite in Italy and some other potentially erionite-bearing deposits. The studied erionite samples show prismatic to extremely fibrous habits and a variable tendency to break down in thin fibrils, which could be potentially pathogenic on inhalation. The chemical data acquired revealed variable amounts of Ca, Na, K and Mg as extra-framework cations, with small amounts of Fe.

In Italy the knowledge of the epidemiology of mesothelioma linked to erionite is extremely scarce, and domestic cases from exposure to airborne erionite fibers are still to be inferred. Identifying the areas in Italy where erionite occurs naturally is a starting point for further specific studies on epidemiology, public health and natural hazards. An effective risk assessment in Italy will require coordinated actions from government agencies, local health authorities, Universities and research centers, in order to record the actual presence of fibrous zeolites, recognizing mineral species and quantifying their abundance in rock deposits.

Ballirano, P., Pacella, A., Cremisini, C., Nardi, E., Fantauzzi, M., Atzei, D., Rossi, A., Cametti G. (2015): Fe (II) segregation at a specific crystallographic site of fibrous erionite: A first step toward the understanding of the mechanisms inducing its carcinogenicity. *Microp. Mesop. Mater.*, **211**, 49-63.

Baris, Y.I., Sahin, A.A., Ozesmi, M., Kerse, I., Ozen, E., Kolacan, B., Altinörs, M., Göktepeli, A. (1978): An outbreak of pleural mesothelioma and chronic fibrosing pleurisy in the village of Karain/Urgüp in Anatolia. *Thorax*, **33**, 181-192.

Carbone, M., Baris, Y.I., Bertino, P., Brass, B., Comertpay, S., Dogan, A.U., Gaudino, G., Jube, S., Kanodia, S., Petridge, C.R., Pass, H.I., Rivera, Z.S., Steele, I., Tuncer, M., Way, S., Yang, H., Miller, A. (2011): Erionite exposure in North Dakota and Turkish villages with mesothelioma. *Proc. Nat. Acad. Sci. USA*, **108**, 13623-13628.

Coffin, D.L., Cook, P.M., Creason, J.P. (1992): Relative mesothelioma induction in rats by mineral fibers: comparison with residual pulmonary mineral fiber number and epidemiology. *Inhal. Toxicol*., **4**, 273-300.

Ilgren, E.B., Kazemian, H., Hoskins, J.A. (2015): Kandovan the next 'Capadoccia'? A potential public health issue for erionite related mesothelioma risk. *Epidemiol. Biostat. Public Health*, **12**, 1-12.

Mattioli, M., Cenni, M., Passaglia, E. (2016): Secondary mineral assemblages as indicators of multi stage alteration processes in basaltic lava flows: Evidence from the Lessini Mountains, Veneto Volcanic Province, Northern Italy. *Per. Mineral*., **85**, 1-24.

Ortega-Guerrero, M.A. & Carrasco-Nùñez, G. (2014): Environmental occurrence, origin, physical and geochemical properties, and carcinogenic potential of erionite near San Miguel de Allande, Mexico. *Environ. Geochem. Health*, **36**, 517-529.

Passaglia, E. & Galli, E. (1974): Levyne and erionite from Sardinia, Italy. *Contrib. Mineral. Petrol*., **43**, 253-259.

Saini-Eidukat, B. & Triplet, J.W. (2014): Erionite and offretite from the Killdeer Mountains, Dunn County, North Dakota, USA. *Am. Mineral*., **99**, 8-15.

Van Gosen, B.S., Blitz, T.A., Plumlee, G.S., Meeker, G.P., Pierson, M.P. (2013). Geologic occurrences of erionite in the United States: an emerging national public health concern for respiratory disease. *Environ. Geochem. Health*, **35**, 419-430.

PRISMATIC TO EXTREMELY FIBROUS OFFRETITE FROM NORTHERN ITALY: MORPHOLOGICAL AND CHEMICAL DATA OF A POTENTIALLY HAZARDOUS ZEOLITE

Giordani M.[1], Mattioli M.*[1], Ballirano P.[2], Boscardin M.[3] & Valentini L.[4]
[1] Dipartimento di Scienze Pure e Applicate, Università "Carlo Bo", Urbino, Italy
[2] Dipartimento di Scienze della Terra, Sapienza Università di Roma, Italy
[3] Museo di Archeologia e Scienze Naturali "G. Zannato", Montecchio Maggiore (VI), Italy
[4] Dipartimento di Scienze Biomolecolari, Università "Carlo Bo", Urbino, Italy
Corresponding email: michele.mattioli@uniurb.it

Keywords: offretite, zeolite, Italy

Offretite, a quite rare zeolite, is hexagonal with space group symmetry *P*6*m*2 and unit-cell parameters *a* = 13.27-13.32 Å, *c* = 7.56-7.61 Å, and has a chemical formula of $KCaMg[Al_5Si_{13}O_{36}]\cdot 16H_2O$. Offretite forms simple hexagonal prisms with pinacoid terminations and the habit is commonly acicular (Passaglia et al., 1998). Due to the structural and chemical similarities with erionite (a mineral recognized to be highly carcinogenic), and because of the possibility of intergrowth of these two species within each crystal, their distinction can be very difficult. The most significant discrimination is based on the Mg/(Ca+Na) cation ratio. Notwithstanding offretite has been reported in various localities from Italy (Passaglia & Tagliavini, 1994; Passaglia et al., 1996, 1998; Boscardin et al., 1998; Guastoni et al., 2002; Mattioli et al., 2016a), the morphologies of offretite crystals have not yet been fully understood and many mineralogical aspects are still unknown.

Here we present new morphological and chemical data of offretite from Northern Italy with two main different habits. The type-1 habit ranges from stocky-prismatic to very thin, needle-like prisms, and thus very similar to those described in the literature for the other Italian offretite. The type-2 habit is very different and is constituted by extremely thin fibers, often with asbestiform appearance, that show a strong tendency to break down into small fibrils, which could potentially be of inhalable size. Preliminary ESEM/EDS analysis on the offretite fibers revealed the occurrence of Mg, K, and Ca as extra-framework cations, and a Mg/(Ca + Na) cation ratio of ≈ 1.

Recent researches on the surface properties of fibrous zeolites (Mattioli et al., 2016b) showed that interaction ability of offretite surface is much lower than that found for erionite, but we can not exclude the fibers of offretite from those able to cause some toxic effect on health. In fact, it is unclear whether the mineralogical distinction between erionite and offretite has any health implications. However, as already seen for the case of asbestos minerals, codification of nomenclature such as specific mineral names or habits into laws or regulations may have consequences in the application of health and legal policy. These data suggest the need for a better understanding of the potential toxicity across the range of erionite and offretite compositions.

Boscardin, M., Checchi, A., Filippi, F., Guglielmino, S., Pegoraro, S., Pretto, G., Zattra, A. (1998): Offretite del Veneto. *Riv. Miner. Ital*., **22**, 25-29.

Guastoni, A., Dugnani, M., Pezzotta, F., Bardelli, G. (2002): Offretite del lago d'Arno in alta Val Saviore, Parco dell'Adamello (Bs). *Atti Soc. It. Nat. Museo Civ. Stor. Nat. Milano*, **143**, 195-207.

Mattioli, M., Cenni, M., Passaglia, E. (2016a): Secondary mineral assemblages as indicators of multi stage alteration processes in basaltic lava flows: evidence from the Lessini Mountains, Veneto Volcanic Province, Northern Italy. *Per. Mineral*., **85**, 1-24.

Mattioli, M., Giordani, M., Dogan, M., Cangiotti, M., Avella, G., Giorgi, R., Dogan, A.U., Ottaviani, M.F. (2016b): Morpho-chemical characterization and surface properties of carcinogenic zeolite fibers. *J. Hazard. Mat.*, **305**, 140-148.

Passaglia, E. & Tagliavini, A. (1994): Chabazite-offretite epitaxial overgrowths in cornubianite from Passo Forcel Rosso, Adamello, Italy. *Eur. J. Mineral*., **6**: 397-405.

Passaglia, E., Artioli, G., Gualtieri, A. (1998): Crystal chemistry of the zeolites erionite and offretite. *Am. Mineral.*, **83**: 577-589.

Passaglia, E., Tagliavini, A., Gutoni, R. (1996): Offretite and other zeolites from Fittà (Verona, Italy). *N. Jb. Mineral. Mh.*, **1996**, 145-156.

THE CRYSTAL STRUCTURES OF MINERAL FIBRES

Gualtieri A.F.*[1], Pollastri S.[1], Bursi Gandolfi N.[1], Perchiazzi N.[2], Plaisier J.R.[3], Lezzerini M.[2] & Gialanella S.[4]
[1] Dipartimento di Scienze Chimiche e Geologiche, Università di Modena e Reggio Emilia, Modena, Italy
[2] Dipartimento di Scienze della Terra, Università di Pisa, Italy
[3] Elettra-Sincrotrone Trieste, Italy
[4] Dipartimento di Ingegneria Industriale, Università di Trento, Italy
Corresponding email: alessandro.gualtieri@unimore.it

Keywords: mineral fibres, structure.

Since 2011, a research project on mineral fibres entitled "*Sviluppo di un modello generale di interazioni tra fibre minerali e cellule biologiche*", has been conducted as part of the long term Italian Research Project of National Interest (PRIN) "*Interazione fra minerali e biosfera: conseguenze per l'ambiente e la salute umana*". The research project is specifically focussed on mineral fibres and is aimed at understanding the biochemical reactions that make them cyto- and geno-toxic and at the development of a general model capable to classify each mineral fibre based on its toxicity potential. The attempt to understand the complex biochemical mechanisms between the mineral fibres and the organic matter requires a basic systematic mineralogical-crystallographic study. Hence, eight mineral fibres samples have been selected for the study based on their socio-economic and industrial importance: three chrysotile of different origin (UICC, Canada; Balangero and Val Malenco, Italy), four amphibole asbestos species (amosite UICC, anthophyllite UICC, crocidolite UICC and tremolite from Val d'Ala) and the fibrous zeolite erionite (from Jersey, Nevada, USA). The surface reactivity and the chemical environment of iron within the crystal structure of these samples have been recently investigated (Pollastri et al., 2014, 2015). In order to complete the crystal structural characterization, X-ray powder and single crystal diffraction experiments have been conducted using both conventional and synchrotron radiation sources (Elettra, Trieste, Italy; SLS, Villigen, Switzerland), for the determination of impurities and the refinement of the crystalline structures. Concerning the chrysotile samples, because of the low to null effect of conventional grinding techniques on chrysotile fibre bundles, we have opted for a cryo-milling process in wet conditions; this procedure allowed to obtain perfectly powder samples. For chrysotile and erionite samples, diffraction patterns were collected with either resonant radiation at the absorption *K*-edge of Fe (≈ 7 k*e*V, λ 1.7428 Å) and with wavelength off of the absorption edge (≈ 10 k*e*V, λ 1.2408 Å) in order to investigate the crystal chemistry of iron within the fibres. The collected data were analysed both with the TOPAS and GSAS. The results of the structural refinements, in particular occupancy and position of the iron atoms within the crystal structures (a primary cause of toxicity as it generate active oxygen species, mobilization by chelators and iron-catalyzed reactions; Hardy & Aust, 1995), were compared to that obtained from the previously performed spectroscopic investigations. The obtained structures of chrysotile samples are similar to each other and quite similar to the only available structure of chrysotile present in literature (Falini et al., 2004). Also the structures of other samples were compared to the few data reported in literature to highlight differences between the fibrous and non fibrous forms of the minerals.

Falini, G., Foresti, E., Gazzano, M., Gualtieri, A.F., Leoni, M., Lesci, I.G., Roveri, N. (2004): Tubular shaped stoichiometric chrysotile nanocrystals. *Chem. - Eur. J.*, **10**, 3043-3049.

Hardy, J.A. & Aust, A.E. (1995). Iron in asbestos chemistry and carcinogenicity. *Chem. Rev.*, **95**, 97-118.

Pollastri, S., D'Acapito, F., Trapananti, A., Colantoni, I., Andreozzi, G.B., Gualtieri, A.F. (2015): The chemical environment of iron in mineral fibres. A combined X-ray absorption and Mössbauer spectroscopic study. *J. Hazard. Mater.*, **298**, 282-293.

Pollastri, S., Gualtieri, A.F., Lassinantti Gualtieri, M., Hanuskova, M., Cavallo, A., Gaudino, G. (2014): The zeta potential of mineral fibres. *J. Hazard. Mater.*, **276**, 469-479.

MINERALS HAZARDS A TO Z: THE ROLE OF THE MINERALOGIST

Gunter M.E.*[1]
[1] Department of Geological Sciences, University of Idaho, Moscow, ID, USA
Corresponding email: mgunter@uidaho.edu

Keywords: asbestos, crystalline silica, zeolites

Clearly there exists a hazard to the inhalation of respirable mineral particles or we would not have convened this session. Generally speaking two negative health effects can occur: 1) a toxic effect (e.g., silicosis or asbestosis), and 2) differing types of cancer (e.g., lung cancer and mesothelioma). The former is dose dependent while the etiology of the latter are less well understood by the medical community. Currently IARC lists 113 “agents and groups of agents” as group 1 human carcinogens; in that list there are three that relate to minerals: 1) asbestos (i.e., chrysotile, crocidolite, amosite, asbestiform anthophyllite, asbestiform tremolite, and asbestiform actinolite), 2) erionite (a rare zeolite), and 3) crystalline silica (quartz and cristobalite).

Since 1999 I have worked as closely with individuals in the medial, regulatory, legal, and government fields as I have with fellow mineralogists and geologists dealing with the health effects of mineral dusts. What is very clear to me is that we – as mineralogist and geologists -- need to dedicate more of our time and energy to educate these other groups in basic mineralogy and geology. One of the biggest issues is much of knowledge from those outside of our field of the main mineral hazard (i.e., asbestos) was gained by working on this issue in built environmental. Unfortunately many of the regulatory definitions for that setting are also being used for the natural setting (Gunter, 2010). Some of these, if directly applied, would result in amphibole “asbestos contamination” of large amounts of farmland (Thompson et al., 2011) as amphiboles occur in many soils. Even more widespread is quartz, basically occurring in all soils (McNamee & Gunter, 2011; Smith et al., 2013). Also, while erionite has been linked to increased rates of mesothelioma, another unfortunate circumstance outside of the geology community is that erionite is now often called asbestos. And like many outside of our community view the term amphibole to be synonymous to asbestos, they are now using the term zeolite to be synonymous with erionite. To me the most ironic aspect of the above is the rarity of asbestos and erionite in the natural environment, while quartz would be the most abundant mineral species in the Earth’s crust. Finally, at least in the USA, litigation of purported asbestos content of various consumer products makes it even more important that we get involved in this area and correctly identify the minerals in these products.

Gunter, M.E. (2010): Defining asbestos: Differences between the built and natural environments. *Chimia*, **64**, 747-752.

McNamee, B.D. & Gunter, M.E. (2104): Evaluating the distribution of minerals listed as group one human carcinogens in soils across the conterminous United States. Geol. Soc. Am. Ann. Meeting, Vancouver, October 2014, abstr.

Smith, D.B., Cannon, W.F., Woodruff, L.G., Solano, F., Kilburn, J.E., Fey, D.L. (2013): Geochemical and mineralogical data for soils of the conterminous United States. U.S. Geological Survey Data Series 801, 19 p.

Thompson, B.D., Gunter, M.E., Wilson, M.A. (2011): Amphibole asbestos soil contamination in the USA: A matter of definition. *Am. Mineral.*, **96**, 690-693.

As SPECIATION IN VICAN IGNIMBRITES: PRELIMINARY XAS DATA

Lepore G.O.*[1], Mazzuoli M.[2-3], Proposito M.[2], Trovato C.[2] & Armiento G.[2]
[1] Istituto Officina dei Materiali, Consiglio Nazionale delle Ricerche, c/o ESRF, Grenoble, France
[2] Laboratorio di Biogeochimica Ambientale, Agenzia Nazionale per le Nuove Tecnologie, l'Energia e lo Sviluppo Economico Sostenibile, Roma, Italy
[3] Dipartimento di Scienze Ecologiche e Biologiche, Università della Tuscia, Viterbo, Italy
Corresponding email: lepore@esrf.fr

Keywords: arsenate, adsorption, ignimbrite

Arsenic frequently occurs in groundwater of volcanic areas due to its presence as a natural constituent of volcanic gasses and geothermal fluids and to the interaction of waters with rocks naturally hosting this element. The determination of the total arsenic (As) concentration in contaminated matrices is however not sufficient for a sound risk assessment due to the fact that As mobility, bioavailability and toxicity vary depending on both the oxidation state and the phases it is associated to. In order to better understand the origin, nature and behaviour of arsenic species in the rocks nearby Viterbo (Northern Latium-Central Italy), XANES and EXAFS measurements have been performed on tuff rocks at the As *K*-edge (11867 *e*V) at the LISA beamline at the European synchrotron Radiation Facility. The analysed samples are ignimbrites belonging to the Sutri formation (Perini et al., 2004); a core sample in the Bagnaccio hydrothermal area, where rocks are affected by upwelling hydrothermal fluids was also collected together with travertine samples (P1 and P2) overlaying ignimbrite (P3).

XANES data on Vican ignimbrites and travertines show that As is always present as As^{5+} except in the case of one sample (TT), where the presence of As^{3+} is also evident. Subsequent analyses highlighted that As^{3+} is concentrated in the scoriae (SN) and As^{5+} in the matrix (MR).

EXAFS analyses show that in all the samples As is bound to oxygen. In the ignimbrites, As^{5+} shows As-O distances ranging from 1.65 to 1.69 Å, compatible with a 4-fold coordination typical of arsenate groups; in SN, As^{3+}-O was found to be 1.77(9) Å, within the characteristic distance range of arsenite groups. No hints of features corresponding to higher coordination shells are shown except for the case of the P3 sample, taken in the hydrothermal area, for which a more detailed data analysis, still in progress, shows the presence of a second coordination shell with As atoms at 3.23(3) Å and thus suggesting the presence of two different As-bearing phases.

The two travertines show As-O distances varying in the same range as in ignimbrites and no clear indication of a second shell coordination.

The absence of detectable second shell signals reveals a poorly ordered environment, probably corresponding to adsorption onto oxide or silicate phases for all the samples except for that coming from the hydrothermal area where the presence of a more ordered As phase is detected.

Perini, G., Francalanci, L., Davidson, J.P., Conticelli, S. (2004): Evolution and genesis of magmas from Vico Volcano, Central Italy: multiple differentiation pathways and variable parental magmas. *J. Petrol.*, **4**, 139-182.

MINERALOGICAL CHARACTERIZATION OF CALCIFICATION AGGREGATIONS IN CEREBRAL ARTERIES

Li Y.[1], Wang C.*[1], Meng F.[1], Li Y.[1], Lu A.[1], Yang C.[2] & Li K.[3]

[1] Key Laboratory of Orogenic Belts and Crustal Evolution, School of Earth and Space Sciences, Beijing University, China

[2] Department of Pathology, Beijing Hospital, Beijing, China

[3] Department of Cardiology, Beijing Hospital, Beijing, China

Corresponding email: liyuan130121@pku.edu.cn

Keywords: pathological mineralization, cerebral artery, carbonate hydroxylapatite

Cerebral artery calcification is frequently observed in computed tomography (CT) of stroke patients, and considered as an independent risk factor of ischemic stroke (Chen et al., 2007). The investigation of mineralogical characteristics of calcification could help reveal the formation and development of calcification process.

Samples were acquired from Beijing Hospital, including three vertebral basilar arteries, one intracranial internal carotid artery, two anterior cerebral arteries and one middle cerebral artery, all belongs to cerebral artery system. The study was approved by the ethics committee of Beijing Hospital.

In hematoxylin-eosin stained sections, calcification appeared in the intima layer of vessel wall. SEM images showed the calcification mainly presented in two different forms: spherical and massive. Spherical calcification either had radiated-concentric structure or concentric layers structure, with a diameter of 0.1-5.0 μm. Spheres distributed along the collagen fiber. Massive calcification appeared in larger scale. The edges of massive calcification were consisted of spherical calcification, and structural remains of spherical calcification were on the fracture surface of massive calcification. This indicated that massive calcification was closely related to spherical calcification.

The micro-area synchrotron radiation X-ray powder diffraction (μ-SRXRD) patterns of the samples match well with CHA (PDF#19-0272). The FT-IR spectra indicated the existence of PO_4^{3-}, CO_3^{2-} and OH^- groups. Therefore, the calcification was identified as carbonate hydroxylapatite. The energy dispersive spectrum (EDS) under SEM showed high contents of Ca, P, O, C and low content of Na, Mg in calcification. Besides, trace elements of Zn, Fe and Sr were observed by Micro-area synchrotron radiation X-ray fluorescence spectroscopy (μ-SRXRF).

The results showed the main mineral phase in calcification is carbonate hydroxylapatite, similar to the minerals in calcification of cardiovascular system. Spherical calcification was speculated to be formed at initial stage of the disease, while the massive calcification was a late stage product.

Chen, X., Lam, W.W.M., Ng, H.K., Fan, Y.H., Wong, K.S. (2007): Intracranial artery calcification: a newly identified risk factor of ischemic stroke. *J. Neuroimag.*, **17**, 300-303.

Li, Y., Wang, X., Zhu, M., Yang, C.Q., Lu, A., Li, K., Meng, F., Wang, C. (2014): Mineralogical characterization of calcification in cardiovascular aortic atherosclerotic plaque: A case study. *Mineral. Mag.*, **78**, 775-786.

Meng, F., Wang, C, Li, Y., Lu A., Mei, F., Liu, J., Du, J., Zhang, Y. (2015): Psammoma bodies in two types of human ovarian tumours: a mineralogical study. *Mineral. Petrol.*, **109**, 357-365.

MAGNETITE AS A POLLUTANT IN THE ATMOSPHERE: EVIDENCE FROM SEM-EDS AND MAGNETIC ANALYSIS OF LEAVES AND PARTICULATE FILTERS

Mantovani L.*[1], Barraco V.[1], Tribaudino M.[1], Solzi M.[1], De Munari E.[2] & Pironi C.[2]
[1] Dipartimento di Fisica e Scienze della Terra "Macedonio Melloni", Università di Parma, Italy
[2] Agenzia Regionale per la Prevenzione, l'Ambiente e l'Energia dell'Emilia-Romagna, Parma, Italy
Corresponding email: luciana.mantovani@unipr.it

Keywords: magnetic minerals, anthropogenic pollution, biomonitoring

The evaluation of health impacts arising from inhalation of pollutant particles < 10 mm (PM_{10}) is an active research area. Usually the PM_{10} particulate is investigated throughout the daily sampling of PM_{10} filter, but in the last decade, some studies have shown that natural bio-monitors like tree leaves could be a good technique for integrate traditional methods and measure the air quality (Lehndorff et al., 2006; Maher et al., 2008; Szonyi et al., 2008; Mitchell & Maher, 2009).

In this work, both PM_{10} filters and leaves are daily collected over a period of five months; filters are taken from an air-quality monitoring stations run by ARPAE-Emilia Romagna and leaves from some *tilia cordata* trees, both located near the central station of Parma. On these samples, magnetic measurements and SEM-EDS analysis has been performed and the results are then compared to the data of several pollutants of anthropogenic origin (heavy metals, O_3, NO_2, C_6H_6, CO).

Saturation isothermal remanent magnetization (SIRM) measurements show that the magnetic fraction of filters and leaves mainly consists of a low coercivity phase, which could be identified as magnetite; the identification was confirmed by SEM-EDS analysis, in which rounded small micrometre particles of magnetite associated with clay minerals and calcite are clearly visible.

The isothermal remanent magnetization (IRM) was measured at liquid nitrogen (77 K) and room temperature (298 K), to assess the grain-size particles distribution: the main part of the magnetic contribution, about 90%, can be attributed to single domain (SD) and superparamagnetic (SP) particles, i.e. the particles with grain size below one micron (Ø < 1 mm). These latter are the most dangerous: being very small, they can penetrate into the alveoli and cause cellular oxidative stress damage (Maher et al., 2008).

Statistical analysis show that significant correlation occurs between the magnetic signals of filters and leaves and the fundamental atmospheric pollutants.

Both filters and leaves show a similar time trend; the magnetic signal increases in the fall-winter period together with NO_2, PM_{10}, $PM_{2.5}$, C_6H_6 and CO content, suggesting a common and predominantly anthropogenic origin of the magnetic particles, probably produced by the combustion process of motor vehicles and by the abrasion of disk brakes (Sagnotti et al., 2009; Saragnese et al. 2011).

The results indicate that a magnetic survey of tree leaves, which is relatively rapid and inexpensive, may be used in addition to the classical air quality monitoring systems to identify and delineate high-polluted areas in urban environments. Furthermore, it should be stressed that leaves are an "easy-to-access" resource even in areas where the PM_{10} sampling units are not present and, for this reason, they may be suitable in monitoring local pollution situations derived, for example, from industrial site or incinerators.

Lehndorff, E., Urbat, M., Schwark, L., (2006): Accumulation histories of magnetic particles on pine needles as function of air quality. *Atmos. Environ.*, **40**, 7082-7096.

Maher, B.A., Moore, C., Matzka, J. (2008): Spatial variation in vehicle-derived metal pollution identified by magnetic and elemental analysis of roadside tree leaves. *Atmos. Environ.*, **42**, 364-373.

Mitchell, R. & Maher, B.A. (2009): Evaluation and application of biomagnetic monitoring of traffic-derived particulate pollution. *Atmos. Environ.*, **43**, 2095-2103.

Sagnotti, L., Taddeucci, J., Winkler, A., Cavallo, A. (2009): Compositional, morphological, and hysteresis characterization of magnetic airborne particulate matter in Rome, Italy. *Geochem. Geophys. Geosyst.*, **10**, 1-17.

Saragnese, F., Lanci, L., Lanza, A. (2010): Nanometric-sized atmospheric particulate studied by magnetic analyses. *Atmos. Environ.*, **45**, 450-459.

Szonyi, M., Sagnotti, L., Hirt, A.M. (2008): A refined biomonitoring study of airborne particulate matter pollution in Rome, with magnetic measurements of *Quercus Ilex* tree leaves. *Geophys. J. Int.*, **173**, 127-141.

EMISSION OF PARTICULATE MATTER FROM SEWAGE SLUDGE THERMAL UTILIZATION PLANT

Michalik M.*[1], Kasina M.[1], Kowalski P.R.[1], Wilczyńska-Michalik W.[2] & Pietras B.[2]
[1] Institute of Geological Sciences, Jagiellonian University, Kraków, Poland
[2] Institute of Geography, Pedagogical University of Kraków, Poland
Corresponding email: marek.michalik@uj.edu.pl

Keywords: sewage sludge thermal utilization, particulate matter emission, particulate matter

Particulate matter (PM) emitted from the sewage sludge thermal utilization plant equipped with fluidized bed boiler was analyzed using scanning electron microscopy fitted with energy dispersive spectrometry. According to the National Centre for Emissions Management (KOBiZE) database in 2013 total emission of PM from the plant was low (ca. 0.17 Mg along with 1.94 Mg of SO_x/SO_2 and 4.20 Mg of NO_x/NO_2). It indicates that the mass of this stream of incineration residue is negligible in comparison with fly ash and air pollution control residues (APC). Significant fractionation of elements between fly ash and APC may suggest higher enrichment of emitted PM in some elements. Results of single particle study are important in interpretation of sources of PM in polluted urban air.

PM contains soot both as dispersed single particles (~ 100-200 nm in size) and agglomerates of particles. Spherical silica particles (1-10 mm) are relatively uniform in chemical composition. Mixed silicates, aluminosilicates, phosphates of Ca, Mg, and Na with low amount of Cl, S, Ba, Zn, and Cu are relatively common. Ca carbonates and Na sulphates occur rarely. Cr containing particles are abundant. They are very variable in size, morphology and chemical composition (beside Cr different content of O, S, Si, Cl, Ca, and Sn can be noted). Fe or Fe-Cu sulphates, sometimes with low content of Si, are also present. Single particles of different composition were noted, e.g. metallic Cr with Ti; Au rich particles with low content of K, S, Si; Fe oxides with Ni and/or Cr; Pb, Zr, Ti, and O.

Particles emitted from the sewage sludge thermal utilization plant are diversified strongly in chemical composition and morphology. Abundance of elements is not correlated with APC residue/fly ash fractionation trend. Emission from sewage sludge thermal utilization plant can be considered as a source of particles with unpredictable chemical composition in urban aerosol.

Acknowledgments: The study was supported by Polish National Science Centre NCN grant No UMO-2014/15/B/ST10/04171

IRON FIXED AS EXTRA-FRAMEWORK CATION POTENTIALLY PLAYS A CRUCIAL ROLE IN INDUCING CARCINOGENICITY IN ERIONITE

Pacella A.[1], Fantauzzi M.[2], Atzei D.[2], Cremisini C.[3], Nardi E.[3], Montereali M.R.[3], Rossi A.[2] & Ballirano P.*[1]

[1] Dipartimento di Scienze della Terra, Sapienza Università di Roma, Italy

[2] Dipartimento di Scienze Chimiche e Geologiche, Università di Cagliari, Italy

[3] Centro Ricerche Casaccia, Agenzia Nazionale per le Nuove Tecnologie, l'Energia e lo Sviluppo Economico Sostenibile, S. Maria di Galeria (RM), Italy

Corresponding email: paolo.ballirano@uniroma1.it

Keywords: erionite, malignant mesothelioma, Fe(III) binding

Erionite is a zeolite with fibrous morphology that has been classified as a Group 1 Human-Carcinogen by the IARC. Its inhalation has been shown to cause malignant mesothelioma (MM), with tumorigenicity 500-800 times greater than that of regulated asbestos. Studies performed on asbestos revealed that several parameters are relevant for the interaction with the biological medium. It has been proposed that the presence and structural coordination of Fe, especially Fe(II), play a primary role in the genotoxic effect of the fibres through the generation of reactive oxygen species (ROS). However, in spite of its high carcinogenicity, erionite is a nominally iron-free phase. Some authors reported the presence of iron in several erionite samples that has been recently shown to be located at the zeolite surface under the form of nano-minerals. Owing to the ion-exchange capabilities of zeolites, the biological activity of erionite has been related to ion-exchanged and/or surface-deposited Fe participating in Fenton chemistry. In particular, Fe(III) is supposed to be mainly fixed at the surface, Fe(II) being ion-exchanged. Recently, Ballirano et al. (2015) provided a detailed picture of the crystal chemical modifications occurring into erionite fibres whenever kept in contact with a source of Fe(II). Results univocally indicate that Fe(II) is segregated within the erionite cavity, at the Ca3 site. This is of particular relevance as it has been shown that in Fe loaded zeolites at rather low Fe content, the most active sites in the ROS generation are those located in well-defined crystallographic positions and possessing a very low nuclearity. Here we report the results of the crystal chemical, structural and surface characterization of erionite-K fibres from Rome (Oregon, USA) after interaction with Fe(III) chloride solutions at different concentrations. In addition, Fe(III) loaded samples were investigated after incubation in ascorbic acid in order to monitor the mobility of reduced Fe(II) and to highlight its possible incorporation as EF cation through ion exchange. Comparison between released and acquired charges under the form of Fe confirms, in perfect agreement with previous studies that Fe(III) is mainly fixed at the fibre surface. Nevertheless, in very diluted Fe(III) solutions (below 50 µM $FeCl_3$) a significant fraction of Fe(III) is segregated by an ion-exchange mechanism in the erionite cavity at the Ca3 site, albeit with a significantly lower efficiency with respect to Fe(II). Incubation in ascorbic acid revealed that only Fe(III) residing at the fibres surface and characterised by low nuclearity is significantly reduced, whereas this reaction does not occur in the case of the ion-exchanged metal. Considering that the total iron in lung fluids occurs at very low concentration our results strongly suggest that the physiological environment unfortunately represents the optimum condition for iron to behave as a very active site.

Ballirano, P., Pacella, A., Cremisini, C., Nardi, E., Fantauzzi, M., Atzei, D., Rossi, A., Cametti, G. (2015): Fe(II) segregation at a specific crystallographic site of fibrous erionite: A first step toward the understanding of the mechanisms inducing its carcinogenicity. *Microp. Mesop. Mater*., **211**, 49-63.

A SURVEY OF ASBESTOS MINERALS IN NEW CALEDONIA: PRELIMINARY RESULTS

Petriglieri J.R.[1-2], Tribaudino M.*[1], Salvioli-Mariani E.[1], Mantovani L.[1], Bersani D.[1], Lottici P.P.[1], Tomatis M.[3] & Laporte-Magoni C.[2]

[1] Dipartimento di Fisica e Scienze della Terra "Macedonio Melloni", Università di Parma, Italy

[2] Pole Pluridisciplinaire de la Matière et de l'Environnement, Université de la Nouvelle Caledonie, Nouméa, New Caledonia

[3] Dipartimento di Chimica, Università di Torino, Italy

Corresponding email: mario.tribaudino@unipr.it

Keywords: asbestos, laterite-saprolite, New Caledonia

The New Caledonia is covered by ultrabasic units for more than a third of its surface, and it is one of the largest world producers of nickel ore which is formed by the alteration of ultramafic rocks. Mining activity, focused on nickel extraction from lateritic ore deposits, must deal with the natural occurrence of asbestos and fibrous minerals. Almost all outcrops of geological units and open mines contain serpentine and amphibole, also as asbestos varieties (Lahondère, 2007).

Owing to humid tropical to sub-tropical conditions, weathering processes and supergene mineralization are the main responsible for fibrogenesis and (neo)formation of asbestos minerals. In fact, spheroidal weathering is a common characteristic of nickel deposits in New Caledonia, where saprolite consists of millimetre- to decimetre-scale blocks, and the intensity of weathering increase from core to the edge. Ni-rich altered serpentines and Fe-oxyhydroxides are the main host minerals (Butt & Cluzel, 2013).

In order to better evaluate the nature and the quantity of these fibrous minerals in the ore deposits, a preliminary characterization of saprolitic and lateritic soils was carried out by X-ray diffraction (XRD) and secondary electron microscopy (SEM). Four soils samples have been analyzed; three of them contain antigorite and/or lizardite varieties, only in one sample serpentine varieties appear in the form of fibers. The saprolite portion shows an homogeneous mineral composition, consisting in quartz, talc and serpentine minerals. On the contrary, the above laterite has a more complex mineral association dominated by Fe-oxyhydroxides, mainly goethite, with subordinate gibbsite, or by a wide variety of Ni-rich hydrous Mg-silicate, such as serpentine, talc, chlorite and smectites.

Moreover, the results of a detailed mineralogical and petrological analysis will be presented on about fifty asbestos samples of serpentine, principally chrysotile and fibrous antigorite varieties, and tremolite, coming from the New Caledonia units. These fibers show different degrees of alteration resulting from the environment conditions. Data obtained with the more traditional analytical techniques - such as optical microscopy, XRD, SEM-EDS, and TEM - will be supported by the employment of more specialized tools as phase contrast microscopy (PCM), Raman spectroscopy, and thermal analysis (DTA).

Finally, these data will be integrated with toxicological analyzes performed on the most representative mineral fibers. Actually, toxicity of fibrous antigorite is still debated; it is considered as asbestos only in New Caledonia and in few other countries.

Butt, C.R. & Cluzel, D. (2013): Nickel laterite ore deposits: weathered serpentinites. *Elements*, **9**, 123-128.

Lahondère, D. (2007): L'amiante environnemental en Nouvelle Calédonie: Expertise géologique des zones amiantifères. Evaluation des actions engagées. BRGM/RP-55894-FR, 55 p.

DISSOLUTION OF MINERAL FIBRES IN CONTACT WITH SIMULATED LUNG FLUID SOLUTIONS

Pollastri S.*[1], Gualtieri A.F.[1], Bursi Gandolfi N.[1], Lassinantti Gualtieri M.[2] & Gherardini D.[1]
[1] Dipartimento di Scienze Chiniche e Geologiche, Università di Modena e Reggio Emilia, Modena, Italy
[2] Dipartimento di Ingegneria "Enzo Ferrari", Università di Modena e Reggio Emilia, Modena, Italy
Corresponding email: simone.pollastri@unimore.it

Keywords: mineral fibres, dissolution, kinetics

Hazardous mineral fibres are the subject of intensive bio-chemical, toxicological and mineralogical investigations worldwide because the cause-effect relationship between exposure to the fibres and the onset lung diseases remain poorly understood. The difficulties arise from the fact that mineral fibres have great chemical variability and molecular arrangements. In addition, fibre size, surface reactivity, biopersistence and iron oxidation state and its coordination number are crucial factors that play a key role on the biogeochemical reactions and mechanisms of cyto- and geno-toxicity should be better defined (Fubini & Mollo, 1995; Hardy & Aust, 1995; Donaldson et al., 2010). For this reasons, the chemical environment of iron in mineral fibres and their surface reactivity has been recently investigated in a systematic way (Pollastri et al. 2014, 2015). As a natural follow up of these works, it is of crucial importance to assess the actual biodurability of mineral fibres. To this aim, representative samples of chrysotile (UICC, Canada; Balangero and Val Malenco, Italy), amphiboles (amosite UICC, anthophyllite UICC, crocidolite UICC and tremolite from Val d'Ala, Italy) and fibrous zeolites (erionite from Jersey, Nevada, USA) have been studied to determine their biodurability *in vitro*. It is important to underline the fact that the innovative aspect of this work is represented by the systematic approach used, since this topic has already been the subject of many studies, which, however, were almost always focused only on specific cases but never following a systematic and standardized protocol. All the experiments were performed in contact with simulated lung fluid (SLF) solutions at acidic *p*H and at 37°C, in order to replicate the chemical environment present within phagolysosomes (intracytoplasmic vacuoles which are formed when a eukaryotic cell incorporates foreign material). The dissolution process was followed by monitoring the weight loss and the amount of crystalline residue with contact time in the organic solution. Both X-ray powder diffraction and scanning electron microscopy (SEM) were used to assess the advancement of the dissolution reaction. The obtained results confirm that chrysotiles have a low biodurability compared to amphiboles and zeolites, with dissolution times in the order of 6 months. A new mathematical model was specifically developed to draw comparable dissolution curves independent of physical parameters such as specific surface. Nevertheless, unexpected differences were observed for the three samples of chrysotile. These differences, which cannot be attributed to the chemical composition, could be related to the different microstructure of the fibres and especially their rolling mode. In fact, chrysotile UICC has a spiral rolling (Yada, 1971) whereas other chrysotiles as that of Balangero possess a concentric cylindrical configuration *sensu stricto* (Mellini, 1987) that is supposed to be more resistant to dissolution.

Donaldson, K., Murphy, F.A., Duffin, R., Poland, C.A. (2010): Asbestos, carbon nanotubes and the pleural mesothelium: a review of the hypothesis regarding the role of long fibre retention in the parietal pleura, inflammation and mesothelioma. *Part. Fibre Toxicol.*, **7**, 1.

Fubini, B. & Mollo, L. (1995): Role of iron in the reactivity of mineral fibers. *Toxicol. Letters*, **82**, 951-960.

Hardy, J.A. & Aust, A.E. (1995): Iron in asbestos chemistry and carcinogenicity. *Chem. Rev.*, **95**, 97-118.

Mellini, M. (1986): Chrysotile and polygonal serpentine from the Balangero serpentinite. *Mineral. Mag.*, **50**, 301-306.

Pollastri, S., Gualtieri, A.F., Lassinantti Gualtieri, M., Hanuskova, M., Cavallo, A., Gaudino, G. (2014): The zeta potential of mineral fibres. *J. Hazard. Mater.*, **276**, 469-479.

Pollastri, S., D'Acapito, F., Trapananti, A., Colantoni, I., Andreozzi, G.B., Gualtieri, A.F. (2015): The chemical environment of iron in mineral fibres. A combined X-ray absorption and Mössbauer spectroscopic study. *J. Hazard. Mater.*, **298**, 282-293.

Yada, K. (1971): Study of microstructure of chrysotile asbestos by high-resolution electron microscopy. *Acta Crystallogr.*, **A27**, 659-664.

MINERALOGICAL ASSESSMENT OF ABANDONED ASBESTOS MINE SITES ALONG THE ORANGE RIVER IN THE KOEGAS AREA, NORTHERN CAPE PROVINCE OF SOUTH AFRICA

Rasmeni S.K.*[1], Ball M.[1] & Negota N.[1]
[1] Mineralogy Division, Mintek, Randburg, South Africa
Corresponding email: Sonwabiler@mintek.co.za

Keywords: asbestos, rehabilitation, Koegas

Asbestos is a naturally-occurring hydrated fibrous silicate mineral of magnesium, iron, sodium, calcium and aluminium, which was formerly widely used in many industries due to its unique properties. It is classified in two mineralogical groups: serpentine group (that includes chrysotile) and amphibole group (that includes crocidolite, amosite, actinolite, anthophyllite and tremolite). Asbestos minerals are considered fibrous (asbestiform) if they contain fibres with the mean aspect ratios of 20:1 or higher. The large scale mining operation in the Koegas area began in the 1890s and continued until its closure in the 1970s. Due to the health risk associated with asbestos exposure, this area was subsequently partially rehabilitated, with the efforts presumably focused on minimising the exposure levels rather than eliminating them. After the banning of the asbestos mining activities, the majority of mines were left derelict and ownerless. The Department of Mineral Resources (DMR) in South Africa has undertaken a project, termed Derelict and Ownerless (D&O) mine rehabilitation as a way of redressing the negative impacts caused by asbestos mining to the environment and communities. Areas that pose immediate danger to the communities through environmental contamination receive priority for rehabilitation.

The study is aimed at investigating the extent of asbestos dispersion around the affected sites with the particular focus on prevailing wind directions for the planned rehabilitation programme. Mining was mainly undertaken on steeply dipping (of 55 to 80 degrees) terrain with some tailing dumps located at about 50 m from the Orange River (the main source of water to the semi-arid Northern Cape Province). Forty-three dry soil samples were collected across the Koegas site and subjected to X-ray diffraction, scanning electron microscopy and optical microscopy. The mineralogical analyses are aimed at determining the bulk mineralogy and the morphology of each asbestos fibre (based on the aspect ratio). Various quantities of crocidolite fibres with the aspect ratio from 52:1 to 251:1 were detected in most of the samples collected around the tailing dumps, the river bank and its tributaries/or streams. Although mining activities in the Koegas area may have ceased many years ago and the area was partially rehabilitated, there is constant environmental contamination, particularly along the Orange River. The results show that tailings dumps located approximately 3 km from the Orange River are mainly contaminated through drainage discharge via the main river tributary or stream. Due to the proximity and higher elevation of the tailing dumps, the asbestos fibre dispersion can be attributed to both drainage discharge and wind action. Therefore, the Koegas area will be prioritized for rehabilitation, as it poses an immediate danger to local communities and downstream areas along the Orange River.

CHARACTERIZATION OF TALC ORE AND WASTE ROCK FROM THE UPPER DORA-MAIRA MASSIF IN THE RODERETTO MINE

Sanchez M.S.*[1]
[1] RJ Lee Group Inc., Monroeville, PA, USA
Corresponding email: msanchez@rjlg.com

Keywords: talc, amphibole, asbestos

Recent allegations of trace level asbestos contamination of cosmetic grade talcum powders in the United States has given rise to increasing consumer concern regarding the widespread use of talc in both cosmetic and pharmaceutical products. The source of some of these are from talc deposits occurring as talc schists and are hosted in the upper crystalline units of the Dora-Maira Massif in Val Gemanasca.

These talcs have been described as “high quality cosmetic grade” by Sandrone & Zucchetti (1988). With the ever-increasing concern towards the use of geologically derived material and their effects on human health this paper addresses further characterization of these ores specific to trace asbestos contamination.

Seventeen (17) samples that represent both talc ore and waste rock were characterized by PLM, XRD, and XRF. Further analysis was conducted employing TEM with EDS and SAED capability. The primary secondary minerals associated with the talc schist are chlorite, calcite and dolomite. Within the talc schist also occur both siliceous and calcareous lenticular lenses where additional minerals such as epidote, rutile, and calcic amphiboles are observed. During the mining operation these pods represent non-talc ore and are removed through beneficiation. No serpentine minerals were observed in the talc schist or lenticular pods, furthermore TEM analysis of these samples found no chrysotile.

Monoclinic amphiboles were observed in the lenticular pods and were further characterized and were determined to be tremolite by EPMA. The occurrence of these tremolites are observable in hand sample and are millimeter sized euhedral crystals. These euhedral tremolites occur both as iso-linear and radial crystals in the plane of the schistose textures. This structural control on crystal orientation further supports that the talc and tremolite formation was cogenetic. In a few instances there is partial replacement of the tremolite by talc thus limited retrograde metamorphism has occurred. No orthorhombic amphiboles were observed. These findings are consistent with the reported literature regarding these important and widespread used deposits.

Sandrone, R. & Zucchetti, S. (1988): Geology of the Italian high-quality cosmetic talc from the Pinerolo district (Western Alps). Zuffar Days – Symposium, Cagliari, 105-113.

SPECIATION AND BIOACCESSIBILITY OF ARSENIC AT THE BAKYRCHIK GOLD MINE, KAZAKHSTAN

Seitkan A.*[1] & Redfern S.A.T.[1]
[1] Department of Earth Sciences, University of Cambridge, United Kingdom
Corresponding email: as2154@cam.ac.uk

Keywords: arsenic, waste, speciation

The Bakyrchik native gold deposit is the largest in Kazakhstan and one of the largest in the world. Gold mining is based on extraction from arsenopyrite and pyrite. Despite the fact that only 10% of the gold ore has been mined to date, it has left behind a dangerous arsenic-containing legacy. Speciation of arsenic (As) in Bakyrchik water bodies (Seitkan & Redfern, 2015) revealed mobility of As, and identified the need for understanding the speciation of As in environmental reservoirs such as sediments, soil, ore, rock and waste material, to shed light on the questions behind the sources of As in water.

Bakyrchik ore, pit-wall rock, tailings, and As-rich residue have been studied by powder X-ray diffraction and electron microprobe analysis. Ore and tailings contained FeAsS, As-bearing FeS_2, as well as their alteration products, comprising Ca, Mg, Zn, Cu, and Al-containing oxidised phases with a wide variation of As (up to 25%). Fe oxides and oxyhydroxides with up to 2.5% As have also been detected. As_2O_3, $Ca_3(AsO_4)_2 \cdot 10H_2O$, $CaAsO_3OH \cdot H_2O$, $Ca_3(AsO_4)_2$ were identified in the As-rich residue. The pit wall rock showed abundance of carbonates and goethite.

Sequential extraction (Larios, 2013) showed that As is mainly associated with Al and amorphous Fe oxyhydroxides in surface water sediments. In oxide waste rocks more than 90% of the As is bound to Al oxyhydroxides, whereas in the sulfidic waste rock As is mainly associated with the refractory fraction. In sediments from the tailings pond As mostly incorporated into refractory minerals. As fractionation in the bottom and surface layers of the exposed tailings followed the similar pattern, with the exception of As associated with poorly crystalline Fe phases found in surface samples. In soil taken far from the mine, As was mainly associated with the organic fraction. In soil close to the mine, As is mostly bound to Al oxyhydroxides and refractory minerals. The main mechanism controlling As mobility at the Bakyrchik is adsorption onto Fe and Al oxy(hydroxides), and co-precipitation of dissolved As with alteration products of sulfide minerals.

The mobility of As can result in subsequent bioavailability and toxicity. We assessed the potential bioaccessibility of As through inhalation by conducting a leaching test using simulated phagolysosomal fluid (PSF) (Stefaniak et al., 2005). The bioaccessibility factor (BF) of As in the <10 μm fraction of samples ranged from 1.23 to 76.83%. This suggests that As bioaccessibility through inhalation is strongly dependent on the mineralogy of As rather than on total As content of the samples. The BF, derived from the PSF test, was used to assess cancer and non-cancer risks through inhalation (Kim et al., 2014). Calculations indicate that all the studied samples are highly hazardous if inhaled, posing significant cancer and non-cancer risks for human health.

Kim, C., Anthony, T., Goldstein, D., Rytuba, J. (2014): Windborne transport and surface enrichment of arsenic in semi-arid mining regions: Examples from the Mojave Desert, California. *Aeolian Res.*, **14**, 85-96.

Larios, R., Fernandez-Martinez, R., Rucandio, I. (2013): Assessment of a sequential extraction procedure for arsenic partitioning and application to samples from different pollution sources. *Anal. Methods*, **5**, 4096-4104.

Seitkan, A. & Redfern, S. (2015): Speciation and distribution of arsenic in water at Bakyrchik Gold Mine, Kazakhstan. In: Goldschmidt Conference 2015, 16-21.08.2015, Prague, Czech Republic.

Stefaniak, A., Guilmette, R., Day, G., Hoover, M., Breysse, P., Scripsick, R. (2005): Characterization of phagolysosomal simulant fluid for study of beryllium aerosol particle dissolution. *Toxicol. in Vitro*, **19**,123-134.

HISTORICAL AND FUTURE ROLE OF HR-TEM AND AR-TEM IN MEDICAL MINERALOGY

Vigliaturo R.*[1], Dražić G.[2] & Petruccione F.[1]
[1] School of Chemistry and Physics, University of KwaZulu-Natal, Durban, South Africa
[2] National Institute of Chemistry, Ljubljana, Slovenia
Corresponding email: ruggero.vigliaturo@gmail.com

Keywords: High Resolution Transmission Electron Microscopy, structure transformation

Health concerns on mineral fibers that are able to induce fibrosis, lung cancer and mesothelioma represent an important topic in medicine and involve several disciplines. Furthermore, they are motivation for a safe nanotechnological development.

The comprehension of these mechanisms goes beyond the simple fiber-like morphology of these materials.

Reactive oxygen species generation mediated by surface properties as defects or metal cations presence is an example of the need to extend consideration about health consequences to a more complex features pattern.

Mineral particles can be considered as a “living system” able to interact with a biological environment in multiple ways and as a heterogeneous population, with various and variable characteristics.

The scientific interest in this field is now moving more to the interaction between mineral-cell interface and exploring transformation that occurs in fibers, the role of HRTEM can become much more pivotal to investigate mineral phases transformation and punctually shed light on fundamental aspects. This is feasible if HRTEM studies are preliminarly supported by strong analytical evidence from other instruments.

Starting from Kühn’s picture of chrysotile bundles to high resolution micrograph of Yada, TEM played an important role in the structure comprehension of these minerals and it has then been used to describe fibers tranformation after complex interaction with the biological material.

With the access to new tools and equipment TEM can greatly contribute to the modeling of interaction processes. Cryo-HRTEM which has not been largely involved in the study of mineral fibers has already demonstrated, for example, that it is possible to visualize the electron beam-sensitive cage structure of erionite after the interaction with the human body. This confirms, together with the chemical analysis, the “sponge-like” behaviour and tetrahedral framework stability of this mineral phase.

Involving more widely spherical aberration corrected AR-STEM combined with EELS, atomic resolution transformations can be visualized, as well as the oxidation state of metals within fibers and cells that play a fundamental role in the reactive oxigen species reaction chain.

With this instrument it is possible to completely describe the structure of fibers and nanoparticles, crystal boundaries, two dimensional defects, etc. Using tomography, where images at different tilting angles are recorded, it is possible to reconstruct the 3D shape of fibres or macromolecules involved in the interaction process.

MAGNETIC COMPONENTS IN SOILS AS A RECORD OF ANTHROPOGENIC IMPACT

Wilczyńska-Michalik W.*[1], Zimirska A.[1], Dietrich A.[2], Maszloch E.[2] & Michalik M.[2]
[1] Institute of Geography, Pedagogical University of Kraków, Poland
[2] Institute of Geological Sciences, Jagiellonian University, Kraków, Poland
Corresponding email: wanda.michalik@post.pl

Keywords: antropogenic components in soil, magnetic particles, Anthropocene

Our study is focused on the identification of anthropogenic components in soils in southern Poland. Soil profiles subjected to deposition of airborne particles were selected, i.e. devoid of direct influx of anthropogenic material (e.g., sites near industrial waste disposal places). Particulate matter (PM) in air in southern Poland, related to numerous sources (household coal and wood burning, vehicular emission, industrial plants, soil erosion and resuspension), is composed of soot, silicate and aluminosilicate particles, metallic or metal oxide particles, sulphates, chlorides. Clear recognition of PM sources is often problematic.

In the magnetic fraction extracted from soil samples (hand magnet separation) from two depth levels (0-10 and 30-40 cm) from eight localizations it was possible to identify anthropogenic particles – Fe metallic or Fe oxide spheres or porous slag particles containing metallic inclusions using SEM-EDS method. Metallic spheres (up to 30 mm in size) of various internal structures originate from iron metallurgy plant or from coal fired power plants. Anthropogenic magnetic fraction was identified in samples from both depths in sites in urban area, in close vicinity of towns as well as situated relatively far from industrial plants (ca 40 km) what indicate long distance airborne transportation of coarse and high density particles.

Because soot particles are the most numerous in polluted air we tried also to identify them in soils. In demineralized samples it was possible to notice particles similar to soot particles but precise identification is ambiguous.

We can consider the easily distinguishable anthropogenic particles in the magnetic fraction of soils as useful marker of the post-second World War rapid industrialization, i.e. so-called “Great Acceleration” considered often as the beginning of the Anthropocene.

Session S27:

Mineral sciences for the understanding of cultural heritage

Conveners:

Gilberto Artioli (Padova – Italy)

Corina Ionescu (Cluj-Napoca – Romania)

Sabine Klein (Frankfurt am Main – Germany)

PORFIDO ROSSO ANTICO – THE IMPERIAL DIMENSION STONE FROM THE EASTERN DESERT OF EGYPT

Abu El-Enen M.M.[1], Lorenz J.[2], Okrusch M.*[2], Kamal A.A.[3], von Seckendorff V.[2], Schüssler U.[2], Brätz H.[4] & Schmitt R.-T.[5]

[1] Department of Geology, El Mansoura University, Egypt
[2] Institut für Geographie und Geologie, Universität Würzburg, Germany
[3] Department of Mineral Resources and Rocks, King Abdulaziz University, Jeddah, Saudi Arabia
[4] GeoZentrum Nordbayern, Universität Erlangen-Nürnberg, Erlangen, Germany
[5] Museum für Naturkunde, Berlin, Germany
Corresponding email: okrusch@uni-wuerzburg.de

Keywords: porfido rosso antico, imperial porphyry, Dokhan subvolcanics

Porfido rosso antico, a famous dimension stone of spectacular purple colour, also known as *Imperial Porphyry*, was quarried in the Mons Porphyrites area north of Jabal Dokhan in the Eastern Desert of Egypt, from the beginning of the first century AD until the middle of the fifth century AD. During this period, the valuable material was processed as decorative stone and used for objects of art, reserved exclusively for the Imperial court of the Roman Empire. After closure of the quarries, only antique spoils of smaller or bigger size have been re-used for these purposes.

Based on field work in each of the Roman quarries and the adjacent valleys, we performed petrological, geochemical and geochronological investigations on rock types that form a subvolcanic intrusion within the Dokhan Volcanic Suite. The predominant rock, best exposed in Wadi Umm Sidri and Wadi Abu Ma'amel, is porphyritic with phenocrysts of plagioclase and amphibole in a matrix of dark greenish gray color. Fissures filled with epidote are frequently present. The sub-volcanic rocks are intruded by, and form xenoliths in, younger (quartz-)syenite that, in turn, is intruded by mafic and acidic dikes. Due to hydrothermal activity, the plutonic and sub-volcanic rocks have been subjected, along fissures, to alteration in deep red colours, whereas younger dikes remained unaffected. Due to hydrothermal overprint, the dark-greenish sub-volcanites were transformed into the*Imperial Porphyry* type, extensively exposed in the Roman quarries, which are situated in the mountain ranges above Wadi Abu Ma'amel. This rock type is distinguished, from the common type of the sub-volcanite, by the famous purplish-gray colour of its matrix that is mainly due to dispersed flakes of haematite. Plagioclase phenocrysts are white or pale pink in colour. The contacts between dark green and red rock types are irregular and gradational, the width of the transition zone ranging from a few centimetres to several metres. Brecciated varieties of Imperial Porphyry, best exposed in the Lepsius Quarries, were especially estimated for manufacturing fine works of art.

We performed XRF analyses of major and trace elements on 17 + 13 samples of common and Imperial Porphyry type, respectively, and LA-ICP-MS analyses of additional trace elements on 10 + 10 samples. In the TAS diagram (Na_2O+K_2O) *vs.* SiO_2, most of the samples analysed plot into the fields of trachyandesite, andesite and dacite. Most, though not all, of the dark-green coloured sub-volcanics are dacitic in composition whereas most data points of the Imperial Porphyry plot in the trachyandesite field or straddle the border with the dacite field. The TAS classification is essentially confirmed e.g. by the diagram (Zr/TiO_2) vs. (Nb/Y). In the MORB-normalized variation diagrams, the Dokhan lavas display positive anomalies of Rb, Ba, K, Th, U, Pb, Al and Ga, and negative anomalies for Ta, Nb, Ti and V. The chondrite-normalized REE-patterns are nearly identical for most of the samples with enrichment factors decreasing from La_N (range 92.85-64.24) to Ho_N (9.08-6.43) and showing very similar values from Er_N (8.34-5.85) to Lu_N (7.25 to 5.56). Confirming earlier published results, we obtained a U-Pb concordia age of 608±6 Ma on zircons from a dark-green trachydacite and similar ages of 600±2.4 Ma and 609±4 Ma on zircons from two Imperial Porphyry samples. The geochemical characteristics of our samples indicate a post-collisional igneous activity within an extensional, basin-and-range type setting, a model proposed already by Stern et al. (1984)

Stern, R.J., Gottfried, D., Hedge, C.E. (1984): Late Precambrian rifting and crustal evolution in the Northeastern Desert of Egypt. *Geology*, **12**, 168-172.

RADIOCARBON DATING OF HISTORICAL AND ARCHAEOLOGICAL MORTARS: TASK IMPOSSIBLE?

Addis A.[1-2], Artioli G.*[1-3], Marzaioli F.[4-5], Passariello I.[5], Preto N.[3], Secco M.[1-6], Terrasi F.[4-5] & Zorzi F.[3]

[1] Centro Interdipartimentale di Ricerca per lo Studio dei Materiali Cementizi e dei Leganti Idraulici, Università di Padova, Italy

[2] Dipartimento dei Beni Culturali: archeologia, storia dell'arte, del cinema e della musica, Università di Padova, Italy

[3] Dipartimento di Geoscienze, Università di Padova, Italy

[4] Dipartimento di Matematica e Fisica, Seconda Università di Napoli, Italy

[5] Centro di Ricerche Isotopiche per i Beni Culturali e Ambientali, Seconda Università di Napoli, Italy

[6] Dipartimento Ingegneria Civile, Edile ed Ambientale, Università di Padova, Italy

Corresponding email: gilberto.artioli@unipd.it

Keywords: lime mortars, radiocarbon dating, AMS ^{14}C

Radiocarbon dating of lime-based mortars was conceptually and experimentally introduced over 50 years ago. The principle is rather simple: lime-based mortars and plasters were and are produced through the carbonation of the slaked lime, and are thus absorbing atmospheric CO_2 during the process of portlandite carbonation. In principle the process takes place rather quickly after the placement of the binder in or on the architectural component. The binder therefore should incorporate the carbon signature of the atmosphere at the time of preparation, and it represent a viable material for radiocarbon dating the architectural structures. However, despite the conceptual simplicity of the method, in practice the application of radiocarbon dating meets with a number of practical difficulties, mainly due to the mineralogical and chemical complexity of the real systems. First of all the carbonate present in the sample may be contaminated by geological carbonate. Even minute quantities of geologically old calcite can produce large errors in the resulting dates. Furthermore the carbonation process after the emplacement may not be so rapid, so that the obtained dates are from calcite produced quite some time after the production. This is often experimentally verified for the so-called "lime lumps". Else there might be subsequent "younger" generations of calcite or CO_2-containing minerals such as hydrotalcite contaminating the original carbonate, due to percolating water, or delayed pozzolanic reactions. The real problem therefore lies in the careful extraction, separation, characterization, and processing of the carbonate fraction in the matrix that correspond to the carbonation of the "original" lime putty of the binder.

The results will be presented on "easy" and "difficult" mortar dating cases. The crucial role of the multi-technique experimental characterization of the carbonate fractions extracted from ancient mortars will be emphasised, because it is fundamental to understand the nature and history of the carbonate fraction to be dated by AMS protocols. The characterization techniques include XRPD, stable C-O isotopes, and cathodoluminescence spectroscopy. The developed methods for separation and characterization of binder fractions have been successfully tested on archaeological mortars of different nature and age.

ARCHAEOMETRIC ANALYSIS OF MOSAIC TESSERAE AND A "RED MARBLE" DECORATIVE STONE FROM THE BIZERE MONASTERY (ARAD COUNTY, WESTERN ROMANIA)

Bajnóczi B.[1], Györkös D.*[1], Mozgai V.[1], Szabó M.[1], Tóth M.[1] & Burnichioiu I.[2]
[1] Institute for Geological and Geochemical Research, Research Centre for Astronomy and Earth Sciences, Hungarian Academy of Sciences, Budapest, Hungary
[2] Faculty of History and Philology, University "1 Decembrie 1918", Alba Iulia, Romania
Corresponding email: dorkagyorkos@gmail.com

Keywords: mosaic tesserae, red marble, Bizere monastery

The Medieval Bizere monastery is situated 15 kms from Arad (Western Romania), south of the valley of River Mureș, on the territory of Frumușeni village. It was founded around the year 1100, and disappeared after the 16th Century. A large variety of building and decorative materials, including masonry blocks, bricks and mosaic tesserae, were discovered during the archaeological excavation of the monastery. Most of the mosaic tesserae were found to be dispersed, however, two surfaces of pavement mosaic, belonging to the basilica of the abbey, were found *in situ* (Burnichioiu & Rusu, 2006, 2011). In order to assess the material usage for decorative elements, several dispersed mosaic tesserae made of rocks and ceramics and a 'red marble' decorative stone were studied by means of optical and cathodoluminescence microscopy, X-ray diffraction, electron microprobe and stable isotope analyses. Based on the mineralogical, petrographic and geochemical characteristics the probable sources (provenance) for the rocks are suggested, whereas the firing conditions (temperature) of the ceramics are established.

Most of the studied tesserae consist of metamorphic rocks such as white marble, quartzite, greenschist, hornfels and "serpentine marble" (ophicalcite). Magmatic rocks (basalt) and sedimentary rocks (sandstone, limestone and breccia) were also identified.

Based on the geology of the region we can assume that most of the rocks have local source in the nearby Southern Apuseni or the Poiana Rusca Mountains. For example, basalt may originate from the Jurassic ophiolitic sequence cropping out in several quarries in the Southern Apuseni Mountains. A potential source of sandstones (quartzarenite and quartz-rich arkose) may be the Upper Cretaceous Gosau succession of the same mountains. Moreover, the Mureș Valley, that is the alluvial pebbles of River Mureș, can be also a possible source for rocks. Some of the white marbles with heteroblastic and cataclastic/mortar texture most probably originate from the Southern Carpathians (Bucova/Zeicani). The possible local or distant source of some white marble mosaics and other unique tesserae made of "serpentine marble" and black-and-white breccia are still to be identified.

The "red marble" decorative stone found at the Bizere site is a bioclastic nodular limestone containing a large amount of Middle Jurassic *Bositra* shell fragments. Although a "red marble" deposit exists in the Apuseni Mountains (at Menyháza/Moneasa), the petrographic and stable isotope characteristics of the studied stone point to a relatively distant source, the Gerecse Mountains in Hungary.

The ceramics studied are diverse in appearance including grey, red and sandwich-structured mosaic tesserae and a red brick. All but one was made from clay intentionally tempered with sand, most probably from the River Mureș. The phase composition of the ceramics suggests a firing temperature of ≤ 650-700°C.

Burnichioiu, I. & Rusu, A.A. (2006): The medieval mosaics from Bizere. Mega, Cluj-Napoca, 55 p. (in Romanian).
Burnichioiu, I. & Rusu, A.A. (2011): Medieval floor mosaics at Bizere Monastery. A brief survey. *Transylvan. Rev.*, **20**, 3-13.

TECHNOLOGICAL STUDIES OF HISTORICAL GLAZES WITH THE USE OF RIGAKU D/MAX RAPID II MICRO-XRD

Bajnóczi B.*[1], Szabó M.[1] & Tóth M.[1]

[1] Institute for Geological and Geochemical Research, Research Centre for Astronomy and Earth Sciences, Hungarian Academy of Sciences, Budapest, Hungary

Corresponding email: bajnoczi@geochem.hu

Keywords: glaze, glass, micro-XRD

Reconstruction of the production technology of historical glazes implies determination of the raw material used including the colouring compounds and opacifying pigments and their preparation and conditions of firing (temperature and atmosphere of the furnace, number of firings).

Crystalline compounds (inclusions), such as unreacted grains and the ones that newly develop during firing (and subsequent cooling) partly due to the reaction between the melt and the ceramic body, are important clues in the reconstruction of the technology and the raw material used. Scanning electron microscopy or electron microprobe analysis is the basic tool to determine the chemical composition of the vitreous groundmass as well as the morphology, size and distribution of the crystalline compounds and their chemical composition using polished cross-sections. The identification of the crystalline compounds using the SEM or electron microprobe techniques is sometimes not straightforward due to the small size of the crystallites, therefore other techniques like Raman microspectroscopy and conventional X-ray diffraction analysis are usually applied.

The micro-X-ray diffraction technique with its high brilliance and low probe size/divergence is an ideal method to analyse the crystalline compounds *in situ* with spot size of tens of μm or even in 10 μm range using the same polished cross-section prepared for SEM or electron microprobe analysis. Synchrotron Radiation micro-X-ray diffraction (SR-μXRD) was used in several studies to identify the crystalline compounds in vitreous materials (glazes, glasses and frits, e.g., Pradell et al., 2010; 2013; Molera et al., 2013; Iñañez et al., 2013, Molina et al., 2014). However, SR-μXRD is not always a cost-effective technique, therefore laboratory micro-XRD instruments provide good alternatives (e.g., Gradmann et al., 2015). In this study a Rigaku D/Max Rapid II micro-X-ray diffractometer was used to analyse crystalline inclusions in glazes and other vitreous materials.

One of the case studies to be presented is the blue glaze of the Anabaptist (Hutterite-Haban) ceramics produced in Eastern-Central Europe in the 16th and 17th Centuries. In addition to the variable amount of tin oxide particles the blue glaze also contains lead-calcium or calcium-lead arsenate crystallites most frequently in the form of needles preferentially deposited inside pores and at the ceramic-glaze interface. The arsenic content of the cobalt pigment used to produce the blue glaze is separated from the cobalt and precipitates as newly-formed arsenate crystals in the vitreous matrix. Micro-XRD analysis indicates that the arsenate is an apatite group mineral, hedyphane.

Gradmann, R., Berthold, C., Schüssler, U. (2015): Composition and colouring agents of historical Islamic glazes measured with EPMA and μ-XRD2. *Eur. J. Mineral.*, **27**, 325-335.

Iñañez, J.G:, Madrid-Fernández, M., Molera, J., Speakman, R.J., Pradell, T. (2013): Potters and pigments: preliminary technological assessment of pigment recipes of American majolica by synchrotron radiation micro-X-ray diffraction (Sr-μXRD). *J. Arch. Sci.*, **40**, 1408-1415.

Molera, J., Coll, J., Labrador, A., Pradell, T. (2013): Manganese brown decorations in 10th to 18th century Spanish tin glazed ceramics. *Appl. Clay Sci.*, **82**, 86-90.

Molina G., Odin, G. P., Pradell, T., Shortland, A.J., Tite, M.S. (2014): Production technology and replication of lead antimonate yellow glass from New Kingdom Egypt and the Roman Empire. *J. Arch. Sci.*, **41**, 171-184.

Pradell, T., Molera, J., Salvadó, N., Labrador, A. (2010): Synchrotron radiation micro-XRD in the study of glaze technology. *Appl. Phys.*, **A99**, 407-417.

Pradell, T., Molina, G., Molera, J., Pla, J., Labrador, A. (2013): The use of micro-XRD for the study of glaze color decorations. *Appl. Phys.*, **A111**, 121-127.

POTTERY PRODUCTION OF THE PITTORE DI LIPARI: CHEMICAL AND MINERALOGICAL ANALYSIS OF THE PIGMENTS

Barone G.[1], Di Bella M.[2], Mastelloni M.A.*[3], Mazzoleni P.[1], Quartieri S.[2], Raneri S.[1], Sabatino G.[2] & Vailati C.[4]

[1] Dipartimento di Scienze Biologiche, Geologiche e Ambientali, Università di Catania, Italy

[2] Dipartimento di Scienze Matematiche e Informatiche, Scienze Fisiche e Scienze della Terra, Università di Messina, Italy

[3] Museo Archeologico Regionale "L. Bernabo Brea", Lipari (ME), Italy

[4] Bruker, Milano, Italy

Corresponding email: mariaamalia.mastelloni@regione.sicilia.it

Keywords: potteries, pigments, Lipari

One of the most impressive Sicilian pottery production is attributed to the so-called Pittore di Lipari, famous for his numerous vessels – found in the archaeological site of Lipari (Eolian Island – Sicily) – decorated with characteristic blue, red and white figures.

From the archaeological point of view, these vessels keep open many questions concerning dating, production technique and cultural background. The chronology proposed by Trendall (Trendall, 1967) – who dated these potteries to the last quarter of the IV B.C. – is questioned on the basis of field observations by Bernabo Brea and Cavalier, who suggest a more recent production (Cavalier, 1976). In this context, new data on the manufacture techniques and on the raw materials used for the pigments may contribute to a deeper comprehension (Mastelloni, 2015; Quartieri et al., 2015).

The importance of the vessels, exposed in the Archaeological Museum of Lipari, imposed the use of non-destructive and *in situ* methods. Specifically, here we present the results of the mineralogical analysis performed by portable Raman spectroscopy (I- Raman Plus - BWTECH) and the chemical data obtained by a portable XRF (Titan System - Bruker).

The results of this study testify the use of a series of different pigments. Among these, only the white one is made by kaolin and gypsum, suggesting the use of a local supply. The blue portions are probably made by Egyptian blue, while two types of pigments were employed for red colors: ochre for the brown-reddish hues and cinnabar for the red purple nuance. The latter one is reported for the first time in the decoration of pottery, while its use is known in Sicilian and Roman wall paintings. Interestingly, the use of cinnabar suggests commercial and cultural relationships between Lipari and the Etruria area, or, subordinately, with Spain, where this mineral was quarried on the Carthaginian and Roman Republican periods.

two types of pigments were employed for red colors: ochre for the brown reddish and cinnabar for the red purple nuance. The latter is reported for the first time in the decoration of pottery, while its use is known in Sicilian and Roman wall paintings. Interestingly, the use of cinnabar suggests commercial and cultural relationships between Lipari and the Etruria area, or, subordinately, with Spain, where this mineral was quarried on the Carthaginian and Roman Republican periods.

Cavalier, M. (1976): Nouveaux documents sur l'art du Peintre de Lipari. Centre Jean Berard, Napoli, 66 p.

Mastelloni, M.A. (2015): I Pittori di Lipari, delle tre Nikai e di Falcone: l'apporto delle analisi alla ricerca. *in* "Lipára ed il teatro in età tardo classica ed ellenistica", Palermo, 73-75.

Quartieri, S., Sabatino, G., Di Bella, M., Gianesella, M., Ardizzone, F., Mastelloni, M.A. (2015): Analisi non distruttive sui pigmenti di materiali prodotti a Lipari tra fine IV e I metà III sec. a.C. *in* "Lipára ed il teatro in età tardo classica ed ellenistica", Palermo.

Trendal, A.D. (1967): The red-figured vases of Lucania, Campania and Sicily. Clarendon, Oxford, 812 p.

EXPLORING THE COROPLASTS "*TECHNE*" IN GREEK ARCHITECTURAL TERRACOTTAS: AN ARCHAEOMETRIC APPROACH

Barone G.[1], Mazzoleni P.[1], Monterosso G.[2], Raneri S.*[1], Santostefano A.[3] & Spagnolo G.[3]
[1] Dipartimento di Scienze Biologiche, Geologiche e Ambientali, Università di Catania, Italy
[2] Museo Regionale "P. Orsi", Siracusa, Italy
[3] Dipartimento di Civiltà Antiche e Moderne, Università di Messina, Italy
Corresponding email: sraneri@unict.it

Keywords: roof revetments, coroplastic art, Sicily

Architectural terracottas represent a key element in the history of ancient Greek architecture; morphological variations, technical features and decorative motifs occur over the time, especially during the archaic period (Winter, 1993). In the western Greek colonies, different styles of roof revetment and decoration are known; among them, the so called "*Siceliote system*" and "*Selinus system*". The numerous fine architectural terracottas fragments found in the South-Eastern area of Sicily during the archeological excavations strongly suggest the existence of important local workshops. However, even if the archaeologists have extensively described this class of artifacts, the scientific debate about fabrics, raw materials supply, manufacturing technology and decoration systems is currently open. One of the most interesting problem concerns the frequent presence of coarse-grained volcanic inclusions in the ceramic paste; this feature seems to be peculiar of many Sicilian architectural terracottas, as testified by several fragments found at Gela, Siracusa and Lentini. Worth of note is that this feature is observable also in area where volcanic rocks don't outcrop suggesting that it is probably due to technological reasons. Another significant aspect regards the painted decoration technique of the revetments (i.e., firing phases, pigments, etc.; Rescigno & Sampaolo, 2005). Even if preliminary studies on some Geloan architectural terracottas specimens have provided really promising results (Barone et al., 2015), the drawing of a complete scenario on the manufacturing features of the regional Sicilian roof revetments needs further investigations.

In order to achieve this goal, we have studied numerous decorated sima and geison fragments and acroteria specimens coming from some of the most important temples of Siracusa and Lentini. Materials have been analysed from petrographic, mineralogical (XRD) and chemical (XRF) point of view. Additionally, in-deep analyses have been carried out on volcanic inclusions, taking advantages from a methodological routine based on clinopyroxenes chemical composition obtained through Scanning Electron Microscopy coupled with Energy-Dispersive Spectrometry (SEM- EDS) measurements (Barone et al., 2010). Finally, an analytical characterization of the polychrome decoration of surfaces has been obtained by performing SEM-EDS and micro-Raman spectroscopy measurements.

All the analytical data have been therefore discussed and compared with the results obtained on Geolan materials in the light of the archaeological interpretations, providing a detailed overview on the local tradition of architectural terracottas production.

Barone, G., Belfiore, C.M., Mazzoleni, P., Pezzino, A., Viccaro, M. (2010): A volcanic temper based approach for provenance studies of archaeological ceramics from Southern Italy. *J Archaeol. Sci.*, **37**, 713-726.

Barone, G., Mazzoleni, P., Raneri, S., Spagnolo, G., Santostefano, A. (2015): Coroplastic art in Sicily: an investigation on provenance and manufacturing technology of the Greek architectural terracottasfrom Gela (Italy), 13th European Meeting on Ancient Ceramics, EMAC2015, Athen, September 24-26, 2015.

Rescigno, C. & Sampaolo, V. (2005): Appunti sull'impiego del colore sulle terrecottearchitettoniche capuane. *in* "Mediterranea". Quaderni annuali dell'Istituto di studi sulle civiltà italiche e del Mediterraneo antico, Consiglio nazionale delle ricerche, **2**, 133-164.

Winter, N.A. (1993): Greek architectural terracottas - From the Prehistoric to the end of the Archaic period. Clarendon, Oxford, 360 p.

NONDESTRUCTIVE CHARACTERIZATION OF ANTIQUE OBJECTS: SYNERGY BY COUPLING X-RAY MICRODIFFRACTION, MICRO-RAMAN SPECTROSCOPY AND MICRO-X-RAY FLUORESCENCE

Berthold C.*[1], Bente K.[1] & Keuper M.[1]
[1] Fachbereich Geowissenschaften - Angewandte Mineralogie, Eberhard Karls Universität Tübingen, Germany
Corresponding email: christoph.berthold@uni-tuebingen.de

Keywords: archaeometry, X-ray diffraction, X-ray fluorescence

Nondestructive and local highly resolved analytics are strongly required characterizing antique objects in relation to raw material provenances, production technologies, abuses and fake determinations as well as to excavation and also to conservation and restoring contexts. For these purposes, archaeometrical interests are focused on combined methods analyzing both, chemical and structural properties. Such kinds of analytics are typically performed using X-ray fluorescence, X-ray diffraction and µ-Raman spectroscopy. Corresponding data should simultaneously be detected in coupled instruments being mobile and easily applicable at the same time. Until today no commercial systems are available combining these devices in one mobile system - especially for local highly resolved analysis.

In the meantime, the progress in development of air-cooled X-ray microfocus tubes as well as X-ray optics but also 2-dimensional X-ray detectors (µ-XRD2) makes these components affordable for mobile systems, thus opening completely new potentials for archaeometric purposes. Fast locally resolved phase mappings even of rough surfaces can be produced within a few minutes without any sample preparation. The integration of fibre optical µ-Raman systems and µ-XRF devices within such a µ-XRD2-setup also allows a high locally resolved, fast, nondestructive and comprehensive chemical and structural characterization of archaeological artifacts at one glance. Inorganic crystalline components and glasses can be analyzed as well as organic compounds thus opening now the field for analyzing a wide spectrum of archaeological artifacts such as ceramics, metals, glasses, and paintings.

In our contribution we will demonstrate the above mentioned advantages of a coupled µ-analysis system showing measurements on different archaeological artifacts such as neolithic to attic ceramics, natural lithic tools and medieval glasses. Additionally, perspectives in further method development will be presented.

GEMMOLOGICAL STUDY OF A RELIQUARY CROSS FROM THE LIÈGE CATHEDRAL, BELGIUM

Bruni Y.*[1], Demaude M.[1], Hatert F.[1], George P.[2] & Strivay D.[3]
[1] Laboratoire de Minéralogie, Université de Liège, Belgium
[2] Trésor de la Cathédrale Saint Paul, Liège, Belgium
[3] Département de Physique, Université de Liège, Belgium
Corresponding email: yannick.bruni@ulg.ac.be

Keywords: gemmology, reliquary cross, Belgium

In 1914, a magnificent reliquary cross was discovered in a safe from the Liège Cathedral. This double-arm cross shows a wooden structure, covered by gold-coated copper on the front, and by carved silver foils on the back. The total length of the cross is 33.5 cm, and it is covered by filigrees, gems, glasswares and pearls on its front. Relics, constituted by fragments of the Holy Cross, were originally inserted in two cavities on the back of the cross; these relics have disappeared. A detailed stylistic investigation by George (2013) showed that the cross was realized in the early XIII Century; in a first approach its style could be compared to the famous gold items realized by Hugo d'Oignies but it is not the same goldsmith's workshop. At that time, Liège was a principality of the German empire with at his head a bishop who governed also a great diocese; in the XII-XIII Centuries the region produces famous pieces of goldsmith's work, as for example the Stavelot Triptych hosted by the Morgan Library & Museum, New York. The style of these pieces of art is called "Mosan art", from the name of the Meuse River located nearby. The reliquary cross was analysed by Raman spectrometry and X-ray fluorescence spectrometry (XRF), to determine the mineralogical and chemical compositions of gems, pearls, glasswares and metals that have been used to decorate the cross. The results confirm the identification of six tiny pearls, six amethysts, twenty five turquoises and two garnets. Twelve coloured glasswares were also identified; their colours are green or blue. A small red cross, located at the centre of the reliquary, is constituted by a nice doublet with red glassware covered by quartz. The filigrees contain Cu and Au, thus confirming that they are constituted by gold-coated copper. These results will help us to confirm the age of the reliquary, and to obtain data on the gem trade during medieval times, in the Liège area.

George, P. (2013): Du prieuré d'Oignies au musée de Namur: le binôme "reliques" et "arts précieux". À propos d'une croix inédite du Trésor de la Cathédrale de Liège. *in* "Actes de la journée d'étude Hugo d'Oignies. Contexte et perspectives.", J. Toussaint, ed., TreMa, Namur, 136-151.

TECHNOLOGICAL CONSTRAINTS FOR LATE NEOLITHIC POTTERY FOUND IN THE SOUTHERN CARPATHIANS (ROMANIA)

Enea-Giurgiu A.*[1], Ionescu C.[1-2-3], Hoeck V.[1-3], Tămaș T.[1] & Roman C.[4]
[1] Department of Geology, Babeș-Bolyai University, Cluj-Napoca, Romania
[2] Archeotechnologies & Archeological Material Sciences Laboratory, Institute of International Relations, History and Oriental Studies, Kazan Federal University, Russia
[3] Department of Geography and Geology, Paris Lodron University, Austria
[4] Museum of Dacian and Roman Civilization, Deva, Romania
Corresponding email: alexandra.giurgiu@ubbonline.ubbcluj.ro

Keywords: pottery, late Neolithic, Romania

The archaeological excavations in the Great Cave of Cerișor, located in the Paleozoic crystalline limestones and dolomites of the Southern Carpathians (Romania), unveiled a complex stratigraphy, which starts in the Late Neolithic and ends in the Bronze Age.

The Late Neolithic finds were assigned to the Turdaș culture, dated between 5000 and 4600 cal. B.C. Twenty Turdaș orange potsherds were studied by optical microscopy (OM), X-ray diffraction (XRD) and electron microprobe (EMP) in order to infer the ceramic technology. Additionally, for provenance investigation, Quaternary cave sediments as well as Miocene mudstones in the area were analyzed by XRD.

Based on the optical characteristics of the matrix, two groups of sherds were distinguished: one with birefringent matrix, the other with low-birefringent to isotropic matrix. The birefringent matrix consists of clay minerals and micas. The isotropic matrix is composed of an amorphous, sometimes vitreous, material. The matrix embeds clasts of quartz, muscovite, chlorite, biotite, feldspar, opaque grains and heavy minerals. Fragments of micaschist, sandstone and quartzo-feldspathic rock, crushed older potsherds and pedogenic concretions are also present.

XRD indicates illite/muscovite, quartz, feldspars, chlorite and some hematite as main mineralogical phases in the sherds. The sherds with isotropic matrix have strongly diminished or no 10 Å illite/muscovite peaks. The Quaternary cave sediments are composed mostly of dolomite, calcite and quartz, with some muscovite/illite and chlorite. The Miocene mudstone consists of illite/muscovite, quartz, feldspars and chlorite.

A coarse matrix composed of well crystallized lamellae of illite, muscovite and rarer chlorite, reaching 100 μm in size is seen in the back-scattered electron (BSE) images. K-feldspar is ubiquitous. Pyroxene, Ti-magnetite, clinozoisite, titanite, ilmenite, apatite and zircon are the heavy minerals.

The optical features of the matrix, the variable intensity of illite/muscovite peaks, and the thermal changes observed in BSE images suggest various firing temperatures, from low (around 800ºC) to high ones (around and over 900ºC). Such a large thermal interval does not necessarily mean different technological choices but rather a normal variation in pottery obtained by bonfire.

The composition of the Miocene mudstone from the area makes it a potential candidate for the clayey raw material. Temper material was, besides some crushed potsherds, alluvial sand containing quartz, feldspars, micas and heavy minerals which are typical for a metamorphic catchment area.

Acknowledgements: The authors acknowledge support of the project PN-II-ID-PCE-2011-3-0881. C.I. also acknowledges subsidy from the Russian Government to support the “Program of competitive growth of Kazan Federal University among world class academic centers and universities”. Dr. S. Tincu (Corvin Castle Museum) is thanked for providing the potsherds.

PROVENANCE OF COPPER USED FOR EGYPTIAN BLUE PIGMENTS OF ANCIENT MEDITERRANEAN ARTEFACTS

Fink-Jensen P.[1], Rodler A.S.*[1], Brøns C.[1], Skriver Hedegaard S.[1] & Klein S.[2]
[1] Ny Carlsberg Glyptotek, Copenhagen, Denmark
[2] Institut für Geowissenschaften, Goethe-Universität Frankfurt am Main, Germany
Corresponding email: alexandra.rodler@reflex.at

Keywords: lead and copper isotope analyses, production centers, trade routes

Egyptian Blue, a calcium copper tetrasilicate compound ($CaCuSi_4O_{10}$), is a bright blue, crystalline pigment, presumably an outcome of the historical developments in glazing techniques, and a synthetic form of the rare mineral cuprorivaite. Further, it is perhaps the earliest artificial pigment that was used in Egypt, Mesopotamia, Greece and the Roman Empire from as early as ca. 2,500 BCE to ca. 800 CE (e.g., Verri, 2009, and references therein). Samples of Egyptian Blue pigments were collected from Egyptian, Etruscan, Roman and south Italian artefacts that are part of the collections of the Ny Carlsberg Glyptotek, Denmark. To elucidate trade and production of the copper-based Egyptian Blue in the ancient Mediterranean area, we employ a powerful combination of lead and copper isotope analyses. Identifying a potential copper ore source can contribute to the reconstruction of ancient trade routes and help to improve our understanding of economic, political and social aspects of ancient civilizations. Variations in Pb isotope composition are rooted in the local geological history and can be useful for fingerprinting geological ore sources. Therefore, lead isotope analysis holds the potential to indicate whether the Egyptian Blue pigments were locally produced or imported. Copper isotope analysis then allows determining the ore type from which the artefacts were manufactured (e.g., Klein *et al.*, 2010), which can provide valuable information on the relative depth exploration of a given mine and thereby on the intensity of the mining activity. Lead isotope data of the Egyptian Blue samples vary considerably and might represent a mixture of ore sources. Processes such as mixing of different alloys, additives during smelting and potential recycling could facilitate the homogenization of lead isotopes and consequently erase original lead isotope signatures (e.g., Boni *et al*., 2000). However, the combination of lead and copper isotope analyses add a valuable dimension to fingerprinting the provenance of raw materials used for the production of Egyptian Blue and might in due course expand our understanding of the distribution of Egyptian Blue workshops and/or their trade routes in the ancient Mediterranean area.

Boni, M., Di Maio, G., Frei, R. Villa, I.M. (2000): Lead isotopic evidence for a mixed provenance for Roman water pipes from Pompeii. *Archaeometry*, **42**, 201-208.

Klein, S., Brey, G.P., Durali-Müller, S., Lahaye, Y. (2010): Characterisation of the raw metal sources used for the production of copper and copper-based objects with copper isotopes. *Archaeol. Anthropol. Sci.*, **2**, 45-56.

Verri, G (2009): The spatially resolved characterisation of Egyptian Blue, Han Blue and Han Purple by photo-induced luminescence digital imaging. *Anal. Bioanal. Chem.*, **394**, 1011-1021.

DEVELOPMENT OF MANGANESE-RICH PATINAS ON THE BUILDING SANDSTONES FROM THE LUNEVILLE CASTLE: FROM INITIAL BEARING PHASES TOWARDS FINAL PHASES

Gatuingt L.*[1-2], Rossano S.[1], Mertz J.-D.[2], Lanson B.[3], Rozenbaum O.[4], Fourdrin C.[1], Reguer S.[5] & Trcera N.[5]

[1] Laboratoire Géomatériaux et Environnement, Université Paris-Est, France

[2] Laboratoire de Recherche des Monuments Historiques, Centre de Recherche sur la Conservation, Champs-sur-Marne, France

[3] Institut des Sciences de la Terre, Université Grenoble Alpes, Centre National de la Recherche Scientifique, Gières, France

[4] Institut des Sciences de la Terre d'Orléans, Université d'Orléans, Centre National de la Recherche Scientifique, Bureau de Recherches Géologiques et Minières, Orléans, France

[5] Synchrotron SOLEIL, Saint-Aubin, France

Corresponding email: laure.gatuingt@culture.gouv.fr

Keywords: sandstone, manganese, patina

Sandstones, used as building stones or in natural settings, are known to develop dark patinas at their surface when subjected for centuries to atmospheric conditions (Nord & Ericsson, 1993; Thomachot & Jeanette, 2004; Mertz, 2010). In January 2003, a violent fire affected the Luneville castle (XVIII Century), located in the east part of France and built with Triassic sandstones. The building materials were submitted to a huge amount of water, resulting from the firemen intervention. A few weeks after – i.e. very quickly – dark stains started developing on some stone blocks located in the burnt parts of the castle. Areas of the castle that have not been submitted to the accidental fire may also present dark patinas.

Chemical analyses have shown that both types of patina are mainly composed of Mn. As these Mn-rich stains are not observed on all building blocks, their formation likely depends on the substrate and possibly results from the dissolution of Mn-bearing compounds in the stone bulk, followed by their migration to the surface as dissolved species, through the porous network. The aims of this work are (i) to infer a formation mechanism for each patina, by comparing its constitutive Mn-bearing minerals with the initial Mn-bearing phases in the sandstone bulk, and (ii) to compare information obtained on different sandstones.

Patinated stones have been sampled on site, both in the burnt and unburnt zones. One patina formed before 2003 in natural conditions, whereas the other one formed consequently to the 2003 fire, in a highly watered area. Optical and electronic microscopies, coupled with Energy-Dispersive X-ray Spectroscopy (EDS) allowed to show that patinas are heterogeneous in thickness and colour and cannot be describe as a continuous coating onto the rock surfaces. Moreover, the patina that developed prior to the 2003 fire is darker, thicker but also richer in Mn than the more recent one. Besides, from these techniques, a correlation was established between the visual aspect of dark spots within the bulk sandstones and their Mn-enrichment. In the bulk, Mn appears to be associated with Ba or Fe at the difference with the patinas. To go further in the understanding of patinas' formation, the speciation of Mn in the core and at the surface of the blocks, have been studied by Raman spectroscopy, X-ray diffraction (XRD) and X-ray absorption spectroscopy (XAS) at the SOLEIL synchrotron (France), on DiffAbs and LUCIA beamlines respectively. Studying Mn-mineralogy in these phases is a real challenge because Mn-oxides frequently have indistinct and broad XRD patterns and are highly sensitive to laser and X-Ray beams. However, we have shown that Mn-bearing phases are different in the bulk and in the patina of a given block, but also from one sandstone to the other in good agreement with our initial assumptions.

Mertz, J-D. (2010): Etat des lieux, diagnostic des pathologies et perspectives. *in* "Un chantier - Restauration des façades des monuments urbains", Ministère de la Culture et de la Communication, OPPIC, 79 p.

Nord, A.G. & Ericsson, T. (1993): Chemical analysis of thin black layers on building stone. *Studies Conserv.*, **38**, 25-35

Thomachot, C. & Jeannette, D. (2004): Effects of iron black varnish on petrophysical properties of building sandstone. *Environ. Geol.*, **47**, 119-131.

ORIGIN AND PROVENANCE OF TUFF FOR THE ROMAN EMPIRE IN *GERMANIA INFERIOR*

Geisweid J.*[1], Hofmeister W.[1] & Schaaff H.[2]

[1] Institut für Geowissenschaften, Johannes Gutenberg-Universität Mainz, Germany

[2] Forschungsbereich Vulkanologie, Archäologie und Technikgeschichte, Römisch-Germanisches Zentralmuseum, Mayen, Germany

Corresponding email: jutta-geisweid@t-online.de

Keywords:

The landscape of the East Eifel (Germany) was created and formed by numerous intensive volcanic events during the Quaternary. Two prominent complexes are well known for the emplacement of tephra layers and diagenetically consolidated tuff:

(1) The Riedener Caldera in the western part of the East Eifel volcanic field is represented by intrusions, domes, tuff and widespread tephra fallout. In the area near the villages of *Rieden*, *Weibern* and *Ettringen* historical as well as recent tuff quarries evidence different sources of tuff stones. The so called *Riedener*, *Weiberner* and *Ettringer* tuff varieties are nowadays mainly used as replacement stones, in particular for restoration.

(2) The eruption of the *Laacher See* Volcano west of the *Neuwied* tectonic basin produced about 5 km^3 of phonolitic material, exclusively as pyroclastics. In addition to fallout pumice and ash deposits which covered the landscape like a blanket, pyroclastic ash flows filled mainly the valleys around the Laacher Lake and partly consolidated by the influence of water to tuff. In particular, worth mentioning here are the ancient mining areas of the *Krufter Bachtal* near the villages of *Kruft*, *Kretz* and *Plaidt* as well as the *Brohlbach* valley. Roman altars dedicated to *Hercules Saxanus* which were donated by members of the Roman Army show a remarkable archaeological evidence for Roman mining sites.

Volcanic tuffs have been used as building stones in many countries and represent a major component of the building mass of ancient monuments not only in Italy, as well as in Germany, the Netherlands, Belgium and Denmark. Tuff, well known by the Romans as a building raw material, was appreciated because of its availability in the Eifel (Germany), its lightness and resistance to physical weathering. Their knowledge of the Neapolitan Yellow Tuff and its similarity to the Rhenish tuff in particular as well as the necessity of building material for the conquered provinces probably caused the extensive exploitation of the tuff deposits in the East Eifel. Besides, the proximity to the Rhine River favoured the easy transportation and further distribution of the tuff blocs in the Roman Empire. Ancient cities like Cologne, Xanten with their Roman heritage as well as technical innovations like a water pipe through the Eifel partly panelled with tuff stone are only a few examples to express the Roman creativity.

According to the increasing archaeological interest in investigating the excavated Roman tuff mining areas in the Eifel and the distribution network in Roman times, it was helpful to find a way to distinguish the tuff properties of the different exploitation sites in order to develop a method for provenance analysis of unknown tuff building material from ancient monuments.

Consequently, the two prominent volcanic complexes of the East Eifel with their economically most important tuff deposits were taken into consideration. Hence, samples of provable historical deposits were examined according to their (1) petrographic and (2) geochemical composition as well as (3) the zeolitization of the tuff as a tracer for the diagenetic evolution abundant at the different site. By means of the distinguishing features and with additional multivariate data analysis it was possible to determine the provenance of the tuff blocs used in roman architecture in *Germania inferior*.

BULK GEOCHEMISTRY *VS.* MICROCHEMISTRY OF PHENOCRYSTS FOR PROVENANCING VOLCANIC STONES FROM THE SAME QUARRY BASIN – THE CASE OF EUGANEAN TRACHYTE

Germinario L.*[1], Hanchar J.M.[2], Maritan L.[1], Mazzoli C.[1] & Sassi R.[1]
[1] Dipartimento di Geoscienze, Università di Padova, Italy
[2] Department of Earth Sciences, Memorial University of Newfoundland, St. John's, Canada
Corresponding email: luigi.germinario@gmail.com

Keywords: provenance, XRF, LA-ICPMS

Bulk-sample chemical analyses have a long tradition in aiding provenance studies of archaeological stone, and have proven to be valid also for characterizing materials of the same rock type but coming from different source regions. Does this still apply to stones quarried in the same basin?

This issue is addressed considering trachytes from the Euganean Hills, an extraction region in northeastern Italy with tens of historical quarries in a 100 km^2 area. Euganean trachyte is a volcanic rock largely exploited in numerous archaeological sites, mainly dated to the Roman times, used for querns, funerary artifacts, road pavings, bridges and monumental architecture. Its widespread use, from northern to central Italy, has led to debates about ancient trade routes, extraction and production activities.

In order to constrain provenance studies of Euganean trachyte in archaeometry, a new reference database of petrographic and geochemical data of samples from 40 quarries has been established. A comparison is presented between the results obtained from bulk-sample and mineral-scale geochemistry of phenocrysts, by X-ray fluorescence (XRF) and laser ablation inductively-coupled plasma mass spectrometry (LA-ICPMS), respectively.

Bulk-sample major- and trace-element geochemistry does not show enough variation among the sampled quarries to provide unique discrimination with good accuracy, in many cases even if supported by a petrographic study. The comparison with previously published data also reveals that experimental conditions and sample quality can severely affect provenance attribution. However, this can be still attempted for some Euganean localities, according to the bivariate statistical analysis of XRF data, checking the clusters of quarries in the following binary plots: V/Nb, TiO_2/Zr, TiO_2/K_2O, Na_2O/Zr, Rb/Zr, Al_2O_3/Sr, Ce/Nd.

Alternatively, LA-ICPMS has proven to be a precise and accurate method for distinguishing nearly all the Euganean quarry sites. Multivariate statistical analysis allowed for the calculation of linear combinations of major- and trace-element concentrations that proved useful for separating different quarries, using binary and ternary plots. Biotite is by far the most informative phase, especially considering the concentrations of Li, Sc, Ti, V, Mn and Co. Good clusters are also provided by the other mafic minerals (augite and kaersutite) and magnetite. The compositions of feldspars (anorthoclase, plagioclase and sanidine) are more homogeneous instead, as revealed by REE patterns and spider diagrams, and the best separations are more frequently achieved combining Li, Ti, Sr, Pb, La and Eu.

Globally, LA-ICPMS provides more reliable criteria for a reference database aimed at provenance recognition, also as stand-alone technique and analyzing very limited amounts of material. At best, even few fine-grained crystals of a single phase might be sufficient, and this is highly advisable when dealing with archaeological materials.

AN ARCHAEOMETRIC STUDY OF THE NEOLITHIC GREENSTONE INDUSTRY OF BRIGNANO FRASCATA (ITALY): ARCHAEOLOGICAL/MINERO-PETROGRAPHIC IMPLICATIONS AND POSSIBLE SUPPLY SOURCES

Giustetto R.*[1], Venturino M.[2], Barale L.[1], d'Atri A.[1] & Compagnoni R.[1]
[1] Dipartimento di Scienze della Terra, Università di Torino, Italy
[2] Soprintendenza Archeologica del Piemonte, Torino, Italy
Corresponding email: roberto.giustetto@unito.it

Keywords: Neolithic greenstone implement, Na-pyroxenite, eclogite

An archaeometric study was performed on the Neolithic greenstone industry of Brignano Frascata (near Alessandria, Northwestern Italy), involving both morpho-typological and minero-petrographic aspects, with the aim to possibly reconstruct the manufacturing techniques and locate the supply sources of the raw materials and ancient trade routes. A pilot comparative study was also made with respect to analogous stone implements collected from close coeval sites of the Grue, Ossona and Curone valleys.

A marked predominance of high-pressure (H*P*) metamorphic lithotypes, namely greenstones from the Piemonte Zone of calc-schists with meta-ophiolites from the Western Alps, is observed. However, in Brignano Frascata "Na-pyroxenites" (42%) slightly prevail upon "Na-pyroxene + garnet rocks" (37%), a trend which is opposite to that observed in other archaeological sites of Northern Italy, where eclogites usually dominate. Lithotypes different than greenstones represent 10% of the population.

Several minero-petrographic features (such as fine grain-size and complex zoning of both pyroxenes and garnets) are observed, which recur also in implements from other archaeological sites of Northern Italy, thus suggesting – in some cases – a common supply source or, instead, the existence of a trade channel way. The morpho-typological exam proved that Brignano Frascata should be considered as an *atelier* for the production and commerce of polished stone implements during Neolithic, as suggested by the great number of retrieved rough casts and fragmented tools probably broken while manufacturing. Presence of several bangle drafts at different steps of their working chain further supports the potential economic importance of the site, as part of these tools might have been addressed to trading.

By combining the morphological and minero-petrographic features of the Brignano Frascata tools, set in the surrounding geologic context, a feasible origin for the raw materials of these implements from pebbles retrieved in secondary conglomeratic deposits is proposed. The Oligocene stratigraphic succession of the Tertiary Piemonte Basin, in fact, includes two lithostratigraphic units located nearby, which contain conglomerate bodies with clasts of meta-ophiolitic rocks (Savignone Conglomerate and Monastero Formation), feasible sources of raw materials for these Neolithic tools. A more accurate location of these deposits, however, is prevented by lack of more specific geological data. Besides, the presence in Brignano Frascata of some tools obtained from granulite suggests that these rocks were probably collected from the alluvial deposits of the Sesia or Po rivers, after their confluence, which is the closest possible area with respect to the studied archaeological sites.

CELTIC FUNERARY POTTERY IN TRANSYLVANIA (ROMANIA): IN THE SEARCH OF RAW MATERIALS

Ionescu C.*[1-2], Berecki S.[3], Hoeck V.[1-4], Simon V.[5] & Enea-Giurgiu A.[1]
[1] Department of Geology, Babeș-Bolyai University, Cluj-Napoca, Romania
[2] Archeotechnologies & Archeological Material Sciences Laboratory, Institute of International Relations History and Oriental Studies, Kazan Federal University, Russia
[3] Mureș County Museum, Târgu Mureș, Romania
[4] Fachbereich Geographie und Geologie, Paris Lodron Universität, Salzburg, Austria
[5] Faculty of Physics & Institute of Interdisciplinary Research on Bio-Nano-Sciences, Babeș-Bolyai University, Cluj-Napoca, Romania
Corresponding email: corina.ionescu@ubbcluj.ro

Keywords: funerary pottery, Celts, Late Iron Age

In Transylvania, the NW part of the today Romania, the Celts dwelt in the Late Iron Age (La Tène period), i.e. from the 4th Century till 2nd Century B.C. In the Celtic settlements and cemeteries, a richness of pottery remnants has been found. The funerary wheel-thrown pottery from the Celtic graves at Fântânele village were studied by optical microscopy (OM), X-ray diffraction (XRD), electron microprobe (EMP) and scanning electron microscopy (SEM). The aim of the study is to find the phase composition of the sherds, as well as specific technological constraints for this peculiar type of pottery. Furthermore, the major, minor, trace and rare earth element chemistry (by ICP-MS) of sherds and Miocene carbonate-rich mudstones sampled in the area were compared, in order to identify the geological formations which provided the clay for ceramic paste.

The funerary pottery was grouped in grey and brown sherds, respectively. Both groups show a similar composition, with an Fe-rich illitic matrix and quartz, plagioclase, K-feldspar, muscovite and chlorite clasts, besides some fragments of metamorphic, magmatic and sedimentary rocks. Fe-rich pedogenic concretions are frequent, whereas carbonate is rare. The change of the optical characteristics of the matrix and the alteration of the XRD patterns indicate a low-to-medium firing temperature, ~ 800°C.

The chemical data obtained for ceramic sherds show ~ 55–66 mass% SiO_2, ~ 14-18 mass% Al_2O_3, ~ 5-7 mass% Fe_2O_3, ~ 1-5 mass% CaO, and ~ 1-2 mass% MgO. The chemical composition of the Miocene sediments shows some systematic differences compared with the ceramics, in particular higher CaO (~ 5-6 mass%) and MgO (~ 1-3 mass%). Other elements, such as Ti and Al are in a good agreement between ceramics and sediments. The content of Fe, Na and Si in ceramics and sediments is similar.

The field work and the chemistry revealed a uniform composition of the Miocene sediments all over in the area. No other rocks, which might be suitable for pottery, crop out. The lower CaO content of the funerary ceramic sherds (low to medium T fired) can be due to burial alteration. On the other hand, the production of the funerary pottery elsewhere cannot be ruled out.

Acknowledgements: The study was supported by Romanian National Authority for Scientific Research, CNCS-UEFISCDI, project PN-II-ID-PCE-2011-3-0881 (granted to CI) and project PN-II-RU-PD-2012-3-0316 (granted to BS). Support of the Sectorial Operational Program for Human Resources Development, co-financed by the European Social Fund was granted to TDL (project POSDRU/159/1.5/S/132400). C.I. also acknowledges subsidy from the Russian Government to support the “Program of competitive growth of Kazan Federal University among world class academic centers and universities”.

“ATLAS OF CZECH MARBLES”: MINERALOGICAL-PETROGRAPHIC AND ISOTOPIC REFERENCE DATABASE FOR PROVENANCE STUDIES

Kucharova A.*[1-2] & Prikryl R.[1-2]
[1] Institute of Geochemistry, Mineralogy and Mineral Resources, Charles University, Prague, Czech Republic
[2]Academy of Fine Arts, Prague, Czech Republic
Corresponding email: astastna@gmail.com

Keywords: marbles, provenance database, Czech Republic

During the past two decades, an effort to establish a complex database and collection (lithotheque) of Czech natural stones used in construction, architecture and sculpture resulted in extensive sampling and laboratory study of many rock types including marbles (i.e., crystalline limestones). This long-term project includes: (a) literature research (published and unpublished data, data from archives), (b) fieldwork (location and description of historic quarries, stone sampling), (c) laboratory studies (mineralogical-petrographic, geochemical, physical, mechanical, and technical properties testing), (d) lithotheque preparation (thin sections, sawn and polished stone slabs, large blocks), and (e) compilation in printed form of the “Atlas of Dimension Stones” (with all available data for each stone type).

Czech Republic shows extensive marble deposits that have been quarried for decorative purposes since Neolithic times. Up until now, around fifty marble quarries from six geological units of investigation (Lugicum, Moravo-Silesian Zone, Kutná Hora-Svratka Crystalline Complex, Moldanubian Zone, Sedlèany-Krásná Hora Metamorphic “Islet” and Krušné Hory Crystalline Complex) located in the Bohemian Massif were examined. Because local marbles frequently form relatively small lenses or deformed and folded tabular bodies in complex metamorphic suites of silicate rocks (such as quartzites, amphibolites, graphitic schists, calc-silicate rocks, etc.), they do not allow full adoption of well-established analytical procedures for provenance studies applicable for white marbles from Mediterranean areas.

Applied methodology included traditional provenancing methods, i.e., the detailed mineralogical-petrographic examination of thin sections (by optical microscopy, cathodoluminescence and petrographic image analysis) and the determination of the C and O stable isotopic ratios of carbonates. Additional methods such as electron microscopy, Raman microspectrometry and magnetic susceptibility measurement were used to determine impure marbles, which included different non-carbonate mineral phases (variously metamorphosed carbonaceous matter, accessory minerals with different magnetic characteristics, etc.).

The gathered data make fundamental quantitative part of a database that will be further employed for provenance studies of specimens obtain from various artefacts.

GOLDEN-SLIP WARE: MANIFACTURING TECHNOLOGY OF A GOLD-LIKE SLIP IN THE FIRST MILLENIUM BC SWAT (NORTHERN PAKISTAN)

Maritan L.*[1], Piovesan R.[1], Dalconi M.C.[1], Vidale M.[2] & Olivieri L.[3]
[1] Dipartimento di Geoscienze, Università di Padova, Italy
[2] Dipartimento di Beni Culturali, Università di Padova, Italy
[3] Dipartimento di Beni Culturali, Università di Bologna, Italy
Corresponding email: lara.maritan@unipd.it

Keywords: talc schist, SEM, XRPD

In the final occupation levels of the early historic site of Barikot (Swat, northern Pakistan), dated at the second half of the third century AD, were found few sherds of a peculiar wheel-thrown ware, called “Golden-slip” for its bright gold-coloured surface and a pearly, very vitreous luster. This slip, making the vessels precious for their aspect, inspired an archaeometric study, aimed at the definition of its manufacturing technology, possible provenance of the raw materials used and production process, including the application technique of the slip and the firing conditions. A multianalytical approach, consisting in the microscopic, microstructural, mineralogical and chemical analysis of both the golden slip and the ceramic paste, was adopted.

The microstructural analysis by optical and electron microscope both indicated that the slip is about 50 mm thick and composed by platy minerals, microchemically identified as talc and chlorite. As the two minerals in some particles are intimately associated, they were probably supplied from a talc-schist bearing chlorite. The ceramic paste contains submillimetric rounded inclusions of green stones (chlorite-schists, serpentinites), and it is mineralogically composed of quartz, plagioclase, illite and hematite.

The raw materials used for both the ceramic paste and the slip were locally supplied, since “green stones” notoriously outcrop as lenses some decimetres to some hundreds meters in the Mingora ophiolites in the Swat valley. The general use of talc-schist in architecture and in the production of Gandharan sculptures, supports that the raw material used for the golden slip was simply obtained from manufacturing residues of a particularly fine rock variety.

The analytical results on the golden-slip samples were compared with those obtained from the analysis of talc-schists fragments from some sculptural fragments and clay materials collected in the Swat valley, near Barikot and, on the basis of the technological constraints analytically defined, were made some replicas, allowing to better describe the manufacturing technology. On the basis of the mineralogical association observed in both the golden slip and ceramic paste, the thermodynamic stability of the pristine mineral phases, as well as the microstructure of both ancient pottery and modern replicas, the golden-slipped pottery underwent firing under oxidising conditions and in the temperature interval between 750 and 800°C.

While the golden look of the slip is a result of the combined light reflectance of the platy structure of the talcose coating and the uniform, bright red colour of the oxidized ceramic background, from a cognitive viewpoint this technique represents a late development of the *long durée* acquaintance of the craftpeople of the Subcontinent with the pyrotechnological transformations of talc and steatite, dating back to Neolithic times.

CUCUTENI - A POTTERY PRODUCTION IN EASTERN ROMANIA: INSIGHTS FROM COMPOSITIONAL ANALYSIS

Matau F.*[1], Breaban I.G.[2], Nica V.[3], Matricala A.-L.[4], Bele A.[4] & Stancu A.[3]
[1] Department of Field Science, ARHEOINVEST Interdisciplinary Research Platform, "Alexandru Ioan Cuza" University, Iași, Romania
[2] Department of Geography, Faculty of Geography and Geology, "Alexandru Ioan Cuza" University, Iași, Romania
[3] Faculty of Physics, "Alexandru Ioan Cuza" University, Iași, Romania
[4] "Petru Poni" Institute of Macromolecular Chemistry, Iași, Romania
Corresponding email: florica.matau@uaic.ro

Keywords: Cucuteni-Trypillia civilization, pottery production, archaeometrical analysis

The aim of this paper is to investigate the relationship between the emergent complexity of the Cucuteni-Trypillia civilization (V-IV millennia BC), starting with the Cucuteni A phase (4600-4050 cal. BC), and the specialization of their ceramic craft production as it is reflected by increasingly homogeneous products. Traditionally, this question has been addressed by typological analysis of sub-sets of larger ceramic assemblages consisting, mainly, of intact painted vessels.

In order to evaluate the changing context of the organization of ceramic production, we engage a robust methodological approach to the analysis of ceramic sherd assemblages, including painted and unpainted pottery, consisting in a combination of analytical techniques. We have used laser ablation induced coupled plasma mass spectrometry (LA-ICP-MS) for spot analysis of the matrix and temper of pottery samples from sites across the eastern region of present-day Romania. X-ray diffraction (XRD) and Fourier-transformed spectroscopy analysis were used to explore the firing temperature and the effects of distinctive tempering agents on the mineralogical transformations due to different firing parameters. The microscopical analysis for detailed study of groundmass microstructure (low magnification) and the degree of vitrification (high magnification) was determined by Environmental Scanning Electron Microscopy (ESEM) analysis.

By determining the chemical and mineralogical composition and the microscopical characteristics of the potshards it was possible to clearly determine the similarities and differences between different groups of pottery determined macroscopically. In addition, the investigation of pottery production process clearly indicated the *technological choices* made by the potters regarding raw material selection, paste recipes and firing process.

MINERALOGICAL AND STABLE ISOTOPIC COMPOSITION OF CORROSION PRODUCTS ON A LATE ROMAN COPPER CAULDRON: AN ATTEMPT TO CHARACTERISE THE BURIAL ENVIRONMENT

Mozgai V.*[1], Bajnóczi B.[1], Fórizs I.[1], Szabó M.[1], Dági M.[2], Mráv Z.[3], Nagy M.[4] & Tóth M.[1]
[1] Institute for Geological and Geochemical Research, Research Centre for Astronomy and Earth Sciences, Hungarian Academy of Sciences, Budapest, Hungary
[2] Museum of Fine Arts, Budapest, Hungary
[3] Hungarian National Museum, Budapest, Hungary
[4] Ministry of Human Resources, Budapest, Hungary
Corresponding email: mozgai.viktoria@csfk.mta.hu

Keywords: copper-alloy, corrosion, incrustation, Late Roman

Corrosion products of a Late Roman copper cauldron with uncertain provenance and now stored in the Hungarian National Museum were examined in this study. The cylindrical cauldron with an originally convex bottom has a stepped wall made of two separate copper sheets joined together with hammering, soldering and riveting. Based on its shape and manufacturing technique, it belongs to a type widespread in the Rhine and Danube regions of the Roman Empire in the 2nd-4th Centuries AD. The southernmost examples of this type were unearthed in the Transdanubian region of Pannonia around Lake Balaton in Hungary. The cauldron is large-sized: 83 cm in diameter and 32.5 cm in height, and was probably made in the 3rd or 4th Century AD.

The aim of this study is to make an attempt to determine the burial environment of the cauldron as corrosion products may contain information about the burial conditions (*p*H, Eh, etc.) of archaeological copper objects. Handheld X-ray fluorescence spectrometry (hXRF), X-ray powder diffraction (XRD), micro-X-ray diffraction (μ-XRD) and electron microprobe analyses were applied to determine the corrosion products. The chemical composition of the cauldron is 98 wt.% copper and 1-2 wt.% lead; other elements (Sb, Sn, Zn) are around or below detection limits of hXRF. The most common corrosion products determined are cuprite (copper oxide, Cu_2O) and malachite (basic copper carbonate, $Cu_2(CO_3)(OH)_2$). The corrosion products form distinct layers, the first product on copper is cuprite followed by malachite. The presence of cuprite indicates that the environment was not reducing, where copper do not corrode, and neither acidic, where copper dissolves (McNeil & Little, 1992). To form malachite, the chemical parameters of the environment changed to more oxidising condition with neutral *p*H.

Rarely paratacamite (copper chloride, $Cu_3(Cu,Zn)(OH)_6Cl_2$) and brochantite (copper sulphate, $Cu_4(SO_4)(OH)_6$) were also identified among the corrosion products. Due to their uneven distribution and as brochantite hardly forms in soils; these minerals are interpreted as products of active corrosion.

Stable carbon and oxygen isotope composition of the malachite corrosion product is -14.2‰ for $\delta^{13}C$ (PDB) and -7.1‰ for $\delta^{18}O$ (PDB). The $\delta^{13}C$ value of -14.2‰ indicates C3 plant dominance on the area of burial, and moderate wetted soil, although the type of soil plays a role as well. The $\delta^{18}O$ value of carbonate minerals formed in soil environment is mostly determined by the $\delta^{18}O$ value of the soil water, the latter is determined by the multiannual mean $\delta^{18}O$ value of the local precipitation. Keeping in mind that the average $\delta^{18}O$ value of the patina malachite in England is -2.2‰ (Smith, 1978), the $\delta^{18}O$ value of -7.1‰ indicates an area on the inner part of the continent or of higher elevation, because these areas are characterized by rather negative $\delta^{18}O$ value of local precipitation.

McNeil, M.B. & Little, B.J. (1992): Corrosion mechanisms for copper and silver objects in near-surface environments. *J. Am. Inst. Conserv.*, **31**, 355-366.

Smith, A.W. (1978): Stable carbon and oxygen isotope ratios of malachite from the patinas of ancient bronze objects. *Archaeometry*, **20**,123-133.

CHARACTERIZATION OF NEWLY-FORMED CALCIUM PHOSPHATES STRATIGRAPHIES CRYSTALLIZED ON CALCIUM CARBONATE SUBSTRATES: A MULTI-ANALYTICAL APPROACH

Possenti E.*[1-2], Colombo C.[2], Conti C.[2], Gatta G.D.[1], Merlini M.[1] & Realini M.[2]

[1] Dipartimento di Scienze della Terra "A. Desio", Università di Milano, Italy

[2] Istituto per la Conservazione e Valorizzazione del Patrimonio Culturale, Consiglio Nazionale delle Ricerche, Milano, Italy

Corresponding email: elena.possenti@unimi.it

Keywords: calcium phosphates, inorganic-mineral treatment, X-ray diffraction techniques

The diammonium hydrogen phosphate [DAP, $(NH_4)_2HPO_4$)] treatment is an effective and promising consolidating agent for carbonatic substrates (Matteini et al., 2011, 2013). The reaction with calcite [CC, $CaCO_3$] at room temperature is non-stoichiometric and induces the formation of hydroxyapatite [HAP, $Ca_5(PO_4)_3(OH)$] (Ni & Ratner, 2003) and other metastable phases (Possenti et al., 2016). Due to the complexity of the DAP reaction mechanism, several studies have been focused on the interaction between the consolidating product and the carbonatic substrate, in order to define the crystallization sequence and the identification of the formed calcium phosphates.

We have recently been carried out a series of experiments on Carrara marble specimens treated by capillarity, paper poultice and immersion in DAP solutions with different molarities. The first experimental findings showed that the treatment involves the formation of a *shell*-like layer around the calcite grains, composed by a mixture of crystalline and amorphous calcium phosphates. These phases are arranged in layers, with different crystals size and morphology. Since the straightforward characterization of calcium phosphates mixture is challenging (Drouet, 2013; Karampas & Kontoyannis, 2013), we have developed and improved a new multi-analytical approach (based on the combination of X-ray diffraction techniques, vibrational spectroscopies and morphological-microchemical analyses). In addition, the reaction kinetics has been investigated (with a non-destructive protocol) with time-resolved experiments performed at the MCX beamline at Elettra (Trieste, Italy). Our first experimental results suggest a correlation between the specific crystalline phase to the morphology and the position of the newly-formed products of the *shell* structure. The reaction products and their position into the porous matrix govern the performance of the mineral-inorganic treatment. The obtained data of this study provide useful recommendation concerning the treatment methodologies in the conservation works (DAP molarities and treatment time).

Drouet, C. (2013): Apatite formation: why it may not work as planned, and how to conclusively identify apatite compounds. *Biomed. Res. Int.* 1-12.

Karampas, I.A. & Kontoyannis, C.G. (2013): Characterization of calcium phosphates mixtures. *Vibr. Spectrosc.*, **64**, 126-133.

Matteini, M., Rescic, S., Fratini, F., Botticelli, G. (2011): Ammonium phosphates as consolidating agents for carbonatic stone materials used in architecture and Cultural Heritage: preliminary research. *Int. J. Archit. Herit. Conserv. Anal. Restor*., **5**, 717-736.

Matteini, M., Colombo, C., Botticelli, G., Casati, M., Conti, C., Negrotti, R., Possenti, E., Realini, M. (2013): Ammonium phosphates to consolidate carbonatic stone materials: an inorganic-mineral treatment greatly promising.*Proc. Built Herit. Monit. Conserv. Manag.*, 1278-1286.

Ni, M. & Ratner, B.D. (2003): Nacre surface transformation to hydroxyapatite in a phosphate buffer solution. *Biomaterials*, **24**, 4323-4331.

Possenti, E., Colombo, C., Bersani, D., Bertasa, M., Botteon, A., Conti, C., Lottici, P.P., Realini, M. (2016): New insight on the interaction of diammonium hydrogenphosphate conservation treatment with carbonatic substrates: A multi-analytical approach. *Microchem. J.*, **127**, 79-86.

MANY A MICKLE MAKES A MUCKLE: Pb ISOTOPE SIGNATURE OF COPPER ORES MAKED BY LEADED INCLUSIONS IN GANGUE MINERALS

Rose T.*[1], Klein S.[1] & Hoefer H.E.[1]
[1] Institut für Geowissenschaften, Goethe-Universität Frankfurt am Main, Germany
Corresponding email: thomas.rose@daad-alumni.de

Keywords: lead isotopes, inclusions, provenancing

In archaeometry, lead isotope studies are commonly used to provenance metallurgical artefacts. However, the regular approach in interpreting Pb isotope data was criticized anew throughout the last years. Greater consideration of geochemical aspects in the application and interpretation of the data was demanded since (e.g., Albarède et al., 2012; Baron et al., 2014). Among others, Baron et al. (2014) presented impressive examples of the pit falls if geochemical aspects are not sufficiently considered.

To contribute to this fruitful discussion, a previously completely unaccounted factor will be presented: the effect of inclusions in gangue minerals with high lead contents on the overall Pb isotopic signature. Ores from Mocissos (Portugal) serve as a case study. Through the powerful combination of electron probe microanalysis (EPMA) and multi-collector mass spectrometry it could be revealed that inclusions with high lead contents are able to corrupt the isotopic signature of ore minerals. Some specimens showed considerable deviations from the originating isotopic field or even the respective geological unit.

The isotopic lead signature of an ore is governed by ore and gangue minerals. For provenance studies, not only is (i) the separation prior to the smelting process unknown and unaccountable and (ii) the purity of the analysed ore sample usually not reported, but most importantly (iii) the isotope data base to which the data are referred is officially established with pure minerals. All these aspects need to be considered as they complicate archaeological interpretation massively.

Although Mocissos represents the oldest evidence for pyrometallurgy outside of settlements on the Iberian Peninsula (Deutsches Archäologisches Institut, 2007), little is known about the site from a geoscientific point of view. Hence, a genetic model of the ore genesis based on thin section analysis and EPMA data is presented. Furthermore the data and methodological approach will be evaluated and limitations are discussed. Comparisons to previously published data and a rough mixing model will be presented to estimate the inclusions' extent on the Pb isotope composition. Finally, implications for the reporting and interpretation of lead isotope data are drawn.

Albarède, F., Desaulty, A., Blichert-Toft, J. (2012): A geological perspective on the use of Pb isotopes in archaeometry. *Archaeometry*, **54**, 853-867.

Baron, S., Tămaş, C.G., Le Carlier, C. (2014): How mineralogy and geochemistry can improve the significance of Pb isotopes in metal provenance studies. *Archaeometry*, **56**, 665-680.

Deutsches Archäologisches Institut (2007): Jahresbericht 2006. Berlin, 264 p.

GLASS COLOURATIONS CAUSED BY Mn-Fe REDOX PAIR

Rossano S.*[1], Khomenko V.[2], Bedidi A.[1], Loisel C.[3], Ferrand J.[1], Sarrasin L.[1], Bertin A.[1] & Perez A.[3]
[1] Laboratoire Géomatériaux et Environnement, Université Paris-Est, Marne-la-Vallée, France
[2] M.P. Semenenko Institute of Geochemistry, Mineralogy and Ore Formation, National Academy of Sciences of Ukraine, Kiev, Ukraine
[3] Laboratoire de Recherche des Monuments Historiques, Champs-sur-Marne, France
Corresponding email: rossano@u-pem.fr

Keywords: glass colouration, manganese, redox

Manganese is a chemical element used as a colourizer in glass industry since antiquity. Its capacity to be present under various oxidation states makes it responsible of a large variety of colourations. In its oxidized state (Mn^{3+}), it imparts a strong purple to violet colour (dependant on matrix composition). Combined with iron, manganese often plays the role of a decolourizer leading to uncoloured glasses mainly used to represent hands and faces in glass windows (see for example Ferrand et al., 2015). The exact understanding of the involved reactions is however not complete and might provide information about the glass technology used in these ancient times.

A series of glasses has been synthesized in order to relate the colouration of glasses with the conditions of synthesis (temperature, atmosphere, glass composition). Two temperatures have been used (1200 and 1550°C). Glasses have been synthesized under air or under reducing atmosphere (H_2/N_2). The glass composition has been chosen on the basis of the average of a large range of medieval glasses compositions for what concerns the main oxides (SiO_2, Al_2O_3, K_2O, Na_2O, CaO, MgO). The MnO (resp. FeO) content has been varied between 1.5-x wt.% (resp. x wt.%), x varying from 0 to 1.5. Glass compositions have been checked by microprobe analysis at the Camparis facility of the Paris 6 university. Optical absorption spectra in the UV-Vis-NIR range have been measured at the Institute of Geochemistry, Mineralogy and Ore Formation in Kiev (UV-Vis) in the range 32000-6000 cm^{-1} and at the Technical University in Berlin (NIR) in the range 7000-1000 cm^{-1}. The colour of the different glasses has been characterized within the CIE 1931 model.

For a given temperature, results show that the addition of Mn in a Fe-rich glass composition implies a decreasing of the concentration in Fe^{2+} and an increase of the concentration in Fe^{3+}. When the uncoloured composition is reached a further increase of the Mn content leads to glasses with a persistent pink colouration. However, results also show that uncoloured glasses are obtained for different contents of Mn according to the temperature used for the synthesis suggesting that the reaction between Mn and Fe is not a simple redox reaction. The content of Mn necessary to decolourize a glass made at 1200°C is much lower than the one at 1550°C. Finally, annealing an uncoloured glass in air leads to the reappearance of the pink colouration characteristic of the presence of Mn^{3+}.

The present set of glasses synthesized in variable conditions helps deciphering the complexity of colour making in ancient times. The effect of temperature combined with atmosphere and glass composition might provide clues to the understanding of ancient glass technology.

Ferrand, J., Rossano, S., Loisel, C., Trcera, N., van Hullebusch, E., Bousta, F., Pallot-Frossard, I. (2015): Browning phenomenon of medieval stained glass windows. *Anal. Chem.*, **87**, 3662-3669.

ARCHAEOMETRIC ANALYSIS OF THE XIONGNU POTTERY (MONGOLIA)

Tengis S.[1], Erdene-Ochir N.-O.[2] & Solongo S.*[1]
[1] Institute of Physics and Technology, Mongolian Academy of Science, Ulaanbaatar, Mongolia
[2] Institute of History and Archaeology, Mongolian Academy of Science, Ulaanbaatar, Mongolia
Corresponding email: saran.solongo@gmail.com

Keywords:

Xiongnu potteries from royal burial mounds at Noin Uul, which are related to the time period from 3th Century BC to 1st Century AD, were investigated by Fourier transform infrared and energy-dispersive X-ray fluorescence spectroscopy and X-ray powder diffraction methods.

Additionally, pottery fragments from different archaeological sites ascribed to the same time period were analyzed to identify the production centre. A preliminary study of provenance analyses suggested the pottery fragments found in burials at Noin Uul may have originated from workshop site at Boroo and Orkhon valley.

GEOCHEMISTRY AND MINERALOGY IN SERVICE OF CULTURAL HERITAGE PRESERVATION: A CASE OF MUSEUM OF ZINC IN KATOWICE, POLAND

Warchulski R.*[1], Gawęda A.[2] & Juszczuk P.[3]
[1] Centre for Polar Studies KNOW (Leading National Research Centre), Faculty of Earth Sciences, University of Silesia, Katowice, Poland
[2] Faculty of Earth Sciences, University of Silesia, Katowice, Poland
[3] Institute of Computer Science, University of Silesia, Katowice, Poland
Corresponding email: rwarchulski@us.edu.pl

Keywords: Zn-Pb slags, geochemistry, cultural heritage

Upper Silesia in Poland is an area famous of extreme amount of mining and smelting industries, their development was related to industrial revolution in XVIII/XIX century. Upper Silesian Industry District covers an area of around 2700 km^2 including 14 large cities, in which over 50 coal and Zn-Pb mines, more than 20 smelters, a few coal-based power plants were/are working.

In Katowice, the capital city of Silesia, Museum of Zinc was funded in 2015 in the place of the former smelting plant. Unfortunately almost all slags produced since 1834 were used for commercial purposes, and as it is common for Polish smelting sites all technological documentation was lost during both World Wars. To restore historical process of zinc smelting three samples historically described as “enriched ore”, “roasted ore” and “roasted ore with coke” were provided for investigations by museum. We were also allowed to sample the slag and lining material directly from the preserved furnaces parts.

On the base of petrographical observations, X-ray diffraction and electron-probe microanalyses it was proven that samples “enriched ore” and “roasted ore” has appropriate phase composition and chemistry for their description. “Roasted ore with coke” description on the other hand was rejected as it was determined that this sample is, in fact, an addition to ore before smelting process, as it contained coke, but was lacking zinc phases necessary for smelting. Analyzed slag has composition similar to material from the other smelting sites in Poland. It is composed of high temperature, low pressure phases like spinel, hematite, pyroxene, cristobalite. It was proven that composition of used lining has good correlation with “roasted ore with coke” composition, thus it is probably re-used as addition.

The new approach included usage of differential evolution algorithm which gave quantitative data about smelting process at site. According to all performed analyses three stage smelting process was used at the site. Firstly “enriched ore” was roasted to remove sulphur. After that “roasted ore” was mixed with additions incorrectly described as “roasted ore with coke” in proportion 1:1.27 and smelted in horizontal muffles forming the furnace. During smelting 62% of batch was volatilized and removed (mainly: Zn, Pb, S, C). Other 38% of material was included to slag, rich in elements like Si, Fe, Ca, Al, Mg and residual S, Pb and Zn. This investigations allowed to create museum exhibition, describing smelting process at the site.

Acknowledgements: This study was supported by NCN 53 grant No. 2014/13/B/ST10/02403 “Zinc and lead metallurgical slags – testing ground for investigation of behaviour of potentially toxic elements in the crystal phase structures and their interaction with environment” given to AG and by the grant of Centre for Polar Studies, University of Silesia, Poland -The Leading National Research Centre (KNOW) in Earth Sciences 2014-2018 given to RW.

Session S28:

Museums and teaching mineral sciences to new generations

Conveners:

Cristiano Ferraris (Paris – France)

Lutz Hecht (Berlin – Germany)

Eleonora Paris (Camerino – Italy)

MONTE AMIATA: THE MINERALOGICAL COLLECTION OF THE NATURAL HISTORY MUSEUM OF THE PISA UNIVERSITY

Biagioni C.[1], Bonaccorsi E.[1], Musetti S.*[1] & Pasero M.[1]
[1] Dipartimento di Scienze della Terra, Università di Pisa, Italy
Corresponding email: silviamusetti1991@gmail.com

Keywords: Monte Amiata, mineral collection, historical specimens

The development and preservation of mineral collections from Tuscan occurrences for research, education, and public exhibitions is one of the missions of the Natural History Museum of the Pisa University. The regional collections are composed by a total of 8238 specimens, representing about 42% of the total mineralogical collections.

The Monte Amiata collection, formed by 171 specimens, is one of the smallest among the regional collections. Several specimens are accompanied by old hand-written labels dating back to the period of activity of Prof. Antonio D'Achiardi (1839-1902) and were described by this author in his *Mineralogia della Toscana* (D'Achiardi, 1872/73).

The specimens belong to three different groups: i) minerals from the Plio-quaternary hydrothermal ore deposits, ii) minerals related to the volcanic rocks of the Monte Amiata, and iii) specimens formed through the action of silica-rich waters.

The first group is representative of one of world-class Hg ore deposits of Monte Amiata (e.g., Rimondi et al., 2015). The mining activity definitively ceased at the end of 1970s and since then the opportunity to collect new specimens has progressively decreased. Consequently, old specimens kept in public or private mineralogical collections are useful for the study of the mineralogy as well as the ore geology of the Monte Amiata. The collection preserves several specimens of cinnabar representive of its different kinds of occurrence in the mining district. Moreover, accessory minerals are present, such as metacinnabar, realgar, orpiment, and stibnite. The occurrence of the high T cubic polymorph of HgS is particularly interesting because its presence was not reported so far in literature. The recent study of some specimens kept in the collection of the Natural History Museum led to the full characterization of metacinnabar from the hydrothermal Hg ores from Monte Amiata.

Minerals related to the volcanic rocks have a particular historical importance, having been collected in the first half of the XIX Century. For example, several loose crystals of sanidine were collected by the naturalist Giorgio Santi (1746-1822). Santi (1795) described (and probably collected) also specimens of "fiorite", a variety of opal from Santa Fiora. These specimens, together with samples of diatomaceous earths, form the third group of specimens constituting the Monte Amiata collection.

In conclusion, the collection is the proof of the mining exploitation carried out in the Monte Amiata area and it has a great historical importance in housing several specimens collected between the end of the XVIII and the beginning of the XIX Century. In this way, the collection is important not only from the scientific point of view but also from an educational perspective, illustrating the evolution of the scientific knowledge and the birth of the mineralogical school at the Pisa University.

D'Achiardi, A. (1872/73): Mineralogia della Toscana. Nistri, Pisa, 678 p.

Rimondi, V., Chiarantini, L., Lattanzi, P., Benvenuti, M., Beutel, M., Colica, A., Costagliola, P., Di Benedetto, F., Gabbani, G., Gray, J.E., Pandeli, E., Pattelli, G., Paolieri, M., Ruggieri, G. (2015): Metallogeny, exploitation and environmental impact of the Mt. Amiata mercury ore district (Southern Tuscany, Italy). *Ital. J. Geosci.*, **134**, 323-336.

Santi, G. (1795): Viaggio al Montamiata. Ranieri Prosperi, Pisa, 356 p.

THE USE OF VIRTUAL WORLDS IN GEOSCIENCE TEACHING/LEARNING

Boniello A.[1] & Paris E.*[1]
[1] Scuola di Scienze e Technologie - Sezione di Geologia, Università di Camerino, Italy
Corresponding email: eleonora.paris@unicam.it

Keywords: virtual worlds, geoscience teaching/learning, immersive environments

Virtual Worlds represent an innovative strategy and an educational opportunity to learn in a socially-interactive learning community and in an immersive environment. However, in spite of the already recognized effectiveness of Virtual World as learning environments, still their application in science teaching-learning is very limited.

To experience this approach and evaluate its applications in Geoscience topics we used a MUVE (Multi User Virtual Environment) to address students of two age groups, 13-15 and 15-18 years old. A virtual island, the UNICAMearth island, was created in 3D using the software Open Sim and the Singularity viewer. Through online access, the students experienced role-play activities built using the Inquiry Based Science Education (IBSE) approach with an adaptive path. Serious games were built to make the students pass ability steps, knowledge tests and solving problems, thus evaluating the acquisition of knowledge and competences. Following the virtual path the students carried out tasks and answered questions, planned to make them acquire specific knowledge as well as general scientific and transversal skills.

Since the use of simulations in virtual environments recreates contexts similar to reality, this characteristic can be effective to study an area and its transformations with time, with interesting possible applications in geoscience topics. In this work, several paths have been created in 3D environments, where the students, as avatars, learn with an immersive training: for example, a volcanic area to simulate eruptions, earthquakes, studying rocks and minerals as well as understand which events may occur in an area at risk of eruption. In each path, through IBSE questions, the students collect data and play the role of a geologist. The possibility to use videos, in-depth cards, links to websites increases the tools available for the teachers to increase the level of difficulty of the path.

The paths have been tested in schools and they were found to be highly involving, increasing also social skills, cooperative working and even connections with the teachers, even for the shiest children or the younger ones. The experimentation has shown that students learned in an engaging way, especially when the environment could be changed by the user. The effectiveness of learning and the interest in approaching these topics were especially high for those students usually lacking interest for science or missing attention and fitting in the traditional school teaching.

Being the first attempt to use the Virtual World in geoscience teaching, it is possible to conclude that their use can be very successful and it is possible to find interesting applications, both in school and in museum or in any educational environment where involvement and a recreation of reality is useful.

LINKING MINERALS AND HEALTH THROUGH THE WIND DUST. AN EDUCATIONAL PROPOSAL

del Buey P.*[1] & Sanz-Montero M.E.[1]
[1] Departamento de Petrología y Geoquímica, Universidad Complutense, Madrid, Spain
Corresponding email: pablodelbuey@ucm.es

Keywords: mineral dust, teaching methodologies, high school

It is well known that minerals and rocks are not interesting for the students of pre-university educational stages. On an attempt of making the teaching of these materials more relevant and consequently more attractive to students we suggest an interdisciplinary approach that links minerals with the human health as well as the environment and the climate at large. The aim of the activity is to raise students' awareness on the impact of natural-sourced atmospheric minerals on human health looking for a real-world example. As in Mediterranean regions, in Madrid (Spain) the main primary source of dust intrusions is the Sahara desert. It consists dominantly of silt, although clay and sand fractions can also be present (Karanasiou et al., 2012). Mineralogically, it is composed by quartz, magnetite/hematite and carbonates. In the finer fractions clays such as palygorskite, illite and kaolinite can also be important, depending on the source area of the dust (Alastuey et al., 2005).

Several activities can be performed to develop this proposal. Specifically, for students in their last years of high school education a visit to the Atmospheric Protecting Service of Madrid Council Head Office was performed. The main objective of this experiment was to show the students the presence of mineralogy in our daily lives, using a real example such as the mineral dust derived from the Sahara desert covering Madrid. Additionally, this activity was designed to motivate them to think about the relation of geology with the environmental and health processes concerning the Earth´s surface. After the theoretical explanation, the visit followed with the observation of the analytical instrumentation used to measure the atmospheric particles. They also provided the data on mineral dust and how the Saharian intrusions increase dramatically their concentration.

To examine the effect of this activity on interest to first course of 16-17 years old students, they were asked to complete a survey. The preliminary most relevant results were that about 50% of the students consider that natural solid atmospheric particles help to a better understanding of our daily relation with minerals by environmental and health issues. In addition, 30% of pupils learned that minerals are part of natural solid atmospheric particles. Other questions of the survey compared this activity with other type of activities and methodologies to teach mineralogy (traditional lessons, practical description of minerals and rocks, and MiniQuest of mineral applications) that they previously had received. As a conclusion of this comparison between different methodologies, the majority of them (60%) considered that mineral applications and their environmental/human health implications were the most useful concepts for studying mineralogy. Therefore, we suggest another kind of activity to link these contents to other parts of the educational programme, for instance: they could look for information about the diseases that breathing natural atmospheric particles caused in our respiratory system.

The results of this preliminary study may be useful and inspiring to integrate more practical methods to teach Geology in high school. In addition, the use of surveys can help to discriminate the most attractive contents of subjects, which could be used to support the design of educational programmes.

Acknowledgements: This work has been possible due to Santa María del Carmen High School, technical staff from the Atmospheric Protecting Service of Madrid Council Head Office and the Spanish Research project CGL2015-66455-R (MINECO).

Alastuey, A., Querol, X., Castillo, S., Escudero, M., Avila, A., Cuevas, E., Torres, C., Romero, P.M., Exposito, F., Garcia, O., Diaz, J.P., Dingenen, R.V., Putaud, J.P. (2005): Characterisation of TSP and PM2.5 at Izaña and Sta. Cruz de Tenerife (Canary Islands, Spain) during a Saharan dust episode. *Atmos. Environ.*, **39**, 4715-4728.

Karanasiou, A., Moreno, N., Moreno, T., Viana, M., de Leeuw, F., Querol, X. (2012): Health effects from Sahara dust particles. ETC/ACM Technical Paper 2011/4,15 p.

THE DEVELOPMENT OF MINERALOGICAL TOOL BOXES: AN EXAMPLE HOW TO STOP THE DISAPPEARANCE OF BASIC GEOSCIENCES IN GERMAN SCHOOL EDUCATION

Hecht L.*[1], Banaszak M.[2], Schmid-Beurmann P.[3], Schmidt B.C.[4] & Stalder R.[5]
[1] Museum für Naturkunde, Leibniz-Institut für Evolutions- und Biodiversitätsforschung, Berlin, Germany
[2] Institut für Angewandte Geowissenschaften, Technische Universität Berlin, Germany
[3] Institut für Mineralogie, Universität Münster, Germany
[4] Abteilung Experimentelle und Angewandte Mineralogie, Universität Göttingen, Germany
[5] Institut für Mineralogie und Petrographie, Universität Innsbruck, Austria
Corresponding email: lutz.hecht@mfn-berlin.de

Keywords: tool boxes, school education, mineralogy

There is no doubt that a basic knowledge of geosciences should be part of a good educational background of our society. We should have some general understanding of our dynamic earth including, e.g., the origin of natural hazards, the formation of mineral deposits, climate change in earth history, the origin and diversification of live on earth etc. The classical subject to teach geosciences at schools is geography. At least in Germany the geography curricula have developed in the last decades more and more towards an almost pure social science with very little aspects of physical geography or general geosciences. Geoscientists from natural history museums, universities, science education labs and other institutions are engaged in several ways to compensate the lack in geoscience education in schools and in the society in general. Sustainable implementation of geosciences at school education requires appropriate formation of school teachers, the supply with teaching materials, and ideally the modification of the school curricular.

A team composed of geoscientists from the German Mineralogical Society (DMG) and school teachers is developing mineralogical tool boxes to better implement and support basic subjects of geosciences in school education. The project was financially supported by the Alexander Tutsek Foundation. Five tool boxes have recently been distributed among several schools all over Germany. One box contains a rather comprehensive selection of rocks, minerals, ores and technical products and is basically meant for various demonstration purposes mainly in geography and chemistry lectures. The other four tool boxes are made to be used by pupils in teamwork. They cover the subjects a) rock identification and classification, b) copper ores and copper recovery, c) the rock cycle, and d) crystal morphology and symmetry.

A close cooperation of geoscientists with teachers in geography but also other natural sciences (chemistry, physics, and biology) is crucial for the development and successful application of such tool boxes in schools or science labs. The tool boxes need to attract pupils, to be feasible for practical teaching, and last but not least be scientifically correct and up to date. We report on and discuss some of our experience in the development of mineralogical tool boxes and the formation of school teachers.

GEOSCIENCE EDUCATION FOR YOUNG GENERATIONS: EMPTY RHETORIC?

Horn S.*[1]
[1] Institut für Geowissenschaften, Johannes Gutenberg-Universität Mainz, Germany
Corresponding email: susanne.horn1@web.de

Keywords: geoscience, education, MINT

Since the adoption of scholar projects in geosciences at most German universities, a lot of innovative concepts have been emerged. It started by talks of professors of the respective departments of geosciences. Following the great success of this campaign, was the increasing demand on the universities by schools and the general public. However, the main focus now is on experimental workshops and field excursions. This is no surprise, because the syllabus of German schools does not give way for the necessary frame for experimenting and extra-school activities. Thus the scholar labs grew at the universities, asking for new positions. Thus the idea of scientists teaching scholars besides their research work, is not possible any more. Preparation of new teaching methods, geared to the needs of the scholars is time consuming.

Projects which have been favoured by sponsors or foundations are still able to provide the required space and staff. However, only a few universities installed new positions to guarantee scholar education for the long term and mostly for chemistry, physics and biology. The lack of geosciences is a problem most concerning!

Now the situation is at a breaking point. The demand is increasing while the financial strain exceeds the budgets of the universities. The reaction is simple: cutting down the projects.

Here I will present a project „volcanism", which has been established for schools, implemented for several years, to show how successful such a project can evolve, generating fruitable networks and new teaching methods.

Volcanoes, which combine disaster and beauty, are far more than pure fascination. A lot of general natural phenomena can be explained. Volcanoes attract scholars, so that we can teach natural science in a most interdisciplinary way.

The project has developed from the start in a setting of close collaboration among scientists and teachers. But unfortunately, related to the education cuts, with no sustainability.

If the challenge of geoscience education for young generations should not decline into empty rhetoric, the conventional approach needs a change and not only be the task of the universities.

The theme of geoscience in this contact is directly correlated to all the disciplines of the so called and widely accepted as future related MINT-faculties. Geosciences directly imply on physics (geophysics = MIN), chemistry (geochemistry, aerosol-chemistry = N), technology (geoengineering = T) and also climate change (anthropocene). Therefore, geosciences are a hotspot for developing a feeling of being responsible for the future of mankind on earth.

Therefore, a particular importance will be due to the geoscience societies and associations as a coordination platform combining all responsible parties:

Schools, universities, museums and governmental departments.

There is only one way open: to build a new structure where to locate and to fund the education in geosciences.

MINERALOGICAL EDUCATION FOR CHILDREN AND GROWNUPS IN THE MINERALOGICAL STATE COLLECTION MUNICH (MUSEUM REICH DER KRISTALLE): A SCIENTIFIC PROGRAM TO UNDERSTAND THE GEOLOGICAL WORK OF SCIENTIST

Kaliwoda M.*[1] & Hochleitner R.[1]

[1] Mineralogische Staatssammlung München, Staatlichen Naturwissenschaftlichen Sammlungen Bayerns, München, Germany

Corresponding email: Melanie.Kaliwoda@lrz.uni-muenchen.de

Keywords: children workshops, mineralogy, museum

Young children from the age of three upwards have a constitutional interest in crystals, rocks and gemstones. If not promoted this interest will be nearly lost with the age of fourteen. This is similar with all natural sciences. So it is important to develop the interest very early and to keep it up over the difficult times of puberty. Therefore the mineralogical state collection programs start with kids in the age of three and accompany them with different age-appropriate offerings to the age of eighteen. The Museum offers special workshops, guided tours through the museum and special exhibitions. Within the tours kids can get an overview to the world of minerals and rocks and the topics of geology, mineralogy and ecology.

Young visitors have the chance to investigate minerals and rocks macroscopically and microscopically. In cooperation with the teachers we offer special lessons which are due to the age and the knowledge of the children and can function as supplements to the normal classes. So it is possible to inform about crystals, minerals and rocks in general or conduct particular research programs like volcanology, plate tectonics, meteorites, environmental and ore mineralogy. Moreover it is possible to create programs together with the teachers. Working groups can do special investigations at the museum and then work out the details at the school under supervision of the respective teacher.

For children at the age of 14 it is possible to work for one week as “young researcher” in the mineralogical state collection during the summer holidays. They can work together with students and scientists in the museum but also in one of our research projects. With this it is possible to become acquainted with scientific equipment as there are electron microprobe or Raman spectroscope and learn to work scientifically. During one year the Mineralogical State Collection has at least 2000 children visiting the museum or book special projects within their kindergarten group or school class.

WORKING WITH MINERALS FROM PRE-SCHOOL AGE TO THE ELDERLY

Kreher-Hartmann B.*[1]
[1] Institut für Geowissenschaften, Friedrich-Schiller-Universität Jena, Germany
Corresponding email: cbk@uni-jena.de

Keywords: special exibiition, pre-school, all school types

The mineralogical collection of the university of Jena/Germany has a long tradition. Arising in 1779 from a typical private natural cabinet it developed to the today existing mineralogical collection. While belonging to an institute of geoscience it is expected to deliver colleagues with material for research and to be used as the base of practical training for students to determine minerals and rocks. Sometimes colleagues are hopefully asking for sample material to be used for bachelor and master thesis or other qualification works.

But is that all? During history in Jena the collection had been closed to the public in between 1945 and 1990. So, since the reopening for the first two or three years only very few people know about the existence of the collection. Very few teachers from the city of Jena came with their pupils along. So some different activities started. First one or two times in the year a special exhibition was opened. With total different themes the curator tried to reach schools of every description. While minerals in myth mainly fascinated kindergarten kids and primary scholars for example ore deposits around the world and technical products formed by ores are in the interest of upper school levels. Dedicating special exhibition from the content near to the course of instruction more pupils are reached. In addition to that some further education for teachers started. Working together with an institute for further training for teachers supplementary themes to the course of instruction should motivate teachers to get in contact with the curator to formulate wishes for a special guided tour to the collection with their classes or to get more experience with the minerals and rocks.

Because of the long tradition in history some specimen came as presents from former very prominent persons to the collection. With the background knowledge and a special history to some objects elderly can be motivated to visit the collection special guided tours or special talk cycles about an object had been created.

All together in this days pupils from distances of more than 100 km came to visit with their classes the collection. There is no kindergarten in Jena who has been not yet for a visit in the collection and special didactic courses for student groups from the chemistry, physics, archaeology as from the school of applied sciences and the professional schools have been created.

There are a lot of interested persons around our collection – we only need to reach and fascinate them!

GEOQUEST - A COMPUTER CLASS ROLE PLAYING GAME

Maraffi S.*[1], Paris E.[1], Sacerdoti F.M.[2] & Scamardella A.[3]
[1] Scuola di Scienze e Tecnologie - Sezione di Geologia, Università di Camerino, Italy
[2] e-voluzione srl, Napoli, Italy
[3] Liceo Scientifico "G. Galilei", Napoli, Italy
Corresponding email: sabina.maraffi@unicam.it

Keywords: Earth sciences, education technology, science education

The aim of the work is to use the latest ICT techniques to create innovative educational products, attractive and easy to use. Our primary topics was Earth Sciences, Mineralogy, Volcanology, History and Mythology, all together in a unique interdisciplinary approach (Maraffi & Sacerdoti, 2016).

The acquisition of knowledge and enhancing skills at actual time requires different approaches, involving students as much as possible. In this perspective, the game seems to be a perfect vehicle, not a single student's playing but a cooperative one (Maraffi & Marinelli, 2016).

GeoQuest is a Computer Class Role Playing Game to teach Earth Science and History. It involves all students using a patented system: the "teaching projector". This system allows the interaction of the class group through the use of smartphones and tablets, and it shows in real-time the game progress to the whole class (Sacerdoti & Maraffi, 2015).

The educational technology is based on the idea to use language which is closer to pupils to improve the teaching/learning process; the laboratory must be considered not only as an equipped classroom, but also as *a situation* close to the real work.

In the our role-playing game the students, divided into several categories (physicist, chemists, disseminators, technicians, historians) have to follow a geological trail in order to discover the present and the past of the Earth.

During the path, students have to pass some *doors* in teamwork; they allow assessment and represent the main sharing/disclosure moment. The *doors* allow to modulate the activities according to single lesson, teaching unit, module.

Main objectives:

1. Working on PC by themselves, students could be even more alone: it needs a best fitting between ICT and cooperative learning. Role-playing helps students to reach their goals easily through cooperation; this in order to avoid the risk of loneliness of Inquiry Based Science Education, preserving entirely the educational value (Maraffi et al., 2016).

2. Science Research now is based on field expert interaction: the role-playing game categories reflect the necessary team to get their goal.

3. The several roles allow everyone to enhance their own skills.

4. The "teaching projector" allows students to comment and to evaluate the groups activities and route them, providing real-time corrections to everybody.

5. The playing categories represent all the aspects of the research areas: from scientists (physicists, chemists), to technicians, to disseminators and historians.

The effective output of the project is guaranteed by the presence of paths with different levels; easier route contains the necessary dispensatory measures and allows the use of compensatory measures for a full inclusion of Special Education Needs (SEN) students.

Maraffi, S. & Marinelli, A. (2016): VALUQuest - A role playing game for skills assessment. Hawaii University International Conferences on Science, Technology & Engineering, Arts, Mathematics and Education (STEAM), Honolulu, 10-12 June 2016.

Maraffi, S. & Sacerdoti, F.M. (2016): GeoQuest - A class role playing engine to teach Earth Science and History. *Eur. J. Sci. Mathem. Educ.*, in press.

Maraffi, S., Sacerdoti, F.M, Scamardella, A. (2016): GeoQuest VESUVIUS - A class role playing game. Hawaii University International Conferences on Science, Technology & Engineering, Arts, Mathematics and Education (STEAM), Honolulu, 10-12 June 2016.

Sacerdoti, F.M. & Maraffi, S. (2015): EVO-RPGE - Aan Interactive role playing engine. International Congress on Education, Innovation and Learning Technologies, Granada, 2015.

WHAT BLIND PEOPLE CAN SEE IN A MINERAL COLLECTION (AND WHAT THEY CAN SHOW US THERE)

Milke R.*[1]
[1] Institut für Geologische Wissenschaften, Freie Universität Berlin, Germany
Corresponding email: milke@zedat.fu-berlin.de

Keywords: collections, museums, outreach

Fascination in minerals and other geological objects often arouses from seeing surprising shapes and colors and other optical effects. Museums make use of eye-catchers in their showroom displays where the often precious specimens are stored in glass cases to prevent them from dust and being stolen. When blind people enter a mineral museum they can hardly feel anything else as glass cases without having a chance to find out which kind of objects are displayed inside.

What fascination can blind people gain from mineral specimens? The same one as people with eyesight, but they need to use all kinds of senses except the optical one. For this purpose, the cases must be opened and the minerals must be handed to them. The mineral and rock collection at Freie Universität Berlin offers guided tours for blind people on a regular basis. Features applied to examine minerals and rocks are shape, surface structure, density, heat capacity, smell, taste, and tentatively sound. The tours take place in small groups.

Accompanying people (including students or trainees) are often astonished by the possibilities to “see” minerals without using the eyes. This changes their own perception of geologic materials. In the presentation I will show examples for all kinds of physical features of specimens used during the guided tours and how I introduce them to the visitors.

MINERALS AT SCHOOL

Pieraccioni F.*[1-2], Bonaccorsi E.[1] & Gioncada A.[1]
[1] Dipartimento di Scienze della Terra, Università di Pisa, Italy
[2] Scuola di Dottorato in Scienze della Terra, Università di Pisa, Italy
Corresponding email: fabio.pieraccioni@for.unipi.it

Keywords: pupils, learning, middle school

Children define “minerals” and “rocks” on the basis of their previous experiences and ideas. In their opinion, minerals are found only in mines and in the subsoil, and rocks only in the mountains. Minerals are always glittering or transparent and rocks are grey or brown and have a opaque appearance. So they often attribute a high economic value to minerals whereas they consider rocks as a natural material without relevance. These ideas are deeply rooted concepts (Stokes et al., 2007) that undermine the building of scientific knowledge about minerals and rocks. It is necessary to be aware of these naive thoughts, to dismount them in order to build a scientific reasoning (Libarkin et al., 2003). The pedagogic literature, as well as our own experience, indicates that the direct experience is a necessary step (even not sufficient) to face with this difficult and delicate passage, through a constructivist approach so that “what the pupil learns he at least understands” (Dewey, 1930).

We describe a didactic research, carried out during a PhD program of Department of Earth Science of University of Pisa, in which we tested an experimental learning sequence about minerals in seven classes of the middle school, involving approximately two hundred pupils.

At first, the teacher divides the class in small work groups, formed by three or four pupils, and gives them three well crystallised minerals. The pupils have to describe what they see. Pupils discuss within each group and - at the end - the teacher asks them to share their ideas. Naive concepts about “minerals” and “rocks” emerge clearly during the discussion; when invited to describe more details, pupils use words such as shape, faces, edges, corners, points etc. and the teacher highlights these words and their relationships with solid geometry. The teacher slowly leads pupils to a shared definition of mineral and then drives them to suggest the possible differences between minerals and rocks. The teacher exhorts pupils to describe the crystal habit of the three minerals by using more scientific words, found in internet through a guided search. At this point the teacher gives nine or ten different minerals to each group, with a form to be filled with some properties of minerals: shape, lustre, transparency, hardness (scratching by fingernail, nail, none of them), streak, cleavage or fractures, specific gravity, magnetism, HCl reaction. Every group tests these properties on each sample and fills in the form. Pupils use the collected information and a dichotomous key to discover the name of their samples.

The starting question-key of this inquiry approach is “What are minerals and rocks for you?”. Pupils have the time to freely observe different samples and they investigate some properties of minerals with simple experiments. This work allows them to reflect individually and in group, developing and sharing new ideas and modifying the old ones, at the light of their new knowledge.

Dewey, J. (1930): Democracy and education. An introduction to the philosophy of education. McMillan, New York. 436 p.

Libarkin, J.C., Beilfuss, M., Kurdziel, J.P. (2003): Research methodologies in science education: Mental models and cognition in education. *J. Geosci. Educ.*, **51**, 121-126.

Stokes, A., King, H., Libarkin, J.C. (2007): Research in science education: Threshold concepts. *J. Geosci. Educ.*, **55**, 434-438.

LARGE AREA SEM IMAGING IN GEOSCIENCES: BRINGING THE WORLD OF NANOSCALE MICROSCOPY TO THE CLASSROOMS AND MUSEUMS AS A TOOL FOR TEACHING AND LEARNING

Schumann D.*[1], Unrau D.[1], Laquerre A.[1], Collins R.[1] & Phaneuf M.W.[1]
[1] Fibics Incorporated, Ottawa, Canada
Corresponding email: dschumann@fibics.com

Keywords: large area SEM imaging, mineralogy, geology

In geoscience, it is very important to be able to investigate and understand mineralogical, textural, and structural relationships of entire samples that are commonly prepared as petrographic thin sections, epoxy mounts, or polished hand specimens. With conventional SEM imaging, the operator examines specific regions of interest preselected through tedious screening using transmitted or reflected light microscopy. This process is time consuming if the goal is the thorough understanding of the mineral associations and textures in the entire sample. Another challenge is usefully and simultaneously displaying of acquired light microscopy, SEM, and chemical data as well as the presentation of it to a large audience. Here we present a novel approach to imaging, analysing, evaluating, displaying, and sharing large area SEM image mosaics of entire samples. Automated high-resolution, large area SEM imaging enabled by the ZEISS Atlas 5 software affords a comprehensive, fast, and user- friendly means of defining, acquiring, observing, and manipulating image mosaics of large areas up to one terabyte in size on Carl Zeiss SEM systems. Atlas 5 allows the user to acquire simultaneously image mosaics of two signals (e.g., BSE-CL, BSE-SE). Background images and overlay images from other sources can be aligned with the SEM image mosaics allowing for the correlation between all data layers (e.g., light microscopy, element maps, automated mineralogy data). All of these data sets can be exported together into a browser based viewer (BBV) format that can be stored on a server and shared on the internet. Light microscopy data or automated mineralogy maps are displayed side by side, together with the SEM image mosaics. Navigation through the image mosaics is with a computer mouse and is similar to using Google Maps©. Any additional information (e.g., high-resolution sub-regions, chemical information, FIB-SEM movie clips) can be linked. The BBV format allows the data to be made publically available for easy use (see www.petapixelproject.com) in universities, high schools, geological surveys, and museums around the world. Large screen touch tables or large wall mounted screens in museums in an interactive exhibit are a useful way to show data sets to visitors who can navigate hands-on through the image mosaics and investigate the smallest details. Data sets of petrographic thin sections can be projected in auditoriums and be used for a wide range of teaching in geology and mineralogy classes. Museums are able to acquire and archive high-resolution large area image mosaics of rare samples that are otherwise not widely accessible (e.g. meteorites, lunar rocks, microfossils, coins). We will demonstrate these capabilities using selected data sets of particularly interesting geological samples comprising large area petrographic light microscopy image mosaics, dual signal SEM image mosaics, element maps, and FIB-SEM nanotomography movies.

PIETRE-PIETANZE / ROCKING RECIPES

Signori G.[1] & Chiesa S.*[2]
[1] Centro Servizi Marmo – Laboratorio Prove, Volargne (VR), Italy
[2] Istituto per la Dinamica dei Processi Ambientali, Consiglio Nazionale delle Ricerche, Milano, Italy
Corresponding email: geo_grace@yahoo.it

Keywords: learning, new generations, rock genetics

The project comes from the need to make it easy to non-geologists to understand and remember in a simple and immediate way different litho-types and genetic processes of rocks.

For our project, non-geologists are either new generations and adults, mainly people from the dimension stone sector, such as manufacturers, designers and users.

The technical terminology of the sector of dimension stones is very poor and does not take into account important features as the composition of rocks, their texture, structure and genetic environment. This exposes designers and users to the risk of generalizing the behavior of different stones and of making wrong choices selecting a stone that is likely to be incompatible with the intended use (non-durable).

The proper use of rock types in fact strongly depends on the correct recognition of composition, texture, structure and genetic environment.

Over the years we have therefore looked for effective ways/examples to make non-geologists understand and retain in memory mineralogical concepts, petrography, textures, genetic environments, etc.

This research led us to approach to neuroscience and to the brain mechanisms related to learning.

Learning is primarily related to the creation of associations and analogies: when we can make some similarities between the daily reality that surrounds us and scientific concepts, it is easier for us to understand and remember the scientific concepts, as we are creating “shortcuts” in our brain.

Our brain likes anything making learning more convenient and effortless.

What’s more: the more associations and analogies are counterintuitive, the more effective and “descent” is the shortcut (Brooks, 2011).

Since cooking shows are overspread on TV, and made it clear even for people who do not like cooking most of the procedures for culinary preparations, we started to associate the genetic processes of rocks to the cooking recipes that could better describe them.

This was quite counterintuitive: rocks can’t be mismatch with food, rocks are very hard, food much softer; rocks are tasteless, food is tasteful, etc.

The response was very positive and effective both by manufacturers and users, and led us in 2014 to extend the proposal also to schools and adults as an interactive workshop at Bergamoscienza, an international science festival being held in Bergamo since 2003.

The workshop is structured as a game, which requires you to match the rocking recipe to the jar containing food and then recognize the associated rock.

It is proposed to classes of primary schools, secondary and high schools, families and adult visitors.

In 2014 and 2015 over 2500 visitors experienced the laboratory.

Among them, students from the local chef school really appreciated the laboratory, and so for 2016 edition they will prepare some special “rocking recipes” for the participants to taste.

Brooks, D. (2011): The social animal: The hidden sources of love, character, and achievement. Random House, New York, 448 p.

SINGLE CRYSTAL GROWTH EXPERIMENT FOR AN EXHIBITION

Simon G.*[1] & Gille P.[2]
[1] Museum Mensch und Natur, Staatliche Naturwissenschaftliche Sammlungen Bayerns, München, Germany
[2] Department für Geo- und Umweltwissenschaften - Sektion Kristallographie, Ludwig-Maximilians-Universität München, Germany
Corresponding email: simon@musmn.de

Keywords: museum exhibition, crystal growth experiment, alum

On the occasion of the 2014 International Year of Crystallography we installed an in-situ crystal growth experiment in the mineralogical exhibition of the Museum Man and Nature in Munich. We started with single crystal growth of potassium alum using the temperature difference technique from an aqueous solution. After five months we earned an almost perfect single crystal with octahedral habit having a weight of 694.9 grams. From the second experiment we yielded a single crystal, which was grown during 4.5 months and showed some defects but had a weight of 956.5 grams.

The second potassium alum was prepared in several steps for a spherical crystal growth experiment. For more than hundred years such experiments have been performed to study growth rates of individual faces (e.g., Spangenberg, 1934, Honigmann, 1958). Our intention was to grow a crystalline sphere that is suited for exhibition purpose: aesthetic and explaining geometrical relationships.

For preparation the alum crystal was first grinded on a rotating disk with abrasive paper and in a second step lapped and polished with a rotating conical metal tool. Subsequently a small hole was drilled for a stand, the sphere was polished with a wet soft cloth. The sphere growth experiment was performed in a well stabilized heating chamber at 30°C for approximately 23 hours with the sphere submerged into three litres of saturated solution using the slow evaporation technique at constant temperature. The result is a pretty sphere showing altogether 86 facets from a cube (6 facets), a rhomb-dodecahedron (12 facets), an octahedron (8 facets), a tetragon-trioctahedron (24 facets) and trigon-trioctahedron (24 facets) and tiny facets of a pentagon-dodecahedron (12 facets).

Our new exhibition concept intends an in-situ crystal growth experiment, an almost perfect alum crystal and the alum sphere. To explain forms and habits we want to integrate animations for crystal mathematics (e.g., mirror plane, rotation axis and inversion axis), crystal growth but also models and hands-on exhibits so that visitors can touch and understand forms (e.g., cube, octahedron and rhomb-dodecahedron) and crystal mathematics (a cube with two-fold axis, a cube with three-fold axis and a cube with four-fold axis). We expect much of playful experience for the visitor and therefore more interest in crystallography.

Honigmann, B. (1958): Experimentelle Methoden zur Bestimmung der Tracht der Gleichgewichtsform und Möglichkeiten zur experimentellen Bestimmung der Gleichgewichtsform selbst. *in* "Gleichgewichts- und Wachstumsformen von Kristallen, vol. 4", B. Honigmann, ed., Steinkopff, Darmstadt, 53-71.

Spangenberg, K. (1934): Wachstum und Auflösung der Kristalle. Handwörterbuch der Naturwissenschaften, 2nd ed., vol. 10, Fischer, Jena, 362 p.

FROM NATURAL HISTORY SPECIMENS TO RECORDS OF EARTH SYSTEM PROCESSES

Walcott R.*[1]
[1] Department of Natural Sciences, National Museum of Scotland, Edinburgh, United Kingdom
Corresponding email: r.walcott@nms.ac.uk

Keywords: National Museum of Scotland, curation, exhibitions

Much of the National Museum of Scotland rock and mineral collection, like many other 19th century natural history collections, was acquired initially to serve as teaching specimens for students at the near-by university. In fact the specimens were used so much that curation of them became a problem. In 1873 the museum decided to sever formal links between the institutions. Since then the nature of the collections has gradually changed over their years and their role as a teaching collection has greatly diminished. In 2009 the Geology department of the museum, which is responsible for the meteorite, petrology and mineralogy collections, was rebranded as the Earth Systems section. One motivation for the change was to try to stimulate more use of the collections by students and researchers, in particular for funded interdisciplinary research projects.

In this presentation I discuss how this rebranding has affected the way the collections have been developed and used. I briefly cover what the change of emphasis has had on collection strategies and storage, exhibition and gallery displays. For example once aspect we have introduced into the main mineral and rock gallery is the role that biology has had on rock and mineral diversity. I end with an assessment how to the collections can be better used.

Technical Session (Sponsors)

SOLUBLE AND INSOLUBLE ELEMENTAL CONTENT IN ANTARCTIC ICE CORES: NEW ADVANCES USING A NEW GENERATION ICP-MS

Baccolo G.[1-2-3], Clemenza M.*[3-5], Delmonte B.[2] & Magarini R.[4]
[1] Dipartimento di Scienze Fisiche, della Terra e dell'Ambiente, Università di Siena, Italy
[2] Dipartimento di Scienze dell'Ambiente, del Territorio e di Scienze della Terra, Università di Milano-Bicocca, Italy
[3] Istituto Nazionale di Fisica Nucleare, Milano, Italy
[4] Perkin Elmer, Monza, Italy
[5] Dipartimento di Fisica, Università di Milano-Bicocca, Italy
Corresponding email: massimiliano.clemenza@mib.infn.it

Keywords: ice cores, trace elements, ICP-MS

Ice cores play a key role among the many natural archives which is possible to use for the reconstruction of past climate and environment. Through the chemical and physical analysis of ice and its content it is possible to obtain precious information about several climatic and environmental parameters for the last hundreds thousands years. Elemental analyses are one of the most important tools dealing with ice cores, providing detailed multi-elemental records that allow to reconstruct past volcanic activity, changes of the atmospheric circulation or biogeochemical cycles. Focusing the attention on more recent periods, the elemental analyses are extremely useful in order to assess the impacts of anthropic activities on remote areas such as Antarctica or Greenland. The definition of the soluble and insoluble elemental fractions is useful in order to distinguish the elemental contribution from atmospheric mineral dust (insoluble fraction) and the soluble one associated to snow precipitations. Analyses have been performed on an advanced ICPMS system equipped with a software package to use Single Particle (SP) technique for evaluation of size distribution and elemental content of insoluble particles, together with the concentration of dissolved fraction. A reaction cell (DRC) was also used for eliminating /reducing spectral interferences on selected isotopes. This study present preliminary results on the simultaneous determination of soluble and insoluble content of selected elements. We determined Al, Si, Ca and Fe in ice samples collected from an Antarctic ice core. These samples correspond to different climatic periods, ranging from few thousand years ago (Holocene), to more than 20 ky ago (last glacial period).

THE EMPYREAN PLATFORM AND NON AMBIENT STUDIES: FEW EXAMPLES FOCUSED ON PYROXENES, BLOSSITE

Casini E.*[1], Nénert G.[2], Prugovecki S.[2], Isobe M.[3], Dadivanyan N. [2], Belik A.[4] & Slobodin B.V.[5]
[1] PANalytical S.R.L., Lissone (MB), Italy
[2] PANalytical B.V., Almelo, Netherlands
[3] Max-Planck-Institut für Festkörperforschung, Stuttgart, Germany
[4] International Center for Materials Nanoarchitectonic, Tsukuba, Japan
[5] Institute of Solid State Chemistry, Ural Branch of the Russian Academy of Sciences, Yekaterinburg, Russia
Corresponding email: eugenio.casini@panalytical.com

Keywords: XRD, non ambient XRD analysis, polymorphism

The relation between crystal structure and properties of minerals and mineral-related materials is the key for technological benefit. The Empyrean multipurpose X-ray diffractometer was used as a platform for the characterization of several types of materials. Initially we focus on the pyroxenes that have been intensively investigated for decades due to their importance in mineralogy. While the silicon based clinopyroxenes have been widely investigated as function of pressure and temperature (Redhammer & Roth, 2004), the germanium based compositions remain poorly investigated. Here we report on the high temperature behavior of Li*M*Ge_2O_6 (*M* = Ge, V) exhibiting a strong first order phase transition between $P2_1/c$ and $C2/c$ symmetries. This study also clarifies the conflicting reports on the symmetry at room temperature of $LiCrGe_2O_6$ ($P2_1/c$ *versus* $C2/c$) (Redhammer, 2008; Matsushita, 2010). Our data confirm the $P2_1/c$ symmetry and a strong first order phase transition around 870°C. Later on we report on the anhydrous copper vanadates that are characteristic minerals of high-temperature volcanic fumaroles (Hughes et al., 1985). Among the list of fumarolic mineral species containing Cu and V, $Cu_2V_2O_7$ appears in the form of either blossite, α-$Cu_2V_2O_7$, or ziesite, β-$Cu_2V_2O_7$. An additional polymorph modification as a γ-form has been also reported which is related to the β-$A_2P_2O_7$ structure-type. These 3 polymorphs are similar in structure but differ markedly in the kinetics of their formation and reversibility of their transformations. $Cu_2V_2O_7$ material has been attracted a lot of attention, not only in mineralogy but also due to its importance as cathode material for rechargeable lithium batteries. Despite a deeper investigation, yet very little is known about the pressure dependence of this material. In order to gain further understanding of $Cu_2V_2O_7$, we have investigated at room conditions the effect of pressure on the crystal structure of blossite treated up to 6 GPa.

Hughes, J.M. & Stoiber, R.E. (1985): Vanadium sublimates from the fumaroles of Izalco volcano, El Salvador. *J. Volcanol. Geotherm. Res.*, **24**, 283-291.

Matsushita, Y., Izumi, F., Isobe, M., Ueda, Y. (2020): Crystal structures of Cr-based magnetic pyroxenes. *Solid St. Sci.*, **12**, 676-679.

Redhammer, G.J. & Roth, G. (2004): Structural changes upon the temperature dependent $C2/c \rightarrow P2_1/c$ phase transition in $LiMe^{3+}Si_2O_6$ clinopyroxenes, Me = Cr, Ga, Fe, V, Sc and In. *Z. Kristallogr.*, **219**, 585-605.

Redhammer, G.J., Roth, G., Amthauer, G. (2008): Chromium-based clinopyroxene-type germanates $NaCrGe_2O_6$ and $LiCrGe_2O_6$ at 298 K. *Acta Crystallogr.*, **C64**, i97-i102.

THE ITALIAN NATIONAL REPOSITORY FOR DISPOSAL OF RADIOACTIVE WASTE: LEARNING FROM THE DURABILITY OF ARCHAEOLOGICAL ANALOGUES OF MODERN BUILDING MATERIALS

Chiaravalli F.[1], Uras S.[1] & Ventura G.*[1]
[1] SOGIN S.p.A, Roma, Italy
Corresponding email: ventura@sogin.it

Keywords: LLW repository, cement durability, archaeological analogues

Safe disposal of radioactive waste needs the complete isolation of radioactive materials from the environment, at least until radioactivity will be mostly reduced. Assessment of the safety of disposal systems for radioactive wastes repositories requires long term forecasting of the performance of the different materials of the disposal system. Both artificial and natural barriers to radionuclides migration must be analyzed in response to the events and processes that might take place over periods of at least several hundreds of years, as well as evaluation of the radiological consequences over the time. The goal is to achieve conditions in which the disposal system leads to exposure level of the same order of magnitude of natural radioactivity. In order to address existing uncertainties, the quantitative safety assessment should be completed with other additional arguments, to increase confidence in safe disposal performance and to communicate and explain it to the stakeholders involved in the disposal decision-making.

The comparative study of modern and ancient construction materials is currently used to speculate about the durability. The durability is one of the most important aspects of material components of disposal structures, and a comparative analysis of modern/ancient materials may also serve as a support for communication to technical and non-technical audiences. Most of the studies on modern building materials and their archaeological analogues have been promoted by waste management agencies and by nuclear safety regulatory bodies, and carried out through international collaboration and the involvement of the International Atomic Energy Agency (IAEA) and the Nuclear Energy Agency (NEA). Although the open literature on modern building materials is broader and deeper, there are still several open questions about the similarities between ancient and modern cements, and in particular about the reaction products able to modify the binding power and strength to the mortar. In addition, the behavior of the amorphous phase at the time scale of hundreds of years is still not entirely clear.

In the framework of the localization and construction of the Italian National Low Level Radioactive Waste Repository, a contribution to the development of studies focalized on factors affecting durability of cement materials will be carried out on ancient works. A comparative analysis between ancient mortars properties and those of more recent ones, in similar environment of construction and conservation, will be done. In particular, the potential effects of time on the mechanical strength, permeability and stability of the crystalline components will be investigated. The study will be conducted on cementitious materials produced in different periods but with similar production protocols. The ancient products to be considered will be those having history of isolation from the degradation agents that may provide analogies with the processes expected by the barriers of the National Deposit. Anthropogenic (e.g., burial and demolition) and weather-climatic stressing factors (e.g., heat and humidity regimes since the construction), along with seismicity (e.g., frequency and intensity), will be considered to better understand laboratory results.

GEOSCIENCE EDUCATION IN A DIGITAL WORLD WITH DIGITAL MICROSCOPY

Graham S.D.[1], Hil E.*[1] & Wittge J.[2]
[1] Carl Zeiss Microscopy, Cambridge, United Kingdom
[2] Carl Zeiss Microscopy, Göttingen, Germany
Corresponding email: edward.hill@zeiss.com

Keywords: digital classroom, light microscopy, mineralogy

Introduction: The ability to understand mineralogy is a fundamental skill all geologists require. For over a hundred years, microscopy has been used to investigate minerals, teach geologists mineralogy and inspire the next generation of geoscientists. However, we now live in a rapidly developing and digital world, which provides us with an opportunity to advance the existing techniques in operation through utilizing the digital capabilities available.

This paper will introduce how optical mineralogy can be taught using “Digital Classroom” technology. In a student laboratory, equipped with ZEISS Primotech light microscopes and iPad technology, all the microscopes are connected to a wireless network, where images can be acquired and shared. Supervisors can view down all the microscopes at once and any images from any microscope can be projected onto the screen.

Digital Microscopy in a Digital World: The world we are living in is changing rapidly, as digital technology is more and more integrated into our everyday lives. Smart phones are common possessions for most, big data is shared, analysed and interpreted around the world using “Cloud” technology and people are continuously connected via the world wide web. It is therefore safe to say, that in the last 10 years, we have truly undergone a third industrial revolution; the digital revolution.

Digital technology is now revolutionising the way we educate and communicate. These digital capabilities are now being applied to Geoscience education and specifically, in this paper, for the microscopy and mineralogy education.

Optical Mineralogy Education with the ZEISS Digital Classroom: The digital classroom allows the supervisors to connect to all Primotech microscopes in the classroom. Using the Zeiss Matscope iPad application, the supervisor is able to view all the images from the microscopes at any time, giving him a comprehensive overview of the students microscopes. The supervisor has the capability to select and share anyone of the student’s microscope images by projecting the image onto the screen.

A simple example of the application of this technology, may be the following scenario. A supervisor is showing his class the features characteristic of an olivine on his light microscope. Now the students will aim to recreate the steps in search for the same features that are used to distinguish an olivine. Whilst overseeing the students microscopes, using the Zeiss Matscope iPad application, the supervisor notes one of the students has an olivine which has been cut perpendicular to the c axis and is showing maximum birefringence. This student’s microscopic image can be easily selected and projected on the front screen, to show the rest of the students this example. Another student may have, in plane polarised light, what appears to be an olivine with high relief, fractured texture and colourless pleochroism; the birefringence is black-grey in colour.

Both examples can be projected live from the students’ microscopes and be used to provide examples of the difference in birefringence based on the orientation of the crystal relative to the crystallographic axis. This is not just a better way of sharing information but also, by involving the students in such exchanges the supervisor can invoke an element of peer-on-peer teaching and greater student engagement with what is being taught.

In addition, students have the benefits of having iPads, which can wirelessly be connected to the microscope. Typically, students within the lecture make observations with the microscope, taking notes and making sketches based on their observations. This is a time intensive process and can result in students spending more time drawing and making notes than interacting with the microscope and the samples. The Zeiss Matscope iPad application therefore allows students and supervisors to acquire and save images, so they are able to build their own library of images. With the Zeiss Matscope iPad application students have the ability to perform measurements, annotate the images or record short videos based on their observations. Therefore, supervisors can create practical exercises, where measurements can be taken to ensure students note the relevant features and observe specific details within the sample. The Matscope iPad application thus allows the students to spend more time focused on the sample and its features and acquiring data from the samples.

Summary Remarks: The digital world we now live in provides us with a great opportunity to revolutionise our education provisions. The ZEISS Digital Classroom is one such evolution taking advantage of the digital

technology available today. The capabilities of the ZEISS Digital Classroom lead the future of how optical mineralogy and microscopy education are evolving.

THE PLANET – A PORTABLE, HIGH-RESOLUTION XRPD

Kinneging A.J.*[1], Verbruggen R. [1] & Huber N.[1]
[1] xplorex GmbH, Rimsting am Chiemsee, Germany
Corresponding email: bert.kinneging@xplorex.eu

Keywords: X-ray powder diffraction, in-field minerals analysis, identification

X-ray diffraction on powders and polycrystalline materials (hereafter XRPD) is the technique of choice when it comes to the identification and quantification of crystalline compounds in minerals. where many rely on X-ray fluorescence spectrometers to determine the elemental composition of their samples, XRPD yields valuable information on the mineralogy of the specimens.

However, the use of XRPD has been limited, due to the fact that diffractometers are either laboratory bound, or cannot generate diffraction patterns of sufficient quality for a complete analysis of the samples at hand. the quality of a diffraction pattern is measured in terms of resolution (FWHM of peaks in deg. 2θ), angular accuracy (band width of the deviation of measured peaks from their theoretical counterpart), angular range and the effective reduction of background radiation in the measurement.

By combining a linear detector with a seemann bohlin optical path, we developed a compact, portable, high resolution powder diffractometer.

In the presentation we will sketch the basic ideas behind the system and we will illustrate the systems performance in terms of resolution, angular accuracy and peak-to-background ratio with measurements on various standard samples like Si and LaB_6.

Furthermore, we will demonstrate the phase identification of some normal samples we obtained from a friendly laboratory.

FAST XRD ANALYSIS OF CLAY OR AMORPHOUS PHASES TOWARDS 1 WT-% ACCURACY

Knorr K.*[1]
[1] Bruker AXS, Karlsruhe, Germany
Corresponding email: karsten.knorr@bruker.com

Keywords:

TOPAS quantitative phase analysis (QPA) of well crystalline material is nowadays a straightforward task with an proven accuracy of about 1 wt-% or better. A growing demand is seen for the quantification of clay, poorly crystalline and amorphous material by X-ray powder diffraction (XRD) as well. A prerequisite for quantifying those materials is the ability to separate their broad but mostly weak signals from the instrument background in the vicinity of the incident primary beam as well as over extended measurement ranges. Energy dispersive linear detectors (LYNXEYE XE) and dynamic beam optimization (DBO) became recently available for BRUKER XRD instruments. As a consequence any user can now easily collect data without the need to reconfigure the instrument. Furthermore, this technology permits rapid measurements in the order of 1 min per sample. It is shown how several amorphous contributions can be separated. For synthetic mixtures an accuracy of about 1 wt-% is demonstrated. This opens the door to routine quality-control XRD on poorly crystalline material.

STRUCTURE ANALYSIS FROM POWDER FOR SAMPLES WITH STRONG ANISOTROPY IN CRYSTAL MORPHOLOGY USING A GANDOLFI ATTACHMENT

Ohbuchi A.[1], Shiramata Y.[1], Konya T.[1], Yamano A.[1], Fujinawa G.[1] & Grässlin J.*[2]
[1] Rigaku Corporation, Tokyo, Japan
[2] Rigaku Europe SE, Ettlingen, Germany
Corresponding email: Juergen.Graesslin@rigaku.com

Keywords: structure analysis, powder diffraction, Gandolfi camera

For structure analysis of new, rare minerals in most cases no crystals of sufficient size and quality for single crystal X-ray diffraction studies are available. Therefore, usually only powder X-ray diffraction remains as option to attempt a structure determination. The most frequent hindrance to a successful structure analysis is the error in the estimation of relative reflection intensities. While ambiguities in partitioning overlapping reflections are inherent to X-ray powder diffraction data, an additional problem can arise from crystallites with strong anisotropy in the morphology resulting in severe preferred orientation. Although samples prepared in rotating capillaries for transmission geometry are less affected compared to flat samples for Bragg-Brentano geometry, the remaining texture can still cause the structure analysis to fail. In that case, a Gandolfi attachment (Gandolfi, 1964), allowing to measure a sample in several orientations, ideally coupled with a fast detector to achieve a reasonable data collection time, can help. A sample of Bismuth oxychloride (BiOCl) was first measured in a rotating capillary using a Rigaku SmartLab 9kW multipurpose X-ray diffractometer equipped with a HyPix-3000 2D Silicon-semiconductor detector. Then an agglomerate of BiOCl-crystallites on a micro-loop from MiTeGen was mounted on the Gandolfi attachment and measured in several orientations to average the intensities. Rietveld structure refinement (Rietveld, 1969; Young, 1995) carried out on this dataset indeed shows a significant improvement compared with the capillary measurement dataset because of the eliminated preferred orientation.

Gandolfi, G. (1964): Metodo per ottenere uno 'spettro di polveri' da un cristallo singolo di picolo dimensioni. *Mineral. Petrogr. Acta,* **10**, 149-156.

Rietveld, H.M. (1969): A profile refinement method for nuclear and magnetic structures. *J. Appl. Crystallogr*., **2**, 65-71.

Young, R.A. (1995): The Rietveld method. Oxford Univ. Press, New York, 308 p.

ONE MICRON HIGH SPATIAL RESOLUTION FT-IR IMAGING: APPLICATIONS IN THE GEOLOGICAL DOMAIN

Scardina P.*[1] & Pasini V.[2]
[1] Agilent Technologies Italia, Milano, Italy
[2] SRA Instruments, Milano, Italy
Corresponding email: paolo.scardina@agilent.com

Keywords:

FT-IR micro-spectroscopy is a technique that allows users to visually see micron sized samples and collect accurate FTIR spectra from small objects. Agilent Cary 620 FTIR Imaging takes this to another level by providing the highest spatial and spectral information from a sample.

The traditional FT-IR mapping has several physical limitations. Indeed, the spatial resolution is limited to 10-15 µm, due to the infrared ray physics. In addition, traditional single point FT-IR takes a lot of time in mapping a sample area, since each spectrum is acquired one by one.

The Agilent Cary 620 FT-IR microscopes and chemical imaging systems represent the latest in cutting-edge performance, delivering unparalleled spatial resolution and sensitivity. It is equipped with a completely new Focal Plane Array detector that overcome all of the traditional FT-IR issues. Thanks to this technology Cary 620 can simultaneously acquires more than 160000, thus increasing the mapping speed and allowing to acquire FT-IR image in less than 10 minutes. In addition, Agilent Cary 620 technology has an incredible spatial capability. It can work in two different ways. Indeed, in the “High Mag” mode it extends the spatial resolution to 1 µm, thus allowing to directly image small objects within a sample; on the other hand, using the low mag mode it can directly image large sample portion, up to the centimeter scale.

Here we present the advantages of Agilent Cary 620 in the geology field. The instrument can be configured to work on hard rock samples using different acquisition parameter. Data clearly shows the ability of Agilent Cary 620 in imaging the rocks mineral distribution and the presence of organic matter micro cluster enclosed within rocks’ samples. Its unique technologies allow to either collect image maps of large sample area, up to several centimeters, and to maps small sample areas with the highest spatial distribution. This features represent a unique solution in the FT-IR spectroscopy to have a complete multi scale knowledge of the investigated samples.

EMU Excellence Medal Talk

QUANTITATIVE INFRARED SPECTROMETRY OF WATER IN NOMINALLY ANHYDROUS MINERALS: FACTS, DOUBTS AND BELIEFS

Kovács I.*[1]
[1] Geological and Geophysical Institute of Hungary, Budapest, Hungary
Corresponding email: kovacs.istvan.janos@mfgi.hu

Keywords: FTIR spectrometry, nominally anhydrous minerals

"Water" (H_2O, OH^- and H^+) in the nominally anhydrous minerals (NAMs) of the lithosphere and upper mantle play a key role in determining rheological and geophysical properties. Both the concentration and the substitution mechanism of "water" are important to formulate this effect on mineral properties. Fourier-transform infrared (FTIR) spectrometry can provide both qualitative and quantitative information simultaneously on the incorporation of "water" into NAMs. In addition it is a cost and labour effective methodology, no wonder that it has become perhaps the most popular analytical technique over the past decades in the field. The quantitative evaluation of micro-FTIR mineral spectra, however, appears to remain a rather controversial topic. To obtain accurate concentrations of "water" in NAMs one should be able to constrain the total polarized absorbance (A_{tot}) satisfactorily and choose appropriate calibration factors (extinction coefficients) to relate A_{tot} to the absolute concentration of "water".

There are several different – sometimes controversial – ways to measure or estimate A_{tot} taking into account the effect of the polarization state of the infrared radiation and the anisotropy of most of the NAMs. Furthermore, there are mineral-, substitution mechanism-, and wavenumber-dependent calibrations factors available to convert A_{tot} to the absolute concentration of water (usually given in ppm wt.%). No wonder that very different absolute water concentrations may be obtained from the very same IR spectrum. Thus, there is certainly a need for an evaluation protocol which would reduce these uncertainties giving clear instructions how A_{tot} should be obtained and what calibrations factors should be used. This talk aims to provide an up-to-date overview on these issues and offers practical tips also to those who are not yet familiar in the field but would be willing to analyse "water" in NAMs in the future. Furthermore several beliefs and doubts will be discussed to hopefully leave the audience with the impression that doing accurate micro-FTIR spectrometry on NAMs is not "rocket science".

Demouchy, S. & Bolfan-Casanova, N. (2016): Distribution and transport of hydrogen in the lithospheric mantle: A review. *Lithos*, **240**, 402-425.

Kovács, I., Hermann, J., O'Neill, H.S.C., FitzGerald, J., Sambridge, M., Horváth, G. (2008): Quantitative absorbance spectroscopy with unpolarized light, Part II: Experimental evaluation and development of a protocol for quantitative analysis of mineral IR spectra. *Am. Mineral.*, **93**, 765-778.

Kovács, I., O'Neill, H.S.C., Hermann, J., Hauri, E. (2010): Site-specific infrared O-H absorption coefficients for water substitution into olivine. *Am. Mineral.*, **95**, 292-299.

Libowitzky, E. & Rossman, G.R. (1996): Principles of quantitative absorbance measurements in anisotropic crystals. *Phys. Chem. Minerals*, **23**, 319-327.

Withers, A.C. (2013): On the use of unpolarized infrared spectroscopy for quantitative analysis of absorbing species in birefringent crystals. *Am. Mineral.*, **98**, 689-697.

Authors' Index

Authors are listed alphabetically: For each contribution, the page number and the session are given. Communicating authors are highlighted in blue.

Thanks to our Platinum Sponsors

COL
Comitato organizzativo locale
del sistema congressuale
della Riviera di Rimini

emc2016 is organized by Società Italiana di Mineralogia e Petrologia, on behalf of:
Deutsche Mineralogische Gesellschaft, Mineralogical Society of Great Britain & Ireland, Mineralogical Society of Finland, Österreichische Mineralogische Gesellschaft, Mineralogical Society of Poland, Russian Mineralogical Society, Sociedad Española de Mineralogía, Société Française de Minéralogie et de Cristallographie, Swiss Society of Mineralogy and Petrology, European Mineralogical Union

Organizing Secretariat: New Aurameeting Srl. e-mail: emc2016@newaurameeting.it